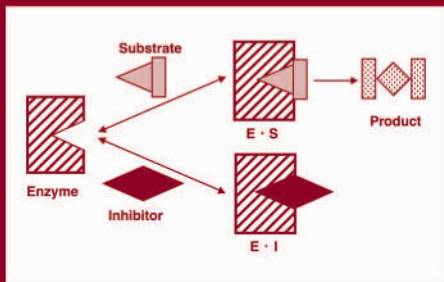


# Drug—Drug Interactions



edited by  
A. David Rodrigues



**ISBN: 0-8247-0283-2**

This book is printed on acid-free paper.

**Headquarters**

Marcel Dekker, Inc.  
270 Madison Avenue, New York, NY 10016  
tel: 212-696-9000; fax: 212-685-4540

**Eastern Hemisphere Distribution**

Marcel Dekker AG  
Hutgasse 4, Postfach 812, CH-4001 Basel, Switzerland  
tel: 41-61-261-8482; fax: 41-61-261-8896

**World Wide Web**

<http://www.dekker.com>

The publisher offers discounts on this book when ordered in bulk quantities. For more information, write to Special Sales/Professional Marketing at the headquarters address above.

**Copyright © 2002 by Marcel Dekker, Inc. All Rights Reserved.**

Neither this book nor any part may be reproduced or transmitted in any form or by any means, electronic or mechanical, including photocopying, microfilming, and recording, or by any information storage and retrieval system, without permission in writing from the publisher.

Current printing (last digit):

10 9 8 7 6 5 4 3 2 1

**PRINTED IN THE UNITED STATES OF AMERICA**

# Preface

Our knowledge of the various human drug metabolizing enzyme systems continues to grow. In recent years, this expansion in knowledge has been fueled by significant advances in molecular biology, the increased availability of human tissue, and the development of reliable model systems and sensitive assay methods for studying drug metabolism *in vitro*. In fact, *in vitro* methodology has become increasingly “standardized” and has been widely accepted by academic institutions, the pharmaceutical industry and regulatory agencies. However, while *in vitro* approaches can be used to screen large numbers of compounds preclinically, it is recognized that accurate forecasting of drug–drug interaction is predicated on sound knowledge of *in vivo* pharmacokinetics and the availability of validated *in vitro*–*in vivo* correlations.

Towards this end, the purpose of *Drug–Drug Interactions* is to relate pharmacokinetic concepts to the Michaelis–Menten kinetics describing *in vitro* enzyme-catalyzed biotransformation reactions. With kinetics as a foundation, the topic of drug–drug interactions is presented in terms of the various *in vitro* models, representative enzyme systems (e.g., cytochromes P450 and UDP-glucuronosyltransferases), and approaches (e.g., kinetics-based *in vitro*–*in vivo* correlations, computer-aided molecular modeling studies and informational databases). Although the subject matter focuses on metabolism-based drug–drug interactions resulting from inhibition and induction of drug-metabolizing enzymes, it is acknowledged that drug–drug interactions can occur via other mechanisms (e.g., competition for drug transporters and binding sites on plasma proteins, or pharmacodynamic drug–drug interactions).

An additional objective of this book is to present the subject of drug–drug interactions from preclinical, clinical, toxicological, regulatory, and marketing

perspectives. Therefore, it is hoped that *Drug–Drug Interactions* will be useful to students and seasoned scientists in the fields of molecular biology, pharmacokinetics, enzymology, toxicology, drug metabolism, pharmacology, clinical pharmacology, medicine, and medicinal chemistry. The subject matter will also appeal to those involved in the marketing of drugs. In the end, the book will have achieved its purpose if it serves merely to provoke constructive debate among individuals within these various disciplines.

*A. David Rodrigues*

# Contents

<i>Preface</i>	<i>iii</i>
<i>Contributors</i>	<i>ix</i>
<i>Useful Information</i>	<i>xiii</i>
1. Introducing Pharmacokinetic and Pharmacodynamic Concepts <i>Malcolm Rowland</i>	1
2. In Vitro Enzyme Kinetics Applied to Drug-Metabolizing Enzymes <i>Kenneth R. Korzekwa</i>	33
3. Human Cytochromes P450 and Their Role in Metabolism-Based Drug–Drug Interactions <i>Stephen E. Clarke and Barry C. Jones</i>	55
4. Review of Human UDP-Glucuronosyltransferases and Their Role in Drug–Drug Interactions <i>Rory P. Remmel</i>	89
5. Drug–Drug Interactions Involving the Membrane Transport Process <i>Hiroyuki Kusuhara and Yuichi Sugiyama</i>	123

6. In Vitro Models for Studying Induction of Cytochrome P450 Enzymes 189  
*Jose M. Silva and Deborah A. Nicoll-Griffith*
7. In Vitro Approaches for Studying the Inhibition of Drug-Metabolizing Enzymes and Identifying the Drug-Metabolizing Enzymes Responsible for the Metabolism of Drugs 217  
*Ajay Madan, Etsuko Usuki, L. Alayne Burton, Brian W. Ogilvie, and Andrew Parkinson*
8. The Role of P-Glycoprotein in Drug Disposition: Significance to Drug Development 295  
*Matthew D. Troutman, Gang Luo, Liang-Shang Gan, and Dhiren R. Thakker*
9. The Role of the Gut Mucosa in Metabolically Based Drug–Drug Interactions 359  
*Kenneth E. Thummel and Danny D. Shen*
10. Mechanism-Based Inhibition of Human Cytochromes P450: In Vitro Kinetics and In Vitro–In Vivo Correlations 387  
*David R. Jones and Stephen D. Hall*
11. Prediction of Metabolic Drug Interactions: Quantitative or Qualitative? 415  
*Jiunn H. Lin and Paul G. Pearson*
12. In Vivo Probes for Studying Induction and Inhibition of Cytochrome P450 Enzymes in Humans 439  
*Grant R. Wilkinson*
13. Molecular Modeling Approaches to Predicting Drug Metabolism and Toxicity 505  
*Anton M. ter Laak, Marcel J. de Groot, and Nico P. E. Vermeulen*
14. Development of a Metabolic Drug Interaction Database at the University of Washington 549  
*Sonia P. Carlson, Isabelle Ragueneau-Majlessi, Thomas E. Bougan, and René H. Levy*

**Contents****vii**

15.	Drug–Drug Interactions: Clinical Perspective <i>David J. Greenblatt and Lisa L. von Moltke</i>	565
16.	Drug–Drug Interactions: Toxicological Perspectives <i>Sidney D. Nelson</i>	585
17.	An Integrated Approach to Assessing Drug–Drug Interactions: A Regulatory Perspective <i>Shiew-Mei Huang, Peter Honig, Lawrence J. Lesko, Robert Temple, and Roger Williams</i>	605
18.	Drug–Drug Interactions: Marketing Perspectives <i>Kevin J. Petty and José M. Vega</i>	633
	<i>Index</i>	645





# Contributors

**Thomas E. Bougan** Applied Technical Systems, Bremerton, Washington

**L. Alayne Burton** XenoTech, LLC, Kansas City, Kansas

**Sonia P. Carlson** Department of Pharmaceutics, University of Washington, Seattle, Washington

**Stephen E. Clarke** Department of Drug Metabolism and Pharmacokinetics, Glaxo SmithKline Pharmaceuticals, Ware, United Kingdom

**Marcel J. de Groot** Molecular Informatics, Structure and Design, Pfizer Global Research & Development, Kent, United Kingdom

**Liang-Shang Gan** Department of Drug Metabolism and Pharmacokinetics, DuPont Pharmaceuticals Company, Newark, Delaware

**David J. Greenblatt** Department of Pharmacology and Experimental Therapeutics, Tufts University School of Medicine, and Division of Clinical Pharmacology, New England Medical Center, Boston, Massachusetts

**Stephen D. Hall** Division of Clinical Pharmacology, Department of Medicine, Indiana University School of Medicine, Indianapolis, Indiana

**Peter Honig** Office of Postmarketing and Drug Risk Assessment, Center for Drug Evaluation and Research, U.S. Food and Drug Administration, Rockville, Maryland

**Shiew-Mei Huang** Office of Clinical Pharmacology and Biopharmaceutics, Center for Drug Evaluation and Research, U.S. Food and Drug Administration, Rockville, Maryland

**Barry C. Jones** Pfizer Global Research & Development, Kent, United Kingdom

**David R. Jones** Division of Clinical Pharmacology, Department of Medicine, Indiana University School of Medicine, Indianapolis, Indiana

**Kenneth R. Korzekwa** Camitro Corporation, Menlo Park, California

**Hiroyuki Kusuhara** Department of Biopharmaceutics, Graduate School of Pharmaceutical Sciences, University of Tokyo and CREST, Japan Science and Technology Corporation, Tokyo, Japan

**Lawrence J. Lesko** Office of Clinical Pharmacology and Biopharmaceutics, U.S. Food and Drug Administration, Rockville, Maryland

**René H. Levy** Department of Pharmaceutics and Department of Neurological Surgery, University of Washington, Seattle, Washington

**Jiunn H. Lin** Drug Metabolism, Merck & Company, West Point, Pennsylvania

**Gang Luo** Department of Drug Metabolism and Pharmacokinetics, DuPont Pharmaceuticals Company, Newark, Delaware

**Ajay Madan** XenoTech, LLC, Kansas City, Kansas

**Sidney D. Nelson** Department of Medicinal Chemistry, School of Pharmacy, University of Washington, Seattle, Washington

**Deborah A. Nicoll-Griffith** Department of Molecular Biology, Merck Frosst Canada, Quebec, Canada

**Brian W. Ogilvie** XenoTech, LLC, Kansas City, Kansas

**Andrew Parkinson** XenoTech, LLC, Kansas City, Kansas

**Paul G. Pearson** Drug Metabolism, Merck & Company, West Point, Pennsylvania

**Kevin J. Petty** Clinical Pharmacology, Merck Research Laboratories, Blue Bell, Pennsylvania

**Isabelle Ragueneau-Majlessi** Department of Pharmaceutics, University of Washington, Seattle, Washington

**Rory P. Remmel** Department of Medicinal Chemistry, University of Minnesota, Minneapolis, Minnesota

**Malcolm Rowland** School of Pharmacy and Pharmaceutical Sciences, University of Manchester, Manchester, United Kingdom

**Danny D. Shen** Department of Pharmaceutics, University of Washington, Seattle, Washington

**Jose M. Silva** Department of Molecular Biology, Merck Frosst Canada, Quebec, Canada

**Yuichi Sugiyama** Department of Biopharmaceutics, Graduate School of Pharmaceutical Sciences, University of Tokyo and CREST, Japan Science and Technology Corporation, Tokyo, Japan

**Robert Temple** Office of Medical Policy, Center for Drug Evaluation and Research, U.S. Food and Drug Administration, Rockville, Maryland

**Anton M. ter Laak** Department of Pharmacochimistry, Vrije Universiteit, Amsterdam, The Netherlands

**Dhiren R. Thakker** Division of Drug Delivery and Disposition, School of Pharmacy, University of North Carolina, Chapel Hill, North Carolina

**Kenneth E. Thummel** Department of Pharmaceutics, University of Washington, Seattle, Washington

**Matthew D. Troutman** Division of Drug Delivery and Disposition, School of Pharmacy, University of North Carolina, Chapel Hill, North Carolina

**Etsuko Usuki** XenoTech, LLC, Kansas City, Kansas

**José M. Vega** Clinical Pharmacology, Merck Research Laboratories, Blue Bell, Pennsylvania

**Nico P. E. Vermeulen** Section of Molecular Toxicology, Department of Pharmacology, Vrije Universiteit, Amsterdam, The Netherlands

**Lisa L. von Moltke** Department of Pharmacology and Experimental Therapeutics, Tufts University School of Medicine, and Division of Clinical Pharmacology, New England Medical Center, Boston, Massachusetts

**Grant R. Wilkinson** Department of Pharmacology, Vanderbilt University School of Medicine, Nashville, Tennessee

**Roger Williams** U.S. Pharmacopeia, Rockville, Maryland

# Useful Information

## WEBSITES

<http://www.dml.georgetown.edu/depts/pharmacology/p450ref2.html>  
<http://www.accp.com/p450.html>  
<http://www.fda.gov/cder/guidance/index.htm>  
<http://www.gentest.com>  
<http://www.panvera.com>  
<http://www.pharmacy.org/wwwdbs.html>  
<http://www.druginfonet.com/faq/faqintac.htm>  
<http://cponline.gsm.com/sample/interact/sample7.htm>  
[http://www.jag.on.ca/asp\\_bin/Drug%20interactions.asp](http://www.jag.on.ca/asp_bin/Drug%20interactions.asp)  
<http://www.unmc.edu/library/pharm/adr.html>  
[http://www.ndmainfo.org/consumerInfo/04\\_02\\_03.html](http://www.ndmainfo.org/consumerInfo/04_02_03.html)  
<http://dmd.aspetjournals.org/>  
<http://jpet.aspetjournals.org/>  
<http://www.xenotechllc.com>  
<http://base.icgeb.trieste.it/p450/>  
<http://www.invitrotech.com>  
<http://216.70.174.79/transporter/>

## BOOKS

GL Amidon. *Mechanisms of Drug Interactions*. New York: Springer, 1996.  
DA Ciraulo. *Drug Interactions in Psychiatry*. Baltimore: Williams and Wilkins, 1995.

- A Emel. Cytochrome P450. New York: Springer-Verlag, 1993.
- PW Erhardt, ed. Drug Metabolism: Databases and High-Throughput Testing During Drug Design and Development. Berlin: Blackwell Science, 1999.
- TBP Geurts. Summary of Drug Interactions with Oral Contraceptives. New York: Parthenon Publishing Group, 1993.
- M Gibaldi. Biopharmaceutics and Clinical Pharmacokinetics. Malvern, PA: Lea and Febiger, 1991.
- GG Gibson, P Skett. Introduction to Drug Metabolism. Glasgow: Blackie Academic and Professional, 1994.
- NJ Gooderham, P Jenner, L Patterson, eds. Drug Metabolism: Towards the Next Millennium. Amsterdam: IOS Press, 1998.
- JP Griffen. A Manual of Adverse Drug Interactions. New York: Elsevier, 1997.
- PD Hansten. Drug Interactions: Clinical Significance of Drug-Drug Interactions. Philadelphia: Lea and Febiger, 1989.
- JG Hardman, LE Limbird, PB Molinoff, RW Ruddon, AG Gilman, eds. The Pharmacological Basis of Therapeutics. New York: McGraw-Hill, 1996.
- W Hori, ed. Drug-Drug Interactions: Analyzing In Vitro-In Vivo Correlations. Southborough, MA: International Business Communications, 1997.
- C Ioannides, ed. Cytochromes P450: Metabolic and Toxicological Aspects. New York: CRC Press, 1996.
- RH Levy, KE Thummel, WF Trager, PD Hansten, M Eichelbaum, eds. Metabolic Drug Interactions. New York: Lippincott, Williams and Wilkins, 2000.
- AP Li. Drug-Drug Interactions: Scientific and Regulatory Perspectives. Advances in Pharmacology, Vol. 43. San Diego: Academic Press, 1997.
- JZ Litt. Pocketbook of Drug Eruptions and Interactions. New York: Parthenon Publishing Group, 1999.
- Office for the Official Publications of the European Communities. European Symposium on the Prediction of Drug Metabolism in Man: Progress and Problems. Luxembourg, 1999.
- PR Ortiz de Montellano, ed. Cytochrome P450: Structure, Mechanism and Biochemistry. New York: Plenum, 1995.
- IR Phillips, EA Shepard, eds. Cytochrome P450 Protocols. Methods in Molecular Biology, Vol. 107. Totowa, NJ: Humana Press, 1998.
- WA Ritschel. Handbook of Basic Pharmacokinetics. Washington, D.C.: American Pharmaceutical Association, 1998.
- M Rowland, TN Tozer. Clinical Pharmacokinetics: Concepts and Applications. Baltimore: Williams & Wilkins, 1995.
- IH Segel. Enzyme Kinetics: Behavior and Analysis of Rapid Equilibrium

- and Steady-State Enzyme Systems. New York: John Wiley and Sons, 1993.
- NT Smith. Drug Interactions in Anesthesia. Philadelphia: Lea and Febiger, 1986.
- IH Stockley. Drug Interactions: A Source Book of Adverse Interactions, Their Mechanisms, Clinical Importance and Management. London: Pharmaceutical Press, 1996.
- PG Welling. Pharmacokinetics: Processes, Mathematics, and Applications. Washington, D.C.: American Chemical Society, 1997.
- PG Welling, FLS Tse, eds. Pharmacokinetics: Regulatory, Industrial, Academic Perspectives. New York: Marcel Dekker, 1999.
- TF Woolf, ed. Handbook of Drug Metabolism. New York: Marcel Dekker, 1999.

## JOURNAL ARTICLES AND BOOK CHAPTERS

- E Albengres, H Le Louet, JP Tillement. Systemic antifungal agents: drug interactions of clinical significance. *Drug Safety* 18:83–97, 1998.
- GD Anderson. A mechanistic approach to antiepileptic drug interactions. *Ann Pharmacother* 21:554–563, 1998.
- T Andersson. Pharmacokinetics, metabolism and interactions of acid pump inhibitors: focus on omeprazole, lansoprazole and pantoprazole. *Clin Pharmacokin* 32:9–28, 1996.
- MS Benedetti, M Bani. Metabolism-based drug interactions involving oralazole antifungals in humans. *Drug Metab Rev* 31:665–717, 1999.
- RJ Bertz, GR Granneman. Use of in vitro and in vivo data to estimate the likelihood of metabolic pharmacokinetic interactions. *Clin Pharmacokin* 32:210–258, 1997.
- P Bonnabry, J Sievering, T Leemann, P Dayer. Quantitative Drug Interactions Prediction and Management System (Q-DIPS): A computer-based prediction and management support system for drug metabolism interactions. *Eur J Clin Pharmacol* 55:341–347, 1999.
- JRBJ Brouwers, PAGM de Smet. Pharmacokinetic-pharmacodynamic drug interactions with nonsteroidal anti-inflammatory drugs. *Clin Pharmacokin* 27:462–485, 1994.
- C Campana, MB Regazzi, I Buggia, M Molinaro. Clinically significant drug interactions with cyclosporin: an update. *Clin Pharmacokin* 30:141–179, 1996.
- R Dal Negro. Pharmacokinetic drug interactions with anti-ulcer drugs. *Clin Pharmacokin* 35:135–150, 1998.
- B Davit, K Reynolds, R Yuan, F Ajayi, D Conner, E Fadiran, B Gillespie,



- C Sahajwalla, SM Huang, LJ Lesko. FDA evaluations using in vitro metabolism to predict and interpret in vivo metabolic drug–drug interactions: impact on labeling. *J Clin Pharmacol* 39:899–910, 1999.
- PJ Eddershaw, M Dickens. Advances in in vitro drug metabolism screening. *Pharm Sci Technol Today* 2:13–19, 1999.
- AG Fraser. Pharmacokinetic interactions between alcohol and other drugs. *Clin Pharmacokin* 33:79–90, 1997.
- JG Gillum, DS Israel, RE Polk. Pharmacokinetic drug interactions with antimicrobial agents. *Clin Pharmacokin* 25:450–482, 1993.
- P Glue, RP Clement. Cytochrome P450 enzymes and drug metabolism: basic concepts and methods of assessment. *Cell Molec Neurobiol* 19:309–323.
- PE Gronroos, KM Irjala, RK Huupponen, H Scheinin, J Forsstrom, JJ Forsstrom. A medication database: a tool for detecting drug interactions in hospital. *Eur J Clin Pharmacol* 53:13–17, 1997.
- JR Halpert. Structural basis of selective cytochrome P450 inhibition. *Ann Rev Pharmacol Toxicol* 35:29–53, 1995.
- PK Honig, BK Gillespie. Clinical significance of pharmacokinetic drug interactions with over-the-counter (OTC) drugs. *Clin Pharmacokin* 35:167–171, 1998.
- K Ito, T Iwatsubo, S Kanamitsu, K Ueda, H Suzuki, Y Sugiyama. Prediction of pharmacokinetic alterations caused by drug–drug interactions: metabolic interaction in the liver. *Pharmacol Rev* 50:387–411, 1998.
- MD Johnson, G Newkirk, JR White. Clinically significant drug interactions: what you need to know before writing prescriptions. *Postgrad Med* 105:193–222, 1999.
- TD Leemann, P Dayer. Quantitative prediction of in vivo drug metabolism and interactions from in vitro data. In: GM Pacifici, GN Fracchia, eds. *Advances in Drug Metabolism in Man*. European Commission, pp 784–830, 1995.
- DF Lewis, M Dickens, PJ Eddershaw, MH Tarbit, PS Goldfarb. Cytochrome P450 substrate specificities, substrate structural templates and enzyme active site geometries. *Drug Metab Drug Interact* 15:1–49, 1999.
- LL Lien, EJ Lien. Preventing potential drug interactions in community pharmacy. *J Clin Pharm Ther* 19:371–379, 1994.
- JH Lin, AYH Lu. Role of pharmacokinetics and metabolism in drug discovery and development. *Pharmacol Rev* 49:403–449, 1997.
- JH Lin, AYH Lu. Inhibition and induction of cytochrome P450 and the clinical implications. *Clin Pharmacokin* 35:361–390, 1998.
- PM Loadman, MC Bibby. Pharmacokinetic drug interactions with anticancer drugs. *Clin Pharmacokin* 26:486–500, 1994.

- LJ Malaty, JJ Kuper. Drug interactions of HIV protease inhibitors. *Drug Safety* 20:147–169, 1999.
- GT McInnes, MJ Brodie. Drug interactions that matter: a critical reappraisal. *Drugs* 36:83–110, 1988.
- EL Michalets. Update: clinically significant cytochrome P450 drug interactions. *Pharmacotherapy* 18:84–112, 1998.
- A Parkinson. An overview of current cytochrome P450 technology for assessing the safety and efficacy of new materials. *Toxicol Pathol* 24:45–57, 1996.
- A Parkinson. Biotransformation of xenobiotics. In: CD Klaassen, ed. *Toxicology: The Basic Science of Poison*. New York: McGraw-Hill, pp 113–186, 1996.
- O Pelkonen, J Maenpaa, P Taavitsainen, A Rautio, H Raunio. Inhibition and induction of human cytochrome P450 (CYP) enzymes. *Xenobiotica* 28:1203–1253, 1998.
- S Pfeifer. Pharmacokinetic drug interactions: part 1, drugs A–C. *Pharmazie* 50:163–179, 1995.
- S Pfeifer. Pharmacokinetic drug interactions: part 2, drugs D–O. *Pharmazie* 50:235–259, 1995.
- S Pfeifer. Pharmacokinetic drug interactions: part 3, drugs P–Z. *Pharmazie* 50:307–332, 1995.
- JR Powell, EW Cate. Induction and inhibition of drug metabolism. In: WE Evans, JJ Schentag, WJ Lesko, H Harrison, eds. *Applied Pharmacokinetics: Principles of Therapeutic Drug Monitoring*. Spokane: Applied Therapeutics, pp 139–186, 1986.
- S Rendic, FJ Di Carlo. Human cytochrome P450 enzymes: a status report summarizing their reactions, substrates, inducers, and inhibitors. *Drug Metab Rev* 29:413–580, 1997.
- R Riva, F Albani, M Coutin, A Baruzzi. Pharmacokinetic interactions between antiepileptic drugs: clinical considerations. *Clin Pharmacokin* 31:470–493.
- AD Rodrigues. Preclinical drug metabolism in the age of high-throughput screening: an industrial perspective. *Pharm Res* 14:1504–1510, 1997.
- AD Rodrigues. Integrated cytochrome P450 reaction phenotyping: attempting to bridge the gap between cDNA-expressed cytochromes P450 and native human liver microsomes. *Biochem Pharmacol* 57:465–480, 1999.
- H Shionoiri. Pharmacokinetic drug interactions with ACE inhibitors. *Clin Pharmacokin* 25:20–58, 1993.
- DA Smith, SM Abel, R Hyland, BC Jones. Human cytochromes P450: selectivity and measurement in vivo. *Xenobiotica* 28:1095–1128, 1998.

- DA Smith, H van de Waterbeemd. Pharmacokinetics and metabolism in early drug discovery. *Curr Opin Chem Biol* 3:373–378, 1999.
- BA Sproule, CA Naranjo, KE Bremmer, PC Hassan. Selective serotonin reuptake inhibitors and CNS drug interactions: a critical review. *Clin Pharmacokin* 33:454–471, 1997.
- AM Taburet, E Singlas. Drug interactions with antiviral drugs. *Clin Pharmacokin* 30:385–401, 1996.
- E Tanaka, S Hisawa. Clinically significant pharmacokinetic drug interactions with psychoactive drugs: antidepressants and antipsychotics and the cytochrome P450 system. *J Clin Pharm Ther* 24:7–16, 1999.
- MH Tarbit, J Berman. High-throughput approaches for evaluating absorption, distribution, metabolism and excretion properties of lead compounds. *Curr Opin Chem Biol* 2:411–416, 1998.
- KE Thummel, GR Wilkinson. In vitro and in vivo drug interactions involving human CYP3A. *Ann Rev Pharmacol Toxicol* 38:389–430, 1998.
- GT Tucker. The rational selection of drug interaction studies: implications of recent advances in drug metabolism. *Int J Clin Pharmacol Ther Toxicol* 30:550–553, 1992.
- LL von Moltke, DJ Greenblatt, J Schmider, CE Wright, JS Harmatz, RI Shader. In vitro approaches to predicting drug interactions in vivo. *Biochem Pharmacol* 55:113–122, 1998.
- GR Wilkinson. Clearance approaches in pharmacology. *Pharmacol Rev* 39:1–47, 1987.
- R Yuan, T Parmlee, JD Balian, RS Uppoor, F Ajayi, A Burnett, LJ Lesko, P Marroum. In vitro metabolic interaction studies: experiences of the Food and Drug Administration. *Clin Pharmacol Ther* 66:9–15, 1999.
- S Zevin, NL Benowitz. Drug interactions with tobacco smoking: an update. *Clin Pharmacokin* 36:425–438, 1999.
- TL Zimbrunnen, MW Jann. Drug interactions with antipsychotic agents: incidence and therapeutic implications. *CNS Drugs* 9:381–401, 1998.

# 1

## Introducing Pharmacokinetic and Pharmacodynamic Concepts

**Malcolm Rowland**

*University of Manchester, Manchester, United Kingdom*

### I. SETTING THE SCENE

All effective drugs have the potential for producing both benefits and risks, associated with desired and undesired effects. The particular response by a patient is driven in one way or another by the concentration of the drug, and sometimes its metabolites, at the effect sites within the body. Accordingly, it is useful to partition the relationship between drug administration and response into two phases, a *pharmacokinetic* phase, which relates drug administration to concentrations within the body produced over time, and a *pharmacodynamic* phase, which relates response (desired and undesired) produced to concentration. In so doing, we can better understand, for example, why patients vary in their response to drugs, which includes genetics, age, disease, and other drugs.

Patients often receive several or more drugs at the same time. Some diseases, such as cancer and AIDS, demand the need for combination therapy, which works better than can be achieved with any one of the drugs alone. In other cases, the patient is suffering from several conditions, each of which is being treated with one or more drugs. Given this situation, and the many potential sites for interaction that exist within the body, it is not surprising that an interaction may occur between them, whereby either the pharmacokinetics or pharmacodynamics of one drug is altered by another. More often than not, however, the interaction is of no clinical significance. This is because the response of most systems within the body is graded, with the intensity of response varying continuously with the concentration of compound producing it. Only when the magnitude of change in response is large enough will an interaction become of clinical significance,

which in turn varies with the drug. For a drug with a narrow therapeutic window, only a small change in response may precipitate a clinically significant interaction, whereas for a drug with a wide margin of safety, large changes in, say, its pharmacokinetics will have no clinical consequence. Also, it is well to keep in mind that some interactions are intentional, being designed for benefit, as often arises in combination therapy. Clearly, the ones of concern are the unintentional ones, which lead to either ineffective therapy through antagonism or lower concentrations of the affected drug or, more worryingly, excessive toxicity, which sometimes is so severe as to limit the use of the offending drug or, if it occurs too often or produces fatality, may result in its removal from the market.

This chapter lays down the conceptual framework for understanding the quantitative and temporal aspects of drug–drug interactions, hereafter called drug interactions, for simplicity. Emphasis is placed primarily on pharmacokinetic aspects, partly because pharmacokinetic interactions are the most common cause of undesirable and, to date, unpredictable interactions and also because most of this book is devoted almost exclusively to this aspect and indeed to one major component of it, drug metabolism. Some pharmacodynamic aspects are also covered, however, for there are many similarities between pharmacokinetic and pharmacodynamic interactions at the molecular level and because ultimately one has to place a pharmacokinetic interaction into a pharmacodynamic perspective to appreciate the likely therapeutic impact. Further reading is provided in the list of references [1–5].

## II. BASIC ELEMENTS OF PHARMACOKINETICS

As depicted in Figure 1 it is useful to divide pharmacokinetic processes in vivo broadly into two parts, absorption and disposition. *Absorption*, which applies to all sites of administration other than direct injection into the bloodstream, comprises all processes between drug administration and appearance in circulating blood. Bioavailability is a measure of the extent of absorption of drug. *Disposition* comprises both distribution of drug into tissues within the body and elimination, itself divided into metabolism and excretion of unchanged drug. Disposition is characterized independently following intravenous administration, when absorption is not involved.

Increasingly, aspects of potential drug interactions are being studied in vitro not only with the aim of providing a mechanistic understanding but also with the hope that the findings can be used to predict quantitatively events in vivo and thereby to avoid or limit undesired clinical interactions. To achieve this aim we need a holistic approach whereby individual processes are nested within a whole body frame. That is, constructs (models) that allow us to explore the impact, for example, of inhibition or induction of a particular metabolic pathway

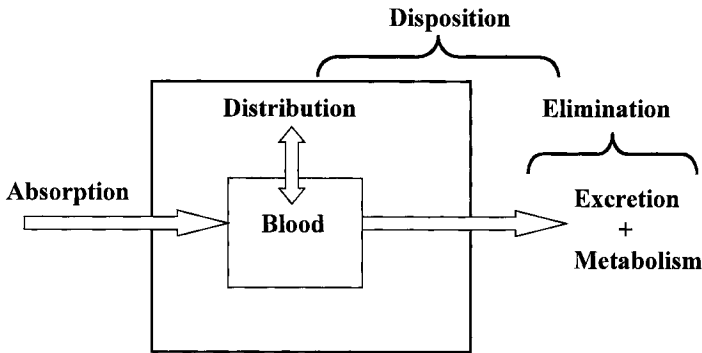


**Figure 1** Schematic representation of processes comprising the pharmacokinetics of a compound. Here terms are defined with respect to measurement in blood or plasma. *Absorption* comprises all events between drug administration and appearance at the site of measurement. *Distribution* is the reversible transfer of drug from and to other parts of the body. *Elimination* is the irreversible loss of drug either as unchanged compound (excretion) or by metabolism. *Disposition* is the movement of drug out of blood by distribution and elimination.

on, say, the concentration–time profile of drug in the circulating plasma or blood, which is delivering drug to all parts of the body, including sites of action and elimination. This approach also allows us to better interpret the underlying events occurring in vivo following a drug interaction. To appreciate this last statement consider the events shown in Figures 2 and 3 and the corresponding summary data given in Table 1.

In Figure 2, pretreatment with the antibiotic rifampin shortened the half-life and decreased the area under the plasma concentration–time (AUC) profile, but not materially the peak concentration, of the oral anticoagulant warfarin, whether given intravenously or orally. In contrast, pretreatment with the sedative hypnotic pentobarbital reduced both the peak concentration and AUC of the anti-hypertensive agent, alprenolol, following oral administration while apparently producing no change in its pharmacokinetics after intravenous dosing. As can be seen, these clinical studies show clear evidence of an interaction, with both actually involving the same mechanism, enzyme induction, but the effect is clearly expressed in different ways. To understand why this is so, we need to deal first with the intravenous data and then the oral data, that is, to separate disposition from absorption.

For many purposes, because distribution is often much faster than elimination, as a first approximation the body can be viewed as a single compartment, of volume  $V$ , into which drugs enter and leave. This is an apparent volume whose

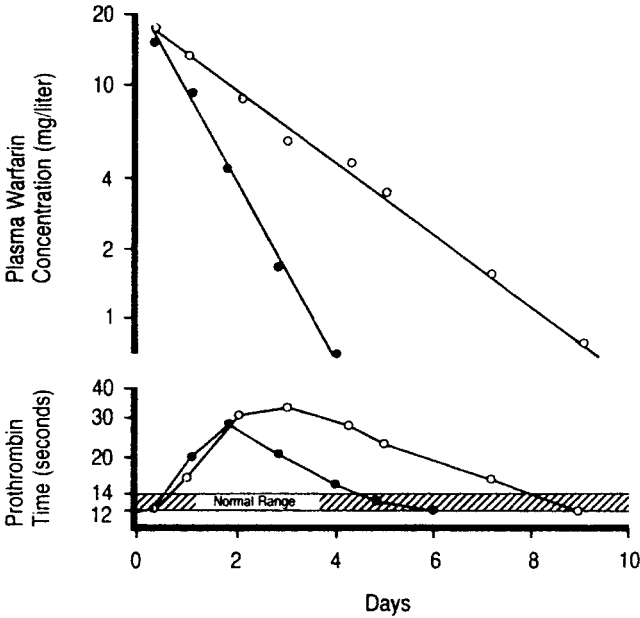


**Figure 2** Half-life of the oral anticoagulant warfarin is shortened and its clearance increased when given as a single dose (1.5 mg/kg) before (○) and while (●) subjects have taken the enzyme inducer, rifampin, 600 mg daily for 3 days prior to and 10 days following warfarin administration. The peak and duration in elevation of the prothrombin time, a measure of the anticoagulant response, are both decreased when rifampin is coadministered. (From Ref. 6. Reproduced with permission.)

value varies widely among drugs, owing to different distribution patterns within the body. The larger the volume, the lower the plasma concentration for a given amount in the body. The other important parameter controlling the plasma concentration ( $C$ )–time profile after an intravenous bolus dose (the disposition kinetics) is clearance ( $CL$ ), a measure of the efficiency of the eliminating organs to remove drug, given by

$$\text{Rate of elimination} = CL \cdot C \quad (1)$$

with units of flow (e.g., mL/min) such that

$$C = \frac{\text{Dose}}{V} \cdot e^{-(CL/V)t} \quad (2)$$

Often, Eq. (2) is recast by substituting  $k$ , the fractional rate of elimination of the drug, for  $CL$  and  $V$ , since

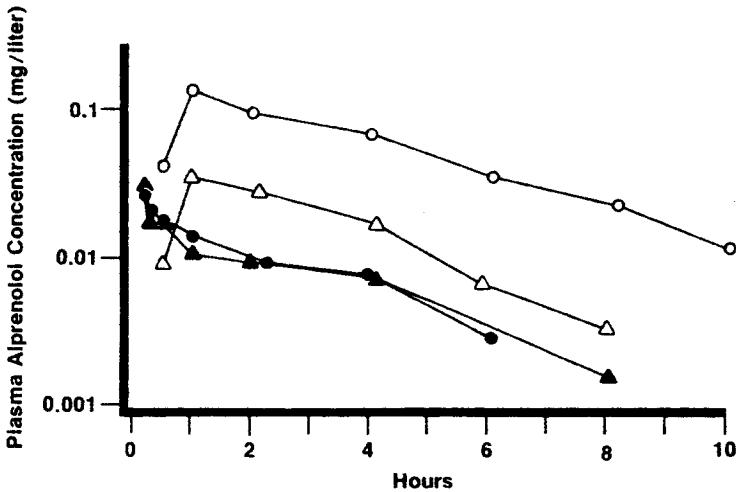


**Figure 3** Enzyme induction of alprenolol metabolism following pentobarbital treatment produces minimal changes in events in plasma following intravenous administration of alprenolol, 5 mg to subjects (● before, ▲ during pentobarbital), but a marked lowering of the plasma concentrations following oral administration of alprenolol, 200 mg (○ before, △ during pentobarbital). (From Ref. 7. Reproduced with permission.)

$$k = \frac{\text{Rate of elimination (CL} \cdot C)}{\text{Amount in body (V} \cdot C)} = \frac{\text{CL}}{V} \quad (3)$$

So

$$C = \frac{\text{Dose}}{V} \cdot e^{-kt} \quad (4)$$

It should be noted that  $k$  is related to half-life ( $t_{1/2}$ ) by

$$t_{1/2} = \frac{0.693}{k} = \frac{0.693 \cdot V}{\text{CL}} \quad (5)$$

Being independent parameters, one a measure of the extent of distribution of drug within the body and the other a measure of the efficiency of the eliminating organs to remove drug from plasma,  $V$  and  $\text{CL}$  are frequently referred to as *primary* pharmacokinetic parameters. While, the dependent ones,  $k$  and  $t_{1/2}$ , are *secondary* parameters, whose values change as a consequence of a change in  $\text{CL}$ ,  $V$ , or both. Thus drugs can have the same half-life but very different values of clearance and volume of distribution, as seen in Figure 4. Also, clearly, once any two parameters are known, the other is readily calculated.



**Table 1** Summary Pharmacokinetic Parameters Before and During Drug Interactions

Warfarin–rifampin interaction								
Warfarin pharmacokinetics <sup>a</sup>								
	Dose (mg/kg)	AUC (mg – hr/L)	CL (L/hr)	<i>t</i> <sub>1/2</sub> (hr)	<i>V</i> (L)			
Warfarin alone	1.5	600	0.18	47	12			
Warfarin + rifampin	1.5	258	0.41	18	11			
Alprenolol–pentobarbital interaction <sup>b</sup>								
Alprenolol pharmacokinetics								
Intravenous				Oral				
	Dose (mg)	AUC (mg-hr/L)	CL (L/hr)	<i>t</i> <sub>1/2</sub> (hr)	Dose (mg)	AUC (mg-hr/L)	<i>t</i> <sub>1/2</sub> (hr)	<i>F</i> (%)
Alprenolol alone	5	0.067	75	2.3	200	0.71	2.3	26
Alprenolol + pentobarbital	5	0.058	86	1.9	200	0.15	2.4	6.5

<sup>a</sup> Abstracted from Ref. 7.<sup>b</sup> Abstracted from Ref. 8.

A further important relationship, which follows by summing (integrating) Eq. (1) over all times, when the total amount eliminated equals the dose, is

$$CL = \left[ \frac{\text{Dose}}{\text{AUC}} \right]_{\text{iv}} \quad (6)$$

which allows the estimation of CL from the plasma data. Armed with these relationships, the changes in the disposition kinetics for the two drugs become clear. For alprenolol, because there was no measurable change in either AUC or *t*<sub>1/2</sub>, there must have been no change in CL or *V* either. In contrast, the smaller AUC during rifampin treatment signifies that the clearance of warfarin has increased, although there was no change in *V*, since substitution of the respective values shows that all the decrease in *t*<sub>1/2</sub> (and increase in *k*) is totally explained by the increase in CL (Table 1). Turning to the oral data, the only other relationship that one needs is

$$F = CL \cdot \left[ \frac{\text{AUC}}{\text{Dose}} \right]_{\text{oral}} \quad (7)$$

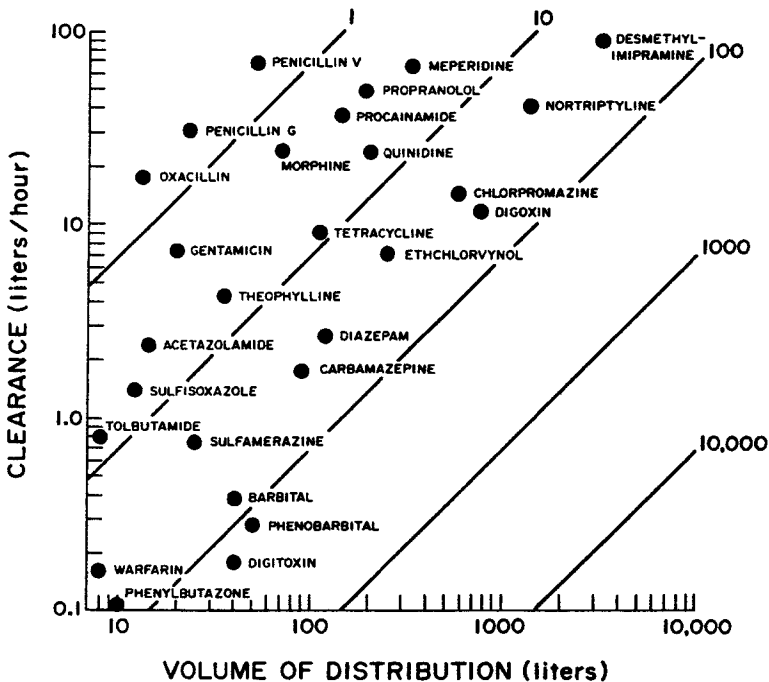


**Figure 4** Log-log plot of clearance versus volume of distribution of various drugs in human illustrating that for a given half-life, clearance and volume of distribution can vary widely. (Adapted from Ref. 8. Reproduced with permission.)

Equation (7) follows from the knowledge that again the total amount eliminated from the body ( $CL \cdot AUC$ ) must equal the total amount entering the systemic circulation ( $F \cdot \text{Dose}$ ), where  $F$  is the extent of absorption, or oral bioavailability, of the drug. Notice, without the intravenous data to provide an estimate of  $CL$ , only the ratio  $F/CL$  can be assessed following oral dosing, severely limiting the interpretation of events. Returning to the two interaction studies, analysis of the combined oral and intravenous plasma data indicates that, whereas there was no change in the oral bioavailability of warfarin (which is totally absorbed) following pretreatment with rifampin, it was reduced from an already low control value of 22% to an even lower value of just 6% for alprenolol after pentobarbital pretreatment (see Table 1).

To gain further insights into these two interactions, we need to place everything, and particularly clearance, on a more physiological footing. To do this, consider the scheme in Figure 5, which depicts events occurring across an elimi-

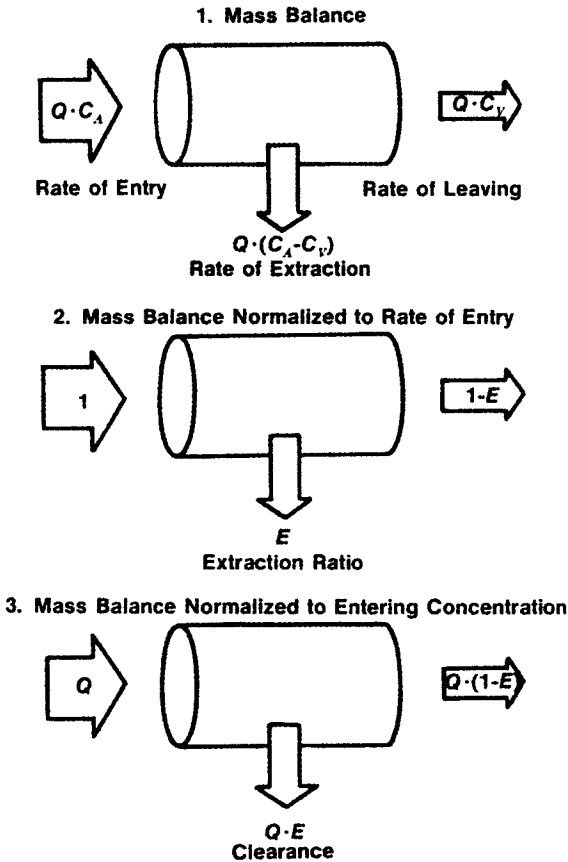


**Figure 5** Schematic of the extraction of a drug by an eliminating organ at steady state, illustrating the interrelationships between blood clearance, extraction ratio, and organ blood flow. See text for appropriate equations. (From Ref. 1. Reproduced with permission.)

nating organ, receiving blood at flow rate  $Q$  containing drug entering at concentration  $C_A$  and leaving at concentration  $C_V$ . Then it follows that

$$\text{Rate of elimination} = Q(C_A - C_V) \quad (8)$$

Often it is useful to express the rate of elimination relative to the rate of presentation ( $Q \cdot C_A$ ) to give the extraction ratio,

$$\text{Extraction ratio, } E = \frac{Q(C_A - C_V)}{Q \cdot C_A} = \frac{C_A - C_V}{C_A} \quad (9)$$

And therefore, from the definition of clearance in Eq. (1), it follows that

$$CL = Q \cdot E \quad (10)$$

It is immediately evident from Eq. (10) that clearance depends on both organ blood flow and extraction ratio. The extraction ratio can vary from 0, when no drug is removed, to 1, when all drug within the blood is removed on a single passage through the organ. Then, CL (strictly based on measurements in whole blood to conserve mass balance) is equal to, and cannot exceed, organ blood flow; clearance is then limited by, and is sensitive to, changes in perfusion rate. For both warfarin and alprenolol, essentially all elimination occurs by hepatic metabolism, and comparison of the estimated respective clearance values (0.18 L/hr and 65 L/hr) with the hepatic blood flow of 81 L/hr reveals that warfarin has a low hepatic extraction ratio ( $E_H$ ), while for alprenolol it is very high, at 0.80. This difference in extraction ratios has a direct impact on oral bioavailability, since all blood perfusing the gastrointestinal tract drains into the liver via the portal vein before entering the general circulation. Consequently, because only drug escaping the liver enters the systemic circulation, the oral bioavailability of a high-extraction-ratio compound, such as alprenolol, is expected to be low due to high *first-pass* hepatic loss. As already mentioned, this is indeed so. Furthermore, its low observed bioavailability (22%) is very close to that predicted assuming the liver is the only site of loss of orally administered compound. Then

$$\text{Predicted oral bioavailability, } F_H = 1 - E_H \quad (11)$$

that is, 20%. In contrast, on this basis warfarin, with its very low estimated hepatic extraction ratio ( $E_H$ ) is expected to have an oral bioavailability close to 100%. This agrees with the experimental findings, supporting the view that such factors as dissolution of the solid drug (administered as a tablet) and permeation through the intestine wall do not limit the overall absorption of this drug.

### A. A Model of Hepatic Clearance

To complete the task of explaining why the effect of induction manifests itself so differently in the pharmacokinetics of warfarin and alprenolol, we need a model that relates quantitatively changes in metabolic enzyme activity to changes in extraction ratio and clearance. Fundamental to all models and indeed to much of both pharmacokinetics and pharmacodynamics is that events are driven by unbound drug in plasma and tissues, the drug bound to proteins and other macromolecules being too bulky to enter cells and interact with sites of elimination and action. The most widely employed model of hepatic clearance in pharmacokinetics, but not the only one, is the well-stirred model [9–12] depicted in Fig-

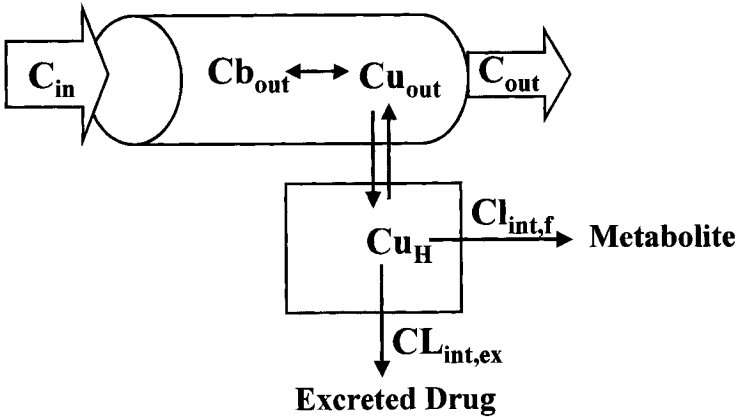


**Figure 6** Well-stirred model of hepatic clearance. Exchange of drug between plasma and hepatocyte and its removal from this cell involves unbound compound. Intrinsic clearance,  $CL_{int}$ , relates the rate of the elimination (by formation of metabolite(s),  $CL_{int,f}$ , and secretion of unchanged compound into bile,  $CL_{int,ex}$ ) to the unbound drug in the cell,  $Cu_H$ .  $Cb_{out}$ ,  $Cu_{out}$  are the bound and unbound concentrations of drug leaving the liver, at total concentration  $C_{out}$ .

ure 6. This model assumes that distribution of drug is so fast in this highly vascular organ that the concentration of unbound drug in the blood leaving it is equal to that in it. For this model,

$$E_H = \frac{fu \cdot CL_{int}}{Q + fu \cdot CL_{int}} \quad (12)$$

and therefore

$$CL = Q \cdot E_H = \frac{Q \cdot fu \cdot CL_{int}}{Q + fu \cdot CL_{int}} \quad (13)$$

which shows that in addition to blood flow  $CL$  and  $E_H$  are controlled by  $fu$ , the fraction of unbound drug in plasma (the ratio of unbound concentration in plasma,  $Cu$ , to the total measured plasma concentration,  $C$ , or strictly  $fu_b$ , the ratio of  $Cu$  to the whole blood concentration, to maintain mass balance across the liver), and  $CL_{int}$  the *intrinsic clearance*.

### 1. Intrinsic Clearance

Like clearance in general, (hepatic) intrinsic clearance is a proportionality constant, in this case between rate of elimination and unbound concentration within

the liver,  $Cu_H$ . That is,  $CL_{int} = (\text{Rate of elimination})/Cu_H$ . Conceptually, it is the value of clearance one would obtain if there were no protein binding or perfusion limitation, and is regarded as a measure of the activity within the cell, divorced from any limitations imposed by events in the perfusing blood. As such, the value of intrinsic clearance is often many orders of magnitude greater than for hepatic blood flow. Inferred through the analysis of in vivo data, where one cannot measure events within the cell, and determined experimentally in vitro, the concept of intrinsic clearance is critical not only to the quantitative interpretation and prediction of drug interactions within the liver, but to pharmacokinetics in general. And, since elimination can be by both metabolism and excretion, often operating additively within an organ to remove drug, under nonsaturating conditions,

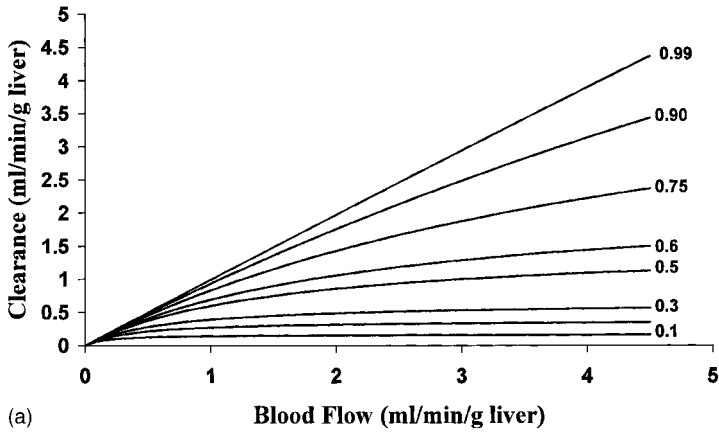
$$CL_{int} = \sum \frac{V_m}{K_m} + \sum \frac{T_m}{K_d} \quad (14)$$

or

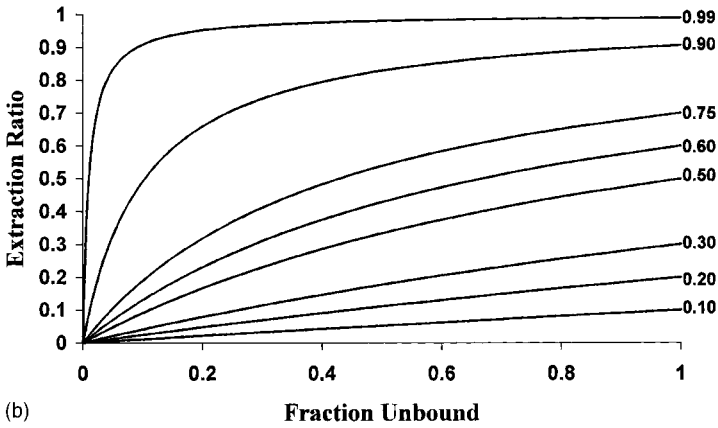
$$CL_{int} = \sum CL_{int,f} + \sum CL_{int,ex} \quad (15)$$

where  $V_m$ ,  $K_m$  are the maximum velocity of metabolism and Michaelis–Menten constant of each of the enzymes involved, alternatively expressed as their ratio, the intrinsic clearance associated with formation of the metabolite,  $CL_{int,f}$ . Similarly,  $T_m$ ,  $K_d$  are the transport maximum and dissociation constant of each of the transporters involved in excretion, with their ratio,  $CL_{int,ex}$  being the intrinsic clearance associated with excretion. Now, recognizing that  $V_m$  is directly proportional to the total amount of the respective enzyme, and induction involves an increase in its synthesis that increases the amount, it follows that the intrinsic clearance of the affected enzyme, and hence total  $CL_{int}$ , also increases during induction.

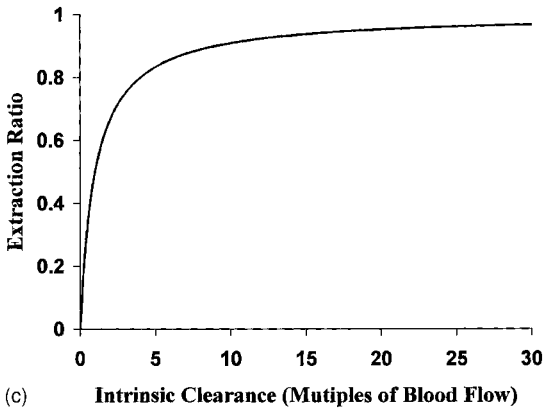
Examination of Eqs. (12) and (13) provides an understanding of the conditions determining the extraction ratio and CL of a drug, and hence the influence of induction itself. These relationships between CL,  $E$ ,  $Q$ ,  $f_u$ , and  $CL_{int}$  are displayed graphically in Figure 7. Also, examination of Eq. (12) reveals that plasma protein binding effectively lowers intrinsic clearance, by decreasing the unbound concentration for a given total concentration delivered in blood. However, when the effective intrinsic clearance ( $f_u \cdot CL_{int}$ )  $\gg Q$ , then it is seen that  $E_H \rightarrow 1$  and  $CL \rightarrow Q$ . Under these circumstances, CL is perfusion rate limited and insensitive to changes in  $CL_{int}$ , which explains why induction of the metabolism of alprenolol produced no noticeable increase in its clearance. Whereas, for a low-extraction drug, such as warfarin (which is both a poor substrate for the metabolic enzymes



(a)



(b)



(c)

**Figure 7** Influence of changes in (a) organ blood flow on clearance; (b) fraction of drug unbound in plasma ( $f_u$ ) on extraction ratio; and (c) intrinsic clearance on extraction ratio, predicted by the well-stirred model of hepatic clearance.

and very highly protein bound,  $f_u = 0.005$ ),  $f_u \cdot CL_{int} \ll Q$ , so

$$CL = f_u \cdot CL_{int} \quad (16)$$

which explains why the increase in intrinsic clearance due to enzyme induction is reflected in direct proportion by the measured clearance.

It remains to resolve the oral data, which is achieved as follows. Substituting Eq. (12) into Eq. (11) gives

$$F_H = \frac{Q}{Q + f_u \cdot CL_{int}} \quad (17)$$

which, when further substituted with Eq. (12) into Eq. (7), provides the useful relationship

$$AUC_{oral} = \frac{\text{Dose}}{f_u \cdot CL_{int}} \quad (18)$$

From Eq. (18) we see that AUC following an oral dose depends only on  $f_u$  and  $CL_{int}$  when, as happens with both warfarin and alprenolol, all administered drug reaches the liver essentially intact. Accordingly, the oral AUC should decrease with enzyme induction, irrespective of whether the drug is of high or low extraction ratio, as was observed.

In summary, changes in (hepatic) intrinsic clearance, whether due to induction or inhibition, are manifest differently in the whole-body pharmacokinetics of a drug, depending upon whether it is of high or low clearance when given alone. For drugs of low hepatic extraction ratio, changes in intrinsic clearance produce changes in total clearance, and half-life, but minimal changes in oral bioavailability. In contrast, for high-extraction-ratio drugs, which obviously must be exceptionally good substrates for the (hepatic) metabolic or excretory transport processes, a change in intrinsic clearance is reflected in a noticeable change in oral bioavailability but not in clearance or half-life.

## 2. Plasma Protein Binding

In drug interactions, the most common cause of altered protein binding is displacement, whereby one drug competes with another for one or more binding sites, increasing  $f_u$  of the affected drug. This can readily be assessed *in vitro* in plasma using one of a variety of methods, such as equilibrium dialysis, ultrafiltration, or ultracentrifugation. However, being a competitive process, the degree of displacement depends on the concentrations of the drugs relative to that of the binding sites. Only when the concentration of one of the drugs approaches the molar concentration of the binding sites will substantial displacement occur. In practice, because most drugs are relatively potent, this does not occur as often as one might have supposed, given so relatively few specific binding sites on



plasma proteins. Even when substantial displacement does occur, it often is of little to no therapeutic importance.

As seen from Eq. (13) (and Fig. 7) and emphasised in Eq. (16), an increase in  $f_u$  will only increase CL of drugs with a low extraction ratio, such as warfarin. When the extraction ratio is high, as with alprenolol, CL is essentially unaffected by a change in  $f_u$ , since clearly all drug, whether initially bound or not, must have been removed on the passage of the drug through the organ. That is, within the contact time of blood within the liver, bound drug dissociates so rapidly that all is available for removal as unbound drug is cleared. Notwithstanding, examination of Eq. (18) shows that, for all drugs, the AUC of the pharmacologically important unbound species ( $f_u \cdot \text{AUC}$ ) should be unaffected by displacement following oral administration, which probably explains why no clinically significant pure displacement interactions have been reported to date. Even so, displacement may affect the half-life of a drug. As now examined, much depends on the overall effect of displacement on the volume of distribution as well as on clearance.

## B. Model of Distribution

In its simplest form, the body may be viewed as comprising two aqueous spaces, the plasma (volume,  $V_p$ ) and the rest of the body ( $V_T$ ), as depicted in Figure 8, with distribution continuing until at equilibrium the unbound concentrations,  $C_u$  and  $C_{uT}$ , respectively, are equal. Then, in each space relating unbound to total drug concentration, though fraction unbound, and noting that the total amount

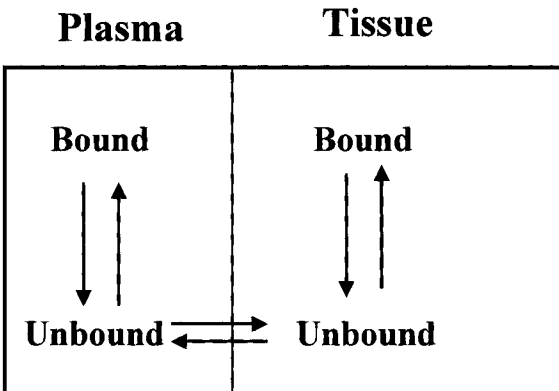


**Figure 8** Simple model of drug distribution, with unbound drug equilibrating between plasma and tissue.

of drug in the body,  $A = V \cdot C = V_p \cdot C + V_T \cdot C_T$ , it follows that

$$V = V_p + V_T \cdot \frac{fu}{fu_T} \quad (19)$$

where  $fu_T$  is the fraction of drug unbound in the tissue. The plasma volume is around 0.05 L/kg. And for drugs that access all the cells,  $V_T$  is 0.55L/kg, giving a total body water space of 0.6L/kg. For many drugs the volume of distribution is quite large, on the order of 1 L/kg or much greater. In these cases, the fraction of drug in the body located in plasma can be ignored, and so  $V$  reduces to  $V_T \cdot fu/fu_T$ , from which it is apparent that the volume of distribution varies directly with  $fu$  and inversely with  $fu_T$ . So displacement in plasma alone will always increase the volume of distribution. For drugs of low volume of distribution,  $<0.2L/kg$ , because they are predominantly located outside of cells, the situation is complicated by the presence of substantial amounts of drug in the interstitial space bathing the cells within tissues, where plasma proteins also reside. Dealing with this situation is beyond the scope of this chapter [1].

Combining Eq. (19) with the model for organ clearance [Eq. (13)] facilitates prediction of the effect of displacement on half-life. For low-extraction-ratio drugs, since  $CL = fu \cdot CL_{int}$ , and  $V = V_T \cdot fu/fu_T$ , both  $CL$  and  $V$  will increase to the same extent with displacement within plasma, so  $t_{1/2}$  ( $= 0.693 V/CL$ ) should remain unchanged. In contrast, half-life is expected to increase with displacement in plasma of high-clearance drugs, since  $V$  always increases but  $CL$  remains unchanged, being limited by organ blood flow.

### III. CHRONIC ADMINISTRATION

Pharmacokinetic information gained following single-dose administration can be used to help predict the likely events following chronic dosing, either as a constant-rate infusion or multiple dosing, which often involves giving a fixed dose at set time intervals.

#### A. Constant-Rate Infusion

During the infusion, the plasma concentration of drug continues to rise until a steady state is reached, when the rate of elimination ( $CL \cdot C$ ) matches the rate of infusion. These relationships, displayed in Figure 9, are defined by:

$$\text{During infusion} \quad C = C_{ss}(1 - e^{-kt}) \quad (20)$$

$$\text{At steady state} \quad C_{ss} = \frac{\text{Rate of infusion}}{CL} \quad (21)$$

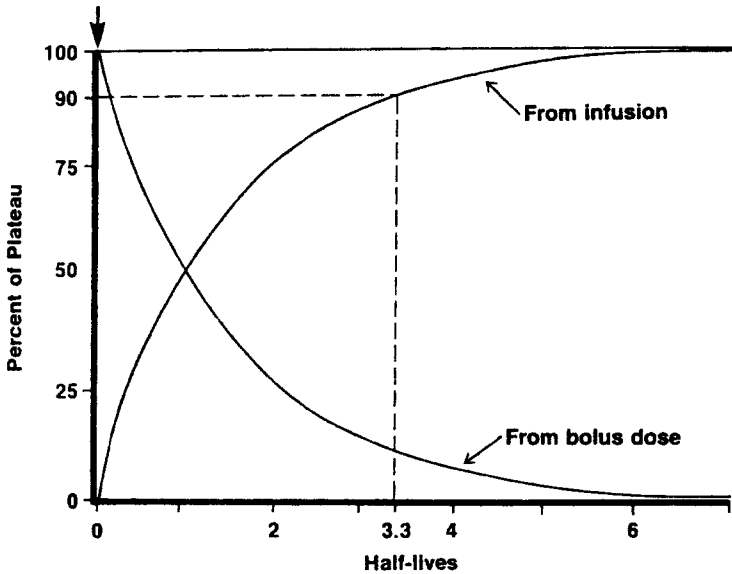


**Figure 9** Approach to plateau following a constant rate of input is controlled solely by the half-life of the drug. Depicted is the situation in which a bolus ( $\downarrow$ ) is immediately followed by an infusion that exactly matches the rate of elimination, thereby maintaining the plasma concentration. As the plasma concentration associated with the bolus falls exponentially, there is a complementary rise in that associated with the infusion. In 3.3 half-lives the plasma concentration associated with the infusion has reached 90% of the plateau value. (From Ref. 1. Reproduced with permission.)

Clearly, events at steady state depend only on clearance, while the time course on approach to the plateau is governed only by  $k$ , and hence half-life, information known from a single-dose study. Furthermore, calculations show that 50% of the plateau is reached in one half-life and 90% in 3.3 half-lives. Accordingly, drugs with short half-lives will reach steady state quickly, and those with half-lives in the order of days will take over a week. Hence, knowing the  $t_{1/2}$  of a drug is important when planning the duration of a study and the frequency of sampling of blood to characterize kinetic events.

## B. Multiple Dosing

Two additional features are observed on multiple dosing, accumulation and fluctuation (Fig. 10). The former arises because there is always drug remaining in the body from preceding doses and the latter because the rate of input varies

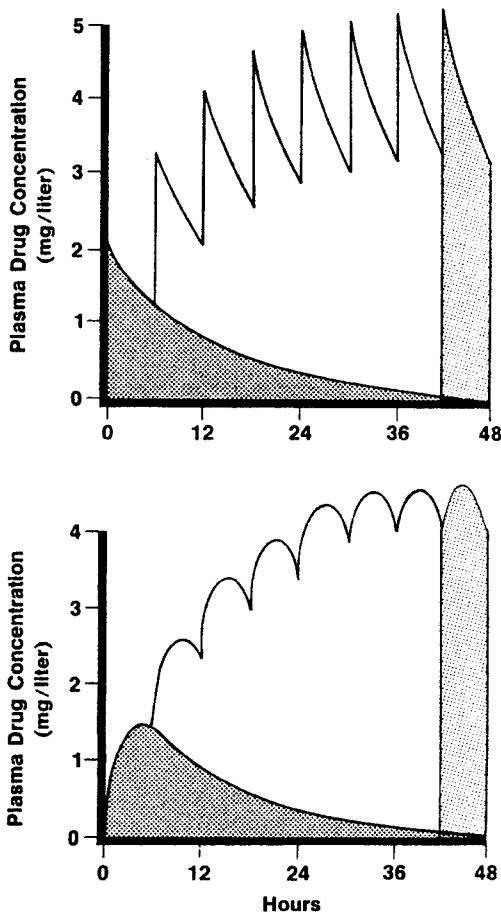


**Figure 10** Plasma concentrations of a drug following a multiple-dosing regimen, of fixed dose and interval, intravenously (top) and orally (bottom). Note that in both cases the area under the plasma concentration–time curve within a dosing interval at plateau is equal to the total area following a single dose. (From Ref. 1. Reproduced with permission.)

throughout each dosing interval. Nonetheless, the rise to the plateau still depends essentially only on the half-life of the drug, while within a dosing interval at plateau, the amount eliminated ( $CL \cdot AUC_{ss}$ ) equals the amount absorbed, i.e.,

$$F \cdot \text{Dose} = CL \cdot AUC_{ss} \quad (22)$$

where  $AUC_{ss}$  is the AUC at plateau. Furthermore, comparison of Eq. (22) with

Eq. (7) provides a useful expectation when the same-size dose is given on a single occasion and after multiple dosing, namely,

$$AUC_{ss} = AUC_{single} \quad (23)$$

Any deviation from this expectation implies that CL,  $F$ , or both must have changed on multiple dosing. If found, the kinetics of the drug are said to be time dependent.

An understanding of these kinetic principles helps in the planning and interpretation of in vivo drug interaction studies, which are of many designs. One goal is often to evaluate the full effects of an interaction, which generally requires exposing the affected drug to the highest concentration of the offending drug, which is at its plateau. So the offending drug needs to be administered for at least 3.3 of its half-lives and often for longer to ensure that the exposure is maintained throughout the time course of the affected drug.

#### IV. A GRADED EFFECT

As already mentioned, practically all drug interactions are graded, being dependent on the concentrations of the interacting drugs and, hence, on their pharmacokinetics as well as manner of administration [1,4]. While many scenarios are possible, for illustrative purposes consider the case of competitive inhibition of one pathway ( $A$ ) of metabolism of a low-clearance drug operating under linear (nonsaturating) conditions in the absence of the inhibitor, all other factors being constant. Then, for the affected pathway,

$$CL_{int,A,inhibited} = \frac{V_m}{K_m \left( 1 + \frac{I}{K_i} \right)} \quad \text{or} \quad CL_{int,A,inhibited} = \frac{CL_{int,A}}{1 + \frac{I}{K_i}} \quad (24)$$

where  $CL_{int,A}$  and  $CL_{int,A,inhibited}$  are the respective intrinsic clearances of the affected pathway in the absence and presence of the inhibitor, at unbound concentration  $I$ . Also characterizing the inhibitor is the inhibitor constant  $K_i$ , defined as the unbound concentration of inhibitor that effectively reduces the value of  $CL_{int,A}$  by one-half. Rearrangement of Eq. (24) gives the degree of inhibition of the affected pathway, DI. Namely,

$$DI = \frac{I/K_i}{1 + I/K_i} \quad (25)$$

which gives an alternative definition for  $K_i$  as the value of  $I$  that produces 50% of the maximum degree of inhibition. It is immediately clear from Eqs. (24) and (25) that the important factor is the ratio  $I/K_i$ . Thus, a compound may potentially

be a potent inhibitor, expressed by a low  $K_i$ , but in practice a significant inhibitory effect will arise only if  $I$  is high enough that  $I/K_i$  is large. Proceeding further, let  $f_m$  be the fraction of the total elimination of drug by the affected pathway in the absence of inhibitor. Then, by reference to previous equations, with appropriate rearrangements, one obtains the following generalized equation that permits exploration of the kinetics of this situation:

$$\begin{aligned}
 R_I &= \frac{C_{ss,\text{inhibited}}}{C_{ss,\text{normal}}} = \frac{AUC_{\text{single},\text{inhibited}}}{AUC_{\text{single},\text{normal}}} = \frac{AUC_{ss,\text{inhibited}}}{AUC_{ss,\text{normal}}} \\
 &= \frac{t_{1/2,\text{inhibited}}}{t_{1/2,\text{normal}}} = \frac{1}{f_m(1 - DI) + (1 - f_m)}
 \end{aligned}
 \tag{26}$$

noting that  $(1 - DI) = 1/(1 + I/K_i)$ . Here  $R_I$  is the ratio of  $C_{ss}$ ,  $AUC_{\text{single}}$ ,  $AUC_{ss}$ , and  $t_{1/2}$  in the presence (inhibited) and absence (normal) of the inhibitor.  $R_I$  might be thought of as the *inhibitor index*, giving a measure of the severity of the impact of the interaction on whole-body events. Figure 11 shows the relationship between  $R_I$  and  $DI$  for various values of  $f_m$ . Immediately apparent is that the increase in  $R_I$  becomes substantial only when  $f_m > 0.5$ , no matter how extensive

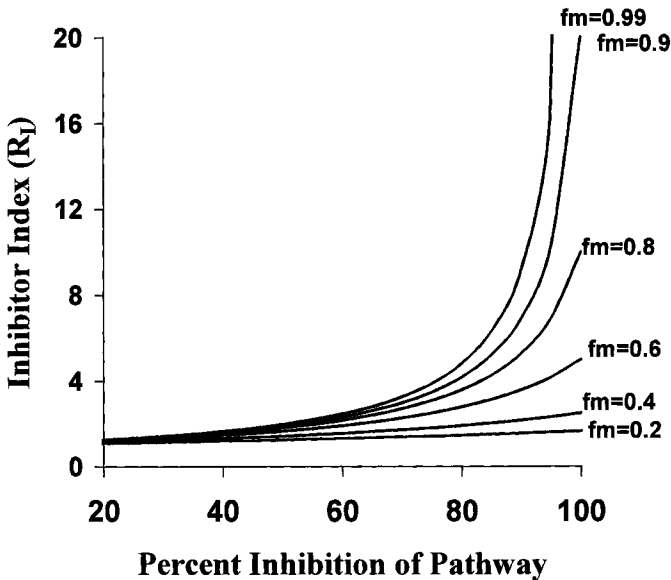


**Figure 11** Relationship between the inhibitor index,  $R_I$ , and the degree of inhibition of a metabolic pathway for various values of the fraction of drug eliminated by that pathway in the absence of the inhibitor,  $f_m$ .

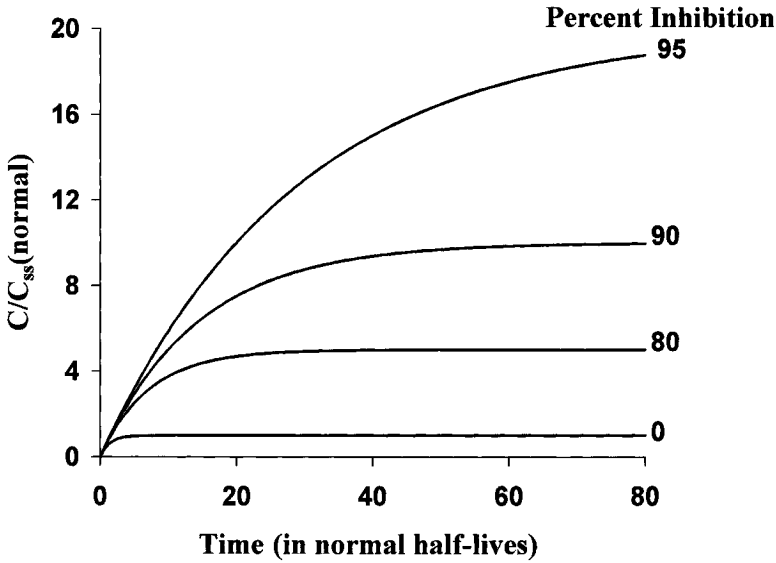


**Figure 12** Effect of inhibition on the rate of accumulation of a drug given as a constant-rate infusion, when  $f_m = 1$ . Note that time is expressed in units of normal half-life and concentration in units of the steady-state concentration in the absence of the inhibitor,  $C_{ss,normal}$ . The greater the degree of inhibition, the longer the half-life and the longer it takes to reach, and the higher is, the plateau.

the degree of inhibition of the affected pathway. Furthermore, note that  $R_I$  increases dramatically to values approaching 10 or greater the closer  $DI$  and  $f_m$  both approach 1. In other words, the problem becomes of very serious concern when the affected pathway is the obligatory route for elimination of the drug and is substantially inhibited. Fortunately, this situation does not arise that often in clinical practice.

The other important aspect is the time scale over which the effect of inhibition is seen in plasma, such as on the time to reach plateau following chronic drug administration, as illustrated in Figure 12 for the extreme case when  $f_m = 1$ . Recall, it takes approximately four half-lives to reach the plateau. So, although greater inhibition results in a substantial increase in the plateau concentration of the affected drug, because its half-life is also progressively increasing, associated with the decrease in clearance, it takes longer and longer to reach the new plateau. This has several implications. First, the full effects of an interaction may occur long after the inhibitor has been added to the dosage regimen of the affected drug, with the danger that any resulting toxicity may not be associated by either the patient or the clinician with the offending drug. Second, in planning *in vivo*

interaction studies during development, administration of the affected drug may need to be maintained for much longer in the presence of the potential inhibitor than based on the normal half-life of the drug. On passing, it is worth noting that a possible exception is inhibition of a drug of high hepatic extraction ratio, such as alprenolol. In this case, for moderate degrees of inhibition of intrinsic clearance, the major changes will be in the AUC and peak plasma concentration, with little change in half-life, because, as discussed previously for such drugs, clearance is blood flow limited. Only when inhibition is so severe that the drug is effectively converted from one of high extraction ratio to one of low extraction will half-life also increase.

Third, the current scenario corresponds to the clinical situation of the affected drug being added to the regimen of an individual already stabilized on the inhibitor. Another, perhaps more common scenario, especially when the inhibitor has just been introduced into clinical practice, is addition of the inhibitor to the maintenance regimen of the affected drug. Then one needs to consider both the pharmacokinetics and dosage regimen of the inhibitor as well as the changing kinetics of the affected drug. This last scenario is illustrated in Figure 13. Upon initiating the regimen of the second drug (inhibitor), its plasma concentration rises toward its plateau with a time scale governed by its half-life. And as it rises, so does the degree of inhibition of the affected drug, which in turn decreases its clearance and prolongs its half-life. The net result is that it takes even longer for the plasma concentration of affected drug to reach its new plateau than anticipated from even its longest half-life, which is at the plateau of the inhibitor. The reason for this is that in essence one has to add on the time that it takes for the inhibitor to reach its plateau. Occasionally, the inhibitor has a much longer half-life than the affected drug, even when inhibited. In this case, the rise of the affected drug to its new plateau virtually mirrors in time the approach of the inhibitor to its plateau.

Also shown in Figure 13 is the return of the affected drug to its previous plateau on withdrawing the offending drug. This return is faster than during the rise in the presence of the inhibitor because as the inhibitor falls, so does the degree of inhibition, which then causes a shortening in the half-life and thus an ever-accelerating decline of the affected drug. It is to be noted, however, that the speed of decline is strongly determined by the kinetics of the inhibitor. If it has a long half-life, its decline may be the rate-limiting step in the entire process, in which case the decline of the inhibited drug parallels that of the inhibitor itself.

## V. ADDITIONAL CONSIDERATIONS

So far analysis has centered on metabolic drug interactions. But there are many pharmacokinetic interactions other than those occurring at enzymatic sites, such as those involving transporters or altered physiological function.



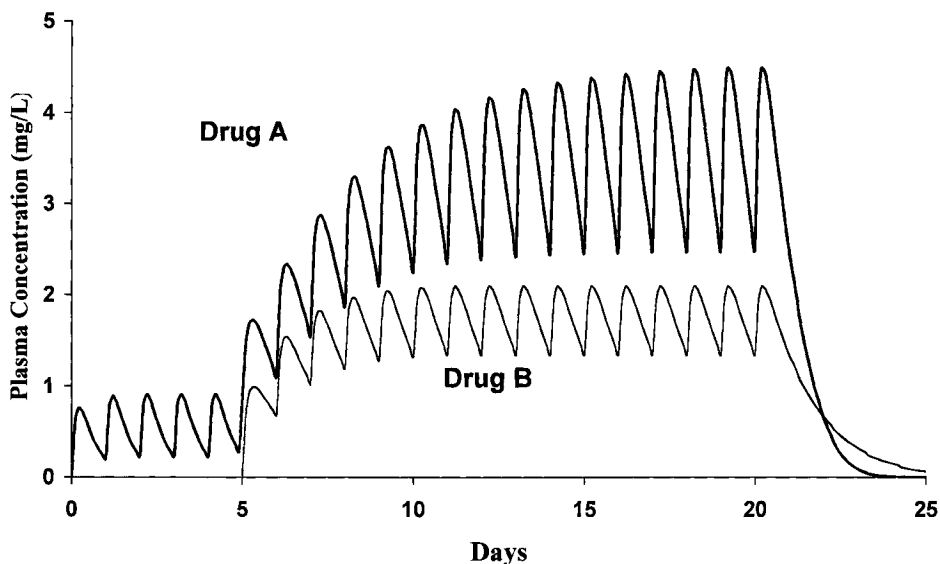


**Figure 13** Simulation of drug interaction kinetics involving competitive inhibition. In this scenario, Drug A is administered as a fixed-oral-dose regimen, first alone until a steady state is reached, and then in the presence of a fixed-oral-dosage regimen of Drug B, which inhibits the obligatory pathway for the elimination of Drug A, that is,  $f_m = 1$ . As the plasma concentration of Drug B rises, so does the degree of inhibition of Drug A, which in turn reduces its clearance and effectively prolongs its half-life. Accordingly, the rise to the new, higher plateau of Drug A takes much longer than when it is given alone, being determined by both the pharmacokinetics and dosage regimen of Drug B as well as the inhibitory potency of Drug B. In the current scenario, the clearance of Drug A is reduced by an average of 86%, and its half-life increased sevenfold during a dosing interval at plateau of Drug B.

## A. Transporters

The quantitative and kinetic conclusions reached with metabolic drug interactions apply equally well to those involving transporters effecting excretion, which reside in organs connected with the exterior, such as the liver via the bile duct, with ultimately removal in feces (see Chap. 5 for more details). This is readily seen by examination of Eq. (15). Being additive, a given change in either a metabolic or an excretory intrinsic clearance ( $CL_{int,f}$  or  $CL_{int,ex}$ ) will produce the same change in the overall intrinsic clearance. Sometimes, a transporter interaction occurs within internal organs, such as the brain, to produce altered drug distribution, not excretion. This occurs, for example, with inhibition of the efflux trans-

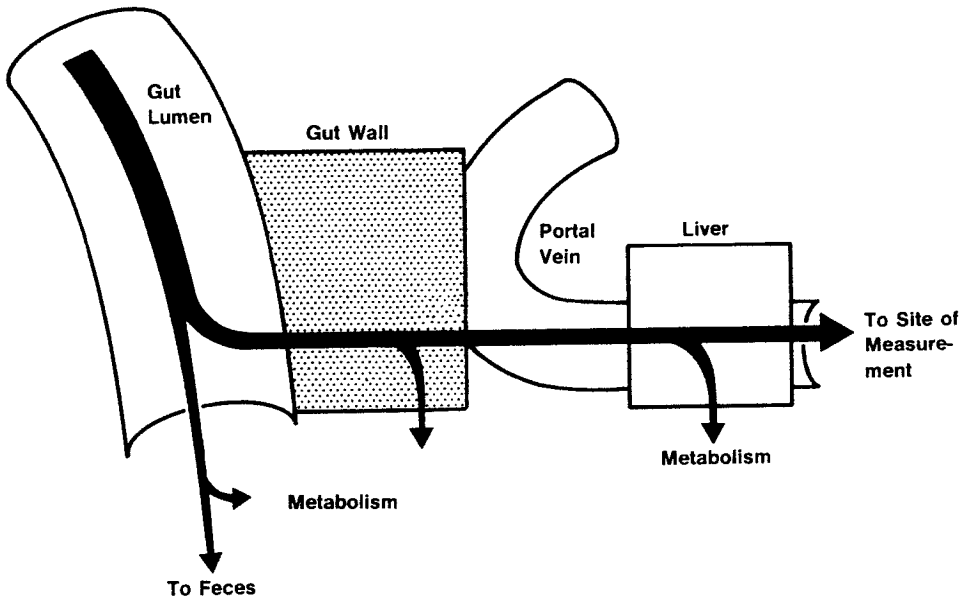


**Figure 14** Schematic depicting events occurring during absorption after oral administration of a drug. Upon dissolution, the drug, in addition to having to permeate the intestinal wall, must pass through the liver to reach the systemic circulation and subsequent sites within the body. Loss of drug can occur at any of these sites, leading to a loss of oral bioavailability. (From Ref. 1. Reproduced with permission.)

porter P-glycoprotein (PGP), located within the blood–brain barrier. For example, normally virtually excluded from the brain by efflux, inhibition of PGP leads to an elevation in brain levels of the substrate cyclosporin [13]. Even so, because brain comprises less than 1% of total body weight, changes in the distribution of drug within it, even when quite profound and of major therapeutic consequence, will have minimal effect on the volume of distribution of the drug,  $V$ , which reflects overall distribution within the body.

## B. Absorption

Many interactions involve a change in either the rate or the extent of drug absorption, particularly following oral administration. There are many potential sites for interaction, within the gastric and intestinal lumen, at or within the gut wall, as well as within the liver (Fig. 14). As indicated in Figure 15, the consequences of a change in absorption kinetics depend on whether the affected drug is given

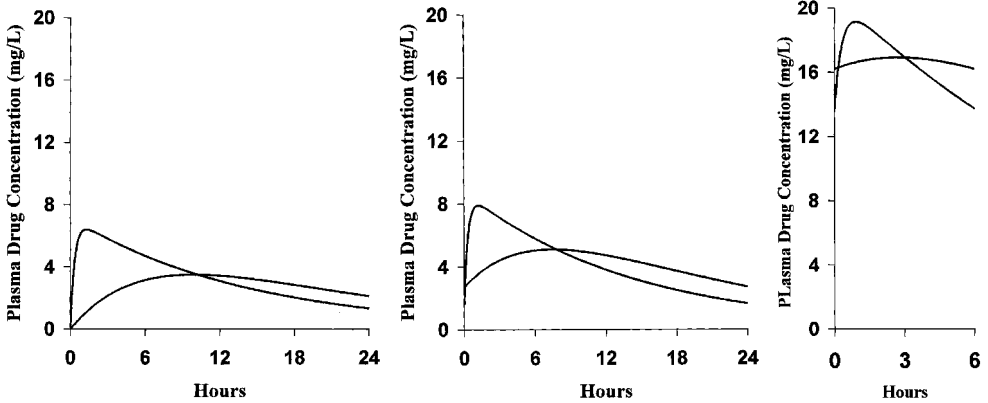


**Figure 15** Impact of dosing frequency on the influence of a change in the kinetics of absorption on events at plateau. Although clear differences are seen after a single dose (left panel), these will also be seen at plateau only if the drug is dosed relatively infrequently (once every 24 hours in this scenario), when little accumulation occurs (middle panel). With frequent dosing (once every 6 hours), accumulation is extensive, so changes in absorption kinetics now have only a minor effect at plateau (right panel).

once or as a multiple-dosing regimen. A slowing in absorption kinetics will always result in a lower and later peak concentration, which could be critical if the affected drug is intended for rapid onset of action, such as for the relief of a headache. However, whether this difference is sustained on multiple dosing depends heavily on the dosing frequency of the affected drug relative to its half-life. When it is given infrequently, there is little accumulation, so the events at plateau are similar to those seen following a single dose. However, when given relatively frequently, because of extensive accumulation the amount absorbed from any one dose is such a small fraction of that in the body at plateau that events at plateau are insensitive to changes in absorption kinetics. In contrast, changes in the extent of absorption seen during single-dose administration, whatever the cause, will still be seen on multiple dosing, irrespective of the frequency of drug administration.

There are many causes of low, particularly oral, bioavailability,  $F$ . Some of these occur in the gastrointestinal lumen, affecting dissolution of solid or its stability, by changing, for example, pH so that only a fraction  $F_A$  of the administered dose reaches the epithelial absorption sites. However, only a fraction of this may permeate through the intestinal wall into the portal blood,  $F_G$ , and then only another fraction,  $F_H$ , escapes the liver and enters the systemic circulation. Accordingly, because these sites of loss are arranged in series, it follows that the

overall systemic oral bioavailability  $F$  is

$$F = F_A \cdot F_G \cdot F_H \quad (27)$$

Notice that overall bioavailability is zero if drug is made total unavailable at any one of the three sites. Also, while measurement of  $F$  is important, which in turn requires the administration of an intravenous dose, it is almost impossible to rationally interpret a drug interaction affecting oral bioavailability without some estimate of the events occurring at at least one of the three sites of loss. It usually requires additional studies to be undertaken to untangle the various events, such as comparing the interaction with both a solution and the usual solid dosage form of the affected drug. Clearly, if no difference is seen, it provides strong evidence that the interaction is not one affecting the dissolution of the drug from the solid. Furthermore, the lack of an interaction following intravenous dosing of the affected drug would then strongly point to the interaction occurring within the intestinal wall.

### C. Displacement

With many drugs highly bound to plasma and tissue proteins, and with activity residing in the unbound drug, there has been much concern that displacement of drug from its binding sites could have severe therapeutic consequences. In practice, this concern is somewhat unfounded. We have seen why this is so following a single dose of a drug (Sec. II.A.2). It is also the case following chronic dosing. Consider again a drug of low clearance, administered as a constant infusion. Then, at steady state, when the rate of elimination ( $CL_{int} \cdot Cu$ ) matches the rate of infusion, it follows that

$$\text{Rate of infusion} = CL \cdot C_{ss} = CL_{int} \cdot Cu_{ss} \quad (28)$$

Now, displacement, by increasing  $f_u$ , will increase  $CL$  (since  $CL = f_u \cdot CL_{int}$ ). But because the events within the cell are unaffected by displacement, it follows that  $CL_{int}$  will not change and so therefore neither will  $Cu_{ss}$ , the therapeutically important unbound concentration at steady state. Consequently, no change in response is expected. Indeed, had no plasma measurements been made, one would have been totally unaware that an interaction had occurred. Furthermore, if plasma measurements are made it is important to determine the fraction of drug unbound and unbound drug concentration; otherwise there is clearly a danger of misinterpretation of the interaction.

## VI. ADDITIONAL COMPLEXITIES

There is a whole variety of factors that further complicate both the interpretation and quantitative prediction of the pharmacokinetic aspects of drug interactions.

Most are either beyond the scope of this introductory chapter or are covered elsewhere in this book. Several, however, are worth mentioning here. One is that sometimes drug interactions are multidimensional, with more than one process affected. For example, although no longer prescribed, the anti-inflammatory compound phenylbutazone interacts with many drugs, as is well documented. One in particular is noteworthy here, namely, the interaction with warfarin causing an augmentation of its anticoagulant effect. On investigation, not only was it found that phenylbutazone markedly inhibits many of the metabolic pathways responsible for warfarin elimination, but it also displaces warfarin from its major binding protein, albumin, making interpretation of the pharmacokinetic events based on total plasma concentration problematic [13,14]. In such situations, and indeed whenever possible, interpretation should be based on the more relevant unbound drug.

Another complexity is the presence of multiple sites for drug elimination. For example, increasing evidence points to the small intestine, in addition to the liver, having sufficient metabolic activity to cause appreciable loss in oral bioavailability of some drugs. Then unambiguous quantitation of the degree of involvement of each organ in an interaction *in vivo* becomes difficult, unless one has a way of separating them physically, such as sampling the hepatic portal vein, which drains the intestine, to assess the amount passing across the intestinal wall, as well as the systemic circulation, to assess the loss of drug on passage through the liver.

Still another is the metabolites themselves, which may possess pharmacological and toxicological activity in their own right. Each metabolite has its own kinetic profile, which often is altered during an interaction, through a change either in its formation or occasionally in its elimination and distribution. Despite these complexities, however, measurement of both drug and its metabolites can often be very informative and provide more definitive insights into an interaction than gained from measurement of drug alone [5].

The last complexity mentioned here is the pharmacokinetics of the interacting drug itself, be it an inhibitor, an inducer, or a displacer. Given that drug interactions are graded, and recognizing that individuals vary widely in their degree of interaction for a given dosage regimen of each drug, it would seem sensible to measure both of them when characterizing an interaction. Unfortunately, this is rarely done. Even *in vitro*, all too often it is assumed that the concentration of the interactant is that added, without any regard to the possibility that it may bind extensively to components in the system or be metabolically degraded. In both cases, the unbound compound of the interacting drug is lower than assumed and if ignored may give a false sense of comfort, suggesting that higher (unbound) concentrations are needed to produce a given degree of interaction than is actually the case. When measured *in vivo* it is usually the interacting drug in the circulating plasma rather than at the site of the interaction, such as the hepatocyte, which

is inaccessible. In addition, the liver receives drug primarily from the portal blood, where the concentration may be much higher than in plasma during the absorption phase of the interactant, making any attempt to generate a meaningful concentration–response relationship more difficult. Finally, because many drug interactions involve competitive processes, the possibility always exists that the interaction is mutual, with both drugs affecting each other, the degree of effect exerted by each on the other depending on the relative concentrations of the two compounds.

Despite these complexities, all is not lost. Through careful planning and subsequent analysis of both *in vitro* and *in vivo* data, progress is being made in our understanding of the mechanisms and pharmacokinetic aspects of drug interactions.

## VII. PHARMACODYNAMIC CONSIDERATIONS

Although when related to a dose the clinical outcome of a drug interaction may appear the same, it is useful to distinguish between pharmacokinetic and pharmacodynamic causes of the interaction. In the former case, the change in response is caused by a change in the concentration of the affected drug, together perhaps with one or more metabolites. In the latter, there may be no change in pharmacokinetics at all.

One feature commonly experienced in pharmacodynamics but much less in pharmacokinetics is saturability, giving rise to nonlinearity. Typically in pharmacodynamics, on raising the concentration of drug, the magnitude of response rises initially sharply and then more slowly on approach to the maximum effect,  $E_{\max}$ . This relationship is characterized in its simplest form, and displayed graphically in Figure 16, by

$$\text{Effect, } E = \frac{E_{\max} \cdot C}{EC_{50} + C} \quad (29)$$

where  $EC_{50}$  is the concentration of drug that causes 50% of the maximum response; it may be regarded as a measure of potency. This relationship is of the same hyperbolic form as that used to describe Michaelis–Menten enzyme kinetics. The reason why saturability is almost the norm in pharmacodynamics and not in pharmacokinetics *in vivo* is that affinity of a drug for its receptor is often many orders of magnitude greater than that for metabolic enzymes, so  $EC_{50}$  values tend to be much lower than  $K_m$  values. Accordingly, the concentrations needed to produce the often desired 50–80% of  $E_{\max}$ , which are already in the saturable part of the concentration–response relationship, are well below the  $K_m$  of the metabolic enzyme systems. It also follows that quite large differences in plasma

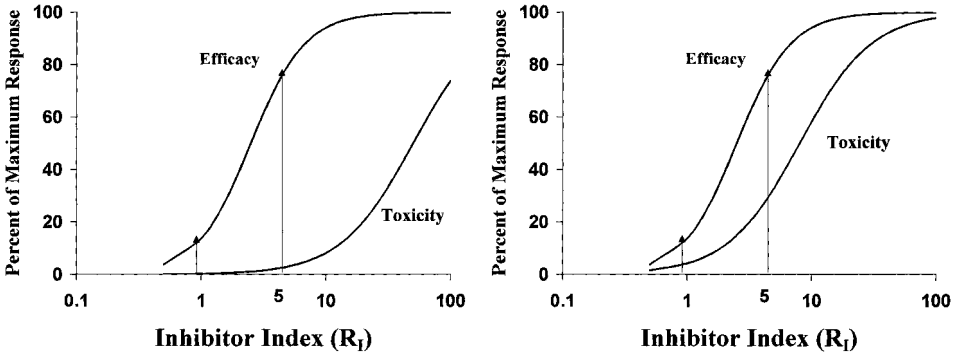


**Figure 16** The wider the therapeutic index of a drug, the smaller the impact that a given degree of inhibition, expressed in terms of the inhibitor index  $R_I$ , has on the likelihood of an increase in the frequency and severity of side effects. In this example, whereas a fivefold increase in  $R_I$  [from 1 (drug alone) to 5] produces a substantial increase in efficacy, it causes only a marked increase in toxicity for the drug with a narrow therapeutic index (right panel). The increase in toxicity for a drug with a wide therapeutic window is minimal (left panel).

concentration of drugs when operating in the 50–80%  $E_{max}$  range will produce relatively small changes in response. So why the concern for pharmacokinetic drug interactions? The answer is complex, but one reason is that as one pushes further toward the maximum possible response,  $E_{max}$ , the body sometimes goes into a hazardous state, putting the patient at risk. An example of this is seen with warfarin, used to lower the concentrations of the clotting factors, thereby decreasing the tendency to form clots, through inhibition of the production of these clotting factors. Normally, inhibition is modest. However, if inhibition is too severe, the clotting factors fall to such low concentrations that internal hemorrhage may occur, with potential fatal consequences. This is clearly an example of the adverse effect being the direct extension of the pharmacological properties of the drug.

In many other cases, the limiting toxicity is not an extension of its desired effect but rather arises from a different effect of the drug, such as excessive intestinal bleeding associated with some anti-inflammatory agents. And, as stated in the introduction, and illustrated in Figure 16, the likelihood of a clinically significant interaction occurring for a given change in plasma concentration of the drug depends on its therapeutic window. The wider the window, the bigger the increase in plasma concentration of a drug needed to produce a significant interaction.

Pharmacodynamic interactions occur when one drug modifies the pharmacodynamic response to the same concentration of another. In most cases the mechanism of the effect of each is known, so the outcome is predictable such that the combination is either used in therapy to benefit or is contraindicated, if it is anticipated to produce undesirable effects. The interaction can result in additivity, but also sometimes in synergism or antagonism, when the response is either greater or less than expected for additivity [16–19]. Additivity occurs when the increase in response produced by the addition of the second drug is that expected from the concentration–response curve for each substance. A common example of additivity is seen with full agonists and antagonisms competing for the same receptor. Then the response to the mixture of compounds, A and B, for full agonists, for example, is

$$\text{Effect } E = \frac{E_{\max}(C_A/EC_{50,A} + C_B/EC_{50,B})}{1 + C_A/EC_{50,A} + C_B/EC_{50,B}} \tag{30}$$

The important features of this type of interaction are that each drug alone produces the same maximum response,  $E_{\max}$ , and that each drug effectively increases the  $EC_{50}$  value of the other. Accordingly, in terms of drug interactions,

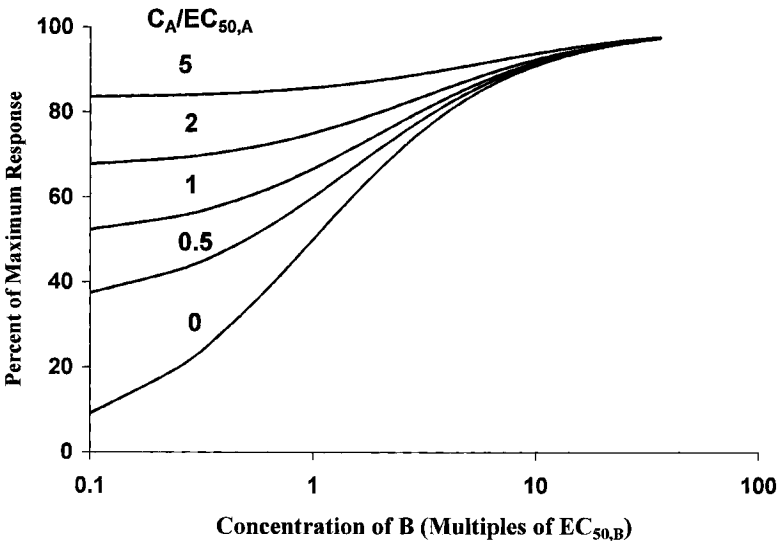


**Figure 17** When two drugs, drug A and drug B, are full competitive agonists (or antagonists) the effect of drug B on drug A depends on the fraction of the maximum effect achieved by drug A in the absence of drug B. As can readily be seen, the closer to  $E_{\max}$  achieved by drug A alone, the smaller the impact of drug B.



as shown in Figure 17, however much drug B is added to drug A, one cannot exceed  $E_{\max}$ , so the nearer the effect is to  $E_{\max}$  with one drug alone, the lower the impact of the addition of the other. The consequences of approaching the  $E_{\max}$  are the same, however, as with a pharmacokinetic interaction, as discussed earlier. The situation is more complex, but the principle is the same, when the interacting drugs are partial agonists or antagonists, each with their own  $E_{\max}$  value, which is less than the maximum possible with a full agonist or antagonist, or a mixture of the two. However, frequently two drugs with the same efficacy will have different toxicity profiles, so for a given degree of efficacy the combination, which requires less of each drug, may well produce less adverse reactions, a clinical advantage.

In summary, a sound understanding of pharmacokinetic and pharmacodynamic concepts not only enables one to place in vitro information into an in vivo framework, but also helps in both the design and the interpretation of in vitro and in vivo drug interaction studies.

## REFERENCES

1. M Rowland, TN Tozer. *Clinical Pharmacokinetics: Concepts and Applications*. 3rd ed. Williams & Wilkins, Baltimore, 1995.
2. WE Evans, JJ Schentag, WJ Jusko, eds. *Applied Pharmacokinetics*. 3rd ed. Applied Therapeutics, San Francisco, 1992.
3. GR Wilkinson. Clearance approaches in pharmacology. *Pharmacol. Rev.* 39:1–47, 1987.
4. M Rowland, SB Matin. Kinetics of drug–drug interactions. *J. Pharmacokinet. Biopharm.* 1:553–567, 1973.
5. PN Shaw, JB Houston. Kinetics of drug metabolism inhibition: use of metabolite concentration–time profiles. *J. Pharmacokinet. Biopharm.* 15:497–510, 1987.
6. RA O'Reilly. Interaction of sodium warfarin and rifampin. *Ann. Int. Med.* 81:337–340, 1974.
7. G Alvan, K Piafsky, M Lind, C von Bahr. Effect of pentobarbital on the disposition of alprenolol. *Clin. Pharmacol. Ther.* 22:316–321, 1977.
8. TN Tozer. Concepts basic to pharmacokinetics. *Pharmacol Therap* 12:109–131, 1982.
9. M Rowland, LZ Benet, GG Graham. Clearance concepts in pharmacokinetics. *J. Pharmacokinet. Biopharm.* 1:123–136, 1973.
10. GR Wilkinson, DG Shand. A physiological approach to hepatic drug clearance. *Clin. Pharmacol. Ther.* 18:377–390, 1975.
11. KS Pang, M Rowland. Hepatic clearance of drugs. I Theoretical considerations of the well-stirred and parallel-tube model. Influence of hepatic blood flow, plasma and blood cell binding, and hepatocellular enzymatic activity on hepatic drug clearance. *J. Pharmacokinet. Biopharm.* 5:625–653, 1977.
12. MS Roberts, JD Donaldson, M Rowland. Models of hepatic elimination: a compari-

- son of stochastic models to describe residence time distributions and to predict the influence of drug distribution, enzyme heterogeneity, and systemic recycling on hepatic elimination. *J. Pharmacokin. Biopharm.* 16:41–83, 1988.
13. C Tanaka, R Kawai, M Rowland. Dose-dependent pharmacokinetics of cyclosporin A in rat: events in tissues. *Drug Metab. Disposition* 28(5):582–589, 2000.
  14. C Banfield, RE O'Reilly, E Chan, M Rowland. Phenylbutazone–warfarin interaction in man: further stereochemical and metabolic considerations. *Brit. J. Clin. Pharmac.* 16:669–675, 1983.
  15. E Chan, AJ McLachlan, R O'Reilly, M Rowland. Stereochemical aspects of warfarin drug interactions: use of a combined pharmacokinetic–pharmacodynamic model. *Clin. Pharmacol. Therap.* 56:286–294, 1994.
  16. NHG Holford, LB Sheiner. Kinetics of pharmacological response. *Pharmacol. Ther.* 16:143–166, 1982.
  17. WR Greco, G Bravo, JC Parsons: The search for strategy: a critical review from a response surface perspective. *Pharmacol. Rev.* 47:331–385, 1995.
  18. T Koizumi, M Kakemi, K Katayama. Kinetics of combined drug effects. *J. Pharmacokin. Biopharm.* 21:593–607, 1993.
  19. MC Berenbaum. The expected effect of a combination of agents. *J. Theor. Biol.* 114:413–431, 1985.



# 2

## In Vitro Enzyme Kinetics Applied to Drug-Metabolizing Enzymes

**Kenneth R. Korzekwa**

*Camitro Corporation, Menlo Park, California*

### I. INTRODUCTION

Most new drugs enter clinical trials with varying amounts of information on the human enzymes that may be involved in their metabolism. Most of this information is obtained from (1) animal studies, (2) human tissue preparations in conjunction with chemical inhibitors or antibodies, and (3) expressed enzymes. This chapter will focus on the techniques used to characterize the in vitro metabolism of drugs. Although many enzymes may play some role in drug metabolism, this chapter will focus on the cytochrome P450 enzymes (P450). The P450 superfamily of enzymes represents the most important enzymes in the metabolism of hydrophobic drugs and other foreign compounds, and many drug–drug interactions result from altering the activities of these enzymes. Although other drug-metabolizing enzymes have not been studied as extensively as the P450 enzymes, most share a characteristic with the P450s that is relatively unique for enzymes: broad substrate selectivity. This versatility has a profound influence on the enzymology and kinetics of these enzymes. Therefore, many of the techniques described for the P450s may apply to other drug-metabolizing enzymes as well.

There is a substantial amount of effort in the area of drug metabolism toward predicting in vivo pharmacokinetic and pharmacodynamic characteristics from in vitro data. If valid, these in vitro–in vivo correlations could be used to predict the potential for drug interactions as well as the genotypic and phenotypic variabilities in the population. A very significant advance in preclinical drug metabolism is the cloning and expression of the human P450 enzymes. This allows the individual human enzymes involved in the metabolism of a particular drug

or other xenobiotic to be identified directly and their kinetic properties ( $K_m$  and  $V_m$ ) characterized. This information can be used to predict which enzymes may be involved at physiologically relevant concentrations, drug–drug interactions, and population variability due to variations in genotype and phenotype.

A simple approach to screen a new drug for metabolism or potential drug interactions is to determine the inhibition kinetics for a standard assay. The use of standard assays precludes the need to develop assays for the metabolites of new drug candidates and allows many compounds to be screened rapidly. With this approach, a standard assay is developed for each P450 enzyme. Metabolism is observed in the presence of varying concentrations of the new compound. Competitive inhibition kinetics suggests that the compound is binding to the P450 active site. If the inhibition constant ( $K_i$ ) is within physiologically relevant concentrations, the compound is likely to be a substrate for that P450 and is likely to have interactions with other drugs metabolized by that P450. The kinetic constants ( $K_m$  and  $V_m$ ) can then be determined for the enzymes that are likely to be important.

Most P450 oxidations and drug interactions can be predicted from inhibition studies, since most P450 inhibitors show competitive Michaelis–Menten kinetics. However, there are examples of unusual kinetics, and most of these are associated with CYP3A oxidations. In this chapter, both Michaelis–Menten kinetics and more complex kinetics will be discussed. General experimental protocols that can be used to obtain and analyze kinetic data will be presented, and the implications of the results when predicting drug interactions will be discussed.

## II. MICHAELIS–MENTEN KINETICS

A drug that binds reversibly to a protein as shown in Figure 1a displays hyperbolic saturation kinetics. At equilibrium, the fraction bound is as described by Eq. (1), where  $K_b = k_{21}/k_{12}$ :

$$\frac{[ES]}{[Et]} = \frac{[S]}{K_b + [S]} \quad (1)$$

The binding affinity and therefore the concentration dependence of the process is described by the binding constant  $K_b$ . Likewise, when a drug binds reversibly to an enzyme, the reaction velocity usually shows hyperbolic saturation kinetics. Under steady-state conditions, the velocity of the simple reaction shown in Figure 1b can be described by the Michaelis–Menten equation:

$$\frac{v}{Et} = \frac{V_m[S]}{K_m + [S]} \quad (2)$$

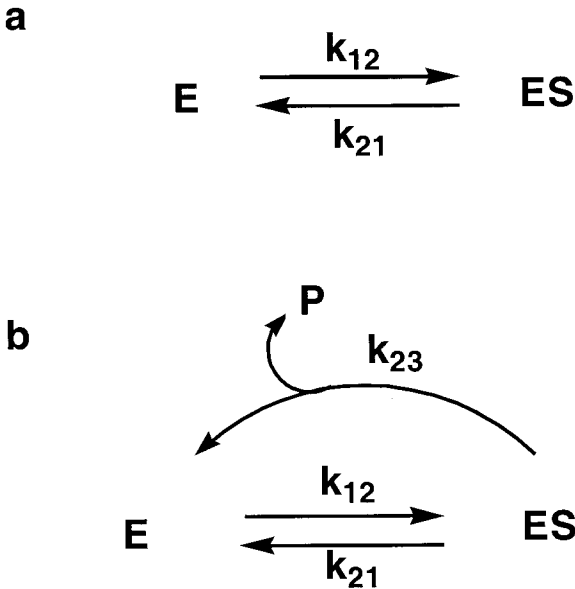


**Figure 1** Simple schemes for (a) protein binding and (b) enzyme catalysis.

In this equation, a hyperbolic saturation curve is described by two constants,  $V_m$  and  $K_m$ . In the simple example in Figure 1b,  $V_m$  is simply  $k_{23}[Et]$  and  $K_m$  is  $k_{12}/(k_{21} + k_{23})$ .  $V_{\max}$  (or  $V_m$ ) is the reaction velocity at saturating concentrations of substrate, and  $K_m$  is the concentration of substrate that achieves half the maximum velocity. Although the constant  $K_m$  is the most useful descriptor of the affinity of the substrate for the enzyme, it is important to note the difference between  $K_m$  and  $K_b$ . Even for the simplest reaction scheme (Fig. 1b) the  $K_m$  term contains the rate constant for conversion of substrate to product ( $k_{23}$ ). If the rate of equilibrium is fast relative to  $k_{23}$ , then  $K_m$  approaches  $K_b$ .

More complex enzymatic reactions usually display Michaelis–Menten kinetics and can be described by Eq. (2). However, the forms of constants  $K_m$  and  $V_m$  can be very complicated, consisting of many individual rate constants. King and Altman [1] have provided a method to readily derive the steady-state equations for enzymatic reactions, including the forms that describe  $K_m$  and  $V_m$ . The advent of symbolic mathematics programs makes the implementation of these methods routine, even for very complex reaction schemes. The P450 catalytic cycle (Fig. 2) is an example of a very complicated reaction scheme. However, most P450-mediated reactions display standard hyperbolic saturation kinetics. Therefore, although the rate constants that determine  $K_m$  and  $V_m$  are generally

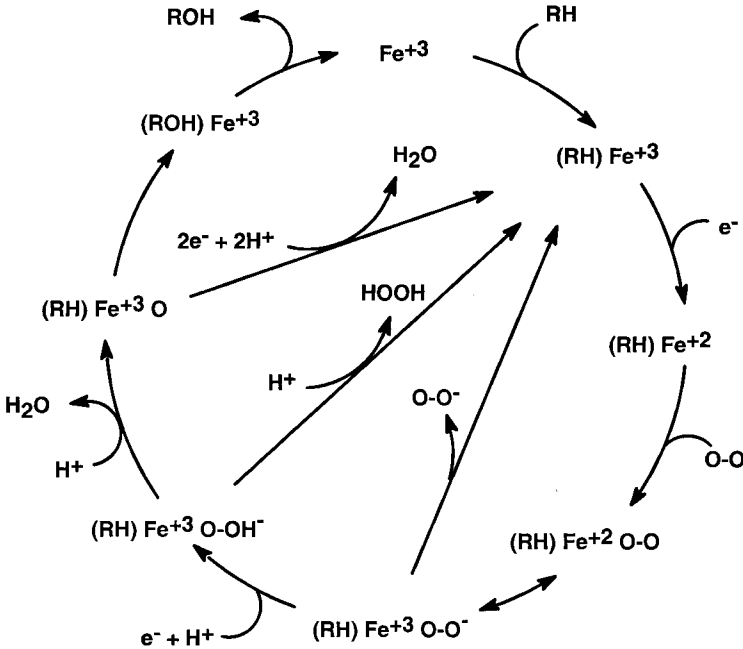


**Figure 2** P450 catalytic cycle.

unknown for the P450 enzymes, the values of  $K_m$  and  $V_m$  can be experimentally determined. Another constant that has important implications in drug metabolism is the ratio of  $V_m$  to  $K_m$ , or  $V/K$ . This is the slope of the hyperbolic saturation curve at low substrate concentrations. Since most P450-mediated reactions have relatively high  $K_m$  values, most drug metabolism occurs in the linear or  $V/K$  region of the saturation curve.

## A. Experimental Determination of In Vitro Kinetic Parameters

### 1. P450 Enzyme Preparations

The P450 enzymes are found primarily in the other membrane of the endoplasmic reticulum. Enzyme activity requires that the enzyme be integrated into a membrane that contains P450 reductase and, for some reactions, cytochrome  $b_5$ . Characterization of the saturation kinetics for the P450 enzymes can be determined using a variety of enzyme preparations, including tissue slices, whole cells, microsomes, and reconstituted, purified enzymes. The more intact the in vitro

preparation, the more likely that the environment of the enzyme will represent the *in vivo* environment. However, intact cell preparations do not generally give kinetic parameters that are observed with microsomal preparations. This could be due to factors such as limiting diffusion into the cells or binding to intracellular proteins. Therefore, when whole-cell preparations are used, observed kinetic characteristics may not provide the true kinetic constants for the enzyme being studied.

Microsomal preparations generally provide reproducible kinetic analyses when only one enzyme is involved in the reaction. However, microsomal preparations (and other intact preparations) contain many different P450 enzymes. Although this characteristic is useful when trying to mimic the metabolic characteristics of an organ, it is a drawback when trying to characterize the kinetic constants of an individual P450 enzyme or when trying to determine which enzyme is involved in the metabolism of a particular drug. Due to the generally broad substrate selectivities of the P450 enzymes, most observed metabolic reactions can be catalyzed by more than one enzyme. Interindividual variability in the content of the different P450s makes it even more difficult to determine the different kinetic parameters when more than one enzyme is involved in a given reaction.

Preparations containing a single P450 isozyme are available as either expression systems or purified, reconstituted enzymes. The P450s have been expressed in bacterial, yeast, insect, and mammalian cells [2]. Most of these enzymes can be used in the membranes in which they are expressed. However, in order to obtain adequate enzyme activity for most expression systems, it is necessary to supplement the membranes with reductase and in some cases  $b_5$ . This is accomplished by either supplementing the membranes with purified coenzymes or by coexpression of the coenzymes. Alternatively, the P450 enzymes can be purified and reconstituted with coenzymes into artificial membranes.

Every enzyme preparation has advantages and disadvantages. Microsomes may more closely represent the *in vivo* activity of a particular organ, but kinetic analyses are complicated by the presence of multiple enzymes. It is not possible to spectrally quantitate the content of any individual enzyme when a mixture of enzymes is present. Expression systems provide isozymically pure preparations, but they also have disadvantages. The P450 enzymes are membrane bound, and for the nonmammalian expression systems the membranes may have different interactions with the P450 proteins. Although expression levels in most of the systems are adequate for spectral quantitation, coexpression of the coenzymes adds variability to different batches. Reconstituted enzymes allow for the exact control of enzyme and coenzyme content. However, the membranes are artificial and can have an influence on enzyme activity. For example, whereas most P450 enzymes can be reconstituted into dilaurylphosphatidylcholine (DLPC) vesicles, the CYP3A enzymes require the presence of both unsaturated lipid and a small



amount of nonionic detergent [3]. Finally, these differences are further complicated by unpredictable influences of ionic strength, pH, etc. of the incubation medium, as will be discussed next.

## 2. Incubation Conditions

Enzyme kinetics are normally determined under steady-state, initial-rate conditions. This places several constraints on the incubation conditions. First, the amount of substrate should greatly exceed the enzyme concentration, and the consumption of substrate should be held to a minimum. Generally, the amount of substrate consumed should be held to less than 10%. This ensures that accurate substrate concentration data is available for the kinetic analyses and minimizes the probability that product inhibition of the reaction will occur. This constraint can be problematic when the  $K_m$  of the reaction is low, since the amount of product (10% of a low substrate concentration) may be below that needed for accurate product quantitation. One method to increase the substrate amount available is to use larger incubation volumes. For example, a 10-ml incubation has 10 times more substrate available than a 1-ml incubation. Another method is to increase the sensitivity of the assay, e.g., using mass spectral or radioisotope assays. When more than 10% of the substrate is consumed, the substrate concentration can be corrected via the integrated form of the rate equation (Dr. James Gillette, personal communication):

$$\frac{v}{Et} = \frac{V_m[\hat{S}]}{K_m + [\hat{S}]} \quad (3)$$

where

$$[\hat{S}] = \frac{[S]_0 - [S]_f}{\ln \frac{[S]_0}{[S]_f}} \quad (4)$$

In Eq. (3),  $[S]_0$  and  $[S]_f$  are starting and ending substrate concentrations.  $[\hat{S}]$  approaches  $[S]$  when substrate consumption is small, and  $[\hat{S}]$  is substituted for  $[S]$  to correct for excess substrate consumption. In these analyses, however, substrate inhibition can be a problem if the product has a similar affinity to the substrate. Fortunately, most P450 oxidations produce products that are less hydrophobic than the substrates, resulting in lower affinities to the enzymes. There are exceptions, including desaturation reactions that produce alkenes from alkanes [4] and carbonyl compounds from alcohols. These products have hydrophobicities that are similar or increased, relative to their substrates.

A second constraint is that the reaction remain linear with time. In the presence of reducing equivalents, the P450 enzymes will generally lose activity over time. Provided that the loss of substrate is not dependent on substrate con-

centration, this will alter the  $V_m$  of the enzyme but not the  $K_m$ . For the P450 reactions, the presence of substrate in the active site can either protect the enzyme or increase its rate of deactivation. Substrate dependence on stability can generate inaccurate saturation curves. Enzyme stabilization can result in a sigmoidal saturation curve for an enzyme showing hyperbolic saturation kinetics, and enzyme destabilization can show substrate inhibition if the enzyme content varies over the incubation time. The reaction should also be linear with enzyme concentration to ensure that other processes, such as saturable, nonspecific binding, do not alter the enzyme saturation profile.

## B. Analysis of Michaelis–Menten Kinetic Data

By far, the best method of determining kinetic parameters is to perform an appropriately weighted least-squares fit to the relevant rate equation [5]. Popular programs available at the time of this writing include *WinNonlin* from Pharsight, *GraFit* by Erithacus Software, and *Axum* from Mathsoft. Although reciprocal plots are useful for determining initial parameters for the regression and for plotting the results, initial parameters for a single enzyme showing hyperbolic saturation kinetics can be obtained by inspection of the data. When more than one enzyme is present, e.g., in microsomes, the data can be fit to combined Michaelis–Menten equations:

$$\frac{v}{[Et]} = \frac{V_{m1}[S]}{K_{m1} + [S]} + \frac{V_{m2}[S]}{K_{m2} + [S]} \dots + \frac{V_{mn}[S]}{K_{mn} + [S]} \quad (5)$$

If the highest substrate concentrations show a linear increase in velocity, the last component of the rate equation should be  $V/K$ , i.e.,  $v_n = (V/K)_n$ . Inclusion of additional rate components should be justified by statistical methods, such as comparing  $F$  values for the regression analyses or the minimum Akaike information criterion estimation (MAICE) [6,7].

## C. Reaction Conditions

In addition to the preceding complexities, the P450 enzymes have some unique characteristics that complicate the design of experimental protocols. Due to the broad substrate selectivities for these enzymes, the enzymes are not optimized for the metabolism of a particular substrate. Therefore, the reaction conditions (i.e., pH, ionic strength, temperature, etc.) that result in optimum velocities for a given reaction are dependent on both the enzyme and the substrate. To further complicate matters, the velocities for these enzymes tend to vary greatly with changes in these reaction conditions. This may well be due to the dependence of the reaction velocity on several pathways in the catalytic cycle.

It is generally accepted that the overall flux through the catalytic cycle (Fig. 2) is dependent on the rates of reduction by P450 reductase [8,9]. However, the actual rates of substrate oxidation are probably dependent on three additional rates: the rate of substrate oxidation and the rates of the decoupling pathways (hydrogen peroxide formation and excess water formation). Thus, the efficiency of the reaction plays a major role in determining the velocity of a P450 oxidation [10]. The sensitivity of the reaction velocities to incubation conditions may be due to changes in the reduction rate as well as to changes in the enzyme efficiency.

Although many P450 reactions show optimal activity in the pH range 7–8, both chlorobenzene and octane metabolism show optimum activity at pH 8.2 in rat liver microsomes [11,12]. This is also the pH at which P450 oxidoreductase optimally reduces cytochrome c [13]. In addition, whereas essentially all in vitro metabolism studies are carried out at 37°C, both of these reactions occur much faster at 25°C. For a given enzyme, the optimum ionic strength is a function of the substrate. For example, the rate of benzphetamine metabolism by reconstituted CYP2B1 increases with increasing ionic strength [14], whereas the optimum for testosterone metabolism by this enzyme is 20 mM potassium phosphate (KPi) buffer and decreases with increasing ionic strength (unpublished results).

Even the optimum ratio of reductase to P450 depends on the substrate and the enzyme. Whereas most reactions are saturated by a reductase:P450 ratio of 10:1, testosterone metabolism by CYP2A1 saturates at much higher reductase ratios. In contrast, essentially all reactions that have a  $b_5$  dependence are saturated at a  $b_5$ :P450 ratio of 1:1.

Thus, many P450 oxidations show a substantial and variable dependence on reaction conditions. This makes it impractical to optimize each reaction. In fact, the optimum reaction conditions may not represent the in vivo reaction environment. It would be difficult to justify a reaction temperature of 25°C in an experiment that will be used for in vitro–in vivo correlations. A more practical approach would be to use a consistent set of reaction conditions that provide adequate velocities. Common reaction conditions include 100 mM KPi, pH 7.4, 37°C, a reductase:P450 ratio of 2:1, and a  $b_5$ :P450 ratio of 1:1.

### III. INHIBITION: MICHAELIS–MENTEN KINETICS

Most P450 oxidations show hyperbolic saturation kinetics and competitive inhibition between substrates. Therefore, both  $K_m$  values and drug interactions can be predicted from inhibition studies. Competitive inhibition suggests that the enzymes have a single binding site and only one substrate can bind at any one time. For the inhibition of substrate A by substrate B to be competitive, the following must be observed:

Substrate A has a hyperbolic saturation curve: Enzymes that bind only one substrate molecule will show hyperbolic saturation kinetics. However, the observation of hyperbolic saturation kinetics does not necessarily mean that only one substrate molecule is interacting with the enzyme (see discussion of non-Michaelis–Menten kinetics in Sec. IV).

The presence of substrate B changes the apparent  $K_m$  but not the  $V_m$  for Substrate A: Saturating concentrations of A must be able to completely displace B from the active site.

Complete inhibition of metabolism is achieved with saturating concentrations of substrate B. Saturating concentrations of B must be able to completely displace A from the active site.

Substrate B does not change the regioselectivity of substrate A: The regioselectivity of the enzyme is determined by the interactions between the substrate and the active site. Since the substrate saturation curve is defined by the  $K_m$  of the enzyme, regioselectivity cannot be a function of substrate or inhibitor concentration [I].

One standard equation for competitive inhibition is given in Eq. (6). This equation shows that the presence of the inhibitor modifies the observed  $K_m$  but not the observed  $V_m$ . A double reciprocal plot gives an  $x$ -intercept of  $-1/K_m(1 + [I]/K_i)$  and a  $y$ -intercept of  $1/V_m$ .

$$\frac{v}{Et} = \frac{V_m[S]}{K_m \left( 1 + \frac{[I]}{K_i} + [S] \right)} \quad (6)$$

Equation (7) gives the fraction activity remaining in the presence of inhibitor, relative to the absence of inhibitor ( $v_i/v_0$ ):

$$\frac{v_i}{v_0} = \frac{K_m + [S]}{K_m \left( 1 + \frac{[I]}{K_i} + [S] \right)} \quad (7)$$

Equation 8 describes the fraction of inhibition, or  $1 - (v_i/v_0)$ .

$$i = 1 - \left( \frac{v_i}{v_0} \right) = \frac{[I]}{[I] + K_i \left( 1 + \frac{[S]}{K_m} \right)} \quad (8)$$

Finally, many reports provide  $IC_{50}$  values (concentration of inhibitor required to achieve 50% inhibition), which are dependent on both substrate concen-

tration and  $K_m$  [Eq. (9)]. Equation (9) shows that when  $[S] = K_m$ , then  $IC_{50} = 2K_i$ :

$$IC_{50} = K_i \left( 1 + \frac{[S]}{K_m} \right) \quad (9)$$

### A. Experimental Design and Analysis of Inhibition Data

By far the best method for characterizing inhibition data is to vary both substrate and inhibitor concentration. The resulting rate data is fit to Eq. (6) by weighted-least-squares regression. Initial estimates for the parameters can be obtained from the control (no inhibitor) data and by a double reciprocal plot. This analysis provides estimates of  $V_m$ ,  $K_m$ , and  $K_i$  from a single experiment. If a minimum of effort is required, the  $K_m$  of the reaction is known, and competitive inhibition is assumed, Equations (6)–(9) can be used to determine the  $K_i$  by varying  $[I]$  at a single substrate concentration. However, neither the  $K_m$  nor the type of inhibition can be validated. Only an observation of partial inhibition indicates that simple competitive inhibition is not involved. If both substrate and inhibitor concentration are varied, the data can also be fit to equations for other types of inhibition, e.g., noncompetitive and mixed type, and the fits can be compared. For the P450 enzymes, the second most prevalent type of inhibition is the partial mixed type of inhibition, which will be discussed later.

## IV. NON-MICHAELIS–MENTEN KINETICS

Most P450 oxidations show standard saturation kinetics and competitive inhibition between substrates. However, some P450 reactions show unusual enzyme kinetics, and most of those identified so far are associated with CYP3A oxidations. The unusual kinetic characteristics of the CYP3A enzymes (and less frequently other enzymes) include five categories: activation, autoactivation, partial inhibition, biphasic saturation kinetics, and substrate inhibition. *Activation* is the ability to be activated by certain compounds; i.e., the rates of a reaction are increased in the presence of another compound. *Autoactivation* occurs when the activator is the substrate itself, resulting in sigmoidal saturation kinetics. For *partial inhibition*, saturation of the inhibitor does not completely inhibit substrate metabolism. *Substrate inhibition* occurs when increasing the substrate beyond a certain concentration results in a decrease in metabolism.

Although most of the observed kinetics are consistent with allosteric binding at two distinct sites [15], studies in our laboratory suggest that the activation of metabolism involves the simultaneous binding of both the activator and the

substrate in the same active site [16,17]. The possibility of binding two substrate molecules to a P450 active site could almost be expected, given the relatively nonspecific nature of the P450–substrate interactions. For example, CYP1A1 is a P450 that metabolizes polycyclic aromatic hydrocarbons (PAHs). The size of the PAHs can vary between naphthalene (two aromatic rings) to very large substrates, such as dibenzopyrenes (six rings). If an active site can accommodate very large substrates, it might be expected that more than one naphthalene molecule can be bound. Indeed, naphthalene metabolism by CYP1A1 has a sigmoidal saturation curve (unpublished results). Finally, it has been shown by NMR studies that both pyridine and imidazole can coexist in the P450cam active site [18]. Thus, even a P450 with rigid structural requirements can simultaneously bind two small substrates.

If enzyme activation and the other unusual kinetic characteristics result from multiple substrates in the active site, kinetic parameters will be difficult to characterize and drug interactions will be more difficult to predict, since they are a function of the enzyme and both of the substrates.

### A. Non-Michaelis–Menten Kinetics for a Single Substrate

If non-Michaelis–Menten kinetics for all P450 enzymes are a result of multiple substrates binding to the enzyme, then the reaction kinetics for the binding of two substrates to an active site can be analyzed as follows: The full kinetic scheme for the two substrate model is given in Figure 3. If product release is fast relative to the oxidation rates, the velocity equation is simplified to Eq. (10):

$$\frac{v}{Et} = \frac{k_{25} \frac{[S]}{K_{m1}} + k_{35} \frac{[S]^2}{K_{m1}K_{m2}}}{1 + \frac{[S]}{K_{m1}} + \frac{[S]^2}{K_{m1}K_{m2}}} \quad (10)$$

In this equation,  $K_{m1} = (k_{21} + k_{24})/k_{12}$  and  $K_{m2} = (k_{23} + k_{35})/k_{32}$ .  $K_{m1}$  would be the standard Michaelis constant for the binding of the first substrate, if  $[ESS] = 0$ .  $K_{m2}$  would be the standard Michaelis constant for the binding of the second substrate, if  $[E] = 0$  (i.e., the first binding site is saturated). In the complete equation, these constants are not true  $K_m$  values, but their form (i.e.,  $K_{m1} = (k_{21} + k_{25})/k_{12}$ ) and significance are analogous. Likewise,  $k_{25}$  and  $k_{35}$  are  $V_{m1}/Et$  and  $V_{m2}/Et$  terms when the enzyme is saturated with one and two substrate molecules, respectively. Equation (10) describes several non-Michaelis–Menten kinetic profiles. Autoactivation (sigmoidal saturation curve) occurs when  $k_{35} > k_{24}$  or  $K_{m2} < K_{m1}$ ; substrate inhibition occurs when  $k_{24} > k_{35}$ ; and a biphasic saturation curve results when  $k_{35} > k_{24}$  and  $K_{m2} \gg K_{m1}$ . This equation was used to fit experimental data for the metabolism of several other substrates, as described next.

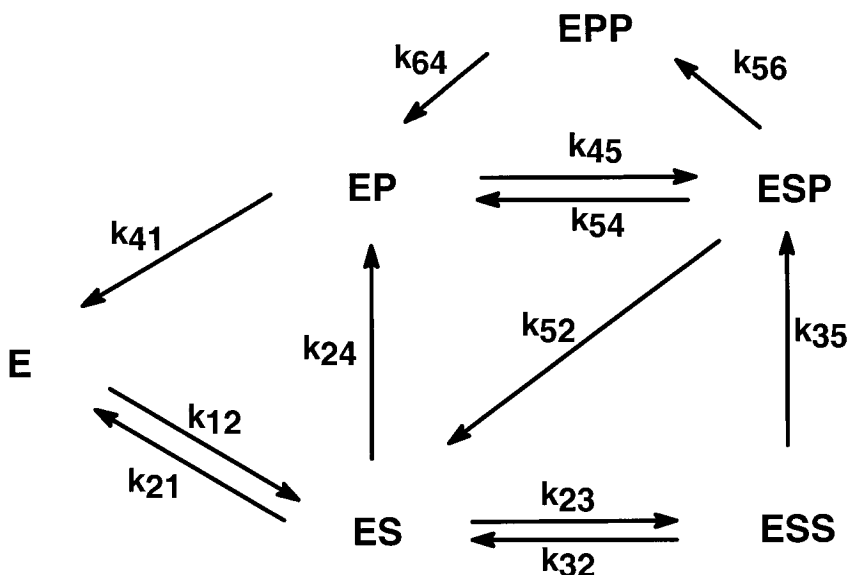


**Figure 3** Proposed kinetic scheme for an enzyme with two binding sites within an active site and a single substrate. (Reprinted with permission from Ref. 17. Copyright 1998, American Chemical Society.)

## 1. Sigmoidal Saturation Kinetics

Although sigmoidal *binding* kinetics can be discussed in terms of binding cooperativity, this is not always the case for enzymes. Sigmoidal saturation kinetics of an enzyme can result when either the second substrate binds to the enzyme with greater affinity than the first or the *ESS* complex is metabolized at a faster rate than the *ES* complex. There have been several reports that describe sigmoidal saturation curves for P450 oxidations [15,19,20], and carbamazepine is a classic CYP3A substrate that shows sigmoidal saturation kinetics (Fig. 4). This figure also shows that quinine converts the sigmoidal curve to a hyperbolic curve. This will be discussed in Sec. V, on interactions between different substrates. For sigmoidal saturation curves, a unique solution for the fit to Eq. (10) is not possible [17]. This becomes apparent when the influence of the second substrate is considered. For this discussion,  $K_m$ ,  $K_{m1}$ ,  $K_{m2}$ ,  $V_{m1}$ , and  $V_{m2}$  are defined as described for Eq. (10). If the second substrate binds with a lower  $K_m$  than the first substrate and has the same rate of product formation, the slope will equal  $(V/K)_1$  at low substrate concentrations, since only one substrate will be bound. As the substrate concentration increases into the range of the second  $K_m$ , much of the *ES* complex

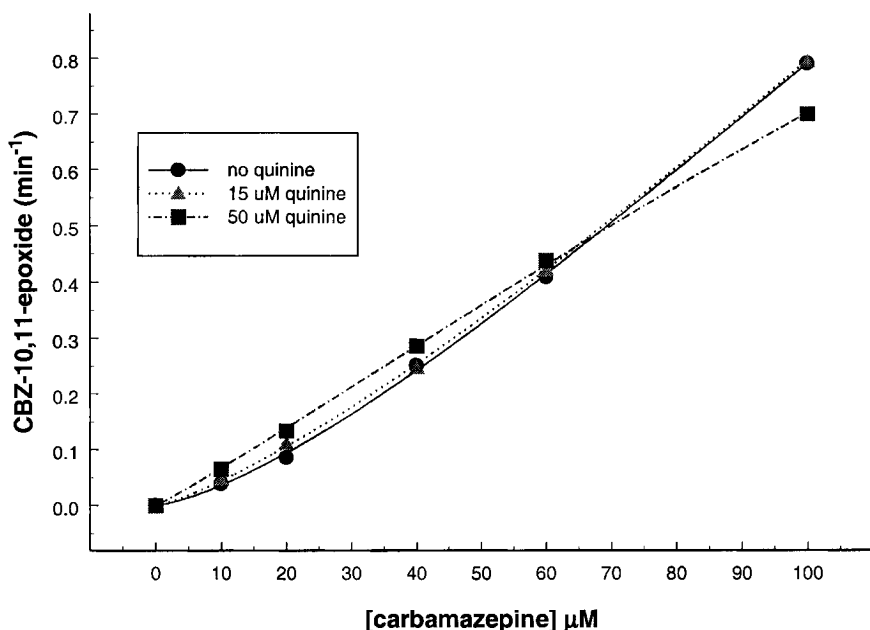


**Figure 4** Effect of quinine on the carbamazepine saturation curve. Quinine makes the sigmoidal saturation curve more hyperbolic. (From K. Nandigama and K. Korzekwa, unpublished results.)

becomes *ESS*. Since the ratio of  $[E]$  to  $[ES]$  is determined by the first  $K_m$ , the *ESS* complex increases at the expense of  $E$ . Therefore, the enzyme becomes saturated faster, resulting in a concave-upward region in the saturation curve. Likewise, if the second substrate binds with a  $K_m$  identical to that of the first substrate but has a higher  $V_m$ , the linear portion of the curve will again have a slope of  $(V/K)_1$ . As the substrate concentration approaches  $K_{m2}$ ,  $[ESS]$  increases. Since the rate of product formation is higher for *ESS*, a concave-upward region results. From a sigmoidal saturation curve one can determine  $(V/K)_1$  from the slope at low substrate concentrations, and  $V_{m2}$  at saturating substrate concentrations. However,  $V_{m1}$ ,  $K_{m1}$ , and  $K_{m2}$  remain undetermined, since  $(V/K)_1$  can have either a  $K_{m1}$  higher than  $K_{m2}$  or a  $V_{m1}$  lower than  $V_{m2}$ . Therefore, multiple solutions are possible when sigmoidal saturation data is fit to Eq. (10).

If a sigmoidal saturation curve is obtained, information relevant to in vitro–in vivo correlations can be obtained from appropriately designed experimental data. The values of  $(V/K)_1$ ,  $V_{m2}$ , and the concave-upward region should be defined if they occur within the therapeutic concentration range. The  $(V/K)_1$  region will



define the rate of metabolism at low substrate concentrations. If the concave-upward region occurs in the therapeutic range, a dose-dependent increase in drug clearance might be expected. On the other hand, if enzyme saturation occurs, a dose-dependent decrease in clearance might be expected. If there is no linear range (i.e., the slope constantly increases at low substrate concentrations), then  $(V/K)_1 = 0$ . This is probably due to  $V_{m1} = 0$ , since an enzyme with a very high  $K_{m1}$  will not be very active at moderate substrate concentrations.

## 2. Biphasic Saturation Kinetics

A second type of nonhyperbolic saturation kinetics became apparent during studies on the metabolism of naproxen to desmethylnaproxen [21]. Studies with human liver microsomes showed that naproxen metabolism has biphasic kinetics and is activated by dapsone (T. Tracy, unpublished results). The unactivated data shows what appears to be a typical concentration profile for metabolism by at least two different enzymes. However, a similar biphasic profile was obtained with expressed enzyme [17]. This biphasic kinetic profile is observed with the two-substrate model when  $V_{m2} > V_{m1}$  and  $K_{m2} \gg K_{m1}$ . The appropriate equation for the two-site model when  $[S] < K_{m2}$  is:

$$\frac{v}{[Et]} = \frac{V_{m1}[S]}{K_{m1} + [S]} + \frac{V_{m2}}{K_{m2}} [S] \quad (11)$$

This equation can be compared to that when two enzymes are present, one with a very high  $K_m$ :

$$\frac{v}{Et} = \frac{V_{m1}[S] + \frac{V_{m2}}{K_{m2}} [S]^2}{K_{m1} + [S]} \quad (12)$$

Fits of experimental data to the two equations are almost indistinguishable. Therefore, saturation kinetic data alone cannot determine the appropriate model when multiple enzymes are present. In addition, higher concentrations of dapsone makes naproxen demethylation kinetics hyperbolic (T. Tracy, unpublished results). This suggests that dapsone is occupying one of the two naproxen-binding regions in the CYP2C9 active site. Again, this will be discussed in Sec. V, on interactions between different substrates.

## 3. Substrate Inhibition

Another kinetic profile, substrate inhibition, occurs when the velocity from *ESS* is lower than that from *ES* (Fig. 5). In this case, the saturation curve will increase to a maximum and then decrease before leveling off at  $V_{m2}$ . For the P450 enzymes,  $V_{m2}$  is usually not zero, when submillimolar concentrations of substrate are in-

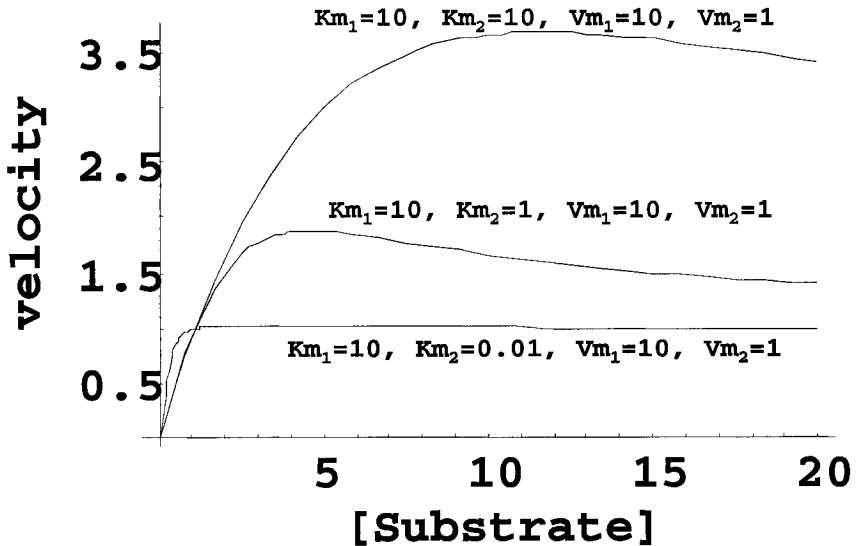
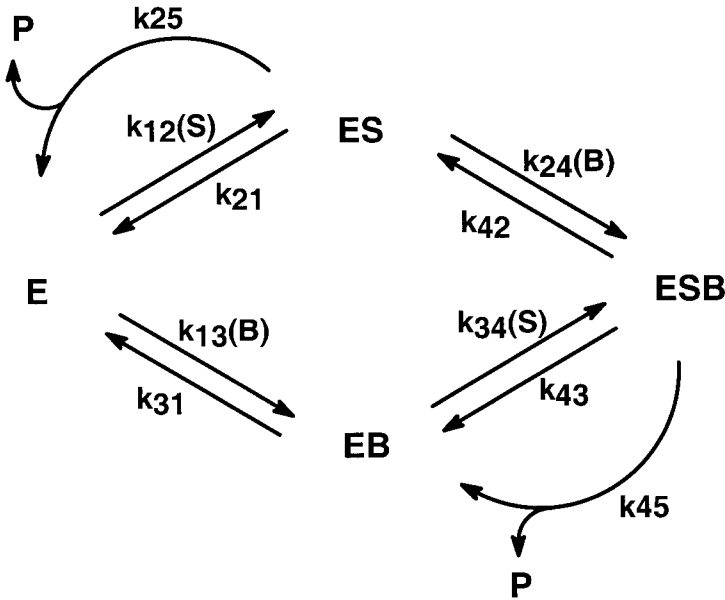


Figure 5 Substrate inhibition saturation curves.

involved. This suggests that *ESS* still has some activity. If substrate inhibition occurs at very high substrate concentrations, non-active-site interactions should be suspected. Substrate inhibition profiles are easily identified, provided that the observed concentration range is appropriate and  $K_{m_2}$  is not much smaller than  $K_{m_1}$  (Fig. 5). However, determining the kinetic constants in Eq. (10) requires adequate experimental data. The number and concentration of data points must be sufficient to define four regions in the saturation curve: the  $(V/K)_1$  region, the concave-downward region, the concave-upward region, and  $V_{m_2}$ .

## V. SIMULTANEOUS BINDING OF DIFFERENT SUBSTRATES TO THE P450 ACTIVE SITES

If two different substrates bind simultaneously to the active site, then the standard Michaelis–Menten equations and competitive inhibition kinetics do not apply. Instead it is necessary to base the kinetic analyses on a more complex kinetic scheme. The scheme in Figure 6 is a simplified representation of a substrate and an effector binding to an enzyme, with the assumption that product release is fast. In Figure 6, *S* is the substrate and *B* is the effector molecule. Product can be formed from both the *ES* and *ESB* complexes. If the rates of product formation



**Figure 6** Simplified kinetic scheme for the interaction between a substrate and an effector molecule for an enzyme with two binding sites within the active site. (Reprinted with permission from Ref. 17. Copyright 1998, American Chemical Society.)

are slow relative to the binding equilibrium, we can consider each substrate independently (i.e., we do not include the formation of the effector metabolites from *EB* and *ESB* in the kinetic derivations). This results in the following relatively simple equation for the velocity:

$$\frac{v}{Et} = \frac{V_m[S]}{K_m \frac{\left(1 + \frac{[B]}{K_b}\right)}{\left(1 + \frac{\beta[B]}{\alpha K_b}\right)} + [S] \frac{\left(1 + \frac{[B]}{\alpha K_b}\right)}{\left(1 + \frac{\beta[B]}{\alpha K_b}\right)}} \quad (13)$$

In this equation, *S* is the substrate, *B* is the effector,  $V_m = k_{25}Et$ ,  $K_m = (k_{21} + k_{25})/k_{12}$  (kinetic constants for substrate metabolism),  $K_B = k_{31}/k_{13}$  (binding constant for effector),  $\alpha$  is the change in  $K_m$  resulting from effector binding and  $\beta$  is

the change in  $V_m$  from effector binding. For inhibitors,  $\beta < 1$ ; for activators,  $\beta > 1$ .

The scheme in Figure 6 provides a general description of the interaction of two molecules with an enzyme, including both inhibition and activation. Since we are considering only the metabolism of  $S$ , the effector molecule can be binding at any other site on the enzyme, e.g., an allosteric site. With respect to P450 activation, at least some P450 effectors are also substrates for the enzymes [16,17]. Also, saturating concentrations of  $S$  will not completely inhibit the metabolism of  $B$ , and saturating concentrations of  $B$  cannot completely inhibit the metabolism of  $S$ . Since the P450 enzymes have only one active site, this data suggests that both molecules bind simultaneously to the active site (i.e., have access to the reactive oxygen). The observation of partial inhibition by another P450 substrate is also consistent with this hypothesis.

To experimentally define these kinds of interactions, it is necessary to vary both substrate and effector concentrations. For Eq. (13), initial parameters can be obtained by first performing double reciprocal plots and then replotting  $1/\Delta$  slope and  $1/\Delta$  intercept versus  $1/[S]$  [22]. The intercept of the  $1/\Delta$  intercept replot is  $\beta V_m/(1 - \beta)$ , which can be used to solve for  $\beta$ . The value for  $\alpha$  can then be obtained from the  $1/\Delta$  slope intercept [ $\beta V_m/K_m(\alpha - \beta)$ ].

If the metabolism of both substrate and effector are measured, the validity of treating the two processes independently can be tested. For example, we reported that 7,8-benzoflavone dramatically increases the  $V_m$  of phenanthrene metabolism by CYP3A4 and that phenanthrene is a partial inhibitor of 7,8-benzoflavone metabolism [16,17]. If the scheme in Figure 6 is valid, then the  $K_m$  when phenanthrene is analyzed as the substrate should equal  $K_B$  when 7,8-benzoflavone is analyzed as the substrate. In addition, since any thermodynamic state is path independent, the  $\alpha$  values and  $K_m\alpha K_B$  values should be similar between experiments. For this pair of substrates, this was shown to be true.

The situation becomes even more complicated when one of the substrates can bind twice to the enzyme, as represented in Figure 7. In this case, inhibition or activation is combined with the nonhyperbolic saturation kinetics for a single substrate described earlier. Analysis of the equation derived for the scheme in Figure 7 suggests that some compounds would be activators at low substrate concentrations and inhibitors at high substrate concentrations. This can occur when the rate of product formation from the intermediates has the order  $ES < ESB < ESS$ . At low substrate concentrations, the reaction is activated by  $B$  by converting  $ES$  to  $ESB$ . At high substrate concentrations, the reaction is inhibited by  $B$  by converting  $ESS$  to  $ESB$ . This is precisely what has been observed in Figure 4. In this figure, quinine converts the sigmoidal carbamazepine saturation curve to a hyperbolic curve (linear double-reciprocal plot), by apparently binding one of the substrate-binding sites. The presence of quinine results in significant

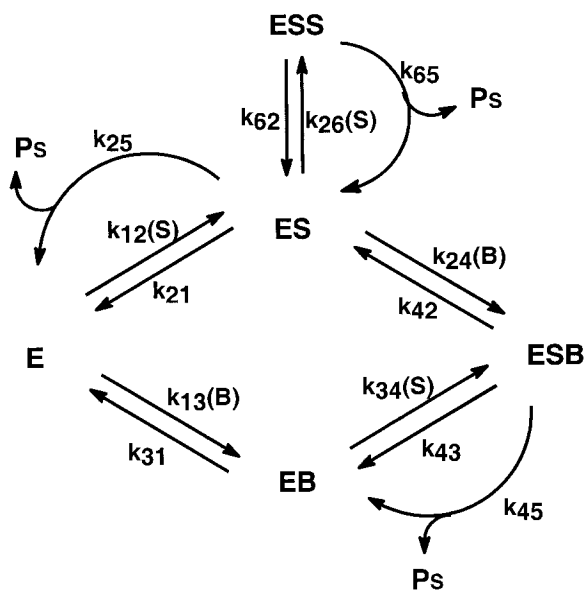


**Figure 7** Kinetic scheme for an enzyme with two binding sites that can bind two substrate molecules and one effector molecule. (Reprinted with permission from Ref. 17. Copyright 1998, American Chemical Society.)

activation at low substrate concentrations and inhibition at high substrate concentrations. This suggests that the reaction velocities from the various substrate complexes have the order  $ES < EB < ESS$ , where  $S$  is carbamazepine and  $B$  is quinine.

Two other examples of sigmoidal reactions that are made linear by an activator include a report by Johnson and coworkers [20], who showed that pregnenolone has a nonlinear double reciprocal plot that was made linear by the presence of  $5 \mu\text{M}$  7,8-benzoflavone, and Ueng et al. [15], who showed that aflatoxin B1 has sigmoidal saturation curve that is made more hyperbolic by 7,8-benzoflavone. Like the effect of quinine on carbamazepine metabolism, 7,8-benzoflavone is an activator at low aflatoxin B1 concentrations and an inhibitor at high aflatoxin B1 concentrations.

Another example of reactions that can be described by Figure 7 is the effect of dapson on naproxen metabolism by CYP2C9. In this case, dapson makes the biphasic naproxen curve more hyperbolic. Finally, one can expect similar influences on reactions that show substrate inhibition. If  $ESB$  has a metabolic rate similar to  $ES$ , one would expect activation at high substrate concentrations.

Conversely, if the rate is similar to  $ESS$ , inhibition would be expected at intermediate substrate concentrations, with little effect at  $V_m$ .

## VI. INFLUENCE OF ATYPICAL KINETICS ON INHIBITION AND DRUG INTERACTION STUDIES

In vitro studies of drug metabolism with human enzymes will become an increasingly important part of preclinical drug development, since they can provide information on the expected genotypic and phenotypic variation within the population and can be used to predict drug interactions. It is common practice to use inhibition of standard assays to determine if a substrate will interact with a particular P450. This is based on the assumption that competitive inhibition occurs and that a given inhibitor will have a  $K_i$  value that is independent of the substrate being inhibited. Although this is true for most P450 oxidations, there is an increasing number of examples where non-Michaelis–Menten kinetics are observed. The foregoing discussion suggests that an effector can either increase or decrease either  $V_m$  or  $K_m$  or both. It is also possible for an effector to bind to the active site and have no influence on a reaction. This can be seen by the effect of quinine on pyrene metabolism by CYP3A4 (Fig. 8). Although quinine is a known CYP3A4 substrate, it appears to have no effect on the reaction. However, if pyrene metabolism is first activated by testosterone or 7,8-benzoflavone, quinine displaces the activator, causing inhibition. This suggests that negative results for one drug cannot always be extrapolated to predict interactions with other drugs. In general, since both  $\alpha$  and  $\beta$  are substrate-pair dependent, drug interactions cannot be extrapolated to other substrates for enzymes that show non-Michaelis–Menten kinetics. This does not mean that inhibition studies are not useful in predicting drug metabolism or drug interactions, only that the limitations of the data should be understood. At an early stage of drug development, it is not practical to perform the extensive kinetic analyses that may be required to define all relevant kinetic parameters. It is still useful to conduct inhibition studies with standard assays to determine the enzymes involved and their approximate binding constants. However, a common result of complex kinetics is the observation of partial inhibition when using an isolated or expressed enzyme preparation. When this occurs, an approximate binding constant for the inhibitor at the given substrate concentration can be obtained by fitting inhibition from the following equation, where  $\beta_{app}$  is the fraction of activity remaining at saturating  $[I]$ :

$$\frac{v}{v_0} = 1 - \frac{(1 - \beta_{app})[I]}{K_{iapp} + [I]} \quad (14)$$

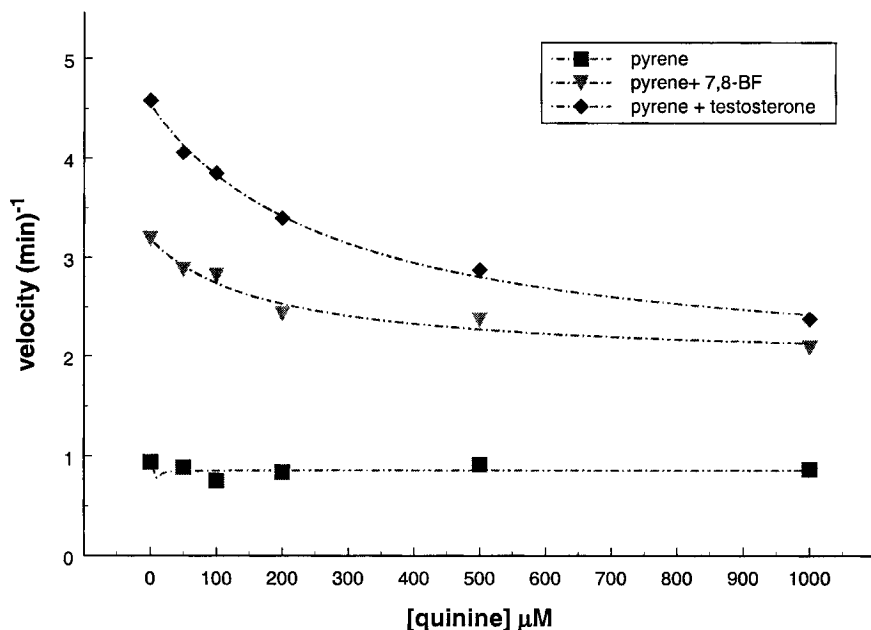


**Figure 8** Effect of quinine on pyrene metabolism. (From K. Nandigama and K. Korzekwa, unpublished results.)

However, values for  $K_i$ ,  $\alpha$ , and  $\beta$  cannot be obtained without performing more complex experiments. More importantly, the observation of partial inhibition indicated that multisubstrate kinetic mechanisms are likely to be involved, and care should be taken in the design and interpretation of future experiments.

## VII. SUMMARY

Most P450 catalyzed reactions show hyperbolic saturation kinetics and competitive inhibition kinetics. Therefore, binding constants can be obtained by inhibition of standard assays. Some P450-catalyzed reactions show atypical kinetics, including activation, autoactivation, partial inhibition, biphasic saturation kinetics, and substrate inhibition. Although atypical kinetics are for metabolism with any P450 enzyme, these phenomena occur most frequently for the CYP3A enzymes. In general, an observation of non-Michaelis–Menten kinetics makes it difficult to interpret results and makes *in vitro*–*in vivo* correlations difficult. In particular, the interactions between two substrates and an enzyme are dependent on both

substrates. This can result in both false negatives and false positives when predicting drug interactions with inhibition studies.

## REFERENCES

1. EL King, C Altman. A schematic method of deriving the rate laws for enzyme-catalyzed reactions. *J. Chem. Phys.* 60:1375–1378, 1956.
2. FJ Gonzalez, KR Korzekwa. Cytochrome P450 expression systems. *Annu. Rev. Pharmacol. Toxicol.* 35:369–390, 1995.
3. DC Eberhart, A Parkinson. Cytochrome P450 IIIA1 (P450p) requires cytochrome b<sub>5</sub> and phospholipid with unsaturated fatty acids. *Arch. Biochem. Biophys.* 291:231–240, 1991.
4. N Hanioka, K Korzekwa, FJ Gonzalez. Sequence requirements for cytochromes P450IIA1 and P450IIA2 catalytic activity: evidence for both specific and non-specific substrate binding interactions through use of chimeric cDNAs and cDNA expression. *Protein Eng.* 3:571–575, 1990.
5. WW Cleland. Statistical analysis of enzyme kinetic data. *Methods Enzymol.* 63:103–138, 1979.
6. T Akaike. A new look at the statistical model identification. *IEEE Trans. Automat. Contr.* 19:716–723, 1974.
7. K Yamaoka, T Nakagawa, T Uno. Application of Akaike's information criterion (AIC) in the evaluation of linear pharmacokinetic equations. *J. Pharmacokinet. Biopharm.* 6:165–175, 1978.
8. JA Peterson, RE Ebel, DH O'Keefe, T Matsubara, RW Estabrook. Temperature dependence of cytochrome P-450 reduction. A model for NADPH-cytochrome P-450 reductase: cytochrome P-450 interaction. *J. Biol. Chem.* 251:4010–4016, 1976.
9. J Grogan, M Shou, D Zhou, S Chen, KR Korzekwa. Use of aromatase (CYP19) metabolite ratios to characterize electron transfer from NADPH-cytochrome P450 reductase. *Biochemistry* 32:12007–12012, 1993.
10. N Hanioka, FJ Gonzalez, NA Lindberg, G Liu, HV Gelboin, KR Korzekwa. Site-directed mutagenesis of cytochrome P450s CYP2A1 and CYP2A2: Influence of the distal helix on the kinetics of testosterone hydroxylation. *Biochemistry* 31:3364–3370, 1992.
11. JP Jones, KR Korzekwa, AE Rettie, WF Trager. Isotopically sensitive branching and its effect on the observed intramolecular isotope effects in cytochrome P-450 catalyzed reactions: a new method for the estimation of intrinsic isotope effects. *J. Am. Chem. Soc.* 108:7074–7078, 1986.
12. KR Korzekwa, DC Swinney, WF Trager. Isotopically labeled chlorobenzenes as probes for the mechanism of cytochrome P-450 catalyzed aromatic hydroxylation. *Biochemistry* 28:9019–9027, 1989.
13. BSS Masters, CH Williams Jr, H Kamin. The preparation and properties of microsomal TPNH-cytochrome c reductase from pig liver. *Methods Enzymol.* 10:565–573, 1967.



14. AI Voznesensky, JB Schenkman. The cytochrome P450 2B4-NADPH cytochrome P450 reductase electron transfer complex is not formed by charge-pairing. *J. Biol. Chem.* 267:14669–14676, 1992.
15. Y-F Ueng, T Kuwabara, Y-J Chun, FP Guengerich. Cooperativity in oxidations catalyzed by cytochrome P450 3A4. *Biochemistry* 36:370–381, 1997.
16. M Shou, J Grogan, JA Mancewicz, KW Krausz, FJ Gonzalez, HV Gelboin, KR Korzekwa. Activation of CYP3A4: Evidence for the simultaneous binding of two substrates in a cytochrome P450 active site. *Biochemistry* 33:6450–6455, 1994.
17. KR Korzekwa, N Krishnamachary, M Shou, A Ogai, RA Parise, AE Rettie, FJ Gonzalez, TS Tracy. Evaluation of atypical cytochrome P450 kinetics with two-substrate models—evidence that multiple substrates can simultaneously bind to cytochrome P450 active sites. *Biochemistry* 37:4137–4147, 1998.
18. L Banci, I Bertini, S Marconi, R Pierattelli, SG Sligar. Cytochrome P450 and aromatic bases: A  $^1\text{H}$  NMR study. *J. Am. Chem. Soc.* 116:4866–4873, 1994.
19. EF Johnson, GE Schwab, LE Vickery. Positive effectors of the binding of an active site-directed amino steroid to rabbit cytochrome P-450 3c. *J. Biol. Chem.* 263:17672–17677, 1988.
20. GE Schwab, JL Raucy, EF Johnson. Modulation of rabbit and human hepatic cytochrome P-450-catalyzed steroid hydroxylations by alpha-naphthoflavone. *Mol. Pharmacol.* 33:493–499, 1988.
21. TS Tracy, C Marra, SA Wrighton, FJ Gonzalez, KR Korzekwa. Involvement of multiple cytochrome P450 isoforms in naproxen O-demethylation. *Eur. J. Clin. Pharmacol.* 52:293–298, 1997.
22. IH Segel. *Enzyme Kinetics*. New York: Wiley, 1975, p 227.

# 3

## Human Cytochromes P450 and Their Role in Metabolism-Based Drug–Drug Interactions

**Stephen E. Clarke**

*Glaxo SmithKline Pharmaceuticals, Ware, United Kingdom*

**Barry C. Jones**

*Pfizer Global Research & Development, Kent, United Kingdom*

### I. INTRODUCTION

Over the last 10–15 years, cytochrome P450 binding has displaced plasma protein binding, renal elimination, and pharmacological effect as the major focus for drug–drug interactions in the pharmaceutical industry. P450 metabolism–based drug–drug interactions, *in vitro* and *in vivo*, have appeared in product labeling and advertising copy in unprecedented and frequently incomprehensible detail. Although this focus has led, on more than one occasion, to undue emphasis on clinically insignificant effects, there does exist in many circumstances a significant risk to patients arising from interactions in the P450 enzyme system. What is more, these interactions can be reasonably well predicted from *in vitro* data and extrapolated from drug to drug, thanks to the large body of available information.

From the authors' survey of the available data on the elimination pathways for 403 drugs marketed in the United States and Europe, the overall importance of P450-mediated clearance can be determined. The elimination of unchanged drug via urine (the most commonly defined), bile, expired air, or feces represented, on average, approximately 25% of the total elimination of dose for these compounds. P450-mediated metabolism represented 55%, with all other metabolic processes making up the remaining 20%. Thus, this focus (or perhaps obsessive compulsion) on studying P450 is somewhat justified.

## II. CYTOCHROME P450 SUPERFAMILY

P450s are ubiquitous throughout nature: they are present in bacteria, plants, and mammals, and there are hundreds of known enzymes that can show tissue- and species-specific expression. This diversity of enzymes has necessitated a systematic nomenclature system [1]. The root name given all cytochrome P450 enzymes is CYP (or *CYP* for the gene). Enzymes showing greater than 40% amino acid sequence homology are placed in the same family, designated by an Arabic numeral. When two or more subfamilies are known to exist within the family, then enzymes with greater than 60% homology are placed in the same subfamily, designated with a letter. Finally this is followed by an Arabic number, representing the individual enzyme, which is assigned on an incremental basis, i.e., first come, first served. As of February 1999 there were approximately 650 P450 enzymes, organized into 96 families, identified in species from alfalfa to the zebra finch; even the humble nematode (*Caenorhabditis elegans*) has over 60 P450s [2]. Only the 35 P450 enzymes described in man (almost certainly an underestimate) (Table 1) are likely to be of any clinical relevance, although only the P450s in families 1, 2, and 3 appear to be responsible for the metabolism of drugs and therefore are potential sites for drug interactions. The P450 enzymes from the other families are generally involved in endogenous processes, particularly hormone biosynthesis. An interaction with these enzymes could have significant toxicological effects, but a pharmacokinetic drug–drug interaction between two ex-

**Table 1** Human Cytochrome P450 Superfamily

Family	Subfamilies	No. of enzymes	Best-described substrates
1	A, B	3	Drugs/xenobiotics
2	A, B, C, D, E, F, J	12	Drugs/xenobiotics
3	A	3	Drugs/xenobiotics
4	A, B, F	4	Fatty acids/leukotrienes
5	A	1	Thromboxane
7	A	1	Cholesterol
8	—	1	Prostacyclin
11	A, B	3	Steroids
17	A	1	Steroids
19	—	1	Estrogen
21	A, B	2	Steroids
24	—	1	Vitamin D/steroids
27	—	1	Vitamin D/steroids
51	—	1	Steroids

ogenous pharmacological agents is highly unlikely. Even of the 18 P450 enzymes in families 1, 2, and 3, perhaps only five or six are quantitatively relevant in the metabolism of pharmaceuticals.

### III. TISSUE DISTRIBUTION AND ABUNDANCE

P450 enzymes can be found throughout the body, particularly at interfaces, such as the intestine, nasal epithelia, and skin. The liver and the intestinal epithelia are the predominant sites for P450-mediated drug elimination and they are also the sites worth considering in most detail with respect to drug–drug interactions. Although P450 enzymes have been well characterized in many other tissues, it is unlikely that these play a significant role in the overall elimination of drugs. These tissues and their P450s may play a role, for example, in tissue-specific production of reactive species and thereby toxicity, but they are unlikely to represent a concern for pharmacokinetic drug interactions.

The complement of intestinal P450s appears to be more restricted than that in the liver. Despite this, many different P450 enzymes have been detected (by activity or mRNA) in the intestine from various species, including man. The available data would suggest that there are measurable levels of at least CYP1A1, CYP2C9, CYP2D6, CYP2E1, and representatives of subfamilies CYP2J and CYP4B present in the intestinal epithelia [3–9]; however, overwhelmingly the most significant P450 enzyme in human intestine is CYP3A4 [10–13]. The other P450 enzymes are clearly present in low quantities and/or are not capable of contributing to the pharmacokinetic profile (e.g., limiting oral bioavailability) via intestinal metabolism. That CYP3A4 is the P450 enzyme of significant concern for drug–drug interactions in the intestine is supported by a number of pharmacokinetic studies.

Although it is not a trivial task to clearly demonstrate the role of a human P450 enzyme in intestinal presystemic elimination, this has been shown for several drugs metabolized by CYP3A4, e.g., cyclosporin [14,15], tacrolimus [16,17], sirolimus [18], midazolam [19], saquinavir [20], felodipine [21,22], and nefazadone [23]. Interestingly, grapefruit juice has been shown to have a significant interaction with a number of these drugs [24]. Grapefruit juice's effect is believed to be limited to the intestine and to be specifically CYP3A4 mediated [22,25,26]. Although still subject to intensive investigation, psoralen derivatives and related compounds are thought to be at least partially involved as the active ingredients in grapefruit juice [27–32]. Interestingly these components are very potent inhibitors (submicromolar inhibitory constants) of CYP1A2, CYP2C9, CYP2C19, and CYP2D6, in addition to any effects they have on CYP3A4 (H. Oldham, personal communication, 1998). Yet the reports of significant interactions *in vivo* appear to be limited to CYP3A4 substrates. This supports the contention that the effect

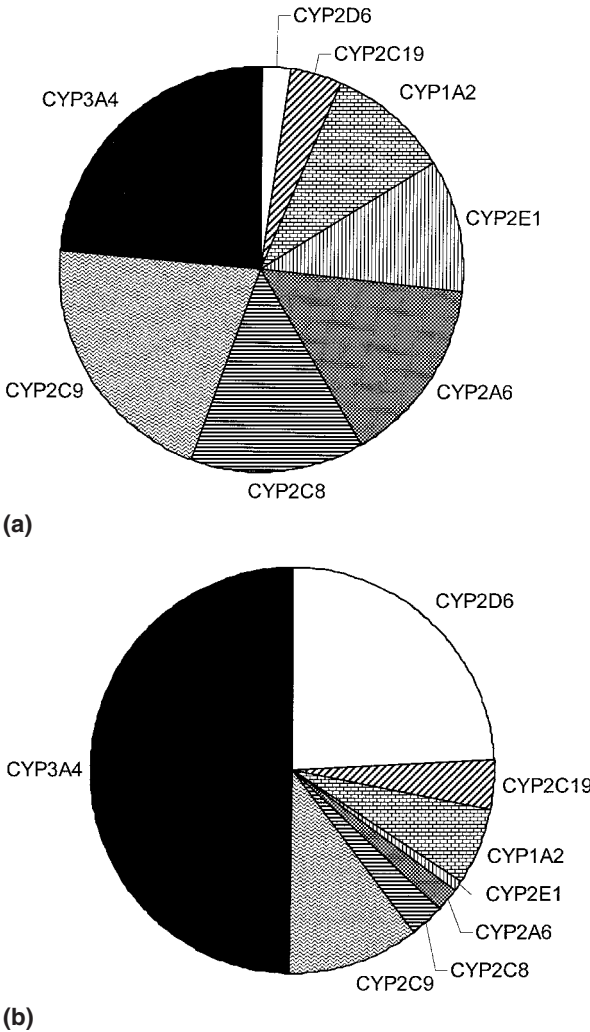


**Figure 1** (a) Relative hepatic abundance of the major cytochromes P450 in man. (b) Relative significance of the major hepatic cytochromes P450 in the P450-mediated clearance of marketed drugs. This figure represents the author's survey of 403 drugs marketed in the United States and/or Europe. Rather than the number of drugs, the values represent the total proportions of drug clearance that each P450 enzyme is responsible for. (Part a adapted from Ref. 33.)

is solely at the intestine, not the liver, and that CYP3A4 is the only P450 that plays a significant role in the intestinal metabolism of drugs. Therefore, the intestine is an important site for P450 drug interactions, but only those mediated via CYP3A4.

In the human liver, the relative content of the major P450 enzymes has been determined in several studies, and a general consensus has emerged. On average, CYP3A4 is quantitatively the most important, with CYP2C8, CYP2C9, CYP2A6, CYP2E1, and CYP1A2 present in somewhat lower quantities; CYP2C19 and CYP2D6 are of relatively minor quantitative importance (Fig. 1a) [33]. However, a very different picture emerges when evaluating the extent to which P450 enzymes are responsible for drug elimination processes (Fig. 1b). CYP3A4 is responsible for approximately 50% of the P450-mediated metabolism of marketed pharmaceuticals, and CYP2D6 has a disproportionate share (~25%) in comparison to the amount of enzyme present in the liver. CYP2C9, CYP1A2, and CYP2C19 make up a progressively less significant proportion of the whole. All the other P450 enzymes make somewhat minor contributions.

It is notable that CYP3A4 appears to be more frequently cited for newly developed drugs than CYP2D6. This increase in the incidence of CYP3A4 substrates follows the increase in lipophilicity, probably a consequence of the paradigm shift in the pharmaceutical industry drug-discovery process, which is now driven by *in vitro* pharmacological screening. It is easy to understand why such a large number of CYP2D6 substrates has been identified. Due to the polymorphic nature of CYP2D6, substrates of this enzyme were among the first and easiest to be defined, even before the molecular basis of the polymorphism was known. Lately, due to the current impracticality of personalizing doses, CYP2D6 substrates are being engineered out or deselected during the drug-discovery and optimization phase, wherever this might provide a competitive advantage. For other P450 enzymes, such as CYP2C8, the tools to investigate and identify substrates have been available only relatively recently, and the importance of these enzymes may be underestimated. These considerations and the data for those drugs where the mechanisms of elimination have yet to be fully elucidated might be expected to alter this overall distribution somewhat; however, it is unlikely that the current picture will change for at least the medium-term future. Thus, from the pharmaceutical industry's perspective, CYP1A2, CYP2C9, CYP2C19, CYP2D6, and CYP3A4 address 95% of the P450 issues and a little over 50% of the total target for pharmacokinetic drug–drug interaction studies.

#### IV. PHARMACOKINETIC CONSIDERATIONS

The pharmacokinetics of drug–drug interactions has been described in detail previously (see Chap. 1); however, there are a number of points that are worth briefly

reiterating in the context of P450. For an inhibition interaction the affected drug clearly must have an appreciable proportion of its clearance via the P450 enzyme being inhibited, i.e., the  $f_m > 0.3$ . For example, if the P450-mediated metabolism was only 20% of the total clearance of a compound, a fivefold reduction in its activity would have a limited effect overall (Fig. 2). Therefore, for inhibition interactions the relative importance of the individual P450 enzymes is simply described by Figure 1b. For induction interactions the degree of effect is less sensitive to the  $f_m$ , and significant pharmacokinetic changes can be seen even if the induced P450 is normally a relatively minor contributor to overall clearance. Using the same example as for inhibition, a fivefold increase in the P450 activity has a significant effect on total clearance, despite the normally minor contribution to clearance (Fig. 2). In such cases the degree of sensitivity is defined by the extent of induction as well as the  $f_m$ . There is evidence of induction for a number of P450 enzymes in man, although some of the most notable inductive effects involve CYP3A4.

It is often thought that drugs with an appreciable  $f_m$  by CYP2D6, that have dangerous interaction potential, have been generally identified (due to the polymorphic nature of this enzyme) and withdrawn. This has been the case, e.g., with perhexiline [34,35] and phenformin [36]. But it has long been recognized that CYP2D6 poor metabolizers and extensive metabolizers coadministered potent

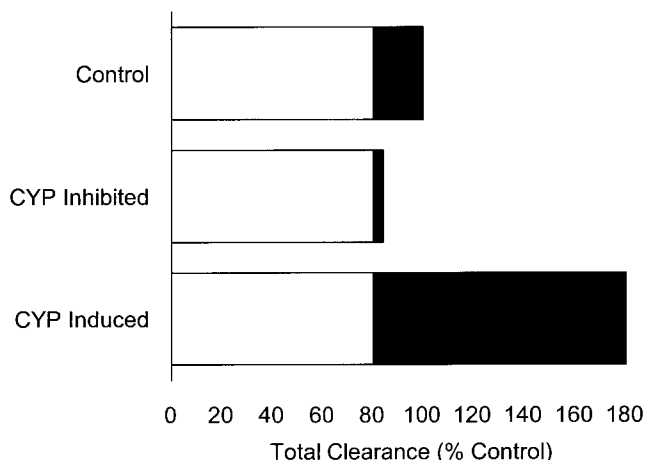


**Figure 2** Influence of  $f_m$  on drug–drug interactions. The control represents a model drug for which cytochrome P450 (dark bar) is responsible for 20% of the clearance, with the remaining 80% being non-P450 mediated (white bar). “CYP Inhibited” and “CYP Induced” illustrate the effect on total clearance of a fivefold reduction or increase in the P450 activity, respectively.

CYP2D6 inhibitors are at particular risk of adverse drug reactions [37]. There are still a large number of CYP2D6 substrates marketed, and serious if not acutely fatal interactions are still possible, despite the existence of a “canary” population that will exhibit very different pharmacokinetics to warn of potential consequences of drug interactions.

The clearance of the target drug can be the most significant arbiter of the severity of interaction for systemic interactions. Using the venous equilibrium model of hepatic elimination, a very highly intrinsically cleared compound (e.g., compound A in Fig. 3) would be relatively insensitive to inhibition interactions. In this case a 75% reduction in enzyme activity would result in virtually no change ( $\sim 6\%$ ) in blood clearance. For a significantly less readily metabolized substrate (e.g., compound B in Fig. 3), such a reduction in enzyme activity would have a significant effect ( $\sim 30\%$ ) on blood clearance. For low-clearance drugs (assuming  $f_m$  is 1), the reduction in clearance exactly reflects the reduction in enzyme activity.

Although systemically low-clearance drugs would be expected to be the most sensitive to drug–drug interactions, such compounds frequently have high oral bioavailability. As such, a coadministered inhibitor will cause little alteration of the  $C_{max}$  on a single oral dose but would need to be able to maintain inhibitory

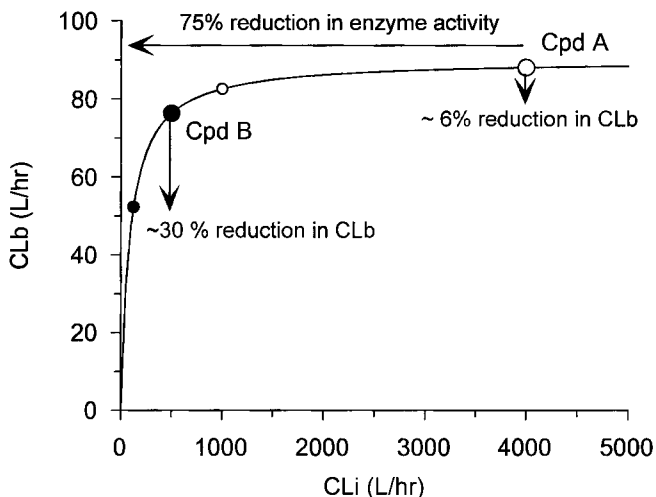


**Figure 3** Influence of clearance on systemic drug–drug interactions. For model compound A (open circles) and compound B (closed circles), the effect on blood clearance of a 75% reduction in intrinsic enzyme activity ( $CL_i$ ) is illustrated. The line represents the relationship between  $CL_i$  and  $CL_b$  that is described by the venous equilibrium, or “well-stirred,” model of hepatic extraction.



levels throughout the dosing interval. At steady state, a large inhibitory effect could be mediated, but the maximum initial “jump” in blood levels of the target drug would be twofold, with each subsequent dose adding at most another unit until the steady state was reached. Such a relatively gentle rate of elevation of blood levels might enable, in some circumstances, known tolerated adverse effects to be identified before serious toxicity is encountered. Many CYP2C9 substrates are high-bioavailability, low-clearance drugs, e.g., glyburide, tolbutamide, phenytoin, and warfarin, as are some CYP1A2 substrates, e.g., caffeine and theophylline. There are also examples of higher-clearance CYP1A2 substrates, for example, ropinirole and tacrine, although most published interaction studies have involved caffeine or theophylline. CYP2D6 and particularly CYP3A4 substrates exhibit a wide range of pharmacokinetic properties, in the latter case involving some of the highest-clearance drugs.

Blood-flow-limited drugs are not only theoretically systemic drug-interaction resistant, but also rarely make good drugs (due to a low oral bioavailability and a high likelihood of a short half-life), and there are few examples marketed, except prodrugs. However, on oral dosing a putative inhibitor of the metabolism of such drugs need only be effective during the first-pass phase to cause a very significant effect. High levels of inhibitory blockade can be achieved due to the concentrations that can be achieved in the gut and the liver during absorption. Since the target drug has a low bioavailability, changes in blood  $C_{max}$  can be quite sudden and of an order of magnitude or more. Currently the greatest concern for low-bioavailability, high-clearance drugs is with certain CYP3A4 substrates. The best-known example is the interaction between potent CYP3A4 inhibitors and terfenadine, where plasma levels of terfenadine have become greatly elevated [38,39] and can result in fatal effects due to the cardiotoxicity of terfenadine.

## V. INCIDENCE OF INHIBITION

P450 inhibitors can be readily identified by *in vitro* methods (see Chaps. 2 and 7), and in the authors' laboratories this has been performed for approximately 400 marketed drugs. For comparison, the probit plots showing the incidence versus potency of these drugs and approximately 2000 typical pharmaceutical company compounds (ca. 1998), are shown in Figure 4.

For the marketed drugs, only 5% had an  $IC_{50}$  of less than 10  $\mu M$  against CYP1A2, and this incidence was increased to approximately 10% for CYP2C9, CYP2C19, and CYP3A4. Many more drugs had a significant inhibitory effect on CYP2D6, with 20% of marketed drugs having an *in vitro*  $IC_{50}$  of less than 10  $\mu M$ . To some degree these results reflect the relative importance of the P450 enzymes in drug clearance (Fig. 1b); however, the results for CYP3A4 are some-

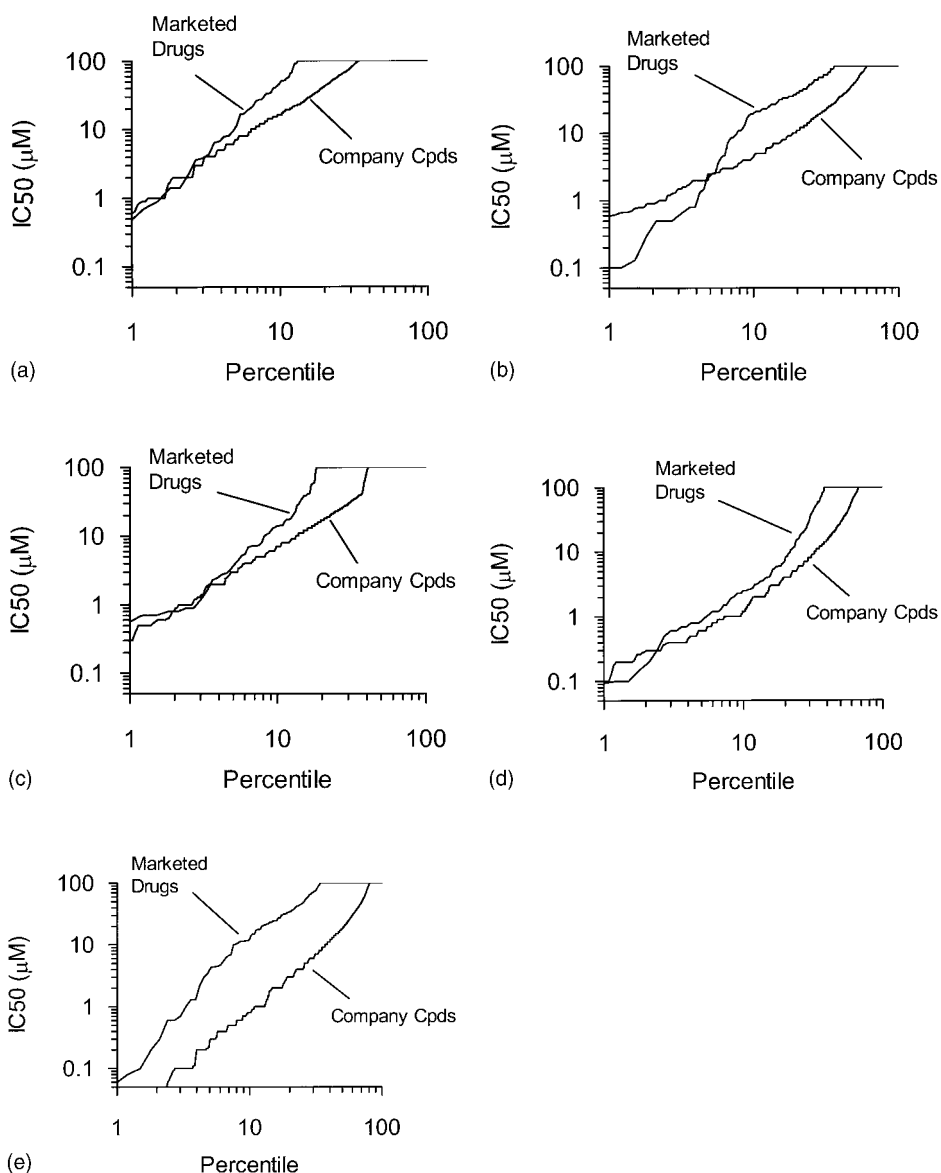


**Figure 4** Incidence of P450 inhibition. Probit plots generated from in vitro P450-inhibition data in the authors' laboratories using heterologously expressed P450s in microsomal membranes. The plots represent data from approximately 400 marketed drugs and 2000 pharmaceutical company compounds synthesized in 1998. (a) CYP1A2; (b) CYP2C9; (c) CYP2C19; (d) CYP2D6; (e) CYP3A4.

what at odds with this. Although there is much concern about CYP3A4-mediated drug interactions, there are not very many marketed drugs that are potent inhibitors of this enzyme. Certainly the majority of research in this area has generally focused on a limited set of azole antifungals and a few macrolide antibiotics. CYP3A4 often has the role of a high-capacity, low-affinity drug-metabolizing enzyme. Equally high-affinity compounds (and therefore potent inhibitors) may have poor pharmacokinetic properties (very high  $V_{\max}/K_m$ , therefore high  $CL_i$ ) that limit their application as pharmaceutical agents, and hence the relatively low incidence of CYP3A4 inhibitors in the marketed drugs.

A more interesting comparison is that of marketed drugs and pharmaceutical company compounds. There is a particularly dramatic difference in the incidence of CYP3A4 inhibition (Fig. 4e). Typical pharmaceutical company compounds are very much more inhibitory to CYP3A4 than are marketed drugs. As more and more drug discovery activity is supported by *in vitro* high-throughput screening, DMSO solubility has become the only limitation to testing. Thus, with high lipophilicity no longer a barrier and the trend to increasing molecular weight, as medicinal chemists “build” additional functionality and selectivity onto their molecular templates, a greater proportion of compounds fulfill the structural requirements for CYP3A4 substrates and inhibitors. This observation is similar to what has been described in the context of permeability and absorption and is part of the basis of the “Lipinski rule of five” [40].

The differences between marketed drugs and pharmaceutical company compounds are less marked for the other major P450 enzymes. For CYP1A2 there are few changes in the incidence of very potent inhibitors, as might be expected. Any increase in lipophilicity, which should improve the affinity of a compound for any P450 enzyme, would be countered by the increased molecular weight, which would make a compound less suitable for the CYP1A2 active site. In fact, CYP1A2, CYP2C9, CYP2C19, and CYP2D6 show broadly similar patterns to one another. There is no increase in the incidence of very potent inhibitors of these P450s in the contemporary company compounds compared to currently marketed drugs. Clearly the specific QSAR attributes that these P450 enzymes exhibit are being no more consistently met now than over the last 20–30 years. However, there are now very many more “midrange” inhibitors and many less “clean” compounds than have been seen previously, due primarily to the general increase in lipophilicity. It is noteworthy that the more recently developed SSRIs and HIV protease inhibitors are less like the majority of other marketed drugs and have a particularly high incidence of interactions with P450. Overall this data would suggest that, unchecked, CYP3A4 inhibition is likely to be the most significant drug–drug interaction challenge facing the pharmaceutical industry in coming years.

Taking all of the foregoing factors into account, the relative importance of each of the major P450 enzymes, with respect to drug–drug interactions, from

a pharmaceutical industry perspective can be ranked (Table 2). Thus, in the authors' opinion, CYP3A4 is of most concern, followed by CYP2C9, CYP2D6, CYP1A2, and CYP2C19, in that order. Clearly the interaction profile of the billion-dollar drug will always be of the most immediate significance, even if it concerns an otherwise relatively insignificant P450 enzyme. However, the majority of the issues of cytochrome P450-mediated drug–drug interactions can be addressed by considering these five enzymes.

## VI. CYP1A2

### A. Selectivity

Initial studies on the CYP1A family characterized the substrates as being lipophilic planar polyaromatic/heteroaromatic molecules, with a small depth and a large area/depth ratio. Later studies have suggested that caffeine interacts with the CYP1A2 via three hydrogen bonds, which orient the molecule so that it can undergo *N*-3-demethylation. Protein homology modeling suggests that the active sites of the CYP1A enzymes are composed of several aromatic residues, which form a rectangular slot and restrict the size and shape of the cavity, so only planar structures are able to occupy the binding site. This is in keeping with the initial observation and could explain the preference of CYP1A enzymes for hydrophobic, planar aromatic species that are able to partake in  $\pi$ – $\pi$  interactions with these aromatic residues. In addition to the aromatic residues there are several residues able to form hydrogen bonds with substrate molecules. Such a model is able to rationalize that caffeine is *N*-demethylated at the 1, 3, and 7 positions by CYP1A2, of which the *N*-3-demethylation is the major pathway. Hence it appears that binding to the active site of CYP1A2 requires certain molecular dimensions and hydrophobicity, together with defined hydrogen bonding and  $\pi$ – $\pi$  interactions.

The domination of the  $\pi$ – $\pi$  interactions is also evident in the inhibitor selectivity of the enzyme. The quinolone antibacterial enoxacin is an inhibitor that directly coordinates via the 4'-nitrogen atom on the piperazine function to the heme iron. In addition, there are aromatic regions and hydrogen bonding functions within the molecule that could be important in forming interactions with residues in the enzyme active site. Indeed, a comparison of a series of quinolone antibiotics has indicated that the keto group, the carboxylate group, and the core nitrogen at position 1 are able to form a similar pattern of hydrogen bonds with the active site, as has been suggested for caffeine.

Unlike some of the other P450s, CYP1A2 does not have a clear preference for acidic or basic molecules. It is able to metabolize basic compounds such as imipramine but is inhibited by acidic compounds such as enoxacin. It is perhaps not surprising then that octanol/buffer partition coefficients or overall lipophilic-

**Table 2** Drug–Drug Interaction Risk Assessment Ranking for Major Human P450 Enzymes

P450	Tissue distribution	Hepatic abundance	Participation in drug clearance	Pharmacokinetic considerations	P450-inhibition incidence		Overall
					Marketed drugs	Company compounds	
1A2	2=	3	4	3	5	5	4
2C9	2=	2	3	2	2=	3	2
2C19	2=	4	5	4=	4	4	5
2D6	2=	5	2	4=	1	2	3
3A4	1	1	1	1	2=	1	1

The major human drug-metabolizing P450 enzymes are ranked for each of the significant factors considered in the text. A rank of 1 represents the greatest risk and that of 5 the least. These rankings are somewhat arbitrary and represent a pharmaceutical industry perspective and are solely the opinion of the authors.

ity is not reflective per se of the interaction between CYP1A2 and its substrates or inhibitors.

## B. Induction

Though CYP1A2 appears to be nonpolymorphic in man [41], it is inducible by environmental factors, such as cigarette smoking [42], which leads to an increased variability of this enzyme. In terms of induction by pharmaceutical agents, probably the most significant example is omeprazole. Omeprazole has been shown to be a CYP1A2 inducer in human hepatocytes [43]. In vivo at higher omeprazole doses (40 and 120 mg for 7 days) there was a significant increase in caffeine metabolism, as shown by urinary metabolic ratios, the caffeine breath test, and caffeine clearance [44]. However, at a low dose of omeprazole (20 mg/day for 7 days) there was no effect on caffeine metabolic ratios [45] or on phenacetin-mediated CYP1A2 metabolism [46], suggesting that omeprazole is a dose-dependent inducer of CYP1A2 in man.

## C. Inhibition

Furafylline, a structural analog of theophylline, was produced as a long-acting substitute for theophylline. Early clinical studies showed that the compound produced marked inhibition of caffeine metabolism. Further in vitro studies showed that furafylline is a selective mechanism-based inhibitor of CYP1A2 [47,48]. Detailed mechanistic studies have indicated that metabolic processing of the C-8 methyl group is involved in the inactivation [48].

The interaction between the quinolone antibacterials and CYP1A2 has been studied in some depth for enoxacin and pefloxacin. Both compounds have been shown to inhibit CYP1A2-mediated metabolism of caffeine in vitro [49]. This in vitro inhibition translated into a twofold decrease in caffeine clearance by pefloxacin and a sixfold decrease in clearance by enoxacin [50]. Because pefloxacin undergoes *N*-demethylation to norfloxacin [51] and norfloxacin is very much more potent as an inhibitor than pefloxacin [50], this suggests that the observed in vivo interaction seen for pefloxacin may, in part, be due to norfloxacin. Many other quinolone antibacterial agents have been investigated for their interaction with theophylline, and ciprofloxacin has also been shown to have notable inhibitory effects [52].

There have been a number of investigations into the ability of the selective serotonin reuptake inhibitors (SSRIs) to inhibit CYP1A2 [53–55]. In general these studies agree that fluvoxamine is the most potent CYP1A2 inhibitor in this class, with  $K_i \sim 0.2 \mu\text{M}$ . Other members of the class, such as fluoxetine, paroxetine, and sertraline, have been shown to be at least 10-fold less potent, with nefazodone and venlafaxine showing low inhibitory potential against CYP1A2. The

potent inhibition of caffeine metabolism by fluvoxamine results in an approximate fivefold decrease in caffeine clearance and sixfold increase in half-life [56].

## D. Substrates

CYP1A2 metabolizes several drug substrates, including phenacetin, tacrine, ropinirole, riluzole, theophylline, and caffeine. Caffeine, although not used therapeutically in the strictest sense, is—given the worldwide consumption of tea, coffee, and other caffeine-containing beverages—of significant interest.

The relative safety of caffeine has led to its widespread use as an *in vivo* probe for CYP1A2 activity in man. The primary route of caffeine metabolism is via *N*-demethylation to paraxanthine, theophylline, and theobromine. The major route of caffeine clearance in man is to paraxanthine [57]. The *N*-3-demethylation of caffeine to paraxanthine has been shown to be mediated by CYP1A2 [58]. However, paraxanthine is further metabolized to a number of different products, and as a consequence urinary metabolic ratios are often used to describe an individual CYP1A2 phenotype.

Such approaches have been used successfully to demonstrate the induction of CYP1A2 by smoking [42]. In addition, this study showed that oral contraceptives produce a small but significant inhibition of CYP1A2. Urinary metabolic ratios have also been used to show that oral AUC of clozapine was correlated with caffeine *N*-3-demethylation [59], a finding supported by some recent *in vitro* data, which has shown that clozapine *N*-demethylation is mediated by CYP1A2 [60].

## VII. CYP2C9

### A. Selectivity

CYP2C9 drug substrates include phenytoin, tolbutamide, various nonsteroidal anti-inflammatory drugs (NSAIDs), and (*S*)-warfarin. In terms of physicochemistry, the majority of the CYP2C9 substrates are acidic or contain areas of hydrogen bonding potential. Therefore, it has been proposed that these groups are important in binding to the active site of CYP2C9. There are a number of substrate template models for CYP2C9, which typically produces template models where the hydrogen bonding groups are positioned at a distance of approximately 8 angstroms and at an angle of 82° from the site of oxidation [61].

At present the key substrate residues within the CYP2C9-active site have yet to be unambiguously identified. However, a homology model based on CYP102 has suggested that there may be two serine residues within the active

site that fulfill this role. In addition there is the suggestion that  $\pi$ - $\pi$  stacking interactions also occur between some of the substrates and the active site [62].

## B. Polymorphism

There are three allelic variants of CYP2C9 that show significantly altered catalytic properties. These variants are termed CYP2C9\*1 (wild type), CYP2C9\*2 (Arg to Cys at position 144), and CYP2C9\*3 (Ile to Leu at position 359). In general, CYP2C9\*2 and CYP2C9\*3 show reduced rates of metabolism toward substrates, relative to CYP2C9\*1 [63,64].

The impact of this reduced rate of metabolism is perhaps best exemplified by warfarin. Warfarin is administered as a racemate, with different P450 enzymes being involved in the metabolism of the different enantiomers. (*R*)-Warfarin is metabolized by various P450s, including CYP1A2, CYP2C19, and CYP3A4 [65–67]. (*S*)-Warfarin, however, is metabolized predominantly by CYP2C9 [68]. Patients who are homozygous for CYP2C9\*1 typically receive doses of between 4 and 8 mg of warfarin per day and have plasma (*S*)-warfarin/(*R*)-warfarin ratios of 0.5. Patients with the CYP2C9\*3 allele are more sensitive to warfarin effects [69], and an individual who was homozygous for CYP2C9\*3 could not receive more than 0.5 mg per day and even at this dose had a plasma (*S*)-warfarin/(*R*)-warfarin ratio of 4 [70].

## C. Inhibition

Sulphaphenazole is perhaps the most potent and selective inhibitor of CYP2C9 [71]. The mode of inhibition is via ligation to the heme iron of CYP2C9, although which nitrogen atom from sulphaphenazole is involved in this ligation is still a matter of debate. Sulphaphenazole is a very commonly used in vitro diagnostic inhibitor for CYP2C9 activity, but it has been less frequently used in vivo for this purpose. The azole antifungal fluconazole also inhibits CYP2C9, and a series of elegant studies has demonstrated the relationship between in vitro  $K_i$  values and the in vivo effect on warfarin clearance [72–74].

There are several other drug classes that have been shown to be inhibitors of CYP2C9. One example is the HMG-CoA reductase inhibitors, which inhibit CYP2C9 in vitro [75]. These compounds are generally lipophilic carboxylic acids and hence might be expected to interact with the CYP2C9-active site. In fact, many of these compounds are relatively weak inhibitors of the enzyme, with the exception of fluvastatin. Racemic fluvastatin was a potent inhibitor of CYP2C9 activity ( $K_i < 1 \mu\text{M}$ ) with the (+)-enantiomer being fivefold more potent than the (–)-enantiomer [75]. This inhibition was also observed in vivo when diclofenac and fluvastatin were coadministered. In this case there was an increase



in diclofenac  $C_{max}$ , a reduction in oral clearance, and a decrease in the 4'-hydroxydiclofenac/diclofenac urinary ratio [76].

## D. Substrates

There are a number of CYP2C9 substrates; however, the use of some of these agents is complicated by their narrow therapeutic margin, e.g., warfarin. This makes this enzyme an important target for drug–drug interactions, but also somewhat less straightforward to investigate clinically. Other than warfarin, there are a substantial number of studies using phenytoin and tolbutamide.

### 1. Phenytoin

Phenytoin is an anticonvulsant that has been shown to be preferentially hydroxylated in the *pro*-(*S*) ring by CYP2C9 [77], which accounts for approximately 80% of its clearance in man [78]. The use of phenytoin is complicated by virtue of its nonlinear kinetics, long half-life, and narrow therapeutic margin. However, it has been used to confirm the *in vitro* finding that phenytoin and tolbutamide are metabolized by the same P450 enzyme [79].

### 2. Tolbutamide

Tolbutamide is metabolized by hydroxylation of the methyl tolyl group in man [80], forming hydroxytolbutamide. Hydroxytolbutamide is further metabolized to carboxytolbutamide [80,81]. However, it is the initial hydroxylation that is rate limiting for elimination, accounting for approximately 85% of the clearance in man. This elimination pattern has enabled urinary ratios to be used to assess tolbutamide interactions, and this gave a good correlation with total clearance upon coadministration with sulphaphenazole [82].

## VIII. CYP2C19

### A. Selectivity

Substrates for this enzyme include (*R*)-mephobarbital, moclobemide, proguanil, diazepam, omeprazole, and imipramine, which do not show obvious structural or physicochemical similarities. Some inferences can be made when the differences between the CYP2C9 substrate phenytoin and the CYP2C19 substrate (*S*)-mephenytoin are considered. Phenytoin is *para*-hydroxylated on the *pro*-(*S*) phenyl ring by CYP2C9, and the (*S*)-enantiomer of mephenytoin is *para*-hydroxylated by CYP2C19. While (*S*)-mephenytoin is structurally similar to phenytoin, the *N*-methyl function in mephenytoin makes donation of a hydrogen bond impossible, which may be why mephenytoin is not a substrate for CYP2C9. CYP2C19

can bind compounds that are weakly basic like diazepam ( $pK_a = 3.4$ ), strongly basic like imipramine ( $pK_a = 9.5$ ), or acidic compounds such as (*R*)-warfarin ( $pK_a = 5.0$ ). One possibility is that CYP2C19 binds substrates via hydrogen bonds, but in a combination of a hydrogen bond donor and acceptor mechanisms.

## B. Polymorphism

The frequency of the CYP2C19 polymorphism shows marked interracial differences, with an occurrence of approximately 3% in Caucasians and between 18 and 23% in Orientals [83]. CYP2C19 poor metabolizers (PMs) lack any functional CYP2C19 activity [84]. The mechanism of this polymorphism has been ascribed largely to two defects in the CYP2C19 gene: A G<sup>681</sup>-to-A mutation in exon 5, resulting in an aberrant splice site, which accounts for between 75 and 85% of PMs in Caucasian and Japanese populations, and a G<sup>636</sup>-to-A mutation in exon 4, which accounts for the remaining PMs in the Japanese population [85]. Further alleles, particularly those accounting for Caucasian PMs, have been identified, with nomenclature reaching CYP2C19\*6 and requiring the use of the subdivision of previously assigned alleles, e.g., CYP2C19\*2a and CYP2C19\*2b [86,87].

## C. Inhibition

There are relatively few clinically relevant inhibitors of CYP2C19, the most significant being the SSRIs. In an in vitro study only citalopram appeared to be a weak inhibitor ( $K_i > 50 \mu\text{M}$ ), with the remaining compounds all having  $K_i$  values of less than  $10 \mu\text{M}$  [88]. A corresponding study indicated that fluoxetine and fluvoxamine were able to inhibit CYP2C19 in vivo [89], although neither compound is selective, since they have marked effects on CYP2D6 and CYP1A2.

## D. Substrates

The metabolic activity of CYP2C19 has most frequently been probed, both in vivo and in vitro, using (*S*)-mephenytoin hydroxylation or mephenytoin S/R ratios. However, other substrates for this enzyme, including diazepam and imipramine, have been identified that have the potential to be used as probes [90,91]. However, the most widely used identified CYP2C19 substrate is omeprazole [92].

### 1. Mephenytoin

Racemic mephenytoin is stereoselectively metabolized in man, with the (*S*)-enantiomer being rapidly hydroxylated in the 4'-position by CYP2C19 and the (*R*)-

enantiomer being slowly metabolized. The (*S*)-mephenytoin phenotype (genotypically conferred or by administration of an inhibitor) is determined following an oral dose by measuring the ratio of (*S*)-mephenytoin to (*R*)-mephenytoin in the 0–8-hour urine [93].

## 2. Imipramine

Imipramine is metabolized mainly by *N*-demethylation and 2-hydroxylation in man. The *N*-demethylation pathway has been shown, *in vitro*, to be mediated by CYP2C19 at low imipramine concentrations [91]. *In vivo* the partial clearance of imipramine, via *N*-demethylation, was shown to be significantly reduced in poor metabolizers of (*S*)-mephenytoin [94]. In addition, a much larger study showed that the S/R ratio for mephenytoin correlated with the *N*-demethylation of imipramine [95].

## 3. Omeprazole

Omeprazole has been shown, *in vitro*, to be metabolized to a number of products, one of which, the 5-hydroxy metabolite, appears to be formed at least in part by CYP2C19 [92]. These *in vitro* metabolism studies correlate with *in vivo* studies that showed that the oral clearance of omeprazole, and the formation of the 5-hydroxy metabolite in three ethnic groups was directly related to CYP2C19 phenotype status [96].

# IX. CYP2D6

## A. Selectivity

The overwhelming majority of CYP2D6 substrates contain a basic nitrogen atom ( $\text{pK}_a > 8$ ), which is ionized at physiological pH. It is the ionic interaction between this protonated nitrogen atom and an aspartic acid residue that governs the binding. All the models of CYP2D6 show essentially the same characteristics, in which there is a 5–7-angstrom distance between this basic nitrogen atom and the site of metabolism. The relative strength of this ionic interaction means that the affinity for substrates can be high and that this P450 enzyme tends to have many examples of low- $K_m$  and  $-K_i$  interactions. Although most of the substrates for CYP2D6 are basic, there are still marked differences in binding affinity. Once the ionic interaction is formed, any difference in binding affinity could be attributed to other  $\pi$ – $\pi$  or hydrophobic interactions. In addition, for very potent CYP2D6 inhibitors, such as ajmalicine, there is a hydrogen acceptor site, in addition to the ion-pair and hydrophobic/lipophilic interaction, which increases the inhibitory potency.

## B. Polymorphism

CYP2D6 was perhaps the first and best characterized of the polymorphic P450 enzymes. The poor metabolism (PM) phenotype is characterized clinically by a marked deficiency in the metabolism of certain compounds, which can result in drug toxicity or reduced efficacy. The prevalence of the PM phenotype shows marked ethnic differences, with a mean value of approximately 7% in Caucasian populations [97] but 1% or less in Orientals [98]. With the latest additions, nearly 70 different CYP2D6 alleles have been identified [99], and the currently applied genotyping methodologies are typically 90% predictive of phenotype [100].

## C. Inhibition

CYP2D6 is inhibited by very low concentrations of quinidine. Although not metabolized by CYP2D6, quinidine conforms closely to the structural requirements of the enzyme [101]; but based on template models, the quinoline nitrogen occupies the position most likely for oxidative attack. Although quinidine is one of the most potent inhibitors of CYP2D6, the most studied class of inhibitory drugs are the SSRIs.

Several studies have been carried out using different substrate probes to determine the inhibitory potency of various members of this class against CYP2D6 [102–105]. The potential implications of CYP2D6 (and other P450 enzymes) inhibition by this class of drugs has been exhaustingly reviewed [106–116] and is not considered further here.

Not all CYP2D6 inhibitors have a basic nitrogen atom. The HIV-I protease inhibitor ritonavir has a weakly basic center but has a relatively strong interaction with CYP2D6 [117]. However, the molecule does have a number of hydrogen bonding groups, which, if there are complementary hydrogen bonding sites in the CYP2D6-active site, may explain the inhibitory potency.

## D. Substrates

There is a wide choice of drugs that are substrates for CYP2D6, but sparteine, debrisoquine, desipramine, dextromethorphan, and metoprolol have been used most frequently, both *in vitro* and *in vivo*. One advantage for *in vivo* drug–drug interaction studies is that most of the substrates were identified in the clinic rather than by the use of a battery of *in vitro* methods.

### 1. Debrisoquine

It was the identification of a group of subjects unable to metabolize debrisoquine [118,119], resulting in a potentially life-threatening drop in blood pressure, which led to the identification of the CYP2D6 polymorphism [120]. Debrisoquine is

metabolized specifically by CYP2D6 [121] to produce 4-hydroxydebrisoquine. Following an oral dose, the metabolite is excreted in the urine along with unchanged drug, and it is this ratio that can determine the CYP2D6 phenotype or the extent of drug interaction. With compromised CYP2D6, debrisoquine is excreted largely unchanged, resulting in a high ratio.

## 2. Dextromethorphan

Dextromethorphan is well tolerated, with few clinically relevant side effects, and it is a readily accessible drug in a large number of countries, making it ideal for drug–drug interaction studies. The major route of metabolism, *O*-demethylation to dextrophan, has been shown, both in vitro and in vivo, to be mediated by CYP2D6 [122]. Dextromethorphan metabolic ratios have been used primarily to identify CYP2D6 PMs, where a metabolic ratio of greater than 0.3 would be indicative of the PM phenotype [123].

## 3. Metoprolol

Metoprolol is a beta-blocker that has been proposed as a pharmacokinetic alternative to debrisoquine in countries where it is difficult to use debrisoquine. Metoprolol is metabolized to desmethylmetoprolol and  $\alpha$ -hydroxymetoprolol by CYP2D6 [124]. The  $\alpha$ -hydroxymetoprolol metabolite has been shown to be bimodally distributed and to correlate with the debrisoquine oxidation phenotype [125]. Again, metoprolol has been used primarily to distinguish between CYP2D6 extensive metabolizers (EMs) and PMs. However, in African populations, the metoprolol metabolic ratio failed to predict the poor metabolizers of debrisoquine [126]. These studies would suggest that in some ethnic groups metoprolol may not be a suitable probe.

## X. CYP3A4

### A. Selectivity

CYP3A4 appears to metabolize lipophilic drugs in positions largely dictated by the ease of hydrogen abstraction in the case of carbon hydroxylation, or electron abstraction in the case of *N*-dealkylation reactions. There are very many drugs that are predominantly eliminated by CYP3A4 and many others where CYP3A4 is a secondary mechanism. The binding of substrates to CYP3A4 seems to be due essentially to lipophilic forces. Generally such binding, if based solely on hydrophilic interactions, is relatively weak and without specific interactions, which allows motion of the substrate in the active site. Thus, a single substrate may be able to adopt more than one orientation in the active site, and there can

be several products of the reaction. Moreover, there is considerable evidence for allosteric behavior, due possibly to the simultaneous binding of two or more substrate molecules to the CYP3A4-active site [127–131]. Such binding can lead to atypical enzyme kinetics and inconsistent drug–drug interactions and is almost diagnostic of CYP3A4 involvement, although other P450 enzymes may, more rarely, be able to exhibit such properties [130,131]. Alternatively, the CYP3A4-active site may undergo substrate-dependent conformational changes [132–134], or there may be an alteration in the pool of active enzyme [135]. Whatever the case, it is not surprising that there is no useful template model for CYP3A4 substrates.

Protein homology models for CYP3A4 have been produced using the soluble bacterial enzymes CYP101 and CYP102. These models suggest the active site pocket to be large and open and made up predominantly of hydrophobic and some neutral residues, together with a small number of polar sidechains. The large number of aromatic side residues allows for the possibility of  $\pi$ – $\pi$  interactions with aromatic substrates. In addition the presence of polar residues suggests the possibility of hydrogen bonds between substrates and the active site.

## B. Induction

CYP3A4 activity can vary considerably between individuals. CYP3A4 can be modulated by dietary factors and hormones as well as pharmaceutical agents, and significant genetic polymorphisms have been identified in the 5' regulatory region [136], which may contribute to this variability. In addition to the upstream response elements, a human orphan nuclear receptor, termed the pregnane X receptor (PXR), has been shown to be involved in the inductive mechanism [137].

It is interesting that most of the pharmaceutical inducers of CYP3A4, in man, either accumulate significantly upon multiple dosing, are given at doses of hundreds of milligrams, or both, e.g., phenobarbital, felbamate, rifampin, phenytoin, carbamazepine, and troglitazone. Therefore the total body burden or liver levels are likely to be high, suggesting that no marketed drugs are highly potent ligands for PXR. With the availability of high-throughput screens [138] and the drive in the pharmaceutical industry for highly potent and selective compounds, resulting in lower doses, new clinically relevant CYP3A4 inducers may become rare.

Meanwhile the currently marketed CYP3A4 inducers can profoundly affect the pharmacokinetics of coadministered CYP3A4 substrates, e.g., rifampin on midazolam [139] or triazolam [140]. Clearly the most frequent outcome is a loss of efficacy, which is perhaps less serious than inhibition interactions, although the consequences of coadministering rifampin with the oral contraceptive pill can lead to contraceptive failure [141–143].

### C. Inhibition

Ketoconazole is a potent, somewhat selective inhibitor of CYP3A4 and is often used *in vitro* and *in vivo* as a diagnostic inhibitor. The drug is basic, partially ionized at physiological pH, and highly lipophilic and is also a substrate for the enzyme, being metabolized in the imidazole ring, the site of its ligation to the heme [144]. This high-energy interaction results in a high potency of enzyme inhibition, with  $K_i$  values typically substantially less than 1  $\mu\text{M}$ . Not surprisingly, oral ketoconazole is contraindicated with many CYP3A4 substrates and can cause life-threatening drug–drug interactions [38]. Other azole antifungals (e.g., itraconazole) also have CYP3A4 inhibitory effects through similar mechanisms, and the drug–drug interactions of these molecules have been extensively reviewed [145,146].

Mechanism-based inhibitors or suicide substrates seem to be particularly prevalent with CYP3A4. Such compounds are substrates for the enzyme, but metabolism is believed to form reactive products that deactivate the enzyme. Several macrolide antibiotics, generally involving a tertiary amine function, are able to inhibit CYP3A4 in this manner [147,148]. Erythromycin is one of the most widely used examples of this type of interaction, although there are other commonly prescribed agents that inactivate CYP3A4 [149–151], a more thorough investigation of this phenomenon might explain a number of interactions that are not readily explained by the conventional *in vitro* data.

Due to the large number of drug molecules metabolized by CYP3A4, potent inhibition, by whatever mechanism, can have a detrimental effect on a compound's marketability. This is exemplified by mibefradil, which was withdrawn from the market during its first year of sales due to its extensive CYP3A4 drug interactions [152–156].

### D. Substrates

There is an enormous choice of CYP3A4 substrates with a wide variety of clinical indications and structural features. Some of these substrates are not ideal targets for investigations of drug–drug interactions, due to potential safety concerns upon inhibition, e.g., terfenadine, or efficacy issues upon induction, e.g., the oral contraceptive pill. Additionally there are increasing concerns about the predictivity of one substrate to another, due to the emerging understanding of the apparent allosteric behavior of CYP3A4. However, the major structural types of CYP3A4 substrates can perhaps be covered by large-molecular-weight molecules derived from natural products, e.g., the macrolides, the benzodiazepines, and the dihydropyridine calcium channel blockers.

### 1. Erythromycin

Although the rate of elimination of this CYP3A substrate can be determined from plasma pharmacokinetics, the erythromycin breath test (ERMBT) is less invasive [157]. The ERMBT involves the intravenous administration of a trace amount of  $^{14}\text{C}$ -*N*-methyl erythromycin. At specified time points, the subject breathes through a one-way valve, into a  $\text{CO}_2$ -trapping solution, and the  $^{14}\text{C}$ - $\text{CO}_2$  is subsequently measured by liquid scintillation counting. This test shows fairly good correlations with trough cyclosporin concentrations [158] and clearly demonstrates the inductive effect of rifampin [157]. However, there was a poor correlation between the ERMBT and the clearance of the CYP3A4 substrate alfentanil [159,160]. The test is still somewhat invasive (intravenous administration) and doesn't assess presystemic effects; a further limitation is the need to administer radioactivity.

### 2. Midazolam

A dose of midazolam in man is eliminated renally (98%), with 1-hydroxymidazolam (the product of CYP3A metabolism) accounting for half of the urinary elimination [161]. Midazolam clearance provides a good estimate of CYP3A activity, and this has been found to correlate with the concentration of CYP3A immunoreactive protein in liver biopsies [162], cyclosporin clearance [163], and the ERMBT [161]. Midazolam clearance has been increased in patients receiving phenytoin [164] and reduced in patients receiving erythromycin [165] or itraconazole [166], showing wide utility for drug–drug interaction studies.

### 3. Nifedipine

Nifedipine was one of the first CYP3A4 substrates to be identified [167,168] and has been the subject of an enormous number of drug–drug interaction studies both *in vitro* and *in vivo*. Pharmacokinetic studies with nifedipine clearly identify inhibitors, such as itraconazole [169] and grapefruit juice [170], and inducers, such as the barbiturates [171] and rifampin [172].

## XI. CONCLUSIONS

There is clear evidence of the extensive involvement of the cytochrome P450 enzyme system in the elimination of pharmaceutical agents and an enormous body of information demonstrating the modulation of activity, via inhibition or induction, with polypharmacy. This fully justifies the intensive research in this area and the pharmaceutical industry focus on such drug–drug interac-



tions. This is reinforced in this volume, in which cytochrome P450 is either the major or the most significant subject of over half the chapters, and inhibition and induction, *in vitro* and *in vivo*, are further exemplified and discussed.

## REFERENCES

1. DR Nelson, T Kamataki, DJ Waxman, FP Guengerich, RW Estabrook, R Feyereisen, FJ Gonzalez, MJ Coon, IC Gunsalus, O Gotoh. The P450 superfamily: update on new sequences, gene mapping, accession numbers, early trivial names of enzymes, and nomenclature. *DNA Cell Biol* 12:1–51, 1993.
2. O Gotoh. Divergent structures of *Caenorhabditis elegans* cytochrome P450 genes suggest the frequent loss and gain of introns during the evolution of nematodes. *Mol Biol Evol* 15:1447–1459, 1998.
3. Y Yamamoto, M Ishizuka, A Takada, S Fujita. Cloning, tissue distribution, and functional expression of two novel rabbit cytochrome P450 isozymes, CYP2D23 and CYP2D24. *J Biochem* 124:503–508, 1998.
4. QY Zhang, G Raner, XX Ding, D Dunbar, MJ Coon, LS Kaminsky. Characterization of the cytochrome P450 CYP2J4—expression in rat small intestine and role in retinoic acid biotransformation from retinal. *Arch Biochem Biophys* 353:257–264, 1998.
5. T Hiroi, S Imaoka, T Chow, Y Funae. Tissue distributions of CYP2D1, 2D2, 2D3 and 2D4 mRNA in rats detected by RT-PCR. *Biochim Biophys Acta* 1380:305–312, 1998.
6. DC Zeldin, J Foley, SM Goldsworthy, ME Cook, JE Boyle, JX Ma, CR Moomaw, KB Tomer, C Steenbergen, S Wu. CYP2J subfamily cytochrome P450s in the gastrointestinal tract—expression, localization, and potential functional significance. *Mol Pharm* 51:931–943, 1997.
7. QY Zhang, J Wikoff, D Dunbar, M Fasco, L Kaminsky. Regulation of cytochrome P4501A1 expression in rat small intestine. *Drug Met Disp* 25:21–26, 1997.
8. T Prueksaritanont, LM Gorham, JH Hochman, LO Tran, KP Vyas. Comparative studies of drug-metabolizing enzymes in dog, monkey, and human small intestines, and in Caco-2 cells. *Drug Met Disp* 24:634–642, 1996.
9. LS Kaminsky, MJ Fasco. Small intestinal cytochromes P450. *Crit Rev Tox* 21:407–422, 1991.
10. PB Watkins, SA Wrighton, EG Schuetz, DT Molowa, PS Guzelian. Identification of glucocorticoid-inducible cytochromes P-450 in intestinal mucosa of rats and man. *J Clin Invest* 90:1871–1878, 1987.
11. JC Kolars, P Schmiedlin-Ren, JD Schuetz, C Fang, PB Watkins. Identification of rifampin-inducible P450III A4 (CYP3A4) in human small bowel enterocytes. *J Clin Invest* 90:1871–1878, 1992.
12. JC Kolars, KS Lown, P Schmiedlinren, M Ghosh, C Fang, SA Wrighton, RM Merion, PB Watkins. CYP3A gene-expression in human gut epithelium. *Pharmacogenetics* 4:247–259, 1994.

13. KS Lown, JC Kolars, KE Thummel, JL Barnett, KL Kunze, SA Wrighton, PB Watkins. Interpatient heterogeneity in expression of CYP3A4 and CYP3A5 in small bowel. Lack of prediction by the erythromycin breath test. *Drug Met Disp* 22:947–955, 1994.
14. CY Wu, LZ Benet, MF Hebert, SK Gupta, M Rowland, DY Gomez, VJ Wachter. Differentiation of absorption, first-pass gut and hepatic metabolism in man: studies with cyclosporine. *Clin Pharmacol Ther* 58:492–497, 1995.
15. LZ Benet, CY Wu, MF Hebert, VJ Wachter. Intestinal drug-metabolism and anti-transport processes—a potential paradigm shift in oral-drug delivery. *J Cont Rel* 39:139–143, 1996.
16. Y Hashimoto, H Sasa, M Shimomura, K Inui. Effects of intestinal and hepatic metabolism on the bioavailability of tacrolimus in rats. *Pharmaceut Res* 15:1609–1613, 1998.
17. A Lampen, U Christians, FP Guengerich, PB Watkins, JC Kolars, A Bader, AK Gonschior, H Dralle, I Hackbarth, KF Sewing. Metabolism of the immunosuppressant tacrolimus in the small intestine: cytochrome P450, drug interactions, and interindividual variability. *Drug Met Disp* 23:1315–1324, 1995.
18. A Lampen, Y Zhang, I Hackbarth, LZ Benet, KF Sewing, U Christians. Metabolism and transport of the macrolide immunosuppressant sirolimus in the small intestine. *J Pharm Exp Ther* 285:1104–1112, 1998.
19. MF Paine, DD Shen, KL Kunze, JD Perkins, CL Marsh, JP McVicar, DM Barr, BS Gillies, KE Thummel. First-pass metabolism of midazolam by the human intestine. *Clin Pharm Ther* 60:14–24, 1996.
20. VJ Wachter, JA Silverman, Y Zhang, LZ Benet. Role of P-glycoprotein and cytochrome P450 3A in limiting oral absorption of peptides and peptidomimetics. *J Pharmaceut Sci* 87:1322–1330, 1998.
21. SX Wang, TA Sutfin, C Baarnhielm, CG Regardh. Contribution of the intestine to the first-pass metabolism of felodipine in the rat. *J Pharm Exp Ther* 250:632–636, 1989.
22. KS Lown, DG Bailey, RJ Fontana, SK Janardan, CH Adair, LA Fortlage, MB Brown, W Guo, PB Watkins. Grapefruit juice increases felodipine oral availability in humans by decreasing intestinal CYP3A protein expression. *J Clin Invest* 99: 2545–2553, 1997.
23. PH Marathe, DE Salazar, DS Greene, J Brennan, UA Shukla, RH Barbhaiya. Absorption and presystemic metabolism of nefazodone administered at different regions in the gastrointestinal tract of humans. *Pharmaceut Res* 12:1716–1721, 1995.
24. B Ameer, RA Weintraub. Drug interactions with grapefruit juice. *Clin Pharmacokin* 33:103–121, 1997.
25. U Fuhr. Drug interactions with grapefruit juice. Extent, probable mechanism and clinical relevance. *Drug Safety* 18:251–272, 1998.
26. EB Feldman. How grapefruit juice potentiates drug bioavailability. *Nutr Rev* 55: 398–400, 1997.
27. DJ Edwards, ME Fitzsimmons, EG Schuetz, K Yasuda, MP Ducharme, LH Warbasse, PM Woster, JD Schuetz, PB Watkins. 6',7'-Dihydroxybergamottin in grapefruit juice and Seville orange juice: effects on cyclosporine disposition, enterocyte CYP3A4, and P-glycoprotein. *Clin Pharm Ther* 65:237–244, 1999.

28. DG Bailey, JH Kreeft, C Munoz, DJ Freeman, JR Bend. Grapefruit juice–felodipine interaction: effect of naringin and 6',7'-dihydroxybergamottin in humans. *Clin Pharm Ther* 64:248–256, 1998.
29. K He, KR Iyer, RN Hayes, MW Sinz, TF Woolf, PF Hollenberg. Inactivation of cytochrome P450 3A4 by bergamottin, a component of grapefruit juice. *Chem Res Tox* 11:252–259, 1998.
30. P Schmiedlin-Ren, DJ Edwards, ME Fitzsimmons, K He, KS Lown, PM Woster, A Rahman, KE Thummel, JM Fisher, PF Hollenberg, PB Watkins. Mechanisms of enhanced oral availability of CYP3A4 substrates by grapefruit constituents. Decreased enterocyte CYP3A4 concentration and mechanism-based inactivation by furanocoumarins. *Drug Met Disp* 25:1228–1233, 1997.
31. K Fukuda, T Ohta, Y Oshima, N Ohashi, M Yoshikawa, Y Yamazoe. Specific CYP3A4 inhibitors in grapefruit juice: furocoumarin dimers as components of drug interaction. *Pharmacogenetics* 7:391–396, 1997.
32. K Fukuda, T Ohta, Y Yamazoe. Grapefruit component interacting with rat and human P450 CYP3A: possible involvement of non-flavonoid components in drug interaction. *Biol Pharmaceut Bull* 20:560–564, 1997.
33. AD Rodrigues. Integrated P450 reaction phenotyping: Attempting to bridge the gap between cDNA-expressed cytochromes P450 and native human liver microsomes. *Biochem Pharm* 57:465–480, 1999.
34. MY Morgan, R Reshef, RR Shah, NS Oates, RL Smith, S Sherlock. Impaired oxidation of debrisoquine in patients with perhexiline liver injury. *Gut* 25:1057–1064, 1984.
35. RR Shah, NS Oates, JR Idle, RL Smith, JD Lockhart. Impaired oxidation of debrisoquine in patients with perhexiline neuropathy. *Br Med J Clin Res* 284:295–299, 1982.
36. NS Oates, RR Shah, JR Idle, RL Smith. Phenformin-induced lacticacidosis associated with impaired debrisoquine hydroxylation. *Lancet* 1(8224):837–838, 1981.
37. JR Idle, NS Oates, RR Shah, RL Smith. Protecting poor metabolizers, a group at high risk of adverse drug reactions. *Lancet* 1(8338):1388, 1983.
38. PK Honig, DC Wortham, K Zamani, DP Conner, JC Mullin, LR Cantilena. Terfenadine–ketoconazole interaction. Pharmacokinetic and electrocardiographic consequences. *JAMA* 269:1513–1518, 1993.
39. PK Honig, RL Woosley, K Zamani, DP Conner, LR Cantilena. Changes in the pharmacokinetics and electrocardiographic pharmacodynamics of terfenadine with concomitant administration of erythromycin. *Clin Pharm Ther* 52:231–238, 1992.
40. CA Lipinski, F Lombardo, BW Dominy, PJ Feeney. Experimental and computational approaches to estimate solubility and permeability in drug discovery and development settings. *Adv Drug Del Rev* 23:3–25, 1997.
41. A Catteau, YC Bechet, N Poisson, PR Betchel, CA Bonaiti-Pellie. Population and family study of CYP1A2 using caffeine urinary metabolites. *Eur J Clin Pharm* 47:423–430, 1995.
42. ME Campbell, SP Speilberg, W Kalow. A urinary metabolite ratio that reflects systemic caffeine clearance. *Clin Pharm Ther* 42:157–165, 1987.
43. R Curi-Pedrosa, M Daujat, L Pichard, JC Ourlin, P Clair, L Gervot, P Lesca, J Domergue, H Joyeux, G Fourtanier, P Maurel. Omeprazole and lansoprazole are

- mixed inducers of CYP1A and CYP3A in human hepatocytes in primary culture. *J Pharm Exp Ther* 269:384–392, 1994.
44. KL Rost, I Roots. Accelerated caffeine metabolism after omeprazole treatment as indicated by urinary metabolite ratios: coincidence with plasma clearance and breath test. *Clin Pharm Ther* 55:402–411, 1994.
  45. T Andersson. Omeprazole drug interaction studies. *Clin Pharmacokin* 21:195–212, 1991.
  46. S Xiaodong, G Gatti, A Bartoli, G Cipolla, G Crema, E Perucca. Omeprazole does not enhance the metabolism of phenacetin, a marker of CYP1A2 activity, in healthy volunteers. *Ther Drug Mon* 16:248–250, 1994.
  47. SE Clarke, AD Ayrton, RJ Chenery. Characterisation of the inhibition of 1A2 by furafylline. *Xenobiotica* 24:517–526, 1994.
  48. KL Kunze, WF Trager. Isoform selective mechanism based inhibition of human cytochrome P4501A2 by furafylline. *Chem Res Tox* 6:649–656, 1993.
  49. U Fuhr, EM Anders, G Mahr, F Sorgel, AH Staib. Inhibitory potency of quinolone antibacterial agents against cytochrome P450IA2 activity in vivo and in vitro. *Antimicrob Agents Chemother* 36:942–948, 1992.
  50. M Kinzig-Schippers, U Fuhr, U Zaigler, J Dammeyer, G Rusing, A Labedzki, J Bulitta, F Sorgel. Interaction of pefloxacin and enoxacin with the human cytochrome P450 enzyme CYP1A2. *Clin Pharm Ther* 65:262–274, 1999.
  51. P Nikolaidis, SE Walker, N Dombros, A Tourkantonis, TW Paton, DG Oreopoulos. Single-dose pefloxacin pharmacokinetics and metabolism in patients undergoing continuous ambulatory peritoneal dialysis (CAPD). *Peritoneal Dialysis Int* 11:59–63, 1991.
  52. RA Robson, EJ Begg, HC Atkinson, DA Saunders, CM Frampton. Comparative effects of ciprofloxacin and lomefloxacin on the oxidative metabolism of theophylline. *Br J Clin Pharm* 29:491–493, 1990.
  53. K Brosen, E Skjelbo, BB Rasmussen, HE Poulsen, S Loft. Fluvoxamine is a potent inhibitor of cytochrome P4501A2. *Biochem Pharm* 45:1211–1214, 1993.
  54. LL Von Moltke, DJ Greenblatt, SX Duan, J Schmider, L Kudchadker, SM Fogelman, JS Harmatz, RI Shader. Phenacetin *O*-deethylation by human liver microsomes in vitro: inhibition by chemical probes, SSRI antidepressants, nefazodone and venlafaxine. *Psychopharmacology* 128:398–407, 1996.
  55. BB Rasmussen, TL Nielsen, K Brosen. Fluvoxamine is a potent inhibitor of the metabolism of caffeine in vitro. *Pharm Tox* 83:240–245, 1998.
  56. U Jeppesen, S Loft, HE Poulsen, K Brosen. A fluvoxamine–caffeine interaction study. *Pharmacogenetics* 6:213–222, 1996.
  57. A Lelo, JO Miners, RA Robson, DJ Birkett. Quantitative assessment of caffeine partial clearances in man. *Br J Clin Pharm* 22:183–186, 1986.
  58. MA Butler, M Iwasaki, FP Guengerich, FF Kadlubar. Human cytochrome P450PA (P450IA2), the phenacetin *O*-deethylase, is primarily responsible for the hepatic 3-demethylation of caffeine and *N*-oxidation of carcinogenic arylamines. *Proc Nat Acad Sci* 86:7696–7700, 1989.
  59. L Bertilsson, JA Carrillo, ML Dahl, A Llerena, C Alm, U Bondesson, L Lindstrom, I Rodriguez-De-La-Rubia, S Ramos, J Benitez. Clozapine disposition covaries with CYP1A2 activity determined by a caffeine test. *Br J Clin Pharm* 38:471–473, 1994.

60. M Pirmohamed, D Williams, S Madden, E Templeton, BK Park. Metabolism and bioactivation of clozapine by human liver in vitro. *J Pharm Exp Ther* 272:984–990, 1995.
61. BC Jones, G Hawksworth, VA Horne, A Newlands, J Morsman, MS Tute, DA Smith. Putative active site model for CYP2C9 (tolbutamide hydroxylase). *Drug Met Disp* 24:1–7, 1996.
62. RL Haining, JP Jones, KR Henne, MB Fisher, DR Koop, WF Trager, AE Rettie. Enzymatic determinants of the substrate specificity of CYP2C9: role of B'-C loop residues in providing the pi-stacking anchor site for warfarin binding. *Biochem* 38: 3285–3292, 1999.
63. RL Haining, AP Hunter, ME Veronese, WF Trager, AE Rettie. Allelic variants of human cytochrome-P450 2C9—baculovirus-mediated expression, purification, structural characterization, substrate stereoselectivity, and prochiral selectivity of the wild-type and I359I mutant forms. *Arch Biochem Biophys* 333:447–458, 1996.
64. H Yamazaki, K Inoue, K Chiba, N Ozawa, T Kawai, Y Suzuki, JA Goldstein, FP Guengerich, T Shimada. Comparative studies on the catalytic roles of cytochrome P450 2C9 and its Cys- and Leu-variants in the oxidation of warfarin, flurbiprofen, and diclofenac by human liver microsomes. *Biochem Pharm* 56:243–251, 1998.
65. LS Kaminsky. Warfarin as a probe of cytochromes P-450 function. *Drug Met Rev* 20:479–487, 1989.
66. Z Zhang, MJ Fasco, Z Huang, FP Guengerich, LS Kaminsky. Human cytochromes P4501A1 and P4501A2—R-warfarin metabolism as a probe. *Drug Met Disp* 23: 1339–1345, 1995.
67. LC Wienkers, CJ Wurden, E Storch, KL Kunze, AE Rettie, WF Trager. Formation of (R)-8-hydroxywarfarin in human liver-microsomes—a new metabolic marker for the (S)-mephenytoin hydroxylase, P4502C19. *Drug Met Disp* 24:610–614, 1996.
68. AE Rettie, KR Korzekwa, KL Kunze, RF Lawrence, AC Eddy, T Aoyama, HV Gelboin, FJ Gonzalez, WF Trager. Hydroxylation of warfarin by human cDNA-expressed cytochrome P-450: a role for P-4502C9 in the etiology of (S)-warfarin–drug interactions. *Chem Res Tox* 5:54–59, 1992.
69. RL Haining, DJ Steward, KR Henne, GA Davis, AE Rettie. Correlation of the cytochrome-P450 2C9 Leu(359) defect with warfarin sensitivity. *Faseb J* 11:130–139, 1997.
70. DJ Steward, RL Haining, KR Henne, AG Davis, TH Rushmore, WF Trager, AE Rettie. Genetic association between sensitivity to warfarin and expression of CYP2C9\*3. *Pharmacogenetics* 7:361–367, 1997.
71. SJ Baldwin, JC Bloomer, GJ Smith, AD Ayrton, SE Clarke, RJ Chenery. Ketoconazole and sulfaphenazole as the respective selective inhibitors of P4503A and 2C9. *Xenobiotica* 25:261–270, 1995.
72. KL Kunze, LC Wienkers, KE Thummel, WF Trager. Warfarin-fluconazole.1. Inhibition of the human cytochrome-P450-dependent metabolism of warfarin by fluconazole—in vitro studies. *Drug Met Disp* 24:414–421, 1996.
73. DJ Black, KL Kunze, LC Wienkers, BE Gidal, TL Seaton, ND McDonnell, JS Evans, E Bauwens, WF Trager. Warfarin-fluconazole. 2. A metabolically based drug-interaction—in vivo studies. *Drug Met Disp* 24:422–428, 1996.

74. KL Kunze, WF Trager. Warfarin-fluconazole. 3. A rational approach to management of a metabolically based drug-interaction. *Drug Met Disp* 24:429–435, 1996.
75. C Transon, T Leemann, P Dayer. In vitro comparative inhibition profiles of major human drug-metabolizing cytochrome-P450 isozymes (CYP2C9, CYP2D6 and CYP3A4) by HMG-CoA reductase inhibitors. *Eur J Clin Pharm* 50:209–215, 1996.
76. C Transon, T Leemann, N Vogt, P Dayer. In vivo inhibition profile of cytochrome P450(tb) (CYP2C9) by (+/–)-fluvastatin. *Clin Pharm Ther* 58:412–417, 1995.
77. CJ Doecke, ME Veronese, SM Pond, JO Miners, DJ Birkett, LN Sansom, ME McManus. Relationship between phenytoin and tolbutamide hydroxylations in human liver microsomes. *Br J Clin Pharm* 31:124–130, 1991.
78. RG Dickerson, WD Hooper, M Patterson, MJ Eadie, B Maguire. Extent of urinary excretion of *p*-hydroxyphenytoin in healthy subjects given phenytoin. *Ther Drug Mon* 7:283–289, 1985.
79. W Tassaneeyakul, ME Veronese, DJ Birkett, CJ Doecke, ME McManus, LN Sansom, JO Miners. Coregulation of phenytoin and tolbutamide metabolism in humans. *Br J Clin Pharm* 34:494–498, 1992.
80. RC Thomas, GJ Ikeda. The metabolic fate of tolbutamide in man and rat. *J Med Chem* 9:507–510, 1966.
81. E Nelson, I O'Reilly. Kinetics of carboxytolbutamide excretion following tolbutamide and carboxytolbutamide administration. *J Pharm Exp Ther* 132:103–109, 1961.
82. ME Veronese, JO Miners, D Randles, D Gregov, DJ Birkett. Validation of the tolbutamide metabolic ratio for population screening with the use of sulfaphenazole to produce model phenotypic poor metabolizers. *Clin Pharm Ther* 47:403–411, 1990.
83. L Bertilsson. Geographical/interracial differences in polymorphic drug oxidation. *Clin Pharmacokin Con* 29:192–209, 1995.
84. JA Goldstein, MB Falletto, M Romkes-Sparks, T Sullivan, S Kitareewan, JL Raucy, JM Lasker, BI Ghanayem. Evidence that CYP2C19 is the major (*S*)-mephenytoin 4'-hydroxylase in humans. *Biochemistry* 33:1743–1752, 1994.
85. JA Goldstein, SMF De Morais. Biochemistry and molecular biology of the human CYP2C subfamily. *Pharmacogenetics* 4:285–299, 1994.
86. GC Ibeanu, J Blaisdell, BI Ghanayem, C Beyeler, S Benhamou, C Bouchardy, GR Wilkinson, P Dayer, AK Daly, JA Goldstein. An additional defective allele, CYP2C19\*5, contributes to the *S*-mephenytoin poor metabolizer phenotype in caucasians. *Pharmacogenetics* 8:129–135, 1998.
87. GC Ibeanu, JA Goldstein, U Meyer, S Benhamou, C Bouchardy, P Dayer, BI Ghanayem, J Blaisdell. Identification of new human CYP2C19 alleles (CYP2C19\*6 and CYP2C19\*2b) in a Caucasian poor metabolizer of mephenytoin. *J Pharm Exp Ther* 286:1490–1495, 1998.
88. K Kobayashi, T Yamamoto, K Chiba, M Tani, T Ishizaki, Y Kuroiwa. The effects of selective serotonin reuptake inhibitors and their metabolites on *S*-mephenytoin 4'-hydroxylase activity in human liver-microsomes. *Br J Clin Pharm* 40:481–485, 1995.
89. U Jeppesen, LF Gram, K Vistisen, S Loft, HE Poulsen, K Broesen. Dose-dependent inhibition of CYP1A2, CYP2C19 and CYP2D6 by citalopram, fluoxetine, fluvoxamine and paroxetine. *Eur J Clin Pharm* 51:73–78, 1996.

90. T Andersson, JO Miners, ME Veronese, DJ Birkett. Diazepam metabolism by human liver microsomes is mediated by both (*S*)-mephenytoin hydroxylase and CYP3A isoforms. *Br J Clin Pharm* 38:131–137, 1994.
91. K Chiba, A Saitoh, E Koyama, M Tani, M Hayashi, T Ishizaki. The role of (*S*)-mephenytoin 4'-hydroxylase in imipramine metabolism by human liver microsomes: a two-enzyme analysis of *N*-demethylation and 2-hydroxylation. *Br J Clin Pharm* 37:237–242, 1994.
92. T Andersson, JO Miners, ME Veronese, W Tassaneeyakul, UA Meyer, DJ Birkett. Identification of human liver cytochrome-P450 isoforms mediating omeprazole metabolism. *Br J Clin Pharm* 36:521–530, 1993.
93. G Tybring, L Bertilsson. A methodological investigation on the estimation of the (*S*)-mephenytoin hydroxylation phenotype using the urinary *S/R* ratio. *Pharmacogenetics* 2:241–243, 1992.
94. E Skjelbo, K Brosen, J Hallas, LF Gram. The mephenytoin oxidation polymorphism is partially responsible for the *N*-demethylation of imipramine. *Clin Pharm Ther* 49, 18–23, 1991.
95. E Skjelbo, LF Gram, K Brosen. The *N*-demethylation of imipramine correlates with the oxidation of (*S*)-mephenytoin (*S/R* ratio). A population study. *Br J Clin Pharm* 35:331–334, 1993.
96. JD Balian, N Sukhova, JW Harris, J Hewett, L Pickle, JA Goldstein, RL Woolsley, DA Flockhart. The hydroxylation of omeprazole correlates with *S*-mephenytoin metabolism: a population study. *Clin Pharm Ther* 57:662–9, 1995.
97. G Alvan, B Bechtel, L Iselius, U Gundert-Remy. Hydroxylation polymorphism of debrisoquine and mephenytoin in European populations. *Eur J Clin Pharm* 39, 533–537, 1990.
98. DR Sohn, SG Shin, CW Park, M Kusaka, K Chiba, T Ishizaki. Metoprolol oxidation polymorphism in a Korean population: comparison with native Japanese and Chinese populations. *Br J Clin Pharm* 32:504–507, 1991.
99. SL Wang, MD Lai, JD Huang. G169R mutation diminishes the metabolic activity of CYP2D6 in Chinese. *Drug Met Disp* 27:385–388, 1999.
100. JS Leathart, SJ London, A Steward, JD Adams, JR Idle, AK Daly. CYP2D6 phenotype–genotype relationships in African-Americans and Caucasians in Los Angeles. *Pharmacogenetics* 8:529–541, 1998.
101. DA Smith, BC Jones. Speculations on the substrate structure–activity relationship (SSAR) of cytochrome P450 enzymes. *Biochem Pharm* 44:2089–2098, 1992.
102. HK Crewe, MS Lennard, GT Tucker, FR Woods, RE Haddock. The effect of selective serotonin re-uptake inhibitors on cytochrome P4502D6 (CYP2D6) activity in human liver microsomes. *Br J Clin Pharm* 34:262–265, 1992.
103. E Skjelbo, K Brosen. Inhibitors of imipramine metabolism by human liver microsomes. *Br J Clin Pharm* 34:256–261, 1992.
104. LL Von Moltke, DJ Greenblatt, MM Cotreaubibbo, SX Duan, JS Harmatz, RI Shader. Inhibition of desipramine hydroxylation in vitro by serotonin-reuptake-inhibitor antidepressants, and by quinidine and ketoconazole—a model system to predict drug-interactions in vivo. *J Pharm Exp Ther* 268:1278–1283, 1994.
105. FM Belpaire, P Wijnant, A Temmerman, BB Rasmussen, K Brosen. The oxidative

- metabolism of metoprolol in human liver microsomes—inhibition by the selective serotonin reuptake inhibitors. *Eur J Clin Pharm* 54:261–264, 1998.
106. HG Zapotoczky, CA Simhandl. Interactions of antidepressants. *Wiener Klinische Wochenschrift* 107:293–300, 1995.
  107. K Brosen. Are pharmacokinetic drug-interactions with the SSRIs an issue. *Int Clin Psychopharm* 11:23–27, 1996.
  108. ML Catterson, SH Preskorn. Pharmacokinetics of selective serotonin reuptake inhibitors—clinical relevance. *Pharm Tox* 78:203–208, 1996.
  109. L Ereshefsky, C Riesenman, YWF Lam. Serotonin selective reuptake inhibitor drug-interactions and the cytochrome-P450 system. *J Clin Psychiatry* 57:17–25, 1996.
  110. RM Lane. Pharmacokinetic drug-interaction potential of selective serotonin reuptake inhibitors. *Int Clin Psychopharm* 11:31–61, 1996.
  111. R Lane, D Baldwin. Selective serotonin reuptake inhibitor-induced serotonin syndrome. *J Clin Psychopharm* 17:208–221, 1997.
  112. F Lopezmunoz, C Alamo, E Cuenca, G Rubio. Effect of antidepressant drugs on cytochrome-P-450 isoenzymes and its clinical relevance—differential profile. *Actas Luso-Espanolas De Neurologia Psiquiatria Y Ciencias Afines* 25:397–409, 1997.
  113. PB Mitchell. Drug interactions of clinical significance with selective serotonin reuptake inhibitors. *Drug Safety* 17:390–406, 1997.
  114. BA Sproule, CA Naranjo, KE Bremner, PC Hassan. Selective serotonin reuptake inhibitors and CNS drug interactions—a critical review of the evidence. *Clin Pharmacokin* 33:454–471, 1997.
  115. GB Baker, J Fang, S Sinha, RT Coutts. Metabolic drug interactions with selective serotonin reuptake inhibitor (SSRI) antidepressants. *Neurosci Biobehav Rev* 22:325–333, 1998.
  116. S Caccia. Metabolism of the newer antidepressants—an overview of the pharmacological and pharmacokinetic implications. *Clin Pharmacokin* 34:281–302, 1998.
  117. LL Von Moltke, DJ Greenblatt, JM Grassi, BW Granda, SX Duan, SM Fogelman, JP Daily, JS Harmatz, RI Shader. Protease inhibitors as inhibitors of human cytochromes P450—high-risk associated with ritonavir. *J Clin Pharm* 38:106–111, 1998.
  118. A Mahgoub, JR Idle, LG Dring, R Lancaster, RL Smith. Polymorphic hydroxylation of debrisoquine in man. *Lancet* 2:584–586, 1977.
  119. M Angelo, LG Dring, R Lancaster, A Latham, RL Smith. A correlation between the response to debrisoquine and the amount of unchanged drug excreted in the urine. *Br J Pharm* 55:264P, 1975.
  120. RL Smith. Introduction. *Xenobiotica* 16:361–365, 1986.
  121. J Gut, T Catin, P Dayer, T Kronbach, U Zanger, UA Meyer. Debrisoquine/sparteine type polymorphism of drug oxidation. *J Biol Chem* 261:11734–11743, 1986.
  122. P Dayer, T Leemann, R Striberni. Dextromethorphan *O*-demethylation in liver microsomes as a prototype reaction to monitor cytochrome P-450 db1 activity. *Clin Pharm Ther* 45:34–40, 1989.
  123. B Schmid, J Bircher, R Preisig, A Kupfer. Polymorphic dextromethorphan metabolism: co-segregation of oxidative *O*-demethylation with debrisoquine hydroxylation. *Clin Pharm Ther* 38:618–624, 1985.



124. SV Otton, HK Crewe, MS Lennard, GT Tucker, HF Woods. Use of quinidine inhibition to define the role of the sparteine/debrisoquine cytochrome P450 in metoprolol oxidation by human liver microsomes. *J Pharm Exp Ther* 247:242–247, 1988.
125. JC McGourty, JH Silas, MS Lennard, GT Tucker, HF Woods. Metoprolol metabolism and debrisoquine oxidation polymorphism—population and family studies. *Br J Clin Pharm* 20:555–566, 1985.
126. MS Lennard, AO Iyuan, PR Jackson, GT Tucker, HF Woods. Evidence for a dissociation in the control of sparteine, debrisoquine and metoprolol metabolism in Nigerians. *Pharmacogenetics* 2:89–92, 1992.
127. GE Schwab, JL Raucy, EF Johnson. Modulation of rabbit and human hepatic cytochrome P-450-catalyzed steroid hydroxylations by alpha-naphthoflavone. *Mol Pharm* 33:493–499, 1988.
128. M Shou, J Grogan, JA Mancewicz, KW Krausz, FJ Gonzalez, HV Gelboin, KR Korzekwa. Activation of CYP3A4—evidence for the simultaneous binding of 2 substrates in a cytochrome-P450 active site. *Biochemistry* 33:6450–6455, 1994.
129. YF Ueng, T Kuwabara, YJ Chun, FP Guengerich. Cooperativity in oxidations catalyzed by cytochrome-P450 3A4. *Biochemistry* 36:370–381, 1997.
130. KR Korzekwa, N Krishnamachary, M Shou, A Ogai, RA Parise, AE Rettie, FJ Gonzalez, TS Tracy. Evaluation of atypical cytochrome-P450 kinetics with 2-substrate models—evidence that multiple substrates can simultaneously bind to cytochrome-P450 active sites. *Biochemistry* 37:4137–4147, 1998.
131. S Ekins, BJ Ring, SN Binkley, SD Hall, SA Wrighton. Autoactivation and activation of the cytochrome P450s. *Int J Clin Pharm Ther* 36:642–651, 1998.
132. AP Koley, JTM Buters, RC Robinson, A Markowitz, FK Friedman. CO Binding-kinetics of human cytochrome-P450 3A4—specific interaction of substrates with kinetically distinguishable conformers. *J Biol Chem* 270:5014–5018, 1995.
133. AP Koley, RC Robinson, FK Friedman. Cytochrome-P450 conformation and substrate interactions as probed by CO binding-kinetics. *Biochimie* 78:706–713, 1996.
134. AP Koley, RC Robinson, A Markowitz, FK Friedman. Drug–drug interactions—effect of quinidine on nifedipine binding to human cytochrome-P450 3A4. *Biochem Pharm* 53:455–460, 1997.
135. AP Koley, JTM Buters, RC Robinson, A Markowitz, FK Friedman. Differential mechanisms of cytochrome-P450 inhibition and activation by alpha-naphthoflavone. *J Biol Chem* 272:3149–3152, 1997.
136. TR Rebbeck, JM Jaffe, AH Walker, AJ Wein, SB Malkowicz. Modification of clinical presentation of prostate tumors by a novel genetic variant in CYP3A4. *J Nat Cancer Inst* 90:1225–1229, 1998.
137. JM Lehmann, DD McKee, MA Watson, TM Willson, JT Moore, SA Kliewer. The human orphan nuclear receptor PXR is activated by compounds that regulate CYP3A4 gene expression and cause drug interactions. *J Clin Invest* 102:1016–1023, 1998.
138. MS Ogg, TJ Gray, GG Gibson. Development of an in vitro reporter gene assay to assess xenobiotic induction of the human CYP3A4 gene. *Eur J Drug Met Pharmacokin* 22:311–313, 1997.
139. JT Backman, KT Olkkola, PJ Neuvonen. Rifampin drastically reduces plasma concentrations and effects of oral midazolam. *Clin Pharm Ther* 59:7–13, 1996.

140. K Villikka, KT Kivisto, JT Backman, KT Olkkola, PJ Neuvonen. Triazolam is ineffective in patients taking rifampin. *Clin Pharm Ther* 61:8–14, 1997.
141. J Domnisse. Oral contraceptive failure due to drug interaction. *S African Med J* 50:796, 1976.
142. DJ Back, AM Breckenridge, FE Crawford, JM Hall, M MacIver, ML Orme, PH Rowe, E Smith, MJ Watts. The effect of rifampicin on the pharmacokinetics of ethynylestradiol in women. *Contraception* 21:135–43, 1980.
143. A Fazio. Oral contraceptive drug interactions: important considerations. *Southern Med J* 84:997–1002, 1991.
144. TK Daneshmend, DW Warnock. Clinical pharmacokinetics of ketoconazole. *Clin Pharmacokin* 14:13–34, 1988.
145. BM Lomaestro, MA Piatek. Update on drug interactions with azole antifungal agents. *Annals Pharmacotherapy* 32:915–928, 1998.
146. E Albengres, H Le Louet, JP Tillement. Systemic antifungal agents. Drug interactions of clinical significance. *Drug Safety* 18:83–97, 1998.
147. TM Ludden. Pharmacokinetic interactions of the macrolide antibiotics. *Clin Pharmacokin* 10:63–79, 1985.
148. M Nahata. Drug interactions with azithromycin and the macrolides: an overview. *J Antimicrob Chemother* 37:133–142, 1996.
149. K He, TF Woolf, PF Hollenberg. Mechanism-based inactivation of cytochrome P-450-3A4 by mifepristone (RU486). *J Pharm Exp Ther* 288:791–797, 1999.
150. RL Voorman, SM Maio, NA Payne, Z Zhao, KA Koeplinger, X Wang. Microsomal metabolism of delavirdine: evidence for mechanism-based inactivation of human cytochrome P450 3A. *J Pharm Exp Ther* 287:381–388, 1998.
151. T Koudriakova, E Iatsimirskaia, I Utkin, E Gangl, P Vouros, E Storozhuk, D Orza, J Marinina, N Gerber. Metabolism of the human immunodeficiency virus protease inhibitors indinavir and ritonavir by human intestinal microsomes and expressed cytochrome P4503A4/3A5: mechanism-based inactivation of cytochrome P4503A by ritonavir. *Drug Met Disp* 26:552–61, 1998.
152. S Krahenbuhl, A Menafoglio, E Giostra, A Gallino. Serious interaction between mibefradil and tacrolimus. *Transplantation* 66:1113–1115, 1998.
153. M Spoendlin, J Peters, H Welker, A Bock, G Thiel. Pharmacokinetic interaction between oral cyclosporin and mibefradil in stabilized post-renal-transplant patients. *Nephrol Dial Transpl* 13:1787–1791, 1998.
154. D Schmassmann-Suhijar, R Bullingham, R Gasser, J Schmutz, WE Haefeli. Rhabdomyolysis due to interaction of simvastatin with mibefradil. *Lancet* 351:1929–1930, 1998.
155. ME Mullins, BZ Horowitz, DH Linden, GW Smith, RL Norton, J Stump. Life-threatening interaction of mibefradil and beta-blockers with dihydropyridine calcium channel blockers. *JAMA* 280:157–158, 1998.
156. Roche, FDA announce new drug-interaction warnings for mibefradil. *Am J Health-Sys Pharmac* 55:210, 1998.
157. PB Watkins, SA Murray, LG Winkelman, DM Heuman, SA Wrighton, PS Guzelian. Erythromycin breath test as an assay of glucocorticoid-inducible liver cytochromes P450. *J Clin Invest* 83:688–697, 1989.
158. PB Watkins, TA Hamilton, TM Annesley, CN Ellis, JC Kolars, JJ Voorhees. The

- erythromycin breath test as a predictor of cyclosporin A blood levels. *Clin Pharm Ther* 48:120–129, 1990.
159. CH Yun, M Wood, AJJ Wood, FP Guengerich. Identification of the pharmacogenetic determinants of alfentanil metabolism: cytochrome P-4503A4. An explanation of the variable elimination clearance. *Anaesthesiology* 77:467–474, 1992.
  160. Y Krivoruk, MT Kinirons, AJJ Wood, M Wood. Metabolism of cytochrome P4503A substrates in vivo administered by the same route: lack of correlation between alfentanil clearance and erythromycin breath test. *Clin Pharm Ther* 56:608–614, 1994.
  161. KS Lown, KE Thummel, PE Benedict, DD Shen, DK Turgeon, S Berent, PB Watkins. The erythromycin breath test predicts the clearance of midazolam. *Clin Pharm Ther* 57:16–24, 1995.
  162. KE Thummel, DD Shen, RL Carithers, P Hartwell, TD Podoll, WF Trager, KL Kunze. Prediction of in vivo midazolam clearance from hepatic CYP3A content and midazolam 1-hydroxylation activity in liver transplant patients. *ISSX Proc* 4: 235, 1993.
  163. KE Thummel, DD Shen, TD Podoll, KL Kunze, WF Trager, PS Hartwell, VA Raisys, CL Marsh, JP McVicar, DM Barr, JD Perkins, RL Carithers. Use of midazolam as a human cytochrome P450 3A probe: 1. in vitro–in vivo correlations in liver transplant patients. *J Pharm Exp Ther* 271:549–556, 1994.
  164. KE Thummel, DD Shen, CE Bacchi, JP McVicar, CL Marsh, JD Perkins, RL Carithers. Induction of human hepatic P4503A3/4 by phenytoin. *Hepatology* 16: 160A, 1992.
  165. KT Olkkola, K Aranko, H Luurila, A Hiller, L Saarnivaara, JJ Himberg, PJ Neuvonen. A potentially hazardous interaction between erythromycin and midazolam. *Clin Pharm Ther* 53:298–305, 1993.
  166. J Ahonen, KT Olkkola, PJ Neuvonen. Effects of itraconazole and terbinafine on the pharmacokinetics and pharmacodynamics of midazolam in healthy volunteers. *Br J Clin Pharm* 40:270–272, 1995.
  167. FP Guengerich, MV Martin, PH Beaune, P Kremers, T Wolff, DJ Waxman. Characterization of rat and human liver microsomal cytochrome P-450 forms involved in nifedipine oxidation, a prototype for genetic polymorphism in oxidative drug metabolism. *J Biol Chem* 261:5051–5060, 1986.
  168. RW Bork, T Muto, PH Beaune, PK Srivastava, RS Lloyd, FP Guengerich. Characterization of mRNA species related to human liver cytochrome P-450 nifedipine oxidase and the regulation of catalytic activity. *J Biol Chem* 264:910–919, 1989.
  169. SA Taylor, AK Gupta, SE Walker, NH Shear. Peripheral edema due to nifedipine–itraconazole interaction: a case report. *Arch Dermatol* 132:350, 1996.
  170. DG Bailey, JD Spence, C Munoz, JM Arnold. Interaction of citrus juices with felodipine and nifedipine. *Lancet* 337:268–269, 1991.
  171. JH Schellens, JH van der Wart, M Brugman, DD Breimer. Influence of enzyme induction and inhibition on the oxidation of nifedipine, sparteine, mephenytoin and antipyrine in humans as assessed by a ‘‘cocktail’’ study design. *J Pharm Exp Ther* 249:638–645, 1989.
  172. N Holtbecker, MF Fromm, HK Kroemer, EE Ohnhaus, H Heidemann. The nifedipine–rifampin interaction. Evidence for induction of gut wall metabolism. *Drug Met Disp* 24:1121–1123, 1996.

# 4

## Review of Human UDP-Glucuronosyltransferases and Their Role in Drug–Drug Interactions

**Rory P. Remmel**

*University of Minnesota, Minneapolis, Minnesota*

### I. INTRODUCTION

The UDP-glycosyltransferases (EC 2.4.21.17) are a group of enzymes that catalyze the transfer of sugars (glucuronic acid, glucose, and xylose) to a variety of acceptor molecules (aglycones). The sugars may be attached at aromatic and aliphatic alcohols, carboxylic acids, thiols, primary, secondary, tertiary, and aromatic amino groups, and acidic carbon atoms. In vivo, the most common reaction occurs by transfer of a glucuronic acid moiety from uridine-diphosphate glucuronic acid (UDP-GA) to an acceptor molecule. This process is termed either *glucuronosylation* or *glucuronidation*. When the enzymes catalyze this reaction, they are also referred to as UDP-glucuronosyltransferases (UGTs). The structure and function of these enzymes have been the subject of several reviews [1–3]. This chapter will review the role of these enzymes in drug–drug interactions that occur in humans.

Glucuronidation is an important step in the elimination of many important endogenous substances from the body, including bilirubin, bile acids, steroid hormones, thyroid hormones, and biogenic amines such as serotonin. Many of these compounds are also substrates for sulfonyltransferases [2]. The interplay between glucuronidation and sulfonylation (sulfation) of steroid and thyroid hormones and the corresponding hydrolytic enzymes,  $\beta$ -glucuronidase and sulfatase, may play an important role in development and regulation. The UGTs are expressed in many tissues, including liver, kidney, intestine, colon, adrenals, spleen, lung,

skin, testes, ovaries, olfactory glands, and brain. Interactions between drugs at the enzymatic level are most likely to occur during the absorption phase (first-pass metabolism) in the intestine and liver or systemically in the liver, kidney, or intestine.

Given the broad array of substrates and the variety of molecular diversity, it is not surprising that there are multiple UGTs. The UGTs have been divided into two families (UGT1 and UGT2) based on their sequence homology. All members of a family have at least 50% sequence identity to one another [4]. The UGT1A family is encoded by a gene complex located on chromosome 2. The large UGT1A gene complex contains 12 variable-region exons that are spliced onto four constant-region exons that encode amino acids on the C-terminus of the enzyme. Consequently, all enzymes in the UGT1 family have an identical C-terminus, but the N-terminus is highly variable, with a sequence homology of only 24–49% [1]. The UGT1A enzymes are named in order of the proximity to the four constant-region exons, i.e., UGT1A1 through UGT1A12 [5]. This arrangement appears to be conserved across all mammalian species studied to date. In humans, all of the gene products are functional except for the pseudogenes, UGT1A2, UGT1A11, and UGT1A12. The UGT1A gene complex is located on chromosome 2 at 2q.37.

The UGT2A subfamily represents olfactory UGTs and will not be further discussed in this review. Human UGT2A1 has recently been cloned by Burchell and coworkers [6]. The UGT2B subfamily consists of a series of complete UGT genes located at 4q12 on chromosome 4. Like the UGT1A enzymes, the C-terminus is highly conserved among all members of the UGT2B genes, with greater variation at the N-terminal half of the protein. Several human UGT2B enzymes have been cloned, expressed, and characterized for a variety of substrates.

Interactions involving glucuronidation have been described in a number of clinical and *in vitro* studies. Apparent decreases in the amount of glucuronide excreted in urine or bile or apparent increases in the AUC have been shown in several studies. These apparent effects on glucuronidation could occur via several different mechanisms, as follows:

1. Direct inhibition of the enzyme by competition with the substrate or with UDPGA
2. Induction of individual UGT enzymes
3. Depletion of the UDPGA cofactor
4. Inhibition of the transport of UDPGA into the endoplasmic reticulum
5. Inhibition of the renal excretion of the glucuronide, with subsequent reconversion to the parent aglycone by beta-glucuronidases (futile cycling)
6. Alteration of endoplasmic reticulum transport, sinusoidal membrane transport, or bile canalicular membrane transport of glucuronides

Major interactions involving individual UGT enzymes will be discussed in detail along with a brief discussion of the function of each enzyme. A table of substrates, inducers, and inhibitors for the human UGT enzymes is provided in the appendix to this chapter.

## II. UGT1A1

UGT1A1 is an important enzyme that is primarily responsible for the glucuronidation of bilirubin in the liver. Cloned, expressed UGT1A1 is a glycosyltransferase that is also capable of catalyzing the formation of bilirubin xylosides and glucosides in the presence of UDP-xylose and UDP-glucose, respectively [7]. In vivo, glucuronidation predominates, but bilirubin xylosides and glucosides have been identified in bile. Drugs that are substrates for UGT1A1 may result in high unconjugated bilirubin concentrations, especially in patients with Gilbert's syndrome. Gilbert's syndrome is an asymptomatic unconjugated hyperbilirubinemia that is most often caused by a genetic polymorphism in the promoter region of the UGT1A1 gene [8]. Decreased expression of UGT1A1 in Gilbert's patients is a result of the presence of a (TA)<sub>7</sub>TAA allele (UGT1A1\*28) in place of the more prevalent (TA)<sub>6</sub>TAA allele [9,10]. Persons who are homozygous for the (TA)<sub>7</sub>TAA allele express approximately 30–50% less UGT1A1 enzyme in liver. Larger screening studies have demonstrated that this regulatory defect occurs in approximately 2–19% of various populations [8]. Older studies in persons with mild hyperbilirubinemia (meeting the criteria for Gilbert's syndrome, but not genetically determined) demonstrated a decreased clearance rate for drugs that are glucuronidated. Clearance of acetaminophen (also catalyzed by other UGT enzymes, especially UGT1A6) was decreased by 30% in six subjects with Gilbert's syndrome [11]. In contrast, a small study by Ullrich et al. demonstrated no difference in the glucuronide/acetaminophen ratio in urine of 11 persons with Gilbert's syndrome [12]. Lorazepam clearance (thought to be catalyzed by UGT2B7), was 20–30% lower in persons with Gilbert's syndrome [13]. Lamotrigine is a triazine anticonvulsant that is metabolized primarily to a quaternary 2-*N*-glucuronide in humans [14]. Oral clearance of lamotrigine was decreased by 32% in persons with Gilbert's syndrome [15]. Lamotrigine is glucuronidated by cloned, expressed UGT1A3 and UGT1A4 but not by UGT1A1. In general these studies were conducted in a small number of Gilbert's patients. There is likely to be a distinct heterogeneity in persons exhibiting mild hyperbilirubinemia that could include patients with Crigler–Najjar Type II who have mutations in the coding region of UGT1A1, persons who are homozygous for the (TA)<sub>7</sub>TAA allele, or patients who have a higher-than-normal breakdown of heme. Since the genetic defect in many Gilbert's patients has only recently been identified, it will be of interest to conduct pharmacokinetic studies in persons who have been

genotyped and are also taking drugs that are known to be UGT1A1 substrates, such as buprenorphine, ethinylestradiol, and SN-38 (an irinotecan metabolite).

Ando et al. completed a small pharmacokinetic study with irinotecan, a water-soluble analog of the antitumor alkaloid camptothecin [16]. Irinotecan is metabolized by carboxylesterase to an active metabolite SN-38, which is cleared primarily by glucuronidation [17]. A single patient that was homozygous for the (TA)<sub>7</sub>TAA allele displayed a much higher SN-38/SN-38 glucuronide metabolic ratio in plasma. Another case report described two additional patients with Gilbert's syndrome who had grade 4 neutropenia while taking irinotecan [18]. Iyer et al. recently compared the liver microsomal glucuronidation rate for SN-38 and bilirubin in 44 patients genotyped for the (TA)<sub>n</sub>TAA allele [19]. A significant correlation between bilirubin glucuronidation and SN-38 glucuronidation was observed ( $r = 0.9$ ) and microsomes from patients homozygous for the (TA)<sub>7</sub>TAA allele ( $n = 4$ ) displayed significantly lower SN-38 glucuronidation rates than microsomes from heterozygotes or homozygotes for the (TA)<sub>6</sub>TAA allele. SN-38 glucuronidation is also catalyzed by cloned, expressed human UGT1A1 but not by UGT1A4 or UGT2B7 [20].

Drug interactions involving UGT1A1 have not been reported for irinotecan. Based on in vitro data, a drug interaction between ethinylestradiol and irinotecan may be hypothesized, since ethinylestradiol glucuronidation also highly correlates with bilirubin glucuronidation in human liver microsomes [21]. Ethinylestradiol has been shown to elevate bilirubin concentrations in plasma, and the 17 $\beta$ -glucuronide is a cholestatic agent. Interactions involving glucuronidation of ethinylestradiol are unlikely, since this steroid is also metabolized by sulfation and CYP3A4. The opioid analog buprenorphine also displays a high intrinsic clearance relative to other opioids in incubations conducted with cloned, expressed UGT1A1, and studies conducted in microsomes from a Crigler–Najjar Type I patient show a 75% reduction in glucuronidation rate [22].

### III. UGT1A3 AND UGT1A4

UGT1A3 and UGT1A4 appear to be important enzymes involved in the catalysis of many tertiary amine drugs to form quaternary ammonium glucuronides [23,24]. UGT1A3, UGT1A4, and UGT1A5 share a high nucleic acid sequence homology of 93–94% in the first variable-region exon and probably have arisen by gene duplication [25,26]. The first exon of this group of enzymes appears to have diverged considerably from UGT1A1 (58% similar to UGT1A4), UGT1A6, and UGT1A7-1A10. UGT1A4 is expressed in human liver, although the level of expression of UGT1A4 mRNA has been reported to be low compared to UGT1A1 mRNA [27]. UGT1A4 has low activity versus bilirubin compared to UGT1A1 and has been sometimes designated as a minor bilirubin form [28].

Both UGT1A3 and UGT1A4 possess similar activity toward a variety of tertiary amines, such as imipramine, cyproheptadine, amitriptyline, triprolidine, and diphenhydramine, with high apparent  $K_m$  values ranging from 0.2 to 2 mM [23,24]. In general, UGT1A4 displays better catalytic activity versus these substrates. There are some significant differences in catalytic activity between UGT1A3 and UGT1A4. UGT1A3 catalyzes the glucuronidation of buprenorphine, norbuprenorphine (low  $K_m$  values), morphine (3-position only), and naltrexone [24]. The enzyme has activity toward a variety of nonsteroidal anti-inflammatory drugs (NSAIDs), simple aromatic phenols (scopoletin, 4-methylumbelliferone, 4-nitrophenol), and flavonoids such as naringenin and quercetin. In contrast, UGT1A4 is inactive toward NSAIDs, but steroidal sapogenins such as hecogenin and diosgenin appear to be excellent substrates, with low  $K_m$  values (7–20  $\mu$ M) [23]. UGT1A4 also has good activity for progestins, especially 5 $\alpha$ -pregnane-3 $\alpha$ ,20 $\alpha$ -diol and androgens such as 5- $\alpha$ -androstane-3 $\alpha$ ,17 $\beta$ -diol. UGT1A3 mRNA is expressed in liver, biliary epithelium, colon, and gastric tissue [26]. UGT1A4 mRNA is expressed in liver, intestine, and colon but not in gastric tissue. UGT1A5 mRNA is not expressed in any of these tissues.

Assuming that UGT1A3 and UGT1A4 are primarily responsible for the glucuronidation of tertiary amine antihistamines and antidepressants, significant drug interactions involving glucuronidation with these substrates have not been reported. This is not unexpected, because typically less than 25% of the dose is excreted as a direct quaternary ammonium glucuronide [29]. The formation of quaternary ammonium glucuronides appears to be highly species specific, with the highest activity in humans and monkeys. Rats are generally incapable of forming quaternary ammonium glucuronides [30]. Lamotrigine, a novel triazine anticonvulsant, is extensively glucuronidated at the 2-position on the triazine ring in humans (90% of the dose excreted in human urine) [31]. It is not significantly glucuronidated in rats and dogs, but 60% of the dose excreted in guinea pig urine is the 2-*N*-glucuronide [14]. Several significant interactions have been reported for lamotrigine in humans. Lamotrigine glucuronidation is induced in patients taking phenobarbital, phenytoin, or carbamazepine, resulting in a twofold decrease in apparent half-life, from 25 hours to approximately 12 hours [32,33]. In contrast, valproic acid inhibits lamotrigine glucuronidation, resulting in a 23 fold increase in half-life [33,34]. The mechanism of this interaction is not clear, although valproic acid is a weak substrate for UGT1A3 [24]. In contrast, lamotrigine had a small but significant effect (25% increase) on the apparent oral clearance (Cl) of valproic acid [35]. This increase could be due to induction of UGTs responsible for valproic acid glucuronidation, since chronic treatment with lamotrigine results in autoinduction [36]. The interaction between acetaminophen and lamotrigine has also been studied. Surprisingly, acetaminophen decreased the AUC by approximately 20% after multiple oral doses in eight human volunteers [37]. Lamotrigine clearance was reported to be 32% lower in seven volun-



teers with Gilbert's syndrome, a regulatory polymorphism in the UGT1A1 gene [15]. However, lamotrigine does not appear to be a substrate for UGT1A1 [38].

#### IV. UGT1A6

UGT1A6 is the most important enzyme for the conjugation of planar phenols. It displays high activity for a variety of aromatic alcohols, including 1-naphthol, 4-nitrophenol, 4-methylumbelliferone, and acetaminophen; however, these planar phenols are also substrates for most other UGT enzymes. Immunoinhibition studies with an antibody raised against a 120-amino-acid N-terminal region UGT1A6 peptide fused to *Staphylococcus aureus* protein A, revealed that approximately 50% of the 1-naphthol glucuronidation activity in human liver microsomes could be inhibited [39]. The first exon sequence of UGT1A6 is divergent from other UGT1A sequences, being most similar to UGT1A9, with only a 54% homology [26]. UGT1A6 may play an important role in the detoxification of carcinogenic aromatic hydrocarbons, since it displays high activity versus hydroxylated metabolites of benzo(a)pyrene and chrysene. The very low toxicity threshold for acetaminophen in cats is apparently due to a genetic defect in UGT1A6, a defect present in all felines [40]. In rats, this enzyme is inducible by polycyclic aromatic hydrocarbons. UGT1A6 is also inducible in human hepatocytes by  $\beta$ -naphthoflavone and in some, but not all, hepatocytes by rifampin [41]. Acetaminophen glucuronidation appears to be increased in smokers, perhaps due to induction of UGT1A6 [42].

#### V. UGT1A7, UGT1A8, AND UGT1A9

There is a 93–94% sequence homology in the first exon of UGT1A7, UGT1A8, UGT1A9, and UGT1A10; however, these enzymes show great variation in their level of tissue expression [26]. This group of UGT1A enzymes is highly divergent from UGT1A3–UGT1A5, with approximately 50% identity in the first exon to UGT1A7–UGT1A10. UGT1A9 is expressed in human hepatic tissues, whereas UGT1A7, UGT1A8, and UGT1A9 are expressed extrahepatically in man [26]. UGT1A7 mRNA is expressed in human esophageal and gastric tissue and sheep intestine [43,44]. In contrast, both rat and rabbit UGT1A7 are expressed in liver as well [45,46]. The rabbit enzyme (UGT1A7I) displays high activity versus a variety of small phenolic compounds, such as 4-methylumbelliferone, *p*-nitrophenol, vanillin, 4-*tert*-butylphenol, and octylgallate. In addition the rabbit enzyme is capable of catalyzing the glucuronidation of imipramine to a quaternary ammonium glucuronide, similar to UGT1A4. Rat UGT1A7 catalyzes the glucuronidation of benzo(a)pyrene phenols and is inducible by both 3-methylcholanthrene and olti-

praz [46]. Recently, Ciotti et al. demonstrated that human UGT1A7 has very high activity for the glucuronidation of 7-ethyl-10-hydroxycamptothecin (SN-38), the active metabolite of irinotecan (see Sec. II) [47]. Thus UGT1A7 may play an important role in the first-pass metabolism of this antitumor drug. The inducibility of human UGT1A7 has not yet been studied, but studies in rats with polycyclic aromatic hydrocarbon inducers suggest that this enzyme may be inducible in smokers.

UGT1A8 mRNA is expressed in human jejunum, colon, and ileum but not in liver or kidney [48]. UGT1A8 has activity versus a variety of planar and bulky phenols, coumarins, flavonoids, anthraquinones, and primary aromatic amines [48]. It also catalyzes the glucuronidation of several endogenous compounds, including dihydrotestosterone, 2- and 4-hydroxyestrone, estradiol, hyocholic acid, trans-retinoic acid, and 4-OH-retinoic acid [121]. Several drugs are also substrates, including opioids (e.g., buprenorphine, morphine, naloxone, and naltrexone), ciprofibrate, diflunisal, furosemide, mycophenolic acid, phenolphthalein, propofol, and 4-OH-tamoxifen. [48,121]. Cloned, expressed UGT1A8 has a high intrinsic clearance for the conjugation of flavonoids such as apigenin and naringenin; thus, drug–food interactions are possible with drug substrates of this enzyme, particularly if the drugs display extensive first-pass glucuronidation in the intestine.

UGT1A9 is expressed in human liver, kidney, and colon [49]. UGT1A9 is expressed in greater amounts in kidney than in liver and is the most prevalent UGT expressed in renal tissue. UGT1A9 is largely responsible for the glucuronidation of a variety of bulky phenols, such as *tert*-butylphenol, and the anesthetic agent propofol [50,51]. Propofol is a specific substrate for UGT1A9, but extrahepatic metabolism of propofol appears to be important, because propofol glucuronide is formed in substantial amounts in cirrhotic patients undergoing surgery with a trans-internal-jugular porto-systemic shunt [52] or during the anhepatic phase of liver transplantation [53]. Propofol is also glucuronidated *in vitro* by human kidney and small intestinal microsomes [52]. Propofol  $V_{\max}$  was 3–3.5 times higher in kidney microsomes compared to liver or small intestinal microsomes on a mg-microsomal protein basis. Propofol Cl is greater than liver blood flow, also suggesting that extrahepatic metabolism is important for this compound [54]. A number of pharmacodynamic interactions have been reported between propofol and benzodiazepines or opioids such as fentanyl and alfentanil. Pharmacokinetic interaction studies with fentanyl or alfentanil revealed that there was a modest decrease (20–50%) in propofol clearance [54,55]. UGT1A9 also catalyzes the glucuronidation of propranolol, valproic acid, clofibrate, and several nonsteroidal anti-inflammatory drugs, and these drugs appear to be glucuronidated at a much faster rate by UGT1A9 than by UGT2B7 on a mg-protein basis in cloned, expressed cells (assuming equivalent levels of expression) [1]. Such NSAIDs may be directly glucuronidated or oxidatively metabolized (primarily by CYP2C9). Relatively few clinical drug interactions with NSAIDs have been

reported [56], although probenecid may inhibit glucuronidation and cause modest increases in NSAID concentrations (see Sec. VIII, on probenecid). UGT1A9 is an inducible enzyme. In the rat, phenobarbital is a good general inducer of the glucuronidation of bulky phenols catalyzed by UGT1A9. UGT1A9 along with UGT1A6 were inducible by 10  $\mu$ M TCDD in Caco-2 cells, a human-derived colon carcinoma cell line [57].

## VI. UGT1A10

UGT1A10 is closely related to UGT1A7, UGT1A8, and UGT1A9. Mojarrabi and Mackenzie cloned the cDNA from human colon [58]. The enzyme was 90% homologous to UGT1A9. UGT1A10 mRNA is not expressed in human liver but is highly expressed in colon, intestine, and kidney [26]. When transfected into COS-7 cells, the enzyme was very active in the conjugation of mycophenolic acid, the major active metabolite of mycophenolate, a newly approved immunosuppressant agent used for the treatment of allograft rejection. In vitro, the enzyme was capable of catalyzing conjugation at both the phenolic hydroxyl at the 7-position and the carboxylic acid moiety to form an acyl glucuronide. The 7-*O*-glucuronide is the predominant conjugate formed in vivo and is the major excretory metabolite of mycophenolate (90% of the dose in humans). An interaction between tacrolimus (FK506) and mycophenolate has been described resulting in a marked increase in mycophenolic acid trough concentrations and AUC [59]. Zucker et al. further studied this phenomenon in vitro and demonstrated that mycophenolic acid glucuronidation activity was 100-fold higher in human kidney microsomes compared to human liver microsomes [60]. With a partially purified preparation of the kidney UGT, tacrolimus was shown to be a potent inhibitor of this mycophenolic acid glucuronidation (presumably catalyzed by UGT1A10), with a  $K_i$  of 27.3 ng/ml compared to a  $K_i = 2158$  ng/ml for cyclosporine A. Since UGT1A10 is present primarily in the extrahepatic tissues and kidney, coadministration of tacrolimus would be expected to significantly inhibit first-pass intestinal metabolism and to decrease CI/F, resulting in the observed increase in the AUC of mycophenolic acid. Other UGT1A enzymes may contribute to mycophenolic acid glucuronidation. For example, Cheng et al. recently reported that the formation of mycophenolic acid glucuronide was 1900 pmole/min/mg protein for UGT1A8 compared to 93 pmole/min/mg protein for UGT1A10 [121]. UGT1A8 mRNA is expressed in intestinal tissues but not in kidney. UGT1A10 appears to have less activity than UGT1A8 for flavonoids, alizarin, and scopoletin [121], but further studies will be needed to determine the relative expression levels of the enzymes in the gut. UGT1A10 has not been as extensively examined for other metabolic activities, but it may be an important enzyme in the extrahepatic metabolism of other drugs such as propofol.

## VII. UGT2B7

UGT2B7 is an important enzyme involved in the glucuronidation of several drug substrates, including the NSAIDs, morphine, and 3-*OH*-benzodiazepines. UGT2B7 has 82% sequence homology to UGT2B4 but has less than 50% homology to UGT1A family enzymes. Ritter et al. initially cloned and expressed UGT2B7 (H), a protein with a His at amino acid 268 [61]. This enzyme had activity toward several steroid substrates, including estriol and androsterone, with low activity for the bile acid hyodeoxycholic acid. Jin et al. cloned and expressed a polymorphic variant from the same cDNA library, UGT2B7 (Y), with a substitution of tyrosine for histidine at position 268 [62]. UGT2B7 (Y) activity expressed in COS-7 cells was more extensively characterized versus a variety of drug substrates. The enzyme catalyzed the conjugation of several NSAIDs (naproxen, ketoprofen, ibuprofen, fenoprofen, zomepirac, diflunisal, and indomethacin), valproic acid, clofibrac acid, temazepam, oxazepam, propranolol, and chloramphenicol. More recently, Tephly and coworkers demonstrated that UGT2B7 catalyzed both the 3-*O*- and 6-*O*-glucuronidation of morphine, codeine 6-*O*-glucuronidation, and the conjugation of several other opioids [63]. This group has also compared the activities of UGT2B7 (Y) and UGT2B7 (H) that were stably expressed in HK293 cells [64]. Both forms displayed similar activity for a range of compounds. Endogenous substrates for UGT2B7 include 4-*OH* estrone, hyodeoxycholic acid, estriol, androsterone, and epitestosterone but not testosterone [64,65].

Based on the substrate activity, one might expect that several drug interactions could result from competition for UGT2B7. Morphine glucuronidation has been well studied; however, relatively few clinical drug–drug interactions with morphine have been reported. In human liver microsomes, the 3-*O*-glucuronidation of morphine is biphasic, with a high-affinity  $K_m$  of 2–7  $\mu\text{M}$  and a low-affinity  $K_m$  of 700–1600  $\mu\text{M}$  [66]. UGT2B7 is the only human UGT expressed in liver that has been shown to glucuronidate morphine to morphine-6-glucuronide. Morphine-6-glucuronide is much more potent in binding to the mu receptor in the CNS than morphine (30–50-fold more potent). However, morphine-6-glucuronide has a poor ability to cross the blood–brain barrier, with a permeability coefficient in rats that was 1/57 that of morphine [67]. Morphine-6-glucuronide has similar analgesic effects to morphine when administered to rats on a mg/kg basis. Since rats are unable to make morphine-6-glucuronide, this reflects a balance of poor permeability and higher CNS potency. In humans, both morphine-3-glucuronide (lacking analgesic activity) and morphine-6-glucuronide are present in higher concentrations than morphine at steady state. Competitive inhibition with other UGT2B7 substrates may not result in a significant effect on analgesic efficiency of morphine, since morphine levels would rise while morphine-6-glucuronide levels would fall. Morphine glucuronidation is inhibited by various benzodiazepines in vitro in rats and oxazepam (20 mg/kg PO) was shown to lower the

morphine-3-glucuronide/morphine ratio in urine. In vitro, the 6-*O*-glucuronidation of codeine by human liver microsomes was inhibited by morphine, amitriptyline, diazepam, probenecid, and chloramphenicol with  $K_i$  values of 3.6, 0.13, 0.18, 1.7, and 0.27 mM, respectively.

Benzodiazepines containing a hydroxyl group at the 3-position, such as lorazepam, oxazepam, and temazepam, are glucuronidated by UGT2B7. (*S*)-oxazepam is a better substrate for glucuronidation in human liver microsomes, with a  $V_{max}/K_m$  ratio of 1.125 ml/min-mg protein versus 0.25 ml/min-mg protein for the (*R*)-isomer [68]. Inhibition studies with racemic ketoprofen in human liver microsomes revealed that racemic ketoprofen competitively inhibited (*S*)-oxazepam glucuronidation, but the inhibition of (*R*)-oxazepam was weaker, and the data did not fit the simple hyperbolic fit expected of a competitive inhibitor of a single enzyme. (*S*)-Oxazepam glucuronidation was inhibited (in order of potency) by hyodeoxycholic acid, estriol, (*S*)-naproxen, ketoprofen, ibuprofen, fenoprofen, and clofibrilic acid. Drug interaction studies with lorazepam and clofibrilic acid in humans have been reported and are summarized in Table 1.

**Table 1** Interactions Involving UGT2B7 Substrates

Precipitant drug	Object drug	Effect	Comments <sup>a</sup>
Valproate	Lorazepam	↑	20% Increase in lorazepam AUC, 31% decrease in formation Cl of lorazepam glucuronide [69]; 40% decrease in lorazepam Cl. [70]
Probenecid	Lorazepam	↑	Lorazepam Cl decreased twofold. Half-life increased from 14 hr to 33 hr. [71]
Neomycin + cholestyramine	Lorazepam		Half-life decreased 19–26%. 34% increase in free oral CL/F. Effect attributed to decreased entero-hepatic circulation. [72]
Probenecid	Clofibrilic acid	↑	Nonrenal Cl <sub>r</sub> decreased by 72%. Free clofibrilic acid C <sub>ss</sub> increased 3.6-fold. [73]
Probenecid	Zomepirac	↑	Zomepirac Cl declined by 64%. Zomepirac glucuronide Cl <sub>r</sub> decreased by 71%. Urinary excretion of zomepirac glucuronide decreased from 72% to 58%. [74]
Oral Contraceptives	Clofibrilic acid	↓	Clofibrilic acid Cl increased 48% in women receiving oral contraceptives. [75]

<sup>a</sup> Source reference numbers are in brackets.

## VIII. INTERACTIONS WITH PROBENECID

Probenecid is a uricosuric agent that is used in the treatment of gout. Probenecid inhibits the active tubular secretion of a number of organic anions, including uric acid and the glucuronides of several different drugs. Detailed studies of clinical interactions between probenecid and several drugs, including clofibrac acid, zidovudine, and several nonsteroidal anti-inflammatory drugs have demonstrated that the rate of excretion of the glucuronides into the urine is decreased, which coincides with the known effects of probenecid upon organic anion transport. Clinical interactions between probenecid and clofibrac acid [73], ketoprofen [76], indomethacin [77], carprofen [78,79], isofezolac [80], naproxen [81], zomepirac [74], and zidovudine [82] have been described. In addition to the expected effect of a decreased rate of glucuronide excretion, these studies have also revealed that the clearance of the parent aglycone is also decreased. In several cases, it has been demonstrated that probenecid affects both the nonrenal and renal clearance of the parent aglycones, suggesting that there are multiple mechanisms for the probenecid effect. The apparent decrease in clearance of the parent drugs has been attributed to three basic mechanisms: (1) inhibition of the renal clearance of the parent drug, (2) direct inhibition of the UGT enzyme responsible for the glucuronidation of the parent drugs, and (3) inhibition of the active secretion of the glucuronide and subsequent hydrolysis of the glucuronide back to the aglycone, resulting in a futile cycle. Several interactions between NSAIDs and probenecid have been reported. Inhibition of direct renal excretion may occur but probably does not significantly contribute, since the excretion of unchanged clofibrac acid and most nonsteroidal anti-inflammatory agents is negligible [76]. Consequently, alternate mechanisms have been proposed. Probenecid has been shown to inhibit the formation clearance of zomepirac glucuronide by 78% in humans, suggesting a direct effect on the UGT enzyme responsible for glucuronidation. Glucuronidation of NSAIDs is catalyzed by several UGT enzymes, including UGT1A9 and UGT2B7, although UGT1A9 may be the most important enzyme for these drugs [1]. An alternate mechanism involving hydrolysis of the glucuronide back to the parent aglycone has also been proposed. This "futile cycle" hypothesis has been well studied in a uranyl nitrate-induced renal failure model in rabbits [83].

The interaction between zidovudine and probenecid has been extensively studied *in vitro* and in several species. The interaction is complex. Probenecid inhibits the renal tubular secretion of both zidovudine and zidovudine glucuronide [82]. Probenecid also directly affects the glucuronidation step, thus decreasing the nonrenal clearance of zidovudine. For example, the nonrenal clearance of zidovudine was significantly decreased from  $10.5 \pm 2.1$  ml/min/kg to  $7.8 \pm 3.3$  ml/min/kg by probenecid in a rabbit model [84]. Probenecid

has been demonstrated to be a direct inhibitor of the glucuronidation of zidovudine in human liver microsomes [85,86]. In freshly isolated rat hepatocytes, probenecid decreased zidovudine-glucuronide by 10-fold [122]. Probenecid also appears to inhibit the efflux of zidovudine from the brain, presumably at the choroid plexus.

## IX. INTERACTIONS WITH ZIDOVUDINE

Zidovudine (3-azido-deoxythymidine, AZT) is an important nucleoside used in the treatment of AIDS. It was the first drug approved for the treatment of AIDS, and as such there are a number of in vitro and in vivo drug interaction studies conducted with this compound. Zidovudine is eliminated in humans primarily by glucuronidation; approximately 75% of the dose is excreted as the glucuronide, with the rest excreted unchanged in urine. A small portion of the drug is reduced to 3'-amino-3'-deoxythymidine, a reaction catalyzed by CYP3A4. The enzyme responsible for zidovudine glucuronidation is not known, and it does not appear to be a substrate for any of the enzymes that have been cloned and expressed. Human liver microsomes from Crigler–Najar Type I patients and Gunn rat liver microsomes do not show diminished zidovudine glucuronidation rates, suggesting that the responsible enzyme is not a member of the UGT1A family of enzymes [20,87]. In rats, zidovudine glucuronidation is inducible by phenobarbital but not by 3MC or clofibrate [88].

Several in vitro drug interaction studies have been conducted in human liver microsomes. In human liver microsomes, the  $K_m$  for zidovudine glucuronidation is approximately 2–3 mM, a concentration well above the typical therapeutic concentration of 0.5–2  $\mu$ M. Turnover of the substrate is also quite slow, which belies the relatively high clearance observed in vivo. Based on determination of  $K_i$  in *N*-octyl- $\beta$ -D-glucoside-solubilized human liver microsomes and comparison to therapeutic concentrations in plasma, Resetar et al. predicted potential interactions of more than 10% with probenecid, chloramphenicol, and (+)-naproxen out of 17 drugs tested [89]. Rajaonarison et al. examined the inhibitory potential of 55 different drugs on zidovudine glucuronidation [87]. By comparison of the relevant therapeutic concentrations, interactions were predicted for cefoperazone, penicillin G, amoxicillin, piperacillin, chloramphenicol, vancomycin, miconazole, rifampicin, phenobarbital, carbamazepine, phenytoin, valproic acid, quinine, phenylbutazone, ketoprofen, probenecid, and propofol. Interactions with beta-lactam antibiotics and vancomycin are not likely to be significant, because these compounds do not penetrate into cells well and are excreted primarily by direct renal elimination, except for cefoperazone. A similar study was conducted by Sim et al. [90]. Indomethacin, naproxen, chloramphenicol, probene-

cid, and ethinylestradiol decreased the glucuronidation of zidovudine (2.5 mM) by over 90% at supratherapeutic concentrations of 10 mM. Other compounds producing some inhibition of zidovudine conjugation were oxazepam, salicylic acid, and acetylsalicylic acid. More recently, Trapnell et al. examined the inhibition of zidovudine at a more relevant concentration of 20  $\mu$ M in bovine serum albumin-activated microsomes by atovaquone, methadone, fluconazole, and valproic acid at therapeutically relevant concentrations [91]. Both fluconazole and valproic acid inhibited zidovudine glucuronidation by more than 50% at therapeutic concentrations. Clinical interaction studies have been conducted with methadone, fluconazole, naproxen, probenecid, rifampicin, and valproic acid (see Table 2).

**Table 2** Clinical Interactions Affecting Zidovudine Glucuronidation

Precipitant drug	Object drug	Effect	Comments <sup>a</sup>
Atovaquone	Zidovudine (ZDV)	↑	ZDV Cl/F decreased by 25%. AUC(m)/AUCp ratio declined from $4.48 \pm 1.94$ to $3.12 \pm 1.1$ with atovaquone [92].
Fluconazole (400 mg)	Zidovudine	↑	Decreased Cl/F by 46%. Decreased ZDV-G Cl <sub>f</sub> by 48%. $A_{e(m)}/A_e$ decreased by 34%. [93]
Methadone	Zidovudine	↑	Oral AUC increased by 41%, i.v. AUC by 19%. Chronic methadone decreased Cl by 26%. ZDV-G Cl <sub>f</sub> decreased by 17%. [94]
Zidovudine	Methadone	N.S.	No significant change in methadone levels.
Naproxen	Zidovudine	N.S.	No alteration in ZDV pharmacokinetics; ZDV-G AUC significantly decreased by 21%. [95]
Probenecid	Zidovudine	↑	ZDV AUC increased more than twofold. [82]
Rifampicin	Zidovudine	↓	Decreased AUC of ZDV by 2–4-fold ( $n = 4$ ). AUC ratio of ZDV-G/ZDV increased in three patients. Ratio returned to baseline in one patient discontinuing rifampin. [96]
Valproate	Zidovudine	↑	ZDV AUC increased twofold. $A_{e(m)}/A_e$ in urine decreased by >50%. [97].

<sup>a</sup> Source reference numbers are in brackets.



## X. IN VITRO APPROACHES TO PREDICTION OF DRUG-DRUG INTERACTIONS

UGT is a membrane-bound enzyme located intracellularly in the endoplasmic reticulum (ER). Unlike P450, the active site is located in the lumen of the ER, and there is good evidence for the existence of an ER transporter for UDPGA, the polar, charged cofactor that is produced in the cytosol [98]. Similarly, the polar glucuronides that are formed in the lumen may require specific transporters for drug efflux from the ER. Microsomes maintain this membrane integrity, and thus both UDPGA and substrate access may be limited in *in vitro* incubations. Consequently, a variety of techniques have been used to “activate enzyme” or to “remove enzyme latency” *in vitro*. The previously cited *in vitro* studies with zidovudine can be used to illustrate these approaches.

Zidovudine glucuronidation has been stimulated by the addition of detergents such as oleoyl lysophosphatidylcholine (0.8 mg/mg protein optimal) [88], Brij 58 (0.5 mg/mg protein) [87], and *N*-octyl- $\beta$ -D-glucoside (0.05%) [89]. Trapnell et al. reported a 15-fold increase in AZT glucuronidation rate with 2.25% bovine serum albumin (BSA) [91]. In our laboratory, we have recently used a pore-forming antibiotic, alamethacin, to stimulate the glucuronidation of zidovudine in human liver microsomes. The advantage of alamethacin is that isozyme-dependent inhibition by detergents can be avoided, but it is still important to determine the optimal concentration for activation for an individual substrate. In our hands, alamethacin stimulated zidovudine glucuronidation activity 3–4-fold, to a slightly higher extent than Fraction V BSA (Remmel RP and Streich JA, unpublished data). Addition of BSA to alamethacin did not substantially increase activation. When low-endotoxin, fatty acid-free BSA was used, almost no activation was observed, suggesting that endotoxin may be involved in a detergent-like effect.

Unlike the situation with cytochrome P450, specific and selective inhibitors of individual UGT enzymes are generally not available. Furthermore, inhibitory antibodies have not been developed because of the high similarity in amino acid content (identical in all UGT1 enzymes) in the constant region containing the UDPGA binding site [99]. Consequently, at this time the only method available to identify isozyme selectivity is to conduct studies with cloned, expressed enzymes. Fortunately, many of these enzymes have recently been commercially available as microsomes prepared from lymphocytes, mammalian cells, insect cells, or bacteria. Procedures for “activation” of UGT activity in cloned, expressed cell systems also vary, but sonication of whole-cell lysates has been commonly used as a convenient method for screening.

## XI. INTERACTIONS INVOLVING DEPLETION OF UDPGA

An alternate mechanism of drug–drug interactions involving glucuronidation may involve depletion of the required cofactor, UDPGA. Several drugs and chemicals have been shown to deplete UDPGA in the rat, including D-galactosamine, diethylether, ethanol, and acetaminophen [100]. In the mouse, Howell et al. [100] demonstrated that valproic acid, chloramphenicol, and salicylamide depleted hepatic UDPGA by greater than 90% at doses of 1–2 mmole/kg. Maximal decreases were noted at 7–15 minutes after injection, but rebounded toward control levels by 2–4 hours after injection. Once depleted, UDPGA levels will be replaced by the breakdown of glycogen stores in the liver. For drugs that are glucuronidated but given at relatively low doses, UDPGA depletion is not likely to be of major importance. Extrahepatic glucuronidation may be more susceptible to depletion of UDPGA, since UDPGA concentrations in liver (279  $\mu$ mole/kg) were reportedly 15 times higher than in intestine, kidney, or lung [101]. However, in patients receiving high doses of certain drugs, such as the NSAIDs, ethanol, acetaminophen, and valproate, depletion of UDPGA stores may influence the rate of glucuronidation, especially if glycogen stores are low. For example, lamotrigine clearance is decreased 2–3-fold in patients also taking valproic acid. Lamotrigine has been shown to be glucuronidated by UGT1A4 [23], and may also be a substrate for UGT1A3, which also catalyzes the glucuronidation of many tertiary amine drugs [24]. Valproic acid is a slow substrate for UGT1A3 and is a weak inhibitor of lamotrigine glucuronidation in microsomes containing excess UDPGA. The maximum recommended dose of valproic acid is 60 mg/kg/day (4200 mg per day), which is equivalent to a dose of 0.14 mmole/kg. Thus, it is conceivable, that UDPGA depletion may play a role in interactions involving valproic acid. A similar case could be made for patients taking high doses of acetaminophen, although in the case of lamotrigine, coadministration of acetaminophen resulted in an unexpected 20% decrease in lamotrigine AUC. Evidence for UDPGA depletion by any drug in humans is lacking, and thus the clinical relevance of this mechanism is unclear.

## XII. INTERACTIONS INVOLVING INDUCTION OF UGT ENZYMES

Regulation of the UGT enzymes has been well studied in animals, especially in the rat. It is clear that many of the enzymes involved in metabolism of xenobiotics share common regulatory sequences (response elements) in the 5'-promoter region that respond to classic inducers such as 3-methylcholanthrene (3-MC), phe-

nobarbital, clofibrate, dexamethasone, and rifampin. Treatment of rats with polycyclic aromatic hydrocarbons (PAH), such as  $\beta$ -naphthoflavone ( $\beta$ -NF), or 3-MC has been shown to increase the transcription of the UGT1A6, an enzyme that conjugates a variety of planar phenols, such as 1-naphthol. UGT1A6, the PAH-inducible P450 enzymes, CYP1A1 and CYP1A2, glutathione transferase Ya (GSTA1-1), NAD(P)H-menadione oxidoreductase, and class 3 aldehyde reductase (ALDH3) are members of an Ah-receptor gene battery, because all of the genes encoding these enzymes contain a xenobiotic-response element (XRE) in their 5'-promoter regions [102]. In humans, omeprazole and cigarette smoking have been shown to induce CYP1A1/2. Cigarette smoking modestly induces the glucuronidation of acetaminophen [103], codeine [104], mexiletine [105], and propranolol [106]. In smokers or patients receiving omeprazole treatment, the *in vitro* glucuronidation of 4-methylumbelliferone (a general substrate for UGT activity) was not significantly induced in duodenal mucosal biopsies [107]. 1-Naphthol glucuronidation (a marker substrate for UGT1A6) was induced fourfold by  $\beta$ -NF in Caco-2 cells, a human colon carcinoma cell line [108]. In contrast, CYP1A1 activity (ethoxyresorufin-deethylation) was induced by more than 100-fold in the same cell line. 1-Naphthol glucuronidation was not affected by the addition of rifampin or clofibrate. Induction of UGT1A6 mRNA and 1-naphthol glucuronidation by  $\beta$ -NF was also demonstrated in a human hepatocarcinoma cell line, KYN-2. However, no induction of 1-naphthol glucuronidation by  $\beta$ -NF was observed in MZ-Hep-1 cells, another human hepatocarcinoma line. Rifampin (100  $\mu$ M) significantly increased this activity in MZ-Hep-1 cells but not in KYN-2 cells. A variable response to induction by rifampin and  $\beta$ -NF was also observed in cultured hepatocytes isolated from five different donors. Fabre et al. also reported that the inducibility of glucuronidation of 1-naphthol by  $\beta$ -NF in human hepatocytes was variable [109].

Induction of glucuronidation by anticonvulsant drugs such as phenobarbital, phenytoin, and carbamazepine has been demonstrated for a number of different drugs, including acetaminophen, chloramphenicol, lamotrigine, valproic acid, and zidovudine. Human liver microsomes obtained from patients treated with phenytoin or phenobarbital displayed two to three times higher activity for the glucuronidation of bilirubin, 4-methylumbelliferone, and 1-naphthol compared to control human liver microsomes [103]. Less is known about the response to induction of the mRNA concentrations of the individual genes, but Sutherland et al. reported that the UGT1A1 mRNA was elevated in livers from individuals treated with phenytoin and phenobarbital [110]. Bilirubin conjugation is also elevated in microsomes prepared from patients taking phenobarbital or phenytoin and rat bilirubin UGT activity was inducible by phenobarbital and clofibrate in H4IIE rat hepatoma cells [111]. However, when a proximal 611bp UGT1A1 promoter/luciferase reporter gene construct was transfected into H4IIE cells, no

induction was observed upon treatment with phenobarbital. Retinoic acid and a combination of retinoic acid and WY 14643 (a potent peroxisome proliferator) both increased luciferase activity [111]. Patients with Crigler–Najjar Type II syndrome (a genetic deficiency in UGT1A1) have been treated with phenobarbital or clofibrate in order to increase bilirubin glucuronidation. The beneficial effect could arise either by increasing the transcription of a poorly functional or poorly expressed UGT1A1 or by inducing UGT1A4 (the minor bilirubin enzyme). Lamotrigine, a triazine anticonvulsant that is metabolized to a quaternary ammonium glucuronide, is a substrate for UGT1A3 and UGT1A4. Lamotrigine clearance is increased approximately twofold in patients taking other inducing anticonvulsants, suggesting that UGT1A4 is inducible by phenobarbital-type inducers.

Induction of the glucuronidation of several drugs by oral contraceptive steroids (OCSs) has been observed. The formation clearance to the acyl glucuronide of diflunisal increased from 3.01 ml/min in control women compared to 4.81 ml/min in OCS users [112]. The urinary recovery of phenprocoumon glucuronide was 14% of the dose in age-matched controls compared to 21% of the dose in OCS users [113]. Ethinylestradiol doubled the fraction of propranolol metabolized to the glucuronide without affecting total body clearance [114]. Oral contraceptives have also been shown to induce the metabolism of acetaminophen [115], clofibric acid, and temazepam.

Rifampin is a potent inducer of several cytochrome P450 enzymes and also appears to be an inducer of glucuronidation as well. Several case reports have documented an induction of methadone withdrawal symptoms upon introduction of antituberculosis therapy that included rifampin [116,117]. Fromm et al. studied the effect of rifampin (600 mg/day for 18 days) on morphine analgesia and pharmacokinetics in healthy volunteers [118]. Morphine CL/F was increased from  $3.58 \pm 0.97$  L/min initially to  $5.49 \pm 2.97$  L/min during rifampin treatment. The AUC of both morphine-6-glucuronide (an active metabolite) and morphine-3-glucuronide were significantly reduced, although the ratio of the morphine AUC/AUCs of the glucuronides was not significantly increased. Since the metabolite/parent ratios in blood were not affected, the authors suggested that rifampin may have affected the absorption of morphine, perhaps by induction of MDR1 (P-glycoprotein) or that an alternate pathway of metabolism or excretion was enhanced, since the urinary recovery of both the glucuronides was decreased. The area under the pain threshold–time curve (cold pressor test) was also significantly reduced by rifampin treatment. Both methadone and morphine are reported substrates for UGT2B7. Rifampin appears to significantly increase the glucuronidation of zidovudine (ZDV) in humans. Burger et al. reported a higher CL/F and significantly increased ratio ZDV-glucuronide/ZDV in plasma in four AIDS patients on rifampin compared to untreated controls [96]. In one patient who had

stopped rifampin, the metabolite/parent AUC ratio also decreased. Rifabutin, a new rifamycin analog, has been reported to decrease zidovudine  $C_{\max}$  and AUC by 48% and 37%, respectively. However, Gallicano et al. reported that 300 mg of rifabutin per day for 7 or 14 days had no significant effect on ZDV pharmacokinetics, except for a statistically significant decrease in half-life from 1.5 to 1.1 hours [119]. Culture of human hepatocytes with 15  $\mu\text{M}$  rifabutin for 48 hours modestly increased the rate of ZDV glucuronidation (28% increase) in one of two donors, but no significant induction was observed with either rifampin or rifapentine, which were more potent inducers of CYP3A4 and CP2C8/9 *in vitro*.

### XIII. CONCLUSIONS

It is clear from the examples just discussed that interactions involving glucuronidation are possible, especially for drugs that are extensively excreted as glucuronides. Due to the overlapping substrate specificity among different UGTs, most interactions (particularly with phenolic substrates) are likely to be relatively modest. Prediction of interactions is possible in human liver microsomes, but it is important to conduct these studies at relevant therapeutic concentrations. With the availability of cloned, expressed enzymes, detailed kinetic studies of inhibitory interactions may be carried out. Induction potential may be accomplished in human hepatocytes or perhaps by utilization of a reporter gene assay similar to studies conducted with cytochrome P450 enzymes [120]. While outside the scope of this review, interactions involving glucuronide transport may be important as well.

### REFERENCES

1. Burchell B, Brierley CH, Rance D. Specificity of human UDP-glucuronosyltransferases and xenobiotic glucuronidation. *Life Sci* 57:1819–1831, 1995.
2. Burchell B, Coughtrie MWH. Genetic and environmental factors associated with variation of human xenobiotic glucuronidation and sulfation. *Environ Health Persp* 105:739–747, 1997.
3. Meech R, Mackenzie PI. Structure and function of uridine diphosphate glucuronosyltransferases. *Clin Exp Pharmacol Physiol* 24:907–915, 1997.
4. Burchell B, Nebert DW, Nelson DR, Bock KW, Iyanagi T, Jansen PLM, Lancet D, Mulder GJ, Roy Chowdhury J, Siest G, Tephly TR, Mackenzie PI. The UDP glucuronosyltransferase gene superfamily: Suggested nomenclature based on evolutionary divergence. *DNA Cell Biol* 10:487–494, 1991.
5. Mackenzie PI, Owens IS, Burchell B, Bock KW, Bairoch A, Belanger A, Fournel-Gigleux S, Green M, Hum DW, Iyanagi T, Lancet D, Louisot P, Magdalou J, Chow-

- dhury JR, Ritter JK, Schachter H, Tephly TR, Tipton KF, Nebert DW. The UDP glucosyltransferase gene superfamily: recommended nomenclature update based on evolutionary divergence. *Pharmacogenetics* 7:255–269, 1997.
- Jedlitschky G, Cassidy AJ, Sales M, Pratt N, Burchell B. Cloning and characterization of a novel human olfactory UDP-glucuronosyltransferase. *Biochem J* 340:837–843, 1999.
  - Bin-Senafi S, Clarke DJ, Burchell B. Investigation of the substrate specificity of a cloned expressed human bilirubin UDP-glucuronosyltransferase: UDP-sugar specificity and involvement in steroid and xenobiotic glucuronidation. *Biochem J* 303: 233–240, 1994.
  - Clarke DJ, Moghrabi N, Monaghan G, Cassidy A, Boxer M, Hume R, Burchell B. Genetic defects of the UDP-glucuronosyltransferase-1 (UGT1) gene that cause familial non-haemolytic unconjugated hyperbilirubinemias. *Clin Chim Acta* 266: 63–74, 1997.
  - Bosma PJ, Chowdhury JR, Bakker C, Gantla S, de Boer A, Oostra BA, Lindhout D, Tytgat GN, Jansen PL, Oude Elferink RP. The genetic basis of the reduced expression of bilirubin UDP-glucuronosyltransferase 1 in Gilbert's syndrome. *New Engl J Med* 333:1171–1175, 1995.
  - Monaghan G, Ryan M, Seddon R, Hume R, Burchell B. Genetic variation in bilirubin UDP-glucuronosyltransferase gene promoter and Gilbert's syndrome. *Lancet* 347:578–581, 1996.
  - de Morais SMF, Uetrecht JP, Wells PG. Decreased glucuronidation and increased bioactivation of acetaminophen in Gilbert's syndrome. *Gastroenterology* 102:577–586, 1992.
  - Ullrich D, Sieg A, Blume R, Bock KW, Schroter W, Bircher J. Normal pathways for glucuronidation, sulphation and oxidation of paracetamol in Gilbert's syndrome. *Eur J Clin Invest* 17:237–240, 1987.
  - Herman RJ, Chaudhary A, Szakacs CB. Disposition of lorazepam in Gilbert's syndrome: effects of fasting, feeding, and enterohepatic circulation. *J Clin Pharmacol* 34:978–984, 1994.
  - Rommel RP, Sinz MW. A quaternary ammonium glucuronide is the major metabolite of lamotrigine in guinea pigs. *In vitro* and *in vivo* studies. *Drug Metab Disp* 19:630–636, 1991.
  - Posner J, Cohen AF, Land G, Winton C, Peck AW. The pharmacokinetics of lamotrigine (BW430C) in healthy subjects with unconjugated hyperbilirubinemia (Gilbert's syndrome). *Br J Clin Pharmacol* 28:117–120, 1989.
  - Ando Y, Saka H, Asai G, Sugiura S, Shimokata K, Kamataki T. UGT1A1 genotypes and glucuronidation of SN-38, the active metabolite of irinotecan. *Ann Oncol* 9:845–847, 1998.
  - Iyer L, King C, Tephly T, Ratain MJ. UGT isoform 1.1 (UGT1.1) glucuronidates SN-38, the active metabolite of irinotecan. *Proc Ann Meet Am Soc Clin Oncol* 16: A707, 1997.
  - Wasserman E, Myara A, Lokiec F, Goldwasser F, Trivin F, Mahjoubi M, Misset JL, Cvitkovic E. Severe CPT-11 toxicity in patients with Gilbert's syndrome: two case reports. *Ann Oncol* 8:1049–1051, 1997.
  - Iyer L, Hall D, Das S, Mortell MA, Ramirez J, Kim S, Di Rienzo A, Ratain MJ.

- Phenotype–genotype correlation of in vitro SN-38 (active metabolite of irinotecan) and bilirubin glucuronidation in human liver tissue with UGT1A1 promoter polymorphism. *Clin Pharmacol Ther* 65:576–582, 1999.
20. Iyer L, King CD, Whittington PF, Green MD, Roy SK, Tephly TR, Coffman BL, Ratain MJ. Genetic predisposition to the metabolism of irinotecan (CPT-11). Role of uridine diphosphage glucuronosyltransferase isoform 1A1 in the glucuronidation of its active metabolite (SN-38) in human liver microsomes. *J Clin Invest* 101: 847–854, 1998.
  21. Ebner T, Rommel RP, Burchell B. Human bilirubin UDP-glucuronosyltransferase catalyzes the glucuronidation of ethinylestradiol. *Mol Pharmacol* 43:649–654, 1993.
  22. King CD, Green MD, Rios GR, Coffman BL, Owens IS, Bishop WP, Tephly TR. The glucuronidation of exogenous and endogenous compounds by stably expressed rat and human UDP-glucuronosyltransferase. *Arch Biochem Biophys* 332:92–100, 1996.
  23. Green MD, Tephly TR. Glucuronidation of amines and hydroxylated xenobiotics and endobiotics catalyzed by expressed human UGT1.4 protein. *Drug Metab Disp* 24:356–363, 1996.
  24. Green MD, King CD, Majarrabi B, Mackenzie PI, Tephly TR. Glucuronidation of amines and other xenobiotics catalyzed by expressed human UDP-glucuronosyltransferase 1A3. *Drug Metab Disp* 26:507–512, 1998.
  25. Mojarrabi B, Butler R, Mackenzie PI. cDNA Cloning and characterization of the human UDP glucuronosyltransferase, UGT1A3. *Biochem Biophys Res Comm* 225: 785–790, 1996.
  26. Strassburg CP, Oldhafer K, Manns MP, Tukey RH. Differential expression of the UGT1A locus in human liver, biliary, and gastric tissue: identification of UGT1A7 and UGT1A10 transcripts in extrahepatic tissue. *Mol Pharmacol* 52:212–220, 1997.
  27. Ritter JK, Crawford JM, Owens IS. Cloning of two human liver bilirubin UDP-glucuronosyltransferase cDNAs with expression in COS-1 cells. *J Biol Chem* 266: 1043–1047, 1991.
  28. Bosma PJ, Seppen J, Goldhoorn B, Bakker C, Elferink RPJO, Roy Chowdhury J, Roy Chowdhury N, Jansen PLM. Bilirubin UDP-glucuronosyltransferase 1 is the only relevant bilirubin glucuronidating isoform in man. *J Biol Chem* 269:17960–17964, 1994.
  29. Hawes EM. N<sup>+</sup>-glucuronidation, a common pathway in human metabolism of drugs with a tertiary amine group. *Drug Metab Disp* 26:830–837, 1998.
  30. Chiu S-HL, Huskey S-EW. Species differences in N-glucuronidation. *Drug Metab Disp* 26:838–847, 1998.
  31. Sinz MW, Rommel RP. Isolation and characterization of a novel quaternary ammonium-linked glucuronide of lamotrigine. *Drug Metab Disp* 19:149–153, 1991.
  32. Binnie CD, van Emde Boas W, Kasteleijn-Nolste-Trenite DGA/de Korte RA/Meijer JW, Meinardi H. Acute effects of lamotrigine (BW430C) in persons with epilepsy. *Epilepsia* 27:248–254, 1986.
  33. Jawad S, Yuen WC, Peck AW, Hamilton MJ, Oxley JR, Richens A. Lamotrigine:

- single-dose pharmacokinetics and initial 1-week experience in refractory epilepsy. *Epilepsy Res* 10:191–200, 1987.
34. Yuen AWC, Land G, Weatherley BC, Peck AW. Sodium valproate inhibits lamotrigine metabolism. *Br J Clin Pharmacol* 33:511–513, 1992.
  35. Anderson GD, Yau MK, Gidal BE, Harris SJ, Levy RH, Lai AA, Wolf KB, Wargin WA, Dren AT. Bidirectional interaction of valproate and lamotrigine in healthy subjects. *Clin Pharmacol Ther* 60:145–156, 1996.
  36. Yau MKK, Adams MA, Wargin WA, Lai AA. A single-dose and steady-state pharmacokinetic study of lamotrigine in healthy male volunteers. In: *Third International Cleveland Clinic-Bethel Epilepsy Symposium on Antiepileptic Drug Pharmacology*, 1992.
  37. Depot M, Powell JR, Messenheimer JA, Cloutier G, Dalton MJ. Kinetic effects of multiple oral doses of acetaminophen on a single oral dose of lamotrigine. *Clin Pharmacol Ther* 48:346–355, 1990.
  38. Remmel RP, Coughtrie MWH, Zihnioglu F, Burchell B. Studies on the N-glucuronidation of lamotrigine by human, guinea pig, and rabbit UDP-glucuronosyltransferases. In: *Proceedings of the 7th International Workshop on Glucuronidation and the UDP-glucuronosyltransferases*, 1993, p 35.
  39. Ouzzine M, Pillot T, Fournel-Gigleux S, Magdalou J, Burchell B, Siest G. Expression and role of the human liver UDP-glucuronosyltransferase UGT1\*6 analyzed by specific antibodies raised against a hybrid protein produced in *Escherichia coli*. *Arch Biochem Biophys* 310:196–204, 1994.
  40. Court MH, Greenblatt DJ. Identification of expressed family 1 UDP-glucuronosyltransferases (UGT1) in cat liver by 5' RACE and RFLP analysis. In: *ISSX Proceedings*, 1999, p 84.
  41. Abid A, Sabolic N, Magdalou J. Expression and inducibility of UDP-glucuronosyltransferases 1-naphthol in human cultured hepatocytes and hepatocarcinoma cell lines. *Life Sciences* 60:1943–1951, 1997.
  42. Bock KW, Wiltfang J, Blume R, Ullrich D, Bircher J. Paracetamol as a test drug to determine glucuronide formation in man: effects of inducers and of smoking. *Eur J Clin Pharmacol* 31:677–683, 1987.
  43. Strassburg CP, Strassburg A, Nguyen N, Li Q, Manns MP, Tukey RH. Regulation and function of family 1 and family 2 UDP-glucuronosyltransferase genes (UGT1A, UGT2B) in human oesophagus. *Biochem J* 338:489–498, 1999a.
  44. Kobayashi T, Tatano A, Yokota H, Onaga T, Watanabe T, Yuasa A. Small intestinal UDP-glucuronosyltransferase sheUGT1A07: partial and cDNA cloning from sheep small intestine. *Arch Biochem Biophys* 364:143–152, 1999.
  45. Bruck M, Li Q, Lamb JG, Tukey RH. Characterization of rabbit UDP-glucuronosyltransferase UGT1A7: tertiary amine glucuronidation is catalyzed by UGT1A7 and UGT1A4. *Arch Biochem Biophys* 348:357–364, 1997.
  46. Metz RP, Ritter JK. Transcriptional activation of the UDP-glucuronosyltransferase 1A7 gene in rat liver by aryl hydrocarbon receptor ligands and oltipraz. *J Biol Chem* 273:5607–5614, 1998.
  47. Ciotti M, Basu N, Brangi M, Owens I. Glucuronidation of 7-ethyl-10-hydroxycamptothecin (SN-38) by the human UDP-glucuronosyltransferases encoded at the UGT1 locus. *Biochem Biophys Res Comm* 260:199–202, 1999.



48. Cheng Z, Radominska-Pandya A, Tephly TR. Cloning and expression of human UDP-glucuronosyltransferase (UGT) 1A8. *Arch Biochem Biophys* 356:301–305, 1998.
49. Strassburg CP, Nguyen N, Manns MP, Tukey RH. UDP-glucuronosyltransferase activity in human liver and colon. *Gastroenterology* 116:149–160, 1999b.
50. Ebner T, Burchell B. Substrate specificities of two stably expressed human liver UDP-glucuronosyltransferases of the UGT1 gene family. *Drug Metab Disp* 21:50–55, 1993.
51. Wooster R, Sutherland L, Ebner T, Clarke D, Da Cruz e Silva O, Burchell B. Cloning and stable expression of a new member of the human liver phenol/bilirubin: UDP-glucuronosyltransferase cDNA family. *Biochem J* 278:465–469, 1991.
52. Raoof AA, Vanobbergh LJ, Degoyet JD, Verbeeck RK. Extrahepatic glucuronidation of propofol in man—possible contribution of gut wall and kidney. *Eur J Clin Pharmacol* 50:91–96, 1996.
53. Gray PA, Park GR, Cockshott ID, Douglas EJ, Shuker B, Simons PJ. Propofol metabolism in man during the anhepatic and reperfusion phases of liver transplantation. *Xenobiotica* 22:105–114, 1992.
54. Pavlin DJ, Coda B, Shen DD, Tschanz J, Nguyen BS, Schaffer R, Donaldson G, Jacobson RL, Chapman CR. Effects of combining propofol and alfentanil on ventilation, sedation, and emesis in human volunteers. *Anesthesiology* 84:23–37, 1996.
55. Cockshott ID, Briggs LP, Douglas EJ, White M. Pharmacokinetics of propofol in female patients. Studies using single bolus injections. *Br J Anaesth* 59:1103–1110, 1987.
56. Verbeeck RK, Blackburn JL, Loewen GR. Clinical pharmacokinetics of non-steroidal antiinflammatory drugs. *Clin Pharmacokin* 8:297–331, 1983.
57. Munzel PA, Schmohl S, Heel H, Kalberer K, Bock-Hennig BS, Bock KW. Induction of human UDP-glucuronosyltransferases (UGT1A6, UGT1A9, and UGT2B7) by *t*-butylhydroxyquinone and 2,3,7,8-tetrachlorodibenzo-p-dioxin in Caco-2 cells. *Drug Metab Disp* 27:569–573, 1999.
58. Mojarabi B, Mackenzie PI. The human UDP glucuronosyltransferase, UGT1A10, glucuronidates mycophenolic acid. *Biochem Biophys Res Comm* 238:775–778, 1997.
59. Zucker K, Rosen A, Tsaroucha A. Unexpected augmentation of mycophenolic acid pharmacokinetics in renal transplant patients receiving tacrolimus and mycophenolate mofetil in combination therapy and analogous in vitro findings. *Transpl Immunol* 5:225–232, 1997.
60. Zucker K, Tsaroucha A, Olson L, Esquenazi V, Tzakis A, Miller J. Evidence that tacrolimus augments the bioavailability of mycophenolate mofetil through inhibition of mycophenolic acid glucuronidation. *Therap Drug Monitor* 21:35–43, 1999.
61. Ritter JK, Sheen YY, Owens IS. Cloning of two human UDP-glucuronosyltransferases in COS-1 cells. *J Biol Chem* 265:7900–7906, 1990.
62. Jin C, Miners JO, Lillywhite KJ, Mackenzie PI. Complementary deoxyribonucleic acid cloning and expression of a human liver uridine diphosphate-glucuronosyltransferase glucuronidating carboxylic acid-containing drugs. *J Pharmacol Exp Ther* 264:475–479, 1992.

63. Coffman BL, Rios GR, King CD, Tephly TR. Human UGT2B7 catalyzed morphine glucuronidation. *Drug Metab Disp* 25:1–4, 1997.
64. Coffman BL, King CD, Rios GR, Tephly TR. The glucuronidation of opioids, other xenobiotics, and androgens by human UGT2B7Y(268) and UGT2B7H(268). *Drug Metab Disp* 26:73–77, 1998.
65. Jin C-J, Mackenzie PI, Miners JO. The regio- and stereo-selectivity of C19 and C21 hydroxysteroid glucuronidation by UGT2B7 and UGT2B11. *Arch Biochem Biophys* 341:207–211, 1997.
66. Miners JO, Lillywhite KJ, Birkett DJ. In vitro evidence for the involvement of at least two forms of human liver UDP-glucuronosyltransferase in morphine-3-glucuronidation. *Biochem Pharmacol* 37:2839–2845, 1988.
67. Wu D, Kang Y-S, Bickel U, Partridge W. Blood–brain barrier permeability to morphine-6-glucuronide is markedly reduced compared to morphine. *Drug Metab Disp* 25:768–771, 1997.
68. Patel M, Tang BK, Kalow W. (S)Oxazepam glucuronidation is inhibited by ketoprofen and other substrates of UGT2B7. *Pharmacogenetics* 5:43–49, 1995.
69. Samara EE, Granneman RG, Witt GF, Cavanaugh JH. Effect of valproate on the pharmacokinetics and pharmacodynamics of lorazepam. *J Clin Pharmacol* 37:442–450, 1997.
70. Anderson GD, Gidal BE, Kantor ED, Wilensky AJ. Lorazepam–valproate interaction: studies in normal subjects and isolated perfused rat liver. *Epilepsia* 35:221–225, 1994.
71. Abernethy DR, Greenblatt DJ, Ameer B, Shader RI. Probenecid impairment of acetaminophen and lorazepam clearance: direct inhibition of ether glucuronide formation. *J Pharmacol Exp Ther* 234:345–349, 1985.
72. Herman RJ, van Pham JD, Szakacs CB. Disposition of lorazepam in human beings: enterohepatic recirculation and first-pass effect. *Clin Pharmacol Ther* 46:18–25, 1989.
73. Veenendaal JR, Brooks PM, Meffin PJ. Probenecid–clofibrate interaction. *Clin Pharmacol Therap* 29:351–358, 1981.
74. Smith PC, Langendijk PN, Bosso JA, Benet LZ. Effect of probenecid on the formation and elimination of acyl glucuronides: studies with zomepirac. *Clin Pharmacol Ther* 38:121–127, 1985.
75. Miners JO, Robson RA, Birkett DJ. Gender and oral contraceptive steroids as determinants of drug glucuronidation: effects on clofibric acid elimination. *Br J Clin Pharmacol* 14:240–243, 1984b.
76. Upton RA, Buskin JN, Williams RL, Holford NHS, Riegelman S. Negligible excretion of unchanged ketoprofen, naproxen, and probenecid in urine. *J Pharm Sci* 69:1254–1257, 1980.
77. Baber N, Halliday L, Sibeon R, Littler T, Orme ML. The interaction between indomethacin and probenecid. *Clin Pharmacol Ther* 24:298–307, 1978.
78. Yu TF, Perel J. Pharmacokinetic and clinical studies of carprofen in gout. *J Clin Pharmacol* 20:347–351, 1980.
79. Spahn H, Spahn I, Benet LZ. Probenecid-induced changes in the clearance of carprofen enantiomers: a preliminary study. *Clin Pharmacol Ther* 45:500–505, 1989.

80. Bannier A, Comet F, Soubeyrand J, Brazier JL, Chauliac F. Effect of probenecid on isofezolac kinetics. *Eur J Clin Pharmacol* 28:433–477, 1985.
81. Runkel R, Mroszczak E, Chaplin M, Sevelius H, Segre E. Naproxen–probenecid interaction. *Clin Pharmacol Ther* 24:706–713, 1978.
82. de Miranda P, Good SS, Yarchoan R, Thomas RV, Blum MR, Myers CE, Broder S. Alteration of zidovudine pharmacokinetics by probenecid in patients with AIDS or AIDS-related complex. *Clin Pharmacol Ther* 46:494–500, 1989.
83. Meffin PJ, Zilm DM, Veenendaal JR. A renal mechanism for the clofibrac acid–probenecid interaction. *J Pharmacol Exp Ther* 227:739–742, 1983.
84. Hedaya MA, Sawchuk RJ. Effect of probenecid on the renal and nonrenal clearance of zidovudine and its distribution into cerebrospinal fluid in the rabbit. *J Pharm Sci* 78:1–7, 1989.
85. Herber R, Magdalou J, Haumont M, Bidault R, van Es H, Siest G. Glucuronidation of 3'-azido-3'-deoxythymidine in human liver microsomes: enzyme inhibition by drugs and steroid hormones. *Biochim Biophys Acta* 1139:20–24, 1992.
86. Kamali F, Rawlins MD. Influence of probenecid and paracetamol (acetaminophen) on zidovudine glucuronidation in human liver in vitro. *Biopharm Drug Disp* 13: 403–409, 1992.
87. Rajaonarison JF, Lacarelle B, De Sousa G, Catalin J, Rahmani R. In vitro glucuronidation of 3'-azido-3'-deoxythymidine by human liver. Role of UDP-glucuronosyltransferase 2 form. *Drug Metab Disp* 19:809–815, 1991.
88. Haumont M, Magdalou J, Lafaurie C, Ziegler JM, Siest G, Colin JN. Phenobarbital inducible UDP-glucuronosyltransferase is responsible for glucuronidation of 3'-azido-3'-deoxythymidine: characterization of the enzyme in human and rat liver microsomes. *Arch Biochem Biophys* 281:264–270, 1990.
89. Resetar A, Minick D, Spector T. Glucuronidation of 3'-azido-3'-deoxythymidine catalyzed by human liver UDP-glucuronosyltransferase. Significance of nucleoside hydrophobicity and inhibition by xenobiotics. *Biochem Pharmacol* 42:559–68, 1991.
90. Sim SM, Back DA, Breckenridge AM. The effect of various drugs on the glucuronidation of zidovudine (azidothymidine; AZT) by human liver microsomes. *Br J Clin Pharmacol* 32:17–21, 1991.
91. Trapnell CB, Klecker RW, Jamis-Dow C, Collins JM. Glucuronidation of 3'-azido-3'-deoxythymidine (zidovudine) by human liver microsomes: relevance to clinical pharmacokinetic interactions with atovaquone, fluconazole, methadone, and valproic acid. *Antimicrob Agents Chemother* 42:1592–1596, 1998.
92. Lee BL, Tauber MG, Sadler B, Goldstein D, Chambers HF. Atovaquone inhibits the glucuronidation and increases the plasma concentrations of zidovudine. *Clin Pharmacol Ther* 59:14–21, 1996.
93. Sahai J, Gallicano, Pakuts A, Cameron DW. Effect of fluconazole on zidovudine pharmacokinetics in patients infected with human immunodeficiency virus. *J Inf Dis* 169:1103–1107, 1994.
94. McCance-Katz EF, Rainey PM, Jatlow P, Friedland G. Methadone effects on zidovudine disposition (AIDS Clinical Trials Group 262). *J Acq Immun Def Syndr Human Retrovir* 18:435–443, 1998.
95. Barry M, Howe J, Back D, Breckenridge A, Brettle R, Mitchell R, Beeching NJ,

- Nye FJ. The effects of indomethacin and naproxen on zidovudine pharmacokinetics. *Br J Clin Pharmacol* 36:82–85, 1993.
96. Burger DM, Meenhorst PL, Koks CHW, Beijnen JH. Pharmacokinetic interaction between rifampin and zidovudine. *Antimicrob Agents Chemother* 37:1426–1431, 1993.
  97. Lertora JJ/Rege AB, Greenspan DL, Akula S, George WJ, Hyslop Jr. NE, Agrawal KC. Pharmacokinetic interaction between zidovudine and valproic acid in patients infected with human immunodeficiency virus. *Clin Pharmacol Ther* 56:272–278, 1994.
  98. Bossuyt X, Blanckaert N. Carrier-mediated transport of intact UDP-glucuronic acid into the lumen of endoplasmic-reticulum-derived vesicles from rat liver. *Biochem J* 302:261–269, 1994.
  99. Rimmel RP, Burchell B. Validation and use of cloned, expressed human drug-metabolizing enzymes in heterologous cells for analysis of drug metabolism and drug–drug interactions. *Biochem Pharmacol* 46:559–566, 1993.
  100. Howell SR, Hazelton GA, Klaassen CD. Depletion of hepatic UDP-glucuronic acid by drugs that are glucuronidated. *J Pharmacol Exp Ther* 236:610–614, 1986.
  101. Cappiello M, Giuliani L, Pacifici GM. Distribution of UDP-glucuronosyltransferase and its endogenous substrate uridine 5'-diphosphoglucuronic acid in human tissues. *Eur J Clin Pharmacol* 41:345–350, 1991.
  102. Nebert DW, Puga A, Vasilou V. Role of the Ah receptor and the dioxin-inducible [Ah] gene battery in toxicity, cancer, and signal transduction. *Ann NY Acad Sci* 685:624–40, 1993.
  103. Bock KW, Bock-Hennig BS. Differential induction of human liver UDP-glucuronosyltransferase activities by phenobarbital-type inducers. *Biochem Pharmacol* 36:4137–4143, 1987.
  104. Yue QY, Tomson T, Sawe J. Carbamazepine and cigarette smoking induce differentially the metabolism of codeine in man. *Pharmacogenetics* 4:193–198, 1994.
  105. Grech-Belanger O, Gilbert M, Turgeon J, LeBlanc PP. Effect of cigarette smoking on mexiletine kinetics. *Clin Pharmacol Ther* 37:638–643, 1985.
  106. Walle T, Walle UK, Cowart TD, Conradi EC, Gaffney TE. Selective induction of propranolol metabolism by smoking: additional effects on renal clearance of metabolites. *J Pharmacol Exp Ther* 241:928–933, 1987.
  107. Buchthal J, Grund KE, Buchmann A, Schrenk D, Beaune P, Bock KW. Induction of cytochrome P4501A by smoking or omeprazole in comparison with UDP-glucuronosyltransferase in biopsies of human duodenal mucosa. *Eur J Clin Pharmacol* 47:431–435, 1995.
  108. Abid A, Bouchon I, Siest G, Sabolovic N. Glucuronidation in the Caco-2 human intestinal cell line: induction of UDP-glucuronosyltransferase 1\*6. *Biochem Pharmacol* 50:557–561, 1995.
  109. Fabre G, Bourrie M, Marti E, Fabre I, Roque C, Saint Aubert B, Joyeux H, Maurel P, Berger Y, Cano JP. *Biochem Pharmacol* 9:79–91, 1990.
  110. Sutherland L, Ebner T, Burchell B. The expression of UDP-glucuronosyltransferases of the UGT1 family in human liver and kidney and in response to drugs. *Biochem Pharmacol* 45:295–301, 1993.
  111. Brierley CH, Bin Senafi S, Clarke D, Hsu M-H, Johnson EF, Burchell B. Regulation

- of the human bilirubin UDP-glucuronosyltransferase gene. *Adv Enz Regul* 36:85–97, 1996.
112. Macdonald JI, Herman RJ, Verbeeck RK. Sex-difference and the effects of smoking and oral contraceptive steroids on the kinetics of diflunisal. *Eur J Clin Pharmacol* 38:175–179, 1990.
  113. Monig H, Baese C, Heidemann HT, Ohnhaus EE, Schulte HM. Effect of oral contraceptive steroids on the pharmacokinetics of phenprocoumon. *Br J Clin Pharmacol* 30:115–118, 1990.
  114. Walle T, Fagan TC, Walle UK, Topmiller MJ. Stimulatory as well as inhibitory effects of ethinyloestradiol on the metabolic clearances of propranolol in young women. *Br J Clin Pharmacol* 41:305–309, 1996.
  115. Miners JO, Attwood J, Birkett DJ. Influence of sex and oral contraceptive steroids on paracetamol metabolism. *Br J Clin Pharmacol* 16:503–509, 1983.
  116. Kreek MJ, Garfield JW, Gutjahr CL, Giusti LM. Rifampin-induced methadone withdrawal. *New Engl J Med* 294:1104–1106, 1976.
  117. Holmes VE. Rifampin-induced methadone withdrawal in AIDS. *J Clin Psychopharm* 10:443, 1990.
  118. Fromm MF, Eckhardt K, Li S, Schanzle G, Hofmann U, Mikus G, Eichelbaum M. Loss of analgesic effect of morphine due to coadministration of morphine. *Pain* 72:261–267, 1997.
  119. Gallicano K, Sahai J, Swick L, Seguin I, Pakuts A, Cameron DW. Effect of rifabutin on the pharmacokinetics of zidovudine in patients infected with human immunodeficiency virus. *Clin Inf Dis* 21:1008–1011, 1995.
  120. Ogg MS, Williams MJ, Tarbit M, Goldfarb PS, Gray TJ, Gibson GG. A reporter gene assay to assess the molecular mechanisms of xenobiotic-dependent induction of the human CYP3A4 gene in vitro. *Xenobiotica* 29:269–279, 1999.
  121. Cheng Z, Radominska-Pandya A, Tephly TR. Studies on the substrate specificity of human intestinal UDP-glucuronosyltransferases 1A8 and 1A10. *Drug Metab Disp* 27:1165–1170, 1999.
  122. Cretton EM, Sommadossi JP. Modulation of 3'-azido-3'-deoxythymidine catabolism by probenecid and acetaminophen in freshly isolated rat hepatocytes. *Biochem Pharmacol* 42:1475–1480, 1991.

**Table 1** UDP-Glucuronosyltransferase Enzymes

Isoenzyme	Trivial names	Species and location	Endogenous substrates	Drug or xenobiotic substrates	Inducibility	Inhibitors
UGT1A1	HP3 HUG-Br1 Rat B1	Human, rat, etc.	Bilirubin Bilirubin monoglucuronide 2- <i>OH</i> -Estrone, 2- <i>OH</i> estadiol	Ethinylestradiol, 1-naphthol, <i>p</i> -nitrophenol, 4-methylumbelliferone, buprenorphine, irinotecan	Phenobarbital? Clofibrate Phenytoin Oltipraz	
Ugt1a1	UgtBr1	Mouse				
UGT1A2P	Rat B2	Rat		Inactive pseudogene in humans	Oltipraz	
UGT1A3	Rat B3	Human liver and colon	Estrone 2- <i>OH</i> -Estrone	Naphthol, <i>p</i> -nitrophenol, <i>N</i> - <i>OH</i> -2-AAF, hydroxy benzo( <i>a</i> )pyrene metabolites (esp. 5- & 12- <i>OH</i> ), tertiary amines		
UGT1A4	HP2 HUG-Br2 Rat B4	Human, rat	Bilirubin (minor form) (0.1% of UGT1A1) 5 $\alpha$ -pregnane-2 $\beta$ ,20 $\alpha$ -diol 5 $\alpha$ -androstene-3 $\alpha$ , 17 $\beta$ -diol	Tertiary amines, e.g., imipramine, amitriptyline, doxepin, cyproheptadine, chlorpromazine, promethazine, ketotifen, chlorpheniramine, clozapine tripelelenamine; lamotrigine, 4-amino-biphenyl, $\alpha$ - & $\beta$ -naphthylamine, benzidine, hecogenin, sapogenin	Phenobarbital Clofibrate Perfluorodecanoate T3-thyroid hormone, lamotrigine?	Valproic acid?
UGT1A5	Rat B5	Human		mRNA not expressed in liver, biliary epithelium, or gastric tissue. Has not yet been cloned and expressed		

Table 1 Continued

Isoenzyme	Trivial names	Species and location	Endogenous substrates	Drug or xenobiotic substrates	Inducibility	Inhibitors
UGT1A6	HP1, UGT1A1 4NP K39	Human kidney, intestine, lung, ovary, & liver, rat		Planar phenols, e.g., acetaminophen, 1- & 2-naphthol (high), <i>p</i> -nitrophenol, 4-methylphenol, 4-ethylphenol, 4-methylumbelliferone, 12- <i>OH</i> and 5- <i>OH</i> benzo( <i>a</i> )pyrene, benzo( <i>a</i> )pyrene-3,6-quinol-2- <i>OH</i> biphenyl, vanillin, $\alpha$ - & $\beta$ -naphthylamine, 5- <i>OH</i> & 8- <i>OH</i> 2AAF	3-MC TCDD BNF	
Ugt1a6 UGT1A7	Rat A2 1g	Mouse Rabbit liver mRNA expressed in human gastric tissue	4- <i>OH</i> -estrone	2- <i>OH</i> & 4- <i>OH</i> biphenyl (low), benzo( <i>a</i> )pyrene 7,8-dihydrodiol and hydroxylated B( <i>a</i> )P-metabolites, 4-methylumbelliferone, 1- & 2-naphthol, <i>p</i> -nitrophenol, irinotecan, 4-isopropylphenol (propofol), 4- <i>tert</i> -butylphenol, octylgallate, propylgallate, vanillin; imipramine (low, rabbit enzyme only)	Oltipraz BNF (rats)	

UGT1A8	Rat A3 1h	Human intestine and colon	2- <i>OH</i> -estrone, 4- <i>OH</i> -estrone, 2- <i>OH</i> -estradiol, 4- <i>OH</i> -estradiol, estrone, dihydrotestosterone, hyocholic acid, hyodeoxycholic acid, trans-retinoic acid, 4- <i>OH</i> -retinoic acid	Alizarin, anthraflavic acid, apigenin, emodin, fisetin, genistein, naringenin, quercetin, quinalizarin, 4-methylumbelliferone, scopolin, carvacrol, eugenol, 1-naphthol, <i>p</i> -nitrophenol, 4-aminobiphenyl, 2- <i>OH</i> -, 3- <i>OH</i> -, and 4- <i>OH</i> -biphenyl, buprenorphine (low), morphine (low), naloxone, naltrexone, ciprofibrate, diflunisal, diphenylamine, furosemide, mycophenolic acid (high), phenolphthalein, propofol, valproic acid	
UGT1A9	HP4 UGT1*02 Rat A4 (pseudogene in rats) li	Human kidney and liver, rat	Estrone 4-hydroxyestrone	Bulky phenols, octyl and propyl gallate; emodin, galangin, quercetin and other flavonoids; carveol, nopol, citronellol, 4- <i>t</i> -butyl-phenol, propofol, labetalol, propranolol, dapsone, bumetanide, $\alpha$ - and $\beta$ -naphthylamine, 4- <i>OH</i> -acetophenone, phenolphthalein, 4-methylumbelliferone, fluorescein, naproxen, ibuprofen, keprofen, ethinylestradiol (minor)	Phenobarbital



**Table 1** Continued

Isoenzyme	Trivial names	Species and location	Endogenous substrates	Drug or xenobiotic substrates	Inducibility	Inhibitors
Ugt1a9 UGT1A10	mUGTBr/P 1j	Mouse Human, colon, biliary epithelium, and gastric tissue (mRNA)	2- <i>OH</i> -estrone (low), 4- <i>OH</i> -estrone (low), dihydrotestosterone	Alizarin, anthraflavic acid, apigenin, emodin, fisetin, genistein, naringenin, quercetin, quinalizarin, 4-methylumbelliferone, scopolletin, carvacrol, eugenol, mycophenolic acid		Tacrolimus
UGT1A11	1k			May be pseudogene, not yet cloned and expressed		
UGT1A12	1l			May be pseudogene, not yet cloned and expressed		
UGT2B1	r-2	Rat liver	Carboxyl group of bile acids, testosterone	4 and 11- <i>OH</i> benzo( <i>a</i> )-pyrene, 4- <i>OH</i> -biphenyl, chloramphenicol, <i>N</i> - <i>OH</i> 2AAF 1- <i>OH</i> -, 2- <i>OH</i> -, 8- <i>OH</i> -, and 9- <i>OH</i> -benzo( <i>a</i> )pyrene, morphine-3- <i>glucuronidation</i> , naloxone, buprenorphine (less than UGT1A1)	Phenobarbital Oltipraz	
UGT2B2	r-4 rlug23	Rat	Carboxyl and hydroxyl groups of bile acids, 3 $\alpha$ - <i>OH</i> group of C19 steroids	1- <i>OH</i> - and 3- <i>OH</i> -2-acetylaminofluorene, <i>N</i> - <i>OH</i> -2-AAF 1-, 4-, 5-, 7-, and 11- <i>OH</i> benzo( <i>a</i> )pyrene, etiocholanolone, androsterone		

UGT2B3	r-3 rlug38	Rat	Testosterone dihydrotestosterone	
UGT2B4	hlug25 h-1 h-20	Human liver	Hyodeoxycholic acid 4-hydroxyestrone, 17- epiestriol, estriol, 2- <i>OH</i> -estriol	4-Nitrophenol, 1-naph- thol, 4- <i>OH</i> -biphenyl, methanol, 2- aminophenol  <i>Note:</i> A clone with small amino acid vari- ations has been de- scribed as UGT2B11 previously.
Ugt2b-5	m-1	Mouse		
UGT2B6	r-5	Rat	17 $\beta$ -hydroxysteroids Testosterone	
UGT2B7	UDPGT-h2 hlug6	Human liver, intestine	4- <i>OH</i> -estrone (high), 2- <i>OH</i> -estrone, hyde- oxycholic acid, es- triol, 2- <i>OH</i> estriol, an- drosterone (low)	Nonsteroidal anti-in- flammatory drugs, e.g., naproxen, keto- profen, ibuprofen, diflunisal, fenopro- fen, tiaprofenic acid, benoxaprofen, indo- methacin, zomepirac, valproic acid, ciprofi- brate, clofibrac acid, temazepam, oxaze- pam, propranolol, chloramphenicol, menthol, 1-naphthol, 4-methylumbellifer- one, morphine 3 <i>OH</i> > 6 <i>OH</i> , buprenor- phine, nalorphine, nal- trexone, codeine (low)

**Table 1** Continued

Isoenzyme	Trivial names	Species and location	Endogenous substrates	Drug or xenobiotic substrates	Inducibility	Inhibitors
UGT2B8		Rat				
UGT2B9		Monkey (90% homology to UGT2B7)		Morphine (3- <i>O</i> - & 6- <i>O</i> -), naloxone, naltrexone, nalorphine, buprenorphine. NSAIDs, e.g., ibuprofen clofibrac acid, propranolol, monoterpenoid alcohols, menthol		
UGT2B10	h-46	Human		Inactive?		
UGT2B11		Human mRNA expressed in many tissues		Beaulieu et al. (BBRC 248:44, 1998) isolated a new sequence with 91% sequence identity to UGT2B10. No activity observed with over 100 substrates. UGT2B10 & 2B11 may form dimers with other forms that alter substrate activity		
UGT2B12	rlug1	Rat				
UGT2B13	EGT10	Rabbit		4- <i>OH</i> -biphenyl, 1-naphthol, 4-nitrophenol, 4-methylumbelliferone, eugenol, acetaminophen, estriol, octylgalate		

UGT2B14	EGT12	Rabbit		Estrone, 17 $\beta$ -estradiol, 1-naphthol, 4-nitrophenol, 4-methylumbelliferone, eugenol
UGT2B15	UDPGT-h3 hlug4	Human liver, brain astrocytes, prostate	5 $\alpha$ -Dihydro-testosterone, estriol 5- $\alpha$ -androstane-3 $\alpha$ ,17 $\beta$ -diol, testosterone (low) 17- <i>O</i> -glucuronidation only	Flavonoids, phenols, anthraquinones, eugenol, 4-methylumbelliferone, esculetin, 4- <i>OH</i> -biphenyl, 8- <i>OH</i> -quinoline, fluorescein, phenolphthalein
UGT2B16		Rabbit	4- <i>OH</i> -estrone	4- <i>tert</i> -butylphenol
UGT2B17		Human liver, skin, kidney, adrenals, testis, uterus, placenta, prostate	3 $\alpha$ - and 17 $\beta$ -androgens, e.g., testosterone, dihydrotestosterone, androstenedione Catalyzes both 3- <i>O</i> - & 17- <i>O</i> -glucuronidation	Eugenol, <i>p</i> -nitrophenol, <i>o,o'</i> -di- <i>OH</i> -biphenyl, <i>p,p</i> -di- <i>OH</i> -biphenyl, 1-naphthol, 4-methylumbelliferone (very low)
UGT2B18		Monkey	Androsterone, dihydrotestosterone, etiocholanolone	1-Naphthol
UGT2B19		Monkey	Testosterone	

Source: Data obtained from Refs. 1, 17, 21, 23–25, 27, 45, 46–50, 62–64.



# 5

## Drug–Drug Interactions Involving the Membrane Transport Process

**Hiroyuki Kusuhara and Yuichi Sugiyama**

*University of Tokyo and CREST, Japan Science and Technology Corporation, Tokyo, Japan*

### I. INTRODUCTION

Drug–drug interactions involving the membrane transport process do not occur when drugs pass through the plasma membrane by passive diffusion, a nonsaturable route. Also, it is possible to estimate the membrane permeability by measuring the physicochemical properties of the drugs, which enables us to predict drug disposition *in silico*. Transporters mediate the membrane transport of a great number of drugs and endogenous compounds. Since the number of binding sites of transporters for drugs is limited, the transport process is saturated at concentrations higher than the  $K_m$  value. Also, when drugs share the same binding sites of transporters, drug–drug interactions may occur, depending on their pharmacokinetic properties. These may alter the drug disposition and/or its pharmacological effects. In addition, it is possible that there are species differences in the affinity and/or maximum transport velocity of drugs and in the transporter responsible for the drugs' disposition. Therefore, it may be difficult in some cases to predict drug–drug interactions in humans from *in vitro* transport experiments using animal models.

The possible sites for drug–drug interactions involving the membrane transport process are summarized in Table 1. Overall, interactions involving

---

Much progress has been achieved in the research area of drug transporters since the chapter was written. We have added as much new information as possible in the proofreading. However, the updated information may not be enough in some areas.

**Table 1** Possible Sites for Drug–Drug Interactions and in Vitro Transport Models

Tissue	Process	Transport direction		In vitro transport experiment
		From	To	
Liver	Uptake	Blood	Parenchymal cells	Isolated and cultured hepatocytes, sinusoidal membrane vesicles, transporter expressions system
	Efflux	Parenchymal cells	Blood	
Kidney	Excretion	Parenchymal cells	Bile	Canalicular membrane vesicles, transporter expression system
	Uptake	Blood	Epithelial cells	Isolated and cultured renal epithelial cells, basolateral membrane vesicles, kidney slices transporter expressions systems
	Efflux	Epithelial cells	Blood	
Small intestine	Excretion	Epithelial cells	Urine	Brush border membrane vesicles, transporter expression system
	Reabsorption	Urine	Epithelial cells	Brush border membrane vesicles, transporter expression system
	Uptake	Digestive tract	Epithelial cells	Everted sac, Ussing-chamber experiments using intestinal epithelium, brush border membrane vesicles, Caco-2 cells, transporter expression systems
	Efflux	Epithelial cells	Digestive tract	Everted sac, Ussing-chamber experiments using intestinal epithelium, basolateral membrane vesicles, Caco-2 cells
Absorption	Epithelial cells	Blood		
BBB	Excretion	Blood	Epithelial cells	Everted sac, Ussing-chamber experiments using intestinal epithelium, basolateral membrane vesicles, Caco-2 cells
	Uptake	Blood	Endothelial cells	Primary cultured cerebral capillary endothelial cells, immortalized cell line
	Uptake	Endothelial cells	Brain parenchyma	
Efflux	Brain parenchyma	Endothelial cells		
BCSFB	Efflux	Endothelial cells	Blood	Primary cultured cerebral capillary endothelial cells, immortalized cell line
	Uptake	Blood	Epithelial cells	Primary cultured choroid epithelial cells, immortalized cell line, membrane vesicles
	Uptake	Epithelial cells	Cerebrospinal fluid	
Tumor	Efflux	Cerebrospinal fluid	Epithelial cells	Primary cultured choroid epithelial cells, immortalized cell line
	Efflux	Epithelial cells	Blood	
	Uptake	Blood	Tumor	Cell line, membrane vesicles
	Efflux	Tumor	Blood	Cell line, membrane vesicles

membrane transporters in organs of elimination (e.g., liver and kidney) and absorption (e.g., intestine) alter the blood concentration time profiles of drugs. On the other hand, comparison, interactions occurring at the blood–brain barrier, at the blood–cerebrospinal fluid barrier, and in tumors will not alter the drug disposition but only the pharmacological and/or toxicological effect of drugs. Unlike the liver, there is a nonspecific and unsaturable elimination route in the kidney, glomerular filtration. In dealing with renal clearance, glomerular filtration, tubular secretion, and reabsorption should be taken into consideration. Since glomerular filtration is a nonspecific elimination route that cannot be saturated, the degree of change in renal clearance caused by drug–drug interactions depends on the contribution of tubular secretion and reabsorption to the overall renal clearance.

Drugs, which are excreted into the bile, may undergo the enterohepatic circulation. It is possible that conjugated metabolites (e.g., glucuronide and sulfate) take part in this enterohepatic circulation; they are excreted into the bile followed by deconjugation in the intestine, then reabsorbed into the blood and in the liver in the intact form. This increases the retention time of a drug in the circulating blood, and interruption of these processes apparently increases the total body clearance. For example, pravastatin (a HMG-Co A reductase inhibitor) undergoes enterohepatic circulation mainly in the intact form [1]. This prolongs the exposure of the liver (target organ) to the drug and minimizes adverse effects in other organs. This enterohepatic circulation is mediated by transporters in every process from gastrointestinal absorption to the biliary transport of pravastatin [2–5].

In this chapter, recent advances in the prediction of transporter-mediated drug–drug interactions and methods for their evaluation are described.

## II. PREDICTION OF DRUG–DRUG INTERACTIONS FROM IN VITRO EXPERIMENTS

We have previously proposed a method for predicting *in vivo* drug–drug interactions from *in vitro* experiments [6]. When predicting drug–drug interactions, it is important to show how to avoid false-negative predictions [6]. We now would like to apply this method to predict *in vivo* drug–drug interactions involving membrane transporters; the procedure is shown in Fig. 1. The pharmacokinetic characteristics of drugs, whose plasma concentration time profiles are significantly affected by drug–drug interactions, are such that their organ clearance is close to their intrinsic clearance (intrinsic clearance-limited drugs) [6]. In addition, any rate-limiting processes should be taken into consideration, because when the uptake is rate limiting, a reduction in secretion will not markedly affect the drug disposition.

Generally speaking, the relationship between intrinsic membrane transport



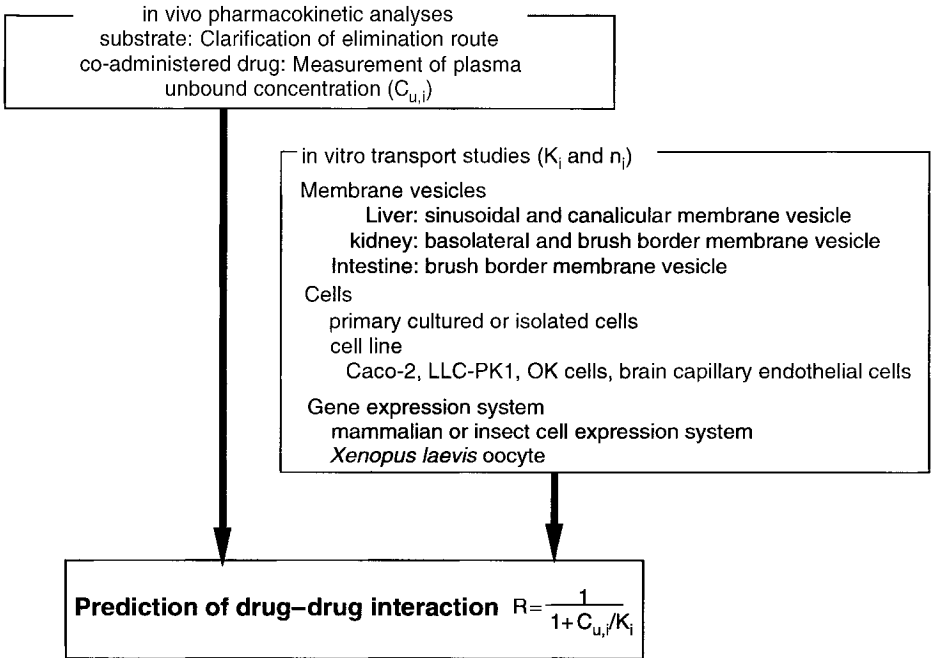


**Figure 1** Schematic diagram for the prediction of drug–drug interactions involving membrane transport from in vitro transport experiments.

clearance ( $PS_{int}$ ) and the unbound concentration of drug ( $C_u$ ) can be described by the Michaelis–Menten equation:

$$PS_{int} = \frac{V_{max}}{K_m + C_u} \quad (1)$$

where  $K_m$  and  $V_{max}$  represent the Michaelis constant and maximal transport velocity, respectively. There are two types of inhibition, competitive and noncompetitive:

$$PS_{int} = \frac{V_{max}}{K_m (1 + C_{u,i}/K_i) + C_u} \quad (\text{competitive})$$

$$PS_{int} = \frac{V_{max}/(1 + C_{u,i}/K_i)}{K_m + C_u} \quad (\text{noncompetitive}) \quad (2)$$

where  $C_{u,i}$  and  $K_i$  represent the unbound concentration of an inhibitor around a transporter and its inhibition constant, respectively. The degree of inhibition depends on the type of inhibition, especially at substrate concentrations higher than

the  $K_m$  value. However, when the substrate concentration is much lower than the  $K_m$  value (this assumption holds true for many drugs at their clinical dosages), the intrinsic membrane transport clearance can be expressed by the following equation, independent of the type of inhibition:

$$PS_{\text{int}} = \frac{V_{\text{max}}}{K_m(1 + C_{u,i}/K_i)} \quad (3)$$

The degree of inhibition ( $R$ ) is defined as follows:

$$R = \frac{PS_{\text{int}}(+\text{inhibitor})}{PS_{\text{int}}(-\text{inhibitor})} = \frac{1}{1 + C_{u,i}/K_i} \quad (4)$$

where  $PS_{\text{int}}(+\text{inhibitor})$  and  $PS_{\text{int}}(-\text{inhibitor})$  represent the intrinsic membrane transport clearance in the presence and absence of inhibitor, respectively.

It is possible that several different transporters participate in the membrane transport of a drug. When they function in parallel, the net intrinsic clearance under linear conditions is described by the sum of all separate intrinsic clearances:

$$PS_{\text{int}} = \sum_j PS_{\text{int},j} \quad (5)$$

Also, the net degree of inhibition is described by the following equation using the contributions of all transporters to the net membrane transport ( $n_j$ ) [7]:

$$R = \sum_j n_j R_j = \sum_j \frac{n_j}{1 + C_{u,i,j}/K_{i,j}} \quad (6)$$

where  $R_j$  represents the degree of inhibition for each transporter. In the case in which drug–drug interactions involve both the uptake and excretion processes, the net degree of inhibition can be approximated by the following equation [7]:

$$R_{\text{net}} \leq R_{\text{uptake}} \times R_{\text{excretion}} \quad (7)$$

This calculated  $R$  value may be a good criterion for initially investigating the possibility of a drug–drug interaction. For this calculation, the unbound concentration of inhibitor ( $C_{u,i}$ ) and inhibition constant ( $K_i$ ) are required. The inhibition constant can be determined by kinetic analysis of the data from an in vitro transport study using isolated or cultured cells, membrane vesicles, gene expression systems, etc. Human-based experimental systems are recommended to determine kinetic parameters. Although animal-based experimental systems are readily available, they are liable to be subject to species differences in the kinetic parameters and the relative contributions of the transporters. Although the unbound concentrations in the capillary and inside the cells are needed to examine the possibility of any drug–drug interaction involving the uptake and excretion processes, respectively, it is impossible to measure these directly in vivo, particularly in

humans. In order to avoid any false-negative predictions, an approximate estimation of the plasma concentration of an inhibitor is necessary. The maximum plasma concentration in the capillaries, i.e., the arterial plasma concentration at the entrance into the tissue, has been used for this purpose [6,8]. When the inhibitor is coadministered orally, the concentration in the inlet to the liver is often higher than the maximum concentration in the circulating plasma. The unbound concentration of inhibitors in the inlet to the liver ( $I_u$ ) can be approximated by the following equation:

$$C_{u,i} \leq C_{i,\max} + \frac{k_a \cdot D \cdot F_a}{Q_H} \quad (8)$$

where  $k_a$ ,  $F_a$ , and  $Q_H$  represent the absorption rate constant, the fraction absorbed from the gastrointestinal tract into the portal vein, and the hepatic blood flow rate, respectively.

Because  $C_{u,i}$  is overestimated in this prediction method, the possibility of a drug–drug interaction can be excluded if an  $R$  value close to unity is obtained by this prediction method. However, it should be kept in mind that overestimation may increase the number of false-positive predictions. Therefore, if this prediction suggests the possibility of drug–drug interactions, then a more accurate prediction of the disposition of coadministered inhibitor and its inhibitory effect must be investigated using a physiologically based pharmacokinetic model.

### III. METHODS TO EVALUATE TRANSPORTER-MEDIATED DRUG INTERACTIONS

Table 1 shows the in vitro methods for evaluating drug–drug interactions. Details of the experimental conditions are readily available in the references cited in this section.

#### A. In Vitro Transport Systems Using Tissues, Cells and Membrane Vesicles

##### 1. Everted Sac

This method is used to measure drug absorption from the mucosal side to the serosal side [9]. A segment of intestine is everted and, thus, the mucosal side is turned to the outside. Drug absorption is evaluated by measuring the amount of drug that appears inside the sac when the everted sac is incubated in the presence of test compound. Since a segment of intestine is used for the assay, not only transport but also metabolism should be taken into consideration. Barr and Riegelman improved this method so that they could measure the drug concentration time profile in one everted intestine [10].

## 2. Ussing Chamber Method

A fragment of small intestine is opened along the mesenteric border to expose the epithelial cells. After the longitudinal muscle fibers have been carefully stripped from the serosal side, it is mounted on the diffusion cell chamber. The transcellular transport of test compound from the mucosal to the serosal side, and vice versa, is measured to evaluate the drug absorption. There are two routes connecting the mucosal and serosal sides, i.e., the transcellular and paracellular routes. The Ussing chamber method allows the determination of electrophysical parameters such as membrane electroresistance, membrane potential, and short circuit current, and the transport via the transcellular and paracellular routes can be evaluated separately [11,12]. The transport of ionized drug via the paracellular route is sensitive to the potential difference, while that via the transcellular route is not because of the high electrical resistance. By measuring the transport rate at a different potential difference (the voltage clamp method), the contribution of transport via the paracellular route can be evaluated. Also, in this system, metabolism should be taken into account.

## 3. Membrane Vesicles

The methods for preparing the brush border membrane vesicles from intestine, kidney, and choroid plexus, basolateral membrane vesicles from kidney, and sinusoidal and canalicular membrane vesicles from liver and luminal and abluminal membrane of the brain capillary endothelial cells are readily available in the literature [13–20]. The advantages of using membrane vesicles for transport studies are as follows: (1) examining the driving force of transport, by changing the ion composition or ATP concentration; (2) the transport across the basolateral or brush border (apical) membrane can be measured separately; and (3) the intracellular binding and metabolism can be ignored. In order to distinguish intravesicular accumulation from adsorption, the uptake is measured at different osmolarities; the intravesicular space decreases with increased osmolarity [21]. The “overshoot” phenomenon is a feature of the uptake into the membrane vesicles: the uptake into membrane vesicles reaches a maximum and then decreases. This is considered to be due to the consumption of the driving force and subsequent release from inside the vesicles. In order to obtain kinetic parameters for drugs whose time profile shows such an overshoot phenomenon, the kinetic analysis or inhibition must be examined during the initial uptake phase, which reflects the transport activity of the transporter.

It is important to characterize the preparation of membrane vesicles in terms of purity and orientation. Purity can be estimated by the enrichment of the relative activity of marker enzymes for the target plasma membrane [17–20]. There are two orientations in the membrane vesicles, i.e., physiological (right side out) and inverted (inside out) [17–20]. In the case of primary active transport, this orienta-

tion is important. Primary active transporters have ATP binding sites in the intracellular domain. Therefore, only inside-out membrane vesicles can use ATP in the medium as driving force. Indeed, Kamimoto et al. demonstrated canalicular membrane vesicles that are oriented inside out but not right side out exhibit ATP-dependent uptake of daunomycin [22]. Therefore, a low fraction of inside-out membrane vesicles makes it difficult to detect the ATP-dependent uptake of drugs. Generally speaking, as far as secondary or tertiary active transporters are concerned, orientation is not important, because the transport mediated by these transporters is generally bidirectional, as indicated by so-called “countertransport” and “trans-stimulation” phenomena.

#### 4. Caco-2 Cells

Caco-2 cells, which are derived from human colorectal tumor, are used as an *in vitro* system for the intestine [23–25]. Caco-2 cells retain the specific features of intestinal epithelial cells, and differentiate to form tight junction and microvilli, but without a mutin layer. The expression of dipeptide transporter (PEPT1), amino acid transporter, monocarboxylic acid transporter, and P-glycoprotein (P-gp) has been confirmed on the apical membrane corresponding to the brush border membrane [26–29]. Therefore, the Caco-2 cell is a useful model for evaluating drug–drug interactions where those transporters are involved. When Caco-2 cells are cultivated on a porous filter, brush border and basolateral membranes are formed on the apical and basal sides, respectively [30]. After they become confluent, they differentiate and form tight junctions and microvilli [30]. The membrane electroresistance and the permeability of mannitol (a marker for paracellular leakage) reach a plateau at 15 days after seeding [30]. Thus, at least a 15-day culture period is needed for such transport studies. Absorption can be evaluated by measuring transcellular transport across a monolayer of Caco-2 cells cultured on a porous filter. Gres et al. examined the correlation between the fraction absorbed and the permeability from the apical to the basal side of Caco-2 cells using 20 different compounds and showed that the compounds with high permeability were highly absorbed (Fig. 2) [31]. However, the gradient of the correlation is steep, and, in case of a drug that shows moderate permeability, the predictability is low. In addition, the permeability of P-gp substrates from the apical to the basal side is lower than that in the opposite direction due to active efflux on the apical side [32], which was diminished in the presence of P-gp inhibitors (verapamil in Fig. 3) [32]. The permeability of P-gp substrates across the epithelial cells is not consistent with their intrinsic membrane permeability predicted from their lipophilicity.

Metabolic enzymes are expressed in Caco-2 cells: alkalinephosphatase, depeptidase IV, and  $\gamma$ -glutamyltranspeptidase on the brush border membrane, phenolsulfotransferase and glucuronidase and glutathione-S-transferase in cytosol, and CYP1A1 and 1A2 in microsomes [33–35]. CYP3A4 is the main P450 iso-

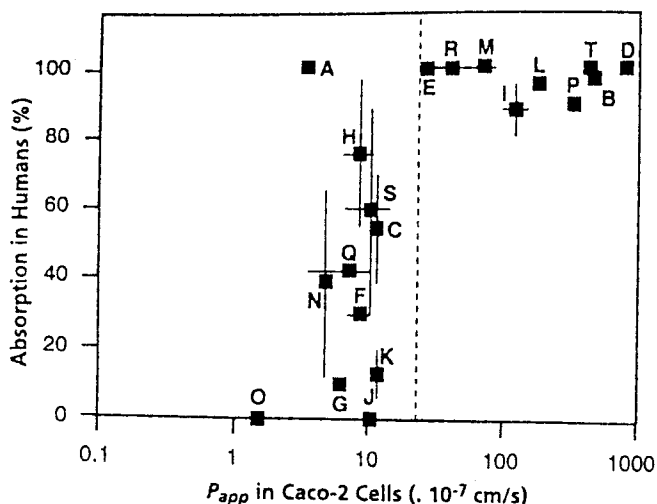


**Figure 2** Correlation between the fraction absorbed and membrane permeability in Caco-2 cells.  $P_{app}$  represents the membrane permeability of the following 20 compounds; it was obtained by measuring the transcellular transport from the apical to the basal side in Caco-2 cells. The fraction absorbed was obtained from the literature. A: amoxicillin; B: antipyrine; C: atenolol; D: caffeine; E: cephalexin; F: cyclosporin A; G: enalaprilate; H: L-glutamine; I: hydrocortisone; J: inulin; K: D-mannitol; L: metoprolol; M: L-phenylalanine; N: PEG-400; O: PEG-4000; P: propranolol; Q: sucrose; R: taurocholate; S: terbutaline; T: testosterone. (From Ref. 31.)

form in human small intestine, but its content in the intestine is not as high as that in the liver [36]. Wachter et al. kinetically demonstrated that the metabolism in the intestine during first pass is not negligible using cyclosporin A as a model compound [36]. However, its expression level is quite low in Caco-2 cells. Schmieclin-Ren et al. and Crespi et al. have established Caco-2 cells with a high CYP3A4 content by culturing in the presence of active vitamin D<sub>3</sub> and gene transfection, respectively [37–39]. They examined the role of CYP3A4 in the first-pass gastrointestinal metabolism of several drugs [37–39]. In addition, Wachter et al. pointed out that the substrates of P-gp overlap those of CYP3A4 and that CYP3A4 and P-gp function cooperatively as a detoxification system in the intestine [40]. Ito et al. investigated this cooperation using a pharmacokinetic model that included metabolism inside the cells and active efflux on the luminal side along the gastrointestinal tract, as well as intracellular diffusion from the luminal to the blood side of the intestinal epithelial cells [41]. When intracellular diffusion is limited ( $\sim 2 \times 10^{-7}$  cm<sup>2</sup>/min), the fraction absorbed after oral administration was elevated by the simultaneous inhibition of both CYP3A4 and P-gp [41].

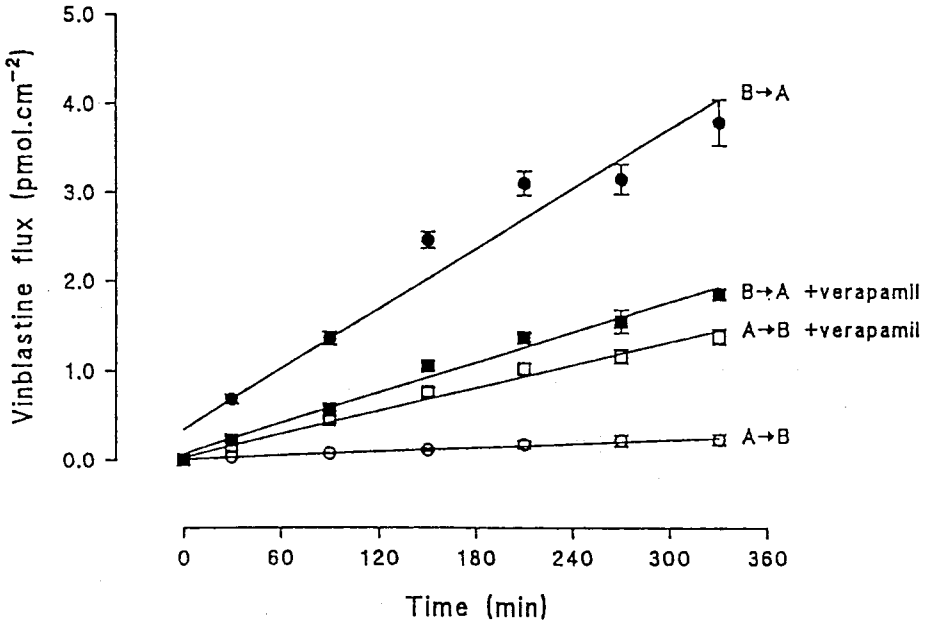


**Figure 3** Time profiles of the transcellular transport of vinblastine in Caco-2 cells, and the effect of verapamil on this transport. The transcellular transport of vinblastine in the presence (+verapamil) and absence of verapamil (100  $\mu$ M) was measured across a monolayer of Caco-2 cells cultured on a porous filter for 14–15 days. B  $\rightarrow$  A corresponds to the transport from the basal to the apical side; A  $\rightarrow$  B is in the opposite direction. (From Ref. 32.)

## 5. LLC-PK1 and OK Cells

Cell lines such as LLC-PK1 and OK cells are used as an in vitro model for the proximal tubule. LLC-PK1 cells are derived from porcine proximal tubule, while OK cells are derived from the kidney of the American opossum. Transcellular transport can be measured across these cells cultured on a porous membrane. Grundemann et al. succeeded in isolating porcine organic cation transporter (OCT2) from LLC-PK1 [42]; therefore, this cell line can be used to examine the urinary excretion of organic cations. However, no transport of *p*-aminohippurate (PAH), a typical substrate of the renal organic anion transporter, was observed in this cell line [43]. In contrast to LLC-PK1 cells, OK cells retain transport activity for PAH in addition to that of cationic compounds such as *N*-methylnicotineamide (NMN) [43,44]. An overshoot phenomenon was observed in the uptake of NMN into apical membrane vesicles prepared from OK cells in the presence

of an outward-directed proton gradient [44]. And, vice versa, the efflux of tetraethylammonium (TEA) was stimulated by an inward-directed proton gradient [44]. This transport property is consistent with that of the brush border membrane of the kidney. The vectorial transcellular transport of organic anions was observed from the basal to the apical side of OK cells [45]. The uptake of PAH from the basal side was inhibited by probenecid [45]. In addition, the efflux of PAH from inside the cells to the apical side was also inhibited by probenecid [45]. This indicates that both uptake and efflux transport are carrier mediated. The efflux of  $\alpha$ -ketoglutarate was stimulated by the addition of PAH to the basal medium [46], which is consistent with the characteristic of an organic anion transporter on the basolateral membrane of the kidney.

## 6. Brain Capillary Endothelial Cells

Primary cultured porcine or bovine brain capillary endothelial cells have been used as an in vitro model for the blood–brain barrier. Recently, an immortalized cell line has been established from mouse, rat, and human brain capillary endothelial cells by infection with Simian virus 40 or transfection of SV40 large T antigen [47–49]. Tatsuta et al. established an immortalized mouse brain capillary endothelial cell line (MBEC4). The activity of  $\gamma$ -glutamyltranspeptidase and alkaline phosphatase, specific marker enzymes for brain capillary endothelial cells, was half that in the brain capillary [47]. Also, P-gp was expressed on the apical membrane of MBEC4 cells, which corresponds to the luminal membrane of the brain capillary [47]. These indicate that MBEC4 cells retain some of the characteristics of brain capillary endothelial cells. It should be noted that *mdr1b*, but not *mdr1a*, is expressed in MBEC4 cells, although *mdr1a* is a predominant subclass in mouse brain capillary endothelial cells [47]. The expression level of *mdr1b* increases in primary cultured rat brain capillary endothelial cells, while that of *mdr1a* decreases [50]. In addition, immortalization and culture increase the expression of multidrug resistance–associated protein 1 (MRP1) [51,52].

## 7. Isolated/Cultured Hepatocytes

Isolated hepatocytes and cultured hepatocytes have been used as an in vitro model of the liver. The hepatic uptake of peptidic endothelin antagonists was measured using isolated rat hepatocytes [53]. When the in vitro uptake clearance of four compounds was extrapolated to give the in vivo uptake clearance based on the assumption of a well-stirred model, they were very close to those obtained by in vivo integration plot analysis (Fig. 4) [53]. Thus, isolated hepatocytes are a good model for evaluating hepatic uptake clearance. Because of progress in cryopreservation techniques, it now seems possible to preserve frozen human hepatocytes in such a way that most of their enzymatic activity is retained [54–56]. They have been used to examine drug metabolism, interactions including induction of meta-



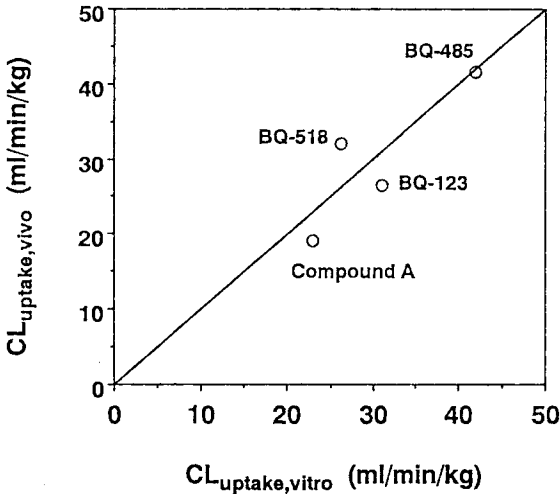


**Figure 4** Comparison between the uptake clearance obtained in vivo and that extrapolated from the in vitro transport study of endothelin antagonists. In vivo uptake clearance of endothelin antagonists (BQ-123, BQ-518, BQ-485, compound A) was evaluated by integration plot analysis using the plasma concentration time profile after intravenous administration (500 nmol/kg) and the amount of drug in the liver and that excreted in the bile. In vitro hepatic uptake clearance was measured using isolated rat hepatocytes and was extrapolated to the in vivo uptake clearance assuming the well-stirred model. (From Ref. 53.)

bolic enzymes. In order to use them to examine drug transport, the degree of transport activity retained in cryopreserved human hepatocytes has to be examined.

Cultured hepatocytes can be applied to measure the hepatic uptake of compounds. Since they attach to the cell-culture dish, it can be washed several times. The expression level of a transporter decreases during culture; a saturable component for the uptake of pravastatin into cultured rat hepatocytes is reduced to 70% by a 6-hour culture, and to 33% by a 24-hour culture, although the nonsaturable component remained constant during culture [2]. The time of culture should be no more than 4–6 hours, the minimum time for cell attachment. Cultured hepatocytes on the collagen-coated dish do not form bile canaliculi, and it is impossible to evaluate the biliary excretion of a drug in this system. LeCluyse et al. demonstrated that a collagen-sandwich configuration made hepatocytes form bile canaliculi [57]. The transport activity was retained to some extent even in 96-hour cultured rat hepatocytes [58]. The cell accumulation of methotrexate, [D-pen<sup>2,5</sup>]-enkephalin and taurocholate was one-fifth to one-half that in a 3-hour culture of hepatocytes and the reduction for salicylate was comparable [58]. Depletion of

$\text{Ca}^{2+}$  disrupts the bile canaliculi [59]. The cumulative biliary excretion of drug in this system is obtained by comparison of the cumulative accumulation in the presence and absence of  $\text{Ca}^{2+}$ . Liu et al. compared in vitro biliary excretion clearance with in vivo intrinsic clearance obtained from biliary excretion clearance based on the well-stirred model and found a good correlation for the five compounds examined (inulin, salicylate, methotrexate, [D-pen<sup>2,5</sup>]enkephalin, and taurocholate) using this system [58].

## B. Gene Expression Systems

The advantage of using a gene expression system is that the kinetic parameters for the target transporter can be obtained. Once the responsible transporters for the drugs in question are identified, the possibility of drug–drug interactions can be examined with the use of the gene expression system. This will save time; otherwise, the uptake or excretion needs to be examined with many possible combinations of drugs. According to our prediction method, the maximum unbound concentration and  $K_i$  are needed to determine the degree of inhibition for each transporter under clinical conditions. They can be obtained from the pharmacokinetic data in clinical trials and from in vitro transport studies, respectively. As mentioned previously, when a drug is transported by several transporters, the contribution of each needs to be estimated to predict the degree of overall drug–drug interaction. In order to determine the contribution, gene knockout mice or animals whose transporter is hereditarily deficient, or specific inhibitors including neutralizing antibody and antisense oligonucleotide, are useful. Animals that are P-gp [Mdr1a (–/–) and Mdr1a/1b (–/–)] or Mrp2/cMOAT deficient (TR<sup>–</sup> rats and Eisai hyperbilirubinemic rats) are available [60,63,64]. Unfortunately, no specific inhibitors have been found; in fact, many inhibitors are known to inhibit multiple transporters. Two approaches have been reported in the literature to evaluate contribution of transporters [65–68]. Injection of cRNA coding a transporter results in its expression on the plasma membrane of *Xenopus laevis* oocytes that have been used for expression cloning or functional analysis. Hybridization of mRNA with antisense oligonucleotide coding a specific sequence for the target transporter reduced the expression of transporter specifically (hybrid depletion method) [65,66]. Comparison of the transport activity in mRNA-injected oocytes in the presence and absence of antisense oligonucleotide gives the contribution of each transporter to the net uptake. Generally speaking, the transport activity of compounds in CRNA-injected oocytes is not as high as that in CRNA-injected oocytes. Thus, this method can be applied to drugs with large uptake clearances. The transport activity of secondary and tertiary active transporter depends on the potential and direction of their driving forces. In order to discuss the contribution quantitatively using this method, it is essential that oocytes mimic the in vivo situation. Kouzuki et al. proposed a method where the contribution of rat

organic anion transporting polypeptide1 (rOatp1) and rat sodium taurocholate co-transporting polypeptide (rNtcp) in cultured rat hepatocytes is evaluated in the uptake of organic anions and bile acids, respectively [67,68]. The scheme for this method is shown in Fig. 5. It is assumed that the relative rOatp1- or rNtcp-mediated transport activity to that of reference compound is not significantly different between cultured rat hepatocytes and cDNA-expressed COS-7 cells in this method. In addition, the reference compound should be a specific substrate; otherwise, the contribution will be overestimated [67,68].

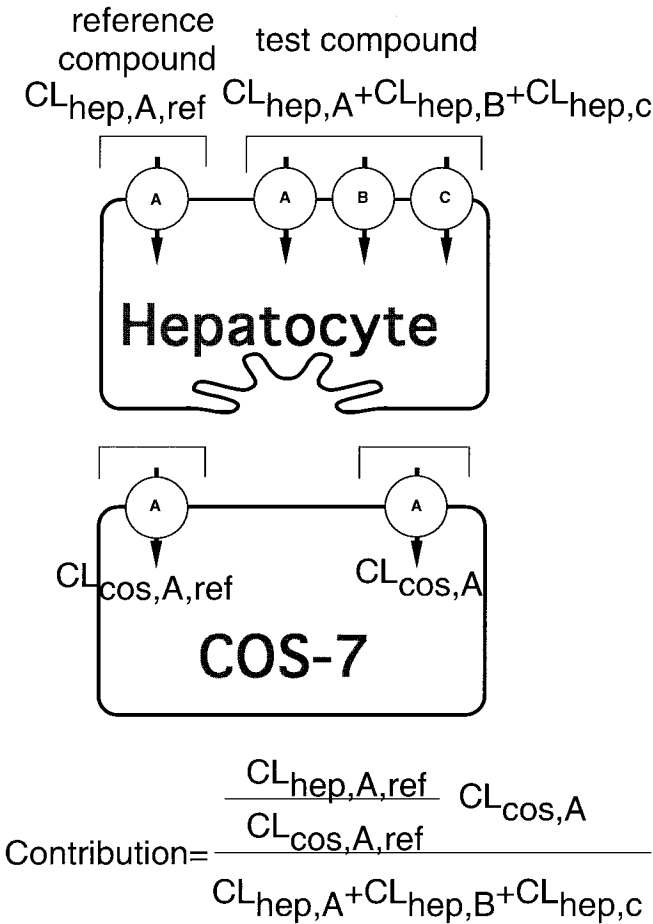


**Figure 5** Schematic diagram to evaluate the contribution of rOatp1 and rNtcp to the hepatic uptake of organic anions.

## IV. TRANSPORTERS

Recently great progress has been made in the identification and isolation of transporter genes. The transporters responsible for drug disposition are summarized in Table 2. In this section, the molecular basis of the transporters is described.

### A. Secondary or Tertiary Active Transporters

#### 1. Organic Cation Transporter (OCT)

The mRNA of rat organic cation transporter 1 (rOCT1) is expressed in both the liver and kidney, although its human counterpart is expressed predominately in the kidney [69,70]. rOCT1 is localized to the sinusoidal membrane surrounding the central vein in the liver and basolateral membrane in the kidney, respectively [71,72]. When rOCT1 is expressed in *Xenopus laevis* oocytes, the uptake of TEA, choline, and NMN was stimulated, and was sensitive to the membrane potential [73]. The OCT1-mediated transport is electrogenic; therefore, it can be detected as a current by electrophysiological methods. Since a current was observed in the presence of type II organic cations such as quinidine, they have been considered to be substrates of rOCT1 [74]. However, no uptake of radiolabeled quinidine was observed using rOCT1-expressed oocytes [75]. Whether they are substrates with a low uptake clearance remains to be clarified. Two homologues (rOCT2 and 3) have been isolated from LLC-PK1 and rat placenta, respectively [42,76]. rOCT2 is expressed in the kidney and brain, while rOCT3 is highly expressed in the placenta and also in the small intestine, brain, and kidney. In contrast to rOCT1, human rOCT2 is localized to the apical membrane of the distal tubule [69]. Comparison of substrate recognition between rOCT1 and rOCT2 was performed using a gene expression system. The inhibition constants of MPP<sup>+</sup>, cimetidine, quinidine, nicotine, NMN, guanidine on rOCT1 or rOCT2-mediated TEA transport were very similar [72]. However, the relative transport activity is different in cDNA transfected HEK 293 cells. For instance, the transport activity of choline relative to MPP<sup>+</sup> was higher in rOCT1 than in rOCT2. Conversely, transport of cimetidine, creatinine, and guanidine was higher in rOCT2 than in rOCT1 [77].

#### 2. Organic Anion Transporting Polypeptide (OATP) Family

rOatp1 was isolated from rat liver as a candidate for sodium-independent uptake of organic anions [78]. Rat oatp1 is localized to the sinusoidal membrane in the liver but is found on the brush border membrane in the kidney and choroid plexus [79,80]. Its substrates include relatively bulky and hydrophobic organic anions and type II organic cations such as *N*-(4,4'-azo-*n*-pentyl)-21-deoxyajmalinium (APDA), *N*-methyl-quinine, and rocuronium, as listed in Table 3 [81–83]. Although rOatp1-mediated transport is active, the driving force has not been identi-

**Table 2** Transporters Responsible for Drug Disposition

	Species	ORF (bp)	AA	Chromosome	Tissue distribution	Localization	Driving force
<b>Facilitate, secondary/tertiary active transporter</b>							
<i>Organic cation transporter</i>							
Oct1	Rat	1668	556		Kidney (proximal tubule), liver, colon	BLM	Membrane potential
Oct1A	Rat	1290	430		ND	ND	ND
OCT1	Human	1659	553	6q25–q26	Liver	ND	ND
Oct2	Rat	1779	593		Kidney, brain	BLM	Membrane potential
OCT2	Porcine	1662	554		ND	ND	ND
OCT2	Human	1665	555	6q25–q26	Kidney (distal tubule)	BBM (?)	ND
Oct3	Rat	1653	551		Placenta, heart, brain, small intestine	ND	Membrane potential
OCTN1	Human	1653	551	5	Ubiquitous (except adult liver), fetal liver, fetal	ND	H <sup>+</sup>
Octn2	Mouse	1671	557		ND	Kidney: BBMV (?)	Na <sup>+</sup> (carnitine)
Octn2/CT1	Rat	1671	557		Ubiquitous	ND	Na <sup>+</sup> (carnitine)
OCTN2	Human	1671	557	5q31	Ubiquitous	Kidney: BBMV (?)	Na <sup>+</sup> (carnitine)
<i>Organic anion transporter</i>							
Oatp1	Rat	2010	670		Liver, brain, liver, kidney	Liver: SM kidney, CPx: BBM	Glutathione
Oatp1	Mouse	2010	670	XA3–A5	Liver, kidney		
Oatp2	Rat	1983	661		Liver, kidney (?), brain, retina	Liver: SM, BCE: LM, ALM, CPx: BLM	ND
Oatp3	Rat	2010	670		Liver (?), kidney (?), retina, brain, small intestine	Small intestine: BBM	ND
Oat-k1	Rat	2007	669		Kidney (proximal tubule)	BBM	Facilitated transport

Oat-k2	Rat	1494	498		Kidney (proximal tubule)	ND	ND
OATP-A	Human	2010	670	12p12	Brain, kidney, liver (?), lung, testes	ND	ND
LST1/Oatp4	Rat	1956/ 2061	652/ 687		Liver	ND	ND
LST1/OATP-C/ OATP2	Human	2073	691	12	Liver	SM	ND
Oatp8	Human	2073	691	12p	Liver	SM	ND
Oat1/NKT	Mouse	1638	546		Kidney, brain	ND	ND
Oat1	Rat	1653	551		Kidney, brain	Kidney: BLM	Dicarboxylate
OAT1	Human	1650	550	11q13.1	Kidney	ND	ND
Oat2/NLT	Rat	1605	535		Liver	Liver: SM	ND
Oat3/Roct	Mouse	1611	537	19		ND	ND
Oat3	Rat	1608	536		Liver, kidney, brain, eye	ND	ND
OAT3	Human	1704	568	11q11.7	Kidney	BLM	ND
OAT4	Human	1650	550		Kidney, placenta	ND	ND
NaPi-1/Npt1	Rat	1395	465		Liver, kidney	Liver: SM	
NaPi-1/NPT1	Rabbit	1395	465		Kidney	Kidney: BBM	
Pept1	Rat	2130	710		Small intestine, kidney	Small intestine, kidney: BBM	H <sup>+</sup>
Pept1	Rabbit	2121	707		Small intestine, liver, brain, kidney	ND	H <sup>+</sup>
PEPT1	Human	2124	708	13q33–q34	Intestine, liver, spleen, kidney, placenta	ND	H <sup>+</sup>
Pept2	Rat	2187	729		Kidney, brain, lung, spleen	Kidney: BBM	H <sup>+</sup>
Pept2	Rabbit	2187	729		Brain, lung, heart, kidney, intestine	ND	H <sup>+</sup>
PEPT2	Human	2187	729	3q13.3–q21	Kidney	ND	H <sup>+</sup>

**Table 2** Continued

	Species	ORF (bp)	AA	Chromosome	Tissue distribution	Localization	Driving force
<b>Primary active transporter</b>							
<i>Organic cation transporter</i>							
Mdr1a	Mouse	3828	1276		Small intestine, heart, brain, liver, kidney, lung, testis	Apical (CM, BBM, LM)	ATP/Mg <sup>2+</sup>
Mdr1b	Mouse	3828	1276		Placenta (during pregnancy), adrenal gland, kidney, heart	Apical (CM, BBM, LM)	ATP/Mg <sup>2+</sup>
MDR1	Human	3840	1280	7.21.1	Brain, liver, kidney, intestine	Apical (CM, BBM, LM)	ATP/Mg <sup>2+</sup>
<i>Organic anion transporter</i>							
Mrp1	Mouse	4584	1528		Muscle, lung, testis, heart, kidney, spleen, brain	Kidney, CPx: BLM	ATP/Mg <sup>2+</sup>
Mrp1	Rat				Choroid plexus		ATP/Mg <sup>2+</sup>
MRP1	Human	4593	1531	16p13.12–13	Lung, spleen, thyroid gland, testis, bladder, adrenal gland	Liver: SM	ATP/Mg <sup>2+</sup>
cMOAT/Mrp2	Rat	4623	1541		Liver, kidney, jejunum	Liver: CM	ATP/Mg <sup>2+</sup>
cMOAT/MRP2	Human	4623	1541	10q24	Liver	Liver: CM	ATP/Mg <sup>2+</sup>
Mrp3	Rat	4569	1523		Intestine, liver (EHBR, TR <sup>-</sup> )	ND	ATP/Mg <sup>2+</sup>
MRP3	Human	4581	1527	17q22	Liver, intestine	Liver: SM	ATP/Mg <sup>2+</sup>

(?): there is a discrepancy; ND: not determined; SM: sinusoidal membrane; CM: canalicular membrane; BLM: basolateral membrane; BBM: brush border membrane; LM: luminal membrane; ALM: abluminal membrane; BCE: brain capillary endothelial cells; CP: choroid plexus.

**Table 3** Substrates of Transporters in Table 2

Transporter	Species	Substrates	Ref. nos.
<b>Facilitate, secondary/tertiary active transporter</b>			
<i>Organic cation transporter</i>			
Oct1	Rat	Adrenaline, choline, cimetidine, creatinine, dopamine, guanidine, 5-hydroxytryptamine, MPP <sup>+</sup> , NMN, noradrenaline, TEA, tyramine	70, 77, 268, 269
OCT1	Human	MPP <sup>+</sup> , NMN, TEA	69, 270, 271
Oct2	Rat	Adrenaline, choline, cimetidine, creatinine, dopamine, guanidine, histamine, 5-hydroxytryptamine, MPP <sup>+</sup> , NMN, noradrenaline, TEA	77, 272, 273
OCT2	Porcine	TEA	42
OCT2	Human	Amantadine, choline, dopamine, histamine, memantine, MPP <sup>+</sup> , NMN, norepinephrine, serotonin	69, 274
Oct3	Rat	Dopamine, guanidine, TEA	76
OCTN1	Human	Carnitine, pyrilamine, quinidine, TEA, verapamil	114, 115
Octn2	Mouse	Carnitine	120, 275
Octn2	Rat	Carnitine	121, 276
OCTN2		Na <sup>+</sup> dependent: acylcarnitine, carnitine, phaloridine, Na <sup>+</sup> independent: pyrilamine, quinidine, TEA, verapamil	116, 117, 121–123
<i>Organic anion transporter</i>			
Oatp1	Rat	Aldosterone, bile acid [TC, GC, TCDC, TUDC], BSP, cortisol, CRC 220, dexamethasone, E3040 sulfate, E217βG, enalaprilat, estrone sulfate, ochratoxin A, ouabain, pravastatin, temocaprilat, <i>N</i> -(4,4'-azo- <i>n</i> -pentyl)-21-deoxyajmalinium, rocuronium	68, 81–83, 86, 98, 277–281
Oatp2	Rat	Biotin, bile acid [TC, CA], DHEAS, digoxin, [D-Pen <sup>2,5</sup> ]enkephalin, Leu-enkephalin, estrone sulfate, ouabain, pravastatin <sup>(b)</sup> , <i>N</i> -(4,4'-azo- <i>n</i> -pentyl)-21-deoxyajmalinium, rocuronium	81, 85–88, 98, 282
Oatp3	Rat	TC, thyroxine, triiodothyronine	88
Oat-k1	Rat	Folate, methotrexate	90
Oat-k2	Rat	Folate, methotrexate, prostaglandin E <sub>2</sub> , TC	89
OATP-A	Human	Bile acid [CA, TC], BSP, estrone sulfate, <i>N</i> -(4,4'-azo- <i>n</i> -pentyl)-21-deoxyajmalinium, <i>N</i> -methyl-quinidine, <i>N</i> -methyl-quinine, rocuronium	81–83, 94, 95



**Table 3** Continued

Transporter	Species	Substrates	Ref. nos.
Lst1/Oatp4	Rat	BSP, estrone sulfate, DHEAS, digoxin, E217 $\beta$ G, leukotriene, C4, TC, prostaglandin E2	99, 305
LST-1/OATP-C/ OATP2	Human	Bilirubin, bilirubin glucuronide DHEAS, eicosanoids, E217 $\beta$ G, estrone sulfate, leukotriene C4, leukotriene E <sub>4</sub> , pravastatin, prostaglandin E <sub>2</sub> , TC, thromboxane B <sub>2</sub> , thyroxine, triiodothyronine	96–98, 306
OATP8	Human	Bile acids [CA, TC], BSP, BQ-123, estrone sulfate, E217 $\beta$ G, DHEAS, digoxin	307, 308
Oat1	Rat	Adefovir, $\alpha$ -ketoglutarate, benzylpenicillin, cAMP, cephaloridine, cGMP, cidofovir, glutarate, indomethacin, methotrexate, ochratoxin A, salicylate, acetylsalicylate, salicyurate, PAH, prostaglandin E <sub>2</sub> , urate	103–107, 283
OAT1	Human	PAH	284, 285
Oat2	Rat	$\alpha$ -Ketoglutarate, acetylsalicylate, methotrexate, PAH, salicylate, prostaglandin E <sub>2</sub>	110
Oat3	Rat	Cimetidine, estrone sulfate, ochratoxin A, PAH	109
OAT3	Human	Cimetidine, E217 $\beta$ G, estrone sulfate, DHEAS, methotrexate, ochratoxin A, PAH, prostaglandin	309
OAT4	Human	DHEAS, estrone sulfate, ochratoxin A, PAH	111
NaPi-1/Npt1	Rat	Benzylpenicillin, mevalonic acid, faropenem, foscarnet	144
NaPi-1	Rabbit	Benzylpenicillin, phenol red, probenecid	143
Pept1	Rat	Di- and tri-peptide, $\beta$ -lactam antibiotics (cefadroxil, cefixime, ceftibuten, cephalixin)	135, 286, 287
Pept1	Rabbit	Di- and tri-peptide, $\beta$ -lactam antibiotics (cyclacillin, cephalixin, cefadroxil)	124, 288
PEPT1	Human	Di- and tri-peptide, $\beta$ -lactam antibiotics (cephalexin, ceftibuten), L-dopa-L-Phe, valacyclovir, L-Val-azidodeoxythymidine	132–134, 289–291
Pept2	Rat	Di- and tri-peptide, bestatin	135
Pept2	Rabbit	Di- and tri-peptide, $\beta$ -lactam antibiotics (cefadroxil)	136
PEPT2	Human	Di- and tri-peptide, $\beta$ -lactam antibiotics (cephalexin)	289, 290, 292
<b>Primary active transporter</b>			
<i>Organic cation transporter</i>			
Mdr1a	Mouse	APM, asimadoline, cyclosporin A, dexamethasone, digoxin, daunorubicin, doxorubicin, domperidone, etoposide, FK-506, HSR-903, indinavir, ivermectin, loperamide, morphine, ondansetron, phenytoin, quinidine, SDZ PSC 833, TBuMA, verapamil, vecuronium, vinblastine	163, 164, 166, 168, 170, 293–299

MDR1	Human	Acebutolol, aldosterone, celiprolol, CPT-11 (carboxylate form), cortisole, cyclosporin A, daunorubicin, dexamethasone, digoxin, diltiazem, domperidone, doxorubicin, estradiol 17 $\beta$ -glucuronide, etoposide, FK506, ivermectine, loperamide, methotrexate, methylprednisolone, morphine, nadolol, nicardipine, ondansetron, phenytoin, ranitidine, rapamycin, rhodamine 123, SN-38 glucuronide, SDZ PSC 833, talinolol, timolol, HIV protease inhibitors (ritonavir, saquinavir, indinavir, nelfinavir), verapamil, vincristine, vinblastine	147, 150, 152–156, 159–162, 169, 300
<i>Organic anion transporter</i>			
MRP1	Human	Calcein, glucuronide conjugates [E217 $\beta$ G, etoposide glucuronide, 6a-hypdeoxycholate glucuronide], glutathione conjugates [aflatoxin B1 glutathione, DNP-SG, ethacynic acid glutathione, GSSG, leukotrienes (C <sub>4</sub> , D <sub>4</sub> , E <sub>4</sub> , NAc), melphalan glutathione], 3 $\alpha$ -sulfatolithocholytaurine, estrone sulfate <sup>(a)</sup> , vincristine <sup>(a)</sup>	177, 182–184
cMOAT/Mrp2	Rat	Ampicilin, cefodizime, ceftriaxone, CPT-11 (carboxylate form), dibromosulfophthalein, glycyrrhizin, glucuronide conjugates [bilirubin glucuronide, cholate 3-glucuronide, E3040 glucuronide, E217 $\beta$ G, grepfloracin glucuronide, liquiritigenin glucuronide, lithocholate 3-glucuronide, naphtol glucuronide, nordeoxycholate 3-glucuronide, SN-38 glucuronide, triiodothyronin glucuronide], glutathione (reduced form), glutathione conjugates [glutathione bimeane, BSP glutathione, bromoisovalerylurea glutathione, DNP-SG, GSSG, leukotrienes (C <sub>4</sub> , D <sub>4</sub> , E <sub>4</sub> , E <sub>4</sub> , NAc),], grepfloracin, methotrexate, 5-methyltetrahydrofolate, 5,10-methylene-tetrahydrofolate, pravastatin, SN-38, temocaprilat, tetrahydrofolate	82, 147, 156, 191–195
cMOAT/MRP2	Human	Leukotriene C <sub>4</sub> , mono- and bis-glucuronosyl bilirubin	301, 302
Mrp3	Rat	Bile acid [TC, GC], glucuronide [6-hydroxy-5,7-dimethyl-2-methylamino-4-(3-pyridylmethyl) benzothiazole (E3040) glucuronide, estradiol 17 $\beta$ -glucuronide], sulfate [TCDC-3-sulfate, tauroolithocholate-3-sulfate]	208, 211

ACE: angiotensin-converting enzyme; E217 $\beta$ G: estradiol 17 $\beta$ -glucuronide; DHEAS: dehydroepiandrosterone sulfate; MPP<sup>+</sup>: 1-methyl-4-phenylpyridinium; NMN: N-methylnicotinamide; TC: taurocholate; a: in the presence of glutathione; b: in oocytes but not transported in the mamrian cells.

fied. Transport activity of taurocholate and leukotriene  $C_4$  was increased and decreased with increased and decreased intracellular concentration of reduced glutathione, respectively [84]. Increased and decreased intracellular glutathione concentration was achieved by the injection of reduced glutathione and treatment with buthionine sulfoximine (BSO) and 1-chloro-2,4-dinitrobenzene (CDNB), respectively [84]. An outward concentration gradient of glutathione, which is abundantly present inside the cells, has been suggested to be the driving force [84]. The contribution of rOatp1 was examined using the method described previously in Sec. II.B. That of taurocholate, cholate, and estrone sulfate was 60, 52, 27%, respectively, when estradiol 17 $\beta$ -glucuronide, a reference compound, is assumed to be transported by only rOatp1 in cultured rat hepatocyte [68]. A large part of the sodium-independent hepatic uptake of organic anions is thought to be mediated by rOatp1. The remainder may be associated with rOatp2 and rLST1/rOatp4 [85,86]. Isoforms of the OATP family—rOatp2, rOatp3, rLST1/rOatp4, rOat-k1, and rOat-k2—have been isolated from rat brain, retina, liver, and kidney, respectively [87–90]. The nucleotide sequences of the rOatp1, rOatp2, and rOatp3 are quite similar, which makes interpretation of Northern blot data difficult. Bands have been detected in the brain, liver, and kidney when full-length rOatp2 cDNA is used as a template for probe preparation [87], although these are detected in the brain and liver when the 3' noncoding region of rOatp2 is used as a template [88]. Since a polyclonal antibody against rOatp2 detected a band in the liver but not in the kidney [85], the expression level of rOatp2 in the kidney may be quite low, if indeed present at all. Immunohistochemical staining revealed the localization of rOatp2 to the sinusoidal membrane of hepatocytes around the central vein, the luminal and abluminal membrane of brain capillary endothelial cells, and the basolateral membrane of choroid epithelial cells [85,86,91]. The substrates of rOatp2 are listed in Table 3. The  $K_m$  values of taurocholate, cholate, estradiol 17 $\beta$ -glucuronide, and estrone sulfate for rOatp2 are quite similar to those for rat rOatp1 [87]. The only exceptions are that rOatp2 shows a threefold-higher affinity for ouabain than rOatp1 [87]. Furthermore, as far as rOatp1 and rOatp2 are concerned, digoxin is a specific substrate of rOatp2, while sulfolithocholate, bromosulphophthalein, leukotriene  $C_4$ , 2,4-dinitrophenyl glutathione (DNP-SG), and gadoxate are specific substrates of rOatp1 [86,87]. rOatp2 also transports type II organic cations such as APDA and rocuronium [81]. Since (1) rOatp2 accepts small peptides such as [D-PEN<sup>2,5</sup>]enkephalin and Leu-enkephalin [85], and (2) it is expressed on the blood–brain barrier [91], rOatp2 may be responsible for the efflux transport of small peptides across the blood–brain barrier [92]. The information available on rOatp3 is limited, but its tissue distribution (liver and kidney) and several substrates (thyroid hormone and taurocholate) have been reported [88]. Both rOat-k1 and rOat-k2 are kidney-specific isoforms of OATP [89,90]. Polyclonal antibody for rOat-k1 detected a band only in the brush border membrane–enriched fraction, but not in the basolateral membrane–enriched fraction [93]. In contrast to other OATPs, rOat-k1-mediated transport was insensitive to an ATP depleter

(sodium azide), suggesting that rOat-k1 is a facilitated transporter [90]. rOat-k2 is a splicing variant of rOat-k1 in the 5' coding region [89], but its substrate specificity is broader than that of rOat-k1. rOat-k1 accepts only folate derivatives, such as methotrexate and folate, while the substrates of rOat-k2 include taurocholate and prostaglandin E<sub>2</sub> in addition to these folate derivatives [89,90].

Human OATP-A (hOATP-A) has been isolated from the liver [94]. hOATP can accept organic anions such as bile acids, a neutral compound ouabain, and type II organic cations such as APDA, *N*-methyl-quinidine, *N*-methyl-quinine, and rocuronium as substrates [81–83,95]. A strong band is observed in the brain using Northern blot analysis [94]. Although hOATP-A mRNA has been detected in the liver and kidney [94], the expression level in the liver remains controversial. When a probe was prepared using the 3'-noncoding region of hOATP as a template, there was no detectable band in the liver [96]. Recently, liver-specific transporter 1 (LST-1, or alternatively referred to as hOATP-C or hOATP2) was isolated from human and rat liver [96–99]. Although the substrate specificity of hLST-1 was similar to rat oatps (Table 3), its amino acid sequence shows at most 40% identity with rat oatps. Both specific expression of hLST-1 in the liver and the observation that pravastatin is also a substrate of hLST-1 but not of hOATP-A [98] suggest that hLST-1, but not hOATP-A, is the dominant isoform responsible for the sodium-independent uptake of organic anions in humans. hOATP-B and hOATP8 have been found on the sinusoidal membrane of the liver [100, 307,308]. Their contribution to the hepatic uptake of organic anions will be examined in the future.

### 3. Organic Anion Transporter (OAT)

Cumulative studies have shown the presence of organic anion transporter on the basolateral membrane of the kidney, and its initial uptake velocity is stimulated by preloading  $\alpha$ -ketoglutarate into the cells or membrane vesicles (the so-called *trans*-stimulation phenomenon) [15,101,102]. rOat1 is a multispecific transporter, and accepts PAH, a typical substrate for this transporter, and relatively hydrophilic organic anions (Table 3) [103–106]. Preincubation of rOat1-expressed oocytes in the presence of  $\alpha$ -ketoglutarate stimulated the initial uptake velocity of PAH, which is consistent with the results obtained using membrane vesicles [106,107]. rOat1 in the kidney was found to localize on the basolateral side [108]. The driving force of rOat1-mediated transport is considered to be an outward concentration gradient of intracellular dicarboxylates.

Three other isoforms—rOat2, rOat3, and human OAT3 and OAT4—have been isolated from rat liver, brain, and human kidney and placenta, respectively [76,109–111]. In contrast to OAT1, the *trans*-stimulation was not observed in these isoforms [109–111,309]. Originally, the sequence of rOat2 was reported as a novel liver-specific transporter (NLT), but it did not show any significant uptake of PAH [76]. However, when Sekine et al. examined the uptake of PAH

in NLT-expressed oocytes, simulated uptake was observed [110]. A single amino acid change occurred in the rOat2 isolated by Sekine, which may affect the transport activity of NLT [110]. The substrate specificity of rOat2 is similar to that of rOat1, as listed in Table 3. Rat rOat3 is expressed in the kidney, liver, eye, and brain [109], while its human counterpart was detected predominantly in the kidney by Northern blot analysis [112,309]. The substrates of OAT3 include estrone sulfate and ochratoxin A [109,309]. Although cimetidine is a cationic compound, it is transported by OAT3. Cimetidine is a bisubstrate, recognized by both organic anion and cation transporters [113]. OAT3 may be partially responsible for the renal uptake of cimetidine. OAT4 is expressed in the kidney and placenta [111]. It accepts sulfate conjugates, ochratoxin A, and PAH, although the transport activity of PAH is quite low [111].

#### 4. OCTN

OCTN1 is strongly expressed in kidney, trachea, bone marrow, and fetal liver, but not in adult liver [114]. When OCTN1 cDNA was transfected to HEK-293 cells, the uptake of TEA was observed [114]. The uptake of TEA via OCTN1 was pH sensitive in HEK-293 cells [114]. An inward proton-concentration gradient stimulated the efflux of TEA in OCTN1-expressed oocytes, indicating that OCTN1-mediated transport couples with proton antiport [115]. The localization of OCTN1 has not yet been described. Since the transport characteristics seem to be consistent with the previous observation using brush border membrane vesicles from the kidney, it is considered to be expressed on the brush border membrane of the kidney. The substrates include quinidine and adriamycin as well as TEA [115]. OCTN2, an isoform of OCTN1, was isolated from human placenta [116]. Although OCTN2 can accept TEA, the transport activity is not as high as that of OCTN1. Carnitine, a zwitter ionic compound, is a cofactor essential for  $\beta$ -oxidation of fatty acids. It has been shown to be an endogenous substrate of OCTN2 [117]. Increased urinary excretion of carnitine due to the lack of the renal reabsorption is specific feature in patients suffering from systemic carnitine deficiency [118,119]. Since OCTN2 is deficient in *jvs* mice, an animal model of systemic carnitine deficiency and several mutations were found in the patients suffering from systemic carnitine deficiency [120], OCTN2 is responsible for the renal absorption. A striking difference was observed in ion requirement for the transport via OCTN2: the transport of carnitine via OCTN2 is sodium dependent, while that of cationic compounds is sodium independent [117,121]. The sodium: carnitine stoichiometry has been reported to be 1:1, and the affinity of carnitine is increased in the presence of sodium [121,122]. In addition to TEA and carnitine, cephaloridine and other cationic compounds, such as verapamil, quinidine, and phryllamine, are substrates of OCTN2 [122,123]. Future studies are required to reveal whether OCTN2 take part in the renal excretion and/or reabsorption of organic cations together with OCTN1.

## 5. Peptide Transporter

In the luminal side of the small intestine, an inward proton-concentration gradient is maintained by an unstirred water layer and  $\text{Na}^+/\text{H}^+$  ATPase. This inward proton-concentration gradient stimulates the uptake of di- or tripeptides into the brush border membrane vesicle prepared from intestine. PEPT1 is expressed in the intestine (duodenum, jejunum, and ileum), kidney, and liver [124,125] and is localized to the brush border membrane [125,126]. The driving force of PEPT1 is an inward proton-concentration gradient, and the stoichiometry differs depending upon the net charge of substrate: the proton:substrate stoichiometry has been reported to be 1:1 for cationic and neutral peptides, and 2:1 for acidic peptides [127]. PEPT1 accepts not only di- and tripeptides, but also several drugs, as listed in Table 3. The substrate recognition was investigated using a series of medium-length fatty acids and revealed that both an amino and a carboxyl group separated by four methylene groups are essential [128]. PEPT1 has attracted attention as a target for drug delivery systems (DDS). Valinyl esterification of the antiviral agent acyclovir showed a three- to fivefold increase in bioavailability [129–131]. Since valacyclovir is a substrate of PEPT1 [132,133], this increase may be due to PEPT1-mediated transport. In addition, this approach has succeeded in improving the intestinal absorption of 2,3-dideoxyazidothymidine (AZT) and L-DOPA modified with L-valine and L-phenylalanine, respectively [133,134].

Unlike PEPT1, PEPT2 is expressed not in the small intestine, but in the kidney and brain [135,136]. In the kidney, PEPT1 is expressed in the early part of the proximal tubule (pars convoluta), while PEPT2 is expressed further along the proximal tubule (pars recta) and localized to the brush border membrane [126,137]; in the brain it is expressed in the glial cells [138]. The transport via PEPT2 is also coupled with the synport of proton. However, the requirement for protons differs between PEPT1 and PEPT2, since the  $\text{H}^+$ :substrate stoichiometry of PEPT2 is 2:1 and 3:1 for neutral and acidic substrates, respectively [139]. PEPT2 generally has a higher affinity for peptides and  $\beta$ -lactam antibiotics, except cefdinir, ceftibuten and cefixime, whose affinities are similar for PEPT1 and PEPT2 [140,141]. There are high- and low-affinity sites responsible for the reabsorption of glycylsarcosine in the brush border membrane of the proximal tubule, and these may correspond to PEPT2 and PEPT1, respectively [142].

## 6. Sodium Phosphate Cotransporter

NaPi-1, alternatively referred to as NPT1, was originally thought to play a role in the reabsorption of phosphate on the brush border membrane to maintain phosphate homeostasis in the body. Saturable uptake of benzylpenicillin was observed in NaPi-1-expressed oocytes [143]. This uptake depends not on sodium and proton, but on chloride [144]. As the extracellular concentration of chloride increases, the uptake of benzylpenicillin falls [144]. The substrates include faro-

penem, foscarnet, and mevalonate as well as benzylpenicillin [144]. In contrast to the kidney, expression is localized to the sinusoidal membrane of the liver [144]. When the direction of the concentration gradient of  $\text{Cl}^-$  is taken into consideration, the transport direction mediated by NaPi-1 is efflux from inside the cells to the blood and urine in the liver and kidney, respectively.

## B. Primary Active Transporters

### 1. P-glycoprotein (P-gp)

It has been found that P-gp is overexpressed on the plasma membrane of multidrug-resistant tumor cells. The mechanism by which P-gp confers multidrug resistance to cells is active efflux of anticancer drugs from inside the cells to outside [145,146]. This results in a reduced intracellular concentration of anticancer drugs. P-gp has two ATP-binding domains (ATP binding cassette; ABC) in the molecule, and efflux transport is a primary active transport process. In normal tissue, P-gp is expressed in the liver, kidney, small and large intestine, and brain capillary endothelial cells and localized to the luminal side, i.e., the brush border membrane in the kidney and intestine, and canalicular membrane in the liver and luminal membrane of the brain capillaries [147–150]. Partridge et al. have suggested that P-gp is expressed not in the brain capillary endothelial cells, but in astrocytes [151].

The rat and mouse counterparts of human MDR1 consist of two isoforms, i.e., Mdr1a (alternatively referred to as Mdr3) and Mdr1b (alternatively referred to as to Mdr1) [147,152–156]. Mdr2, the other isoform of P-gp, does not confer multidrug resistance, but translocates phospholipid in the canalicular membrane [157,158]. The substrate specificity of P-gp is broad, and so P-gp-overexpressed cells show resistance to a variety of drugs with unrelated chemical structures [147,152–156]. The substrates are characterized by their high lipophilicity and planar structure [147,152–154,155,156]. Generally speaking, the substrate carries an overall positive charge or else no charge [147,152–156]. Nevertheless, the carboxylate form of CPT-11, estradiol 17 $\beta$ -glucuronide, and methotrexate have been suggested to be substrates, in spite of their negative charge [159–162].

Together with the localization of P-gp, cumulative studies suggest the role of P-gp in biliary, urinary, and intestinal excretion [147–150,156]. The development of P-gp knockout mice confirmed the contribution of P-gp to biliary, urinary, and intestinal excretion. Disruption of *mdr1b* did not alter the tissue distribution of digoxin [60]. In the *Mdr1a* knockout mouse, the expression level of *Mdr1b* is increased in the liver and kidney, which may compensate for the deficiency of *Mdr1a* [163]. Smit et al. reported a pharmacokinetic analysis of tri-*n*-butylmethylammonium (TBuMA), azidoprocaïnamide methoiodide (APM), and vecuronium [164]. The biliary excretion clearance, renal clearance, and intestinal

excretion clearance of TBuMa fell to 20, 66, and 14% of the normal value, respectively [164]. For APM and vecuronium these were 25, 73, and 9% and 43, 570, and 48%, respectively [164]. In addition, the amounts of digoxin and paclitaxel excreted into the intestine, bile, and urine have been investigated [165,166]. Although the amount excreted into the intestine fell markedly, that into the bile and urine did not differ significantly from normal [165,166]. Even in the *mdr1a/1b* double knockout mouse, the amount of digoxin excreted into the bile fell to half the normal value, while that of paclitaxel was unchanged [60]. Thus, passive diffusion and/or another mechanism are involved in biliary and urinary excretion of digoxin and paclitaxel.

As described previously, a cooperative role of P-gp and CYP3A4 is suggested in the detoxification system of the small intestine [36,40]. We have found that L-754,394 and SDZ PSC 833 are specific inhibitors for CYP3A4 and P-gp, respectively; there was a 200-fold difference in the  $IC_{50}$ , which was determined by examining the inhibition of the metabolism of midazolam using intestinal and liver microsomes and transcellular transport of vinblastine across Caco-2 cells, respectively [167]. These compounds are useful for examining the contribution of metabolism and active efflux to the low fraction of absorption of a drug in question.

The distribution in the brain of P-gp substrate increased considerably relative to the normal value, even when the increased plasma concentration was taken into consideration [163,165,166,168–170]. Since the integrity of the blood–brain barrier is maintained in the *Mdr1a* knockout mouse [171], this was attributed to dysfunction of P-gp in the blood–brain barrier.

## 2. Multidrug-Resistance-Associated Protein1 (MRP1)

MRP1 was isolated from non-P-gp multidrug-resistance tumor cells, HL60AR [172]. The spectrum of the resistance profile in MRP1-expressed tumor cells is quite similar to that of P-gp. MRP1 exhibits resistance to doxorubicin, daunorubicin, epirubicin, vincristine, vinblastine, and etoposide [173,174]. Since the cell accumulation of anticancer drugs in MRP1-expressed cells was reduced relative to that in their parent cells, the mechanism by which MRP1 confers resistance has been attributed to active efflux from the cells [173,175,176]. However, there was no ATP-dependent uptake of these anticancer drugs into the membrane vesicles prepared from MRP1-expressed tumor cells [177,178]. The role of glutathione deserves attention because of the following observations: (1) Buthionine sulfoximine (BSO) is an inhibitor of glutamyl cystein synthetase, which catalyzes the rate-limiting step of the production of GSH, and the concentration of GSH falls in the presence of BSO. The efflux of daunorubicin is reduced in the presence of BSO [179,180]. (2) ATP-dependent uptake of vincristine into membrane vesicles from MRP1-expressed cells was observed only in the presence of GSH [181].



(3) The substrates include glutathione and glucuronide conjugates [177,182–184]. To overcome MRP1-mediated multidrug resistance, inhibitors have been sought; genistein, MK-571, SDZ PSC 833, and verapamil have been identified as potential candidates [177].

Northern blot analysis and RNase protection assay indicated that MRP1 is expressed in the lung, spleen, thymus, testis, bladder, and adrenal gland [175]. The mouse counterpart is also abundantly expressed in muscle [174]. When its cDNA is transfected to LLC-PK1, it is localized to the basal membrane that corresponds to the basolateral membrane under physiological conditions [185]. The physiological role of MRP1 was examined using gene knockout mice. The sensitivity of etoposide increased in the Mrp1 knockout mice [61]. The ATP-dependent uptake of DNP-SG into membrane vesicles prepared from red blood cells was dramatically reduced in Mrp1 knockout mice, which was accompanied by decreased efflux of leukotriene C<sub>4</sub> with increased intracellular accumulation in bone-marrow-derived cells of Mrp1 knockout mice. This causes decreased inflammatory response induced by arachidonic acid in Mrp1 knockout mice [61]. There was no significant difference in the plasma concentration of etoposide between Mdr1a/1b and Mdr1a/1b/Mrp1 knockout mice, while the concentration in the cerebrospinal fluid in Mdr1a/1b/Mrp1 knockout mice was tenfold greater than that in Mdr1a/1b knockout mice, indicating the role of mrp1 in the efflux transport of etoposide from the cerebrospinal fluid [186].

The role of MRP1 in the blood–brain barrier and blood–cerebrospinal fluid barrier was suggested to involve protection at the brain from invasion of xenobiotics in studies using primary cultured and immortalized mouse brain capillary endothelial cells and isolated rat choroid plexus [14,51,52,187,188]. However, the physiological role of MRP1 in the blood–brain barrier is controversial, because increased expression of MRP1 in immortalized or cultured brain capillary endothelial cells has been reported, and the endogenous level of MRP1 in brain capillary endothelial cells is not high [51,52]. In the choroid plexus, there is an efficient excretion system for estradiol 17 $\beta$ -glucuronide [187]. Rapid elimination of estradiol 17 $\beta$ -glucuronide from CSF was observed in rats after intracerebroventricular administration [187]. In addition, a large part of the intracellularly formed 1-naphthol  $\beta$ -glucuronide (~75%) by preloading naphthol into the cells was excreted into the basal side of the primary cultured choroid epithelial cells on a porous membrane [189]. Together with UDP glucuronosyltransferase, MRP1 functions in the detoxification system in the choroid plexus as an efflux transporter on the basolateral membrane.

### 3. Canalicular Multispecific Organic Anion Transporter (cMOAT/MRP2/cMRP)

The mutant rats, such as TR<sup>-</sup> rats and Eisai hyperbilirubinemic rats (EHBR), exhibit hyperbilirubinemia due to a deficiency in biliary excretion of bilirubin

glucuronide [63,64,190]. Canalicular multispecific organic anion transporter (cMOAT) was initially characterized by comparison of *in vivo* biliary excretion clearance and ATP-dependent uptake into the canalicular membrane vesicles between normal and mutant rats [82,147,156,191–195]. The substrates include organic anions such as glutathione conjugates, glucuronides, and relatively lipophilic organic anions with carboxyl group [82,147,156,191–195]. The isolated cDNA that encodes rat cMOAT shows a degree of similarity to MRP1 in the amino acid level [196–198]. Because of the similarity in the amino acid sequence and substrate specificity, cMOAT is alternatively referred to as MRP2. cMOAT is localized to the canalicular membrane in the liver [199] and is not observed in liver from patients suffering from Dubin–Johnson syndrome [196,199]. In addition, a strong band was detected in the jejunum and, to a lesser degree, in the duodenum by Northern blot analysis [197]. There was a negligible difference in the appearance of 1-naphthol  $\beta$ -glucuronide, formed intracellularly from 1-naphthol, in the lumen between normal and mutant rats [200]. In contrast, reduced intestinal excretion of glutathione conjugates was observed in EHBR after intravenous administration of CDNB [201]. This was confirmed using Ussing chamber and everted sac. DNP-SG showed 1.5-fold greater serosal-to-mucosal flux than the opposite direction in normal rats, whereas a similar flux was observed in both directions in EHBR [201]. In addition, metabolic inhibitors reduced the preferential serosal-to-mucosal flux of DNP-SG in normal rats [201]. In everted sac studies, intestinal secretion clearance, defined as the efflux rate of DNP-SG into the mucosal side divided by the area under the curve on the serosal side, was significantly lower in the jejunum of EHBR than that in SD rats [201]. The ATP-dependent uptake of DNP-SG and estradiol 17 $\beta$ -glucuronide was observed in brush border membrane vesicles prepared from Caco-2 cells [202]. Northern blot analysis indicated extensive expression of cMOAT and MRP3 and only minimal expression of MRP1 and MRP5 in Caco-2 cells [202]. These observations suggest a role for cMOAT in active efflux on the brush border membrane.

The human counterpart was isolated from cisplatin-resistant tumor cells (KCP4), where the expression level of cMOAT increased four- to sixfold relative to the parent cells [203]. Antisense oligonucleotide enhances the toxicity of cisplatin, SN-38, vincristine, and doxorubicin to the host cells (HepG2), in parallel with the reduced expression of cMOAT, four- to sixfold, indicating that cMOAT is involved in one of the mechanisms that confer drug resistance in tumor cells [204]. The transport activity of human cMOAT was compared with that of the rat counterpart using canalicular membrane vesicles. The uptake clearance of glutathione conjugates in humans was 10-fold to 40-fold lower than that in rats, while that of glucuronide conjugates was more comparable with that in rats (2-fold to 4-fold lower) [205]. Although the expression level was not normalized, the low transport clearance was due to the low affinity for glutathione conjugates in human [205]. It is not the case in the studies using brush border membrane

vesicles from Caco-2 cells [202]. The  $K_m$  value of DNP-SG was comparable to that in rats [202]. Further studies are required to investigate this discrepancy.

#### 4. MRP3

MRP3 is expressed in the small and large intestine, and in the liver specifically in humans [206–208]. Although the expression level of rat Mrp3 (rMrp3) was below the limit of detection in normal liver, increased expression was detected in the liver of EHBR and TR<sup>-</sup> rat. The localization of MRP3 in the liver is controversial. Orlicz et al. found that it was expressed predominantly in the canalicular membrane in TR<sup>-</sup> rats [209], while König et al. detected a strong signal in the basolateral membrane of two patients with Dubin–Johnson syndrome [210]. In contrast to MRP1 and cMOAT, the transport activity of rMrp3 for glutathione conjugates was quite low, while glucuronides are good substrates of rMrp3 [208]. Striking differences within the MRP family were observed in taurocholate transport. Mrp3 accepts taurocholate and glycocholate as substrate, while the other member does not [211].

### V. EXAMPLES OF DRUG–DRUG INTERACTIONS INVOLVING MEMBRANE TRANSPORT

In this section, examples of the drug–drug interactions involving membrane transport will be described.

#### A. MDR Modulators: Interactions with P-gp

In order to overcome P-gp-mediated multidrug resistance, inhibitors of P-gp have been sought; these are referred to as MDR modulators [212–216]. This is a unique example of a clinical application of a drug–drug interaction aimed at reinforcing the effect of anticancer drugs. Although there are drugs that can inhibit the function of P-gp, their clinical application is limited because of their own pharmacological and/or adverse effects [212–216]. Drugs aimed at overcoming drug resistance have been investigated, and several candidates have been identified, such as SDZ PSC 833 [212–216]. Coadministration of an MDR modulator increases both the intracellular accumulation of anticancer drugs and the survival rate of tumor-bearing mice. Two possible direct and indirect mechanisms have been proposed for the increased intracellular accumulation of anticancer drugs in tumors: (1) inhibition of P-gp-mediated active efflux in the tumor cells and (2) increased plasma retention by inhibiting the elimination of anticancer drugs. P-gp mediates the biliary and urinary excretion of its substrates [147,148] and limits the intestinal absorption of its substrates [150]. Inhibition of P-gp will either reduce the hepatic and renal clearance or increase the bioavailability. In rats given SDZ PSC

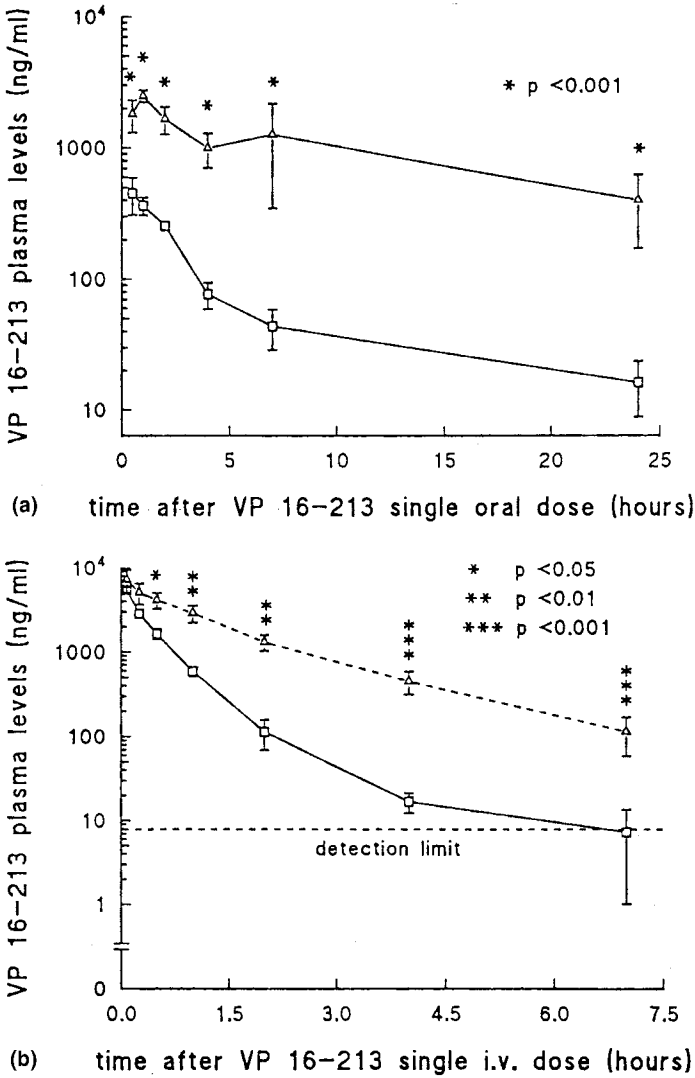


**Figure 6** Alteration of the disposition of etoposide (VP 16-213) by SDZ PSC 833 treatment. Rats were given intravenous SDZ PSC 833 (50 mg/kg;  $\Delta$ ) or solvent ( $\square$ ) for 10 days. On day 6, etoposide (VP 16-213) was administered (a) intravenously (5 mg/kg) or (b) orally (30 mg/kg). (From Ref. 217. Copyright © 1992 American Cancer Society. Reprinted by permission of Wiley-Liss, Inc., a subsidiary of John Wiley & Sons, Inc.)

833, the plasma concentration of etoposide increased considerably (Fig. 6) [217]. The AUC after oral and intravenous administration of etoposide (VP 16-213) exhibited, respectively, 13- and 3-fold increase in SDZ PSC 833-treated rats [217]. It should be noted that MDR modulator may also inhibit the metabolic pathway mediated by CYP3A4, as described previously.

The brain distribution of P-gp substrates is increased significantly in *Mdr1a* and *Mdr1a/1b* knockout mice compared with that in wild type, even when the increased plasma concentration in P-gp knockout mice is taken into consideration [60,163,166,168–171]. Coadministration of MDR modulator produced a similar result [168,218–221]. The brain uptake clearance of quinidine increased 16-fold in rats given intravenous SDZ PSC 833, compared with the uptake clearance in control rats (Fig. 7) [168]. SDZ PSC 833 did not affect the brain uptake of manni-

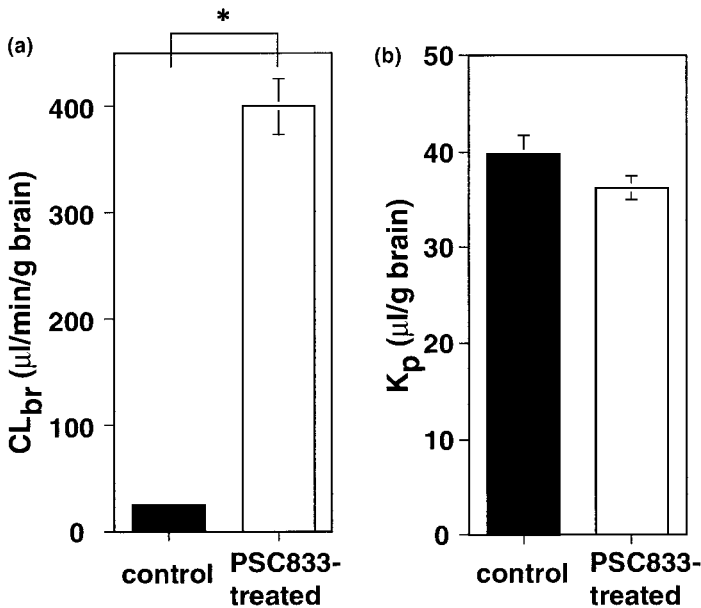


**Figure 7** Effect of SDZ PSC 833 on the brain uptake of (a) quinidine and (b) mannitol in rats. Soon after SDZ PSC 833 (10 mg/kg) or solvent was administered intravenously, quinidine or mannitol was also administered intravenously. The brain uptake clearance of quinidine was determined by integration plot analysis using the plasma concentration–time profile and the amount in the brain. The brain uptake of mannitol was evaluated using the tissue-to-plasma partition coefficient at 5 min after the administration.  $*P < 0.05$ . (From Ref. 168.)

tol [168], indicating that the increase is not due to a nonspecific effect. SDZ PSC 833 had no effect in Mdr1a knockout mice in which the brain distribution of quinidine is significantly increased [168]. Therefore, the effect of SDZ PSC 833 is attributed to inhibition of the efflux transport of quinidine via P-gp at the blood–brain barrier.

## B. Digoxin-Quinidine and -Quinine

Digoxin undergoes both biliary and urinary excretion [222]. The drug–drug interactions between digoxin and quinidine or quinine (a stereoisomer of quinidine) are very well known [222]. The degree of inhibition by quinidine and quinine of the biliary and urinary excretion of digoxin are different; quinine reduced the biliary excretion clearance of digoxin to 65% of the control value, while quinidine reduced both the biliary and renal clearance to 42% and 60%, respectively (Fig. 8) [222]. In proportion to the reduction in total body clearance, coadministration of quinine and quinidine increases the plasma concentration of digoxin 1.1- and 1.5-fold, respectively [222]. In addition to these agents, verapamil has an inhibitory effect, but specifically on the biliary excretion [223]. In another report, a

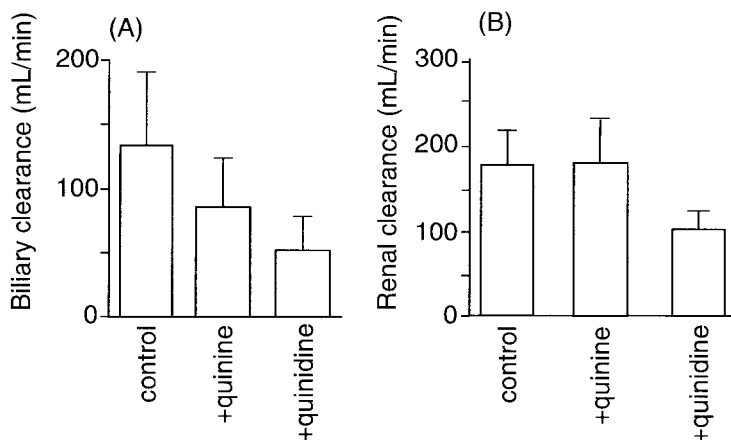


**Figure 8** Change in the biliary and renal clearance of digoxin caused by treatment with quinidine or quinine. After a steady-state concentration of quinine or quinidine was achieved by multiple oral administration, the plasma concentration and the biliary and urinary excretion of digoxin after oral administration were measured in healthy volunteers. The steady-state concentrations of quinine and quinidine were  $7.0 \pm 2.5$ ,  $4.5 \pm 0.5$   $\mu\text{M}$ , respectively. (From Ref. 222.)

slight effect of verapamil on the renal excretion was reported [224]. This may be due to the difference in the plasma concentration of verapamil between two separate clinical trials.

Both the uptake and excretion processes involved in biliary and urinary excretion need to be taken into consideration. No inhibitory effect of quinine and quinidine was obtained in isolated human hepatocytes at a concentration of 50  $\mu\text{M}$  [225]. In contrast to the human situation, stereoselective inhibition of quinine and quinidine has been observed in isolated rat hepatocytes [226]. Quinine inhibits uptake into isolated hepatocytes at the concentration of 50  $\mu\text{M}$ , while the effect of quinidine was minimal (at most a 20% reduction) [226]. Substrates of P-gp, such as vinblastine, daunorubicin, and reserpine, as well as quinine, quinidine, and verapamil, also inhibit the renal excretion of digoxin, although typical substrates for organic cation and anion transport on the basolateral membrane (TEA and PAH) do not [227]. These observations suggest that P-gp is a possible site for this interaction. A pharmacokinetic change in digoxin disposition was observed in Mdr1a and Mdr1a/1b knockout mice [60,165]. The cumulative biliary excretion of digoxin was reduced to 66% (not significantly different) and 50% in mdr1a and mdr1a/1b knockout mice, respectively, compared with that in wild-type mouse [60,165]. On the other hand, the plasma concentration of digoxin increased in Mdr1a and Mdr1a/1b knockout mice was increased twice [60,165]. Taken together, the biliary excretion clearance was considered to be significantly reduced in P-gp knockout mice. In contrast, the role of P-gp in the urinary excretion of digoxin was unclear because of increased cumulative urinary excretion amount in Mdr1a knockout mice [165]. The role of P-gp in this drug–drug interaction has been examined using Mdr1a knockout mice [228]. Coadministration of quinidine caused a 73% increase in the plasma concentration of digoxin in normal mice, whereas it had little effect (20% increase) in Mdr1a knockout mice at the same plasma concentration of quinidine (Fig. 9) [228].

The drug–drug interaction between digoxin and quinidine has been observed in the intestinal absorption of digoxin [229]. The appearance of digoxin on the luminal side of an everted sac of the jejunum and ileum increased in the presence of quinidine or an unhydrolyzed ATP analog, AMPPNP, indicating active efflux into the lumen [229]. Indeed, the intestinal secretion of digoxin was significantly reduced in Mdr1a and Mdr1a/1b knockout mice [60,165]. Therefore, the interaction of quinidine and digoxin involving intestinal absorption may be due to the inhibition of P-gp function.

### **C. Human Immunodeficiency Virus (HIV) Protease Inhibitor: Ritonavir and Saquinavir**

Saquinavir is a potent HIV protease inhibitor with a low bioavailability (0.7%), while ritonavir is well absorbed [230]. Oral coadministration of ritonavir and

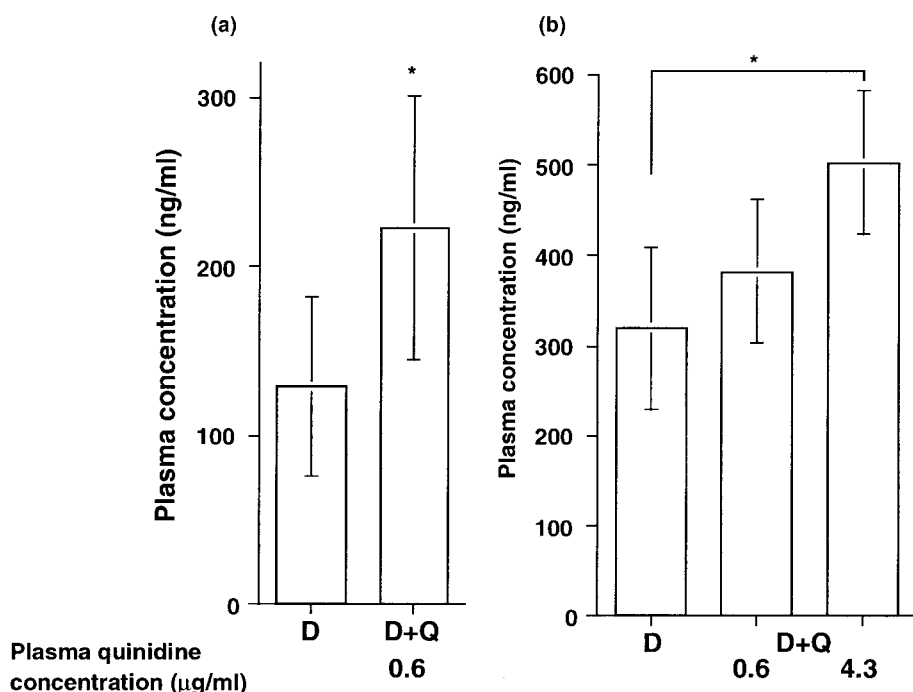


**Figure 9** Effect of quinidine on the plasma concentration of digoxin in (a) wild-type and (b) Mdr1a knockout mice. Plasma concentrations of digoxin 4 hours after intravenous administration (0.5 mg/kg) are shown. Quinidine (40 mg/kg or 100 mg/kg) was administered intraperitoneally 30 min prior to the administration of digoxin. D and D + Q represent the plasma concentration of digoxin administered alone and in combination with quinidine, respectively. \* $P < 0.05$ . (From Ref. 228.)

saquinavir caused a 50- to 100-fold increase in the AUC of saquinavir but did not affect the AUC of ritonavir (Fig. 10) [231]. Both saquinavir and ritonavir are metabolized by CYP3A4 [232,233]. Since ritonavir is a potent inhibitor of CYP3A4, whose  $IC_{50}$  is 150-fold lower than that of saquinavir [233], metabolism may be involved in this drug–drug interaction. In addition, the involvement of P-gp was suggested. The basal-to-apical transport of saquinavir and ritonavir was 50–70 and 15–25 times greater than in the opposite direction in Caco-2 cells [234]. This vectorial transport of saquinavir was abolished completely in the presence of an MDR modulator, GF120918 [234]. These observations indicate that P-gp plays a role in the low bioavailability of saquinavir in addition to the CYP3A4-mediated metabolism [234].



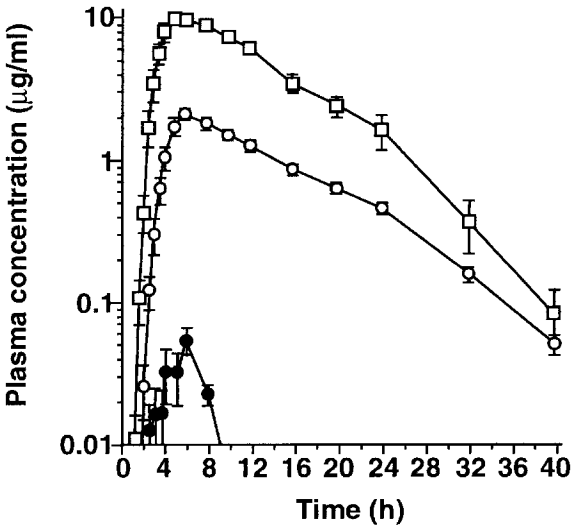


**Figure 10** Change in the disposition of saquinavir caused by ritonavir treatment. Plasma concentration–time profiles for saquinavir administered alone (●) and in combination with ritonavir (□) and for ritonavir administered in combination with saquinavir (□) are shown. Ritonavir (600 mg) and saquinavir (400 mg) were administered in single doses to healthy volunteers. (From Ref. 231.)

#### D. HMG-CoA Reductase Inhibitor: Cerivastatin and Cyclosporin A

In kidney transplant recipients treated with cyclosporin A, the AUC of cerivastatin was 3.8-fold larger than that in healthy volunteers [235]. Since the renal clearance of cerivastatin is negligible, the increased AUC of cerivastatin in the recipients may be caused by a drug–drug interaction [236]. The details of this interaction have not been elucidated. CYP3A4 is responsible for one route of two metabolic pathways of cerivastatin [237]. Since cyclosporin A is a substrate for CYP3A4, metabolism is possibly involved in this interaction. However, the effect of erythromycin, a suicide substrate of CYP3A4, on the AUC of cerivastatin was minimal, suggesting that this hypothesis may not be valid [238]. The hepatobiliary transport of pravastatin, an HMG-CoA reductase inhibitor, has been shown to be carrier mediated (oatp and cMOAT) [4,5]. That of cerivastatin is also expected to be carrier mediated. Since the main elimination route of cerivastatin is metabolism, the most likely site for the drug–drug interaction between cerivastatin and cyclosporin A is the hepatic uptake process.

### **E. Transport via Large Neutral Amino Acid Transporter (LNAAT) Is Affected by Diet**

The pharmacological effect of L-DOPA is affected by diet [239]. The “off” period in Parkinsonian patients treated with L-DOPA is a clinical problem, since the efficacy of the drug fails suddenly. Because of the inverse relationship between the plasma levels of LNAA and the clinical performance of Parkinsonian patients [239], and the fact that the transcellular transport of L-leucine is inhibited by L-DOPA [240] across primary cultured bovine brain capillary endothelial cells, the “off” period may be attributed to the membrane transport of L-DOPA via LNAAT at the blood–brain barrier. In addition to L-DOPA, baclofen and melphalan are suggested to be taken up into the brain via amino acid transport by examining the inhibitory effect of L-leucine and phenylalanine, respectively [240,241]. This indicates that brain transport might be affected by the plasma concentration of large neutral amino acids.

### **F. Bromosulphothalein (BSP)-Probenecid**

Bromosulphothalein and its glutathione conjugate are excreted mainly into the bile under normal conditions [242]. Coadministration of probenecid caused a 3.7-fold increase in the total plasma concentration of BSP and its glutathione conjugate [242]. The hepatic uptake and biliary excretion of BSP are carrier mediated. oatp and cMOAT are responsible for this in rats (see Sec. IV). Since probenecid is an inhibitor of both oatp and cMOAT, the interaction between probenecid and BSP may involve membrane transport.

### **G. Methotrexate–Organic Anions**

A large portion of intravenously administered methotrexate is excreted into the urine in humans [243]. When the renal clearance of methotrexate was measured in the monkey under steady-state conditions, it was three times greater than the glomerular filtration clearance, indicating secretion is involved in the renal excretion [244]. Since the renal excretion of methotrexate is saturable, transporters are responsible for the renal secretion of methotrexate [244]. Coadministration of probenecid (700 mg/m<sup>2</sup>) reduced the renal clearance to the glomerular filtration clearance [244]. The site where methotrexate undergoes secretion was examined using the stop-flow method [245]. A peak appeared at the site corresponding to the proximal tubule in the monkey, indicating that excretion of methotrexate occurs at the proximal tubule, and benzylpenicillin reduced the peak value to 33% of the control value [245]. The interaction between methotrexate and benzylpenicillin was also examined using kidney slices [245]. The uptake of methotrexate

into kidney slices was inhibited by benzylpenicillin in a concentration-dependent manner, and the saturable component was completely inhibited by benzylpenicillin [245]. The molecular mechanism for the excretion of methotrexate has not been identified. Since rOat-k1, rOat-k2, and rOat1 can accept methotrexate as substrate, they may be involved in the renal excretion of methotrexate.

#### **H. Benzylpenicillin-Probenecid**

Benzylpenicillin disappears from the blood very rapidly (the elimination half-life is 30 min in the adult), and 60–90% of the dose is excreted in the urine [243]. The renal clearance is approximately equal to the blood flow rate, indicating a high secretion clearance [243]. In Table 4, the inhibition constant of several organic anions on the uptake of benzylpenicillin into rabbit kidney slices is shown [246]. When the effect of these organic anions on the total body clearance of benzylpenicillin was examined, it was found that probenecid and phenylbutazone reduced its renal clearance to 60%, while sulfipyrazone reduced it to 40% of the control value [246]. Since benzylpenicillin exhibits blood-flow-limited elimination, reduced intrinsic secretion clearance does not affect the renal clearance as much. rOat1 [103] and ratNpt1 [143] are candidates for the transporter responsible for the renal excretion of benzylpenicillin on the basolateral and brush border membranes, respectively, although their individual contributions have not yet been determined.

#### **I. Ranitidine-Probenecid**

The renal clearance of ranitidine accounts for 53% of the total body clearance in the beagle dog. Although ranitidine is a cationic compound, probenecid treatment reduced the total body clearance and renal clearance to 60% and 52% of the control value, respectively [247]. Whether the reduction in nonrenal clearance is ascribable to the inhibition of membrane transport remains to be clarified. According to an analysis using a physiological pharmacokinetic model, the drug–drug interaction between ranitidine and probenecid is due to inhibition of transport across the basolateral membrane. Probenecid reduces the transport on the basolateral membrane to 20% of the control value, but not the transport via the brush border membrane [247]. In the uptake process, both renal organic anion and cation transporters are involved [113].

#### **J. Ciprofloxacin-Probenecid and Furosemide-Probenecid**

Renal clearance accounts for 61% of the total body clearance of ciprofloxacin in humans [243]. Coadministration of probenecid reduces the total body and renal clearance to 59% and 36% of the control value, respectively, but has no effect

**Table 4** Possible Drug–Drug Interactions Involving Renal Excretion

Substrate	Inhibitor	Species	$K_{i, \text{in vitro}}^a$ ( $\mu\text{M}$ )	$\text{CL}_r/\text{CL}_c^b$	$C_{ui}^c$ ( $\mu\text{M}$ )	$R$
Benzylpenicillin	Probenecid <sup>d</sup>	Human	10	0.39	30	0.25
Benzylpenicillin	Phenylbutazone <sup>e</sup>	Human	8.1	0.42	19.6	0.29
Benzylpenicillin	Sulfapyrazone <sup>f</sup>	Human	3.8	0.61	0.9	0.81
Benzylpenicillin	Salicylate <sup>g</sup>	Human	370	0.62	36	0.91
Benzylpenicillin	Indomethacin <sup>h</sup>	Human	40	0.82	0.38	0.99
Benzylpenicillin	Chlorothiazide <sup>i</sup>	Human	24	0.86	0.75	0.97
Benzylpenicillin	Sulfamethoxypyridazine <sup>j</sup>	Human	750	1.18	126	0.86
Methotrexate	Probenecid <sup>k</sup>	Monkey	50 <sup>p</sup>	0.68	80	0.38
			10 <sup>q</sup>			0.11
Ciprofloxacin	Probenecid <sup>l</sup>	Human	50 <sup>p</sup>	0.36	30	0.63
			10 <sup>q</sup>			0.25
Furosemide	Probenecid <sup>m</sup>	Human	50 <sup>p</sup>	0.34	30	0.63
			10 <sup>q</sup>			0.25
Ranitidine	Probenecid <sup>n</sup>	Beagle dog	50 <sup>p</sup>	0.52	4.2 <sup>o</sup>	0.92
			10 <sup>q</sup>			0.70

<sup>a</sup> Inhibition constant determined rabbit kidney slice.

<sup>b</sup> The ratio of renal clearance in the presence ( $\text{CL}_r$ ) and absence ( $\text{CL}_c$ ) of inhibitor. In the case of methotrexate and benzylpenicillin, the ratios of total body clearances are shown. Since their main elimination pathway is urinary excretion, they correspond to the decrease in the renal clearance.

<sup>c</sup> The pharmacokinetic data were obtained from Refs. 243 and 303 for human and monkey, respectively.

<sup>d</sup> 2 g/day for 5–7 days (oral).

<sup>e</sup> 600 mg/day for 5–7 days (oral).

<sup>f</sup> 600 mg/day for 5–7 days (oral).

<sup>g</sup> 3 g/day for 5–7 days (oral).

<sup>h</sup> 75 mg/day for 5–7 days (oral).

<sup>i</sup> 2 g/day for 5–7 days (oral).

<sup>j</sup> 500 mg/day for 5–7 days (oral).

<sup>k</sup> 700 mg/m<sup>2</sup>.

<sup>l</sup> 500 mg and 1000 mg 10 and 2 hr before ciprofloxacin infusion, and 500 mg 4, 10, and 16 hr after the ciprofloxacin infusion.

<sup>m</sup> 1 g (oral).

<sup>n</sup> A loading dose of 375 mg, followed by a constant infusion of 0.5% probenecid (7 ml/hr).

<sup>o</sup> the concentration was available from Ref. 246, and human plasma unbound fraction is used for the calculation.

<sup>p</sup>  $K$  value for uptake into the rabbit kidney slice (Ref. 304).

<sup>q</sup>  $K$  value for uptake into the rabbit kidney slice (Ref. 246).

on the nonrenal clearance [248]. Frusemide undergoes both renal excretion and glucuronidation. Probenecid treatment resulted in a 2.7-fold increase in the AUC of plasma frusemide after oral administration to healthy volunteers [249]. Probenecid reduced the renal clearance of frusemide to 34% of the normal value [249].

### K. Cefadroxil-Cephalexin

Both the dose-normalized AUC of the plasma concentration for 2 hours after administration and the maximum plasma concentration exhibited nonlinearity, when cefadroxil, a  $\beta$ -lactam antibiotic, was administered at different oral doses from 5 to 30 mg/kg orally [250]. Coadministration of cephalexin (15 mg/kg) reduced both the AUC and  $C_{\max}$  of cefadroxil [250]. Since cefadroxil and cephalexin are substrates of PEPT1 [251], this interaction may be accounted for by an interaction at the binding site of PEPT1 [250].

### L. Tolbutamide-Sulfonylurea

Coadministration of tolbutamide and sulfonylurea derivatives causes severe hypoglycemia [252]. Two possible mechanisms for this interaction have been proposed: (1) a change in the plasma protein binding of tolbutamide, and (2) inhibition of metabolism [253,254]. Sulfaphenazole treatment increased the tissue-to-plasma partition coefficient ( $K_p$ ) of tolbutamide in rats. This was due to an increase in the unbound concentration of tolbutamide, since the  $K_{p,f}$  values obtained via division of the  $K_p$  value by the unbound fraction were comparable in all tissues except the brain and spleen [255]. The mechanism in the spleen remains to be clarified. The active efflux transport at the BBB is ascribed to an increase of  $K_{p,f}$  of tolbutamide in the brain based on the following observations: The  $K_{p,f}$  of tolbutamide in the brain increased with the increase in brain concentration [256]. The basal-to-apical transport of tolbutamide was greater than in the opposite direction in MBEC4 cells cultured on porous filters [256]. Since sulfonylurea derivatives, such as sulfaphenazole, sulfadimethoxine, and sulfamethoxazole, inhibit this efflux transport, interactions at the blood-brain barrier may be accounted for by inhibition of the efflux transport of tolbutamide [256]. Neither cyclosporin A nor verapamil affects the cellular accumulation of tolbutamide, suggesting the presence of an efflux transporter other than P-gp [256].

## VI. EXAMPLES OF THE PREDICTION OF DRUG-DRUG INTERACTIONS BASED ON LITERATURE DATA

In this section, the methodology described earlier has been applied to the prediction of in vivo drug-drug interactions from in vitro data gathered from the literature.

### A. Quinidine-Digoxin

Since the pharmacokinetic parameters of quinidine are available from the literature, the prediction of an interaction between digoxin and quinidine is examined in this section. Neither quinidine nor quinine inhibits the uptake of digoxin into isolated human hepatocytes at a concentration of 50  $\mu\text{M}$  [25]. Hedman and Meijer reported that quinidine has a slight effect on the hepatic uptake of digoxin; while quinine inhibited the hepatic uptake of digoxin almost completely at 50  $\mu\text{M}$  in isolated rat hepatocyte [226]. However, according to Okudaira et al., both quinidine and quinine have inhibitory effect in rats [257]. The minimum inhibition constant (50  $\mu\text{M}$ ) estimated from Okudaira's report is used in order to avoid a false-negative prediction. The drug-drug interaction between quinidine and digoxin in healthy volunteers was examined under steady-state conditions. The steady-state concentration of quinidine was 4.5  $\mu\text{M}$ . The plasma unbound fraction is 0.13, and its unbound concentration is estimated as 0.59  $\mu\text{M}$ . Since quinidine and digoxin were administered orally, the inlet concentration needs to be estimated according to the Eq. (8), and the value is estimated to be 4.0  $\mu\text{M}$  using  $Q_H = 1.6 \text{ L/min}$ ,  $F_a = 0.8$ ,  $k_a = 0.1 \text{ min}^{-1}$ , and  $f_u = 0.13$ . Therefore,  $R$  value is calculated as 0.92 indicating that the interaction between quinidine and digoxin on the basolateral side is none or minimal:

$$R = \frac{1}{1 + C_{u,i}/K_i} = \frac{1}{1 + 4.6/50}$$

The  $K_i$  value of quinidine for the transport of digoxin on the bile canaliculi has not been determined. The ATP-dependent uptake of quinidine into canalicular membrane vesicles was saturable with a  $K_m$  value of 5  $\mu\text{M}$  [258]. Since quinidine is a substrate of P-gp [168], it may represent the  $K_m$  value for P-gp, i.e., the  $K_i$  value for digoxin transport via P-gp. In the prediction of drug-drug interaction in excretion process from inside the cells, intracellular unbound concentration of coadministered drug is necessary to be estimated. To measure the tissue unbound concentration is practically impossible in humans. As a safety margin, the cell-to-plasma unbound concentration ratio is assumed to be 10. The  $R$  value of the interaction between digoxin and quinidine is calculated as 0.098 under such approximation, while it can be calculated as 0.52 when the cell-to-plasma unbound concentration ratio is assumed to be 1. Thus, quinidine treatment will reduce the biliary excretion to 9.8–52% of the normal value. To predict a drug-drug interaction in the renal excretion, the  $R$  value can be calculated for renal clearance as 0.46 and 0.89 when the concentration ratio is assumed to be 10 and 1, respectively. Thus, the renal clearance may be affected, but not so much as observed in the liver.

### B. Drug-Drug Interactions with MDR Modulators

An MDR modulator, SDZ PSC 833, increases the brain uptake clearance of quinidine in rats [168]. For quantitative prediction, the intracellular unbound concen-

tration of SDZ PSC 833 is required. Since SDZ PSC 833 is a very lipophilic compound, the uptake process is considered to involve passive diffusion. Therefore, the intracellular unbound concentration is assumed to be the same as the plasma unbound concentration in the brain capillaries. The plasma concentration of SDZ PSC 833 was 12.4–18.5  $\mu\text{M}$  up to 10 min after intravenous administration of 10 mg/kg to rats [259], and the plasma unbound concentration was estimated to be 0.25–0.56  $\mu\text{M}$  using the human plasma unbound fraction (0.02–0.03) [260]. The  $K_i$  value of SDZ PSC 833 for P-gp was determined to be 0.06 or 0.3  $\mu\text{M}$ . The former was determined from the ability to overcome multidrug resistance in P-gp-expressed murine monocytic leukemia P388 [261], and the latter was determined by the degree of inhibition of the ATP-dependent uptake of daunomycin into canalicular membrane vesicles [262]. Since the maximum value of  $C_{u,i}/K_i$  is 9.3, inhibition of the active efflux via P-gp leads to a 90% reduction, as calculated by the following equation:

$$R = \frac{1}{1 + 0.56/0.06} = 0.097$$

Indeed, the brain uptake clearance of quinidine was increased 20-fold in the presence of SDZ PSC 833.

### C. Interactions of Methotrexate and Benzylpenicillin with Other Organic Anions

Table 4 summarizes the  $K_i$  values of coadministered drugs for the uptake of methotrexate, benzylpenicillin, ranitidine, and ciprofloxacin into rabbit kidney slices, the degree of reduction in renal clearance, and the  $R$  values [245]. Because the plasma concentration of inhibitors was not measured,  $C_{u,i}$  was estimated in proportion to the maximum plasma concentration produced by the clinical dose [243]. Good agreement is observed between  $R$  values and the renal clearance change caused by coadministered drug in the combinations of benzylpenicillin-probenecid, benzylpenicillin-phenoxybutazone, benzylpenicillin-sulfamethoxy-pyridazine, and methotrexate-probenecid (Table 4). However,  $R$  values in other combinations do not suggest the reduction by coadministration, because it was observed in vivo. This may be due partially to an inaccurate estimation of the plasma concentration and a species difference in the  $K_i$  value between rabbits and humans. It is also possible that the drug–drug interaction does not involve uptake, but rather excretion.

Indomethacin has been reported to inhibit rOat1 and rOat-k1 [104,263] but not rOat3 [14]. The possibility of a drug–drug interaction via these transporters has been examined. Although indomethacin is also a substrate of rOat1, the transport activity is not high enough to determine the kinetic parameters [104]. The

$K_i$  value of indomethacin for the transport of PAH via rOat1 is adopted in the calculation. When it is taken into consideration that the maximum plasma concentration of indomethacin under clinical conditions is  $0.07 \mu\text{M}$  [243], the drug–drug interaction involving indomethacin via rOat1 is negligible (the  $R$  value is 1). In rats, rOat-k1 and rOat-k2 can accept methotrexate [89,90], and nonsteroidal anti-inflammatory drugs inhibit the transport via rOat-k1 [263]. However, the  $K_i$  value ( $1.0 \text{ mM}$ ) is significantly greater than the maximum plasma unbound concentration, even although a tenfold concentration ratio is assumed. The possibility of a drug–drug interaction by indomethacin via rOat-k1 is negligible.

#### D. Bromosulfophthalein (BSP)-Probenecid

As described earlier, the hepatobiliary transport of BSP is mediated by organic anion transporters. The clinical dose of probenecid is, at most, 1 g. The maximum plasma concentration after oral administration of 1 g was about  $250 \mu\text{M}$  [264]. The concentration of the inlet to the liver is calculated as  $550 \mu\text{M}$  using  $Q_H = 1.2 \text{ L/min/60 kg body weight}$ ,  $F_a = 100\%$ , and  $k_a = 0.1 \text{ min}^{-1}$ . Although the plasma protein binding exhibits nonlinearity, the plasma unbound fraction is 0.08–0.12 over this concentration range where the possibility of drug–drug interaction is examined [264]. Thus, the maximum plasma unbound concentration is found to be  $66 \mu\text{M}$ .

Although the  $K_i$  value of probenecid on the hepatic uptake of BSP has not been determined, the  $K_i$  value of probenecid for oatp1 is reported to be approximately  $100 \mu\text{M}$  [265]. Although all oatps are expressed in the liver [78,87,88], their contribution to the hepatic uptake of BSP has not been determined. Assuming that the  $K_i$  values of probenecid for members of the OATP family are not significantly different, the  $R$  value can be calculated as 0.60. And BSP is excreted into the bile by cMOAT [266]. The  $K_i$  value of probenecid has been determined to be  $44 \mu\text{M}$  using rat canalicular membrane vesicles (unpublished data), so the  $R$  value can be calculated to be 0.40 and 0.063 when the concentration ratio of probenecid is assumed to be 1 and 10, respectively. Thus, the net  $R$  value, obtained by multiplying the  $R$  values of the uptake and excretion processes, is 0.24 and 0.038, respectively. The increase in the plasma concentration of BSP (including glutathione conjugates) caused by probenecid was 3.7-fold [242]. The  $R$  value was, thus, considerably underestimated when the concentration ratio was taken as 10.

#### E. Cefadroxil and Cephalexin

Both the  $C_{\text{max}}$  and AUC up to 2 hours after oral administration of cefadroxil were reduced by coadministration of cephalexin [250]. Quantitative prediction of the interactions involving absorption is quite difficult, because of the diffi-



culty in estimating the unbound concentration in the lumen, where drugs undergo absorption. Both cefadroxil (5 mg/kg) and cephalixin (45 mg/kg) were administered as a 200-ml suspension [250]. If this suspension is assumed not to undergo any dilution during transit into the small intestine followed by drug dissolution, the concentration of 200 ml is equal to the unbound concentration in the lumen. When the calculated drug concentration exceeds the solubility, this solubility should be used in any further calculations. Based on this assumption, the following unbound substrate and inhibitor concentrations were obtained:

$$I = \frac{\text{dose}}{200 \text{ ml}} = \frac{5666}{200} = 28.3 \text{ mM}$$

$$S = \frac{\text{dose}}{200 \text{ ml}} = \frac{787}{200} = 3.94 \text{ mM}$$

The  $K_m$  value of cephalixin (7.5 mM) determined using Caco-2 cells is used as the  $K_i$  value in this prediction [23]. Since the  $K_m$  value of cefadroxil was found to be 5.9 mM using the rat in situ perfusion method [267], the substrate concentration is not low enough to be negligible relative to its  $K_m$  value. Therefore, the substrate concentration should be taken into consideration, and the  $R$  value is obtained from the following equation:

$$R = \frac{5.9 + 3.94}{5.9 \times (1 + 28.3/7.5) + 3.94} = 0.31$$

Therefore, coadministration of cephalixin reduces the absorption clearance to 30%. In this calculation, the same concentration is assumed from entrance to exit. However, this is unrealistic because drugs undergo absorption and, thus, the concentration at exit is lower than that at entrance. And the dilution in the gastrointestinal tract is not taken into consideration.

## F. Sulfonamide and Tolbutamide

The plasma concentration of sulfamethoxazole at the steady-state concentration was found to be 2.0 mM [255]. Since the human plasma unbound fraction of sulfamethoxazole is 0.48 [243], the unbound plasma concentration can be calculated as 0.96 mM. The inhibition constant was estimated to be 2.0 mM from the inhibitory effect of sulfamethoxazole on the transcellular transport of tolbutamide from the basal to the apical side. Thus, the  $R$  value can be calculated as 0.68,

which is not so much different from in vivo observation; the  $K_{p,f}$  of tolbutamide exhibited a threefold increase in sulfamethoxazole-treated rats [255]. In the estimation of the inhibition constant of sulfamethoxazole, it was assumed that sulfamethoxazole does not affect the uptake process, and there is not a significant difference in the inhibition constant between mice and rat and between the MBEC4 cell-to-medium and brain capillary endothelial cell-to-plasma concentration ratio of sulfamethoxazole.

The clinical dose of sulfamethoxazole is 1 g (twice a day). When 1000 mg sulfamethoxazole is administered orally, the maximum plasma concentration is 304  $\mu\text{M}$  using a distribution volume = 13 L/60 kg body weight and  $F_a = 100\%$ . Thus, the unbound concentration can be calculated to be 146  $\mu\text{M}$ . If the species difference in the  $K_i$  value and concentration ratio of sulfamethoxazole between mice and humans is negligible, the  $R$  value is 0.93. Under clinical conditions, no drug–drug interaction involving the active efflux of tolbutamide will occur under such assumptions.

## VII. SUMMARY

In addition to P450 enzymes, transporters play an important role in drug disposition and, therefore, it is possible that drug–drug interactions at the site of transporters alter the plasma concentration–time profiles. Indeed, the interactions between drugs like quinidine-digoxin and probenecid-benzylpenicillin are transporter-mediated. We also reviewed in vitro experimental models for investigation of these drug–drug interactions. In addition, a procedure is described that allows the prediction of such interactions using maximum plasma unbound concentration at the clinical dosage and inhibition constant of a coadministered drug for the membrane transport process of the drug in question. This method is useful for initial investigations, but more precise pharmacokinetic analyses are subsequently required for quantitative prediction when the prediction suggests that a drug–drug interaction is likely.

Transporters are also summarized in this chapter. Multispecific transporters for both organic anions and cations, which accept structurally unrelated substances, play a significant role in the hepatobiliary and renal transport processes. They can be classified into several families, such as OCT, OATP, OAT, MDR, and MRP, in terms of the similarities in the amino acid sequence and substrate specificity. There are drugs that are recognized by several transporters localized on the same membrane, and multiple transporters are expected to be involved in the membrane transport process. Therefore, the contribution of each transporter to the net membrane transport process is taken into consideration when the observations in gene expression systems are extrapolated to in vivo situations.

## ACKNOWLEDGMENTS

We would like to thank Hiroshi Suzuki, Yukio Kato, Kiyomi Ito, Kosei Ito, Yoshihisa Shitara, Daisuke Sugiyama, and Yoko Ootsubo-Mano for sharing meaningful discussions with us, giving us useful suggestions, and helping collect information to prepare this manuscript. This work was supported by CREST, Japan Science and Technology Corporation.

## REFERENCES

1. T Komai, K Kawai, T Tokui, Y Tokui, C Kuroiwa, E Shigehara, M Tanaka. Disposition and metabolism of pravastatin sodium in rats, dogs and monkeys. *Eur J Drug Metab Pharmacokinet* 17:103–113, 1992.
2. M Ishigami, T Tokui, T Komai, K Tsukahara, M Yamazaki, Y Sugiyama. Evaluation of the uptake of pravastatin by perfused rat liver and primary cultured rat hepatocytes. *Pharm Res* 12:1741–1745, 1995.
3. I Tamai, H Takanaga, H Maeda, T Ogihara, M Yoneda, A Tsuji. Proton-cotransport of pravastatin across intestinal brush-border membrane. *Pharm Res* 12:1727–1732, 1995.
4. M Yamazaki, S Akiyama, K Ni'inuma, R Nishigaki, Y Sugiyama. Biliary excretion of pravastatin in rats: contribution of the excretion pathway mediated by canalicular multispecific organic anion transporter. *Drug Metab Dispos* 25:1123–1129, 1997.
5. M Yamazaki, H Suzuki, M Hanano, T Tokui, T Komai, Y Sugiyama. Na(+)-independent multispecific anion transporter mediates active transport of pravastatin into rat liver. *Am J Physiol* 264:G36–44, 1993.
6. K Ito, T Iwatsubo, S Kanamitsu, K Ueda, H Suzuki, Y Sugiyama. Prediction of pharmacokinetic alterations caused by drug–drug interactions: metabolic interaction in the liver. *Pharmacol Rev* 50:387–412, 1998.
7. K Ueda, Y Kato, K Komatsu, Y Sugiyama. Inhibition of biliary excretion of methotrexate by probenecid in rats: Quantitative prediction of interaction from in vitro data. *J Pharmacol Exp Ther* (in press).
8. K Ito, T Iwatsubo, S Kanamitsu, Y Nakajima, Y Sugiyama. Quantitative prediction of in vivo drug clearance and drug interactions from in vitro data on metabolism, together with binding and transport. *Annu Rev Pharmacol Toxicol* 38:461–499, 1998.
9. T Wilson, G Wiselman. The use of sacs of everted small intestine for the study of the transference of substances from the mucosal to serosal surface. *J Physiol* 123: 116–125, 1954.
10. WH Barr, S Riegelman. Intestinal drug absorption and metabolism. II. Kinetic aspects of intestinal glucuronide conjugation. *J Pharm Sci* 59:164–168, 1970.
11. RA Frizzell, MJ Koch, SG Schultz. Ion transport by rabbit colon. I. Active and passive components. *J Membr Biol* 27:297–316, 1976.

12. RA Frizzell, SG Schultz. Ionic conductances of extracellular shunt pathway in rabbit ileum. Influence of shunt on transmural sodium transport and electrical potential differences. *J Gen Physiol* 59:318–346, 1972.
13. R Kannan, A Mittur, Y Bao, T Tsuruo, N Kaplowitz. GSH transport in immortalized mouse brain endothelial cells: evidence for apical localization of a sodium-dependent GSH transporter. *J Neurochem* 73:390–399, 1999.
14. H Kusuvara, H Suzuki, M Naito, T Tsuruo, Y Sugiyama. Characterization of efflux transport of organic anions in a mouse brain capillary endothelial cell line. *J Pharmacol Exp Ther* 285:1260–1265, 1998.
15. JB Pritchard, DS Miller. Mechanisms mediating renal secretion of organic anions and cations. *Physiol Rev* 73:765–796, 1993.
16. MM Sanchez del Pino, RA Hawkins, DR Peterson. Neutral amino acid transport by the blood-brain barrier. Membrane vesicle studies. *J Biol Chem* 267:25951–25957, 1992.
17. H Murer, P Gmaj, B Steiger, B Hagenbuch. Transport studies with renal proximal tubular and small intestinal brush border and basolateral membrane vesicles: vesicle heterogeneity, coexistence of transport system. *Methods Enzymol* 172:346–364, 1989.
18. JL Boyer, PJ Meier. Characterizing mechanisms of hepatic bile acid transport utilizing isolated membrane vesicles. *Methods Enzymol* 192:517–533, 1990.
19. E Kinne-Saffran, RK Kinne. Isolation of luminal and contraluminal plasma membrane vesicles from kidney. *Methods Enzymol* 191:450–469, 1990.
20. PJ Meier, JL Boyer. Preparation of basolateral (sinusoidal) and canalicular plasma membrane vesicles for the study of hepatic transport processes. *Methods Enzymol* 192:534–545, 1990.
21. PJ Meier, A St. Meier-Abt, C Barrett, JL Boyer. Mechanisms of taurocholate transport in canalicular and basolateral rat liver plasma membrane vesicles. Evidence for an electrogenic canalicular organic anion carrier. *J Biol Chem* 259:10614–10622, 1984.
22. Y Kamimoto, Z Gatmaitan, J Hsu, IM Arias. The function of Gp170, the multidrug resistance gene product, in rat liver canalicular membrane vesicles. *J Biol Chem* 264:11693–11698, 1989.
23. AH Dantzig, L Bergin. Uptake of the cephalosporin, cephalixin, by a dipeptide transport carrier in the human intestinal cell line, Caco-2. *Biochim Biophys Acta* 1027:211–217, 1990.
24. G Wilson. Cell culture techniques for the study of drug transport. *Eur J Drug Metab Pharmacokin* 15:159–163, 1990.
25. L Barthe, J Woodley, G Houin. Gastrointestinal absorption of drugs: methods and studies. *Fundam Clin Pharmacol* 13:154–168, 1999.
26. R Kekuda, V Torres-Zamorano, YJ Fei, PD Prasad, HW Li, LD Mader, FH Leibach, V Ganapathy. Molecular and functional characterization of intestinal Na(+) -dependent neutral amino acid transporter B0. *Am J Physiol* 272:G1463–1472, 1997.
27. I Tamai, H Takanaga, H Maeda, Y Sai, T Ogihara, H Higashida, A Tsuji. Participation of a proton-cotransporter, MCT1, in the intestinal transport of monocarboxylic acids. *Biochem Biophys Res Commun* 214:482–489, 1995.
28. SK Basu, J Shen, KJ Elbert, CT Okamoto, VH Lee, H von Grafenstein. Develop-

- ment and utility of anti-PepT1 anti-peptide polyclonal antibodies. *Pharm Res* 15: 338–342, 1998.
29. J Hunter, MA Jepson, T Tsuruo, NL Simmons, BH Hirst. Functional expression of P-glycoprotein in apical membranes of human intestinal Caco-2 cells. Kinetics of vinblastine secretion and interaction with modulators. *J Biol Chem* 268:14991–14997, 1993.
  30. V Meunier, M Bourrie, Y Berger, G Fabre. The human intestinal epithelial cell line Caco-2: pharmacological and pharmacokinetic applications. *Cell Biol Toxicol* 11:187–194, 1995.
  31. MC Gres, B Julian, M Bourrie, V Meunier, C Roques, M Berger, X Boulenc, Y Berger, G Fabre. Correlation between oral drug absorption in humans, and apparent drug permeability in TC-7 cells, a human epithelial intestinal cell line: comparison with the parental Caco-2 cell line. *Pharm Res* 15:726–733, 1998.
  32. J Hunter, BH Hirst, NL Simmons. Drug absorption limited by P-glycoprotein-mediated secretory drug transport in human intestinal epithelial Caco-2 cell layer. *Pharm Res* 10:743–749, 1993.
  33. A Baranczyk-Kuzma, JA Garren, IJ Hidalgo, RT Borchardt. Substrate specificity and some properties of phenol sulfotransferase from human intestinal Caco-2 cells. *Life Sci* 49:1197–1206, 1991.
  34. I Chantret, A Barbat, E Dussaulx, MG Brattain, A Zweibaum. Epithelial polarity, villin expression, and enterocytic differentiation of cultured human colon carcinoma cells: a survey of twenty cell lines. *Cancer Res* 48:1936–1942, 1988.
  35. X Boulenc, M Bourrie, I Fabre, C Roque, H Joyeux, Y Berger, G Fabre. Regulation of cytochrome P450IA1 gene expression in a human intestinal cell line, Caco-2. *J Pharmacol Exp Ther* 263:1471–1478, 1992.
  36. VJ Wachter, JA Silverman, Y Zhang, LZ Benet. Role of P-glycoprotein and cytochrome P450 3A in limiting oral absorption of peptides and peptidomimetics. *J Pharm Sci* 87:1322–1330, 1998.
  37. P Schmiedlin-Ren, KE Thummel, JM Fisher, MF Paine, KS Lown, PB Watkins. Expression of enzymatically active CYP3A4 by Caco-2 cells grown on extracellular matrix-coated permeable supports in the presence of 1 alpha, 25-dihydroxyvitamin D3. *Mol Pharmacol* 51:741–754, 1997.
  38. CL Crespi, BW Penman, M Hu. Development of Caco-2 cells expressing high levels of cDNA-derived cytochrome P4503A4. *Pharm Res* 13:1635–1641, 1996.
  39. M Hu, Y Li, CM Davitt, SM Huang, K Thummel, BW Penman, CL Crespi. Transport and metabolic characterization of Caco-2 cells expressing CYP3A4 and CYP3A4 plus oxidoreductase. *Pharm Res* 16:1352–1359, 1999.
  40. VJ Wachter, CY Wu, LZ Benet. Overlapping substrate specificities and tissue distribution of cytochrome P450 3A and P-glycoprotein: implications for drug delivery and activity in cancer chemotherapy. *Mol Carcinog* 13:129–134, 1995.
  41. K Ito, H Kusuhara, Y Sugiyama. Effects of intestinal CYP3A4 and P-glycoprotein on oral drug absorption—theoretical approach. *Pharm Res* 16:225–231, 1999.
  42. D Grundemann, J Babin-Ebell, F Martel, N Ordning, A Schmidt, E Schomig. Primary structure and functional expression of the apical organic cation transporter from kidney epithelial LLC-PK1 cells. *J Biol Chem* 272:10408–10413, 1997.

43. R Hori, M Okamura, A Takayama, K Hirozane, M Takano. Transport of organic anion in the OK kidney epithelial cell line. *Am J Physiol* 264:F975–980, 1993.
44. G Yuan, RJ Ott, C Salgado, KM Giacomini. Transport of organic cations by a renal epithelial cell line (OK). *J Biol Chem* 266:8978–8986, 1991.
45. M Takano, K Hirozane, M Okamura, A Takayama, J Nagai, R Hori. *p*-Aminohippurate transport in apical and basolateral membranes of the OK kidney epithelial cells. *J Pharmacol Exp Ther* 269:970–975, 1994.
46. J Nagai, I Yano, Y Hashimoto, M Takano, K Inui. Efflux of intracellular alpha-ketoglutarate via *p*-aminohippurate/dicarboxylate exchange in OK kidney epithelial cells. *J Pharmacol Exp Ther* 285:422–427, 1998.
47. T Tatsuta, M Naito, T Oh-hara, I Sugawara, T Tsuruo. Functional involvement of P-glycoprotein in blood-brain barrier. *J Biol Chem* 267:20383–20391, 1992.
48. KI Hosoya, T Terasaki, K Tetsuka, T Nagura, S Ontsuki, H Takanaga, M Ueda, N Yanai, M Obitani, T Terasaki. mRNA expression and transport characterization of conditionally immortalized rat brain capillary endothelial cell lines: A new in vitro bbb model for drug targeting. *J Drug Target* 8:357–370, 2000.
49. DJ Begley, D Lechardeur, ZD Chen, C Rollinson, M Bardoul, F Roux, D Scherman, NJ Abbott. Functional expression of P-glycoprotein in an immortalized cell line of rat brain endothelial cells, RBE4. *J Neurochem* 67:988–995, 1996.
50. MA Barrand, KJ Robertson, SF von Weikersthal. Comparisons of P-glycoprotein expression in isolated rat brain microvessels and in primary cultures of endothelial cells derived from microvasculature of rat brain, epididymal fat pad and from aorta. *FEBS Lett* 374:179–183, 1995.
51. S Seetharaman, MA Barrand, L Maskell, RJ Scheper. Multidrug resistance–related transport proteins in isolated human brain microvessels and in cells cultured from these isolates. *J Neurochem* 70:1151–1159, 1998.
52. A Regina, A Koman, M Piciotti, B El Hafny, MS Center, R Bergmann, PO Couraud, F Roux. Mrp1 multidrug resistance–associated protein and P-glycoprotein expression in rat brain microvessel endothelial cells. *J Neurochem* 71:705–715, 1998.
53. Y Kato, S Akhteruzzaman, A Hisaka, Y Sugiyama. Hepatobiliary transport governs overall elimination of peptidic endothelin antagonists in rats. *J Pharmacol Exp Ther* 288:568–574, 1999.
54. AP Li, P Maurel, MJ Gomez-Lechon, LC Cheng, M Jurima-Romet. Preclinical evaluation of drug–drug interaction potential: present status of the application of primary human hepatocytes in the evaluation of cytochrome P450 induction. *Chem Biol Interact* 107:5–16, 1997.
55. AP Li, PD Gorycki, JG Hengstler, GL Kedderis, HG Koebe, R Rahmani, G de Sousas, JM Silva, P Skett. Present status of the application of cryopreserved hepatocytes in the evaluation of xenobiotics: consensus of an international expert panel. *Chem Biol Interact* 121:117–123, 1999.
56. AP Li, C Lu, JA Brent, C Pham, A Fackett, CE Ruegg, PM Silber. Cryopreserved human hepatocytes: characterization of drug-metabolizing enzyme activities and applications in higher throughput screening assays for hepatotoxicity, metabolic stability, and drug–drug interaction potential. *Chem Biol Interact* 121:17–35, 1999.
57. EL LeCluyse, KL Audus, JH Hochman. Formation of extensive canalicular net-

- works by rat hepatocytes cultured in collagen-sandwich configuration. *Am J Physiol* 266:C1764–1774, 1994.
58. X Liu, JP Chism, EL LeCluyse, KR Brouwer, KL Brouwer. Correlation of biliary excretion in sandwich-cultured rat hepatocytes and in vivo in rats. *Drug Metab Dispos* 27:637–644, 1999.
  59. X Liu, EL LeCluyse, KR Brouwer, RM Lightfoot, JI Lee, KL Brouwer. Use of  $\text{Ca}^{2+}$  modulation to evaluate biliary excretion in sandwich-cultured rat hepatocytes. *J Pharmacol Exp Ther* 289:1592–1599, 1999.
  60. AH Schinkel, U Mayer, E Wagenaar, CAAM Mol, L van Deemter, JJM Smit, MA van der Valk, AC Voordouw, H Spits, O van Tellingen, JMJM Zijlmans, WE Fibbe, P Borst. Normal viability and altered pharmacokinetics in mice lacking *mdr1*-type (drug-transporting) P-glycoproteins. *Proc Natl Acad Sci USA* 94:4028–4033, 1997.
  61. J Wijnholds, R Evers, MR van Leusden, CA Mol, GJ Zaman, U Mayer, JH Beijnen, M van der Valk, P Krimpenfort, P Borst. Increased sensitivity to anticancer drugs and decreased inflammatory response in mice lacking the multidrug resistance-associated protein. *Nat Med* 3:1275–1279, 1997.
  62. F Kuipers, M Enserink, R Havinga, AB van der Steen, MJ Hardonk, J Fevery, RJ Vonk. Separate transport systems for biliary secretion of sulfated and unsulfated bile acids in the rat. *J Clin Invest* 81:1593–1599, 1988.
  63. PL Jansen, WH Peters, WH Lamers. Hereditary chronic conjugated hyperbilirubinemia in mutant rats caused by defective hepatic anion transport. *Hepatology* 5: 573–579, 1985.
  64. S Hosokawa, O Tagaya, T Mikami, Y Nozaki, A Kawaguchi, K Yamatsu, M Shamoto. A new rat mutant with chronic conjugated hyperbilirubinemia and renal glomerular lesions. *Lab Animal Sci* 42:27–34, 1992.
  65. B Hagenbuch, BF Scharschmidt, PJ Meier. Effect of antisense oligonucleotides on the expression of hepatocellular bile acid and organic anion uptake systems in *Xenopus laevis* oocytes. *Biochem J* 316:901–904, 1996.
  66. I Tamai, T Nakanishi, K Hayashi, T Terao, Y Sai, T Shiraga, K Miyamoto, E Takeda, H Higashida, A Tsuji. The predominant contribution of oligopeptide transporter PepT1 to intestinal absorption of beta-lactam antibiotics in the rat small intestine. *J Pharm Pharmacol* 49:796–801, 1997.
  67. H Kouzuki, H Suzuki, K Ito, R Ohashi, Y Sugiyama. Contribution of sodium taurocholate co-transporting polypeptide to the uptake of its possible substrates into rat hepatocytes. *J Pharmacol Exp Ther* 286:1043–1050, 1998.
  68. H Kouzuki, H Suzuki, K Ito, R Ohashi, Y Sugiyama. Contribution of organic anion transporting polypeptide to uptake of its possible substrates into rat hepatocytes. *J Pharmacol Exp Ther* 288:627–634, 1999.
  69. V Gorboulev, JC Ulzheimer, A Akhoundova, I Ulzheimer-Teuber, U Karbach, S Quester, C Baumann, F Lang, AE Busch, H Koepsell. Cloning and characterization of two human polyspecific organic cation transporters. *DNA Cell Biol* 16:871–881, 1997.
  70. D Grundemann, V Gorboulev, S Gambaryan, M Veyhl, H Koepsell. Drug excretion mediated by a new prototype of polyspecific transporter. *Nature* 372:549–552, 1994.
  71. F Meyer-Wentrup, U Karbach, V Gorboulev, P Arndt, H Koepsell. Membrane lo-

- calization of the electrogenic cation transporter roct1 in rat liver. *Biochem Biophys Res Commun* 248:673–678, 1998.
72. Y Urakami, M Okuda, S Masuda, H Saito, K Inui. Functional characteristics and membrane localization of rat multispecific organic cation transporters, oct1 and oct2, mediating tumular secretion of cationic drugs. *J Pharmacol Exp Ther* 287: 800–805, 1998.
  73. H Koepsell. Organic cation transporters in intestine, kidney, liver, and brain. *Annu Rev Physiol* 60:243–266, 1998.
  74. AE Busch, S Quester, JC Ulzheimer, S Waldegger, V Gorboulev, P Arndt, F Lang, H Koepsell. Electrogenic properties and substrate specificity of the polyspecific rat cation transporter rOCT1. *J Biol Chem* 271:32599–32604, 1996.
  75. G Nagel, C Volk, T Friedrich, JC Ulzheimer, E Bamberg, H Koepsell. A reevaluation of substrate specificity of the rat cation transporter rOCT1. *J Biol Chem* 272: 31953–31956, 1997.
  76. R Kekuda, PD Prasad, X Wu, H Wang, YJ Fei, FH Leibach, V Ganapathy. Cloning and functional characterization of a potential-sensitive, polyspecific organic cation transporter (OCT3) most abundantly expressed in placenta. *J Biol Chem* 273: 15971–15979, 1998.
  77. D Grundemann, G Liebich, N Kiefer, S Koster, E Schomig. Selective substrates for non-neuronal monoamine transporters. *Mol Pharmacol* 56:1–10, 1999.
  78. E Jacquemin, B Hagenbuch, B Stieger, AW Wolkoff, PJ Meier. Expression cloning of a rat liver Na(+)-independent organic anion transporter. *Proc Natl Acad Sci USA* 91:133–137, 1994.
  79. AJ Bergwerk, X Shi, AC Ford, N Kanai, E Jacquemin, RD Burk, S Bai, PM Novikoff, B Stieger, PJ Meier, VL Schuster, AW Wolkoff. Immunologic distribution of an organic anion transport protein in rat liver and kidney. *Am J Physiol* 271: G231–238, 1996.
  80. RH Angeletti, PM Novikoff, SR Juvvadi, JM Fritschy, PJ Meier, AW Wolkoff. The choroid plexus epithelium is the site of the organic anion transport protein in the brain. *Proc Natl Acad Sci USA* 94:283–286, 1997.
  81. JE van Montfoort, B Hagenbuch, KE Fattinger, MI M, GM Groothuis, DK Meijer, PJ Meier. Polyspecific organic anion transporting polypeptides mediate hepatic uptake of amphipathic type II organic cations. *J Pharmacol Exp Ther* 291:147–152, 1999.
  82. M Muller, PL Jansen. Molecular aspects of hepatobiliary transport. *Am J Physiol* 272:G1285–1303, 1997.
  83. PJ Meier, U Eckhardt, A Schroeder, B Hagenbuch, B Stieger. Substrate specificity of sinusoidal bile acid and organic anion uptake systems in rat and human liver. *Hepatology* 26:1667–1677, 1997.
  84. L Li, TK Lee, PJ Meier, N Ballatori. Identification of glutathione as a driving force and leukotriene C4 as a substrate for oatp1, the hepatic sinusoidal organic solute transporter. *J Biol Chem* 273:16184–16191, 1998.
  85. M Kakyō, H Sakagami, T Nishio, D Nakai, R Nakagomi, T Tokui, T Naitoh, S Matsuno, T Abe, H Yawo. Immunohistochemical distribution and functional characterization of an organic anion transporting polypeptide 2 (oatp2). *FEBS Lett* 445: 343–346, 1999.



86. C Reichel, B Gao, J Van Montfoort, V Cattori, C Rahner, B Hagenbuch, B Stieger, T Kamisako, PJ Meier. Localization and function of the organic anion-transporting polypeptide oatp2 in rat liver. *Gastroenterol* 117:688–695, 1999.
87. B Noe, B Hagenbuch, B Stieger, PJ Meier. Isolation of a multispecific organic anion and cardiac glycoside transporter from rat brain. *Proc Natl Acad Sci USA* 94:10346–10350, 1997.
88. T Abe, M Kakyo, H Sakagami, T Tokui, T Nishio, M Tanemoto, H Nomura, SC Hebert, S Matsuno, H Kondo, H Yawo. Molecular characterization and tissue distribution of a new organic anion transporter subtype (oatp3) that transports thyroid hormones and taurocholate and comparison with oatp2. *J Biol Chem* 273:22395–22401, 1998.
89. S Masuda, K Ibaramoto, A Takeuchi, H Saito, Y Hashimoto, KI Inui. Cloning and functional characterization of a new multispecific organic anion transporter, OAT-K2, in rat kidney. *Mol Pharmacol* 55:743–752, 1999.
90. H Saito, S Masuda, K Inui. Cloning and functional characterization of a novel rat organic anion transporter mediating basolateral uptake of methotrexate in the kidney. *J Biol Chem* 271:20719–20725, 1996.
91. B Gao, B Stieger, B No, JM Fritschy, PJ Meier. Localization of the organic anion transporting polypeptide 2 (oatp2) in capillary endothelium and choroid plexus epithelium of rat brain. *J Histochem Cytochem* 47:1255–1264, 1999.
92. WA Banks, AJ Kastin. Passage of peptides across the blood-brain barrier: pathophysiological perspectives. *Life Sci* 59:1923–1943, 1996.
93. S Masuda, H Saito, H Nonoguchi, K Tomita, K Inui. mRNA distribution and membrane localization of the OAT-K1 organic anion transporter in rat renal tubules. *FEBS Lett* 407:127–131, 1997.
94. GA Kullak-Ublick, B Hagenbuch, B Stieger, CD Scheingart, AF Hofmann, AW Wolkoff, PJ Meier. Molecular and functional characterization of an organic anion transporting polypeptide cloned from human liver. *Gastroenterology* 109:1274–1282, 1995.
95. X Bossuyt, M Muller, PJ Meier. Multispecific amphipathic substrate transport by an organic anion transporter of human liver. *J Hepatol* 25:733–738, 1996.
96. T Abe, M Kakyo, T Tokui, R Nakagomi, T Nishio, D Nakai, H Nomura, M Unno, M Suzuki, T Naitoh, S Matsuno, H Yawo. Identification of a novel gene family encoding human liver-specific organic anion transporter LST-1. *J Biol Chem* 274:17159–17163, 1999.
97. J Konig, Y Cui, AT Nies, D Keppler. A novel human organic anion transporting polypeptide localized to the basolateral hepatocyte membrane. *Am J Physiol* 278:G156–G164, 2000.
98. B Hsiang, Y Zhu, Z Wang, Y Wu, V Sasseville, WP Yang, TG Kirchgessner. A novel human hepatic organic anion transporting polypeptide (OATP2). Identification of a liver-specific human organic anion transporting polypeptide and identification of rat and human hydroxymethylglutaryl-CoA reductase inhibitor transporters. *J Biol Chem* 274:37161–37168, 1999.
99. M Kakyo, M Unno, T Tokui, R Nakagomi, T Nishio, H Iwasashi, D Nakai, M Seki, M Suzuki, T Naitoh, S Matsuno, H Yawo, T Abe. Molecular characterization and functional regulation of a novel rat liver-specific organic anion transporter rlst-1. *Gastroenterology* 117:770–775, 1999.

100. T Nagase, K Ishikawa, N Miyajima, A Tanaka, H Kotani, N Nomura, O Ohara. Prediction of the coding sequences of unidentified human genes. IX. The complete sequences of 100 new cDNA clones from brain which can code for large proteins in vitro. *DNA Res* 5:31–39, 1998.
101. JV Moller, MI Sheikh. Renal organic anion transport system: pharmacological, physiological, and biochemical aspects. *Pharmacol Rev* 34:315–358, 1983.
102. KJ Ullrich, G Rumrich. Renal transport mechanisms for xenobiotics: chemicals and drugs. *Clin Invest* 71:843–848, 1993.
103. S Jariyawat, T Sekine, M Takeda, N Apiwattanakul, Y Kanai, S Sophasan, H Endou. The interaction and transport of beta-lactam antibiotics with the cloned rat renal organic anion transporter 1. *J Pharmacol Exp Ther* 290:672–677, 1999.
104. N Apiwattanakul, T Sekine, A Chairoungdua, Y Kanai, N Nakajima, S Sophasan, H Endou. Transport properties of nonsteroidal anti-inflammatory drugs by organic anion transporter 1 expressed in *Xenopus laevis* oocytes. *Mol Pharmacol* 55:847–854, 1999.
105. M Tsuda, T Sekine, M Takeda, SH Cha, Y Kanai, M Kimura, H Endou. Transport of ochratoxin A by renal multispecific organic anion transporter 1. *J Pharmacol Exp Ther* 289:1301–1305, 1999.
106. T Sekine, N Watanabe, M Hosoyamada, Y Kanai, H Endou. Expression cloning and characterization of a novel multispecific organic anion transporter. *J Biol Chem* 272:18526–18529, 1997.
107. DH Sweet, NA Wolff, JB Pritchard. Expression cloning and characterization of ROAT1. The basolateral organic anion transporter in rat kidney. *J Biol Chem* 272:30088–30095, 1997.
108. A Tojo, T Sekine, N Nakajima, M Hosoyamada, Y Kanai, K Kimura, H Endou. Immunohistochemical localization of multispecific renal organic anion transporter 1 in rat kidney. *J Am Soc Nephrol* 10:464–471, 1999.
109. H Kusuvara, T Sekine, N Utsunomiya-Tate, M Tsuda, R Kojima, SH Cha, Y Sugiyama, Y Kanai, H Endou. Molecular cloning and characterization of a new multispecific organic anion transporter from rat brain. *J Biol Chem* 274:13675–13680, 1999.
110. T Sekine, SH Cha, M Tsuda, N Apiwattanakul, N Nakajima, Y Kanai, H Endou. Identification of multispecific organic anion transporter 2 expressed predominantly in the liver. *FEBS Lett* 429:179–182, 1998.
111. SH Cha, T Sekine, H Kusuvara, E Yu, JY Kim, DK Kim, Y Sugiyama, Y Kanai, H Endou. Molecular cloning and characterization of multispecific organic anion transporter 4 expressed in the placenta. *J Biol Chem* 275:4507–4512, 2000.
112. JE Race, SM Grassl, WJ Williams, EJ Holtzman. Molecular cloning and characterization of two novel human renal organic anion transporters (hOAT1 and hOAT3). *Biochem Biophys Res Commun* 255:508–514, 1999.
113. KJ Ullrich, G Rumrich, C David, G Fritzsche. Bisubstrates: substances that interact with renal contraluminal organic anion and organic cation transport systems. I. Amines, piperidines, piperazines, azepines, pyridines, quinolines, imidazoles, thiazoles, guanidines and hydrazines. *Pflugers Arch* 425:280–299, 1993.
114. I Tamai, H Yabuuchi, J Nezu, Y Sai, A Oku, M Shimane, A Tsuji. Cloning and characterization of a novel human pH-dependent organic cation transporter, OCTN1. *FEBS Lett* 419:107–111, 1997.
115. H Yabuuchi, I Tamai, J Nezu, K Sakamoto, A Oku, M Shimane, Y Sai, A Tsuji.

- Novel membrane transporter OCTN1 mediates multispecific, bidirectional, and pH-dependent transport of organic cations. *J Pharmacol Exp Ther* 289:768–773, 1999.
116. X Wu, PD Prasad, FH Leibach, V Ganapathy. cDNA sequence, transport function, and genomic organization of human OCTN2, a new member of the organic cation transporter family. *Biochem Biophys Res Commun* 246:589–595, 1998.
  117. I Tamai, R Ohashi, J Nezu, H Yabuuchi, A Oku, M Shimane, Y Sai, A Tsuji. Molecular and functional identification of sodium ion-dependent, high affinity human carnitine transporter OCTN2. *J Biol Chem* 273:20378–20382, 1998.
  118. J Kerner, C Hoppel. Genetic disorders of carnitine metabolism and their nutritional management. *Annu Rev Nutr* 18:179–206, 1998.
  119. V Tanphaichitr, P Leelahagul. Carnitine metabolism and human carnitine deficiency. *Nutrition* 9:246–254, 1993.
  120. J Nezu, I Tamai, A Oku, R Ohashi, H Yabuuchi, N Hashimoto, H Nikaido, Y Sai, A Koizumi, Y Shoji, G Takada, T Matsuishi, M Yoshino, H Kato, T Ohura, G Tsujimoto, J Hayakawa, M Shimane, A Tsuji. Primary systemic carnitine deficiency is caused by mutations in a gene encoding sodium ion-dependent carnitine transporter. *Nat Genet* 21:91–94, 1999.
  121. X Wu, W Huang, PD Prasad, P Seth, DP Rajan, FH Leibach, J Chen, SJ Conway, V Ganapathy. Functional characteristics and tissue distribution pattern of organic cation transporter 2 (OCTN2), an organic cation/carnitine transporter. *J Pharmacol Exp Ther* 290:1482–1492, 1999.
  122. R Ohashi, I Tamai, H Yabuuchi, JI Nezu, A Oku, Y Sai, M Shimane, A Tsuji. Na(+)-dependent carnitine transport by organic cation transporter (OCTN2): its pharmacological and toxicological relevance. *J Pharmacol Exp Ther* 291:778–784, 1999.
  123. ME Ganapathy, W Huang, DP Rajan, AL Carter, M Sugawara, K Iseki, FH Leibach, V Ganapathy. Beta-lactam antibiotics as substrates for OCTN2, an organic cation/carnitine transporter. *J Biol Chem* 275:1699–1707, 2000.
  124. YJ Fei, Y Kanai, S Nussberger, V Ganapathy, FH Leibach, MF Romero, SK Singh, WF Boron, MA Hediger. Expression cloning of a mammalian proton-coupled oligopeptide transporter. *Nature* 368:563–566, 1994.
  125. H Ogihara, H Saito, BC Shin, T Terado, S Takenoshita, Y Nagamachi, K Inui, K Takata. Immuno-localization of H<sup>+</sup>/peptide cotransporter in rat digestive tract. *Biochem Biophys Res Commun* 220:848–852, 1996.
  126. H Shen, DE Smith, T Yang, YG Huang, JB Schnermann, FC Brosius. 3rd Localization of PEPT1 and PEPT2 proton-coupled oligopeptide transporter mRNA and protein in rat kidney. *Am J Physiol* 276:F658–655, 1999.
  127. A Steel, S Nussberger, MF Romero, WF Boron, CA Boyd, MA Hediger. Stoichiometry and pH dependence of the rabbit proton-dependent oligopeptide transporter PepT1. *J Physiol* 498:563–569, 1997.
  128. F Doring, J Will, S Amasheh, W Clauss, H Ahlbrecht, H Daniel. Minimal molecular determinants of substrates for recognition by the intestinal peptide transporter. *J Biol Chem* 273:23211–23218, 1998.
  129. S Weller, MR Blum, M Doucette, T Burnette, DM Cederberg, P de Miranda, ML Smiley. Pharmacokinetics of the acyclovir pro-drug valaciclovir after escalating single- and multiple-dose administration to normal volunteers. *Clin Pharmacol Ther* 54:595–605, 1993.

130. PJ Shinko, PV Sinko, PV Balimane. Carrier-mediated intestinal absorption of valacyclovir, the L-valyl ester prodrug of acyclovir: 1. Interactions with peptides, organic anions and organic cations in rats. *Biopharm Drug Dispos* 19:209–217, 1998.
131. J Soul-Lawton, E Seaber, N On, R Wootton, P Rolan, J Posner. Absolute bioavailability and metabolic disposition of valacyclovir, the L-valyl ester of acyclovir, following oral administration to humans. *Antimicrob Agents Chemother* 39:2759–2764, 1995.
132. ME Ganapathy, W Huang, H Wang, V Ganapathy, FH Leibach. Valacyclovir: a substrate for the intestinal and renal peptide transporters PEPT1 and PEPT2. *Biochem Biophys Res Commun* 246:470–475, 1998.
133. H Han, RL de Vrueh, JK Rhie, KM Covitz, PL Smith, CP Lee, DM Oh, W Sadee, GL Amidon. 5'-Amino acid esters of antiviral nucleosides, acyclovir, and AZT are absorbed by the intestinal PEPT1 peptide transporter. *Pharm Res* 15:1154–1159, 1998.
134. I Tamai, T Nakanishi, H Nakahara, Y Sai, V Ganapathy, FH Leibach, A Tsuji. Improvement of L-dopa absorption by dipeptidyl derivation, utilizing peptide transporter PepT1. *J Pharm Sci* 87:1542–1546, 1998.
135. H Saito, T Terada, M Okuda, S Sasaki, K Inui. Molecular cloning and tissue distribution of rat peptide transporter PEPT2. *Biochim Biophys Acta* 1280:173–177, 1996.
136. M Boll, M Hergert, M Wagener, WM Weber, D Markovich, J Biber, W Clauss, H Murer, H Daniel. Expression cloning and functional characterization of the kidney cortex high-affinity proton-coupled peptide transporter. *Proc Natl Acad Sci USA* 93:284–289, 1996.
137. DE Smith, A Pavlova, UV Berger, MA Hediger, T Yang, YG Huan, JB Schnermann. Tubular localization and tissue distribution of peptide transporters in rat kidney. *Pharm Res* 15:1244–1249, 1998.
138. ST Dieck, H Heuer, J Ehrchen, C Otto, K Bauer. The peptide transporter PepT2 is expressed in rat brain and mediates the accumulation of the fluorescent dipeptide derivative. *Glia* 25:10–20, 1998.
139. XZ Chen, T Zhu, DE Smith, MA Hediger. Stoichiometry and kinetics of the high-affinity H<sup>+</sup>-coupled peptide transporter PepT2. *J Biol Chem* 274:2773–2779, 1999.
140. T Terada, H Saito, M Mukai, K Inui. Recognition of beta-lactam antibiotics by rat peptide transporter, PEPT1 and PEPT2, in LLC-PK1 cells. *Am J Physiol* 273: F706–F711, 1997.
141. S Ramamoorthy, W Liu, YY Ma, TL Yang-Feng, V Ganapathy, FH Leibach. Proton/peptide cotransporter (PEPT 2) from human kidney: functional characterization and chromosomal localization. *Biochim Biophys Acta* 1240:1–4, 1995.
142. K Takahasi, N Nakamura, T Terada, T Okano, T Futami, H Saito, K Inui. Interaction of beta-lactam antibiotics with H<sup>+</sup> peptide cotransporters in rat renal brush border membranes. *J Pharmacol Exp Ther* 286:1037–1042, 1998.
143. AE Busch, A Schuster, S Waldeger, CA Wagner, G Zempel, S Broer, J Biber, H Murer, F Lang. Expression of a renal type I sodium/phosphate transporter (NaPi-1) induces a conductance in *Xenopus* oocytes permeable for organic and inorganic anions. *Proc Natl Acad Sci USA* 93:5347–5351, 1996.

144. H Yabuuchi, I Tamai, K Morita, T Kouda, K Miyamoto, E Takeda, A Tsuji. Hepatic sinusoidal membrane transport of anionic drugs mediated by anion transporter Npt1. *J Pharmacol Exp Ther* 286:1391–1396, 1998.
145. K Dano. Active outward transport of daunomycin in resistant Ehrlich ascites tumor cells. *Biochim Biophys Acta* 323:466–483, 1973.
146. T Skovsgaard. Mechanisms of resistance to daunorubicin in Ehrlich ascites tumor cells. *Cancer Res* 38:1785–1791, 1978.
147. RPJ Oude Elferink, DKF Meijer, F Kuipers, PLM Jansen, AK Groen, GMM Groothuis. Hepatobiliary secretion of organic compounds: molecular mechanisms of membrane transport. *Biochim Biophys Acta* 1241:215–268, 1995.
148. NL Simons, J Hunter, MA Jepson. Renal secretion of xenobiotics mediated by P-glycoprotein: importance to renal function in health and exploitation for targeted drug delivery to epithelial cysts in polycystic kidney disease. *Adv Drug Deliv Rev* 25:243–256, 1997.
149. A Tsuji, I Tamai. Blood-brain barrier function of P-glycoprotein. *Adv Drug Deliv Rev* 25:285–298, 1997.
150. J Hunter, BH Hirst. Intestinal secretion of drugs. The role of P-glycoprotein and related drug efflux systems in limiting oral drug absorption. *Adv Drug Deliv Rev* 25:129–157, 1997.
151. WM Pardridge, PL Golden, YS Kang, U Bickel. Brain microvascular and astrocyte localization of P-glycoprotein. *J Neurochem* 68:1278–1285, 1997.
152. WT Bellamy. P-glycoproteins and multidrug resistance. *Ann Rev Pharmacol Toxicol* 36:161–183, 1996.
153. MM Gottesman, I Pastan. Biochemistry of multidrug resistance mediated by the multidrug transporter. *Ann Rev Biochem* 62:385–427, 1993.
154. MM Gottesman, CA Hrycyna, PV Schoenlein, UA Germann, I Pastan. Genetic analysis of the multidrug transporter. *Ann Rev Genet* 29:607–649, 1995.
155. AR Safa multidrug resistance. In: RL Schilsky, GA Milano, MJ Ratain, et al. *Principles of Antineoplastic Drug Development and Pharmacology*. New York: Marcel Dekker, 1996, pp 457–786.
156. H Kusuhara, H Suzuki, Y Sugiyama. The role of P-glycoprotein and canalicular multispecific organic anion transporter in the hepatobiliary excretion of drugs. *J Pharm Sci* 87:1025–1040, 1998.
157. JJ Smit, AH Schinkel, RPJ Oude Elferink, AK Groen, E Wagenaar, L van Deemter, CAAM Mol, R Ottenhoff, NM van der Lugt, MA van Roon, MA van der Valk, GJ Offerhaus, AJM Berns, P Borst. Homozygous disruption of the murine *mdr2* P-glycoprotein gene leads to a complete absence of phospholipid from bile and to liver disease. *Cell* 75:451–462, 1993.
158. S Ruetz, P Gros. Phosphatidylcholine translocase: a physiological role for the *mdr2* gene. *Cell* 77:1071–1081, 1994.
159. D de Graaf, RC Sharma, EB Mechetner, RT Schimke, IB Roninson. P-Glycoprotein confers methotrexate resistance in 3T6 cells with deficient carrier-mediated methotrexate uptake. *Proc Natl Acad Sci USA* 93:1238–1242, 1996.
160. MD Norris, D De Graaf, M Haber, M Kavallaris, J Madafiglio, J Gilbert, E Kwan, BW Stewart, EB Mechetner, AV Gudkov, IB Roninson. Involvement of MDR1 P-glycoprotein in multifactorial resistance to methotrexate. *Int Natl Cancer* 65:613–619, 1996.

161. XY Chu, Y Kato, Y Sugiyama. Possible involvement of P-glycoprotein in biliary excretion of CPT-11 in rats. *Drug Metab Dispos* 27:440–441, 1999.
162. L Huang, T Hoffman, M Vore. Adenosine triphosphate-dependent transport of estradiol-17-beta(beta-D-glucuronide) in membrane vesicles by MDR1 expressed in insect cells. *Hepatology* 28:1371–1377, 1998.
163. AH Schinkel, JJ Smit, O van Tellingen, JH Beijnen, E Wagenaar, L van Deemter, CAAM Mol, MA van der Valk, EC Robanus-Maandag, HP te Riele, AJM Berns, P Borst. Disruption of the mouse *mdr1a* P-glycoprotein gene leads to a deficiency in the blood-brain barrier and to increased sensitivity to drugs. *Cell* 77:491–502, 1994.
164. JW Smit, AH Schinkel, M Muller, B Weert, DKF Meijer. Contribution of the murine *mdr1a* P-glycoprotein to hepatobiliary and intestinal elimination of cationic drugs as measured in mice with an *mdr1a* gene disruption. *Hepatology* 27:1056–1063, 1998.
165. U Mayer, E Wagenaar, JH Beijnen, JW Smit, DK Meijer, J van Asperen, P Borst, AH Schinkel. Substantial excretion of digoxin via the intestinal mucosa and prevention of long-term digoxin accumulation in the brain by the *mdr 1a* P-glycoprotein. *Br J Pharmacol* 119:1038–1044, 1996.
166. A Sparreboom, J van Asperen, U Mayer, AH Schinkel, JW Smit, DK Meijer, P Borst, WJ Nooijen, JH Beijnen, O van Tellingen. Limited oral bioavailability and active epithelial excretion of paclitaxel (Taxol) caused by P-glycoprotein in the intestine. *Proc Natl Acad Sci USA* 94:2031–2035, 1997.
167. M Achira, H Suzuki, K Ito, Y Sugiyama. Comparative studies to determine the selective inhibitors for P-glycoprotein and cytochrome P450 3A4. *AAPS Pharm Sci* 1, 1999. (available from <http://www.pharmsci.org/journal>)
168. H Kushihara, H Suzuki, T Terasaki, A Kakee, M Lemaire, Y Sugiyama. P-glycoprotein mediates the efflux of quinidine across the blood-brain barrier. *J Pharmacol Exp Ther* 283:574–580, 1997.
169. AH Schinkel, E Wagenaar, CAAM Mol, L van Deemter. P-Glycoprotein in the blood-brain barrier of mice influences the brain penetration and pharmacological activity of many drugs. *J Clin Invest* 97:2517–2524, 1996.
170. AH Schinkel, E Wagenaar, L van Deemter, CAAM Mol, P Borst. Absence of the *mdr1a* P-glycoprotein in mice affects tissue distribution and pharmacokinetics of dexamethasone, digoxin, and cyclosporin A. *J Clin Invest* 96:1698–1705, 1995.
171. EC de Lange, G de Bock, AH Schinkel, AG de Boer, DD Breimer. BBB transport and P-glycoprotein functionality using MDR1A (–/–) and wild-type mice. Total brain versus microdialysis concentration profiles of rhodamine-123. *Pharm Res* 15: 1657–1665, 1998.
172. SP Cole, G Bhardwaj, JH Gerlach, JE Mackie, CE Grant, KC Almquist, AJ Stewart, EU Kurz, AM Duncan, RG Deeley. Overexpression of a transporter gene in a multidrug-resistant human lung cancer cell line. *Science* 258:1650–1654, 1992.
173. SPC Cole, KE Sparks, K Fraser, DW Loe, CE Grant, GM Wilson, RG Deeley. Pharmacological characterization of multidrug resistant MRP-transfected human tumor cells. *Cancer Res* 54:5902–5910, 1994.
174. BD Stride, CE Grant, DW Loe, DR Hipfner, SPC Cole, RG Deeley. Pharmacological characterization of the murine and human orthologs of multidrug-resistance protein in transfected human embryonic kidney cells. *Mol Pharmacol* 52:344–353, 1997.

175. GJ Zaman, CH Versantvoort, JJ Smit, EW Eijndems, M de Haas, AJ Smith, HJ Broxterman, NH Mulder, EG de Vries, F Baas, P Borst. Analysis of the expression of MRP, the gene for a new putative transmembrane drug transporter, in human multidrug resistant lung cancer cell lines. *Cancer Res* 53:1747–1750, 1993.
176. S Ruetz, M Brault, C Kast, C Hemenway, J Heitman, CE Grant, SP Cole, RG Deeley, P Gros. Functional expression of the multidrug resistance-associated protein in the yeast *Saccharomyces cerevisiae*. *J Biol Chem* 271:4154–4160, 1996.
177. DW Loe, RG Deeley, SPC Cole. Biology of the multidrug resistance-associated protein, MRP. *Eur J Cancer* 32A: 945–957, 1996.
178. G Jedlitschky, I Leier, U Buchholz, K Barnouin, G Kurz, D Keppler. Transport of glutathione, glucuronate, and sulfate conjugates by the MRP gene-encoded conjugate export pump. *Cancer Res* 56:988–994, 1996.
179. GJ Zaman, J Lankelma, O van Tellingen, J Beijnen, H Dekker, C Paulusma, RPJ Oude Elferink, F Baas, P Borst. Role of glutathione in the export of compounds from cells by the multidrug-resistance-associated protein. *Proc Natl Acad Sci USA* 92:7690–7694, 1995.
180. CH Versantvoort, HJ Broxterman, T Bagrij, RJ Scheper, PR Twentymen. Regulation by glutathione of drug transport in multidrug-resistant human lung tumor cell lines overexpressing multidrug resistance-associated protein. *Br J Cancer* 72:82–89, 1995.
181. DW Loe, KC Almquist, RG Deeley, SP Cole. Multidrug resistance protein (MRP)-mediated transport of leukotriene C4 and chemotherapeutic agents in membrane vesicles. Demonstration of glutathione-dependent vincristine transport. *J Biol Chem* 271:9675–9682, 1996.
182. D Lautier, Y Canitrot, RG Deeley, SPC Cole. Multidrug resistance mediated by the multidrug resistance protein (MRP) gene. *Biochem Pharmacol* 52:967–977, 1996.
183. SP Cole, RG Deeley. Multidrug resistance mediated by the ATP-binding cassette transporter protein MRP. *Bioessays* 20:931–940, 1998.
184. RG Deeley, SP Cole. Function, evolution and structure of multidrug resistance protein (MRP). *Semin Cancer Biol* 8:193–204, 1997.
185. R Evers, GJ Zaman, L van Deemter, H Jansen, J Calafat, LC Oomen, RPJ Oude Elferink, P Borst, AH Schinkel. Basolateral localization and export activity of the human multidrug resistance-associated protein in polarized pig kidney cells. *J Clin Invest* 97:1211–1218, 1996.
186. J Wijnholds, EC de Lange, GL Scheffer, DJ van Den Berg, CA Mol, M van Der Valk, AH Schinkel, RJ Scheper, DD Breimer, P Borst. Multidrug resistance protein 1 protects the choroid plexus epithelium and contributes to the blood-cerebrospinal fluid barrier. *J Clin Invest* 105:279–285, 2000.
187. J Nishino, H Suzuki, D Sugiyama, T Kitazawa, K Ito, M Hanano, Y Sugiyama. Trans epithelial transport of organic anions across the choroid plexus: possible involvement of organic anion transporter and multidrug resistance-associated protein. *J Pharmacol Exp Ther* 290:289–294, 1999.
188. VV Rao, JL Dahlheimer, ME Bardgett, AZ Snyder, RA Finch, AC Sartorelli, D Piwnica-Worms. Choroid plexus epithelial expression of MDR1 P-glycoprotein and multidrug resistance-associated protein contribute to the blood-cerebrospinal-fluid drug-permeability barrier. *Proc Natl Acad Sci USA* 96:3900–3905, 1999.

189. N Strazielle, JF Ghersi-Egea. Demonstration of a coupled metabolism-efflux process at the choroid plexus as a mechanism of brain protection toward xenobiotics. *J Neurosci* 19:6275–6289, 1999.
190. T Mikami, T Nozaki, O Tagaya, S Hosokawa, T Nakura, H Hori, S Kondou. *Cong Anom* 26:250–251, 1986.
191. B Stieger, PJ Meier. Bile acid and xenobiotic transporters in liver. *Curr Opin Cell Biol* 10:462–467, 1998.
192. H Suzuki, Y Sugiyama. Excretion of GSSG and glutathione conjugates mediated by MRP1 and cMOAT/MRP2. *Semin Liver Dis* 18:359–376, 1998.
193. J Konig, AT Nies, Y Cui, I Leier, D Keppler. Conjugate export pumps of the multidrug resistance protein (MRP) family: localization, substrate specificity, and MRP2-mediated drug resistance. *Biochim Biophys Acta* 1461:377–394, 1999.
194. P Borst, R Evers, M Kool, J Wijnholds. The multidrug resistance protein family. *Biochim Biophys Acta* 1461:347–357, 1999.
195. M Kuwano, S Toh, T Uchiumi, H Takano, K Kohno, M Wada. Multidrug resistance-associated protein subfamily transporters and drug resistance. *Anticancer Drug Des* 14:123–131, 1999.
196. CC Paulusma, PJ Bosma, GJ Zaman, CT Bakker, M Otter, GL Scheffer, RJ Scheper, P Borst, RP Oude Elferink. Congenital jaundice in rats with a mutation in a multidrug resistance-associated protein gene. *Science* 271:1126–1128, 1996.
197. K Ito, H Suzuki, T Hirohashi, K Kume, T Shimizu, Y Sugiyama. Molecular cloning of canalicular multispecific organic anion transporter defective in EHBR. *Am J Physiol* 272:G16–22, 1997.
198. M Buchler, J Konig, M Brom, J Kartenbeck, H Spring, T Horie, D Keppler. cDNA cloning of the hepatocyte canalicular isoform of the multidrug resistance protein, cMrp, reveals a novel conjugate export pump deficient in hyperbilirubinemic mutant rats. *J Biol Chem* 271:15091–15098, 1996.
199. J Kartenbeck, U Leuschner, R Mayer, D Keppler. Absence of the canalicular isoform of the MRP gene-encoded conjugate export pump from the hepatocytes in Dubin–Johnson syndrome. *Hepatology* 23:1061–1066, 1996.
200. MH de Vries, FA Redegeld, AS Koster, J Noordhoek, JG de Haan, RP Oude Elferink, PL Jansen. Hepatic, intestinal and renal transport of 1-naphthol-beta-D-glucuronide in mutant rats with hereditary-conjugated hyperbilirubinemia. *Naunyn-Schmiedebergs Arch Pharmacol* 340:588–592, 1989.
201. Y Gotoh, H Suzuki, S Kinoshita, T Hirohashi, Y Kato, Y Sugiyama. Involvement of an organic anion transporter (canalicular multispecific organic anion transporter/multidrug resistance-associated protein 2) in gastrointestinal secretion of glutathione conjugates in rats. *J Pharmacol Exp Ther* 292:433–439, 2000.
202. T Hirohashi, H Suzuki, XY Chu, I Tamai, A Tsuji, Y Sugiyama. Function and expression of multidrug resistance-associated protein family in human colon adenocarcinoma cells (Caco-2). *J Pharmacol Exp Ther* 292:265–270, 2000.
203. K Taniguchi, M Wada, K Kohno, T Nakamura, T Kawabe, M Kawakami, K Kago-tani, K Okumura, S Akiyama, M Kuwano. A human canalicular multispecific organic anion transporter (cMOAT) gene is overexpressed in cisplatin-resistant human cancer cell lines with decreased drug accumulation. *Cancer Res* 56:4124–4129, 1996.



204. K Koike, T Kawabe, T Tanaka, S Toh, T Uchiumi, M Wada, S Akiyama, M Ono, M Kuwano. A canalicular multispecific organic anion transporter (cMOAT) antisense cDNA enhances drug sensitivity in human hepatic cancer cells. *Cancer Res* 57: 5475–5479, 1997.
205. K Niinuma, Y Kato, H Suzuki, CA Tyson, V Weizer, JE Dabbs, R Froehlich, CE Green, Y Sugiyama. Primary active transport of organic anions on bile canalicular membrane in humans. *Am J Physiol* 276:G1153–1164, 1999.
206. Y Kiuchi, H Suzuki, T Hirohashi, CA Tyson, Y Sugiyama. cDNA cloning and inducible expression of human multidrug resistance associated protein 3 (MRP3). *FEBS Lett* 433:149–152, 1998.
207. T Uchiumi, E Hinoshita, S Haga, T Nakamura, T Tanaka, S Toh, M Furukawa, T Kawabe, M Wada, K Kagotani, K Okumura, K Kohno, S Akiyama, M Kuwano. Isolation of a novel human canalicular multispecific organic anion transporter, cMOAT2/MRP3, and its expression in cisplatin-resistant cancer cells with decreased ATP-dependent drug transport. *Biochem Biophys Res Commun* 252:103–110, 1998.
208. T Hirohashi, H Suzuki, Y Sugiyama. Characterization of the transport properties of cloned rat multidrug resistance-associated protein 3 (MRP3). *J Biol Chem* 274: 15181–15185, 1999.
209. DF Ortiz, S Li, R Iyer, X Zhang, P Novikoff, IM Arias. MRP3, a new ATP-binding cassette protein localized to the canalicular domain of the hepatocyte. *Am J Physiol* 276:G1493–1500, 1999.
210. J Konig, D Rost, Y Cui, D Keppler. Characterization of the human multidrug resistance protein isoform MRP3 localized to the basolateral hepatocyte membrane. *Hepatology* 29:1156–1163, 1999.
211. T Hirohashi, H Suzuki, H Takikawa, Y Sugiyama. ATP-dependent transport of bile salts by rat multidrug resistance-associated protein 3 (Mrp3). *J Biol Chem* 275: 2905–2910, 2000.
212. T Tsuruo, A Tomida. Multidrug resistance. *Anti-Cancer Drugs* 6:213–218, 1995.
213. WT Beck In: RF Ozols, ed. *Molecular and Clinical Advances in Anticancer Drug Resistance*. Boston: Kluwer, 1991, pp 151–170.
214. JM Ford, WN Hait. Pharmacology of drugs that alter multidrug resistance in cancer. *Pharmacol Rev* 42:155–199, 1990.
215. JM Ford. Modulators of multidrug resistance. Preclinical studies. *Hematol Oncol Clin North America* 9:337–361, 1995.
216. MM Gottesman, GH Mickisch, I Pastan. In vivo models of P-glycoprotein-mediated multidrug resistance. *Cancer Treat Res* 73:107–128, 1994.
217. RP Keller, HJ Altermatt, P Donatsch, H Zihlmann, JA Laissue, PC Hiestand. Pharmacologic interactions between the resistance-modifying cyclosporine SDZ PSC 833 and etoposide (VP 16-213) enhance in vivo cytostatic activity and toxicity. *Int Natl Cancer* 51:433–438, 1992.
218. S Desrayaud, P Guntz, JM Scherrmann, M Lemaire. Effect of the P-glycoprotein inhibitor, SDZ PSC 833, on the blood and brain pharmacokinetics of colchicine. *Life Sci* 61:153–163, 1997.
219. A Sakata, I Tamai, K Kawazu, Y Deguchi, T Ohnishi, A Saheki, A Tsuji. In vivo evidence for ATP-dependent and P-glycoprotein-mediated transport of cyclosporin A at the blood-brain barrier. *Biochem Pharmacol* 48:1989–1992, 1994.

220. Q Wang, H Yang, DW Miller, WF Elmquist. Effect of the P-glycoprotein inhibitor, cyclosporin A, on the distribution of rhodamine-123 to the brain: an in vivo microdialysis study in freely moving rats. *Biochem Biophys Res Commun* 211:719–726, 1995.
221. Q Wang, H Yang, WF Elmquist. The effect of LY-335979 on the distribution kinetics of quinidine to the brain: an in vivo microdialysis study in freely moving rats. *Pharm Res* 13:S-456, 1996.
222. A Hedman, B Angelin, A Arvidsson, R Dahlqvist, B Nilsson. Interactions in the renal and biliary elimination of digoxin: stereoselective difference between quinine and quinidine. *Clin Pharmacol Ther* 47:20–26, 1990.
223. A Hedman, B Angelin, A Arvidsson, O Beck, R Dahlqvist, B Nilsson, M Olsson, K Schenck-Gustafsson. Digoxin–verapamil interaction: reduction of biliary but not renal digoxin clearance in humans. *Clin Pharmacol Ther* 49: 256–262, 1991.
224. J Kuhlmann. Effects of verapamil, diltiazem, and nifedipine on plasma levels and renal excretions of digitoxin. *Clin Pharmacol Ther* 38:667–673, 1985.
225. P Olinga, M Merema, IH Hof, MJ Slooff, JH Proost, DK Meijer, GM Groothuis. Characterization of the uptake of rocuronium and digoxin in human hepatocytes: carrier specificity and comparison with in vivo data. *J Pharmacol Exp Ther* 285: 506–510, 1998.
226. A Hedman, DK Meijer. Stereoselective inhibition by the diastereomers quinidine and quinine of uptake of cardiac glycosides into isolated rat hepatocytes. *J Pharm Sci* 87:457–461, 1998.
227. R Hori, N Okamura, T Aiba, Y Tanigawara. Role of P-glycoprotein in renal tubular secretion of digoxin in the isolated perfused rat kidney. *J Pharmacol Exp Ther* 266: 1620–1625, 1993.
228. MF Fromm, RB Kim, CM Stein, GR Wilkinson, DM Roden. Inhibition of P-glycoprotein-mediated drug transport: A unifying mechanism to explain the interaction between digoxin and quinidine. *Circulation* 99:552–557, 1999.
229. Y Emi, D Tsunashima, K Ogawara, K Higaki, T Kimura. Role of P-glycoprotein as a secretory mechanism in quinidine absorption from rat small intestine. *J Pharm Sci* 87:295–299, 1998.
230. HH Kupferschmidt, KE Fattinger, HR Ha, F Follath, S Krahenbuhl. Grapefruit juice enhances the bioavailability of the HIV protease inhibitor saquinavir in man. *Br J Clin Pharmacol* 45:355–359, 1998.
231. A Hsu, GR Granneman, G Cao, L Carothers, T el-Shourbagy, P Baroldi, K Erdman, F Brown, E Sun, IM Leonard. Pharmacokinetic interactions between two human immunodeficiency virus protease inhibitors, ritonavir and saquinavir. *Clin Pharmacol Ther* 63:453–464, 1998.
232. ME Fitzsimmons, JM Collins. Selective biotransformation of the human immunodeficiency virus protease inhibitor saquinavir by human small-intestinal cytochrome P4503A4: potential contribution to high first-pass metabolism. *Drug Dispos* 25:256–266, 1997.
233. VA Eagling, DJ Back, MG Barry. Differential inhibition of cytochrome P450 isoforms by the protease inhibitors, ritonavir, saquinavir and indinavir. *Br J Clin Pharmacol* 44:190–194, 1997.
234. J Alsenz, H Steffen, R Alex. Active apical secretory efflux of the HIV protease

- inhibitors saquinavir and ritonavir in Caco-2 cell monolayers. *Pharm Res* 15:423–428, 1998.
235. W Muck, I Mai, L Fritsche, K Ochmann, G Rohde, S Unger, A Johne, S Bauer, K Budde, I Roots, HH Neumayer, J Kuhlmann. Increase in cerivastatin systemic exposure after single and multiple dosing in cyclosporine-treated kidney transplant recipients. *Clin Pharmacol Ther* 65:251–261, 1999.
236. W Much, W Ritter, K Ochmann, S Unger, G Ahr, W Wingender, J Kuhlmann. Absolute and relative bioavailability of the HMG-CoA reductase inhibitor cerivastatin. *Int J Clin Pharmacol Ther* 35:255–260, 1997.
237. M Boberg, R Angerbauer, P Fey, WK Kanhai, W Karl, A Kern, J Ploschke, M Radtke. Metabolism of cerivastatin by human liver microsomes in vitro. Characterization of primary metabolic pathways and of cytochrome P450 isozymes involved. *Drug Metab Dispos* 25:321–331, 1997.
238. W Muck, K Ochmann, G Rohde, S Unger, J Kuhlmann. Influence of erythromycin pre- and co-treatment on single-dose pharmacokinetics of the HMG-CoA reductase inhibitor cerivastatin. *Eur J Clin Pharmacol* 53:469–473, 1998.
239. JH Pincus, K Barry. Protein distribution diet restores motor function in patients with dopa-resistant “off” period. *Neurology* 38:481–483, 1988.
240. KL Audus, RT Borchardt. Characterization of the large neutral amino acid transport system of bovine brain microvessel endothelial cell monolayers. *J Neurochem* 47:484–488, 1986.
241. NH Greig, S Momma, DJ Sweeney, QR Smith, SI Rapoport. Facilitated transport of melphalan at the rat blood-brain barrier by the large neutral amino acid carrier system. *Cancer Res* 47:1571–1576, 1987.
242. SH Blondheim. Effect of probenecid on excretion of bromosulphthalein. *J Clin Invest* 7:529–532, 1955.
243. AG Gilman, TW Rall, AS Nies, P Taylor. In: Goodman and Gilman’s *The Pharmacological Basis of Therapeutics*. 8th ed. New York: Pergamon press, 1990.
244. RS Bourke, G Chheda, A Bremer, O Watanabe, DB Tower. Inhibition of renal tubular transport of methotrexate by probenecid. *Cancer Res* 35:110–116, 1975.
245. WM Williams, TS Chen, KC Huang. Effect of penicillin on the renal tubular secretion of methotrexate in the monkey. *Cancer Res* 44:1913–1917, 1984.
246. DW Nierenerg. Drug inhibition of penicillin tubular secretion: concordance between in vitro and clinical findings. *J Pharmacol Exp Ther* 240:712–716, 1987.
247. SP Boom, I Meyer, AC Wouterse, FG Russel. A physiologically based kidney model for the renal clearance of ranitidine and the interaction with cimetidine and probenecid in the dog. *Biopharm Drug Dispos* 19:199–208, 1998.
248. U Jaehde, F Sorgel, A Reiter, G Sigl, KG Naber, W Schunack. Effect of probenecid on the distribution and elimination of ciprofloxacin in humans. *Clin Pharmacol Ther* 58:532–541, 1995.
249. TB Vree, M Van den Biggelaar-martea, CPWGM Verwey-van Wissen. Probenecid inhibits the renal clearance of frusemide and its acylglucuronide. *Br J Clin Pharmacol* 39:692–695, 1995.
250. TM Garrigues, U Martin, JE Peris-Ribera, LF Prescott. Dose-dependent absorption and elimination of cefadroxil in man. *Eur J Clin Pharmacol* 41:179–183, 1991.
251. JPF Bai, GL Amidon. Structural specificity of mucosal-cell transport and metabo-

- lism of peptide drugs: implication for oral peptide drug delivery. *Pharm Res* 9: 969–978, 1992.
252. LK Christensen, JM Hansen, M Kristensen. Sulfaphenazole-induced hypoglycaemic attacks in tolbutamide treated diabetics. *Lancet* 2:1298–1301, 1963.
253. M Rowland, SB Martin. Kinetics of drug–drug interactions. *J Pharmacokinet Biopharm* 1:553–567, 1973.
254. J Shibasaki, R Konishi, K Yamazaki. Tolbutamide–sulphaphenazole interaction in rabbits. *J Pharmacokinet Biopharm* 5:277–290, 1977.
255. O Sugita, Y Sawada, Y Sugiyama, T Iga, M Hanano. Physiological based pharmacokinetics of drug–drug interaction: a study of tolbutamide–sulfonamide interaction in rats. *J Pharmcokin Biopharm* 10:297–316, 1982.
256. H Takanaga, H Murakami, N Koyabu, H Matsuo, M Naito, T Tsuruo, Y Sawada. Efflux transport of tolbutamide across the blood-brain barrier. *J Pharm Pharmacol* 50:1027–1033, 1998.
257. K Okudaira, Y Sawada, Y Sugiyama, T Iga, M Hanano. Effects of basic drugs on the hepatic transport of cardiac glycosides in rats. *Biochem Pharmacol* 37:2949–2955, 1988.
258. PW Wigler, KL Lyon, K Patterson, AJ Loggia, H Diazarauzo, MS Reddy, JM Cook. Epoxide metabolite of quinine and inhibition of the multidrug resistance pump in human leukemic lymphoblasts. *Mol Pharmacol* 46:563–567, 1994.
259. S Song, H Suzuki, R Kawai, C Tanaka, I Akasaka, Y Sugiyama. Dose-dependent effects of PSC 833 on its tissue distribution and on the biliary excretion of endogenous substrates in rats. *Drug Metab Dispos* 26:1128–1133, 1998.
260. N Simon, E Dailly, S Combes, E Malaurie, M Lemaire, JP Tillement, S Urien. Role of lipoprotein in the plasma binding of SDZ PSC 833, a novel multidrug resistance–reversing cyclosporin. *Br J Clin Pharmacol* 45:173–175, 1998.
261. D Boesch, K Muller, A Poutier-Manzanedo, F Loor. Restoration of daunomycin retention in multidrug-resistant P388 cells by submicromolar concentrations of SDZ PSC 833, a nonimmunosuppressive cyclosporin derivative. *Exp Cell Res* 196: 26–32, 1991.
262. M Bohme, G Jedlitschky, I Leier, M Buchler, D Keppler. ATP-dependent export pumps and their inhibition by cyclosporins. *Adv Enzyme Regulation* 34:371–380, 1994.
263. S Masuda, H Saito, K Inui. Interactions of nonsteroidal anti-inflammatory drugs with rat renal organic anion transporter, OAT-K1. *J Pharmacol Exp Ther* 283: 1039–1042, 1997.
264. BM Emanuelsson, B Beermann, LK Paalzow. Non-linear elimination and protein binding of probenecid. *Eur J Clin Pharmacol* 32:395–401, 1989.
265. N Kanai, R Lu, Y Bao, AW Wolkoff, VL Schuster. Transient expression of oatp organic anion transporter in mammalian cells: identification of candidate substrates. *Am J Physiol* 270:F319–325, 1996.
266. T Kitamura, P Jansen, C Hardenbrook, Y Kamimoto, Z Gatmaitan, IM Arias. Defective ATP-dependent bile canalicular transport of organic anions in mutant (TR-) rats with conjugated hyperbilirubinemia. *Proc Natl Acad Sci USA* 87:3557–3561, 1990.
267. PJ Sinko, GL Amidon. Characterization of the oral absorption of beta-lactam anti-

- otics. I. Cephalosporins: determination of intrinsic membrane absorption parameters in the rat intestine in situ. *Pharm Res* 5:645–650, 1988.
268. AE Busch, S Quester, JC Ulzheimer, V Gorboulev, A Akhoundova, S Waldegger, F Lang, H Koepsell. Monoamine neurotransmitter transport mediated by the polyspecific cation transporter rOCT1. *FEBS Lett* 395:153–156, 1996.
269. T Breidert, F Spitzenberger, D Grundemann, E Schomig. Catecholamine transport by the organic cation transporter type 1 (OCT1). *Br J Pharmacol* 125:218–224, 1998.
270. L Zhang, ME Schaner, KM Giacomini. Functional characterization of an organic cation transporter (hOCT1) in a transiently transfected human cell line (HeLa). *J Pharmacol Exp Ther* 286:354–361, 1998.
271. L Zhang, MJ Dresser, AT Gray, SC Yost, S Terashita, KM Giacomini. Cloning and functional expression of a human liver organic anion transporter. *Mol Pharmacol* 51:913–921, 1997.
272. M Okuda, H Saito, Y Urakami, M Takano, K Inui. cDNA cloning and functional expression of a novel rat kidney organic cation transporter, OCT2. *Biochem Biophys Res Commun* 224:500–507, 1996.
273. D Grundemann, S Koster, N Kiefer, T Breidert, M Engelhardt, F Spitzenberger, N Obermuller, E Schomig. Transport of monoamine transmitters by the organic cation transporter type 2, OCT2. *J Biol Chem* 273:30915–30920, 1998.
274. AE Busch, U Karbach, D Miska, V Gorboulev, A Akhoundova, C Volk, P Arndt, JC Ulzheimer, MS Sonders, C Baumann, S Waldegger, F Lang, H Koepsell. Human neurons express the polyspecific cation transporter hOCT2, which translocates monoamine neurotransmitters, amantadine, and memantine. *Mol Pharmacol* 54:342–352, 1998.
275. Y Zhu, MC Jong, KA Frazer, E Gong, RM Krauss, JF Cheng, D Boffelli, EM Rubin. Genomic interval engineering of mice identifies a novel modulator of triglyceride production. *Proc Natl Acad Sci USA* 97:1137–1142, 2000.
276. T Sekine, H Kusuhara, N Utsunomiya-Tate, M Tsuda, Y Sugiyama, Y Kanai, H Endou. Molecular cloning and characterization of high-affinity carnitine transporter from rat intestine. *Biochem Biophys Res Commun* 251:586–591, 1998.
277. U Eckhardt, JA Horz, E Petzinger, W Stuber, M Reers, G Dickneite, H Daniel, M Wagener, B Hagenbuch, B Stieger, PJ Meier. The peptide-based thrombin inhibitor CRC 220 is a new substrate of the basolateral rat liver organic anion-transporting polypeptide. *Hepatology* 24:380–384, 1996.
278. U Eckhardt, A Schroeder, B Stieger, M Hochli, L Landmann, R Tynes, PJ Meier, B Hagenbuch. Polyspecific substrate uptake by the hepatic organic anion transporter Oatp1 in stably transfected CHO cells. *Am J Physiol* 276:G1037–1042, 1999.
279. KS Pang, PJ Wang, AY Chung, AW Wolkoff. The modified dipeptide, enalapril, an angiotensin-converting enzyme inhibitor, is transported by the rat liver organic anion transport protein. *Hepatology* 28:1341–1346, 1998.
280. M Kontaxi, U Eckhardt, B Hagenbuch, B Stieger, PJ Meier, E Petzinger. Uptake of the mycotoxin ochratoxin A in liver cells occurs via the cloned organic anion transporting polypeptide. *J Pharmacol Exp Ther* 279:1507–1513, 1996.
281. H Ishizuka, K Konno, H Naganuma, K Nishimura, H Kouzuki, H Suzuki, B Stieger,

- PJ Meier, Y Sugiyama. Transport of temocaprilat into rat hepatocytes: role of organic anion transporting polypeptide. *J Pharmacol Exp Ther* 287:37–42, 1998.
282. T Tokui, D Nakai, R Nakagomi, H yawo, T Abe, Y Sugiyama. Pravastatin, an HMG-CoA reductase inhibitor, is transported by rat organic anion transporting polypeptide, oatp2. *Pharm Res* 16:904–908, 1999.
283. T Cihlar, DC Lin, JB Pritchard, MD Fuller, DB Mendel, DH Sweet. The antiviral nucleotide analogs cidofovir and adefovir are novel substrates for human and rat renal organic anion transporter 1. *Mol Pharmacol* 56:570–580, 1999.
284. M Hosoyamada, T Sekine, Y Kanai, H Endou. Molecular cloning and functional expression of a multispecific organic anion transporter from human kidney. *Am J Physiol* 276:F122–128, 1999.
285. R Lu, BS Chan, VL Schuster. Cloning of the human kidney PAH transporter: narrow substrate specificity and regulation by protein kinase C. *Am J Physiol* 276: F295–303, 1999.
286. H Saito, M Okuda, T Terada, S Sasaki, K Inui. Cloning and characterization of a rat H<sup>+</sup>/peptide cotransporter mediating absorption of beta-lactam antibiotics in the intestine and kidney. *J Pharmacol Exp Ther* 275:1631–1637, 1995.
287. A Tsuji, I Tamai. Carrier-mediated intestinal transport of drugs. *Pharm Res* 13: 963–977, 1996.
288. M Boll, D Markovich, WM Weber, H Korte, H Daniel, H Murer. Expression cloning of a cDNA from rabbit small intestine related to proton-coupled transport of peptides, beta-lactam antibiotics and ACE-inhibitors. *Pflugers Arch* 429:146–149, 1994.
289. ME Ganapathy, M Brandsch, PD Prasad, V Ganapathy, FH Leibach. Differential recognition of beta-lactam antibiotics by intestinal and renal peptide transporters, PEPT 1 and PEPT2. *J Biol Chem* 270:25672–25677, 1995.
290. ME Ganapathy, PD Prasad, B Mackenzie, V Ganapathy, FH Leibach. Interaction of anionic cephalosporins with the intestinal and renal peptide transporters PEPT 1 and PEPT 2. *Biochim Biophys Acta* 1324:296–308, 1997.
291. R Liang, YJ Fei, PD Prasad, S Ramamoorthy, H Han, TL Yang-Feng, MA Hediger, V Ganapathy, FH Leibach. Human intestinal H<sup>+</sup>/peptide cotransporter. Cloning, functional expression, and chromosomal localization. *J Biol Chem* 270:6456–6463, 1995.
292. W Liu, R Liang, S Ramamoorthy, YJ Fei, ME Ganapathy, MA Hediger, V Ganapathy, FH Leibach. Molecular cloning of PEPT 2, a new member of the H<sup>+</sup>/peptide cotransporter family, from human kidney. *Biochim Biophys Acta* 1235:461–466, 1995.
293. NH Hendrikse, AH Schinkel, EG de Vries, E Fluks, WT Van der Graaf, AT Willemssen, W Vaalburg, EJ Franssen. Complete in vivo reversal of P-glycoprotein pump function in the blood-brain barrier visualized with positron emission tomography. *Br J Pharmacol* 124:1413–1418, 1998.
294. S Desrayaud, EC De Lange, M Lemaire, A Bruelisauer, AG De Boer, DD Breimer. Effect of the Mdr1a P-glycoprotein gene disruption on the tissue distribution of SDZ PSC 833, a multidrug resistance-reversing agent, in mice. *J Pharmacol Exp Ther* 285:438–443, 1998.
295. K Yokogawa, M Takahashi, I Tamai, H Konishi, M Nomura, S Moritani, K Miya-

- moto, A Tsuji. P-glycoprotein-dependent disposition kinetics of tacrolimus: studies in *mdr1a* knockout mice. *Pharm Res* 16:1213–1218, 1999.
296. RB Kim, MF Fromm, C Wandel, B Leake, AJ Wood, DM Roden, GR Wilkinson. The drug transporter P-glycoprotein limits oral absorption and brain entry of HIV-1 protease inhibitors. *J Clin Invest* 101:289–294, 1998.
297. J van Asperen, O van Tellingen, F Tijssen, AH Schinkel, JH Beijnen. Increased accumulation of doxorubicin and doxorubicinol in cardiac tissue of mice lacking *mdr1a* P-glycoprotein. *Br J Cancer* 79:108–113, 1999.
298. JW Jonker, E Wagenaar, L van Deemter, R Gottschlich, HM Bender, J Dasenbrock, AH Schinkel. Role of blood-brain barrier P-glycoprotein in limiting brain accumulation and sedative side effects of asimadoline, a peripherally acting analgesic drug. *Br J Pharmacol* 127:43–50, 1999.
299. M Murata, I Tamai, H Kato, O Nagata, A Tsuji. Efflux transport of a new quinolone antibacterial agent, HSR-903, across the blood-brain barrier. *J Pharmacol Exp Ther* 290:51–57, 1999.
300. JW Polli, JL Jarrett, SD Studenberg, JE Humphreys, SW Dennis, KR Brouwer, JL Woolley. Role of P-glycoprotein on the CNS disposition of amprenavir (141W94), an HIV protease inhibitor. *Pharm Res* 16:1206–1212, 1999.
301. T Kawabe, ZS Chen, M Wada, T Uchiumi, M Ono, S Akiyama, M Kuwano. Enhanced transport of anticancer agents and leukotriene C4 by the human canalicular multispecific organic anion transporter (cMOAT/MRP2). *FEBS Lett* 456:327–331, 1999.
302. T Kamisako, I Leier, Y Cui, J Konig, U Buchholz, J Hummel-Eisenbeiss, D Keppler. Transport of monoglucuronosyl and bisglucuronosyl bilirubin by recombinant human and rat multidrug resistance protein 2. *Hepatology* 30:485–490, 1999.
303. CWN Chiang, LZ Benet. Dose-dependent kinetics of probenecid in rhesus monkeys-intravenous bolus studies. *Pharmacology* 23:326–336, 1981.
304. MI Sheikh, J Maxild. Kinetics studies on the renal transport of probenecid in vitro. *Biochim Biophys Acta* 514:356–361, 1978.
305. V Cattori, B Hagenbuch, N Hagenbuch, B Steiger, R Ha, KE Winterhalter, PJ Meier. Identification of organic anion transporting polypeptide 4 (Oatp4) as a major full-length isoform of the liver-specific transporter-1 (*rlst-1*) in rat liver. *FEBS Lett* 474:242–245, 2000.
306. Y Cui, J Konig, II Leier, U Buchholz, D Keppler. Hepatic uptake of bilirubin and its conjugates by the human organic anion-transporting polypeptide 2 (symbol SLC21A6). *J Biol Chem* 27:27, 2000.
307. J Konig, Y Cui, AT Nies, D Keppler. Localization and genomic organization of a new hepatocellular organic anion transporting polypeptide. *J Biol Chem* 275:23161–23168, 2000.
308. GA Kullak-Ublick, MG Ismail, B Steiger, L Landmann, R Huber, F Pizzagalli, K Fattinger, PJ Meier, B Hagenbuch. Organic anion-transporting polypeptide B (OATP-B) and its functional comparison with three other OATPs of human liver. *Gastroenterology* 120:525–533, 2001.
309. SH Cha, T Sekine, J Fukushima, Y Kanai, Y Kobayashi, T Goya, H Endou. Identification and characterization of human organic anion transporter 3 expressing predominantly in the kidney. *Mol Pharmacol* 59:1277–1286, 2001.

# 6

## In Vitro Models for Studying Induction of Cytochrome P450 Enzymes

**Jose M. Silva and Deborah A. Nicoll-Griffith**

*Merck Frosst Canada, Quebec, Canada*

### I. INTRODUCTION

Cytochrome P450 (CYP) enzymes form a gene superfamily that are involved in the metabolism of a variety of chemically diverse substances ranging from endogenous compounds to xenobiotics, including drugs, carcinogens, and environmental pollutants. Although CYP regulation is only now beginning to be understood, it is well known that several of the CYP genes are induced by many drugs. This may cause variability in enzymatic activity, with different groups of patients producing unexpected pharmacological outcomes of some drugs as a result of drug–drug interactions [1,2]. For example, induction of CYP3A has been shown to result in a significant loss of efficacy for the contraceptive steroids [3,4]. Thus, regulatory agencies now request that new drugs be tested for their potential to induce CYP enzymes. Until recently, this involved treating laboratory animals with the test compound, followed by analysis of liver CYP enzymes *ex vivo*. This raises four major issues: First, there is the requirement of large numbers of animals; reduction in animal usage should be encouraged where possible. Second, large amounts of test compound have to be synthesized; this imposes a heavy burden on the synthetic chemistry efforts and is not compatible with combinatorial chemistry strategies. Thirdly, *in vivo* studies are not high throughput, this in a time where advancements in combinatorial chemical synthesis have greatly increased the number of drug candidates being produced at the drug discovery stage. And finally, it is well known that species differences in CYP induction exist [5], making the extrapolation from animals to humans unreliable. Therefore, it is desirable to have *in vitro* models, in particular of human origin,



to address CYP induction of drug candidates before costly clinical trials are conducted.

Unfortunately, there are no hepatoma cell lines able to express most of the major forms of adult CYP enzymes. However, various *in vitro* models for assessing enzyme induction have been described and include precision-cut liver slices, primary hepatocytes, and reporter gene constructs. The last model involves transfecting recombinant DNA encoding a reporter enzyme, such as chloramphenicol acetyl transferase, under the control of the regulatory element of the specific CYP of interest. In this chapter we will discuss all three models but will focus mostly on the primary hepatocyte model which, in our opinion, is the gold standard for predicting CYP induction in both laboratory animals and human. In addition, a case study involving a drug candidate ('DFP') will be discussed along with strategies for managing CYP induction in drug candidates.

## II. MODELS

### A. Primary Hepatocytes

Isolation of viable hepatocytes was first demonstrated by Howard et al. and rapidly increased in popularity with the further development of a high-yield preparative technique by Berry and Friend [6,7]. Compared to liver slices, isolated hepatocytes are easier to manipulate and show a superior range of activities [8]. For a detailed description of rat and human hepatocyte isolation techniques the reader is referred to other reviews [8,9].

While primary hepatocytes maintained under conventional culture conditions tend to undergo rapid loss of liver-specific functions, great progress has been made in the last decade to slowing this process. In our opinion the three most important factors in retaining CYP responsiveness in primary hepatocyte are: media formulation, matrix composition, and cell-cell contacts [10–13].

There are several commercially available media that have been reported to support CYP-inducible hepatocytes in culture, including: Dubecco's modified Eagle's medium, Liebovitz L-15 medium, Waymouth 752/1 and modified Williams' E medium, to name a few [11]. In summary, these are all enriched media containing a high amino acid content. High concentrations of certain amino acids have been reported to decrease protein degradation while stabilizing some levels of mRNA [14]. Serum has routinely been used as a media supplement with many immortalized cell lines and is thought to improve cell attachment, survival, and morphology. However, with primary hepatocytes, serum is generally thought to promote growth and therefore has a dedifferentiation effect on hepatocytes, resulting in a loss of CYP expression [15]. As a result, serum is used in the initial cell attachment stage (<24 hr) but is usually not included for the duration of the

culture. Other supplements usually include dexamethasone and insulin. A low concentration of dexamethasone (<100 nM) has been reported to improve the viability of hepatocytes in culture [8] as well as to improve the responsiveness to CYP inducers [12,16,17]. Insulin is also considered to be beneficial for the long-term survival of cultured hepatocytes [11].

Another culture condition known to be important in the maintenance of differentiated hepatocytes is the extracellular matrix. These comprise simple matrices, such as rat tail collagen, as well as more complex matrices, including: fibronectin [18], extracts from rat liver [19], and, more recently, Matrigel, a bio-matrix preparation derived from the Engelbreth-Holm-Swarm sarcoma [10,12]. In our laboratory, we initially compared both rat and human primary hepatocytes cultured on collagen compared to Matrigel and found that while CYP3A responsiveness was not affected, basal CYP3A levels were better maintained in hepatocytes on Matrigel. In contrast, responsiveness to CYP2B1 in rat hepatocytes was markedly affected by the substratum used. As shown in Figure 1, Western blots of rat hepatocytes treated with phenobarbital show marked induction in CYP2B1 protein, while a poor response was observed in cells cultured on collagen [12].

Another substratum model developed to preserve liver function in hepatocytes in culture is the collagen-sandwich model. It was first demonstrated by Dunn et al. [20] that overlaying cultured rat hepatocytes with a top layer of collagen preserved the liver-specific phenotype, including CYP inducibility [21]. In addition, cells cultured under these conditions re-established cell polarity and developed a structurally and functionally normal bile canalicular network [22]. More recently, LeCluyse et al. [23] reported that the matrix conditions considered to be optimal for maintaining cellular integrity, protein yields, and CYP enzyme induction in primary human hepatocytes are a collagen-sandwich model in combination with modified Chee's medium containing insulin and dexamethasone.

Figure 2 illustrates the standard induction protocol that we follow in our laboratory. Freshly isolated hepatocytes are cultured on 60-mm dishes or multiwell plates precoated with Matrigel for a minimum of two days. This allows the cells to recover from the damage endured during isolation and allows the cells to adapt to the culture environment. It's been reported that during this initial culture period a rapid loss in constitutive CYP expression is observed in the first 24 hr, followed by a recovery period after which the cells are capable to respond to CYP inducers [12,24]. The cells are then challenged with the test compounds and allowed to incubate for a period of 24–48 hr. Response to inducers is rapid, as shown by the Northern blots of rat hepatocytes treated with dexamethasone and phenobarbital in Figure 3. CYP3A and CYP2B1 mRNA levels increased within 2 hr, reaching a maximum at 24 hr. Corresponding CYP protein induction requires at least 8 hr before a significant rise is observed.

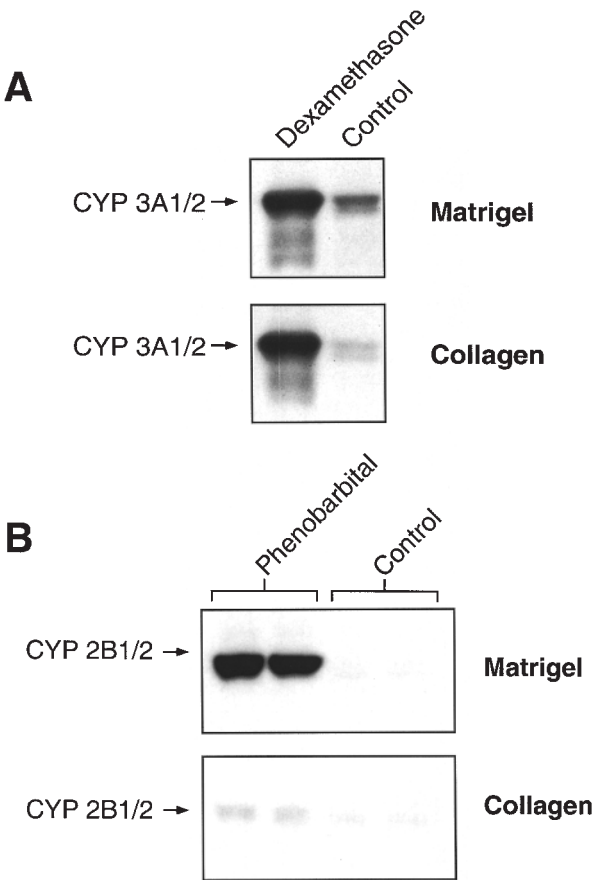


**Figure 1** Immunoblot analysis of CYP3A (panel A) and CYP2B (panel B) protein in rat hepatocytes cultured on Matrigel and collagen. Cells were incubated in the presence of 10  $\mu$ M dexamethasone or 50  $\mu$ M phenobarbital for 48 hr. (From Ref. 12.)

### 1. Interpretation of Induction Data

Induction of CYP expression by xenobiotics has been reported in mainly three ways: induction potential (fold induction over control);  $EC_{50}$  (effective concentration for 50% maximal induction); and ‘potency index’ (the ratio of induction response of the test compound compared to that of a gold standard). In our laboratory, we have defined CYP induction as a *potency index*, or a percentage of a classic inducer, rather than as fold increase over a control (induction potential). The reason for this is twofold: First, the basal levels of some CYPs may be low

## Cytochrome P450 Induction Assay in Primary Cultured Hepatocytes

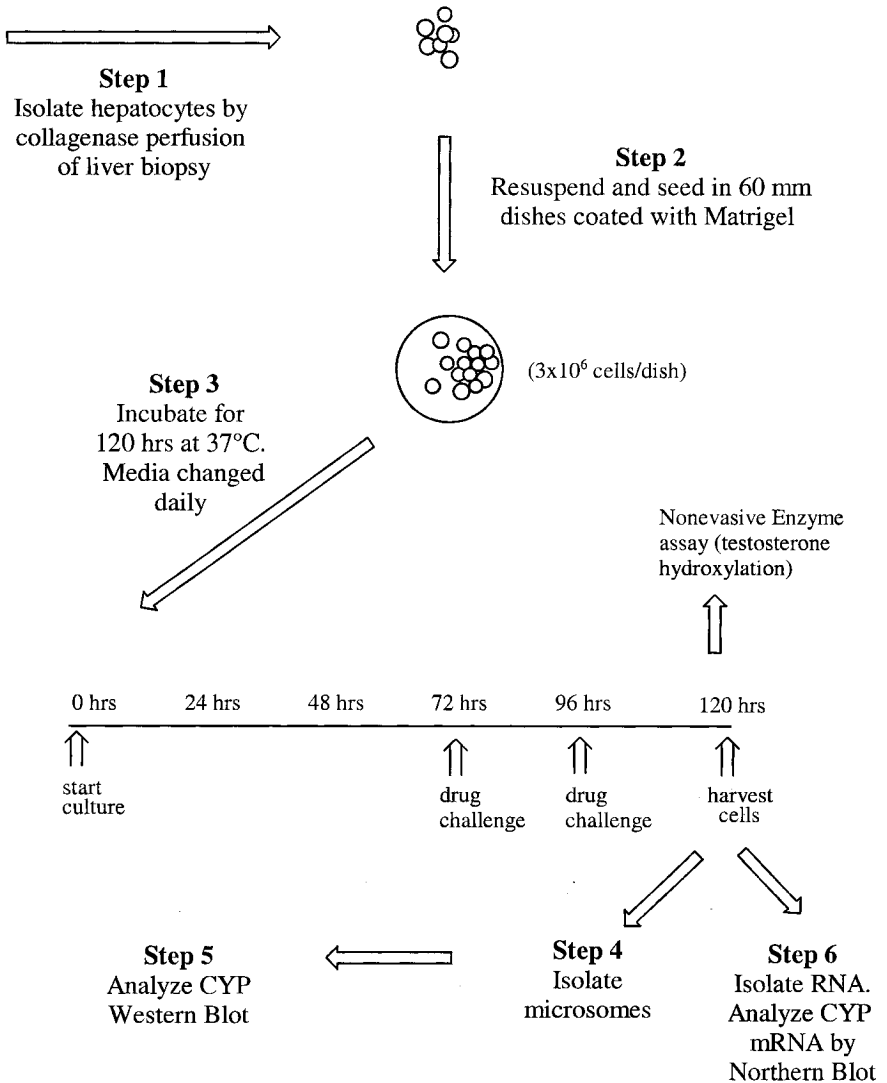
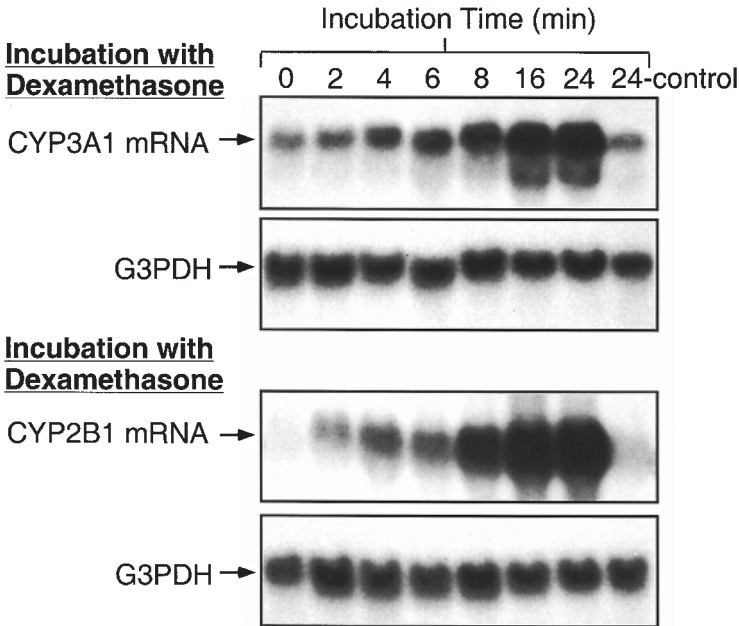
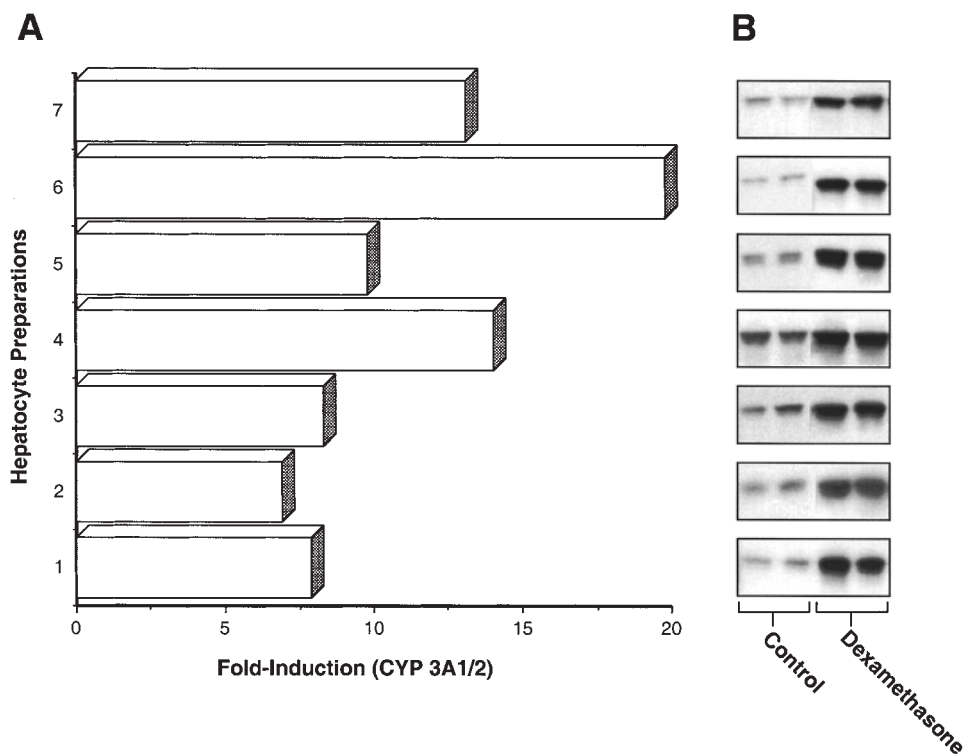


Figure 2 Hepatocyte induction protocol.



**Figure 3** Northern blot analysis of CYP3A and 2B mRNAs in rat hepatocytes cultured on Matrigel. Cells were incubated in the presence of 10  $\mu$ M dexamethasone or 50  $\mu$ M phenobarbital for 48 hr. (From Ref. 12.)

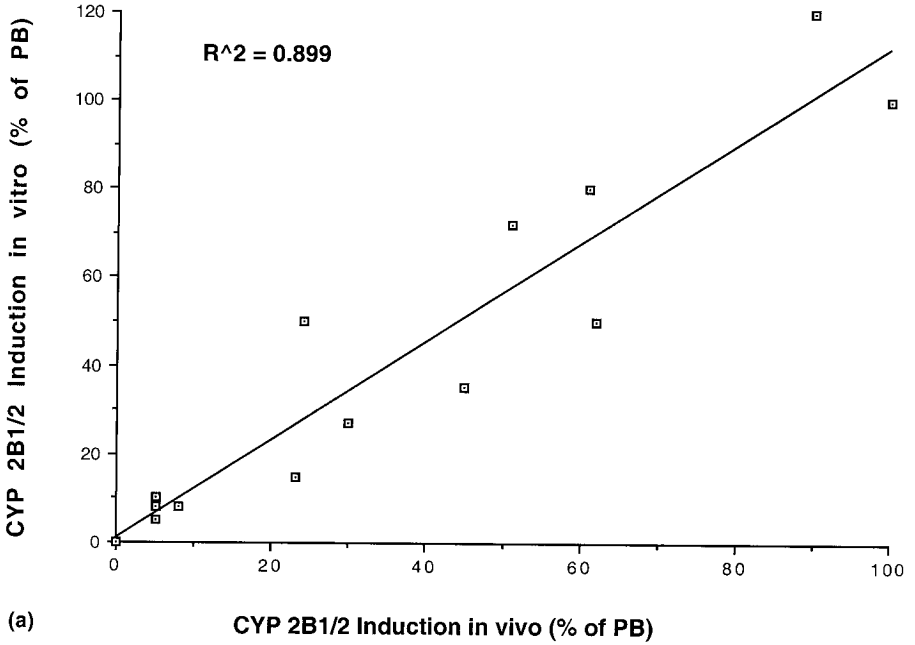
and therefore difficult to accurately quantitate. Second, we, and others, have found that basal CYP levels in culture may be highly variable between different hepatocyte preparations, while the maximum induction levels are more consistent. For example, we have found that induction of CYP3A protein in dexamethasone-treated rat hepatocyte cultures from different preparations varies from a  $\sim$ 7- to a  $\sim$ 20-fold increase (Fig. 4) [12]. In human primary cultures, induction of CYP3A4 by a drug candidate, calculated as a fold increase, also varied from a 2- to an 8-fold increase in hepatocytes from four different donors [12]. In contrast, when the results were expressed as a percentage of a classic inducer (rifampicin), the range was from 16 to 34% [12]. Interestingly, Kostrubsky et al. reported that variation in the basal level of CYP3A4 expression in human primary hepatocytes was up to fivefold between different donors [25]. However, the maximal CYP3A activity detected after treatment with rifampicin was similar in six separate human hepatocyte cultures. Another study, by Chang et al., reported that induction of oxazaphosphorine 4-hydroxylation activity by rifampicin in human



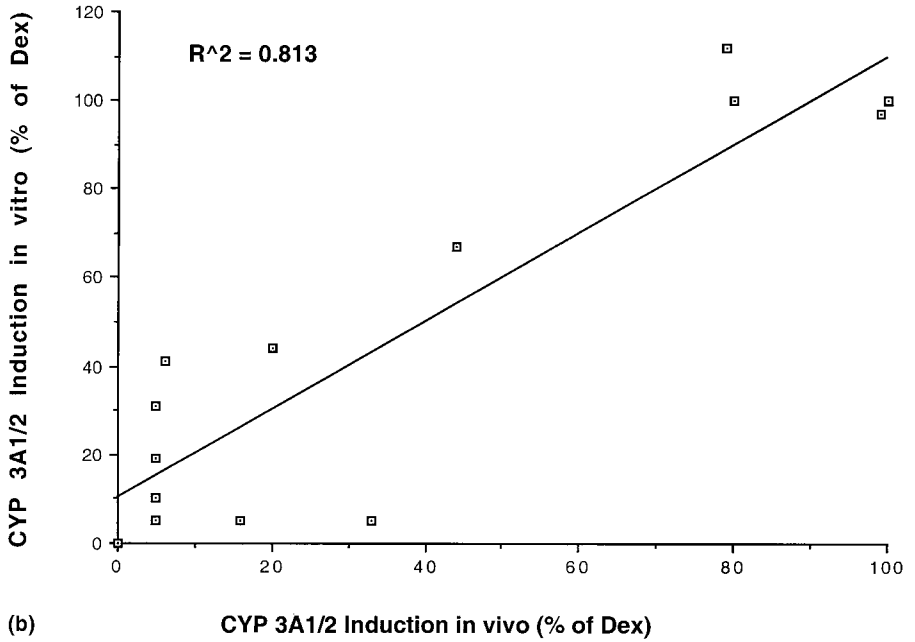
**Figure 4** Variability in CYP3A induction in rat hepatocytes from seven different preparations. Panel A represents fold increase in CYP3A protein from dexamethasone-treated cells over nontreated cells. (From Ref. 12.)

hepatocyte cultures was inversely related to the basal activity [26]. These results suggest that CYP activity after maximal induction is similar between separate cultures and that differences in fold induction result from variation in basal expression. It is therefore prudent to include a positive control to address the variability between different hepatocyte preparations. This is particularly important when comparing the potency indices of different drug candidates that may not have been incubated with the cells from the same donor.

In order to further validate this approach, we recently compared induction potency indices for a series of compounds *in vivo*, in rats, with those obtained in the rat hepatocyte model [12]. As shown in Figure 5, results demonstrated an excellent correlation for CYP3A and 2B expression.



(a)



(b)

## 2. In Vitro Induction Screening

One of the drawbacks of using protein level measurements in hepatocytes for induction screening is the relatively large amount of time and labor required for cell harvest and preparation of samples for CYP analysis. In addition, large numbers of cells are required per dish. This is particularly undesirable when using human hepatocytes, an increasingly limited resource. The immediate challenge, therefore, is to modify the model to accommodate a higher-throughput format. In our laboratory this has been achieved by developing a 96-well format and using analytical methodology that allows for the measurement of CYP expression in fewer cells.

In regards to culturing hepatocytes in a 96-well plate format, we have adapted the same conditions that we use when culturing cells in 60-mm dishes and 24-well plates [12] and simply scaled them down to a 96-well-plate format. The 96-well plates are precoated with Matrigel and are commercially available (Collaborative Biomedical Products) or, alternatively, normal plates can be coated with diluted Matrigel and dried overnight [27]. Hepatocytes cultured on collagen-coated 96-well plates have also been reported to be suitable for CYP induction [28].

With respect to higher-throughput analytical methodologies, we have taken two approaches: The first involves the addition of CYP-selective substrates to cell culture and measuring the formation of the relevant metabolites in the media (CYP activity assays). The second approach is to measure CYP mRNA levels using newly developed technologies compatible with 96-well-culture formats.

*a. CYP Activity Assays.* The first example of using activity probes for determining CYP expression in intact hepatocytes cultured on 96-well plates was described by Donato et al. [28]. In this study the authors used two derivatives of phenoxazone, namely, 7-ethoxyresorufin (EROD) and 7-pentoxyresorufin (PROD), to determine activity of CYP1A1 and 2B1, respectively, in rat and human hepatocytes. These two compounds are specifically *O*-dealkylated to a highly fluorescent metabolite, resorufin. Therefore, in this assay the substrates are added directly to the cells in the presence of dicumarol, to prevent further reduction of the quinone moiety by DT-diaphorase, and incubated for a period of time (~30 min). Aliquots of the media are then transferred to microplates to fluorometrically determine amount of product (resorufin) formed. Because resorufin is also known to be further conjugated by glucuronic acid and sulfate in the

---

**Figure 5** Induction of CYP2B (Panel a) and CYP3A (Panel b) in vitro vs. induction in vivo. Cultured rat hepatocytes and Sprague Dawley rats were treated with 13 drug candidates at a dose of 50  $\mu$ M and 400 mg/kg, respectively. Potency indexes for all the compounds in vitro were compared to ones found in vivo. (From Ref. 12.)



intact cell, a mixture of  $\beta$ -glucuronidase and arylsulfatase is added to the microplate to hydrolyze either conjugate back to resorufin. Validation of this method was examined by comparing the results obtained in intact cultured hepatocytes with the activity determined in the microsomal fraction. An excellent correlation between the two assays was found for EROD ( $r = 0.95$ ) and PROD ( $r = 0.94$ ) activities [28].

The classical CYP3A probe is testosterone, which is known to undergo CYP3A4-dependent  $6\beta$ -hydroxylation [29]. This probe has been well characterized and is widely used to determine CYP3A activity in human liver microsomes. Testosterone has also been used to determine CYP3A4 activity in human primary hepatocytes (as carefully described in Ref. 25). In our laboratory we have used both Western blot analysis and testosterone  $6\beta$ -hydroxylation activity assays to determine CYP3A4 induction in human hepatocytes and have found good agreement (Fig. 6). However, HPLC or LC/MS analysis is required for the

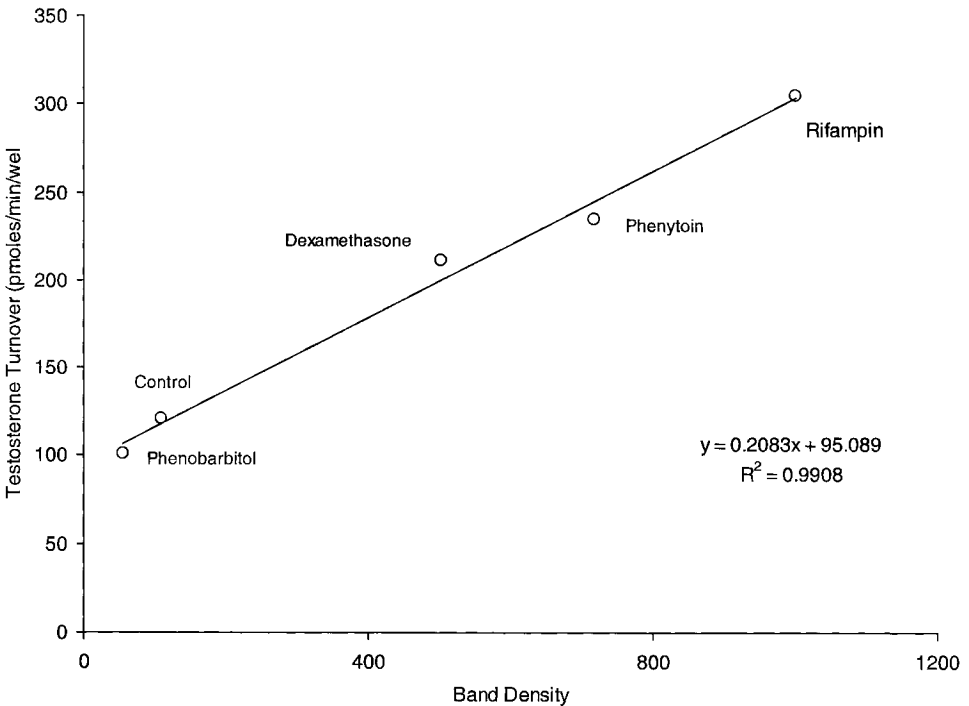


**Figure 6** Correlation between testosterone  $6\beta$ -hydroxylation and CYP3A protein levels, as determined by Western blot, in human hepatocytes incubated with several prototypical inducers.

quantification of the  $6\beta$ -hydroxytestosterone metabolite, resulting in a tedious and time-consuming assay. Two other probes, benzyloxyquinoline and benzylox-yltrifluorocoumarin (BFC), have also been identified as potential CYP3A fluorescent probes [30]. A recent study by Price et al. demonstrated that BFC is metabolized in microsomes from cells expressing recombinant human CYP1A, 2B, 2C, and 3A isoforms. In primary rat hepatocytes, however, BFC was shown to be a good substrate for assessing the induction of CYP1A, 1A2, and 2B1 isoforms but not CYP3A [31].

A recent paper by Chauret et al. described the discovery of a novel fluorescent probe that is selectively metabolized by CYP3A in human liver microsomes [32]. This probe, DFB (3,4-difluorobenzyl)-4-(4methylsulfonylphenyl)-5,5-dimethyl-(5H) furan-2-one), is metabolized to DFH, which has fluorescent characteristics (Fig. 7). In vitro CYP reaction phenotyping studies (cDNA-expressed CYP proteins and immunoinhibition experiments with highly selective anti-CYP3A4 antibodies) demonstrated that DFB was metabolized primarily by CYP3A4 (Fig. 8). Furthermore, metabolism studies performed with human liver microsomes obtained from different donors indicated that DFB dealkylation and testosterone  $6\beta$ -hydroxylation correlated well (Fig. 9).

In our laboratory we have further characterized the use of this probe for assessing CYP3A4 induction in cultured human hepatocytes [33,34]. In this assay, hepatocytes cultured in 96-well plates are incubated with DFB for 15 min. An aliquot of the media is then transferred to a microplate and DFH quantified using a fluorescent plate reader. During the course of the reaction, the fluorescent metabolite DFH is not metabolized and there is no need for further manipulation of the sample. Figure 10 shows the correlation of CYP3A4 activity obtained with DFB and testosterone in human hepatocytes treated with several inducers. The DFB assays afford a quick and simple readout of CYP3A4 activity. Furthermore, because the cells are not adversely affected, multiple assays can be performed at different times. Indeed, it may even be possible to use the same cells to test more than one compound after an adequate washout period. Ferrini et al. have described

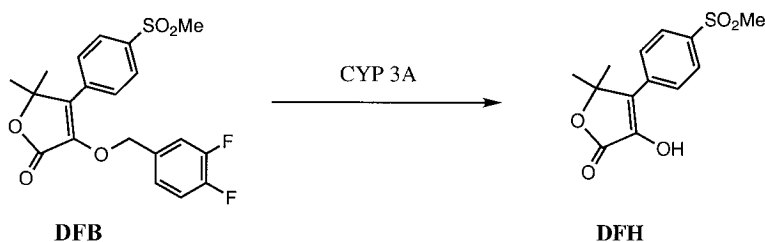


**Figure 7** Metabolic pathway for DFB.

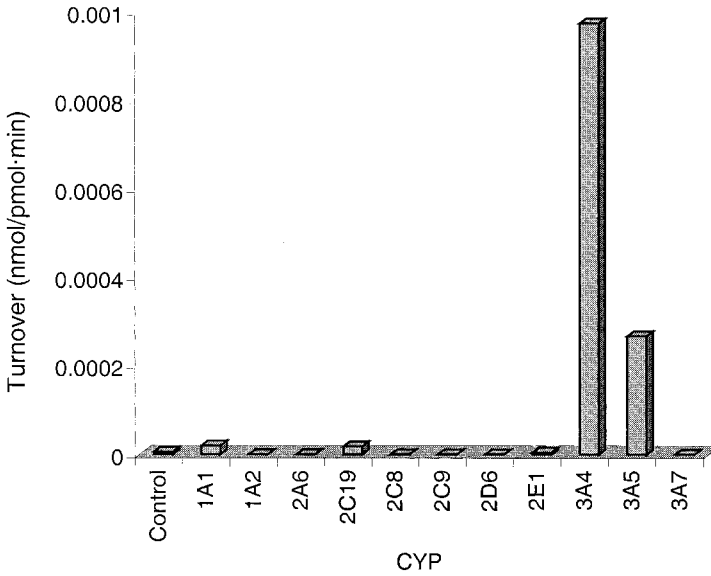


**Figure 8** Turnover of DFB to DFH in microsomes prepared from cell lines expressing a single CYP. (From Ref. 32.)

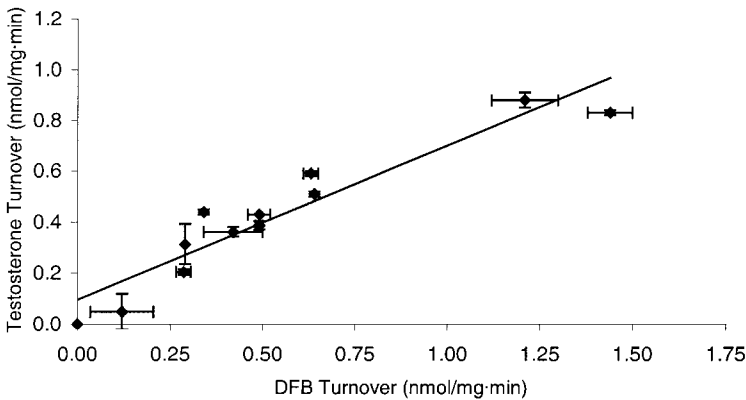


**Figure 9** Correlation between testosterone 6 $\beta$ -hydroxylation and DFB debenzoylation in various human liver microsomes. (From Ref. 32.)

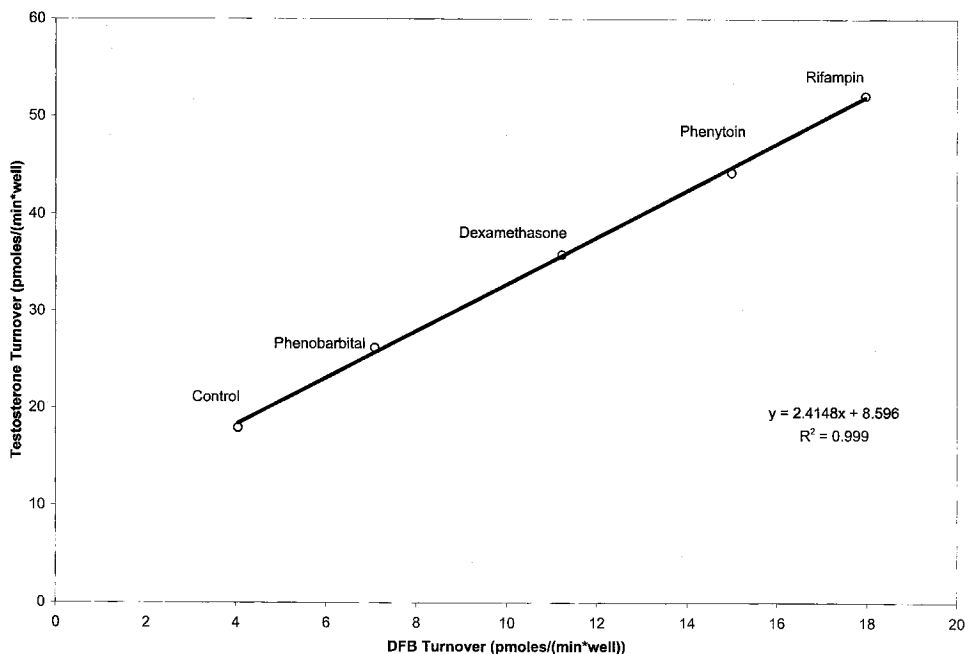


**Figure 10** Correlation between testosterone 6 $\beta$ -hydroxylation and DFB debenzoylation in human hepatocytes treated with several prototypical inducers.

culture conditions to maintain human hepatocytes for several weeks while retaining CYP inducibility [35]. In this latter study, the authors demonstrated that CYP3A4 expression would return to basal levels after removal of the inducer, at which time another round of testing by other compounds could be attempted.

Some compounds may have inducing properties as well as being mechanism-based inhibitors of the same CYP enzyme. It is therefore prudent, when analyzing CYP expression with activity probes, to verify that the compound being tested does not inhibit the CYP enzyme activity. In our laboratory we routinely test for this by incubating cells for  $\sim 2$  hr with the test compound prior to measurement of CYP enzyme activity. If, after thoroughly washing the cells, the activity in induced cells is reduced, it is likely that inhibition of CYP 3A4 has occurred. This will indicate whether the test compound is a time-dependent inhibitor.

#### *b. mRNA Analysis.*

QUANTITATIVE REAL-TIME REVERSE TRANSCRIPTASE-POLYMERASE CHAIN REACTION (RT-PCR). In addition to using immunodetection of apoprotein and

substrate metabolism, it is possible to screen for induction by analyzing expression of CYP mRNA. However, such methodology does not detect CYP induction resulting from posttranslational stabilization of proteins. An example of this latter case is with induction of CYP2E1 by isoniazid where an increase in mRNA is not observed [36].

Precise quantification of mRNA expression is difficult using conventional methods such as Northern blotting. By comparison, RT-PCR is more quantitative; however, the methodology is not suitable for a reasonable throughput [37,38] and may lead to semiquantitative data [39]. Recently, a more efficient technology for precise analysis of mRNA has been developed in the form of real-time RT-PCR [40,41]. The assay is based on the use of a 5'-nuclease assay and the detection of fluorescent PCR products [42]. The method uses the 5'-nuclease activity of *Taq* polymerase to cleave a nonextendable oligonucleotide probe that hybridizes to the target cDNA and is labeled with a fluorescent reporter dye [FAM(6-carboxyfluorescein)] on the 5' end and a quencher dye on the 3' end [TAMRA(6-carboxy-tetramethyl-rhodamine)] (Fig. 11). When the probe is intact, the fluorescent signal is quenched due to the close proximity of the fluorescent and quencher dyes. However, during PCR, the nuclease degradation of the hybridization probe releases the quenching of the reporter dye, resulting in an increase in fluorescent emission. Real-time analysis of fluorescence products after each PCR cycle is determined using the ABI Prism 7700 Sequence Detection System (PE Biosystems). The PCR amplification is done in a 96-well-plate format, and accumulation of PCR products is determined in real time by fluorescence detection. The mRNA copy number of the targeted gene is obtained by determining the PCR threshold cycle number generated when the fluorescent signal reaches a threshold value (see Ref. 42 for more details). Commonly, induction of gene expression is obtained by comparing fold increase of targeted mRNA from treated cells over mRNA from untreated cells.

The application of this technology for determining CYP induction in primary hepatocytes was first described by Strong et al. [40]. To further demonstrate the potential of this technology, a study was conducted in our laboratory using primary human primary hepatocytes cultured on a 96-well plate precoated with Matrigel [34]. Cells were treated with increasing doses of rifampicin (0.08–50  $\mu$ M) and at various intervals (3, 6, 12, and 24 hr). CYP3A4 activity was assessed with DFB prior to RNA isolation. CYP3A4, 5, and 7 mRNA analysis using real-time TaqMan PCR was then conducted. As shown in Figure 12, induction of CYP3A4 activity was clearly demonstrated after 24 hr in a dose-dependent manner. However, CYP3A4 mRNA was markedly elevated 3 hr after rifampicin dosing and continued to increase over 24 hr (Fig. 13A). These results demonstrate not only that rifampicin causes induction in CYP3A4 mRNA leading to a concomitant increase in CYP3A4 activity, but also that the increase in mRNA is a

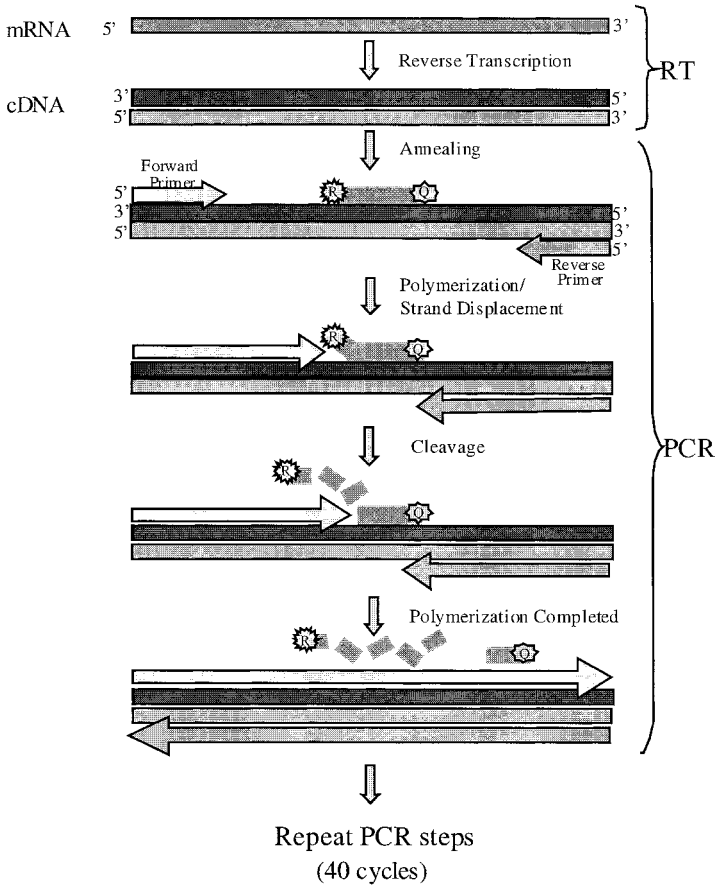


**Figure 11** TaqMan RT-PCR assay.

much earlier event compared to alteration in enzyme activity. In contrast to CYP3A4 mRNA, CYP3A5 and 3A7 mRNA were not significantly elevated by rifampicin (Fig. 13B, C). This clearly demonstrates the advantage of this technology in its ability to differentiate between closely related CYPs. A recent study by Bowen et al. has also demonstrated the use of quantitative real-time RT-PCR to measure the expression of CYP1A1 and 3A4 in human hepatocytes [41]. The more conventional analytical methodology exemplified by Western blot and substrate probes lack the sensitivity and selectivity to profile all CYPs. Another advantage to this method is the ability to store the isolated mRNAs in order to

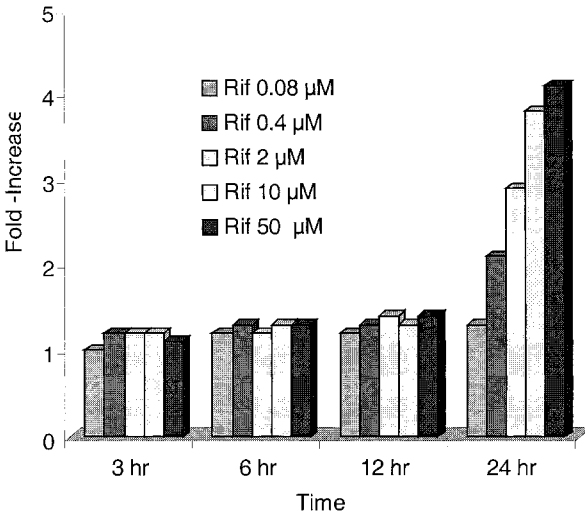
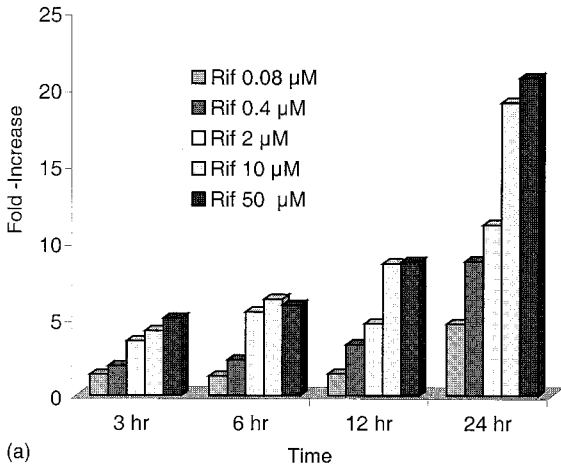


**Figure 12** Dose- and time-dependent induction of CYP3A activity in human cultured hepatocytes incubated with rifampicin. Cells cultured on Matrigel-coated 96-well plates were incubated with increasing doses of rifampicin, and CYP3A was determined by probing the cells with DFB prior to RNA isolation.

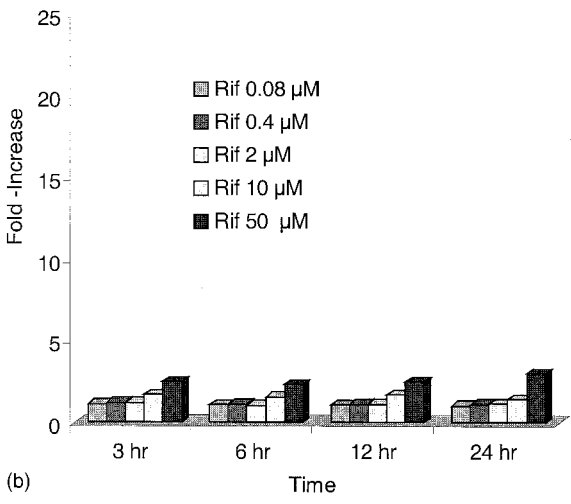
perform further analysis of other genes at a later date. The cells, however, are terminated at the end of the experiment and, therefore, cannot be recycled for further studies.

*c. Ribonuclease Protection Assays.* Surrey et al. reported a new assay to quantify mRNA levels for CYP isoforms 1A1, 1A2, 3A, and 4A1 in rat hepatocytes [43]. This assay uses a set of oligonucleotide probes end-labeled with [ $^{35}$ S]dATP to hybridize to mRNA in rat hepatocytes cultured on Cytostar-T\* 96-well scintillating microplates, precoated with Matrigel. After treating the cells with potential inducers, hepatocytes were fixed with formaldehyde followed by in situ hybridization with specific [ $^{35}$ S]ATP-labeled oligonucleotide probes developed to hybridize to specific sites on CYP mRNA. While the probes for CYP1A1,

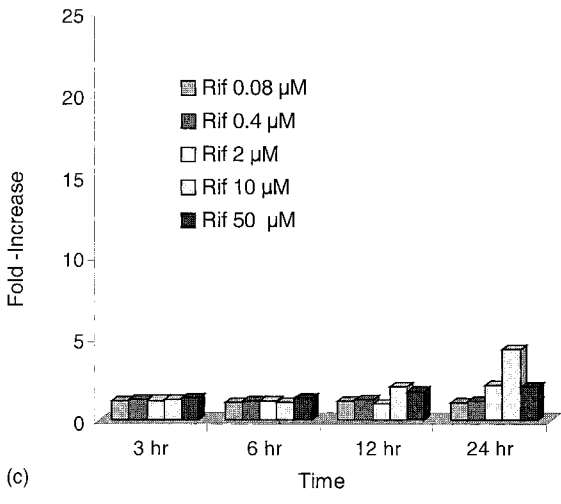
**Figure 13** Dose- and time-dependent induction of CYP3A4 (panel a), 3A5 (panel b), and 3A7 (panel c) mRNAs in human cultured hepatocytes incubated with rifampicin. Cells cultured on Matrigel-coated 96-well plates were incubated with increasing doses of rifampicin, and RNA was harvested at times indicated. Specific CYP mRNAs were determined by TaqMan RT-PCR.



(a)



(b)



(c)



1A2, and 4A1 were selective, the set for CYP3A did not discriminate between CYP3A1, 3A2, 3A18, and 3A23. In this study the authors demonstrated that the CYP3A mRNA levels obtained in rat hepatocytes treated with various compounds correlated well with testosterone 6 $\beta$ -hydroxylase activities in hepatic microsomes from *in vivo* studies [43].

The advantage of such a technique is that mRNA does not need to be isolated. The procedure, from culture to hybridization to detection, takes place within a single 96-well plate. A limitation to this assay is that only one CYP may be analyzed per well and samples cannot be stored for analysis of other genes at a later date.

*d. bDNA Technology.* Another recently developed technology to measure CYP mRNA levels is the branched DNA (bDNA) signal amplification assay [44,45]. This technology involves a nonpolymerase chain reaction and nonradioactive detection method resembling the enzyme-linked immunosorbent assay (ELISA). One of the advantages of this assay is the capability to use total RNA or cell extract for the analysis. The assay comprises a multiple of oligonucleotides to capture the mRNA of interest (see Ref. 45 for details). Three types of hybrid target probes are used and include capture probes, label extender, and blocker probes. Capture probes are designed so that a portion hybridizes to an oligonucleotide that is fixed to the well surface of a 96-well plate and another portion hybridizes to the target mRNA. Label extender oligonucleotide probes are designed so that a portion hybridizes to the mRNA target and the other portion hybridizes to the branched DNA molecule that is essential for the amplification of the hybridization signal. Blocker oligonucleotide probes fill in the gaps in the mRNA between the capture and the label extender probes (this minimizes RNase-mediated mRNA degradation). Detection of target CYP mRNA is then accomplished by adding an enzyme (alkaline phosphatase) conjugated to an oligonucleotide, which hybridizes to the branches of the bDNA molecule. Upon addition of a substrate, dioxetane, a chemiluminescent signal is produced and measured. This technology has recently been used to analyze the expression of CYP1A1, 1A2, 2B1/2, 2E1, 3A1/23, and 4A2/3 in rats treated with classical enzyme-inducing compounds [45].

## B. Liver Slices

Tissue slices have been used for several decades to study basic pathways of intermediary metabolism as well as hepatotoxicity [46–48]. However, procurement of the slices was performed by handheld instruments, and therefore the quality of the slices tended to vary between different preparations as well as between different laboratories [49]. It was not until 1985 that the first paper described

the development of a mechanical tissue slicer, where it was possible to obtain reproducible slices of specified thickness [50]. More recently, this model has gained popularity and acceptance. There are now two commercially available instruments to produce slices of reproducible thickness, the Krumdieck slicer and the Brendel-Vitron slicer (see Ref. 49 for a review). Although liver slices have been widely used for drug metabolism and toxicity studies, their use for CYP induction studies have been limited. Several groups have shown that it is possible to culture slices for several days while retaining CYP inducibility [51–54]. To overcome the problems associated with long-term culture of tissue slices, a roller culture system has been developed that allows the upper and lower surfaces of the cultured slice to be exposed to the gas phase during the course of incubation [49]. Precision-cut rat and human liver slices cultured in this way are reported to survive for up to 72 hours while still retaining CYP inducibility [55]. The same authors demonstrated induction of CYP2B1/2 and 3A in rat liver slices when treated with phenobarbital, CYP1A2 when treated with  $\beta$ -naphthoflavone, and CYP1A2, 2B1/2, and 3A when treated with Aroclor 1254 [55]. In cultured human liver slices, rifampicin has also been shown to induce CYP 3A4 [56].

This model offers the advantage of maintaining tissue architecture and cell-to-cell communication. Moreover, slices may be prepared from a range of tissues, including liver, heart kidney, lung, and spleen, from laboratory animals and humans. The main disadvantage of this model is in the handling of the slices. Because a complex culture system is required, the number of samples that can be handled at any one time is limited. The model is also not amenable to automation, unlike a 96-well cell-culture format. In addition, slices have a limited lifespan in culture (~7 days), and several investigators have expressed concerns about the ability of a test compound to penetrate through a layer of damaged cells to reach viable cells [57,58].

### C. Reporter Gene Constructs

Kliwiler et al. first identified a new member of the steroid/thyroid receptor family termed PXR (“pregnane X receptor”) to be responsible for mediating the activation of CYP3A gene expression [59]. Their conclusions were based on three lines of evidence: First, both dexamethasone and PCN were potent activators of PXR; second, PXR binds as a heterodimer with RXR (retinoic acid receptor) to the conserved DR-3 motifs in the CYP3A23 and 3A2 gene promoters; and finally, PXR was found to be tissue selective, expressed mainly in liver, intestine, and kidney. These tissues are the ones reported to express inducible CYP3A genes in response to both dexamethasone and pregnenolone 16 $\alpha$ -carbonitrile [60]. This was immediately followed by another report by the same group [61] with the

identification of a human PXR that bound to the rifampicin response element in the CYP3A4 promoter as a heterodimer with RXR. Comparison of the human PXR with the recently cloned mouse PXR revealed significant differences in their activation by several drugs. This further supports the hypothesis that the molecular reasoning for the observed species differences in CYP3A expression was due to species specificity in PXR. Furthermore, with the cloning of PXRs from other species, including rabbit and rat, observed species-specific xenobiotic activation of CYP3A *in vivo* and in primary hepatocytes has so far correlated with the activation of PXR *in vitro* [62]. This prompted the suggestion to use PXR binding and activation assays to assess the potential for drug candidates to induce CYP3A. A recent study on St. John's wort, a herbal remedy used for the treatment of depression, demonstrated that hyperforin, a constituent of St. John's wort, induced CYP3A4 in human primary hepatocytes and was a potent PXR ligand [63]. Moreover, CV-1 cells cotransfected with an expression vector for human PXR and a reporter gene resulted in the activation of PXR comparable to that achieved with rifampicin. These data further support the hypothesis that PXR is a key regulator of CYP3A expression in different species. However, it's important to note that activation of PXR may not be the only possible mechanism resulting in the induction of CYP3A.

These type of assays have great potential as screening tools for CYP induction without having to use valuable human hepatocytes. The human hepatocyte model could be reserved to confirm results of a lead compound after exhaustive screening with such reporter gene-construct models.

### III. CASE STUDY

An example of an *in vitro*–*in vivo* correlation was recently demonstrated in a study involving autoinduction [64]. The major oxidative pathway of a cyclooxygenase-2 inhibitor, DFP (5,5-dimethyl-3-(2-propoxy)-4-(4-methanesulfonylphenyl)-2(5*H*)-furanone), gives rise to DFH, a dealkylated product (Fig. 14). This process is mediated by CYP3A enzymes in the rat, as demonstrated by incubations of DFP with hepatic microsomes from rats treated with dexamethasone (CYP3A23) and with recombinant rat CYPs 3A1 and 3A2. DFP is also a potent inducer of CYP3A in the rat hepatocyte induction model, as measured by Western blot or enzyme activity, using both testosterone and DFP as probe substrates (Fig. 15). Thus, the CYP3A-mediated pathway of DFP was induced in hepatocytes that had been treated for 48 hours with 2, 10, and 50  $\mu\text{M}$  DFP, in a dose-dependent manner. *In vivo* rat pharmacokinetic studies at oral doses of 10, 30, and 100 mg/kg gave  $C_{\text{max}}$  concentrations of circa 20, 40, and 80  $\mu\text{M}$ , respectively (Fig. 16A), indicating that the *in vitro* concentrations approximated *in vivo* concentrations. Based on this data, it was predicted that autoinduction should occur *in vivo*,

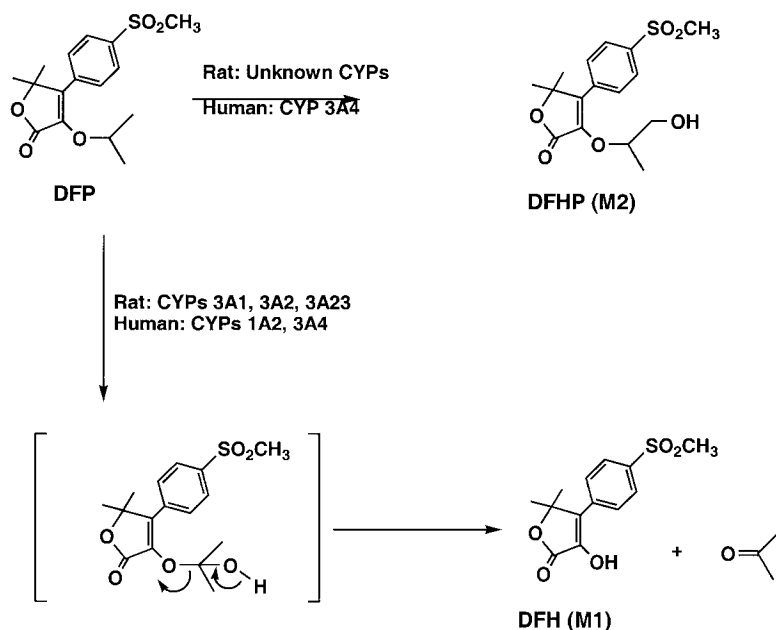


**Figure 14** Proposed metabolic pathway for DFP. (From Ref. 64.)

giving rise to altered pharmacokinetic parameters such as lowered  $C_{\max}$  and AUC values.

Induction of rat CYP3A was confirmed *in vivo* by dosing rats with DFP at 100 mg/kg for 4 days. Microsomes prepared from the excised livers showed that DFP gave 55% ( $\pm 7\%$  s.d.,  $n = 4$ ) of the induction observed with dexamethasone, as determined by Western blot analysis. *In vivo*, treatment of rats with DFP (10–100 mg/(kg-day) for 13 weeks) indicated that DFP induced its own metabolism. The  $C_{\max}$  and plasma drug area-under-the-curve (AUC) values during the 13th week were significantly lower than that on the first day, and the effect was dose dependent (Fig. 16). Thus, at the lowest dose, the changes in  $C_{\max}$  and AUC were modest or insignificant. However, at the top dose, reductions in both parameters were marked. The  $C_{\max}$  was reduced by about 50% and the AUC was reduced by about 80%. Thus, autoinduction was realized *in vitro* and *in vivo*. In both cases, the observed metabolic autoinduction is consistent with the hypothesis that it is caused by CYP3A induction.

Subsequent studies with DFP indicated that the human oxidative pathways were catalysed by CYPs 3A and 1A, as demonstrated by turnover with recombinant CYP enzymes. Induction studies in the human hepatocyte model demon-

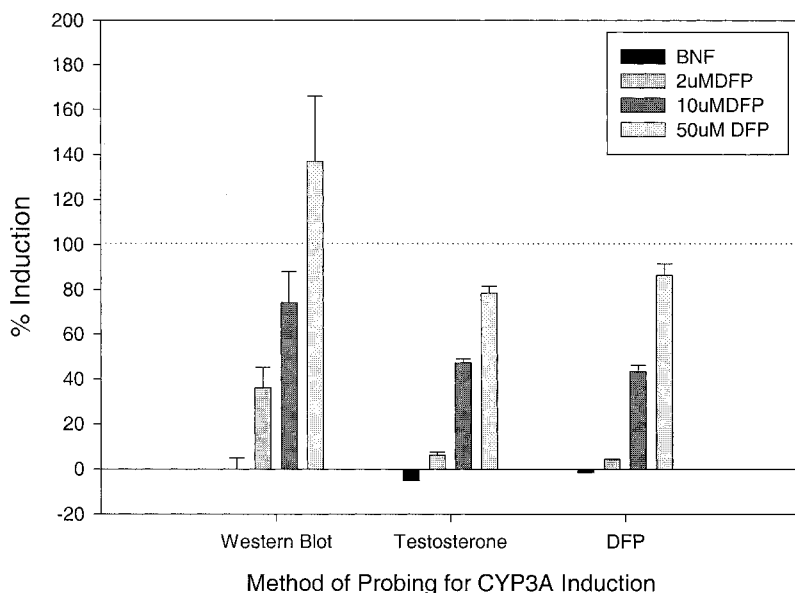


**Figure 15** CYP3A potency indices of DFP in cultured rat hepatocytes as determined by Western blots, testosterone 6 $\beta$ -hydroxylation, and DFP turnover. (From Ref. 64.)

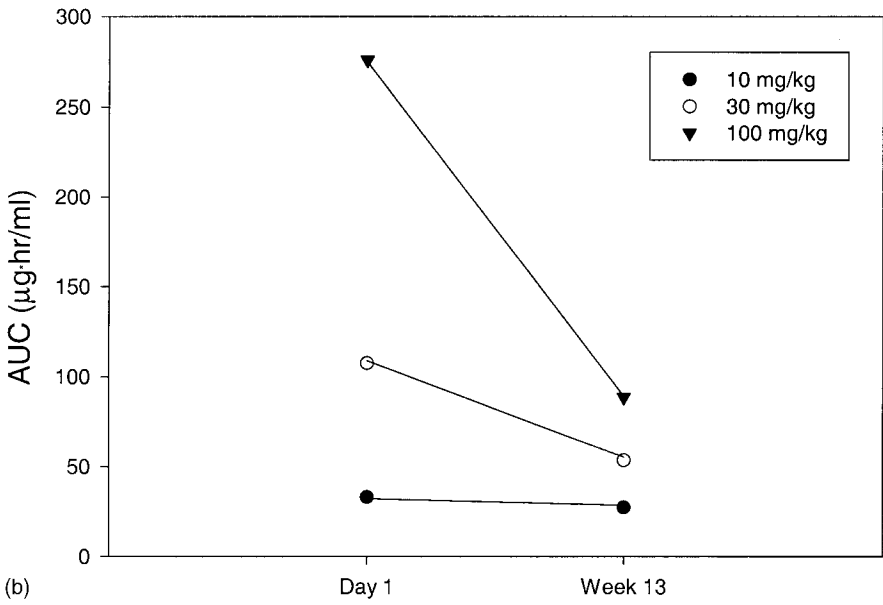
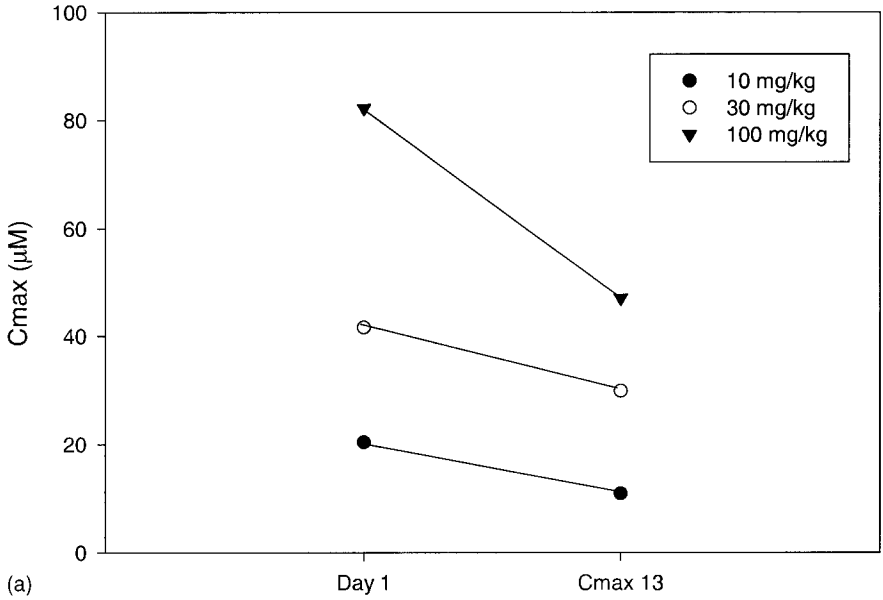
stated that human CYP3A was not significantly induced by DFP. Therefore, despite the autoinduction observed in rats, this compound was carried forward into clinical trials.

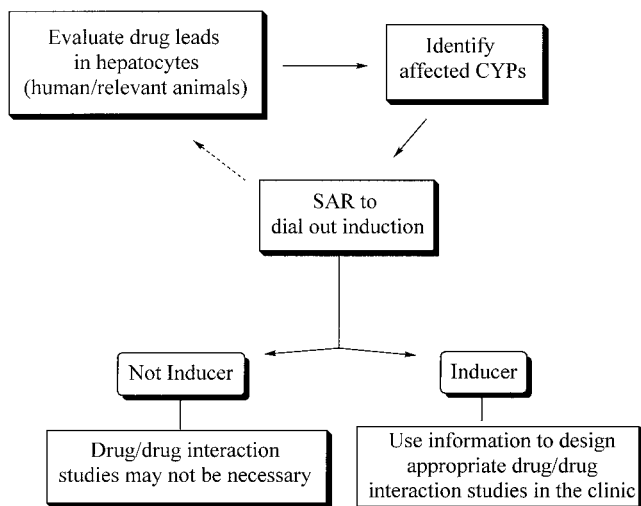
#### IV. STRATEGIES FOR MANAGING POTENTIAL CYP INDUCERS

Figure 17 summarizes strategies for screening for and dealing with possible CYP inducers at the drug discovery and development stages. The first step involves incubating a lead compound in the human hepatocyte model to determine CYP

---

**Figure 16** Changes to pharmacokinetic parameters over 13-week dosing regimen. (Panel a) Maximum plasma concentration ( $C_{max}$ ) of DFP determined after single doses of 10, 30, or 100 mg/kg of DFP compared to the  $C_{max}$  after 13 weeks of dosing. (Panel b) Area under the plasma concentration versus time curve (AUC) after a single dose of 10, 30, or 100 mg/kg of DFP compared to the  $C_{max}$  after 13 weeks of dosing. (From Ref. 64.)





**Figure 17** Strategies for dealing with CYP induction in drug discovery.

potency indices over a wide range of concentrations. If human hepatocytes are not readily available, hepatocytes from a relevant species may be used. For example, rabbit hepatocytes appear to be a better predictor for CYP 3A4 induction compared to rat hepatocytes [5,12]. If results show that the compound is a potent inducer of a particular CYP, then other, closely related analogs may be tested to determine the feasibility of reducing the induction potential within a chemical series. In the case where it may not be possible to identify a noninducing analog, this information can be used as a guide to plan relevant drug–drug interaction studies in the clinic.

## ACKNOWLEDGMENTS

The authors would like to thank Dr. Thomas Rushmore, Dr. Karen Richards, and Ms. Kristie Strong-Basalysa for their contribution in the development of the Quantitative Real-Time Reverse Transcriptase-Polymerase Chain Reaction assay for CYP analysis in primary hepatocytes.

## REFERENCES

1. NK Wadhwa, TJ Schroeder, AJ Pesce, AS Myre, CW Clardy, MR First. Cyclosporin drug interactions: A review. *Ther Drug Monit* 9:399–406, 1987.

2. JP Whitlock, MS Denison. Induction of cytochrome P450 enzymes that metabolize xenobiotics. In: Ortiz de Montellano PR, ed. *Cytochrome P450: Structure, Mechanism and Biochemistry*. 2nd ed. Plenum Press, New York, 1995, pp 367–390.
3. AM Breckenridge, DJ Back, FE Crawford, M MacCiver, N Orme, PH Rowe. Drug interactions with oral contraceptives: clinical and experimental studies. *Int Congress Sympos Series—Royal Soc Med* 31:1–11, 1980.
4. FP Guengerich. Oxidation of 17  $\alpha$ -ethenylestradiol by human liver cytochrome P-450. *Molecular Pharmac* 33:500–508, 1988.
5. TA Kocarek, EG Schuetz, SC Strom, RA Fisher, PS Guzelian. Comparative analysis of cytochrome CYP 3A induction in primary cultures of rat, rabbit, and human hepatocytes. *Drug Metab Dispos* 23:415–421, 1994.
6. RB Howard, AK Christensen, FA Gibbs, LA Pesch. The enzymatic preparation of isolated intact parenchymal cells from rat liver. *J Cell Biol* 35:675–684, 1967.
7. MN Berry, DS Friend D. High-yield preparation of isolated rat liver parenchymal cells: a biochemical and fine structural study. *J Cell Biol* 43:506–520, 1969.
8. MN Berry, AM Edwards, GK Barrit, eds. *Isolated Hepatocytes: Preparation, Properties and Applications*. Elsevier, New York, 1991.
9. AP Li, MA Roque, DJ Beck, DL Kaminski. Isolation and culturing of hepatocytes from human livers. *J Tissue Culture Methods* 14:139–146, 1992.
10. EG Schuetz, D Li, CJ Omiecinski, UA Muller-Eberhard, HK Kleinman, B Elswick, PS Guzelian. Regulation of gene expression in adult rat hepatocytes cultured on basement membrane matrix. *J Cell Physiol* 143:309–323, 1988.
11. EL LeCluyse, PL Bullock, A Parkinson, JH Hochman. Cultured rat hepatocytes. *Pharm Biotechnol* 8:121–159, 1996.
12. JM Silva, PE Morin, SH Day, BP Kennedy, P Payette, T Rushmore, JA Yergey, DA Nicoll-Griffith. Refinement of an in vitro cell model for cytochrome P450 induction. *Drug Metab Dispos* 26:490–496, 1998.
13. P Maurel. The use of adult human hepatocytes in primary culture and other in vitro systems to investigate drug metabolism in man. *Adv Drug Dev Rev* 22:105–132, 1996.
14. PO Seglen, PB Gordon, A Poli. Amino acid inhibition of autophagic/lysosomal pathway of protein degradation in isolated rat hepatocytes. *Biochim Biophys Acta* 630: 103–118, 1980.
15. R Enat, DM Jefferson, N Ruiz-Opaza, Z Gatmaitan, A Leinwand, LM Reid. Hepatocyte proliferation in vitro: its dependence on the use of serum-free hormonally defined medium and substrata of extracellular matrix. *Proc Natl Acad Sci USA* 81: 1411–1415, 1984.
16. DJ Waxman, JJ Morrissey, S Naik, HO Jauregui. Phenobarbital induction of cytochrome P450: high-level long-term responsiveness of primary rat hepatocyte cultures to drug induction, and glucocorticoid dependence of the phenobarbital response. *Biochem J* 271:113–119, 1990.
17. JS Sidhu, CJ Omiecinski. Modulation of xenobiotic-inducible cytochrome CYP gene expression by dexamethasone in primary rat hepatocytes. *Pharmacogenetics* 5:24–36, 1995.
18. S Johansson, M Hook. Substrate adhesion of rat hepatocytes: on the mechanism of attachment of fibronectin. *J Cell Biol* 98:810–817, 1984.



19. LM Reid, Z Gaitmaitan, I Arias, P Ponce, M Rojkind. Long-term cultures of normal rat hepatocytes on liver biomarkers. *Ann NY Acad Sci* 349:70–76, 1980.
20. JC Dunn, ML Yarmush, HG Kowbe, RG Tompkins. Hepatocyte function and extracellular matrix geometry: long-term culture in a sandwich configuration. *FASEB J* 3:174–177, 1989.
21. JS Sidhu, FM Farin, CJ Omiecinski. Influence of extracellular matrix overlay on phenobarbital-mediated induction of CYP2B1, 2B2, and 3A1 genes in primary adult rat hepatocyte culture. *Arch Biochem Biophys* 30:103–113, 1993.
22. EL LeCluyse, KL Audus, JK Hochman. Formation of extensive canalicular networks by rat hepatocytes cultured on collagen-sandwich configuration. *Am J Physiol* 266: C1764–C1774, 1994.
23. EL LeCluyse, A Madan, G Hamilton, K Carroll, R DeHaan, A Parkinson. Expression and regulation of cytochrome P450 enzymes in primary cultures of human hepatocytes. *J Biochem Molecular Tox* 14:177–188, 2000.
24. TA Kocarek, EG Schuetz, PS Guzelian. Expression of multiple forms of cytochrome P450 mRNAs in primary cultures of rat hepatocytes maintained on Matrigel. *Mol Pharmacol* 43:328–334, 1992.
25. VE Kostrubsky, V Ramachandran, R Venkataramanan, K Dorko, JE Esplen, S Zhang, JF Sinclair, SA Wrighton, SC Strom. The use of human hepatocyte cultures to study the induction of cytochrome P-450. *Drug Metab Dispos* 27:887–894, 1999.
26. TK Chang, L Yu, P Maurel, DJ Waxman. Enhance cyclophosphamide and ifosfamide activation in primary human hepatocyte cultures: response of cytochrome P-450 inducers and autoinduction by oxazaphosphorines. *Cancer Res* 57:1946–1954, 1997.
27. DD Surry, G McAllister, G Meneses-Lorente, DC Evans DC. High-throughput ribonuclease protection assay for the determination of CYP3A mRNA induction in cultured rat hepatocytes. *Xenobiotica* 29:827–838, 1999.
28. MT Donato, MJ Gomez-Lechon, JV Castell. A microassay for measuring cytochrome P4501A1 and P4502B1 activities in intact human and rat hepatocytes cultured on 96-well plates. *Analytical Biochem* 213:29–33, 1993.
29. DJ Waxman, C Attisano, FP Guengerich, DP Lapenson. Human liver microsomal steroid metabolism: identification of the major microsomal steroid hormone 6 beta-hydroxylase cytochrome P-450 enzyme. *Arch Biochem Biophys* 263:424–436, 1988.
30. CL Crespi, VP Miller, JM Ackermann, DM Streser, WF Busby. Novel high-throughput fluorescent P450 assays (abstr). *Toxicologist* 48:323, 1999.
31. RJ Price, D Surry, AB Renwick, G Menses-Lorente, BG Lake, DC Evans. CYP isoform induction screening in 96-well plates: use of 7-benzoyloxy-4-trifluoromethylcoumarin as a substrate for studies with rat hepatocytes. *Xenobiotica* 30:781–795, 2000.
32. N Chauret, N Tremblay, R Lackman, JY Gauthier, JM Silva, J Marois, J Yergey, DA Nicoll-Griffith. Description of a 96-well plate assay to measure cytochrome P4503A inhibition in human liver microsomes using a selective fluorescent probe. *Analytical Biochem* 276:215–226, 1999.
33. JM Silva, S Day, N Chauret, DA Nicoll-Griffith. Fluorescent probe for CYP 3A activity in human hepatocytes cultured on a 96-well plate. *ISSX Proc* 15:204, 1999.
34. JM Silva, HTS for assessing cytochrome P450 induction in primary hepatocytes. *Drug Metab Rev* 32, 168, 2000.

35. JB Ferrini, L Prichard, J Domergue, P Maurel. Long-term primary cultures of adult human hepatocytes. *Chem Biol Interact* 107:31–45, 1997.
36. KS Park, DH Sohn, RL Veech, BJ Song. Translational activation of ethanol-inducible cytochrome P450 (CYP2E1) by isoniazid. *European J Pharmacol Environmental Tox Pharmacol Section* 248:7–14, 1993.
37. J Greuet, L Pichard, JC Ourlin, C Bonfils, J Domergue, P Le Treut, P Maurel. Effect of cell density and epidermal growth factor on the inducible expression of CYP3A and CYP1A genes in human hepatocytes in primary culture. *Hepatology* 25:1166–1175, 1997.
38. MT Donato, MJ Gomez-Lechon, R Jover, T Nakamura, JV Castell. Human hepatocyte growth factor down-regulates the expression of cytochrome P450 isozymes in human hepatocytes in primary culture. *J Pharmacol Exp Ther* 284:760–767, 1998.
39. LD Murphy, CE Herzog, JB Rudick, AT Fojo, SE Bates. Use of the polymerase chain reaction in the quantitation of *mdr-1* gene expression. *Biochem* 29:10351–10356, 1990.
40. KL Strong, TH Rushmore, KM Richards. Quantitation of human CYP3A4, 3A5 and 3A7 RNA levels in cultured primary hepatocytes using real-time RT-PCR. *ISSX Proc* 15:69, 1999.
41. WP Bowen, J Carey, A Miah, HF McMurray, PW Munday, RS James, RA Coleman, AM Brown. Measurement of cytochrome P450 gene induction in human hepatocytes using quantitative real-time reverse transcriptase-polymerase chain reaction. *Drug Metab Dispos* 28:781–788, 2000.
42. CA Heid, J Stevens, KJ Livak, PM Williams. Real time quantitative PCR. *Genome Res* 6:986–994, 1996.
43. DD Surry, G Meneses-Lorente, R Heavens, A Jack, DC Evans. Rapid determination of rat hepatocyte mRNA induction potential using oligonucleotide probes for CYP1A1, 1A2, 3A and 4A1. *Xenobiotica* 30:441–456, 2000.
44. TP Burris, PD Pelton, L Zhou, MC Osborne, E Cryan, KT Demarest. A novel method for analysis of nuclear receptor function at natural promoters: peroxisome proliferator-activated receptor  $\gamma$  agonist actions on a P2 gene expression detected using branched DNA messenger RNA quantitation. *Molecular Endocrinology* 13:410–417, 1999.
45. DP Hartley, CD Klaassen. Detection of chemical-induced differential expression of rat hepatic cytochrome P450 mRNA transcripts using branched DNA signal amplification technology. *Drug Metab Dispos* 28:608–616, 2000.
46. O Warburg. Experiments on surviving carcinoma tissue. *Methods Biochem Z* 142:317–333, 1923.
47. HA Krebs. Body size and tissue respiration. *Biochim Biophys Acta* 4:249–269, 1950.
48. CG Fraga, BE Leibovitz, AL Tappel. Halogenated compounds as inducers of lipid peroxidation in tissue slices. *Free Radic Biol Med* 3:119–123, 1987.
49. AR Parrish, AJ Gandolfi, K Brendel K. Minireview precision-cut tissue slices: applications in pharmacology and toxicology. *Life Sci* 57:1887–1905, 1995.
50. PF Smith, AJ Gandolfi, CL Krumdieck, CW Putnam, CF Zukoski, WM Davis, K Brendel. Dynamic organ culture of precision liver slices for in vitro toxicology. *Life Sci* 13:1367–1375, 1985.

51. BG Lake, JA Beamand, AC Japenga, A Renwick, S Davies, RJ Price. Induction of cytochrome P-450-dependent enzyme activities in cultured rat liver slices. *Food Chem Toxicol* 31:377–386, 1993.
52. MS Gokhale, TE Buntton, J Zurlo, JD Yager. Cytochrome P-450 1A1/1A2 induction, albumin secretion, and histological changes in cultured liver slices. *In Vitro Toxicol* 8:357–368, 1995.
53. AT Drahusuk, BP McGarrigle, HL Tai, S Kitareewan, JA Goldstein, J Olson. Validation of precision-cut liver slices in a dynamic organ culture as an invitro model for studying CYP1A1 and CYP1A2 induction. *Toxic Appl Pharmacol* 140:393–403, 1996.
54. D Muller, R Glockner, M Rost. Nonooxygenation, cytochrome P4501A1-mRna in rat liver slices exposed to beta-naphthoflavone and dexamethasone in vitro. *Exper Tox Pathol* 48:433–438, 1996.
55. BG Lake, C Charzat, JM Tredger, AB Renwick, JA Beamand, RJ Price. Induction of cytochrome P450 isoenzymes in cultured precision-cut rat and human liver slices. *Xenobiotica* 26:297–306, 1996.
56. BG Lake, SE Ball, AB Renwick, JM Tredger, J Kao, JA Beamand, RJ Price. Induction of CYP3A isoforms in cultured precision-cut human liver slices. *Xenobiotica* 27:1165–1173, 1997.
57. S Ekins, GI Murray, JA Williams, MD Burke, NC Marchant, GM Hawksworth. Quantitative differences in phase I and II enzyme activities between rat precision-cut liver slices and isolated hepatocytes. *Drug Metab Dispos* 23:1274–1279, 1995.
58. S Ekins, JA Williams, GI Murray, MD Burke, NC Marchant, J Engeset, GM Hawksworth. Xenobiotic metabolism in rat, dog and human precision-cut liver slices, freshly isolated hepatocytes, and vitrified precision-cut liver slices. *Drug Metab Dispos* 24:990–995, 1996.
59. SA Kliewer, JT Moore, L Wade, JL Staudinger, MA Watson, SA Jones, DD McKee, BB Oliver, TM Wilson, RF Zetterstrom, T Perlmann, JM Lehmann. An orphan nuclear receptor activated by pregnanes defines a novel steroid signaling pathway. *Cell* 92:73–82, 1998.
60. K Debri, AR Boobis, DS Davis, RJ Edwards. Distribution and induction of CYP3A1 and CYP3A2 in rat liver and extrahepatic tissues. *Biochem Pharmacol* 50:2047–2056, 1995.
61. JM Lehmann, DD McKee, MA Watson, TM Wilson, TJ Moore, SA Kliewer. The human orphan nuclear receptor PXR is activated by compounds that regulate CYP3A4 gene expression and cause drug interactions. *J Clin Invest* 102:1016–1023, 1998.
62. SA Jones, LB Moore, JL Shenk, GB Wisely, GA Hamilton, DD McKee, NC Tomkinson, EL LeCluyse, MH Lambert, TM Wilson, SA Kliewer, JT Moore. The pregnane X receptor: a promiscuous xenobiotic receptor that has diverged during evolution. *Molecular Endocrinol* 14:27–39, 2000.
63. LB Moore, B Goodwin B, SA Jones, GB Wisely, CJ Serabjit-Singh, TM Wilson, JL Collins, SA Kliewer. St. John's wort induces hepatic drug metabolism through activation of the pregnane X receptor. *PNAS* 97:7500–7502, 2000.
64. DA Nicoll-Griffith, JM Silva, N Chauret, S Day, Y Leblanc, P Roy, J Yergey, R Dixit, D Patrick. Application of rat hepatocyte culture to predict in vivo metabolic auto-induction: studies with DFP, a cyclooxygenase-2 inhibitor. *Drug Metab Dispos* 29:159–165, 2001.

# 7

## In Vitro Approaches for Studying the Inhibition of Drug-Metabolizing Enzymes and Identifying the Drug-Metabolizing Enzymes Responsible for the Metabolism of Drugs

**Ajay Madan, Etsuko Usuki, L. Alayne Burton, Brian W. Ogilvie, and Andrew Parkinson**

*XenoTech, LLC, Kansas City, Kansas*

### I. INTRODUCTION

The reactions catalyzed by drug (xenobiotic)-biotransforming enzymes are generally divided into two groups, namely, phase I and phase II reactions (Table 1). Phase I reactions involve hydrolysis, reduction, and oxidation, whereas phase II biotransformation reactions include glucuronidation, sulfation, acetylation, methylation, conjugation with glutathione (mercapturic acid synthesis), and conjugation with amino acids (such as glycine, taurine, and glutamic acid) [1]. Phase I biotransformation of drugs often precedes and is slower than phase II biotransformation. For this reason, phase I biotransformation (such as oxidation of drugs by cytochrome P450) tends to be the rate-limiting step in the overall metabolism and, at times, the elimination of drugs. Therefore, a decrease or increase in the content/activity of phase I drug-metabolizing enzymes often results in alteration of the pharmacokinetics of drugs [1–5]. Decreased content/activity of an enzyme may result from the following mechanisms:

1. Expression of a mutant enzyme (e.g., mutation in the gene sequence of CYP2D6 leads to no enzyme expression or the expression of an inactive enzyme)

**Table 1** Localization of Drug-Metabolizing Enzymes and Example Substrates

Reaction	Enzyme	Localization	Example substrates
<i>Phase I</i>			
Hydrolysis	Carboxylesterase	Microsomes, cytosol	Procaine, procainamide, spironolactone, cocaine, succinylcholine
	Peptidase	Blood, lysosomes	Variety of endogenous and exogenous peptides benzo[a]pyrene 4,5-oxide, <i>cis</i> - and <i>trans</i> -stilbene oxide
Reduction	Epoxide hydrolase	Microsomes, cytosol	
	Azo- and nitro-reduction	Microflora, microsomes, cytosol	Prontosil, chloramphenicol, nitrobenzenes
	Carbonyl reduction	Cytosol	Haloperidol, chloral hydrate, pentoxifylline
	Disulfide reduction	Cytosol	Disulfiram
	Sulfoxide reduction	Cytosol	Sulindac
	Quinone reduction	Cytosol, microsomes	Menadione
Oxidation	Reductive dehalogenation	Microsomes	Halothane, carbon tetrachloride
	Alcohol dehydrogenase	Cytosol	Methanol, ethanol
	Aldehyde dehydrogenase	Mitochondria, cytosol	Formaldehyde, acetaldehyde
	Aldehyde oxidase	Cytosol	<i>N</i> <sup>1</sup> -Methylnicotinamide, 6-methylpurine
	Xanthine oxidase	Cytosol	Hypoxanthine, xanthine, allopurinol, pthalazine
	Monoamine oxidase	Mitochondria	Serotonin, tyramine, phenelzine, catecholamines, milacemide, <i>N</i> -desisopropylpropranolol, 1-methyl-4-phenyl-1,2,5,6-tetrahydropyridine

<i>Phase II</i>	Diamine oxidase	Cytosol	Putrescine
	Prostaglandin H synthase	Microsomes	Arachidonic acid, acetaminophen, 2-aminonaphthalene, butylated hydroxytoluene, butylated hydroxyanisole, phenylbutazone
	Flavin-monoxygenases	Microsomes	Nicotine, dimethylaniline, 2-acetylamino fluorene, acetylhydrazine, cysteamine, cimetidine, methimazole, thiobenzamide, diphenylmethylphosphine
	Cytochrome P450	Microsomes	See Chapter 3
	Glucuronide conjugation	Microsomes	Valproic acid, acetaminophen, zidovudine, codeine, chloramphenicol, oxazepam, lamotrigine, ketoprofen
	Sulfate conjugation	Cytosol	4-Nitrophenol, dopamine, estrone, dehydroepiandrosterone, quercetin
	Glutathione conjugation	Cytosol, microsomes	Acetaminophen, chlorobenzene, ethacrynic acid, diethylmaleate
	Amino acid conjugation	Mitochondria, microsomes	Benzoic acid, <i>N</i> -hydroxy-4-aminoquinoline-1-oxide
	Acetylation	Mitochondria, cytosol	Isoniazid, 4-aminobenzoic acid
	Methylation	Cytosol	Captopril, 6-mercaptopurine, spirironolactone, azathioprine, diethyldithiocarbamate, phenols, catechols

2. Inhibition of the activity of a pre-existing enzyme (e.g., inhibition of CYP3A4 by ketoconazole)
3. Inactivation of a pre-existing enzyme (e.g., inactivation of CYP3A4 by erythromycin)
4. Suppression of the expression of an enzyme (e.g., suppression of P450 enzymes by cytokines released in response to infection or inflammation)

On the other hand, an increase in the content/activity of an enzyme may result from the following mechanisms:

1. Expression of several copies of the gene (e.g., some individuals have multiple copies of CYP2D6)
2. Stimulation of the activity of a pre-existing enzyme (e.g., enhanced activity of CYP3A4 by  $\alpha$ -naphthoflavone, although this may be largely an in vitro phenomenon)
3. Increased expression or induction of an enzyme (e.g., induction of CYP3A4 by rifampin)

The involvement of drug transporters (e.g., P-glycoprotein) in drug interactions has recently been recognized and reviewed [6–13]. It is becoming increasingly evident that drug transporters (uptake transporters, efflux transporters, bile duct transporters, etc.) are primarily responsible for determining the intracellular concentration of a large number of drugs. Consequently, inhibition or induction of these transporters may alter the absorption (e.g., intestine), distribution (e.g., blood-brain barrier) or elimination (e.g., liver and kidney) of drugs, thereby altering the pharmacokinetics of drugs. The role of drug transporters in drug interactions is discussed in Chapter 5 and 8 of this book.

Metabolic drug interactions have received considerable attention in the 1990s because some prominent drugs (e.g., terfenadine) were shown to cause life-threatening adverse effects when prescribed with other commonly used drugs (e.g., antibiotics). At about the same time, in vitro technology was developed to study interactions of drugs with individual *human* P450 enzymes by using either enzyme selective substrates or recombinant P450 enzymes. The development of this in vitro technology, along with guidance documents issued by the U.S. Food and Drug Administration (FDA) and the European Agency for the Evaluation of Medicinal Products has made evaluation of drug interactions an integral part of the drug development process [14,15].

It should be emphasized that the mechanisms of drug interactions just noted are examples of *pharmacokinetic* drug interactions, which represent only a subset of drug interactions. The other major type of drug interactions is *pharmacodynamic* in nature and occurs when two concomitantly administered drugs have additive or synergistic pharmacological effects (see Chap. 1). For example, aspirin inhibits the synthesis of prostaglandins that are responsible not only for medi-

ating pain and inflammation but also for the aggregation of platelets. Therefore, administration of aspirin with warfarin (an anticoagulant) can lead to hemorrhagic tendencies due to an exaggerated anticoagulant effect. Pharmacodynamic drug interactions have been well studied and documented and are beyond the scope of this chapter.

Drug interactions resulting from an increase in enzyme content/activity (enzyme induction) are discussed elsewhere in this book (see Chap. 6). This chapter will focus on *in vitro* systems for studying the inhibition of drug-metabolizing enzymes and the identification of drug-metabolizing enzymes involved in the metabolism of a drug. To this end, various experimental designs, their advantages and pitfalls, and extrapolation of *in vitro* data to the clinical situation will be discussed. Particular attention will be paid to cytochrome P450 enzymes, because most of the clinically relevant pharmacokinetic drug interactions are, in one way or another, related to P450 enzymes.

### **A. Cytochrome P450 Enzymes and Their Role in Drug Metabolism**

Liver microsomes from all mammalian species contain numerous P450 enzymes, each with the potential to catalyze various types of reactions. In other words, all of the P450 enzymes expressed in liver microsomes have the potential to catalyze xenobiotic hydroxylation, epoxidation, dealkylation, oxygenation, and dehydrogenation. The broad and often-overlapping substrate specificity of liver microsomal P450 enzymes precludes the possibility of naming these enzymes for the reactions they catalyze (see Chap. 6). The amino acid sequence of numerous P450 enzymes has been determined, largely by recombinant DNA techniques, and such sequences now form the basis for classifying and naming P450 enzymes. In general, P450 enzymes with less than 40% amino acid sequence identity are assigned to different gene families (gene families 1, 2, 3, 4, etc.). P450 enzymes that are 40–55% identical are assigned to different subfamilies (e.g., 2A, 2B, 2C, 2D, 2E, etc.). P450 enzymes that are more than 55% identical are classified as members of the same subfamily (e.g., 2A1, 2A2, 2A3, etc.). The liver microsomal P450 enzymes involved in xenobiotic biotransformation belong to three main P450 gene families: CYP1, CYP2, and CYP3. Liver microsomes also contain P450 enzymes encoded by the CYP4 gene family, substrates for which include several fatty acids and eicosanoids but relatively few xenobiotics. The liver microsomal P450 enzymes in each of these gene families generally belong to a single subfamily (e.g., CYP1A, CYP3A, and CYP4A). A notable exception is the CYP2 gene family, which contains five subfamilies (i.e., CYP2A, CYP2B, CYP2C, CYP2D, and CYP2E). The number of P450 enzymes in each subfamily differs from one species to the next [1,2,4,5,16–19].

Human liver microsomes can contain a dozen or more different P450 en-



zymes [CYP1A2, 2A6, 2B6, 2C8, 2C9, 2C18, 2C19, 2D6, 2E1, 3A4, 3A5, 3A7 (fetal), 4A9, and 4A11] that biotransform xenobiotics and/or endogenous substrates. Other P450 enzymes in human liver microsomes have been described, but they appear to be allelic variants of the aforementioned enzymes rather than distinct gene products. For example, CYP2C10 and CYP3A3 appear to be allelic variants of CYP2C9 and CYP3A4, respectively. Unfortunately, a nomenclature system based on structure does not guarantee that structurally related proteins in different species will perform the same function (examples of such functional differences are given later). Some P450 enzymes have the same name in all mammalian species, whereas others are named in a species-specific manner. For example, all mammalian species contain two P450 enzymes belonging to the CYP1A subfamily, and in all cases these are known as CYP1A1 and CYP1A2 because the function and regulation of these enzymes are highly conserved among mammalian species. The same is true of CYP1B1 and CYP2E1. In other words, CYP1A1, CYP1A2, CYP1B1, and CYP2E1 are not species-specific names, but rather they are names given to proteins in all mammalian species. In all other cases, functional or evolutionary relationships are not immediately apparent, so the P450 enzymes are named in a species-specific manner, and the names are assigned in chronological order regardless of the species of origin. For example, human liver microsomes express CYP2A6, but this is the only functional member of the CYP2A subfamily found in human liver. The other members of this subfamily (i.e., CYP2A1–CYP2A5) are the names given to rat and mouse proteins, which were sequenced before the human enzyme. With the exception of CYP1A1, CYP1A2, CYP1B1, and CYP2E1, the names of all of the other P450 enzymes in human liver microsomes refer specifically to human P450 enzymes [1,2,4,5,16,18,19].

Without exception, the levels and activity of each P450 enzyme have been shown to vary from one individual to the next, due to environmental and/or genetic factors. Allelic variants, which arise by point mutations in the wild-type gene, are another source of interindividual variation in P450 activity. Amino acid substitutions can increase or, more commonly, decrease P450 enzyme activity, although the effect is generally substrate dependent. The environmental factors known to affect P450 levels/activity include medications (e.g., anticonvulsants, rifampin, isoniazid, antifungals, macrolide antibiotics), foods (e.g., cruciferous vegetables, charcoal-broiled beef), social habits (e.g., alcohol consumption, cigarette smoking), and disease status (diabetes, inflammation, infection, hyper- and hypothyroidism).<sup>\*</sup> When environmental factors influence P450 enzyme levels, considerable variation may be observed during repeated measures of xenobiotic biotransformation (e.g., drug metabolism) in the same individual. Such variation is not observed when alterations in P450 activity are determined genetically [1,2].

---

\* Liver and kidney disease in general will impair the elimination of hepatically and renally cleared drugs, respectively.

Due to their broad substrate specificity, it is possible that two or more P450 enzymes can contribute to the metabolism of a single compound. For example, two P450 enzymes, designated CYP2D6 and CYP2C19, both contribute significantly to the metabolism of propranolol in humans: CYP2D6 oxidizes the aromatic ring to give 4-hydroxypropranolol, whereas CYP2C19 oxidizes the isopropanolamine sidechain to give naphthoxylactic acid. Consequently, changes in either CYP2D6 or CYP2C19 do not markedly affect the disposition of propranolol. Three human P450 enzymes—CYP1A2, CYP2E1, and CYP3A4—can convert the commonly used analgesic acetaminophen to its hepatotoxic metabolite, *N*-acetylbenzoquinoneimine. It is also possible for a single P450 enzyme to catalyze two or more metabolic pathways for the same drug. For example, CYP2D6 catalyzes the *O*-demethylation and 5-hydroxylation (aromatic ring hydroxylation) of methoxyphenamine, and CYP3A4 catalyzes the 3-hydroxylation and *N*-oxygenation of quinidine, the M1-, M17-, and M21-oxidation of cyclosporin, the 1'- and 4-hydroxylation of midazolam, the *tert*-butyl-hydroxylation and *N*-dealkylation of terfenadine, and several pathways of testosterone oxidation, including 1 $\beta$ -, 2 $\beta$ -, 6 $\beta$ -, and 15 $\beta$ -hydroxylation and dehydrogenation to 6-dehydrotestosterone [1].

The pharmacologic or toxic effects of certain drugs are exaggerated in a significant percentage of the population due to a heritable deficiency in a P450 enzyme. Two major cytochrome P450 deficiencies have been identified to date: CYP2D6 and CYP2C19. Deficiencies of these enzymes are inherited as autosomal recessive traits, which result from a variety of mutations. Individuals lacking CYP2D6 or CYP2C19 were initially identified as poor metabolizers of debrisoquine and *S*-mephenytoin, respectively. However, because each P450 enzyme has a broad substrate specificity, each genetic defect affects the metabolism of several drugs. The incidence of the poor-metabolizer phenotype varies among different ethnic groups. For example, 5–10% of Caucasians are poor metabolizers of debrisoquine (an antihypertensive drug metabolized by CYP2D6), whereas less than 1% of Japanese subjects are defective in CYP2D6 activity. In contrast, ~20% of Japanese subjects are poor metabolizers of *S*-mephenytoin (an anticonvulsant metabolized by CYP2C19), whereas less than 5% of Caucasians are so affected. Some individuals have been identified as poor metabolizers of phenacetin, coumarin, or tolbutamide, which are metabolized by CYP1A2, CYP2A6, and CYP2C9, respectively. However, the incidence of each of these phenotypes is apparently less than 1% [1,18].

The observation that individuals who are genetically deficient in a particular P450 enzyme are poor metabolizers of one or more drugs illustrates a very important principle: The rate of elimination of drugs can be largely determined by a single P450 enzyme. This observation seems to contradict the fact that P450 enzymes have broad and overlapping substrate specificities. The resolution to this apparent paradox lies in the fact that, although more than one human P450 enzyme can catalyze the biotransformation of a xenobiotic, they may do

so with markedly different affinities. Consequently, xenobiotic biotransformation *in vivo*, where only low substrate concentrations are usually achieved, is often determined by the P450 enzyme with the highest affinity (lowest apparent  $K_m$ ) for the xenobiotic. For example, the *N*-demethylation of diazepam and the 5-hydroxylation of omeprazole are both catalyzed by two human P450 enzymes: CYP2C19 and CYP3A4. However, these reactions are catalyzed by CYP3A4 with such low affinity that the *N*-demethylation of diazepam and the 5-hydroxylation of omeprazole *in vivo* appear to be dominated by CYP2C19 [20–29]. When several P450 enzymes catalyze the same reaction, their relative contribution to xenobiotic biotransformation is determined by the kinetic parameter,  $V_{max}/K_m$ , which is a measure of *in vitro* intrinsic clearance at low substrate concentrations (<10% of  $K_m$ ).

## B. Inhibition of Cytochrome P450 Enzymes

If a drug is metabolized by a P450 enzyme, it will potentially inhibit the metabolism of other drugs that are metabolized by the same P450 enzyme. The inhibitory effects may not be limited to those P450 enzymes involved in its metabolism, because some chemicals competitively inhibit P450 enzymes that play no role in their metabolism. For example, quinidine and terbinafine are potent inhibitors of, but not substrates for, CYP2D6 [30–31]. Whether a reversible inhibitor of cytochrome P450 will cause a clinically significant impairment of drug metabolism will depend on the  $K_i$  and  $K_m$  values of the drugs (i.e., measures of the affinity with which each chemical binds to cytochrome P450) and the dose of each drug (or more importantly the hepatic concentration of each drug).

Metabolism by cytochrome P450 represents the rate-limiting step in the metabolism of a large number of drugs; hence, inhibition of cytochrome P450 is recognized by the FDA and other regulatory agencies as an important cause of drug interactions [14,15]. Inhibitory drug interactions can cause symptoms of drug overdose, including an exaggerated pharmacological response and/or drug toxicity. Inhibitory drug interactions generally fall into two categories. The first involves “direct” inhibition of the metabolism of one drug by the other. Direct inhibition may exhibit Michaelis–Menten kinetics characteristic of competitive, noncompetitive, uncompetitive, or mixed (competitive and noncompetitive) inhibition. For example, omeprazole and diazepam are both metabolized by CYP2C19. When the two drugs are administered simultaneously, omeprazole decreases the plasma clearance of diazepam and prolongs its plasma half-life [20,21,25,32]. The inhibition of diazepam metabolism by omeprazole is known to involve competition for metabolism by CYP2C19, because no such inhibition occurs in individuals who, for genetic reasons, lack this polymorphically expressed P450 enzyme (*Note*: 2–5% of Caucasians and 12–23% of Asians lack CYP2C19) [20,21,25,32]. Second, some drugs can inhibit P450 enzymes (and cause inhibitory drug interactions) even if they are not metabolized by the af-

fects P450 enzyme. The inhibition of dextromethorphan metabolism by quinidine is a good example of this type of drug interaction. The clearance of dextromethorphan is determined by its rate of metabolism by CYP2D6, which *O*-demethylates dextromethorphan to dextrophan, which can then be conjugated with glucuronic acid and excreted in urine. Dextromethorphan clearance is impaired in individuals lacking CYP2D6 (*Note*: 5–10% of Caucasians lack this polymorphically expressed enzyme) [33] and when this antitussive agent is taken with quinidine, a potent inhibitor of CYP2D6 [34]. However, quinidine is not metabolized by CYP2D6, even though it binds to this enzyme with high affinity ( $K_i \sim 100$  nM) [35]. Quinidine is actually metabolized by CYP3A4 and is a weak competitive inhibitor of this enzyme ( $K_i > 100$   $\mu$ M) [30]. The lesson to be learned from quinidine is that a new chemical entity can potentially inhibit P450 enzymes that are not involved in its metabolism. Similarly, (1) terbinafine, an antimycotic agent, is metabolized by several P450 enzymes (but not CYP2D6), and it is a potent inhibitor of CYP2D6 [31,36]; and (2) celecoxib, a cyclooxygenase-2 inhibitor, is metabolized by CYP2C9 (but not CYP2D6) and is a potent inhibitor of CYP2D6 [37].

The second type of drug interaction results from “irreversible” (or “quasi-irreversible”) inhibition of cytochrome P450 and often involves metabolism-dependent inhibition or suicide inactivation of cytochrome P450 [38]. The inhibition of terfenadine metabolism by erythromycin is an example of this type of drug interaction. Terfenadine, the active ingredient in the antihistamine Seldane®, is converted to a carboxylic acid metabolite (fexofenadine) by CYP3A4 [39]. This metabolite blocks H1-histamine receptors but does not cross the blood–brain barrier, which is why Seldane® is a nonsedating antihistamine [40–42]. Erythromycin inhibits CYP3A4 and blocks the conversion of terfenadine to fexofenadine [43–45]. Under such conditions, terfenadine enters the systemic circulation. In addition to blocking H1-histamine receptors, terfenadine blocks  $K^+$  channels in the heart, which can lead to Torsades de Pointes [40–42]. Inhibition of terfenadine metabolism by erythromycin has caused fatal ventricular arrhythmias [40–42]. Fatal interactions have also been reported between erythromycin and the gastrokinetic drug cisapride [46]. Like terfenadine, erythromycin is a substrate for CYP3A4. However, the pronounced inhibition of terfenadine metabolism by erythromycin does not result simply from competition between the two drugs for metabolism by CYP3A4. In fact, erythromycin is a relatively poor competitive inhibitor of CYP3A4 ( $K_i \sim 130$   $\mu$ M) [47]. The reason erythromycin is so effective at inhibiting terfenadine metabolism is that CYP3A4 converts erythromycin to a metabolite that binds so tightly to the heme moiety of CYP3A4 that it is not released from the enzyme’s active site [48]. In other words, CYP3A4 converts erythromycin to a metabolite that irreversibly (or quasi-irreversibly) inhibits the enzyme. This type of inhibition of a P450 enzyme by a metabolism-dependent irreversible inhibitor can completely block the metabolism of other drugs. As the fatal interactions between erythromycin and terfenadine and cisapride indicate,

irreversible inhibition of cytochrome P450 can have profound consequences. Other examples of irreversible or quasi-irreversible metabolism-dependent inhibitors, which inhibit CYP1A2, CYP2A6, and CYP2C9, respectively, include furafylline [49], 8-methoxypsoralen [50–51], and tienilic acid [52].

A variation of this second type of inhibition is when a drug causes metabolism-dependent “reversible” inhibition. This type of inhibition is rare but is possible if a drug is converted to a metabolite that is more potent than the parent drug as a direct or metabolism-dependent inhibitor of cytochrome P450 enzymes. For example, fluoxetine and norfluoxetine (the *N*-demethylated metabolite of fluoxetine) are equipotent in their ability to inhibit CYP2D6, but norfluoxetine is approximately six times more potent than fluoxetine in inhibiting CYP3A4 [53–55]. It is speculated that, if tested, fluoxetine would test positive as a metabolism-dependent “reversible” inhibitor of CYP3A4.

## II. EVALUATION OF DRUGS AS INHIBITORS OF P450 ENZYMES

The primary purpose of evaluating drugs as inhibitors of P450 enzymes in vitro is to determine their potential to cause drug interactions in the clinic. However, identifying a drug as an inhibitor of a given P450 enzyme does not necessarily imply that the drug will cause clinically relevant drug interactions.

For example, if CYP2C19 is potently inhibited by a drug, it cannot be simply assumed that the drug will significantly interact with all substrates for CYP2C19. The inhibition must be considered in the following context:

1. The pharmacokinetics of the inhibitory drug
2. The potential of administering the inhibitory drug together with other drugs that are CYP2C19 substrates (each of which must be considered individually)
3. The extent to which drug clearance is dependent on CYP2C19<sup>†</sup>
4. The potential for saturating the capacity of CYP2C19
5. The clinical consequences of alteration of pharmacokinetics of the affected drug (which may or may not be a cause for concern, depending on the drug’s therapeutic index)

---

<sup>†</sup> If a drug were metabolized by CYP2C19, the extent to which it is cleared by CYP2C19 in the liver could depend on several factors, including (1) the role of extrahepatic metabolism, (2) liver disease (decrease in blood flow), (3) whether the CYP2C19 is the wild type or an allelic variant, (4) the extent of protein binding, (5) the role of other enzymes, including phase II enzymes, in the clearance of the drug, and (6) whether hepatic metabolism represents the primary mechanism of clearance of the drug, as opposed to renal clearance, for example.

The experimental studies described herein provide a tool for *predicting* the potential for drug interactions. Needless to say, a well-designed study can be a powerful predictor; however, it is possible to design an analytically sound experiment that provides meaningless data.

### A. Theoretical Concepts

Two types of inhibition are possible: “direct” inhibition and metabolism-dependent inhibition. Direct (“reversible” or “metabolism-independent”) inhibition occurs when a drug inhibits P450 enzymes without requiring biotransformation. Metabolism-dependent inhibition occurs when a drug has to be converted to a metabolite in order to inhibit P450 enzymes; in this case, the inhibition may be “reversible,” “quasi-irreversible,” or “irreversible.”

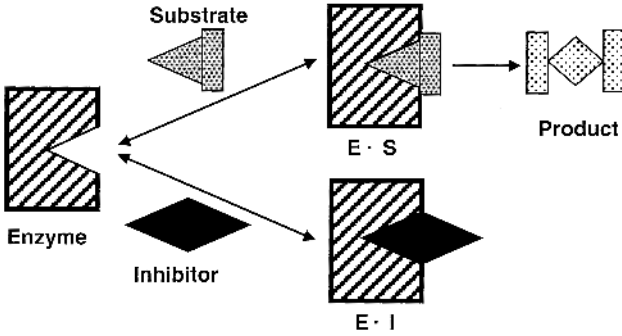
“Direct” inhibition has traditionally been divided into three categories: competitive, noncompetitive, and uncompetitive. All three models of “direct” inhibition are depicted in Figure 1. However, in practice, mixed (competitive and noncompetitive) inhibition is frequently observed. Competitive inhibition occurs when the inhibitor and substrate compete for binding to the active site of the enzyme. Noncompetitive inhibition occurs when the inhibitor binds to a site on the enzyme that is different from the active site to which the substrate binds. In the case of uncompetitive inhibition, the inhibitor binds to the enzyme when the substrate is bound to it; the binding site may be the same as or different from the active site (substrate binding site). Finally, mixed (competitive-noncompetitive) inhibition occurs when the inhibitor binds to the active site as well as to another site on the enzyme; or the inhibitor binds to the active site but does not block the binding of the substrate. The kinetics and the affinity with which an inhibitor binds to an enzyme are best described by the dissociation constant for the enzyme–inhibitor complex. This dissociation constant is referred to as the *inhibition constant*, or the  $K_i$  value. Transformations of the Michaelis–Menten equation are used not only for calculating  $K_i$  values but also for graphical depiction of the type of inhibition (Table 2 and Fig. 2).

The affinity with which an inhibitor binds to an enzyme is defined by its  $K_i$  value, whereas the affinity with which the substrate binds is often defined by its  $K_m$  value. Both definitions should be taken with a grain of salt, because they are based on three assumptions:

1. The dissociation of the enzyme–inhibitor or enzyme–substrate complex is the rate-limiting step.
2. The concentration of the enzyme is negligible compared with the concentration of the substrate/inhibitor.
3. The “free” (unbound) concentration of the substrate/inhibitor is known or well approximated by the total concentration of substrate/inhibitor.

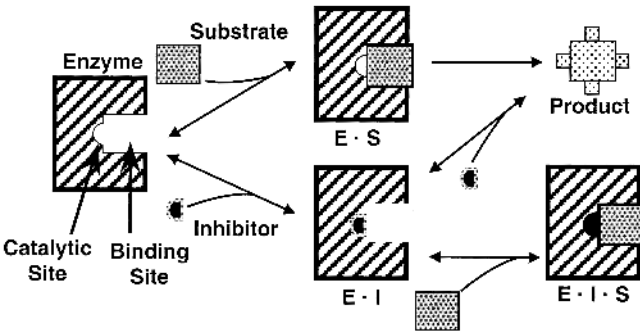
**Competitive inhibition**

I and S bind to the same site on the enzyme.  
 $V_{max}$  is unchanged,  $K_m$  increases



**Noncompetitive inhibition**

I and S bind to different sites on the enzyme.  
 $V_{max}$  decreases,  $K_m$  is unaffected.



**Uncompetitive inhibition**

I binds to enzyme-substrate complex.  
 $V_{max}$  decreases,  $K_m$  decreases

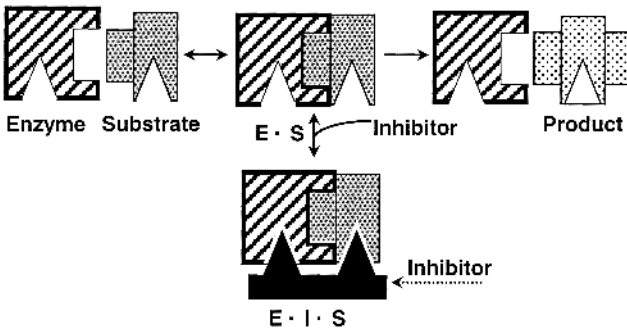


**Figure 1** Various mechanisms of enzyme inhibition.

**Table 2** Michaelis–Menten Equations and Their Transformations Used for Evaluating Drugs as Inhibitors of P450 Enzymes In Vitro and In Vivo

Inhibition type	Michaelis–Menten	Eadie–Hofstee ( $y = \text{rate}, x = \text{rate}/[S]$ for $y = mx + c$ )	In vitro to in vivo extrapolation (Fractional inhibition = $i$ )
No inhibition	$v = \frac{V_{\max} \cdot [S]}{K_m + [S]}$	$y = -K_m \cdot [S] + V_{\max}$	Not applicable
Competitive	$v = \frac{V_{\max} \cdot [S]}{K_m \cdot (1 + [I]/K_i) + [S]}$	$y = -K_m \cdot (1 + [I]/K_i) \cdot [S] + V_{\max}$	$i = [I]/([I] + K_i \cdot (1 + [S]/K_m))$ For $[S] \ll K_m, [S]/K_m \rightarrow 0$ ; $\therefore i = [I]/([I] + K_i)$ .
Noncompetitive	$v = \frac{V_{\max} \cdot [S]}{K_m \cdot (1 + [I]/K_i) + (1 + [I]/K_i) \cdot [S]}$	$y = -K_m \cdot [S] + \frac{V_{\max}}{(1 + [I]/K_i)}$	$i = [I]/([I] + K_i)$
Uncompetitive	$v = \frac{V_{\max} \cdot [S]}{K_m + (1 + [I]/K_i) \cdot [S]}$	$y = \frac{-K_m \cdot [S]}{(1 + [I]/K_i)} + \frac{V_{\max}}{(1 + [I]/K_i)}$	$i = [I]/([I] + K_i \cdot [1 + K_m/[S]])$ For $[S] \ll K_m, K_m/[S] \rightarrow \infty; \therefore i = 0$ . However, as $[S] \rightarrow K_m, i$ becomes significant.
Mixed inhibition (competitive-noncompetitive)	$v = \frac{V_{\max} \cdot [S]}{K_m (1 + [I]/K_i) + (1 + [I]/K'_i) \cdot [S]}$	$y = \frac{-K_m \cdot (1 + [I]/K_i) \cdot [S]}{(1 + [I]/K'_i)} + \frac{V_{\max}}{(1 + [I]/K'_i)}$	$i = [I]/([I] + K_i) \quad \text{for } [S] \ll K_m$

$v$  = the initial rate of the reaction;  $[S]$  = the substrate concentration;  $[I]$  = the inhibitor concentration.

$V_{\max}$  and  $K_m$  are the kinetic constants for a given enzyme, and  $K_i$  is the inhibition constant. Fractional inhibition ( $i$ ) is the predicted inhibition of a P450 enzyme in vivo in the presence of an inhibitor with an inhibition constant equal to  $K_i$  and free or total plasma concentration equal to  $[I]$  [4,88].



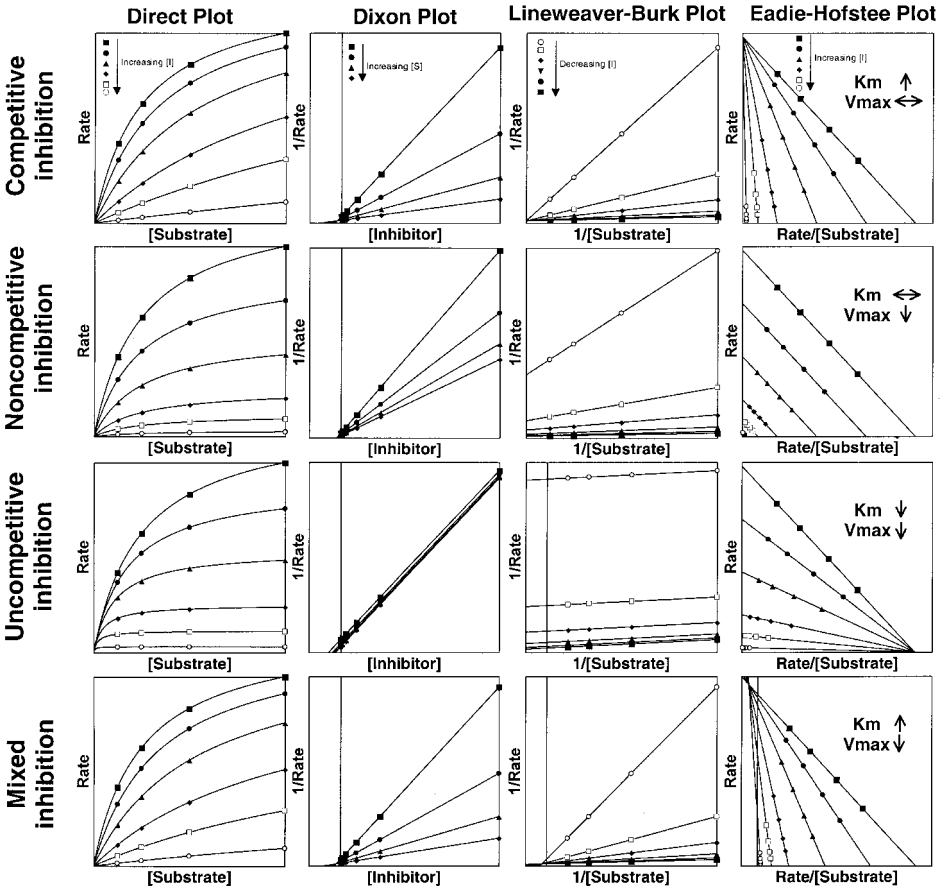


**Figure 2** Graphical representation of enzyme inhibition: Direct plot ([substrate] versus initial rate of product formation) and various transformations of the direct plot (i.e., Dixon, Lineweaver–Burk, and Eadie–Hofstee plots) are depicted. All graphs and the corresponding fit are based on theoretical data; hence, they appear “perfect.” It should be noted that the Eadie–Hofstee plots are most useful in differentiating one type of inhibition from the other and are therefore preferred.

All three assumptions can be violated in the case of cytochrome P450 enzymes, depending on the *in vitro* system used. For example, cytochromes P450 are membrane-bound enzymes; therefore, when rates of reaction are measured in human liver microsomes, a significant fraction of the substrate/inhibitor may be bound to the lipid membrane and/or to proteins embedded therein. In other

words, the ‘free’ concentration of substrate/inhibitor may differ significantly from the total concentration. Additionally, the potency of some inhibitors (e.g., the CYP3A inhibitors ketoconazole, clotrimazole) is such that the free concentration of the inhibitor tends to approach the concentration of the enzyme [56], a violation of the second assumption. Theoretically, this problem can be overcome by lowering the concentration of the enzyme (i.e., the microsomal protein concentration); however, this is not always possible because of limitations of the analytical methods. Alternatively, an ‘‘apparent’’  $K_i$  can be estimated by correcting for the fraction of the inhibitor that is bound to the enzyme, which is calculated as the product of the fractional inhibition in the presence of a given inhibitor concentration and enzyme content [56].

It is important to note that the foregoing discussion puts emphasis on the  $K_i$  value for inhibition rather than the  $IC_{50}$  value. The  $K_i$  value is an inhibition constant that defines the affinity of the inhibitor for the enzyme, whereas,  $IC_{50}$  is the concentration of inhibitor required to cause 50% inhibition under a given set of experimental conditions. It is preferable to determine the inhibition constant ( $K_i$ ) rather than an  $IC_{50}$  value for the following reasons:

1.  $K_i$  values are intrinsic constants, whereas  $IC_{50}$  values are extrinsic constants. Consequently,  $IC_{50}$  values, in contrast to  $K_i$  values, are dependent on the type of substrate, the concentration of substrate, and incubation conditions (protein concentration or incubation times, etc.).
2. Because they are intrinsic constants,  $K_i$  values can be reproduced from one laboratory to another.
3. The pharmaceutical industry in general and, perhaps more importantly, the FDA have accepted the method of predicting the potential for drug interactions by a drug based on  $K_i$  values and the (free) plasma concentration of the drug.
4. The size of the experiment necessary to determine  $K_i$  values is only slightly larger than that required to determine  $IC_{50}$  values. Therefore, determination of  $IC_{50}$  values is cost effective and time saving only when several (>3) drugs are to be screened for their potential to inhibit cytochrome P450.

Several classes of drugs, including alkylamines, heterocyclic amines, hydrazines, methylenedioxybenzenes, and macrolide antibiotics, can be metabolized by P450 enzymes to form stable complexes with heme, thus inactivating the P450 enzyme in a ‘‘quasi-irreversible’’ manner [38]. Alternatively, chemicals containing terminal double or triple bonds can be oxidized to radical intermediates that alkylate heme, thus inhibiting the enzyme in an irreversible manner [38]. It should be noted, however, that covalent modification (and irreversible inhibition) of the apoprotein is also possible. For example, tienilic acid is converted to a thiophene sulfoxide by CYP2C9, which is an electrophilic reactive

intermediate that can covalently bind to the nucleophilic group of an amino acid residue in the active site of CYP2C9 [52]. The kinetics of metabolism-dependent “irreversible” or “quasi-irreversible” inhibitors are complex [38]; this is the subject of Chap. 10 of this book. The kinetics of “reversible” metabolism-dependent inhibition are dependent on the inhibitory metabolite. Therefore, when further study of such inhibition is warranted, the inhibitory metabolite should be used as a “direct” inhibitor instead of the parent compound.

The drugs under investigation can be evaluated for their ability to inhibit various human P450 enzymes, including CYP1A2, CYP2A6, CYP2B6, CYP2C8, CYP2C9, CYP2C19, CYP2D6, CYP2E1, CYP3A4/5, and CYP4A9/11, using the enzyme-selective marker substrate reactions listed in Tables 3 and 4 (although alternate enzyme substrates are available; see Chap. 3).

## **B. In Vitro Systems for the Study of Inhibition of P450 Enzymes**

The systems that have been used include purified reconstituted P450 enzymes, microsomes from cell lines transfected with the cDNA encoding a given human P450 enzyme, human liver microsomes, isolated/cultured hepatocytes, and liver slices. The two systems used most often are human liver microsomes and cDNA-expressed enzymes. However, all systems have distinct advantages and disadvantages; therefore, the selection of a given system should be based on the desired endpoint. In reality, the choice of the *in vitro* system used for the evaluation of drugs as inhibitors of P450 enzymes is a controversial subject. This is primarily because the principles of Michaelis–Menten enzyme kinetics (“pure thoughts”) are often applied to these (“impure”) systems. Needless to add that all three aforementioned assumptions (see Sec. II.A, “Theoretical Concepts”) can be violated depending on the *in vitro* system. Each of these systems is discussed with respect to their utility, advantages, and disadvantages.

### **1. Human Liver Microsomes**

Human liver microsomes contain all of the P450 enzymes expressed in human liver, although their levels can vary from one sample to the next. To circumvent the problem of variability, several individual samples of human liver microsomes are pooled, and this pool serves as the *in vitro* test system for evaluating drugs as inhibitors of human P450 enzymes. Since human liver microsomes are pooled from several individuals, they contain the “average” levels of all P450 enzymes expressed in human livers. (Such pooled human liver microsomes are commercially available from several sources.) In addition, the ratio of NADPH-cytochrome P450 reductase to P450 in human liver microsomes and the amount of cytochrome  $b_5$  and the type of lipids are the same as those in the intact liver.

**Table 3** P450 Enzymes, Examples of Their Marker Substrate Reactions, and Respective Reversible and Metabolism-Dependent Inhibitors

P450	Marker reactions	Reversible inhibitors	Metabolism-dependent inhibitors
CYP1A2	7-Ethoxyresorufin <i>O</i> -dealkylation Phenacetin <i>O</i> -deethylation Caffeine <i>N</i> <sub>3</sub> -demethylation	$\alpha$ -Naphthoflavone Fluvoxamine	Furafylline
CYP2A6	Coumarin 7-hydroxylation	Letrozole <sup>a</sup>	8-Methoxypsoralen
CYP2B6	S-Mephenytoin <i>N</i> -demethylation 7-Ethoxy-4-trifluoromethylcoumarin <i>O</i> -dealkylation	Orphenadrine (?)	Chloramphenicol (?)
CYP2C8	Paclitaxel 6 $\alpha$ -hydroxylation Retinol 4-hydroxylation	Quercetin (?)	None available
CYP2C9	Diclofenac 4'-hydroxylation Tolbutamide methylhydroxylation S-Warfarin 7-hydroxylation	Sulfaphenazole	Tienilic acid Methylenedioxyphenyl compounds <sup>a</sup>
CYP2C19	S-Mephenytoin 4'-hydroxylation	Modafinil <sup>a</sup> Omeprazole	None available
CYP2D6	Dextromethorphan <i>O</i> -demethylation Bufuralol 1'-hydroxylation Debrisoquine 4-hydroxylation	Quinidine	RO115-1954 <sup>a</sup> Methylenedioxyphenyl compounds <sup>a</sup>
CYP2E1	Chlorzoxazone 6-hydroxylation	4-Methylpyrazole	3-Aminotriazole
CYP3A4/5	Testosterone 6 $\beta$ -hydroxylation Midazolam 1'- and 4-hydroxylation Nifedipine oxidation Erythromycin <i>N</i> -demethylation Cyclosporin oxidation	Ketoconazole	Troleandomycin Erythromycin Gestodene Methylenedioxyphenyl compounds <sup>a</sup>
CYP4A9/11	Lauric acid 12-hydroxylation	10-(Imidazolyl)-decanoic acid <sup>b</sup>	None available

(?): The selectivity of these inhibitors has not yet been established.

<sup>a</sup> Information gathered from several review articles (Refs. 1, 17, 19, and 36), with the exception of letrozole, modafinil, methylenedioxyphenyl compounds, and RO115-1954 (Refs. 137–140).

<sup>b</sup> From Ref. 55a.

**Table 4** Typical Incubation Conditions and Kinetic Constants of Marker Substrate Reactions of Human P450 Enzymes in a Pool of Human Liver Microsomes

P450 Enzyme	Marker reaction	Pool of nine human liver microsomal samples			
		[Protein] (mg/ml)	Incubation time (min)	$K_m^c$ ( $\mu$ M)	$V_{max}^c$ (pmol/min/mg)
CYP1A2	7-Ethoxyresorufin <i>O</i> -dealkylation	0.1	10	$0.26 \pm 0.01$	$120 \pm 2$
CYP2A6	Coumarin 7-hydroxylation	$0.05^a$	$5^a$	$0.57 \pm 0.02$	$1300 \pm 12$
CYP2B6	<i>S</i> -Mephenytoin <i>N</i> -demethylation	$1.0^b$	$30^b$	$1700 \pm 40$	$1900 \pm 30$
CYP2C8	Paclitaxel 6 $\alpha$ -hydroxylation	0.1	10	$14 \pm 1$	$530 \pm 30$
CYP2C9	Diclofenac 4'-hydroxylation	0.1	$5^a$	$3.7 \pm 0.2$	$3600 \pm 59$
CYP2C19	<i>S</i> -Mephenytoin 4'-hydroxylation	$1.0^b$	$30^b$	$35 \pm 2$	$380 \pm 4$
CYP2D6	Dextromethorphan <i>O</i> -demethylation	0.1	10	$5.5 \pm 0.5$	$360 \pm 13$
CYP2E1	Chlorzoxazone 6-hydroxylation	0.1	10	$27 \pm 2$	$2500 \pm 100$
CYP3A4/5	Testosterone 6 $\beta$ -hydroxylation	0.1	10	$110 \pm 10$	$9800 \pm 490$
CYP4A9/11	Lauric acid 12-hydroxylation	0.1	$5^a$	$7.6 \pm 1.2$	$2200 \pm 100$

<sup>a</sup> The protein concentration and incubation time were less than 0.1 mg/ml and 10 min, respectively, to avoid overmetabolism of the substrate.

<sup>b</sup> The protein concentration and/or incubation time were 1.0 mg/ml and 30 min, respectively, because of low sensitivity of the assays.

<sup>c</sup> The kinetic constants were determined at XenoTech (unpublished data) with a pool of nine human liver microsomal samples and are consistent with published literature values. (Note:  $V_{max}$  values can vary enormously from one microsomal sample to the next, but the  $K_m$  values should be within a factor of 2 or 3.)

Another advantage is that the same sample of pooled human liver microsomes (and often the same experimental conditions, i.e., protein concentration and incubation time) can be used to study all P450 enzymes of interest. Human liver microsomes are also the system of choice for evaluating drugs as metabolism-dependent inhibitors of P450 enzymes, for they contain the complete enzymatic machinery to metabolize drugs that can inhibit P450 enzymes. This is an important consideration because the enzyme that converts a drug to an inhibitory metabolite may not be the one that is inhibited. The major disadvantage of using pooled human liver microsomes is that these microsomes contain a large amount of lipids and proteins that can decrease the free concentration of drug in the medium. However, to various degrees, this is a disadvantage of all available in vitro systems. Another disadvantage is that human liver microsomes are an exhaustible resource; therefore, each batch of microsomes is slightly different, although the variability can be minimized by pooling samples from a large number of individuals and by preparing large batches and by careful selection of samples that will become a part of the pool. Indeed, when these measures are taken, pooled human liver microsomes may be one of the most consistent in vitro systems. Finally, with human liver microsomes, enzyme-selective substrates must be used. This is less of a problem now that enzyme-selective substrates are available for all major P450 enzymes. However, most of the enzyme-selective assays are HPLC assays; therefore they are time consuming and less amenable to high throughput.

## 2. cDNA-Expressed P450 Enzymes

Microsomes containing cDNA-expressed enzymes for all known P450 enzymes are commercially available from several sources. The major advantage of this system is its simplicity, because such microsomes contain only one P450 enzyme. Another advantage is that the selection of the substrate need not be limited to enzyme-specific substrates, as in the case of human liver microsomes [57–59]. In fact, a substrate that was metabolized by all P450 enzymes would be particularly valuable for use with recombinant enzymes. It is noteworthy that, for certain P450 enzymes, these microsomes are now available with very high activities (Supersomes®, Gentest Corp., Woburn, MA; Baculosomes®, Panvera, Madison, WI). However, the Supersomes® and Baculosomes® have not been thoroughly characterized with regard to their kinetic properties and substrate/inhibitor specificities. Additionally, a significant portion of total cytochrome P450 in the Supersomes® is the apoprotein, which is catalytically inactive because it is not bound to heme. Another problem of cDNA-expressed enzymes is the variable expression of cytochrome b<sub>5</sub> and/or NADPH-cytochrome P450 reductase, which can affect the turnover number ( $V_{\max}$ ) for a given enzyme [60–61], although the “affinity” ( $K_m$  value) of P450 enzymes toward marker substrates is generally comparable between recombinant enzymes and human liver microsomes [62].

The exception to this generalization is in cases where multiple P450 enzymes can metabolize a drug in human liver microsomes and hence the observed  $K_m$  value is found to be different from that observed with recombinant enzymes [63]. For example, testosterone 6 $\beta$ -hydroxylation is catalyzed by both CYP3A4 and CYP3A5 in human liver microsomes, and these two enzymes have different affinity for testosterone [64]. For this reason, recombinant proteins are more appropriate when it is necessary to differentiate between the inhibitory potency of a drug toward two functionally similar enzymes, such as CYP3A4 and CYP3A5.

Recombinant P450 enzymes are not suitable for metabolism-dependent inhibition experiments, where the inhibitory metabolite has little or no effect on the enzyme responsible for its formation, but has the ability to inhibit other enzymes [59]. For example, spironolactone is metabolized to an *S*-oxide by flavin-containing monooxygenases (FMO) to a metabolite that can covalently bind to protein and inhibit cytochrome P450 [65]. Presumably, this phenomenon would not be observed if individual cDNA-expressed P450 enzymes were used.

Finally, certain P450 enzymes, e.g., CYP2C9, CYP2C18, CYP2C19, and CYP2D6, exist in several polymorphic forms. For example, CYP2C9 and its allelic variants differ by one to four amino acids and are allelic variants rather than distinct gene products [18,66,67]. Therefore, if the variant CYP2C9\*2 were selected as a source of the enzyme, then that preparation would be representative of ~10% of the population. Although the variant forms of P450 enzymes differ from the wild-type forms by only a few amino acids, there are numerous examples where a single amino acid substitution can alter the catalytic properties of cytochrome P450 [18,67].

### 3. Purified Reconstituted P450 Enzymes

Several human P450 enzymes have been purified to homogeneity. NADPH-cytochrome P450 reductase is required to reconstitute a functional P450 enzyme, as is the presence of a lipid bilayer, and, in some cases, cytochrome  $b_5$ . A functional P450 enzyme can be reconstituted with NADPH-cytochrome P450 reductase and phospholipids (and cytochrome  $b_5$ ) by mixing the ingredients in empirically determined proportions. The major advantages of this system are its simplicity and the ease with which its components can be manipulated. The disadvantages are: not all enzymes are available in purified form; it is often difficult to reconstitute them reproducibly; and the concentration of NADPH-cytochrome P450 reductase, which is often added in saturating amounts, is several times higher than that present in human liver microsomes. This system is rarely used for the evaluation of drugs as inhibitors of P450 enzymes, having largely been replaced by cDNA-expressed P450 enzymes. However, purified reconstituted P450 enzymes are the system of choice for detailed mechanistic studies.

#### 4. Isolated Hepatocytes, Cultured Hepatocytes, and Liver Slices

Human hepatocytes (fresh or cryopreserved) are now commercially available. However, the quality, stability, and availability of the commercial preparations remain questionable. Nevertheless, the simple fact that they are available has prompted some use of hepatocytes for evaluating drugs as inhibitors of P450 enzymes. Hepatocytes offer limited advantages over the well-established systems, such as pooled human liver microsomes or cDNA-expressed enzymes, but are subject to a plethora of additional problems. Because hepatocytes are a complex system, none of the Michaelis–Menten equations for enzyme kinetics readily applies to them. It has been argued that, because hepatocellular uptake of drugs in isolated hepatocytes mimics the *in vivo* situation better, the drug-interaction studies using hepatocytes would be more predictive [68]. However, drugs may compete for the uptake pathways as well, which makes it extremely difficult to interpret the data mechanistically. The mechanistic interpretation of the data is what is needed to make *in vitro* to *in vivo* predictions using marker substrates. Additionally, phase II metabolism of marker substrate (or its metabolite) may complicate the determination of initial rates of metabolite formation. Hepatocytes might be an appropriate system to study interactions between two *specific* drugs that may be concomitantly administered, but not to evaluate a drug against marker substrates. There are other *in vitro* systems to evaluate drug interactions involving inhibition, transport, and/or phase II metabolism [69].

Isolated hepatocytes are a scarce resource, and pooled hepatocytes are not yet available; thus, it is often difficult to repeat experiments or to compare results from one laboratory to another. In the opinion of the authors, the use of hepatocytes should be reserved for induction or integrated-metabolism studies (i.e., studies that cannot be conducted readily with subcellular fractions). Cultured hepatocytes present even a greater problem, because the expression of P450 enzymes is markedly diminished (if not lost) when hepatocytes are placed in culture [70,71]. Similarly, liver slices, in addition to being plagued with the same problems as noted for isolated hepatocytes, have a barrier to the diffusion of drugs to cells in the core of the liver slice [72].

#### C. Selection of the Concentrations of Marker Substrate

A range of substrate concentrations (between  $0.2K_m$  and  $5K_m$ ) that gives a wide variation in the rates of substrate turnover and is in the nonlinear part of the rate versus substrate concentration curve is recommended. We typically use  $K_m/2$ ,  $K_m$ ,  $2K_m$ , and  $4K_m$  for all major hepatic P450 enzymes. Figure 3 illustrates the consequences of selecting an inappropriate substrate concentration range (too



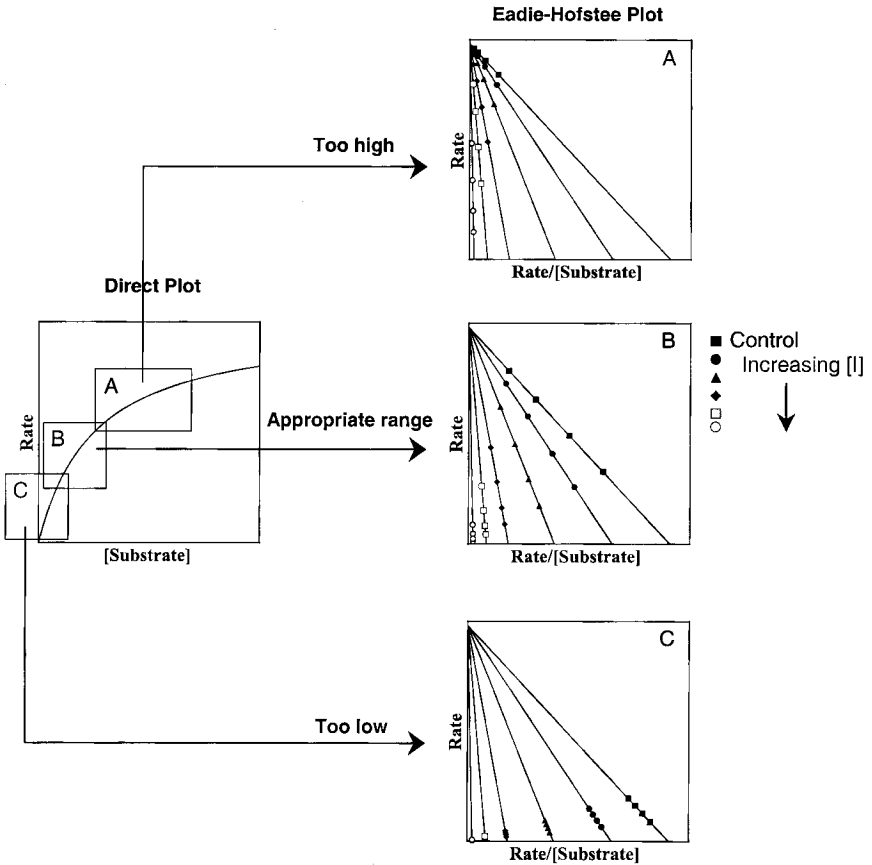


**Figure 3** Consequences of selecting an inappropriate range of substrate concentration on Eadie–Hofstee plots of enzyme inhibition: All graphs and the corresponding fit are based on theoretical data. Selecting a range of substrate concentrations that is too high results in an Eadie–Hofstee plot that has a cluster of data points toward  $V_{max}$ , whereas selecting a concentration range that is too low has the opposite effect. In either case, a slight experimental error can have a large influence on the slope of the regression lines and hence introduce an error in the calculated  $K_i$  value. Also, a “too-high” or “too-low” concentration range makes it harder to discriminate between different types of inhibition (not shown). The “appropriate range” is found between  $0.2K_m$  and  $5K_m$ ; the substrate concentrations shown in the middle Eadie–Hofstee plot, entitled “Appropriate range,” are  $K_m/2$ ,  $K_m$ ,  $2K_m$ , and  $4K_m$ , which is what the authors recommend (solubility permitting).

low or too high) on the results of an inhibition experiment. When a substrate concentration range between  $0.2K_m$  and  $5K_m$  is selected, the Eadie–Hofstee plot provides the largest spread of points on the entire graph, thus making the  $K_i$  value determination more accurate.

#### D. Selection of the Concentration of Drug

Several concentrations of the drug are studied, which normally cover a range that spans at least two orders of magnitude. The concentration of the drug is selected based on (but not equal to) the known or anticipated maximum plasma concentration ( $C_{\max}$ ) of the drug in vivo. The plasma  $C_{\max}$  is multiplied by a factor of 10, 100, or even 1000, which then becomes the highest concentration to be studied. The multiplication factors are important for several reasons: (1) Most lipophilic drugs are believed to be concentrated in the liver; therefore, the concentration at the active site of the P450 enzyme may be higher than the plasma  $C_{\max}$  [73]. (2) A significant portion of all lipophilic drugs is bound to microsomal proteins and lipids, thus reducing the “free” drug available to inhibit the enzyme [74–76]. (3) The most important (but often neglected) reason for studying a superphysiological concentration is that the concentration of the marker substrates is also superphysiological. For instance, the concentrations of the marker substrates are centered around the  $K_m$  value, which may be orders of magnitude higher than the plasma  $C_{\max}$  value.

It is important to study superphysiological concentrations of the marker substrates because (1) the analytical methods available are not able to detect initial rates of product formation at very low concentration of substrate, and (2) it will be difficult to distinguish between the various types of inhibition. (Fig. 3). *Since, the concentration of the substrate is raised artificially, the concentration of the drug in question must also be increased artificially.*

It is noteworthy that the methods available for in vitro to in vivo extrapolations of the inhibition data (discussed later) are independent of the concentrations of the inhibitor studied. This is another advantage of designing experiments with the aim of determining  $K_i$  values rather than  $IC_{50}$  values. Quite often, the discussion of multiplication factors is futile because the limit of the aqueous solubility of drugs determines the highest concentration of the drug that can be studied. In the absence of information on actual or anticipated plasma concentrations, it is recommended that  $1000\ \mu\text{M}$  or the limit of aqueous solubility of the drug (whichever is highest) be selected as the highest concentration to be studied in vitro. Typically, four or more concentrations of the drug are studied that cover at least two orders of magnitude; for example, if the highest concentration of the drug is  $1000\ \mu\text{M}$ , the lower concentrations may be 250, 50, 10, 2.5, and  $1\ \mu\text{M}$ . The consequences of selecting a too-low or too-high concentration range of drug on an Eadie–Hofstee plot are shown in Figure 4. The experiment should be repeated

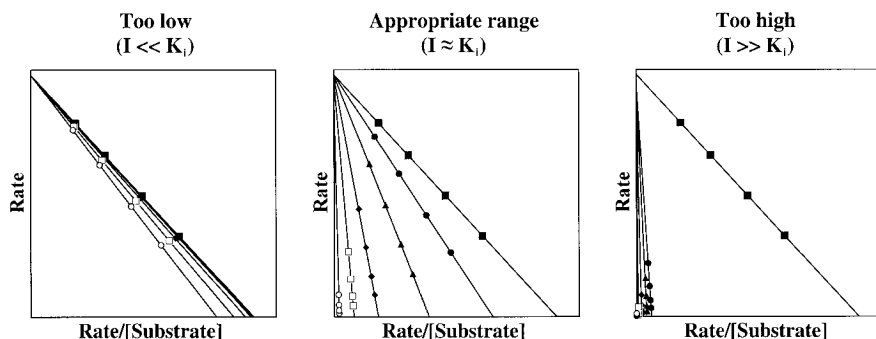


**Figure 4** Consequences of selecting an inappropriate range of inhibitor concentration on Eadie–Hofstee plots of enzyme inhibition: All graphs and the corresponding fit are based on theoretical data. Selecting a range of inhibitor (drug) concentration that is “too inhibitory” results in an Eadie–Hofstee plot with a cluster of steep regression lines, whereas selecting a concentration range that is “not inhibitory enough” results in a cluster of shallow lines. In either case, a slight experimental error can have a large influence on the slope of the regression lines and hence introduce an error in the calculated  $K_i$  value. Furthermore, both extremes make it harder to discriminate between different types of inhibition (not shown). The “appropriate range” is centered around the estimated  $K_i$  value, and spans two orders of magnitude; the inhibitor concentrations shown in the middle Eadie–Hofstee plot, entitled “Appropriate range,” are  $0.4K_i$ ,  $1.3K_i$ ,  $4K_i$ ,  $10K_i$ , and  $40K_i$ . The experiment should be repeated if the concentration range selected is “too high” such that the concentration range does not bracket the observed  $K_i$  value. It may not be necessary or desirable to repeat the experiment if the observed  $K_i$  value exceeds the concentration range of the drug, in which case a minimum estimated  $K_i$  value may be calculated (described in the text, Sec. II.H.1).

if the concentration range selected were too high such that the concentration range does not bracket the observed  $K_i$  value. It may not be necessary or desirable to repeat the experiment if the observed  $K_i$  value exceeds the concentration range of the drug, in which case a minimum estimated  $K_i$  value may be calculated (discussed later).

## E. Selection of Incubation Conditions

A well-designed pool of human liver microsomes is more suitable than a random selection of human liver microsomes. This is because human liver microsomes contain variable amounts of P450 enzymes and consequently catalyze the metabolism of marker substrates at variable rates. With a random pool of human liver microsomes, for each of the ten P450 enzyme assays, variable amounts of microsomes and/or incubation times are required to allow the generation of sufficient

metabolites that can be detected easily and reliably. Equally important is to perform experiments under initial-rate conditions, such that the percentage of metabolism of substrate does not exceed 20%. To accommodate these two requirements, a variety of incubation conditions must be used for different P450 enzyme reactions. For example, there are assays (e.g., coumarin 7-hydroxylase) that are carried out in the presence of 0.01 mg/mL of microsomal protein, while others are carried out in presence of 2.0 mg/mL of protein (e.g., *S*-mephenytoin 4'-hydroxylation). In other words, there can be a 200-fold variation in the concentration of microsomal protein in the incubations. Similarly, incubation conditions may vary from 2 min to 30 min, resulting in a 15-fold difference in incubation time.

The variation in incubation conditions (protein amount and incubation time) is a concern and a potential flaw of these studies, for two reasons. First, drugs can bind to microsomes in a manner that influences their ability to inhibit the enzyme being evaluated. Therefore, it is possible to have a 100-fold variation in binding, depending on the assay, which would result in a 100-fold variation in the concentration of unbound (free) drug. Second, the drugs under investigation are often high-turnover substrates for P450 enzymes. In other words, the drugs may not be metabolically stable during the incubation period. A variable incubation time and protein amount may cause the drug to be completely metabolized under assay conditions of high protein amount and long incubation times, but not under conditions of low protein and short incubation times. The consequence of both excessive binding and excessive metabolism is that the drug may no longer be available to inhibit the P450 enzyme [56,74–77].

The solution to this problem is to use a “tailor-made” pool of human liver microsomes, which contains the right blend of P450 enzyme activities that will allow assays of P450 enzymes under identical conditions of protein amount and incubation time. For *most* assays, the “tailor-made” pool will allow the evaluation of drugs under conditions of constant protein binding and constant metabolism of the drug. Both the extent of protein binding and the percentage of metabolism (metabolic stability) can be experimentally determined prior to the initiation of an inhibition study, and the amount of drug in the incubations can be increased to compensate for loss due to binding or metabolism. In our laboratory, we have successfully prepared a pool that allows the evaluation of CYP1A2, CYP2C8, CYP2C9, CYP2D6, CYP2E1, CYP3A4/5, and CYP4A9/11 at a constant protein concentration of 0.1 mg/ml, and CYP1A2, CYP2C8, CYP2D6, CYP2E1, and CYP3A4/5 for constant incubation time of 10 min.

## F. Experimental Design for Evaluating Drugs as Inhibitors of P450 Enzymes

The drugs under investigation can be evaluated for their ability to inhibit various human P450 enzymes, including CYP1A2, CYP2A6, CYP2B6, CYP2C8, CYP2C9, CYP2C19, CYP2D6, CYP2E1, CYP3A4/5, and CYP4A9/11, using

the enzyme-selective marker substrate reactions listed in Tables 3 and 4 (although alternate enzyme substrates are available; see Chap. 3). Table 4 also provides the kinetic constants for each of the P450 enzymes.

### 1. Determination of $IC_{50}$ Values for “Direct” Inhibition of Human P450 Enzymes

Each drug is incubated with human liver microsomes in the presence of the marker substrate. Reactions are initiated with NADPH, which is added immediately before the samples are incubated at 37°C. (If the microsomes are incubated at 37°C in the absence of NADPH, considerable FMO activity may be lost.) If no pharmacokinetic data is available, the final concentration of the drug is typically equal to zero, 0.5, 2.5, 10, 50, 250, or 1000  $\mu\text{M}$  (solubility permitting). The concentration of each marker substrate is equal to its  $K_m$ . Incubations containing no drug contain the organic solvent used to dissolve the drug (negative controls), which may not be sufficiently water soluble to be added as an aqueous solution. It may be necessary to repeat the experiment if the lower concentrations of the drug cause virtually complete inhibition of P450 activity. Data is plotted on a percent control activity versus drug concentration curve, and  $IC_{50}$  values are calculated by nonlinear regression of the data (see Fig. 5).

### 2. Determination of $K_i$ Values for the Inhibition of Human P450 Enzymes

Each drug is incubated with human liver microsomes in the presence of the marker substrate. Reactions are initiated with NADPH. If no pharmacokinetic data is available, the final concentrations of the drug are typically equal to zero, 0.5, 2.5, 10, 50, 250, and 1000  $\mu\text{M}$  (solubility permitting). The concentration of each marker substrate is equal to  $K_m/2$ ,  $K_m$ ,  $2K_m$ , and  $4K_m$  (solubility permitting). Incubations containing no drug contain the organic solvent used to dissolve the drug (negative controls), which may not be sufficiently water soluble to be added as an aqueous solution. Additional incubations are carried out in the presence of a known inhibitor of P450 enzymes (positive controls). It may be necessary to repeat the experiment if the lower concentrations of the drug cause virtually complete inhibition of P450 activity even at the highest substrate concentration. Data is analyzed by means of an Eadie–Hofstee plot (rate versus rate/[substrate]), the type of inhibition is ascertained, and the  $K_i$  values are calculated via nonlinear regression of the data (see Fig. 6).

### 3. Evaluation of the Drug as a Metabolism-Dependent Inhibitor of Human P450 Enzymes

These experiments are designed based on the results obtained from direct inhibition experiments (see Sec. II.F.1). It is for this reason that the evaluation of the

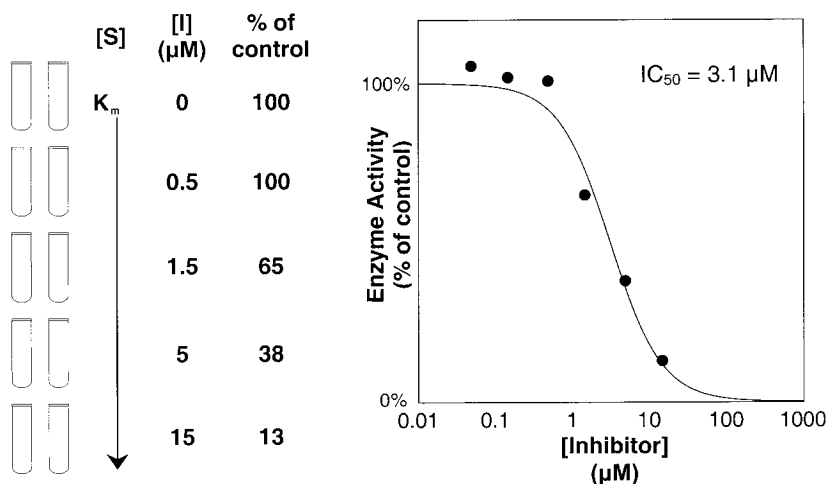


**Figure 5** Design of and graphical representation (semilog plot) of an  $IC_{50}$  determination experiment: Actual data obtained with a proprietary compound is shown. Duplicate incubations containing a pool of human liver microsomes and the marker substrate (at concentration equal to  $K_m$ ) were performed in the absence or presence of varying concentrations of the inhibitor. Reactions were initiated with an NADPH-generating system. The incubations were stopped after a predetermined incubation time. The data is plotted on a semilog plot with log [inhibitor] on the x-axis and percentage of control activity on the y-axis. The concentration of the inhibitor that causes 50% inhibition (or 50% of control) represents the  $IC_{50}$  value. The  $IC_{50}$  value forms the basis for designing an experiment for the determination of the  $K_i$  value (see Fig. 6).

drug as a direct inhibitor should precede its evaluation as a metabolism-dependent inhibitor.

a. *“Reversible” Metabolism-Dependent Inhibition.* To examine a drug as a “reversible” metabolism-dependent inhibitor, a pool of human liver microsomes is preincubated with the drug and NADPH for 0 and 15 min to allow for the generation of metabolites that could inhibit cytochrome P450. After the preincubation period, the marker substrate is added and the incubation continued to measure residual P450 activity. The concentration of the drug is the highest concentration of the drug that causes no more than 30% inhibition when tested as a direct inhibitor. The concentration of marker substrate is equal to its  $K_m$ . Preincubations containing no drug (but containing the solvent in which the drug is dissolved) and incubations that contain drug but are not preincubated serve as negative controls. Such an experimental design and typical data obtained are illustrated in Fig. 7. If substantial inhibition is observed, then the inhibitory me-

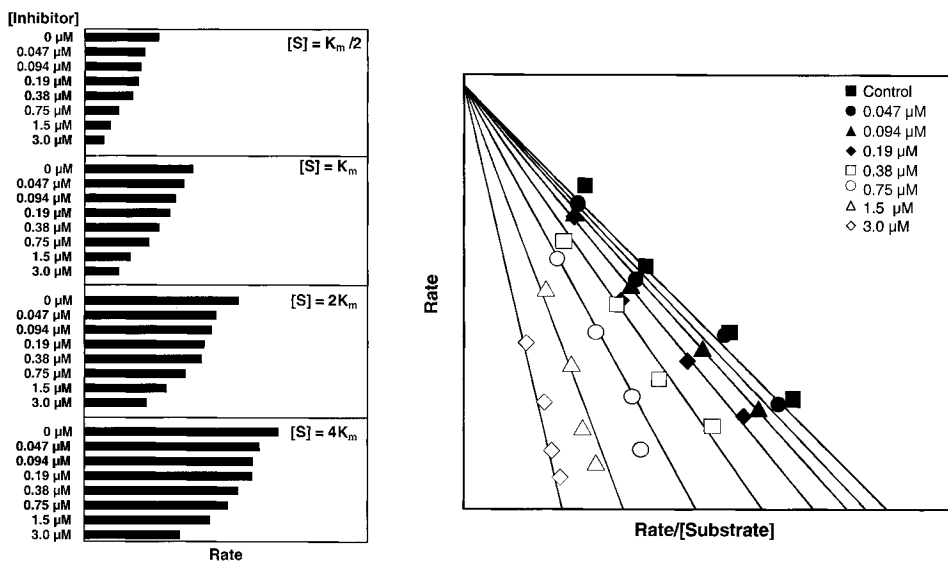


**Figure 6** Design and graphical representation of a  $K_i$  determination experiment: Actual data obtained with a proprietary compound is shown. Duplicate incubations containing a pool of human liver microsomes and the marker substrate (at concentrations equal to  $K_m/2$ ,  $K_m$ ,  $2K_m$ , and  $4K_m$ ) were performed in the presence of varying concentrations of the inhibitor. Reactions were initiated with an NADPH-generating system and stopped after a predetermined incubation time. The bar graphs (left) show the effect of inhibitor concentration on enzyme activity at various inhibitor concentrations. The Eadie-Hofstee plot (right) suggests that the inhibition is competitive in nature, with a  $K_i$  value of 0.91  $\mu\text{M}$ .

tabolite should be identified and its potency ( $K_i$  value) for inhibition of a given P450 enzyme should be evaluated.

*b. Metabolism-Dependent “Irreversible” or “Quasi-Irreversible” Inhibition.* To evaluate a drug as an “irreversible” or “quasi-irreversible” inhibitor, a pool of human liver microsomes is preincubated with the drug and NADPH for 0 and 15 min to allow for the generation of intermediates that inhibit cytochrome P450 irreversibly or quasi-irreversibly. After the preincubation period, an aliquot of microsomes is removed and added to incubation mixtures containing the marker substrate, and another incubation is carried out to measure the residual marker P450 activity. This type of preincubation allows the drug to be diluted by a factor of 10 (dilution factor) for the final incubation with the marker substrate, thereby minimizing any “reversible” inhibition effects. The highest con-

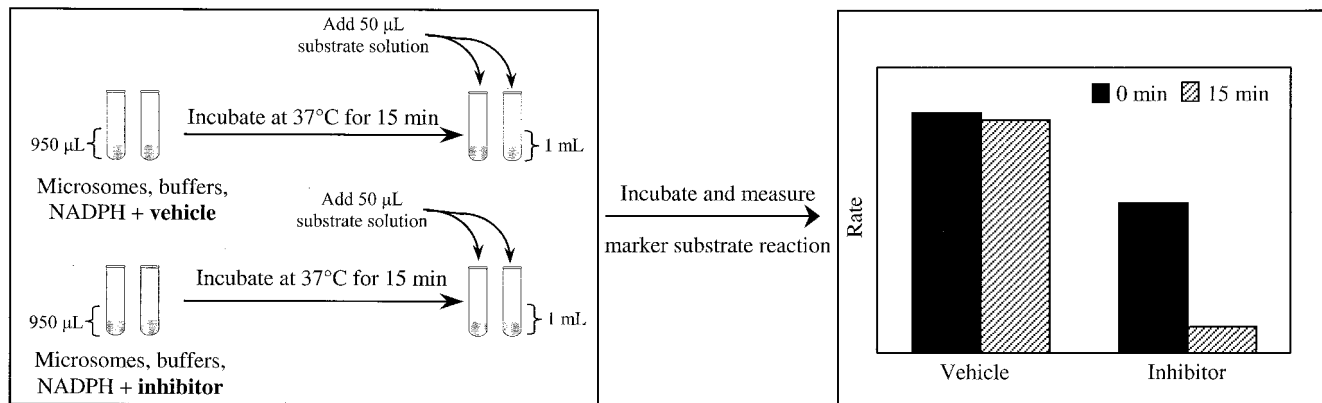


**Figure 7** Design and graphical representation of “reversible” metabolism-dependent inhibition—preliminary experiment: Actual data obtained with a proprietary compound is shown. Duplicate “preincubations” containing a pool of human liver microsomes were performed in the absence or presence of the inhibitor. Reactions were initiated with an NADPH-generating system. After a predetermined “preincubation” period (e.g., 15 min), the marker substrate (final concentration equal to  $K_m$ ) was added in a small volume (1/20 of the total incubation volume), and the “incubation” is continued to allow for the formation of metabolite(s) of the marker substrate. The incubations were stopped after a predetermined incubation time. The data is plotted on a bar graph as indicated. A marked increase in inhibition due to the 15-min preincubation compared with the 0-min preincubation is an indication of metabolism-dependent inhibition. The vehicle control gives an estimate of the loss of enzyme activity due to the preincubation or the vehicle. It should be noted that an “irreversible” or “quasi-irreversible” metabolism-dependent inhibitor (Fig. 8) is likely to show marked inhibition when tested as a “reversible” metabolism-dependent inhibitor. However, the converse is not true. Therefore, a “reversible” metabolism-dependent inhibitor can be identified only when little or no inhibition is observed in the experiment described in Fig. 8, but marked inhibition is observed in the experiment described in this figure.



centration of the drug that causes less than 30% inhibition as a “reversible” inhibitor is multiplied by the dilution factor to give the concentration of inhibitor at which the preincubations are carried out. For example, if 10  $\mu\text{M}$  drug causes 30% inhibition of a P450 activity with the concentration of marker substrate equal to  $K_m$ , then the irreversible or quasi-irreversible inhibition experiments are conducted with 100  $\mu\text{M}$  drug (with 10 times the usual concentration of microsomal protein). After the preincubation period, an aliquot would be diluted 10-fold to measure residual P450 activity, at which point the final concentration of the drug would be 10  $\mu\text{M}$ , which, if the drug is strictly a reversible inhibitor, would cause only a 30% inhibition of P450 activity. The concentration of marker substrate is equal to  $K_m$  (although this is not absolutely necessary, because such metabolism-dependent inhibitors exhibit kinetics similar to those observed with noncompetitive inhibitors, the inhibitory capacity of which is not affected by substrate concentration). Preincubations containing no drug (but containing the solvent in which the drug is dissolved) and incubations that contain drug but are not preincubated serve as negative controls. Such an experimental design and typical data obtained are illustrated in Fig. 8; they are similar to those described in the literature [49,52,78].

If substantial inhibition is observed, an additional experiment may be carried out at multiple concentrations of the drug and multiple preincubation times to determine the rate of inactivation ( $K_{\text{inact}}$ ) and  $K_i$  value [49,52,78]. The concentrations of drug and preincubation times are chosen such that percentage inhibition ranging from 10 to 90% is observed after preincubation. For each inhibitor concentration, the preincubation time ( $x$ -axis) is plotted against the natural log of the fraction of remaining enzyme activity ( $y$ -axis) (see Fig. 9). The reciprocal of inhibitor concentration is then plotted against the *initial* rates of inactivation of the enzyme (slope of the lines in Fig. 9); the  $y$ -intercept and the negative reciprocal of the  $x$ -intercept of this plot give the  $K_{\text{inact}}$  value and  $K_i$  value, respectively (Fig. 9). For metabolism-dependent irreversible or quasi-irreversible inhibitors, the  $K_{\text{inact}}$  value is defined as the fraction of the total enzyme that is inactivated each minute at saturating concentrations of the inhibitor, and the  $K_i$  value is defined as the dissociation constant of the initial (and reversible) enzyme–inhibitor complex.

#### 4. Sample-to-Sample Variation in Inhibition of P450 Enzymes

When significant direct or metabolism-dependent inhibition is observed, it is prudent to check the sample-to-sample variation in the inhibition of P450 enzymes. This is because the preceding experiments are performed with a pool of human liver microsomes or cDNA-expressed enzymes; and since there is enormous sample-to-sample variation in the expression of P450 enzymes in human liver, it is important to check if the inhibitory potency varies with differential expression

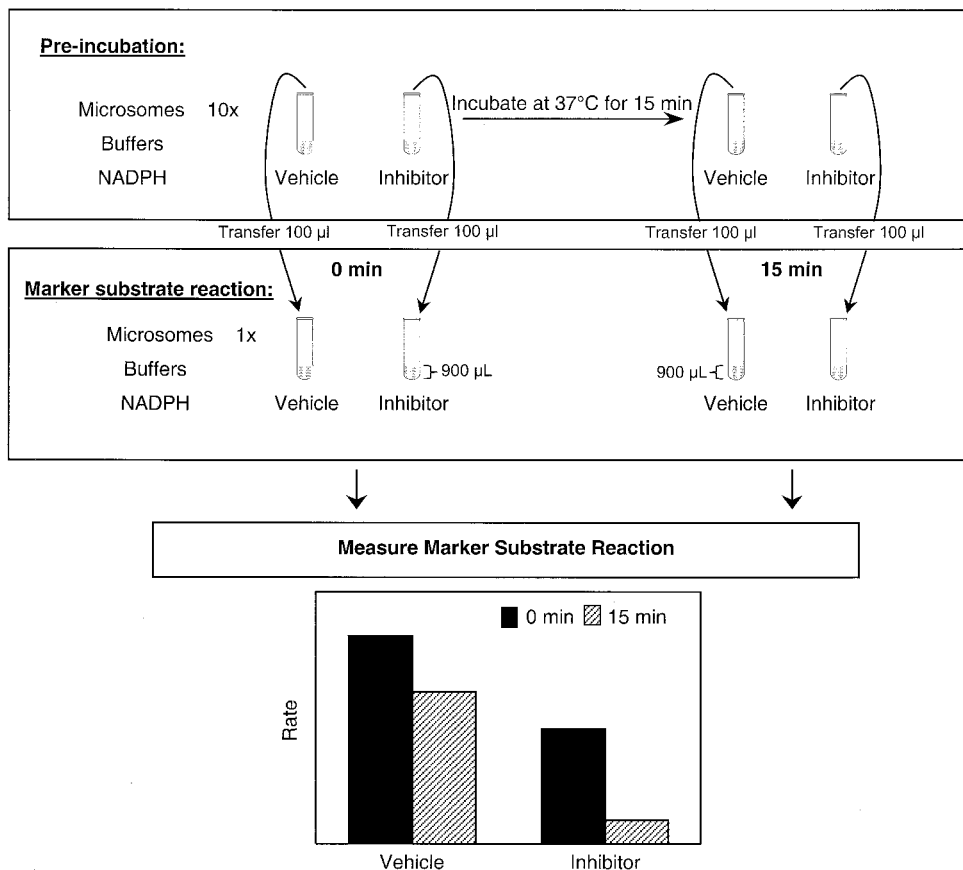


**Figure 8** Design and graphical representation of “irreversible” or “quasi-irreversible” metabolism-dependent inhibition—typical result of the preliminary screening experiment: Actual data obtained with a proprietary compound is shown. “Preincubations” containing a pool of human liver microsomes (at 10 times the “normal” concentration) were performed in the absence or presence of the inhibitor. Reactions were initiated with an NADPH-generating system. After a predetermined “preincubation” period (e.g., 15 min), an aliquot of the reaction mixture (typically, 100  $\mu$ L) was transferred to another “incubation” (final volume 1000  $\mu$ L) containing the marker substrate, NADPH-generating system. (*Note:* This resulted in the dilution of the microsomes to the “normal” protein concentration and the dilution of the inhibitor to 1/10 its original concentration, which minimizes the direct inhibitory effects of the inhibitor.) The “incubation” was then continued to allow for the formation of metabolite(s) of the marker substrate. The incubations were stopped after a predetermined incubation time. The data is plotted on a bar graph as indicated. A marked increase in inhibition as a result of the 15-min preincubation compared with the 0-min preincubation is an indication of metabolism-dependent “irreversible” inhibition. The vehicle control gives an estimate of the loss of enzyme activity due to the preincubation or the vehicle. If a drug shows potential for inhibition as “irreversible” or “quasi-irreversible” inhibition, an additional experiment may be necessary to determine the  $K_{\text{inact}}$  values (see Fig. 9).

**Pre-incubation      Marker substrate incubation**

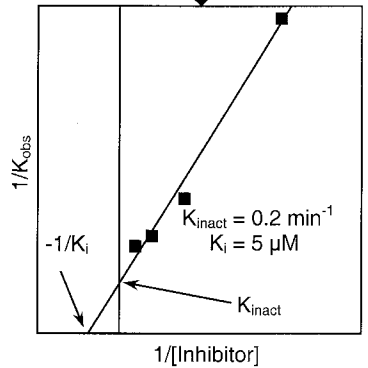
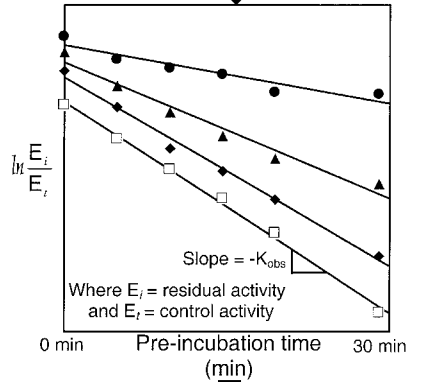
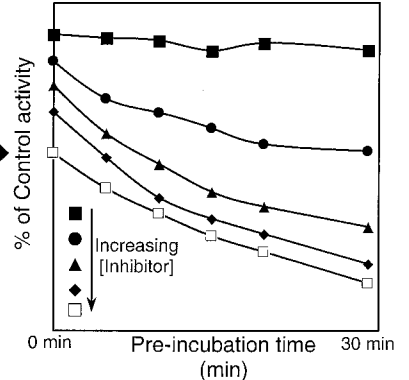
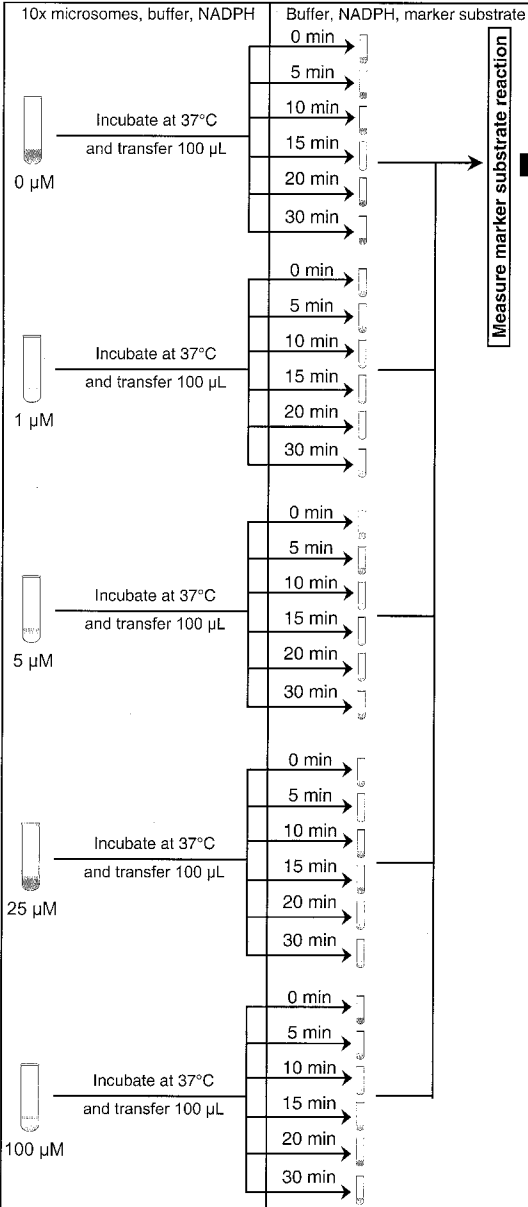


**Figure 9** Design and graphical representation of “irreversible” or “quasi-irreversible” metabolism-dependent inhibition—determination of  $K_{\text{inact}}$  and  $K_i$  values: Actual data obtained with a proprietary compound is shown. “Preincubations” containing a pool of human liver microsomes (at 10 times the “normal” concentration) were performed in the absence or presence of varying concentrations of the inhibitor. (The concentration range of the inhibitor and the preincubation times were chosen based on the results shown in Fig. 8 and are such that percentage inhibition ranging from 10 to 90% is observed after preincubation.) Reactions were initiated with an NADPH-generating system. After several predetermined “preincubation” periods (e.g., 5, 10, 15, 20, and 30 min), an aliquot of the reaction mixture (typically, 100  $\mu\text{L}$ ) was transferred to another “incubation” (final volume 1000  $\mu\text{L}$ ) containing the marker substrate, and a NADPH-generating system. (Note: This resulted in the dilution of the microsomes to the “normal” protein concentration and the dilution of the inhibitor to 1/10 its original concentration, which minimizes the direct inhibitory effects of the inhibitor.) The “incubation” was then continued to allow for the formation of metabolite(s) of the marker substrate. The incubations are stopped after a predetermined incubation time. The data is plotted on a line graph (top) with incubation time on the  $x$ -axis and percentage of control activity on the  $y$ -axis. Subsequently, for each inhibitor concentration, the preincubation time ( $x$ -axis) is plotted against the natural log of fraction of remaining enzyme activity ( $y$ -axis) (middle graph). The reciprocal of inhibitor concentration is then plotted against the *initial* rates of inactivation of the enzyme (slope of the lines in the middle graph); the  $y$ -intercept and the negative reciprocal of the  $x$ -intercept of this plot give the  $K_{\text{inact}}$  value and  $K_i$  value, respectively (bottom graph). For metabolism-dependent “irreversible” or “quasi-irreversible” inhibitors, the  $K_{\text{inact}}$  value is defined as the fraction of the total enzyme that is inactivated each minute at saturating concentrations of the inhibitor, and the  $K_i$  value is defined as the dissociation constant of the initial (and reversible) enzyme–inhibitor complex.

of a given enzyme. Additionally, several P450 enzymes (such as, CYP2C9, CYP2C19, and CYP2D6) are polymorphically expressed; therefore, the inhibitory effects of a drug between allelic variants may not be similar. While such experiments are generally performed with recombinant P450 enzymes, not all polymorphic enzymes may be commercially available or have been identified. For example, quinidine is a potent and selective inhibitor of CYP2D6 in a pool of human liver microsomes or in an individual human liver microsomal sample with high CYP2D6 activity, as measured by dextromethorphan *O*-demethylation (Fig. 10). However, when quinidine is added to microsomes from an individual donor who expresses allelic variants of CYP2D6 (namely, the \*4 and \*5 alleles<sup>‡</sup>), it has little or no inhibitory effect (Fig. 10). These allelic variants of CYP2D6 have no enzyme activity [79], and the low dextromethorphan *O*-demethylase ac-

<sup>‡</sup> Genotyping data graciously provided by Developmental Pharmacology and Experimental Therapeutics Laboratory, The Children’s Mercy Hospital, Kansas City, MO.

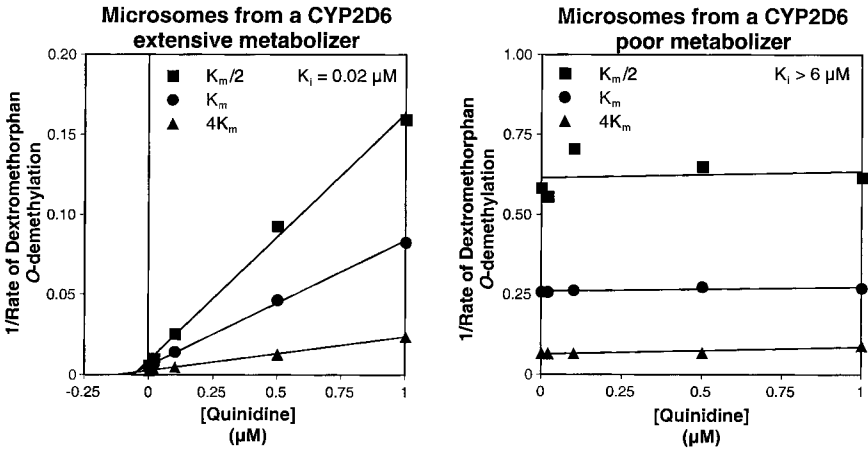


**Figure 10** Effect of quinidine on dextromethorphan *O*-demethylation by two different samples of human liver microsomes (Dixon plots): Several concentrations of quinidine (0, 0.02, 0.1, 0.5, and 1.0  $\mu\text{M}$ ) and dextromethorphan (2, 4, and 16  $\mu\text{M}$ ) were incubated in two individual human liver microsomal samples, and the formation of dextrophan was measured by HPLC with fluorescence detection. Microsomal sample 14 was obtained from a donor containing the \*1\*2 alleles of CYP2D6, which makes it an extensive metabolizer (EM), whereas microsomal sample 20 was from a donor containing the \*4\*5 alleles of CYP2D6, which makes it a poor metabolizer (PM) [79]. The data was plotted on a Dixon plot. Quinidine inhibited CYP2D6 in the EM microsomal sample (#14) but not in the PM microsomal sample (#20). (Genotyping data provided by the Developmental Pharmacology and Experimental Therapeutics Laboratory, The Children's Mercy Hospital, Kansas City, MO.)

tivity observed in this sample is catalyzed by CYP2C19 and CYP2C9 [80], enzymes that are not potently inhibited by quinidine [81].

Another important consideration for determining sample-to-sample variation in inhibition is in the case of metabolism-dependent inhibitors. For example, spironolactone is metabolized to an *S*-oxide by flavin-containing monooxygenases (FMO) to a metabolite that can covalently bind proteins and inhibits cytochrome P450. The extent of such inhibition is dependent on the concentration of FMO present in a given sample of human liver microsomes [65,82].

Since the purpose of the experiments designed to evaluate sample-to-sample variation is simply to check the results obtained from a pooled sample, these experiments need not be as detailed. For example, if a drug competitively inhibits a P450 enzyme with a  $K_i$  value of 50  $\mu\text{M}$ , it would be expected to inhibit 50% of the P450 enzyme activity when the substrate concentration is equal to  $K_m$  and the inhibitor concentration is 100  $\mu\text{M}$  ( $2K_i$ ;  $IC_{50} = 2K_i$  when the substrate

concentration is equal to  $K_m$  and inhibition is competitive). Therefore, a single experiment can be performed with individual liver microsomal samples (typically  $n \geq 10$ ), where the substrate concentration is equal to  $K_m$  and the drug concentration is equal to  $2K_i$ . (In this experiment, rates of marker substrate reaction by a given P450 enzyme should be inhibited by 50% in all of the microsomal samples.) An example of such an experiment and data obtained are shown in Figure 11. It should be noted that if the inhibition is noncompetitive, then the concentration of the drug examined in such an experiment should be equal to its  $K_i$  value.

### G. Pitfalls of In Vitro Evaluation of Drugs as Inhibitors of P450 Enzymes

Several pitfalls relating to the selection of the in vitro system (protein binding, selection of drug concentrations, and metabolic stability of the drug) were discussed in the preceding sections. In addition, there are several other factors complicating the interpretation of in vitro inhibition data. These include aqueous solubility of the drug, failure to measure initial rates of marker substrate reaction,

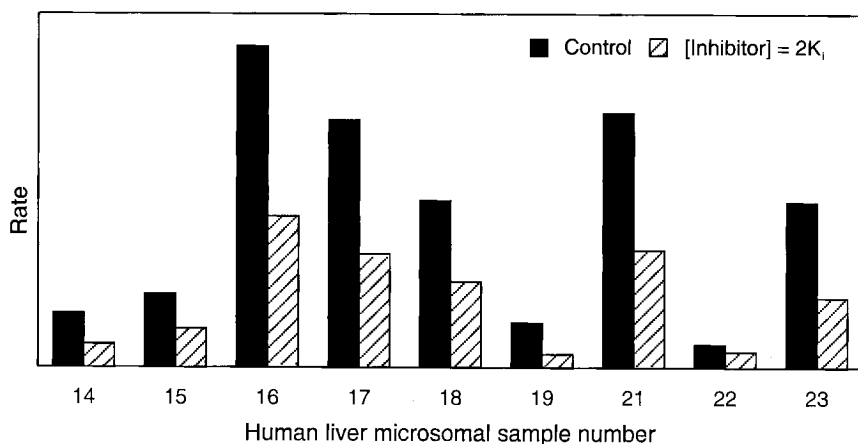


**Figure 11** Sample-to-sample variation in inhibition of *S*-mephenytoin 4'-hydroxylase (CYP2C19): A bank of human liver microsomes was incubated with *S*-mephenytoin (final concentration equal to  $K_m$ ) in the absence (solid bars) or presence of a proprietary drug (hatched bars). (The drug had been previously determined to be a competitive inhibitor of CYP2C19 with a pool of human liver microsomes with a  $K_i$  equal to 40  $\mu\text{M}$ .) The concentration of the drug for this experiment was equal approximately to  $2K_i$ , which, if the drug is a competitive inhibitor, should yield approximately 50% inhibition in all the samples examined.

interference by the drug or its metabolite(s) with the analytical measurement of the marker substrate reaction, and selective inhibition of P450 enzymes by the organic solvents often used to dissolve drugs.

## 1. Solubility

Most new drugs tend to have poor aqueous solubility at physiological pH. This limits the highest concentration of the drug that can be achieved *in vitro*. Two methods are typically used to circumvent this problem. The first method involves dissolving the drug in an organic solvent [such as methanol, acetonitrile, ethanol, or dimethyl sulfoxide (DMSO)] or weakly acidic solutions and delivering the drug to the incubation mixtures. (The impact of organic solvents is discussed later.) The second method relies on the lipophilicity of the biological membranes (microsomes) to solubilize the drug. To this end, stock solutions of the drug are added to a solution containing microsomes to achieve a concentration of the drug that exceeds its aqueous solubility. This means that the drug is bound to microsomes and, therefore, is unavailable to interact with the enzyme. Theoretically, only the free concentration of the drug is available to interact with the enzyme. The impact of binding of drug to microsomes on the extrapolation of *in vitro* data to the clinical situation has been discussed by Obach [74–76]. Nonspecific binding of drugs to proteins and lipid membranes *in vitro* is analogous to the binding of drugs to plasma *in vivo*, so much so that the *in-vitro-to-in-vivo* predictions are better when the total (bound + free) drug concentrations *in vitro* and *in vivo* are used in the prediction of intrinsic clearances and drug interactions [74–76].

## 2. Organic Solvents

Several studies have demonstrated that organic solvents can potently and selectively inhibit P450 enzymes [50,83–86]. This is not surprising, because organic solvents tend to be substrates for P450 enzymes. Additionally, considering that a 1% (v/v) concentration of organic solvents in the final incubation mixture translates to a molar concentration of >100 mM, it is not surprising that the solvents have the potential to inhibit cytochrome P450. The most susceptible enzyme is CYP2E1, which is almost completely inhibited by organic solvents. Finally, some solvents are better than others in their ability to cause inhibition of P450 enzymes. For example, 0.1% DMSO causes almost complete inhibition of CYP2E1, and it markedly inhibits several enzymes, including CYP2C9, CYP2C19, and CYP3A4/5 (unpublished observations). In contrast, 1.0% methanol does not inhibit CYP2C19 and CYP3A4/5, but it does markedly inhibit CYP2E1 and to a lesser extent CYP2C9. (Acetonitrile has little or no inhibitory effect on CYP2C9 activity.) The take-home points are that no one organic solvent is optimal for all

P450 enzymes and that the final concentration of the organic solvent should be minimized as much as possible (<1.0% and preferably <0.1%).

There are two potential solutions to this dilemma. First, an attempt should be made to dissolve the drug in water or aqueous buffers (solubility permitting); often, it is possible to dissolve drugs in acidic buffers (pH 2.5–5.0), provided the buffering capacity of the incubation buffer (pH 7.4) is not overwhelmed by the acid. With a careful experimental design, it is actually possible to deliver the drug in a volume of the incubation medium that represents almost 80% of the final incubation volume. Subsequently, an attempt may be made to dissolve the drug in PEG400. In our hands, up to 0.5% (v/v) PEG400 (final concentration) had minimal effect on cytochrome P450 enzyme activities, including CYP2E1 (unpublished results).

In practice, most drugs are dissolved in organic solvents for drug inhibition studies. The concentration of organic solvent is kept as low as possible (0.1–1.0% depending on the organic solvent). In the case of CYP2E1, which is potently inhibited by most organic solvents, drugs are typically dissolved in methanol and then added to empty incubation tubes; the methanol is evaporated under a gentle stream of inert gas and the drug reconstituted with microsomal protein and incubation buffers. Regardless of the approach, each experiment should include a no-vehicle control (no-solvent control) and a vehicle (solvent) control to demonstrate the effect of the solvent under the conditions of a given experiment. The effect of the drug is compared against the vehicle (solvent) control.

### 3. Initial Rates

The P450 marker substrate reactions should be studied under conditions where formation of metabolite is directly proportional to incubation time and protein concentration and the percentage metabolism of the substrate does not exceed 20% (preferably 10%). In other words, reaction rates should be determined under initial-rate conditions. This concept can be easily forgotten or overlooked. For example, it is very easy to overmetabolize coumarin in human liver microsomes when studying coumarin 7-hydroxylation, a marker reaction for CYP2A6. Assuming that the incubation volume is 1.0 ml, protein concentration is 0.1 mg/ml, incubation time is 10 min, [coumarin] is 0.5  $\mu\text{M}$  ( $K_m$ ; 500 pmol/1-mL incubation), and the average initial rate of the coumarin 7-hydroxylation in a *random* pool of human liver microsomes at [coumarin] =  $K_m$  is  $\sim 1000$  pmol/min/mg protein. This means that under the experimental conditions described, 500 pmol of coumarin can be turned over twice if the reaction were operating at initial rates. If a given concentration of a drug inhibited coumarin 7-hydroxylase by 50% at  $K_m$ , the total product formed will be 500 pmol/incubation (which is the same as that formed in absence of the inhibitor). This would lead to an erroneous conclusion that the drug does not inhibit CYP2A6, when in fact it does. The



example provided is one extreme. In reality, the net effect of overmetabolizing the marker substrate is reflected in a decrease in overall inhibitory capacity of the drug and an increase in the  $K_i$  value.

#### 4. Choice of Marker Substrate

In the case of CYP3A4, the inhibitory potency of a drug has been shown to be dependent on the choice of marker substrate [87]. For example, the rank order of potency of inhibition of 18 flavonoids toward CYP3A4 activity was found to be different depending upon whether triazolam 1'-hydroxylation or testosterone 6 $\beta$ -hydroxylation was chosen as the marker substrate reaction [87]. Additionally, CYP3A4 is susceptible to activation or inhibition by substrate, which is demonstrated by an S-shaped or bell-shaped rate versus [substrate] curve [19]. It is believed that the active site of CYP3A4 is sufficiently large as to allow simultaneous binding of two molecules of either the substrate or one molecule each of the substrate and a modulator (activator or inhibitor). This has been proposed to be the mechanism for substrate-mediated activation of CYP3A4 and for the activation of CYP3A4 by flavonoids (e.g.,  $\alpha$ -naphthoflavone). This of course complicates the interpretation of data obtained with a single marker substrate. In order to get a good appreciation for the inhibitory effects of a drug on CYP3A4 and to extrapolate the *in vitro* findings to the clinical situation, the inhibition of CYP3A4 can be evaluated with several marker substrates.

#### 5. Interference by Drug

The drug being tested or a metabolite of the drug can interfere with the analytical measurement of the marker substrate reaction. Therefore, it is nearly impossible to evaluate the specificity of the analytical method. The use of marker substrates that permit analysis by HPLC with fluorimetric, diode-array, radiometric, or mass spectrometric detection minimizes (but does not exclude) the chances of interference. For each experiment, additional control incubations should be performed in which the drug is incubated with microsomal protein and NADPH in the *absence* of the marker substrate to ascertain whether the drug and its metabolites interfere with the analytical method.

#### 6. Time-Dependent Loss of Cytochrome P450 Enzymes in Incubations

Preincubation of human liver microsomes with NADPH in the absence of substrate results in a marked loss of P450 enzyme activity (see Figs. 8 and 9). This loss is attributed to inactivation of P450 enzymes either by activated oxygen or by microsomal heme oxygenase, both of which are NADPH dependent. Therefore, appropriate controls are required to compensate for this loss of activity to avoid

confusing the loss of activity with inhibition of activity. Conversely, incubating microsomes at 37°C without NADPH leads to inactivation of FMO.

## H. Statistical Methods

When inhibition of P450 enzymes is observed,  $K_i$  values are calculated via computer software (e.g., *GraFit*, Erithacus Software Limited, London, UK). The data is plotted on an Eadie–Hofstee plot (see Fig. 2) for a visual inspection of the type of inhibition. For determination of  $K_i$  values, the entire data set (i.e., rates at all concentrations of drug at all concentrations of substrate) is fitted to the Michaelis–Menten equations for competitive, noncompetitive, uncompetitive, and mixed (competitive–noncompetitive) inhibition (Table 2) by nonlinear regression analysis with simple weighting. The term *simple weighting* implies that the weighting applied for nonlinear regression is based on the assumption that the percentage error associated with each data point is the same. (Alternative weighting methods should be used if necessitated by the analytical measurement.) It should be noted that, at times, nonlinear regression lines will not correlate with the data points depicted on the Eadie–Hofstee plots. This is because the software (*GraFit*) attempts to fit all data to a single equation. The goodness of fit to each equation for competitive, noncompetitive, uncompetitive, and mixed inhibition is indicated by a lower reduced chi-square value, which provides the basis for selection of the type of inhibition. A relatively high standard error associated with  $K_i$  values suggests that the nonlinear regression does not fit the data very well, and a visual inspection of the Eadie–Hofstee plot may be necessary to confirm the nature of inhibition. This approach is reliable for calculating  $K_i$  values only when the  $K_i$  value lies with the concentration range of inhibitor studied. Therefore, when extrapolation or interpolation  $K_i$  values beyond the concentration range studied are required, these values should be treated as estimates only.

It is possible to determine if the nonlinear regression lines for two different types of inhibition (e.g., competitive versus noncompetitive) are statistically significantly different from each other. However, if such robust determination of the type of inhibition is required, then additional concentrations of drug *and* the marker substrate should be studied. This is typically not necessary or required, because, as discussed later, the methods used for extrapolation of the in vitro  $K_i$  value to the clinical potential for inhibition have been simplified such that they are independent of the nature of the inhibition. A circular argument can be made that since the  $K_i$  value is dependent on the type of inhibition, it is important to ascertain unequivocally the mechanism of inhibition. The largest difference in  $K_i$  value is obtained between competitive and noncompetitive inhibitors. For example, if 10  $\mu\text{M}$  drug causes 50% inhibition at a substrate concentration equal to  $K_m$ , the  $K_i$  value for competitive inhibition will be 5  $\mu\text{M}$  and that for noncom-

petitive inhibition will be 10  $\mu\text{M}$ . Depending on the application of the data, it may or may not be important to determine the  $K_i$  value with a high degree of accuracy. Of course, the discussion of an “accurate” determination of the  $K_i$  value must involve percent binding of the drug to microsomal protein, and therefore the determination should be based on the free concentration of the drug. Other factors, such as metabolic stability of the drug and the marker substrate, should be considered as well. For applications where the  $K_i$  value is more than 10 times the “free” plasma concentration of the drug, the nuances related to accuracy of the  $K_i$  determination are probably not relevant.

### 1. Estimation of the Minimum $K_i$ Value When No Inhibition is Observed

When little or no concentration-dependent inhibition is observed, a minimum  $K_i$  value can be assigned to the drug as follows. Assuming that the inhibition is competitive and that there is up to 10% experimental error in determination of initial enzymatic rates ( $v$ ) at the highest inhibitor concentration, then:

$$v = v \pm 0.1v$$

In other words, the rate,  $v$ , can range from  $0.9v$  to  $1.1v$  ( $\pm 10\%$  variation). Based on the conservative assumption that the observation of  $0.9v$  (10% inhibition) at the highest concentration of drug (e.g., 100  $\mu\text{M}$ ) and the lowest concentration of substrate, (e.g.,  $K_m/2$ ; note that at  $K_m/2$ ,  $v = V_{\max}/3$ ) is masked by experimental error, the estimated minimum  $K_i$  value can be calculated from equations shown in Table 2 as follows:

$$\begin{aligned} \text{Estimated minimum } K_i &= \frac{0.9v[100]K_m}{3v[0.5K_m] - 0.9v(K_m + 0.5K_m)} \\ &= 600 \mu\text{M} \end{aligned} \quad (1)$$

Therefore, based on the conservative assumption that 10% inhibition of P450 activity by 100  $\mu\text{M}$  drug at a substrate concentration equal to  $K_m/2$  could have been masked by experimental error, the  $K_i$  value for drug as an inhibitor of that P450 enzyme could be as low as 600  $\mu\text{M}$  (six times the highest concentration studied).

## I. In Vitro to In Vivo Extrapolations

### 1. Calculation of Fractional Inhibition by “Reversible” or Direct Inhibitors

The predicted fractional inhibition,  $i$ , of the metabolism of a drug by a P450 inhibitor may be calculated from the following equations [4,88]:

For noncompetitive inhibition:

$$i = \frac{[I]}{[I] + K_i} \quad (2)$$

For competitive inhibition:

$$i = \frac{[I]}{[I] + K_i(1 + [S]/K_m)} \quad (3)$$

For uncompetitive inhibition:

$$i = \frac{[I]}{[I] + K_i(1 + K_m/[S])} \quad (4)$$

In these equations,  $[I]$  is the “free” plasma concentration of the inhibitor in humans,  $K_i$  is the inhibition constant of the inhibitor for the human P450 enzyme in question,  $K_m$  is the Michaelis constant for the metabolism of the drug by the P450 enzyme in question, and  $[S]$  is the plasma or “free” hepatic concentration of the drug. When the concentration of substrate is substantially less than  $K_m$ , the  $[S]/K_m$  term tends to zero and, conversely,  $K_m/[S]$  tends to infinity ( $\infty$ ). Under this condition, Eq. (3) simplifies to Eq. (2), and Eq. (4) tends to zero. Therefore, taking a conservative approach, the fractional inhibition ( $i$ ) of metabolism of drugs by a P450 inhibitor can be calculated from Eq. (2) for competitive and noncompetitive inhibition. For this same reason, the fractional inhibition by mixed (competitive and noncompetitive) inhibitors can be determined from Eq. (2). However, for uncompetitive inhibitors (where the inhibition increases as the substrate concentration increases),  $K_m/[S]$  tends to infinity and  $i$  tends to zero. In other words, uncompetitive inhibitors are clinically relevant only when the plasma concentration of the drug in question approaches (or exceeds)  $K_m$  for a given reaction *and* the plasma concentration of the inhibitor approaches (or exceeds) its  $K_i$  value for a given P450 enzyme. (There are no known clinically relevant drug interactions that have been attributed to uncompetitive inhibition of P450 enzymes.)

## 2. Predicted Inhibition by Metabolism-Dependent “Irreversible” Inhibitors

The potential for metabolism-dependent inhibitors to cause clinically significant drug interactions is dependent on the amount of cytochrome P450 inactivated, which is a function of the amount of drug consumed, the amount of drug converted to the inhibitory metabolite, and the amount of new cytochrome P450 synthesized between drug treatments. Erythromycin and ethinylestradiol are both metabolism-dependent inhibitors of CYP3A4, which is the most abundant P450 enzyme in human liver microsomes [89–92]. However, these two drugs differ

**Table 5** Prediction of Clinical Significance of Metabolism-Dependent ‘‘Irreversible’’ or ‘‘Quasi-Irreversible’’ Inhibition of CYP3A4/5 by Erythromycin and Gestodene Using In Vitro Data Enzymes

Parameter	Erythromycin	Gestodene
Dose	2,700 $\mu\text{mol/day}$	0.25 $\mu\text{mol/day}$
Average total hepatic CYP3A4 <sup>a</sup>	1,000 nmol <sup>a</sup>	1,000 nmol <sup>a</sup>
Partition ratio <sup>b</sup>	0.01 (assumption)	0.12
% metabolized by CYP3A4 <sup>c</sup>	100% (assumption)	100% (assumption)
Amount of CYP3A4 inactivated/day	27 $\mu\text{mol/day}$	0.019 $\mu\text{mol/day}$
% CYP3A4 inactivated/day <sup>d</sup>	2700%	3%
Turnover half-life of P450 <sup>e</sup>	24 hr	24 hr

<sup>a</sup> Average total CYP3A4 in human liver estimated to be 1000 nmol [89,93].

<sup>b</sup> Partition ratio is the number of molecules of P450 inactivated/number of molecules of inhibitor metabolized by the pathway that leads to inactivation. For erythromycin the partition ratio was deduced (with some assumptions) [48,141], whereas for gestodene the partition ratio has been experimentally determined [93].

<sup>c</sup> Amount of CYP3A4 inactivated/day = partition ratio  $\times$  dose.

<sup>d</sup> % CYP3A4 inactivated/day = (Amount of CYP3A4 inactivated/day)  $\times$  100/(Average total hepatic CYP3A4 content).

<sup>e</sup> Turnover half-life of P450 enzyme is estimated to be approximately 24 hr based on work done in rats [142,143].

markedly in their potential to inactivate CYP3A4 under clinically relevant conditions because of marked differences in dosage regimen. The recommended dose of erythromycin is 2 g/day (2,700  $\mu\text{mol/day}$ ), compared with 75  $\mu\text{g/day}$  for gestodene (0.25  $\mu\text{mol/day}$ ). Although the two drugs may differ in the degree to which they are converted to inhibitory metabolites (i.e., although they may have different partition ratios), it is clear that the  $\sim$ 1,000-fold difference in dose likely explains why recommended daily doses of erythromycin causes clinically significant inhibition of CYP3A4, whereas gestodene and related contraceptive steroids do not [93,94]. This extrapolation is summarized in Table 5 and discussed in detail elsewhere in this book (see Chap. 10).

### III. IDENTIFICATION OF P450 ENZYMES INVOLVED IN A GIVEN REACTION: REACTION PHENOTYPING

*Reaction phenotyping* (also known as *enzyme mapping*) is the process of identifying the P450 enzyme(s) responsible for a given reaction. Although the experimental approaches described here are specifically for P450 enzymes, similar approaches can be used for other enzyme systems. Important distinctions must be

made between identifying the P450 enzyme involved in a given reaction and evaluating a drug for its ability to inhibit P450 enzymes. As stated in the previous section, if a drug is metabolized by a P450 enzyme, it will inhibit that P450 enzyme, depending on the affinity of the drug for the enzyme. However, the converse is not true. In other words, a drug is *not* necessarily metabolized by a given P450 enzyme just because it inhibits that P450 enzyme. For example, although quinidine, terbinafine, and celecoxib are potent inhibitors of CYP2D6, they are metabolized by other P450 enzymes [30,31,36,37]. Additionally, reaction phenotyping serves to predict the effect of polymorphisms, environmental factors, and other drugs on the overall metabolism and elimination of the drug of interest. (P450 inhibition studies predict the effect of the drug of interest on the overall metabolism and elimination of other drugs.) This is the reason why both types of studies must be performed independently in order to predict the potential for drug–drug interactions.

If a drug is metabolized by a polymorphic P450 enzyme (such as CYP2D6), the pharmacokinetics of the drug will be determined by the expression of that enzyme. In some instances, reaction phenotyping serves to predict (or explain) the failure of drug therapy in a certain population. For example, codeine must be metabolized by CYP2D6 to morphine, the active metabolite, before an analgesic effect is observed. This means that CYP2D6 poor metabolizers fail to convert sufficient codeine to morphine to observe the desired therapeutic effect. Similarly, it was speculated that proguanil, an antimalarial prodrug, which is metabolized by CYP2C19 to its active metabolite, cycloguanil, would be ineffective in CYP2C19 poor metabolizers [95]. This is especially notable because CYP2C19 is not expressed in up to 71% of certain populations, such as, the Vanuatu islands in Melanesia, a region where malaria is quite prevalent [95]. However, recent work performed by Kaneko et al. [96,97] suggest that, although Vanuatu CYP2C19 poor metabolizers exhibit reduced conversion of proguanil to cycloguanil, the therapeutic efficacy of proguanil for malaria is not compromised compared with their CYP2C19 extensive metabolizer counterparts. This is presumably due to the higher resistance of Vanuatu to malaria and/or the formation of other metabolites of proguanil that may be pharmacologically active. Nevertheless, the potential clearly exists for poor metabolizers to fail to convert prodrugs to their pharmacologically active metabolites.

### A. Multiple Approaches for Reaction Phenotyping

Several approaches are available for reaction phenotyping [1,2], and these include the following:

1. Correlation analysis of the metabolism of the drug with the sample-to-sample variation in P450 enzyme activity

2. Chemical and antibody inhibition of the metabolism of the drug
3. Metabolism of the drug by recombinant P450 enzymes

Each approach has advantages and disadvantages, and a combination of approaches is usually required to identify which human P450 enzyme is responsible for metabolizing a xenobiotic. It should be emphasized that reaction phenotyping *in vitro* is not always carried out with pharmacologically or toxicologically relevant substrate concentrations; hence, the P450 enzyme that appears responsible for biotransforming the drug *in vitro* may not be the P450 enzyme responsible for biotransforming the drug *in vivo*. Furthermore, the identification of P450 enzymes involved in a given reaction may have little or no clinical significance if that reaction is not the rate-limiting step in the overall clearance of that drug [26,76,98–106]. Each approach is briefly described next; the details of the experimental design are provided in the succeeding sections.

*Correlation analysis* involves measuring the rate of xenobiotic metabolism by several samples of human liver microsomes and correlating reaction rates with the variation in the level or activity of the individual P450 enzymes in the same microsomal samples.

*Chemical and antibody inhibition* involves an evaluation of the effects of known P450 enzyme inhibitors or inhibitory antibodies on the metabolism of a xenobiotic by human liver microsomes. This approach to reaction phenotyping can be accomplished with a single sample of human liver microsomes and is usually carried out with a pooled sample.

*Biotransformation by cDNA-expressed human P450 enzymes* can establish whether a particular P450 enzyme can or cannot biotransform a xenobiotic, but it does not readily address whether that P450 enzyme contributes substantially to reactions catalyzed by human liver microsomes. However, the utility of cDNA-expressed human P450 enzymes in the reaction phenotyping can be significantly increased by determining the intrinsic clearance ( $V_{\max}/K_m$ ) of a drug by each enzyme and predicting the role these enzymes may play in human liver microsomes.

## B. Stepwise Method for Reaction Phenotyping

To identify which P450 enzyme or enzymes are primarily responsible for metabolizing a particular xenobiotic, the xenobiotic (hereafter called Drug X) is incubated with each of the individual or pooled human liver microsomal samples or with recombinant P450 enzymes (preferably at a pharmacologically relevant drug concentration and under initial-rate conditions [i.e., under conditions where metabolite formation or substrate disappearance is directly proportional to incubation time and microsomal protein concentration *and* the percentage metabolism of the substrate does not exceed 20%]). These experiments are preceded by a

series of experiments to establish incubation conditions and analytical methods suitable for reaction phenotyping.

### Step 1. Development of the Analytical Procedure and Evaluation of Its Suitability

A procedure must be developed to measure the rate of formation of metabolites of the drug. This invariably involves chromatographic separation of the analytes by HPLC followed by a variety of detection techniques, such as UV-VIS, radiometric, fluorimetric, or MS/MS. Methods that have been developed for the analysis of the parent drug in formulations and in stability testing are often unsuitable, because they are not designed to separate the parent drug from the metabolites, although they do provide a good starting point. The metabolites can be generated by incubating the parent drug with a pool of human liver microsomes in the presence of NADPH or an NADPH-generating system. A rather high concentration of microsomal protein (1–2 mg/mL) and drug (1–100  $\mu$ M) and long incubation times (30–120 min) are initially employed for this preliminary experiment to maximize the detection of all possible metabolites.

Briefly, liver microsomes (e.g., 1 mg/mL) are incubated at  $37 \pm 1^\circ\text{C}$  in 0.5-ml incubation mixtures (final volume) containing potassium phosphate buffer (50 mM, pH 7.4),  $\text{MgCl}_2$  (5 mM), EDTA (1 mM), and the drug (e.g., 1, 10, 100  $\mu$ M) with and without an NADPH-generating system, at the final concentrations indicated. The NADPH-generating system consists of NADP (1 mM), glucose-6-phosphate (5 mM), and glucose-6-phosphate dehydrogenase (1 unit/mL). If it is sufficiently water soluble, the drug is added to the incubation mixtures in water. Otherwise, the drug is added to each incubation in PEG400, methanol, DMSO, or another suitable organic solvent (such that the concentration of the vehicle does not exceed 1%; 0.2% in the case of DMSO). Reactions are started by the addition of the NADPH-generating system or by the addition of the drug, and stopped after 30 min by the addition of a stop reagent (e.g., organic solvent, acid, or base). Zero-time, zero-protein, and zero-substrate incubations serve as blanks. Precipitated protein is removed by centrifugation (400–2,500 g for 5–15 min at  $5\text{--}15^\circ\text{C}$ ), and an aliquot (up to 200  $\mu$ L) of the supernatant fraction is analyzed by HPLC.

The profile of the metabolites in the HPLC chromatogram of an incubated sample is compared with blanks or zero-time incubations. These incubation mixtures are used for developing the appropriate HPLC separation and detection techniques.

At this point, it is highly desirable (although not absolutely necessary) to establish the identity of the metabolites by traditional spectrometric techniques. The metabolite identification is important to predict the enzyme system involved in a given reaction. For example, if a metabolite is formed by *N*-oxidation or *S*-



oxygenation, both FMO and P450 would need to be considered potential contributors to this reaction. Alternatively, if a metabolite is a hydrolysis product of the parent drug, it points to involvement of carboxylesterases, especially if the reaction does not require NADPH. More importantly, the identity of the metabolite can establish whether it is a primary or secondary metabolite. The methodology for reaction phenotyping described here is not suitable for studying the pathways involved in the formation of secondary metabolites. In most cases, it is only necessary to focus on the *major* and *primary* metabolites of the parent drug, for which it may be necessary to fine-tune the HPLC method.

Once an analytical HPLC method is established, it is then necessary to evaluate its suitability using traditional procedures, which are beyond the scope of this chapter. The desired criteria for evaluating method suitability include determination of limits (lower and upper) of quantification, inter- and intraday precision, specificity of the method, and linearity of the calibration curves [107]. The evaluation of method suitability must be performed in the presence of the representative biological matrix that will be used in reaction phenotyping. The matrix of choice is a pool of human liver microsomes. It is not feasible to repeat the suitability evaluation when the biological matrix changes slightly. For example, a switch from the pool of human liver microsomes to individual human liver microsomal samples, dog liver microsomal samples, or recombinant P450 enzymes does not necessitate that the suitability of the method be reevaluated. Appropriate controls can be included with individual experiments to establish that the method is suitable for the slightly different biological matrix.

## Step 2. Effect of Time and Protein

Step 2 establishes if the metabolite formation is proportional to incubation time and protein concentration, which in turn will help determine whether the metabolites of the drug are primary metabolites (no lag in formation) or secondary metabolites (lag in formation). For example, dextromethorphan is *O*-demethylated to dextrorphan by CYP2D6 and *N*-demethylated to 3-methoxymorphinan by CYP2B6 and CYP3A4 [108–110]. Both dextrorphan and 3-methoxymorphinan are *N*-demethylated and *O*-demethylated, respectively, resulting in the formation of 3-hydroxymorphinan. In vitro formation of 3-hydroxymorphinan is always preceded by formation of dextrorphan or 3-methoxymorphinan and exhibits a time lag in its formation (unpublished results).

The experimental design for evaluating the effect of incubation time and protein concentration on metabolite formation is often influenced by the results of the experiments described previously, but the overall design will remain essentially the same. The drug (e.g., 1, 10, and 100  $\mu\text{M}$ ) is incubated with three concentrations of human liver microsomes (e.g., 0.125, 0.5, and 2.0 mg protein/mL) for a fixed time period (e.g., 0, 15 min). Additionally, the drug (e.g., 1, 10, and

100  $\mu\text{M}$ ) is incubated with a single concentrations of human liver microsomes (e.g., 0.5 mg protein/mL) for multiple time periods (e.g., 0, 5, 10, 15, 20, 30, 45, 60 min). In addition to human liver microsomes and the drug, the incubation mixtures contain 50 mM potassium phosphate (50 mM, pH 7.4),  $\text{MgCl}_2$  (3 mM), EDTA (1 mM), and an NADPH-generating system (1 mM NADP, 5 mM glucose-6-phosphate, and 1 unit/mL glucose-6-phosphate dehydrogenase). The remaining procedure is identical to that described previously.

If incubating as much as 100  $\mu\text{M}$  drug with liver microsomal protein for 120 min in the presence of NADPH results in no detectable formation of metabolites, and if incubating as little as 1  $\mu\text{M}$  drug with liver microsomal protein for 120 min in the presence of NADPH results in no detectable loss of parent compound, it is usually safe to assume that the drug is minimally metabolized by cytochrome P450 and/or FMO, unless other compelling data (such as in vivo pharmacokinetic data) is available that strongly suggests involvement of these enzymes.

It is unlikely that the formation of a metabolite would be proportional to protein concentration and incubation time at all three concentrations of substrate examined; however, appropriate ranges of protein concentration and incubation time become evident. If the percentage metabolism of substrate does not exceed 20%, it is pragmatic to expect a doubling of metabolite formation when the incubation time is doubled, but this doubling is not always observed when the protein concentration is doubled. This is because, as the microsomal protein concentration increases, the bound fraction of the substrate increases, which results in a lowering of the free concentration of the substrate and a lowering of the initial rate of reaction [56].

### Step 3. Determination of Kinetic Constants ( $K_m$ and $V_{\max}$ )

If the ultimate goal is to use in vitro intrinsic clearance data ( $V_{\max}/K_m$ ) to predict in vivo clearances via a given enzymatic pathway, it is important to design this experiment very carefully. If kinetic parameters are determined with the individual samples of human liver microsomes, it will generally be found that  $V_{\max}$  values vary enormously from one sample to the next, whereas  $K_m$  values remain relatively constant. The sample-to-sample variability in the  $V_{\max}$  values in a bank of human liver microsomes is related directly to the specific content of the given enzyme in the microsomal sample. However, the  $K_m$  value (the concentration of the substrate at which the reaction proceeds at one-half the maximum velocity) should not be influenced by the specific content (although it may be if those samples with high  $V_{\max}$  value result in overmetabolism of the substrate such that initial-rate conditions are not observed). For example, if the levels of a particular P450 enzyme vary 20-fold in a bank of human liver microsomes, then  $V_{\max}$  values for a reaction catalyzed by that particular P450 enzyme would also be expected

to vary 20-fold. However,  $K_m$  values would be expected to remain constant from one sample to the next because  $K_m$  is an intrinsic property of an enzyme and, as such, is not dependent on the amount of enzyme present. (A simple analogy will serve to underscore this point. Freezing point is an intrinsic property of liquids. Water, for example, freezes at 0°C, and it does so regardless of the amount of water being frozen, for which reason ice cubes and icebergs freeze at the same temperature.)

Although  $K_m$  values would be expected to be constant, there are reports of  $K_m$  varying from one sample to the next. When  $K_m$  is found to increase with  $V_{\max}$ , it is more than likely that the metabolism of the substrate was not determined under initial-rate conditions. Therefore, sample-to-sample variation in  $K_m$  values, particularly when such variation coincides with the variation in  $V_{\max}$  values, is usually an experimental artifact. For example, coumarin 7-hydroxylation is catalyzed by CYP2A6 in human liver microsomes; we observed little sample-to-sample variability in the  $K_m$  for coumarin 7-hydroxylation, which was approximately 0.5  $\mu\text{M}$  regardless of whether the microsomal samples had high or low levels of CYP2A6 [50,111]. However, it should be noted that great care was taken to measure initial rates of coumarin 7-hydroxylation. The percentage of substrate converted to 7-hydroxycoumarin in our studies ranged from less than 1% to about 15%. We suspect that reports of higher  $K_m$  values for the 7-hydroxylation of coumarin by human liver microsomes, such as a  $K_m$  of 10  $\mu\text{M}$  reported by Yamazaki et al. [112], stem from excessive metabolism of the substrate such that reaction rates did not reflect initial velocities.

The experiment designed to evaluate the effect of incubation time and protein concentration on the formation of metabolites (Step 2) provides the preliminary data necessary to select a range of substrate concentrations and experimental conditions to determine  $K_m$  and  $V_{\max}$  for the metabolism of the drug by human liver microsomes. A crude estimation of the  $K_m$  can be obtained from the three concentration points used in Step 2, provided the rate data represents initial reaction velocities. A range of substrate concentrations (0.1–10 $K_m$ ) is usually sufficient; however, this may have to be expanded if the kinetic constants for formation of more than one metabolite are to be determined or if two kinetically distinct enzymes are involved in metabolite formation. The kinetic constants ( $K_m$  and  $V_{\max}$ ) for a given reaction are determined with a pool of human liver microsomes from several individuals.

Typically, the pool of human liver microsomes (e.g., 10–100  $\mu\text{g}$ ) are incubated in duplicate for a specified time period (e.g., 5–30 min) at  $37 \pm 1^\circ\text{C}$  in 1-ml (final volume) incubation mixtures containing potassium phosphate buffer (50 mM, pH 7.4),  $\text{MgCl}_2$  (3 mM), EDTA (1 mM), NADP (1 mM), glucose-6-phosphate (5 mM), glucose-6-phosphate dehydrogenase (1 unit/ml), drug (0.1 $K_m$ , 0.2 $K_m$ , 0.3 $K_m$ , 0.4 $K_m$ , 0.5 $K_m$ , 0.6 $K_m$ , 0.7 $K_m$ , 0.8 $K_m$ , 0.9 $K_m$ ,  $K_m$ , 1.25 $K_m$ , 1.6 $K_m$ , 2 $K_m$ , 4 $K_m$ , 7 $K_m$ , and 10 $K_m$ , where  $K_m$  is the crude estimate

obtained from data generated in Step 2) at the final concentrations indicated. For all substrate concentrations, the rate of reaction is measured under initial-rate conditions; that is, the product formation is directly proportional to protein concentration and incubation time and the percentage metabolism of the substrate does not exceed 20%. Initial-rate conditions are achieved by varying the incubation time or the protein concentration.

Note that, in some cases where the solubility of the drug is limiting, it may be difficult to achieve concentrations equal to multiples of  $K_m$ . Alternatively, it may be impractical to study concentrations equal to fractions of  $K_m$  because of the low sensitivity limits of detecting metabolites.

Data was plotted on an Eadie–Hofstee plot, and the kinetic constants were calculated with computer software, such as *GraFit* (Version 4.0, Erithacus Software Limited, London, UK), using nonlinear regression analysis with simple weighting, unless otherwise indicated (see Fig. 12). The term *simple weighting* implies that the weighting applied for nonlinear regression is based on the assumption that the percent error associated with each data point is the same. It should be noted that, at times, nonlinear regression lines do not appear to correlate with the data points depicted on the Eadie–Hofstee plots. This is because the computer software attempts to fit all data to a single equation. A relatively high standard error associated with  $K_m$  values suggests that the nonlinear regression did not fit the data very well. When extrapolation or interpolation  $K_m$  values beyond the concentration range studied are required, the  $K_m$  values should be treated as estimates only. If the standard error associated with the  $K_m$  value is large (>25%) and/or if the  $K_m$  value falls outside the range of substrate concentrations studied, it is prudent to repeat this experiment using the most recently determined  $K_m$  as an initial estimate.

Alternatively, the Eadie–Hofstee plot may suggest involvement of two or more kinetically distinct enzymes, in which case the data should be fit into a dual-enzyme model given by the following equation:

$$v_{\text{total}} = v_1 + v_2 = \frac{V_{\text{max}_1} \cdot [S]}{K_{m_1} + [S]} + \frac{V_{\text{max}_2} \cdot [S]}{K_{m_2} + [S]} \quad (5)$$

where  $v_{\text{total}}$  is the overall rate of metabolite formation at substrate  $[S]$ ,  $V_{\text{max}_1}$  and  $V_{\text{max}_2}$  are the maximal velocities of the reaction and  $K_{m_1}$  and  $K_{m_2}$  are the Michaelis constants for enzyme 1 and enzyme 2, respectively. Since the high- $K_m$  enzyme (i.e.,  $K_{m_2}$ ) most likely has a negligible contribution toward  $V_{\text{total}}$  at low substrate concentrations (this range of  $[S]$  can be selected by a visual inspection of the Eadie–Hofstee plot; Fig. 13), it can be assumed that  $v_{\text{total}} = v_1$ ; the data is plotted on an Eadie–Hofstee plot to obtain  $K_{m_1}$  and  $V_{\text{max}_1}$ . Subsequently,  $v_2$  (which equals  $v_{\text{total}} - v_1$ ) is calculated, and the data is plotted on an Eadie–Hofstee plot to obtain  $K_{m_2}$  and  $V_{\text{max}_2}$ . As a rule of thumb, only data points for which  $v_2 > 0.2v_{\text{total}}$  should

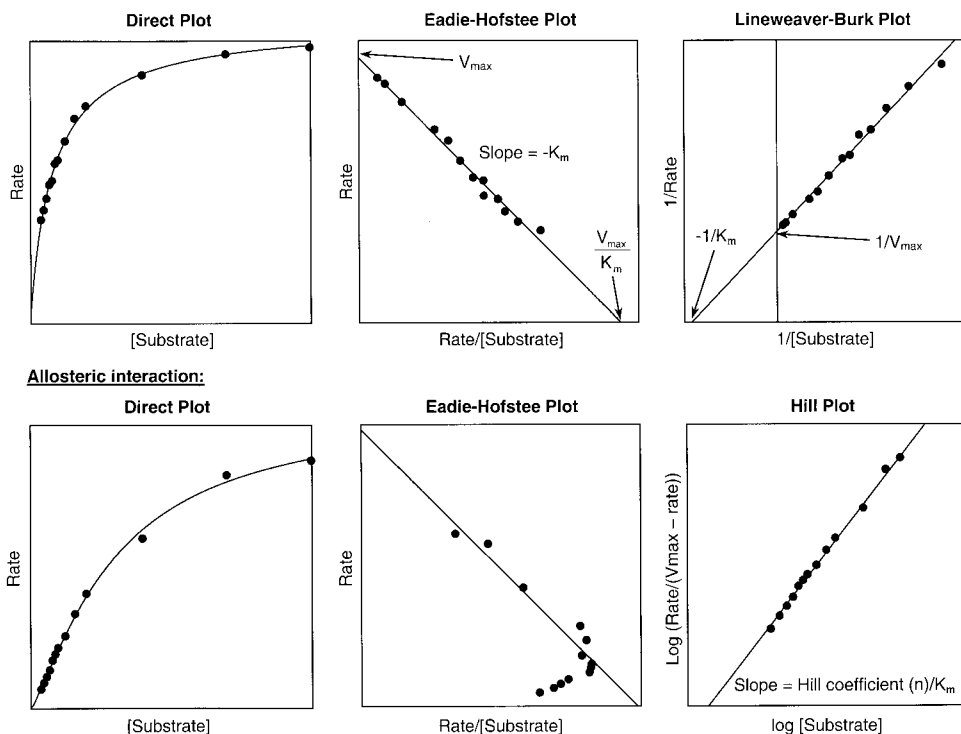


**Figure 12** Examples of enzyme kinetic plots used for determination of  $K_m$  and  $V_{max}$  for a normal and an allosteric enzyme: Direct plot ([Substrate] versus initial rate of product formation) and various transformations of the direct plot (i.e., Eadie–Hofstee, Lineweaver–Burk, and/or Hill plots) are depicted for an enzyme exhibiting traditional Michaelis–Menten kinetics (coumarin 7-hydroxylation by CYP2A6) and one exhibiting allosteric substrate activation (testosterone 6 $\beta$ -hydroxylation by CYP3A4/5). The latter exhibits an S-shaped direct plot and a ‘hook’-shaped Eadie–Hofstee plot; such plots are frequently observed with CYP3A4 substrates.  $K_m$  and  $V_{max}$  are Michaelis–Menten kinetic constants for enzymes.  $K'$  is a constant that incorporates the interaction with the two (or more) binding sites but that is not equal to the substrate concentration that results in half-maximal velocity, and the symbol ‘ $n$ ’ (the Hill coefficient) theoretically refers to the number of binding sites. See Sec. III.B.3 for additional details.

be included in the latter determinations, because the experimental error associated with determination of  $v_{total}$  can give highly erroneous values for  $v_2$ .

Simply because a reaction fits the single-enzyme model well and gives a straight line on an Eadie–Hofstee plot, it cannot be concluded that only a single enzyme participates in the reaction, although this is one possibility. Two enzymes

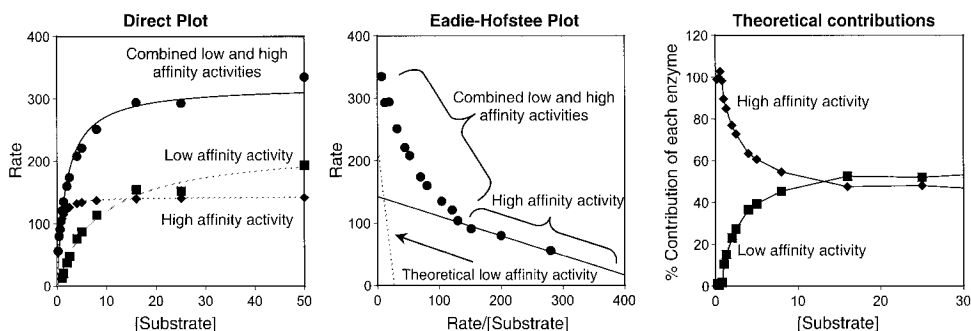


**Figure 13** Depictions of a reaction catalyzed by two kinetically distinct enzymes: The effect of substrate concentration on the *O*-deethylation of 7-ethoxy-4-trifluoromethylcoumarin (7-EFC) in a pool of human liver microsomes is depicted to illustrate the method used to determine the kinetic constants when two enzymes are involved in the same reaction (unpublished results). The 7-EFC *O*-dealkylation is catalyzed by CYP2B6 (high  $K_m$ ) and CYP1A2 (low  $K_m$ ). Note that the direct plot (left) does not effectively indicate that two enzymes might be involved in a given reaction. However, this is readily achieved by a concave-appearing Eadie–Hofstee plot (middle graph). The kinetic constants ( $K_m$  and  $V_{max}$ ) of the high-affinity (low- $K_m$ ) enzyme, CYP1A2, are determined using the initial rates observed at low substrate concentrations (solid line in the middle graph). Then the contribution of the low- $K_m$  enzyme, CYP1A2, is subtracted using Eq. (5) and the kinetic constants for the high- $K_m$  enzyme, CYP2B6, determined (dotted line in the middle graph). The theoretical contributions of the individual enzymes, CYP1A2 and CYP2B6, in 7-EFC *O*-dealkylation at various concentrations of 7-EFC are shown (right). It is evident that the relative contribution of the high- $K_m$  enzyme increases (and that of the low- $K_m$  enzyme decreases) as the substrate concentration is increased.

with similar  $K_m$  values toward the same substrate have frequently been observed, and these will result in an Eadie–Hofstee plot consistent with single-enzyme kinetics. Applying the dual-enzyme model for such situations will not help; instead, reaction-phenotyping data must be used to tease out the role of the two enzymes. Some cytochrome P450 enzymes (CYP2B6 and CYP3A4) have been shown to exhibit kinetics consistent with allosteric interaction of the substrate with the enzyme, which is also known as *substrate activation* [17,19,113,114]. These result in an S-shaped [Substrate] versus rate curve and a “hook”-shaped Eadie–Hofstee plot. When allosteric interactions are observed, the Hill equation and a Hill plot can be used to calculate kinetic constants [19,22,23] (Fig. 12). The Hill equation is [19]:

$$v = \frac{V_{max} \cdot [S]^n}{K' + [S]^n} \quad (6)$$

where  $K'$  is a constant that incorporates the interaction with the two (or more) binding sites but that is not equal to the substrate concentration that results in half-maximal velocity, and the symbol " $n$ " (the Hill coefficient) theoretically refers to the number of binding sites. When " $n$ " is greater than 1, it indicates positive cooperativity; when " $n$ " is less than 1, it indicates negative cooperativity [19]. It should be noted that " $n$ " need not be an integer. For instance, if a Hill coefficient of 2 were observed, it would indicate that there are two catalytically active binding sites, whereas a Hill coefficient of 1.3 would indicate that there are two binding sites and that only one is catalytically active while the other activates the reaction by the catalytically active site.

#### Step 4. Role of FMO and Cytochrome P450 in the Metabolism of the Drug

The knowledge of the structural features of the parent compound and the metabolite are useful in predicting whether or not a given reaction can be catalyzed by FMO. Flavin-containing monooxygenases tend to catalyze *N*-oxidation and *S*-oxidation reactions but never *C*-oxidation reactions. On the other hand, P450s tend to catalyze *C*-oxidation and *S*-oxidation reactions and only some *N*-oxidation reactions. Therefore, if the reaction in question is an *S*-oxidation or *N*-oxidation, it is advisable to determine the relative contribution of FMO and P450. Cytochrome P450 enzymes can be inhibited by the detergent Emulgen 911 and by a nonselective P450 enzyme inhibitor, 1-benzylimidazole. Although there are no selective inhibitors of FMO, this enzyme can be inactivated by heating microsomes in the absence of NADPH to 50°C for 1 min. Under these conditions, the loss of cytochrome P450 is minimal compared with that of FMO activity. Finally, FMO-3, the predominant form of human FMO [82], is now commercially available as a recombinant enzyme. This enzyme preparation may be used to ascertain whether FMO-3 is capable of catalyzing a given reaction.

Briefly, human liver microsomes are incubated at  $37 \pm 1^\circ\text{C}$  in 1-ml incubation mixtures (final volume) containing potassium phosphate buffer (50 mM, pH 7.4),  $\text{MgCl}_2$  (3 mM), EDTA (1 mM), the drug, and an NADPH-generating system in the presence or absence of 1-benzylimidazole (100–1000  $\mu\text{M}$ ) or Emulgen 911 (final concentration 1% v/v). The concentration of microsomal protein and the drug and the incubation time are based on the results of experiments outlined previously. Reactions are started by the addition of the NADPH-generating system, which consists of NADP (1 mM), glucose-6-phosphate (5 mM), and glucose-6-phosphate dehydrogenase (1 unit/mL), at the final concentrations indicated. Metabolite formation is determined by HPLC, as outlined previously.

Heat inactivation of microsomal FMO may be carried out by the method of Poulsen et al. [115]. A concentrated suspension of microsomes (10 mg/mL) in 100 mM potassium phosphate buffer (pH 7.4) containing 200

$\mu\text{M}$  butylated hydroxytoluene is rapidly heated to  $50^\circ\text{C}$  and maintained at  $50^\circ\text{C}$  for 1 min, immediately after which the tubes are chilled in ice. This procedure results in 20–30% loss of cytochrome P450 and complete inactivation of FMO [116]. These microsomes are used for studying the metabolism of the drug, as described earlier.

Some procedures for preparing human liver microsomes result in considerable loss of FMO activity [117]. In addition, FMO activity can be lost when liver microsomes are incubated at  $37^\circ\text{C}$  in the absence of NADPH [118]. This is because FMO is extremely susceptible to heat degradation, especially in the absence of NADPH. It is for this reason that we advise against preincubating reaction mixtures to  $37^\circ\text{C}$  in the absence of NADPH before initiating a reaction. Another important experimental consideration regarding FMO enzymes is that they cannot be inhibited by polyclonal antibodies, even though these antibodies recognize FMO on a Western immunoblot.

#### Step 5. Correlation Analysis: Sample-to-Sample Variation in the Metabolism of the Drug

For this step, the drug is incubated with a bank of human liver microsomes to determine interindividual differences in metabolite formation. The experimental conditions for examining the in vitro metabolism of the drug by this bank of human liver microsomes are based on the results from experiments described in Step 3 (i.e., experiments designed to establish the  $K_m$  and  $V_{\max}$ ). The metabolism of the drug by human liver microsomes is examined with a low, pharmacologically relevant concentration of the drug. This is at times not possible when the plasma concentration of the drug is submicromolar, because the formation of metabolite at low substrate concentrations is very difficult. It may also be necessary to study the sample-to-sample variation under several substrate concentrations.

This experiment is carried out with a bank of human liver microsomes (e.g.,  $n = 16$ ) that has been analyzed to determine the sample-to-sample variation in the activity of several P450 enzymes (namely, CYP1A2, CYP2A6, CYP2B6, CYP2C8, CYP2C9, CYP2C19, CYP2D6, CYP2E1, CYP3A4/5, and CYP4A9/11) [119]. Such banks of human liver microsomes are commercially available as kits (e.g., reaction phenotyping kit), and the manufacturers provide data on individual P450 enzyme activity in each sample. *Caution:* it is important to select a bank of human liver microsomes (kit) in which the P450 enzyme activities do not correlate with each other. In other words, the independent variables (marker P450 enzyme activities supplied with the kits) must exhibit independent correlations. Differences in the rates of formation of the drug metabolites are compared with the sample-to-sample variation in the activities of P450 enzymes shown in Table 3 and Figure 14. This is done by simple regression analysis ( $r^2 =$  regression



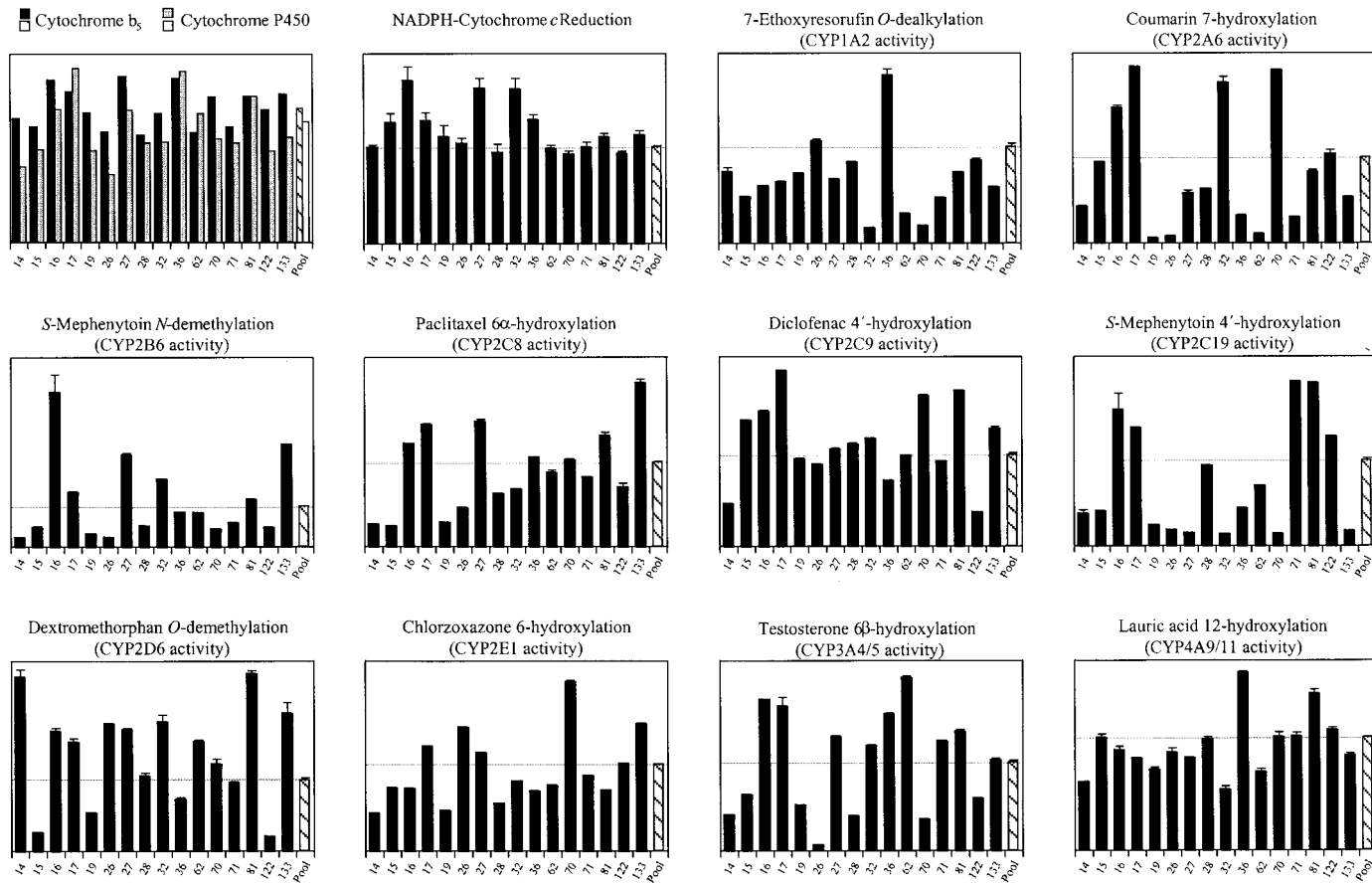


**Figure 14** Sample-to-sample variation in activity of P450 enzymes in a bank of human liver microsomes: Data accompanying the Reaction Phenotyping Kit available through Xeno Tech, LLC. Dotted line represents activity in pooled human liver microsomal samples.

coefficient or coefficient of determination) or by Pearson's product moment correlation analysis ( $r$  = correlation coefficient), where the marker P450 enzyme activity is the independent variable and the rate of formation drug metabolite is the dependent variable. The latter determination also provides statistical significance of the relationships. However, the statistical significance should be treated cautiously, because as the sample size increases and as the number of P450s increase, it is quite common to get statistically significant correlations by chance alone. For example, 7-ethoxy-4-trifluoromethylcoumarin *O*-dealkylation is primarily catalyzed by CYP2B6, and therefore this activity correlates highly with *S*-mephenytoin *N*-demethylase (CYP2B6) activity in human liver microsomes but not with any other P450 activity (Fig. 15).

Additionally, the significant correlations should always be confirmed with a visual inspection of the graph. There are two hallmark characteristics of a misleadingly high correlation coefficient: (1) the regression line has a high intercept, and/or (2) there is an outlying data point that is skewing the correlation analysis (see Fig. 16). Also note that the latter can cause otherwise well-correlated data to skew the analysis toward a low correlation coefficient; this is quite common when the immunoreactive protein is used as the independent variable. This is because allelic variants of a P450 enzyme (which have lowered enzyme activity) often have the same cross-reactivity with the wild-type forms of the enzyme.

When two (or more) P450 enzymes *significantly* participate in the metabolism of a drug at pharmacologically relevant concentrations, the identity of the enzymes involved can be assessed by multivariate regression analysis [120]. This approach is successful when the participation of both enzymes is significant. For example, on average, if CYP3A4 is primarily (~90%) responsible for the metabolism of a drug and CYP1A2 is a minor contributor (~10%), a high correlation will be observed with CYP3A4 but not with CYP1A2. It is unlikely that the application of multivariate regression analysis will be helpful in such a case. Conversely, however, on average, if the contributions of CYP3A4:CYP1A2 were 60:40, the multivariate regression analysis would readily identify the hidden regressor. The graphical representation of this approach is illustrated in Figure 17, where multivariate correlation analysis successfully revealed that both CYP1A2 and CYP2B6 significantly contribute toward the formation of 7-ethoxy-4-trifluoromethyl coumarin *O*-demethylase activity.

If two kinetically distinct enzymes are involved in a given reaction, the sample-to-sample variation experiments may be performed at multiple concentrations to identify the enzyme that is more relevant at a given substrate concentrations. For example, the 5-hydroxylation of lansoprazole is catalyzed by two P450 enzymes, CYP3A4 and CYP2C19 [121]. At high substrate concentrations (~100  $\mu$ M), the 5-hydroxylation of lansoprazole by human liver microsomes is dominated by CYP3A4, a low-affinity, high-capacity enzyme. However, at pharmaco-

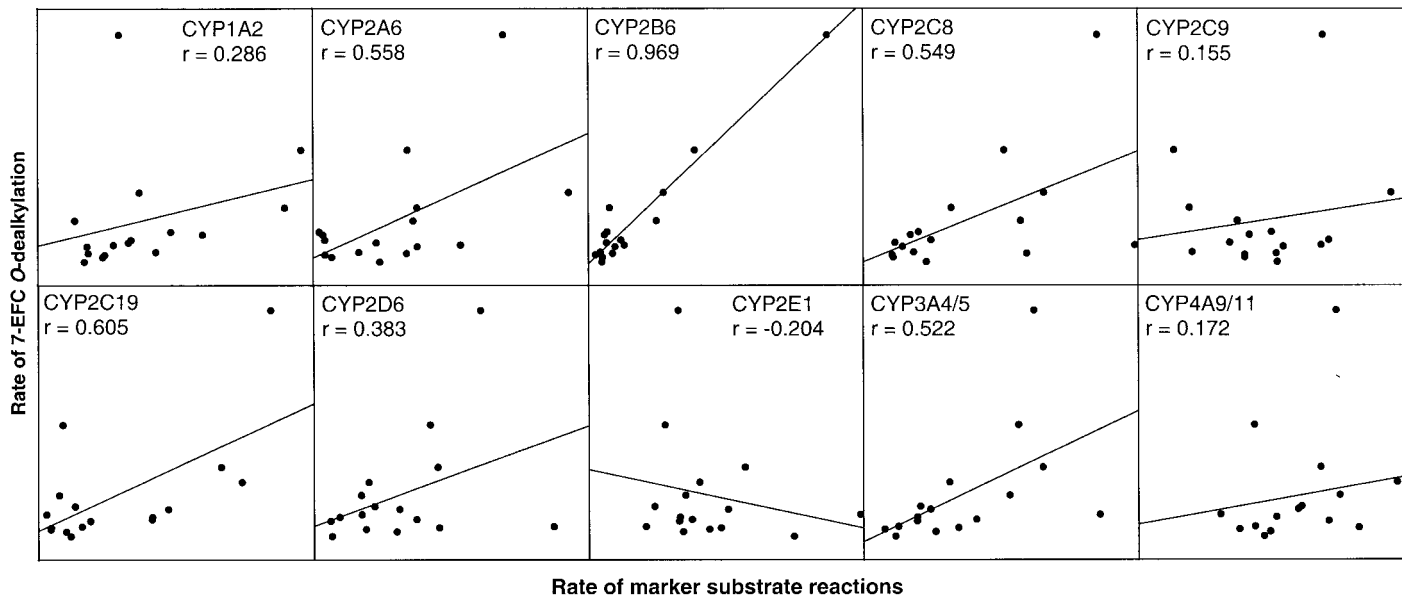
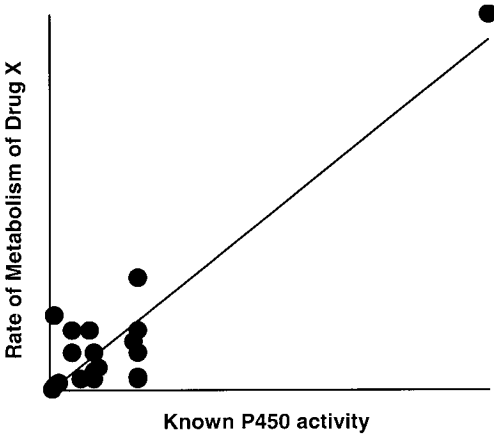


**Figure 15** Correlation analysis of the sample-to-sample variation in 7-ethoxy-4-trifluoromethyl coumarin (7-EFC) *O*-dealkylase activity in a bank of human liver microsomes with marker P450 activities: The *O*-dealkylation of 7-EFC was determined in 16 human liver microsomal samples by a fluorometric method [144]. The sample-to-sample variation in 7-EFC *O*-dealkylase activity was correlated with the sample-to-sample variation in various P450 enzyme activities shown in Figure 14.  $r$  = Pearson's product moment correlation coefficient. The highest correlation was observed with CYP2B6, which is misleading, because this reaction is substantially catalyzed also by CYP1A2. (Note also the y-axis intercept on the graph showing high correlation of 7-EFC *O*-dealkylase activity with *S*-mephenytoin 4'-hydroxylase activity.)

**Pitfall: Outlier data point**



**Pitfall: High intercept on the y axis**

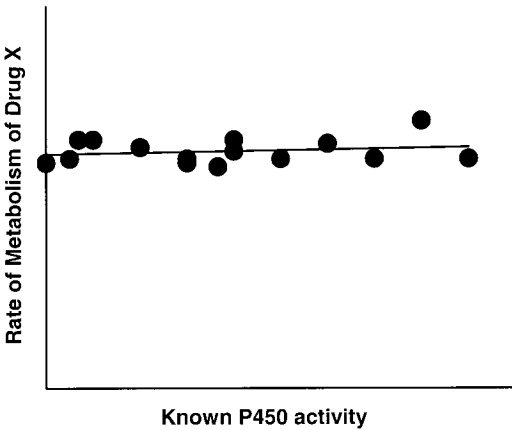


**Figure 16** Common pitfalls in correlation analysis: All graphs and the corresponding fit are based on theoretical data. An outlier microsomal sample, which is very high in several P450 enzyme activities, can yield a high correlation coefficient (top). Similarly, a high correlation coefficient is obtained with a high y-axis intercept, which suggests that the sample-to-sample variation in the drug reaction of interest cannot be explained solely by the sample-to-sample variation in a given P450 enzyme activity (bottom).

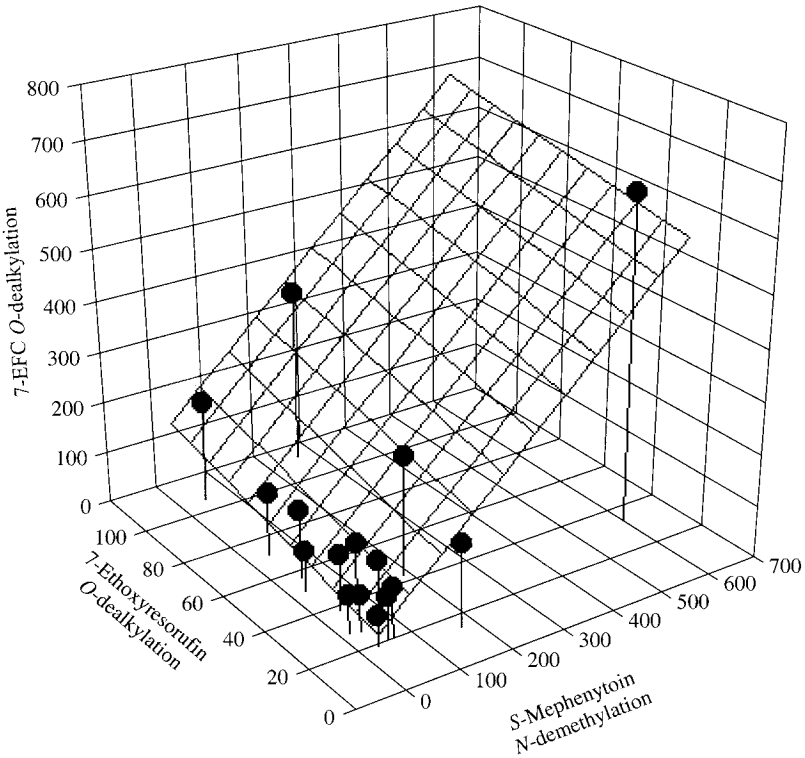


**Figure 17** Multivariate correlation analysis of sample-to-sample variation in 7-ethoxy-4-trifluoromethyl (7-EFC) coumarin *O*-dealkylase activity in a bank of human liver microsomes with CYP2B6 and CYP1A2 activity: The sample-to-sample variation in the 7-EFC *O*-dealkylation in a bank of human liver microsomes was correlated with *S*-mephenytoin *N*-demethylase (CYP2B6) and 7-ethoxyresorufin *O*-dealkylase (CYP1A2) activities (pmol/mg/min) by multivariate regression analysis. The regression coefficient of 7-EFC *O*-dealkylase activity improved from 0.939 (for CYP2B6 alone) to 0.999 when CYP1A2 activity was included in the analysis. Note that all points fall on the 3-dimensional plane best described by a combination of both CYP1A2 and CYP2B6 activity and that the bottom-left corner of the plane is very close to zero for 7-EFC *O*-dealkylase activity. This is in contrast to the positive *y*-axis intercept observed in Figure 15.

logically relevant concentrations ( $\sim 1 \mu\text{M}$ ), the 5-hydroxylation of lansoprazole is catalyzed primarily by CYP2C19, as it is *in vivo*. In the study by Pearce et al. [121], the correlation of CYP2C19 activity with lansoprazole 5-hydroxylation improved dramatically when the substrate concentration was lowered from 125 to  $1 \mu\text{M}$  and, conversely, the correlation of the same activity with CYP3A4 pro-

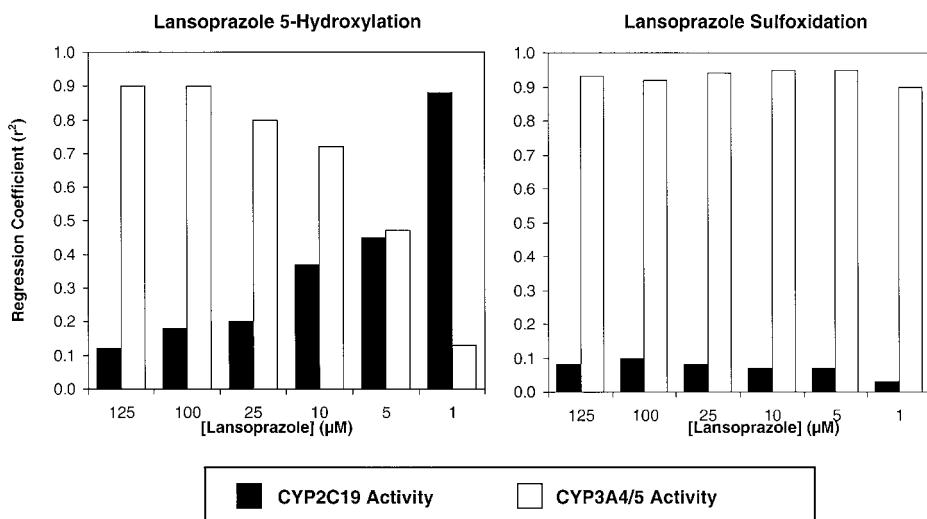


**Figure 18** Relationship between the rates of *S*-mephenytoin 4'-hydroxylation (CYP2C19) or testosterone 6 $\beta$ -hydroxylation (CYP3A4/5) and the rates of lansoprazole 5-hydroxylation and lansoprazole sulfoxidation by human liver microsomes at substrate concentrations varying from 1 to 125  $\mu$ M: Human liver microsomes were incubated with lansoprazole (1–125  $\mu$ M) in the presence of an NADPH-generating system. The rates of lansoprazole 5-hydroxylation were compared with the rates of *S*-mephenytoin 4'-hydroxylation (a marker for CYP2C19 activity) or testosterone 6 $\beta$ -hydroxylation (a marker for CYP3A4/5 activity). Note that the correlation of CYP2C19 activity with lansoprazole 5-hydroxylation improved dramatically when the substrate concentration was lowered from 125 to 1  $\mu$ M and, conversely, the correlation of the same activity with CYP3A4 progressively worsened. This is because, at low lansoprazole concentrations, lansoprazole 5-hydroxylation is catalyzed primarily by CYP2C19, but the contribution of CYP3A4/5 predominates at high concentrations of lansoprazole. In contrast, the correlation of lansoprazole sulfoxidation with CYP2C19 was poor, and that with CYP3A4/5 was good, regardless of lansoprazole concentration. This is because CYP3A4/5 is the primary enzyme responsible for lansoprazole sulfoxidation in human liver microsomes.

gressively worsened (Fig. 18). Similarly, oxidative bioactivation of halothane is catalyzed by CYP2E1 at low substrate concentrations, but at high concentrations CYP2E1 is inhibited by halothane, and the role of other enzymes becomes more prominent [122].

Finally, as described in the next section, it is possible to selectively inhibit a P450 enzyme (preferably with a metabolism-dependent "irreversible" or "quasi-irreversible" inhibitor or a selective inhibitory antibody) [123–125]. Therefore, studying the metabolism of the drug in a bank of human liver microsomes in

the absence *and* presence of the inhibitor can establish the identity (and the relative contribution) of the enzymes involved. For example, the *O*-dealkylation of 7-ethoxy-4-trifluoromethylcoumarin (7-EFC) is catalyzed primarily by CYP2B6, but with significant contributions from CYP1A2. (CYP1A2 is the high-affinity but low-capacity enzyme for this reaction, and CYP2B6 is the low-affinity but high-capacity enzyme). A correlation analysis of uninhibited rates of 7-EFC *O*-dealkylation in a bank of human liver microsomes revealed a high correlation with CYP2B6 but not with CYP1A2 (Fig. 19). When this same reaction was conducted with a bank of human liver microsomes in which CYP1A2 had been inhibited by furafylline, the activity remaining revealed an almost perfect correlation with CYP2B6, and the inhibited activity revealed a high correlation with CYP1A2 (Fig. 19). A similar approach implicated CYP3A4 and CYP2D6 in the conversion of loratidine to desloratidine [125].

#### Step 6. Chemical and Antibody Inhibition

Experiments outlined in Step 5 will likely provide information on which human P450 enzyme or enzymes are responsible for metabolizing the drug. The postulated role of a particular P450 enzyme in the metabolism of the drug can be verified by inhibiting the reaction with chemicals or antibodies known to inhibit that enzyme. Human liver microsomes pooled from several individuals are used for these studies. As stated previously for correlation analysis, chemical inhibition experiments are conducted at the pharmacologically relevant concentration of the drug or at the lowest possible concentration of the drug at which metabolite formation can be reasonably detected. One or more of the inhibitors shown in Table 3 are used to preferentially inhibit certain P450 enzymes. For example, inhibition of 7-ethoxy-4-trifluoromethyl coumarin *O*-dealkylase activity in a pool of human liver microsomes by chemical inhibitors of human P450 enzymes is shown in Figure 20.

It is important to know the selectivity of the inhibitors and the appropriate concentration of the inhibitors for various P450 enzymes before applying them. For example, ketoconazole is a potent inhibitor of human CYP3A4/5 ( $K_i < 20$  nM) but is capable of inhibiting several P450 enzymes ( $K_i$  in  $\mu$ Molar range) [19,126]. Additionally, an estimate of the metabolic stability of the inhibitors should be available. For example, coumarin is a selective substrate of CYP2A6 ( $K_m \sim 0.5 \mu$ M) [50,111]; therefore, it should be a good competitive inhibitor of this enzyme. However, in practice, coumarin is a poor inhibitor because it is so rapidly metabolized under typical microsomal incubation conditions. Finally, if the drug reaction is catalyzed with a very high affinity, the concentration of a *competitive* inhibitor must be increased accordingly. A good rule of thumb is to

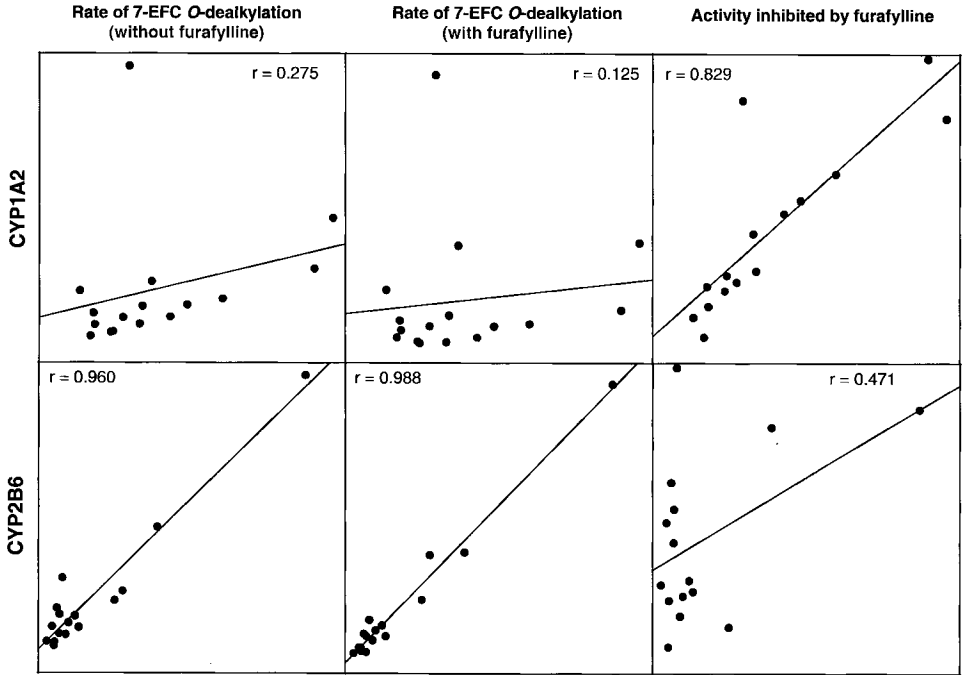


**Figure 19** Correlation analysis of the sample-to-sample variation in 7-ethoxy-4-trifluoromethyl coumarin (7-EFC) *O*-dealkylase activity in a bank of human liver microsomes with CYP2B6 and CYP1A2 activity in the absence or presence of 5  $\mu$ M furafylline: A bank of 16 human liver microsomal samples were preincubated with an NADPH-generating system in the absence or presence of furafylline (10  $\mu$ M) for 10 min at 37°C. The microsomal samples were then diluted 10-fold into an incubation containing the marker substrate, 7-EFC, and the 7-EFC *O*-dealkylation activity was determined. The 7-EFC *O*-dealkylase activity was correlated with 7-ethoxyresorufin *O*-dealkylase (CYP1A2) and *S*-mephenytoin *N*-demethylase (CYP2B6) activities in the absence of furafylline (a metabolism-dependent CYP1A2 inhibitor). The 7-EFC *O*-dealkylase activity remaining in the presence of furafylline and the activity inhibited by furafylline were also correlated with CYP1A2 and CYP2B6 activities. Note that the correlation with CYP2B6 improved from 0.960 to 0.988 in the presence of furafylline, whereas 7-EFC *O*-dealkylase activity inhibited by furafylline was well correlated with CYP1A2 activity ( $r = 0.829$ ) but not with CYP2B6 activity ( $r = 0.471$ ).



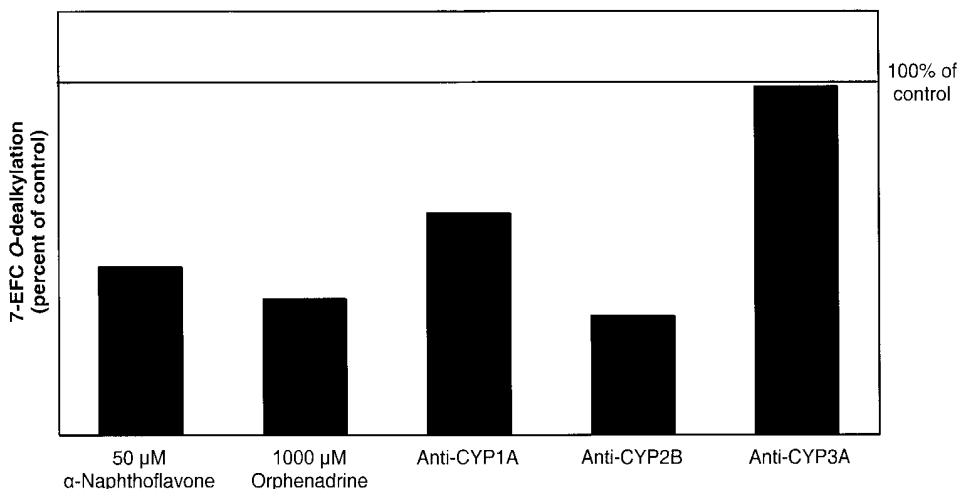


**Figure 20** Inhibition of 7-ethoxy-4-trifluoromethyl coumarin (7-EFC) *O*-dealkylase activity in a pool of human liver microsomes by selective chemical inhibitors of P450 enzymes and polyclonal antibodies: The *O*-dealkylation of 7-EFC by a pool of human liver microsomes was studied in the presence of  $\alpha$ -naphthoflavone (CYP1A2 inhibitor) or orphenadrine (CYP2B6 inhibitor). Similarly, 7-EFC *O*-dealkylation was determined in the presence of selective inhibitory polyclonal antibodies against CYP1A, CYP2B, and CYP3A enzymes. The data shows that both CYP1A2 and CYP2B6 significantly contribute to this reaction.

use multiples (1, 2, 5, and 10) of the lowest inhibitor concentration, which is calculated by the following equation:

$$\text{Lowest [Inhibitor]} = \frac{[\text{Drug}] \times K_{i(\text{inhibitor})}}{K_{m(\text{Drug})}} \quad (7)$$

where [Drug] is the concentration of the drug at which the experiment will be performed,  $K_i$  is the inhibition constant of the inhibitor for a given enzyme, and  $K_m$  is the Michaelis constant of the drug reaction determined in Step 3. For example, if the lowest concentration of the inhibitor were calculated to be 1  $\mu\text{M}$ , then the concentrations of inhibitor applied may be 1, 2, 5, and 10  $\mu\text{M}$ . It is imperative to study several inhibitor concentrations to ensure that the inhibition is concentration dependent. (*Note*: Equation (7) does not apply for noncompetitive inhibitors.)

There are a couple of practical problems associated with the use of chemical inhibitors: (1) They may interfere with the chromatographic analysis of the metabolite of interest, and (2) they are often dissolved in organic solvents [50,83–

86], which tend to be inhibit some P450 enzymes. Selection of water-soluble inhibitors and/or studying appropriate solvent controls helps in interpretation of the data.

Since the selectivity of some inhibitors is questionable [17,19,50,84,126–131], selective inhibitory polyclonal, monoclonal, or antipeptide antibodies against individual P450 enzymes are the best reagents for inhibiting a drug reaction [132,133]. The inhibition observed is noncompetitive and is therefore independent of the substrate concentration. However, a large antibody-to-microsomes ratio is often required to achieve marked inhibition, which can increase the cost of such experiments. Additionally, selective inhibitory antibodies are commercially available only for selected P450s; therefore, the role of some but not all enzymes can be evaluated by this approach. For example, inhibition of 7-ethoxy-4-trifluoromethyl coumarin *O*-dealkylase activity in a pool of human liver microsomes by inhibitory antibodies is shown in Figure 20.

### Step 7. cDNA-Expressed Human P450 Enzymes

Several human P450 enzymes have been cloned and expressed individually in various cell lines. Microsomes from these cells, which contain a single human P450 enzyme, are commercially available. The recombinant P450 enzymes differ in their catalytic competency, and they are not expressed in cells at concentrations that reflect their levels in human liver microsomes. Therefore, a simple evaluation of metabolism by a bank of recombinant P450 enzymes (such as the one shown in Fig. 21) does not establish the *extent* to which a P450 enzyme contributes to the metabolism of a particular drug, only that a particular P450 enzyme *can* metabolize that drug. Also, the recombinant P450 enzymes are expressed with additional NADPH-cytochrome P450 reductase such that there is at least an order of magnitude difference in the P450-to-reductase ratio in recombinant P450 enzymes versus native human liver microsomes. This makes it difficult to interpret the results obtained with recombinant enzymes. To circumvent this issue, a useful tool has been recently summarized by Rodrigues [90]: The kinetic constants ( $K_m$  and  $V_{max}$ ) for each enzyme are experimentally determined. Only those enzymes that are implicated in the metabolism of the drug (from the results of Steps 5 and 6) are selected for this determination. (It is impractical to determine the kinetic constants for all recombinant P450 enzymes.)

Care must be taken in the determination of kinetic constants, as described previously in Step 3, and the methodology is very similar to those described previously. The  $V_{max}$  (expressed as pmol product formed/min/pmol of P450) obtained with the recombinant P450 is multiplied by the specific content (expressed as average pmol P450/mg of human liver microsomes) of that P450 in native human liver microsomes [89–92,134], which gives the predicted  $V_{max}$  in an average (or a pooled) sampled of human liver microsomes. The predicted  $V_{max}$  is

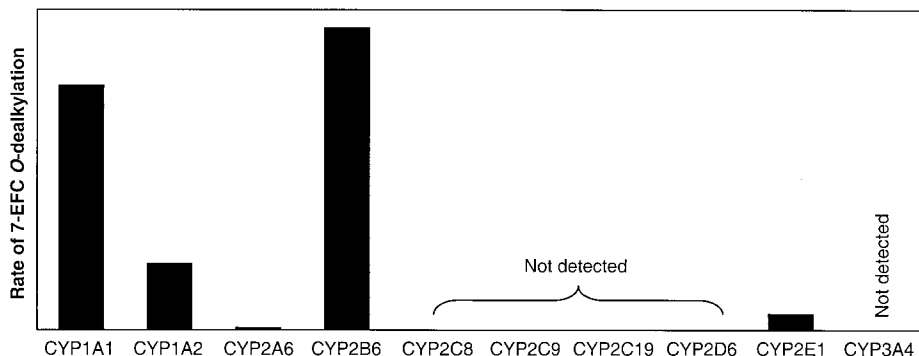


**Figure 21** 7-Ethoxy-4-trifluoromethyl coumarin (7-EFC) *O*-dealkylation by a bank of recombinant human P450 enzymes: The *O*-dealkylation of 7-EFC was studied in a bank of recombinant human P450 enzymes from Gentest (Woburn, MA). The data shows that, in addition to CYP1A2 and CYP2B6, CYP1A1 and CYP2E1 have the capacity to catalyze this reaction. The contribution of CYP1A1 is expected to be minimal, because this enzyme is not expressed at detectable levels in human liver. In contrast, the contribution of CYP2E1 may have been underestimated because *O*-dealkylation of 7-EFC was studied in the presence of 0.5% DMSO, and CYP2E1 is potently inhibited by DMSO.

divided by the  $K_m$  value determined with the recombinant P450 enzyme to give the predicted intrinsic clearance in human liver microsomes, which indicates the rate at which each P450 will clear the drug when  $[\text{substrate}] \ll K_m$ . The sum total of the predicted clearance by each individual P450 enzyme should be similar to the experimentally determined intrinsic clearance value with a pool of human liver microsomes (Step 3). If this is not the case, then one or more of the major contributing P450 enzymes must have been excluded from the analysis. The predicted percentage contribution of each P450 enzyme can then be easily calculated. (This method is illustrated in Table 6.) The limitation of this approach is that the turnover numbers in recombinant enzymes can at times be affected by the presence or absence of cytochrome  $b_5$ , and the amount of NADPH-cytochrome P450 reductase [19,61], and hence they are different from what would be observed in human liver microsomes.

An alternative approach is to determine a “relative activity factor,” which is a measure of catalytic activity of a known marker substrate reaction in human liver microsomes (expressed as pmol/min/mg protein) versus a given recombinant enzyme (also expressed as pmol/min/mg) [58,135]. The relative activity factor is then multiplied by the observed rates of the P450 reaction in question in a bank of recombinant P450 enzymes to give predicted rates in human liver microsomes. This approach has not been fully validated. For example, it would

**Table 6** Predicting Relative Contribution of CYP1A2 and CYP3A4 Toward a Reaction in an Average Human Liver Microsomal (HLM) Sample Based on Theoretical Kinetic Data from Recombinant Enzymes

Microsomes	Observed kinetic constants by recombinant P450 enzyme		Specific content <sup>a</sup> (pmol P450/mg HLM)	Predicted $V_{\max}$ in HLM <sup>b</sup> (pmol/min/mg HLM)	Predicted intrinsic clearance <sup>c</sup> (CL <sub>in</sub> )	Percent contribution <sup>d</sup>
	$V_{\max}$ (pmol/min/pmol P450)	$K_m$ ( $\mu$ M)				
Recombinant CYP1A2	10	1	45	450	450	70%
Recombinant CYP3A4	10	10	96	960	96.0	14%

<sup>a</sup> Specific content: From Ref. 89.

<sup>b</sup> Predicted  $V_{\max}$ : Observed  $V_{\max} \times$  Specific content.

<sup>c</sup> Predicted intrinsic clearance: Predicted  $V_{\max}$ /Observed  $K_m$ .

<sup>d</sup> Percent contribution: (CL<sub>in</sub> of one enzyme/CL<sub>in</sub> of all enzymes)  $\times$  100.

be important to establish whether the relative activity factor remains constant for several marker substrate reactions catalyzed by the same P450 enzymes. A limitation of this approach, if it were to be validated, is that the relative activity factor must be empirically determined for each lot of recombinant P450 enzyme and pooled human liver microsomes in the same laboratory. Additionally, the presence of allelic variants and enzymes that cannot be easily distinguished based on marker substrate reaction (e.g., CYP3A4 and CYP3A5) in human liver microsomes complicate the use of relative activity factors.

### C. Potential Pitfalls with Approaches for Reaction Phenotyping

The potential pitfalls associated with each step in reaction phenotyping were addressed earlier (see Sec. III.B). There are additional potential pitfalls in reaction phenotyping that do not apply simply to any one approach, but apply to all of the experimental approaches to identifying which P450 enzyme is primarily responsible for metabolizing a drug. The two most common errors follow.

1. The metabolism of the substrate (drug) is not measured under initial-rate conditions: Prior to initiating reaction phenotyping, a pool of human liver microsomes should always be used to establish initial-rate conditions (i.e., conditions under which metabolite formation is proportional to protein concentration and incubation time), *and* total substrate consumed should be less than 20%. Whenever possible, the amount of substrate consumed during the reaction should be less than 10% in order to measure initial rates of metabolite formation.
2. The metabolism of the substrate (drug) is not measured at pharmacologically relevant concentrations: Even if a  $K_m$  value is determined appropriately (i.e., at appropriate substrate concentrations and under initial-rate conditions), it should not be used as a basis for selecting the concentration of substrate for reaction phenotyping studies unless such concentrations are pharmacologically relevant. Selecting a substrate concentration for reaction phenotyping based on  $K_m$  values is also problematic when the substrate is converted to two metabolites with different  $K_m$  values. Reaction phenotyping should be conducted, whenever possible, with pharmacologically relevant concentrations of drugs. When reaction phenotyping is carried out with high (nonpharmacologically relevant) substrate concentrations, the P450 enzyme that appears to be responsible for metabolizing the drug *in vitro* may not be the P450 enzyme responsible for metabolizing the drug *in vivo*. This important principle is illustrated in a study of lansoprazole metabolism. Pearce et al. [121] demonstrated that the 5-hydroxylation of lansopra-

zole can be catalyzed by two P450 enzymes, CYP3A4 and CYP2C19. At high substrate concentrations, the 5-hydroxylation of lansoprazole by human liver microsomes is dominated by CYP3A4, a low-affinity, high-capacity enzyme. However, at pharmacologically relevant concentrations, the 5-hydroxylation of lansoprazole is catalyzed primarily by CYP2C19, as it is in vivo. In the study by Pearce et al. [121], the contribution of CYP2C19 to lansoprazole 5-hydroxylation by human liver microsomes became increasingly important as the substrate concentration was decreased and, conversely, the contribution of CYP3A4 progressively declined. Such trends are particularly useful when it is difficult to estimate a pharmacologically relevant substrate concentration or when it is difficult to conduct experiments at pharmacologically relevant concentrations for analytical reasons (i.e., low analytical sensitivity). Such trends allow results obtained at relatively high substrate concentrations to be extrapolated to lower, pharmacologically relevant concentrations.

3. If a drug is converted to several metabolites, the temptation is to phenotype all of the reactions. This is necessary when all of the metabolites are formed in vivo or are important from a pharmacological or toxicological viewpoint. The  $K_m$  and  $V_{max}$  experiment should give a clear indication of the major pathways by which the drug is metabolized, and the minor pathways should be ignored for most practical purposes. Additionally, the minor metabolites tend to be secondary metabolites (i.e., they are metabolites of metabolites), in which case, the principles described here can be easily compromised. If a secondary metabolic pathway must be characterized, it is best to use the metabolite of the parent drug as the substrate and repeat Steps 1 through 7.

The inherent limitations of in vitro studies should also be kept in mind. Metabolites may be formed in vivo but not in vitro, or they may be formed in one in vitro system but not in another. Although a lot has been done to characterize these systems, it is important to remember that the results generated from in vitro systems must be extrapolated with caution to the in vivo situation.

#### **D. In Vitro to In Vivo Extrapolation of Reaction Phenotyping Data**

Information on which P450 enzyme is primarily responsible for metabolizing a drug is useful for explaining or predicting pharmacokinetic variability, which may occur when a drug is metabolized by a polymorphically expressed P450 enzyme. Additionally, reaction phenotyping is useful for explaining or predicting certain drug interactions, which may occur with concomitantly administered

drugs. For example, if a drug were found to be metabolized primarily by CYP3A4, it would point to the possibility that the rate of metabolism of the drug might be increased by rifampin and other drugs that induce this P450 enzyme. Conversely, a prediction can be made that the rate of metabolism of the drug might be decreased by ketoconazole and other drugs that inhibit CYP3A4. Consequently, rifampin and related inducers might diminish the therapeutic effect of a drug that is metabolized by CYP3A4, whereas ketoconazole and related inhibitors might enhance the pharmacologic and toxic effects of the drug.

#### IV. TIMING OF IN VITRO DRUG INTERACTION STUDIES

Like most phases of drug development, the sequence of studies required to establish that a potential drug (new chemical entity, drug) is therapeutically efficacious and safe differs from one pharmaceutical company to the next and from one drug to the next. When reaction phenotyping should be carried out will depend on such factors as the chemical structure of the drug, its intended clinical application, its potential for coadministration with other drugs, and problems associated with structurally related drugs or preapproved drugs in the same therapeutic class. Many pharmaceutical companies evaluate the interaction of drugs with human P450 enzymes, either as substrates or inhibitors, as part of their criteria for selecting drug candidates.

At what stage of drug development should studies be conducted to identify the enzymes responsible for the metabolism of drugs or to evaluate the potential for drugs to inhibit the drug-metabolizing enzymes? What is an acceptable experimental design and/or endpoint? The answers to such questions depend on the number of new chemical entities (drugs) available for a given application, the history of the class of drug, the structural features of the drug, and the intended use of the drugs.

#### REFERENCES

1. Parkinson, A. Biotransformation of xenobiotics. In: Casarett and Doull's Toxicology. The Basic Science of Poisons. (5th ed.) (Klaassen, CD, ed.) McGraw-Hill, New York, 1996, pp 113–186.
2. Parkinson, A. An overview of current cytochrome P450 technology for assessing the safety and efficacy of new materials. *Toxicologic Pathol* 24:45–57, 1996.
3. Bertz, RJ, and Granneman, GR. Use of in vitro and in vivo data to estimate the likelihood of metabolic pharmacokinetic interactions. *Clin Pharmacokinet* 32:210–258, 1997.
4. Lin, JH, and Lu, AYH. Inhibition and induction of cytochrome P450 and the clinical implications. *Clin Pharmacokinet* 35:361–390, 1998.

5. Omiecinski, CJ, Rimmel, RP, and Hosagrahara, VP. Concise review of the cytochrome P450s and their roles in toxicology. *Toxicological Sci* 48:151–156, 1999.
6. Lu, AY. Drug-metabolism research challenges in the new millennium: individual variability in drug therapy and drug safety. *Drug Metab Dispos* 26:1217–1222, 1998.
7. Wachter, VJ, Silverman, JA, Zhang, Y, and Benet, LZ. Role of P-glycoprotein and cytochrome P450 3A in limiting oral absorption of peptides and peptidomimetics. *J Pharm Sci* 87:1322–1330, 1998.
8. Stieger, B, and Meier, PJ. Bile acid and xenobiotic transporters in liver. *Curr Opin Cell Biol* 10:462–467, 1998.
9. Wandel, C, Kim, RB, Kajiji, S, Guengerich, P, Wilkinson, GR, and Wood, AJ. P-Glycoprotein and cytochrome P-450 3A inhibition: dissociation of inhibitory potencies. *Cancer Res* 59:3944–3948, 1999.
10. Kim, RB, Wandel, C, Leake, B, Cvetkovic, M, Fromm, MF, Dempsey, PJ, Roden, MM, Belas, F, Chaudhary, AK, Roden, DM, Wood, AJ, and Wilkinson, GR. Interrelationship between substrates and inhibitors of human CYP3A and P-glycoprotein. *Pharm Res* 16:408–14, 1999.
11. Smith, DA, and van-de-Waterbeemd, H. Pharmacokinetics and metabolism in early drug discovery. *Curr Opin Chem Biol* 3:373–378, 1999.
12. Ambudkar, SV, Dey, S, Hrycyna, CA, Ramachandra, M, Pastan, I, and Gottesman, MM. Biochemical, cellular, and pharmacological aspects of the multidrug transporter. *Annu Rev Pharmacol Toxicol* 39:361–398, 1999.
13. Hall, SD, Thummel, KE, Watkins, PB, Lown, KS, Benet, LZ, Paine MF, Mayo, RR, Turgeon, DK, Bailey, DG, Fontana, RJ, and Wrighton, SA. Molecular and physical examination of the first-pass extraction. *Drug Metab Dispos* 27:161–166, 1999.
14. US Food and Drug Administration, Center for Drug Evaluation and Research (CDER). Guidance for industry: drug metabolism/drug interaction studies in the drug development process: Studies in vitro. [www.fda.gov/cder/guidance.html](http://www.fda.gov/cder/guidance.html).
15. The European Agency for the Evaluation of Medicinal Products: Note for guidance on the investigation of drug interactions (CPMP/EWP/560/95). [www.eudra.org/humandocs/humans/EWP.html](http://www.eudra.org/humandocs/humans/EWP.html).
16. Pelkonen, O., Mäenpää, J, Taavitsainen P, Rautio, A, and Raunio, H, Inhibition and induction of human cytochrome P450 enzymes. *Xenobiotica* 12:1203–1253, 1998.
17. Smith, DA, Abel SM, Hyland, R, and Jones BC. Human cytochrome P450s: selectivity and measurement in vivo. *Xenobiotica* 12:1095–1128, 1998.
18. Ingelman-Sundberg M, Oscarson, M, and McLellan RA. Polymorphic human cytochrome P450 enzymes: an opportunity for individualized drug treatment. *TIPS* 20: 342–349, 1999.
19. Clarke SE. In vitro assessment of human cytochrome P450. *Xenobiotica* 12:1167–1202, 1998.
20. Bertilsson, L, Henthorn, TK, Sanz, E, Tybring, G, Sawe, J, and Villen, T. Importance of genetic factors in the regulation of diazepam metabolism: relationship to S-mephenytoin, but not debrisoquin, hydroxylation phenotype. *Clin Pharmacol Ther* 45:348–355, 1989.



21. Andersson, T, Cederberg, C, Edvardsson, G, Heggelund, A, and Lundbord, P. Effect of omeprazole treatment on diazepam plasma levels in slow versus normal rapid metabolizers of omeprazole. *Clin Pharmacol Ther* 47:79–85, 1990.
22. Andersson, T, Miners JO, Veronese, ME, and Birkett, DJ. Diazepam metabolism by human liver microsomes is mediated by both *S*-mephenytoin hydroxylase and CYP3A isoforms. *Br J Clin Pharmacol* 38:192–198, 1994.
23. Andersson, T, Miners JO, Veronese, ME, and Birkett, DJ. Identification of human liver cytochrome P450 isoforms mediating secondary omeprazole metabolism. *Br J Clin Pharmacol* 37:597–604, 1994.
24. Andersson, T, Miners JO, Veronese, ME, Tassaneeyakul, W, Meyer, UA, and Birkett, DJ. Identification of human liver cytochrome P450 isoforms mediating omeprazole metabolism. *Br J Clin Pharmacol* 36:521–530, 1993.
25. Andersson, T. Pharmacokinetics, metabolism and interactions of acid pump inhibitors: focus on omeprazole, lansoprazole and pantoprazole. *Clin Pharmacokinet* 31: 9–28, 1996.
26. Houston, JB. Utility of in vitro drug metabolism data in predicting in vivo metabolic clearance. *Biochem Pharmacol* 47:1469–1479, 1994.
27. Kato, R, and Yamazoe, Y. The importance of substrate concentration in determining cytochromes P450 therapeutically relevant in vivo. *Pharmacogenetics* 4:359–362, 1994.
28. Kohl, C, and Steinkellner, M. Prediction of pharmacokinetic drug/drug interactions from in vitro data: interactions of the nonsteroidal anti-inflammatory drug lornoxicam with oral anticoagulants. *Drug Metab Dispos* 28:161–168, 2000.
29. Kenworthy, KE, Bloomer, JC, Clarke, SE, and Houston, JB. CYP3A4 drug interactions: correlation of 10 in vitro probe substrates. *Br J Clin Pharmacol* 48:716–727, 1999.
30. Guengerich, FP, Muller, ED, and Blair, IA. Oxidation of quinidine by human liver cytochrome P-450. *Mol Pharmacol* 30:287–295, 1986.
31. Vickers, AEM, Sinclair, JR, Zollinger, M, Heitz, F, Glänzel, U, Johanson, L, and Fischer, V. Multiple cytochrome P450s involved in the metabolism of terbinafine suggest a limited potential for drug–drug interactions. *Drug Metab Dispos* 27: 1029–1038, 1999.
32. Parkinson, A, and Hurwitz, A. Omeprazole and the induction of human cytochrome P450: a response to concerns about potential adverse effects. *Gastroenterology* 100: 1157–1164, 1991.
33. Schmid, B, Bircher, J, Preisig, R, and Kupfer, A. Polymorphic dextromethorphan metabolism: co-segregation of oxidative *O*-demethylation with debrisoquine hydroxylation. *Clin Pharmacol Ther* 38:618–624, 1985.
34. Zhang, Y, Britto, MR, Valderhaug, BA, Wedlund, PJ, and Smith, RA. Dextromethorphan: enhancing its systemic availability by way of low-dose quinidine-mediated inhibition of cytochrome P450 2D6. *Clin Pharmacol Ther* 51:647–655, 1992.
35. Stobl, GR, von Kruedener, S, Sstockigt, J, Guengerich, FP, and Wolff T. Development of a pharmacophore for inhibition of human liver cytochrome P-450 2D6: molecular modeling and inhibition studies. *J Med Chem* 36:1136–1145, 1993.
36. Abdel-Rahman, SM, Marcucci, KM, Boge, T, Gotschall, RR, Kearns, GL, and

- Leeder, JS. Potent inhibition of cytochrome-P450-mediated dextromethorphan *O*-demethylation by terbinafine. *Drug Metab Dispos* 27:770–775, 1999.
37. Celebrex™ (Celecoxib capsules). Physicians Desk Reference, 54th ed. Montvale, NJ: Medical Economics, 2000, pp 2334–2337.
  38. Ortiz De Montellano, PR. Structure, mechanism and inhibition of cytochrome P450. 23:1181–1187, 1995.
  39. Yun, CH, Okerholm, RA, and Guengerich, FP. Oxidation of the antihistaminic drug terfenadine in human liver microsomes. Role of CYP3A(4) in *N*-dealkylation and *C*-oxidation. *Drug Metab Dispos* 21:403–409, 1993.
  40. Monahan, BP, Ferguson, CL, Killeavy, ES, Lloyd, BK, Troy, J, and Cantilena LR. Torsades de pointes occurring in association with terfenadine use. *JAMA* 264: 2788–2790, 1990.
  41. Woosley, RL, Chen, Y, Freiman, JP, and Gillis RA. Mechanism of the cardiotoxic actions of terfenadine. *JAMA* 269:1532–1536, 1993.
  42. Kivisto, KT, Neuvonen, PJ, and Klotz, U. Inhibition of terfenadine metabolism: pharmacokinetic and pharmacodynamic consequences. *Clin Pharmacokinet* 27:1–5, 1994.
  43. Honig, PK, Woosley, RL, Zamani, K, Conner, DP, and Cantilena Jr, LR. Changes in the pharmacokinetics and electrocardiographic pharmacodynamics of terfenadine with concomitant administration of erythromycin. *Clin Pharmacol Ther* 52:231–238, 1992.
  44. Honig, PK, Wortham, DC, Zamani, K, Conner, DP, Mullin, JC, and Cantilena, LR. Terfenadine–ketoconazole interactions: pharmacokinetic and electrocardiographic consequences. *JAMA* 269:1513–1518, 1993.
  45. von Moltke, LL, Greenblatt, DJ, Duan, SX, Harmatz, JS, and Shader, RI. In vitro prediction of the terfenadine–ketoconazole pharmacokinetic interaction. *J Clin Pharmacol* 34:1222–1227, 1994.
  46. Bedford, TA, and Rowbotham, DJ. Cisapride: Drug interactions of clinical significance [Published erratum in *Drug Saf* 17:196, 1997]. *Drug Saf* 15:167–175, 1996.
  47. Draper, AJ, Madan, A, Smith, K, and Parkinson, A. Development of a non-HPLC assay to determine testosterone hydroxylase (CYP3A) activity in human liver microsomes. *Drug Metab Dispos* 26:199–305, 1998.
  48. Mansuy, D. Formation of reactive intermediates and metabolites: effects of macrolide antibiotics on cytochrome P450. *Pharmacol Ther* 33:41–45, 1987.
  49. Kunze, KL, and Trager, WF. Isoform-selective mechanism-based inhibition of human cytochrome P450 1A2 by furafylline. *Chem Res Toxicol* 6:649–656, 1993.
  50. Draper, A, Madan, A, and Parkinson, A. Inhibition of coumarin 7-hydroxylase in human liver microsomes. *Arch Biochem Biophys* 341:47–61, 1997.
  51. Koenigs LL, Peter, RM, Thompson, SJ, Rettie, AE, and Trager, WF. Mechanism-based inactivation of human liver cytochrome P450 2A6 by 8-methoxypsoralen. *Drug Metab Dispos* 25:1407–1415, 1997.
  52. Lopez-Garcia, MP, Dansette, PM, and Mansuy, D. Thiophene derivatives as new mechanism-based inhibitors of cytochromes P-450: inactivation of yeast-expressed human liver cytochrome P-450 2C9 by tielinic acid. *Biochemistry* 33:166–175, 1994.

53. Caccia, S. Metabolism of the newer antidepressants: an overview of the pharmacological and pharmacokinetic implications. *Clin Pharmacokinet* 34:281–302, 1998.
54. Greenblatt, DJ, von Moltke, LL, Schmider, J, Harmatz, JS, and Shader, RI. Inhibition of human cytochrome P450-3A isoforms by fluoxetine and norfluoxetine: in vitro and in vivo studies. *J Clin Pharmacol* 36:783–791, 1996.
55. von Moltke, LL, Greenblatt, DJ, Schmider, J, Duan, SX, Wright, CE, Harmatz, JS, and Shader, RI. Midazolam hydroxylation by human liver microsomes in vitro: inhibition by fluoxetine, norfluoxetine and byazole antifungal agents. *J Clin Pharmacol* 36:783–791, 1996.
- 55a. Ogilvie, BW, Otradovec, SM, Paris, BP, Scheinkoenig, JA, Carrott, PW, Loecker, SL, Hanzlik, RP, Parkinson, A, and Madan, A. 10(Imidazolyl)-decanoic acid (10-IDA) is a selective and potent inhibitor of CYP4A9/11. *Drug Metab Rev* 32:230, 2000.
56. Gibbs, MA, Kunze, KL, Howald, WN, and Thummel, KE. Effect of inhibitor depletion on inhibitory potency: tight binding inhibition of CYP3A by clotrimazole. *Drug Metab Dispos* 27:596–599, 1999.
57. Crespi, CL, Miller, VP, and Penman, BW. Microtiter plate assays for inhibition of human, drug-metabolizing cytochrome P450. *Anal Biochem* 248:188–190, 1997.
58. Crespi, CL, and Miller, VP. The use of heterologously expressed drug metabolizing enzymes—state of the art and prospects for the future. *Pharmacol Ther* 84:121–131, 1999.
59. Moody, GC, Griffin, SJ, Mather, AN, McGinnity, DF, and Riley, RJ. Fully automated analysis of activities catalyzed by the major human liver cytochrome P450 (CYP) enzymes: assessment of human CYP inhibition potential. *Xenobiotica* 29:53–75, 1999.
60. Yamazaki, H, Gillam, EMJ, Dong, MS, Johnson, WW, Guengerich, FP, and Shimada T. Reconstitution of recombinant cytochrome P450 2C10(2C9) and comparison with cytochrome P450 3A4 and other forms: effects of cytochrome P450-P450 and cytochrome P450-b5 interactions. *Arch Biochem Biophys* 342:329–337, 1997.
61. Yamazaki, H, Nakajima, M, Nakamura, M, Asahi, S, Shimada, N, Gillam, EM, Guengerich, FP, Shimada, T, and Yokoi, T. Enhancement of cytochrome P-450 3A4 catalytic activities by cytochrome b5 in bacterial membranes. *Drug Metab Dispos* 27:999–1004, 1999.
62. McGinnity, DF, Griffin, SJ, Moody, GC, Voice, M, Hanlon, S, Friedberg, T, and Riley, RJ. Rapid characterization of the major drug-metabolizing human hepatic cytochrome P-450 enzymes expressed in *Escherichia coli*. *Drug Metab Dispos* 27:1017–1023, 1999.
63. Friedberg, T, Pritchard, MP, Bandera, M, Hanlon, SP, Yao, D, McLaughlin, LA, Ding S, Burchell, B, and Wolf, CR. Merits and limitations of recombinant models for study of human P450-mediated drug metabolism and toxicity: an intralaboratory comparison. *Drug Metab Rev* 31:523–544, 1999.
64. Lee, CA, Kadwell, SH, Kost, TA, and Serabjit-Singh, CJ. CYP3A4 expressed by insect cells infected with a recombinant baculovirus containing both CYP3A4 and human NADPH-cytochrome c reductase is catalytically similar to human liver microsomal CYP3A4. *Arch Biochem Biophys* 319:157–167, 1995.
65. Decker, CJ, Cashman JR, Sugiyama, K, Maltby, D, and Correia, MA. Formation

- of glutathionyl-spirolactone disulfide by rat liver cytochrome P450 or hog liver monooxygenase: a functional probe of two-electron oxidations of the thio-steroid? *Chem Res Toxicol* 4:669–677, 1991.
66. Rettie, AE, Wienkers, LC, Gonzalez, FJ, Trager, WF, and Korzekwa, KR. Impaired (*S*)-warfarin metabolism catalysed by the R144C allelic variant of CYP2C9. *Pharmacogenetics* 4:39–42, 1994.
  67. Miners, JO, and Birkett, DJ. Cytochrome P4502C9: an enzyme of major importance in human drug metabolism. *Br J Clin Pharmacol* 45:525–539, 1998.
  68. Li, AP. Preclinical evaluation of drug–drug interactions using human in vitro experimental systems. *IDrugs* 1:311–314, 1998.
  69. Borchardt, RT, Smith, PL, and Wilson, G, eds. Models for assessing drug absorption and metabolism. *Pharmaceutical Technol* 8:1996.
  70. Kocarek, TA, Schuetz, EG, and Guizelian, PS. Expression of multiple forms of cytochrome P450 mRNA in primary cultures of rat hepatocytes maintained on matrigel. *Mol Pharmacol* 43:328–334, 1993.
  71. Woodcroft, KJ, and Novak, RF. Xenobiotic-enhanced expression of cytochrome P4502E1 and 2B in primary cultured rat hepatocytes. *Drug Metab Dispos* 26:372–378, 1998.
  72. Ekins, S, Murray, GI, Burke, MD, Williams, JA, Marchant, NC, and Hawksworth, GM. Quantitative differences in phase I and II metabolism between rat precision-cut liver slices and isolated hepatocytes. *Drug Metab Dispos* 23:1274–1279, 1995.
  73. von Moltke, LL, Greenblatt, DJ, Schmider, J, Wright, CE, Harmatz, JS, and Shader, RI. In vitro approaches to predicting drug interactions in vivo. *Biochem Pharmacol* 55:113–122, 1998.
  74. Obach, RS. The importance of nonspecific binding in in vitro matrices, its impact on enzyme kinetic studies of drug metabolism reactions, and implications for in vitro-in vivo correlations. *Drug Metab Dispos* 24:1047–1049, 1996.
  75. Obach, RS. Nonspecific binding to microsomes: impact on scale-up of in vitro intrinsic clearance to hepatic clearance as assessed through examination of warfarin, imipramine, and propranolol. *Drug Metab Dispos* 25:1359–1369, 1997.
  76. Obach, RS. Prediction of human clearance of twenty-nine drugs from hepatic microsomal intrinsic clearance data: an examination of in vitro half-life approach and nonspecific binding to microsomes. *Drug Metab Dispos* 27:1350–1359, 1999.
  77. Gibbs, MA, Thummel, KE, Shen, DD, and Kunze, KL. Inhibition of cytochrome P-450 3A (CYP3A) in human intestinal and liver microsomes: comparison of  $K_i$  values and impact of CYP3A5 expression. *Drug Metab Dispos* 27:180–187, 1999a.
  78. Kitz, R, and Wilson, IB. Esters of methanesulfonic acid as irreversible inhibitors of acetylcholinesterase. *J Biol Chem* 237:3245–3249, 1962.
  79. Daly, AK, Brockmüller, J, Broly, F, Eichelbaum, M, Evans, WE, Gonzalez, FJ, Huang, JD, Idle, JR, Ingelman-Sundberg, M, Ishizaki, T, Jacqz-Aigrain, E, Meyer, UA, Nebert, DW, Steen, VM, Wolf, CR, and Zanger, UM. Nomenclature of human CYP2D6 alleles. *Pharmacogenetics* 6:193–201, 1996.
  80. von Moltke, LL, Greenblatt, DJ, Grassi, JM, Granda, BW, Venkatakrishnan, K, Schmider, J, Harmatz, JS, and Shader, RI. Multiple human cytochromes contribute to biotransformation of dextromethorphan in vitro: role of CYP2C9, CYP2C19, CYP2D6 and CYP3A4. *J Pharm Pharmacol* 50:997–1004, 1998.

81. Mankowski, D. The role of CYP2C19 in the metabolism of (+/-) bufuralol, the prototypic substrate of CYP2D6. *Drug Metab Dispos* 27:1024–1028, 1999.
82. Cashman, JR. Structural and catalytic properties of the mammalian flavin-containing monooxygenase. *Chem Res Toxicol* 8:165–181, 1995.
83. Binkley, SN, Ring, BJ, VandenBranden, MR, and Wrighton, SA. The effect of solvents on the activity of CYP2C9, 2C19, 2D6 and 3A. *Cytochrome P450 meeting*, Purdue, IN, 1994.
84. Hickman, D, Wang, JP, and Unadkat, JD. Evaluation of the selectivity of in vitro probes and suitability of organic solvents for the measurement of human cytochrome P450 monooxygenase activities. *Drug Metab Dispos* 26:207–215, 1998.
85. Chauret, N, Gauthier, A, and Nicolle-Griffith, DA. Effect of common organic solvents on in vitro cytochrome P450-mediated metabolic activities in human liver microsomes. *Drug Metab Dispos* 27:1–4, 1998.
86. Busby, WF, Ackermann, JM, and Crespi, CL. Effect of methanol, ethanol, dimethyl sulfoxide, and acetonitrile on in vitro activities of cDNA-expressed human cytochromes P450. *Drug Metab Dispos* 27:246–249, 1999.
87. Schrag ML, and Wiekens, LC. Interactions with CYP3A4 are substrate dependent. *ISSX Proceedings* 15:394, 1999.
88. Rowland, M, and Martin, SB. Kinetics of drug–drug interactions. *J Pharmacokinet Biopharm* 1:553–567, 1973.
89. Shimada, T, Yamazaki, H, Mimura, M, Inui, Y, and Guengerich, FP. Interindividual variations in human liver cytochrome P450 enzymes involved in the oxidations of drugs, carcinogens and toxic chemicals: studies with liver microsomes of 30 Japanese and 30 Caucasians. *J Pharmacol Exp Ther* 270:414–423, 1994.
90. Rodrigues, AD. Integrated cytochrome P450 reaction phenotyping: attempting to bridge the gap between cDNA-expressed cytochromes P450 and native human liver microsomes. *Biochem Pharmacol* 57:465–480, 1999.
91. Tateishi, T, Nakura H, Asoh, M, Watanabe, M, Tanaka, M, Kumai, T, Takashima, S, Imaoka, S, Funae, Y, Yabusaki, Y, Kamataki, T, and Kobayashi, S. A comparison of hepatic cytochrome P450 protein expression between infancy and postinfancy. *Life Sciences* 61:2567–2574, 1997.
92. Klose, TS, Blaisdell, JA, and Goldstein, JA. Gene structure of CYP2C8 and extrahepatic distribution of the human CYP2Cs. *J Biochem Mol Tox* 13:289–295, 1999.
93. Guengerich, FP. Mechanism-based inactivation of human liver cytochrome P-450 IIIA4 by gestodene. *Chem Res Toxicol* 3:363–371, 1990.
94. Guengerich, FP. Inhibition of oral contraceptive steroid-metabolizing enzymes by steroids and drugs. *Am J Obstet Gynecol* 163:2159–2162, 1990b.
95. Kaneko A, Kaneko O, Taleo, G, Björkman, A, and Kobayakawa, T. High frequencies of CYP2C19 mutations and poor metabolism of proguanil in Vanuatu. *Lancet* 349:921–922, 1997.
96. Kaneko, A, Bergqvist, Y, Takechi, M, Kalkoa, M, Kaneko, O, Kobayakawa, T, Ishizaki, T, and Björkman, A. Intrinsic efficacy of proguanil against falciparum and vivax malaria independent of the metabolite cycloguanil. *J Infect Dis* 179: 974–979, 1999.
97. Kaneko, A, Bergqvist, Y, Taleo, G, Kobayakawa, T, Ishizaki, T, and Björkman,

- A. Proguanil disposition and toxicity in malaria patients from Vanuatu with high frequencies of CYP2C19 mutations. *Pharmacogenetics* 9:317–328, 1999.
98. Ashforth, EIL, Carlile, DJ, Chenery, R, and Houston, JB. Prediction of in vivo disposition from in vitro systems: clearance of phenytoin and tolbutamide using rat hepatic microsomal and hepatocyte data. *J Pharmacol Exp Ther* 274:761–766, 1995.
  99. Schmider, J, Greenblatt, DJ, von Moltke, LL, and Shader, RI. Relationship of in vitro data on drug metabolism to in vivo pharmacokinetics and drug interactions: implications for diazepam disposition in humans. *J Clin Psychopharmacol* 16:267–272, 1996.
  100. Iwatsubo, T, Hirota, N, Ooie, T, Suzuki, H, Shimada, N, Chiba, K, Ishizaki, T, Green, CE, Tyson, CA, and Sugiyama, Y. Prediction of in vivo drug metabolism in the human liver from in vitro metabolism data. *Pharmacol Ther* 73:147–171, 1997.
  101. Carlile, DJ, Zomorodi, K, and Houston, BJ. Scaling factors to relate drug metabolic clearance in hepatic microsomes, isolated hepatocytes, and the intact liver. *Drug Metab Dispos* 25:903–911, 1997.
  102. Obach, RS, Baxter JG, Liston, TE, Silber, MB, Jones, BC, MacIntyre, F, Rance, DJ, and Wastall, P. The prediction of human pharmacokinetic parameters from preclinical and in vitro metabolism data. *J Pharmacol Exp Ther* 283:46–58, 1997.
  103. Carlile, DJ, Hakooz, N, and Houston, BJ. Kinetics of drug metabolism in rat liver slices: IV. Comparison of ethoxycoumarin clearance by liver slices, isolated hepatocytes, and hepatic microsomes from rats treated with known modifiers of cytochrome P450 activity. *Drug Metab Dispos* 27:526–532, 1999.
  104. Carlile, DJ, Stevens, AJ, Ashforth, EIL, Waghela, D, and Houston JB. In vivo clearance of ethoxycoumarin and its prediction from in vitro systems: use of drug depletion and metabolite formation methods in hepatic microsomes and isolated hepatocytes. *Drug Metab Dispos* 26:216–221, 1998.
  105. Ito, K, Iwatsubo, T, Kanamitsu, S, Ueda, K, Suzuki, H, and Sugiyama, Y. Prediction of pharmacokinetic alterations caused by drug–drug interactions: metabolic interaction in the liver. *Pharmacol Rev* 50:387–411, 1998.
  106. Davit, B, Reynolds, K, Yuan, R, Ajayi, F, Conner, D, Fadiran, E, Gillespie, B, Sahajwalla, C, Huang, SM, and Lesko, LJ. FDA evaluations using in vitro metabolism to predict and interpret in vivo metabolic drug–drug interactions: impact on labeling. *J Clin Pharmacol* 39:899–910, 1999.
  107. Johnson, J, and Van Buskirk, G. Analytical method validation. *J Validation Tech* 2:88–105, 1996.
  108. Kronbach, T. Bufuralol, dextromethorphan, and debrisoquine as prototype substrates for human P450IID6. *Meth Enzymol* 206:509–517, 1991.
  109. Gorksi, JC, Jones, DR, Wrighton, SA, and Hall, SD. Characterization of dextromethorphan *N*-demethylation by human liver microsomes: contribution of the cytochrome P450 3A (CYP3A) subfamily. *Biochem Pharmacol* 48:173–182, 1994.
  110. McIntyre, CJ, Madan, A, and Parkinson, A. Investigation of the role of CYP2B6 in the *N*-demethylation of dextromethorphan by human liver microsomes. *ISSX Proceedings* 10:231, 1996.

111. Pearce, R, Greenway, D, and Parkinson, A. Species differences and interindividual variation in liver microsomal cytochrome P450 2A enzymes: effects on coumarin, dicumarol, and testosterone oxidation. *Arch Biochem Biophys* 298:211–225, 1992.
112. Yamazaki, H, Mimura, M, Sugahara, C, and Shimada, T. Catalytic roles of rat and human cytochrome P450 2A enzymes in testosterone 7 alpha- and coumarin 7-hydroxylations. *Biochem Pharmacol* 48:1524–1527, 1994.
113. Thummel, KE, and Wilkinson, GR. In vitro and in vivo drug interactions involving human CYP3A. *Annu Rev Pharmacol Toxicol* 38:389–430, 1998.
114. Ekins, S, VandenBranden, M, Ring BJ, Gillespie, JS, Yang, TJ, Gelboin, HV, and Wrighton, SA. Further characterization of the expression in liver and catalytic activity of CYP2B6. *J Pharmacol Exp Ther* 286:1253–1259, 1998.
115. Poulsen, LL, Hyslop, RM, and Ziegler, DM. *S*-oxygenation of *N*-substituted thioureas catalyzed by the pig liver microsomal FAD-containing monooxygenase. *Arch Biochem Biophys* 198:78–88, 1979.
116. Madan, A, Parkinson, A, and Faiman, MD. Role of flavin-containing monooxygenases and P450 enzymes in the sulfoxidation of *S*-methyl *N,N*-diethylthiolcarbamate. *Biochem Pharmacol* 46:2291–2297, 1993.
117. Serabjit, CS. Non-P450-dependent metabolism. In: *A Primer of Drug Metabolism, Pathology and Toxicology in the Non-Clinical Safety Assessment of New Pharmaceuticals*. Arlington, VA: Pharmaceutical Education and Research Institute, 1999, section 13b.
118. Kaderlik, KR, Poulsen, LL, and Ziegler, DM. Studies on the mechanism for the thermal inactivation of hog liver flavin containing monooxygenase. *Progress Pharmacol Clin Pharmacol* 8:47–55, 1990.
119. Pearce, RE, Coulter, CJ, Madan, A, Sanzgiri, U, Draper, AJ, Bullock, PL, Cook, DC, Burton, LA, Latham, JL, Nevins, CJ, and Parkinson, A. Effects of freezing, thawing and storing human liver microsomes on cytochrome P450 activity. *Arch Biochem Biophys* 331:145–169, 1996.
120. Sharer, JE, and Wrighton, SA. Identification of the human cytochrome P450 involved in the in vitro oxidation of antipyrine. *Drug Metab Dispos* 24:487–494, 1996.
121. Pearce, RE, Rodrigues, AD, Goldstein, JA, and Parkinson A. Identification of the human P450 enzymes involved in the metabolism of lansoprazole. *J Pharmacol Exp Ther* 277:805–816, 1996.
122. Madan, A, and Parkinson, A. Characterization of the NADPH-dependent covalent binding of [<sup>14</sup>C]-halothane to human liver microsomes: a role for CYP2E1 at low substrate concentrations. *Drug Metab Dispos* 24:1307–1313, 1996.
123. Madan, A, Parkinson, A, and Faiman, MD. Identification of the human and rat P450 enzymes responsible for the sulfoxidation of *S*-methyl *N,N*-diethylthiolcarbamate (DETC-Me): the terminal step of disulfiram bioactivation. *Drug Metab Dispos* 23: 1153–1162, 1995.
124. Madan, A, Parkinson, A, and Faiman, MD. Identification of the human and rat P450 enzymes responsible for the sulfoxidation and thiono-oxidation of diethyldithiolcarbamate methyl ester (DDTC-Me). *Alcohol Clin Exp Ther* 22:1212–1219, 1998.

125. Yumibe, N, Huie, K, Chen, KJ, Snow, M, Clement, RP, and Cayen, MN. Identification of human liver cytochrome P450 enzymes that metabolize the non-sedating antihistamine loratadine. *Biochem Pharmacol* 51:165–172, 1996.
126. Newton, DJ, Wang, RW, and Lu, AYH. Cytochrome P450 inhibitors—evaluation of specificities in the in vitro metabolism of therapeutic agents by human liver microsomes. *Drug Metab Dispos* 23:154–158, 1995.
127. Chang TKH, Gonzalez, FJ, and Waxman, DJ. Evaluation of triacetyloleandomycin,  $\alpha$ -naphthoflavone and diethylthiocarbamate as selective chemical probes for inhibition of human cytochromes P450. *Arch Biochem Biophys*. 311:437–442, 1994.
128. Rodrigues, AD, Kukulka, MJ, Surber, BW, Thomas, SB, Uchic, JT, Rotert, GA, Michel, G, Thomekromer, B, and Machinist, JM. Measurement of liver microsomal cytochrome-P450 (CYP2D6) activity using [*O*-methyl-*C*-14] dextromethorphan. *Anal Biochem* 219:309–320, 1994.
129. Rodrigues, AD. Use of in vitro human metabolism studies in drug development—an industrial perspective. *Biochem Pharmacol*. 48:2147–2156, 1994.
130. Halpert, JR. Structural basis of selective cytochrome P450 inhibition. *Annu Rev Pharmacol Toxicol* 35:29–53, 1995.
131. Bourrié, M, Meunier, V, Berger, Y, and Fabre, G. Cytochrome P450 isoform inhibitors as a tool for the investigation of metabolic reactions catalyzed by human liver microsomes. *J Pharmacol Exp Ther* 277:321–332, 1996.
132. Gelboin, HV, Krausz, KW, Gonzalez, FJ, and Yang, TJ. Inhibitory monoclonal antibodies to human cytochrome P450 enzymes: a new avenue for drug discovery. *TIPS* 20:432–438, 1999.
133. Stresser, DM, and Kupfer, D. Monospecific antipeptide antibody to cytochrome P-450 2B6. *Drug Metab Dispos* 27:517–525, 1999.
134. Äbelö, A, Andersson TB, Bredberg, U, Skånberg, I, and Weidolf, L. Stereoselective metabolism by human liver CYP enzymes of a substituted benzimidazole. *Drug Metab Dispos* 28:58–64, 2000.
135. Crespi, CL, Code EL, Penman, BW, and Waxman, DJ. An activity-based method for integrating metabolism data from cDNA-expressed cytochrome P450 enzymes to the balance of enzymes in human liver microsomes. *ISSX Proceedings* 8:40, 1995.
136. Rendic, S, and Di Carlo, FJ. Human cytochrome P450 enzymes: a status report summarizing their reactions, substrates, inducers and inhibitors. *Drug Metab Rev* 29:413–580, 1997.
137. Wirz, B, Valles, B, Parkinson, A, Madan, A, Probst Alessandro, Zimmerlin, A, and Gut, J. CYP3A4 and CYP2A6 are involved in the biotransformation of Letrozole (©FEMARA). *ISSX Proceedings (7th North American ISSX Meeting, San Diego, CA)* 10:49, 1996.
138. Robertson, P, Madan, A, Carroll, K, Mudra, D, Heyn, H, Stong, D, and Parkinson, A. In vitro inhibition and induction of human hepatic cytochromes P450 by modafinil (Provigil). 12th International Symposium on Microsomes and Drug Oxidation (Montpelleir, France), 1998.
139. Nakajima, M, Suzuki, M, Yamaji, R, Takashina, H, Shimada N, Yamazaki, H, and Yokoi, T. Isoform selective inhibition and inactivation of human cytochrome P450s by methylenedioxyphenyl compounds. *Xenobiotica* 29:1191–1202, 1999.
140. Soohoo, D, Van Natta, KL, and Carlson, TJ. Potent and selective mechanism-based



- inhibition of CYP2D6 by RO115-1954. ISSX Proceedings (9th North American ISSX Meeting, San Diego, CA) 15:130, 1996.
141. Yamazaki, H, and Shimada, T. Comparative studies of in vitro inhibition of cytochrome P450 3A4-dependent testosterone 6 $\beta$ -hydroxylation by roxithromycin and its metabolites, troleandomycin, and erythromycin. *Drug Metab Dispos* 26:1053–1057, 1998.
  142. Parkinson, A, Thomas, PE, Ryan, DE, and Levin, W. The in vivo turnover of rat liver microsomal epoxide hydrolase and both the apoprotein and heme moieties of specific cytochrome P-450 isozymes. *Arch Biochem Biophys* 225:216–236, 1983.
  143. Shiraki, H, and Guengerich, FP. Turnover of membrane proteins: kinetics of induction and degradation of seven forms of rat liver microsomal cytochrome P-450, NADPH-cytochrome P-450 reductase, and epoxide hydrolase. *Arch Biochem Biophys* 235:86–96, 1984.
  144. Buters, JT, Schiller, CD, and Chou, RC. A highly sensitive tool for the assay of cytochrome P450 activity in rat, dog and man: direct fluorescence monitoring of the deethylation of 7-ethoxy-4-trifluoromethylcoumarin. *Biochem Pharmacol* 46: 1577–1584, 1993.

# 8

## The Role of P-Glycoprotein in Drug Disposition: Significance to Drug Development

**Matthew D. Troutman**

*University of North Carolina, Chapel Hill, North Carolina*

**Gang Luo and Liang-Shang Gan**

*DuPont Pharmaceuticals Company, Newark, Delaware*

**Dhiren R. Thakker**

*University of North Carolina, Chapel Hill, North Carolina*

### I. INTRODUCTION

The most preferred route of administration for low-molecular-weight conventional drugs is oral administration. Among the important questions that must be asked in the course of drug development is how well the compound is orally absorbed and what factors affect this parameter. The intestine is far from a passive barrier to drug absorption as was once thought. The intestine contains several elements that can affect oral absorption and ultimately oral bioavailability. Some of the more important and well-documented factors include the micro-environment (e.g., pH) present at the intestinal surface, the anatomical and physiological state of the intestine, intestinal metabolism, specificity for endogenous transport systems, and specificity for efflux pumps, namely, P-glycoprotein (P-gp), whose existence in the gastrointestinal tract has been well established [1]. The importance of P-gp as a biochemical barrier has been recognized only recently. Since the recognition of its role in limiting the oral absorption of certain drugs [2–7], P-gp has emerged as an important determinant of the oral bioavailability of drug molecules. In this chapter, the structure and function of P-gp are reviewed, with

a specific emphasis on its role in all aspects of drug disposition, i.e., absorption, distribution, metabolism, and excretion. Also described are *in vitro* and *in vivo* models for studying this biochemical barrier.

P-gp was initially discovered by Juliano and Ling as a transmembrane protein that was overexpressed in Chinese hamster ovary cells treated with various chemotherapeutic agents that had become resistant to these cytotoxic drugs [8,9]. In several cancerous tissues, overexpression of this protein is often associated with conferring the multidrug-resistance (MDR) phenotype that involves the removal of a variety of structurally unrelated compounds from within cells. The discovery of P-gp can certainly be considered a milestone in biomedical science. This finding has helped scientists elucidate one of the more active mechanisms involved in the multidrug-resistance phenotypes so often seen in refractory cancers. More recently, it has been recognized that P-gp is constitutively expressed in many normal tissues, namely, epithelial and endothelial barrier tissues, where it provides a biochemical mechanism to modulate the trafficking of endogenous compounds and xenobiotics across these barriers.

Extensive studies have been carried out to further understand the structure and function of P-gp. These include isolation of its isoforms from human, mouse, rat, hamster, and pig; identification of its tissue specific expression; elucidation of protein structure; recognition of its physiological function and impacts on clinical drug therapy; validation of laboratory assays to determine its activity; and development of various *in vitro* and *in vivo* models to demonstrate P-gp based drug-drug interactions. It is currently thought that P-gp's primary physiological role involves the protection of the cell from foreign cytotoxic compounds. The substrate specificity of P-gp is quite broad: It mediates secretion of steroid hormones, blocks intestinal absorption and brain entry of foreign compounds, accelerates elimination of xenobiotics, and extrudes toxins out of cells [1,10,11]. Thus, it should not be difficult to understand that P-gp affects drug absorption, distribution, metabolism, and excretion; this, in turn could lead to unexpected changes in exposure to therapeutic agents and their efficacy and/or toxicity. In this chapter, we will expand on the role played by P-gp in altering drug disposition, with particular emphasis on the methodologies used to assess it (see also Chap. 5).

## II. P-GLYCOPROTEIN AND RELATED TRANSPORTERS

### A. Nomenclature

Genetic analysis has revealed the existence of multiple mammalian MDR genes [12]. Members of the MDR gene family can be divided into three classes (Table 1) based on the sequence homology [13]. In humans, the genes are denoted

**Table 1** Nomenclature and Function of Mammalian P-Glycoprotein Gene Family

Species	Member	Function	Refs.
Human	MDR1 (ABCB1) <sup>a</sup>	Multidrug resistance	14,15
	MDR2/3 (ABCB4) <sup>a</sup>	Phosphatidylcholine translocation	16,17
Mouse	mdr3 (mdr1a)	Multidrug resistance	18–20,26
	mdr1 (mdr1b)	Multidrug resistance	
	mdr2	Phosphatidylcholine translocation	
Rat	mdr3	Multidrug resistance	27
	mdr1	Multidrug resistance	21
	mdr2	Phosphatidylcholine translocation	
Hamster	pgp1	Multidrug resistance	12,13,22,227
	pgp2	Multidrug resistance	
	pgp3	Phosphatidylcholine translocation	

<sup>a</sup> In the new nomenclature system, human MDR1 and MDR2/3 are named ABCB1 and ABCB4, respectively. Readers are referred to the following web site: <http://www.gene.ucl.ac.uk/users/hester/abc.html>.

MDR1 (class I) [14,15] and MDR3 (class III) [16,17]. In mice, the genes are denoted mdr3 (mdr1a, class I), mdr1 (mdr1b, class II), and mdr2 (class III) [18–20]. In rats, the genes are denoted as mdr3 (class I), mdr1 (class II), and mdr2 (class III) [21]. In hamsters, these genes are named pgp1 (class I), pgp2 (class II), and pgp3 (class III) [13,22]. In pigs, five members of the P-gp superfamily have been identified: four class I genes and one class III gene [23].

It has been shown experimentally that only the class I and class II (human MDR1, rodent mdr3 and mdr1) confer the multidrug-resistance phenotypes [15,18,20,24,25]. The human MDR3 and rodent mdr2 genes encode a protein expressed in the bile canalicular membrane that translocates phosphatidylcholine from the inner to the outer leaflet of this membrane [26,27]. In this chapter, only the gene products conferring the multidrug-resistance phenotype will be discussed, because these proteins are implicated in drug disposition.

## B. Expression In Vivo

P-gp is constitutively expressed in nearly all barrier tissues. Techniques involving Northern blots [28] or Western blots with monoclonal antibodies such as C219 [29] and MRK 16 [30] have been used extensively to determine the tissue distribution of P-gp. It is highly expressed in adrenal cortex [1], kidney, liver, intestine, and pancreas [29,31,32], endothelial cells at blood–tissue barriers, namely, the central nervous system, the testis, and the papillary dermis [29,33,34]. P-Glyco-

protein displays specific subcellular localization in epithelial cells with a polarized excretion or absorption function. More specifically, P-gp is found at the apical canalicular surface of hepatocytes, in the apical membrane of the columnar epithelial cells of colon and intestine [1], and at the apical brush border of the renal proximal tubule epithelium [35].

### C. Expression In Vitro

Expression of P-gp has been demonstrated in some cell lines, such as Caco-2 [36–38], Madine–Darby canine kidney (MDCK) cells [39–41], and LS180/AD50 cells [42]. There are some reports that P-gp expression in the cell lines can be induced with chemicals such as vinblastine [38], reserpine, rifampicin, and many others [42]. Overexpression of P-gp has frequently been observed in certain untreated tumors, derived from tissues known to normally express P-gp at a high level. P-gp overexpression has not been observed in all tumors though; for example, P-gp was not detected in breast carcinomas, endometrial carcinoma, or melanoma derived from tissues known not to express P-gp [29].

### D. Physiological Functions

The tissue-specific expression and cellular localization of P-gp has provided some insight regarding its physiological function and roles in pharmacology. Several likely physiological functions of P-gp have been postulated by Borst and Schinkel [43], Borst and associates [44], and Lum and Gosland [45]: (1) P-gp protects against the entry of exogenous toxins ingested with food, evidenced by expression in small intestine, colon, and blood–tissue barrier sites. It extrudes toxic compounds from the central nervous system and testis [33,34]. The literature is replete with examples of P-gp-mediated efflux from barrier-forming cells. (2) P-gp excretes toxins or metabolites, as evidenced by its expression in liver canalicular membrane and kidney; for example, rat liver canalicular membrane vesicles actively transport daunomycin [46]. Recently, evidence has been presented to show how P-gp-mediated efflux can make the intestine an important organ of drug elimination [5–7]. (3) P-gp transports steroid hormones; P-gp is expressed in adrenal gland, and it was demonstrated that it transports cortisol, corticosterone, and aldosterone [10]. (4) P-gp extrudes polypeptides, as seen by the ability of P-gp to efflux cyclosporin A and tacrolimus [47,48]. (5) It activates endogenous chloride channel activity. P-gp itself is not a volume-sensitive chloride channel; however, P-gp has been shown to play an indirect role in chloride channel activation. It also enhances the ability of cells to down-regulate their volume through modulation of volume sensitivity of the chloride channel in a manner independent of its ATPase activity [49,50].

## E. P-Glycoprotein–Related Transporters

### 1. Multidrug Resistance–Associated Proteins (MRPs)

In addition to P-gp, MDR-associated protein (MRP) plays an important role in multidrug resistance of cancer therapy, and affects the behavior of other drug substrates. MRP1 is a member of a relatively large protein family consisting of at least six members—MRP1, MRP2, MRP3, MRP4, MRP5, and MRP6 [51,52]—each with diverse specificities, structure, and function. MRP2, also called canalicular membrane organic anion transporter (cMOAT), is highly expressed in canalicular membrane and plays a critical role in biliary excretion of organic anionic compounds [51–55]. MRP1 consists of 1531 amino acid residues, with a molecular weight of 190 kDa. Like P-gp, MRP1 is glycosylated posttranslationally (at two sites, versus one site seen for P-gp), and thus the actual molecular weights are greater than those predicted from the primary sequences of amino acid residues. The amino acid sequences for P-gp and MRP1 show only 15% similarity [11]. Other differences in their protein structure include different numbers of transmembrane segments (12 for MDR1 and 17 for MRP1) and different orientation of their N-termini [see Table 2 for comparison of P-gp (MDR1) and MRP1].

The differential expression of MDR1 and MRP1 in various tissues suggests that they may have different physiological functions and that they play different roles in the pharmacology and toxicology of their substrates. P-gp is expressed in the apical membranes of certain normal human tissue cells and in tumor cells, as described earlier. Pharmacologically, P-gp plays a role in preventing intestinal drug absorption and brain entry, and in eliminating drugs by excretion into bile and urine. MRP1 is extensively expressed in lung (bronchial epithelia), bladder, spleen, and testes (haploid spermatid), but to a lesser extent in kidney, stomach, liver, and colon [56–58]. Unlike P-gp, MRP1 is localized to the basolateral membranes of cells [59].

Both P-gp and MRP1 exhibit broad but different spectrums of substrate specificity. Generally speaking, P-gp transports hydrophobic compounds and MRP1 effluxes hydrophilic chemicals. For example, P-gp transports hydrophobic molecules that often possess a positive charge, a nitrogen group, and an aromatic group; whereas MRP1 has been shown to transport heavy metal oxyanions, glutathione conjugates, glucuronide conjugates, and sulfate conjugates (the reader is cautioned that these are very general characteristics of P-gp and MRP1 substrates, and numerous deviations exist in each case). Despite their very different substrate selectivity, they do exhibit some overlap in their activity toward some substrates. As listed in Table 2, verapamil, cyclosporin A, doxorubicin, vincristine, and tamoxifen are examples of substrates that can be readily effluxed by both MDR1 and MRP1.

**Table 2** Comparison of Human MDR1 Gene Product and MRP1

	MDR1	MRP1
Family members	MDR1 and MDR3	MRP1, MRP2, MRP3, MRP4, MRP5, MRP6
Protein Chemistry		
Amino acid residues	1,280	1,531
Molecular weight (kDa)	~170	~190
Glycosylation sites	1	2
Transmembrane segments	12	17
Extracellular N-terminus	No	Yes
Molecular Biology		
Locus on chromosome	7q21.1	16p13.12-13
Gene expression		
In normal tissues	Adrenal cortex, liver, kidney, intestine, brain, testes, placenta, lymphocytes	High in lung, bladder, spleen, thyroid, testes, adrenal gland, low in kidney, stomach, liver, colon
In tumor tissues	High in colon, renal, and adrenal carcinomas, rarely in lung and gastric carcinomas	
Substrates and Inhibitors		
Calcium channel blockers (verapamil)	Yes	Yes
Immunosuppressants (cyclosporin A)	Yes	Yes
Anthracycline (doxorubicin)	Yes	Yes
Vinca alkaloids (vincristine)	Yes	Yes
Calmodulin antagonists (trifluoperazine)	Yes	Yes
Toxic peptides (valinomycin)	Yes	Yes
Steroids (tamoxifen)	Yes	Yes
Glucuronide conjugates	No	Yes
Glutathione conjugates	No	Yes
Sulfate conjugates	No	Yes
Others		
Colchine	Yes	No
Taxol	Yes	No
Heavy metal oxyanions	No	Yes
Specific inhibitors	PSC833, GF120918	Genestein

## 2. Sister of P-Glycoprotein (SPGP)

SPGP, a 160-kDa ABC transport protein, is closely related to the P-gp family. Recent results have suggested that SPGP is the major canalicular bile salt export pump expressed in mammalian liver [60]. The expression of SPGP (determined by RT-PCR) is high in the liver, and significant in the brain grey cortex and large-gut mucosa [61]. Unlike P-gp, SPGP has presently not been detected in the kidney or the blood–brain barrier [61]. The subcellular distribution of SPGP in the liver (determined by immunofluorescence and immunogold-labeling experiments) appears to be localized to the canalicular microvilli and to subcanalicular vesicles [62]. SPGP appears to be important in the biliary secretion of taurocholate, taurochenodeoxycholate, tauroursodeoxycholate, glycocholate, and cholate [62].

Although SPGP is related to P-gp, its substrate specificity is different. The actions of SPGP on several known P-gp substrates were examined by expressing SPGP cDNA in LLC-PK1 and MDCKII cells. Cells expressing SPGP displayed decreased uptake of taurocholate and vinblastine compared to control cells, and the accelerated efflux of vinblastine was observed in the cells [63]. SPGP has no effect on the uptake of the P-gp substrates vincristine, daunomycin, paclitaxel, digoxin, and rhodamine 123, but does efflux calcein acetoxymethyl ester (calcein-AM) [63]. The transport of calcein-AM via SPGP-mediated efflux was not inhibited by the P-gp inhibitors cyclosporin A or reserpine, but transport was inhibited by ditekiren (a linear hexapeptide) [63]. The involvement of this protein in drug transport has only recently been explored, and its role in drug elimination will become clearer as more studies are performed to address the significance of SPGP-mediated efflux of drugs.

## III. BIOCHEMISTRY OF P-GLYCOPROTEIN

### A. Protein Structure and Transport

P-Glycoprotein is as a member of the superfamily of transporters known as ATP binding cassette transporters, or ABC transporters. To date, more than 200 membrane transporters have been identified as members of the ABC transporter family [64]. Some of the better-known members of this family include the sodium potassium ATPase, the calcium ATPase, and the outwardly rectifying chloride ion channel, CFTR [64]. Certainly, as biochemical and molecular biology methods improve, the list of known ABC transporters is likely to grow even further. All ABC transporters have a similar architectural plan comprising four major domains: two membrane-bound domains, each with six transmembrane segments, and two cytosolic ATP-binding motifs, commonly known as the Walker A and B domains, that bind and hydrolyze ATP (also known as the nucleotide-binding



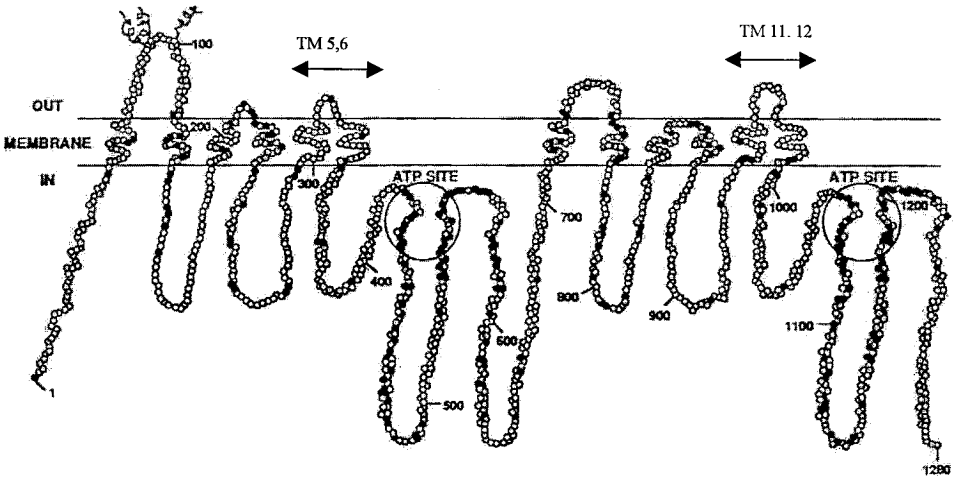


**Figure 1** Model of human P-glycoprotein derived from sequence analysis. Transmembrane domains 5, 6, 11, and 12 are thought to compose the binding site(s). (From Refs. 22, 67.)

domains, or NBDs) (see Fig. 1). All four domains of mammalian P-gp are encoded by one gene, as opposed to being constructed from the subunits derived from several genes [65]. Although attempts to extrapolate the information known about some of the well-characterized ABC transporters to P-gp have met with mixed results, some basic elements are conserved for all of these ABC transporters. Indeed, there exists a high degree of homology among many of these transporters, and certain structural features are conserved between highly related members of the family (most notably between the NBDs). The most significant differences come mainly from the substrate-binding region, which will be discussed in detail later.

The human MDR1 gene product (P-gp) is a protein consisting of 1,280 amino acid residues with a large degree of homology between a carboxy terminal half and an amino terminal half [14,66]. Each of the homologous halves contains a hydrophobic membrane-associated domain, consisting of approximately 300 amino acids, and a hydrophilic nucleotide-binding domain, also consisting of approximately 300 amino acids [66–69]. Chemotherapeutic drugs or chemosensitizers do not inhibit ATP binding, suggesting that separate ATP- and drug-binding sites exist (see Fig. 1) [66].

P-gp is synthesized as a nonglycosylated precursor with a molecular weight of 120–140 kDa. The protein is processed to the mature glycosylated form with a half-life of 1–2 hr in humans and 20–30 min in rodents. The mature form of P-gp has a molecular size ranging between 160–180 kDa, depending on the cell

type and species [70,71]. The first extracellular loop of P-gp contains N-linked carbohydrate moieties that do not appear to be important in protein function or ATPase activity [70–77]. It has been postulated that the carbohydrate moiety, rather than participating in P-gp-mediated efflux activity, contributes to the proper folding and routing of P-gp. It has been further proposed that this glycosylation may confer stability to the protein as it is transported to the plasma membrane and further stability within the plasma membrane [77]. This hypothesis has been supported with experiments in which tunicamycin treatment (tunicamycin prevents posttranslational N-linked glycosylation of proteins) of colon cancer cells resulted in reduced levels of cell-surface-associated P-gp. These results suggest that glycosylation is important for effective translocation of P-gp to the plasma membrane [78]. This finding was further supported by mutational analysis in which one or all of the N-linked glycosylation sites in the first extracellular loop were deleted. These deletions resulted in unaltered protein activity but less P-gp expression at the membrane [78].

Functional P-gp is phosphorylated by multiple kinases, including protein kinase A (PKA), protein kinase C (PKC), and perhaps a serine threonine kinase. Despite the presence of multiple consensus sites for PKA and PKC phosphorylation distributed throughout the primary structure of human P-gp, only a cluster of maximally four serine residues is phosphorylated by kinases. These serine residues are all located in a central cytosolic linker region that connects the homologous halves of P-gp [79,80]. Efforts have been made to associate the degree of phosphorylation with the drug efflux activity, much the way CFTR activity is regulated by varying degrees of phosphorylation [79]. It has been postulated that inhibiting phosphorylation would inactivate P-gp and thus reverse the MDR phenotype it confers. The results of several experiments studying the effects of phosphorylation of P-gp have been unclear. Indeed, some experiments have shown that P-gp in different phosphorylation states has different efflux activity; however, some of the compounds used to inhibit or promote phosphorylation were shown to upregulate P-gp at the transcriptional and translational levels [79,80]. Recently, evidence has been presented to refute the claims that phosphorylation state determines efflux activity [81].

Several early hypotheses have suggested that the broad substrate specificity of P-gp was the result of P-gp's ability to change physical parameters of the surrounding medium, such as modifying pH or influencing the osmotic gradient similar to a chloride ion channel or an ATP channel [64,82,83]. These models were also used to rationalize the high apparent basal ATPase activity of P-gp. Whole-cell patch-clamp experiments aimed at following the flux of chloride ions with human intestinal cells that constitutively expressed P-gp and with those that did not (expression blocked by treatment with antisense oligonucleotides) have provided definite evidence that P-gp is not a chloride channel. It was shown that (1) the magnitude of chloride current activated by osmotic swelling was identical for both sets of cells, (2) antibodies to P-gp had no effect on chloride channel

activity, and (3) the P-gp inhibitor verapamil and the P-gp substrates daunomycin and vincristine did not affect the chloride current [84]. Based on these results, it was concluded that P-gp itself is not a volume-sensitive chloride channel in these human small intestinal epithelial cells [84]. Multiple studies have provided significant evidence that P-gp directly effluxes its substrates in the manner of a primary ATPase [64]. The most convincing evidence comes from the studies with acetoxymethyl esters of fluorescent dyes, fluorescently labeled daunorubicin, and the measurement of structural changes associated with substrate efflux [64,66,85].

Both the N- and C-terminal halves must be present for drug transport to occur [86]. Further, it has been shown that both halves must be present and acting in a cooperative manner for optimum activity [86]. Indeed, both halves independently show basal ATPase activity, but coupling of drug binding to increased ATPase activity is observed only when both halves of the protein are expressed [87].

Several studies have been performed to identify the specific regions involved in drug transport. Based on mutational deletions and insertions, a model has been proposed by Gottesman et al. in which the transmembrane segments 5, 6, 11, and 12 come together with the two NBDs to form the drug-binding region [88]. Photoaffinity labeling with azidopine or azidoprazosin shows that the binding site is located in two regions, TM 5 and 6, and TM 11 and 12 [67,89]. This hypothesis has also been supported by a mutational analysis done by Loo and Clark in which two cysteine residues were introduced into transmembrane segments 6 and 12. It was found that these residues could be oxidatively crosslinked and that this bonding could be blocked by introduction of verapamil or vinblastine, two classic P-gp substrates. This suggests that TM segments 6 and 12 are maximally 7 angstroms apart in the tertiary structure of P-gp [64,67,89,90]. Loo and Clark have also identified important point mutations in transmembrane segment 6 that affect drug resistance profiles, and a mutation at serine 344 that results in a complete loss of function [90–92]. A single substitution of serine with phenylalanine in TM 11 had a significant effect on the substrate specificity and modulatory effects of verapamil and progesterone [93–95].

The amino acid sequence of transmembrane segments 5, 6, 11, and 12, which compose the binding pocket (determined with photoaffinity-labeling experiments with azidopine and azidoprazosin) contain several aromatic side chains shown to be important in binding and transport of substrates [89,96]. P-gp contains a high amount of aromatic amino acids compared to other ABC transporters, and these residues are highly conserved across species [97]. The presence of aromatic and hydrophobic amino acid residues in the binding region of P-gp is thought to comprise a hydrophobic channel that provides binding sites for hydrophobic molecules with P-gp. This channel reduces the interactions of P-gp's hydrophobic substrates with the lipid bilayer, making the transport of these substrates across the membrane more favorable [68]. Using molecular modeling, Pagawi et al. [98] have presented evidence to show how aromatic amino acid

side chains play a role in the binding and transport of drugs by P-gp. These researchers demonstrated how rhodamine 123 could readily intercalate between several phenylalanine side chains contained in transmembrane helices 5, 6, 11, and 12 [98]. They proposed that the transport path followed by P-gp substrates may involve an internal channel lined by aromatic amino residues facing the inside of the helices. The compounds may interact with the protein via gaps between externally oriented aromatic side chains at interfaces between the transmembrane helices and the surrounding lipid [98]. The proposed involvement of several aromatic rich helices (located in the binding region, TMs 5, 6, 11, 12) in drug binding and transport gives P-gp the conformational flexibility needed to interact with several chemically unrelated substrates of various sizes and shapes [97].

These results have led to the most widely accepted current hypothesis, which states that amino acid residues of both N- and C-terminal halves of P-gp interact and cooperate to form one major drug interaction pore [68,89]. This model allows for multiple sites for drug recognition, and rationalizes the finding that different classes of drugs bind to different, possibly allosterically coupled regions within P-gp [64,100–102]. Recent evidence has shown that P-gp-mediated efflux activity toward certain compounds can be increased in the presence of other P-gp substrates, perhaps by some unknown allosteric mechanism. By using isolated P-gp-containing plasma membrane vesicles from Chinese hamster ovary cells, the kinetics of transport of rhodamine 123 and Hoechst 33342 were determined under various conditions. It was found that each substrate stimulated the transport of the other [103]. Additionally, it was found that colchicine and quercetin stimulated rhodamine 123 efflux and inhibited Hoechst 33342 transport [103]. Anthracyclines were found to have the opposite effect, as the P-gp-mediated efflux of Hoechst 33342 was increased in the presence of these compounds, whereas that of rhodamine 123 was decreased [103]. These results have supported early reports that a wide range of flavonoids, including quercetin, increased the P-gp-mediated efflux of adriamycin from HCT-15 colon cells and 7,12-dimethylbenz(a)anthracene from breast cancer cells possessing the MDR phenotype [104,105].

## B. Substrate Transport Models

It is becoming increasingly clear that P-gp does not act like a classical transporter; more specifically, P-gp is not enzyme-like. Transporters that act to aide hydrophilic molecules in crossing the membrane bilayer bind the substrate like an enzyme, which results in a conformational change and the resulting transport activity of the transmembrane protein. The structural parameters that promote interactions of the compounds with the binding site of the proteins constitute the most important factors in determining whether or not a compound may be a substrate for these types of carriers. P-gp also interacts with its substrates, like

other ABC transporters; but unlike most transporters that have been studied to date, P-gp can bind to its substrates while they are associated with the plasma membrane. By use of fluorescent dye esters it has been shown that P-gp interacts with its substrates within the plasma membrane, from both the inner and the outer leaflet. As these dyes cross the membranes, esterases quickly hydrolyze these compounds to their free acid forms that accumulate in the cytoplasm. Multidrug-resistance cells showed no accumulation of these dyes in the cytoplasm, clearly illustrating that P-gp can efflux substrates directly from the membrane [85]. Therefore, the behavior of the compound within the lipid bilayer becomes important in determining how P-gp acts to efflux its substrates. Two hypotheses currently exist to explain this phenomena and to rationalize some of the discrepancies seen between the efflux action of P-gp and the action of other ABC transporters. Both hypotheses present new views of transporter action, quite different from the classical enzyme-like mechanism used to describe several other transporters.

### 1. Hydrophobic Vacuum Cleaner Model

Higgins and Gottesman have postulated that P-gp acts as a hydrophobic vacuum cleaner, clearing the plasma membrane of substrates before they enter the cytoplasm [67,106]. This hypothesis serves to explain two deviations from the classical transporter model. First, by acting to remove substrates directly from the membrane, the primary determinant of substrate specificity is the ability of the drug to interact with the plasma membrane, and the secondary determinant would be the ability of the drug to interact with the protein itself. This serves to explain the broad substrate specificity of P-gp and to explain why nearly all P-gp substrates are lipophilic. The second deviation is often associated with the kinetics of transport. It is usually quite difficult to correlate the initial rate of drug efflux with drug concentration in MDR cells. The vacuum cleaner model hypothesizes that the actual concentration seen by the transporter would not correspond to the concentration of drug used in the experiment, but actually would depend on both the ability of the drug to partition into the lipid bilayer as well as the lipid composition of the membrane [67,106]. Indeed, changes in the membrane fluidity have been shown to alter the drug transport via P-gp in rat CMV cells [107].

### 2. Flippase Model

A second widely accepted model builds on the vacuum cleaner model to explain how P-gp actually translocates substrates. It has been proposed that P-gp acts like a flippase to “flip” substrates from the inner leaflet to the outer leaflet or aqueous space [106]. According to this model, the concentration of the substrate in the outer leaflet and the extracellular space is in equilibrium. There also exists an equilibrium between the inner leaflet and the cytoplasm; and finally an equilibrium exists between the leaflets of the plasma membrane. The pump would create

a gradient by flipping the substrate from the inner to the outer leaflet and thus force the substrate to partition from the outer leaflet into the extracellular space.

The large degree of homology (75%) seen between the MDR1 and MDR3 gene products has led to the formulation of hypotheses aimed at correlating the functional activity of these two structurally related proteins [108]. It has been shown that the MDR3 gene product is able to translocate phosphatidylcholine from the apical surface of the canalicular membrane into the bile [17]. Recent studies have shown that like MDR3 P-gp, MDR1 P-gp can also translocate short-chain derivatives of phospholipids from the inner to the outer leaflet of epithelial cells [108], and it is quite possible that MDR1 P-gp may translocate drug substrates in a similar manner.

These hypotheses provide a framework for developing a more refined understanding regarding the mechanism of action of P-gp. It is clear that additional factors need to be considered to fully understand the interactions between substrates and P-gp as well as the mechanism by which the substrates are pumped out when they bind to the protein. Given that P-gp effluxes its substrates directly from the plasma membrane, it is clear that understanding the behavior of drugs in membranes is critical.

### **C. Relationship Between P-Glycoprotein, the Membrane Environment, and the Structure of Substrates/Inhibitors**

It is well established that the substrate specificity of P-gp is quite broad with respect to both chemical structure and size. The structural diversity of P-gp substrates (and inhibitors) is so broad that it is difficult to define specific structural features that are required for the substrates/inhibitors of P-gp. However, some of the properties that are shared by many P-gp substrates include the presence of a nitrogen group, aromatic moieties, planar domains, large molecular size (>300), often the presence of a positive charge at physiological pH, amphipathicity, and lipophilicity. In attempts to further elucidate the criteria for P-gp efflux, several researchers have developed structure–activity relationships; this information is available in Ref. 109–115.

P-gp functional activity has been shown to be intimately related to both the chemical composition and the physical state of the membrane. P-gp, reconstituted into lipid vesicles, displays a dependence on the phospholipid composition of the vesicles for catalytic activation [97]. It was also shown that the NBDs, which are thought to reside in the cytoplasm, are also dependent on the phospholipid environment and the resulting phase of the lipid bilayer [97]. Contrary to other membrane transporters, P-gp binds ATP with higher affinity when the membrane is in the gel state [97]. Furthermore, P-gp also causes the efflux of drugs more efficiently in gel-phase membranes versus liquid crystalline–phase mem-

branes [97]. Membrane fluidizers such as benzyl alcohol, chloroform, and diethyl ether can abolish the ATPase activity of P-gp and thus render the pump ineffective at removing substrates from the cell [116]. It is known that epithelial cells have a specialized apical membrane composition that is composed of a 1-to-1 ratio of sphingolipids to cholesterol in the outer leaflet and nearly 1-to-1 ratio of phosphatidylcholine to cholesterol in the inner leaflet [117]. The presence of the sphingolipids in the outer leaflet makes the membrane less fluid due to the capacity of these lipids for extensive hydrogen bonding interactions [117]. It is possible that P-gp requires this specialized membrane environment for optimal activity. Because the substrates of P-gp interact with it within the membrane, the behavior of the compounds in the bilayer is as important to the substrate specificity of P-gp as their interactions with the protein. Multilamellar vesicles (MLV) and large unilamellar vesicles (LUV) have been used to measure the transbilayer movement of both MDR-type drugs and modulators [118,119]. Multidrug-resistance-type drugs were shown to cross these membranes at much lower rates than the MDR modulators [118]. These modulators act in a competitive manner to occupy P-gp by crossing the membrane as fast as or faster than efflux can occur [118]. The importance of the membrane environment on substrate specificity has been clearly illustrated by transfection of P-gp into cells with dissimilar lipid composition [106]. The relative abilities of P-gp to efflux vinblastine and daunorubicin are reversed when the efflux pump is transfected in insect cells that have different membrane compositions than mammalian cells [106].

Surfactants have been used to efficiently inhibit P-gp efflux [120,121]. These compounds could likely inhibit P-gp by some alteration of the membrane fluidity rather than by interactions with the protein. The change of membrane fluidity is thought either to increase the permeability of the compound or to alter the tertiary structure of P-gp (abolishing ATPase activity), making it less effective at effluxing compounds [116,121]. Presently, the actual mechanism is unclear, and it is possible that a combination of these effects may be contributing to the inhibitory activity.

#### IV. EXPERIMENTAL MODELS

The involvement of P-gp in the absorption and consequent distribution of orally administered xenobiotics has been extensively studied in *in vitro*, *in situ*, and *in vivo* models. Some routinely used systems include cultured cell lines, isolated intestinal segments, everted sacs, and brush border membranes. Organ (brain, liver, and kidney) perfusion and gene knockout mice have also been used. Each of these models has certain advantages and disadvantages. A brief description of the models that have been used to evaluate the role of P-gp in the disposition of drug molecules follows.

## A. In Vitro Models

### 1. Caco-2 Cells

Of the many cell types utilized to model drug behavior in the human intestine, the immortalized human colorectal carcinoma-derived cell line, Caco-2, is the most widely accepted in vitro model to date. This cell line has demonstrated several advantages over others that have made it the cell line of choice in both academia and the pharmaceutical industry [36,122–128]. Perhaps the most attractive feature of the Caco-2 cell line is the spontaneous differentiation into mature enterocytes that occurs on porous polycarbonate membranes under normal culturing conditions. Accompanying this differentiation is the expression of several biochemical and anatomical features common to normal intestinal enterocytes. Caco-2 monolayers become polarized and display a well-defined brush border membrane located in the apical domain. Due to the various enzyme and transport activities associated with the brush border, the expression of this feature in cell lines used to model intestinal enterocytes is critical. The brush border contains several transporters, metabolic enzymes, and efflux pumps, such as P-gp, whose expression is both stable and functional [2,48,129,130]. The expression of P-gp has been demonstrated by Western blot analysis and by polarized transport of P-gp substrates, such as cyclosporin A, that is reversed (i.e., polarity is abolished) by P-gp inhibitors, such as verapamil [2,36,37,48,130,131].

The function of P-gp in Caco-2 cells has been extensively evaluated with respect to various methodological factors, such as culture time and passage number. Western blot analysis demonstrated that P-gp was expressed as early as day 7 of culturing [37]. Experiments with cyclosporin-A transport showed that apical-to-basolateral transport was relatively constant from day 5 of culturing (treatment with the P-gp inhibitor verapamil significantly increased apical-to-basolateral permeability, consistent with inhibition of an apically polarized efflux mechanism) [37]. The basolateral-to-apical permeability increased until day 17, at which time this permeability became constant. These results suggest that the biochemical barrier posed by P-gp is not fully functional until day 17. This is most likely due to the amount of expression of P-gp per cell and the subsequent increase in this number to day 17. Interestingly, P-gp is functional in cytosolic vesicles released from the Golgi apparatus, suggesting that the protein does not need to be incorporated into the apical membrane to be functional [132–134].

Passage number has also been considered as a variable that may affect the amount of P-gp present in the apical brush border. Although Caco-2 cells of lower passage numbers (~22) have been shown to have a shorter doubling time than those of higher passage number (~72), resulting in an increased number of cells and, thus, an increased amount of membrane protein [131], several reports have stated that Caco-2 cells at higher passage numbers (>90) contain signifi-



cantly more P-gp than those at lower passage numbers. P-gp expression in Caco-2 cells has been shown to be stable, and this allows relatively accurate comparison of data from various monolayers as long as they represent a relatively narrow range of passage numbers.

Expression of specific proteins can be easily induced in Caco-2 cells using simple culturing techniques. For example, the induction and overexpression of cytochrome P450 3A4 (CYP3A4) was achieved by culturing the cells with  $1\alpha$ -25 dihydroxyvitamin D3 beginning at confluence, and this expression was shown to be dose and duration dependent [135]. Expression of P-gp can also be easily induced in the Caco-2 cell line by culturing with vinblastine, verapamil, or celi-prolol [38,136]. Conversely, metkephamid has been used to decrease the level of P-gp expression [136]. No morphological differences were noticed for vinblastine-cultured cells with respect to appearance, formation of tight monolayers, or transepithelial resistance [38].

## 2. Madine–Darby Canine Kidney Cells

Examples of studies involving P-gp-mediated efflux of therapeutic compounds in immortalized MDCK cells are far less numerous than those utilizing the Caco-2 cell line. Both have been used to follow the passive diffusion of compounds across monolayers. The most significant advantage the MDCK cell line has over the Caco-2 cell line is the much shorter culture time. Studies by Simons et al. have shown that these cells are polarized and contain a well-defined apical brush border membrane with a membrane composition similar to that of the intestine [117,137]. The spontaneous differentiation of MDCK into polarized cell monolayers with defined apical and basolateral domains makes studying the actions of transporters expressed in a polarized fashion facile. In addition, this cell line has also been transfected with other drug-effluxing transporters (expressed in either apical or basolateral domain) to study their effects on altering the flux of a compound as it crosses a polarized monolayer [41].

Although there is a widespread perception that wild-type MDCK cells contain insignificant levels of P-gp, it has been demonstrated that this is not the case. It was shown that the transport of vinblastine sulfate across MDCK monolayers was indeed apically polarized [39]. These results were duplicated by Hirst et al. using the same test compound, vinblastine, in two different strains of MDCK cells [40]. The transport profiles of vinblastine showed polarity in both a high-resistance strain (TEER  $\sim 2000$  ohms  $\cdot$  cm<sup>2</sup>) and a low resistance strain (TEER  $\sim 200$  ohms  $\cdot$  cm<sup>2</sup>) [40]. Recently, parallel studies were performed measuring the transport of a novel peptide, KO2 across both MDCK and Caco-2 cells. The results showed nearly identical profiles for the apical-to-basolateral and basolateral-to-apical transport of this agent in both cell types [41]. Although it is unlikely that all P-gp substrates will behave identically in both cell lines, these studies

indicate that there is sufficient P-gp expression in MDCK cells to affect transport studies. Thus, MDCK cells can be used to evaluate the transport of compounds that are suspected to be substrates of P-gp.

MDCK cells have been transfected with the cDNA encoding the multispecific organic anion transporter (cMOAT or MRP2) to further elucidate the substrate specificity and actions of this transporter. Using these transfected MDCK cells, it was shown that cMOAT can mediate the transport of vinblastine and organic anions (specifically several glutathione conjugates), and this transport was inhibited (to a small degree) by inhibitors of MRP1 [138]. The human MDR1 gene has also been transfected into MDCK cells. The expression of MDR1 gene product in these MDCK cells was shown to be nearly tenfold higher than that seen in Caco-2 cells (as determined by Western blot analysis) [41].

### 3. Brain Microvessel Endothelial Cells (BMECs)

The delivery of therapeutic agents into the central nervous system (CNS) poses a particularly difficult problem, because the transport of compounds across the very formidable barrier formed by the specialized endothelial cells lining the capillaries that perfuse the brain, the blood–brain barrier (BBB), is not easy [139,140]. The BBB is a blood–tissue barrier within the CNS that regulates the transport of nutrients into the brain and that limits exposure of the brain to toxic compounds via mechanisms such as P-gp. As is the case with the intestinal epithelium, P-gp plays an important role in limiting the transport of drugs across the BBB [141,142]. Because the primary pharmacological targets of many drugs are receptors within the CNS and because many of these drugs have been shown to be substrates for P-gp in other organs and in various *in vitro* systems, investigation of the processes surrounding the transport of compounds across the BBB (specifically the susceptibility of compounds to P-gp-mediated efflux in the BBB) remains an important area of research.

One of the most extensively used *in vitro* models to study drug behavior at the BBB are cultured brain microvessel endothelial cells (BMECs), a primary culture that forms confluent monolayers 9–12 days after initial seeding [143]. These cultured cells have been shown to retain many morphological and biochemical properties of their *in vivo* counterparts, including distinguishable luminal and abluminal membrane domains that are functionally and biochemically distinct [144–155]. One of the major advantages of BMECs is that these cells can be grown on collagen-coated or fibronectin-treated polycarbonate membranes, and thus this system can be used to study transport across the monolayer by various mechanisms (i.e., passive diffusion, transcytosis, endocytosis, inwardly directed carrier proteins, polarized efflux, and uptake in both luminal and abluminal directions) [143]. One limitation of the system is that the tight junctional complexes of BMECs are not as developed as those seen *in vivo*, and

thus the contribution of paracellular permeability to the overall permeability of a compound is much greater in this *in vitro* system than what would be seen for a compound crossing the BBB *in vivo* [156].

The expression of P-gp in the luminal membrane of BMECs cultured on polycarbonate membranes has been confirmed by both functional assays (vincristine transport [155] and rhodamine 123 transport [157]) and biochemical assays involving immunohistochemical analysis [155,158]. Additionally, the expression of P-gp in BMEC was shown by immunohistochemical methods to be constant and at a high level in 5–7-day-old primary cultures [158]. Like many other barrier-forming cells, BMECs appear to express other efflux proteins; for example, RT-PCR and immunoblot analysis have shown the presence of MRP1 in rat BMECs [159,160]. Functional evidence has also been presented to confirm the expression of MRP1 in BMECs [161].

The BMECs have been used to study various aspects of the P-gp-mediated efflux of compounds from the endothelial cells that comprise the BBB. Several examples have demonstrated the usefulness of this system to study polarized efflux via P-gp. For example, the influence P-gp expressed in brain capillary endothelial cells has on the transport of cyclosporin A [162,163], vincristine [155], protease inhibitors (amprenavir, saquinavir, and indinavir) [164,165], rhodamine 123 [157,166], opioid peptides [166–168], and the  $\beta$ -blocking agent bunolol [169] has been determined using this system.

#### 4. Membrane Vesicles

Membrane vesicles are typically formed from intact cells and require some skill for their preparation. Given this limitation, the use of membrane vesicles as a rapid screen for P-gp efflux activity has not been extensive, and has proven a better tool for studying the microscopic aspects of P-gp-mediated efflux.

Rat liver canalicular membrane vesicles (CMVs) have been used to examine the mechanisms of uptake of P-gp substrates such as daunomycin, daunorubicin, and vinblastine, whose biliary excretion is extensive [46,107,170,171]. Early work with plasma membrane vesicles, partially purified from MDR human KB carcinoma cells that accumulated [ $^3$ H]vinblastine in an ATP-dependent manner, definitively showed how P-gp can act to efflux substrates from cancer cells [172]. Additionally, these vesicles have been used to study microscopic aspects of P-gp-mediated efflux, such as the relationship of P-gp function to membrane fluidity [107].

Brush border membrane vesicles (BBMVs) prepared from the rat intestine were used to elucidate the function of P-gp in this organ and to show that the subcellular distribution of P-gp is localized to the apical membrane [173]. The differences in P-gp-mediated efflux seen in the ileum, jejunum, and duodenum rat intestine were studied by preparing BBMVs from each of these distinct regions

and then determining the Michaelis–Menten parameters,  $K_m$  and  $V_{max}$ , associated with the P-gp-mediated efflux of several substrates and inhibitors, and the corresponding ATPase activity associated with efflux [174]. Renal BBMVs have been used to show P-gp actions on its substrates in the kidney [175].

Membrane vesicles prepared from Chinese hamster ovary cells have been used to determine the kinetic parameters associated with P-gp efflux [109,112]. Factors such as the ATP hydrolysis rate associated with the transport of various substrates has been studied along with the Michaelis–Menten parameters of efflux for P-gp substrates [109,112].

## 5. Isolated Intestinal Segments

In these studies, the intestine is removed and either mounted in a diffusion apparatus (Ussing chamber) or everted to make an everted sac [176–179]. Factors affecting the transport of drugs (i.e., metabolism and efflux) can be studied by determining the fate of the test compound as it crosses the intestinal epithelium.

The transport characteristics of verapamil were determined for each region of the rat intestine as well as the colon with this model system. The duodenum and jejunum showed the most P-gp activity, followed by lower activity in the colon and, surprisingly, none in the ileum [176]. Polarized transport of quinidine due to P-gp efflux was demonstrated by using intestinal segments mounted in Ussing chambers [177]. Further studies using everted sacs showed that P-gp inhibition by quinidine caused an altered drug absorption of digoxin and explained the interaction seen with coadministration of these agents [179]. Metabolism and P-gp-mediated efflux of the macrolide antibiotic tacrolimus were studied in perfusion studies and in everted sacs [178]. It was shown that inhibiting P-gp with miconazole (a P-gp inhibitor) greatly increased the amount of tacrolimus in the tissue [178]. The results of these experiments provided evidence that P-gp is active in limiting tissue exposure to drugs and also that the intestinal metabolism of certain compounds can be significant.

## 6. Expression Systems

The availability of full-length cDNA for functional mammalian MDR genes has made it possible to evaluate protein structure and structure–activity relationships, and to determine substrate-binding affinity through the in vitro P-gp expression system. Presently, the MDR1 gene has been successfully expressed in *E. coli* [180,181], in Sf9 cells using a recombinant baculovirus [74,76], in *Xenopus* oocytes [182], and in yeast [75,183,184]. P-gp expressed in these in vitro systems is thought to function normally (analogous to the function seen in in vivo systems), even though the former lacks glycosylation at the N-terminus. Despite the normal functional activity of P-gp, researchers found it difficult to use P-gp expressed in *E. coli* for functional assay, because many drugs cannot penetrate the

cell walls. To solve this problem, Beja and Bibi developed a method to express P-gp in “leaky” *E. coli* cells [180]. The results of these assays may be significantly different from those obtained in studies performed with mammalian cells, due to differences that exist between bacteria, the insect cells, and mammalian cells.

## 7. Experimental Methods and Design

The use of appropriate experimental design can provide definitive evidence that P-gp-mediated efflux is altering the transport of a compound, and can provide further mechanistic information regarding the transport of a compound. Many of the following techniques can be applied to any of the in vitro model systems described above.

*a. Transport Assay.* The most direct method of identifying the effect of P-gp on drug absorption is to measure the transport of drug molecules in both apical-to-basolateral (mucosal-to-serosal, the absorptive pathway) and basolateral-to-apical (serosal-to-mucosal, the secretory pathway) directions. A significantly larger effective permeability in the basolateral-to-apical direction provides evidence that some form of secretory pump such as P-gp is enhancing the transport of the test compound in the secretory direction above what is expected from simple passive diffusion. As a consequence of this secretory mechanism, the apical-to-basolateral transport is reduced, whereas the basolateral-to-apical transport is enhanced. For a typical P-gp substrate, a plot of flux in the secretory direction versus concentration has both a passive-diffusion component and a saturable (Michaelis–Menten) component. Demonstration of saturable efflux in the secretory direction provides direct evidence that an efflux pump such as P-gp, which has a finite capacity, is active in the transport of the test compound [185]. Modeling programs can be used to determine the apparent  $K_m$  and  $V_{max}$  for the P-gp-mediated transport of the compound.

In order to verify the role of P-gp in the polarized transport of a compound, a known inhibitor of P-gp can be added to abolish the vectorial transport. Some of the well-known inhibitors of P-gp efflux include verapamil, cyclosporin-A, progesterone, quinidine, chlorpromazine, reserpine, and the antibody MRK16 [109–113]. By inhibiting P-gp efflux, the additional secretory component is removed and transport is expected to resemble a passive diffusion process; i.e., transport in each direction should converge to a common value.

*b. Competition Assay.* Fluorescent dyes such as calcein-AM and rhodamine derivatives have been demonstrated to be P-gp substrates [186–193]. These compounds can be used in competition assays in which the test compound is added with these dyes. Any reduction in the dye efflux would be indicative of the inhibitory properties of the test compounds toward P-gp. Both rhodamine 123 and calcein-AM have been used in high-throughput assays, including the NCI assay, to screen large numbers of compounds as inhibitors of P-gp in several cell types [187–190,192].

Calcein-AM itself is a weakly fluorescent molecule. When the acetoxy-methyl ester group is cleaved by intracellular esterases, the fluorescent intensity of the metabolite calcein increases significantly [187,190,192]. The amount of P-gp inhibition can be correlated directly with the amount of intracellular fluorescence. This is because calcein-AM is transported via P-gp, and thus the efflux pump attenuates its intracellular accumulation, unless it is inhibited by another P-gp substrate and/or inhibitor. However, calcein is not significantly transported by P-gp, due to the negative charge and subsequent lack of binding to membranes; thus it accumulates in the cytoplasm when formed by hydrolysis of intracellular calcein-AM [187,190,192].

These competition assays are also applicable to cells grown on porous membranes. Rhodamine 123 has been used in conjunction with cell monolayers grown on polycarbonate membranes to detect the presence of P-gp in the apical cell membrane and to assess its inhibition by a variety of compounds in a competition-style assay [191,193]. The use of a radioligand such as  $^3\text{H}$ -verapamil to test drug affinity for P-gp in Caco-2 cells has been described by Doppenschmitt et al. [38,194].

It is important to note that P-gp inhibition by a compound for the efflux of any of these ligands does not correlate directly with the ability of P-gp to efflux the compound of interest. Such is the case with paclitaxel, which is considered an excellent P-gp substrate but a poor inhibitor [118], as determined by the dye-efflux method. The converse is seen with progesterone, which is a good inhibitor of P-gp-mediated efflux and yet a poor substrate. This is not surprising, considering the fact that P-gp has multiple binding sites and many factors other than the affinity for P-gp can affect the substrate/inhibitory properties of compounds.

*c. Uptake Assay.* An alternative method to assess the function of P-gp in specific membrane components of the cell (i.e., canalicular membrane) is to determine the uptake of substrates into membrane vesicles [46,170]. Kamimoto et al. [46] prepared canalicular membrane vesicles (CMVs) and sinusoidal membrane vesicles (SMVs) from rat liver, and demonstrated that in the presence of ATP [ $^3\text{H}$ ]daunomycin was taken up only by CMV but not by SMV. This transport was temperature dependent, osmotically sensitive, and saturable. In addition, P-gp substrates such as adriamycin, quinidine, verapamil, vincristine, and vinblastine inhibited uptake of daunomycin by CMVs. Similarly, Bohme et al. have demonstrated the P-gp-mediated uptake of daunorubicin in rat CMVs was inhibited by PSC 833, a P-gp inhibitor with low nanomolar potency [195]. These results suggest that P-gp mediates the efflux of its substrates from hepatocytes into bile, thus affecting the clearance of xenobiotics.

*d. ATPase Activity Assay.* P-Glycoprotein-associated ATPase is vanadate sensitive. A membrane product prepared from baculovirus-infected insect cells containing this activity is now commercially available from GENTEST (Woburn, MA). Substrates of P-gp such as verapamil have been shown to stimu-

late this vanadate-sensitive membrane ATPase [76]. By determination of inorganic phosphate liberated in the reaction containing a P-gp preparation and a test compound in the presence and absence of vanadate, one can determine if the test compound is a substrate/inhibitor of P-gp [76,196]. Any compound that binds to P-gp will stimulate the magnesium-dependent ATPase; thus, this method cannot distinguish between a substrate and an inhibitor of P-gp.

## B. In Situ Models

Some efforts have been made to determine the effect of P-gp has on the disposition of its substrates by use of in situ perfusion methods, including intestinal perfusion [197,198], liver perfusion [199–201], kidney perfusion [202], and brain perfusion [203–205]. These experiments allow the researcher to study the transport of compounds in a physiologically relevant environment in which the integrity of the organ is preserved with regard to cell polarity and representation of all cell types seen in the organ.

### 1. Intestinal Perfusion

In situ intestinal perfusion studies are typically done with live animals in which a perfusion loop has been inserted into the intestine [197,198]. Depending on the experimental protocol, the system can offer a relatively unbiased view of intestinal transport with respect to the normal expression of transporters in healthy animals. One limitation of this protocol is that the disappearance rather than the appearance of a compound is often determined (appearance can be determined by collection of blood in the vessels perfusing the section of intestine studied, a process requiring significant surgical skill). Estimates of the polarity of transport imparted by P-gp are difficult to assess and typically can be determined only by using an inhibitor or antibody to P-gp, each of which may have unknown effects on the passive transport of the test compound. Often the animal is anesthetized, and the anesthetic agent can further affect the results (altered membrane fluidity, possible inhibitory effects on P-gp-mediated efflux activity) [116]. There are some other obvious limitations. Using the intact intestine adds more levels of complexity, which can further confound studies meant to elucidate the role of transporters, which act at the cellular level. It is possible that results will differ by intestinal region and also due to the presence of the Peyer's patches, which have different physiological roles from enterocytes [176,177]. Furthermore, these studies suffer from an interspecies variability (rats are typically the test subjects). Despite certain disadvantages, these studies, if conducted with appropriate controls involving known P-gp substrates, can provide valuable insights on how to correlate the effect of P-gp observed in cellular transport studies to that expressed in the absorption of drugs in vivo.

By measuring the intestinal absorption from rat small intestine *in situ*, Saitoh et al. studied the differences between the oral bioavailabilities of methylprednisolone, prednisolone, and hydrocortisone, three structurally related glucocorticoids. Compared to prednisolone and hydrocortisone, methylprednisolone absorption was significantly retarded in jejunum and ileum by an intestinal efflux system. In the presence of verapamil and quinidine, the attenuation in the absorption of methylprednisolone was reversed, suggesting that P-gp is responsible for the attenuated absorption of methylprednisolone absorption [198]. This study provides a good example of the usefulness of an intestinal perfusion experiment in further determining the regional differences in intestinal drug absorption modulated by P-gp that would otherwise be impossible to deduce in experiments performed with cell culture models or with whole-animal systems.

## 2. Liver Perfusion

The rat isolated perfused liver has been extensively used because of the minimal surgical manipulation needed, and the size of the rat liver allows the use of a hemoglobin free perfusate (organs of less than 25 g are needed to ensure adequate oxygen delivery at the flow rates used in these experiments) [199]. The isolated perfused liver system provides an excellent model for studying the hepatobiliary disposition of compounds without the confounding influences that may be seen *in vivo*, such as influences on hepatic metabolism, and additional metabolism or excretion by other organs of clearance [199,200]. The isolated perfused rat liver can be used to study the biochemical regulation of hepatic metabolism, the synthetic function of liver, and the mechanism of bile formation and secretion [200]. This model has provided important results regarding the influence of MDR modulators on the hepatobiliary disposition of chemotherapeutic agents [206,207].

The effects of the P-gp inhibitor GF120918 on the hepatobiliary disposition (biliary excretion) of doxorubicin were determined using a perfused rat liver system [200]. Biliary excretion is the rate-limiting process for doxorubicin elimination. In the presence of GF120918, the biliary excretion of doxorubicin and its major metabolite, doxorubicinol, was decreased significantly without alterations in doxorubicin perfusate concentrations or doxorubicin and doxorubicinol liver concentrations. In a similar study on the hepatic elimination of two other P-gp substrates, vincristine and daunorubicin, it was reported that canalicular P-gp plays a significant role in the biliary secretion of these compounds [201,208].

## 3. Kidney Perfusion

Because the kidney is typically involved in the excretion of hydrophilic compounds, and because most of the substrates of P-gp are hydrophobic and likely to be cleared mainly by biliary excretion or intestinal secretion, few studies have



been performed with the isolated perfused kidney. The isolated perfused rat kidney model demonstrated that digoxin is actively secreted by P-gp located on the luminal membrane of renal tubular epithelial cells and that clinically important interactions with quinidine and verapamil are caused by the inhibition of P-gp activity in the kidney [202]. These results provide an excellent example of how the isolated perfused kidney model can be used to definitively conclude that P-gp-mediated efflux is involved in the renal excretion of a compound, and also to elucidate possible drug–drug interactions that might arise in the kidney following the coadministration of P-gp substrates/inhibitors.

#### 4. Brain Perfusion

The brain perfusion system has been used to study the disposition of several compounds across a functionally intact BBB that has been shown to possess nearly identical structural and functional features as those seen in the BBB *in vivo*, including the presence of multiple tight junctional complexes between cells and P-gp [33,203–205]. This *in situ* technique involves stopping the heart and perfusing the brain via the carotid artery at a flow rate that does not alter the integrity of the BBB [205,209]. The brain capillary endothelium, the choroid plexus, and the arachnoid membrane, which comprise the functional BBB *in vivo*, are all present in this technique, and this provides a major advantage over *in vitro* models used to study the BBB (e.g., BMEC). One major advantage this technique has over an *in vivo* experiment involves the perfusion fluid used in the experiment. The composition of the solution can be controlled with respect to test compounds, plasma proteins, nutrients, and metabolic cofactors [205]. However, the use of a perfusate solution can also be a disadvantage, for it may not be possible to provide all the necessary nutrients or metabolic cofactors that would be present *in vivo* and thus may lead to incorrect conclusions [204]. The major disadvantages of the model with respect to *in vitro* models include the lack of control of the extracellular fluid concentration for studies of drug efflux from the brain and the greater complexity that the brain matrix provides [204]. As with other perfusion systems, this technique requires anesthesia, and this may act to confound the results.

Some of the more notable applications of this *in situ* model system in the study of CNS drug disposition have involved the determination of drug permeability across the BBB, drug uptake kinetics, transport mechanisms (uptake and efflux), elucidation of the CNS metabolic pathways (the drug has no access to peripheral metabolism), and the effects of plasma protein binding [204]. This model has been used to study the effects of P-gp-mediated efflux in the BBB on antibacterial agents [210], colchicine [211,212], and vinblastine [211], and has been used to evaluate a prodrug strategy for increasing doxorubicin uptake into

the brain [213]. The system has also been used to determine the effects of P-gp modulators, such as verapamil [214] and PSC833 [215], on the BBB transport of P-gp substrates. Recently, the system has been adopted and validated for use in the gene knockout [*mdr1a(-/-)*] mice (see Sec. IV.C.1). Results obtained from this model compared with those from experiments performed in wild-type mice can be used to gauge the overall effect of P-gp-mediated efflux on the transport of P-gp substrates across the BBB [216].

These *in situ* techniques can be powerful tools to gauge the actual extent of P-gp efflux that can be expected *in vivo*. However, there are confounding factors that must be addressed when interpreting data obtained from these studies. As with all biological models, the appropriate controls must be used to ensure that the observed effects are in fact due to P-gp-mediated efflux activity.

## C. In Vivo Models

### 1. Gene Knockout Mice [*mdr1a(-/-)*]

Schinkel et al. have generated mice with individual disruptions of the *mdr1a*, *mdr1b*, or *mdr2* genes [43,217–222]. In addition, they have generated a double knockout, in which both *mdr1a* and *mdr1b* are disrupted [223]. In mice, *mdr1a* and *mdr1b* genes encode two separate P-gp proteins that are analogous to the MDR1 gene product expressed in humans [219]. The *mdr1a* RNA is found abundantly in the brain, intestine, liver, and testis [224], while *mdr1b* RNA is usually associated with the adrenal cortex, placenta, ovarium, and uterus [225]. Both are expressed in the kidney, heart, lung, thymus, and spleen [219,224]. The relative sequence identity of the human P-gp with the mouse *mdr1a* P-gp is 82% [226–228]. The greatest homology of the two proteins is seen in ATP-binding regions, the second, fourth, and eleventh transmembrane domains, and the first and second intracytoplasmic loops in each half of the molecule [22,226,229]. The proteins show the least homology in the first extracellular loop, in the connecting region between the homologous halves, and at both terminal ends [22,226,229].

Schinkel et al. have concluded that *mdr1*-type P-gp has no essential physiological function, since no gross disturbance in corticosteroid metabolism, or in bile formation was observed in *mdr1a(-/-)* mice. However, the absence of P-gp would alter the profile of metabolism and disposition of drugs that are substrates of P-gp. For example, the concentration of ivermectin and vinblastine in the brain of *mdr1a(-/-)* mice was 87-fold and 22-fold over that of wild-type *mdr1a(+/+)* mice [219]. Thus, the knockout or reversal of P-gp function leads to increased toxicity of the drugs in organs normally protected by P-gp [219].

Although the mouse *mdr1a* P-gp is not totally homologous to the human P-gp, mice that are dominant negative for the *mdr1a* gene provide excellent in

vivo information about the effects of P-gp on the absorption, distribution, metabolism, and elimination of drugs [219,221,230,231].

## 2. Transgenic Mice

A transgenic mouse model involving MDR1 has been used to study the function of P-gp. A transgenic system was developed to express human MDR1 gene in the marrow of mice [232–235] leading to bone marrow that is resistant to the cytotoxic effect of anticancer drugs that are substrates of P-gp. When exposed to anticancer agents, the transgenic mice showed normal peripheral white blood cell counts, which implies that the MDR1 P-gp protects the marrow [234]. When the efflux activity of the MDR1 P-gp expressed in these mice was inhibited with other P-gp substrates or MRK16, an antibody to an external epitope of P-gp, the mice became sensitized to cytotoxic drug therapy, which manifested in a drop in the white blood cell counts [234]. This model has seen widespread use in evaluating the safety of chemotherapeutic agents. However, this and other transgenic models have not yet found use in the evaluation of the effects of P-gp on drug pharmacokinetics.

## D. In Vitro–In Vivo Correlations (IVIVC)

In vitro models have provided invaluable information about properties of compounds that affect their in vivo transport and absorption. Regardless of how closely these in vitro systems model in vivo conditions, they do not completely represent what may be seen in vivo. It is important to compare the results obtained from some key in vitro and in vivo experiments so that the magnitude of certain processes seen in vitro can be gauged properly and so that any disconnect between the in vitro and in vivo systems can be identified. Although it is certain that these relationships will not hold for all drug compounds, a comparison of the data with a limited set of compounds is useful.

In cell lines such as Caco-2 and MDCK, P-gp expression can vary from clone to clone, and thus the magnitudes of efflux for various substrates are likely to be affected [37,40,131]. Cells in which P-gp has been induced are not likely to represent actual levels seen in vivo for normal tissues. It has been estimated that cells displaying the MDR phenotype can contain between  $8 \times 10^5$  and  $3 \times 10^6$  copies of MDR gene per cell, which would give rise to nearly 30% (mean) of all membrane proteins [236]. Certainly this high level of expression is likely to skew the results of a P-gp assay. The variation in expression of P-gp, along with other factors, makes information obtained by the use of cell lines qualitative in nature. Certainly compounds that display a greater propensity to interact with P-gp in vitro are expected to be influenced by this efflux pump to a greater extent

in vivo. However, as yet there are no reliable parameters to relate the P-gp activity seen in vitro with that seen in vivo. Despite our inability to predict quantitatively the influence P-gp may have on the in vivo transport of substrates in normal tissues with respect to other processes, in vitro experiments remain the best means of demonstrating that a compound is a substrate for polarized efflux. Nearly all experiments designed to study the extent of P-gp efflux of test compounds in vivo require adequate in vitro data to support the hypothesis [185,237–239].

In vitro studies on P-gp substrates such as vinblastine, paclitaxel, cyclosporin-A talinolol, acebutolol, and digoxin have provided a good indication of the effect of P-gp on the in vivo pharmacokinetic behavior of these compounds [185,230,237–240]. These studies show that results from the in vitro studies provide a qualitative picture of the influence of P-gp on its in vivo pharmacokinetic behavior. Findings such as these give confidence that results from in vitro experiments can be extrapolated to explain the modulation of drug disposition by P-gp efflux.

## V. EFFECT OF P-GLYCOPROTEIN ON DRUG DISPOSITION

Much of the information known about the role of P-gp in determining the pharmacokinetic profile of drugs has come from in vivo experimentation. These experiments can be classified roughly into two categories: studies performed in the P-gp-deficient mouse model, as done by Schinkel et al. [219,221,230,231,239], and those performed to determine the pharmacokinetic parameters of P-gp substrates in normal mice and man [185,226,238,241–246]. These studies have helped to elucidate the overall importance of P-gp in affecting the absorption, distribution, metabolism, and elimination of its substrates. The following is a brief review of some of the important findings from each aspect of drug pharmacokinetics.

### A. Absorption

All orally administered drugs must pass through the gastrointestinal tract and thus pass the barrier formed by the mucosal cells (enterocytes) in the intestine. For years, low first-pass bioavailability of a drug was attributed mainly either to clearance via hepatic metabolism and biliary clearance or to poor absorption in the intestine due to poor solubility or intrinsic permeability properties. Although these are certainly important factors in determining the overall oral bioavailability of certain drugs, recent studies have shown that P-gp-mediated efflux also plays a very significant role in attenuating oral absorption of many drug molecules [6,179,185,198,239,240,246,248]. It has been shown through studies with *mdr1a(-/-)* mice that the mean absorption time (reduced in the knockout mice)

of P-gp substrates is altered by the apically directed efflux activity of P-gp [185,219,221,230,231].

The effects of P-gp on paclitaxel pharmacokinetics were determined in the *mdr1a(-/-)* mice. As expected, the plasma AUC values for the *mdr1a(-/-)* mice were indeed several times higher following oral administrations of paclitaxel (10 mg/kg) compared to values obtained in wild-type mice [239]. The oral bioavailability of paclitaxel was 35% for the *mdr1a(-/-)* mice versus 11% for the wild-type mice [239]. Similar studies have been performed with other P-gp substrates, such as cyclosporin-A and fexofenadine, and an increased oral absorption of all these substrates was observed in the P-gp-deficient mice [221,249].

The nonlinear oral bioavailability (with dose) has been particularly perplexing in the case of the beta-adrenoceptor antagonists. The dose-normalized AUC was found to increase with dose, but the oral clearance was found to decrease with increasing dose [185]. These findings were not compatible with the saturable first-pass effect. The polarized transport of talinolol observed in Caco-2 cells was attributed to P-gp efflux [7]. The  $t_{\max}$  and mean absorption times of orally administered talinolol were significantly reduced with coadministration of verapamil. By using verapamil to alter the pharmacokinetic properties (specifically the intestinal absorption) of the beta adrenoceptor antagonist talinolol, it has been clearly shown in an intact model that the absorption of this drug is significantly affected by P-gp present in the intestine [185].

## B. Distribution

In some instances, P-gp can significantly affect the profile of the drug distribution, most notably in tissues that possess a specialized blood-tissue barrier, such as the brain. Experiments with the *mdr1a(-/-)* mice have shown how P-gp affects the distribution of its substrates into certain tissues [185,219,221,230,231]. A few examples are described here to demonstrate the role played by P-gp in the tissue distribution of drugs.

Some of the most informative results came from a study involving altered behavior of vinblastine in *mdr1a(-/-)* mice. At moderate doses of vinblastine (1 mg/kg), the concentrations of the parent drug in heart, muscle, brain, and plasma were 3, 7, 20, and 2 times higher, respectively, in the *mdr1a(-/-)* mice compared to the normal mice (results summarized in Table 3) [219]. The levels in the other tissues expressing the *mdr1a* P-gp were two to three times higher in *mdr1a(-/-)* mice [219]. At a dose of 6 mg/kg, the differences in tissue distribution were still significant, but reduced, most likely due to saturation of P-gp [219]. A 12-fold increase in brain concentration was seen at this dose, and plasma and tissue differences of approximately twofold were seen [219]. These results demonstrate the importance of P-gp efflux in the distribution of drugs.

**Table 3** Relative Influence of P-gp on the Biliary and Intestinal Excretion of P-gp Substrates<sup>a</sup>

Drug (dose)	Plasma level <sup>b</sup> (ng/ml)		Biliary excretion <sup>c</sup> (% of administered dose)		Intestinal excretion <sup>c</sup> (% of administered dose)		Ref.
	Wild type	mdr1a(-/-)	Wild type	mdr1a(-/-)	Wild type	mdr1a(-/-)	
Paclitaxel (5 mg/kg)	289 ± 38	327 ± 44	25.7 ± 4.5	26.6 ± 2.90	4.63 ± 0.49	1.52 ± 0.05	239
Digoxin (0.2 mg/kg)	125 ± 10	216 <sup>d</sup> ± 14	24.0 ± 4.8	15.8 ± 2.9	16.4 ± 2.6	2.2 <sup>d</sup> ± 0.4	260
Vinblastine (1 mg/kg)	NA <sup>e</sup>	NA <sup>e</sup>	26.7 ± 1.3	28.9 ± 2.0	10.4 ± 0.4	6.8 <sup>d</sup> ± 0.5	261
Doxorubicin (5 mg/kg)	150 ± 22	166 ± 23	13.3 ± 1.7	2.4 <sup>d</sup> ± 0.3	10.5 ± 0.5	10.0 ± 0.4	261

<sup>a</sup> Biliary and intestinal excretion of total [<sup>3</sup>H] label of the drugs (parent and metabolites) in the first 90 min after i.v. bolus administration was determined in the wild-type and mdr1a(-/-) mice with a cannulated gallbladder.

<sup>b</sup> Plasma concentration at *t* = 90 min.

<sup>c</sup> Data (means ± S.E.) are represented as a percentage of the administered dose.

<sup>d</sup> *p* < 0.05 versus wild-type mice.

<sup>e</sup> NA: not available.

The distribution of other P-gp substrates into various tissues has also displayed altered patterns in the *mdr1a*(-/-) mice compared to that seen in wild-type mice. The concentration of ivermectin and vinblastine were found to be 87 and 22 times higher, respectively, in the brain of *mdr1a*(-/-) mice than in that of the wild-type mice. Not surprisingly, compared to the wild-type mice, the *mdr1a*(-/-) mice displayed an increased sensitivity to ivermectin (100-fold) and vinblastine (3-fold), respectively [219].

The effects of P-gp on opioid peptide pharmacodynamics was studied using *mdr1a*(-/-) mice. The brain tissue concentration of DPDPE was found to be two to four times higher in the *mdr1a*(-/-) mice, and the dose required to elicit a comparable antinociception was nearly 30 times lower in the *mdr1a*(-/-) mice [250].

The treatment of mice with the P-gp inhibitor GF120918 resulted in a 13-fold and 3.3-fold increase in brain and CSF concentration of amprenavir, respectively, over that in the vehicle-treated mice [165].

Similar studies have been performed with the P-gp substrates dexamethasone, digoxin, and cyclosporin-A [221,230]. The differences seen in plasma and tissue concentrations between the *mdr1a*-deficient mice and the normal mice differ from drug to drug, but a common theme observed in the *mdr1a* deficient mice was the increased tissue accumulation of these substrates [230]. For a more thorough review of the findings for these compounds, please see Ref. [230].

### C. Metabolism

P-Glycoprotein can play a role in the oxidative metabolism of its substrates that are also substrates of CYP3A4. Several factors have led to the observation that P-gp and CYP3A4 may act in concert to limit the oral absorption of drugs. These barrier-forming proteins are colocalized to the apical region of the enterocytes that form the epithelial lining of the small intestine [251]. P-gp and CYP3A4 can be induced by many of the same compounds, although it has recently been shown that these proteins are not coregulated [252]. It is well known that there exists a large degree of overlap between the broad substrate specificities of P-gp and of CYP3A4 [253]. Given this fact, it seems reasonable that the combined actions of P-gp and CYP3A4 could account in some part for the low oral bioavailability determined for many of these dual substrates.

Until recently, intestinal metabolism via CYP3A4-mediated metabolic pathways was thought to be insignificant due to lower levels of CYP3A4 expression compared to that seen in the liver, and because of slower metabolic rates measured for intestinal microsomes [246]. However, similar  $K_m$  values have been reported for midazolam 1'-hydroxylation by microsomes obtained in the upper intestine and the liver [254]. This correlation indicates that the upper intestine and hepatic CYP3A4 are functionally equivalent. Such findings further establish

the importance of the intestine in the elimination of substrates for CYP3A4-mediated metabolic pathways that are administered orally. Additionally, coadministration of substrates/inhibitors that may alter the function of these proteins (induction, inhibition) could be further responsible for the variability in intestinal absorption (drug interactions) seen for some drugs.

Although there is only limited mechanistic information regarding the interplay between P-gp and CYP3A4, the results from the few *in vitro* experiments have presented an interesting possibility that these two proteins may act in concert (see Fig. 2). Studies involving cyclosporin-A transport across Caco-2 cell monolayers have shown how P-gp and CYP3A4 may act coordinately to enhance the attenuation of apical-to-basolateral transport of this drug. It was observed that cyclosporin-A metabolism was much greater when the compound was transported

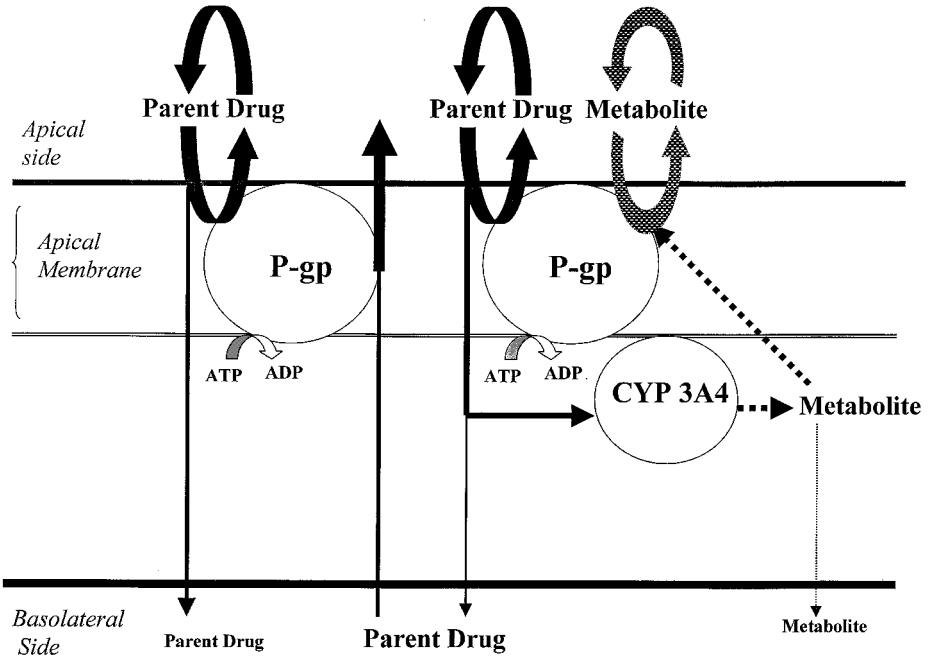


**Figure 2** Apically directed P-gp-mediated efflux of drugs across intestinal epithelium and synergistic interactions of P-gp with CYP3A4 in attenuating the absorptive transport. Heavy arrows versus light arrows indicate relative magnitudes of the flux. This exemplifies an elimination mechanism that a dual substrate of P-gp and CYP3A4 may encounter in the enterocyte. Conceivably, the metabolite may or may not be a substrate for P-gp (as drawn, it is a substrate).



in the apical-to-basolateral (absorptive) direction than in the basolateral-to-apical (secretory) direction [240]. Hence, the reduction in the apical-to-basolateral flux of cyclosporin-A caused by apically directed P-gp efflux enhanced the exposure of the compound to CYP3A4, and thus a greater amount of metabolism was achieved [240]. A corollary to the former statement dictates that the actions of P-gp to reduce the rate of absorption of these dual substrates will reduce the amount of enzyme expression needed for significant catalytic activity, which could affect the bioavailability of the drugs.

Quantification of the distribution of the primary metabolites formed in these experiments has also provided some interesting observations. The metabolites of cyclosporin-A generated by a CYP3A4-like enzyme were preferentially transported to the apical side, indicating that these metabolites were also P-gp substrates [240]. Similar results were obtained in experiments following the metabolism of midazolam as it diffused across Caco-2 cells induced to express CYP3A4 [255]. Fisher et al. found that the distribution of 1'-hydroxymidazolam and 4-hydroxymidazolam, two primary metabolites of midazolam generated by the CYP3A4-mediated metabolism, were preferentially transported to the apical compartment regardless of the transport direction of midazolam [255]. This is interesting because midazolam is not subject to polarized efflux but does interact with P-gp in an inhibitory fashion [256]. These results suggest that CYP3A4-mediated metabolism of midazolam makes the P-gp-mediated efflux of this compound (via its metabolites) more efficient. The oxidative metabolism mediated by CYP3A4 may possibly reduce the passive membrane permeability of the metabolites (e.g., 1'-hydroxymidazolam), thus allowing P-gp to more effectively establish a concentration gradient. Furthermore, the addition of oxygen may act to increase the affinity of P-gp for these metabolites with similar structures. Formation of metabolites that are a better substrate of P-gp than the parent drug also has consequences for the catalytic activity of CYP3A4. If the efflux of primary metabolites is more efficient than that of the parent, the amount of competing secondary oxidative metabolism will be reduced, and thus the primary metabolism of the parent will be more complete [257].

These findings have raised several interesting questions regarding how these proteins may act in concert to maximize their protective activities. It is not well understood what parameters (substrate affinity, protein expression, substrate permeability properties, etc.) will determine that this coordinate elimination pathway existing in the intestine will be significant. It does appear that P-gp can increase the susceptibility of some compounds to CYP3A4-mediated metabolic pathways both at the cellular level and at the organ level (most notably the intestine) [240,255,258,259]. It is very likely that P-gp-mediated efflux activity may also influence the activity of other enzymes (i.e., other cytochrome P450 isozymes) involved in the metabolic transformation of P-gp substrates that are substrates for these various enzymes.

## D. Excretion

In addition to affecting absorption, distribution, and possibly the metabolism of drugs, P-gp can also facilitate the excretion of its substrates in the liver, kidney, and intestine. The processes underlying biliary excretion of drugs via a P-gp-mediated pathway and those involved in the renal secretion of drugs have been described (see Sec. IV.B.2 and IV.B.3). The mechanisms demonstrating how P-gp acts to make the intestine an important route of elimination are only now being elucidated. Certain drugs administered via the intravenous route are indeed eliminated to a high degree in the intestine by means of a process other than biliary excretion [219,221,230,231,238,239,241,242]. The enormous surface area of the intestine ( $\sim 200 \text{ m}^2$  in adult man) allows the organ to act as a giant dialysis membrane for drugs as the concentrations in the plasma exceed those in the intestinal lumen, and passive diffusion across the mucosa into the gut lumen can occur [242]. Some of the same driving forces that affect the intestinal absorption of drugs also exist for exsorptional elimination. These factors include physicochemical properties such as lipophilicity, and molecular size. Other biochemical and physiological factors that are likely to affect this process include protein binding, blood flow to the gut, and substrate specificity for the intestinal P-gp transporter [185,242]. P-gp can affect the rate at which drugs are eliminated from tissues and from the plasma via elimination through the liver, intestine, and/or kidney [219,221,230,231]. The oral, systemic, and tissue clearances (rate of elimination) are affected by P-gp efflux, and thus the terminal half-lives of P-gp substrates may be related to the efflux activity seen in the organism [185].

The effect of P-gp-mediated efflux activity on excretion has been clearly shown through experiments with vinblastine and paclitaxel in *mdr1a(-/-)* mice. The results of these experiments have shown how P-gp-mediated efflux activity accelerates tissue clearances and also the systemic clearances of its substrates. Additionally, these studies have highlighted the role of the intestine in elimination. While the role of intestinally expressed P-gp in limiting absorption is recognized, these experiments have helped elucidate its role in making the intestine a significant route of elimination, a process that has not been appreciated until recently.

In normal mice, the elimination of vinblastine in the feces within 24 hours of administration was determined to be approximately 25% of the dose as unchanged drug at two doses (1 mg/kg and 6 mg/kg) [231]. In the *mdr1a*-deficient mice, the amount of unchanged drug recovered in the feces was reduced to 9.4% for the 1-mg/kg dose and 3.4% for the 6-mg/kg dose [231]. The amount of vinblastine remaining in the brain tissue of the P-gp-deficient mice was approximately 1000 ng/g tissue at the 6-mg/kg dose 24 hours after administration, whereas the amount of vinblastine remaining in the brain tissue of normal mice at the same dose was only 22 ng/g tissue [231]. The normal mice showed much

more rapid elimination of vinblastine from both the plasma and tissue than the *mdr1a*-deficient mice, and a significant reduction in terminal elimination half-life and reduced clearances of vinblastine were observed at each of these doses for the P-gp-deficient mice [219,231]. Obviously P-gp can dramatically alter the elimination profiles of its substrates as well as altering the absorption. The protective role of the *mdr1a* P-gp in the mouse, presumably via its effect on the distribution and elimination of vinblastine, is evident in the significantly higher LD50 value (22 mg/kg) for the normal mice compared to that for the *mdr1a*(-/-) mice (6 mg/kg) [231].

As seen with vinblastine, clearances of paclitaxel were reduced and elimination half-life increased in the *mdr1a*(-/-) mice [239]. Nearly 90% of the radioactivity following an IV dose of paclitaxel was recovered in the feces of the wild-type mice, mainly as unchanged drug or hydroxylated metabolites [239]. For the *mdr1a* deficient mice, a mere 1.5% of the dose was recovered in the feces, and approximately 45% of the dose was recovered in the urine as unknown metabolites [239]. Following an oral dose (10 mg/kg), 90% of the dose was recovered in feces of the wild-type mice, compared to only 2% seen in the *mdr1a*-deficient mice [239]. The levels of the hydroxylated metabolites excreted by the *mdr1a*-deficient mice were not dependent on the route of elimination, whereas in wild-type mice, three times as much hydroxylated paclitaxel was collected following an IV dose [239].

The contributions of the *mdr1a* P-gp to the hepatic and intestinal clearances of paclitaxel, digoxin, vinblastine, and doxorubicin have been determined by comparing the amounts of biliary and intestinal secretion of each drug in wild-type and *mdr1a*(-/-) mice (Table 3). The amounts of biliary excretion of paclitaxel and the hydroxylated metabolites were not significantly different between the wild-type mice and the *mdr1a*-deficient mice [239]. Further, when the biliary excretion into the intestinal lumen was blocked, nearly three times the amount of a 10-mg/kg IV dose was recovered in the lumen of the wild-type mice versus the *mdr1a*(-/-) mice within 90 minutes of administration [239]. Like paclitaxel, absence of the *mdr1a* P-gp seems to have a minimal effect on the biliary secretion of digoxin and vinblastine, whereas the intestinal secretion of these compounds is significantly affected [260,261]. An opposite situation exists for the intestinal and biliary secretion of doxorubicin. Nearly five times the amount of unchanged doxorubicin was secreted into the bile of the wild-type mice versus the *mdr1a*(-/-) mice, whereas the intestinal secretion of doxorubicin was approximately equal (~10% of the dose) in both sets of mice [261]. These results illustrate that in mice, *mdr1a* P-gp is active in the intestinal excretion of paclitaxel, digoxin, and vinblastine, and that the mouse liver has the ability to utilize alternate pathways of elimination for these compounds. Conversely, the biliary excretion of doxorubicin in mice appears to be highly dependent on *mdr1a* P-gp-mediated efflux

activity, whereas intestinal *mdr1a* P-gp plays less of a role in the intestinal excretion of doxorubicin (see Table 3).

## VI. CLINICAL TRIALS WITH P-GLYCOPROTEIN MODULATORS

A large area of research has involved determining the possible use of P-gp modulators to reverse the MDR phenotype associated with P-gp-mediated efflux in an attempt to improve the efficacy of chemotherapeutic agents and chemotherapeutic regimens. Clinical trials have been performed to assess the use of P-gp modulators (i.e., verapamil, cyclosporin A, etc.) to improve the intracellular delivery/efficacy of chemotherapeutic agents (i.e., doxorubicin, vinblastine, and etoposide). However, the interpretation of the results of these clinical trials involving the use of P-gp inhibitors in an attempt to reverse the MDR phenotype has been complicated by unknown pharmacokinetic interactions between the target cytotoxic drug and the modulator [262]. Results obtained from trials with first-generation inhibitors have been somewhat disappointing; however, some promising results were obtained in hematolymphoid malignancies [262,263]. There are several possible reasons why this line of therapy has not been successful. Difficulties in detecting the MDR1 phenotype in clinical practice, the inability to achieve target concentrations of the modulator, the methodology of the trial, and the multifaceted array of chemoresistance mechanisms could all act to confound the results of these trials [263]. Therefore, further clinical studies that allow the dissection of the pharmacokinetic effects of these modulators from their cellular effects of inhibiting P-gp-mediated efflux must be designed. The following sections provide a brief summary of what has been learned from trials performed with the first generation of P-gp modulators and the subsequent improvements achieved in the clinical outcomes with the second and third generations of P-gp modulators.

### A. First-Generation P-Glycoprotein Modulators

These agents represent drugs in clinical use for other indications that had been shown to inhibit P-gp efflux through *in vitro* experiments. Due to the relatively low binding affinity of these compounds for P-gp and the need to increase the doses of these modulators to toxic levels, few of these agents have been further studied for use in clinical modulation of P-gp. However, early trials with these drugs have provided invaluable information regarding the consequences of inhibiting P-gp. These first-generation inhibitors include verapamil, cyclosporin A, tamoxifen, quinidine, and quinine.

## 1. Verapamil

Many of the early trials aimed at reversing the MDR phenotype associated with the overexpression of P-gp involved coadministration of the phenylalkamine voltage-dependent L-type calcium channel blocker verapamil. Racemic verapamil was shown to reverse P-gp-mediated resistance to vincristine and vinblastine *in vitro* and *in vivo* in P388 leukemia [264]. These early findings and the fact that verapamil was a clinically used drug with an established record of safety provided the rationale for its use clinically as a P-gp modulator.

The maximum tolerated dose of verapamil has been reported to be 480 mg/day orally (leading to blood levels of 1 mM), with the dose-limiting toxicity being hypotension [265]. Dose escalation studies with intravenously administered verapamil showed that for the dose range 0.15–0.6 mg/kg/hr, cardiovascular toxicities may be seen along with edema and weight gain [266].

Oral verapamil has been shown to increase peak plasma levels, prolong the terminal half-life, and increase the volume of distribution at steady state of doxorubicin [267]. Similar studies were performed by Gigante et al. [268], in which the pharmacokinetics of doxorubicin in combination with verapamil given at high doses intravenously were followed in 17 patients with advanced neoplasms. The steady-state concentration, and systemic and renal clearances were found to be statistically similar for various doses of verapamil and doxorubicin and for doxorubicin administered alone [268].

Additionally, trials were designed to assess the usefulness of verapamil in improving the efficacy of chemotherapeutic regimens for the treatment of small-cell lung cancer [269,270], refractory multiple myeloma [271], and breast cancer [272]. The results of these trials showed that verapamil had only a modest positive effect on the overall effectiveness of the regimen.

## 2. Cyclosporin A

The immunosuppressive cyclic undecapeptide cyclosporin A has been used in several clinical trials as a modulator of P-gp. Cyclosporin A readily inhibits CYP3A metabolism and may lead to significant pharmacokinetic interactions [273]. Several studies have been performed using cyclosporin A as a P-gp modulator in combination with etoposide, doxorubicin, and paclitaxel.

Background work with mice was performed to assess the feasibility of using cyclosporin A as a modulator of P-gp-mediated drug resistance. The AUC of doxorubicin in the liver, kidney, and adrenals increased nearly two to three times with respect to the levels measured in control animals 30 minutes after a single intraperitoneal injection of cyclosporin A [274]. The serum levels of doxorubicin following cyclosporin A treatment were unchanged, indicating that cyclosporin A might alter the drug concentrations in the tumor without affecting its plasma concentration [274].

The effects of cyclosporin A on the pharmacokinetics of etoposide have been determined and were shown to be dose dependent. In a patient population with a range of cyclosporin A concentrations (297–5073 ng/ml), it was observed that patients with higher cyclosporin A concentrations also had larger increases in etoposide AUC [275]. Results from studies using clinically relevant plasma concentrations of cyclosporin A (1000–5000 ng/ml) as a P-gp inhibitor resulted in mean 48%, 52%, and 52% decreases in the systemic, renal, and nonrenal clearances of intravenously administered etoposide [248,275]. A similar decrease in the systemic, renal, and nonrenal clearances of doxorubicin were observed with the administration of cyclosporin A [248,276].

### 3. Tamoxifen, Quinine, and Quinidine

Quinine and quinidine are both alkaloid drugs (quinine is the S-diastereoisomer of quinidine) used as antiarrhythmic drugs. Both have been shown to modulate P-gp-mediated efflux *in vitro*, with quinidine being the stronger inhibitor of the two [101,277]. Few positive results have been seen with the use of these agents in reversing MDR in clinical trials [278–281]. The relatively low affinity of each of these compounds has limited their use clinically to reverse MDR.

Tamoxifen is an estrogen receptor antagonist that weakly binds to P-gp and exerts inhibitory effects *in vitro* at concentrations above 1  $\mu\text{M}$  [282]. Tamoxifen is used clinically for the treatment of breast cancer, and initial trials with this P-gp inhibitor have focused on using this drug not only to treat breast cancer but also to reverse P-gp-mediated MDR. In a dose escalation study, the vinblastine and tamoxifen combination proved to be neurotoxic [283]. Neurotoxicity also occurred in a trial with high-dose tamoxifen and etoposide, and at this dose the plasma concentration of tamoxifen was below the concentration reported to reverse etoposide resistance in P-gp-expressing cell lines [282,283]. Tamoxifen has very complex pharmacokinetics that are not fully understood presently. The drug exhibits high plasma protein binding (98%), enterohepatic recirculation, distribution into fatty tissue, and a long terminal half-life [284]. Other trials with tamoxifen have been performed, all of which have reported adverse toxic effects without much success at reversing MDR [285,286]. Because of these severe toxic effects of tamoxifen, such as dizziness, tremor, unsteady gait, grand mal seizure, and myelosuppression [283], no further trials have been conducted with this drug.

## B. Second-Generation P-Glycoprotein Modulators

These compounds represent a more focused attempt to develop potent P-gp modulators that would be much less toxic than first-generation inhibitors, so that adequate P-gp inhibitory concentrations can be achieved clinically without risk of the toxic effects. The second-generation modulators include dexniguldipine (B8509-035), dexverapamil (R-verapamil), and S9788.

The (–) isomer of the L-type calcium channel blocker (+)-niguldipine is dexniguldipine. This agent binds to an intracellular domain of P-gp with a  $K_i$  of 10 nM [102]. In addition, this compound can block RNA synthesis at 5  $\mu$ M [287] and possesses some anticancer activity. Currently, only a few studies have been conducted to evaluate the use of this compound as a P-gp modulator. Definitive results have yet to be reported.

Dexverapamil is just as effective at blocking P-gp-mediated efflux as its enantiomer S-verapamil, but this compound is seven times less potent at inhibiting the contractile force of isolated human heart muscle tissue [288]. This reduction in the dose-limiting factor of verapamil has led to clinical trials with dexverapamil as a possible P-gp reversing agent. A clinical trial was conducted to evaluate the effect of dexverapamil in Hodgkin's and 154 non-Hodgkin's lymphoma refractory to EPOCH chemotherapy. The combination therapy was well tolerated, but the results showed that the effect of dexverapamil in improving the EPOCH chemotherapeutic regimen was minimal at best [289,290]. A trial involving combination therapy of dexverapamil and paclitaxel in heavily pretreated patients with metastatic breast cancer showed that the combination resulted in hematological toxicity that was greater than with paclitaxel alone, along with increased mean peak paclitaxel concentrations and delayed mean paclitaxel clearance [291].

S9788 has been shown to be five times more potent than verapamil in inhibiting P-gp in vitro [292]. The triazonoamino-piperidine derivative S9788 represents one of the first attempts at the development of a high-affinity agent used specifically to reverse P-gp-mediated resistance. It is possible to achieve nontoxic plasma concentrations of S9788 that are known to reverse P-gp-mediated efflux in vitro [293]. The adverse effects of this compound seem to involve cardiotoxic events, including A-V blocks and QT prolongation leading to ventricular arrhythmia and torsade de pointe, which occur at the maximum tolerated dose (96 mg/m<sup>2</sup>) [293,294]. In a preliminary study, coadministration of S9788 did not enhance the toxicity of doxorubicin, and the pharmacokinetic profile of doxorubicin was not altered by S9788 [294]. Further clinical trials are in progress with this compound as a P-gp modulator.

### C. Third-Generation P-Glycoprotein Modulators

Like the second-generation modulators, these compounds represent further attempts to produce agents whose primary activity involves the inhibition of P-gp-mediated efflux with reduced toxic effects. Many of these compounds have been shown to possess low nM potency as P-gp inhibitors in vitro. These compounds include GF120918 (GW918), valsopodar (PSC833), and CGP41251.

GF120918 (GW918) is an acridonecarboxamide derivative that has been

shown to inhibit P-gp with an EC<sub>50</sub> of 20 nM, making it one of the most potent P-gp modulators reported [295]. Initial trials were performed to assess the alteration in the pharmacokinetic profile of doxorubicin that may occur with coadministration of GF120918. The results indicate that plasma concentrations of GF120918 that modulate P-gp *in vitro* were obtainable, and at these concentrations the pharmacokinetics and pharmacodynamic toxicity (involving myelotoxicity) of doxorubicin appear to be unaltered by GF120918 [296].

Valspodar (PSC833) is an analog of cyclosporin D, but it has no immunosuppressive activity. Results from *in vitro* assays have shown that PSC833 may be as much as 20 times more potent an inhibitor of P-gp as cyclosporin A [195,297,298]. Several clinical trials have been performed with PSC833 with some promising results. Patients with relapsed acute myelogenous leukemia (AML) were administered PSC833 with mitoxantrone and etoposide, and it was concluded that this regimen was tolerable and had antileukemic activity [299,300]. Plasma concentrations of PSC833, shown to reverse P-gp-mediated efflux *in vitro*, were achievable in patients treated with other P-gp substrates, without any PSC833-associated toxicity. However, the toxicity of the chemotherapeutic agents tends to be somewhat pronounced when they are coadministered with PSC833 [301,302]. The effectiveness of PSC833 in increasing the efficacy of chemotherapeutic agents/regimens appears promising, but more trials must be performed to confirm these initial results.

CGP41251 is the *N*-benzyl derivative of staurosporine and appears to have some affinity for protein kinase C (PKC) along with an ability to inhibit P-gp-mediated efflux [284]. There have been few clinical studies performed with this agent to date.

## VII. DRUG-DRUG INTERACTIONS BETWEEN P-GLYCOPROTEIN SUBSTRATES

Although drug-drug interactions are typically associated with a change in a compound's metabolic profile, it has recently become apparent that interactions between P-gp substrates can also lead to significant alterations in the pharmacokinetic profiles of these drugs. The actions of transporters in the elimination of their substrates in the liver, kidney, and intestine (exsorption) has recently been elucidated. It is now known that primary active transport mechanisms contribute greatly to the biliary excretion of various cytotoxic agents, organic cations and anions, and compounds that have been conjugated via phase II metabolism [303]. The elimination of organic cations by the kidney is highly dependent on active transport [304]. It is known that intestinally expressed P-gp can act to limit the absorption of its substrates and, like the liver and kidney, the presence of P-gp in



the intestine can make this an efficient organ of elimination. Due to the extensive distribution and physiologically protective nature of P-gp, it is inevitable that drug–drug interactions between substrates of this pump will be seen, given the importance of P-gp in determining the absorption, distribution, and elimination of its substrates [305]. Knowledge regarding the importance of these interactions is presently limited. The following sections contain examples of drug interactions caused by the coadministration of compounds that affect P-gp-mediated efflux.

### A. Digoxin

The cardiac glycoside digoxin, widely used for the treatment of congestive heart failure, has a very narrow therapeutic window, and any interactions that alter the blood concentration of this agent are potentially dangerous [306,307]. Digoxin has been shown to be a substrate of P-gp both in vitro [308] and in vivo [202]. Because of the strict monitoring of digoxin pharmacokinetics, valuable information regarding the interaction between this agent and other P-gp substrates has been elucidated.

The ratio of renal clearance of digoxin to creatinine clearance decreased with the coadministration of clarithromycin (0.64 and 0.73) and was restored (1.30) after the administration of clarithromycin had stopped [309]. The role of P-gp efflux in this interaction was confirmed using an in vitro kidney epithelial cell line [309]. The administration of itraconazole, a P-gp inhibitor, with digoxin resulted in an increased trough concentration and a decrease in the amount of renal clearance, possibly by an inhibition of the renal tubular secretion of digoxin via P-gp [310]. The P-gp modulator verapamil has been shown to decrease the renal clearance of digoxin [311].

It is well known that a drug–drug interaction occurs between digoxin and quinidine. It has been shown that quinidine can alter the secretion of digoxin in the kidney and also in the intestine [179]. The plasma concentrations of digoxin following intravenous injection increased twofold when quinidine (1 mg/h) was coadministered [179]. The total clearance decreased from  $318 \pm 19.3$  to  $167 \pm 11.0$  ml/hr [179]. The coadministration of quinidine decreased the amount of digoxin appearing in the intestine by approximately 40% [179]. The intestinal clearance also decreased from  $28.8 \pm 1.7$  to  $11.1 \pm 1.6$  ml/hr following quinidine coadministration [179]. These studies demonstrate how quinidine can affect the absorption and secretion of digoxin.

In some cases of atrial fibrillation, both digoxin and verapamil are used [306,307]. Observations from this coadministration have shown how the P-gp modulation affected by verapamil altered the distribution and elimination of digoxin [202,230,312–315].

Dietary factors and herbal agents can also lead to drug interactions. The effects of Saint John's wort (*Hypericum perforatum*), a widely used herbal antide-

pressant, on digoxin were examined in a single blind placebo controlled clinical trial, designed to study the changes in the pharmacokinetics of digoxin used in combination with this supplement. This herbal extract was shown to have significant effects on the pharmacokinetic profile of digoxin [316]. The results of this study indicate that Saint John's wort extract appears to increase the elimination of digoxin.

Another interaction that has been reported to affect digoxin pharmacokinetics involves the induction of P-gp. It has been shown clinically that the blood concentration of digoxin decreases significantly for patients receiving rifampin [317]. A clinical trial was designed to confirm that this decrease was indeed due to the induction of P-gp; the single-dose pharmacokinetics of digoxin (oral and IV) were determined before and after administration of rifampin. The rifampin treatment increased the level of P-gp in the intestine 3.5-fold [317]. The AUC of orally administered digoxin was significantly lower after the administration of rifampin, whereas the decrease in intravenously administered digoxin was affected to a lesser degree [317]. Additionally, the renal clearance and half-life of digoxin were found to be unaltered by rifampin [317]. These findings led the authors to postulate that the digoxin–rifampin interaction occurs largely at the level of the intestine and that this interaction seems to have a large effect on the absorption of digoxin [317]. The ability of orally administered rifampin to induce intestinally expressed P-gp may have further consequences for the intestinal absorption of other P-gp substrates/inhibitors.

## B. Cyclosporin A

Like digoxin, the plasma concentrations of cyclosporin A are strictly monitored. The determination of the effects of other agents on the pharmacokinetic profile of cyclosporin A has provided valuable information regarding possible drug–drug interactions involving P-gp-mediated efflux.

A toxic interaction between escalating doses of intravenously administered cyclosporin A (6–27 mg/kg/day, median: 19.5 mg/kg/day) and a standard chemotherapeutic regimen was observed in patients diagnosed with soft-tissue sarcoma [305,318]. The regimen consisted of courses of etoposide and ifosfamide (days 1 and 2) (VP16/Ifos cycles), alternating with courses of vincristine, dactinomycin, and cyclophosphamide (days 1 and 5) (VAC cycles) [318]. The administration of cyclosporin A dramatically increased the systemic toxicity of the VAC cycle, but only mildly increased the systemic toxicity of the VP16/Ifos cycle [318]. A possible mechanism for this increased toxicity was proposed to involve increases in serum concentrations (due to decreased elimination) of etoposide, vincristine, and dactinomycin, all of which are P-gp substrates, following the inhibition of P-gp by cyclosporin A [318].

An enhancement in the absorption of orally administered cyclosporin A

(10 mg) was observed, as evidenced by an increase in the AUC, when a solution of vitamin E was given concomitantly with one of the cyclosporin A doses in a randomized trial [319]. The levels of metabolites of cyclosporin were unchanged by oral administration of the vitamin E solution. This led the researchers to conclude that the vitamin E solution acted either to enhance the absorptive transport or to decrease the countertransport of cyclosporin in the intestine by inhibition of P-gp [319].

## VIII. CONCLUSIONS

Originally discovered as an adaptive response of cancer cells that are exposed to high concentrations of toxic drugs, P-gp is now recognized as a widely distributed constitutive protein that plays a pivotal role in the systemic disposition of a wide variety of hormones, drugs, and other xenobiotics. Furthermore, recent investigations have uncovered a large family of efflux proteins, with diverse and overlapping substrate specificities, that play a critical role in the disposition of therapeutic agents. The scope of the biochemical, cellular, physiological, and clinical implications of these proteins is just beginning to be recognized. An exhaustive review of this vast and complex area of emerging research is beyond the scope of this chapter. Instead, we have focused on the most extensively investigated protein, P-gp, as a prototype of the efflux pump family. The studies presented here have demonstrated the dual role played by P-gp in minimizing the systemic and tissue/organ exposure to foreign agents—it acts as a biochemical barrier in preventing the entry (absorption) of drugs across epithelial or endothelial tissues, and it provides a driving force for the excretion of drugs and metabolites by mediating their active secretion into the excretory organs. By virtue of its presence in epithelial and endothelial cells, P-gp can also play a decisive role in the tissue and organ distribution of a drug. The most notable example of this is the role played by P-gp (as a component of the blood–brain barrier) in attenuating the access of drugs to brain tissues. P-gp, when colocalized with metabolic enzymes in certain tissues (e.g., CYP3A in intestinal epithelium), can modulate the metabolic transformation of some drugs markedly, both at the cellular and tissue/organ levels. Hence, in designing drugs with an optimal pharmacokinetic profile, it is imperative that the role of P-gp (and other efflux proteins) in the absorption, distribution, metabolism, and elimination of the drug candidates be elucidated. It is equally important to recognize that other factors—i.e., coadministered drug(s), diet, disease, etc.—can significantly affect the disposition of a given therapeutic agent by modulating the activity of P-gp (and other efflux proteins), resulting in serious incidents of therapeutic failure or unexpected toxicity. Hence, investigation of P-gp and other efflux proteins across a wide array of scientific disciplines promises to be a very fertile area of research in the years to come.

## REFERENCES

1. Thiebaut F, Tsuruo T, Hamada H, Gottesman MM, Pastan I, Willingham MC. Cellular localization of the multidrug-resistance gene product P-glycoprotein in normal human tissues. *Proc Natl Acad Sci USA* 1987, 84(21):7735–7738.
2. Hunter J, Hirst BH, Simmons NL. Drug absorption limited by P-glycoprotein-mediated secretory drug transport in human intestinal epithelial Caco-2 cell layers. *Pharm Res* 1993, 10(5):743–749.
3. Hunter J, Hirst BH, Simmons NL. Epithelial secretion of vinblastine by human intestinal adenocarcinoma cell (HCT-8 and T84) layers expressing P-glycoprotein. *Br J Cancer* 1991, 64(3):437–444.
4. Ince P, Elliott K, Appleton DR, Moorghen M, Finney KJ, Sunter JP, Harris AL, Watson AJ. Modulation by verapamil of vincristine pharmacokinetics and sensitivity to metaphase arrest of the normal rat colon in organ culture. *Biochem Pharmacol* 1991, 41(8):1217–1225.
5. Gramatte T, Oertel R, Terhaag B, Kirch W. Direct demonstration of small intestinal secretion and site-dependent absorption of the beta-blocker talinolol in humans. *Clin Pharmacol Ther* 1996, 59(5):541–549.
6. Meyers MB, Scotto KW, Sirotnak FM. P-glycoprotein content and mediation of vincristine efflux: correlation with the level of differentiation in luminal epithelium of mouse small intestine. *Cancer Commun* 1991, 3(5):159–165.
7. Wetterich U, Spahn-Langguth H, Mutschler E, Terhaag B, Rosch W, Langguth P. Evidence for intestinal secretion as an additional clearance pathway of talinolol enantiomers: concentration- and dose-dependent absorption in vitro and in vivo. *Pharm Res* 1996, 13(4):514–522.
8. Juliano RL, Ling V. A surface glycoprotein modulating drug permeability in Chinese hamster ovary cell mutants. *Biochim Biophys Acta* 1976, 455(1):152–162.
9. Kartner N, Riordan JR, Ling V. Cell surface P-glycoprotein associated with multidrug resistance in mammalian cell lines. *Science* 1983, 221(4617):1285–1288.
10. Ueda K, Okamura N, Hirai M, Tanigawara Y, Saeki T, Kioka N, Komano T, Hori R. Human P-glycoprotein transports cortisol, aldosterone, and dexamethasone, but not progesterone. *J Biol Chem* 1992, 267(34):24248–24252.
11. Kusuhara H, Suzuki H, Sugiyama Y. The role of P-glycoprotein and canalicular multispecific organic anion transporter in the hepatobiliary excretion of drugs. *J Pharm Sci* 1998, 87(9):1025–1040.
12. Juranka PF, Zastawny RL, Ling V. P-glycoprotein: multidrug-resistance and a superfamily of membrane-associated transport proteins. *FASEB J* 1989, 3(14):2583–2592.
13. Ng WF, Sarangi F, Zastawny RL, Veinot-Drebot L, Ling V. Identification of members of the P-glycoprotein multigene family. *Mol Cell Biol* 1989, 9(3):1224–1232.
14. Chen CJ, Chin JE, Ueda K, Clark DP, Pastan I, Gottesman MM, Roninson IB. Internal duplication and homology with bacterial transport proteins in the *mdr1* (P-glycoprotein) gene from multidrug-resistant human cells. *Cell* 1986, 47(3):381–389.

15. Fardel O, Lecureur V, Guillouzo A. The P-glycoprotein multidrug transporter. *Gen Pharmacol* 1996, 27(8):1283–1291.
16. van der Blik AM, Kooiman PM, Schneider C, Borst P. Sequence of *mdr3* cDNA encoding a human P-glycoprotein. *Gene* 1988, 71(2):401–411.
17. Smith AJ, Timmermans-Hereijgers JL, Roelofsen B, Wirtz KW, van Blitterswijk WJ, Smit JJ, Schinkel AH, Borst P. The human MDR3 P-glycoprotein promotes translocation of phosphatidylcholine through the plasma membrane of fibroblasts from transgenic mice. *FEBS Lett* 1994, 354(3):263–266.
18. Gros P, Croop J, Housman D. Mammalian multidrug resistance gene: complete cDNA sequence indicates strong homology to bacterial transport proteins. *Cell* 1986, 47(3):371–380.
19. Gros P, Raymond M, Bell J, Housman D. Cloning and characterization of a second member of the mouse *mdr* gene family. *Mol Cell Biol* 1988, 8(7):2770–2778.
20. Devault A, Gros P. Two members of the mouse *mdr* gene family confer multidrug resistance with overlapping but distinct drug specificities. *Mol Cell Biol* 1990, 10(4):1652–1663.
21. Deuchars KL, Duthie M, Ling V. Identification of distinct P-glycoprotein gene sequences in rat. *Biochim Biophys Acta* 1992, 1130(2):157–165.
22. Devine SE, Hussain A, Davide JP, Melera PW. Full length and alternatively spliced *pgp1* transcripts in multidrug-resistant Chinese hamster lung cells. *J Biol Chem* 1991, 266(7):4545–4555.
23. Childs S, Ling V. Duplication and evolution of the P-glycoprotein genes in pig. *Biochim Biophys Acta* 1996, 1307(2):205–212.
24. Ueda K, Cardarelli C, Gottesman MM, Pastan I. Expression of a full-length cDNA for the human “MDR1” gene confers resistance to colchicine, doxorubicin, and vinblastine. *Proc Natl Acad Sci USA* 1987, 84(9):3004–3008.
25. Schurr E, Raymond M, Bell JC, Gros P. Characterization of the multidrug resistance protein expressed in cell clones stably transfected with the mouse *mdr1* cDNA. *Cancer Res* 1989, 49(10):2729–2733.
26. Buschman E, Gros P. The inability of the mouse *mdr2* gene to confer multidrug resistance is linked to reduced drug binding to the protein. *Cancer Res* 1994, 54(18):4892–4898.
27. Oude Elferink RPJ, tytgat GNJ, Groen AK. The role of *mdr2* P-glycoprotein in hepatobiliary lipid transport. *FASEB J* 1997, 11:19–28.
28. Fojo AT, Ueda K, Slamon DJ, Poplack DG, Gottesman MM, Pastan I. Expression of a multidrug-resistance gene in human tumors and tissues. *Proc Natl Acad Sci USA* 1987, 84(1):265–269.
29. Cordon-Cardo C, O’Brien JP, Boccia J, Casals D, Bertino JR, Melamed MR. Expression of the multidrug resistance gene product (P-glycoprotein) in human normal and tumor tissues. *J Histochem Cytochem* 1990, 38(9):1277–1287.
30. Hamada H, Tsuruo T. Functional role for the 170- to 180-kDa glycoprotein specific to drug-resistant tumor cells as revealed by monoclonal antibodies. *Proc Natl Acad Sci USA* 1986, 83(20):7785–7789.
31. Sugawara I, Kataoka I, Morishita Y, Hamada H, Tsuruo T, Itoyama S, Mori S. Tissue distribution of P-glycoprotein encoded by a multidrug-resistant gene as revealed by a monoclonal antibody, MRK 16. *Cancer Res* 1988, 48(7):1926–1929.

32. Sugawara I, Nakahama M, Hamada H, Tsuruo T, Mori S. Apparent stronger expression in the human adrenal cortex than in the human adrenal medulla of Mr 170,000–180,000 P-glycoprotein. *Cancer Res* 1988, 48(16):4611–4614.
33. Cordon-Cardo C, O'Brien JP, Casals D, Rittman-Grauer L, Biedler JL, Melamed MR, Bertino JR. Multidrug-resistance gene (P-glycoprotein) is expressed by endothelial cells at blood-brain barrier sites. *Proc Natl Acad Sci USA* 1989, 86(2):695–698.
34. Thiebaut F, Tsuruo T, Hamada H, Gottesman MM, Pastan I, Willingham MC. Immunohistochemical localization in normal tissues of different epitopes in the multidrug transport protein P170: evidence for localization in brain capillaries and cross-reactivity of one antibody with a muscle protein. *J Histochem Cytochem* 1989, 37(2):159–164.
35. Lieberman DM, Reithmeier RA, Ling V, Charuk JH, Goldberg H, Skorecki KL. Identification of P-glycoprotein in renal brush border membranes. *Biochem Biophys Res Commun* 1989, 162(1):244–252.
36. Gan LS, Thakker, DR. Applications of the Caco-2 model in the design and development of orally active drugs: elucidation of biochemical and physical barriers posed by the intestinal epithelium. *Adv. Drug Delivery Rev.* 1997, 23(1–3):77–98.
37. Hosoya KI, Kim KJ, Lee VH. Age-dependent expression of P-glycoprotein gp170 in Caco-2 cell monolayers. *Pharm Res* 1996, 13(6):885–890.
38. Doppenschmitt S, Spahn-Langguth H, Regardh CG, Langguth P. Radioligand-binding assay employing P-glycoprotein-overexpressing cells: testing drug affinities to the secretory intestinal multidrug transporter. *Pharm Res* 1998, 15(7):1001–1006.
39. Horio M, Chin KV, Currier SJ, Goldenberg S, Williams C, Pastan I, Gottesman MM, Handler J. Transepithelial transport of drugs by the multidrug transporter in cultured Madin–Darby canine kidney cell epithelia. *J Biol Chem* 1989, 264(25):14880–14884.
40. Hunter J, Hirst BH, Simmons NL. Transepithelial secretion, cellular accumulation and cytotoxicity of vinblastine in defined MDCK cell strains. *Biochim Biophys Acta* 1993, 1179(1):1–10.
41. Zhang Y, Benet LZ. Characterization of P-glycoprotein mediated transport of K02, a novel vinylsulfone peptidomimetic cysteine protease inhibitor, across MDR1-MDCK and Caco-2 cell monolayers. *Pharm Res* 1998, 15(10):1520–1524.
42. Schuetz EG, Beck WT, Schuetz JD. Modulators and substrates of P-glycoprotein and cytochrome P4503A coordinately up-regulate these proteins in human colon carcinoma cells. *Mol Pharmacol* 1996, 49(2):311–318.
43. Borst P, Schinkel AH. What have we learnt thus far from mice with disrupted P-glycoprotein genes? *Eur J Cancer* 1996, 32A(6):985–990.
44. Borst P, Schinkel AH, Smit JJ, Wagenaar E, Van Deemter L, Smith AJ, Eijdem EW, Baas F, Zaman GJ. Classical and novel forms of multidrug resistance and the physiological functions of P-glycoproteins in mammals. *Pharmacol Ther* 1993, 60(2):289–299.
45. Lum BL, Gosland MP. MDR expression in normal tissues. Pharmacologic implications for the clinical use of P-glycoprotein inhibitors. *Hematol Oncol Clin North Am* 1995, 9(2):319–336.

46. Kamimoto Y, Gatmaitan Z, Hsu J, Arias IM. The function of Gp170, the multidrug resistance gene product, in rat liver canalicular membrane vesicles. *J Biol Chem* 1989, 264(20):11693–11698.
47. Pournier-Manzanedo A, Boesch D, Loo F. FK-506 (fujimycin) reverses the multidrug resistance of tumor cells in vitro. *Anticancer Drugs* 1991, 2(3):279–283.
48. Augustijns PF, Bradshaw TP, Gan LS, Hendren RW, Thakker DR. Evidence for a polarized efflux system in CACO-2 cells capable of modulating cyclosporin A transport. *Biochem Biophys Res Commun* 1993, 197(2):360–365.
49. Valverde MA, Bond TD, Hardy SP, Taylor JC, Higgins CF, Altamirano J, Alvarez-Leefmans FJ. The multidrug resistance P-glycoprotein modulates cell regulatory volume decrease. *EMBO J* 1996, 15(17):4460–4468.
50. Miwa A, Ueda K, Okada Y. Protein kinase C-independent correlation between P-glycoprotein expression and volume sensitivity of Cl<sup>-</sup> channel. *J Membr Biol* 1997, 157(1):63–69.
51. Kool M, de Haas M, Scheffer GL, Scheper RJ, van Eijk MJ, Juijn JA, Baas F, Borst P. Analysis of expression of cMOAT (MRP2), MRP3, MRP4, and MRP5, homologues of the multidrug resistance-associated protein gene (MRP1), in human cancer cell lines. *Cancer Res* 1997, 57(16):3537–3547.
52. Kool M, van der Linden M, de Haas M, Baas F, Borst P. Expression of human MRP6, a homologue of the multidrug resistance protein gene MRP1, in tissues and cancer cells. *Cancer Res* 1999, 59(1):175–182.
53. Masuda M, Iizuka Y, Yamazaki M, Nishigaki R, Kato Y, Ni'inuma K, Suzuki H, Sugiyama Y. Methotrexate is excreted into the bile by canalicular multispecific organic anion transporter in rats. *Cancer Res* 1997, 57(16):3506–3510.
54. Jansen PL, Peters WH, Lamers WH. Hereditary chronic conjugated hyperbilirubinemia in mutant rats caused by defective hepatic anion transport. *Hepatology* 1985, 5(4):573–579.
55. Fernandez-Checa JC, Takikawa H, Horie T, Ookhtens M, Kaplowitz N. Canalicular transport of reduced glutathione in normal and mutant Eisai hyperbilirubinemic rats. *J Biol Chem* 1992, 267(3):1667–1673.
56. Zaman GJ, Versantvoort CH, Smit JJ, Eijdemans EW, de Haas M, Smith AJ, Broxterman HJ, Mulder NH, de Vries EG, Baas F. Analysis of the expression of MRP, the gene for a new putative transmembrane drug transporter, in human multidrug resistant lung cancer cell lines. *Cancer Res* 1993, 53(8):1747–1750.
57. Stride BD, Valdimarsson G, Gerlach JH, Wilson GM, Cole SP, Deeley RG. Structure and expression of the messenger RNA encoding the murine multidrug resistance protein, an ATP-binding cassette transporter. *Mol Pharmacol* 1996, 49(6):962–971.
58. Flens MJ, Zaman GJ, van der Valk P, Izquierdo MA, Schroeijers AB, Scheffer GL, van der Groep P, de Haas M, Meijer CJ, Scheper RJ. Tissue distribution of the multidrug resistance protein. *Am J Pathol* 1996, 148(4):1237–1247.
59. Evers R, Zaman GJ, van Deemter L, Jansen H, Calafat J, Oomen LC, Oude Elferink RP, Borst P, Schinkel AH. Basolateral localization and export activity of the human multidrug resistance-associated protein in polarized pig kidney cells. *J Clin Invest* 1996, 97(5):1211–1218.

60. Muller M, Jansen PL. Molecular aspects of hepatobiliary transport. *Am J Physiol* 1997, 272(6 Pt. 1):G1285–G1303.
61. Torok M, Gutmann H, Fricker G, Drewe J. Sister of P-glycoprotein expression in different tissues. *Biochem Pharmacol* 1999, 57(7):833–835.
62. Gerloff T, Stieger B, Hagenbuch B, Madon J, Landmann L, Roth J, Hofmann AF, Meier PJ. The sister of P-glycoprotein represents the canalicular bile salt export pump of mammalian liver. *J Biol Chem* 1998, 273(16):10046–10050.
63. Lecureur V, Sun D, Hargrove P, Schuetz EG, Kim RB, Lan LB, Schuetz JD. Cloning and expression of murine sister of P-glycoprotein reveals a more discriminating transporter than MDR1/P-glycoprotein. *Mol Pharmacol* 2000, 57(1):24–35.
64. Sharom FJ. The P-glycoprotein efflux pump: how does it transport drugs? *J Membr Biol* 1997, 160(3):161–175.
65. Higgins CF. ABC transporters: from microorganisms to man. *Annu Rev Cell Biol* 1992, 8:67–113.
66. Leveille-Webster CR, Arias IM. The biology of the P-glycoproteins. *J Membr Biol* 1995, 143(2):89–102.
67. Gottesman MM, Pastan I. Biochemistry of multidrug resistance mediated by the multidrug transporter. *Biochemistry* 1993, 62:385–427.
68. German UA. P-glycoprotein—a mediator of multidrug resistance in tumour cells. *Eur J Cancer* 1996, 32A(6):927–944.
69. Endicott JA, Ling V. The biochemistry of P-glycoprotein-mediated multidrug resistance. *Annu Rev Biochem* 1989, 58:137–171.
70. Richert ND, Aldwin L., Nitecki D, Gottesman MM, Pastan I. Stability and covalent modification of P-glycoprotein in multidrug-resistant. *Biochemistry* 1988, 27(20):7607–7613.
71. Greenberger LM, Lothstein L, Williams SS, Horwitz SB. Distinct P-glycoprotein precursors are overproduced in independently isolated drug-resistant cell lines. *Proc Natl Acad Sci USA* 1988, 85(11):3762–3766.
72. Beck WT, Cirtain MC. Continued expression of vinca alkaloid resistance by CCRF-CEM cells after treatment with tunicamycin or pronase. *Cancer Res* 1982, 42(1):184–189.
73. Ling V, Kartner N, Sudo T, Siminovitch L, Riordan JR. Multidrug-resistance phenotype in Chinese hamster ovary cells. *Cancer Treat Rep* 1983, 67(10):869–874.
74. Germann UA, Willingham MC, Pastan I, Gottesman MM. Expression of the human multidrug transporter in insect cells by a recombinant baculovirus. *Biochemistry* 1990, 29(9):2295–2303.
75. Kuchler K, Thorner J. Functional expression of human mdr1 in the yeast *Saccharomyces cerevisiae*. *Proc Natl Acad Sci USA* 1992, 89(6):2302–2306.
76. Sarkadi B, Price EM, Boucher RC, Germann UA, Scarborough GA. Expression of the human multidrug resistance cDNA in insect cells generates a high activity drug-stimulated membrane ATPase. *J Biol Chem* 1992, 267(7):4854–4858.
77. Schinkel AH, Kemp S, Dolle M, Rudenko G, Wagenaar E. N-glycosylation and deletion mutants of the human MDR1 P-glycoprotein. *J Biol Chem* 1993, 268(10):7474–7481.
78. Kramer R, Weber TK, Areci R, Ramchurren N, Kastriakis WV, Steele GJ, Sum-



- merhayes IC. Inhibition of N-linked glycosylation of P-glycoprotein by tunicamycin results in a reduced multidrug resistance phenotype. *Br J Cancer* 1995, 71(4):670–675.
79. Chambers TC, Germann UA, Gottesman MM, Pastan I, Kuo JF, Ambudkar SV. Bacterial expression of the linker region of human MDR1 P-glycoprotein and mutational analysis of phosphorylation sites. *Biochemistry* 1995, 34(43):14156–14162.
  80. Orr GA, Han EK, Browne PC, Nieves E, O'Connor BM, Yang CP, Horwitz SB. Identification of the major phosphorylation domain of murine *mdr1b* P-glycoprotein. Analysis of the protein kinase A and protein kinase C phosphorylation sites. *J Biol Chem* 1993, 268(33):25054–25062.
  81. Scala S, Dickstein B, Regis J, Szallasi Z, Blumberg PM, Bates SE. Bryostatin 1 affects P-glycoprotein phosphorylation but not function in multidrug-resistant human breast cancer cells. *Clin Cancer Res* 1995, 1(12):1581–1587.
  82. Higgins CF. P-glycoprotein and cell volume-activated chloride channels. *J Bioenerg Biomembr* 1995, 27(1):63–70.
  83. Boyum R, Guidotti G. Effect of ATP binding cassette/multidrug resistance proteins on ATP efflux of *accharomyces cerevisiae*. *Biochem Biophys Res Commun* 1997, 230(1):22–26.
  84. Tominaga M, Tominaga T, Miwa A, Okada Y. Volume-sensitive chloride channel activity does not depend on endogenous P-glycoprotein. *J Biol Chem* 1995, 270(46):27887–27893.
  85. Homolya L, Hollo Z, Germann UA, Pastan I, Gottesman MM, Sarkadi B. Fluorescent cellular indicators are extruded by the multidrug resistance protein. *J Biol Chem* 1993, 268(29):21493–21496.
  86. Currier SJ, Ueda K, Willingham MC, Pastan I, Gottesman MM. Deletion and insertion mutants of the multidrug transporter. *J Biol Chem* 1989, 264(24):14376–14381.
  87. Loo TW, Clarke DM. Reconstitution of drug-stimulated ATPase activity following co-expression of each half of human P-glycoprotein as separate polypeptides. *J Biol Chem* 1994, 269(10):7750–7755.
  88. Gottesman MM, Hrycyna CA, Schoenlein PV, Germann UA, Pastan I. Genetic analysis of the multidrug transporter. *Annu Rev Genet* 1995, 29:607–649.
  89. Bruggemann EP, Currier SJ, Gottesman MM, Pastan I. Characterization of the azidopine and vinblastine binding site of P-glycoprotein. *J Biol Chem* 1992, 267(29):21020–21026.
  90. Loo TW, Clarke DM. Inhibition of oxidative cross-linking between engineered cysteine residues at positions 332 in predicted transmembrane segments (TM) 6 and 975 in predicted TM12 of human P-glycoprotein by drug substrates. *J Biol Chem* 1996, 271(44):27482–27487.
  91. Loo TW, Clarke DM. Functional consequences of phenylalanine mutations in the predicted transmembrane domain of P-glycoprotein. *J Biol Chem* 1993, 268(27):19965–19972.
  92. Loo TW, Clarke DM. Mutations to amino acids located in predicted transmembrane segment 6 (TM6) modulate the activity and substrate specificity of human P-glycoprotein. *Biochemistry* 1994, 33(47):14049–14057.

93. Ueda K, Taguchi Y, Morishima M. How does P-glycoprotein recognize its substrates? *Semin Cancer Biol* 1997, 8(3):151–159.
94. Kajiji S, Talbot F, Grizzuti K, Van Dyke-Phillips V, Agresti M, Safa AR, Gros P. Functional analysis of P-glycoprotein mutants identifies predicted transmembrane domain 11 as a putative drug binding site. *Biochemistry* 1993, 32(16):4185–4194.
95. Gros P, Dhir R, Croop J, Talbot F. A single amino acid substitution strongly modulates the activity and substrate specificity of the mouse *mdr1* and *mdr3* drug efflux pumps. *Proc Natl Acad Sci USA* 1991, 88(16):7289–7293.
96. Germann VA, Pastan I, Gottesman MM. P-glycoproteins: mediators of multidrug resistance. *Semin Cell Biol* 1993, 4(1):63–76.
97. Sharom FJ. The P-glycoprotein multidrug transporter: interactions with membrane lipids, and their modulation of activity. *Biochem Soc Trans* 1997, 25(3):1088–1096.
98. Pawagi AB, Wang J, Silverman M, Reithmeier RA, Deber CM. Transmembrane aromatic amino acid distribution in P-glycoprotein. A functional role in broad substrate specificity. *J Mol Biol* 1994, 235(2):554–564.
99. Schinkel AH, Roelofs EM, Borst P. Characterization of the human MDR3 P-glycoprotein and its recognition by P-glycoprotein-specific monoclonal antibodies. *Cancer Res* 1991, 51(10):2628–2635.
100. Tamai I, Safa AR. Azidopine noncompetitively interacts with vinblastine and cyclosporin A binding to P-glycoprotein in multidrug resistant cells. *J Biol Chem* 1991, 266(25):16796–16800.
101. Ferry DR, Russell MA, Cullen MH. P-glycoprotein possesses a 1,4-dihydropyridine-selective drug acceptor site which is allosterically coupled to a vinca-alkaloid-selective binding site. *Biochem Biophys Res Commun* 1992, 188(1):440–445.
102. Ferry DR, Malkhandi PJ, Russell MA, Kerr DJ. Allosteric regulation of [3H]vinblastine binding to P-glycoprotein of MCF-7 ADR cells by dexniguldipine. *Biochem Pharmacol* 1995, 49(12):1851–1861.
103. Shapiro AB, Ling V. Positively cooperative sites for drug transport by P-glycoprotein with distinct drug specificities. *Eur J Biochem* 1997, 250(1):130–137.
104. Critchfield JW, Welsh CJ, Phang JM, Yeh GC. Modulation of adriamycin accumulation and efflux by flavonoids in HCT-15 colon cells. Activation of P-glycoprotein as a putative mechanism. *Biochem Pharmacol* 1994, 48(7):1437–1445.
105. Phang JM, Poore CM, Lopaczynska J, Yeh GC. Flavonol-stimulated efflux of 7,12-dimethylbenz(a)anthracene in multidrug-resistant breast cancer cells. *Cancer Res* 1993, 53(24):5977–5981.
106. Higgins CF, Gottesman MM. Is the multidrug transporter a flippase? *Trends Biochem Sci* 1992, 17(1):18–21.
107. Sinicrope FA, Dudeja PK, Bissonnette BM, Safa AR, Brasitus TA. Modulation of P-glycoprotein-mediated drug transport by alterations in lipid fluidity of rat liver canalicular membrane vesicles. *J Biol Chem* 1992, 267(35):24995–25002.
108. van Helvoort A, Smith AJ, Sprong H, Fritzsche I, Schinkel AH, Borst P, van Meer G. MDR1 P-glycoprotein is a lipid translocase of broad specificity, while MDR3 P-glycoprotein specifically translocates phosphatidylcholine. *Cell* 1996, 87(3):507–517.
109. Litman T, Zeuthen T, Skovsgaard T, Stein WD. Structure–activity relationships of

- P-glycoprotein interacting drugs: kinetic characterization of their effects on ATPase activity. *Biochim Biophys Acta* 1997, 1361(2):159–168.
110. Seelig A. A general pattern for substrate recognition by P-glycoprotein. *Eur J Biochem* 1998, 251(1–2):252–261.
  111. Scala S, Akhmed N, Rao US, Paull K, Lan LB, Dickstein B, Lee JS, Elgemeie GH, Stein WD, Bates SE. P-glycoprotein substrates and antagonists cluster into two distinct groups. *Mol Pharmacol* 1997, 51(6):1024–1033.
  112. Litman T, Zeuthen T, Skovsgaard T, Stein WD. Competitive, non-competitive and cooperative interactions between substrates of P-glycoprotein as measured by its ATPase activity. *Biochim Biophys Acta* 1997, 1361(2):169–176.
  113. Etievant C, Schambel P, Guminski Y, Barret JM, Imbert T, Hill BT. Requirements for P-glycoprotein recognition based on structure–activity relationships in the podophyllotoxin series. *Anticancer Drug Des* 1998, 13(4):317–336.
  114. Bain LJ, LeBlanc GA. Interaction of structurally diverse pesticides with the human MDR1 gene product P-glycoprotein. *Toxicol Appl Pharmacol* 1996, 141(1):288–298.
  115. Ford JM, Prozialeck WC, Hait WN. Structural features determining activity of phenothiazines and related drugs for inhibition of cell growth and reversal of multidrug resistance. *Mol Pharmacol* 1989, 35(1):105–115.
  116. Regev R, Assaraf YG, Eytan GD. Membrane fluidization by ether, other anesthetics, and certain agents abolishes P-glycoprotein ATPase activity and modulates efflux from multidrug-resistant cells. *Eur J Biochem* 1999, 259(1–2):18–24.
  117. Simons K, van Meer G. Lipid sorting in epithelial cells. *Biochemistry* 1988, 27(17):6197–6202.
  118. Eytan GD, Regev R, Oren G, Assaraf YG. The role of passive transbilayer drug movement in multidrug resistance and its modulation. *J Biol Chem* 1996, 271(22):12897–12902.
  119. Regev R, Eytan GD. Flip-flop of doxorubicin across erythrocyte and lipid membranes. *Biochem Pharmacol* 1997, 54(10):1151–1158.
  120. Nerurkar MM, Burton PS, Borchardt RT. The use of surfactants to enhance the permeability of peptides through Caco-2 cells by inhibition of an apically polarized efflux system. *Pharm Res* 1996, 13(4):528–534.
  121. Nerurkar MM, Ho NF, Burton PS, Vidmar TJ, Borchardt RT. Mechanistic roles of neutral surfactants on concurrent polarized and passive membrane transport of a model peptide in Caco-2 cells. *J Pharm Sci* 1997, 86(7):813–821.
  122. Pinto M., Robine-Leon S., Appay M.-D., Kedinger M., Triadou N., Dussaulx E.B., Croix B., Simon-Assmann P., Haffen K., Fogh J., Zweibbaum A. Enterocyte-like differentiation and polarization of the human colon carcinoma cell line Caco-2 in culture. *Biol. Cell* 1983, 47:323–330.
  123. Hidalgo IJ, Raub TJ, Borchardt RT. Characterization of the human colon carcinoma cell line (Caco-2) as a model system for intestinal epithelial permeability. *Gastroenterology* 1989, 96(3):736–749.
  124. Artursson P. Epithelial transport of drugs in cell culture. I: a model for studying the passive diffusion of drugs over intestinal absorptive (Caco-2) cells. *J Pharm Sci* 1990, 79(6):476–482.
  125. Artursson P. Cell cultures as models for drug absorption across the intestinal mucosa. *Crit Rev Ther Drug Carrier Syst* 1991, 8(4):305–330.

126. Wilson G, Hassan I, Dix C, Williamson I, Shah R, Mackay M, Artursson P. Transport and permeability properties of human Caco-2 cells: an in vitro model of the intestinal epithelial cell barrier. *J Control. Release* 1990, 11:25–40.
127. Hilgers AR, Conradi RA, Burton PS. Caco-2 cell monolayers as a model for drug transport across the intestinal mucosa. *Pharm Res* 1990, 7(9):902–910.
128. Cogburn JN, Donovan MG, Schasteen CS. A model of human small intestinal absorptive cells. 1. Transport barrier. *Pharm Res* 1991, 8(2):210–216.
129. Chantret I, Barbat A, Dussaulx E, Brattain MG, Zweibaum A. Epithelial polarity, villin expression, and enterocytic differentiation of cultured human colon carcinoma cells: a survey of twenty cell lines. *Cancer Res* 1988, 48(7):1936–1942.
130. Burton PS, Conradi RA, Hilgers AR, Ho NF. Evidence for a polarized efflux system for peptides in the apical membrane of Caco-2 cells. *Biochem Biophys Res Commun* 1993, 190(3):760–766.
131. Briske-Anderson MJ, Finley JW, Newman SM. The influence of culture time and passage number on the morphological and physiological development of Caco-2 cells. *Proc Soc Exp Biol Med* 1997, 214(3):248–257.
132. Lankelma J, Mulder HS, van Mourik F, Wong Fong Sang HW, Kraayenhof R, van Grondelle R. Cellular daunomycin fluorescence in multidrug resistant 2780AD cells and its relation to cellular drug localisation. *Biochim Biophys Acta* 1991, 1093(2–3):147–152.
133. Molinari A, Cianfriglia M, Meschini S, Calcabrini A, Arancia G. P-glycoprotein expression in the Golgi apparatus of multidrug-resistant cells. *Int J Cancer* 1994, 59(6):789–795.
134. Schuurhuis GJ, van Heijningen TH, Cervantes A, Pinedo HM, de Lange JH, Keizer HG, Broxterman HJ, Baak JP, Lankelma J. Changes in subcellular doxorubicin distribution and cellular accumulation alone can largely account for doxorubicin resistance in SW-1573 lung cancer and MCF-7 breast cancer multidrug resistant tumour cells. *Br J Cancer* 1993, 68(5):898–908.
135. Schmiedlin-Ren P, Thummel KE, Fisher JM, Paine MF, Lown KS, Watkins PB. Expression of enzymatically active CYP3A4 by Caco-2 cells grown on extracellular matrix-coated permeable supports in the presence of 1 alpha,25-dihydroxyvitamin D3. *Mol Pharmacol* 1997, 51(5):741–754.
136. Anderle P, Niederer E, Rubas W, Hilgendorf C, Spahn-Langguth H, Wunderli-Allenspach H, Merkle HP, Langguth P. P-Glycoprotein (P-gp) mediated efflux in Caco-2 cell monolayers: the influence of culturing conditions and drug exposure on P-gp expression levels. *J Pharm Sci* 1998, 87(6):757–762.
137. Simons K, Fuller SD. Cell surface polarity in epithelia. *Annu Rev Cell Biol* 1985, 1:243–288.
138. Evers R, Kool M, van Deemter L, Janssen H, Calafat J, Oomen LC, Paulusma CC, Oude Elferink RP, Baas F, Schinkel AH, Borst P. Drug export activity of the human canalicular multispecific organic anion transporter in polarized kidney MDCK cells expressing cMOAT (MRP2) cDNA. *J Clin Invest* 1998, 101(7):1310–1319.
139. Pardridge WM. CNS drug design based on principles of blood–brain barrier transport. *J Neurochem* 1998, 70(5):1781–1792.
140. Bradbury MW. The blood-brain barrier. *Exp Physiol* 1993, 78(4):453–472.

141. Schinkel AH. P-glycoprotein, a gatekeeper in the blood-brain barrier. *Adv Drug Delivery Rev* 1999, 36:179–194.
142. Tsuji A, Tamai I. Blood–brain barrier function of P-glycoprotein. *Adv Drug Delivery Rev* 1997, 25(2,3):287–298.
143. Audus KL, Ng L, Wang W, Borchardt RT. Models for assessing drug absorption and metabolism. In: RT Borchardt, G Wilson, eds. *Brain Microvessel Endothelial Cell Culture Systems*, 1996, New York: Plenum Press, pp 239–258.
144. Audus KL, Borchardt RT. Characteristics of the large neutral amino acid transport system of bovine brain microvessel endothelial cell monolayers. *J Neurochem* 1986, 47(2):484–488.
145. Audus KL, Borchardt RT. Bovine brain microvessel endothelial cell monolayers as a model system for the blood–brain barrier. *Ann N Y Acad Sci* 1987, 507:9–18.
146. Betz AL, Firth JA, Goldstein GW. Polarity of the blood–brain barrier: distribution of enzymes between the luminal and antiluminal membranes of brain capillary endothelial cells. *Brain Res* 1980, 192(1):17–28.
147. Borges N, Shi F, Azevedo I, Audus KL. Changes in brain microvessel endothelial cell monolayer permeability induced by adrenergic drugs. *Eur J Pharmacol* 1994, 269(2):243–248.
148. Drewes LD, Lidinsky WA. Studies of cerebral capillary endothelial membrane. *Adv Exp Med Biol* 1980, 131:17–27.
149. Guillot FL, Audus KL. Angiotensin peptide regulation of fluid-phase endocytosis in brain microvessel endothelial cell monolayers. *J Cereb Blood Flow Metab* 1990, 10(6):827–834.
150. Miller DW, Audus KL, Borchardt RT. Application of cultured endothelial cells of the brain microvasculature in the study of the blood–brain barrier. *J Tissue Cult Methods* 1992, 14:217–224.
151. Raub TJ, Audus KL. Adsorptive endocytosis and membrane recycling by cultured primary bovine brain microvessel endothelial cell monolayers. *J Cell Sci* 1990, 97(Pt 1):127–138.
152. Joo F. The blood–brain barrier in vitro: ten years of research on microvessels isolated from the brain. *Neurochem Int* 1985, 7:1–25.
153. Joo F. The cerebral microvessels in culture, an update. *J Neurochem* 1992, 58(1): 1–17.
154. Joo F. The blood–brain barrier in vitro: the second decade. *Neurochem Int* 1993, 23(6):499–521.
155. Tsuji A, Terasaki T, Takabatake Y, Tenda Y, Tamai I, Yamashita T, Moritani S, Tsuruo T, Yamashita J. P-glycoprotein as the drug efflux pump in primary cultured bovine brain capillary endothelial cells. *Life Sci* 1992, 51(18):1427–1437.
156. Crone C. The blood–brain barrier as a tight epithelium: where is information lacking? *Ann NY Acad Sci* 1986, 481:174–185.
157. Fontaine M, Elmquist WF, Miller DW. Use of rhodamine 123 to examine the functional activity of P-glycoprotein in primary cultured brain microvessel endothelial cell monolayers. *Life Sci* 1996, 59(18):1521–1531.
158. Lechardeur D, Scherman D. Functional expression of the P-glycoprotein mdr in primary cultures of bovine cerebral capillary endothelial cells. *Cell Biol Toxicol* 1995, 11(5):283–293.

159. Regina A, Koman A, Piciotti M, El Hafny B, Center MS, Bergmann R, Couraud PO, Roux F. Mrpl multidrug resistance-associated protein and P-glycoprotein expression in rat brain microvessel endothelial cells. *J Neurochem* 1998, 71(2):705–715.
160. Seetharaman S, Barrand MA, Maskell L, Scheper RJ. Multidrug resistance-related transport proteins in isolated human brain microvessels and in cells cultured from these isolates. *J Neurochem* 1998, 70(3):1151–1159.
161. Huai-Yun H, Secrest DT, Mark KS, Carney D, Brandquist C, Elmquist WF, Miller DW. Expression of multidrug resistance-associated protein (MRP) in brain microvessel endothelial cells. *Biochem Biophys Res Commun* 1998, 243(3):816–820.
162. Shirai A, Naito M, Tatsuta T, Dong J, Hanaoka K, Mikami K, Oh-hara T, Tsuruo T. Transport of cyclosporin A across the brain capillary endothelial cell monolayer by P-glycoprotein. *Biochim Biophys Acta* 1994, 1222(3):400–4004.
163. Tsuji A, Tamai I, Sakata A, Tenda Y, Terasaki T. Restricted transport of cyclosporin A across the blood-brain barrier by a multidrug transporter, P-glycoprotein. *Biochem Pharmacol* 1993, 46(6):1096–1099.
164. Glynn SL, Yazdanian M. In vitro blood–brain barrier permeability of nevirapine compared to other HIV antiretroviral agents. *J Pharm Sci* 1998, 87(3):306–310.
165. Polli JW, Jarrett JL, Studenberg SD, Humphreys JE, Dennis SW, Brouwer KR, Woolley JL. Role of P-glycoprotein on the CNS disposition of amprenavir (141W94), an HIV protease inhibitor. *Pharm Res* 1999, 16(8):1206–1212.
166. Letrent SP, Polli JW, Humphreys JE, Pollack GM, Brouwer KR, Brouwer KL. P-glycoprotein-mediated transport of morphine in brain capillary endothelial cells. *Biochem Pharmacol* 1999, 58(6):951–957.
167. Egleton RD, Abbruscato TJ, Thomas SA, Davis TP. Transport of opioid peptides into the central nervous system. *J Pharm Sci* 1998, 87(11):1433–1439.
168. Henthorn TK, Liu Y, Mahapatro M, Ng KY. Active transport of fentanyl by the blood-brain barrier. *J Pharmacol Exp Ther* 1999, 289(2):1084–1089.
169. Matsuzaki J, Yamamoto C, Miyama T, Takanaga H, Matsuo H, Ishizuka H, Kawahara Y, Kuwano M, Naito M, Tsuruo T, Sawada Y. Contribution of P-glycoprotein to bunitrolol efflux across blood–brain barrier. *Biopharm Drug Dispos* 1999, 20(2):85–90.
170. Bohme M, Jedlitschky G, Leier I, Buchler M, Keppler D. ATP-dependent export pumps and their inhibition by cyclosporins. *Adv Enzyme Regul* 1994, 34:371–380.
171. Kwon Y, Kamath AV, Morris ME. Inhibitors of P-glycoprotein-mediated daunomycin transport in rat liver canalicular membrane vesicles. *J Pharm Sci* 1996, 85(9):935–939.
172. Horio M, Gottesman MM, Pastan I. ATP-dependent transport of vinblastine in vesicles from human multidrug-resistant cells. *Proc Natl Acad Sci USA* 1988, 85(10):3580–3584.
173. Hsing S, Gatmaitan Z, Arias IM. The function of Gp170, the multidrug-resistance gene product, in the brush border of rat intestinal mucosa. *Gastroenterology* 1992, 102(3):879–885.
174. Makhey VD, Guo A, Norris DA, Hu P, Yan J, Sinko PJ. Characterization of the regional intestinal kinetics of drug efflux in rat and human intestine and in Caco-2 cells. *Pharm Res* 1998, 15(8):1160–1167.

175. Dutt A, Heath LA, Nelson JA. P-glycoprotein and organic cation secretion by the mammalian kidney. *J Pharmacol Exp Ther* 1994, 269(3):1254–1260.
176. Saitoh H, Aungst BJ. Possible involvement of multiple P-glycoprotein-mediated efflux systems in the transport of verapamil and other organic cations across rat intestine. *Pharm Res* 1995, 12(9):1304–1310.
177. Emi Y, Tsunashima D, Ogawara K, Higaki K, Kimura T. Role of P-glycoprotein as a secretory mechanism in quinidine absorption from rat small intestine. *J Pharm Sci* 1998, 87(3):295–299.
178. Hashimoto Y, Sasa H, Shimomura M, Inui K. Effects of intestinal and hepatic metabolism on the bioavailability of tacrolimus in rats. *Pharm Res* 1998, 15(10):1609–1613.
179. Su SF, Huang JD. Inhibition of the intestinal digoxin absorption and exsorption by quinidine. *Drug Metab Dispos* 1996, 24(2):142–147.
180. Beja O, Bibi E. Functional expression of mouse Mdr1 in an outer membrane permeability mutant of *Escherichia coli*. *Proc Natl Acad Sci USA* 1996, 93(12):5969–5974.
181. Evans GL, Ni B, Hrycyna CA, Chen D, Ambudkar SV, Pastan I, Germann UA, Gottesman MM. Heterologous expression systems for P-glycoprotein: *E. coli*, yeast, and baculovirus. *J Bioenerg Biomembr* 1995, 27(1):43–52.
182. Castillo G, Vera JC, Yang CP, Horwitz SB, Rosen OM. Functional expression of murine multidrug resistance in *Xenopus laevis* oocytes. *Proc Natl Acad Sci USA* 1990, 87(12):4737–4741.
183. Saeki T, Shimabuku AM, Azuma Y, Shibano Y, Komano T, Ueda K. Expression of human P-glycoprotein in yeast cells—effects of membrane component sterols on the activity of P-glycoprotein. *Agric Biol Chem* 1991, 55(7):1859–1865.
184. Raymond M, Gros P, Whiteway M, Thomas DY. Functional complementation of yeast ste6 by a mammalian multidrug resistance mdr gene. *Science* 1992, 256(5054):232–234.
185. Spahn-Langguth H, Baktir G, Radschuweit A, Okyar A, Terhaag B, Ader P, Hanafy A, Langguth P. P-glycoprotein transporters and the gastrointestinal tract: evaluation of the potential in vivo relevance of in vitro data employing talinolol as model compound. *Int J Clin Pharmacol Ther* 1998, 36(1):16–24.
186. Bucana CD, Giavazzi R, Nayar R, O'Brian CA, Seid C, Earnest LE, Fan D. Retention of vital dyes correlates inversely with the multidrug-resistant phenotype of adriamycin-selected murine fibrosarcoma variants. *Exp Cell Res* 1990, 190(1):69–75.
187. Dhar S, Nygren P, Liminga G, Sundstrom C, de la Torre M, Nilsson K, Larsson R. Relationship between cytotoxic drug response patterns and activity of drug efflux transporters mediating multidrug resistance. *Eur J Pharmacol* 1998, 346(2–3):315–322.
188. Efferth T, Lohrke H, Volm M. Reciprocal correlation between expression of P-glycoprotein and accumulation of rhodamine 123 in human tumors. *Anticancer Res* 1989, 9(6):1633–1637.
189. Lee JS, Paull K, Alvarez M, Hose C, Monks A, Grever M, Fojo AT, Bates SE. Rhodamine efflux patterns predict P-glycoprotein substrates in the National Cancer Institute drug screen. *Mol Pharmacol* 1994, 46(4):627–638.

190. Liminga G, Nygren P, Larsson R. Microfluorometric evaluation of calcein acetoxy-methyl ester as a probe for P-glycoprotein-mediated resistance: effects of cyclosporin A and its nonimmunosuppressive analogue SDZ PSC 833. *Exp Cell Res* 1994, 212(2):291–296.
191. Takano M, Hasegawa R, Fukuda T, Yumoto R, Nagai J, Murakami T. Interaction with P-glycoprotein and transport of erythromycin, midazolam, and ketoconazole in CaCo-2 cells. *Eur J Pharmacol* 1998, 358(3):284–294.
192. Tiberghien F, Loor F. Ranking of P-glycoprotein substrates and inhibitors by a calcein-AM fluorometry screening assay. *Anticancer Drugs* 1996, 7(5):568–578.
193. Yumoto R, Murakami T, Nakamoto Y, Hasegawa R, Nagai J, Takano M. Transport of rhodamine 123, a P-glycoprotein substrate, across rat intestine and Caco-2 cell monolayers in the presence of cytochrome P-450 3A-related compounds. *J Pharmacol Exp Ther* 1999, 289(1):149–155.
194. Doppenschmitt S, Langguth P, Regardh CG, Andersson TB, Hilgendorf C, Spahn-Langguth H. Characterization of binding properties to human P-glycoprotein: development of a [<sup>3</sup>H]verapamil radioligand-binding assay. *J Pharmacol Exp Ther* 1999, 288(1):348–357.
195. Bohme M, Buchler M, Muller M, Keppler D. Differential inhibition by cyclosporins of primary-active ATP-dependent transporters in the hepatocyte canalicular membrane. *FEBS Lett* 1993, (1–2):193–196.
196. Drucekes P, Schinzel R, Palm D. Photometric microtiter assay of inorganic phosphate in the presence of acid-labile organic phosphates. *Anal Biochem* 1995, 230(1):173–177.
197. Lennernas H. Human jejunal effective permeability and its correlation with preclinical drug absorption models. *J Pharm Pharmacol* 1997, 49(7):627–638.
198. Saitoh H, Hatakeyama M, Eguchi O, Oda M, Takada M. Involvement of intestinal P-glycoprotein in the restricted absorption of methylprednisolone from rat small intestine. *J Pharm Sci* 1998, 87(1):73–75.
199. Brouwer KLR, Thrumen RG. Isolated perfused liver. In: Borchardt RT, Smith PL, Wilson G, eds. *Models for Assessing Drug Absorption and Metabolism*. 1996, New York: Plenum Press, pp 161–192.
200. Booth CL, Brouwer KR, Brouwer KL. Effect of multidrug resistance modulators on the hepatobiliary disposition of doxorubicin in the isolated perfused rat liver. *Cancer Res* 1998, 58(16):3641–3648.
201. Watanabe T, Miyauchi S, Sawada Y, Iga T, Hanano M, Inaba M, Sugiyama Y. Kinetic analysis of hepatobiliary transport of vincristine in perfused rat liver. Possible roles of P-glycoprotein in biliary excretion of vincristine. *J Hepatol* 1992, 16(1–2):77–88.
202. Hori R, Okamura N, Aiba T, Tanigawara Y. Role of P-glycoprotein in renal tubular secretion of digoxin in the isolated perfused rat kidney. *J Pharmacol Exp Ther* 1993, 266(3):1620–1625.
203. Smith QR, Takasato Y. Kinetics of amino acid transport at the blood-brain barrier studied using an in situ brain perfusion technique. *Ann NY Acad Sci* 1986, 481: 186–201.
204. Smith QR. Brain perfusion systems for studies of drug uptake and metabolism in the central nervous system. In: Borchardt RT, Wilson G, Smith PL, eds. *Models*



- for Assessing Drug Absorption and Metabolism. 1996, New York: Plenum Press, pp 285–307.
205. Takasato Y, Rapoport SI, Smith QR. An in situ brain perfusion technique to study cerebrovascular transport in the rat. *Am J Physiol* 1984, 247(3 Pt 2):H484–H493.
  206. Smit JW, Duin E, Steen H, Oosting R, Roggeveld J, Meijer DK. Interactions between P-glycoprotein substrates and other cationic drugs at the hepatic excretory level. *Br J Pharmacol* 1998, 123(3):361–370.
  207. Booth CL, Pollack GM, Brouwer KL. Hepatobiliary disposition of valproic acid and valproate glucuronide: use of a pharmacokinetic model to examine the rate-limiting steps and potential sites of drug interactions. *Hepatology* 1996, 23(4):771–780.
  208. Hayes JH, Soroka CJ, Rios-Velez L, Boyer JL. Hepatic sequestration and modulation of the canalicular transport of the organic cation, daunorubicin, in the Rat. *Hepatology* 1999, 29(2):483–493.
  209. Smith QR, Nagura H, Takada Y, Duncan MW. Facilitated transport of the neurotoxin, beta-*N*-methylamino-L-alanine, across the blood–brain barrier. *J Neurochem* 1992, 58(4):1330–1337.
  210. Murata M, Tamai I, Kato H, Nagata O, Tsuji A. Efflux transport of a new quinolone antibacterial agent, HSR-903, across the blood–brain barrier. *J Pharmacol Exp Ther* 1999, 290(1):51–57.
  211. Drion N, Lemaire M, Lefauconnier JM, Scherrmann JM. Role of P-glycoprotein in the blood–brain transport of colchicine and vinblastine. *J Neurochem* 1996, 67(4):1688–1693.
  212. Drion N, Risede P, Cholet N, Chanez C, Scherrmann JM. Role of P-170 glycoprotein in colchicine brain uptake. *J Neurosci Res* 1997, 49(1):80–88.
  213. Rousselle C, Clair P, Lefauconnier JM, Kaczorek M, Scherrmann JM, Tamsamani J. New advances in the transport of doxorubicin through the blood–brain barrier by a peptide vector-mediated strategy. *Mol Pharmacol* 2000, 57(4):679–686.
  214. Chikhale EG, Burton PS, Borchardt RT. The effect of verapamil on the transport of peptides across the blood–brain barrier in rats: kinetic evidence for an apically polarized efflux mechanism. *J Pharmacol Exp Ther* 1995, 273(1):298–303.
  215. Lemaire M, Bruelisauer A, Guntz P, Sato H. Dose-dependent brain penetration of SDZ PSC 833, a novel multidrug resistance-reversing cyclosporin, in rats. *Cancer Chemother Pharmacol* 1996, 38(5):481–486.
  216. Dagenais C, Rousselle C, Pollack GM, Scherrmann JM. Development of an in situ mouse brain perfusion model and its application to mdr1a P-glycoprotein-deficient mice. *J Cereb Blood Flow Metab* 2000, 20:381–386.
  217. Groen AK, Van Wijland MJ, Frederiks WM, Smit JJ, Schinkel AH, Oude Elferink RP. Regulation of protein secretion into bile: studies in mice with a disrupted mdr2 P-glycoprotein gene. *Gastroenterology* 1995, 109(6):1997–2006.
  218. Oude Elferink RP, Ottenhoff R, van Wijland M, Smit JJ, Schinkel AH, Groen AK. Regulation of biliary lipid secretion by mdr2 P-glycoprotein in the mouse. *J Clin Invest* 1995, 95(1):31–38.
  219. Schinkel AH, Smit JJ, van Tellingen O, Beijnen JH, Wagenaar E, van Deemter L, Mol CA, van der Valk MA, Robanus-Maandag EC, te Riele HPJ, Berns, AJM, Borst P. Disruption of the mouse mdr1a P-glycoprotein gene leads to a deficiency

- in the blood-brain barrier and to increased sensitivity to drugs. *Cell* 1994, 77(4): 491–502.
220. Schinkel AH, Mol CA, Wagenaar E, van Deemter L, Smit JJ, Borst P. Multidrug resistance and the role of P-glycoprotein knockout mice. *Eur J Cancer* 1995, 31A(7–8):1295–1298.
221. Schinkel AH. Pharmacological insights from P-glycoprotein knockout mice. *Int J Clin Pharmacol Ther* 1998, 36(1):9–13.
222. Smit JJ, Schinkel AH, Oude Elferink RP, Groen AK, Wagenaar E, van Deemter L, Mol CA, Ottenhoff R, van der Lugt NM, van Roon MA. Homozygous disruption of the murine *mdr2* P-glycoprotein gene leads to a complete absence of phospholipid from bile and to liver disease. *Cell* 1993, 75(3):451–462.
223. Smit JW, Schinkel AH, Weert B, Meijer DK. Hepatobiliary and intestinal clearance of amphiphilic cationic drugs in mice in which both *mdr1a* and *mdr1b* genes have been disrupted. *Br J Pharmacol* 1998, 124(2):416–424.
224. Croop JM, Raymond M, Haber D, Devault A, Arceci RJ, Gros P, Housman DE. The three mouse multidrug resistance (*mdr*) genes are expressed in a tissue-specific manner in normal mouse tissues. *Mol Cell Biol* 1989, 9(3):1346–1350.
225. Arceci RJ, Croop JM, Horwitz SB, Housman D. The gene encoding multidrug resistance is induced and expressed at high levels during pregnancy in the secretory epithelium of the uterus. *Proc Natl Acad Sci USA* 1988, 85(12):4350–4354.
226. van de Vrie W, Marquet RL, Stoter G, De Bruijn EA, Eggermont AM. In vivo model systems in P-glycoprotein-mediated multidrug resistance. *Crit Rev Clin Lab Sci* 1998, 35(1):1–57.
227. Endicott JA, Sarangi F, Ling V. Complete cDNA sequences encoding the Chinese hamster P-glycoprotein gene family. *DNA Seq* 1991, 2(2):89–101.
228. Silverman JA, Raunio H, Gant TW, Thorgeirsson SS. Cloning and characterization of a member of the rat multidrug resistance (*mdr*) gene family. *Gene* 1991, 106(2): 229–236.
229. Hsu SI, Lothstein L, Horwitz SB. Differential overexpression of three *mdr* gene family members in multidrug-resistant J774.2 mouse cells. Evidence that distinct P-glycoprotein precursors are encoded by unique *mdr* genes. *J Biol Chem* 1989, 264(20):12053–12062.
230. Schinkel AH, Wagenaar E, van Deemter L, Mol CA, Borst P. Absence of the *mdr1a* P-Glycoprotein in mice affects tissue distribution and pharmacokinetics of dexamethasone, digoxin, and cyclosporin A. *J Clin Invest* 1995, 96(4):1698–1705.
231. van Asperen J, Schinkel AH, Beijnen JH, Nooijen WJ, Borst P, van Tellingen O. Altered pharmacokinetics of vinblastine in *mdr1a* P-glycoprotein-deficient mice. *J Natl Cancer Inst* 1996, 88(14):994–999.
232. Galski H, Sullivan M, Willingham MC, Chin KV, Gottesman MM, Pastan I, Merlino GT. Expression of a human multidrug resistance cDNA (MDR1) in the bone marrow of transgenic mice: resistance to daunomycin-induced leukopenia. *Mol Cell Biol* 1989, 9(10):4357–4363.
233. Mickisch GH, Pastan I, Gottesman MM. Multidrug resistant transgenic mice as a novel pharmacologic tool. *Bioessays* 1991, 13(8):381–387.
234. Mickisch GH, Merlino GT, Galski H, Gottesman MM, Pastan I. Transgenic mice that express the human multidrug-resistance gene in bone marrow enable a rapid

- identification of agents that reverse drug resistance. *Proc Natl Acad Sci USA* 1991, 88(2):547–551.
235. Mickisch GH, Rahman A, Pastan I, Gottesman MM. Increased effectiveness of liposome-encapsulated doxorubicin in multidrug-resistant-transgenic mice compared with free doxorubicin. *J Natl Cancer Inst* 1992, 84(10):804–805.
236. Stein WD. Kinetics of the multidrug transporter (P-glycoprotein) and its reversal. *Physiol Rev* 1997, 77(2):545–590.
237. Walle UK, Walle T. Taxol transport by human intestinal epithelial Caco-2 cells. *Drug Metab Dispos* 1998, 26(4):343–346.
238. Terao T, Hisanaga E, Sai Y, Tamai I, Tsuji A. Active secretion of drugs from the small intestinal epithelium in rats by P-glycoprotein functioning as an absorption barrier. *J Pharm Pharmacol* 1996, 48(10):1083–1089.
239. Sparreboom A, van Asperen J, Mayer U, Schinkel AH, Smit JW, Meijer DK, Borst P, Nooijen WJ, Beijnen JH, van Tellingen O. Limited oral bioavailability and active epithelial excretion of paclitaxel (Taxol) caused by P-glycoprotein in the intestine. *Proc Natl Acad Sci USA* 1997, 94(5):2031–2035.
240. Gan LS, Moseley MA, Khosla B, Augustijns PF, Bradshaw TP, Hendren RW, Thakker DR. CYP3A-like cytochrome P450-mediated metabolism and polarized efflux of cyclosporin A in Caco-2 cells. *Drug Metab Dispos* 1996, 24(3):344–349.
241. Ferry DR. Testing the role of P-glycoprotein expression in clinical trials: applying pharmacological principles and best methods for detection together with good clinical trials methodology. *Int J Clin Pharmacol Ther* 1998, 36(1):29–40.
242. Arimori K, Nakano M. Drug exsorption from blood into the gastrointestinal tract. *Pharm Res* 1998, 15(3):371–376.
243. Ling V. Multidrug resistance: molecular mechanisms and clinical relevance. *Cancer Chemother Pharmacol* 1997, 40(40 Suppl):S3–S8.
244. Aszalos A, Ross DD. Biochemical and clinical aspects of efflux pump related resistance to anti-cancer drugs. *Anticancer Res* 1998, 18(4C):2937–2944.
245. Wang Q, Yang H, Miller DW, Elmquist WF. Effect of the P-glycoprotein inhibitor, cyclosporin A, on the distribution of rhodamine-123 to the brain: an in vivo microdialysis study in freely moving rats. *Biochem Biophys Res Commun* 1995, 211(3):719–726.
246. Hebert MF. Contributions of hepatic and intestinal metabolism and P-glycoprotein to cyclosporine and tacrolimus oral drug delivery. *Adv Drug Delivery Rev* 1997, 27(2,3):201–214.
247. Smit JW, Schinkel AH, Muller M, Weert B, Meijer DK. Contribution of the murine *mdr1a* P-glycoprotein to hepatobiliary and intestinal elimination of cationic drugs as measured in mice with an *mdr1a* gene disruption. *Hepatology* 1998, 27(4):1056–1063.
248. Relling MV. Are the major effects of P-glycoprotein modulators due to altered pharmacokinetics of anticancer drugs? *Ther Drug Monit* 1996, 18(4):350–356.
249. Cvetkovic M, Leake B, Fromm MF, Wilkinson GR, Kim RB. OATP and P-glycoprotein transporters mediate the cellular uptake and excretion of fexofenadine. *Drug Metab Dispos* 1999, 27(8):866–871.
250. Chen C, Pollack GM. Altered disposition and antinociception of [D-penicilla-

- mine(2,5)] enkephalin in *mdr1a*-gene-deficient mice. *J Pharmacol Exp Ther* 1998, 287(2):545–552.
251. Kolars JC, Lown KS, Schmiedlin-Ren P, Ghosh M, Fang C, Wrighton SA, Merion RM, Watkins PB. CYP3A gene expression in human gut epithelium. *Pharmacogenetics* 1994, 4(5):247–259.
  252. Seree E, Villard PH, Hever A, Guigal N, Puyou F, Charvet B, Point-Somma H, Lechevalier E, Lacarelle B, Barra Y. Modulation of MDR1 and CYP3A expression by dexamethasone: evidence for an inverse regulation in adrenals. *Biochem Biophys Res Commun* 1998, 252(2):392–395.
  253. Wachter VJ, Wu CY, Benet LZ. Overlapping substrate specificities and tissue distribution of cytochrome P450 3A and P-glycoprotein: implications for drug delivery and activity in cancer chemotherapy. *Mol Carcinog* 1995, 13(3):129–134.
  254. Paine MF, Khalighi M, Fisher JM, Shen DD, Kunze KL, Marsh CL, Perkins JD, Thummel KE. Characterization of interintestinal and intrainestinal variations in human CYP3A-dependent metabolism. *J Pharmacol Exp Ther* 1997, 283(3):1552–1562.
  255. Fisher JM, Wrighton SA, Watkins PB, Schmiedlin-Ren P, Calamia JC, Shen DD, Kunze KL, Thummel KE. First-pass midazolam metabolism catalyzed by 1 $\alpha$ ,25-dihydroxy vitamin D<sub>3</sub>-modified Caco-2 cell monolayers. *J Pharmacol Exp Ther* 1999, 289(2):1134–1342.
  256. Kim RB, Wandel C, Leake B, Cvetkovic M, Fromm MF, Dempsey PJ, Roden MM, Belas F, Chaudhary AK, Roden DM, Wood AJ, Wilkinson GR. Interrelationship between substrates and inhibitors of human CYP3A and P-glycoprotein. *Pharm Res* 1999, 16(3):408–414.
  257. Watkins PB. The barrier function of CYP3A4 and P-glycoprotein in the small bowel. *Adv Delivery Rev* 1997, 27(2,3):161–170.
  258. Benet LZ, Izumi T, Zhang Y, Silverman JA, Wachter VJ. Intestinal MDR transport proteins and P-450 enzymes as barriers to oral drug delivery. *J Controlled Release* 1999, 62(1–2):25–31.
  259. Wachter VJ, Silverman JA, Zhang Y, Benet LZ. Role of P-glycoprotein and cytochrome P450 3A in limiting oral absorption of peptides and peptidomimetics. *J Pharm Sci* 1998, 87(11):1322–1330.
  260. Mayer U, Wagenaar E, Beijnen JH, Smit JW, Meijer DK, van Asperen J, Borst P, Schinkel AH. Substantial excretion of digoxin via the intestinal mucosa and prevention of long-term digoxin accumulation in the brain by the *mdr1a* P-glycoprotein. *Br J Pharmacol* 1996, 119(5):1038–1044.
  261. van Asperen J, van Tellingen O, Beijnen JH. The role of *mdr1a* P-glycoprotein in the biliary and intestinal secretion of doxorubicin and vinblastine in mice. *Drug Metab Dispos* 2000, 28(3):264–267.
  262. Kaye SB. Multidrug resistance: clinical relevance in solid tumours and strategies for circumvention. *Curr Opin Oncol* 1998, 10(Suppl 1):S15–S19.
  263. Leveque D, Jehl F. P-glycoprotein and pharmacokinetics. *Anticancer Res* 1995, 15(2):331–336.
  264. Tsuruo T, Iida H, Tsukagoshi S, Sakurai Y. Overcoming of vincristine resistance in P388 leukemia *in vivo* and *in vitro* through enhanced cytotoxicity of vincristine and vinblastine by verapamil. *Cancer Res* 1981, 41(5):1967–1972.

265. Cantwell B, Buamah P, Harris AL. Phase I and II study of oral verapamil and intravenous vindesine. *Proc Am Soc Clin Oncol* 1985, 42:161.
266. Pennock GD, Dalton WS, Roeske WR, Appleton CP, Mosley K, Plezia P, Miller TP, Salmon SE. Systemic toxic effects associated with high-dose verapamil infusion and chemotherapy administration. *J Natl Cancer Inst* 1991, 83(2):105–110.
267. Kerr DJ, Graham J, Cummings J, Morrison JG, Thompson GG, Brodie MJ, Kaye SB. The effect of verapamil on the pharmacokinetics of adriamycin. *Cancer Chemother Pharmacol* 1986, 18(3):239–242.
268. Gigante M, Toffoli G, Boiocchi M. Pharmacokinetics of doxorubicin co-administered with high-dose verapamil. *Br J Cancer* 1995, 71(1):134–136.
269. Millward MJ, Cantwell BM, Munro NC, Robinson A, Corris PA, Harris AL. Oral verapamil with chemotherapy for advanced non-small cell lung cancer: a randomized study. *Br J Cancer* 1993, 67(5):1031–1035.
270. Milroy R. A randomized clinical study of verapamil in addition to combination chemotherapy in small cell lung cancer. West of Scotland Lung Cancer Research Group, and the Aberdeen Oncology Group. *Br J Cancer* 1993, 68(4):813–818.
271. Dalton WS, Crowley JJ, Salmon SS, Grogan TM, Laufman LR, Weiss GR, Bonnet JD. A phase III randomized study of oral verapamil as a chemosensitizer to reverse drug resistance in patients with refractory myeloma. A southwest Oncology Group study. *Cancer* 1995, 75(3):815–820.
272. Taylor CW, Dalton WS, Mosley K, Dorr RT, Salmon SE. Combination chemotherapy with cyclophosphamide, vincristine, adriamycin, and dexamethasone (CVAD) plus oral quinine and verapamil in patients with advanced breast cancer. *Breast Cancer Res Treat* 1997, 42(1):7–14.
273. Kronbach T, Fischer V, Meyer UA. Cyclosporine metabolism in human liver: identification of a cytochrome P-450III gene family as the major cyclosporine-metabolizing enzyme explains interactions of cyclosporine with other drugs. *Clin Pharmacol Ther* 1988, 43(6):630–635.
274. Colombo T, Zucchetti M, D'Incalci M. Cyclosporin A markedly changes the distribution of doxorubicin in mice and rats. *J Pharmacol Exp Ther* 1994, 269(1):22–27.
275. Lum BL, Kaubisch S, Yahanda AM, Adler KM, Jew L, Ehsan MN, Brophy NA, Halsey J, Gosland MP, Sikic BI. Alteration of etoposide pharmacokinetics and pharmacodynamics by cyclosporine in a phase I trial to modulate multidrug resistance. *J Clin Oncol* 1992, 10(10):1635–1642.
276. Bartlett NL, Lum BL, Fisher GA, Brophy NA, Ehsan MN, Halsey J, Sikic BI. Phase I trial of doxorubicin with cyclosporine as a modulator of multidrug resistance. *J Clin Oncol* 1994, 12(4):835–842.
277. Tsuruo T, Iida H, Kitatani Y, Yokota K, Tsukagoshi S, Sakurai Y. Effects of quinidine and related compounds on cytotoxicity and cellular accumulation of vincristine and adriamycin in drug-resistant tumor cells. *Cancer Res* 1984, 44(10):4303–4307.
278. Wishart GC, Plumb JA, Morrison JG, Hamilton TG, Kaye SB. Adequate tumour quinidine levels for multidrug resistance modulation can be achieved in vivo. *Eur J Cancer* 1992, 28(1):28–31.
279. Verrelle P, Meissonnier F, Fonck Y, Feillel V, Dionet C, Kwiatkowski F, Plagne R, Chassagne J. Clinical relevance of immunohistochemical detection of multidrug

- resistance P-glycoprotein in breast carcinoma. *J Natl Cancer Inst* 1991, 83(2):111–116.
280. Solary E, Caillot D, Chauffert B, Casasnovas RO, Dumas M, Maynadie M, Guy H. Feasibility of using quinine, a potential multidrug resistance-reversing agent, in combination with mitoxantrone and cytarabine for the treatment of acute leukemia. *J Clin Oncol* 1992, 10(11):1730–1736.
281. Wigler PW. Cellular drug efflux and reversal therapy of cancer. *J Bioenerg Biomembr* 1996, 28(3):279–284.
282. Stuart NS, Philip P, Harris AL, Tonkin K, Houlbrook S, Kirk J, Lien EA, Carmichael J. High-dose tamoxifen as an enhancer of etoposide cytotoxicity. Clinical effects and in vitro assessment in p-glycoprotein expressing cell lines. *Br J Cancer* 1992, 66(5):833–839.
283. Trump DL, Smith DC, Ellis PG, Rogers MP, Schold SC, Winer EP, Panella TJ, Jordan VC, Fine RL. High-dose oral tamoxifen, a potential multidrug-resistance-reversal agent: phase I trial in combination with vinblastine. *J Natl Cancer Inst* 1992, 84(23):1811–1816.
284. Ferry DR, Traunecker H, Kerr DJ. Clinical trials of P-glycoprotein reversal in solid tumours. *Eur J Cancer* 1996, 32A(6):1070–1081.
285. Samuels BL, Hollis DR, Rosner GL, Trump DL, Shapiro CL, Vogelzang NJ, Schilsky RL. Modulation of vinblastine resistance in metastatic renal cell carcinoma with cyclosporine A or tamoxifen: a cancer and leukemia group B study. *Clin Cancer Res* 1997, 3(11):1977–1984.
286. Smith DC, Trump DL. A phase I trial of high-dose oral tamoxifen and CHOPE. *Cancer Chemother Pharmacol* 1995, 36(1):65–68.
287. Wilisch A, Haussermann K, Noller A, Probst H, Gekeler V. MDR modulating and antineoplastic effects of B859-035, the (–) isomer of niguldipine. *J Cancer Res Clin Oncol* 1991, 117:S110.
288. Ferry DR, Glossmann H, Kaumann AJ. Relationship between the stereoselective negative inotropic effects of verapamil enantiomers and their binding to putative calcium channels in human heart. *Br J Pharmacol* 1985, 84(4):811–824.
289. Wilson WH, Bates SE, Fojo A, Chabner BA. Modulation of multidrug resistance by dexverapamil in EPOCH-refractory lymphomas. *J Cancer Res Clin Oncol* 1995, 121 Suppl 3:R25–R29.
290. Wilson WH, Jamis-Dow C, Bryant G, Balis FM, Klecker RW, Bates SE, Chabner BA, Steinberg SM, Kohler DR, Wittes RE. Phase I and pharmacokinetic study of the multidrug resistance modulator dexverapamil with EPOCH chemotherapy. *J Clin Oncol* 1995, 13(8):1985–1994.
291. Tolchner AW, Cowan KH, Solomon D, Ognibene F, Goldspiel B, Chang R, Noone MH, Denicoff AM, Barnes CS, Gossard MR, Retsch PA, Berg SL, Balis FM, Venzon DJ, O'Shaughnessy JA. Phase I crossover study of paclitaxel with r-verapamil in patients with metastatic breast cancer. *J Clin Oncol* 1996, 14(4):1173–1184.
292. Dhainaut A, Regnier G, Atassi G, Pierre A, Leonce S, Kraus-Berthier L, Prost JF. New triazine derivatives as potent modulators of multidrug resistance. *J Med Chem* 1992, 35(13):2481–2496.
293. Punt CJ, Voest EE, Tueni E, Van Oosterom AT, Backx A, De Mulder PH, Hecquet B, Lucas C, Gerard B, Bleiberg H. Phase IB study of doxorubicin in combination

- with the multidrug resistance reversing agent S9788 in advanced colorectal and renal cell cancer. *Br J Cancer* 1997, 76(10):1376–1381.
294. Tranchand B, Catimel G, Lucas C, Sarkany M, Bastian G, Evene E, Guastalla JP, Negrier S, Rebattu P, Dumortier A, Foy M, Grossin F, Mazier B, Froudarakis M, Barbet N, Clavel M, Ardiet C. Phase I clinical and pharmacokinetic study of S9788, a new multidrug-resistance reversal agent given alone and in combination with doxorubicin to patients with advanced solid tumors. *Cancer Chemother Pharmacol* 1998, 41(4):281–291.
295. Hyafil F, Vergely C, Du Vignaud P, Grand-Perret T. In vitro and in vivo reversal of multidrug resistance by GF120918, an acridonecarboxamide derivative. *Cancer Res* 1993, 53(19):4595–4602.
296. Sparreboom A, Planting AS, Jewell RC, van der Burg ME, van der Gaast A, de Bruijn P, Loos WJ, Nooter K, Chandler LH, Paul EM, Wissel PS, Verweij J. Clinical pharmacokinetics of doxorubicin in combination with GF120918, a potent inhibitor of MDR1 P-glycoprotein. *Anticancer Drugs* 1999, 10(8):719–728.
297. te Boekhorst PA, van Kapel J, Schoester M, Sonneveld P. Reversal of typical multidrug resistance by cyclosporin and its non-immunosuppressive analogue SDZ PSC 833 in Chinese hamster ovary cells expressing the *mdr1* phenotype. *Cancer Chemother Pharmacol* 1992, 30(3):238–242.
298. Glisson B, Gupta R, Hodges P, Ross W. Cross-resistance to intercalating agents in an epipodophyllotoxin-resistant Chinese hamster ovary cell line: evidence for a common intracellular target. *Cancer Res* 1986, 46(4 Pt 2):1939–1942.
299. Advani R, Visani G, Milligan D, Saba H, Tallman M, Rowe JM, Wiernik PH, Ramek J, Dugan K, Lum B, Villena J, Davis E, Paietta E, Litchman M, Covelli A, Sikic B, Greenberg P. Treatment of poor prognosis AML patients using PSC833 (valspodar) plus mitoxantrone, etoposide, and cytarabine (PSC-MEC). *Adv Exp Med Biol* 1999, 457:47–56.
300. Kornblau SM, Estey E, Madden T, Tran HT, Zhao S, Consoli U, Snell V, Sanchez-Williams G, Kantarjian H, Keating M, Newman RA, Andreeff M. Phase I study of mitoxantrone plus etoposide with multidrug blockade by SDZ PSC-833 in relapsed or refractory acute myelogenous leukemia. *J Clin Oncol* 1997, 15(5):1796–1802.
301. Lee EJ, George SL, Caligiuri M, Szatrowski TP, Powell BL, Lemke S, Dodge RK, Smith R, Baer M, Schiffer CA. Parallel phase I studies of daunorubicin given with cytarabine and etoposide with or without the multidrug resistance modulator PSC-833 in previously untreated patients 60 years of age or older with acute myeloid leukemia: results of cancer and leukemia group B study 9420. *J Clin Oncol* 1999, 17(9):2831–2839.
302. Giaccone G, Linn SC, Welink J, Catimel G, Stieltjes H, van der Vijgh WJ, Eeltink C, Vermorken JB, Pinedo HM. A dose-finding and pharmacokinetic study of reversal of multidrug resistance with SDZ PSC 833 in combination with doxorubicin in patients with solid tumors. *Clin Cancer Res* 1997, 3(11):2005–2015.
303. Yamazaki M, Suzuki H, Sugiyama Y. Recent advances in carrier-mediated hepatic uptake and biliary excretion of xenobiotics. *Pharm Res* 1996, 13(4):497–513.
304. Adams DJ, Knick VC. P-glycoprotein mediated resistance to 5'-nor-anhydro-vinblastine (Navelbine). *Invest New Drugs* 1995, 13(1):13–21.

305. Yu DK. The contribution of P-glycoprotein to pharmacokinetic drug–drug interactions. *J Clin Pharmacol* 1999, 39(12):1203–1211.
306. Mackstaller LL, Alpert JS. Atrial fibrillation: a review of mechanism, etiology, and therapy. *Clin Cardiol* 1997, 20(7):640–650.
307. Cobbe SM. Using the right drug. A treatment algorithm for atrial fibrillation. *Eur Heart J* 1997, 18 Suppl C:C33–C39.
308. de Lannoy IA, Silverman M. The MDR1 gene product, P-glycoprotein, mediates the transport of the cardiac glycoside, digoxin. *Biochem Biophys Res Commun* 1992, 189(1):551–557.
309. Wakasugi H, Yano I, Ito T, Hashida T, Futami T, Nohara R, Sasayama S, Inui K. Effect of clarithromycin on renal excretion of digoxin: interaction with P-glycoprotein. *Clin Pharmacol Ther* 1998, 64(1):123–128.
310. Alderman CP, Allcroft PD. Digoxin-itraconazole interaction: possible mechanisms: *Ann Pharmacother* 1997, 31(4):438–440.
311. Ito S, Woodland C, Harper PA, Koren G. P-glycoprotein-mediated renal tubular secretion of digoxin: the toxicological significance of the urine-blood barrier model. *Life Sci* 1993, 53(2):PL25–PL31.
312. Brody TM, Larner J, Minneman RG. *Human Pharmacology: Molecular to Clinical*. 3rd ed. 1998, St. Louis: Mosby-Year Book.
313. Kelly RA, Smith TW. Pharmacological treatment of heart failure. In: Hardman JG, Limbird LE, Molinoff PB, Ruddon RW, Gilman AG, eds. *The pharmacological basis of therapeutics*. 9th ed. 1996, New York: McGraw-Hill, pp 809–838.
314. Koren G, Woodland C, Ito S. Toxic digoxin-drug interactions: the major role of renal P-glycoprotein. *Vet Hum Toxicol* 1998, 40(1):45–46.
315. Pedersen KE. Digoxin interactions. The influence of quinidine and verapamil on the pharmacokinetics and receptor binding of digitalis glycosides. *Acta Med Scand Suppl* 1985, 697:1–40.
316. John A, Brockmoller J, Bauer S, Maurer A, Langheinrich M, Roots I. Pharmacokinetic interaction of digoxin with an herbal extract from St John's wort (*Hypericum perforatum*). *Clin Pharmacol Ther* 1999, 66(4):338–345.
317. Greiner B, Eichelbaum M, Fritz P, Kreichgauer HP, von Richter O, Zundler J, Kroemer HK. The role of intestinal P-glycoprotein in the interaction of digoxin and rifampin. *J Clin Invest* 1999, 104(2):147–153.
318. Theis JG, Chan HS, Greenberg ML, Malkin D, Karaskov V, Moncica I, Koren G, Doyle J. Increased systemic toxicity of sarcoma chemotherapy due to combination with the P-glycoprotein inhibitor cyclosporin. *Int J Clin Pharmacol Ther* 1998, 36(2):61–64.
319. Chang T, Benet LZ, Hebert MF. The effect of water-soluble vitamin E on cyclosporine pharmacokinetics in healthy volunteers. *Clin Pharmacol Ther* 1996, 59(3):297–303.





# 9

## The Role of the Gut Mucosa in Metabolically Based Drug–Drug Interactions

**Kenneth E. Thummel and Danny D. Shen**

*University of Washington, Seattle, Washington*

### I. INTRODUCTION

#### A. Background

The gastrointestinal mucosa represents a major physical and enzymatic barrier to the systemic availability of orally ingested, pharmacologically active molecules. A critical component of that barrier is a collection of biotransforming enzymes localized at the apical aspect of the columnar epithelium (enterocytes). Although drug absorption can occur along the entire length of the gastrointestinal tract, it is most favored in the proximal (duodenum and jejunum) small intestine because of surface area considerations. The liver is generally considered to be the major site of drug metabolism, but it is becoming increasingly clear that, for some drug molecules (e.g., midazolam, nifedipine, verapamil, saquinavir, terfenadine), the small intestine can also make a significant contribution to first-pass drug elimination. Indeed, some prodrugs have been developed that take advantage of the enzymatic activity of the intestinal mucosa to promote the absorption and subsequent release of pharmacologically active drug into the hepatic portal circulation. Of particular importance are the carboxyesterases, but cytochrome P450–catalyzed oxidations have also been described.

In addition to drug metabolism, there is growing recognition that expression of drug transporters, such as P-glycoprotein, at the apical membranes of mucosal enterocytes promotes the efflux of drugs from intracellular sites into the gut lumen. In the case of P-glycoprotein, expression of the transporter occurs along

the entire length of the intestine, including the ileum and colon. Thus, for other orally administered drugs (e.g., cyclosporine and digoxin), extensive apically directed drug efflux appears to effectively reduce the intestinal and absolute bioavailability.

In this chapter, we review the expression and localization of intestinal enzymes and transporters that have been implicated in drug–drug interactions and the pharmacokinetic and clinical consequences of those interaction events.

## B. Pharmacokinetic Principles

If a metabolically based drug–drug interaction is to have clinical significance, the affected process of drug metabolism or transport must represent an appreciable part of the overall drug elimination scheme (see Chap. 1). In the case of intestinal metabolism, it is the fraction of a dose metabolized by the gut mucosa on first pass ( $F_M$ ) that is most relevant. In general, intestinal mucosal enzymes that contribute significantly to the first-pass metabolism of a drug have a much lower contribution to the systemic clearance of the same molecule [1]. Thus, important drug interactions involving gut metabolism will generally be associated with drugs that have an appreciable first-pass mucosal extraction ratio.

The role of the gut wall in a drug–drug interaction is usually inferred from the difference in the observed magnitude of AUC change after oral and intravenous dosing of the affected drug (except in the case of a very high-extraction drug with blood flow rate–limited systemic clearance). Because most intestinal enzymes are also found in the liver, an overall change in AUC may reflect an interaction with both hepatic and intestinal components. As seen from the following equation, the oral AUC is a function of the systemic clearance (Cl) of the drug, the product of the intestinal mucosal and liver availability fractions ( $F_M$  and  $F_L$ ), and the fraction absorbed ( $F_{Abs}$ ):

$$\text{AUC}^{po} = \frac{(F_{Abs} \cdot F_M \cdot F_L) \cdot \text{Dose}}{\text{Cl}} \quad (1)$$

Embedded within each metabolic component ( $F_M$ ,  $F_L$ , Cl) is an intrinsic clearance term ( $V_{max}/K_m$ ) that can be modified by an enzyme/transporter inducer or inhibitor. If drug elimination were exclusively hepatic, the systemic AUC observed in the presence of a modulator (\*) would be inversely related to the modification of intrinsic clearance [2,3], as indicated in the following equation:

$$\frac{\text{AUC}^{po*}}{\text{AUC}^{po}} = \frac{f_B \cdot \text{Cl}_L^{\text{in}}}{f_B \cdot \text{Cl}_L^{\text{in}*}} \quad (2)$$

When both liver and intestine contribute significantly to the metabolic elimination of an orally administered drug, the resulting mathematical relationship between the oral AUC for the affected drug and organ intrinsic clearance will be more complex. If we consider the pharmacokinetic model depicted in Figure 1 for a drug that is metabolized in the liver and intestine but is not subject to intestinal or hepatic efflux processes, a series of equations can be derived with the following simplifying assumptions:

1. Complete absorption of the oral dose ( $f_{abs} = 1$ )
2. Sequential mucosal and liver first-pass metabolic extraction

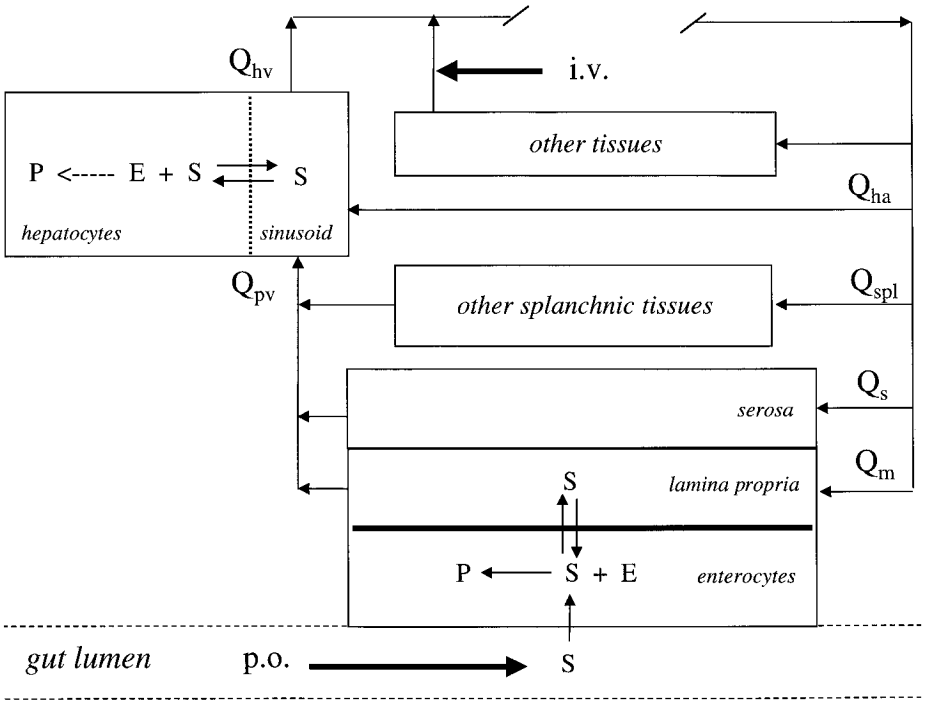


**Figure 1** Physiological model for sequential intestinal and hepatic first-pass metabolism. Blood flow to the small intestine is functionally divided into mucosal ( $Q_m$ ) and serosal ( $Q_s$ ) flow. Mucosal blood flow in the lamina propria perfuses the enterocyte epithelium. Portal blood flow ( $Q_{pv}$ ), which perfuses the liver, is composed of blood leaving the small intestine and other splanchnic organs, such as the stomach and spleen. Blood flow leaving the liver ( $Q_{hv}$ ) represents the sum of hepatic arterial flow ( $Q_{ha}$ ) and  $Q_{pv}$ . First-pass metabolism of an orally administered substrate ( $S$ ) to product ( $P$ ) may occur in the enterocyte or hepatocyte.

3. Systemic clearance (Cl) = liver clearance (Cl<sub>L</sub>), i.e., no significant renal or intestinal contributions to systemic clearance
4. Flow-limited organ extraction
5. First-order liver and intestinal metabolism

$$\frac{\text{Dose}^{po}}{\text{AUC}^{po}} = \frac{\text{Cl}_L}{F_M \cdot F_L} \quad (3)$$

$$F_M = \frac{Q_M}{(f_B \cdot \text{Cl}_M^{\text{int}}) + Q_M} \quad \text{and} \quad F_L = \frac{Q_L}{(f_B \cdot \text{Cl}_L^{\text{int}}) + Q_L} \quad (4)$$

Substituting, we get

$$\frac{\text{Dose}^{po}}{\text{AUC}^{po}} = \frac{f_B \cdot \text{Cl}_L^{\text{in}}}{\frac{Q_M}{Q_M + f_B \cdot \text{Cl}_M^{\text{in}}}} \quad (5)$$

where  $f_B$  is the free fraction in blood,  $\text{Cl}_M^{\text{in}}$  and  $\text{Cl}_L^{\text{in}}$  are the unbound intrinsic clearances of the intestinal mucosa and liver, respectively, and  $Q_M$  and  $Q_L$  are blood flows to the intestinal mucosa and liver, respectively. In the presence of a modulating drug, the AUC ratio in the absence and presence of a modulating drug can be expressed as the following:

$$\frac{\text{AUC}^{po*}}{\text{AUC}^{po}} = \frac{Q_M + f_B \cdot \text{Cl}_M^{\text{in}}}{Q_M + f_B \cdot \text{Cl}_M^{\text{in}*}} \cdot \frac{f_B \cdot \text{Cl}_L^{\text{in}}}{f_B \cdot \text{Cl}_L^{\text{in}*}} \quad (6)$$

What is apparent from the foregoing relationship is the multiplicative effect that a change in hepatic and intestinal intrinsic clearance can have on the systemic AUC, as illustrated in Figures 2 and 3 for midazolam. For example, a fourfold increase in hepatic and mucosal intrinsic clearances, as a consequence of enzyme induction, can cause as much as a 94% (16-fold) reduction in systemic AUC, depending on the initial mucosal extraction ratio (Fig. 2). Without mucosal first-pass extraction, only a 75% (fourfold) reduction is predicted from a fourfold increase in hepatic intrinsic clearance. In addition, systemic blood levels can be up to fourfold lower for the drug that exhibits an extensive intestinal first-pass, in comparison to one that does not.

From the perspective of inhibitory interactions, fourfold reductions in hepatic and intestinal intrinsic clearance may cause up to a 16-fold increase in systemic AUC compared with control, as illustrated in Figure 3 for midazolam. In the case of rapidly reversible enzyme inhibitors, the change in intrinsic clearance can be expressed as a function of the  $K_i$  and inhibitor concentration ( $I$ ):

$$\frac{f_B \cdot \text{Cl}_L^{\text{in}}}{f_B \cdot \text{Cl}_L^{\text{in}(I)}} = 1 + \frac{I_L}{K_i} \quad \text{and} \quad \frac{f_B \cdot \text{Cl}_M^{\text{in}}}{f_B \cdot \text{Cl}_M^{\text{in}(I)}} = 1 + \frac{I_M}{K_i} \quad (7)$$

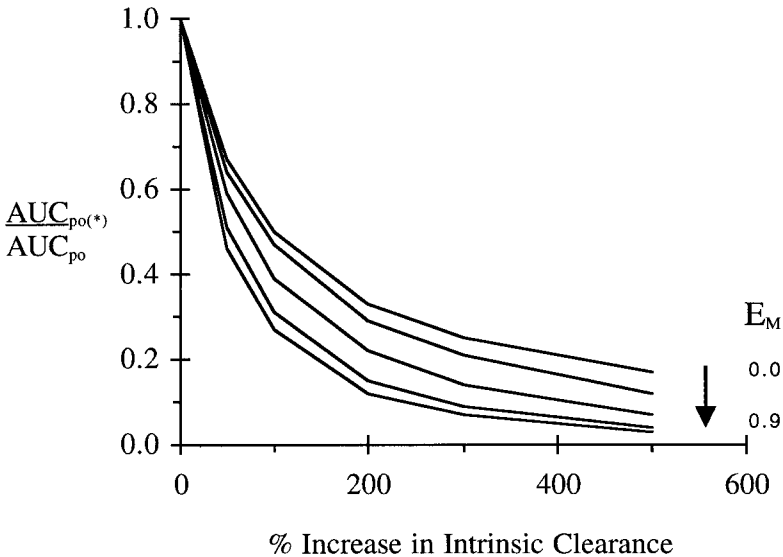


**Figure 2** Simulation of the effect of enzyme induction on oral midazolam AUC. Hepatic extraction in the absence of an inducer was set at 0.44. The inducer was assumed to cause an equivalent change in hepatic and intestinal intrinsic clearance. Mucosal and hepatic plasma flows were assumed to be 240 and 780 ml/min. Simulations were obtained from Eq. (6), assuming an initial intestinal extraction ratio of 0.00, 0.07, 0.27, 0.43, 0.60, and 0.88.

Substitution of Eq. (7) into Eq. (6) yields an expression [Eq. (8)] that again illustrates the multiplicative effect that an enzyme/transporter inhibitor can have on the systemic exposure to an orally administered drug:

$$\frac{AUC^{po(I)}}{AUC^{po}} = \frac{Q_M + f_B \cdot Cl_M^{in}}{Q_M + \frac{f_B \cdot Cl_M^{in}}{1 + \frac{I_M}{K_i}}} \cdot \left( 1 + \frac{I_L}{K_i} \right) \quad (8)$$

Note that the effect of the inhibitor in the liver is independent of blood flow. This is not the case for the intestine, where the relative magnitude of blood flow compared to the baseline intrinsic clearance and the apparent intrinsic clearance in the presence of inhibitor must be considered. When the baseline mucosal intrinsic clearance is negligible compared to mucosal blood flow (i.e., low mucosal extraction), Eq. (8) will collapse into a much simpler and better-recognized equation (see Chap. 1) for a hepatic inhibitory interaction [2]:

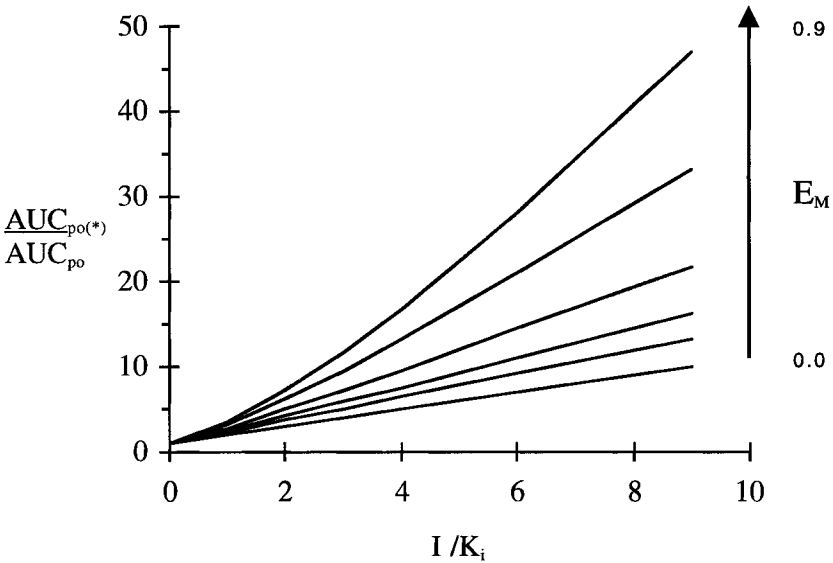


**Figure 3** Simulation of the effect of enzyme inhibition on oral midazolam AUC. Hepatic extraction in the absence of an inhibitor was set at 0.44. The inhibitor/ $K_i$  ratio was assumed to be equivalent for inhibition of hepatic and intestinal metabolism. Mucosal and hepatic plasma flows were assumed to be 240 and 780 ml/min. Simulations were obtained from Eq. (8), assuming an initial intestinal extraction ratio of 0.00, 0.27, 0.43, 0.60, 0.78, and 0.88.

$$\frac{AUC_{po(I)}}{AUC_{po}} = 1 + \frac{I_L}{K_i} \tag{9}$$

For an orally administered drug that is completely absorbed from the gastrointestinal tract and subject to first-pass intestinal extraction, one can assign a lower limit for the mucosal extraction ratio that merits attention. For example, complete inhibition of an initial intestinal extraction that is 25% would result in a 1.33-fold increase in AUC, independent of any changes in hepatic metabolism. The lower the mucosal extraction ratio, the closer that interaction will be defined by the liver. For interactions involving induction of intestinal processes, a lower limit of significance for the initial mucosal extraction is more difficult to assign. However, given the magnitude of change in enzyme/transporter expression commonly observed in a clinical setting (4- to 6-fold), induction of an intestinal process that removes no more than a few percent of the oral dose in the initial state

is unlikely to have an appreciable effect on the AUC of the affected drug. Again, when the initial mucosal extraction ratio is moderate to high, both induction and inhibition of mucosal intrinsic clearance will have a pronounced effect on the oral AUC [Eq. (6)].

It is also possible to have a modulator of drug metabolism/transport that exerts an intestinally selective effect. Under the right dosing conditions, constituents of grapefruit juice appear to selectively inhibit CYP3A and drug transporters in the intestinal mucosa, but not those of the liver. As discussed later, the magnitude of AUC changes observed in vivo are generally modest when a single glass of regular-strength juice is ingested, and the effects are dependent on the initial intestinal extraction efficiency for any given individual. The greater the intestinal first-pass extraction, the greater the change in oral AUC that is possible. Conversely, if  $E_M$  is already low, grapefruit juice will cause little change to the intestinal availability and to the oral AUC.

Another important consideration for understanding metabolically based drug–drug interactions is that the level of exposure of the liver and intestinal mucosa to an inhibitor or inducer may not be identical, particularly during the periabsorptive phase, when intracellular concentrations of the modulator may be much greater for the intestinal mucosa than for the liver. It is also important to recognize that intracellular machinery implicated in the mechanism of an interaction (e.g., transacting factors for induction) may not be present at the same level in the intestine and the liver and functioning to the same degree. Consequently, the extent of induction or inhibition at each site of metabolism/transport following acute or chronic administration of an interacting drug could be quite different.

## II. INTERACTIONS INVOLVING DRUG METABOLISM

The presence of drug-metabolizing enzymes in the human intestinal mucosal has been recognized for some time. The most important of these from the perspective of drug–drug interactions are the cytochrome P450s. The specific P450 content of microsomes isolated from mucosal epithelium of the proximal small intestine is roughly 1/6 to 1/8 of that found in liver microsomes [4,5]. Some P450 isozymes, such as CYP3A4, CYP3A5, and CYP2C, are expressed more prominently than others [6]. Several UDP-glucuronosyltransferase and sulfotransferase isozymes are also found in the human intestine [7–9]. As discussed later, each of these enzymes can contribute significantly to the overall first-pass elimination of some orally administered drugs, and recognition of their role in first-pass metabolism helps to define the effects of enzyme modulators.



## A. CYP3A

### 1. Localization and Function

CYP3A4 mRNA has been detected in numerous organs of the body, but the enzyme is expressed predominantly within columnar epithelial cells lining the gastrointestinal tract, proximal tubules of the kidney, bile duct epithelium, and hepatic parenchymal cells [10]. Purification of the human hepatic isozyme and production of an isozyme-selective antibody led to the first characterization of functionally active CYP3A4 in the human gastrointestinal tract [11]. Subsequent studies have revealed the expression of both CYP3A5 and CYP3A4 in the enterocytes of the small intestine. CYP3A4 is the dominant P450 isozyme in the small intestine [12,13]. The related isozyme CYP3A5 is generally found in the small intestine at lower levels and, in some individuals, is difficult to detect [4,14].

The expression of CYP3A along the gastrointestinal tract is not uniform. Mucosal enzyme concentration is greatest within the duodenal and jejunal sections of the small intestine and declines distally and proximally. DeWaziers et al. [6] reported mean microsomal CYP3A contents that were approximately 2.5% (esophagus), 4.3% (stomach), 48% (duodenum), 25% (jejunum), 15% (ileum), and 1.5% (colon) of mean hepatic microsomal CYP3A content. In a more recent study of 20 full-length donor intestines and livers, Paine et al. [4] reported a median value of 70 (4–262), 31 (<2–91), 23 (<2–98), and 17 (<2–60) pmol/mg protein in mucosal microsomes isolated from liver, duodenum, jejunum, and ileum, respectively. A similar regional pattern was described for CYP3A-catalyzed midazolam 1'-hydroxylation activity.

Significant expression of CYP3A4 in the gastrointestinal tract appears to be restricted to the small intestine. Within mucosa of the colon and stomach, CYP3A5 protein and mRNA appear to be more prominent than corresponding CYP3A4 measures [12,13]. For example, Gervot et al. [15] detected CYP3A5 protein, but not CYP3A4, in colonic mucosa from 40 different uninduced tissue donors. These authors suggested that any CYP3A4 in colonic tissue is likely to be a consequence of prior treatment of the donor with an enzyme inducer. CYP3A5 also appears to be the dominant CYP3A isozyme expressed at relatively low levels in various colonic-derived cells [15,16]. In this respect, these cell lines may represent an excellent model for xenobiotic metabolism in the human colon and its role in tissue mutagenesis or cytotoxicity. However, increased expression of CYP3A4 in the Caco-2 cell line by vitamin D<sub>3</sub> treatment [16] or stable transfection [17] would be desirable if it is to be used as a model for first-pass drug metabolism.

Total CYP3A content within a defined region of small bowel varies considerably between individuals. Lown et al. [14] found an 11-fold difference in immunoreactive CYP3A protein and an 8-fold difference in CYP3A4 mRNA in an analysis of duodenal pinch biopsies obtained from 20 "normal" volunteers. Even

greater variability (>50-fold) was described by Paine et al. [4] in an analysis of CYP3A protein content in duodenal and jejunal mucosal scrapings from 20 organ donors. Although some of this extreme variability in the latter study could be the result of events preceding the procurement of tissue (i.e., reduced nutritional intake, antibiotic administration, treatment with known CYP3A inducers, and brain death), it does suggest a remarkably dynamic system of enzyme expression that may respond to a variety of dietary, therapeutic, and pathophysiological conditions. For example, exposure of volunteers to the known hepatic inducer rifampin will cause an increase in duodenal CYP3A4 content [18]. In contrast, acute and chronic ingestion of grapefruit juice will result in a lower level of duodenal CYP3A4 content [19].

Despite years of effort, we have only limited knowledge about the regulation of CYP3A4 expression by constitutive factors in humans. Studies in rodents indicate tight control of hepatic CYP3A by the pituitary secretion of growth hormone as well as by thyroid hormone. Expression of CYP3A4 in cultured human hepatocytes is also affected by growth hormone (positively) and thyroxine (negatively) treatment [20], and this may form the basis for regulation of constitutive expression *in vivo*. Recent data also suggest a role for the nuclear hormone receptor PXR/SXR in the regulation of hepatic CYP3A4, but nothing is known about its involvement in constitutive intestinal CYP3A4 expression. Interestingly, a recent study with Caco-2 cells suggests a role for another hormone in the regulation of intestinal CYP3A. Treatment of these cells with  $1\alpha,25$ -dihydroxy vitamin D<sub>3</sub> stimulated CYP3A4 expression and its associated midazolam 1'-hydroxylation activity tremendously [16]. Dihydroxy vitamin D<sub>3</sub> also plays important physiological roles in calcium homeostasis, including an effect on luminal enterocytes of the small intestine. Binding of the hormone to a specific intracellular receptor triggers a cascade of events that promote calcium absorption. Thus, delivery of the fully active hormone, which is produced in the kidney ( $1\alpha$ -hydroxylation of hepatically generated 25-hydroxy vitamin D<sub>3</sub>), and interaction with vitamin D<sub>3</sub> receptors within the liver and small intestine may regulate hepatic and intestinal CYP3A4 gene transcription.

Mucosal homogenate and microsomes from human intestine have been shown to catalyze the metabolism of a number of CYP3A substrates, including the oxidation of flurazepam [21], ethinylestradiol [22], erythromycin [11], cyclosporine [11], midazolam [23], tacrolimus [24], saquinavir [25], terfenadine [25], and rifabutin [26]. Not surprisingly, some of the compounds that have been studied appear to undergo significant first-pass metabolic extraction after oral administration. CYP3A-catalyzed metabolic reactions appear to contribute to the low oral bioavailability of midazolam [27], verapamil [28], nifedipine [29], and tirilazad [30]. Given the extensive first-pass metabolic extraction that occurs *in vivo*, intestinal extraction is also likely to be an important determinant of the low oral bioavailability of terfenadine [31] and saquinavir [32].

Significant first-pass intestinal extraction occurs despite the fact that total CYP3A content of the entire gut mucosa is much less than total hepatic CYP3A; 70 nmol vs. 5490 nmol [4]. More important than total enzyme mass, however, is the comparable intracellular (parenchymal vs. enterocyte) enzyme concentration and the obligatory nature of drug passage through the enterocyte if it follows transcellular absorption. Thus, a more appropriate variable for comparison might be the microsomal intrinsic clearance activity. In studies that compared both hepatic and intestinal (duodenal or jejunal) microsomes, mean metabolic rates for intestinal microsomes were 45–118% of hepatic microsomal rates for erythromycin [11], midazolam [4], and tacrolimus [24]. Based on these limited studies, mean mucosal intrinsic clearances may be within 2- to 3-fold of the corresponding mean hepatic intrinsic clearance. Whether or not there will be a similarity in first-pass extraction for a given drug is more difficult to predict, since total oral dose, enzyme saturability ( $K_m$ ), and the region and rate of drug absorption become relevant. Should the dose be high enough to cause enzyme saturation, it is possible that a drug with a high hepatic and intestinal intrinsic clearance could largely escape intestinal first-pass extraction but not hepatic extraction.

## 2. Induction of Intestinal CYP3A4

Induction of intestinal CYP3A4 by orally administered drugs has been demonstrated at both the biochemical and functional levels. The response to inducers is presumably mediated by the PXR receptor. In their initial characterization of human intestinal CYP3A4, Kolars et al. [18] noted its inducibility in healthy volunteers by rifampin administration. CYP3A4 mRNA in biopsies of the duodenal mucosa were elevated 5- to 8-fold compared with untreated control biopsies. In vivo, rifampin profoundly reduces the AUC of selective probe substrates of CYP3A4 that exhibit a moderate to high first pass. For example, oral midazolam AUC is reduced by 96% when subjects are pretreated with rifampin (600 mg/day) for 5 days [33]. This corresponds approximately to a 23-fold increase in the apparent oral clearance ( $Cl/F$ ). Although the systemic midazolam clearance is also induced by rifampin [34], the modest magnitude of change (2.6-fold) suggests that rifampin can increase both intestinal and hepatic first-pass extraction. As presented in Eq. (6), one would expect a CYP3A4 inducer to have a multiplicative effect on the total oral bioavailability through separate reductions in the mucosal and hepatic availability terms. Other orally administered CYP3A4 substrates that are affected to a similar degree by rifampin include nifedipine, 92% AUC reduction [29]; verapamil, 97% AUC reduction [28]; triazolam, 95% AUC reduction [35]; buspirone, 90% AUC reduction [36]; tamoxifen, 86% AUC reduction [37]; and toremifene, 87% AUC reduction [37].

Analysis of intravenous and oral AUC data, before and during treatment with CYP3A inducers, has been used to implicate the intestinal mucosa as a major site of enzyme induction [28,29]. However, as Lin et al. [38] have pointed

out, such analyses are based on the assumption that the intestinal mucosa does not contribute significantly to the systemic clearance of the CYP3A substrate. This assumption may be true under basal conditions but might be inappropriate after treatment with the inducer, particularly if the inducer exerts a more profound effect on the gut wall enzyme compared to hepatic enzyme.

Importantly, ignoring a possible contribution of the intestinal mucosa to systemic clearance will lead to an underestimation of the true intestinal first-pass extraction. It has also been noted by Lin et al. that portal and total hepatic blood flow may be altered by an enzyme inducer such as rifampin and that failure to take this into account can lead to an overestimation of the pharmacokinetic effect of intestinal CYP3A4 induction. However, Reichel et al. [39] carefully examined the effect of 7 days of rifampin administration (600 mg/day) on portal blood flow and liver volume, as assessed by color Doppler ultrasound and magnetic resonance volumetry, respectively, and found no change in portal blood flow and less than a 10% increase in liver volume. These findings lend support to the conclusion that the *in vivo* effects of rifampin on the AUC of some orally administered drugs are mediated, in part, by induction of intestinal CYP3A4 and intestinal first-pass drug metabolism.

The CYP3A4 inducers phenytoin and carbamazepine [40] also exert a pronounced effect on oral midazolam AUC in patients receiving the drugs for seizure control [41], presumably through an induction of intestinal and hepatic CYP3A4. In this case, administration of the inducers led to a 94% reduction in midazolam AUC compared with an untreated control population.

### 3. Inhibition of Intestinal CYP3A

Over the past few years considerable interest has been directed toward understanding the effect of potent CYP3A inhibitors on the first-pass extraction of relatively high intrinsic clearance drugs. This interest stemmed initially from the observation that ketoconazole profoundly alters the AUC of orally administered terfenadine, resulting in a prolonged QT interval that could lead to a serious adverse event. It was estimated that oral terfenadine AUC increased 16- to 73-fold following multiple-dose ketoconazole administration [42]. Although some of the pharmacokinetic changes observed were surely the result of an interaction in the liver, it is likely that the enzyme/transporter barrier at the intestinal mucosa was also affected by ketoconazole. Both CYP3A-dependent first-pass metabolism and P-glycoprotein-mediated active efflux processes in the intestinal mucosa are likely to be inhibited by ketoconazole.

Inhibitory intestinal drug–drug interactions can also occur with other CYP3A substrates. In a study of the effect of ketoconazole on tirilazad pharmacokinetics, Fleishaker et al. [30] reported a 67% and 309% increase in tirilazad AUC after an intravenous and an oral dose, respectively. Further analysis of the data suggested that tirilazad underwent significant intestinal first-pass metabolism

and that ketoconazole inhibited both intestinal and hepatic metabolic processes. Itraconazole also appears to have a profound inhibitory effect on intestinal CYP3A4, as illustrated by an increase in oral midazolam bioavailability from 39% to 96% following 6 days of oral itraconazole (200 mg/day) administration [43]. Similarly, 5 days of saquinavir administration (1200 mg, tid) inhibited the metabolic clearance of intravenous and oral midazolam [44]. The oral bioavailability of midazolam increased from 41% to 90%, which is consistent with an inhibition of both hepatic and intestinal midazolam extraction.

Ketoconazole, itraconazole, and saquinavir are potent reversible inhibitors of CYP3A4 *in vitro*; their respective  $K_i$  values are 20 nM [45], 270 nM [46], and 700 nM [25]. Thus, their inhibition of intestinal drug metabolism is not unexpected. Of equal interest, but less predictable, is the inhibition of intestinal CYP3A by drugs that must themselves be metabolized before an effect is manifested. For example, clarithromycin is not a particularly potent inhibitor of CYP3A4 under routine microsomal incubation conditions ( $K_i = 10\text{--}28 \mu\text{M}$ ) [26,47], but it is an effective inhibitor of both hepatic and intestinal midazolam metabolism *in vivo*. In a study with healthy volunteers, Gorski et al. [48] found that administration of clarithromycin (500 mg, bid) for 7 days increased the hepatic midazolam availability from 74% to 90% and the intestinal availability from 42% to 83%. Overall, the inhibition of intestinal midazolam metabolism by clarithromycin had a much greater impact on the absolute midazolam bioavailability than did inhibition of hepatic midazolam metabolism. The effect of clarithromycin, as well as troleandomycin and erythromycin on CYP3A activity [34,49] appears to be mediated through the time-dependent formation of a metabolite that can generate a stable enzyme–inhibitor complex, or MI complex [50]. Presumably, CYP3A MI-complex formation can occur in both the human liver and intestinal mucosa.

Another form of intestinal CYP3A inhibition is that observed following the ingestion of grapefruit juice. Beginning with a serendipitous discovery that a grapefruit juice vehicle used for oral alcohol administration could increase the AUC of oral felodipine [51,52], there has been a flood of studies documenting the effect of grapefruit juice on the metabolism of drugs that exhibit significant first-pass metabolic extraction. These include midazolam [53], buspirone [54], lovastatin [55], simvastatin [56], terfenadine [57], cyclosporine [58], and nifedipine [59]. (For reviews, see Refs. 60–62.) Although the identity of the inhibitory constituents in grapefruit juice remain in question, a striking aspect of the interaction is that normal consumption (1 glass of regular-strength juice a day) appears to alter only the function of intestinal CYP3A and not hepatic CYP3A. For example, the AUC of midazolam is increased 52% after oral but not intravenous administration [53]. A similar observation was made with cyclosporine [58] and nifedipine [59]. Also, the Erythromycin Breath Test, a probe for hepatic CYP3A activity, is unaltered by grapefruit juice consumption [19].

The magnitude of the grapefruit juice interaction can vary widely between

individuals and is clearly dependent on the strength of the juice and the frequency of administration. Repeated ingestion of 200 ml of double-strength grapefruit juice, three times a day, for 2 days caused a 9-fold increase in mean oral buspirone AUC [54] and a 15-fold and 16-fold increase in mean oral lovastatin [55] and simvastatin [56] AUC, respectively. In comparison, a single 250-ml volume of regular-strength grapefruit juice elicited a 149% and 50% increase in felodipine [63] and cisapride [64] AUC, respectively. The impact of dosing regimen on the magnitude of the grapefruit juice interaction is further illustrated by a recent report that consumption of 250 ml of regular-strength juice, once a day (a.m.), for 3 days had a much more modest effect on lovastatin AUC (30% increase) when lovastatin was dosed on the evening of the last day of grapefruit juice consumption, mimicking a more “typical” pattern of juice consumption and statin administration [65]. These authors suggested that a more vigorous regimen of grapefruit juice consumption might alter hepatic CYP3A function, in addition to intestinal CYP3A, resulting in a more profound interaction, as described earlier.

Another interesting aspect of the grapefruit juice effect is that it appears to be highly variable in a given population. Some subjects/patients will experience significant changes, whereas the change for others is minor or nonexistent [58,64,66]. It has been suggested that the magnitude of the grapefruit juice interaction will depend on the basal level of intestinal CYP3A expression [19]. Higher levels of intestinal CYP3A4 are associated with a greater magnitude of interaction, and vice versa.

It was originally postulated that the inhibitory component of grapefruit juice might be naringenin, quercetin, or a related flavanoid molecule [67,68]. More recent studies *in vitro* and *in vivo* point toward a furanocoumarin molecule such as 6',7'-dihydroxybergamottin [69–71] or a furanocoumarin dimer [72]. These molecules may inhibit intestinal CYP3A by both reversible [72] and suicide inactivation [19,70] mechanisms.

## **B. CYP2C9, CYP2C19, and CYP2D6**

Three other intestinal P450 isozymes that merit consideration from the perspective of oral drug bioavailability are CYP2C9, CYP2C19, and CYP2D6. Although DeWaziers et al. [6] reported the detection of what was described as CYP2C8–10 in mucosal microsomes, it was found only in the small intestine and preferentially in the proximal region. Subsequent studies indicate that CYP2C9 and CYP2C19 are the major forms expressed in the human small intestine [73]. In our own analysis of 14 different duodenal microsomal preparations, we have detected two proteins that were reactive with CYP2C-selective anti-CYP2C19 antibody and that comigrated with authentic cDNA-expressed CYP2C19 and CYP2C9 protein standards (unpublished research). Duodenal CYP2C9 protein content varied approximately fourfold among the different preparations, with a

median value that was 15% of the median hepatic microsomal specific content [38 (range, 10–101) pmol/mg protein vs. 10 (range, 4.2–18) pmol/mg protein]. Duodenal CYP2C19 content was equally variable, but comparable to the hepatic enzyme content [4.1 (range, 1–10.4) pmol/mg protein vs. 2.9 (range, 1.1–7.3) pmol/mg protein for liver and duodenal microsomes, respectively].

Very little has been reported to date about intestinal CYP2C-specific metabolic activity. Prueksaritanont et al. [74] reported on a relatively low level of tolbutamide hydroxylase activity that they ascribed to “CYP2C8-10” isozyme. In our characterization of human duodenal CYP2C activity, we found significant but variable turnover of (*S*)-warfarin and (*S*)-mephenytoin to their respective CYP2C9- and CYP2C19-catalyzed 7- and 4-hydroxylated metabolites.

Based on an incomplete oral bioavailability, several CYP2C substrates may undergo significant first-pass intestinal metabolism, including the CYP2C9 substrates verapamil [75], losartan [76], and diclofenac [77] and the CYP2C19 substrates (*S*)-mephenytoin [78] and omeprazole [79]. However, although functional CYP2C9, CYP2C19 proteins are expressed in the human intestinal enterocyte and they may play a role in first-pass drug metabolism, there is no evidence to date to indicate that the intestinal enzymes are involved in drug–drug interactions.

Identification of CYP2D6 in human intestinal microsomes was also first described by DeWaziers et al. [6]. Like CYP3A4, it is localized within mucosal enterocytes and most concentrated within the proximal small intestine. The mean specific enzyme content of duodenal and jejunal microsomes was reported to be approximately 20% of hepatic CYP2D6 microsomal content. However, it was undetected in ileum and colon. The expression of CYP2D6 in the human gastrointestinal tract has been confirmed by other investigators. In separate studies, Prueksaritanont and coworkers detected CYP2D6 in mucosal microsomes from several human donors [74,80]. In addition, they reported observing microsomal 1'-hydroxylation activity toward the CYP2D6 substrate (+)-bufuralol in all preparations. Further, the activity was largely inhibited by the known CYP2D6 inhibitors, quinidine and ajmaline, as well as anti-CYP3A1 IgG [80].

In a more comprehensive study, Madani et al. [81] quantitated CYP2D6 protein in 20 human jejunum and 31 human livers. They found that the median microsomal specific CYP2D6 content was less than 8% of the hepatic microsomal content (0.85 vs. 12.8 pmol/mg) and that there was extensive interindividual variability in protein content for both tissues. These investigators also characterized the catalytic activity of the same jejunal microsomes toward the recognized CYP2D6 substrate metoprolol and found that the  $\alpha$ -hydroxylation reaction rate was significantly correlated with CYP2D6 protein content ( $r = 0.75$ ).

Although there are many CYP2D6 substrates that undergo extensive first-pass metabolism and that are the objects of inhibitory drug interactions, it is not likely that the gut wall contributes significantly to the elimination process. For example, duodenal and jejunal microsomal intrinsic clearances for metoprolol oxidation reactions were found to be only a fraction of the hepatic intrinsic clear-

ance [81]. Consequently, the first pass hepatic and intestinal extraction ratios for metoprolol were predicted to be 61% and 2% for liver and small intestine, respectively. Thus, any potential inhibition of intestinal CYP2D6 activity should have little impact on the systemic bioavailability of the drug.

## C. Glucuronosyltransferases and Sulfotransferases

### 1. Localization and Function

It is rapidly becoming apparent that the human UDP-glucuronosyltransferase (UGT) family of drug-metabolizing enzymes is as complex as the cytochromes P450. Like the P450 family, several UGT isoforms are expressed within the human intestinal mucosa [82] and can catalyze first-pass drug metabolism. Within the UGT1A family, mRNA coding for UGT1A1, UGT1A3, UGT1A4, and UGT1A9 has been identified [8]. In addition, full-length cDNA for UGT1A8 and UGT1A10 has been isolated and shown to be catalytically active toward both endogenous molecules and drugs. Both UGT1A8 and UGT1A10 appear to be expressed selectively within the intestine [8], potentially playing a major role in the metabolism of dietary xenobiotics and some drugs [8,83,84]. A major opioid-metabolizing isoform, UGT2B7 [85], is also found in human intestinal mucosa [7], with preferential expression in the small intestine.

Microsomes isolated from human intestine display appreciable glucuronidation activity toward several drugs, including estradiol and 17 $\beta$ -estradiol, ethinylestradiol, acetaminophen, morphine, propofol, amitriptyline, desipramine, imipramine, and ibuprofen [8,22,86–90]. In the case of propofol, first-pass intestinal metabolism has been implicated as a contributing factor to its incomplete oral bioavailability [91,92]. It is likely that many substrates for UGTs will undergo at least some first-pass metabolism by the intestinal mucosa. However, the relative importance of this process in comparison to hepatic extraction remains to be elucidated.

The human small intestine also metabolizes substrates for sulfotransferases, including ethinylestradiol, terbutaline, isoproterenol, and acetaminophen [9,22, 74,86,93]. At least four isoforms of sulfotransferase have been identified (either directly or indirectly with substrate probes) in the human intestinal mucosa [9]. Although data is limited, it has been suggested that gut wall sulfotransferases contribute to the first-pass metabolism of the  $\beta_2$ -agonists, terbutaline, isoproterenol [93,94], and ethinylestradiol [22].

### 2. Drug Interactions Involving Intestinal UDP-Glucuronosyltransferase and Sulfotransferase

Evidence for the involvement of human intestinal sulfotransferases in drug–drug interactions is limited and, in some cases, circumstantial. For example, first-pass sulfation of isoproterenol in the dog can be reduced by coadministration of com-



petitive substrates, salicylamide [95] and ascorbic acid [96]. Also, both oral acetaminophen [97] and ascorbate [98] administration increase the bioavailability of ethinylestradiol through an inhibition of sulfotransferase activity. Inhibitors of sulfotransferases may exert their effect by competition for the enzyme or the cofactor, PAPS. The effects of acetaminophen and ascorbate were attributed to a reduction in first-pass intestinal ethinylestradiol sulfation, via depletion of the intracellular sulfate pool.

Intestinal UGTs also appear to be involved in oral drug interactions. In humans, amitriptyline will inhibit [99,100] the glucuronidation of the low-bioavailability UGT2B7 substrate morphine [85] *in vitro* and will cause substantial increases in the AUC of morphine when coadministered *in vivo* [101]. Given the presence of UGT2B7 in the intestinal mucosa [7], it is possible that inhibition of first-pass intestinal metabolism contributes to the pharmacokinetic interaction.

A similar scenario can be invoked for an interaction between tacrolimus and mycophenolic acid. UGT1A8 and UGT1A10 are expressed in human intestine but not liver [8], and will catalyze the 7-*O*-glucuronidation of mycophenolic acid [83,84], the active metabolite produced from ester hydrolysis of mycophenolate mofetil. Ester hydrolysis of mycophenolate mofetil can occur in the intestine, liver, and blood. Tacrolimus is reportedly a good inhibitor of mycophenolic acid conjugation, both *in vitro* [102] and *in vivo* [103]. Thus, it is possible that the drug–drug interaction that occurs in patients is, in part, a consequence of the inhibition of first-pass intestinal UGT1A8/10 activity.

### III. P-GLYCOPROTEIN

#### A. Localization and Function

P-Glycoprotein (P-gp) is an active plasma membrane transporter belonging to the family of ATP-binding cassette (ABC) proteins that act to remove drugs and other xenobiotic molecules from an intracellular domain of a variety of cell types, including epithelial cells lining the gastrointestinal tract and renal tubules and the bile canalicular membrane of hepatocytes. In the intestine, P-gp is localized on the apical plasma membrane surface [104] of the mucosa and operates as an efflux pump to remove drug molecules that have diffused into the enterocytes from either the lumen or the blood circulation into the lumen of the gut [105,106]. P-gp is one of several hepatic and intestinal transporters that may function in humans to limit the systemic bioavailability of orally administered drugs [105,107]. It is the best characterized of the efflux transporters in terms of function and potential involvement in drug–drug interactions. Analysis of tissue mRNA reveals P-gp distribution throughout the length of the gastrointestinal tract, with the highest level of expression in the small and large intestine [108]. P-gp is able to transport a broad range of structurally diverse molecules [109], some of which are also substrates or inhibitors of CYP3A4 [110]. The overlap

of active-site ligands between the two systems is not perfect and perhaps coincidental [111], as illustrated by the development of P-gp-selective inhibitors such as PSC833 for adjunctive use in cancer chemotherapy [112].

Investigations of P-gp function require the use of intact cell systems or whole-animal models or humans. Characterization of substrate diversity and relative efficiency of a polarized efflux process and susceptibility to inducers and inhibitors is most commonly performed with an immortalized human cell line, such as Caco-2, TC7, or LS180 [107,111–114]. For many drugs, experiments with cultured confluent monolayers have demonstrated time- and concentration-dependent efflux of substrate molecules in a manner that is consistent with a role for P-gp in limiting oral drug bioavailability. Drugs that show incomplete oral bioavailability and are also substrates for intestinal efflux transporters include paclitaxel [115], vinblastine [107], terfenadine [114], cyclosporine [116], tacrolimus [116], sirolimus [117], digoxin [111], saquinavir [118], ritonavir [118], and lovastatin [111].

More definitive proof of the *in vivo* relevance of intestinal P-gp for some of these drugs (paclitaxel and vinblastine) has come from pharmacokinetic studies with knockout mice in which the gene coding for intestinal P-gp (*mdr1a*) has been removed from the genome. Active excretion of these drugs from blood into the gut lumen is impaired in knockout mice compared with wild-type mice, and there is an improvement in oral bioavailability [105,119]. In humans, there has been one study in which it was reported that the expression of P-gp, measured in human duodenal biopsies, was positively correlated with the oral bioavailability of the known P-gp substrate cyclosporine [120]. In addition, the extent of cyclosporine absorption was inversely correlated with the level of P-gp mRNA content in intestinal mucosal tissue [121]. However, the implied importance of regional differences in P-gp expression in the gastrointestinal tract is clouded by the possibility of reduced cyclosporine uptake into the distal (colon) mucosa as a consequence of reduced surface area for drug diffusion.

## B. Drug Interactions Involving P-Glycoprotein

### 1. Induction of Drug Efflux

In comparison to CYP3A4, less is known about the ability of various drugs to induce intestinal P-gp expression and function. However, studies with an LS180 human colon carcinoma cell line have revealed that a number of drugs, including reserpine, rifampin, phenobarbital, and verapamil, can up-regulate P-gp expression (more than 10-fold for these examples) [113]. The inductive effect of rifampin has also been demonstrated *in vivo*. Treatment of healthy volunteers with rifampin (600 mg/day) for 10 days resulted in a 3.5-fold increase in duodenal P-gp levels and a 58% reduction in digoxin AUC following oral administration but no change after intravenous administration [122]. Interestingly, the ab-

sence of an effect of rifampin on the systemic clearance of digoxin suggests that induction of P-gp altered only intestinal digoxin bioavailability and not systemic clearance pathways. This finding is in contrast to the significant changes in systemic digoxin clearance that occurred in a P-gp knockout mouse, which was attributed in part to the loss of intestinal digoxin excretion mediated by mucosal P-gp [123].

Similar interactions might be expected between rifampin and other P-gp inducers and low-oral-bioavailability P-gp substrates, such as saquinavir and terfenadine.

## 2. Inhibition of Drug Efflux

Most comprehensive studies describing the inhibitory effects of various drugs on P-gp function have been examined at the cellular level, using model substrates. For example, Kim et al. [111] recently determined the effect of a series of CYP3A4 substrates and inhibitors on the transport of digoxin in Caco-2 cell monolayers. The most notable inhibitors were terfenadine, quinidine, ketoconazole, verapamil, PSC-833, amiodarone, lovastatin, and erythromycin; all inhibited digoxin transport by at least 50% at a nominal concentration of 10  $\mu$ M. Other drugs that effectively inhibit P-gp function in a cell monolayer system, and at a similar concentration, include cyclosporine A and tacrolimus [112].

As already discussed, evidence for the clinical importance of intestinal P-gp comes from in vivo drug–drug interaction studies. Some of the first-generation inhibitors of P-gp were found to increase the oral bioavailability of recognized P-gp substrates when coadministered to patients or healthy volunteers. Examples include an interaction between quinidine and digoxin [122], cyclosporine and etoposide [124,125], cyclosporine and paclitaxel [126], and ketoconazole and cyclosporine A [127]. In addition, the pronounced effect of ketoconazole on the oral bioavailability of terfenadine [42] and saquinavir [128] is likely to be mediated in part by an inhibition of intestinal P-gp function. However, it should be emphasized that although intestinal transport processes have been implicated, some of the effects of these P-gp inhibitors on oral drug bioavailability could also be mediated through an inhibition of intestinal and/or hepatic oxidative metabolism.

A more definite example of the inhibition of P-gp function by ketoconazole is illustrated by the drug's effect on oral fexofenadine AUC. Fexofenadine is the active metabolite (antihistaminic) of terfenadine and is not a substrate for CYP3A4 but is transported by P-gp [129]. Coadministration of ketoconazole or erythromycin with fexofenadine (Allegra<sup>®</sup>) results in a 164% and 109% increase, respectively, in steady-state fexofenadine concentration in blood (*Physicians Desk Reference*, 1998). Because P-gp is expressed in both the intestinal mucosa and the bile canaliculi, the interaction may occur at one or both sites.

## REFERENCES

1. KE Thummel, KL Kunze, DD Shen. Enzyme-catalyzed processes of first-pass hepatic and intestinal drug extraction. *Adv Drug Deliv Rev* 27:99–127, 1997.
2. M Rowland, SB Matin. Kinetics of drug–drug interactions. *J Pharmacokinet Biopharm* 1:553–567, 1973.
3. PN Shaw, JB Houston. Kinetics of drug metabolism inhibition: use of metabolite concentration–time profiles. *J Pharmacokinet Biopharm* 15:497–510, 1987.
4. MF Paine, M Khalighi, JM Fisher, DD Shen, KL Kunze, CL Marsh, JD Perkins, KE Thummel. Characterization of inter- and intra-intestinal differences in human CYP3A-dependent metabolism. *J Pharmacol Exp Ther* 283:1552–1562, 1997.
5. Q-Y Zhang, D Dunbar, A Ostrowska, S Zeisloft, J Yang, L Kaminsky. Characterization of human small intestinal cytochromes P-450. *Drug Metab Dispos* 27:804–809, 1999.
6. I DeWaziers, PH Cugnenc, CS Yang, J-P Leroux, PH Beaune. Cytochrome P450 isoenzymes, epoxide hydrolase and glutathione transferases in rat and human hepatic and extrahepatic tissues. *J Pharmacol Exp Ther* 253:387–394, 1990.
7. A Radomska-Pandya, J Little, J Pandya, T Tephly, C King, G Barone, J-P Raufman. UDP-glucuronosyltransferases in human intestinal mucosa. *Biochim Biophys Acta* 1394:199–208, 1998.
8. C Strassburg, N Nguyen, M Manns, R Tukey. UDP-glucuronosyltransferase activity in human liver and colon. *Gastroenterology* 116:149–160, 1999.
9. C Her, C Szumlanski, I Aksoy, R Weinshilboum. Human jejunal estrogen sulfotransferase and dehydroepiandrosterone sulfotransferase. Immunochemical characterization of individual variation. *Drug Metab Dispos* 24:1328–1335, 1996.
10. GI Murray, TS Barnes, HF Sewell, SWB Ewen, WT Melvin, MD Burke. The immunocytochemical localisation and distribution of cytochrome P-450 in normal hepatic and extrahepatic tissues with a monoclonal antibody to human cytochrome P-450. *Br J Clin Pharmacol* 25:465–475, 1988.
11. PB Watkins, SA Wrighton, EG Schuetz, PS Guzelian. Identification of glucocorticoid-inducible cytochromes P-450 in the intestinal mucosa of rats and man. *J Clin Invest* 80:1029–1036, 1987.
12. JC Kolars, KS Lown, P Schmiedlin-Ren, M Ghosh, C Fang, SA Wrighton, RM Merion, PB Watkins. CYP3A gene expression in human gut epithelium. *Pharmacogenetics* 4:247–259, 1994.
13. R McKinnon, W Burgess, PdIM Hall, S Roberts-Thomson, F Gonzalez, M McManus. Characterization of CYP3A gene subfamily expression in human gastrointestinal tissues. *Gut* 36:259–267, 1995.
14. KS Lown, JC Kolars, KE Thummel, JL Barnett, KL Kunze, SA Wrighton, PB Watkins. Interpatient heterogeneity in expression of CYP3A4 and CYP3A5 in small bowel: lack of prediction by the erythromycin breath test. *Drug Metab Dispos* 22:947–955, 1994.
15. L Gervot, V Carrière, P Costet, P-H Cugnenc, A Berger, P Beaune, I deWaziers. CYP3A5 is the major cytochrome P450 3A expressed in human colon and colonic cell lines. *Environ Toxicol Pharmacol* 2:381–388, 1996.

16. P Schmiedlin-Ren, KE Thummel, JM Fisher, MF Paine, KS Lown, PB Watkins. Expression of enzymatically active CYP3A4 by Caco-2 cells grown on extracellular matrix-coated permeable supports in the presence of  $1\alpha,25$ -dihydroxyvitamin D<sub>3</sub>. *Mol Pharmacol* 51:741–754, 1997.
17. M Hu, Y Li, CM Davitt, SM Huang, K Thummel, BW Penman, CL Crespi. Transport and metabolic characterization of Caco-2 cells expressing CYP3A4 and CYP3A4 plus oxidoreductase. *Pharm Res* 16:1352–1359, 1999.
18. JC Kolars, P Schmiedlin-Ren, JD Schuetz, C Fang, PB Watkins. Identification of rifampin-inducible P450III A4 (CYP3A4) in human small bowel enterocytes. *J Clin Invest* 90:1871–1878, 1992.
19. KS Lown, DG Bailey, RJ Fontana, SK Janardan, CH Adair, LA Fortlage, MB Brown, W Guo, PB Watkins. Grapefruit juice increases felodipine oral availability in humans by increasing intestinal CYP3A protein expression. *J Clin Invest* 99: 2545–2553, 1997.
20. C Liddle, B Goodwin, J George, M Tapner, G Farrell. Separate and interactive regulation of cytochrome P450 by triiodothyronine, dexamethasone, and growth hormone in cultured hepatocytes. *J Clin Endocrinol Metab* 83:2411–2416, 1998.
21. WA Mahon, T Inaba, RM Stone. Metabolism of flurazepam by the small intestine. *Clin Pharmacol Ther* 22:228–233, 1977.
22. SM Rogers, DJ Back, ML Orme. Intestinal metabolism of ethinyloestradiol and paracetamol in vitro: studies using Ussing chambers. *Br J Clin Pharmacol* 23:727–734, 1987.
23. KE Thummel, D O'Shea, MF Paine, DD Shen, KL Kunze, JD Perkins, GR Wilkinson. Oral first-pass elimination of midazolam involves both gastrointestinal and hepatic CYP3A-mediated metabolism. *Clin Pharmacol Ther* 59:491–502, 1996.
24. A Lampen, U Christians, FP Guengerich, PB Watkins, JC Kolars, A Bader, A-K Gonschior, H Dralle, I Hackbarth, K-F Sweing. Metabolism of the immunosuppressant tacrolimus in the small intestine: cytochrome P450, drug interactions, and interindividual variability. *Drug Metab Dispos* 23:1315–1324, 1995.
25. ME Fitzsimmons, JM Collins. Selective biotransformation of the human immunodeficiency virus protease inhibitor saquinavir by human small-intestinal cytochrome P4503A4. *Drug Metab Dispos* 25:256–266, 1997.
26. E Iatsimirskaia, S Tulebaev, E Storozhuk, I Utkin, D Smith, N Gerber, T Koudriakova. Metabolism of rifabutin in human enterocyte and liver microsomes: kinetic parameters, identification of enzyme systems, and drug interactions with macrolides and antifungal agents. *Clin Pharmacol Ther* 61:554–562, 1997.
27. MF Paine, DD Shen, KL Kunze, JD Perkins, CL Marsh, JP McVicar, DM Barr, BS Gillies, KE Thummel. First-pass metabolism of midazolam by the human intestine. *Clin Pharmacol Ther* 60:14–24, 1996.
28. MF Fromm, D Busse, HK Kroemer, M Eichelbaum. Differential induction of prehepatic and hepatic metabolism of verapamil by rifampin. *Hepatology* 24:796–801, 1996.
29. N Holtbecker, M Fromm, HK Kroemer, EE Ohnhaus, H Heidemann. The nifedipine–rifampin interaction. Evidence for induction of gut wall metabolism. *Drug Metab Dispos* 24:1121–1123, 1996.

30. JC Fleishaker, PG Pearson, LC Wienkers, LK Pearson, GR Graves. Biotransformation of tirilazad in humans: 2. Effect of ketoconazole on tirilazad clearance and oral bioavailability. *J Pharmacol Exp Ther* 277:991–998, 1996.
31. DA Garteiz, RH Hook, BJ Walker, RA Okerholm. Pharmacokinetics and biotransformation studies of terfenadine in man. *Arzneimittelforschung* 32:1185–1190, 1982.
32. PEO Williams, GJ Muirhead, MJ Madigan, AM Mitchell, T Shaw. Disposition and bioavailability of the HIV-proteinase inhibitor, Ro 31-8959, after single doses in healthy volunteers. *Br J Clin Pharmacol* 34:155P–156P, 1992.
33. JT Backman, KT Olkkola, PJ Neuvonen. Rifampin drastically reduces plasma concentrations and effects of oral midazolam. *Clin Pharmacol Ther* 59:7–13, 1996.
34. ED Kharasch, M Russell, D Mautz, KE Thummel, KL Kunze, AT Bowdle, K Cox. The role of cytochrome P450 3A4 in alfentanil clearance. Implications for interindividual variability in disposition and perioperative drug interactions. *Anesthesiology* 87:36–50, 1997.
35. K Villikka, KT Kivisto, JT Backman, KT Olkkola, PJ Neuvonen. Triazolam is ineffective in patients taking rifampin. *Clin Pharmacol Ther* 61:8–14, 1997.
36. TS Lamberg, KT Kivisto, PJ Neuvonen. Concentrations and effects of buspirone are considerably reduced by rifampicin. *Br J Clin Pharmacol* 45:381–385, 1998.
37. KT Kivisto, K Villikka, L Nyman, M Anttila, PJ Neuvonen. Tamoxifen and toremifene concentrations in plasma are greatly decreased by rifampin. *Clin Pharmacol Ther* 64:648–654, 1998.
38. J Lin, M Chiba, T Baillie. Is the role of the small intestine in first-pass metabolism overemphasized? *Pharmacol Rev* 51:135–157, 1999.
39. C Reichel, W Block, T Skodra, F Traber, P Schiedermaier, U Spengler, R Nuber, HH Schild, T Sauerbruch. Relationship between cytochrome P-450 induction by rifampicin, hepatic volume and portal blood flow in man. *Eur J Gastroenterol Hepatol* 9:975–979, 1997.
40. L Pichard, I Fabre, G Fabre, J Domergue, BS Aubert, G Mourad, P Maurel. Cyclosporin A drug interactions. Screening for inducers and inhibitors of cytochrome P-450 (cyclosporin A oxidase) in primary cultures of human hepatocytes and in liver microsomes. *Drug Metab Dispos* 18:595–605, 1990.
41. JT Backman, KT Olkkola, M Ojala, H Laaksovirta, PJ Neuvonen. Concentrations and effects of oral midazolam are greatly reduced in patients treated with carbamazepine or phenytoin. *Epilepsia* 37:253–257, 1996.
42. PK Honig, DC Wortham, K Zamani, DP Conner, LR Cantilena. The terfenadine–ketoconazole interaction: pharmacokinetic and electrocardiographic consequences. *JAMA* 269:1513–1518, 1993.
43. KT Olkkola, J Ahonen, PJ Neuvonen. The effect of systemic antimycotics, itraconazole and fluconazole, on the pharmacokinetics and pharmacodynamics of intravenous and oral midazolam. *Anesthes Analges* 82:511–516, 1996.
44. VJ Palkama, J Ahonen, PJ Neuvonen, KT Olkkola. Effect of saquinavir on the pharmacokinetics and pharmacodynamics of oral and intravenous midazolam. *Clin Pharmacol Ther* 66:33–39, 1999.
45. MA Gibbs, KE Thummel, DD Shen, KL Kunze. Inhibition of CYP3A in human

- intestinal and liver microsomes: comparison of  $K_i$  values and impact of CYP3A5 expression. *Drug Metab Dispos*, 27:161–166, 1999.
46. LLv Moltke, DJ Greenblatt, J Schmider, SX Duan, CE Wright, JS Harmatz, RI Shader. Midazolam hydroxylation by liver microsomes in vitro: inhibition by fluoxetine, norfluoxetine, and by azole antifungal agents. *J Clin Pharmacol* 36:783–791, 1996.
  47. M Jurima-Romet, K Crawford, T Cyr, T Inaba. Terfenadine metabolism in human liver. In vitro inhibition by macrolide antibiotics and azole antifungals. *Drug Metab Dispos* 22:849–857, 1994.
  48. JC Gorski, DR Jones, BD Haehner-Daniels, MA Hamman, EM O'Mara, SD Hall. The contribution of intestinal and hepatic CYP3A to the interaction between midazolam and clarithromycin. *Clin Pharmacol Ther* 64:133–143, 1998.
  49. KT Olkkola, K Aranko, H Luuila, A Hiller, L Saarnivaara, J-J Himberg, PJ Neuvonen. A potentially hazardous interaction between erythromycin and midazolam. *Clin Pharmacol Ther* 53:298–305, 1993.
  50. M Tinel, V Descatoire, D Larrey, J Loeper, G Labbe. Effects of clarithromycin on cytochrome P-450. Comparison with other macrolides. *J Pharmacol Exp Ther* 250:746–751, 1989.
  51. DG Bailey, JD Spence, B Edgar, CD Bayliff, JM Arnold. Ethanol enhances the hemodynamic effects of felodipine. *Clin Invest Med* 12:357–362, 1989.
  52. DG Bailey, JD Spence, C Munoz, JMO Arnold. Interaction of citrus juices with felodipine and nifedipine. *Lancet* 377:268–269, 1991.
  53. HHT Kupferschmidt, HR Ha, WH Ziegler, PJ Meier, S Krähenbühl. Interaction between grapefruit juice and midazolam in humans. *Clin Pharmacol Ther* 58:20–28, 1995.
  54. JJ Lilja, KT Kivisto, JT Backman, TS Lamberg, PJ Neuvonen. Grapefruit juice substantially increases plasma concentrations of buspirone. *Clin Pharmacol Ther* 64:655–660, 1998.
  55. T Kantola, KT Kivisto, PJ Neuvonen. Grapefruit juice greatly increases serum concentrations of lovastatin and lovastatin acid. *Clin Pharmacol Ther* 63:397–402, 1998.
  56. JJ Lilja, KT Kivisto, PJ Neuvonen. Grapefruit juice–simvastatin interaction: effect on serum concentrations of simvastatin, simvastatin acid, and HMG-CoA reductase inhibitors. *Clin Pharmacol Ther* 64:477–483, 1998.
  57. RE Benton, PK Honig, K Zamani, LR Cantalina, RL Woosley. Grapefruit juice alters terfenadine pharmacokinetics, resulting in prolongation of repolarization on the electrocardiogram. *Clin Pharmacol Ther* 59:383–388, 1996.
  58. MP Ducharme, LH Warbasse, DJ Edwards. Disposition of intravenous and oral cyclosporine after administration with grapefruit juice. *Clin Pharmacol Ther* 57:485–491, 1995.
  59. TJ Rashid, U Martin, H Clarke, DG Waller, AG Renwick, CF George. Factors affecting the absolute bioavailability of nifedipine. *Br J Clin Pharmacol* 40:51–58, 1995.
  60. B Ameer, RA Weintraub. Drug interactions with grapefruit juice. *Clin Pharmacokin* 33:103–121, 1997.

61. U Fuhr. Drug interactions with grapefruit juice. Extent, probable mechanism and clinical relevance. *Drug Saf* 18:251–272, 1998.
62. DG Bailey, J Malcolm, O Arnold, JD Spence. Grapefruit juice–drug interactions. *Br J Clin Pharmacol* 46:101–110, 1998.
63. DG Bailey, JR Bend, JMO Arnold, LT Tran, JD Spence. Erythromycin–felodipine interaction: magnitude, mechanism, and comparison with grapefruit juice. *Clin Pharmacol Ther* 60:25–33, 1996.
64. AS Gross, YD Goh, RS Addison, GM Shenfield. Influence of grapefruit juice on cisapride pharmacokinetics. *Clin Pharmacol Ther* 65:395–401, 1999.
65. JD Rogers, J Zhao, L Liu, RD Amin, KD Gagliano, AG Porras, RA Blum, MF Wilson, M Stepanavage, JM Vega. Grapefruit juice has minimal effects on plasma concentrations of lovastatin-derived 3-hydroxy-3-methylglutaryl coenzyme A reductase inhibitors. *Clin Pharmacol Ther* 66:358–366, 1999.
66. DG Bailey, JMO Arnold, JD Spence. Grapefruit juice and drugs. How significant is the interaction? *Clin Pharmacokinet* 26:91–98, 1994.
67. FP Guengerich, DH Kim. In vitro inhibition of dihydropyridine oxidation and aflatoxin B1 activation in human liver microsomes by naringenin and other flavanoids. *Carcinogenesis (Oxford)* 11:2275–2279, 1990.
68. A Miniscalco, J Lundahl, CG Regardh, B Edgar, UG Eriksson. Inhibition of dihydropyridine metabolism in rat and human liver microsomes by flavonoids found in grapefruit juice. *J Pharmacol Exp Ther* 261:1195–1199, 1992.
69. DJ Edwards, FH Bellevue III, PM Woster. Identification of 6',7'-dihydroxybergamottin, a cytochrome P450 inhibitor, in grapefruit juice. *Drug Metab Dispos* 24:1287–1290, 1996.
70. P Schmiedlin-Ren, DJ Edwards, ME Fitzsimmons, K He, KS Lown, PM Woster, A Rahman, KE Thummel, JM Fisher, PF Hollenberg, PB Watkins. Mechanisms of enhanced oral availability of CYP3A4 substrates by grapefruit constituents: decreased enterocyte CYP3A4 concentration and mechanism-based inactivation by furanocoumarins. *Drug Metab Dispos* 25:1228–1233, 1997.
71. DJ Edwards, ME Fitzsimmons, EG Schuetz, K Yasuda, MP Ducharme, LH Warbasse, PM Woster, JD Schuetz, P Watkins. 6',7'-Dihydroxybergamottin in grapefruit juice and Seville orange juice: effects on cyclosporine disposition, enterocyte CYP3A4, and P-glycoprotein. *Clin Pharmacol Ther* 65:237–244, 1999.
72. K Fukuda, T Ohta, Y Oshima, N Ohashi, M Yoshikawa, Y Yamazoe. Specific CYP3A4 inhibitors in grapefruit juice: furocoumarin dimers as components of drug interaction. *Pharmacogenetics* 7:391–396, 1997.
73. TS Klose, JA Blaisdell, JA Goldstein. Gene structure of CYP2C8 and extrahepatic distribution of the human CYP2Cs. *J Biochem Mol Toxicol* 13:289–295, 1999.
74. T Prueksaritanont, LM Gorham, JH Hochman, LO Tran, KP Vyas. Comparative studies of drug-metabolizing enzymes in dog, monkey, and human small intestines, and in Caco-2 cells. *Drug Metab Dispos* 24:634–642, 1996.
75. D Busse, J Cosme, P Beaune, HK Kroemer, M Eichelbaum. Cytochromes of the P450 2C subfamily are the major enzymes involved in the *O*-demethylation of verapamil in humans. *Naunyn Schmiedebergs Arch Pharmacol* 353:116–121, 1995.
76. RA Stearns, PK Chakravarty, R Chen, SH Chiu. Biotransformation of losartan to its



- active carboxylic acid metabolite in human liver microsomes. Role of cytochrome P4502C and 3A subfamily members. *Drug Metab Dispos* 23:207–215, 1995.
77. T Leemann, M Kondo, J Zhao, C Transon, P Bonnabry, P Dayer. [The biotransformation of NSAIDs: a common elimination site and drug interactions.] *Schweiz Med Wochenschr* 122:1897–1899, 1992.
  78. JA Goldstein, MB Faletto, M Romkes-Sparks, T Sullivan, S Kitareewan, JL Raucy, JM Lasker, BI Ghanayem. Evidence that CYP2C19 is the major (*S*)-mephenytoin 4'-hydroxylase in humans. *Biochemistry* 33:1743–1752, 1994.
  79. JM Lasker, MR Wester, E Aramsombatdee, JL Raucy. Characterization of CYP2C19 and CYP2C9 from human liver: respective roles in microsomal tolbutamide, *S*-mephenytoin, and omeprazole hydroxylations. *Arch Biochem Biophys* 353:16–28, 1998.
  80. T Prueksaritanont, LM Dwyer, AE Cribb. (+)-bufuralol 1'-hydroxylation activity in human and rhesus monkey intestine and liver. *Biochem Pharmacol* 50:1521–1525, 1995.
  81. S Madani, MF Paine, L Lewis, KE Thummel, DD Shen. Comparison of CYP2D6 content and metoprolol oxidation between microsomes isolated from human livers and small intestines. *Pharm Res* 16:1199–1205, 1999.
  82. SN de Wildt, GL Kearns, JS Leeder, JN van der Anker. Glucuronidation in humans. Pharmacogenetic and developmental aspects. *Clin Pharmacokinet* 36:439–452, 1999.
  83. B Mojarrabi, PI Mackenzie. The human UDP glucuronosyltransferase, UGT1A10, glucuronidates mycophenolic acid. *Biochem Biophys Res Commun* 238:775–778, 1997.
  84. Z Cheng, A Radominska-Pandya, TR Tephly. Studies on the substrate specificity of human intestinal UDP-glucuronosyltransferases 1A8 and 1A10. *Drug Metab Dispos* 27:1165–70, 1999.
  85. BL Coffman, GR Rios, CD King, TR Tephly. Human UGT2B7 catalyzes morphine glucuronidation. *Drug Metab Dispos* 25:1–4, 1997.
  86. DJ Back, M Bates, AM Breckenridge, A Ellis, JM Hall, M Maciver, ML Orme, PH Rowe. The in vitro metabolism of ethinyloestradiol, mestranol and levonorgestrel by human jejunal mucosa. *Br J Clin Pharmacol* 11:275–278, 1981.
  87. GM Pacifici, C Bencini, A Rane. Presystemic glucuronidation of morphine in humans and rhesus monkeys: subcellular distribution of the UDP-glucuronosyltransferase in the liver and intestine. *Xenobiotica* 16:123–128, 1986.
  88. E Diczfalusy, C Franksson, B Lisboa, B Martinsen. Formation of oestrone glucuronide by the human intestinal tract. *Acta Endocrinol* 40:537–551, 1962.
  89. AA Raoof, LJ van Obbergh, J de Ville de Goyet, RK Verbeeck. Extrahepatic glucuronidation of propofol in man: possible contribution of gut wall and kidney. *Eur J Clin Pharmacol* 50:91–96, 1996.
  90. M Cappiello, L Giuliani, GM Pacifici. Distribution of UDP-glucuronosyltransferase and its endogenous substrate uridine 5'-diphosphoglucuronic acid in human tissues. *Eur J Clin Pharmacol* 41:345–350, 1991.
  91. PA Gray, GR Park, ID Cockshott, EJ Douglas, B Shuker, PJ Simons. Propofol metabolism in man during the anhepatic and reperfusion phases of liver transplantation. *Xenobiotica* 22:105–114, 1992.

92. P Veroli, B O'Kelly, F Bertrand, JH Trouvin, R Farinotti, C Ecoffey. Extrahepatic metabolism of propofol in man during the anhepatic phase of orthotopic liver transplantation. *Br J Anaesth* 68:183-186, 1992.
93. GM Pacifici, M Eligi, L Giuliani. (+) and (-)terbutaline are sulphated at a higher rate in human intestine than in liver. *Eur J Clin Pharmacol* 45:483-487, 1993.
94. ME Conolly, DS Davies, CT Dollery, CD Morgan, JW Paterson, M Sandler. Metabolism of isoprenaline in dog and man. *Br J Pharmacol* 46:458-472, 1972.
95. PN Bennett, E Blackwell, DS Davies. Competition for sulphate during detoxification in the gut wall. *Nature* 258:247-248, 1975.
96. JB Houston, HJ Wilkens, G Levy. Potentiation of isoproterenol effect by ascorbic acid. *Res Commun Chem Pathol Pharmacol* 14:643-650, 1976.
97. SM Rogers, DJ Back, PJ Stevenson, SF Grimmer, ML Orme. Paracetamol interaction with oral contraceptive steroids: increased plasma concentrations of ethinyloestradiol. *Br J Clin Pharmacol* 23:721-725, 1987.
98. DJ Back, AM Breckenridge, M MacIver, ML Orme, H Purba, PH Rowe. Interaction of ethinyloestradiol with ascorbic acid in man. *Br Med J (Clin Res Ed)* 282:1516, 1981.
99. A Wahlstrom, L Lenhammar, B Ask, A Rane. Tricyclic antidepressants inhibit opioid receptor binding in human brain and hepatic morphine glucuronidation. *Pharmacol Toxicol* 75:23-27, 1994.
100. Q Yue, C von Bahr, I Odar-Cederlof, J Sawe. Glucuronidation of codeine and morphine in human liver and kidney microsomes: effect of inhibitors. *Pharmacol Toxicol* 66:221-226, 1990.
101. V Ventafridda, M Bianchi, C Ripamonti, P Sacerdote, F De Conno, E Zecca, AE Panerai. Studies on the effects of antidepressant drugs on the antinociceptive action of morphine and on plasma morphine in rat and man. *Pain* 43:155-162, 1990.
102. K Zucker, A Tsaroucha, L Olson, V Esquenazi, A Tzakis, J Miller. Evidence that tacrolimus augments the bioavailability of mycophenolate mofetil through the inhibition of mycophenolic acid glucuronidation. *Ther Drug Monit* 21:35-43, 1999.
103. K Zucker, A Rosen, A Tsaroucha, L de Faria, D Roth, G Ciancio, V Esquenazi, G Burke, A Tzakis, J Miller. Augmentation of mycophenolate mofetil pharmacokinetics in renal transplant patients receiving Prograf and CellCept in combination therapy. *Transplant Proc* 29:334-336, 1997.
104. J Hunter, MA Jepson, T Tsuruo, NL Simmons, BH Hirst. Functional expression of P-glycoprotein in apical membranes of human intestinal Caco-2 cells. Kinetics of vinblastine secretion and interaction with modulators. *J Biol Chem* 268:14991-14997, 1993.
105. J Van Asperen, O Van Tellingen, JH Beijnen. The pharmacological role of P-glycoprotein in the intestinal epithelium. *Pharmacol Res* 37:429-435, 1998.
106. K Arimori, M Nakano. Drug exsorption from blood into the gastrointestinal tract. *Pharm Res* 15:371-376, 1998.
107. J Hunter, BH Hirst, NL Simmons. Drug absorption limited by P-glycoprotein-mediated secretory drug transport in human intestinal epithelial Caco-2 cell layers. *Pharm Res* 10:743-749, 1993.
108. AT Fojo, K Ueda, DJ Slamon, DG Poplack, MM Gottesman, I Pastan. Expression

- of a multidrug-resistance gene in human tumors and tissues. *Proc Natl Acad Sci USA* 84:265–269, 1987.
109. A Seelig. A general pattern for substrate recognition by P-glycoprotein. *Eur J Biochem* 251:252–261, 1998.
  110. VJ Wachter, CY Wu, LZ Benet. Overlapping substrate specificities and tissue distribution of cytochrome P450 3A and P-glycoprotein: implications for drug delivery and activity in cancer chemotherapy. *Mol Carcinog* 13:129–134, 1995.
  111. RB Kim, C Wandel, B Leake, M Cvetkovic, MF Fromm, PJ Dempsey, MM Roden, F Belas, AK Chaudhary, DM Roden, AJ Wood, GR Wilkinson. Interrelationship between substrates and inhibitors of human CYP3A and P-glycoprotein. *Pharm Res* 16:408–414, 1999.
  112. C Wandel, RB Kim, S Kajiji, P Guengerich, GR Wilkinson, AJ Wood. P-Glycoprotein and cytochrome P-450 3A inhibition: dissociation of inhibitory potencies. *Cancer Res* 59:3944–3948, 1999.
  113. EG Schuetz, WT Beck, JD Schuetz. Modulators and substrates of P-glycoprotein and cytochrome P4503A coordinately up-regulate these proteins in human colon carcinoma cells. *Mol Pharmacol* 49:311–318, 1996.
  114. SD Raeissi, IJ Hidalgo, J Segura-Aguilar, P Artursson. Interplay between CYP3A-mediated metabolism and polarized efflux of terfenadine and its metabolites in intestinal epithelial Caco-2 (TC7) cell monolayers. *Pharm Res* 16:625–632, 1999.
  115. UK Walle, T Walle. Taxol transport by human intestinal epithelial Caco-2 cells. *Drug Metab Dispos* 26:343–346, 1998.
  116. T Saeki, K Ueda, Y Tanigawara, R Hori, T Komano. Human P-glycoprotein transports cyclosporin A and FK506. *J Biol Chem* 268:6077–6080, 1993.
  117. VC Dias, RW Yatscoff. Investigation of rapamycin transport and uptake across absorptive human intestinal cell monolayers. *Clin Biochem* 27:31–36, 1994.
  118. J Alsenz, H Steffen, R Alex. Active apical secretory efflux of the HIV protease inhibitors saquinavir and zalcitabine in Caco-2 cell monolayers [published erratum appears in *Pharm Res* 15(6):958, 1998]. *Pharm Res* 15:423–428, 1998.
  119. A Sparreboom, J van Asperen, U Mayer, AH Schinkel, JW Smit, DK Meijer, P Borst, WJ Nooijen, JH Beijnen, O van Tellingen. Limited oral bioavailability and active epithelial excretion of paclitaxel (Taxol) caused by P-glycoprotein in the intestine. *Proc Natl Acad Sci USA* 94:2031–2035, 1997.
  120. KS Lown, RR Mayo, AB Leichtman, H-L Hsiao, K Turgeon, P Schmiedlin-Ren, MB Brown, W Guo, SJ Rossi, LZ Benet, PB Watkins. Role of intestinal P-glycoprotein (mdr1) in interpatient variation in the oral bioavailability of cyclosporine. *Clin Pharmacol Ther* 62:248–260, 1997.
  121. G Fricker, J Drewe, J Huwyler, H Gutmann, C Beglinger. Relevance of P-glycoprotein for the enteral absorption of cyclosporin A: in vitro–in vivo correlation. *Br J Pharmacol* 118:1841–1847, 1996.
  122. B Greiner, M Eichelbaum, P Fritz, HP Kreichgauer, O von Richter, J Zundler, HK Kroemer. The role of intestinal P-glycoprotein in the interaction of digoxin and rifampin. *J Clin Invest* 104:147–153, 1999.
  123. U Mayer, E Wagenaar, JH Beijnen, JW Smit, DK Meijer, J van Asperen, P Borst, AH Schinkel. Substantial excretion of digoxin via the intestinal mucosa and preven-

- tion of long-term digoxin accumulation in the brain by the *mdr 1a* P-glycoprotein. *Br J Pharmacol* 119:1038–1044, 1996.
124. BL Lum, S Kaubisch, AM Yahanda, KM Adler, L Jew, MN Ehsan, NA Brophy, J Halsey, MP Gosland, BI Sikic. Alteration of etoposide pharmacokinetics and pharmacodynamics by cyclosporine in a phase I trial to modulate multidrug resistance. *J Clin Oncol* 10:1635–1642, 1992.
  125. BL Lum, GA Fisher, NA Brophy, AM Yahanda, KM Adler, S Kaubisch, J Halsey, BI Sikic. Clinical trials of modulation of multidrug resistance. Pharmacokinetic and pharmacodynamic considerations. *Cancer* 72:3502–3514, 1993.
  126. JM Meerum Terwogt, JH Beijnen, WW ten Bokkel Huinink, H Rosing, JH Schellens. Co-administration of cyclosporin enables oral therapy with paclitaxel [letter] [published erratum appears in *Lancet* 352:824, 1998]. *Lancet* 352:285, 1998.
  127. DY Gomez, VJ Wachter, SJ Tomlanovich, MF Hebert, LZ Benet. The effects of ketoconazole on the intestinal metabolism and bioavailability of cyclosporine. *Clin Pharmacol Ther* 58:15–19, 1995.
  128. E Albengres, H Le Louet, JP Tillement. Systemic antifungal agents. Drug interactions of clinical significance. *Drug Saf* 18:83–97, 1998.
  129. M Cvetkovic, B Leake, MF Fromm, GR Wilkinson, RB Kim. OATP and P-glycoprotein transporters mediate the cellular uptake and excretion of fexofenadine. *Drug Metab Dispos* 27:866–871, 1999.



# 10

## Mechanism-Based Inhibition of Human Cytochromes P450: In Vitro Kinetics and In Vitro–In Vivo Correlations

**David R. Jones and Stephen D. Hall**

*Indiana University School of Medicine, Indianapolis, Indiana*

### I. INTRODUCTION

Over the past decade there has been a substantial improvement in the ability to predict metabolism-based in vivo drug interactions from kinetic data obtained in vitro. This advance has been most evident for interactions that occur at the level of cytochrome P450 (CYP) catalyzed oxidation and reflects the availability of human tissue samples, cDNA-expressed CYPs, and well-defined substrates and inhibitors of individual enzymes. The most common paradigm in the prediction of in vivo drug interactions has been first to determine the enzyme selectivity of a suspected inhibitor and subsequently to estimate the constant that quantifies the potency of reversible inhibition in vitro. This approach has been successful in identifying clinically important potent competitive inhibitors, such as quinidine, fluoxetine, and itraconazole. However, there is a continuing concern that a number of well-established and clinically important CYP-mediated drug interactions are not predictable from the classical approach that assumes reversible mechanisms of inhibition are ubiquitous.

Irreversible inhibition is an additional mechanism by which the catalytic activity of an enzyme may be reduced both in vitro and in vivo. This mechanism has been extensively characterized in vitro and is particularly common for CYP-mediated biotransformations, in part because of the high-energy intermediates that are characteristic of these reactions. A seminal illustration of the importance of an irreversible mechanism of inhibition is provided by erythromycin, the

widely used macrolide antibiotic. Steady-state plasma concentrations of erythromycin are far below the *in vitro* estimated constant for competitive inhibition of CYP3A4 [1,2], and consequently no *in vivo* drug interactions are expected with CYP3A4 substrates. However, in clinical practice erythromycin is a well-established inhibitor of CYP3A-mediated biotransformation [1]. This is not surprising in view of the ample evidence demonstrating that both human and animal CYP3A enzymes convert erythromycin to a metabolite that complexes with heme to cause inactivation [3]. Thus, the goal of this text is to describe the scope of irreversible inhibition of drug metabolizing enzymes and to indicate how the prediction of *in vivo* drug interactions can be incorporated into this phenomenon.

## II. CHARACTERISTICS OF IRREVERSIBLE INHIBITORS

In general, three types of CYP inhibition have been described [4]. The most common type of inhibition is displayed by agents that reversibly bind to CYP and is displayed by all substrates of an enzyme at sufficiently high concentrations. A second type of inhibition occurs when substrates or their metabolites form quasi-irreversible complexes with the prosthetic heme; this is typified by the inhibition of CYP3A enzymes by macrolide antibiotics. The third type of inhibition occurs when a substance binds irreversibly to structural motifs of the CYP apoprotein or to the prosthetic heme group or accelerates the degradation of the prosthetic heme group. The latter two modes of inhibition are most commonly displayed by inhibitors that are dependent on the enzyme itself to reveal their inhibition, and they are therefore commonly referred to as *mechanism-based inhibitors* [5]. A mechanism-based inhibitor must first bind and then become catalytically activated by the enzyme. The activated species irreversibly alters the enzyme and removes it permanently from the pool of active enzyme. For a substance to be classified as a direct mechanism-based inhibitor it should meet the following rigorous criteria proposed by Silverman [5]:

1. Under conditions that support catalysis, a time-dependent loss of enzyme activity is observed.
2. The rate of enzyme inactivation is proportional to low inactivator concentration but is independent at high inactivator concentration [Eq. (1)].
3. The rate of inactivation is slower in the presence of a competing substrate than in its absence.
4. Enzyme activity does not return upon physical removal of inactivator, e.g., by dialysis, filtration, or centrifugation.
5. A catalytic step for the conversion of inactivator to a reactive intermediate can be proposed.

6. There is no lag time for inactivation; the presence of exogenous nucleophiles has no effect on the inactivation rate; following inactivation, a second, equal addition of enzyme results in the same rate of inactivation as the first addition in the absence of inactivator and cofactor depletion.

### III. TYPES OF IRREVERSIBLE INHIBITORS

#### A. Compounds That Covalently Bind to the Protein

Examples of xenobiotics that bind to proteins and fall into this class of mechanism-based inhibitor include tienilic acid, cannabidiol, chloramphenicol, secobarbital, some psoralens, spironolactone, and mifepristone.

Tienilic acid is oxidized by CYP2C9 to form metabolites that appear to covalently bind to the protein at the active site, thus rendering the enzyme inactive [6,7]. Evidence suggests that an electrophilic sulfoxide metabolite of tienilic acid is the reactive species. When tienilic acid was incubated with CYP2C9 and NADPH, three protein species were detected: native CYP2C9, a monoadduct of CYP2C9 and tienilic acid, and a diadduct that incorporated two molecules of tienilic acid in CYP2C9. Further evidence suggested that each tienilic acid that was covalently adducted to CYP2C9 contained a hydroxyl group, which is consistent with initial ring oxidation and/or with initial sulfoxide formation, provided the attached sulfoxide does not dehydrate [8].

Preincubation of human liver microsomes with cannabidiol decreased the formation of all detectable metabolites of cyclosporine, a substrate of CYP3A [9]. Cannabidiol is metabolized by CYP3A to form a cannabidiol-hydroxyquinone. This metabolite binds to the apoprotein of CYP3A and renders it inactive [10].

Chloramphenicol and secobarbital exhibit properties similar to those of tienilic acid, but they have not been studied in humans [11,12]. Oxidative dechlorination of chloramphenicol with formation of reactive acyl chlorides appears to be an important metabolic pathway for irreversible inhibition of CYP. Chloramphenicol binds to CYP, and subsequent substrate hydroxylation and product release are not impaired. The inhibition of CYP oxidation and the inhibition of endogenous NADPH oxidase activity suggest that some modification of the CYP has taken place, which inhibits its ability to accept electrons from the CYP reductase [11]. Secobarbital completely inactivates rat CYP2B1 functionally, with partial loss of the heme chromophore. Isolation of the *N*-alkylated secobarbital-heme adduct and the modified CYP2B1 protein revealed that the metabolite partitioned between heme *N*-alkylation, CYP2B1 protein modification, and epoxidation. A small fraction of the prosthetic heme modifies the protein and also contributes to the CYP2B1 inactivation [13].



Psoralens, e.g., 8-methoxypsoralen, are a family of furanocoumarin derivatives that have been used in part to treat diseases like psoriasis and cutaneous T-cell lymphoma. Additionally, 8-methoxypsoralen has been shown to inhibit CYP2A6 [14]. The mechanism of inhibition by this compound appears to be an initial oxidation to generate an epoxide that reacts with a nucleophilic amino acid at the active site [15].

CYP inactivation by spironolactone is due to a reactive species that binds covalently to the protein and/or modifies the heme group [16]. However, this has not been investigated in human tissue. More recently, mifepristone (RU 486) was characterized as a mechanism-based inhibitor of CYP3A4 [17]. Mifepristone irreversibly modified the CYP3A4 apoprotein at the active site. The proposed mechanism of inactivation involved addition of reactive oxygen to the carbon-carbon triple bond of mifepristone to yield a highly reactive ketene intermediate that reacts with a nucleophilic residue at the enzyme active site [17].

## **B. Compounds That Quasi-Irreversibly Coordinate to the Prosthetic Heme**

These compounds are catalytically oxidized to intermediates or products that coordinate tightly to the prosthetic heme of the CYP. This coordination can only be displaced under special nonphysiological experimental conditions (e.g., potassium ferricyanide). Many nitrogen-containing compounds, usually amines, are found in this group. Primary amines are required for the metabolic intermediate complex (MIC) formation, although secondary and tertiary amines are appropriate precursors. The primary amines are hydroxylated and then further oxidized to a nitroso group that appears to chelate to the heme, which results in a more stable (ferrous) state of iron. This ferrous state exhibits a spectrum with an absorbance maximum of 445–455 nm [18]. Nonnitrogenous compounds, composed primarily of methylenedioxybenzene derivatives, also form MIC and exhibit absorbance peaks at ~430 nm and 455 nm when the iron is in the ferrous state. However, the MIC formed by these compounds can also be observed at ~437 nm when the iron is in the ferric state. The MIC formed by the nonnitrogenous compounds may be a result of metabolism at the methylene carbon [18]. Table 1 lists all the drugs (or metabolites) that have formed MICs in human liver microsomes, cDNA-expressed CYPs, or rat liver microsomes.

## **C. Compounds That Covalently Bind to the Prosthetic Heme**

This class of compounds irreversibly inactivates CYP by the covalent attachment of the inhibitor, or a derivative of the inhibitor, to the prosthetic heme group. Compounds that fall into this class are terminal acetylenes, e.g., gestodene [19]

**Table 1** Drugs That Form Metabolic Intermediate Complexes

Drug (or metabolite)	MIC Formation			Ref.
	Human liver microsomes	Expressed CYP3A	Rat liver microsomes	
Clarithromycin	+	+		Unpublished data
<i>N</i> -desmethylclarithromycin	+	+		Unpublished data
Didesmethylclarithromycin			+	73
14- <i>OH</i> clarithromycin			+	73
Clarithromycin <i>N</i> -oxide			+	73
Dirithromycin	+			74
Erythromycin	+			74
<i>N</i> -desmethylerythromycin			+	37
Didesmethylerythromycin			+	37
Triacetyloleandomycin	+			75
Oleandomycin			+	75
<i>N</i> -desmethylroxithromycin			+	75
Amitriptyline	+			Unpublished data
Nortriptyline	+	+		Unpublished data
Fluoxetine	+	+		Unpublished data
Norfluoxetine	+	+		Unpublished data
Fluvoxamine	+	+		Unpublished data
Imipramine			+	34
Desipramine			+	34
Amphetamine			+	18
Methamphetamine			+	18
Benzphetamine			+	18
Fenfluramine			+	18
Phenmetrazine			+	18
Clorgyline			+	77
Diltiazem	+	+		36
<i>N</i> -desmethyldiltiazem	+	+		Unpublished data
Lidocaine			+	34
Diphenhydramine			+	34
Propoxyphene			+	18
Norpropoxyphene			+	18
Ritonavir	+/-	+/-		Unpublished data
Indinavir	+	+		Unpublished data
Tamoxifen			+	34
Desmethyldtamoxifen			+	34
Dapsone			+	18
Sulfanilamide			+	18
Orphenadrine			+	78
Tofenacine			+	78

and ethynylestradiol [20], which selectively inactivate CYP3A, furafylline, which selectively inactivates CYP1A1/2 [21], hydrazines, e.g., phenelzine [22], and other xenobiotics, e.g., griseofulvin [23], and phencyclidine, which has been shown to be a substrate and inhibitor of CYP3A [24,25]. Phenelzine and griseofulvin have exhibited mechanism-based inhibition in mouse or rat liver microsomes but have not been investigated with human tissue.

#### D. Compounds That Degrade the Prosthetic Heme Group

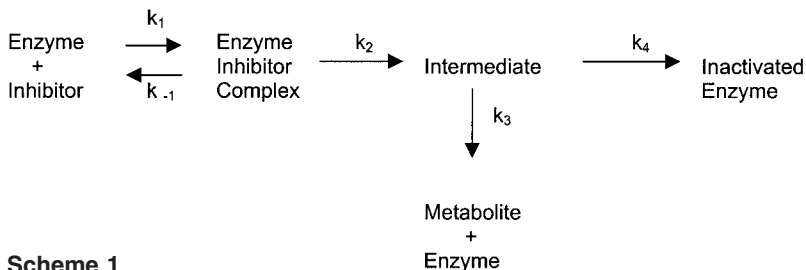
Certain CYPs undergo mechanism-based inactivation as a result of conversion of their prosthetic heme groups to products that irreversibly bind to the protein. Hydrogen peroxide and cumene hydroperoxide partially degrade the prosthetic heme to monopyrrole and dipyrrole fragments that bind to the protein [26,27]. Presently, no drugs have been shown to fall into this class.

#### E. Miscellaneous Compounds

Other drugs and compounds have been shown to be mechanism-based inhibitors of CYP but do not fall into one of the preceding categories, or too little information has been generated to determine which category each represents. Grapefruit juice causes mechanism-based inhibition through accelerated degradation of CYP3A, but the causative component(s) of grapefruit juice and the mechanism of this effect remain to be established. Two of the high-activity antiretroviral treatments for HIV infection, ritonavir and delavirdine, have also exhibited properties that are consistent with mechanism-based inhibition of CYP3A4; again, the mechanism by which this occurs is unknown [28,29].

### IV. KINETICS OF MECHANISM-BASED INHIBITION

Scheme 1 is the simplest one that is consistent with the inactivation of an enzyme while a drug is metabolized [30]. As with conventional enzyme kinetics, there is an initial, reversible step that combines the inhibitor and free enzyme to form an enzyme-inhibitor complex.



Scheme 1

In the absence of catalysis, the inhibitor concentration and the ratio of  $k_1$  to  $k_{-1}$ , the equilibrium association constant, will define the fraction of the enzyme bound with inhibitor at a given enzyme concentration. The enzyme–inhibitor complex proceeds to transform the inhibitor to an intermediate that may decompose to form a metabolite or react with the enzyme to form an inactive complex. First-order rate constants  $k_2$ ,  $k_3$ , and  $k_4$  determine the rates of these reactions and the concentration of intermediate at a given concentration of inhibitor and enzyme.

Most commonly the rate of formation of the inactivated enzyme, under steady-state conditions, can be described by the rectangular hyperbolic function often associated with the traditional Henri–Michaelis–Menten function [30,31]:

$$\text{Rate of inactive enzyme formation} = I_{\max} \cdot \frac{I}{K_I + I} = k_{\text{inact}} \cdot E \cdot \frac{I}{K_I + I} \quad (1)$$

where  $I$  is the concentration of inhibitor or inactivator,  $K_I$  is the inhibitor concentration that supports half the maximal rate of inactivation, and  $I_{\max}$  is the maximal rate of inactivation (when  $I \gg K_I$ ). The symbol  $K_I$  is employed in the context of inactivation kinetics to distinguish it from the equilibrium inhibition constant  $K_i$  (see Chap. 2) that is commonly used in the description of reversible enzyme inhibition [5]. The maximal rate of inactivation,  $I_{\max}$ , will occur when inhibitor binds to all of the available enzyme:

$$\text{Maximal rate of formation of inactive enzyme} = E \cdot k_{\text{inact}} \quad (2)$$

Thus,  $k_{\text{inact}}$  is the first-order rate constant that relates the maximal rate of formation of inactive enzyme to the active enzyme concentration. Tatsunami et al. demonstrated that under steady-state conditions the following relationships exist for the reaction displayed in Scheme 1 [32]:

$$K_I = \frac{k_{-1} + k_2}{k_1} \cdot \frac{k_3 + k_4}{k_2 + k_3 + k_4} \quad (3)$$

$$k_{\text{inact}} = \frac{k_2 \cdot k_4}{k_2 + k_3 + k_4} \quad (4)$$

It is clear from Eqs. (3) and (4) that  $K_I$  and  $k_{\text{inact}}$  are complex functions of several microrate constants. It is important to note that only under restrictive conditions can  $k_{\text{inact}}$  be equated with  $k_2$ , e.g., when  $k_4$  is much greater than  $k_2$  plus  $k_3$ . Similarly,  $K_I$  cannot simply be equated with the inverse of the equilibrium association constant for inhibitor and free enzyme.

Analogous relationships exist for the rate of metabolite formation in this enzymatic scheme:

$$\text{Rate of metabolite formation} = V_{\max} \cdot \frac{I}{K_I + I} = k_{\text{cat}} \cdot E \cdot \frac{I}{K_I + I} \quad (5)$$

where  $V_{\max}$  is the maximal rate of metabolite formation (when  $I \gg K_I$ ) and  $K_I$  is the inhibitor concentration that supports half the maximal rate of metabolite formation and is exactly the same as the constant defined in Eqs. (1) and (3).  $k_{\text{cat}}$  is the first-order rate constant that relates maximal rate of metabolite formation to  $E$  and that is analogous to  $k_{\text{inact}}$  and can also be defined as a function of the microrate constants:

$$k_{\text{cat}} = \frac{k_2 \cdot k_3}{k_2 + k_3 + k_4} \quad (6)$$

In the context of mechanism-based inactivation,  $k_{\text{cat}}$  does not have the same definition as that commonly used in metabolite formation kinetics;  $k_{\text{cat}}$  is not equivalent to  $k_2$  unless  $k_3$  greatly exceeds  $k_2$  and  $k_4$ , which may occur when the inactivation pathway is minor in comparison to the formation of metabolite.

A useful index of the propensity for an enzyme to undergo inactivation, as opposed to metabolite formation, is the partition ratio,  $r$  [33], defined as the ratio of the rate of metabolite formation to the rate of inactive enzyme formation. Thus, by combining Eqs. (1) and (5):

$$r = \frac{k_{\text{cat}}}{k_{\text{inact}}} \quad (7)$$

Furthermore from the relationships in Eqs. (4) and (6) that include the microrate constants of Scheme 1:

$$r = \frac{k_3}{k_4} \quad (8)$$

From Eqs. (7) and (8) it is clear that, in the context of the current model,  $r$  is independent of inhibitor concentration. The value of  $r$  varies from infinity, when the inactivation reaction is a very rare event, to a value of zero, where inactivation of enzyme occurs during every catalytic cycle.

It should be noted that the mechanism depicted in Scheme 1 is the simplest that is consistent with mechanism-based inhibition. The mechanism for a given inactivator and enzyme may be considerably more complex, due to (1) multiple intermediates (for example, MIC formation often involves four or more intermediates [34]), (2) detectable metabolite that may be produced from more than one intermediate, and (3) the fact that enzyme–inhibitor complex may produce a metabolite that is mechanistically unrelated to the inactivation pathway. Events such as these will necessitate alternate definitions for  $k_{\text{inact}}$ ,  $K_I$ , and  $r$  in terms of the microrate constants of the appropriate model. The hyperbolic relationship be-

tween rate of inactivation and inhibitor concentration will, however, remain, unless nonhyperbolic kinetics characterize this interaction. Silverman discussed this possibility from the perspective of an allosteric interaction between inhibitor and enzyme [5]. Nonhyperbolic kinetics have been observed for the interaction of several drugs with members of the CYPs [35].

## V. DETERMINATION OF ENZYME CONSTANTS IN VITRO

Characterization of a mechanism-based inactivator may involve the estimation of the constants described in Sec. IV, namely,  $k_{\text{inact}}$ ,  $K_I$ ,  $k_{\text{cat}}$ , and  $r$ . The most common approach has been to incubate inactivator, enzyme, and cofactors together and to determine the decline in enzyme activity with time [31]. In practice this approach often employs the measurement of residual enzyme activity in a subsequent incubation with a specific substrate under conditions that limit further inactivation and competitive inhibition by the inactivator, usually by an appropriate dilution (tenfold or greater) of the original incubate [5].

Based on the foregoing discussion, the rate of change of enzyme activity in the presence of an inactivator concentration  $I$  is given by:

$$\frac{dE_{(t)}}{dt} = -k_{\text{inact}} \cdot I \cdot \frac{E_{(t)}}{K_I + I} \quad (9)$$

where  $E_{(t)}$  is the enzyme concentration at some time  $t$ . This expression can be integrated to provide a relationship that has been widely used to estimate the desired parameters:

$$E_{(t)} = E_{(0)} \cdot e^{-(k_{\text{inact}} \cdot I / (K_I + I)) \cdot t} \quad (10)$$

where  $E_{(0)}$  is the initial enzyme concentration or activity. Thus a plot of  $E_{(t)}$  against time can be generated for a range of inhibitor concentrations that encompass  $K_I$  to estimate  $k_{\text{inact}}$  and  $K_I$ . Alternatively, by taking the natural log of Eq. (10),

$$\ln\left(\frac{E_{(t)}}{E_{(0)}}\right) = -\left(k_{\text{inact}} \cdot \frac{I}{K_I + I}\right) \cdot t \quad (11)$$

Equation (11) indicates that a plot of log fractional enzyme activity against time will be linear, and the negative of the slope will be equivalent to  $k_{\text{inact}} \cdot I / (K_I + I)$  [31]. The family of curves obtained by varying inhibitor concentration should share the same value of  $\ln(E_{(t)}/E_{(0)}) = 1$  at  $t = 0$ , unless the experiment

is confounded by the occurrence of significant competitive inhibition (Fig. 1a). The relationship between the slope of these plots and inhibitor concentration can be analyzed by nonlinear regression [see Eq. (1)] or double reciprocal plots to estimate  $k_{\text{inact}}$  and  $K_I$  (Figs. 1b and 2). Many mechanism-based inhibitors have been characterized in this manner. Estimates of  $k_{\text{inact}}$  and  $K_I$  were quantified for diltiazem, clarithromycin, and delavirdine, mechanism-based inhibitors of CYP3A4, in this manner [36, unpublished data, 29]. Similarly, the furanocouma-

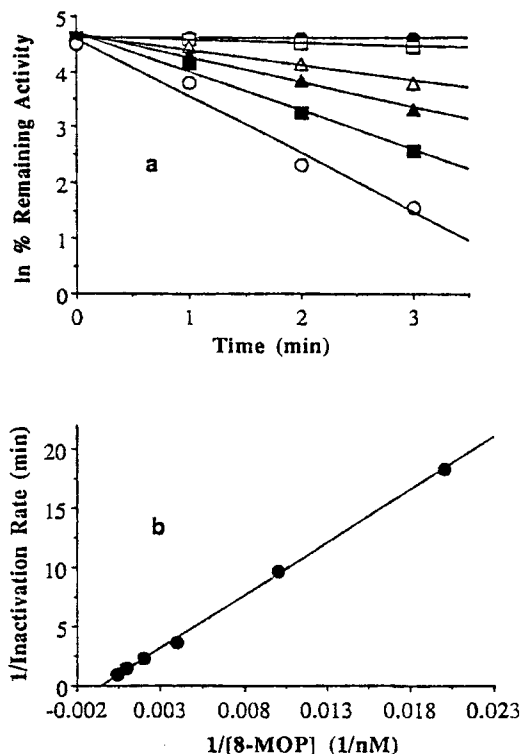


**Figure 1** (a) 8-Methoxypsoralen (8-MOP) mediated inactivation of P450 2A6 activity in human liver microsomes (HL109) in the presence of a NADPH-generating system and (b) double-reciprocal plot of the relationship between inactivation rate and 8-MOP concentration. The concentrations of 8-MOP present in the inactivation assay were 0  $\mu\text{M}$  (●), 0.05  $\mu\text{M}$  (□), 0.25  $\mu\text{M}$  (△), 0.5  $\mu\text{M}$  (▲), 1  $\mu\text{M}$  (■), and 2.5  $\mu\text{M}$  (○). The reversible binding constant ( $K_I$ ) and the rate constant for inactivation ( $k_{\text{inact}}$ ) associated with microsomal P450 2A6 and 8-MOP were calculated, using nonlinear regression, to be 1.8  $\mu\text{M}$  and 2  $\text{min}^{-1}$ , respectively. The rate of turnover for the uninhibited reaction in microsomes (HL109) was 5.21 nmol/nmol P450/min. (From Ref. 14.)

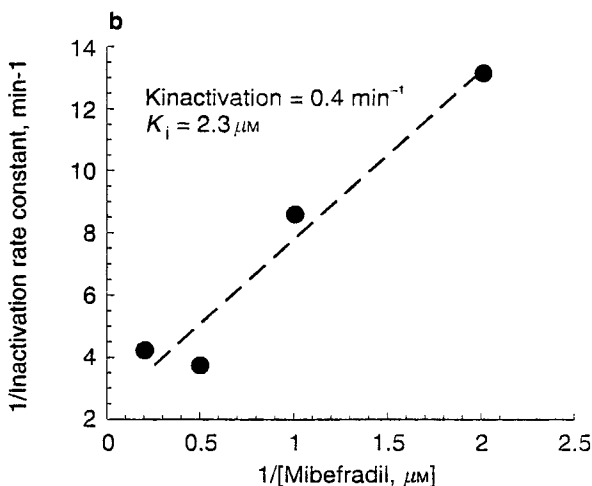


**Figure 2** Double reciprocal plot of the initial CYP3A4 inactivation rate constant (obtained using 250  $\mu\text{M}$  testosterone at mibefradil concentrations of 0.5, 2.5, 5, and 10  $\mu\text{M}$ ) and the corresponding mibefradil concentrations.  $K_{\text{inactivation}} \equiv k_{\text{inact}}$ ;  $K_i \equiv K_I$ . (From Ref. 72.)

rins and 8-methoxypsoralen were shown to be mechanism-based inhibitors of CYP2A6 using this procedure [14,15]. Representative inactivators and target enzymes and estimated values of kinetic constants are presented in Table 2. These approaches assume a constant inhibitor concentration equal to the starting concentration and that loss of enzyme activity is due only to the specific effect of the inactivator. Preliminary experiments are indicated to verify these assumptions.

In some cases the rate of enzyme inactivation can be quantified without an assay for enzyme activity. For example, inactivation of CYPs due to MIC formation can be directly quantified spectrophotometrically, which avoids the potential artifacts introduced by the measurement of catalytic activity. Microsomes, or purified enzymes, are incubated with a substrate and NADPH then is monitored for MIC formation over time in a spectrophotometer. An example of MIC formation by diltiazem in human liver microsomes is shown in Figure 3 [36]. The MIC exhibits an absorbance maximum between 448 nm and 456 nm when the heme iron is in the reduced state [18]. Extinction coefficients of MIC are approximately  $64 \text{ mM}^{-1} \text{ cm}^{-1}$  [37]. Thus, MIC formation by diltiazem in the example is 59% of the total CYP, which would be consistent with inactivation of most of the CYP3A in the microsomes.

The value of  $k_{\text{cat}}$  and  $K_i$  can also be estimated by quantifying the rate of metabolite formation from the inhibitor either simultaneously with the decline



**Table 2** Mechanism-Based Inhibitors and Estimates of Their In Vitro Constants

Compound	Tissue	$K_I$ ( $\mu\text{M}$ )	$k_{\text{inact}}$ ( $\text{min}^{-1}$ )	$k_{\text{cat}}$ ( $\text{min}^{-1}$ )	Partition ratio $r$	$k_{\text{inact}}/K_I$ ( $\mu\text{L} \cdot \text{min}^{-1} \cdot \text{pmol}^{-1}$ )	Ref.
Furafylline	CYP1A1	1000	0.16	?	?	<0.01	21
	CYP1A2	6.9	0.07	?	?	0.01	
Furanocoumarins (8-MOP)	CYP2A6	1.9	2	22	11	1.05	14
( <i>R</i> )-(+)-menthofuran	CYP2A6	0.84	0.25	0.88	3.5	0.30	79
Tienillic acid	CYP2C10	4.3	0.22	2.6	12	0.05	6
Delavirdine	Liver microsomes	9.5	0.44	18	41	0.05	29
Diltiazem	CYP3A4	2.2	0.17	14.6	86	0.08	36
Gestodene	Liver microsomes	46	0.39	3.5	9	0.01	19
Ritonavir	CYP3A4	?	0.135	1.4	10	?	28

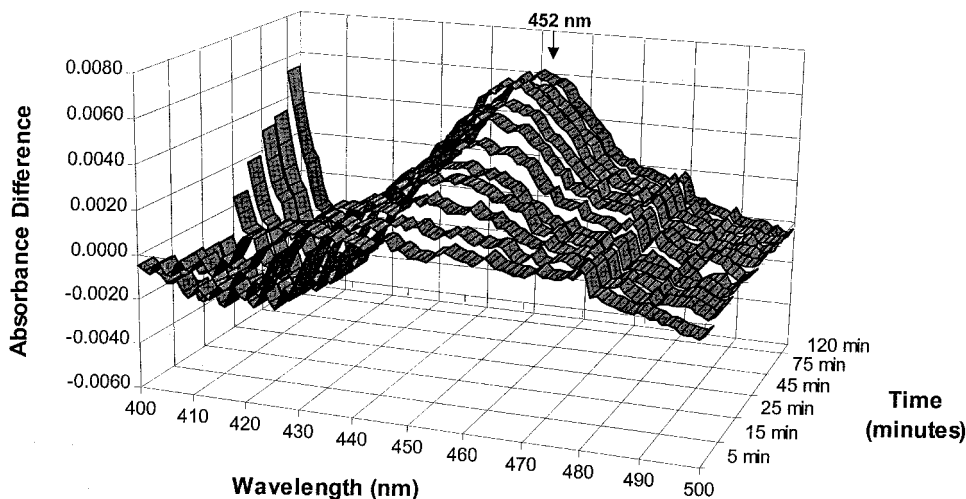


**Figure 3** Metabolic intermediate complex formation by diltiazem (5  $\mu\text{M}$ ) in human liver microsomes. The sample cuvette contained human liver microsomes, diltiazem, and NADPH, whereas the reference cuvette contained human liver microsomes, buffer, and NADPH. The ribbons represent the change in absorbance difference for scans from 5 to 120 min. (From Ref. 36.)

in enzyme activity or under the same incubation conditions. The rate of change of metabolite,  $dM(t)/dt$ , is given by

$$\frac{dM(t)}{dt} = \frac{k_{\text{cat}} \cdot I}{K_I + I} \cdot E_{(0)} \cdot e^{-(k_{\text{inact}} \cdot I / (K_I + I)) \cdot t} \quad (12)$$

If the rate of metabolite formation can be determined over a time period that is sufficiently short that significant enzyme inactivation does not occur ( $k_{\text{cat}} > k_{\text{inact}}$ ), then the exponential term in Eq. (12) approaches unity and may be ignored. Equation (12) illustrates that the apparent  $V_{\text{max}}$  for formation of a metabolite will decline as the incubation time increases when simultaneous enzyme inactivation occurs (Fig. 4).

The partition ratio can be obtained from estimates of  $k_{\text{inact}}$  and  $k_{\text{cat}}$  or can be determined directly. This is achieved by simultaneously quantifying the moles of enzyme inactivated and the moles of metabolite formed for given incubation conditions. Clearly, if any two parameters from  $k_{\text{inact}}$ ,  $k_{\text{cat}}$ , and  $r$  are known, then the third can be calculated (Table 2).

Under conditions where it is not possible to approximate the steady state, i.e., constant inactivator concentration, it is possible to estimate  $k_{\text{inact}}$  and  $K_I$  if

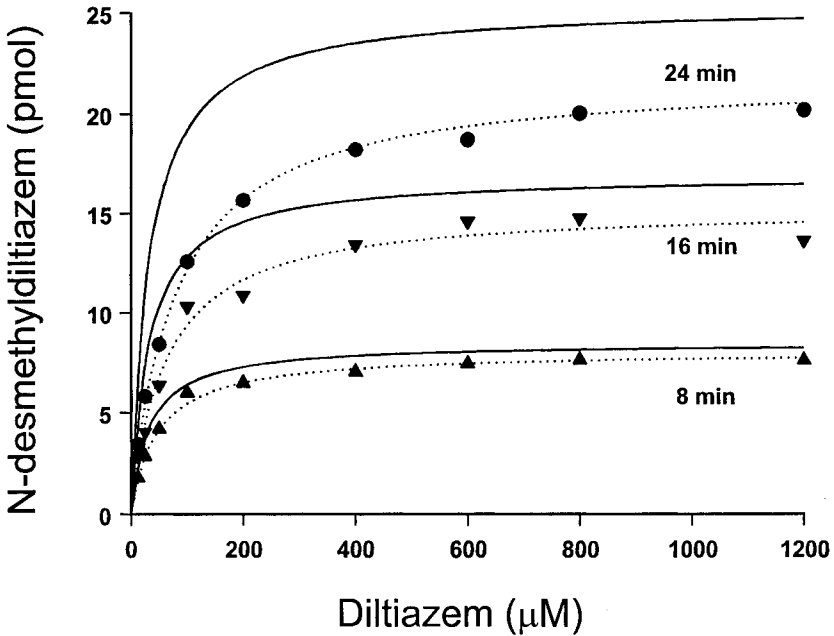


**Figure 4** Effect of incubation time on the formation of *N*-desmethyldiltiazem (MA) in human liver microsomes. Human liver microsomes (50  $\mu\text{g}$ ) were incubated with diltiazem (12.5–1200  $\mu\text{M}$ ) and NADPH (1 mM) at 37° for 8 ( $\blacktriangle$ ), 16 ( $\blacktriangledown$ ), and 24 ( $\bullet$ ) minutes. The dashed line is the line of best fit of the data with the Michaelis–Menten equation. The solid line is the line that represents the predicted MA formation at the corresponding time using instantaneous formation rates. (From unpublished data.)

the inactivator concentration and residual enzyme activity are quantified simultaneously. If a fixed quantity of enzyme and inactivator are combined under non-steady-state conditions that support catalysis, then the rate of formation of inactive enzyme at some time  $t$ ,  $dIE_{(t)}/dt$ , is given by

$$\frac{dIE_{(t)}}{dt} = k_{\text{inact}} \cdot E_{(t)} \cdot \frac{I_{(t)}}{K_I + I_{(t)}} \quad (13)$$

The corresponding decline in inhibitor concentration at some time  $t$ ,  $-dI_{(t)}/dt$ , will be given by the rate of metabolite formation plus the rate of inactive enzyme formation:

$$\frac{-dI_{(t)}}{dt} = (k_{\text{inact}} + k_{\text{cat}}) \cdot E_{(t)} \cdot \frac{I_{(t)}}{K_I + I_{(t)}} \quad (14)$$

Equation (14) can also be written to include the partition ratio:

$$\frac{-dI_{(t)}}{dt} = (1 + r) \cdot k_{\text{inact}} \cdot E_{(t)} \cdot \frac{I_{(t)}}{K_I + I_{(t)}} \quad (15)$$

## VI. PREDICTION OF DRUG INTERACTIONS IN VIVO

### A. Extent of Interaction

When one drug has the capability to inactivate an enzyme, the elimination of a second drug that relies on that enzyme may be impaired. The net effect of exposure to an enzyme inactivator is to enhance the rate of degradation of active enzyme from the endogenous pool. Under baseline conditions the rate of change of active enzyme concentration,  $dE_{(t)}/dt$ , is determined by the balance between the rate of de novo synthesis and the rate of degradation. Enzyme synthesis rate is generally assumed to be a zero-order process, whereas the rate of degradation is a first-order process [38]:

$$\frac{dE_{(t)}}{dt} = R_0 - k_E \cdot E_{(t)} \quad (16)$$

where  $R_0$  is the rate of enzyme synthesis and  $k_E$  is the endogenous degradation rate constant. Therefore, at steady state ( $dE_{(t)}/dt = 0$ ) the enzyme concentration,  $E_{SS}$ , is given by

$$E_{SS} = \frac{R_0}{k_E} \quad (17)$$

In turn the steady-state enzyme concentration in the liver determines the baseline hepatic intrinsic clearance,  $CL_{\text{int}}$ , for the metabolism of a drug substrate by the enzyme. When substrate concentration,  $S$ , is low relative to the Michaelis constant,  $K_m$ , for a particular biotransformation,

$$CL_{\text{int}} = \frac{V_{\text{max}}}{K_m} = E_{SS} \cdot \frac{k_{\text{cat}}}{K_m} \quad (18)$$

where  $V_{\text{max}}$  is the maximal rate of substrate metabolism and  $k_{\text{cat}}$  is the first-order rate constant that relates  $V_{\text{max}}$  to  $E_{SS}$ . In the presence of an inactivator of the enzyme, the rate of change of active enzyme,  $dE'_{(t)}/dt$ , is given by:

$$\frac{dE'_{(t)}}{dt} = R_0 - k_E \cdot E_{(t)} - k_I \cdot E_{(t)} \quad (19)$$

where  $k_I$  is the rate constant for inactivation of enzyme. Consequently, the steady-state enzyme concentration in the presence of inactivator,  $E'_{SS}$ , is reduced:

$$E'_{SS} = \frac{R_0}{k_E + k_I} \quad (20)$$

The inactivator will therefore produce a corresponding reduction in intrinsic clearance to  $CL'_{int}$ .

$$CL'_{int} = E'_{SS} \cdot \frac{k_{cat}}{K_m} \quad (21)$$

The ratio of the intrinsic clearances in the absence and presence of an inactivator is given by

$$\frac{CL_{int}}{CL'_{int}} = \frac{E_{SS}}{E'_{SS}} = \frac{k_E + k_I}{k_E} = 1 + \frac{k_I}{k_E} \quad (22)$$

For a drug that is eliminated exclusively by the liver and that is completely absorbed following oral administration, the intrinsic clearance can be related to the area under the plasma concentration–time curve ( $AUC_{po}$ ) if the well-stirred model of hepatic elimination is assumed (see Refs. 39 and 40 plus other chapters in this book):

$$CL_{int} \cdot f_u = \frac{\text{Dose}_{po}}{AUC_{po}} \quad (23)$$

where  $AUC_{po}$  is obtained from time zero to infinity following a single oral dose or over a dosing interval when drug is administered orally to steady state;  $f_u$  is the fraction of drug unbound in plasma. Thus, for a drug that is eliminated from the body by a single hepatic pathway that is the target of an inactivator, the following relationship describes the predicted increase  $AUC_{po}$  from the baseline state to the inactivated state  $AUC'_{po}$ :

$$\frac{AUC'_{po}}{AUC_{po}} = \frac{CL_{int}}{CL'_{int}} = 1 + \frac{k_I}{k_E} \quad (24)$$

If the inactivated pathway is only one of multiple elimination pathways in the liver, then the predictive model of Eq. (24) becomes

$$\frac{AUC'_{po}}{AUC_{po}} = \frac{1}{(fm_1/(1 + k_I/k_E)) + 1 - fm_1} \quad (25)$$

where  $fm_1$  represents the fraction of the total hepatic elimination at baseline that is due to the pathway that is susceptible to inactivation.

From Eqs. (24) and (25) it is clear that in order to predict the effect of an inactivator on the  $AUC_{po}$  of a coadministered drug, the determinants of  $k_I$  must be understood. From our earlier discussion, the rate of formation of inactive enzyme is given by

$$\text{Rate of inactive enzyme formation} = k_{\text{inact}} \cdot E \cdot \frac{I}{K_I + I} \quad (26)$$

From Eq. (19) the rate of inactivation of enzyme is also given by  $k_I \cdot E$ ; therefore, when  $K_I \gg I$ ,

$$k_I = k_{\text{inact}} \cdot \frac{I}{K_I} \quad (27)$$

Consequently, the predicted effect of inactivator on  $\text{AUC}_{po}$  is given by

$$\frac{\text{AUC}'_{po}}{\text{AUC}_{po}} = 1 + \left( k_{\text{inact}} \cdot \frac{I}{K_I \cdot k_E} \right) \quad (28)$$

An analogous expression can readily be derived from Eq. (22). Thus estimates of  $k_{\text{inact}}$  and  $K_I$  determined in vitro can be combined with estimates of baseline enzyme turnover ( $1/k_E$ ) and in vivo concentration of inhibitor to predict the extent (fold increase in AUC) of an interaction. This expression is reminiscent of the model used to predict interactions involving reversible, competitive inhibition (see Chap. 1), with the substitution of  $k_{\text{inact}}/K_I \cdot k_E$  for  $1/K_i$  [41]. The ratio of  $k_{\text{inact}}$  to  $K_I$  is a useful parameter that can be considered the intrinsic efficiency of inactivation independent of inhibitor concentration (Table 2). The concentration of inhibitor that should be used in this predictive model is either a time-average concentration or a steady-state concentration at the enzyme, but in practice plasma concentrations are often used as a surrogate. However, if the assumption that  $K_I \gg I$  is not appropriate, the function that is nonlinear with respect to inhibitor concentration [Eq. (26)] must be employed and the time-average concentration would not be appropriate. In this nonlinear system, the effect of an inactivator on steady-state enzyme concentrations can be predicted by iteratively solving the differential equations that describe the rate of change of enzyme and inactivator concentration.

## B. Time Course of Inactivation

An important characteristic of inhibition of drug metabolism by an inactivator is the time dependence of both the onset and offset of the effect. The time course of the change in enzyme concentration from the baseline,  $E_{SS}$ , to that in the presence of inactivator,  $E'_{SS}$ , is given by

$$E_{(t)} = E_{SS} \cdot e^{-k_I t} + E'_{SS} \quad (29)$$

where  $E_{(t)}$  is the enzyme concentration at some time  $t$ . This relationship indicates that the half-life of the decline in enzyme concentration ( $0.693/k_I$ ) is dependent on  $k_I$ , which in turn is a function of  $k_{\text{inact}}$ ,  $K_I$ , and  $I$  [Eq. (27)]. Therefore, the

greater the potency of the inactivator, the faster the onset of the interaction. In contrast, the rate of offset of the interaction is given by

$$E(t) = E'_{ss} + R_0 \cdot (1 - e^{-k_E t}) \quad (30)$$

In this case the half-life for the return to baseline enzyme concentration ( $0.693/k_E$ ) is controlled by the turnover of the enzyme. Thus the offset of the interaction is independent of the properties of a given inactivator.

### C. Intestinal Wall Metabolism

For many drugs, particularly those that are substrates for CYP3A4, it is inappropriate to assume that all metabolism occurs in the liver, because intestinal enterocytes also contribute to first-pass elimination of these substrates (see Chap. 9). When intestinal wall metabolism contributes to the “first-pass” effect, our prediction of the effect of inactivation on  $AUC_{po}$  must be modified as follows [42]:

$$\frac{AUC'_{po}}{AUC_{po}} = \left( \frac{F'_G}{F_G} \right) \cdot \left[ 1 + \left( \frac{k_{inact} \cdot I}{K_I \cdot k_E} \right) \right] \quad (31)$$

where  $F_G$  and  $F'_G$  are the intestinal wall availabilities in the absence and presence of inhibitor, respectively. In turn  $F_G$  is a function of the intrinsic clearance at the intestinal wall,  $CL_{int,G}$  [43]:

$$F_G = \frac{A}{A + CL_{int,G}} \quad (32)$$

where  $A$  is the absorption constant, which may be a function of epithelial permeability or intestinal blood flow. The ratio  $F'_G/F_G$  can therefore be estimated from the relative change in  $CL_{int,G}$  caused by the inactivator at the concentration in contact with the enterocytes. This assumes that  $A$  is unaffected by the presence of inactivator.

## VII. EXAMPLES OF INTERACTIONS DUE TO IRREVERSIBLE INHIBITION

Although a number of mechanisms of irreversible inhibition are possible, the most common is MIC formation. A good illustration of inhibition by MIC formation is exhibited by the interaction of clarithromycin with midazolam. Intravenous and oral midazolam was administered in the absence and presence of clarithromycin [44]. Clarithromycin decreased hepatic extraction and increased hepatic and gut wall bioavailability of midazolam. There was no significant relationship

between the clarithromycin-induced changes in midazolam clearance and the plasma concentration of inhibitor. These data suggest that clarithromycin may not be acting as a competitive inhibitor of CYP3A enzymes. A steady-state concentration of  $\sim 0.9 \mu\text{M}$  and the high equilibrium inhibition constant ( $\sim 10 \mu\text{M}$ ) for clarithromycin as a competitive inhibitor of CYP3A in human liver microsomes also suggest that competitive inhibition is unlikely to occur in vivo [45]. Clarithromycin caused the inhibition of midazolam metabolism by MIC formation, which our laboratory has confirmed. The finding that greater baseline CYP3A4 activity resulted in a greater inhibition with clarithromycin can also be explained by MIC formation. Subjects with a low endogenous enzyme degradation rate will have the highest baseline CYP3A4 activity, at a given enzyme synthesis rate. These same subjects will be most affected by the increased rate of enzyme degradation in the presence of a MIC-forming inhibitor and therefore have the greatest interaction. The increased susceptibility to drug interactions in subjects with the highest CYP3A4 activity should be expected whenever the dominant mechanism of inhibition involves stable MIC formation in vivo, as predicted by Eq. (28).

Application of in vitro data obtained with clarithromycin illustrates that accurate predictions of drug inhibition by compounds that form MICs can be made in vivo. For example, applying Eq. (28) and in vitro estimates of  $K_I$  ( $= 5.5 \mu\text{M}$ ),  $k_{\text{inact}}$  ( $= 0.07 \text{ min}^{-1}$ ), and  $I$  ( $= 0.9 \mu\text{M}$ ) for clarithromycin in cDNA-expressed CYP3A4(+b5) (Gentest Corp., Woburn, MA) and  $k_E$  ( $= 0.00026 \text{ min}^{-1}$ ) for CYP3A, quantitative predictions can be made on the effect of clarithromycin on the  $\text{AUC}_{po}$  of a CYP3A substrate, i.e., midazolam (from unpublished data and Ref. 38). Applying these in vitro estimates with midazolam as the CYP3A4 substrate, the predicted  $\text{AUC}'_{po}/\text{AUC}_{po}$  was 45, whereas the observed  $\text{AUC}'_{po}/\text{AUC}_{po}$  was 7, when all the subjects were included [44]. However, if it is assumed that the unbound fraction of inactivator is 0.1, then the predicted  $\text{AUC}'_{po}/\text{AUC}_{po}$  becomes 5, compared to the observed ratio of 7.

Additional drug interactions of clarithromycin with other CYP3A substrates can be illustrated. Carbamazepine exhibited an increased concentration despite a dose reduction and a doubling of the concentration/dose ratio in a patient taking clarithromycin [46]. Clarithromycin statistically increased the AUC, peak plasma concentration, and terminal half-life of ritonavir, an HIV protease inhibitor [47]. Clarithromycin increased cyclosporin A AUC approximately two-fold but decreased the terminal elimination rate constant only 15% [48]. A compound known to induce CYP3A, rifabutin, exhibited increased concentrations of more than 400% in patients receiving concomitant clarithromycin [49].

Many clinical studies have shown that diltiazem, a calcium channel blocker, inhibits the metabolism of CYP3A substrates, e.g., nifedipine, cyclosporin A, triazolam, quinidine, midazolam, alfentanil, and lovastatin, by MIC formation. Intravenous and oral diltiazem increased the mean plasma concentration–time curves of midazolam by 24% and that of alfentanil by 40%. In addition, the mean



half-life of midazolam was 43% longer and that of alfentanil was 50% longer in patients receiving diltiazem [50]. Coadministration of diltiazem for 1 week increased the whole-blood cyclosporin A trough levels by 45% [51]. Pretreatment with diltiazem significantly increased the AUC of quinidine approximately two-fold [52]. These studies illustrate the diverse group of compounds that are affected by diltiazem.

In vitro estimates of  $K_I$  and  $k_{\text{inact}}$  in c-DNA-expressed CYP3A4(+b5) (Gen-test Corp., Woburn, MA) were 2.2  $\mu\text{M}$  and 0.17  $\text{min}^{-1}$  for diltiazem and 0.77  $\mu\text{M}$  and 0.03  $\text{min}^{-1}$  for the major metabolite of diltiazem, *N*-desmethyldiltiazem, respectively (from Ref. 36 and unpublished data). When the in vitro estimates of diltiazem are applied to Eq. (28) with a diltiazem concentration of 0.3  $\mu\text{M}$ , the predicted change in  $\text{AUC}_{po}$  is a 90-fold increase. However, if the fraction unbound is equal to 0.2 for diltiazem, then the estimated ratio change would be  $\sim 18$ . If the estimates for *N*-desmethyldiltiazem were used in Eq. (28) with an estimated concentration of 0.15  $\mu\text{M}$ , the change in AUC would be an anticipated 23-fold increase; applying the fraction unbound of 0.2, the change would be approximately 5-fold.

Three studies have observed the effect of diltiazem on the AUC of CYP3A substrates. In one study with lovastatin, an HMG-CoA reductase inhibitor, a steady-state diltiazem concentration of  $\sim 0.3 \mu\text{M}$  significantly increased the oral lovastatin  $\text{AUC}'_{po}/\text{AUC}_{po}$  3.6-fold [42]. However, the in vitro  $K_I$  for diltiazem is  $\sim 60 \mu\text{M}$  [53], which illustrates that some type of inhibition of CYP3A metabolism is ongoing other than reversible inhibition. Another study reported that the  $\text{AUC}_{po}$  for midazolam increased approximately fourfold after volunteers were administered diltiazem [54]. Additionally, diltiazem increased the mean AUC of triazolam threefold and the  $t_{1/2}$  and peak plasma concentration twofold [55]. Thus, the change in AUC for the CYP3A substrates in the presence of diltiazem is less than expected based on the in vitro estimates of  $K_I$  and  $k_{\text{inact}}$ . The reason for this is unknown at present, but there appears to be some evidence from our laboratory that a metabolite of diltiazem inhibits the formation of the intermediate that forms the MIC.

Erythromycin is a CYP3A substrate that has been shown to inhibit other CYP3A substrates probably by MIC formation. In an early clinical study, liver specimens were removed by surgical biopsy in patients receiving erythromycin. In vivo MIC formation and an increased CYP concentration were observed in microsomes from these liver specimens [3]. Clinically reported drug interactions with CYP3A substrates include midazolam, dextromethorphan, cyclosporine A, alfentanil, triazolam, alprazolam, and carbamazepine. Erythromycin steady-state concentrations of 4  $\mu\text{M}$  inhibited midazolam metabolism [1], whereas the reported in vitro  $K_I$  of erythromycin was 148  $\mu\text{M}$  [2]. The in vitro  $K_I$  is 35 times greater than the steady-state plasma concentrations, which would suggest that no inhibition of midazolam metabolism would be observed by erythromycin at that

concentration. Nevertheless, erythromycin substantially inhibited midazolam hydroxylation in vivo [1]. Erythromycin significantly increased the dextromethorphan/3-methoxymorphinan urinary metabolic ratio corresponding to a 34% inhibition of activity [56]. Erythromycin decreased the clearance of oral carbamazepine by 20% without affecting the elimination rate constant and apparent volume of distribution [57]. Erythromycin decreased triazolam clearance by 52%, decreased the apparent volume of distribution by 30%, and significantly increased the half-life [58]. Erythromycin significantly increased the plasma  $AUC_{po}$  less than threefold, decreased the apparent oral clearance, and increased the elimination half-life of alprazolam, another CYP3A substrate [59,60]. Cyclosporine A pharmacokinetics have also been affected by erythromycin. Erythromycin significantly increased the AUC of cyclosporine A twofold and increased the maximum serum concentration [61]. The alfentanil plasma clearance significantly decreased by 26%, whereas the elimination half-life significantly increased after erythromycin administration [62]. Even though erythromycin has been shown to inhibit many CYP3A substrates, no in vitro estimates of  $K_i$  and  $k_{inact}$  have been determined.

Fluvoxamine, a selective serotonin uptake inhibitor, has been shown to inhibit compounds that are metabolized by CYP3A. The effect of fluvoxamine on alprazolam hydroxylation is another example of an in vitro  $K_i$  overestimating the concentration needed to cause an in vivo drug interaction. The in vitro  $K_i$  of fluvoxamine is 10  $\mu\text{M}$  [63]. However, the fluvoxamine steady-state concentration of  $\approx 0.3 \mu\text{M}$  caused inhibition of alprazolam metabolism in vivo [64]. Specifically, fluvoxamine increased plasma concentrations of alprazolam by 100% and increased the mean  $t_{1/2}$  from 20 to 34 hours [64]. Fluvoxamine has also been shown to inhibit the *N*-demethylation of imipramine, clomipramine, amitriptyline, and maprotiline in depressed patients [65]. CYP3A4 is one enzyme that contributes to the *N*-demethylation of tricyclic antidepressants. When fluvoxamine was added to a constant dosage of carbamazepine, a substantial increase in plasma concentrations of carbamazepine was observed [66]. Our laboratory has demonstrated that fluvoxamine forms an MIC with CYP3A4, which would help explain the multiple interactions of fluvoxamine with CYP3A substrates.

Fluoxetine is another selective serotonin reuptake inhibitor that has been shown to be an inhibitor of CYP. Fluoxetine increased desipramine maximum plasma concentration fourfold, and the  $AUC_{po}$  was increased fivefold [67]. Desipramine is hydroxylated to 2-*OH* desipramine by CYP2D6 and *N*-demethylated in part by CYP3A [68]. Fluoxetine significantly prolonged alprazolam half-life and reduced alprazolam clearance [69]. The in vitro estimated  $K_i$  of fluoxetine for alprazolam hydroxylation is  $\sim 50 \mu\text{M}$  [63]. However, fluoxetine concentrations of  $\sim 0.15 \mu\text{M}$  [69] inhibited alprazolam metabolism in vivo, which illustrates that additional mechanisms of inhibition by fluoxetine are ongoing in regard to CYP3A metabolism. Our laboratory has demonstrated that fluoxetine also

forms an MIC with CYP3A4. Estimates of  $K_i$  and  $k_{\text{inact}}$  in cDNA-expressed CYP3A4(+b5) were  $5.3 \mu\text{M}$  and  $0.02 \text{ min}^{-1}$ , respectively [unpublished data]. Nevertheless, few clinical interactions of CYP3A substrates with fluoxetine have been reported.

The clinical significance of the mechanism-based inactivation of CYP3A by gestodene and ethynyl estradiol is still unclear. Nevertheless, these compounds are given daily and could affect CYP3A. Gestodene exhibits a low partition ratio (Table 2), but it is unclear how much effect the irreversible inactivation on CYP3A would result from a normal dosage of  $\sim 75 \mu\text{g/day}$ . Guengerich hypothesized that gestodene would inactivate only about 3% of total CYP3A per day if the in vitro partition ratio was the same in vivo [19,20].

Another nonlinear kinetic component that may be a result of mechanism-based inhibition is the time-dependent inhibition of one drug by another that has been observed with inhibitors of CYP3A. When grapefruit juice was consumed 24 hours prior to felodipine, an inhibition of felodipine metabolism was observed. Specifically, higher felodipine  $C_{\text{max}}$  was evident when grapefruit juice was consumed 24 hours before the drug, and the half-life of the grapefruit juice effect was 12 hours [70]. A preincubation of grapefruit juice solids with cDNA-expressed CYP3A4 produced a time-dependent inactivation of the enzyme prior to testosterone  $6\beta$ -hydroxylation, which illustrates that grapefruit juice indeed mechanistically inhibits CYP3A [71].

## VIII. CONCLUSION

Many drugs are mechanism-based inhibitors of CYP. This property could affect a drug's own metabolism or the metabolism of coadministered drugs, which could lead to serious drug interactions. Even though in vitro  $K_i$ 's have been determined for a number of drugs and have been used to predict an in vivo interaction, the effect of mechanism-based inhibitors can be observed at in vivo concentrations below that  $K_i$ . This effect can be predicted if in vitro estimates of kinetic constants (e.g.,  $K_i$  and  $k_{\text{inact}}$ ) for mechanism-based inhibitors are known. A theoretical basis and application have been presented that applies in vitro estimates of mechanism-based inhibitors to accurately predict in vivo drug interactions.

## REFERENCES

1. KT Olkkola, K Aranko, H Luurila, A Hiller, L Saarnivaara, J-J Himberg, PJ Neuvonen. A potentially hazardous interaction between erythromycin and midazolam. Clin Pharmacol Ther 53:298–305, 1993.

2. M-P Gascon, P Dayer. In vitro forecasting of drugs which may interfere with the biotransformation of midazolam. *Eur J Clin Pharmacol* 41:573–578, 1991.
3. D Larrey, C Funck-Brentano, P Breil, J Vitaux, C Theodore, G Babany, D Pessayre. Effects of erythromycin on hepatic drug-metabolizing enzymes in humans. *Biochem Pharmacol* 32:1063–1068, 1983.
4. PR Ortiz de Montellano, MA Correia. Inhibition of cytochrome P450 enzymes. In: PR Ortiz de Montellano, ed. *Cytochrome P450 Structure, Mechanism, and Biochemistry*. 2nd ed. New York: Plenum Press, 1995, pp 305–364.
5. RB Silverman. *Mechanism-Based Enzyme Inactivation: Chemistry and Enzymology*. Vol I. Boca Raton, FL: CRC Press, 1988, pp 3–30.
6. MP López-García, PM Dansette, D Mansuy. Thiophene derivatives as new mechanism-based inhibitors of cytochromes P-450: inactivation of yeast-expressed human liver cytochrome P-450 2C9 by tienilic acid. *Biochem* 33:166–175, 1994.
7. P Jean, P López-García, P Dansette, D Mansuy, JL Goldstein. Oxidation of tienilic acid by human yeast-expressed cytochromes P-450 2C8, 2C9, 2C18 and 2C19: evidence that this drug is a mechanism-based inhibitor specific for cytochrome P-450 2C9. *Eur J Biochem* 241:797–804, 1996.
8. LL Koenigs, RM Peter, AP Hunter, RL Haining, AE Rettie, T Friedberg, MP Pritchard, M Shou, TH Rushmore, WF Trager. Electrospray ionization mass spectrometric analysis of intact cytochrome P450: identification of tienilic acid adducts to P450 2C9. *Biochem* 38:2312–2319, 1999.
9. W Jaeger, LZ Benet, LM Bornheim. Inhibition of cyclosporine and tetrahydrocannabinol metabolism by cannabidiol in mouse and human microsomes. *Xenobiotica* 26:275–284, 1996.
10. LM Bornheim, MP Grillo. Characterization of cytochrome P450 3A inactivation by cannabidiol: possible involvement of cannabidiol-hydroxyquinone as a P450 inactivator. *Chem Res Toxicol* 11:1209–1216.
11. J Halpert, B Näslund, I Betnér. Suicide inactivation of rat liver cytochrome P-450 by chloramphenicol in vivo and in vitro. *Mol Pharmacol* 23:445–452, 1983.
12. JM Lunetta, K Sugiyama, MA Correia. Secobarbital-mediated inactivation of rat liver cytochrome P450<sub>2</sub>: A mechanistic reappraisal. *Mol Pharmacol* 35:10–17, 1989.
13. K He, AM Falick, B Chen, F Nilsson, MA Correia. Identification of the heme adduct and an active site peptide modified during mechanism-based inactivation of rat liver cytochrome P450 2B1 by secobarbital. *Chem Res Toxicol* 9:614–622, 1996.
14. LL Koenigs, RM Peter, SJ Thompson, AE Rettie, WF Trager. Mechanism-based inactivation of human liver cytochrome P450 2A6 by 8-methoxypsoralen. *Drug Metab Dispos* 25:1407–1415, 1997.
15. LL Koenigs, WF Trager. Mechanism-based inactivation of P450 2A6 by furanocoumarins. *Biochem* 37:10047–10061, 1998.
16. CJ Decker, MS Rashed, TA Baillie, D Maltby, MA Correia. Oxidative metabolism of spironolactone: evidence for the involvement of electrophilic thiosteroid species in drug-mediated destruction of rat hepatic cytochrome P450. *Biochem* 28:5128–5136, 1989.
17. K He, TF Woolf, PF Hollenberg. Mechanism-based inactivation of cytochrome P-450-3A4 by mifepristone (RU486). *J Pharamcol Exp Ther* 288:791–797, 1999.

18. MR Franklin. Inhibition of mixed-function oxidations by substrates forming reduced cytochrome P-450 metabolic-intermediate complexes. *Pharmac Ther* 2:227–245, 1977.
19. FP Guengerich. Mechanism-based inactivation of human liver microsomal cytochrome P-450 IIIA4 by gestodene. *Chem Res Toxicol* 3:363–371, 1990.
20. FP Guengerich. Oxidation of 17  $\alpha$ -ethynylestradiol by human liver cytochrome P-450. *Mol Pharmacol* 33:500–508, 1988.
21. W Tassaneeyakul, DJ Birkett, ME Veronese, ME McManus, RH Tukey, JO Miners. Direct characterization of the selectivity of furafylline as an inhibitor of human cytochromes P450 1A1 and 1A2. *Pharmacogen* 4:281–284, 1994.
22. SF Muakkassah, WCT Yang. Mechanism of the inhibitory action of phenelzine on microsomal drug metabolism. *J Pharmacol Exp Ther* 219:147–155, 1981.
23. F De Matteis, AH Gibbs. Drug-induced conversion of liver haem into modified porphyrins. *Biochem J* 187:285–288, 1980.
24. EM Laurenzana, SM Owens. Metabolism of phencyclidine by human liver microsomes. *Drug Metab Dispos* 25:557–563, 1997.
25. SM Owens, M Gunnell, EM Laurenzana, JL Valentine. Dose- and time-dependent changes in phencyclidine metabolite covalent binding in rats and the possible role of CYP2D1. *J Pharmacol Exp Ther* 265:1261–1266, 1993.
26. WH Schaefer, TM Harris, FP Guengerich. Characterization of the enzymatic and nonenzymatic peroxidative degradation of iron porphyrins and cytochrome P-450 heme. *Biochem* 24:3254–3263, 1985.
27. K Yao, AM Falick, N Pater, MA Correia. Cumene hydroperoxide-mediated inactivation of cytochrome P450 2B1. Identification of an active site heme-modified peptide. *J Biol Chem* 268:59–65, 1993.
28. T Koudriakova, E Iatsimirskaia, I Utkin, E Gangl, P Vouros, E Storozhuk, D Orza, J Marinina, N Gerber. Metabolism of the human immunodeficiency virus protease inhibitors indinavir and ritonavir by human intertinal microsomes and expressed cytochrome P4503A4/3A5: Mechanism-based inactivation of cytochrome P4503A by ritonavir. *Drug Metab Dispos* 26:552–561, 1998.
29. RL Voorman, SM Maio, NA Payne, Z Zhao, KA Koeplinger, X Wang. Microsomal metabolism of delavirdine: evidence for mechanism-based inactivation of human cytochrome P450 3A. *J Pharmacol Exp Ther* 287:381–388, 1998.
30. SG Waley. Kinetics of suicide substrates. *Biochem J* 185:771–773, 1980.
31. SG Waley. Kinetics of suicide substrates. Practical procedures for determining parameters. *Biochem J* 227:843–849, 1985.
32. S Tatsunami, N Yago, M Hosoe. Kinetics of suicide substrates. Steady-state treatments and computer-aided exact solutions. *Biochim Biophys Acta* 662:226–235, 1981.
33. C Walsh, T Cromartie, P Marcotte, R Spencer. Suicide substrates for flavoprotein enzymes. *Meth Enzymol* 53:437–448, 1978.
34. C Bensoussan, M Delaforge, D Mansuy. Particular ability of cytochromes P450 3A to form inhibitory P450-iron-metabolite complexes upon metabolic oxidation of aminodrugs. *Biochem Pharmacol* 49:591–602, 1995.
35. KR Korzekwa, N Krishnamachary, M Shou, A Ogai, RA Parise, AE Rettie, FJ Gonzalez, TS Tracy. Evaluation of atypical cytochrome P450 kinetics with two-substrate

- models: evidence that multiple substrates can simultaneously bind to cytochrome P450 active sites. *Biochem* 37:4137–4147, 1998.
36. DR Jones, JC Gorski, MA Hamman, BS Mayhew, S Rider, SD Hall. Diltiazem inhibition of CYP3A activity is due to metabolite intermediate complex formation. *J Pharmacol Exp Therap* 290:1116–1125, 1999.
  37. LK Pershing, MR Franklin. Cytochrome P-450 metabolic-intermediate complex formation and induction by macrolide antibiotics: a new class of agents. *Xenobiotica* 12:687–699, 1982.
  38. L Pichard, I Fabre, M Daujat, J Domergue, H Joyeux, P Maurel. Effect of corticosteroids on the expression of cytochromes P450 and on cyclosporin A oxidase activity in primary cultures of human hepatocytes. *Mol Pharmacol* 41:1047–1055, 1992.
  39. GR Wilkinson, DG Shand. A physiological approach to hepatic drug clearance. *Clin Pharmacol Ther* 18:377–390, 1975.
  40. JB Houston. Drug metabolite kinetics. *Pharmacol Ther* 15:521–552, 1982.
  41. E Jacqz, SD Hall, RA Branch, GR Wilkinson. Polymorphic metabolism of mephenytoin in man: pharmacokinetic interaction with a co-regulated substrate, mephobarbital. *Clin Pharmacol Ther* 6:646–653, 1986.
  42. NE Azie, DC Brater, PA Becker, DR Jones, SD Hall. The interaction of diltiazem with lovastatin and pravastatin. *Clin Pharmacol Ther* 64:369–377, 1998.
  43. TN Tozer. Concepts basic to pharmacokinetics. *Pharmac Ther* 12:109–131, 1981.
  44. JC Gorski, DR Jones, BD Haehner-Daniels, MA Hamman, EM O'Mara Jr, SD Hall. The contribution of intestinal and hepatic CYP3A to the interaction between midazolam and clarithromycin. *Clin Pharmacol Ther* 64:133–143, 1998.
  45. M Jurima-Romet, K Crawford, T Cyr, T Inaba. Terfenadine metabolism in human liver. In vitro inhibition by macrolide antibiotics and azole antifungals. *Drug Metab Dispos* 22:849–857, 1994.
  46. F Albani, R Riva, A Baruzzi. Clarithromycin–carbamazepine interaction: a case report. *Epilepsia* 34:161–162, 1993.
  47. D Ouellet, A Hsu, GR Granneman, G Carlson, J Cavanaugh, H Guenther, JM Leonard. Pharmacokinetic interaction between ritonavir and clarithromycin. *Clin Pharmacol Ther* 64:355–362, 1998.
  48. IS Sketris, MR Wright, ML West. Possible role of the intestinal P-450 enzyme system in a cyclosporine–clarithromycin interaction. *Pharmacother* 16:301–305, 1996.
  49. G Apseloff, G Foulds, L LaBoy-Goral, S Willavize, J Vincent. Comparison of azithromycin and clarithromycin in their interactions with rifabutin in healthy volunteers. *J Clin Pharmacol* 38:830–835, 1998.
  50. J Ahonen, KT Olkkola, M Salmenperä, M Hynynen, PJ Neuvonen. Effect of diltiazem on midazolam and alfentanil disposition in patients undergoing coronary artery bypass grafting. *Anesthesiology* 85:1246–1252, 1996.
  51. J Brockmüller, H-H Neumayer, K Wagner, W Weber, G Heinemeyer, H Kewitz, I Roots. Pharmacokinetic interaction between cyclosporin and diltiazem. *Eur J Clin Pharmacol* 38:237–242, 1990.
  52. S Laganière, RF Davies, G Carignan, K Foris, L Goernert, K Carrier, C Pereira, I McGilveray. Pharmacokinetic and pharmacodynamic interactions between diltiazem and quinidine. *Clin Pharmacol Ther* 60:255–264, 1996.
  53. L Pichard, I Fabre, G Fabre, J Domergue, BS Aubert, G Mourad, P Maurel. Cyclo-

- sporin A drug interactions. Screening for inducers and inhibitors of cytochrome P-450 (Cyclosporin A Oxidase) in primary cultures of human hepatocytes and in liver microsomes. *Drug Metab Dispos* 18:595–606, 1990.
54. JT Backman, KT Olkkola, K Aranko, J-J Himberg, PJ Neuvonen. Dose of midazolam should be reduced during diltiazem and verapamil treatments. *Br J Clin Pharmacol* 37:221–225, 1994.
  55. A Varhe, KT Olkkola, PJ Neuvonen. Oral triazolam is potentially hazardous to patients receiving systemic antimycotics ketoconazole or itraconazole. *Clin Pharmacol Ther* 56:601–607, 1994.
  56. DR Jones, JC Gorski, BD Haehner, EM O'Mara Jr, SD Hall. Determination of cytochrome P450 3A4/5 activity in vivo with dextromethorphan *N*-demethylation. *Clin Pharmacol Ther* 60:374–384, 1996.
  57. YY Wong, TM Ludden, RD Bell. Effect of erythromycin on carbamazepine kinetics. *Clin Pharmacol Ther* 33:460–464, 1983.
  58. JP Phillips, EJ Antal, RB Smith. A pharmacokinetic drug interaction between erythromycin and triazolam. *J Clin Psychopharmacol* 6:297–299, 1986.
  59. JC Gorski, DR Jones, MA Hamman, SA Wrighton, SD Hall. Biotransformation of alprazolam by members of the human cytochrome P450 3A subfamily. *Xenobiotica* 29:931–944, 1999.
  60. N Yasui, K Otani, S Kaneko, T Ohkubo, T Osanai, K Sugawara, K Chiba, T Ishizaki. A kinetic and dynamic study of oral alprazolam with and without erythromycin in humans: in vivo evidence for the involvement of CYP3A4 in alprazolam metabolism. *Clin Pharmacol Ther* 59:514–519, 1996.
  61. DJ Freeman, R Martell, SG Carruthers, D Heinrichs, PA Keown, CR Stiller. Cyclosporin–erythromycin interaction in normal subjects. *Br J Clin Pharmacol* 23:776–778, 1987.
  62. RR Bartkowski, ME Goldberg, GE Larijani, T Boerner. Inhibition of alfentanil metabolism by erythromycin. *Clin Pharmacol Ther* 46:99–102, 1989.
  63. LL von Moltke, DJ Greenblatt, MH Court, SX Duan, JS Harmatz, RI Shader. Inhibition of alprazolam and desipramine hydroxylation in vitro by paroxetine and fluvoxamine: comparison with other selective serotonin reuptake inhibitor antidepressants. *J Clin Psychopharmacol* 15:125–131, 1995.
  64. JC Fleishaker, LK Hulst. A pharmacokinetic and pharmacodynamic evaluation of the combined administration of alprazolam and fluvoxamine. *Eur J Clin Pharmacol* 46:35–39, 1994.
  65. S Hartter, H Wetzel, E Hammes, C Hiemke. Inhibition of antidepressant demethylation and hydroxylation by fluvoxamine in depressed patients. *Psychopharmacol* 110:302–308, 1993.
  66. J Fritze, B Unsorg, M Lanczik. Interaction between carbamazepine and fluvoxamine. *Acta Psychiat Scand* 84:583–584, 1991.
  67. SH Preskorn, J Alderman, M Chung, W Harrison, M Messig, S Harris. Pharmacokinetics of desipramine coadministered with sertraline or fluoxetine. *J Clin Psychopharmacol* 14:90–98, 1994.
  68. K Brosen, JG Hansen, KK Nielsen, SH Sindrup, LF Gram. Inhibition by paroxetine of desipramine metabolism in extensive but not in poor metabolizers of sparteine. *Eur J Clin Pharmacol* 44:349–355, 1993.

69. DJ Greenblatt, SH Preskorn, MM Cotreau, WD Horst, JS Harmatz. Fluoxetine impairs clearance of alprazolam but not of clonazepam. *Clin Pharmacol Ther* 52:479–486, 1992.
70. J Lundahl, CG Regårdh, B Edgar, G Johnson. Relationship between time of intake of grapefruit juice and its effect on pharmacokinetics and pharmacodynamics of felodipine in healthy volunteers. *Eur J Clin Pharmacol* 49:61–67, 1995.
71. WK Chan, LT Nguyen, VP Miller, RZ Harris. Mechanism-based inactivation of human cytochrome P450 3A4 by grapefruit juice and red wine. *Life Sci* 62:135–142, 1998.
72. T Prueksaritanonont, B Ma, C Tang, Y Meng, C Assang, P Lu, PJ Reider, JH Lin, TA Baillie. Metabolic interactions between mibefradil and HMG-CoA reductase inhibitors: an in vitro investigation with human liver preparations. *Br J Clin Pharmacol* 47:291–298, 1999.
73. S Ohmori, I Ishii, S-I Kuriya, T Taniguchi, T Rikihisas, S Hirose, Y Kanakubo, M Kitada. Effects of clarithromycin and its metabolites on the mixed function oxidase system in hepatic microsomes of rats. *Drug Metab Dispos* 21:358–363, 1993.
74. TD Lindstrom BR Hanssen, SA Wrighton. Cytochrome P-450 complex formation by dirithromycin and other macrolides in rat and human livers. *Antimicrobial Agents Chemother* 37:265–269, 1993.
75. MR Franklin. Cytochrome P450 metabolic intermediate complexes from macrolide antibiotics and related compounds. *Meth Enzymol* 206:559–573, 1991.
76. H Yamazaki, T Shimada. Comparative studies of in vitro inhibition of cytochrome P450 3A4-dependent testosterone 6 $\beta$ -hydroxylation by roxithromycin and its metabolites, troleandomycin, and erythromycin. *Drug Metab Dispos* 26:1053–1057, 1998.
77. U Sharma, ES Roberts, PF Hollenberg. Formation of a metabolic intermediate complex of cytochrome P4502B1 by clorgyline. *Drug Metab Dispos* 24:1247–1253, 1996.
78. A Bast, FA van Kemenade, EM Savenije-Chapel, J Noordhoek. Product inhibition in orphenadrine metabolism as a result of a stable cytochrome P-450-metabolic intermediate complex formed during the disposition of mono-*N*-desmethylophenadrine (tofenacine) in the rat. *Res Comm Chem Pathol Pharmacol* 40:391–403, 1983.
79. SC Khojasteh-Bakht, LL Koenigs, RM Peter, WF Trager, SD Nelson. (*R*)-(+)-menthofuran is a potent, mechanism-based inactivator of human liver cytochrome P450 2A6. *Drug Metab Dispos* 26:701–704, 1998.





# 11

## Prediction of Metabolic Drug Interactions: Quantitative or Qualitative?

**Jiunn H. Lin and Paul G. Pearson**

*Merck & Company, West Point, Pennsylvania*

### I. INTRODUCTION

Patients, particularly the elderly, frequently suffer from multiple medical conditions or diseases, and an effective therapy often requires the concurrent use of multiple medications. Whenever two or more drugs are administered at the same time, there is always a concern for drug–drug interactions. Although interactions can be pharmacokinetic or pharmacodynamic in nature, in many cases the interactions have a pharmacokinetic, rather than pharmacodynamic, basis. There are many underlying mechanisms responsible for pharmacokinetic interactions, and reversible inhibition of cytochrome P450 (CYP) enzymes is probably the most common cause for pharmacokinetic interactions. This is because the CYP enzyme system comprises a superfamily of isoforms that play an important role in the metabolism of many chemically diverse drugs.

Irrespective of the type of inhibition, enzyme inhibition always results in a decrease in the intrinsic clearance ( $V_{\max}/K_m$ ) of drugs and hence an increase in drug concentrations in plasma that may lead to undesirable pharmacological responses and toxicity. Several prominent drugs have been withdrawn from the market in recent years because of serious adverse reactions as the result of drug interactions [1,2].

Because of potential adverse effects and toxicity, metabolic drug interactions are considered to be an undesirable property of new drug candidates. Therefore, from an industrial perspective, the potential of metabolic drug interactions

has become one of the important factors in selecting a new drug candidate for further development. It is highly desirable not to develop new drug candidates that are potent CYP inhibitors and are not susceptible to the effects of known CYP inhibitors. Over the past 10 years, great advances have been made in characterizing the various isoforms of human CYP and defining the selectivity of substrates and inhibitors. With our knowledge about human CYPs, and the ready availability of human tissue preparations and recombinant human CYPs, *in vitro* enzyme systems have been used extensively as screening tools for predicting *in vivo* drug interactions in the earlier stages of drug discovery [3]. In fact, the use of *in vitro* enzyme systems for investigating the ability of a drug to inhibit the metabolism of other drugs provides some of the most useful information in predicting drug interactions.

Although it is relatively easy to assess *in vitro* drug interactions, the interpretation and extrapolation of *in vitro* interaction data to *in vivo* situations is not as straightforward and can be highly controversial. Can *in vivo* drug interactions be predicted accurately from *in vitro* metabolic studies? Should the prediction be qualitative or quantitative? These are the questions that industrial drug metabolism scientists must confront daily. Some scientists believe that quantitative prediction of drug interactions is possible, whereas others are less optimistic and consider quantitative prediction of *in vivo* drug interactions as being very difficult. The difficulty stems from the complexities in enzyme kinetics and factors involved in drug interactions. The purpose of this chapter is to briefly review the principles of enzyme kinetics and to examine the factors that may complicate the prediction of drug interactions. Because reversible inhibition is the major mechanism responsible for drug interactions, the main focus of this review will be on reversible inhibition involving CYP enzymes.

## II. THEORETICAL CONSIDERATIONS

The mechanisms of CYP inhibition can be categorized grossly as: reversible inhibition, quasi-irreversible inhibition, and irreversible inhibition [4]. Of these, reversible inhibition is the most common mechanism responsible for the documented drug interactions. Both quasi-irreversible and irreversible inhibition are caused by the formation of reactive metabolites. Quasi-irreversible inhibition involves the formation of metabolic intermediate (MI) complex (see Chap. 10), while irreversible inhibition is caused by enzyme inactivation (destruction) resulting from the formation of reactive intermediates. Although MI complexation does not destroy the enzyme, the MI complex is so stable *in vivo* that the enzyme involved in the complex is unavailable for drug metabolism. Therefore, MI complexation can be considered as irreversible inhibition *in vivo*. Depending on whether enzyme inhibition is a reversible or irreversible process, pharmacokinetic

consequences caused by inhibition can be quite different. Reversible enzyme inhibition is transient; the normal function of CYP enzymes continues after the inhibitor has been eliminated from the body. In contrast, the loss of enzyme activity by irreversible inactivation persists even after elimination of the inhibitor, and de novo biosynthesis of enzymes is the only means to restore the functional activity. Kinetically, reversible inhibitors show only dose-dependent inhibition, while irreversible inhibitors always exhibit time- and dose-dependent inhibitory effects on the disposition of substrates [5,6]. It is, therefore, of importance to understand the mechanisms of inhibition and to differentiate between reversible inhibition and irreversible inhibition.

Time-dependent loss of enzyme activity is one of the most important features in distinguishing between reversible and irreversible inhibition, and the simplest way to test whether a new drug candidate in vitro is a reversible or irreversible inhibitor is to preincubate the drug candidate with enzyme preparations prior to the addition of marker substrates. If preincubation results in loss of enzyme activity as a function of time, it is highly possible that the drug candidate is an irreversible inhibitor. Otherwise, the drug candidate is a reversible inhibitor. However, it should be noted that time-dependent inhibition may also result from the formation of inhibitory metabolite(s) of the inhibitor. For example, the time-dependent inhibitory effect of diltiazem on testosterone 6 $\beta$ -hydroxylation in human liver microsomes is at least partly due to metabolite inhibition. Sutton et al. [7] have shown that *N*-desmethyl and *N,N*-didesmethyl metabolites of diltiazem were more potent inhibitors of CYP3A4-mediated testosterone 6 $\beta$ -hydroxylation than the parent drug. The human microsomal  $K_i$  values for *N,N*-didesmethylated, *N*-desmethylated diltiazem and diltiazem were 0.1, 2, and 60  $\mu$ M, respectively. The generation of inhibitory metabolites is believed to be partly responsible for the time-dependent inhibition observed with diltiazem in vitro. As in the case of diltiazem, norfluoxetine, a principal metabolite of fluoxetine, is a more potent competitive inhibitor of midazolam  $\alpha$ -hydroxylation and 4-hydroxylation than the parent drug [8]. Norfluoxetine is eight and four times more potent as an inhibitor of midazolam  $\alpha$ -hydroxylation and 4-hydroxylation, respectively, as compared to fluoxetine. Thus, caution should be exercised in distinguishing reversible and irreversible inhibition by examining the potential contribution of inhibitory metabolites.

Kinetically, reversible inhibition can be further classified as a competitive, noncompetitive, or uncompetitive process (see Chaps. 2 and 7). In the case of competitive inhibition, the binding of inhibitor prevents binding of substrate to the active site of the enzyme; in the case of noncompetitive inhibition, the inhibitor binds to a site other than the active site of the enzyme and has no effect on binding of substrate. The enzyme-substrate-inhibitor complex is nonproductive. In the case of uncompetitive inhibition, the inhibitor, instead of binding the free enzyme, binds to the enzyme-substrate complex, and again the enzyme-

substrate–inhibitor complex is nonproductive [9]. To differentiate whether a reversible inhibition is a competitive, noncompetitive, or uncompetitive process, data is often analyzed by graphical methods (e.g., Dixon, Lineweaver–Burk plots) that linearize an inherently nonlinear relationship [10]. However, the usefulness of the graphical methods has been questioned. Ideally, nonlinear regression fitting should be used to analyze enzyme kinetic data and to establish the type of inhibition [11].

In the case of Michaelis–Menten kinetics, the velocity ( $v$ ) of an enzymatic reaction can be expressed as Eq. (1),

$$v = \frac{V_{\max} \cdot [S]}{K_m + [S]} \quad (1)$$

where  $V_{\max}$  is the maximum velocity of metabolism,  $K_m$  is the Michaelis–Menten constant of the substrate, and  $[S]$  is the substrate concentration (see Chap. 2). To extrapolate the in vitro kinetic data to metabolic ability in vivo, the concept of intrinsic clearance ( $CL_{\text{int}}$ ) is important and very useful. Kinetically, the intrinsic clearance is considered as the cornerstone for the in vitro//in vivo extrapolation. *Intrinsic clearance* is defined as the velocity divided by the substrate concentration  $[S]$ . In the absence of inhibitor, the intrinsic clearance ( $CL_{\text{int},o}$ ) can be described by Eq. (2), while the intrinsic clearance in the presence of inhibitor ( $CL_{\text{int},i}$ ) can be expressed by Eqs. (3), (4), and (5) for competitive, noncompetitive, and uncompetitive inhibition, respectively:

$$CL_{\text{int},o} = \frac{V_{\max}}{K_m + [S]} \quad (2)$$

$$CL_{\text{int},i} = \frac{V_{\max}}{K_m \left( 1 + \frac{[I]}{K_i} \right) + [S]} \quad (3)$$

$$CL_{\text{int},i} = \frac{V_{\max}}{K_m \left( 1 + \frac{[I]}{K_i} \right) + [S] \left( 1 + \frac{[I]}{K_i} \right)} = \frac{\frac{V_{\max}}{\left( 1 + \frac{[I]}{K_i} \right)}}{K_m + [S]} \quad (4)$$

$$CL_{\text{int},i} = \frac{V_{\max}}{K_m + [S] \left( 1 + \frac{[I]}{K_i} \right)} = \frac{\frac{V_{\max}}{\left( 1 + \frac{[I]}{K_i} \right)}}{\frac{K_m}{\left( 1 + \frac{[I]}{K_i} \right)} + [S]} \quad (5)$$

where  $K_i$  is the inhibition constant of the inhibitor, and  $[I]$  is the inhibitor concentration. As indicated in Eqs. (3) and (4), a competitive inhibitor acts only to increase the apparent  $K_m$  and has no effect on the  $V_{max}$ , while a classic noncompetitive inhibitor decreases the  $V_{max}$  but has no effect on the  $K_m$ . On the other hand, an uncompetitive inhibitor decreases both the  $V_{max}$  and  $K_m$  to the same extent [Eq. (5)]. Depending on the type of inhibition, the  $V_{max}$  value of a drug can be decreased, or the  $K_m$  value can be increased. However, regardless of the type, enzyme inhibition always results in a decreased intrinsic clearance [Eqs. (3)–(5)].

If a drug is metabolized exclusively by the liver, the total clearance ( $CL_{total}$ ) of the drug approximates the hepatic clearance ( $CL_H$ ), which can be expressed as Eq. (6) or (7), according to the well-stirred model or parallel-tube model, respectively [12]:

$$CL_{total} = CL_H = Q_H \cdot E = \frac{Q_H \cdot fu \cdot CL_{int}}{Q_H + fu \cdot CL_{int}} \quad (6)$$

$$CL_{total} = CL_H = Q_H \cdot E = Q_H(1 - e^{-fu \cdot CL_{int}/Q_H}) \quad (7)$$

where  $Q_H$  is the hepatic blood flow,  $E$  is the hepatic extraction ratio, and  $fu$  is the unbound fraction of drug in the blood. Drugs can be further classified as low- or high-clearance compounds, depending on whether their clearance is enzyme limited or flow limited [12].

Because the hepatic first-pass metabolism reflects the hepatic intrinsic clearance ( $CL_{int}$ ), hepatic bioavailability ( $F_H$ ) can be expressed as Eq. (8) or (9), depending on the well-stirred model or parallel-tube model, respectively:

$$F_H = 1 - E = \frac{Q_H}{Q_H + fu \cdot CL_{int}} \quad (8)$$

$$F = 1 - E = e^{-fu \cdot CL_{int}/Q_H} \quad (9)$$

As shown in Eqs. (8) and (9), a decrease in the  $CL_{int}$  caused by enzyme inhibition will result in a decrease in first-pass metabolism, leading to an increase in bioavailability, regardless of the hepatic model.

Importantly, the pharmacokinetic consequences of enzyme inhibition, independent of the type of mechanism involved, should always be an increase in plasma concentrations, because enzyme inhibition will cause a decrease in the hepatic metabolism and an increase in bioavailability. A simple and direct way of assessing the effect of enzyme inhibition in vivo is to compare the plasma AUC of a substrate before and after coadministration of an inhibitor. The AUC after oral (po) administration can be expressed as Eq. (10) or (11):

$$AUC_{po} = \frac{F_H \cdot fa \cdot Dose}{CL_H} = \frac{fa \cdot Dose}{fu \cdot CL_{int}} \quad (10)$$

$$\text{AUC}_{po} = \frac{F_H \cdot fa \cdot \text{Dose}}{\text{CL}_H} = \frac{fa \cdot \text{Dose}(e^{-fu \cdot \text{CL}_{int}/Q_H})}{Q_H(1 - e^{-fu \cdot \text{CL}_{int}/Q_H})} \quad (11)$$

where  $fa$  is the fraction of dose absorbed from the gastrointestinal lumen. On the other hand, the AUC following intravenous (iv) administration can be expressed as Eq. (12) or (13):

$$\text{AUC}_{iv} = \frac{\text{Dose}}{\text{CL}_H} = \frac{\text{Dose}}{\left[ \frac{Q_H \cdot fu \cdot \text{CL}_{int}}{Q_H + fu \cdot \text{CL}_{int}} \right]} \quad (12)$$

$$\text{AUC}_{iv} = \frac{\text{Dose}}{\text{CL}_H} = \frac{\text{Dose}}{Q_H(1 - e^{-fu \cdot \text{CL}_{int}/Q_H})} \quad (13)$$

To illustrate the effect of enzyme inhibition on the AUCs after oral and intravenous administration, computer simulations were carried out for high-, intermediate-, and low-clearance drugs by using Eqs. (10–13) (Figs. 1 and 2). For low-clearance drugs ( $E < 0.5$ ), a decrease in the  $\text{CL}_{int}$  caused by enzyme inhibition yields an almost proportional increase in the AUC, regardless of the route of administration or the choice of hepatic models. However, for high-clearance drugs ( $E > 0.9$ ), changes in the AUC are more profound after oral administration than after intravenous dosing. Interestingly, a reduction of the  $\text{CL}_{int}$  has little effect on the  $\text{AUC}_{iv}$  of high-clearance drugs following intravenous administration. A significant increase in the  $\text{AUC}_{iv}$  is observed only when more than 80% of the  $\text{CL}_{int}$  is inhibited, namely, when the ratio of  $\text{CL}_{int}$  (inhibited)/ $\text{CL}_{int}$  (control) is equal to or less than 0.2 (Fig. 2). It is interesting to note that the parallel-tube model appears to be more sensitive to enzyme inhibition for high-clearance drugs. This is particularly true after oral administration. It should be noted that the parallel-tube model describes kinetics more accurately for high-clearance drugs [12]. Thus, simulations according to the parallel-tube model, rather than the well-stirred model, more accurately reflect the in vivo situations for high-clearance drugs. Overall, these computer simulations show that pharmacokinetic consequences of enzyme inhibition are dependent on the route of substrate administration and kinetic properties of the substrate (high or low clearance) (see Chap. 1).

The indinavir–ketoconazole interaction exemplifies the route- and substrate-dependence of drug–drug interaction. Both indinavir (an HIV protease inhibitor) and ketoconazole (an antifungal agent) are extensively metabolized by CYP3A enzymes in rats. The former is a high-clearance drug in rats, while the latter is a low-clearance drug. In vitro studies with rat liver microsomes indicated that indinavir and ketoconazole competitively inhibited each other, with a  $K_i$  value of 0.25  $\mu\text{M}$  for ketoconazole and 4.5  $\mu\text{M}$  for indinavir. Coadministration of ketoconazole (25 mg/kg) had little effect on indinavir clearance and AUC after

ORAL DOSE

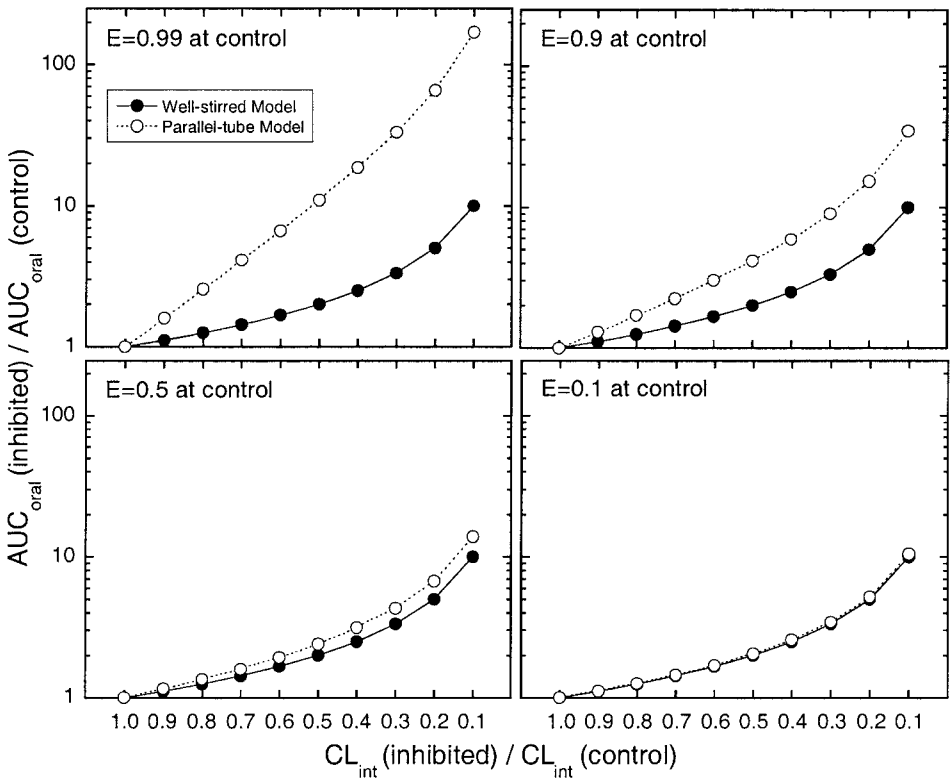


**Figure 1** Simulated effect of drug inhibition on the area under the concentration–time curve (AUC) after oral administration of a high-clearance ( $E = 0.99$  and  $E = 0.9$ ), intermediate-clearance ( $E = 0.5$ ), and low-clearance ( $E = 0.1$ ) drug. The fraction of drug absorbed from the gastrointestinal tract is assumed to be unity. The hepatic blood flow used in the calculation is 20 ml/min/kg, and the dose is 10,000 nmol/kg.

an intravenous dose of indinavir (10 mg/kg). The plasma clearance of indinavir decreased from 87 ml/min/kg in control rats to 83 ml/min/kg in ketoconazole-administered rats. However, coadministration of ketoconazole significantly increased the oral AUC and bioavailability of indinavir by more than fourfold. On the other hand, administration of 20 mg/kg indinavir significantly increased the AUC of ketoconazole by approximately twofold after both intravenous and oral administration of ketoconazole. The clearance of ketoconazole in rats decreased from 0.51 ml/min/kg when given alone to 0.27 ml/min/kg when given with



## IV DOSE

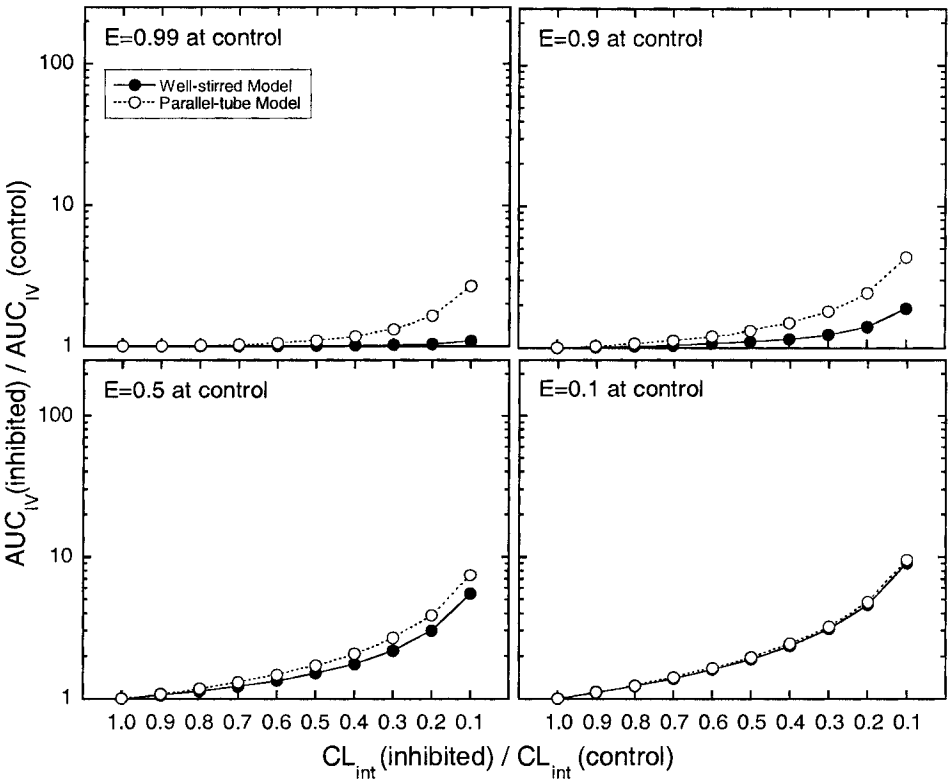


**Figure 2** Simulated effect of drug inhibition on the area under the concentration–time curve (AUC) after intravenous administration of a high-clearance ( $E = 0.99$  and  $E = 0.9$ ), intermediate-clearance ( $E = 0.5$ ), and low-clearance ( $E = 0.1$ ) drug. The hepatic blood flow used in the calculation is 20 ml/min/kg, and the dose is 10,000 nmol/kg.

indinavir [13]. Similarly, a route-dependent interaction also was observed with a ketoconazole–midazolam interaction in humans [14]. Midazolam is a moderate-clearance compound, with a clearance value of 8–10 ml/min/kg in humans. It was expected that ketoconazole would have less of an effect on midazolam AUC after intravenous dosing than oral administration of midazolam. As expected, coadministration of midazolam with ketoconazole (three doses of 200 mg) caused a fourfold increase in AUC of midazolam after intravenous dosing (56 versus 222 ng · hr/ml) as opposed to an 11-fold increase in oral AUC (54 versus 651 ng · hr/ml).

### III. ASSESSMENT OF DRUG INTERACTION POTENTIAL

Two key questions need to be addressed when assessing the potential of drug interactions for a new drug candidate. Will the new drug candidate be a potent CYP inhibitor, thereby altering the elimination or bioavailability of existing drugs? Will the new drug candidate be susceptible to effects of known CYP inhibitors? To avoid the potential of drug interactions, it is important to develop new drug candidates that are not potent CYP inhibitors and are not readily inhibited by other CYP inhibitors. While assessment of the susceptibility of a new drug candidate to CYP inhibitors is relatively simple, determining whether a new drug candidate is a potent CYP inhibitor is not as straightforward.

#### A. Assessment of Inhibitory Potency

There are two ways, quantitative or qualitative, of predicting the potential drug interactions for new drug candidates. Quantitative assessment is to accurately predict the extent of drug interactions, while qualitative assessment is to forecast the likelihood of a drug interaction. As indicated in Eqs. (3)–(5), the inhibitory potency of a new drug candidate is determined by its inhibition constant ( $K_i$ ) and concentration [I] at the enzyme active site. Thus for quantitative prediction,  $K_i$  and [I] values for the drug candidate must be accurately obtained. Although direct measurement of unbound inhibitor concentration at the active site of enzymes is very difficult, the unbound inhibitor concentration in plasma is often used as an approximation. Unfortunately, human plasma concentration data for new drug candidates is not available at the discovery stage. Therefore, it is almost impossible to quantitatively predict in vivo drug interactions of new drug candidates without the knowledge of their unbound plasma concentrations [I]. As a result, assessment of inhibitory potency of a new drug candidate at the stage of drug discovery has to be qualitative and solely relies on in vitro  $K_i$  (or  $IC_{50}$ ) values.

To determine whether a new drug candidate is a potent or weak CYP inhibitor, it is necessary to use an arbitrary range of  $K_i$  values. A weak inhibitor is arbitrarily defined as having a  $K_i$  value greater than 10  $\mu\text{M}$ , while a potent inhibitor has a  $K_i$  value less than 1  $\mu\text{M}$ . However, for drugs with intermediate potency ( $K_i$  ranging between 1 and 10  $\mu\text{M}$ ), evaluation of inhibitory potential becomes problematic. Care must be taken to avoid premature termination of the development of a new drug candidate. For example, a new drug candidate having a  $K_i$  value of 1  $\mu\text{M}$  is defined as a potent inhibitor. However, a clinically significant interaction will not occur if the maximal concentrations of the inhibitor in plasma are not expected to exceed 0.5  $\mu\text{M}$ . In addition, plasma protein binding has to be taken into consideration. If a potent inhibitor ( $K_i = 1 \mu\text{M}$ ) binds extensively to plasma proteins (>95%), a significant drug interaction will not occur, even when the maximal concentration of the inhibitor reaches 10  $\mu\text{M}$ . This is because

the unbound inhibitor concentration is less than 0.5  $\mu\text{M}$ . It is generally believed that only an unbound inhibitor can compete for enzymes. Furthermore, the overall benefit-to-risk balance also has to be taken into consideration when considering a new drug candidate for further development. The introduction of the HIV protease inhibitors (saquinavir, zidovudine, and zalcitabine) is a good example whereby the benefits of antiretroviral therapy outweighed the risks of drug interactions. All of these HIV protease inhibitors are potent CYP3A4 inhibitors with  $K_i$  values  $\leq 1$   $\mu\text{M}$  [15–17].

Today, it is common practice to screen for inhibitory potency using only one marker substrate per CYP enzyme. For example, the commonly used probe substrates for CYP3A4 and CYP2D6 include testosterone and bufuralol, respectively. As will be discussed later, the  $K_i$  values of a given inhibitor are often substrate dependent, where differences in  $K_i$  values can be as much as 10- or 20-fold. Thus, it is possible that a new drug candidate can be identified as a potent CYP inhibitor of one marker substrate but a weak inhibitor of a second substrate. To avoid such substrate dependences, *in vitro*  $K_i$  values should be measured using several marker substrates, ideally using substrates that are expected to be administered concurrently. However, it should be emphasized that it would not be cost effective to apply the multiple-substrate approach to the screening of compounds at the early drug discovery stage. The multiple-substrate approach should be applied only to lead candidates.

## 1. Estimation of Inhibition Constant

As stated earlier, quantitative prediction of *in vivo* drug interactions requires both accurate estimation of *in vitro*  $K_i$  values and measurement of unbound inhibitor concentration in plasma. Even when the information on plasma concentrations of inhibitor becomes available from clinical studies during drug development, quantitative prediction is still very difficult. The difficulty stems from the inaccuracy of  $K_i$  estimation. There are numerous factors that may affect the accuracy of  $K_i$  estimation. Obviously, inaccuracy in  $K_i$  estimation may result from inappropriate experimental conditions.

When an inhibitor is also a substrate for the same enzyme or when an inhibitor binds extensively to microsomal proteins, significant depletion of inhibitor concentration may occur during the incubation as a result of metabolism and nonspecific binding. Therefore, the  $K_i$  value of the inhibitor may be overestimated when a high microsomal protein concentration is used. The effect of microsomal protein concentration on inhibitory potency has recently been studied for three antifungal agents [18]. The degree of inhibition toward the metabolism of midazolam by clotrimazole and ketoconazole, but not fluconazole, was decreased substantially when the amount of microsomal protein in the incubate increased. As the concentration of microsomal protein in the incubate increased from 25 to 500  $\mu\text{g/ml}$ , the degree of inhibition by clotrimazole (3 nM) decreased from 95% to

6%. These results are consistent with depletion of inhibitors through nonspecific binding, because both clotrimazole and ketoconazole bind extensively to proteins, whereas fluconazole binds weakly. To minimize the problem of inhibitor depletion in  $K_i$  estimation, it is important to shorten the incubation time and to lower the microsomal protein concentration for inhibition studies. With the advent of sensitive liquid chromatography–mass spectrometric (LC-MS) methods, this is possible.

The nonspecific binding and metabolism of ketoconazole can also explain the huge differences observed in the  $K_i$  values of ketoconazole–CYP3A4 interactions in human liver microsomes. Ketoconazole strongly inhibited  $\alpha$ -hydroxylation of midazolam with a  $K_i$  value of 0.0037  $\mu\text{M}$  when a low microsomal protein concentration (0.25 mg/ml) was used [8], while the  $K_i$  value for ketoconazole–tacrolimus interaction was estimated to be 8  $\mu\text{M}$  when a high microsomal protein concentration (1.5 mg/ml) was used [19]. A sixfold increase in the microsomal protein resulted in a 2200-fold increase in the estimated  $K_i$  values of ketoconazole. Although it is not expected that the  $K_i$  values of ketoconazole will be the same for different substrates, such as midazolam and tacrolimus, the differences in protein concentration used can certainly contribute significantly to the huge discrepancy seen in the  $K_i$  values between these two substrates.

The large discrepancy in the  $K_i$  values of ketoconazole for midazolam and tacrolimus may also be partly attributed to multiple binding sites (apoprotein) of CYP3A4 with which these substrates and inhibitor interact. Although there is only one single catalytic site (prosthetic heme) for CYP3A4, this enzyme may have more than one binding site. Orientation of substrate and inhibitor molecules in relation to their binding sites and catalytic site may result in different  $K_i$  values. In support of the hypothesis of multiple binding sites of CYP3A4, Shou et al. [20] have successfully described the enzyme kinetics of CYP3A4-mediated metabolism of diazepam and its derivatives with a kinetic model that consists of two substrate-binding sites and one catalytic site. Recently, Wang et al. [21] have demonstrated that in vitro drug–drug interaction patterns are substrate dependent. Mutual inhibition, partial inhibition, and activation were observed in the testosterone–terfenadine, testosterone–midazolam, and terfenadine–midazolam interactions. These results are consistent with the hypothesis of multiple binding sites and suggest that CYP3A4-mediated drug interactions do not always follow classical Michaelis–Menten kinetics.

Interestingly, although there is a widespread assumption that the  $K_i$  value of a given inhibitor is an intrinsic activity of the inhibitor and that the inhibitor should have the same  $K_i$  value for all substrates that are catalyzed by the same enzyme [22,23], marked differences in the  $K_i$  values of a given inhibitor between different substrates and between different metabolic pathways of the same substrate have been observed. For example, the differences in ketoconazole  $K_i$  values for the CYP3A4-mediated midazolam  $\alpha$ -hydroxylation (0.0037  $\mu\text{M}$ ) and 4-hydroxylation (0.047  $\mu\text{M}$ ) are more than 12-fold (Table 1) [8]. Similar results

**Table 1**  $K_m$  Values for Metabolism of Midazolam, Triazolam, and Terfenadine and Corresponding  $K_i$  Values for Ketoconazole in Human Liver Microsomes

Metabolic pathways	$K_m$ ( $\mu\text{M}$ )	$K_i$ ( $\mu\text{M}$ )
Midazolam $\alpha$ -hydroxylation	3.3	0.0037
Midazolam 4-hydroxylation	57.4	0.047
Terfenadine dealkylation	3.9	0.024
Terfenadine hydroxylation	12.6	0.237
Triazolam $\alpha$ -hydroxylation	74.2	0.006
Triazolam 4-hydroxylation	305	0.023

Source: Refs. 8, 24, 25.

were also observed for terfenadine and triazolam. Both drugs are transformed into two metabolites by CYP3A4, and the ketoconazole  $K_i$  values for each metabolic pathway are considerably different (Table 1) [24,25]. Moreover, the  $K_i$  values of ketoconazole are quite different among these three substrates (midazolam, terfenadine, and triazolam). As shown in Table 1, the ketoconazole  $K_i$  values for terfenadine metabolism are approximately 10 times higher than those for midazolam metabolism [8,24]. In addition to the CYP3A4 enzyme, different  $K_i$  values of sulfaphenazole for different substrates of CYP2C9 have also been reported. The sulfaphenazole  $K_i$  value for ibuprofen and naproxen is 0.12  $\mu\text{M}$  and 1.6  $\mu\text{M}$ , respectively [23]. Similarly, quinidine has been shown to exhibit different  $K_i$  values with multiple CYP2D6 substrate. The quinidine  $K_i$  value for debrisoquine 4-hydroxylation is 0.6  $\mu\text{M}$  [26], while it is 0.05  $\mu\text{M}$  for desipramine hydroxylation [27]. It should be noted that the *in vitro* experimental conditions used for quinidine inhibition studies in the two laboratories were quite similar; hence, the 12-fold difference in quinidine  $K_i$  value cannot be completely explained by the experimental conditions. Collectively, the examples clearly demonstrate that inhibition is substrate dependent, and it should not be assumed that a given inhibitor will have the same  $K_i$  value for all substrates of the same enzyme or the same  $K_i$  value for all metabolic reactions of a given substrate catalyzed by the same enzyme. This is particularly true for the CYP3A4 enzyme, which has a relatively larger pocket site, allowing different orientations of various substrates for binding and catalytic sites, as compared to other CYP isoforms [28,29].

The choice of *in vitro* enzyme systems, such as hepatocytes, liver microsomes, cDNA-based vector systems, and liver slices, is also an important factor that may affect the  $K_i$  estimation. The  $K_i$  values of omeprazole against 3-hydroxylation and *N*-demethylation of diazepam were 28 and 59  $\mu\text{M}$ , respectively, when rat hepatocytes were used, while the corresponding  $K_i$  values were 108 and 226  $\mu\text{M}$  when rat liver microsomes were used [30]. Under *in vivo* conditions, where

diazepam clearance was measured in rats receiving infusion of omeprazole to achieve a wide range of steady-state omeprazole concentrations, the *in vivo*  $K_i$  value of 57  $\mu\text{M}$  more closely reflected the hepatocyte data. In an attempt to explain the discrepancy of  $K_i$  values between hepatic microsomes and hepatocytes, the investigators suggested that the lower  $K_i$  values in hepatocytes may result from omeprazole's high tendency to bind cytosolic proteins, providing a cellular reservoir within the hepatocytes. Alternatively, an active transporter involved in the uptake of omeprazole into hepatocytes could also result in a higher intracellular omeprazole concentration and hence lower  $K_i$  values. Regardless of mechanisms involved, these results suggest that hepatocytes may prove to be a better *in vitro* model for the assessment of drug–drug interaction potential.

Recently, Gibbs et al. [31] investigated the effect of ketoconazole on midazolam  $\alpha$ -hydroxylation using human liver microsomes, cDNA-expressed CYP3A4, and CYP3A5 microsomes. For liver microsomes that contained only CYP3A4, the ketoconazole  $K_i$  value (0.015  $\mu\text{M}$ ) was similar to that for cDNA-expressed CYP3A4 microsomes (0.026  $\mu\text{M}$ ). However, the ketoconazole  $K_i$  value was 0.055  $\mu\text{M}$  for liver microsomes that contained both CYP3A4 and CYP3A5. This value was more than three times greater than the  $K_i$  value obtained with human liver microsomes containing only CYP3A4. The reason the ketoconazole  $K_i$  was higher in the liver microsomes containing CYP3A4 and CYP3A5 than the liver microsomes containing only CYP3A4 was that ketoconazole exhibited a much higher  $K_i$  value (0.109  $\mu\text{M}$ ) with CYP3A5 than with CYP3A4 (0.026  $\mu\text{M}$ ). In this same study, similar observations were obtained for fluconazole. The  $K_i$  values for fluconazole's inhibitory effect on cDNA-expressed CYP3A4 were comparable to the  $K_i$  values obtained from incubations with liver microsomes containing only CYP3A4 (9.2  $\mu\text{M}$  versus 10.4  $\mu\text{M}$ ), whereas the  $K_i$  values for cDNA-expressed CYP3A5 was approximately ninefold higher (85  $\mu\text{M}$ ). These examples illustrate the point that inaccuracy of  $K_i$  estimation may occur when more than one isoform is involved in formation of the measured metabolic product of a given substrate. The situation may be made even more complicated if the relative amounts of each isoform differ between liver microsomal preparations.

Liver slices are considered to be a useful model for drug metabolism studies because of the retained architectural and cellular integrity; however, there are few reports examining drug interactions with this model. Rodrigues et al. [32] have compared the effect of ketoconazole on terfenadine metabolism in human liver slices, microsomal preparations, and cDNA-expressed CYP3A4. At concentrations of 5–10  $\mu\text{M}$ , ketoconazole completely inhibited terfenadine metabolism in all three enzyme models. In this report, no attempts were made to compare the  $K_i$  values of ketoconazole in these three enzyme models. In fact, the usefulness of liver slices in obtaining kinetic parameters has been proven to be limited [33]. The values of intrinsic clearance ( $V_{\max}/K_m$ ) of a series of drugs determined from rat liver slices were consistently less than those obtained from hepatocytes by a

factor ranging from 2 to 20, depending on the drug's lipophilicity. These results strongly suggest that a distribution equilibrium is not achieved between cells within the slices and incubation media, probably due to the slice thickness (~260  $\mu\text{m}$ ). It is quite possible that the  $K_i$  value of inhibitors can be overestimated when liver slices are used.

Accumulation of potent inhibitory metabolites in the incubation medium may also result in inaccurate estimation of  $K_i$  values. Sutton et al. [7] have shown that *N*-desmethyl and *N,N*-didesmethyl metabolites of diltiazem are more potent in inhibiting CYP3A4-mediated testosterone 6 $\beta$ -hydroxylation than the parent drug. The  $K_i$  values for *N,N*-didesmethylated, *N*-desmethylated diltiazem and diltiazem were 0.1, 2 and 60  $\mu\text{M}$ , respectively. As in the case of diltiazem, norfluoxetine, a principal metabolite of fluoxetine, is a more potent competitive inhibitor for midazolam  $\alpha$ -hydroxylation and 4-hydroxylation than the parent drug. The  $K_i$  values of norfluoxetine for midazolam  $\alpha$ -hydroxylation and 4-hydroxylation were 1.44 and 17.0  $\mu\text{M}$ , respectively, while the corresponding values of fluoxetine were 11.5 and 67.3  $\mu\text{M}$  [8].

The  $K_i$  value of a given inhibitor varies significantly when the type of inhibition is assigned arbitrarily. For example, depending on the assignment of inhibition type, the calculated in vitro ketoconazole  $K_i$  values for triazolam  $\alpha$ -hydroxylation and 4-hydroxylation pathways differ significantly [25]. Using the same data set, the ketoconazole  $K_i$  values were 0.006  $\mu\text{M}$  for the  $\alpha$ -hydroxylation pathway and 0.023  $\mu\text{M}$  for the 4-hydroxylation pathway when competitive inhibition was assigned, while the corresponding ketoconazole  $K_i$  values were 0.06  $\mu\text{M}$  and 0.08  $\mu\text{M}$  when noncompetitive inhibition was assumed. Similarly, the ketoconazole  $K_i$  values for midazolam  $\alpha$ -hydroxylation varied when a different type of inhibition was assigned. When ketoconazole was designated as a noncompetitive inhibitor of midazolam  $\alpha$ -hydroxylation, the  $K_i$  value was estimated to be 0.11  $\mu\text{M}$  [3], while the  $K_i$  value was 0.0037  $\mu\text{M}$  when ketoconazole was considered a competitive inhibitor of the same midazolam  $\alpha$ -hydroxylation [8]. The observed 30-fold difference in the  $K_i$  values cannot be entirely attributed to the microsomal protein concentrations used in these two laboratories, because there were only small differences in microsomal protein concentrations (0.25 mg/ml versus 0.5 mg/ml). From the examples just cited, it is clear that unless the in vivo intracellular milieu can be replicated by in vitro experimental conditions, accurate estimation of inhibitor  $K_i$  value from in vitro studies is almost impossible. Since the predictability of in vivo drug-drug interactions is critically dependent on the accuracy of  $K_i$  estimation, it follows that inaccuracy of  $K_i$  estimation prevents meaningful quantitative prediction of in vivo drug interactions.

## 2. Inhibitor Concentration at the Active Site of Enzymes

In addition to the problems of estimating  $K_i$  values, another critical issue in predicting in vivo drug interactions is an accurate measurement of inhibitor concen-

tration  $[I]$  at the active site of the target enzyme. Ideally, the inhibitor concentrations at the active site should be directly measured. Although direct measurement of unbound drug concentrations at the active site is seldom possible, the unbound drug concentration in plasma is used in lieu of unbound concentration at the active site, assuming that the drug binds reversibly to plasma and tissue protein and that equilibrium of unbound drug occurs readily between plasma and tissues. In fact, this assumption is one of the most important tenets for the practical elucidation of pharmacokinetics and drug metabolism.

Many reports are available to support the assumption that only the unbound inhibitor competes with substrate at the active site. For example, plasma protein binding has to be taken into consideration to predict the inhibitory effect of ketoconazole on antipyrine clearance [34]. In this study, ketoconazole was infused intravenously into rats to obtain a wide range of steady-state plasma concentrations of this drug. Analysis of the relationship between steady-state plasma concentrations of ketoconazole and the degree of inhibition of antipyrine clearance yielded an *in vivo*  $K_i$  value of 3  $\mu\text{M}$  based on total (bound + unbound) plasma concentrations, and 0.07  $\mu\text{M}$  based on unbound ketoconazole concentrations. The *in vivo*  $K_i$  value of ketoconazole based on unbound concentration showed closer agreement with the reported *in vitro*  $K_i$  values. Similarly, a good prediction of the interaction between tolbutamide and sulfaphenazole in animals was obtained only when unbound plasma concentrations were used [35].

However, there are many studies that contradict the hypothesis of unbound concentration. Von Moltke et al. [24] have found that ketoconazole competitively inhibited the biotransformation of terfenadine to its desalkyl- and hydroxymetabolites in human liver microsomes, with a  $K_i$  value of 0.024  $\mu\text{M}$  for the desalkyl terfenadine pathway and 0.27  $\mu\text{M}$  for terfenadine hydroxylation. Instead of unbound concentration, the total plasma concentration of ketoconazole gave a better prediction of ketoconazole–terfenadine interaction *in vivo* when the  $K_i$  values and the clinical plasma concentration of ketoconazole were incorporated into a mathematic model. Similarly, Tran et al. [36] reported that stiripentol significantly inhibited the metabolism of carbamazepine in humans and that the *in vivo*  $K_i$  values of stiripentol for carbamazepine metabolism were more consistent with the *in vitro*  $K_i$  values when total plasma concentrations of stiripentol, rather than unbound concentrations, were used to estimate the *in vivo*  $K_i$  values. Recently, a good agreement between the *in vitro* and *in vivo*  $K_i$  values of ritonavir in ritonavir–saquinavir interaction has been reported in humans [37]. The *in vivo*  $K_i$  (based on total plasma concentration) for ritonavir inhibition on saquinavir metabolism was estimated to be 0.0164  $\mu\text{g}/\text{ml}$ , which was comparable to the *in vitro*  $\text{IC}_{50}$  (0.025  $\mu\text{g}/\text{ml}$ ) for ritonavir inhibition. All of the three inhibitors just cited (ketoconazole, stiripentol, and ritonavir) were bound extensively to plasma protein (>95%).

In some cases, even the use of total plasma concentrations of inhibitor failed to predict (underestimated) the degree of drug interaction *in vivo*. Both



fluoxetine and its principal metabolite, norfluoxetine, are competitive inhibitors of desipramine hydroxylation in human liver microsomes, with  $K_i$  values of 3.0 and 3.5  $\mu\text{M}$ , respectively [27]. A substantial increase in steady-state plasma concentration of desipramine was observed in healthy volunteers after three weeks of desipramine and fluoxetine coadministration. The mean steady-state concentration of desipramine increased from 36 ng/ml before fluoxetine coadministration to 162 ng/ml during coadministration, reflecting an 80% decrease in the clearance. At this time, the mean plasma levels of fluoxetine and norfluoxetine were 92 and 102 ng/ml, respectively. Using  $K_i$  values (3.0  $\mu\text{M}$  for fluoxetine and 3.5  $\mu\text{M}$  for norfluoxetine) from the *in vitro* study and total plasma concentration determined *in vivo*, the prediction of the decreases in desipramine clearance were much less (23% decrease) than the clinical observations [27]. These results led to a speculation that the concentration of fluoxetine and its metabolite at the active site of enzymes is much higher than plasma concentration because of a high liver/plasma partition ratio, which was later estimated to be 12 for fluoxetine and 14 for norfluoxetine, respectively [27]. When the calculated liver concentrations of fluoxetine and norfluoxetine were used, the predicted percent inhibition (82%) was in excellent agreement with the clinical observations [27]. In another report by von Moltke et al. [8], the predicted inhibition of midazolam (84%) by itraconazole was in good agreement with the observed interactions in clinical studies (ranging from 83% to 95%) if liver concentrations of itraconazole calculated from a liver/plasma ratio of 10 were used. Similar approaches have been used for the prediction of a ketoconazole–triazolam interaction. Using the plasma ketoconazole concentration together with liver/plasma partition ratios and the *in vitro*  $K_i$  values, the predicted percentage inhibition of triazolam clearance by ketoconazole was consistent with that observed *in vivo* [25]. The use of the liver/plasma partition ratio has also been adopted by other laboratories. For example, Preskorn and Magnus [38] have reported that the extent of the inhibitory effect of fluoxetine (plus norfluoxetine) on the oral clearance of desipramine was best predicted when the liver/plasma partition ratios were taken into consideration.

The liver/plasma partition approach implies that the enzyme exposure is related to the total (bound and unbound), rather than the unbound, concentration of inhibitor in the liver. Obviously, this approach challenges the fundamental assumption of pharmacokinetics that the rate of metabolism is a function of unbound drug concentration in the liver. Some scientists believe that the success in predicting an *in vivo* interaction by way of the liver/plasma partition approach may simply be fortuitous. Using the rat as animal model, Yamano et al. [39] demonstrated that the extent of itraconazole inhibitory effect on midazolam metabolism could be predicted quantitatively based on the unbound concentrations of itraconazole in the liver and its  $K_i$  value for midazolam metabolism when the active transport of itraconazole was taken into consideration. Because of the active hepatic uptake of itraconazole, the unbound azole concentration in the liver

was about 10-fold higher than the unbound concentration in plasma. Taking these findings together, these investigators concluded that the inability in predicting in vivo interactions from in vitro  $K_i$  values using unbound plasma concentrations was simply due to neglecting the active uptake of some inhibitors by the liver. The possible involvement of active transport of inhibitors further complicates the predictability of in vivo drug interactions.

Given the problems associated with the inaccuracy in estimating in vitro  $K_i$  values and insufficient methods in measuring the unbound inhibitor concentration [I] at the active site of enzymes, it is very difficult to quantitatively predict in vivo drug interactions. This means that one can only assess whether there is a likelihood of drug interactions, namely, “highly possible” or “less likely,” rather than a prediction of quantitative changes of plasma concentrations of a given substrate before and during enzyme inhibition.

## B. Susceptibility to CYP Inhibitors

From an industrial perspective, it is equally important not to develop new drug candidates that are potent CYP inhibitor and new drug candidates that are readily inhibited by other known CYP inhibitors. Surprisingly, most drug metabolism scientists have focused only on the question of whether new drug candidates are potent CYP inhibitors, rather than on the question of whether new drug candidates are susceptible to the effects of known CYP inhibitors. Depending on the kinetic properties of drugs, the increase in the AUC of drugs can be as much as 100-fold. For example, coadministration of ritonavir resulted in a greater than 100-fold increase in the plasma AUC of saquinavir in human volunteers [37,40].

To determine whether a new drug candidate is readily inhibited by other CYP inhibitors, it is important to identify the elimination pathways of the drug candidate and the relative contribution of metabolic fraction to overall elimination. From a kinetic standpoint, ideal drugs are eliminated by multiple mechanisms (metabolism, renal and biliary excretion). A significant drug interaction will not occur unless two of these three elimination processes are completely inhibited. Rowland and Martin [41] developed a pharmacokinetic model to evaluate the relative contribution of the metabolic fraction ( $f_m$ ) on the degree of drug interaction (see Chap. 1). They concluded that a significant drug interaction occurs only when a particular pathway being inhibited is greater than 50% of total elimination pathways.

At the stage of drug discovery, the information on the relative contribution of metabolic fraction in humans is not available. Therefore, the metabolic fraction ( $f_m$ ) of new drug candidates can be estimated only indirectly from animal species. If the metabolic fraction of a given drug candidate is similar among three or four different animal species tested, then it is reasonable to assume that humans will have a similar fraction [42].

If a new drug candidate is eliminated mainly (>50%) by CYP-mediated metabolism, it is important to identify which CYP isoforms are responsible for each metabolic pathway of the drug and to establish the relative contribution of each CYP isoform to the overall metabolism of the drug. In some cases, all metabolic pathways of a drug are catalyzed by a single isoform, while in other cases a single metabolic pathway may involve multiple isoforms. If a new drug candidate is eliminated exclusively by a single oxidative metabolic reaction that is mediated by only a single CYP isoform, the clearance of this drug would readily be inhibited by other drugs. In contrast, if a new drug candidate is metabolized by multiple metabolic pathways that are catalyzed by multiple isoforms, the elimination of this drug would not readily be altered by other drugs.

To identify the CYP(s) responsible for a specific metabolic reaction of a drug candidate, several methods must be considered [43,44]. These include (a) use of CYP-form selective inhibitors; (b) use of CYP-form selective antibodies; (c) measure of catalytic activity of each individual recombinant human CYP toward the drug candidate; (d) inhibition of marker substrates by the drug candidate for each CYP isoform; and (e) metabolic correlation of activity with marker substrates for each CYP isoform. Each approach has its advantages and disadvantages, and a combination of approaches is usually required to accurately identify the CYP isoform responsible for the metabolic reaction of a given drug [17,45].

Although the identification of CYP involvement is relatively straightforward, inappropriate experimental conditions may lead to misidentification. For example, *N*-dealkylation is the major metabolic pathway for diazepam in humans receiving a clinical dose. However, *in vitro* studies in human liver microsomes showed that 3-hydroxylation was the major pathway when a high concentration (100  $\mu\text{M}$ ) was employed [46]. When a clinically relevant concentration of diazepam (2  $\mu\text{M}$ ) was used, *N*-demethylation became the major metabolic pathway of the drug [47]. It should be noted that *N*-demethylation of diazepam is mainly catalyzed by CYP2C19, while 3-hydroxylation is mediated by CYP3A4 [48,49]. Similarly, inappropriate use of high drug concentration will also result in misidentification of the CYP isoform involved in the metabolism of lansoprazole. At clinically relevant concentrations, CYP2C19-mediated 5-hydroxylation is the major metabolic pathway of lansoprazole, whereas at high concentrations the drug is catalyzed mainly by CYP3A4 to form sulfoxide metabolite [50].

Susceptibility to CYP inhibition is also dependent on the kinetic property of drugs. As shown in Figure 1, a high-clearance drug is subject to extensive first-pass metabolism and is more susceptible to CYP inhibition than low-clearance drugs when given orally. This is because coadministration of a high-clearance drug with an inhibitor will change the plasma AUC of the drug by increasing bioavailability through inhibition of first-pass metabolism and decreasing the hepatic clearance. For low-clearance drugs, the first-pass metabolism is minor, and the inhibitory effect is observed only on hepatic clearance [Eqs. (10) and (11)].

Therefore, the degree of inhibition for high-clearance drugs caused by inhibitors is always more profound than that of low-clearance drugs.

In a recent clinical study, Greenblatt et al. [51] demonstrated that ketoconazole causes a more profound increase in the oral AUC of triazolam in healthy volunteers than in the oral AUC of alprazolam. While both triazolam and alprazolam are anxiolytic agents that are metabolized predominantly by human CYP3A4, the human pharmacokinetics of the two drugs differ substantially. Triazolam has a clearance (8–10 ml/min/kg) in the intermediate range relative to hepatic blood flow and an absolute bioavailability of approximately 50%, probably due in large part to its first-pass metabolism. In contrast, alprazolam has a clearance of less than 5% of hepatic blood flow and an absolute bioavailability exceeding 90%. Coadministration of the same oral dose of ketoconazole resulted in a 14-fold increase of plasma AUC of triazolam but only a 4-fold increase of alprazolam AUC.

The results of the foregoing study strongly support the notion that high-clearance drugs are more sensitive to enzyme inhibition. Therefore, it is important to determine whether a new drug candidate is a high- or low-clearance compound at the stage of drug discovery in order to preferably avoid the development of a high-clearance drug that is highly susceptible to CYP inhibition. With the increased availability of human hepatocytes and liver microsomes, hepatic clearance of drugs in humans can be estimated reasonably well from *in vitro* metabolic data [52–56]. At Merck, we routinely use the *in vivo/in vitro* approach for the prediction of human hepatic clearance of new drug candidates. With this approach, detailed enzyme kinetic studies can be conducted to determine the  $K_m$  and  $V_{max}$  values of new drug candidates in rat, dog, and monkey microsomes (or hepatocytes). The *in vitro* hepatic clearance is then calculated from the  $V_{max}/K_m$  values and compared with the *in vivo* hepatic clearance in rats, dogs, and monkeys after intravenous administration of the drug candidates. If *in vivo* hepatic clearance in animal species can be extrapolated reasonably well from *in vitro* clearance, then the  $V_{max}/K_m$  values from human liver microsomes can be used to predict human hepatic clearance of new drug candidates. This approach was used successfully to predict human hepatic clearance for several drugs, including indinavir, an HIV protease inhibitor [57].

In summary, three steps are needed to properly assess whether a drug is susceptible to CYP inhibition. First, it is important to estimate the relative contribution of metabolism (*fm*) of a drug to its overall elimination from animal species. If the *fm* is greater than 30–50%, the second step is to identify which human CYP enzymes are involved in the metabolism. Thirdly, it is important to predict whether the drug has a high or low hepatic clearance, particularly when only one CYP enzyme is involved in its metabolism. Without sufficient supporting data and without more thoughtful integration of all of the aforementioned information, a meaningful assessment of susceptibility to CYP inhibition cannot be obtained.

Finally, it also should be emphasized that, like the prediction of inhibitory potency, the assessment of susceptibility of a new drug to CYP inhibition can be made only in a qualitative sense, namely, "highly likely," "possible," or "least likely," but not quantitatively.

#### IV. CONCLUSION

Assessment of the potential drug interactions for new drug candidates can be looked at from two perspectives: whether the new drug candidates are potent CYP inhibitors and whether they are susceptible to effects of known CYP inhibitors. Although it is highly desirable to have an early and accurate assessment of drug interaction potential, it is very difficult to quantitatively predict the extent of drug interactions. The difficulty in quantitatively predicting the inhibitory potency of new drug candidates stems from the inaccuracy of *in vitro*  $K_i$  estimation and insufficient methods for direct measurement of inhibitor concentration at the active site of enzymes. On the other hand, the difficulty in quantitatively predicting the susceptibility of new drug candidates stems from the uncertainty in the estimation of metabolic fraction in humans at the stage of drug discovery. Until optimal experimental conditions can be established for accurate  $K_i$  estimation and suitable techniques can be developed to enable direct measurement of unbound inhibitor concentrations at the site of target enzymes, information obtained from *in vitro* metabolic studies can be used only for qualitative prediction, namely, whether there is a "lack of an interaction" or "probability of an interaction."

#### REFERENCES

1. Lazarou J, Pomeranz BH, and Corey PN. Incidence of adverse drug reaction in hospitalized patients: a meta-analysis of prospective studies. *JAMA* 279:1200–1205, 1998.
2. Duchateau A. Posicor: Veni, vidi and gone. *Pharm. Weekblad.* 133:1294–1295, 1998.
3. Wrighton SA, and Ring BJ. Inhibition of human CYP 3A catalyzed 1'-hydroxy midazolam formation by ketoconazole, nifedipine, erythromycin, cimetidine and nizatidine. *Pharm. Res.* 11:921–924, 1994.
4. Lin JH, and Lu AYH. Inhibition and induction of cytochrome P450 and the clinical implications. *Clin. Pharmacokinet.* 35:361–390, 1998.
5. Lin JH, Chiba M, Chen I-W, Vastag KJ, Nishime JA, and Dorsey BD. Time- and dose-dependent pharmacokinetics of L-754,394, an HIV protease inhibitor, in rats, dogs and monkeys. *J. Pharmacol. Exp. Ther.* 274:264–269, 1995.
6. Mico BA, Federowicz DA, Ripple MG, and Kerns W. *In vivo* inhibition of oxidative

- drug metabolism by, and acute toxicity of 1-aminobenzotriazole (ABT): a tool for biochemical toxicology. *Biochem. Pharmacol.* 37:2515–2519, 1988.
7. Sutton D, Butler AM, Nadin L, and Murray M. Role of CYP 3A4 in human hepatic diltiazem *N*-demethylation inhibition of CYP 3A4 activity by oxidized diltiazem metabolites. *J. Pharmacol. Exp. Ther.* 282:294–300, 1997.
  8. von Moltke LL, Greenblatt DJ, Schmider J, Duan SX, Wright CE, Harmatz JS, and Shader RI. Midazolam hydroxylation by human liver microsomes in vitro: inhibition by fluoxetine, norfluoxetine and byazole antifungal agents. *J. Clin. Pharmacol.* 36: 783–791, 1996b.
  9. Segel IH. Simple inhibition systems. In: *Enzyme Kinetics*. Wiley-Interscience, New York, 1975, pp 100–160.
  10. Cornish-Bowden A. A simple graphical method for determining the inhibition constants of mixed, uncompetitive and non-competitive inhibitors. *Biochem. J.* 137: 143–144, 1973.
  11. Kakkar T, Boxenbaum H, and Mayersohn M. Estimation of  $K_i$  in a competitive enzyme-inhibition model: comparison among three methods of data analysis. *Drug. Metab. Dispos.* 27:756–762, 1999.
  12. Wilkinson GR. Clearance approaches in pharmacology. *Pharmacol. Rev.* 39:1–47, 1987.
  13. Lin JH. In vitro and in vivo drug interaction with indinavir. Symposium on Recent Advances in Drug–Drug interaction, Washington, D.C., December 10–11, 1996.
  14. Tsunoda SM, Velez RL, von Moltke LL, and Greenblatt DJ. Differentiation of intestinal and hepatic cytochrome P450 3A activity with use of midazolam as an in vivo probe: effect of ketoconazole. *Clin. Pharmacol. Ther.* 66:461–471, 1999.
  15. Fitzsimmons ME, and Collins JM. Selective biotransformation of the human immunodeficiency virus protease inhibitor saquinavir by human small-intestinal cytochrome P4503A4: potential contribution to high first-pass metabolism. *Drug Metab. Dispos.* 25:256–266, 1997.
  16. Kumar GN, Rodrigues AD, Buko AM, and Denissen JF. Cytochrome P450-mediated metabolism of the HIV-1 protease inhibitor (ABT-538) in human liver microsomes. *J. Pharmacol. Exp. Ther.* 277:423–431, 1996.
  17. Chiba M, Hensleigh M, Nishime JA, and Lin JH. Role of CYP 3A4 in human metabolism of MK-639, a potent HIV protease inhibitor. *Drug Metab. Dispos.* 24:307–314, 1996.
  18. Gibbs MA, Kunze KL, Howald WN, and Thummel KE. Effect of inhibitor depletion on inhibitory potency: tight binding inhibition of CYP 3A by clotrimazole. *Drug Metab. Dispos.* 27:596–599, 1999.
  19. Lampen A, Christians U, Guengerich FP, Watkins PB, Kolars JC, Bader A, Gonschior A-K, Dralle H, Hackbarth I, and Sewing K-F. Metabolism of the immunosuppressant tacrolimus in the small intestine: cytochrome P450, drug interaction and interindividual variability. *Drug Metab. Dispos.* 23:1315–1324, 1995.
  20. Shou M, Mei Q, Ettore MW, Dai R, Baillie TA, and Rushmore TH. Sigmoidal kinetic model for two cooperative substrate-binding sites in a cytochrome P450 3A4 active site: an example of the metabolism of diazepam and its derivatives. *Biochem. J.* 340:845–853, 1999.
  21. Wang RW, Newton DJ, Liu N, Atkins WM, and Lu AYH. Human cytochrome P450

- 3A4: in vitro drug–drug interaction patterns are substrate-dependent. *Drug Metab. Dispos.* 28:360–366, 2000.
22. Tucker GT. Extrapolating concentrations—in vitro to in vivo. In: Boobis AR, Kremers P, Pelkonen O, and Pithan K, eds. *European Symposium on the Prediction of Drug Metabolism in Man: Progress and Problem*. European Communities, 1999, pp 237–246.
  23. Pelkonen O, Maenpaa J, Taavitsainen P, Rautio A, and Raunio H. Inhibition and induction of human cytochrome P450 (CYP) enzymes. *Xenobiotica* 28:1203–1253, 1998.
  24. von Moltke LL, Greenblatt DJ, Duan SX, Harmatz JS, and Shader RI. In vitro prediction of the terfenadine–ketoconazole pharmacokinetic interaction. *J. Clin. Pharmacol.* 34:1222–1227, 1994.
  25. von Moltke LL, Greenblatt DJ, Harmatz JS, Duan SX, Harrel LM, Cotreau-Bibbo MM, Pritchard GA, Wright CE, and Shader RI. Triazolam biotransformation by human liver microsomes in vitro: effects of metabolic inhibitors and clinical confirmation of a predicted interaction with ketoconazole. *J. Pharmacol. Exp. Ther.* 276: 370–379, 1996.
  26. Kobayashi S, Murray S, Watson D, Sesardic D, Davies DS, Boobis AR. The specificity of inhibition of debrisoquine 4-hydroxylase activity by quinidine and quinine in the rat is the reverse of that in man. *Biochem. Pharmacol.* 38:2795–2799, 1989.
  27. von Moltke LL, Greenblatt DJ, Cotreau-Bibbo MM, Duan SX, Harmatz JS, and Shader RI. Prediction of desipramine hydroxylation in vitro by serotonin-reuptake-inhibitor antidepressants, and by quinidine and ketoconazole: a model system to predict drug interaction in vivo. *J. Pharmacol. Exp. Ther.* 268:1278–1283, 1994.
  28. Lewis DFV, Eddershaw PJ, Goldfarb PS, and Tarbit MH. Molecular modelling of CYP3A4 from an alignment with CYP102: identification of key interactions between putative active site residues and CYP3A-specific chemicals. *Xenobiotica* 26:1067–1086, 1996.
  29. Lewis DFV, Eddershaw PJ, Goldfarb PS, Tarbit MH. Molecular modelling of cytochrome P450 2D6 (CYP2D6) based on an alignment with CYP102: structure studies on specific CYP2D6 substrate metabolism. *Xenobiotica* 27:319–340, 1997.
  30. Zomorodi K, and Houston JB. Effect of omeprazole on diazepam disposition in the rat: in vitro and in vivo studies. *Pharm. Res.* 12:1642–1646, 1995.
  31. Gibbs MA, Thummel KE, Shen DD, and Kunze KL. Inhibition of cytochrome P450 3A (CYP 3A) in human intestinal and liver microsomes: Comparison of  $K_i$  values and impact of CYP 3A5 expression. *Drug Metab. Dispos.* 27:180–187, 1999b.
  32. Rodrigues AD, Mulford DJ, Lee RD, Surber BW, Kukulka MJ, Ferrero JL, Thomas SB, Shet MS, and Estabrook RW. In vitro metabolism of terfenadine by a purified recombinant fusion protein containing cytochrome P450 3A4 and NADPH-P450 reductase: comparison to human liver microsomes and precision-cut liver tissue slices. *Drug Metab. Dispos.* 23:765–775, 1995.
  33. Worboys PD, Bradbury A, and Houston B. Kinetics of drug metabolism in rat liver slices II: comparison clearance by liver slices and freshly isolated hepatocytes. *Drug Metab. Dispos.* 24:676–681, 1996.
  34. Ervine CM, Matthew DE, Brennan B, and Houston JB. Comparison of ketoconazole and fluconazole as cytochrome P450 inhibitors: use of steady-state infusion approach

- to achieve plasma concentration–response relationship. *Drug Metab. Dispos.* 24: 211–215, 1996.
35. Sugita O, Sawada Y, Sugiyama Y, Iga T, and Hanano M. Prediction of drug interaction from in vitro plasma protein binding and metabolism. *Biochem. Pharmacol.* 30: 3347–3354, 1981.
  36. Tran A, Rey E, Pons G, et al. Influence of stiripentol on cytochrome P450-mediated metabolic pathways in humans: in vitro and in vivo comparison and in vivo inhibition constants. *Clin. Pharmacol. Ther.* 62:490–504, 1997.
  37. Hsu A, Granneman GR, Cao G, Carothers L, El-Shourbagy T, Baroldi P, Erdman K, Brown F, Sun E, and Leonard M. Pharmacokinetic interactions between two human immunodeficiency virus protease inhibitors, ritonavir and saquinavir. *Clin. Pharmacol. Ther.* 63:453–464, 1998.
  38. Preskorn SH, and Magnus RD. Inhibition of hepatic P450 isoenzymes by serotonin selective reuptake inhibitors: in vitro and in vivo findings and their implications for patient care. *Psychopharmacol. Bull.* 30:251–259, 1994.
  39. Yamano K, Yamamoto K, Kotaki H, Sawada Y, and Iga T. Quantitative prediction of metabolic inhibition of midazolam by itraconazole and ketoconazole in rats: implication of concentrative uptake of inhibitors into liver. *Drug Metab. Dispos.* 27: 395–402, 1999.
  40. Kempf DJ, Marsh KC, Kumar G, Rodrigues AD, Denissen JF, McDonald E, Kulkula MJ, Hsu A, Granneman GR, Baroldi PA, Sun E, Pizzati D, Plattner JJ, Norbeck DW, and Leonard JM. Pharmacokinetic enhancement of inhibitors of human immunodeficiency virus protease by combination with ritonavir. *Antimicrob. Agents Chemother.* 41:654–660, 1997.
  41. Rowland M, and Martin SB. Kinetics of drug–drug interactions. *J. Pharmacokinet. Biopharm.* 1:553–567, 1973.
  42. Lin JH. Species similarities and differences in pharmacokinetics. *Drug Metab. Dispos.* 23:1008–1021, 1995.
  43. Guengerich FP, and Shimada T. Human cytochrome P450 enzymes and chemical carcinogenesis. In: Jeffery EH, ed. *Human Drug Metabolism: From Molecular Biology to Man*. Boca Raton, FL: CRC Press, 1992, pp 5–12.
  44. Guengerich FP. Catalytic selectivity of human cytochrome P450 enzymes: relevance to drug metabolism and toxicity. *Toxicol Lett.* 70:133–138, 1994.
  45. Chiba M, Xu, X, Nishime JA, Balani SK, and Lin JH. Hepatic microsomal metabolism of montelukast, a potent leukotriene D<sub>4</sub> receptor antagonist, in humans. *Drug Metab. Dispos.* 25:1022–1031, 1997.
  46. Inaba T, Tait A, Nakano M, Mahon WA, and Kalow W. Metabolism of diazepam in vitro by human liver: independent variability of *N*-demethylation and C3-hydroxylation. *Drug Metab. Dispos.* 16:605–608, 1988.
  47. Yasumori T, Nagata K, Yang SK, Chen L-S, Murayama N, Yamazoe Y, and Kato R. Cytochrome P450 mediated metabolism of diazepam in human and rat: involvement of human CYP2C in *N*-demethylation in the substrate concentration-dependent manner. *Pharmacogenetics* 3:291–301, 1993.
  48. Jung F, Richardson TH, Raucy JL, and Johnson EF. Diazepam metabolism by cNDA-expressed human 2C P450s: identification of P4502C18 and P4502C19 as low  $K_m$  diazepam *N*-demethylases. *Drug Metab. Dispos.* 25:133–139, 1997.



49. Ono S, Hatanaka T, Miyazawa S, Tsutsui M, Aoyama T, Gonzalez FJ, and Satoh T. Human liver microsomal diazepam metabolism using cDNA-expressed cytochrome P450s: role of CYP2B6, 2C19 and the 3A subfamily. *Xenobiotica* 26:1155–1166, 1996.
50. Pearce RE, Rodrigues AD, Goldstein JA, and Parkinson A. Identification of the human P450 enzymes involved in lansoprazole metabolism. *J. Pharmacol. Exp. Ther.* 277:805–816, 1996.
51. Greenblatt DJ, Wright CE, von Moltke LL, Harmatz JS, Ehrenberg BL, Harrel HK, Counihan M, Tobias S, and Shader RI. Ketoconazole inhibition of triazolam and alprazolam clearance: differential kinetic and dynamic consequences. *Clin. Pharmacol. Ther.* 64:237–247, 1998.
52. Lin JH, and Lu AYH. Role of pharmacokinetics and metabolism in drug discovery and development. *Pharmacol. Rev.* 49:403–449, 1997.
53. Iwatsubo T, Hirota N, Ooie T, Suzuki H, Chiba K, Ishizaki T, Green CE, Tyson CA, and Sugiyama Y. Prediction of in vivo drug metabolism in human liver from in vitro metabolism data. *Pharmacol. Rev.* 73:141–171, 1997.
54. Lave T, Coassolo P, and Reigner B. Prediction of hepatic metabolic clearance based on interspecies allometric scaling techniques and in vitro–in vivo correlations. *Clin. Pharmacokinet.* 36:211–231, 1999.
55. Houston JB. Utility of in vitro drug metabolism data in predicting in vivo metabolic clearance. *Biochem. Pharmacol.* 47:1469–1479, 1994.
56. Houston JB, and Carlile DJ. Prediction of hepatic clearance from microsomes, hepatocytes and liver slices. *Drug Metab. Rev.* 29:891–922, 1997.
57. Lin JH. Role of pharmacokinetics in the discovery and development of indinavir. *Advanced Drug Delivery Rev.* 39:33–49, 1999.

# 12

## In Vivo Probes for Studying Induction and Inhibition of Cytochrome P450 Enzymes in Humans

**Grant R. Wilkinson**

*Vanderbilt University School of Medicine, Nashville, Tennessee*

The discovery of cytochrome P450 (EC1.14.14.1, CYP) in the early 1960s resulted in an explosion of knowledge about this monooxygenase system that still continues today. However, even before this critical event, it was apparent that the oxidative metabolism of drugs often exhibits large interindividual variability; moreover, drug-metabolizing activity may be modulated by environmental, pathophysiological, and genetic factors [1]. Research during the subsequent four decades has largely focused on determining the mechanisms involved in such variability and, in the case of drug metabolism in humans, its clinical significance and importance. In certain situations, genotyping with respect to the presence of allelic variants can be of some value in accounting for this interindividual variability, especially if a strong genetic determinant is involved [2,3]. However, even when genetic polymorphism is present, considerable variability is often present within a phenotypic group [2]; moreover, genotyping cannot take into account the modulation of catalytic activity by environmental and disease-state factors. In vitro approaches using tissue preparations, e.g., liver microsomes and recombinant expressed enzymes, have considerable merit in this regard (see Chaps. 2, 3, and 7). However, the application of such invasive procedures to the clinical situation is obviously limited, especially when studying healthy subjects. Accordingly, so-called “noninvasive” procedures, utilizing readily available fluids such as plasma and saliva or excretions like urine and expired air, form the basis for measuring in vivo metabolizing ability. These measures are generally applied to two related types of experimental questions: what is the basal level

of catalytic activity in an individual subject, i.e., phenotyping, and what are the determinants of interindividual variability within or between populations, e.g., the effects of drug and environmental interactions, genetics, and disease states? The use of “model” compounds, or, as currently termed, *in vivo* probes, has been extensively applied for these purposes since its conception some 30 years ago [4]. This chapter considers the rationale, development, validation, and application of currently useful *in vivo* probes to assess the catalytic activity of specific human CYP isoforms in individual subjects.

## I. ENDOGENOUS COMPOUNDS AS *IN VIVO* PROBES

By analogy to the use of creatinine clearance as an indicator of kidney function and the renal excretion of drugs, attempts have been made to identify an endogenous compound that could be used to assess drug-metabolizing activity. The plasma levels of  $\gamma$ -glutamyltransferase and bilirubin as markers of hepatic dysfunction and the urinary excretion of endogenous 6 $\beta$ -hydroxycortisol and D-glucuronic acid have been sporadically investigated for this purpose over the years [5,6]. With the exception of 6 $\beta$ -hydroxycortisol, these approaches have proven fruitless, but even measurement of the hydroxysteroid's excretion has limitations.

6 $\beta$ -Hydroxycortisol is a minor metabolite of cortisol that is subsequently excreted unchanged in the urine; changes in adrenal corticoid generation, rather than formation of the metabolite, are accounted for by expressing 6 $\beta$ -hydroxycortisol excretion relative to that of cortisol. A number of drugs, e.g., rifampin and anticonvulsant agents, increase the excretion of this metabolite, consistent with the induction of a CYP-mediated pathway [5,6]. CYP3A appears to be the major enzyme involved in the formation of 6 $\beta$ -hydroxycortisol [7,8]; therefore, it has been inferred that changes in the metabolite's excretion reflect modulation of this isoform. Unfortunately, studies to investigate the relationship between 6 $\beta$ -hydroxycortisol excretion and the basal level of CYP3A activity using other *in vivo* probes, such as the erythromycin breath test and midazolam's hydroxylation (Sec. VIII), have been consistently unsuccessful [9–12]. Furthermore, troleandomycin—a mechanism-based inhibitor of CYP3A—was not found to consistently affect the urinary excretion of endogenous 6 $\beta$ -hydroxycortisol, despite the fact the erythromycin breath test was markedly affected by such pretreatment [9]. Collectively, this data raises serious questions regarding the nature and interpretation of any measured increase in urinary 6 $\beta$ -hydroxycortisol excretion over its basal level. It does not appear to reflect hepatic CYP3A alone, and possibly the localization of the isoform in other organs such as the kidney and intestinal epithelium may be contributory to 6 $\beta$ -hydroxycortisol's overall urinary excretion [9,13]. Regardless, the current status of this endogenous probe would appear to be limited to its use as a relatively nonspecific indicator of enhanced oxidative

metabolism following pretreatment with a putative inducing agent [14–16]. As such, any change in the 6 $\beta$ -hydroxycortisol:cortisol ratio requires further investigation with respect to the specific CYP isoform(s) affected, the magnitude of induction, and in the case of CYP3A, whether this occurs in the liver and/or the intestinal epithelium and possibly other extrahepatic tissues.

## II. EXOGENOUS COMPOUNDS AS IN VIVO PROBES

### A. Desirable Phenotypic Trait Characteristics

Beginning with the use of antipyrine [4], administration of a “model” drug to quantitatively assess oxidative drug-metabolizing activity has been an important experimental tool. A number of compounds have been investigated for this purpose. However, with the recognition that cytochrome P450 is a multigene superfamily of related heme-thiolate proteins with separate but potentially overlapping substrate specificities, the goal in recent years has been to develop and use specific probe drugs for the individual isoforms. The major effort has focused on isoforms of the CYP1, CYP2, and CYP3 families, since in humans these appear to be responsible for the metabolism of most drugs and other xenobiotics.

Although the liver is the major organ involved in CYP-mediated drug metabolism, other tissues, including the intestinal epithelium, kidney, and additional organs, all have a similar potential, depending on the individual isoform. However, available *in vivo* probes provide a collective estimate of the measured catalytic function within the body. That is, assessment of activity by an individual organ is usually not possible, despite the fact that this may be critical to interpreting the phenotyping result. For example, it is not unreasonable to suggest that CYP2E1 and CYP2A6 localization within the lung is more important than the isoforms’ hepatic levels in lung carcinogenesis resulting from the metabolic activation of environmental chemicals. However, such a level of refinement is not currently possible.

Following administration of an *in vivo* probe, an experimental measure characterizing the enzyme’s functional activity is obtained. Ideally, this phenotypic trait should exclusively reflect the catalytic activity of a single pathway of metabolism mediated by the isoform of interest. In practice, evidence of such absolute specificity is difficult, if not impossible, to obtain *in vivo*, so the trait measure should be considered a primary, rather than an exclusive, reflection of the isoform’s activity. It is also desirable that the trait measure be sensitive to changes/differences in the enzyme’s catalytic activity produced, for example, by a drug interaction or a genetic factor. Unless this characteristic is present, small changes/differences in activity will not be recognized. Additionally, differences in enzyme activity should ideally result in a linear change in the phenotypic value so that discrimination between values is readily interpretable. If other relation-

ships are present, e.g., the rectangular hyperbola associated with debrisoquine's urinary metabolic ratio used for phenotyping CYP2D6 activity (Sec. VI), large differences in the trait value do not necessarily reflect comparable differences in catalytic activity. It also makes common sense and is esthetically more satisfying if the value of the trait measure increases with an increase in catalytic activity. From a practical standpoint, the phenotyping procedure and associated chemical analyses should be robust so that reliable and reproducible results are obtained regardless of the particular circumstances under which the testing is performed. This is especially important in the case of field studies, where a relatively sophisticated research environment and facilities may not be present, especially with regard to analysis of the biological sample. Also, from the perspective of the individual being phenotyped, it is important that the involved procedure be simple, rapid, and as noninvasive as possible. A further practical issue relates to the availability of the *in vivo* probe and its measured metabolite in the specific locale where the study is being conducted. Ideally, the *in vivo* probe should be available and approved for clinical use worldwide and the phenotypic trait not be affected by the particular dosage form used. In practice, regulatory factors sometimes limit the use of a specific *in vivo* probe; e.g., sparteine is not approved by the Food and Drug Administration in the United States and, therefore, has not been used for investigating CYP2D6 activity in that country.

## B. Pharmacokinetic Basis of Phenotypic Traits

### 1. Plasma Clearance Values

The most appropriate and closest *in vivo* measure of an enzyme's catalytic activity is a drug's intrinsic clearance ( $CL_{int,u}$ ) in terms of its unbound concentration in the plasma [17]. At low drug concentrations relative to the enzyme's  $K_m$  value, i.e., first-order conditions, this may be viewed as the ratio of the apparent  $V_{max}$  to the  $K_m$  value describing metabolism by an individual enzyme. Intrinsic clearance associated with hepatic drug metabolism is closely reflected in a drug's clearance following oral administration ( $CL_o$ ) rather than by intravenous or any other route; moreover, this applies regardless of the rate-limiting process of hepatic clearance, i.e., intrinsic clearance or hepatic blood flow [17]. In addition, any CYP-mediated metabolism occurring in the intestinal epithelium, e.g., CYP3A, is also reflected in the first-pass effect following an oral dose. Accordingly, the "gold standard" approach to estimating the level of metabolic activity of a drug-metabolizing enzyme is to express the ratio of the total area under the plasma concentration–time curve ( $AUC_o$ ) for unbound drug to the administered oral dose ( $D_o$ ) in order to provide an estimate of oral clearance [Eq. (1)]. In practice, the fraction of the drug unbound in plasma ( $f_u$ ) and any changes/differences are rarely taken into

account, but they may be a factor when this parameter is altered. Thus, the estimated intrinsic clearance ( $CL_o$ ) is generally based on total drug concentrations.

$$\frac{D_o}{AUC_o} = CL_o \sim CL_{int} = f_u \cdot CL_{int,u} \quad (1)$$

If more than one metabolic pathway is present and several different enzymes are involved, this must be taken into account by “partitioning” the intrinsic clearance value according to the relative contributions of each enzyme/pathway [17,18]. This is generally accomplished by correcting the total oral clearance by the fraction of the administered dose that is metabolized along the pathway of interest ( $f_{m1}$ ) based on the total amount of the individual metabolite and any associated secondary metabolites excreted in urine ( $Ae_{\infty,m1}$ , where  $m1$  represents a single route of metabolism) [Eq. (2)]:

$$CL_{O,m1} = f_{m1} \cdot CL_o = \frac{Ae_{\infty,m1}}{D_o} \cdot CL_o \quad (2)$$

The major advantage of (fractional) oral clearance as a phenotypic trait is that its value is linearly related to the enzyme’s catalytic activity, provided that first-order conditions are present. This requirement, along with any safety considerations, is the main reason the dose of an in vivo probe should be as low as possible, consistent with analytical considerations. Furthermore, it is possible to directly extrapolate this type of trait measure to the disposition of other drugs whose metabolism is mediated by the measured enzyme and also to place the trait value within a therapeutic context. On the other hand, estimation of oral clearance requires multiple blood and urine collections, often over many hours, that are an inconvenience for the study subject and require considerable amounts of analytical time and effort. Because of this, simpler and less time-consuming approaches have often been used. However, it is not always appreciated that such phenotyping tests provide only an indirect measure of metabolizing activity and may be affected by factors other than the enzyme’s intrinsic clearance. In addition, it is difficult to relate an indirect trait measure to parameters that are of clinical importance, such as the drug’s clearance.

## 2. Urinary Metabolic Ratios

Because it requires only a single measure involving the relative excretion of unchanged drug and metabolite, the urinary metabolic ratio (MR) is the commonest indirect approach used for characterizing drug metabolizing ability. It was first applied with respect to debrisoquine in order to identify individuals with absent or low CYP2D6 activity, i.e., poor metabolizers (Sec. VI.B). This type of trait value expresses the ratio of the amount of unchanged drug, e.g., debrisoquine, to

that of metabolite formed by the isoform of interest, e.g., 4-hydroxydebrisoquine, excreted in a fixed period, e.g., 0–8 hr, following administration of a single oral dose of the *in vivo* probe. Such a ratio provides the greatest discrimination between poor metabolizers (PMs) and extensive metabolizers (EMs), since impaired metabolism results in a large numerator and a small denominator that provide a multiplier effect. As a result, the higher the metabolic activity, the smaller the trait value, and the relationship is a rectangular hyperbola. More important is the fact that a urinary metabolic ratio is an entirely empirical trait measure that reflects pharmacokinetic factors besides that of the enzyme's intrinsic clearance, in particular, the renal clearance of the *in vivo* probe [18]. In the case of debrisoquine, not only is this latter value relatively large but it is time dependent, decreasing from a value approximating renal plasma flow to that of the glomerular filtration rate during the 0–8-hr urine collection period [19]. An alternative approach for calculating a urinary metabolic ratio is to express the amount of metabolite excreted over a fixed time period relative to the sum of this amount and that of unchanged drug [20–21]. This relative recovery ratio (RR) approach, which is similar in form to the fractional urinary recovery of the metabolite, has the attraction that the trait value increases with increasing metabolic activity; however, its value also reflects the probe's renal clearance [18]. In addition, interpretation of such approaches is critically dependent on the completeness of the urine collection; an incomplete specimen will result in underestimation of metabolizing ability.

With certain drugs that have been used as *in vivo* probes, e.g., coumarin, chlorzoxazone, and mephenytoin, essentially no drug is excreted unchanged into the urine; thus, a metabolic ratio approach cannot be used. In the case of mephenytoin (Sec. V.B.1), a ratio expressing the administered oral dose of *S*-mephenytoin to the amount of 4'-hydroxymephenytoin formed by CYP2C19 over a fixed period after dosing—the hydroxylation index (HI)—has been used to discriminate between poor and extensive metabolizers [22,23]. This relationship is similar to the inverse of the urinary recovery of metabolite; therefore, the trait value reflects not only the intrinsic clearance of the isoform of interest but, in addition, the intrinsic clearance values associated with other metabolic pathways and enzymes [18]. Finally, it must be recognized that in the presence of renal dysfunction the validity of a urinary metabolic ratio is highly questionable, because of the trait value's dependency on the renal clearance of the *in vivo* probe and/or its measured metabolite [24].

### 3. Plasma Metabolic Ratios

The urinary metabolic ratio should provide similar information to that of the ratio of the plasma AUC values of the *in vivo* probe drug and metabolite over the collection time period, but it has the practical advantage of a single urine collec-

tion, compared to multiple plasma samples. In order to simplify a plasma-based trait measure, the plasma concentration ratio of metabolite to unchanged drug at a single time point after drug administration has also been used, e.g., plasma 6-hydroxychlorzoxazone:chlorzoxazone ratio as a measure of CYP2E1 activity [25,26]. In this situation, choice of an appropriate sampling time is critical. Sufficient time must elapse for a significant amount of metabolism to have occurred. But if the selected time is too soon after drug administration (1–2 hr), the metabolic ratio will reflect the absorption characteristics of the probe drug in addition to its metabolism. This may vary not only between individuals but also between different manufacturers' products, especially for a generic drug. Sampling during the elimination phase obviates this potential problem; for metabolites whose elimination is formation limited, this represents the best approach, since the ratio should be a constant value over this time period [27]. On the other hand, when removal from the body of the metabolite is elimination limited, e.g., 6-hydroxychlorzoxazone [28], then the plasma levels of drug and metabolite do not decline in parallel. As a result, the metabolic ratio depends not only on the formation of the involved metabolite but also on its elimination relative to that of the parent drug [27]. Unfortunately, such pharmacokinetic considerations rarely appear to be appreciated when such trait measures are developed.

#### 4. CO<sub>2</sub> Breath Tests

*N*-Demethylation is a common CYP-mediated metabolic pathway, and the resulting formaldehyde subsequently enters the one-carbon pool and appears ultimately in the exhaled breath as CO<sub>2</sub>. Labeling of the methyl group of an appropriate in vivo probe with either <sup>14</sup>C or <sup>13</sup>C and measurement of the expired radio- or stable-isotope, therefore, provides an index of the *N*-demethylation process. This is the basis of a number of CO<sub>2</sub> breath tests that have been used to evaluate in vivo drug metabolism. Experimental approaches include both the assessment of the complete time course of exhalation of labeled CO<sub>2</sub> in the breath as well as a more limited sampling including a single time point determination. Moreover, the involved quantitative collection procedure for expired CO<sub>2</sub> is now relatively simple; in certain instances, e.g., erythromycin breath test, a simple kit including all needed items is commercially available. Not only is a CO<sub>2</sub> breath test noninvasive, other than for drug administration, but by using a stable-labeled in vivo probe, studies may be performed in young infants and pregnant women, contrary to the situation when a radiolabel is used, with its associated radiation exposure. A breath test is generally sensitive and reproducible but suffers a major disadvantage in that it is an indirect measure of the responsible *N*-demethylating enzyme and a number of potentially limiting assumptions are involved [29].

The pathway from *N*-demethylation to exhaled CO<sub>2</sub> involves a number of steps many of which are also metabolic, but catalyzed by several enzyme systems



distinct from the initiating CYP isoform. A critical assumption is that all steps prior to (e.g., absorption for a probe that is not administered parenterally) or subsequent to *N*-demethylation are not rate limiting. In general, the steps involved in intermediary metabolism of the one-carbon pool meet this criterion. However, a percentage, estimated to be between 37% and 57%, of labeled *N*-demethylated groups is lost in transit through the one-carbon pool, and this exhibits interindividual variability [29], which is generally not accounted for. A further potential complication is the fact that endogenous CO<sub>2</sub> production is not constant and depends on a number of factors, including physical activity, food intake, body temperature, age, and body size. Accordingly, the use of a mean CO<sub>2</sub> production rate based on either body weight or surface area only partially normalizes for this factor, even if the *in vivo* probe is administered after a period of fasting and the subject under investigation remains recumbent for the period of the study [29]. A final limitation is related to the fact that a CO<sub>2</sub> breath test is a measure of the rate of excretion of the labeled carbon. Accordingly, it is dependent on the volume of distribution of the *in vivo* probe; i.e., a large volume of distribution will result in a reduction in the breath test result, even though the enzyme's intrinsic activity is the same [30,31]. However, interindividual variability in such a parameter is common with all drugs; therefore, the assumption that a constant value is applicable to all subjects results in some error in evaluating the involved enzyme's activity.

### C. Validation of a Phenotypic Trait Measure

Following the *in vitro* discovery that a particular metabolic pathway is mediated by a single CYP isoform and that such metabolism is a major route of elimination, it is not uncommon to speculate that appropriate assessment of the formation of the metabolite *in vivo* could serve as a phenotypic trait measure. Moreover, knowledge of the disposition of the drug and metabolite may indicate a putative quantitative trait for this purpose, e.g., urinary metabolic ratio. However, considerably greater effort and information is, in fact, required before such a trait value can be accepted as a valid measure of the enzyme's metabolic activity. Unfortunately, several of the earlier-developed *in vivo* probes were not rigorously evaluated prior to their application, and interpretation of differences/changes in their trait values is therefore not easy.

Ideally, the trait measure should be correlated directly with the target enzyme's intrinsic clearance as measured, for example, in a tissue biopsy, e.g., liver from the same subjects. However, from a practical standpoint this "gold standard" approach is difficult, especially in health subjects. Moreover, even if applied, it does not address the issue of any extrahepatic metabolism. On the other hand, if the target enzyme exhibits genetic polymorphism such that a null phenotype exists, e.g., CYP2C19 and CYP2D6 (Secs. V.B and VI), advantage of this experiment of nature can be taken. However, in general, the best practical valida-

tion approach would appear to be the demonstration of a close and meaningful correlation between the putative trait value and the in vivo probe's fractional oral clearance determined by a conventional pharmacokinetic study. Care must be taken in such a correlation to ensure that a large enough population size, perhaps 50 or more subjects, be investigated for this purpose and that the data is not inappropriately weighted by individuals with metabolic activities at the extremes of the distribution curve, i.e., subjects having inhibited or induced metabolizing activity. A false and overly positive impression of the trait measure may be obtained if these two factors are not adequately considered; in this regard it is important to recognize that the appropriate statistical measure of the potential usefulness of any correlation is the coefficient determination ( $r^2$ ) and not the regression coefficient ( $r$ ). As a corollary, it is also important to demonstrate that the phenotypic trait also correlates with the fractional clearances of other substrates metabolized by the same target enzyme. Such correlations are particularly critical in establishing that factors other than metabolism are not rate limiting. Additional validation steps generally focus on modulating the target enzymes' activity and its effect on the trait value. Enzyme induction and inhibition, especially involving mechanism-based inhibitors, are usually used for this purpose, with the trait measure appropriately increasing or decreasing. Finally, if metabolism is limited to the liver or if a liver-specific test is required, then changes in the trait value would be expected in the presence of severe liver disease. In this regard, advantage may be taken of the anhepatic period during a liver transplant operation, when no functioning liver is present.

Importantly, no single criterion is sufficient by itself to validate a particular phenotypic trait value; rather, several of the described approaches must provide collective and consistent evidence. Finally, it should be recognized that to some extent validation depends on the purpose to which the in vivo probe is to be applied. For example, if evidence is required to demonstrate the presence or absence of a drug interaction, a less rigorous level of validation might be acceptable than if a quantitative measure of the extent of modulation of metabolic activity is necessary. Thus, the erythromycin breath test (Sec. VIII.B) is a useful in vivo probe for answering such a semiquantitative question, despite the fact that it only reflects hepatic CYP3A4 and not that localized in the intestinal epithelium, which importantly contributes to first-pass metabolism after oral drug administration. Similarly, a trait measure that discriminates between poor and extensive metabolizers associated with a genetic polymorphism may not necessarily be suitable for quantifying smaller within-phenotype differences in metabolism.

#### D. In Vivo Probe Cocktails

Determination of the activity of individual CYP isoforms by use of a single in vivo probe has the advantage that only the enzyme of interest is targeted, and metabolic or other types of interaction occurring because of coadministration of

other drugs can be disregarded. On the other hand, such a narrow focus has disadvantages, given that multiple CYP isoforms are present and more than one of these may be of interest. In this case, a single probe strategy would require multiple sequential studies using different *in vivo* probes to assess each individual enzyme. Not only is this time consuming, but it also results in an inefficient use of resources. To overcome these disadvantages, a “cocktail” approach has been applied based on the simultaneous administration of more than one *in vivo* probe, each of which assesses the metabolic activity of a different enzyme. This concept was originally developed using nonspecific model drugs, such as antipyrine and hexobarbital [32], but more recently it has been applied with cocktails of several ( $n = 2-6$ ) different selective *in vivo* probes. For example, various combinations of debrisoquine or dextromethorphan with mephenytoin, caffeine, nifedipine, coumarin, and chlorzoxazone have been used to simultaneously assess CYP2D6, CYP2C19, CYP1A2, CYP3A, CYP2A6, and CYP2E1 activities, respectively [33–36].

The “cocktail” approach appears to be particularly suited to indirect phenotypic trait values based on a single time-point determination, e.g., metabolic ratios, where only one or two samples are sufficient for the experimental objective. For example, it is an attractive strategy for investigating the CYP isoform selectivity of enzyme inhibition or induction of a drug prior to more focused studies [34,37]. However, a critical issue in the application of any “cocktail” study is whether one or more of the individual drugs interacts with another in the mixture. This may occur within the body through a metabolic interaction such as inhibition of another CYP isoform’s catalytic activity, or a pharmacodynamic interaction may occur that either affects the phenotypic trait value of another drug or results in an undesirable clinical effect. Accordingly, it is important to establish prior to application not only that combining two or more *in vivo* probes has no effect on any of the individual phenotypic trait values but also that the combination is safe. A second potential complicating factor is that multiple drugs and their metabolites are present and must be analyzed in the same biological sample. Accordingly, the involved analytical methodologies must be not only sufficiently sensitive but also specific so that no analytical interference is present.

A related approach to using a “cocktail” strategy that has been suggested is based on measuring the metabolism of a single *in vivo* probe in which two or more metabolites are formed involving different CYP isoforms. For example, the *O*-demethylation of dextromethorphan (DTM) to dextrorphan (DT) is mediated by CYP2D6, whereas CYP3A is importantly involved in the *N*-demethylation pathway leading to the formation of 3-methoxymorphinan (3MM) [38]. Accordingly, it has been proposed that the urinary metabolic ratios DTM:DT and DTM:3MM could be used to separately assess the metabolic activities of the two involved isoforms [39,40].

However, the demonstration that enzymes other than CYP3A may also significantly contribute to *N*-demethylation raises questions as to the reliability and validity of the DTM:3MM metabolic ratio as a measure of CYP3A activity [41]. In principle, the stereo- and regioselective metabolism of warfarin could also serve to assess the activity of multiple CYP isoforms. For example, *S*-warfarin is primarily metabolized to 7-hydroxywarfarin by CYP2C9, whereas CYP1A2 is responsible for *R*-enantiomer's 6- and 8-hydroxylation; also, CYP3A is importantly involved in the formation of 10-hydroxy-*R*-warfarin, and hydroxylation of *R*-warfarin at the 8-position is mediated mainly by CYP2C19 [42,43]. However, this approach has yet to be extended to the in vivo situation, probably because of analytical considerations, which would be further complicated by the small dose of warfarin that would need to be used for safety purposes in healthy subjects undergoing such phenotyping. Nevertheless, the overall strategy of a single probe and multiple enzymes appears to be worthwhile pursuing further.

### III. CYTOCHROME P450 1A2 (CYP1A2)

The CYP1A subfamily consists of two members, CYP1A1 and CYP1A2, which are both important in the metabolic activation of chemical procarcinogens. However, unlike its related isoform, CYP1A1 is not constitutively expressed in the liver and is primarily an extrahepatic enzyme; moreover, it is not involved in the metabolism of therapeutically useful drugs. Accordingly, the in vivo probes investigated for this subfamily have been directed almost exclusively toward CYP1A2. Drugs whose metabolism importantly involves CYP1A2 include phenacetin (*O*-de-ethylation), caffeine (*N*1-, *N*3-, and *N*7-demethylation), theophylline (*N*1- and *N*3-demethylation), tacrine (1- and 7-hydroxylation), tamoxifen (*N*-demethylation), *R*-warfarin (6- and 8-hydroxylation), and acetaminophen (ring oxidation) [44]. A number of these substrates have been studied and applied as in vivo probes in humans.

#### A. Caffeine

Caffeine (1,3,7-trimethylxanthine) is one of the most widely and frequently consumed xenobiotics throughout the world. The diet is the principal source of such intake, with estimates of per capita daily consumption in Europe and North America exceeding 200 mg/day. Following oral administration, caffeine is rapidly and completely absorbed, and it is then eliminated essentially completely (>95%) by metabolism. Such metabolism is complex, with at least 17 metabolites being formed and excreted in the urine. However, these arise from three primary pathways that contribute to over 95% of the drug's overall metabolic clearance; *N*3-demethylation to form paraxanthine (80%), *N*1-demethylation to

form theobromine (11%), and *N*7-demethylation to form theophylline (4%). *C*8-Hydroxylation and *C*8–*N*9 bond scission together account for the remaining 5% or so of caffeine’s metabolism. Subsequently, these primary metabolites are extensively further metabolized (Fig. 1). Importantly, CYP1A2 is almost exclusively responsible for all three of the initial *N*-demethylation steps, especially after small doses. At high in vitro substrate concentrations, CYP2E1 and possibly other CYP isoforms are contributory, but this is of little relevance to caffeine exposure in vivo. Not surprising, therefore, caffeine has become the most widely used in vivo probe for assessing CYP1A2 activity [45,46].

1. Caffeine Oral Clearance

Over 95% of caffeine’s plasma clearance can be accounted for by the three *N*-demethylation pathways, all of which are mediated exclusively by CYP1A2 [45,46]. Accordingly, measurement of the in vivo probe’s oral clearance is the “gold standard” by which this isoform’s activity can be evaluated. This notion is supported by reasonably strong correlation ( $r = 0.74, p < 0.01$ ) between this parameter and caffeine’s intrinsic clearance with regard to *N*3-demethylation, as

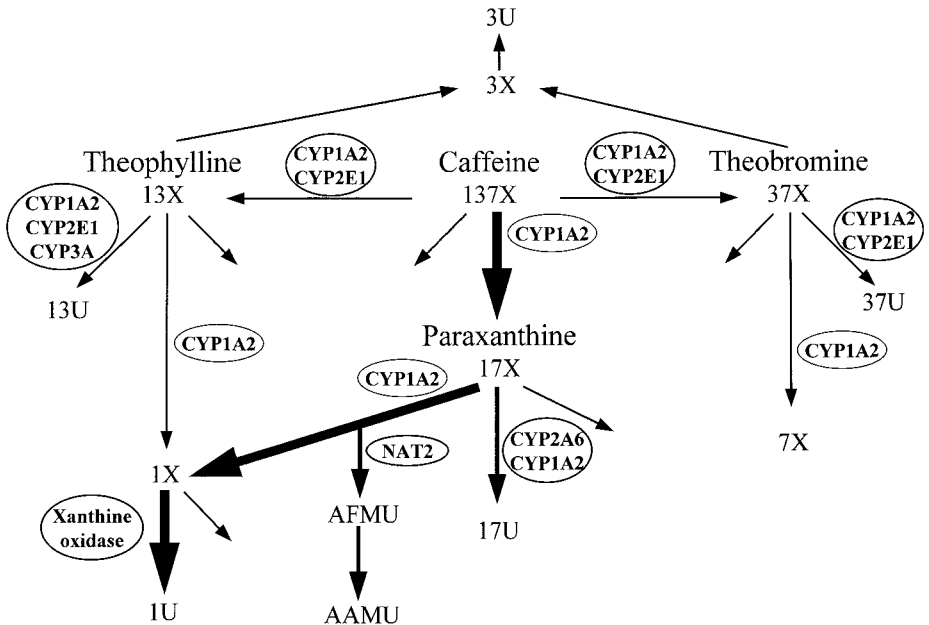


**Figure 1** Pathways of caffeine metabolism and involved CYP isoforms (abbreviations described in text).

estimated *in vitro* from liver microsomes obtained from the same subjects studied *in vivo* [47]. In practice, phenotyping is a simple procedure involving the oral administration of a single 100–200-mg dose of caffeine followed by serial blood sampling over 12–24 hr and appropriate HPLC measurement of caffeine's plasma level and pharmacokinetic analysis. The caffeine may be given in the form of an available over-the-counter formulation or as a measured amount of coffee of known caffeine content or similarly as a cola drink. Some investigators have administered caffeine intravenously and used systemic clearance as the phenotypic trait measure [48,49]. However, since caffeine is a low-clearance drug, the potential value of this approach is not particularly great and is outweighed by the disadvantage of administering the caffeine by intravenous injection. Because caffeine is ubiquitous in the diet, phenotyping involves a caffeine-free period of 1–3 days prior to and also during the study period. However, if measurable caffeine is present in the plasma prior to administration of the *in vivo* probe, a pharmacokinetically-based correction can take this into account [47]. Several studies have demonstrated that caffeine's oral clearance is appropriately altered by factors that have been shown to modulate CYP1A2 activity either *in vitro* or in animals, e.g., tobacco usage and administration of other inducers, oral contraceptives, and mechanism-based inhibitors [46]. In addition, this phenotypic trait value is robust and reproducible when studied in the same subjects over a 4-month period [50]. In order to minimize the number of required blood samples, it has been suggested that estimation of caffeine's elimination half-life based on three or four postabsorption plasma levels could provide an alternative phenotypic trait measure [51,52]. Since caffeine's volume of distribution is similar to total body water, such an estimate can also be used to obtain an approximate value of the probe's clearance [48]. However, such approaches still require that the blood sampling period be sufficiently long to accurately define caffeine's elimination half-life, which ranges from about 2 to 12 hr in healthy subjects but can be considerably longer in patients with liver disease or when CYP1A2 is inhibited because of a drug interaction. This factor probably accounts for the lower accuracy and higher intrasubject variability found with foreshortened sampling protocols [49]. Recently, a Bayesian estimation of caffeine clearance based on a single plasma level obtained at either 12 hr or 24 hr after intravenous administration of the probe was shown to be well correlated with the directly determined value [49]. Further study of this simple approach would appear warranted.

Caffeine is not extensively bound to plasma proteins; therefore, it readily distributes into saliva with a saliva:plasma concentration ratio of total drug between 0.74 and 0.94 [52,53]. Not surprisingly, therefore, a close correlation exists between saliva and plasma caffeine levels and derived pharmacokinetic parameters. Accordingly, an alternative approach for estimating caffeine's oral clearance following administration of the *in vivo* probe is to measure salivary levels of the drug [47,52–55]. Because of its noninvasiveness, even when salivary flow rate

is stimulated by chewing Parafilm® or by the application of citric acid to the tongue, a large number of samples may be obtained for pharmacokinetic analysis, and collection can be extended beyond the clinical setting. Indeed, comparisons of caffeine's oral clearance values independently determined from plasma and saliva concentrations are essentially the same [47,53–55].

In an attempt to further simplify the caffeine phenotyping test, a trait measure based on the plasma or salivary paraxanthine:caffeine concentration ratio between 3 hr and 7 hr after administration of the probe has been suggested [56]. High linear correlations ( $>0.89$ ) have been observed between this trait value and caffeine's oral clearance, and if necessary, a predicted caffeine clearance value may be calculated from the ratio [56]. Currently, this phenotyping approach appears to be the simplest and most noninvasive means of readily assessing CYP1A2 activity using caffeine as a probe; in addition, the method is reproducible and appears to be robust [56], despite the theoretical dependency of the trait value on the urine flow rate [51].

## 2. Caffeine and Phenacetin Breath Tests

The use of radiolabeled caffeine to determine drug-metabolizing ability based on a  $^{14}\text{CO}_2$  breath test was an early example of the applicability of this general approach [57,58], even before it was recognized that this was a measure of CYP1A2 activity. Generally, labeling has been at the *N*-3 methyl position, since this is the site of the major pathway of caffeine metabolism; however, labeling of all three *N*-methyl groups [58] and *N*-7 labeling has also been investigated [59]. Additionally, both radio- ( $^{14}\text{C}$ ) and stable- ( $^{13}\text{C}$ ) labeling has been successfully used [57–64]. The need for mass spectrometry-based analytical methodology in the case of stable-labeled caffeine is in most instances outweighed by the safety issue related to exposure to radioactivity associated with the use of radiolabeled carbon. Other than equipment requirements, the caffeine breath test is simple to perform and for [ $^{13}\text{C}$ ]-(*N*-3-methyl) caffeine a commercial kit is available for this purpose. Typically, exhaled breath is collected at several intervals up to 1–8 hr following an oral dose of labeled caffeine. Either the cumulative amount [57–63] or the hourly rate [64] of labeled  $\text{CO}_2$  excretion is used as the phenotypic trait value. The caffeine breath test appears to be reproducible, although extensive testing of this characteristic has not been reported. However, excellent correlations ( $r = 0.84\text{--}0.90$ ) have been found between the 2-hr cumulative caffeine breath test and the drug's oral clearance [58,62,63]. In addition, the breath test has been shown to alter in response to modulating conditions that either decrease or increase CYP1A2 activity [45,60,61].

The *O*-de-ethylation of phenacetin is CYP1A2-mediated and results in the liberation of acetaldehyde that is subsequently metabolized to acetate and then  $\text{CO}_2$ . Thus, a breath test based on the use of phenacetin labeled with  $^{14}\text{C}$  in the

1-position of the ethyl side chain could function to assess CYP1A2 activity. Early studies demonstrated the feasibility of this approach and its potential application to evaluating hepatic function [65,66]. No extensive validation was attempted, so it is difficult to determine how well this test reflects the enzyme's intrinsic clearance, rather than perhaps some other determinant, such as liver blood flow. However, the situation appears to be moot, since phenacetin is no longer an approved drug worldwide, because of its renal side effects following chronic dosing; accordingly, further studies of this approach are unlikely.

### 3. Urinary Metabolic Ratios

Following initial *N*-demethylation, caffeine's primary metabolites undergo extensive further metabolism (Fig. 1). For example, the major metabolite paraxanthine (17X) is demethylated to form 1-methylxanthine (1X), 1-methylurate (1U), and 5-acetylamino-6-formylamino-3-methyluracil (AFMU), which spontaneously degrades, especially under basic assay conditions, to 5-acetylamino-6-amino-3-methyluracil (AAMU) [45]. These metabolites account for about 20%, 40%, and 15%, respectively, of the urinary recovery of caffeine-derived products. In addition, approximately 10% of 17X is excreted unchanged and another 20% is hydroxylated to form 1,7-dimethylurate (17U). Theobromine (37X) is in part excreted unchanged (~10%), and about 20% is metabolized to 3-methylurate (37U) and approximately 50% to 7-methylxanthine (7X). About 10–15% of theophylline (13X) is excreted into urine, with about 50% of this primary metabolite being metabolized to 1,3-demethylurate (13U) and some 23% to 1-methylurate (1U). Finally, a small amount of caffeine is excreted unchanged in urine, and some additional minor metabolites are formed [45,51].

CYP1A2 is primarily responsible for the *N*1-, *N*3-, and *N*7-monodemethylations of 17X, 37X, and 13X, respectively, and also the 8-hydroxylation of these primary metabolites. However, other CYP isoforms, e.g., CYP2A6, CYP2E1, and CYP3A, are also importantly involved in the formation of the various dimethyluric acids (Fig. 1). Polymorphic *N*-acetyltransferase-2 (NAT2) mediates the conversion of an unstable 17X intermediate to AFMU, and xanthine oxidase is responsible for the oxidation of 1X to 1U [45,51]. Thus, the metabolism of caffeine results in a complex urinary recovery profile involving multiple primary and secondary metabolites as well as unchanged drug (Fig. 1).

Because CYP1A2 is predominantly involved in caffeine's primary and secondary metabolism, a urinary metabolic ratio approach has been applied with an expectation that this would provide a simple and convenient noninvasive means of assessing the isoform's metabolic activity. Over 12 different urinary molar metabolic ratios have been suggested as putative trait measures of CYP1A2 activity, generally based on a 0–24-hr urine collection following an oral dose of caffeine, although "spot" sampling within a shorter defined time period (2–6 hr)



has also been used [45,51,67–69]. The most common of these are shown in Table 1. A major difficulty in the application of these phenotypic trait measures is that they are essentially all empirical, and until recently their limitations were not understood or, more importantly, appreciated. From the metabolic scheme shown in Fig. 1, it is clear that CYP1A2 activity affects both the numerator and the denominator of the metabolic ratios to a varying extent. Also, CYP isoforms other than CYP1A2 and urine flow rate affect the excretion of caffeine and several of its metabolites [51,70]. All of these factors exhibit intra- and interindividual variability, so it is not surprising that in a study involving 237 healthy subjects, the common metabolic ratios appeared to reflect three different parameters, and no one ratio correlated particularly well with any other [68]. Ratios 1, 2, and 5 (Table 1) were the best correlated ratios ( $r = 0.73$ – $0.88$ ), but, even so, considerable variability was present within the relationship. A rigorous sensitivity analysis based on a pharmacokinetic model of caffeine's metabolism and urinary excretion profile identified a number of confounding variables that contributed to this situation [51]. Moreover, this analysis concluded that none of the caffeine urinary metabolic ratios are specific for CYP1A2, although Ratio 4 may be useful when studying the modulation of CYP1A2 activity within the same subject. It was also suggested that the plasma–saliva ratio of 17X:137X measured a short time after caffeine administration might be a robust CYP1A2 marker. Experimental investi-

**Table 1** Common Caffeine Urinary Metabolite Ratios Used as Phenotypic Measures of CYP1A2 Activity

		Refs.
Ratio 1	$\frac{(17X)}{(137X)}$	47,56,61,83
Ratio 2	$\frac{(17U) + (17X)}{(137X)}$	47,56,61,69–73,81
Ratio 3	$\frac{(AFMU) + (1X) + (1U)}{(17X)}$	69,74
Ratio 4	$\frac{(AFMU) + (1X) + (1U)}{(17U)}$	45,47,54,56,69,70,75–80
Ratio 5	$\frac{(AFMU) + (1X) + (1U) + (17X)}{(137X)}$	68
Other ratios	Various	51,69,78

For simplicity AFMU is used in all equations when the actual analyte is AAMU after converting all AFMU to AAMU.

gations have subsequently confirmed these theoretical findings. For example, significant correlations were obtained between Ratio 4 and caffeine's oral clearance ( $r = 0.66\text{--}0.77$ ,  $p < 0.002$ ) by several different investigators [47,69,70]. By contrast, the correlations between Ratios 1 and 2 and caffeine clearance were generally much poorer [47,69,70]; other, less common metabolic ratios were also found to be poor measures of caffeine clearance [69]. Thus, with the exception of Ratio 4, the validity of other urinary metabolic ratios would appear to be questionable; however, considerable experimental data indicates that this urinary metabolic ratio is a robust and reproducible trait measure that is sensitive to the modulation of CYP1A2 activity [45].

Unfortunately, many investigators have used various of the caffeine urinary metabolic ratios without recognizing their potential limitations. As a result, conclusions drawn from the interpretation of such flawed data may be inaccurate. One area where this may exist and remains a controversial issue concerns the population distribution of inferred CYP1A2 activity. For example, several studies using Ratio 1 or 2 have concluded that CYP1A2 activity is either bi- or trimodally distributed within the population, and "slow," "intermediate," and "rapid" phenotypes can be identified; additionally, interethnic and racial differences in the frequency of these putative phenotypes exist [71–73]. These observations are in strong contrast to similar studies by other investigators, using Ratio 4 as an index of CYP1A2 activity, where a log-normal distribution has been found [70,75–80]. Moreover, numerous studies based on the determination of caffeine's plasma clearance in large numbers of subjects have not provided any evidence of discrete subgroups with either low or high values within a log-normal distribution. Modeling analysis also indicates the likelihood that the polymodal distribution could be an artifact [51]; this is supported by the observations that despite the fact that the frequency distributions of Ratio 4 and caffeine clearance were unimodal, the distribution for Ratio 2 in the same subjects was bimodal [70]. Also, the effects of cigarette smoking on CYP1A2 activity, as measured by Ratio 2, was noted to depend on racial background [71,81], an observation that again is inconsistent with data based on clearance or Ratio 4 measures and one that is difficult to mechanistically explain. These discordances might be considered trivial except for the potential value of identifying the level of CYP1A2 activity as a possible risk factor for the development of certain types of cancer [81]. Use of a valid *in vivo* probe would appear to be critical for such studies.

Although the validity of the urinary metabolic ratio approach for assessing CYP1A2 activity is debatable, there is substantial evidence indicating that its use for determining *N*-acetyltransferase-2 (NAT2) activity is appropriate. This application is based on the involvement of NAT2 in the formation of AFMU, and both the molar ratios of urinary AFMU:1MX and AFMU:(AFMU + 1X + 1U) have been demonstrated to be reliable phenotypic indicators that categorize populations into three subgroups according to genotype [45–47,67,80,82–85]. In

practice, pretreatment of the urine to convert all of the AFMU to AAMU is advisable to avoid misclassification [45,85]. Similarly, the molar ratios 1U:1X and 1U:(1X + 1U) have been used to determine xanthine oxidase activity [74,76,80].

The metabolism of theophylline (1,3-dimethylxanthine) is similar to that of caffeine but less complex (*vide supra*). Consequently, some consideration has been given to using it as a CYP1A2 probe. However, potential analytical sensitivity problems and, more importantly, safety considerations do not suggest that theophylline has any advantage over caffeine for this purpose [86].

In summary, caffeine is an acceptable and validated *in vivo* probe for assessing CYP1A2 activity in humans. The “gold standard” approach depends on determination of the drug’s oral clearance following a single phenotyping dose under dietary caffeine-free conditions. Both plasma and saliva concentrations may be used for this purpose. Comparisons of caffeine’s elimination half-life may be an alternative approach when within-subject changes in CYP1A2 activity are being investigated. However, such temporal monitoring applicable to drug interactions is probably best accomplished by the 17X:1X plasma/saliva concentration ratio determined at a single time point after caffeine administration. Alternatively, a caffeine breath test can similarly provide such within-subject information. Interpretation of caffeine urinary metabolic ratios is more difficult than with other approaches, and that based on the molar ratio (AFMU + 1X + 1U):17U (Ratio 4) is probably the best of those developed. However, given the comparable simplicity and noninvasiveness of the salivary 17X:1X ratio, it is difficult to justify why even urinary Ratio 4 should continue to be used.

#### IV. CYTOCHROME P450 2A6 (CYP2A6)

CYP2A6 appears to be the only catalytically active isoform of the CYP2A subfamily that is expressed in humans. Activity is localized mainly in the liver; however, extrahepatic distribution is also present, especially in the nasal epithelium and lung. Such localization is likely to be critically important, since CYP2A6 mediates the metabolism and activation of nicotine, cotinine, and tobacco-smoke-related nitrosamines like 4-(methylnitrosamino)-1-(3-pyridyl)-1-butanone (NNK), 4-(methylnitrosamino)-1-(3-pyridyl)-1-butanol (NNAL), and *N*-nitrosornicotine (NNN), which are among the most potent of known lung carcinogens. CYP2A6 also activates a number of other established procarcinogens, many of which are also metabolized by CYP2E1 [44]. Only a small number of drugs are currently known to be importantly metabolized by CYP2A6; these include coumarin [87,88], methoxyflurane [89], halothane [90], valproic acid [91], disulfiram [92], losigamone [93], letrozole [94], and (+)-*cis*-3,5-dimethyl-2(3-pyridyl) thiazolidine-4-one (SM-12502) [95]. Importantly, genetic polymorphisms are present in the CYP2A6 gene, and, although current data is relatively

limited, these appear to have functional consequences. At least three defective alleles have been reported, the most prevalent of which (CYP2A6\*2) appears to be a Leu 160 His substitution that yields an inactive enzyme [96–99]. By contrast, a deletion mutation (CYP2A6\*4) is the most common variant (15–20%) in Asian populations (100). Duplication of the CYP2A6 gene also occurs and appears to be associated with increased catalytic activity (101).

The 7-hydroxylation of coumarin (1,2-benzopyrone) is a major urinary metabolic pathway that accounts for about 60% of an orally administered dose [102]. This pathway is almost exclusively mediated by CYP2A6 [87,88] and forms the basis of the “coumarin index” or “2-hr coumarin test” used to measure *in vivo* CYP2A6 activity. The phenotypic trait measure is simply the percentage of a 5-mg dose of coumarin excreted in urine as 7-hydroxycoumarin over the 0–2-hr period following oral administration in the fasted state [102]. Because the 7-hydroxy metabolite is excreted mainly as a conjugate, urine is pretreated with  $\beta$ -glucuronidase prior to analysis, and a methodology based on chromatographic separation would appear to be preferable to one using solvent extraction [103]. Application of this phenotyping procedure to various population groups has shown that the trait measure exhibits considerable interindividual variability, and it is unimodally distributed in a normal fashion [102–104]. While a few individuals with lower values could be identified, no clear polymorphism was apparent, consistent with the low frequency of the CYP2A6\*2 allele in Caucasians. On the other hand, a gene dose effect has been reported with respect to individual CYP2A6\*1 homozygotes, CYP2A6\*1/CYP2A6\*2 heterozygotes, and CYP2A6\*2 homozygotes [105]. Accordingly, it would be expected that in the general population all three phenotypes (extensive, intermediate, and poor) would be present.

The “coumarin index,” however, has several problems that make it less than ideal as a CYP2A6 trait measure. First, is the fact that the trait value is entirely empirical and has been validated and characterized to only a very limited extent. Accordingly, its sensitivity to determinants of CYP2A6 activity are largely unknown, other than that its value is reduced by age [106] and the administration of grapefruit juice [107] but not disulfiram [108], and that it is increased by antiepileptic drugs [109]. As expected, severe but not mild liver disease reduces the urinary recovery of 7-hydroxycoumarin, but, not unexpectedly, renal dysfunction has also been found to affect the trait value [109]. A second difficulty is that the “coumarin index” is an indirect measure of CYP2A6 activity, and perhaps, more importantly, it is unlikely that it can ever be validated against a “gold standard” such as the formation clearance of 7-hydroxycoumarin. This is because of the extreme analytical difficulties associated with measuring plasma coumarin levels because of its relatively high volatility, and this problem is further compounded by the low dose used for phenotyping (5 mg). Coumarin is also excreted in the urine as a result of dietary and environmental exposure through

fragrances and other sources. Such daily exposure may be as high as 25 mg [110], which probably accounts for the finding that in certain subjects the urinary molar recovery of 7-hydroxycoumarin exceeds the molar dose of coumarin administered to determine the trait value [103,110]. An additional consideration, especially in North America, is the absence of an available approved formulation containing coumarin, which was removed from the market 45 years ago because of its hepatotoxicity and carcinogenic properties in animals [111]. More recently, limited use of coumarin in certain types of cancer has been investigated [112], but the strength of the available tablet is 100 mg, i.e., 20-fold greater than the dose used to determine the "coumarin index." Because of these problems, attempts have been made to develop an alternative phenotyping method to assess *in vivo* CYP2A6 activity.

A potential method that was recently reported is based on a metabolic ratio approach, namely, the 2-hydroxyphenylacetic acid:7-hydroxycoumarin ratio in a 0–8-hr urine sample following oral administration of 2 mg coumarin [110]. 2-Hydroxyphenylacetic acid is the terminal metabolite of an alternative pathway of coumarin metabolism besides 7-hydroxylation, and usually accounts for about 2.5–30% of the administered dose. The frequency distribution of this trait measured in 103 subjects identified two individuals with values markedly greater than the remainder of the population. Moreover, within the major subgroup, there was evidence of overlapping bimodality. Unfortunately, the CYP2A6 genotypes of the subjects were not determined to show that the apparent phenotypes reflected the genetic polymorphism. Future studies will undoubtedly investigate this possibility and demonstrate the value of this urinary metabolic ratio as an indicator of CYP2A6 activity.

The major human urinary metabolites of nicotine are cotinine, nicotine *N'*-oxide, and *trans*-3'-hydroxycotinine [113]. CYP2A6 appears to be the major enzyme responsible for formation of an iminium ion that is the first step in the C-5 oxidation of nicotine to cotinine and also the subsequent 3-hydroxylation of this metabolite [114,115]. These facts, coupled with the known acute safety profile and wide use of nicotine through tobacco smoking, suggests that appropriate measurement of the drug's metabolism might provide a means to assess *in vivo* CYP2A6 activity. One reported approach is based on the 30-min intravenous infusion of a 50:50 mixture (2  $\mu$ g base/kg) of 3',3'-dideuterium-labeled nicotine and 2,4,5,6-tetradeutero cotinine followed by serial blood sampling over the following 96 hr and a 0–8-hr urine collection [116,117]. Using gas chromatography–mass spectrometric–based assays, the levels of nicotine and cotinine derived from each stable-labeled form are measured. Appropriate pharmacokinetic analysis then allows estimation of nicotine's formation clearance to cotinine and also the latter's clearance. To date, this methodology has been applied primarily to investigating nicotine's metabolism within the context of cigarette smoking and addiction [116,117]. It should be noted, however, that an individual deficient in

the CYP2A6-mediated conversion of nicotine to nicotine was identified using this approach [118]. Clearly, substantial further research is required before a simple and routine nicotine/cotinine-based phenotyping procedure for CYP2A6 is established. Despite the need for stable-labeled drugs and the associated sophisticated instrumentation for their measurement, such an approach would provide a “gold-standard” against which alternative trait measures such as the “coumarin index” or others could be evaluated and validated. Possibly, a simpler, single-point plasma- or urine-based measure could be developed using nicotine/cotinine. Finally, if the new drug candidate SM-12502 ever becomes clinically available, it is possible that an appropriate phenotyping measure could be developed using this drug since a genotype:phenotype relationship appears to be present [95,100].

## V. CYTOCHROME P450 2C (CYP2C)

Four closely related CYP2C9 genes have been definitively identified in humans: CYP2C8, CYP2C9, CYP2C18, and CYP2C19. However, additional genes/gene-like sequences are present. At one time, CYP2C10 was thought to be a discrete protein but is now considered to be an allelic variant of CYP2C9 or possibly a cloning artifact. Little information is currently available regarding CYP2C8, especially substrates that are preferentially metabolized by this isoform. One such reaction is the 6 $\alpha$ -hydroxylation of taxol, and the 4-hydroxylations of retinol and retinoic acid also appear to be CYP2C8-mediated. CYP2C18 appears to be a minor member of the CYP2C subfamily; to date, no metabolic reactions have been demonstrated to be selectively catalyzed by this enzyme [44]. On the other hand, many drugs are substrates of CYP2C9 and CYP2C19, and in many instances the involved metabolic reactions are highly specific. Accordingly, these two isoforms have received the most attention with regard to the development and application of in vivo probes.

### A. Cytochrome P450 2C9 (CYP2C9)

CYP2C9 is importantly involved in the oxidation of a large number of drugs, many of them widely used in clinical practice. Such drugs for which the isoform catalyzes the formation of a principal metabolite include phenytoin, tolbutamide, fluoxetine, losartan, *S*-warfarin, torsemide, valproic acid, and many nonsteroidal anti-inflammatory agents (diclofenac, ibuprofen, naproxen, piroxicam, suprofen, and tenoxicam). Thus, most, but not all, CYP2C9 substrates are weak acids with pKa values between 3.8 and 8.1 [119]. Increasing evidence indicates that genetic polymorphisms are present in the CYP2C9 gene that have functional consequences. Three alleles resulting from Arg  $\rightarrow$  Cys and Ile  $\rightarrow$  Leu substitutions at amino acids 144 and 359 have been noted. CYP2C9\*1 (Arg<sup>144</sup>/Ile<sup>359</sup>) represents

the wild-type protein, whereas CYP2C9\*2 (Cys<sup>144</sup>/Ile<sup>359</sup>) and CYP2C9\*3 (Arg<sup>144</sup>/Leu<sup>359</sup>) appear to be relatively rare variants. As with many other genetic polymorphisms, population frequency distributions differ according to racial ancestry; for example, CYP2C9\*2 has not yet been found in Asian groups (Chinese and Japanese), and its prevalence is also very low in African-Americans [119].

In vitro studies with human liver microsomes and expressed CYP2C9 allelic variants have found markedly impaired catalytic activity of CYP2C9\*3 compared to CYP2C9\*1 [119]. Furthermore, this difference has also been noted to be present in patients receiving warfarin therapy, where a gene-dose effect leads to reduced clearance of the anticoagulant's *S*-enantiomer [120–122]. As a result, a dangerously exacerbated therapeutic response to normal doses of racemic warfarin is produced in CYP2C9\*3/CYP2C9\*3 homozygotes [120]. Similarly, an individual identified as a poor metabolizer of tolbutamide was also subsequently found to be homozygous for CYP2C9\*3 [123]; in the clinical trials associated with the development of losartan, two subjects, corresponding to <1% of the study population, had markedly impaired conversion of the drug to an active metabolite and both were CYP2C9\*3/CYP2C9\*3 homozygotes [124]. Comparable information regarding CYP2C9\*2 is currently less definitive, since in vitro studies provide conflicting data on the effect of the Arg 144 Cys substitution [119]. And, while the median warfarin maintenance dose was 20% lower in CYP2C9\*1/CYP2C9\*2 heterozygotes compared to homozygous wild-type patients, there was considerable overlap in the dosage requirements [125].

Thus, valuable information on CYP2C9 activity in vivo has been obtained through studies of warfarin's metabolism, and it has even been suggested that the drug's *S*:*R* enantiomeric concentration ratio in plasma could be used to identify homozygous CYP2C9\*3 patients [121]. However, for safety and analytical reasons it is unlikely that the anticoagulant could be used as an in vivo probe in healthy subjects. A similar safety issue also would appear to apply to phenytoin, despite the fact that its major route of metabolism, viz, 4-hydroxylation, is mediated by CYP2C9. Moreover, the plasma clearance of phenytoin exhibits nonlinearity due to saturable metabolism, and a urinary 4-hydroxyphenytoin:phenytoin metabolic ratio has been shown to be overly variable and of limited usefulness as a phenotypic trait measure of CYP2C9 activity [126]. Accordingly, efforts have been directed toward other potential drugs.

## 1. Tolbutamide

The metabolism of tolbutamide (1-butyl-3-*p*-tolysulfonylurea) in humans involves a single pathway, with the initial and rate-limiting step being tolyl methylhydroxylation to form hydroxytolbutamide, which is further oxidized to carboxy-tolbutamide by alcohol and aldehyde dehydrogenases. Overall, this pathway of metabolism accounts for up to 85% of tolbutamide's clearance and is exclusively mediated by CYP2C9 [119]. Accordingly, determination of tolbutamide's (frac-

tional) clearance following a single oral dose (500 mg) has been used as a phenotypic trait value for assessing in vivo CYP2C9 activity [127]. Since the drug's half-life ranges between 4 and 12 hr, this approach requires not only multiple blood samples but collection over a considerable time period (24–36 hr). An alternative and simpler metabolic ratio approach has also been developed based on the relative recovery of metabolites and unchanged drug excreted into urine over the 6–12-hr period following a 500-mg oral dose of tolbutamide. Initially, this ratio—(hydroxytolbutamide + carboxytolbutamide):tolbutamide—was shown to be sensitive to the inhibition of CYP2C9 activity by pretreatment with sulfaphenazole [128]. Subsequently, the trait measure was shown to be unimodally distributed in an Australian population of 106 healthy subjects [129], which is not surprising given the low frequency of the CYP2C9\*3 allele (vide supra). Also, a previously identified poor metabolizer, who was later shown to be a CYP2C9\*3 homozygote [123], was found to have a markedly lower value than the reference population [129]. It therefore appears that tolbutamide is a useful in vivo probe for CYP2C9. However, such use is not without problems, in particular, the safety issue associated with the hypoglycemic response produced by tolbutamide administration. This is not usually a problem in subjects who have been fed. However, in fasted individuals, blood glucose levels may be significantly reduced by tolbutamide and require reversal using glucose supplementation [130]; use of a lower dose (250 mg) may obviate this problem. Clearly, this limits application of the test to a controlled clinical situation.

## 2. Nonsteroidal Anti-Inflammatory Agents (NSAIDs)

The NSAIDs are relatively safe drugs, and, since CYP2C9 is a major determinant in the metabolism of many of these agents, measurement of the involved pathway in principle could serve as an indicator of the isoform's activity. For example, the oral clearance of diclofenac, which reflects primarily CYP2C9-mediated 4'-hydroxylation, was found to be reduced following pretreatment with fluvastatin, an established in vitro inhibitor of the enzyme [131]. A decrease was also noted in a urinary metabolic ratio (4'-hydroxydiclofenac:diclofenac) based on a 0–4-hr collection period but not over 4–8 hr. Unfortunately, validation of neither of these putative trait measures using diclofenac has been reported. More recently, the 4'-hydroxylation of flurbiprofen has been investigated in a similar fashion, with the intent to develop this drug as a CYP2C9 in vivo probe [132]. Such preliminary information will obviously require appropriate substantiation before the described trait measures will be widely accepted.

## B. Cytochrome P450 2C19 (CYP2C19)

The enzyme now known as CYP2C19 [133,134] was first identified because of its major involvement in the 4'-hydroxylation of the *S*-enantiomer of mephenytoin



[22,23]. Although, its substrate specificity was originally thought to be limited to related anticonvulsant agents, the *in vivo* metabolism of an increasing number of structurally unrelated drugs appear to be mediated by this isoform. These include *R*-mephobarbital (4'-hydroxylation) [135], hexobarbital (3'-hydroxylation) [136], proguanil (ring cyclization) [137], omeprazole and related proton pump inhibitors (5'-methylhydroxylation) [138–140], diazepam (*N*-demethylation) [141], certain tricyclic antidepressants (*N*-demethylation) [142–144], carisoprodil (*N*-dealkylation) [145], citalopram (*N*-demethylation) [146], moclobemide (*C*-hydroxylation) [147], propranolol (side-chain oxidation) [148], and nelfinavir (methylhydroxylation) [149]. A major characteristic of CYP2C19 is the presence of a genetic polymorphism that subdivides populations into "poor" metabolizers (PMs) and "extensive" metabolizers (EMs) [150]. The molecular genetic basis of such phenotypes is now well recognized. The two most common defects involve null alleles arising from G → A base pair mutations in exon 5 (CYP2C19\*2) and exon 4 (CYP2C19\*3), respectively [3], and they account for over 99% of defective alleles in populations with Asian ancestry but only in about 87% in individuals of Caucasian origin [151–153]. A transition mutation in the initiation codon (CYP2C19\*4) accounts for an additional 3% of defective alleles in Caucasian PMs [154], and three rare mutations (CYP2C19\*5, CYP2C19\*6, and CYP2C19\*7) have also been identified [155–158]. Not unexpectedly, the population allelic frequencies [159] and phenotypes, *i.e.*, EMs, representative of both wild-type homozygotes and heterozygotes, and PMs (homozygous mutants), varies according to racial/geographical origin. For example, in populations of European descent the frequency of the PM phenotypes ranges from 1.3 to 6.1%, with a mean value of about 3.5% [160]. A similar low prevalence rate is also present in Africans and African Americans [161–163]. By contrast, a much higher frequency (13–23%) is found in indigenous populations living in Southeast Asia, such as Chinese, Japanese, and Koreans [138,164–168]. Importantly, the impaired metabolism present in PMs is often associated with marked differences in a substrate's disposition and pharmacokinetics [150]. Moreover, drug interactions involving CYP2C19 can occur only in individuals with the EM phenotype, since no enzyme is present in PMs (169). These factors have led to the development of *in vivo* probes to classify individuals according to phenotype.

## 1. Mephenytoin

The genetic polymorphism in CYP2C19 was first discovered serendipitously during clinical studies to investigate the enantioselective metabolism of racemic mephenytoin at Vanderbilt University [150]. Subsequently, two alternative phenotyping procedures were developed that have been widely used throughout the world by numerous investigators. Both of these are based on the fact that CYP2C19 metabolizes racemic mephenytoin to its 4'-hydroxy metabolite, and this is essentially complete and stereospecific for the *S*-enantiomer.

*a. Urinary S:R Enantiomeric Ratio.* The 4'-hydroxylation of *S*-mephenytoin is not only extensive but also rapid, and this is in contrast to metabolism of the *R*-enantiomer, which involves mainly *N*-demethylation [150]. Accordingly, only a small fraction of an administered oral dose of racemic mephenytoin (50–100 mg) is excreted into urine over 0–8 hr as the unchanged *S*-enantiomer in EMs, whereas a much larger amount of *R*-mephenytoin is excreted. In the absence of CYP2C19 activity, i.e., PMs, impaired metabolism of *S*-mephenytoin by 4'-hydroxylation results in increased excretion of this enantiomer; Because the metabolism of *R*-mephenytoin is not different between EMs and PMs, the *S*:*R* enantiomeric concentration ratio in a 0–8-hr urine sample is increased [23]. Thus, the *S*:*R* ratio ranges from less than 0.03 to 0.8 in EMs and 0.9 to 1.2 in PMs [150]. The pharmacokinetic basis of the trait measure has been described, and studies have confirmed that the urinary *S*:*R* ratio is the same as the comparable ratio of the areas under the plasma concentration–time profiles of the enantiomers during the collection period, which in turn reflects the relative intrinsic clearances of the two isomers [169]. Also, this trait value has been found to be reproducible in individuals over a long period of time [170]. Although the *S*:*R* ratio is widely used, it has a reciprocal and, therefore, rectangular hyperbolic relationship with CYP2C19 activity. For this reason, there is some merit in using the *R*:*S* ratio, which is linearly related to such activity, so the smaller its value, the lower the 4'-hydroxylating activity [21,171].

A minor route of metabolism of *S*-mephenytoin results in the formation and urinary excretion of an acid-labile conjugate that is probably a cysteinyl derivative [172]. This pathway appears to be associated with CYP2C19, since it is present only in EMs [173]. The significance of this urinary metabolite is that it is easily hydrolyzed back to *S*-mephenytoin, and this can occur to an unpredictable extent during sample storage, even at  $-20^{\circ}\text{C}$  [173]. The resulting artifactual *S*:*R* ratio value may, therefore, misclassify an individual's phenotype. Several approaches have been used to obviate or minimize this problem. The most widely used procedure is to obtain a repeat *S*:*R* value but following acid hydrolysis of the urine sample prior to analysis. The enantiomeric ratio is significantly increased by such pretreatment in EMs but remains essentially unchanged in PMs [173–175]. Another approach [176] includes measurement of the *S*:*R* ratio in a urine sample collected 24–32 hr after drug administration, since little or no acid-labile metabolite is present at this time. However, the *S*:*R* ratio in EMs at this later time is smaller (0.16–0.5) than that in a 0–8-hr sample, whereas the value in PMs is still close to unity. Also, it is possible to extract the collected urine immediately after collection and store the dried extract at  $-20^{\circ}\text{C}$  until subsequent analysis [176].

The major advantage of using the urinary *S*:*R* ratio as a phenotypic trait for assessing CYP2C19 activity is that the method is fairly robust with regard to any incompleteness of urine collection or noncompliance with respect to dose administration. This is because the *R*-enantiomer serves as an in vivo “internal

standard.’’ On the other hand, the required enantiospecific assay uses chiral capillary column gas chromatography with a nitrogen-specific detector, and such instrumentation is not commonly available. For this reason, an alternative phenotypic trait measure based on the formation and urinary elimination of 4'-hydroxymephenytoin has also been frequently used.

*b. Urinary 4'-Hydroxymephenytoin Excretion.* After its formation, 4'-hydroxymephenytoin is glucuronidated and excreted in this form into the urine. Accordingly, the aglycone must be liberated prior to determination of the amount of CYP2C19-mediated metabolite formed, using either  $\beta$ -glucuronidase pretreatment or acid hydrolysis [176]. In EMs, the 0–8-hr urinary recovery of 4'-hydroxymephenytoin is between 5 and 52% (25–240  $\mu\text{mol}$ ) of the administered 100-mg (460  $\mu\text{mol}$ ) phenotyping dose of racemic mephenytoin (mean 18–20%) [150]. By contrast, in PMs from undetectable to 3% of the dose (mean 0.5–0.8%) is excreted [150]. An alternative phenotypic trait measurement based on excretion of the 4'-hydroxy metabolite is the mephenytoin hydroxylation index (HI):

$$\text{HI} = \frac{\text{molar doses of } S\text{-mephenytoin (230 } \mu\text{mol in 100-mg racemic dose)}}{\mu\text{mol 4'-hydroxymephenytoin excreted in 0–8 hr}} \quad (3)$$

In EM individuals this value ranges from about 0.6 to 20, whereas a much higher value (30–2500) is observed in PMs [22,23,150]. Importantly, the metabolite's concentration in urine samples from PM subjects is often close to the lower limit of sensitivity of the HPLC-based assay. Thus, an antimodal value that discriminates between the two phenotypes cannot be defined with absolute precision and varies between laboratories. As a result, phenotypic misclassification may occur when the 0–8-hr urinary recovery is in the range of about 15 to 25  $\mu\text{mol}$ . A further interpretive difficulty is the trait's dependency on a complete 0–8-hr urine collection, since a low recovery of the 4'-hydroxy metabolite can also reflect poor subject compliance. Some investigators, therefore, confirm the completeness of urine collection in putative PMs by measurement of the amount of creatinine in the sample (>50 mg in 0–8 hr). Alternatively, the phenotype is determined by combining the information provided by both the excretion of 4'-hydroxymephenytoin and the urinary *S*:*R* ratio.

Despite the described approaches and precautions, the trait values of a small number of individuals may not be consistent with genotypic information or are uninterpretable based on the assumption that only two phenotypes are present. One reason for this is the very low frequency of ‘‘intermediate metabolizers’’ who have an *S*:*R* enantiomeric ratio consistent with the PM phenotype (>0.9) but who excrete more (20–60  $\mu\text{mol}$ ) of the 4'-hydroxy metabolite than would be expected if this was the case but at a rate less than that in EMs [176]. It is likely that such rare individuals have an as-yet-unidentified allelic variant of CYP2C19 with reduced catalytic activity compared to the wild-type enzyme, as

occurs with CYP2D6 (Sec. VI). It is possible that the urinary *S*:*R* ratio measured at 24–32 hr may also identify such individuals, since occasional subjects have been noted to have values between 0.2 and 0.5, whereas in most EMs this trait value is about 0.1 [175,177].

Mephenytoin has been extensively used for phenotyping purposes; however, such use is not without practical problems. For example, sedation is often observed in PMs, especially those of small body size, e.g., children and Southeast Asians, following administration of a 100-mg dose usually used for phenotyping [178]. Accordingly, a dose of 50 mg mephenytoin is often used to phenotype such individuals. A further complicating factor is that racemic mephenytoin (Mesantoin<sup>®</sup>, Sandoz/Novartis) is not available in many parts of the world. For these reasons, other in vivo probes have been investigated.

## 2. Omeprazole

The 5'-hydroxylation of omeprazole cosegregates with CYP2C19 activity both in vitro using human liver microsomes [179–181] and in vivo in several different populations [138,182]. In addition, the drug has a short elimination half-life (1–2 hr) and has a far wider therapeutic ratio than mephenytoin, resulting in better tolerability by subjects. Accordingly, trait measures reflective of in vivo CYP2C19 activity have been investigated.

In general, phenotyping has been performed following oral administration of a single 20-mg oral dose of omeprazole and obtaining a single blood sample for determination of the plasma concentrations of omeprazole and its 5'-hydroxy metabolite by HPLC. However, different sampling times and trait values have been used by different investigators. A metabolic ratio (omeprazole:5'-hydroxy-omeprazole) determined 3 hr after administration of the probe was able to identify EMs who had trait values between 0.05 and 5.6, whereas individuals with the PM phenotype had larger ratios [183]. In fact, the presence of metabolite in the plasma was not always detectable in PMs. A metabolic ratio of about 7 appeared to be the antimode of the population distribution curve in 160 Swedish Caucasians [184]. A similar approach, but based on sampling at 2 hr after omeprazole administration and using the logarithm of the metabolic ratio—termed the “omeprazole hydroxylation index”—was also able to discriminate, using an antimode of 1, between the two CYP2C19 phenotypes in 85 healthy subjects of various racial backgrounds [185,186] and 77 African Americans [163]. A third trait value, using a single 4-hr blood sample, has also been used: (omeprazole + omeprazole sulfone):5'-hydroxyomeprazole [187]. Again, phenotypic classification was possible based on an antimode value of 12. Regardless of the precise trait value used, concordance was noted in the various studies between the measured CYP2C19-mediated omeprazole metabolism and the urinary *S*:*R* ratio for mephenytoin and also the genotype of the individual. This suggests that measurement of omepra-

zole's 5'-hydroxylation using a single time-point plasma metabolic ratio is a valid approach for CYP2C19 phenotyping. However, wider application of the methods will probably be necessary before omeprazole replaces mephenytoin as the "gold standard" in vivo probe for assessing CYP219 activity. For example, analytical sensitivity issues may limit omeprazole's wider application, since in one population study 23 of 100 subjects could not be phenotyped because of unmeasurable concentration of omeprazole and/or its 5'-hydroxy metabolite [185,186]. Also, omeprazole sulfone formation is mediated primarily by CYP3A [180], which exhibits considerable interindividual variability in its activity (Sec. VIII). Accordingly, the metabolic ratio incorporating this metabolite's concentration into its estimation would be affected by this factor and presumably altered if CYP3A was inhibited or induced by drug administration in addition to the in vivo probe [187].

### 3. Proguanil

The antimalarial effects of proguanil (chloroguanide) are dependent on its metabolic activation to cycloguanil. This pathway is mediated in large part by CYP2C19, and the formation clearance of the metabolite cosegregates with the mephenytoin phenotype [188]. Furthermore, the relative amounts of cycloguanil and unchanged drug excreted in urine collected 0–8 hr after an oral dose of 200 mg proguanil has been shown to be dependent on the CYP2C19 phenotype [137,189–194]. Also, a good correlation ( $r = 0.96$ ) was found between the urinary proguanil:cycloguanil metabolic ratio and the formation clearance of 4-proguanil to cycloguanil [195], and an antimode of 10 was able to discriminate between EMs and PMs [190,192]. However, in other studies this value did not necessarily separate the two phenotypes [191,193], and a better antimode was suggested to be 15 [196]. More recent studies based on genotype:phenotype relationships have found a gene-dose effect in the proguanil metabolic ratio [197,198]. However, there was substantial overlap in the metabolic ratio in subjects of different CYP2C19 genotypes [198], and it was difficult to define an exact antimode [197]. Additional reservations about this phenotyping approach have also been expressed based on the observation that no correlation was found between the proguanil metabolic ratio and mephenytoin's hydroxylation index [199,200]. This may reflect the fact that the cyclization of proguanil to cycloguanil is mediated not only by CYP2C19 but also by CYP3A [201]. Such considerations indicate that the proguanil urinary metabolic ratio approach may have limitations as the method of choice for CYP2C19 phenotyping.

## VI. CYTOCHROME P450 2D6 (CYP2D6)

CYP2D6 is the most thoroughly investigated human CYP isoform because of its genetic polymorphism and involvement in the metabolism of many drugs of clini-

cal importance. Accordingly, a plethora of reports and reviews addressing various aspects of the enzyme have been published (for example, Refs. 202 and 203). The genetic polymorphism was discovered independently by three groups of investigators, two studying the metabolism of debrisoquine [204,205] and another interested in sparteine [206]. With both drugs, a bimodal frequency distribution was observed in the urinary excretion of measured metabolites and unchanged drug, and the subgroups were termed EMs and PMs. More recently, based on genetic analysis, an “intermediate” metabolizer phenotype (IM) has been defined [207], and in addition, “ultrarapid” metabolizers (UMs) have been described [208]. The molecular genetic bases of the CYP2D6 polymorphism are now well established. Currently, some 48 mutations resulting in 53 alleles are known, and additional rare ones continue to be identified [203,207,209]. However, the five most common alleles represent over 95% of the variants [209], and a formal nomenclature scheme has been adopted [210]. Many types of null mutations result in impaired CYP2D6 activity, and homozygosity is associated with the PM phenotype, e.g., CYP2D6\*3, CYP2D6\*4, CYP2D6\*5, and CYP2D\*6. Other variant alleles, such as CYP2D6\*9, CYP2D6\*10, and CYP2D6\*17, lead to an enzyme with reduced catalytic activity compared to the wild-type allele (CYP2D6\*1). Finally, gene duplication and amplification up to 13 copies (CYP2D6\*2XN, where *N* indicates the number of genes) is associated with ultrarapid metabolism [210].

Considerable heterogeneity is present in the frequencies of these various alleles in different worldwide populations, dependent upon racial/geographic factors [203,207]. Consequently, the frequencies of CYP2D6 phenotypes differs among these groups. Most information is available on the PM phenotype, which is present in about 4–10% (mean 7.4%) of populations of European descent [160]. By contrast, a lower frequency, 0.6–1.5%, has been observed in Southeast Asians, such as Japanese [165], Chinese [166], and Koreans [167]. Also, the population distribution curve of CYP2D6 activity is shifted to the right in Chinese and Koreans, compared to Caucasians, as a consequence of the lower frequency of CYP2D6\*4 and the increased prevalence of CYP2D6\*10 alleles. In general, a similar low phenotypic frequency also appears to be the case with populations of African descent, due to the fact that CYP2D6\*17 is more common than CYP2D6\*4 [211–213]. However, considerable heterogeneity also appears to be present among various African populations (Sec. VI.E).

A large number of drugs, estimated to be over 50, have been shown to be metabolized by CYP2D6. These include, for example,  $\beta$ -adrenoceptor blockers (metoprolol, propranolol, timolol), antiarrhythmic agents (sparteine, propafenone, mexilitene, encainide, flecainide), antidepressants (tricyclics, selective serotonin reuptake inhibitors), neuroleptics (haloperidol, perphenazine, thioridazine, zuclopenthixol), opioids (codeine, dihydrocodeine, dextromethorphan), amphetamines (methamphetamine, methylenedioxymethylamphetamine—“ecstasy,” fenfluramine), and various other drugs [202]. Although such drugs exhibit

diverse chemical structures, a critical characteristic appears to be a basic nitrogen atom, which is ionized at physiological pH and interacts with an aspartic acid residue in the active site of CYP2D6. In those cases where CYP2D6-mediated metabolism is of major importance in the overall elimination of a drug, differences in drug disposition and pharmacokinetics is present between the two phenotypes, and this may be quite marked [202]. The clinical consequences in PMs of such differences [202] include a higher propensity to develop adverse drug reactions following a conventional dose or a reduced clinical effect because an active metabolite is not formed, e.g., the conversion of codeine to morphine [214]. In addition, therapeutic failure may occur in UMs as a result of inefficacious drug levels [215]. These clinical considerations and general interest in the CYP2D6 genetic polymorphism have resulted in the development and application of a number of *in vivo* probes for assessing the enzyme's activity.

### A. Sparteine

A polymorphism in sparteine metabolism was initially identified because of the involvement of CYP2D6 in the formation of 2- and 5-dehydrosparteine [206]. This led to the development of a urinary metabolic ratio type of phenotypic trait measure (sparteine:dehydrosparteines) based on a 0–8-hr or 0–12-hr urine collection following oral administration of 100 mg sparteine. Such a phenotyping approach is robust and has been applied to several thousand individuals. An anti-mode value greater than 20 appears to reliably distinguish PMs from EMs. More recently, subphenotyping within the conventional EM phenotype has been suggested [2]. For example: a sparteine metabolic ratio of 2–20 reflects the IM phenotype, who are generally CYP2D6\*2/CYP2D6 null heterozygotes; a value from 0.2 to 2 is indicative of wild-type homozygotes and some heterozygotes; and values below 0.2 are usually associated with UMs who have duplicated/amplified genes. However, overlap in the trait values between the various subphenotypic groups does not permit any useful predictability of genotype from the sparteine metabolic ratio, or vice-versa.

Unfortunately, sparteine is not marketed and approved for clinical use in many countries, including North America and the United Kingdom, and analytical reference compounds required for the GLC analytical procedure are not readily available. Accordingly, the use of sparteine for CYP2D6 phenotyping has had limited use outside a small number of mainly European investigators.

### B. Debrisoquine

CYP2D6 mediates the alicyclic hydroxylation of debrisoquine at the 1-, 3-, and 4-positions [216]. However, formation of 4-hydroxydebrisoquine is quantitatively the most important of these pathways, accounting for between 1 and 30%

of an administered dose, depending on genotype, and the metabolite is almost exclusively of the *S*-enantiomer configuration [19]. This urinary metabolic profile led to the empirical development of the commonly used CYP2D6 trait measure of the 0–8-hr urinary metabolic ratio (debrisoquine:4-hydroxydebrisoquine) determined following an oral 10-mg dose of debrisoquine [204,205]. An alternative “urinary recovery ratio” (4-hydroxydebrisoquine: (debrisoquine + 4-hydroxydebrisoquine)) has also been used, but to a far lesser extent [21,35]. In most populations, a metabolic ratio above 12.6 has generally been used to discriminate PMs from EMs. Also, within the latter phenotype, there is a general trend for the metabolic ratio to decrease as the number of functional alleles increases, and IM (2.0–12.6), EM (0.1–2.0), and UM (<0.1) subphenotypes may be defined [19,217]. However, there is considerable overlap in the phenotypic trait value between the various subgenotypes, so the debrisoquine metabolic ratio cannot be used to identify a particular genotype, and vice-versa.

Many thousands of individuals worldwide have been phenotyped with debrisoquine. This extensive experience by numerous investigators has established that it is safe even in PMs, and it provides a reproducible and robust method for determining in vivo CYP2D6 activity [170]. Moreover, the metabolic ratio appears to be sufficiently sensitive to modulation of CYP2D6 activity for it to be used to identify determining factors [202]. However, a significant practical problem associated with debrisoquine (Declinax<sup>®</sup>, Hoffman La-Roche) is its lack of availability and regulatory approval in several countries, including the United States. As a result, alternative drugs suitable for in vivo CYP2D6 phenotyping in such places have been investigated.

### C. Metoprolol

Over 95% of an administered dose of metoprolol is metabolized in humans to a number of metabolites, including  $\alpha$ -hydroxymetoprolol, which accounts for up to 10% of the eliminated dose [218]. Considerable interindividual variability is present in the  $\beta$ -adrenoceptor blocker’s oral clearance, and this was found to be determined by the CYP2D6 polymorphism as assessed by debrisoquine [219] and sparteine metabolic ratios [220]. These observations led to the development and application of a 0–8-hr urinary metoprolol: $\alpha$ -hydroxymetoprolol metabolic ratio approach for CYP2D6 phenotyping following an oral dose of 100 mg metoprolol tartrate [221,222]. A good correlation was observed between this ratio and the debrisoquine metabolic ratio, with an antimode value of about 12.5, clearly separating EMs from PMs. Although metoprolol’s urinary excretion may be affected by urinary pH [218] and the drug’s metabolism exhibits stereoselectivity [223], neither of these factors appears to be an important variable in the trait measure, which has been shown to be reproducible with respect to phenotypic assignment [220]. A single-point, 3-hr postdose metabolic ratio approach has also



been suggested based on its good agreement with the equivalent urinary trait measure [224]; however, its use has been limited.

Despite the relative safety of metoprolol and its general availability for clinical studies, the metoprolol metabolic ratio has been used to only a limited extent as an *in vivo* probe for assessing CYP2D6 activity. Such use has been directed mainly toward the investigation of racial/geographic differences in CYP2D6 and the dissociation between measures of such activity provided by different *in vivo* probes (Sec. VI.E). One reason for this limited use has been the application of an even safer and more widely used drug for phenotyping purposes, namely, dextromethorphan.

#### D. Dextromethorphan

Dextromethorphan (3-methoxy-17-methylmorphinan) is a widely used and effective non-narcotic antitussive. After oral administration, it is rapidly and extensively metabolized in humans by *O*- and *N*-demethylation to form dextrorphan and 3-methoxymorphinan; a small amount of secondary metabolite, 3-hydroxymorphinan, is also formed. *N*-Demethylation is mediated mainly by CYP3A, whereas the formation of the major metabolite, dextrorphan, is determined by CYP2D6 [38]. This dependency led to the suggestion that the conversion of dextromethorphan to dextrorphan could be used to assess *in vivo* CYP2D6 activity [225]. Moreover, its high safety profile and global availability would permit its universal application, even in subjects where use of unapproved drugs like sparteine and debrisoquine was not possible (e.g., children, pregnant women).

A 0–8-hr urinary metabolic ratio (dextromethorphan:dextrorphan) is usually used as the trait measure following an oral dose of 15–40 mg dextromethorphan hydrobromide in a solid dosage form or as cough syrup. Because dextrorphan is conjugated prior to excretion, hydrolysis of the urine by pretreatment with  $\beta$ -glucuronidase is usually performed, although some investigators have suggested that this may not be necessary [226]. Using the conventional approach, an antimode of 0.3 is able to discriminate between EMs and PMs [225]. Pharmacokinetic studies have substantiated that the urinary metabolic ratio reflects the plasma levels of the unchanged drug to its metabolite [227], and possible factors affecting the trait measure have been investigated [228]. It is also possible to determine a single time-point, dextromethorphan metabolic ratio in plasma within 2–5 hr after an oral dose or in a 6-hr saliva sample [229,230]; however, neither of these alternative approaches has been widely used.

In general, excellent agreement has been obtained between CYP2D6 phenotypic assignment based on the use of dextromethorphan compared to debrisoquine, both *in vitro* [231,232] and *in vivo* [38,225,233]. Furthermore, concordance between EM and PM CYP2D6 genotypes and dextromethorphan's metabolic ratio has more recently been established [217,233–235]. On the other

hand, this trait measure appears less suitable for defining subphenotypes within the EM phenotype, since there is considerable overlap in the trait value between the groups [217]. Accordingly, it is not possible to identify ultrarapid or intermediate metabolizers. However, the dextromethorphan urinary metabolic ratio is modulated by factors that alter CYP2D6 activity, such as inhibition by quinidine and substrates like selective serotonin-reuptake inhibitors [236,237].

### E. Correlations Between Different CYP2D6 Probes

In populations of European descent, good agreement in the CYP2D6 phenotype has generally been found regardless of the particular in vivo probe that has been used. For example, a high correlation ( $r = 0.81$ ) was observed in a white British population between the metabolic ratios of debrisoquine and metoprolol [221]. In Japanese, similar good relationships ( $r = 0.78$ – $0.83$ ) were obtained between alternative probes [238]. However, discordances have been noted in other populations, especially African. For example, in Ghanaians and Zambians much lower correlations ( $r = 0.41$  and  $0.60$ ) were found between the urinary metabolic ratios of sparteine, metoprolol, and debrisoquine [239,240]. Also, in another study the correlation between the metabolic ratios of debrisoquine, sparteine, and dextromethorphan were considerably weaker in Ghanaians compared to Caucasians and Chinese [241]. Moreover, no polymorphism was apparent in the population distribution curve in Nigerians using either debrisoquine or sparteine [212,242], and no significant relationship ( $r = 0.31$ ) was found between debrisoquine and sparteine metabolic ratios [243]. Studies in black Africans of the Venda have also indicated dissociations between the various in vivo CYP2D6 probes, namely, a log-normal distribution of the sparteine metabolic ratio with no evidence of a PM subgroup, whereas phenotyping with debrisoquine identified a 4% prevalence of this phenotype [244,245]. However, the metoprolol metabolic ratio indicated a PM incidence of 7.4% [246]. Similarly, only 1 of 18 PMs in a San Bushmen population in South Africa phenotyped with debrisoquine [247] were subsequently found to have impaired metabolism of metoprolol [246], and a similar discordance was noted in Zimbabweans [211]. It has been speculated that such dissociations might reflect poor patient compliance with the clinical protocol or that the antimode value established in populations of European descent does not always apply to other populations. However, a more likely explanation, which is also consistent with the shift to the right of the frequency distribution curve of the phenotypic trait measure in African populations compared to those of European descent, involves differences in allele frequency, especially CYP2D6\*17. This variant allele, which expresses a protein with reduced catalytic activity compared to the wild-type gene [248,249], is not present in Europeans but is common among black African populations [203,207,248]. Significantly, such decreased CYP2D6 activity is associated with reduced affinity for some CYP2D6 substrates and al-

tered substrate specificity [249], which could also account for the insensitivity of Africans to the effect of quinidine on CYP2D6 [241]. Alternatively, a presently unidentified CYP2D6 variant may be present in such populations.

In summary, any of the described *in vivo* probes and associated trait measures provide safe, simple, and practical approaches for identifying CYP2D6 EMs and PMs, and these have been validated and successfully applied by numerous investigators, especially in non-African populations. The choice of probe depends mainly on the local regulatory situation and the availability of the particular drug and its metabolites. Debrisoquine and sparteine appear to be more suitable than dextromethorphan for subphenotyping within the EM population. However, in neither case does it appear possible to identify an individual's genotype on the basis of the subphenotypic trait value. Just as important is the reverse situation, namely, the CYP2D6 genotype does not predict the level of CYP2D6 catalytic activity within EMs, which can be established only by phenotyping. Likewise, modulation of such activity requires the use of an *in vivo* probe, and all three of the widely used approaches appear to be sufficiently sensitive for this purpose. The situation in various African and possibly other populations [250,251] is less clear because of the high prevalence of CYP2D6\*17, which appears to have different substrate and inhibitor specificities than other allelic variants. As a result, identification of PMs in such groups by phenotyping is not as clear-cut as in European- and Southeast Asian-derived populations; this problem is compounded by the low prevalence of this subgroup in these populations. This would appear to be one situation in which putative classification as a PM requires confirmation by genotyping.

## VII. CYTOCHROME P450 2E1 (CYP2E1)

CYP2E1 is importantly involved in the metabolic activation of a large number of environmental xenobiotics many of which have carcinogenic or toxic effects, for example, *N*-nitrosamines, benzene, styrene, and halogenated hydrocarbons. Thus, along with CYP2A6 (Sec. IV) this isoform is considered to be important in the etiology of and individual susceptibility to disease states associated with exposure to such agents. CYP2E1 also mediates the metabolism of a small number of drugs, which include ethanol, acetaminophen, chlorzoxazone, and certain fluorinated anesthetic agents [44,252]. The regulation of CYP2E1 is complex and can be affected by both physiological and exogenous factors, such as drug-induced inhibition and induction. Thus, *in vivo* CYP2E1 activity varies quite markedly within a population, with the basal variability being about 4- to 5-fold; however, this can be greater if obese individuals and chronic alcoholics are included [25,28]. In addition, CYP2E1 activity is normally distributed; to date, no evidence

of polymorphism or rare individuals with unexplained impairment have been described [28].

Several genetic polymorphisms have been identified in the CYP2E1 gene [253–256]. This has led to considerable speculation regarding their possible involvement as risk factors in, for example, alcoholic liver disease and cancer. Efforts to address such issues are complicated by the fact that the frequencies of the polymorphisms vary substantially according to the racial/geographic characteristics of the study population. As a result, such molecular epidemiological findings have become controversial, since the resulting data is often conflicting and suffers from low statistical power. The latter problem also applies to population studies attempting to relate genotype to phenotype. In general, CYP2E1 activity as measured both *in vitro* [256–259] and *in vivo* [28,259,260] by the 6-hydroxylation of chlorzoxazone does not appear to be under genetic regulation by the various identified allelic variants. However, a recent study investigating the *Rsa*I restriction fragment length polymorphism in the 5′-regulatory sequence of the CYP2E1 gene (C1019T) found that chlorzoxazone's oral clearance was greatest in homozygous wild-type individuals ( $c_1/c_1$ ) and decreased with the number of variant  $c_2$  alleles [261]. However, the difference in CYP2E1 activity between the two homozygous groups was less than 2-fold. In addition, a recent report has described a further mutation in the 5′-regulatory region that appears to be involved in the inducibility of CYP2E1 activity [255]. It is also not clear what role, if any, such genetic factors may have in the 30–40% lower CYP2E1 activity noted in populations of Japanese ancestry and possibly other Southeast Asians compared to those of European descent [259,261].

The only *in vivo* probe developed and used for assessing human CYP2E1 activity has been chlorzoxazone, based on the finding that this isoform selectively mediates the drug's 6-hydroxylation [262]. Subsequent studies also found that CYP1A1 was able to catalyze this reaction [263,264]; however, this is not a constitutive isoform, and its affinity for chlorzoxazone is much less than that of CYP2E1. Accordingly, its overall role *in vivo* is likely to be very minor [264]. This probability is supported by the observation that chlorzoxazone's metabolism is similar in nonsmokers and smokers in whom CYP1A1 would be expected to be induced [25]. Preliminary *in vitro* evidence has been presented showing that recombinant CYP1A2 also mediates chlorzoxazone's 6-hydroxylation [265], but this has not been confirmed [264]. Similarly, it is not clear whether CYP3A has a role in the *in vivo* formation of chlorzoxazone's 6-hydroxy metabolite as has been suggested by studies *in vitro* [266]. Overall, the current available evidence indicates that the *in vivo* 6-hydroxylation of chlorzoxazone in humans is predominantly, if not exclusively, mediated by CYP2E1, and its measurement provides a valid estimate of the enzyme's activity.

Chlorzoxazone (5-chloro-2(3*H*)-benzoxazolone) is a skeletal muscle relax-

ant that has been approved for clinical use for over 40 years. Single-dose (250 mg) oral administration is safe and well tolerated, and 6-hydroxylation is the major pathway of elimination, accounting for about 50–80% of the dose [25,28]. This metabolite is rapidly conjugated; therefore, determination of its concentration in either plasma or urine requires pretreatment with either  $\beta$ -glucuronidase or acid, respectively [25,267,268]. The “gold standard” for assessing CYP2E1 activity is estimation of chlorzoxazone’s fractional oral clearance to its 6-hydroxy metabolite, following an overnight fast, based on determination of the drug’s plasma level–time profile over 8 hr and measurement of the metabolite’s 0–8-hr or 0–12-hr urinary recovery [28,259,269]. Because ethanol is an inhibitor of CYP2E1 while present in the body and an inducer after chronic use, it is important that alcoholic beverages not be consumed for about 72 hr prior to phenotyping. Such a clearance approach has been validated in humans by a number of studies demonstrating that factors known to alter CYP2E1 activity in animals or in vitro also modulate chlorzoxazone’s clearance in an appropriate fashion. These include mechanism-based inhibition by disulfiram [269], chlormethiazole [270], and phytochemicals in watercress [271], as well as induction by obesity [267] and pretreatment with isoniazid [272,273]. Importantly, the last interaction is masked by the antitubercular agent’s inhibition of CYP2E1 while it is present in the body. In contrast to findings in animals, fasting over 36 hr reduces CYP2E1 activity compared to a standard 8–12-hr overnight fast [267]. The main practical disadvantage of this clearance approach is the need to obtain multiple blood samples over 8 hr to define the plasma concentration–time profile along with collection of urine for 8–12 hr. Because 6-hydroxylation is the major route of elimination of chlorzoxazone, use of the probe’s oral clearance is probably as informative as the formation clearance estimate. Besides simplifying the phenotyping procedure, another advantage of this latter trait measure is that it reduces the error of the value’s estimation associated, for example, with incomplete collection of urine. However, extensive blood sampling is still required; for this reason, a simpler metabolic ratio approach has been advocated.

Chlorzoxazone is generally rapidly absorbed, with a peak value approximately 2 hr after oral administration, and plasma levels of the 6-hydroxy metabolite are detectable prior to this time [25,28]. Thus, a single-time-point, plasma metabolic ratio (6-hydroxychlorzoxazone:chlorzoxazone) is readily determinable. Different investigators have used different times to determine this trait measure. Many employ a value determined 2 hr after oral chlorzoxazone administration, based on a high correlation ( $r = 0.88$ ) between it and the clearance of chlorzoxazone to its 6-hydroxy metabolite [25,268]. Also, the ratio of the areas under the plasma concentration–time curves for the chlorzoxazone and its 6-hydroxy metabolite has been found to correlate with the metabolic ratio [25]. Others have suggested that a 4-hr sampling time point is more optimal and similarly have reported a high correlation (0.89) between the two trait measures [26].

However, in larger population studies such correlations have been found to be much lower; for example,  $r = 0.42\text{--}0.53$  [28]. Nevertheless, chlorzoxazone's plasma metabolic ratio undoubtedly reflects CYP2E1 activity and is reduced by inhibition, e.g., chlormethiazole [274] and liver disease [275,276], and increased by induction, e.g., ethanol [25,277]. Moreover, it has been demonstrated to provide a simple method for investigating temporal aspects associated with changes in CYP2E1 activity, as, for example, following the effects of ethanol withdrawal in chronic alcoholics [277].

Phenotypic trait measures based solely on the urinary excretion of 6-hydroxychlorzoxazone have also been reported based on the amount of metabolite excreted in 0–8 hr [278], or a ‘hydroxylation index’ approach [279], or estimating the elimination half-life of the metabolite [280]. However, the validity of these approaches is highly questionable, so they have not been widely applied.

### VIII. CYTOCHROME P450 3A (CYP3A)

The human CYP3A subfamily includes at least three functional proteins, CYP3A4, CYP3A5, and CYP3A7; however, the last one is not found in significant amounts in adults. The substrate specificities of CYP3A4 and CYP3A5 are in general similar, although some important distinctions do exist; for example, erythromycin and quinidine do not appear to be metabolized by CYP3A5, although they are good CYP3A4 substrates [44,281]. Because of this and the current difficulty in distinguishing between the individual CYP3A isoforms, which may be present in different amounts in the same tissue, they are collectively referred to as CYP3A. Importantly, CYP3A is the most abundant of all of the human CYP isoforms and constitutes, on average, about 30% of total CYP protein in the liver. CYP3A is also present in the small intestinal epithelium, particularly in the apical region of mature enterocytes at the tip of the microvillus, where it accounts for about 70% of total CYP protein and is present at about 50% of the hepatic level. Catalytic activity, mainly associated with CYP3A5, is also present in the kidney [44,281].

The substrate specificity of CYP3A is very broad; accordingly, an extremely large number of structurally divergent chemicals are metabolized by a variety of different pathways, often in a regio- and stereo-selective fashion [44]. Estimates, based primarily on in vitro studies, suggest that the metabolism of about 40–50% of drugs used in humans involves CYP3A, and frequently such biotransformation is extensive. Moreover, because of its localization in the intestinal epithelium and liver, CYP3A is an important factor in the first-pass metabolism of drugs following their oral administration [282]. A further characteristic

of CYP3A is the large interindividual variability in activity, which reflects both genetic and environmental factors. Basal variability appears to be about 5-fold, but this range can be significantly increased by inhibition or induction. In this respect, CYP3A is extremely prone to both types of interactions [281]. Furthermore, the distribution of CYP3A activity is unimodal, and to date no evidence of a functional polymorphism has been reported. Recently, it has been recognized that the substrate/inhibitor specificity of CYP3A overlaps with that of the membrane efflux transporter termed P-glycoprotein [283]. However, this overlap is not complete, and it is probably a fortuitous one that reflects the broad substrate specificities of the individual proteins [284]. In fact, several important CYP3A substrates, such as nifedipine and midazolam, are not transported by P-glycoprotein [284]. Nevertheless, the colocalization of the two proteins at important sites for drug disposition, such as the enterocyte and hepatocyte, results in an interrelationship that functions in a concerted fashion to reduce the intracellular drug concentration. Thus, the hepatic elimination, for example, of erythromycin—a substrate for both P-glycoprotein and CYP3A—is determined by both proteins. In addition, the coadministration of two CYP3A substrates can result in drug interactions that reflect inhibition of metabolism alone, reduced P-glycoprotein efflux only, or a combination of both effects [281].

The overall importance of CYP3A in human drug metabolism and the propensity of this isoform's activity to be readily modulated by drug interactions have resulted in considerable effort to identify a suitable *in vivo* probe. In principle, any of the many drugs metabolized by CYP3A could be used to determine the enzyme's activity in the body. This, of course, is the approach used to determine whether a significant interaction occurs between a specific CYP3A substrate and a known inhibitor or inducer. On the other hand, investigation of whether a new drug candidate interacts with CYP3A and studying determinants of the enzyme's activity require a more focused approach. It is now recognized that measurement of the endogenous 6- $\beta$ -hydroxylation of cortisol does not fulfill this requirement (Sec. I), and therefore alternative approaches have been investigated [285].

### A. Dapsone

Dapsone (4,4'-diaminodiphenylsulfone) has been widely used for phenotyping with respect to acetylation by NAT-2; however, the drug is also *N*-hydroxylated. Formation of the hydroxylamine metabolite by human liver microsomes was found to be selectively mediated by CYP3A [286]; this led to the development of a 0–8-hr urinary metabolic recovery ratio approach (dapsone hydroxylamine: dapsone + dapsone hydroxylamine) to quantitatively assess this pathway of metabolism [287,288]. Subsequently, the trait measure has been applied as part of

a “cocktail” approach [35] in a number of studies investigating the putative role of CYP3A as a risk factor in cancer [289–291] and other disease states [288,292,293].

Attempts to correlate the dapson recovery ratio to other measures of CYP3A activity have, however, been disappointing [11,294]. This lack of success is not surprising, since it is now recognized that several CYP isoforms besides CYP3A contribute to dapson's *N*-hydroxylation, including CYP2E1 [295] and CYP2C9 [296]. Furthermore, CYP3A is involved to a major extent only at high concentrations that are not achieved in vivo [295]. Additionally, it has been found that the dapson urinary recovery ratio is not altered by pretreatment with ketoconazole, even though this markedly affects CYP3A activity as measured by the erythromycin breath test [297]. Collectively, this evidence strongly suggests that the dapson recovery ratio is not a useful trait measure to selectively measure CYP3A activity. Nevertheless, there may be some merit in continuing its use as an in vivo probe in certain types of investigations, since a high trait value appears to be associated with a reduced risk of developing aggressive bladder cancer [289–291].

## B. Erythromycin

CYP3A selectively *N*-demethylates erythromycin, and if [<sup>14</sup>C]-*N*-methyl drug is used, the carbon of the methyl group is eventually excreted as <sup>14</sup>CO<sub>2</sub>. Measurement of radioactivity present in a breath sample collected after intravenous administration and expressing this as a fraction of the dose excreted per hour is the basis of the erythromycin breath test [285]. Since the first introduction of this phenotyping procedure, the sampling schedule has changed from multiple collections over 1–2 hr [31,298,299] to a single sample 20 min after drug administration [300–303]. Considerable validation and application of this simple and rapid phenotyping approach have been reported [31,285,298–304], and there is no question that the erythromycin breath test provides a measure of CYP3A activity under certain circumstances and for some types of investigation.

A limiting factor of this breath test is that it appears to measure only CYP3A4-mediated metabolism and not that involving CYP3A5; thus, overall CYP3A activity is underestimated, especially in the 25–30% of individuals with significant hepatic levels of this isoform [281]. More important, however, is the fact that the erythromycin breath test reflects predominantly CYP3A4 activity only in the liver and, therefore, metabolism in the intestinal tract is not measured. This is an obvious limitation with respect to an orally administered drug and may account, in part, for the relatively poor correlation between this trait measure and the oral clearance of several other CYP3A substrates [10,11,294]. Similar poor relationships have also been observed with regard to the breath test and the sys-



temic clearance of drugs that are CYP3A substrates [12,305], which is somewhat unexpected, since the intravenous route of administration is common to both these estimates of drug metabolism. It is, therefore, unclear what the erythromycin breath test is exactly measuring. Clearly this is not erythromycin's clearance or the CYP3A-mediated formation clearance to the *N*-demethylated metabolite, since the antibiotic's half-life is 1–2 hr and breath sampling is at 20 min. The recent findings that erythromycin is a substrate for P-glycoprotein [284,306] and that this probably contributes to the significant biliary excretion of erythromycin [307] further complicate the situation.

Despite these questions and limitations, the erythromycin breath test provides a practical and useful means of assessing CYP3A activity, especially in studies involving its potential modulation. For example, serial monitoring of relative CYP3A activity has proven of value in the drug development process for identifying whether a drug candidate or a new drug affects CYP3A activity and would, therefore, potentially produce a drug interaction with other CYP3A substrates. Even though the findings reflect only hepatic CYP3A4, they should be sufficient evidence that an interaction does [302,304,308] or does not [309,310] occur. Only in the former situation would further targeted studies with additional CYP3A substrates be necessary. However, the need for an *in vivo* probe that takes into account the CYP3A activity involved in presystemic metabolism related to the oral first-pass effect has led to the investigation of approaches other than the erythromycin breath test.

### C. Midazolam

In humans, midazolam is rapidly and almost completely metabolized to its primary 1'-hydroxy metabolite and, to a much lesser extent, to 4-hydroxymidazolam. Both of these pathways are selectively mediated by CYP3A [311,312]. In addition, both intestinal and hepatic microsomes exhibit high midazolam hydroxylation activity, which in the case of the liver is significantly correlated with the drug's systemic clearance [313]. Moreover, scale-up of such *in vitro* measures [282] was found to provide an excellent prediction of the *in vivo* extraction ratios of the two organs [313,314]. Liver dysfunction markedly impairs midazolam's elimination [315,316], and plasma levels during the anhepatic phase of liver transplantation are elevated [317]. A further characteristic of midazolam's metabolism is that it is readily altered by administration of known CYP3A inhibitors (e.g.,azole antifungal agents, certain macrolide antibiotics, HIV protease inhibitors, grapefruit juice) and inducing agents (e.g., anticonvulsants and rifampin) [281]. Collectively, these characteristics fulfill most of the criteria usually accepted for validation of an *in vivo* probe (Sec. II.C).

A plasma-metabolic-ratio (1'-hydroxymidazolam:midazolam) approach

based on a single time-point value at 30 min following an intravenous dose of the probe has been considered as a possible simple phenotypic trait value [313,318]. However, this trait measure now appears to be less valid and useful than originally suggested [314]. Accordingly, a clearance approach is currently the only available way to assess CYP3A activity with this *in vivo* probe. Ideally, a formation clearance, involving measurement of the amount of 1'-hydroxy metabolite formed and eliminated as conjugate in the urine, provides the "gold standard." However, simply using the drug's plasma clearance without "partitioning" this into its individual pathways would also appear to be a valid approach, since midazolam's metabolism and systemic elimination appear to be predominantly, if not exclusively, mediated by CYP3A.

Since midazolam's elimination half-life is only 1–2 hr, phenotyping consists of determining the drug's plasma concentration–time curve by obtaining multiple samples for 6–8 hr following administration of a suitable dose and, if required, a 0–8-hr or 0–12-hr urine collection. If midazolam is given by the oral route, then the measure of CYP3A activity reflects both intestinal and hepatic CYP3A activity. Thus, the phenotypic trait allows quantification of CYP3A function in a way that can be related to therapeutic situations involving oral drug administration. So long as the oral midazolam dose is 5–7.5 mg, adverse effects associated with the drug's sedative effect are generally minimal, unless CYP3A activity is impaired, when a lower dose should be used. Significantly, midazolam's oral clearance is very sensitive to modulation of CYP3A and, therefore, is capable of detecting small changes/differences in the level of activity. For example, rifampin pretreatment was found to reduce the area under the drug's plasma concentration–time curve by 96% [319], whereas ketoconazole increased this parameter by 15-fold [320]. Accordingly, the full range of CYP3A activity that is possible *in vivo* is several 100-fold. Moreover, more modest changes [281], including no effect at all [321–323], can be readily detected.

Midazolam may also be safely administered in doses below about 2 mg by the intravenous route, but in some subjects this is accompanied by mild sedation, which requires appropriate clinical monitoring. Thus, estimation of the drug's systemic clearance resulting from CYP3A-mediated metabolism is possible, and in contrast to the drug's oral clearance, this measure appears to reflect predominantly hepatic elimination; i.e., the contribution of extrahepatic CYP3A is relatively small [317]. This probably reflects the fact that intestinal CYP3A is localized in the apical region of the enterocytes and, therefore, access of drug in the systemic blood is limited. Moreover, midazolam is extensively bound to plasma proteins (>98%), which further impairs midazolam's distribution to this site. Accordingly, a second CYP3A trait measure is available that focuses mainly on the enzyme's activity in the liver. By appropriate analysis of both of these clearance values determined in the same individual, it is possible to further char-

acterize CYP3A activity by estimating the separate contributions of the intestine and the liver to the overall metabolism of midazolam [314]. These two clearance estimates may be obtained by serially administering midazolam by the two routes of administration on separate occasions. However, a more desirable approach, which removes any error associated with intrasubject variability in CYP3A activity, employs the simultaneous administration of a stable-labeled [ $^{15}\text{N}_3$ ] form of the drug along with unlabeled drug by the other route. Recent applications of this elegant approach have found that CYP3A in the intestine contributes almost equally to midazolam's first-pass metabolism after an oral dose [314]. Also, the inhibition of CYP3A activity by pretreatment with clarithromycin affects mainly the intestinal enzyme, which in turn is the major determinant of the drug's interindividual variability and not hepatic CYP3A activity [324]. The potential to obtain further mechanistic understanding about drug:drug interaction involving CYP3A using this approach would appear to be considerable.

Both the erythromycin breath test and estimation of the oral and/or intravenous clearances of midazolam appear to provide practical and useful information of the *in vivo* level of CYP3A activity. However, it is clear that these different phenotypic trait values reflect different aspects of such activity. Accordingly, selection of the more appropriate approach depends to a large extent on the particular question being addressed. In general, the erythromycin breath test provides a simple but relative measure that is well suited for temporal monitoring of hepatic CYP3A4 activity, as would be applicable to detect alterations in this enzyme's activity associated with inhibition or induction caused by a drug interaction. On the other hand, the use of midazolam provides a more absolute measure, and, in the case of the drug's oral clearance, this finding can be quantitatively extrapolated to other CYP3A substrates when these are used in a therapeutic situation. Attempts have been successfully made to combine the use of the two *in vivo* probe drugs by administering them concurrently [325]. However, the simultaneous administration of midazolam by the oral and intravenous routes would appear to be a more rigorous and informative approach [314,324], providing the necessary analytical instrumentation is available.

## IX. PERSPECTIVES

Over the past decade, considerable progress has occurred in the development and application of *in vivo* probes suitable for assessing the catalytic activity of individual CYP isoforms in human subjects. CYP2C19 and CYP2D6 have benefited most from this effort, which has focused mainly on phenotypic classification because of the extremely large interindividual variability in enzyme activity

across the population distribution curve, i.e., from ultrarapid/extensive to poor metabolizers. It is likely that a similar level of investigation will occur with the other isoforms that have more recently been shown to have rare or polymorphic variant alleles, e.g., CYP2A6, CYP2C9, and CYP2E1. Undoubtedly, molecular genetic approaches will continue to identify new genomic polymorphisms for these and possibly other CYP isoforms, similar to the situation that has been found with the more established genetic polymorphisms. A future critical issue, therefore, will be to establish any functional significance of these mutant alleles by appropriate *in vitro* approaches and, importantly, to confirm that a genotype:phenotype relationship exists and is important in the *in vivo* setting. Such studies will be facilitated by the availability of new, simple, reliable, and valid phenotypic trait measures for the isoforms of interest.

In general, the *in vivo* activity of most of the characterized and expressed CYP isoforms that are important in the metabolism of drugs and other xenobiotics of toxicologic interest can currently be assessed, at least at the level of the whole organism. The exception is CYP2B6; an isoform whose role and importance in the metabolism of xenobiotics has yet to be adequately defined. Recent studies suggest that CYP2B6 may be more important than previously considered, despite the fact that it is a minor hepatic CYP [326,327]. However, identification of a selective probe, even for *in vitro* studies, has been problematic [326,328], although the *N*-demethylation of *S*-mephenytoin to nirvanol shows promise in this regard [328,329]. Unfortunately, the substrate concentrations used with this putative probe make it unsuitable for *in vivo* phenotyping, since they are rarely encountered in humans [329]. CYP2B6 was the only one of 10 recombinant expressed human CYP isoforms able to *trans*-hydroxylate the investigational drug RP 73401 [330]. Since this is the primary route of metabolism of this compound *in vivo*, it is possible that a suitable phenotypic trait measure for CYP2B6 could be developed using RP73401, if the drug becomes clinically available.

All of the available *in vivo* probes and associated trait measures appear to be sufficiently sensitive and suitable for evaluating changes/differences in the particular isoform's level of activity. Accordingly, they may be applied to investigating the presence or absence of a drug interaction and provide insight into its mechanism. Selection of the most appropriate approach, when several *in vivo* probes or trait measures are available for a particular isoform, depends to a large extent on the purpose of the study. Indirect trait values based on a single point determination such as a saliva/plasma/urine metabolic ratio are well suited to screening studies designed to answer the question of whether an interaction occurs or not. Incorporating several *in vivo* probes into a "cocktail" strategy further facilitates this goal. On the other hand, more quantitative questions related to the extent to which metabolism is inhibited or induced and to sites of interaction (intestine versus liver) may require the use of trait values based on more direct

measures, such as clearance approaches. Regardless, interpretation of any change in the trait measure is critically dependent on an understanding of its basis and limitations. Finally, it should be appreciated that the *in vivo* evaluation of enzyme activity is in most cases complementary to information obtained by applying the approaches of molecular genetics. However, it has the added advantage that it also reflects the contributions of other determinants, including the effects of environmental factors and disease states; moreover, in many instances, phenotyping has direct therapeutic relevance.

## ACKNOWLEDGMENT

This work was supported, in part, by grants GM31304 and CA76020 from the United States Public Health Service.

## REFERENCES

1. JR Gillette. Keynote address: man, mice, microsomes, metabolites, and mathematics—40 years after the revolution. *Drug Metab Rev* 27:1–44, 1995.
2. E-U Griese, UM Zanger, U Brudermanns, A Gaedigk, G Mikus, K Mörike, T Stüven, M Eichelbaum. Assessment of the predictive power of genotypes for the *in vivo* catalytic function of CYP2D6 in a German population. *Pharmacogenetics* 8: 15–26, 1998.
3. JA Goldstein, J Blaisdell. Genetic tests which identify the principal defects in CYP2C19 responsible for the polymorphism in mephenytoin metabolism. In: EF Johnson, MR Waterman, eds. *Cytochrome P450, Part B: Methods in Enzymology*, San Diego, CA: Academic Press, 272:210–218, 1996.
4. ES Vesell, JG Page. Genetic control of drug levels in man: antipyrine. *Science* 161: 72–73, 1968.
5. BK Park. Assessment of urinary 6 $\beta$ -hydroxycortisol as an *in vivo* index of mixed-function oxygenase activity. *Br J Clin Pharmacol* 12:97–102, 1981.
6. GR Wilkinson. Prediction of interpatient variability of drug metabolizing ability. In: GR Wilkinson, MD Rawlins, eds. *Drug Metabolism and Disposition: Considerations in Clinical Pharmacology*, Lancaster, PA: MTP Press, 1985, pp 183–209.
7. DJ Waxman, C Attisano, FP Guengerich, DP Lapenson. Human liver microsomal steroid metabolism: identification of the major microsomal steroid hormone 6 $\beta$ -hydroxylase cytochrome P-450 enzyme. *Arch Biochem Biophys* 263:424–436, 1988.
8. C Ged, JM Rouillon, L Pichard, J Combalbert, N Bressot, P Bories, H Michel, P Beaune, P Maurel. The increase in urinary excretion of 6 $\beta$ -hydroxycortisol as a marker of human hepatic cytochrome P450III<sub>A</sub> induction. *Br J Clin Pharmacol* 28: 373–387, 1989.
9. PB Watkins, DK Turgeon, P Saenger, KS Lown, JC Kolars, T Hamilton, K Fish-

- man, PS Guzelian, JJ Voorhees. Comparison of urinary 6-beta-cortisol and the erythromycin breath test as measures of hepatic P450III<sub>A</sub> (CYP3A) activity. *Clin Pharmacol Ther* 52:265–273, 1992.
10. CM Hunt, PB Watkins, P Saenger, GM Stave, N Barlascini, CO Watlington, JT Wright Jr, PS Guzelian. Heterogeneity of CYP3A isoforms metabolizing erythromycin and cortisol. *Clin Pharmacol Ther* 51:18–23, 1992.
  11. MT Kinirons, D O'Shea, TE Downing, AT Fitzwilliam, L Joellenbeck, JD Groopman, GR Wilkinson, AJJ Wood. Absence of correlations among three putative in vivo probes of human cytochrome P4503A activity in young healthy men. *Clin Pharmacol Ther* 54:621–629, 1993.
  12. MT Kinirons, D O'Shea, JD Groopman, KE Thummel, AJJ Wood, GR Wilkinson. Route of administration does not explain the lack of correlation between putative in vivo probes of cytochrome P4503A. *Br J Clin Pharmacol* 37:501P–502P, 1994.
  13. J Seidegård, K Dahlström, A Kullberg. Effect of grapefruit juice on urinary 6 $\beta$ -hydroxycortisol/cortisol excretion. *Clin Exp Pharmacol Physiol* 25:379–381, 1998.
  14. SJ Kovacs, DE Martin, DE Everitt, SD Patterson, DK Jorkasky. Urinary excretion of 6-beta-hydroxycortisol as an in vivo marker for CYP3A induction: applications and recommendations. *Clin Pharmacol Therap* 63:617–622, 1998.
  15. JC Fleishaker, LK Pearson, GR Peters. Induction of tirilazad clearance by phenytoin. *Biopharmaceut Drug Disp* 19:91–96, 1998.
  16. B Monsarrat, E Chatelut, I Royer, P Alvinerie, J Dubois, A Dezeuse, H Roche, S Cros, M Wright, P Canal. Modification of paclitaxel metabolism in a cancer patient by induction of cytochrome P450 3A4. *Drug Metab Disp* 26:229–233, 1998.
  17. GR Wilkinson. Clearance approaches in pharmacology. *Pharmacol Rev* 39:1–47, 1987.
  18. PR Jackson, GT Tucker, MS Lennard, HF Woods. Polymorphic drug oxidation: pharmacokinetic basis and comparison of experimental indices. *Br J Clin Pharmacol* 22:541–550, 1986.
  19. P Dálen, M-L Dahl, M Eichelbaum, L Bertilsson, GR Wilkinson. Disposition of debrisoquine in Caucasians with different CYP2D6-genotypes including those with multiple genes. *Pharmacogenetics* 9:697–706, 1999.
  20. T Inaba, SV Otton, W Kalow. Debrisoquine hydroxylation capacity: problems of assessment in two populations. *Clin Pharmacol Ther* 29:218–223, 1981.
  21. A Kaisary, P Smith, E Jacqz, CB McAllister, GR Wilkinson, WA Ray, RA Branch. Genetic predisposition to bladder cancer: ability to hydroxylate debrisoquine and mephenytoin as risk factors. *Cancer Res* 47:5488–5493, 1987.
  22. A Küpfer, R Preisig. Pharmacogenetics of mephenytoin: a new drug hydroxylation polymorphism in man. *Eur J Clin Pharmacol* 26:753–759, 1984.
  23. PJ Wedlund, WS Aslanian, CB McAllister, GR Wilkinson, RA Branch. Mephenytoin hydroxylation deficiency in Caucasians: frequency of a new oxidative drug metabolism polymorphism. *Clin Pharmacol Ther* 36:773–780, 1984.
  24. J-P Kévorkian, C Michel, U Hofmann, E Jacqz-Aigrain, HK Kroemer, M-N Peraldi, M Eichelbaum, P Jaillon, C Funck-Brentano. Assessment of individual CYP2D6 activity in extensive metabolizers with renal failure: comparison of sparteine and dextromethorphan. *Clin Pharmacol Ther* 59:583–592, 1996.

25. C Girre, D Lucas, E Hispand, C Menez, S Dally, J-F Menez. Assessment of cytochrome P4502E1 induction in alcoholic patients by chlorzoxazone pharmacokinetics. *Biochem Pharmacol* 47:1503–1508, 1994.
26. Frye RF, A Adedoyin, K Mauro, GR Matzke, RA Branch. Use of chlorzoxazone as an in vivo probe of cytochrome P450 2E1: choice of dose and phenotypic trait measure. *J Clin Pharmacol* 38:82–89, 1998.
27. JB Houston. Drug metabolite kinetics. *Pharmac Ther* 15:521–552, 1982.
28. RB Kim, D O’Shea, GR Wilkinson. Interindividual variability of chlorzoxazone 6-hydroxylation in men and women and its relationship to CYP2E1 genetic polymorphisms. *Clin Pharmacol Ther* 57:645–655, 1995.
29. GH Lambert, AN Kotake, D Schoeller. The CO<sub>2</sub> breath tests as monitors of the cytochrome P450 dependent mixed function monooxygenase system. *Prog Clin Biol Res* 135:119–145, 1983.
30. EA Lane, I Parashos. Drug pharmacokinetics and the carbon dioxide breath test. *J Pharmacokinetic Biopharm* 14:29–49, 1986.
31. KS Lown, KE Thummel, PE Benedict, DD Shen, DK Turgeon, S Berent, PB Watkins. The erythromycin breath test predicts the clearance of midazolam. *Clin Pharmacol Ther* 57:16–24, 1995.
32. DD Breimer, JHM Schellens. A “cocktail” strategy to assess in vivo oxidative drug metabolism in humans. *Trends Pharmacol Sci* 11:223–225, 1990.
33. EJ Sanz, T Villén, C Alm, L Bertilsson. *S*-Mephenytoin hydroxylation phenotypes in a Swedish population determined after coadministration with debrisoquin. *Clin Pharmacol Ther* 45:495–499, 1989.
34. JHM Schellens, H Ghabrial, HHH van der Wart, EN Bakker, GR Wilkinson, DD Breimer. Differential effects of quinidine on the disposition of nifedipine, sparteine, and mephenytoin in humans. *Clin Pharmacol Ther* 50:520–528, 1991.
35. RF Frye, GR Matzke, A Adedoyin, JA Porter, RA Branch. Validation of the five-drug “Pittsburgh cocktail” approach for assessment of selective regulation of drug-metabolizing enzymes. *Clin Pharmacol Ther* 62:365–376, 1997.
36. HGE Endres, L Henschel, U Merkel, M Hippus, A Hoffman. Lack of pharmacokinetic interaction between dextromethorphan, coumarin and mephenytoin in man after simultaneous administration. *Pharmazie* 51:46–51, 1996.
37. A Adedoyin, RF Frye, K Mauro, RA Branch. Chloroquine modulation of specific metabolizing enzymes activities: investigation with selective five drug cocktail. *Br J Clin Pharmacol* 46:215–219, 1998.
38. E Jacqz-Aigrain, C Funck-Brentano, T Cresteil. CYP2D6- and CYP3A-dependent metabolism of dextromethorphan in humans. *Pharmacogenetics* 3:197–204, 1993.
39. DR Jones, JC Gorski, MA Hamman, SD Hall. Quantification of dextromethorphan and metabolites: a dual phenotypic marker for cytochrome P450 3A4/5 and 2D6 activity. *J Chromatog B* 678:105–111, 1996.
40. J Ducharme, S Abdullah, IW Wainer. Dextromethorphan as an in vivo probe for the simultaneous determination of CYP2D6 and CYP3A activity. *J Chromatog B* 678:113–128, 1996.
41. J Schmider, DJ Greenblatt, SM Fogelman, LV von Moltke, RI Shader. Metabolism of dextromethorphan in vitro: involvement of cytochromes P450 2D6 and 3A3/4, with a possible role of 2E1. *Biopharmaceut Drug Disp* 18:227–240, 1997.

42. LS Kaminsky, Z-Y Zhang. Human P450 metabolism of warfarin. *Pharmacol Ther* 73:67–74, 1997.
43. LC Wienkers, CJ Wurden, E Storch, KL Kunze, AE Rettie, WF Trager. Formation of (*R*)-8-hydroxywarfarin in human liver microsomes—a new metabolic marker for the (*S*)-mephenytoin hydroxylase, P450C19. *Drug Metab Disp* 24:610–614, 1996.
44. FP Guengerich. Human cytochrome P450 enzymes. In: *Cytochrome P450: Structure, Mechanism, and Biochemistry*. PR Ortiz de Montellano, ed. New York: Plenum, pp 473–535, 1995.
45. W Kalow, B-K Tang. The use of caffeine for enzyme assays: a critical appraisal. *Clin Pharmacol Ther* 53:503–514, 1993.
46. JO Miners, DJ Birkett. The use of caffeine as a metabolic probe for human drug metabolizing enzymes. *Gen Pharmac* 27:245–249, 1996.
47. U Fuhr, KL Rost, R Engelhardt, M Sachs, D Liermann, C Belloc, P Beaune, S Janezic, D Grant, UA Meyer, AH Staib. Evaluation of caffeine as a test drug for CYP1A2, NAT2 and CYP2E1 phenotyping in man by in vivo versus in vitro correlations. *Pharmacogenetics* 6:159–176, 1996.
48. RA Nagel, LY Dirix, KM Hayllar, R Preisig, JM Tredger, R Williams. Use of quantitative liver function tests—caffeine clearance and galactose elimination capacity—after orthotopic liver transplantation. *J Hepatol* 10:149–157, 1990.
49. CP Denaro, P Jacob III, NL Benowitz. Evaluation of pharmacokinetic methods used to estimate caffeine clearance and comparison with a Bayesian forecasting method. *Ther Drug Monit* 20:78–87, 1998.
50. A Balogh, S Harder, R Vollandt, AH Staib. Intra-individual variability of caffeine elimination in healthy subjects. *Int J Clin Pharmacol Ther Toxicol* 30:383–387, 1992.
51. A Rostami-Hodjegan, S Nurminen, PR Jackson, GT Tucker. Caffeine urinary metabolite ratios as markers of enzyme activity: a theoretical assessment. *Pharmacogenetics* 6:121–149, 1996.
52. G Jost, A Wahlländer, U von Mandach, R Preisig. Overnight salivary caffeine clearance: a liver function test suitable for routine use. *Hepatology* 7:338–344, 1987.
53. U Fuhr, K Klittich, AH Staib. Inhibitory effect of grapefruit juice and its bitter principal, naringenin, on CYP1A2 dependent metabolism of caffeine in man. *Br J Clin Pharmacol* 35:431–436, 1993.
54. ME Campbell, SP Spielberg, W Kalow. A urinary metabolite ratio that reflects systemic caffeine clearance. *Clin Pharmacol Ther* 42:157–165, 1987.
55. A Wahlländer, S Mohr, G Paumgartner. Assessment of hepatic function—comparison of caffeine clearance in serum and saliva during the day and at night. *J Hepatol* 10:129–137, 1990.
56. U Fuhr, KL Rost. Simple and reliable CYP1A2 phenotyping by the paraxanthine/caffeine ratio in plasma and in saliva. *Pharmacogenetics* 4:109–116, 1994.
57. H Wietholtz, M Voegelin, MJ Arnaud, J Bircher, R Preisig. Assessment of the cytochrome P-448 dependent liver enzyme system by a caffeine breath test. *Eur J Clin Pharmacol* 21:53–59, 1981.
58. AN Kotake, DA Schoeller, GH Lambert, AL Baker, DD Schaffer, H Josephs. The



- caffeine CO<sub>2</sub> breath test: dose response and route of *N*-demethylation in smokers and nonsmokers. *Clin Pharmacol Ther* 32:261–269, 1982.
59. Y Horsmans, X De Koninck, AP Geubel, S Pauwels. Microsomal function in hepatitis B surface antigen healthy carriers: assessment of cytochrome P450 1A2 activity by the <sup>14</sup>C-caffeine breath test. *Pharmacol Toxicol* 77:247–249, 1995.
  60. KL Rost, H Brösicke, J Brockmöller, M Scheffler, H Helge, I Roots. Increase of cytochrome P4501A2 activity by omeprazole: evidence by the <sup>13</sup>C-[*N*-3-methyl]-caffeine breath test in poor and extensive metabolizers of *S*-mephenytoin. *Clin Pharmacol Ther* 52:170–180, 1992.
  61. KL Rost, I Roots. Accelerated caffeine metabolism after omeprazole treatment is indicated by urinary metabolite ratios: coincidence with plasma clearance and breath test. *Clin Pharmacol Ther* 55:402–411, 1994.
  62. E Renner, H Wietholtz, P Huguenin, MJ Arnaud, R Preisig. Caffeine: a model compound for measuring liver function. *Hepatology* 4:38–46, 1984.
  63. G Pons, J-C Blais, E Rey, M Plissonnier, M-O Richard, O Carrier, P D'Athis, C Moran, J Badoual, G Olive. Maturation of caffeine *N*-demethylation in infancy: a study using the <sup>13</sup>CO<sub>2</sub> breath test. *Pediatr Res* 23:632–636, 1988.
  64. RJ Fontana, DK Turgeon, TF Woolf, MJ Knapp, NL Foster, PB Watkins. The caffeine breath test does not identify patients susceptible to tacrine hepatotoxicity. *Hepatology* 23:1429–1435, 1996.
  65. KJ Breen, RW Bury, IV Calder, PV Desmond, M Peters, ML Mashford. A [<sup>14</sup>C] phenacetin breath test to measure hepatic function in man. *Hepatology* 4:47–52, 1984.
  66. DA Schoeller, AN Kotake, GH Lambert, PS Krager, AL Baker. Comparison of the phenacetin and aminopyrine breath tests: effect of liver disease, inducers and cobaltous chloride. *Hepatology* 5:276–281, 1985.
  67. B-K Tang, D Kadar, L Quian, J Iriah, J Yip, W Kalow. Caffeine as a metabolic probe: validation of its use for acetylator phenotyping. *Clin Pharmacol Ther* 49: 648–657, 1991.
  68. LJ Notarianni, SE Oliver, P Dobrocky, PN Bennett, BW Silverman. Caffeine as a metabolic probe: a comparison of the metabolic ratios used to assess CYP1A2 activity. *Br J Clin Pharmacol* 39:65–69, 1995.
  69. CP Denaro, M Wilson, P Jacob III, NL Benowitz. Validation of urine caffeine metabolite ratios with use of stable isotope-labeled caffeine clearance. *Clin Pharmacol Ther* 59:284–296, 1996.
  70. B-K Tang, Y Zhou, D Kadar, W Kalow. Caffeine as a probe for CYP1A2 activity: potential influence of renal factors on urinary phenotypic trait measurements. *Pharmacogenetics* 4:117–124, 1994.
  71. MA Butler, NP Lange, JF Young, NE Caporaso, P Vineis, RB Hayes, CH Teitel, JP Messingill, MF Lawsen, FF Kadlubar. Determination of CYP1A2 and NAT2 phenotypes in human populations by analysis of caffeine urinary metabolites. *Pharmacogenetics* 2:116–127, 1992.
  72. M Nakajima, T Yokoi, M Mizutani, S Shin, FF Kadlubar, T Kamataki. Phenotyping of CYP1A2 in Japanese population by analysis of caffeine urinary metabolites: absence of mutation prescribing the phenotype in the CYP1A2 gene. *Cancer Epidemiol Biomarkers Prevention* 3:413–421, 1994.

73. T Yokoi, M Sawada, T Kamataki. Polymorphic drug metabolism: studies with recombinant Chinese hamster cells and analyses in human populations. *Pharmacogenetics* 5:S65–S69, 1995.
74. MV Relling, J-S Lin, GD Ayers, WE Evans. Racial and gender differences in *N*-acetyltransferase, xanthine oxidase, and CYP1A2 activities. *Clin Pharmacol Ther* 52:643–658, 1992.
75. W Kalow, B-K Tang. Caffeine as a metabolic probe: exploration of the enzyme-inducing effect of cigarette smoking. *Clin Pharmacol Ther* 49:44–48, 1991.
76. W Kalow, B-K Tang. Use of caffeine metabolite ratios to explore CYP1A2 and xanthine oxidase activities. *Clin Pharmacol Ther* 50:508–19, 1991.
77. K Vistisen, HE Poulsen, S Loft. Foreign compound metabolism capacity in man measured from metabolites of dietary caffeine. *Carcinogenesis* 13:1561–1568, 1992.
78. JA Carrillo, J Benítez. Caffeine metabolism in a healthy Spanish population: *N*-acetylator phenotype and oxidation pathways. *Clin Pharmacol Ther* 55:293–304, 1994.
79. A Catteau, YC Bechtel, N Poisson, PR Bechtel, C Bonaiti-Pellie. A population and family study of CYP1A2 using caffeine urinary metabolites. *Eur J Clin Pharmacol* 47:423–430, 1995.
80. BB Rasmussen, K Brøsen. Determination of urinary metabolites of caffeine for the assessment of cytochrome P4501A2, xanthine oxidase, and *N*-acetyltransferase activity in humans. *Therap Drug Monit* 18:254–262, 1996.
81. NP Lang, MA Butler, J Massengill, M Lawson RC Stotts, M Hauer-Jensen, FF Kadlubar. Rapid metabolic phenotypes of acetyltransferase and cytochrome P4501A2 and putative exposure to food-borne heterocyclic amines increase the risk for colorectal cancer or polyps. *Cancer Epidemiol Biomarkers Prevention* 3:675–682, 1994.
82. AJ Kilbane, LK Silbart, M Manis, IZ Beitins, WW Weber. Human *N*-acetylation genotype determination with urinary caffeine metabolites. *Clin Pharmacol Ther* 47:470–477, 1990.
83. SH McQuilkin, DW Nierenberg, E Bresnick. Analysis of within-subject variation of caffeine metabolism when used to determine cytochrome P4501A2 and *N*-acetyltransferase-2 activities. *Cancer Epidemiol Biomarkers Prevention* 4:139–146, 1995.
84. BG Hardy, C Lemieux, SE Walker, WR Bartle. Interindividual and intraindividual variability in acetylation: characterization with caffeine. *Clin Pharmacol Ther* 44:152–157, 1988.
85. BK Tang, D Kadar, W Kalow. An alternative test for acetylator phenotyping with caffeine. *Clin Pharmacol Ther* 42:509–513, 1987.
86. BB Rasmussen, K Brøsen. Theophylline has no advantages over caffeine as a putative model drug for assessing CYP1A2 activity in humans. *Br J Clin Pharmacol* 43:253–258, 1997.
87. H Raunio, T Syngelmä, M Pasanen, R Juvonen, P Honkakoski, MA Kairaluoma, E Sotaniemi, MA Lang, O Pelkonen. Immunochemical and catalytical studies on hepatic coumarin 7-hydroxylase in man, rat, and mouse. *Biochem Pharmacol* 37:3889–3895, 1988.

88. JS Miles, AW McLaren, LM Forrester, MJ Glancey, MA Lang, CR Wolf. Identification of the human liver cytochrome P-450 responsible for coumarin 7-hydroxylase activity. *Biochem J* 267:365–371, 1990.
89. ED Kharasch, DC Hankins, KE Thummel. Human kidney methoxyflurane and sevoflurane metabolism. Intrarenal fluoride production as a possible mechanism of methoxyflurane nephrotoxicity. *Anesthesiology* 82:689–699, 1995.
90. DK Spracklin, DC Hankins, JM Fisher, KE Thummel, ED Kharasch. Cytochrome P4502E1 is the principal catalyst of human oxidative halothane metabolism in vitro. *J Pharmacol Exp Ther* 281:400–411, 1997.
91. AJM Sadeque, MB Fisher, KR Korzekwa, FJ Gonzalez, AE Rettie. Human CYP2C9 and CYP2A6 mediate formation of the hepatotoxin 4-ene-valproic acid. *J Pharmacol Exp Ther* 283:698–703, 1997.
92. A Madan, A Parkinson, MD Faiman. Identification of the human and rat P450 enzymes responsible for the sulfoxidation of *S*-methyl *N,N*-diethylthiolcarbamate (DETC-ME). The terminal step in the bioactivation of disulfiram. *Drug Metab Disp* 23:1153–1163, 1995.
93. CD Torchin, PJ McNeilly, IM Kapetanovic, JM Strong, HJ Kupferberg. Stereoselective metabolism of a new anticonvulsant drug candidate, losigamone, by human liver microsomes. *Drug Metab Disp* 24:1002–1008, 1996.
94. B Wirz, B Valles, A Parkinson, A Madan, A Probst, A Zimmerlin, J Gut. CYP3A4 and CYP2A6 are involved in the biotransformation of letrozole. *ISSX Proc* 10: 359, 1996.
95. KI Nunoya, T Yokoi, K Kimura, T Kodama, M Funayama, K Inoue, K Nagashima, Y Funae, N Shimada, C Green, T Kamataki. (+)-Cis-3,5-dimethyl-2-(3-pyridyl)thiazolidin-4-one hydrochloride (SM-12502) as a novel substrate for cytochrome P450 2A6 in human liver microsomes. *J Pharmacol Exp Ther* 277:768–774, 1996.
96. S Yamano, J Tatsuno, FJ Gonzalez. The CYP2A3 gene product catalyzes coumarin 7-hydroxylation in human liver microsomes. *Biochemistry* 29:1322–1329, 1990.
97. H Hadidi, K Zahlsen, JR Idle, S Cholerton. A single amino acid substitution (Leu160His) in cytochrome P450 CYP2A6 causes switching from 7-hydroxylation to 3-hydroxylation of coumarin. *Food Chem Toxic* 35:903–907, 1997.
98. M Oscarson. Genetic polymorphisms in the cytochrome P450 2A6 (CYP2A6) gene: implications for interindividual differences in nicotine metabolism. *Drug Metab Disp* 29:91–95, 2001.
99. P Fernandez-Salguero, SM Hoffman, S Cholerton, H Mohrenweiser, H Raunio, A Rautio, O Pelkonen, JD Huang, WE Evans, JR Idle Jr. A genetic polymorphism in coumarin 7-hydroxylation: sequence of the human CYP2A genes and identification of variant CYP2A6 alleles. *Am J Hum Genet* 57:651–660, 1995.
100. K Nunoya, T Yokoi, K Kimura, K Inoue, T Kodama, M Funayama, K Nagashima, Y Funae, C Green, M Kinoshita, T Kamataki. A new deleted allele in the human cytochrome P4502A6 (CYP2A6) gene found in individuals showing poor metabolic capacity to coumarin and (+)-cis-3,5-dimethyl-2-(3-pyridyl)thiazolidin-4-one hydrochloride (SM-12502). *Pharmacogenetics* 8:239–249, 1998.
101. Y Rao, E Hoffmann, M Zia, L Bodin, M Zeman, EM Sellars, RF Tyndale. Duplications and defects in the CYP2A6 gene: identification, genotyping and in vivo effects on smoking. *Mol Pharmacol* 58:747–755, 2000.

102. A Rautio, H Kraul, A Kojo, E Salmela, O Pelkonen. Interindividual variability of coumarin 7-hydroxylation in healthy volunteers. *Pharmacogenetics* 2:227–233, 1992.
103. S Cholerton, ME Idle, A Vas, FJ Gonzalez, JR Idle. Comparison of a novel thin-layer chromatographic-fluorescence detection method with a spectrofluorometric method for the determination of 7-hydroxycoumarin in human urine. *J Chromatog* 575:325–330, 1992.
104. M Iscan, H Rostami, M Iscan, T Güray, O Pelkonen, A Rautio. Interindividual variability of coumarin 7-hydroxylation in a Turkish population. *Eur J Clin Pharmacol* 47:315–318, 1994.
105. M Oscarson, H Gullstén, A Rautio, ML Bernal, B Sinues, M-L Dahl, JH Stengård, O Pelkonen, H Raunio, M Ingelman-Sundberg. Genotyping of human cytochrome P4502A6 (CYP2A6), a nicotine C-oxidase. *FEBS Letters* 438:201–205, 1998.
106. EA Sotaniemi, P Lumme, P Arvela, A Rautio. Age and CYP3A4 and CYP2A6 activities marked by the metabolism of lignocaine and coumarin in man. *Thérapie* 51:363–366, 1996.
107. U Merkel, H Sigusch, A Hoffmann. Grapefruit juice inhibits 7-hydroxylation of coumarin in healthy volunteers. *Eur J Clin Pharmacol* 46:175–177, 1994.
108. ED Kharasch, DC Hankins, PJ Baxter, KE Thummel. Single-dose disulfiram does not inhibit CYP2A6 activity. *Clin Pharmacol Ther* 64:39–45, 1998.
109. EA Sotaniemi, A Rautio, M Bäckstrom, P Arvela, O Pelkonen. CYP3A4 and CYP2A6 activities marked by the metabolism of lignocaine and coumarin in patients with liver and kidney diseases and epileptic patients. *Br J Clin Pharmacol* 39: 71–76, 1995.
110. H Hadidi, Y Irshaid, CB Vågbo, A Brunsvik, S Cholerton, K Zahlens, JR Idle. Variability of coumarin 7- and 3-hydroxylation in a Jordanian population is suggestive of a functional polymorphism in cytochrome P450 CYP2A6. *Eur J Clin Pharmacol* 54:437–441, 1998.
111. D Egan, R O’Kennedy, E Moran, D Cox, ENA Posser, RD Thornes. The pharmacology, metabolism, analysis, and applications of coumarin and coumarin-related compounds. *Drug Metab Rev* 22:503–529, 1990.
112. ME Marshall, JL Mohler, K Edmonds, B Williams, K Butler, M Ryles, L Weiss, D Urban, A Bueschen, M Markiewicz, G Cloud. An updated review of the clinical development of coumarin (1,2-benzopyrene) and 7-hydroxycoumarin. *J Cancer Res Clin Oncol* 120:S39–S42, 1994.
113. P Jacob III, NL Benowitz, AT Shulgin. Recent studies of nicotine metabolism in humans. *Pharmacol Biochem Behav* 30:249–253, 1988.
114. ES Messina, RF Tyndale, EM Sellers. A major role for CYP2A6 in nicotine C-oxidation by human liver microsomes. *J Pharmacol Exp Ther* 282:1608–1614, 1997.
115. M Nakajima, T Yamamoto, K-I Nunoya, T Yokoi, K Nagashima, K Inoue, Y Funae, N Shimada, T Kamataki, Y Kuroiwa. Characterization of CYP2A6 involved in 3’-hydroxylation of cotinine in human liver microsomes. *J Pharmacol Exp Ther* 277:1010–1015, 1996.
116. NL Benowitz, P Jacob III. Metabolism of nicotine to cotinine studied by a dual stable isotope method. *Clin Pharmacol Ther* 56:483–493, 1994.

117. EJ Pérez-Stable, B Herrera, P Jacob III, NL Benowitz. Nicotine metabolism and intake in Black and White smokers. *JAMA* 280:152–156, 1998.
118. NL Benowitz, P Jacob III, DPL Sachs. Deficient C-oxidation of nicotine. *Clin Pharmacol Ther* 57:590–594, 1995.
119. JO Miners, DJ Birkett. Cytochrome P4502C9: an enzyme of major importance in human drug metabolism. *Br J Clin Pharmacol* 45:525–538, 1998.
120. DJ Steward, RL Haining, KR Henne, G Davis, TH Rushmore, WF Trager, AE Rettie. Genetic association between sensitivity to warfarin and expression of CYP2C9\*3. *Pharmacogenetics* 7:361–376, 1997.
121. KR Henne, A Gaedigk, G Gupta, JS Leeder, AE Rettie. Chiral phase analysis of warfarin enantiomers in patient plasma in relation to CYP2C9 genotype. *J Chromatograph B* 710:143–148, 1998.
122. H Takahashi, T Kashima, Y Nomizo, N Muramoto, T Shimizu, K Nasu, T Kubota, S Kimura, H Echizen. Metabolism of warfarin enantiomers in Japanese patients with heart disease having different CYP2C9 and CYP2C19 genotypes. *Clin Pharmacol Ther* 63:519–528, 1998.
123. CR Bhasker, JO Miners, S Coulter, DJ Birkett. Allelic and functional variability of cytochrome P4502C9. *Pharmacogenetics* 7:51–58, 1997.
124. JB McCrea, A Cribb, T Rushmore, B Osborne, L Gillen, M-W Lo, S Waldman, T Bjornsson, S Spielberg, M Goldberg. Phenotypic and genotypic investigations of a healthy volunteer deficiency in the conversion of losartan to its active metabolite E-3174. *Clin Pharmacol Ther* 65:348–352, 1999.
125. H Furuya, P Fernandez-Salguero, W Gregory, H Taber, A Steward, FJ Gonzalez, JR Idle. Genetic polymorphism of CYP2C9 and its effect on warfarin maintenance dose requirement in patients undergoing anticoagulation therapy. *Pharmacogenetics* 5:389–392, 1995.
126. W Tassaneeyakul, DJ Birkett, MC Pass, JO Miners. Limited value of the urinary phenytoin metabolic ratio for the assessment of cytochrome P4502C9 activity in vivo. *Br J Clin Pharmacol* 42:774–778, 1996.
127. RG Knodell, SD Hall, GR Wilkinson, FP Guengerich. Hepatic metabolism of tolbutamide: characterization of the form of cytochrome P-450 involved in methyl hydroxylation and relationship in vivo disposition. *J Pharmacol Exp Ther* 241:1112–1119, 1987.
128. ME Veronese, JO Miners, D Randles, D Gregov, DJ Birkett. Validation of the tolbutamide metabolic ratio for population screening with use of sulfaphenazole to produce model phenotypic poor metabolizers. *Clin Pharmacol Ther* 47:403–411, 1990.
129. ME Veronese, JO Miners, DLP Rees, DJ Birkett. Tolbutamide hydroxylation in humans: lack of bimodality in 106 healthy subjects. *Pharmacogenetics* 3:86–93, 1993.
130. YSR Krishnaiah, S Satyanarayana, D Visweswaram. Interaction between tolbutamide and ketoconazole in healthy subjects. *Br J Clin Pharmacol* 37:205–207, 1994.
131. C Transon, T Leemann, N Vogt, P Dayer. In vivo inhibition profile of cytochrome P450TB (CYP2C9) by ( $\pm$ )-fluvastatin. *Clin Pharmacol Ther* 58:412–417, 1995.
132. RF Frye, TS Tracy, JM Hutzler, KR Korzekwa, Y Cannon, M Pauli, S-M Huang,

- RA Branch. Flurbiprofen as a selective in vivo probe of CYP2C9 activity. *Clin Pharmacol Ther* 67:109, 2000.
133. SA Wrighton, JC Stevens, GW Becker, M VandenBraden. Isolation and characterization of human liver cytochrome P4502C19: correlation between 2C19 and *S*-mephenytoin 4'-hydroxylation. *Arch Biochem Biophys* 306:240–245, 1993.
  134. JA Goldstein, MB Faletto, M Romkes-Sparks, T Sullivan, S Kitareewan, JL Raucy, JM Lasker, BI Ghanayem. Evidence that CYP2C19 is the major (*S*)-mephenytoin 4'-hydroxylase in humans. *Biochemistry* 33:1743–1752, 1994.
  135. A Küpfer, RA Branch. Stereoselective mephobarbital hydroxylation cosegregates with mephenytoin hydroxylation. *Clin Pharmacol Ther* 38:414–418, 1985.
  136. A Adedoyin, C Prakash, D O'Shea, IA Blair, GR Wilkinson. Stereoselective disposition of hexobarbital and its metabolites: relationship to the *S*-mephenytoin polymorphism in Caucasian and Chinese subjects. *Pharmacogenetics* 4:27–38, 1994.
  137. SA Ward, NA Helsby, E Skjelbo, K Brøsen, LF Gram, AM Breckenridge. The activation of the biguanide antimalarial proguanil co-segregates with the mephenytoin oxidation polymorphism—a panel study. *Br J Clin Pharmacol* 31:689–692, 1991.
  138. T Andersson, C-G Regardh, Y-C Lou, Y Zhang, M-L Dahl, L Bertilsson. Polymorphic hydroxylation of *S*-mephenytoin and omeprazole metabolism in Caucasian and Chinese subjects. *Pharmacogenetics* 2:25–31, 1992.
  139. D-R Sohn, J-T Kwon, H-K Kim, T Ishizaki. Metabolic disposition of lansoprazole in relation to the *S*-mephenytoin 4'-hydroxylation phenotype status. *Clin Pharmacol Ther* 61:574–582, 1997.
  140. M Tanaka, T Ohkubo, K Otani, A Suzuki, S Kaneko, K Sugawara, Y Ryokawa, H Hakusui, S Yamamori, T Ishizaki. Metabolic disposition of pantoprazole, a proton pump inhibitor, in relation to *S*-mephenytoin 4'-hydroxylation phenotype and genotype. *Clin Pharmacol Ther* 62:619–628, 1997.
  141. L Bertilsson, TK Henthorn, E Sanz, G Tybring, J Säwe, T Villén. Importance of genetic factors in the regulation of diazepam metabolism: relationship to *S*-mephenytoin, but not debrisoquin hydroxylation phenotype. *Clin Pharmacol Ther* 45:348–355, 1989.
  142. E Skjelbo, K Brøsen, J Hallas, LF Gram. The mephenytoin oxidation polymorphism is partially responsible for the *N*-demethylation of imipramine. *Clin Pharmacol Ther* 49:18–23, 1991.
  143. KK Nielsen, K Brøsen, MGJ Hansen, LF Gram. Single-dose kinetics of clomipramine: relationship to the sparteine and *S*-mephenytoin oxidation polymorphisms. *Clin Pharmacol Ther* 55:518–527, 1994.
  144. U Breyer-Pfaff, B Pfandl, K Nill, E Nusser, C Monney, M Jonzier-Perey, D Baettig, P Baumann. Enantioselective amitriptyline metabolism in patients phenotyped for two cytochrome P450 isozymes. *Clin Pharmacol Ther* 52:350–358, 1992.
  145. P Dálen, G Alvan, M Wakelkamp, H Olsen. Formation of meprobamate from carisoprodol is catalyzed by CYP2C19. *Pharmacogenetics* 6:387–394, 1996.
  146. SH Sindrup, K Brøsen, MGJ Hansen, T Aaes-Jørgensen, KF Overø, LF Gram. Pharmacokinetics of citalopram in relation to the sparteine and the mephenytoin oxidation polymorphisms. *Ther Drug Monit* 15:11–17, 1993.
  147. LF Gram, TW Guentert, S Grange, K Vistisen, K Brøsen. Moclobemide, a substrate

- of CYP2C19 and an inhibitor of CYP2C19, CYP2D6, and CYP1A2: a panel study. *Clin Pharmacol Ther* 57:670–677, 1995.
148. SA Ward, T Walle, UK Walle, GR Wilkinson, RA Branch. Propranolol's metabolism is determined by both mephenytoin and debrisoquine hydroxylase activities. *Clin Pharmacol Ther* 45:72–79, 1989.
  149. JH Lillibridge, CA Lee, YK Pithavala, TM Sandoval, EY Wu, KE Zhang, EL Mazabel, M Zhang, BM Kerr. The role of CYP2C19 in the formation of nelfinavir hydroxy-*t*-butylamide (M8): in vitro/in vivo correlation. *ISSX Proc* 13:55, 1998.
  150. GR Wilkinson, FP Guengerich, RA Branch. Genetic polymorphism of *S*-mephenytoin hydroxylation. *Pharmac Ther* 43:53–76, 1989.
  151. SMF de Morais, GR Wilkinson, J Blaisdell, K Nakamura, UA Meyer, JA Goldstein. The major genetic defect responsible for the polymorphism of *S*-mephenytoin in humans. *J Biol Chem* 269:15419–15422, 1994.
  152. SMF de Morais, GR Wilkinson, J Blaisdell, K Nakamura, UA Meyer, JA Goldstein. Identification of a new genetic defect responsible for the polymorphism of *S*-mephenytoin metabolism in Japanese. *Mol Pharmacol* 46:594–598, 1994.
  153. K Brøsen, SMF de Morais, UA Meyer, JA Goldstein. A multifamily study on the relationship between CYP2C19 genotype and *S*-mephenytoin oxidation phenotype. *Pharmacogenetics* 5:312–317, 1995.
  154. RJ Ferguson, SMF deMorais, S Benhamou, C Bouchardy, J Blaisdell, G Ibeanu, GR Wilkinson, TC Sarich, JM Wright, P Dayer, JA Goldstein. A novel defect in human CYP2C19: mutation of the initiation codon is responsible for poor metabolism of *S*-mephenytoin. *J Pharmacol Exp Ther* 284:356–361, 1998.
  155. GC Ibeanu, J Blaisdell, BI Ghanayem, C Beyeler, S Benhamou, C Bouchardy, GR Wilkinson, P Dayer, AK Daly, JA Goldstein. An additional defective allele, CYP2C19\*5, contributes to the *S*-mephenytoin poor metabolizer phenotype in Caucasians. *Pharmacogenetics* 8:129–135, 1998.
  156. Z-S Xiao, JA Goldstein, H-G Xie, J Blaisdell, W Wang, C-H Jiang, F-X Yan, N He, S-L Huang, Z-H Xu, H-H Zhou. Differences in the incidence of the CYP2C19 polymorphism affecting the *S*-mephenytoin phenotype in Chinese Han and Bai populations and identification of a new rare CYP2C19 mutant allele. *J Pharmacol Exp Ther* 281:604–609, 1997.
  157. GC Ibeanu, JA Goldstein, U Meyer, S Benhamou, C Bouchardy, P Dayer, BI Ghanayem, J Blaisdell. Identification of new human CYP2C19 alleles (CYP2C19\*6 and CYP2C19\*2B) in a Caucasian poor metabolizer of mephenytoin. *J Pharmacol Exp Ther* 286:1490–1495, 1998.
  158. GC Ibeanu, J Blaisdell, RJ Ferguson, BI Ghanayem, K Brøsen, S Benhamou, C Bouchardy, P Dayer, GR Wilkinson, JA Goldstein. A novel transversion in intron 5 donor splice junction of CYP2C19 and a sequence polymorphism in exon 3 contribute to the poor metabolism of the anticonvulsant drug *S*-mephenytoin. *J Pharmacol Exp Ther* 290:635–640, 1999.
  159. JA Goldstein, T Ishizaki, K Chiba, SMF de Morais, D Bell, PM Krahn, DAP Evans. Frequencies of the defective CYP2C19 alleles responsible for the mephenytoin poor metabolizer phenotype in various Oriental, Caucasian, Saudi Arabian and American black populations. *Pharmacogenetics* 7:59–64, 1997.
  160. G Alván, P Bechtel, L Iselius, U Gundert-Remy. Hydroxylation polymorphisms of

- debrisoquine and mephenytoin in European populations. *Eur J Clin Pharmacol* 39: 533–537, 1990.
161. C Masimirembwa, L Bertilsson, I Johnansson, JA Hasler, M Ingelman-Sundberg. Phenotyping and genotyping of *S*-mephenytoin hydroxylase (cytochrome P450 2C19) in a Shona population of Zimbabwe. *Clin Pharmacol Ther* 57:656–661, 1995.
  162. TI Edeki, JA Goldstein, SMF de Morais, L Hajiloo, M Butler, P Chapdelaine, GR Wilkinson. Genetic polymorphism of *S*-mephenytoin 4'-hydroxylation in African-Americans. *Pharmacogenetics* 6:357–360, 1996.
  163. JS Marinac, JD Balian, JW Foxworth, SK Willsie, JC Daus, R Owens, DA Flockhart. Determination of CYP2C19 in phenotype in black Americans with omeprazole: correlation with genotype. *Clin Pharmacol Ther* 60:138–144, 1996.
  164. M Jurima, T Inaba, D Kadar, W Kalow. Genetic polymorphism of mephenytoin *p*(4')-hydroxylation: difference between Orientals and Caucasians. *Br J Clin Pharmacol* 19:483–487, 1985.
  165. K Nakamura, F Goto, WA Ray, CB McAllister, E Jacqz, GR Wilkinson, RA Branch. Interethnic differences in genetic polymorphism of debrisoquin and mephenytoin hydroxylation between Japanese and Caucasian populations. *Clin Pharmacol Ther* 38:402–408, 1985.
  166. L Bertilsson, Y-Q Lou, Y-L Du, Y Liu, T-Y Kuang, X-M Liao, K-Y Wang, J Reviriego, L Iselius, F Sjöqvist. Pronounced differences between native Chinese and Swedish populations in the polymorphic hydroxylations of debrisoquin and *S*-mephenytoin. *Clin Pharmacol Ther* 51:388–397, 1992.
  167. H-K Roh, M-L Dahl, I Johansson, M Ingelman-Sundberg, Y-N Cha, L Bertilsson. Debrisoquine and *S*-mephenytoin hydroxylation phenotypes and genotypes in a Korean population. *Pharmacogenetics* 6:441–447, 1996.
  168. D-R Sohn, M Kusaka, T Ishizaki, S-G Shin, I-J Jang, J-G Shin, K Chiba. Incidence of *S*-mephenytoin hydroxylation deficiency in a Korean population and the interphenotypic differences in diazepam pharmacokinetics. *Clin Pharmacol Ther* 52: 160–169, 1992.
  169. E Jacqz, SD Hall, RA Branch, GR Wilkinson. Polymorphic metabolism of mephenytoin in man: pharmacokinetic interaction with a co-regulated substrate, mephobarbital. *Clin Pharmacol Ther* 39:646–653, 1986.
  170. A LLerena, MJ Valdivielso, J Benítez, L Bertilsson. Reproducibility over time of mephenytoin and debrisoquine hydroxylation phenotypes. *Pharmacol Toxicol* 73: 46–48, 1993.
  171. RE Bluhm, GR Wilkinson, R Shelton, RA Branch. Genetically determined drug-metabolizing activity and desipramine-associated cardiotoxicity: a case report. *Clin Pharmacol Ther* 53:89–95, 1993.
  172. G Tybring, J Nordin, T Bergman, L Bertilsson. An *S*-mephenytoin cysteine conjugate identified in urine of extensive but not of poor metabolizers of *S*-mephenytoin. *Pharmacogenetics* 7:355–360, 1997.
  173. PJ Wedlund, BJ Sweetman, GR Wilkinson, RA Branch. Pharmacogenetic association between the formation of 4-hydroxymephenytoin and a new metabolite of *S*-mephenytoin in man. *Drug Metab Dispos* 15:277–279, 1987.
  174. Y Zhang, RA Blouin, PJ McNamara, J Steinmetz, PJ Wedlund. Limitation to the



- use of the urinary *S*-/*R*-mephenytoin ratio in pharmacogenetic studies. *Br J Clin Pharmacol* 31:350–352, 1991.
175. G Tybring, L Bertilsson. A methodological investigation on the estimation of the *S*-mephenytoin hydroxylation phenotype using the urinary *S*/*R* ratio. *Pharmacogenetics* 2:241–243, 1992.
176. PJ Wedlund, GR Wilkinson. In vivo and in vitro measurement of CYP2C19 activity. In: EF Johnson, MR Waterman, eds. *Cytochrome P450, Part B: Methods in Enzymology*. San Diego: Academic Press, 272:105–114, 1996.
177. EJ Sanz, T Villén, C Alm, L Bertilsson. *S*-mephenytoin hydroxylation phenotypes in a Swedish population determined after coadministration with debrisoquin. *Clin Pharmacol Ther* 45:495–499, 1989.
178. R Setiabudy, K Chiba, M Kusaka, T Ishizaki. Caution in the use of a 100 mg dose of racemic mephenytoin for phenotyping Southeastern Oriental subjects. *Br J Clin Pharmacol* 33:665–666, 1992.
179. K Chiba, K Kobayashi, K Manabe, M Tani, T Kamataki, T Ishizaki. Oxidative metabolism of omeprazole in human liver microsomes: cosegregation with *S*-mephenytoin 4'-hydroxylation. *J Pharmacol Exp Ther* 266:52–59, 1993.
180. T Andersson, JO Miners, ME Veronese, W Tassaneeyakul, W Tassaneeyakul, UA Meyer, DJ Birkett. Identification of human liver cytochrome P450 isoforms mediating omeprazole metabolism. *Br J Clin Pharmacol* 36:521–530, 1993.
181. WG Karam, JA Goldstein, JM Lasker, BI Ghanayem. Human CYP2C19 is a major omeprazole 5-hydroxylase, as demonstrated with recombinant cytochrome P450 enzymes. *Drug Metab Disp* 24:1081–1087, 1996.
182. D-R Sohn, K Kobayashi, K Chiba, K-H Lee, S-G Shin, T Ishizaki. Disposition kinetics and metabolism of omeprazole in extensive and poor metabolizers of *S*-mephenytoin 4'-hydroxylation recruited from an Oriental population. *J Pharmacol Exp Ther* 262:1195–1202, 1992.
183. M Chang, G Tybring, M-L Dahl, E Götharson, M Sagar, R Seensalu, L Bertilsson. Interphenotype differences in disposition and effect on gastrin levels of omeprazole—suitability of omeprazole as a probe for CYP2C19. *Br J Clin Pharmacol* 39: 511–518, 1995.
184. M Chang, M-L Dahl, G Tybring, E Götharson, L Bertilsson. Use of omeprazole as a probe drug for CYP2C19 phenotype in Swedish Caucasians: comparison with *S*-mephenytoin hydroxylation phenotype and CYP2C19 genotype. *Pharmacogenetics* 5:358–363, 1995.
185. I Ieiri, T Kubota, A Urae, M Kimura, Y Wada, K Mamiya, S Yoshioka, S Irie, T Amamoto, K Nakamura, S Nakano, S Higuchi. Pharmacokinetics of omeprazole (a substrate of CYP2C19) and comparison with two mutant alleles, CYP2C19<sub>m1</sub> in exon 5 and CYP2C19<sub>m2</sub> in exon 4, in Japanese subjects. *Clin Pharmacol Ther* 59: 647–653, 1996.
186. JD Balian, N Sukhova, JW Harris, J Hewett, L Pickle, JA Goldstein, RL Woosley, DA Flockhart. The hydroxylation of omeprazole correlates with *S*-mephenytoin metabolism: a population study. *Clin Pharmacol Ther* 57:662–669, 1995.
187. KL Rost, J Brockmöller, F Esdorn, I Roots. Phenocopies of poor metabolizers of omeprazole caused by liver disease and drug treatment. *J Hepatology* 23:268–277, 1995.

188. R Setiabudy, M Kusaka, K Chiba, I Darmansjah, T Ishizaki. Metabolic disposition of proguanil in extensive and poor metabolisers of *S*-mephenytoin 4'-hydroxylation recruited from an Indonesian population. *Br J Clin Pharmac* 39:297–303, 1995.
189. SA Ward, WM Watkins, E Mberu, JE Saunders, DK Koech, HM Gilles, RE Howells, AM Breckenridge. Inter-subject variability in the metabolism of proguanil to the active metabolite cycloguanil in man. *Br J Clin Pharmacol* 27:781–787, 1989.
190. NA Helsby, SA Ward, G Edwards, RE Howells, AM Breckenridge. The pharmacokinetics and activation of proguanil in man: consequences of variability in drug metabolism. *Br J Clin Pharmacol* 30:593–598, 1990.
191. K Brösen, E Skjelbo, H Flachs. Proguanil metabolism is determined by the mephenytoin oxidation polymorphism in Vietnamese living in Denmark. *Br J Clin Pharmac* 36:105–108, 1993.
192. S Wanwimolruk, EL Pratt, JR Denton, SCW Chalcraft, PA Barron, JR Broughton. Evidence for the polymorphic oxidation of debrisoquine and proguanil in a New Zealand Maori population. *Pharmacogenetics* 5:193–198, 1995.
193. S Wanwimolruk, MR Thou, DJ Woods. Evidence for the polymorphic oxidation of debrisoquine and proguanil in a Khmer (Cambodian) population. *Br J Clin Pharmacol* 40:166–169, 1995.
194. E Skjelbo, TK Mutabingwa, I Bygbjerg, KN Nielsen, LF Gram, K Brösen. Chloroguanide metabolism in relation to the efficacy in malaria prophylaxis and the *S*-mephenytoin oxidation in Tanzanians. *Clin Pharmacol Ther* 59:304–311, 1996.
195. AA Somogyi, HA Reinhard, F Bochner. Pharmacokinetic evaluation of proguanil: a probe phenotyping drug for the mephenytoin hydroxylase polymorphism. *Br J Clin Pharmac* 41:175–179, 1996.
196. NE Basci, A Bozkurt, S Kortunay, A Isimer, A Sayal, SO Kayaalp. Proguanil metabolism in relation to *S*-mephenytoin oxidation in a Turkish population. *Br J Clin Pharmacol* 42:771–773, 1996.
197. JK Coller, AA Somogyi, F Bochner. Association between CYP2C19 genotype and proguanil oxidative polymorphism. *Br J Clin Pharmacol* 43:659–660, 1997.
198. JM Hoskins, GM Shenfield, AS Gross. Relationship between proguanil metabolic ratio and CYP2C19 genotype in a Caucasian population. *Br J Clin Pharmacol* 46:499–504, 1998.
199. C Funck-Brentano, O Bosco, E Jacqz-Aigrain, A Keundjian, P Jaillon. Relation between chloroguanide bioactivation to cycloguanil and the genetically determined metabolism of mephenytoin in humans. *Clin Pharmacol Ther* 51:507–512, 1992.
200. C Partovian, E Jacqz-Aigrain, A Keundjian, P Jaillon, C Funck-Brentano. Comparison of chloroguanide and mephenytoin for the in vivo assessment of genetically determined CYP2C19 activity in humans. *Clin Pharmacol Ther* 58:257–263, 1995.
201. DJ Birkett, D Rees, T Andersson, FJ Gonzalez, JO Miners, ME Veronese. In vitro proguanil activation to cycloguanil by human liver microsomes is mediated by CYP3A isoforms as well as by *S*-mephenytoin hydroxylase. *Br J Clin Pharmac* 37:413–420, 1994.
202. M Eichelbaum, AS Gross. The genetic polymorphism of debrisoquine/sparteine metabolism-clinical aspects. *Pharmac Ther* 46:377–394, 1990.

203. UA Meyer, UM Zanger. Molecular mechanisms of genetic polymorphisms of drug metabolism. *Ann Rev Pharmacol Tox* 37:269–296, 1997.
204. A Mahgoub, JR Idle, LG Dring, R Lancaster, RL Smith. Polymorphic hydroxylation of debrisoquine in man. *Lancet* 2:584–586, 1977.
205. GT Tucker, JH Silas, AO Iyun, MS Lennard, AJ Smith. Polymorphic hydroxylation of debrisoquine. *Lancet* 2:718, 1977.
206. M Eichelbaum, N Spannbrucker, B Steincke, HJ Dengler. Defective *N*-oxidation of sparteine in man: a new pharmacogenetic defect. *Eur J Clin Pharmacol* 16:183–187, 1979.
207. AK Daly. Molecular basis of polymorphic drug metabolism. *J Mol Med* 73:539–553, 1995.
208. I Johansson, E Lundqvist, L Bertilsson, M-L Dahl, F Sjöqvist, M Ingelman-Sundberg. Inherited amplification of an active gene in the cytochrome P450 2D-locus as a cause of ultrarapid metabolism of debrisoquine. *Proc Natl Acad Sci* 90:11825–11829, 1993.
209. D Marez, M Legrand, N Sabbagh, J-M Lo Guidice, C Spire, J-J Lafitte, UA Meyer, F Broly. Polymorphism of the cytochrome P450 CYP2D6 gene in a European population: characterization of 48 mutations and 53 alleles, their frequencies and evolution. *Pharmacogenetics* 7:193–202, 1997.
210. AK Daly, J Brockmüller, F Broly, M Eichelbaum, WE Evans, FJ Gonzalez, J-D Huang, JR Idle, M Ingelman-Sundberg, T Ishizaki, E Jacqz-Aigrain, UA Meyer, DW Nebert, VM Steen, CR Wolf, UM Zanger. Nomenclature of human CYP2D6 alleles. *Pharmacogenetics* 6:193–201, 1996.
211. C Masimirembwa, J Hasler, L Bertilsson, I Johansson, O Ekberg, M Ingelman-Sundberg. Phenotype and genotype analysis of debrisoquine hydroxylase (CYP2D6) in a black Zimbabwean population—reduced enzyme activity and evaluation of metabolic correlation of CYP2D6 probe drugs. *Eur J Clin Pharmacol* 51: 117–122, 1996.
212. AO Iyun, MS Lennard, GT Tucker, HF Woods. Metoprolol and debrisoquin metabolism in Nigerians: lack of evidence for polymorphic oxidation. *Clin Pharmacol Ther* 40:387–394, 1986.
213. MV Relling, J Cherrie, MJ Schell, WP Petros, WH Meyer, WE Evans. Lower prevalence of the debrisoquin oxidative poor metabolizer phenotype in American black versus white subjects. *Clin Pharmacol Ther* 50:308–313, 1991.
214. SH Sindrup, K Brøsen. The pharmacogenetics of codeine hypoalgesia. *Pharmacogenetics* 5:335–346, 1995.
215. L Bertilsson, M-L Dahl, F Sjöqvist, Å Abert-Wistedt, M Humble, I Johansson, E Lundqvist, M Ingelman-Sundbert. Molecular basis for rational megaprescribing in ultrarapid hydroxylators of debrisoquine. *Lancet* 341:63, 1993.
216. B Eiermann, PO Edlund, A Tjernberg, P Dalén, M-L Dahl, L Bertilsson. 1- and 3-hydroxylations, in addition to 4-hydroxylation, of debrisoquine are catalyzed by cytochrome P450 2D6 in humans. *Drug Metab Disp* 26:1096–1101, 1998.
217. C Sachse, J Brockmüller, S Bauer, I Roots. Cytochrome P450 2D6 variants in a Caucasian population: allele frequencies and phenotypic consequences. *Am J Hum Genet* 60:284–295, 1997.

218. C-G Regårdh, G Johnsson. Clinical pharmacokinetics of metoprolol. *Clin Pharmacokinet* 5:557–569, 1980.
219. MS Lennard, JH Silas, S Freestone, LE Ramsay, GT Tucker, HF Woods. Oxidation phenotype—a major determinant of metoprolol metabolism and response. *New Eng J Med* 307:1558–1560, 1982.
220. DWJ Clark. Genetically determined variability in acetylation and oxidation. Therapeutic implications. *Drugs* 29:342–375, 1985.
221. JC McGourty, JH Silas, MS Lennard, GT Tucker, HF Woods. Metoprolol metabolism and debrisoquine oxidation polymorphism—population and family studies. *Br J Clin Pharmacol* 20:555–566, 1985.
222. D-R Sohn, S-G Shin, C-W Park, M Kusaka, K Chiba, T Ishizaki. Metoprolol oxidation polymorphism in a Korean population: comparison with native Japanese and Chinese populations. *Br J Clin Pharmacol* 32:504–507, 1991.
223. MS Lennard, GT Tucker, JH Silas, S Freestone, LE Ramsay, HF Woods. Differential stereoselective of metoprolol in extensive and poor debrisoquin metabolisers. *Clin Pharmacol Ther* 34:732–737, 1983.
224. D-R Sohn, M Kusaka, S-G Shin, I-J Jang, K Chiba, T Ishizaki. Utility of a one-point (3-hour postdose) plasma metabolic ratio as a phenotyping test using metoprolol in two East Asian populations. *Therap Drug Monit* 14:184–189, 1992.
225. B Schmid, J Bircher, R Preisig, A Küpfer. Polymorphic dextromethorphan metabolism: co-segregation of oxidative *O*-demethylation with debrisoquin hydroxylation. *Clin Pharmacol Ther* 38:618–624, 1985.
226. NE Basci, A Bozkurt, SO Kayaalp, A Sayal, A Isimer. Omission of the deconjugation step in urine analysis and the unaltered outcome of CYP2D6 phenotyping with dextromethorphan. *Eur J Drug Metab Pharmacokinet* 23:1–5, 1998.
227. DA Capon, F Bochner, N Kerry, G Mikus, C Danz, AA Somogyi. The influence of CYP2D6 polymorphism and quinidine on the disposition and antitussive effect of dextromethorphan in humans. *Clin Pharmacol Ther* 60:295–307, 1996.
228. A Küpfer, B Schmid, G Pfaff. Pharmacogenetics of dextromethorphan *O*-demethylation in man. *Xenobiotica* 16:421–433, 1986.
229. Z-Y Hou, LW Pickle, PS Meyer, RL Woosley. Salivary analysis of determination of dextromethorphan metabolic phenotype. *Clin Pharmacol Ther* 49:410–419, 1991.
230. O Y-P Hu, H-S Tang, H-Y Lane, W-H Chang, T-M Hu. Novel single-point plasma or saliva dextromethorphan method for determining CYP2D6 activity. *J Pharmacol Exp Therap* 285:955–960, 1998.
231. P Dayer, T Leemann, R Striberni. Dextromethorphan *O*-demethylation in liver microsomes as a prototype reaction to monitor cytochrome P-450 db<sub>1</sub> activity. *Clin Pharmacol Ther* 45:34–40, 1989.
232. NL Kerry, AA Somogyi, F Bochner, G Mikus. The role of CYP2D6 in primary and secondary oxidative metabolism of dextromethorphan: in vitro studies using human liver microsomes. *Br J Clin Pharmacol* 38:243–248, 1994.
233. WE Evans, MV Relling. Concordance of P450 2D6 (debrisoquine hydroxylase) phenotype and genotype: inability of dextromethorphan metabolic ratio to discriminate reliably heterozygous and homozygous extensive metabolizers. *Pharmacogenetics* 1:143–148, 1991.

234. C Funck-Brentano, G Thomas, E Jacqz-Algrain, J-M Poirier, T Simon, G Béréziat, P Jaillon. Polymorphism of dextromethorphan metabolism: relationships between phenotype, genotype and response to the administration of encainide in humans. *J Pharmacol Exp Ther* 263:780–786, 1992.
235. T Zimmermann, R Schlenk, G Pfaff, P Lach, A Wildfeuer. Prediction of phenotype for dextromethorphan *O*-demethylation by using polymerase chain reaction in healthy volunteers. *Arzneim-Forsch/Drug Res* 45:41–43, 1995.
236. L Ereshefsky, C Riesenman, YW Lam. Antidepressant drug interactions and the cytochrome P450 system—the role of cytochrome P4502D6. *Clin Pharmacokinet* 29(Suppl 1):10–19, 1995.
237. E Richelson. Pharmacokinetic drug interactions of new antidepressants: a review of the effects of the metabolism of other drugs. *Mayo Clin Proc* 72:835–847, 1997.
238. Y Horai, J Taga, T Ishizaki, K Ishikawa. Correlations among the metabolic ratios of three test probes (metoprolol, debrisoquine and sparteine) for genetically determined oxidation polymorphism in a Japanese population. *Br J Clin Pharmacol* 29: 111–115, 1990.
239. NM Woolhouse, M Eichelbaum, NS Oates, JR Idle, RL Smith. Dissociation of co-regulatory control of debrisoquin/phenformin and sparteine oxidation in Ghanaians. *Clin Pharmacol Ther* 37:512–521, 1985.
240. OO Simooya, E Njunju, AR Hodjegan, MS Lennard, GT Tucker. Debrisoquine and metoprolol oxidation in Zambians: a population study. *Pharmacogenetics* 3: 205–208, 1993.
241. K Droll, K Bruce-Mensah, SV Otton, A Gaedigk, EM Sellers, RF Tyndale. Comparison of three CYP2D6 probe substrates and genotype in Ghanaians, Chinese and Caucasians. *Pharmacogenetics* 8:325–333, 1998.
242. JC Ritchie, SC Mitchell, RL Smith. Sparteine metabolism in a Nigerian population. *Drug Metab Disp Interact* 13:129–135, 1996.
243. MS Lennard, AO Iyun, PR Jackson, GT Tucker, HF Woods. Evidence for a dissociation in the control of sparteine, debrisoquine and metoprolol metabolism in Nigerians. *Pharmacogenetics* 2:89–92, 1992.
244. De K Sommers, J Moncrieff, J Avenant. Non-correlation between debrisoquine and metoprolol polymorphisms in the Venda. *Human Toxicol* 8:365–368, 1989.
245. De K Sommers, J Moncrieff, JC Avena. Absence of polymorphism of sparteine oxidation in the South African Venda. *Human Exp Toxicol* 10:175–178, 1991.
246. De K Sommers, J Moncrieff, J Avenant. Metoprolol  $\alpha$ -hydroxylation polymorphism in the San Bushmen of Southern Africa. *Human Toxicol* 8:39–43, 1989.
247. De K Sommers, J Moncrieff, J Avenant. Polymorphism of the 4-hydroxylation of debrisoquine in the San Bushmen of Southern Africa. *Human Toxicol* 7:273–276, 1988.
248. D Masimirembwa, I Persson, L Bertilsson, J Hasler, M Ingelman-Sundberg. A novel mutant variant of the CYP2D6 gene (CYP2D6\*17) common in a black African population: association with diminished debrisoquine hydroxylase activity. *Br J Clin Pharmacol* 42:713–719, 1996.
249. M Oscarson, M Hidestrand, I Johansson, M Ingelman-Sundberg. A combination of mutations in the CYP2D6\*17 (CYP2D6Z) allele causes alterations in enzyme function. *Mol Pharmacol* 52:1034–1040, 1997.

250. HF Al-Hadidi, YM Irshaid, NM Rawashdeh. Metoprolol  $\alpha$ -hydroxylation is a poor probe for debrisoquine oxidation (CYP2D6) polymorphism in Jordanians. *Eur J Clin Pharmacol* 47:311–314, 1994.
251. YM Irshaid, HF Al-Hadidi, A Latif, F Awwadi, M Al-Zoubi, NM Rawashdeh. Dextromethorphan metabolism in Jordanians: dissociation of dextromethorphan *O*-demethylation from debrisoquine 4-hydroxylation. *Eur J Clin Metab Pharmacokinet* 21:301–307, 1996.
252. MJJ Ronis, KO Lindros, M Ingelman-Sundberg. The CYP2E1 subfamily. In: C Ioannides, ed. *Cytochromes P450: Metabolic and Toxicological Aspects*. Boca Raton, FL: CRC Press, 1996, pp 211–239.
253. F Uematsu, H Kikuchi, T Ohmachi, I Sagami, M Motomiya, T Kamataki, M Komori, M Watanabe. Two common RFLPs of the human CYP2E gene. *Nucleic Acids Res* 19:2803, 1991.
254. Y Hu, M Oscarson, I Johansson, Q-Y Yue, M-L Dahl, M Tabone, S Arinco, E Albano, M Ingelman-Sundberg. Genetic polymorphism of human CYP2E1: characterization of two variant alleles. *Mol Pharmacol* 51:370–376, 1997.
255. DG McCarver, R Byun, RN Hines, M Hichme, W Wegenek. A genetic polymorphism in the regulatory sequence of human CYP2E1: association with increased chlorzoxazone hydroxylation in the presence of obesity and ethanol intake. *Tox Appl Pharmacol* 152:276–281, 1998.
256. KS Fairbrother, J Grove I de Waziers, DT Steimel, CP Day, CL Crespi, AK Daly. Detection and characterization of novel polymorphisms in the CYP2E1 gene. *Pharmacogenetics* 8:543–552, 1998.
257. V Carrière, F Berthou, S Baird, C Belloc, P Beaune, I deWaziers. Human cytochrome P450 2E1 (CYP2E1): from genotype of phenotype. *Pharmacogenetics* 6: 203–211, 1996.
258. H Powell, NR Kitteringham, M Pirmohamed, DA Smith, BK Park. Expression of cytochrome P4502E1 (CYP2E1) in human liver: assessment of mRNA, genotype and phenotype. *Pharmacogenetics* 8:411–421, 1998.
259. RB Kim, H Yamazaki, K Chiba, D O'Shea, M Mimura, FP Guengerich, T Ishizaki, T Shimada, GR Wilkinson. In vivo and in vitro characterization of CYP2E1 activity in Japanese and Caucasians. *J Pharmacol Exp Ther* 279:4–11, 1996.
260. D Lucas, C Ménez, C Girre, F Berthou, P Bodénez, I Joannet, E Hispard, L-G Bardou, J-F Ménez. Cytochrome P450 2E1 genotype and chlorzoxazone metabolism in healthy and alcoholic Caucasian subjects. *Pharmacogenetics* 5:298–304, 1995.
261. L Le Marchand, GR Wilkinson, LR Wilkens. Genetic and dietary predictors of CYP2E1 activity: a phenotyping study in Hawaii Japanese using chlorzoxazone. *Cancer Epidemiol Biomarkers Prevention* 8:495–500, 1999.
262. R Peter, R Böcker, PH Beaune, M Iwasaki, FP Guengerich, CS Yang. Hydroxylation of chlorzoxazone as a specific probe for human liver cytochrome P450III<sub>E1</sub>. *Chem Res Toxicol* 3:566–73, 1990.
263. V Carriere, T Goasduff, D Ratanasavanh, F Morel, J-C Gautier, A Guillouzo, P Beaune, F Berthou. Both cytochromes P450 2E1 and 1A1 are involved in the metabolism of chlorzoxazone. *Chem Res Tox* 6:852–857, 1994.
264. H Yamazaki, Z Guo, FP Guengerich. Selectivity of cytochrome P4502E1 in chlorzoxazone 6-hydroxylation. *Drug Metab Disp* 23:438–440, 1995.

265. S Ono, T Hatanaka, H Hotta, M Tsutsui, T Satoh, FJ Gonzalez. Chlorzoxazone is metabolized by human CYP1A2 as well as by human CYP2E1. *Pharmacogenetics* 5:141–148, 1995.
266. JC Gorski, DR Jones, SA Wrighton, SD Hall. Contribution of human CYP3A subfamily members to the 6-hydroxylation of chlorzoxazone. *Xenobiotica* 27:243–256, 1997.
267. D O'Shea, SN Davis, RB Kim, GR Wilkinson. Effect of fasting and obesity in humans on the 6-hydroxylation of chlorzoxazone: a putative probe of CYP2E1 activity. *Clin Pharmacol Ther* 56:359–367, 1994.
268. D Lucas, J-F Menez, F Berthou. Chlorzoxazone: an in vitro and in vivo substrate probe for liver CYP2E1. In: EF Johnson, MR Waterman, eds. *Cytochrome P450, Part B: Methods in Enzymology*. San Diego, CA: Academic Press, 272:115–123, 1996.
269. ED Kharasch, KE Thummel, J Mhyre, JH Lillibridge. Single-dose disulfiram inhibition of chlorzoxazone metabolism: a clinical probe for P4502E1. *Clin Pharmacol Ther* 53:643–650, 1993.
270. CB Eap, C Schnyder, J Besson, L Savary, T Buclin. Inhibition of CYP2E1 by chlormethiazole as measured by chlorzoxazone pharmacokinetics in patients with alcoholism and in healthy volunteers. *Clin Pharmacol Ther* 64:52–57, 1998.
271. I Leclercq, J-P Desager, Y Horsmans. Inhibition of chlorzoxazone metabolism, a clinical probe for CYP2E1, by a single ingestion of watercress. *Clin Pharmacol Ther* 64:144–149, 1998.
272. R Zand, SD Nelson, JT Slattery, KE Thummel, TF Kalhorn, SP Adams, JM Wright. Inhibition and induction of cytochrome P4502E1-catalyzed oxidation by isoniazid in humans. *Clin Pharmacol Ther* 54:142–149, 1993.
273. D O'Shea, RB Kim, GR Wilkinson. Modulation of CYP2E1 activity by isoniazid in rapid and slow *N*-acetylators. *Br J Clin Pharmacol* 43:99–103, 1997.
274. AC Gebhardt, D Lucas, J-F Ménez, HK Seitz. Chlormethiazole inhibition of cytochrome P450 2E1 as assessed by chlorzoxazone hydroxylation in humans. *Hepatology* 26:957–961, 1997.
275. K Dilger, J Metzler, JC Bode, U Klotz. CYP2E1 activity in patients with alcoholic liver disease. *J Hepatol* 27:1009–1014, 1997.
276. I Dupont, D Lucas, P Clot, C Ménez, E Albano. Cytochrome P4052E1 inducibility and hydroxyethyl radical formation among alcoholics. *J Hepatol* 28:564–572, 1998.
277. D Lucas, C Ménez, C Girre, P Bodénez, E Hispard, J-F Ménez. Decrease in cytochrome P4502E1 as assessed by the rate of chlorzoxazone hydroxylation in alcoholics during the withdrawal phase. *Alcohol Clin Exp Res* 19:362–366, 1995.
278. RB Kim, D O'Shea, GR Wilkinson. Relationship in healthy subjects between CYP2E1 genetic polymorphisms and the 6-hydroxylation of chlorzoxazone—a putative measure of CYP2E1 activity. *Pharmacogenetics* 4:162–165, 1994.
279. AW Dreisbach, N Ferencz, NE Hopkins, MG Fuentes, AB Rege, WJ George, JLL Lertora. Urinary excretion of 6-hydroxychlorzoxazone as an index of CYP2E1 activity. *Clin Pharmacol Ther* 58:498–505, 1995.
280. ES Vesell, T DeAngelo Seaton, YI A-Rahim. Studies on interindividual variations

- of CYP2E1 using chlorzoxazone as an *in vivo* probe. *Pharmacogenetics* 5:53–57, 1995.
281. KE Thummel, GR Wilkinson. *In vitro* and *in vivo* drug interactions involving human CYP3A. *Annu Rev Pharmacol Toxicol* 38:389–430, 1998.
  282. KE Thummel, KL Kunze, DD Shen. Enzyme-catalyzed processes of first-pass hepatic and intestinal drug extraction. *Adv Drug Del Rev* 27:99–127, 1997.
  283. VJ Wacher, C-Y Wu, LZ Benet. Overlapping substrate specificities and tissue distribution of cytochrome P4503A and P-glycoprotein: implications for drug delivery and activity in cancer chemotherapy. *Mol Carcin* 13:129–134, 1995.
  284. RB Kim, C Wandel, B Leake, M Cvetkovic, MF Fromm, PJ Dempsey, MM Roden, F Belas, AK Chaudhary, DM Roden, AJJ Wood, GR Wilkinson. Interrelationship between substrates and inhibitors of human CYP3A and P-glycoprotein. *Pharm Res* 16:408–414, 1999.
  285. PB Watkins. Noninvasive tests of CYP3A enzymes. *Pharmacogenetics* 4:171–184, 1994.
  286. CM Fleming, RA Branch, GR Wilkinson, FP Guengerich. Human liver microsomal *N*-hydroxylation of dapsone by cytochrome P-4503A4. *Mol Pharmacol* 41:975–980, 1992.
  287. DG May, J Porter, GR Wilkinson, RA Branch. Frequency distribution of dapsone *N*-hydroxylase, a putative probe for P4503A4 activity, in a white population. *Clin Pharmacol Ther* 55:492–500, 1994.
  288. DG May, PA Arns, WO Richards, J Porter, D Ryder, CM Fleming, GR Wilkinson, RA Branch. The disposition of dapsone in cirrhosis. *Clin Pharmacol Ther* 51:689–700, 1992.
  289. CM Fleming, A Kaisary, GR Wilkinson, P Smith, RA Branch. The ability to 4-hydroxylate debrisoquine is related to recurrence of bladder cancer. *Pharmacogenetics* 2:128–134, 1992.
  290. CM Fleming, R Persad, A Kaisary, P Smith, A Adedoyin, J Porter, GR Wilkinson, RA Branch. Low activity of dapsone *N*-hydroxylation as a susceptibility risk factor in aggressive bladder cancer. *Pharmacogenetics* 4:199–207, 1994.
  291. RA Branch, HD Chern, A Adedoyin, M Romkes-Sparks, TG Lesnick, R Persad, GR Wilkinson, CM Fleming, AJ Dickinson, G Sibley, P Smith. The procarcinogen hypothesis for bladder cancer: activities of individual drug metabolizing enzymes as risk factors. *Pharmacogenetics* 5:S97–S102, 1995.
  292. DG May, CM Black, NJ Olsen, ME Csuka, SB Tanner, L Bellino, JA Porter, GR Wilkinson, RA Branch. Scleroderma is associated with differences in individual routes of metabolism: a study with dapsone, debrisoquin, and mephenytoin. *Clin Pharmacol Ther* 48:286–295, 1990.
  293. C Black, G May, ME Csuka, S Lupoli, GR Wilkinson, RA Branch. Activity of oxidative routes of metabolism of debrisoquine, mephenytoin, and dapsone is unrelated to the pathogenesis of vinyl chloride-induced disease. *Clin Pharmacol Ther* 52:659–667, 1992.
  294. CM Stein, MT Kinirons, T Pincus, GR Wilkinson, AJJ Wood. Comparison of the dapsone recovery ratio and the erythromycin breath test as *in vivo* probes of CYP3A activity in patients with rheumatoid arthritis receiving cyclosporine. *Clin Pharmacol Therap* 59:47–51, 1996.



295. AK Mitra, KE Thummel, TF Kalhorn, ED Kharasch, JD Unadkat, JT Slattery. Metabolism of dapsone to its hydroxylamine by cytochrome P-450 2E1 in vitro and in vivo. *Clin Pharmacol Ther* 58:556–566, 1995.
296. HJ Gill, MD Tingle, BK Park. *N*-Hydroxylation of dapsone by multiple enzymes of cytochrome P450: implications for inhibition of haemotoxicity. *Br J Clin Pharmacol* 40:531–538, 1995.
297. MT Kinirons, Y Krivoruk, GR Wilkinson, AJJ Wood. Effects of ketoconazole on the erythromycin breath test and the dapsone recovery ratio. *Br J Clin Pharmacol* 47:223–224, 1999.
298. PG Watkins, TA Hamilton, TM Annesley, CN Ellis, JC Kolars, JJ Voorhees. The erythromycin breath test as a predictor of cyclosporine blood levels. *Clin Pharmacol Ther* 48:120–129, 1990.
299. DK Turgeon, DP Normolle, AB Leichtman, TM Annesley, DE Smith, PB Watkins. Erythromycin breath test predicts oral clearance of cyclosporine in kidney transplant recipients. *Clin Pharmacol Ther* 52:471–478, 1992.
300. DK Turgeon, AB Leichtman, KS Lown, DP Normolle, GM Deeb, RM Merion, PB Watkins. P4503A activity and cyclosporine dosing in kidney and heart transplant recipients. *Clin Pharmacol Ther* 56:253–260, 1994.
301. DK Turgeon, AB Leichtman, DS Blake, RL Schmouder, KS Lown, TM Annesley, PB Watkins. Prediction of interpatient and inpatient variation in OG 37-325 dosing requirements by the erythromycin breath test: a prospective study in renal transplant recipients. *Transplantation* 57:1736–1741, 1994.
302. C-L Cheng, DE Smith, PL Carver, SR Cox, PB Watkins, DS Blake, CA Kauffman, KM Meyer, GL Amidon, PL Stetson. Steady-state pharmacokinetics of delavirdine in HIV-positive patients: effect on erythromycin breath test. *Clin Pharmacol Ther* 61:531–543, 1997.
303. D Wagner. CYP3A4 and the erythromycin breath test. *Clin Pharmacol Ther* 64:129–130, 1998.
304. PB Watkins, SA Murray, LG Winkelman, DM Heuman, SA Wrighton, PS Guzelian. Erythromycin breath test as an assay of glucocorticoid-inducible liver cytochromes P-450. Studies in rats and patients. *J Clin Invest* 83:688–697, 1989.
305. Y Krivoruk, MT Kinirons, AJJ Wood, M Wood. Metabolism of cytochrome P4503A substrates in vivo administered by the same route: lack of correlation between alfentanil clearance and erythromycin breath test. *Clin Pharmacol Ther* 56:608–614, 1994.
306. EG Schuetz, K Yasuda, K Arimori, JD Schuetz. Human MDR1 and mouse *mdr1a* P-glycoprotein alter the cellular retention and disposition of erythromycin, but not of retinoic acid or benzo(*a*)pyrene. *Arch Biochem Biophys* 350:340–347, 1998.
307. P Chelvan, JMT Hamilton-Miller, W Brumfitt. Biliary excretion of erythromycin after parenteral administration. *Br J Clin Pharmacol* 8:233–235, 1979.
308. CA Jamis-Dow, ML Pearl, PB Watkins, DS Blake, RW Klecker, JM Collins. Predicting drug interactions in vivo from experiments in vitro: human studies with paclitaxel and ketoconazole. *Am J Clin Oncol* 20:592–599, 1997.
309. T Tateishi, SG Graham, Y Krivoruk, AJJ Wood. Omeprazole does not affect measured CYP3A4 activity using the erythromycin breath test. *Br J Clin Pharmacol* 40:411–412, 1995.

310. PI Craig, M Tapner, GC Farrell. Interferon suppresses erythromycin metabolism in rats and human subjects. *Hepatology* 17:230–235, 1993.
311. T Kronbach, D Mathys, M Umeno, FJ Gonzalez, UA Meyer. Oxidation of midazolam and triazolam by human liver cytochrome P450III<sub>A4</sub>. *Mol Pharmacol* 36:89–96, 1989.
312. JC Gorski, SD Hall, DR Jones, M VandenBraden, SA Wrighton. Regioselective biotransformation of midazolam by members of the human cytochrome P4503A (CYP3A) subfamily. *Biochem Pharmacol* 47:1643–1653, 1994.
313. KE Thummel, DD Shen, TD Podoll, KL Kunze, WF Trager, PS Hartwell, VA Raisys, CL Marsh, JP McVicar, DM Barr, JD Perkins, RL Carithers Jr. Use of midazolam as a human cytochrome P450 3A probe: I. In vitro-in vivo correlations in liver transplant patients. *J Pharmacol Exp Ther* 271:549–556, 1994.
314. KE Thummel, D O’Shea, MF Paine, DD Shen, KL Kunze, JD Perkins, GR Wilkinson. Oral first-pass elimination of midazolam involves both gastro-intestinal and hepatic CYP3A-mediated metabolism. *Clin Pharmacol Ther* 59:491–502, 1996.
315. AJ MacGilchrist, GG Birnie, A Cook, G Scobie, T Murray, G Watkinson, MJ Brodie. Pharmacokinetics and pharmacodynamics of intravenous midazolam in patients with severe alcoholic cirrhosis. *Gut* 27:190–195, 1986.
316. PJ Pentikäinen, L Välisalmi, J-J Himberg, C Crevoisier. Pharmacokinetics of midazolam following intravenous and oral administration in patients with chronic liver disease and in healthy subjects. *J Clin Pharmacol* 29:272–277, 1989.
317. MF Paine, DD Shen, KL Kunze, JD Perkins, CL Marsh, JP McVicar, DM Barr, BS Gillies, KE Thummel. First-pass metabolism of midazolam by the human intestine. *Clin Pharmacol Ther* 60:14–24, 1996.
318. KE Thummel, DD Shen, TD Podoll, KL Kunze, WF Trager, CE Bacchi, CL Marsh, JP McVicar, DM Barr, JD Perkins, RL Carithers Jr. Use of midazolam as a human cytochrome P450 3A probe: II. Characterization of inter- and intra-individual hepatic P4503A variability after liver transplantation. *J Pharmacol Exp Ther* 271:557–566, 1994.
319. JT Backman, KT Olkkola, PJ Neuvonen. Rifampin drastically reduces plasma concentrations and effects of oral midazolam. *Clin Pharmacol Ther* 59:7–13, 1996.
320. KT Olkkola, JT Backman, PJ Neuvonen. Midazolam should be avoided in patients receiving the systemic antimycotics ketoconazole or itraconazole. *Clin Pharmacol Ther* 55:481–485, 1994.
321. JT Backman, KT Olkkola, PJ Neuvonen. Azithromycin does not increase plasma concentrations of oral midazolam. *Int J Clin Pharmacol Ther* 33:356–359, 1995.
322. MJ Mattila, J Vanakoski, JJ Idänpään-Heikkilä. Azithromycin does not alter the effects of oral midazolam on human performance. *Eur J Clin Pharmacol* 47:49–52, 1994.
323. J Ahonen, KT Olkkola, PJ Neuvonen. Effect of itraconazole and terbinafine on the pharmacokinetics and pharmacodynamics of midazolam in healthy volunteers. *Br J Clin Pharmacol* 40:270–272, 1995.
324. JC Gorski, DR Jones, BD Haehner-Daniels, MA Hamman, EM O’Mara Jr, SD Hall. The contribution of intestinal and hepatic CYP3A to the interaction between midazolam and clarithromycin. *Clin Pharmacol Ther* 64:133–143, 1998.
325. J McCrea, T Prueksaritanont, BJ Gertz, A Carides, L Gillan, S Antonello, MJ

- Brucker, C Miller-Stein, B Osborne, S Waldman. Concurrent administration of the erythromycin breath test (EBT) and oral midazolam (MDZ) as in vivo probes for CYP3A activity. *J Clin Pharmacol Ther* 39:1212–1220, 1999.
326. S Ekins, M VandenBraden, BJ Ring, SA Wrighton. Examination of purported probes of human CYP2B6. *Pharmacogenetics* 7:165–179, 1997.
327. EL Code, CL Crespi, BW Penman, FJ Gonzalez, TK Chang, DJ Waxman. Human cytochrome P4502B6: interindividual hepatic expression, substrate specificity, and role in procarcinogen activation. *Drug Metab Disp* 25:985–993, 1997.
328. S Ekins, M VandenBraden, BJ Ring, JS Gillespie, TJ Yang, HV Gelboin, SA Wrighton. Further characterization of the expression in liver and catalytic activity of CYP2B6. *J Pharmacol Exp Ther* 286:1253–1259, 1998.
329. JW Ko, Z Desta, DA Flockhart. Human *N*-demethylation of (*S*)-mephenytoin by cytochrome P450s 2C9 and 2B6. *Drug Metab Disp* 26:775–778, 1998.
330. JC Stevens, RB White, SH Hsu, M Martinet. Human liver CYP2B6-catalyzed hydroxylation of RP 73401. *J Pharmacol Exp Ther* 282:1389–1395, 1997.

# 13

## Molecular Modeling Approaches to Predicting Drug Metabolism and Toxicity

**Anton M. ter Laak and Nico P. E. Vermeulen**

*Vrije Universiteit, Amsterdam, The Netherlands*

**Marcel J. de Groot**

*Pfizer Global Research & Development, Kent, United Kingdom*

### I. INTRODUCTION

Biotransformation enzymes catalyze various metabolic reactions in xenobiotic and endogenous compounds, e.g., oxidation, reduction, and conjugation reactions. In order to get more insight into the mechanism of action of an enzyme, the substrate selectivity of an enzyme, and the factors determining whether or not a compound will be metabolized by a certain enzyme, a detailed description of the shape and the physicochemical properties of the active site is a prerequisite [1]. As the crystal structure of only a few biotransformation enzymes is available, there are many different strategies to characterize the mechanisms of actions and the active sites of these enzymes, such as (a) chemical modification and affinity labeling, (b) site-directed mutagenesis, (c) spectroscopic techniques, (d) crystallography, (e) structure-activity relationships, and (f) pharmacophore and homology modeling. For cytosolic glutathione *S*-transferase all of these approaches have been applied, as previously reviewed [1]. In cases of membrane-bound enzymes such as cytochromes P450 (CYPs), crystallography, one of the most valuable techniques to elucidate protein structures, has not yet been as successful for the enzyme systems. In recent years, this lack of knowledge has resulted in the prediction of various enzymes structures using computer-aided molecular modeling techniques.

The primary aim of this chapter is to summarize and discuss the requirements and the assumptions for the various computer modeling techniques used, predict the substrate selectivity of enzymes, elucidate the drawbacks and limitations of these modeling techniques, and indicate some of the possible experimental methods to validate the modeled structures of the proteins and, specifically, the active sites. One important class of enzymes will be used to illustrate these aspects, viz the cytochromes P450 (CYPs). In addition, we discuss some of the best known computational methods to predict toxicities.

The cytochromes P450 constitute a large superfamily of heme-containing enzymes capable of oxidizing and reducing substrates of endogenous and exogenous origin. The CYPs belong to a separate family when the primary sequence homology with any other family is equal to or less than 40% [2]. For mammalian CYP amino acid sequences within the same subfamily, the identity is usually over 55% [2].

Cytochromes P450 generally detoxify potentially dangerous compounds, but in a number of cases nontoxic compounds are bioactivated to toxic reactive intermediates, and procarcinogens are activated into their ultimate carcinogens [3]. The CYPs also catalyze key reactions in steroidogenesis in animals, and many yield resistance in insects and plants or affect flower coloring [4]. The metabolic activities of CYPs can be divided into (1) monooxygenase activity, usually resulting in the incorporation of an oxygen atom into the substrate, (2) oxydase activity, resulting in the formation of superoxide anion radicals and hydrogen peroxide (uncoupling of the catalytic cycle [5]), and (3) reductase activity, usually producing free radical intermediates under anaerobic conditions [5–7].

The CYPs can also be classified according to the electron transfer chain delivering the electrons required for the one-electron reductions from NAD(P)H: class I CYPs are found in the mitochondrial membranes of eukaryotes and in bacteria and require a flavin adenine dinucleotide (FAD) containing reductase and an iron-sulfur protein (putidaredoxin) [4,8], while class II CYPs are bound to the endoplasmic reticulum and interact directly with a cytochrome P450 reductase [containing FAD and flavin mononucleotide (FMN)] [4,9].

## II. METHODOLOGICAL ASPECTS OF PHARMACOPHORE MODELS

One possibility to derive a model for the active site of an enzyme is the creation of a small molecule model, or pharmacophore model. With this technique, information on the active site is derived (indirectly) from the shape, electronic properties, and conformations of substrates, inhibitors, or metabolic products. Various substrates, inhibitors, or metabolic products are aligned by superimposing chemically similar groups. By using this approach a template is created that de-

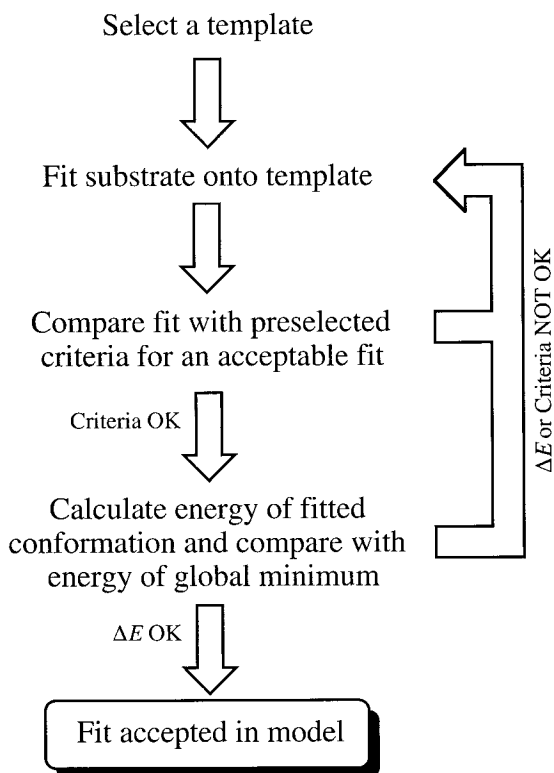


**Figure 1** General procedure for the construction of a small molecule (pharmacophore) model.

scribes the size of the active site and the electrostatic distribution therein. The general procedure followed to construct a pharmacophore model is depicted in Fig. 1. A pharmacophore model for substrates will be used as an example, although pharmacophore models for inhibitors or metabolites can be obtained in a similar manner.

### A. Requirements

In order to build a pharmacophore model for substrates of a specific enzyme, a main requisite is a template molecule upon which the model will be built. The template molecule is usually a substrate which ideally: (a) is specifically metabolized by the (iso)enzyme under investigation, (b) is large, (c) is relatively rigid,

in order to limit conformational freedom, (d) contains essential functional groups, and (e) is regio- and/or stereoselectively metabolized. Further requisites are the availability of appropriate enzyme kinetic and metabolic data concerning a variety of additional substrates, which are specifically metabolized by the (iso)enzyme under investigation and computer programs containing the molecular forcefield parameters required for modeling the substrates under investigation.

After selection of a template molecule, additional substrates are superimposed onto the template molecule. Some predefined fit criteria have to be met; otherwise the fit onto the template is rejected. When the fit is accepted, an energy calculation is performed in order to determine the energy difference between the global minimum energy conformation and the fitted conformation. If this energy difference ( $\Delta E$ ) is within a predefined range, the fit of the compound on the template molecule is accepted in the model [10,11].

## B. Assumptions

The construction of the pharmacophore model would not be possible without taking certain assumptions into account. The primary assumption for pharmacophore modeling is that all substrates will be oriented in a similar manner (both electronically and sterically) in the active site of the enzyme. The second assumption is that the geometry of the substrates obtained from energy-minimization corresponds to the geometry necessary for the biologically active geometry. This is true for in vacuo generated geometries only when (1) the active site of the enzyme is mainly hydrophobic in nature, (2) charge stabilization by the apoprotein is not significant during the reaction, and (3) the metabolic reaction of the substrate is "chemical-like" and does not strictly require specific interactions between the substrate and the apoprotein, thereby altering the geometry of the substrate [13,14]. Geometries derived from crystal structures, on the other hand, are usually influenced by crystal-packing effects. The geometries used, derived either from calculations or from crystal structures, *do not necessarily* correspond to the biologically active conformation.

## C. Drawbacks of Pharmacophore Models

In pharmacophore models, steric, electronic, and other interactions with the protein are not explicitly modeled. However, if a substrate can be accommodated in a pharmacophore model but experimentally the formation of a certain metabolite does not occur, this does not necessarily imply a steric (or electronic) restriction that is neglected by the model. Possibly, other metabolic pathways and/or (iso)enzymes compete with the specific metabolic reaction of the (iso)enzyme for the substrate under the experimental conditions applied. The absence of a certain (predicted) metabolite may also be due to kinetic rather than thermody-

namic effects [13], for example, when the specific metabolic conversion is very slow compared to other metabolic reactions.

Substrate geometries taken directly from the CSD [12] are usually influenced by packing effects that are absent in a biological environment. In a similar way, the geometries of the substrates/inhibitors obtained by using semiempirical or *ab initio* optimizations are not necessarily identical to the geometries in a biological environment (as indicated earlier).

Pharmacophore models for inhibitors are generally more difficult to construct compared to substrates or metabolic products. The specific site of reaction (e.g., oxidation or conjugation) is lacking in inhibitor models and can therefore not be used as an easily identifiable site to be superimposed.

#### D. Experimental Validation

After building a pharmacophore model, metabolic predictions can in principle be made using the model. In order to validate the model and its predictions, experiments can be designed to test the hypotheses. Generally, the predicted metabolites of a substrate have to be identified in incubations using the purified or heterologously expressed (iso)enzyme. When using microsomes for such experiments, other (iso)enzymes can be responsible for the metabolites as well. The metabolite pattern found in the metabolism experiments can subsequently be compared with the predicted metabolites. In case the predicted metabolite is not detected experimentally, this does not unequivocally indicate that the pharmacophore model is erroneous (as indicated in Sec. II.c).

Several easily accessible parameters, such as Michaelis–Menten constants ( $K_m$ ), inhibition constants ( $K_i$ ), and binding constants ( $K_s$ ) do not appear very useful for the validation of pharmacophore models. The most useful constant is  $K_s$ , for a pharmacophore model can give information only on the binding of substrates and not on overall reaction rates. However, for a series of substrate of glutathione *S*-transferase (see later [15]), recent experiments indicated that although the  $K_m$  values appeared to correlate well with differences observed in the pharmacophore model, the differences in  $K_s$  (and to a lesser extent the differences in  $K_i$ ) were almost indistinguishable for the various substrates.

### III. PHARMACOPHORE MODELS FOR CYTOCHROME P450 ISOENZYMES

Pharmacophore models have been derived for only a limited number of P450 isoenzymes. In recent years, more elaborate computational techniques were used, compared to the relative simple calculations performed in the 1980s.



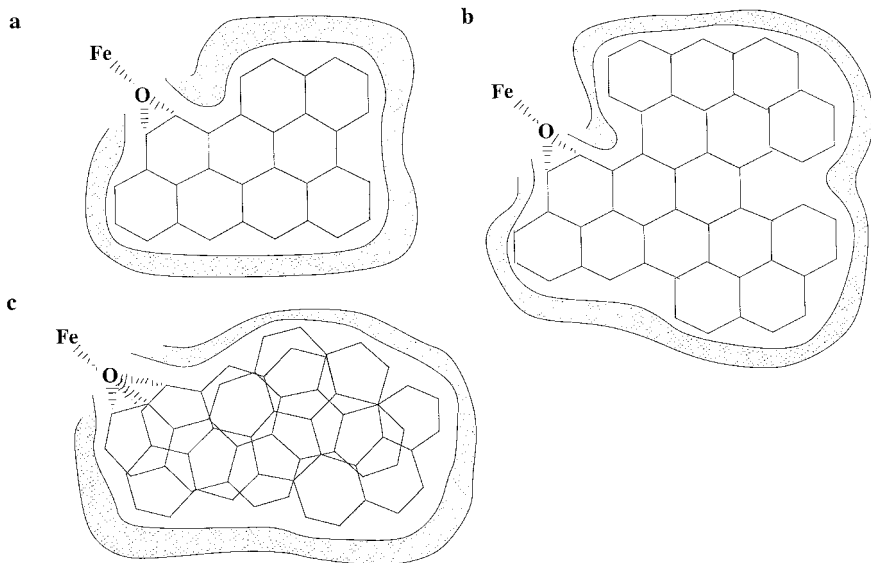


**Figure 2** (a) Steric model of the active site of CYP1A1 based on the metabolism of benzo[*a*]pyrene. The binding site is asymmetrically positioned toward the activated oxygen species bound at the iron atom [16]. (b) Expansion of model (a) in order to accommodate several other PAHs [17,18]. (c) Proposed model in which some flexibility in the angle of the oxygen addition to the substrate is allowed [16]. (From Ref. 19.)

## A. CYP1A1

A very simple pharmacophore model for rat CYP1A1 was first derived by Jerina and coworkers [16] using benzo[*a*]pyrene and a variety of other polycyclic aromatic hydrocarbons (PAHs) (Fig. 2a). Benzo[*a*]pyrene is converted stereoselectively via 7,8-epoxidation by CYP1A1, via hydration by epoxide hydrolase, and via 9,10-epoxidation by CYP1A1 to the ultimate carcinogen benzo[*a*]pyrene 7(*R*),8(*S*)-diol 9(*S*),10(*R*)-epoxide. Based on the PAH substrates used, this model described the active site of CYP1A1 as a hydrophobic cleft, asymmetrically oriented relative to the heme. This original model of CYP1A1 substrates was later extended to accommodate several other PAHs [17,18]. The original model had to be extended considerably (Fig. 2b), or a certain degree of flexibility in the position of the substrates had to be incorporated (Fig. 2c).

Rat CYP1A1 is also known to metabolize, in a regio- and stereoselective manner, a variety of small non-PAH substrates, such as 7-ethoxycoumarin and

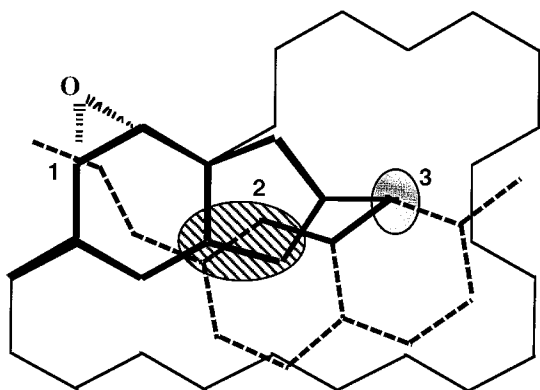


**Figure 3** Pharmacophore model for CYP1A1 for small non-PAH substrates. 7-Ethoxycoumarine (solid line) and zoxazolamine (dashed line) are shown when superimposed onto the steric model for PAHs as shown in Fig. 2a [16] with (1) the site of oxidation, (2) the region of presumed  $\pi$ - $\pi$  interactions between substrates and protein, and (3) the location of heteroatoms in the substrates proposed to form a hydrogen bonding interaction with the protein. (From Ref. 19.)

zoxazolamine [19]. The binding and orientation of these small substrates in the active site of CYP1A1 was suggested to be the result of a hydrogen bonding interaction and aromatic interactions with protein [19]. The sites of oxidation and the heteroatoms responsible for the hydrogen bonding interaction with the protein were superimposed, as indicated in Fig. 3 [19]. The combination of the model for PAHs [16,18] and the model for pharmacophores [19] presents a rough pharmacophore model that can accommodate many substrates of rat CYP1A1.

## B. CYP1A1/1A2

Computational analysis of compounds oxidized by rat CYP1A1 and 1A2 indicated that these isoenzymes preferentially catalyze the hydroxylation of essentially flat molecules, further characterized by a small depth and a large area/depth ratio [20,21]. These studies used substrate geometries from crystal structures and from MINDO/3 semiempirical calculations [20]. Because crystal structures may be influenced by crystal-packing effects, a direct comparison is, however, not necessarily warranted (see Sec. II.A). The substrates were fitted onto each other, based on only size and shape; no functional groups within the substrates were superimposed [20].

### C. CYP2B1/2B2

A simple computational analysis of compounds metabolized by rat CYP2B1 and 2B2<sup>1</sup> suggested these substrates to be rather bulky, nonplanar molecules characterized by small area/depth ratios and a larger flexibility in molecular conformation, when compared to substrates of the rat CYP1A1 and 1A2 [20,21]. Again crystal structures and MINDO/3 optimized geometries were used interchangeably. The substrates were not superimposed in this study, and only sizes and shapes were compared [20].

### D. CYP2C9

Human CYP2C9 is an isoenzyme involved in the metabolism of a large number of antiinflammatory drugs, which exist as anions at physiological pH [21]. Based on 12 substrates, a pharmacophore model for CYP2C9 has been derived phenytoin and (*S*)-warfarin, as templates [21]. The geometries of the substrates were derived partially from crystal structures and partially from molecular mechanical calculations using the “consistent valence forcefield” [21]. It was possible to superimpose the substrates with their sites of hydroxylation and to bring all anionic heteroatoms in the various substrates at a distance between 3.5 Å and 4.8 Å from a common (hypothetical) cationic interaction site within the CYP2C9 protein [21] (Fig. 4). Since the positions of the anionic heteroatoms were rather different for the various substrates, a hydrogen bond to the protein was suggested not to be possible with all the substrates. Instead, a purely cation–anion interaction was presumed [21]. This model was updated to reflect studies done with sulfaphenazole (a very potent inhibitor of 2C9), thus including a hydrophobic zone between the hydroxylation site and the cationic site of the protein. This indicated that the tight binding of sulfaphenazole was due to a ligand interaction between the aniline nitrogen of sulfaphenazole and the heme iron [21]. A second 2C9 pharmacophore model was first described by Jones et al. [43] and later updated by overlaying 8 substrates and 1 inhibitor, using phenytoin as the template molecule and ensuring sites of metabolism and the hydrogen bond donor were superimposed [44]. In contrast to the purely cation–anion interaction suggested by Mancy et al. [21], this model used a hydrogen bond donor–hydrogen bond acceptor interaction and results in a larger active site cavity for CYP2C9 [44].

### E. CYP2D6

Human CYP2D6 is a polymorphic member of the CYP superfamily and is absent in 5–9% of the Caucasian population as a result of a recessive inheritance of gene mutations [22,23]. This results in deficiencies in drug oxidations known as the debrisoquine/sparteine polymorphism that affect the metabolism of numerous

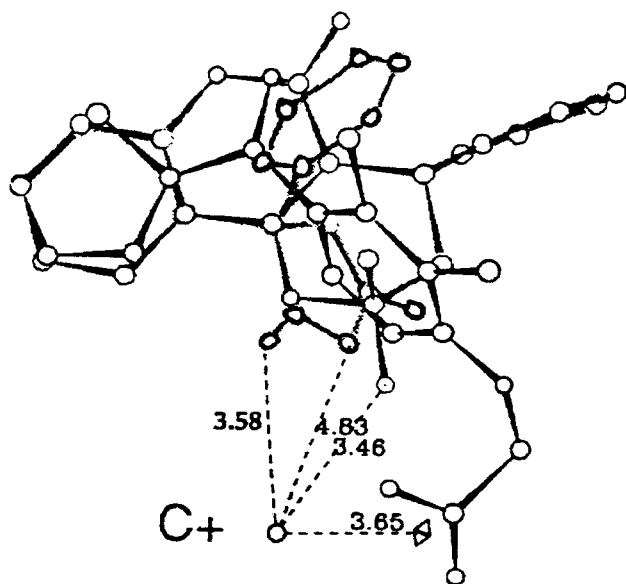


**Figure 4** Superposition of the hydroxylation sites and hydroxylated aromatic rings of warfarin, phenytoin, and tienilic acid. Possible interaction of their anionic sites with a cationic site of CYP2C9 ( $C^+$ ) is shown. (From Ref. 21.)

drugs. A decreased metabolism of these drugs is found in poor metabolizers that have two nonfunctional CYP2D6 alleles, compared to extensive metabolizers with at least one functional allele. Pharmacophore models predicting the involvement of CYP2D6 may identify potential problems for poor metabolizers when either a drug is not metabolized or a prodrug is not activated due to the dependence on the lacking CYP2D6.

The first substrate models were based on substrates containing a basic nitrogen atom at a distance of either 5 Å (Fig. 5a) [24] or 7 Å [27] from the site of oxidation and an aromatic ring system, which was coplanar in both models [24,27]. In the 5-Å model no substrates were actually fitted onto each other [24]. The main problem of these initial models was that neither could explain the other group of substrates.

An extended model was derived by Islam et al. [28] who combined these models by indicating a distance between a basic nitrogen atom and the site of oxidation between 5 and 7 Å. This pharmacophore model also contained the heme moiety and the crystal structure of CYP101 (CYP<sub>cam</sub> [29]) with an oxygen atom bond to the iron of the heme moiety. Above this moiety the template molecule of this pharmacophore model (debrisoquine) was positioned arbitrarily [28],

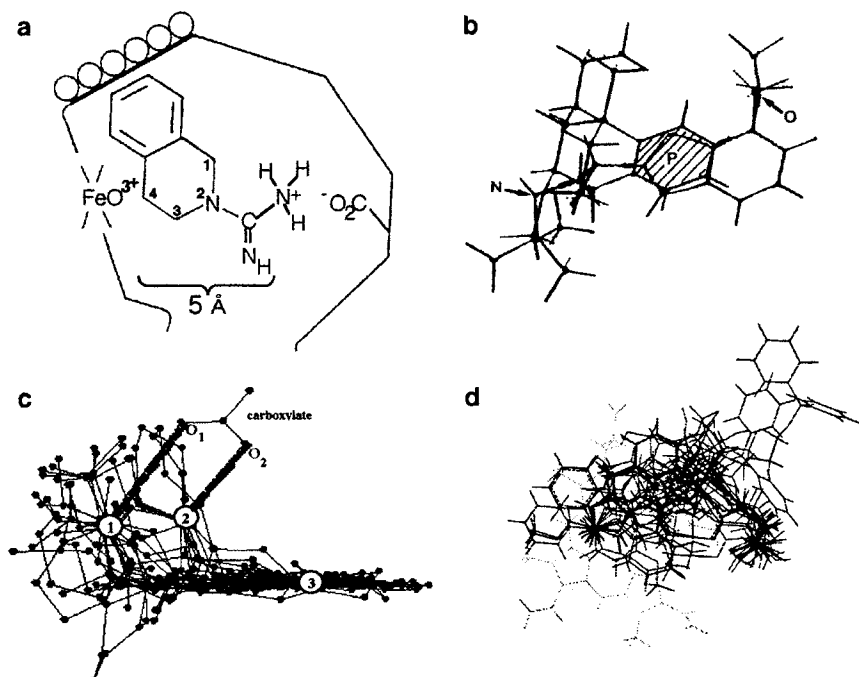


**Figure 5** (a) Initial 5-Å pharmacophore model for CYP2D6. Debrisoquine is shown at the active center, with the basic nitrogen atom attached to a carboxyl group and the site of oxidation adjacent to the iron-oxo complex. The heavy line and six circles denote a hydrophobic region (From Ref. 24). (b) Initial 7-Å pharmacophore model for CYP2D6. Juxtaposition of dextromethorphan and bufuralol, with N: basic nitrogen atom, P: lipophilic plane, and O: oxidation site (From Ref. 28). (c) Combined 5-Å-7-Å pharmacophore model for CYP2D6 [11]. Oxidation sites (3) of all molecules are superimposed. Basic nitrogen atoms are fitted either on the basic nitrogen atom of debrisoquine (2) or onto that of dextromethorphan (1) and interact with one of the carboxylic oxygen atoms (O<sub>1</sub> or O<sub>2</sub>) (From Ref. 19). (d) Refined pharmacophore model for CYP2D6, containing the heme moiety (gray) and aspartic acid residue 301 derived from a protein model for CYP2D6 [31]. (Adapted from Ref. 10.)

in a manner resembling the orientation of camphore in the CYP101 crystal structure [30]. A set of 15 compounds was fitted onto the template debrisoquine onto which some of the known substrates of CYP2D6 (e.g., sparteine and amitriptyline) could not be fitted [28]. One prediction based on this model, that NNK (4-(*N*-methyl-*N*-nitrosamino)-1-(3-pyridyl)-1-butanone) is not a substrate for CYP2D6, was experimentally confirmed using human liver microsomes [28].

Another pharmacophore model for CYP2D6 was derived by Koymans et al. [11]. This model suggested a hypothetical carboxylate group within the protein to be responsible for a well-defined distance of either 5 Å or 7 Å between the basic nitrogen atom and the site of oxidation within the substrate. This model used debrisoquine and dextromethorphan as templates for the 5 Å and 7 Å compounds, respectively. The oxidation sites of the two templates were superimposed, and the areas next to the sites of oxidation were fitted coplanarily, while the basic nitrogen atoms were placed 2.5-Å apart, interacting with different oxygen atoms of the postulated carboxylate group in the protein. The final model (Fig. 5c) consisted of 16 substrates, accounting for 23 metabolic reactions, with their sites of oxidation and basic nitrogen atoms fitted onto the sites of oxidation of the templates and one of the basic nitrogen atoms of the template molecules, respectively. The model was verified by predicting the metabolism of four compounds giving 14 possible CYP-dependent metabolites. In vivo and in vitro metabolism studies with these substrates showed that 13 out of 14 predictions (3 positive and 10 negative predictions) were correct [11], indicating the relatively high predictive value of the model. More recently, the predictive value of the model was further confirmed as two metabolites of 1-[-2[bis(4-fluoro-phenyl)methoxy]ethyl]-4-(3-phenyl-propyl)-piperazine (GBR 12909) were also correctly predicted and shown to be formed by heterologously expressed CYP2D6 [14]. The relatively large GBR 12909 extended considerably from the region described by the pharmacophore model, indicating an extension of the model in certain directions to be necessary [14].

In a next step, the actual positions of the heme moiety and the I-helix, containing Asp301 (derived from a protein model of CYP2D6; see later) [31] were added to this pharmacophore model, thereby incorporating some steric restrictions and orientational preferences into the pharmacophore model [10]. Involvement of Asp301 in substrate binding was initially predicted using homology modeling techniques [32] and recently confirmed, with site-specific mutation and expression experiments, to be important for the activity of CYP [33]. In this refined pharmacophore model, an aspartic acid residue is coupled to the basic nitrogen atom of the substrates, thus enhancing the pharmacophore model with the direction of the hydrogen bond between the aspartic acid in the protein and the (protonated) basic nitrogen [10] using debrisoquine and dextromethorphan again as template molecules. The site of oxidation above the heme moiety was one of the two possible sites of oxidation, as suggested by the recently derived protein model for CYP2D6 (see later) [31], and is located above pyrrole ring B of the heme moiety. In this model the sites of hydroxylation or *O*-demethylation in the substrates were fitted onto the defined oxidation site above pyrrole ring B of the heme moiety, while the C<sub>α</sub> and C<sub>β</sub> atoms of the attached aspartic acid moiety were fitted onto the C<sub>α</sub> and C<sub>β</sub> atoms of Asp301, respectively [10]. A schematic representation of the refined pharmacophore model of CYP2D6 is

given in Figure 5d. A variety of substrates fitted in the original substrate model for CYP2D6 [11,14,34] were successfully fitted into the refined substrate model (for example, GBR 12909), indicating that the refined substrate model for CYP2D6 (with extra steric and directional restraints) can accommodate the same variety in molecular structures as the original substrate model. The refined pharmacophore model also gives a more accurate description of the active site of CYP2D6. This model was recently used successfully to design a novel and selective CYP2D6 substrate suitable for high-throughput screening [127] and to provide an understanding of the hydroxylation of debrisoquine [58]. A similar pharmacophore model containing 40 substrates with 57 different metabolic pathways has been combined with a protein homology model of CYP2D6 [35]. This combined model demonstrated a high level of complementarity of the model with the CYP2D6 substrate binding site which underlines the justification to use pharmacophore models for metabolism predictions. A second substrate pharmacophore has been derived specifically for 14 substrates that are *N*-dealkylated by CYP2D6 [36]. This pharmacophore was also successfully merged with the protein 2D6 model and showed a more important role for the interaction of the aromatic region in the *N*-dealkylated substrates with Phe481, compared with the hydroxylated *O*-demethylated substrates. It was speculated that this aromatic–aromatic interaction contributes more significantly to CYP2D6 binding because the *N*-dealkylated substrates lack an interaction of a basic nitrogen atom with Asp301.

Parallel to the substrate models for CYP2D6, an inhibitor model has been derived using 6 strong reversible inhibitors of CYP2D6 fitted onto each other at template [25]. The basic nitrogen atoms were superimposed and the aromatic planes of these inhibitors were fitted coplanar. All inhibitors used were relatively flexible, resulting in various low-energy conformations. The final template consisted of those conformations of ajmalicine, quinidine, chlorpromazine, trifluperidol, prodipine, and lobeline that could be fitted relatively well onto each other [37]. Consecutively, other inhibitors, such as derivatives of ajmalicine and quinidine, were fitted onto the derived template. The derived preliminary pharmacophore model consisted of a tertiary nitrogen atom (protonated at physiological pH) and a flat hydrophobic region [37]. Furthermore, there appeared to be a region in which functional groups with lone pairs seemed to cause enhanced inhibitory potency, while in another region hydrophobic groups seemed to be allowed but caused no enhanced inhibitory effect [25]. The inhibition data was obtained from experiments using human liver microsomes and bufuralol as substrate [25]. The uncertainties in both the template used and the inhibition experiments used to verify this model were relatively large [11,14]. The features derived for this inhibitor-based pharmacophore model [25] were very similar to the features of the proposed substrate models of CYP [10,11,28]. For this reason it is not unlikely that the substrate-based and inhibitor-based pharmacophore models can be combined.

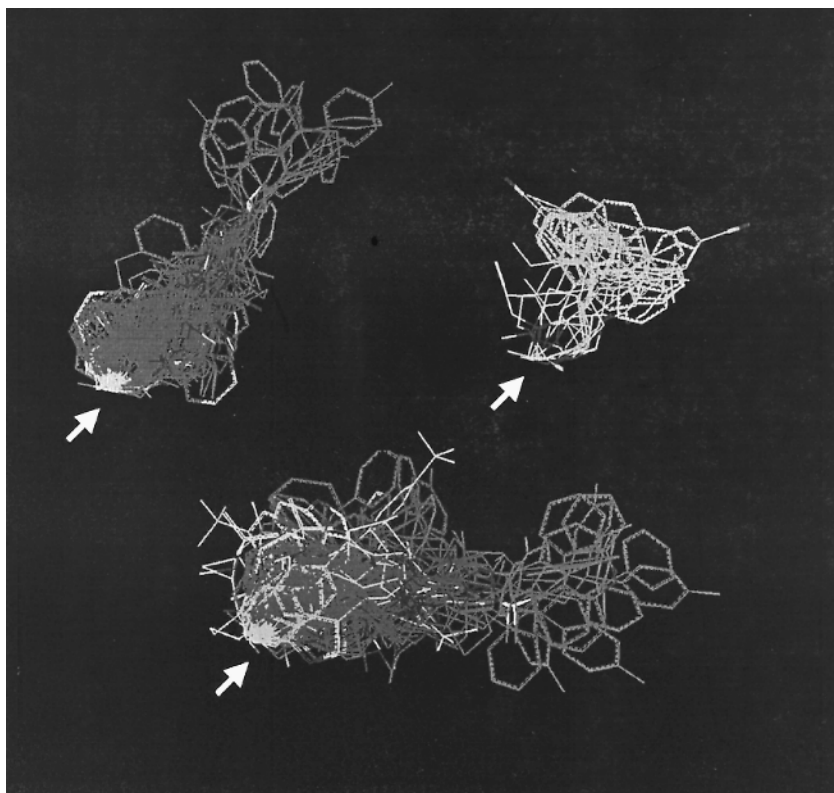


**Figure 6** Separate pharmacophore models for CYP2D6 catalyzed hydroxylation and O-demethylation reactions (top left: dark gray substrates with oxidation sites colored light gray) [35] and for N-dealkylation reactions (top right: light gray substrates with nitrogen atoms colored dark gray). All 51 substrates have been energy minimized in the active site of a CYP2D6 protein homology model and combined in one pharmacophore model. Sites of oxidation are indicated by white arrows. (From Ref. 36.)

## F. CYP3A4

To gain better understanding and find a good description of the active site of CYP3A4, Ekins and coworkers recently built a pharmacophore of CYP3A4 substrates using the program *Catalyst* [130]. In this study, a three-dimensional quantitative structure—activity relationship model was constructed based on the structures and  $K_m$  values of 38 substrates measured in human liver microsomal CYP3A4. After validation of the model by randomizing the activity values and the substrate structures, a significant representation of the CYP3A4 substrate site



was generated. The resulting CYP3AF pharmacophore consisted of four features: two hydrogen-bond-acceptor groups, one hydrogen-bond-donor group, and one hydrophobic region. These results correspond relatively well with the results from docking studies into a CYP3A4 protein model using a large number of substrates, as performed by Lewis et al. [129] (see also Sec. IV.F.4). In that study, it was concluded that CYP3A4 substrates are characterized by the presence of an electronegative atom lying between 5.5 and 7.8 Å from the site of metabolism and that some substrates contain an aromatic ring between 2 and 4 Å from the electronegative atom, optimal for aromatic stacking within the CYP3A4 binding site [129]. The *Catalyst* substrate 3D model has been validated further by predicting the  $K_m$  values of a test set of 12 substrates not used for constructing the model. The residuals of the predictions were all within 1 log unit from the experimental values using the fast fitting method of *Catalyst*, demonstrating a successful example of in silico prediction from a pharmacophore model.

## G. Summary

A wide variety of substrates specifically metabolized by a given CYP isoenzyme is generally available. This usually enables the selection of a suitable template for the pharmacophore model. When suitable template molecule is available, a combination of several structurally different compounds may also be successfully used as a template. The earliest reported substrate models for CYPs are relatively crude pharmacophore models, while the more recently derived models are much more advanced and are constructed using more sophisticated computational modeling techniques. The latter models demonstrate a clear potential to predict the possible involvement of specific CYP isoenzymes in the metabolism of selected substrates and the nature of hypothetical interaction sites in the active site of the protein. For the polymorphic isoenzyme CYP2D6, pharmacophore models have already been used to predict its involvement, in order to identify potentially large interindividual differences between extensive and poor metabolizers. This may pose risks to poor metabolizers in case either a drug is not metabolized or a prodrug is not activated due to dependence on a lacking CYP2D6.

## IV. PROTEIN MODELS

### A. Introduction

Another computer-assisted approach to obtain structural information on the active site of a protein (e.g., an enzyme) is the construction of a homology model (direct modeling). Homology modeling yields information on the active site by constructing a three-dimensional model of the protein based on the amino acid sequence and the crystal structure of one or more similar proteins. This method

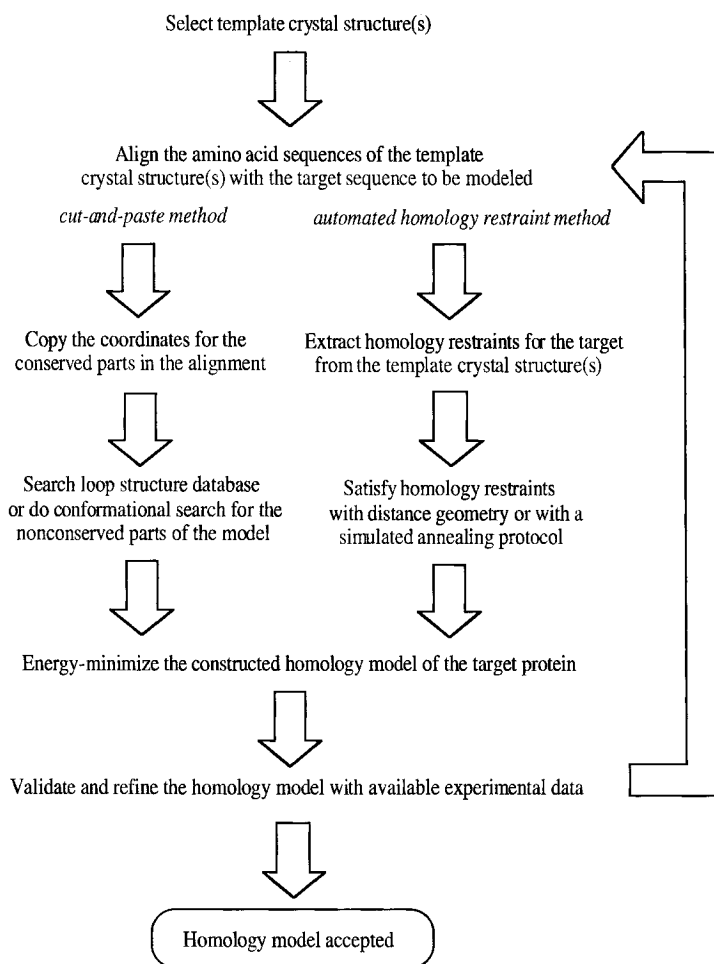


**Figure 7** General procedures for the construction of homology (protein) models. Left-hand side: “Cut-and-paste” method. Right-hand side: Automated modeling using homology restraints as implemented in CONSENSUS [38] or in MODELLER [39].

affords a three-dimensional representation of the protein and more specifically of its active site, as well as information on amino acids (potentially) involved in binding and on catalysis [13]. Briefly, there are two methods for constructing protein homology models, as depicted in Figure 7: the “cut-and-paste” method and “comparative protein modeling by satisfaction of homology restraints” as included in CONSENSUS [38] or in MODELLER [39].

In both cases, an alignment is made between the amino acid sequences of the unknown structure and one or more crystallized template proteins, ideally supplemented with structural or biochemical data. In the “cut-and-paste” protocol, homologous regions present in both the crystal structure(s) and the unknown structure are copied directly from the crystal structure(s) to the homology model, while the nonidentical parts are calculated for the model or subtracted from loop structure databases (Fig. 7, left-hand side). In the case of comparative homology modeling (Fig. 7, right-hand side), many distance and dihedral restraints on the target sequence are calculated from the alignment with the template X-ray structures. Several slightly different 3D structures of the target protein that all satisfy the large set of spatial restraints can then be obtained using distance geometry [38] or a simulated annealing protocol [39]. The variability among these models can be used to estimate the errors in the corresponding regions of the fold.

In both methods presented in Figure 7 the homology model is energy-minimized in the last step using molecular mechanical methods. In the minimized homology model, substrates, inhibitors, or metabolites can be docked. The constructed homology model can also be validated and refined with experimental data (e.g., from site-directed mutagenesis and/or site-specific modification experiments).

Although a good amino acid alignment between similar proteins is a prerequisite for the construction of a protein model, it is not our aim to discuss the various methods and software programs used to obtain (automatic) alignments.

## B. Requirements

In order to build a homology model of a protein, at least one crystal structure of a similar protein is required, as well as an alignment describing corresponding amino acids in the protein under investigation and the crystallized protein(s). The crystal structure(s) should preferably have a high resolution (1.5–2.5 Å) and a high (primary sequence) homology with the protein under investigation. Ideally, the crystallized protein(s) belong(s) to the same family of proteins [(iso)enzymes]. The reliability of the alignment depends on the homology between the crystal structure(s) used and the protein under investigation. When the homology is relatively low, the alignment will contain parts of questionable reliability, and consequently various alignments will be possible for such regions. In the case of low homology, the algorithm used to derive the alignment also has an important influence on the final homology model, because different algorithms give rise to different alignments and, consequently, to different protein models. Generally, an automatically generated alignment needs to be adjusted manually based on available additional information, such as site-directed mutagenesis [40]. Use of multialignment techniques and secondary-structure predictions can also help aligning specific regions with a very low homology [41].

### C. Assumptions

The most important assumption inherent to homology modeling is that the three-dimensional structure of the protein constructed is similar to that of the crystallized protein used as a “template.” The validity of this assumption, of course, depends on the specific protein under investigation and the availability of homologous crystal structures.

An important factor determining the quality of a homology model is the forcefield used for the molecular mechanical calculations. Various programs, employing a variety of forcefields, can be used to build a homology model, to energy-minimize the model, and to dock the substrates, inhibitors, or metabolites. Because the energy terms and parameters in the different forcefields are not identical, no direct comparison can generally be made of total energies obtained for homology models of the same protein by different programs. Structural comparisons can be made to a certain extent. However, differences in the forcefields employed will usually have consequences for the final geometry of the protein model. When selecting a forcefield, one should first determine whether that specific forcefield gives an appropriate description of all aspects of the protein model under construction, e.g., that it contains the correct parameters, in the case of CYPs, for example, for the description of a heme moiety. Ab initio calculations would circumvent the dependency of homology models on forcefields, but protein/enzyme structures are generally far too large for ab initio approaches.

### D. Drawbacks of Homology Models

The drawbacks of homology models are closely related to the assumptions mentioned earlier. A homology model will to a certain extent resemble the crystal structure from which it was derived. This resemblance might be real or merely a consequence of the methodology used. When the homology between the available crystal structure(s) and the protein/enzyme for which the model is constructed is relatively low, the alignment of the respective sequences is not straightforward. In the modeling studies mentioned in Sec. III, several alignment programs were used. Most of the automated alignments were manually adjusted to incorporate additional information (e.g., site-directed mutagenesis data) and to remove errors (e.g., insertions or deletions in  $\alpha$ -helices). Although these manual adjustments introduce uncertainties, different authors have nevertheless independently derived almost identical alignments [9,31,40].

The dependence of the geometry of the final protein model on the forcefield used is another drawback. It is therefore advisable to perform the geometry optimization calculations used to construct and optimize the homology model also on the crystal structure(s) used as a template, and to determine first the changes occurring in the template structure(s) due to this procedure. As several homology

modeling programs and forcefields have been used to geometry-optimize the resulting protein models, a comparison of the various models has to be considered carefully. Even when identical software is used, the forcefield parameters used in the various optimization procedures are not always identical and, unfortunately, often not mentioned in publications.

## E. Experimental Validation

The validation of protein models has to come from crystallization experiments or from other methods, such as three-dimensional NMR. Often, however, homology modeling techniques are used when protein structure determinations using three-dimensional NMR or crystallization have not been successful. Predictions as to, e.g., the possible role of specific amino acids in binding of substrates and/or inhibitors and in the mechanism of catalysis can often be verified experimentally using site-directed mutagenesis experiments or site-specific modification experiments. Predictions concerning available space in the active site above different pyrrole rings can be assessed using reactions between arylhydrazines or aryl diazenes with heme proteins, leading to different iron *N*-arylporphyrins [44]. Such information can be derived from NMR spin-relaxation studies as well, as performed recently for a number of CYP2D6 substrates [45].

## F. Homology Models for CYP Isoenzymes

### 1. Overview

Despite extensive efforts, no eukaryotic, membrane-bound CYPs have been crystallized so far. However, crystal structures have been resolved for several soluble bacterial CYPs: thus CYP101 (CYP<sub>cam</sub>, schematically shown in Fig. 8a) without substrate [23,26] with camphor as bound substrate [30], with adamantanone, adamantane, camphane, norcamphor, or thiocamphor as bound substrate analogs [26,46], with metyrapone or 1-, 2-, or 4-phenylimidazole as bound inhibitors [47], with both enantiomers of a chiral, multifunctional inhibitor bound [48], and with 5-*exo*-hydroxycamphor as bound catalytic product [49]. Later on, crystal structures of CYP102 (CYP<sub>BM3</sub>, schematically shown in Fig. 8b) without substrate [8,37,50], CYP 107A (CYP<sub>eryF</sub>) with 6-deoxyerythronolide B as bound substrate [51,52], and CYP108 (CYP<sub>terp</sub>) without substrate [37,53] and the CYP51 in *M. tuberculosis* [59] have been described as well. Also, a crystal structure has been published for a soluble eukaryotic *Fusarium oxysporum* CYP55 (CYP<sub>nor</sub>) [54] that in contrast to other CYPs does not possess mono-oxygenase activity, but reduces nitric oxide instead [55]. Furthermore, the crystal structures of the rabbit CYP2C5/3, a solubilized mammalian chimera, has recently become available [132,133]. The core region of CYPs, containing the D-, E-, I-, and L-helices and

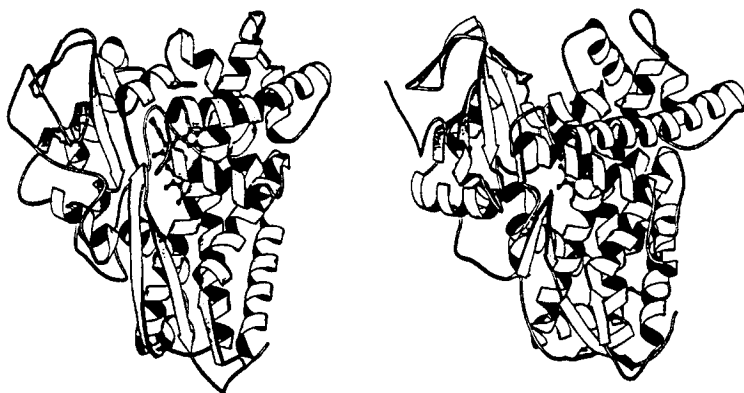


**Figure 8** Schematic diagram of (left) CYP101 and (right) CYP102. Helices are represented as rods and  $\beta$ -sheets as flat arrows. (From Ref. 55.)

the heme coordination region, of all available crystal structures is very similar [4,9,52,56,57], indicating that the three-dimensional structure of these regions is well conserved despite a low sequence homology, while other regions (e.g., the active site region containing the B'-helix [4,52,57], the loops between the C- and D-helices, the region spanning the F- and G-helices, and some parts of the  $\beta$ -sheets) are less similar [4,9,52,56,57]. For this reason, the core region of homology models of CYPs based on these crystal structures will likely be a reliable representation, while other parts will remain speculative.

Table 1 summarizes homology models built so far based on the available CYP crystal structures. In principle, a crystal structure of a membrane bound CYP would be the best starting point for a homology modeling study on a membrane bound CYP. In the absence of such a crystal structure, CYP102 and CYP2C5/3 represent the best starting points for homology modeling.

The most reliable homology models so far have been constructed based on multiple alignments and use site-directed mutagenesis data to enhance the reliability of the alignment [61,62]. Some models have been experimentally validated by site-directed mutagenesis experiments, while in other cases the site-directed mutagenesis experiments were based on initial predictions from the homology models. Recently, a set of protein models for CYP2D6 was reported that incorporated distance restraints derived from NMR data in order to enhance the quality of these models [45,63,64]. Although several homology models are based on multiple alignments methods, site-directed mutagenesis data is less widely used [13,31,45,65–69].

Examples of recently constructed homology models using all available

**Table 1** Overview of Homology Models Built for Cytochromes P450, the Crystal Structure(s) Used as a Template, and Some Specifications of the Homology Models

Enzyme model	Template CYP(s)	Specification <sup>a</sup> and reference(s)
CYP1 <sup>b</sup>	101	Complete CYP model. Little specific information about this model is indicated [102].
CYP1A1	101	Complete CYP model [103]. Alignment in conflict with experimental data for CYP2A4/2A5.
CYP1A1	101	Complete CYP model [104].
CYP1A1/1A2	102	Complete CYP model [105].
CYP1A1/1A2/1A6	102	Complete CYP model [109].
CYP1A2	102	Complete CYP model [107].
CYP1A2	102	Complete CYP model [108].
CYP1A2	101/102/107A/108	Complete CYP model. Comparison with CYP2D6 and CYP3A4 [83].
CYP2A1/2A4/2A5	102	Complete CYP models [69].
CYP2A6	102	Complete CYP model. Incorporates data from a variety of site-directed mutagenesis studies to improve/adjust the alignment. A limited amount of specific information about this model is indicated [68].
CYP2A6	102	Complete CYP model [106].
CYP2B <sup>b</sup>	101	Complete CYP model. Little specific information about this model is indicated [102].
CYP2B1	101	Complete CYP models, which do not explain all site-directed mutagenesis results [67].
CYP2B1	102	Complete CYP model, including a suggestion for membrane attachment [78].
CYP2B1/2B4	102	Complete CYP model. Incorporates data from a variety of site-directed mutagenesis studies to improve/adjust the alignment [68].
CYP2B4	101/102/107A/108	Complete CYP model [110].
CYP2B1/2B4/2B5	102/2C5	Complete CYP models. In agreement with site-directed mutagenesis antibody-recognition site residues associated with binding redox partner residues [77,60].
CYP2B6	101/102/107A/108	Complete CYP model [111].
CYP2C3/2C9	102	Complete CYP model. Incorporates data from a variety of site-directed mutagenesis studies to improve/adjust the alignment. A limited amount of specific information about this model is indicated [68].

CYP2C9	101	Complete CYP model. Site-directed mutagenesis data used to improve the multialignment of the 2-family [13].
CYP2C9	101/102/107A/108	Complete CYP models [112].
CYP2C9/2C18/ 2C19	101/102/107A/108	Complete CYP models [113].
CYP2C9/2C19	102	Complete CYP models [90,91].
CYP2D1/2D6	102	Complete CYP models. Incorporates data from a variety of site-directed mutagenesis studies to improve/adjust the alignment. A limited amount of specific information about this model is indicated [68].
CYP2D6	101	Preliminary CYP model, containing only active site regions of the protein (11 segments). Indicated Asp <sup>301</sup> as an important amino acid for catalytic activity [32].
CYP2D6	101/102/108	A set of 13 complete CYP models. Uses structural alignment method, multiple alignment (16 CYP sequences), and NMR-derived distance restraints [45].
CYP2D6	101/102/108	Semicomplete CYP model containing active site region and well-conserved regions (three segments, only highly variable loops omitted). Uses structural alignment method and multiple alignment (66 CYP sequences). Incorporates data from site-directed mutagenesis results concerning the 2-family to improve/adjust the alignment [31].
CYP2D6	102	Complete CYP model. Incorporates data of allelic variants and site-directed mutagenesis studies [114].
CYP2D6	101/102/107A/108	Complete CYP models [63,64].
CYP2D6	101/102/108	Complete CYP model including 51 docked substrates [35,36].
CYP2D6	101/102/107A/108	Complete CYP model. Comparison with CYP1A2 and CYP3A4 [83].
CYP2E1	102	Complete CYP model. Includes data of species differences between rat, mouse, and man [115,116].
CYP3A4 (CYP <sub>NF</sub> )	101	Complete CYP model. Only partially geometry optimized [117].
CYP3A4	102	Complete CYP model [129].
CYP3A4	101/102/107A/108	Complete CYP model [61,62].
CYP3A4	101/102/107A/108	Complete CYP model. Comparison with CYP1A2 and CYP2D6 [83].
CYP4A1/4A4/ 4A11	102	Complete CYP model. Incorporates data from a variety of site-directed mutagenesis studies to improve/adjust the alignment [118].



**Table 1** Continued

Enzyme model	Template CYP(s)	Specification <sup>a</sup> and reference(s)
CYP4A11	102	Complete CYP model [119].
CYP5 (TXAS)	101 or 102	Complete CYP models. Comparisons of models derived from CYP101 or CYP102 [60].
CYP11A (CYP <sub>SCC</sub> )	101	Complete CYP model [120].
CYP17 (CYP <sub>17α</sub> )	101	Complete CYP model [84].
CYP17 (CYP <sub>17α</sub> )	101	Complete CYP model [66].
CYP17 (CYP <sub>17α</sub> )	101 or 102	Complete CYP models. Comparisons of models derived from CYP101 or CYP102 [121].
CYP17 (CYP <sub>17α</sub> )	101	Complete CYP model [122].
CYP19 (CYP <sub>arom</sub> )	101	Partial CYP model containing only heme region and I-helix [65].
CYP19 (CYP <sub>arom</sub> )	101	Complete CYP model. Little specific information about this model is indicated [102].
CYP19 (CYP <sub>arom</sub> )	101	Complete CYP model [84].
CYP19 (CYP <sub>arom</sub> )	101/102/108	Semicomplete CYP model [56].
CYP19 (CYP <sub>arom</sub> )	101/102/108	Partial CYP model containing heme moiety, I-helix, and C-terminus [123].
CYP19 (CYP <sub>arom</sub> )	101 or 102	Complete CYP models. Comparisons of models derived from CYP101 or CYP102 [88].
CYP51 (CYP <sub>14α</sub> )	101	Complete CYP model [49].
CYP51 (CYP <sub>14α</sub> )	101	Complete CYP model [124].
CYP51 (CYP <sub>14α</sub> )	102	Complete CYP model [125].
CYP105A1/B1 (CYPSU1/SU2)	101	Complete CYP models generated with different alignments [126].

<sup>a</sup> Complete CYP model = model constructed for complete enzyme, including regions with (very) low homology; partial CYP model = regions with low homology have been omitted; semicomplete/preliminary CYP model = regions with low homology, nonessential for catalytic activity, have been omitted.

<sup>b</sup> Specific isoenzyme not given.

CYP crystal structures and a variety of site-directed mutagenesis data (Table 1) will be discussed next: CYP2B1 [40], CYP2D6 [31], CYP3A4 [61,62], and CYP19 [56].

## 2. CYP2B1

CYP2B1 is one of the most active and versatile cytochromes CYP in the rat, which catalyzes the 16  $\beta$ -hydroxylation of androstenedione with a high degree of specificity [70]. A homology model for CYP2B1 was constructed using a consensus modeling method in which the coordinates of the model are weighted averages of the coordinates of the three crystal structures [40]. The alignment of the sequences of the three crystal structures was done using a structure-based alignment [9], in which positions of secondary structure elements were aligned based on a structural superposition rather than on primary amino acid sequences. Molecular mechanical and molecular dynamical techniques were used to optimize the protein model [40]. The substrates androstenedione and progesterone were docked into the active site area of the protein model, and all site-directed mutagenesis data available for CYP2B1 could be explained by this model, in contrast to previous homology models constructed based on CYP101 alone [67]. This indicates the superiority of homology models that use all available crystal structures and combine these with site-directed mutagenesis experiments or other protein biochemistry data, relative to models constructed solely from the crystal structure of CYP101. A stereo view of androstenedione docked into the active site of the homology model for CYP2B1 [40] is shown in Figure 9.

The active site could be distinguished in an upper part containing residues Ile114 and Ile290 (not shown in Fig. 9) and a lower part with residues Gly478 and Ile480, which were shown to be important for activity [70–76]. These two groups of residues could not interact with the substrate androstenedione simultaneously when it is docked in a 16 $\alpha$ - or 16 $\beta$ -binding orientation. The key amino acids indicated by site-directed mutagenesis experiments were changed in the model, after which androstenedione was docked into the mutant protein model in 16 $\alpha$ -, 16 $\beta$ -, and 15 $\alpha$ -binding orientations, thereby confirming key roles of residues Ile114, Phe206, Ile290, Thr302, Val363, and Gly478, in agreement with site-directed mutagenesis data [70–76] and with the previously derived homology model for CYP2B1 [67]. Other complete models of CYP2B1 based on CYP102 have also been described [77,78]. Recently, the first protein homology models of CYP2B1, 2B4, and 2B5 based on the new crystal structure of mammalian CYP2C5 [132/133] have been published [60]. This molecular modeling and mutagenesis study has revealed a molecular basis for difference in inhibition of CYP2B1, 2B4, and 2B5 by 4-phenylimidazole showing the importance of residues Ile114, Ser294, Ile363, and Val367 in the active site of CYP2B1 (Fig. 9) [60].

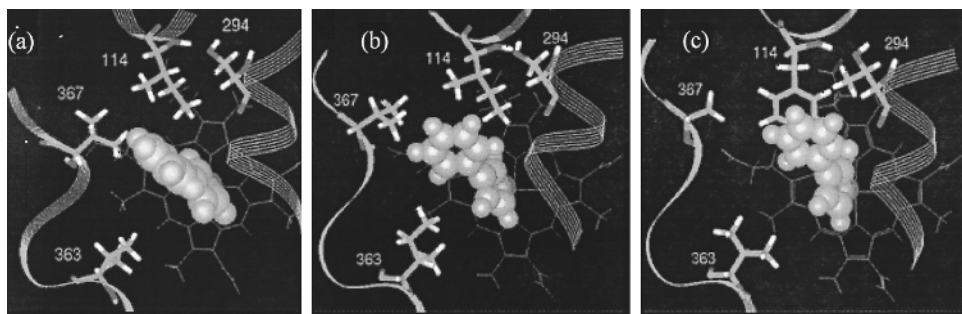


**Figure 9** Cytochrome P450 homology models of CYP2B1 (a), CYP2B4 (b) and CYP2B5 (c) based on the recently published crystal structure of mammalian CYP2C5 [132,133]. Together with results from mutation studies, the homology models reveal that amino acids 114, 294, 363, and 367 in the active sites of the CYP2B enzymes are responsible for observed differences in inhibition constants of 4-phenylimidazole. The view is perpendicular to the heme group shown as “lines,” 4-phenylimidazole is shown as “ball-and-stick” with the dark gray nitrogen atom close to the heme iron. (From Ref. 60.)

### 3. CYP2C8, 9, 18, and 19

Characteristic substrates of the CYP2C subfamily are anions or polar hydrogen-bond-accepting substrates of a variety of shapes and sizes. Among these are warfarin, phenytoin, tolbutamide, and thienilic acid [131]. Substrate binding to P450 2C isoenzymes is believed to involve hydrogen and ion-pair interactions with a significant selectivity for substrate recognition between the various 2C-isoenzymes. Recently, 3D-homology models of CYP2C9 [112], 2C18, and 2C19 [113] were built, assessed, and used to explain substrate selectivities. Unconstrained molecular dynamics (MD) simulations were used to test the stability of the protein models and to calculate sites of hydroxylation in the 2C-substrates.

### 4. CYP2D6

A homology model was recently constructed for human CYP2D6, a polymorphic member of the CYP superfamily absent in 5–9% of the Caucasian population [22,23,79]. First, the sequences of the crystal structures of the bacterial CYP101, CYP102, and CYP108 isoenzymes were structurally aligned [31] using a method similar to that described by Hasemann et al. [9]. Then a multialignment for 66 members of the CYP2-family was constructed [31], which facilitated the alignment of CYP2D6 with the structural alignment of the three crystal structures. This multialignment also enabled the use of site-directed mutagenesis data of

other members of the CYP2 family to improve the alignment between CYP2D6 and the structural alignment of the sequences of the three crystal structures [31]. Molecular mechanical calculations were used to optimize the constructed homology model [31]. The active site consisted of the heme moiety, the F-, I-, and K-helices, the loop between helices B and B', the loop between the B' and the C-helix, and  $\beta$ -sheets 3 and 5. Three known substrates (debrisoquine, dextromethorphan, and GBR 12909) and one inhibitor (ajmalicine) were docked into the active site of the CYP2D6 model [31], indicating the protein model to be able to accommodate large substrates, which extended considerably the boundaries of the previously derived pharmacophore model for CYP2D6 [11,14] described in a previous section.

The orientation of the substrates relative to each other when docked into the active site, the position of the heme moiety, and the position of the I-helix containing Asp301 (an amino acid proposed [32] and shown [33] to be crucial for the catalytic activity of CYP2D6) were used to improve the previously described pharmacophore model for CYP2D6 substrates (see Figs. 5c [11] and 5d [10]). The two amino acids in CYP2D6 for which site-directed mutagenesis data is available, namely, Asp301 [33] and Val374 [80,81], were indeed part of the active site of the derived protein model [31]. Asp301 is an especially important residue for catalytic activity because it forms a hydrogen bond with the basic nitrogen atom present in the substrates of CYP2D6 (as indicated earlier). Because no further site-directed mutagenesis data is available for CYP2D6 as yet, no validation could be given of the importance of other amino acids in the active site of CYP2D6 indicated by the model. The homology model indicated a region of the active site to be a hydrophobic envelope in which only planar substrates could be accommodated, in close agreement with previously derived pharmacophore for CYP2D6 [10,11,27,29,82]. Recently, 51 substrates were docked and evaluated in a refined model of CYP2D6 explaining 72 metabolic pathways catalyzed by CYP2D6. It appeared that this model could predict correctly six out of eight metabolites observed in a "test set" of seven compounds [30,35,36]. A comparable complete CYP2D6 model was recently published together with models of CYP1A2 and CYP3A4 based on four bacterial crystal structures [83]. In total, 14 CYP2D6 substrates and four nonspecific substrates known to be metabolized by CYP2D6 were successfully docked into the active site. It was found that almost all substrates have important VDW interactions with Val370, Phe483, and Leu484 in the active site, whereas Asp301 is always involved in charge-reinforced hydrogen bonds with the protonated nitrogen atom of the substrates. This chapter also gives a suggestion for membrane attachment of mammalian CYPs 1A2, 2D6, and 3A4 [83] (Fig. 10).

One of several successful applications of substrate and protein modeling in the case of CYP2D6 was recently reported, i.e., the design, and subsequent synthe-

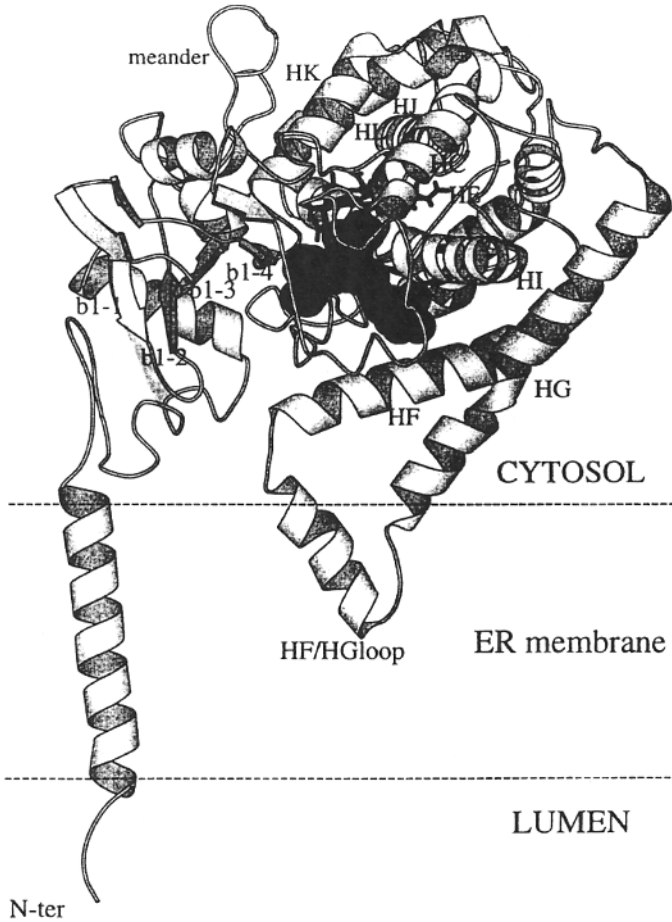


**Figure 10** Sketch of the CYP2D6 model after De Rienzo et al. [83]. Labels indicate some of the relevant protein regions. The heme group is represented as a black-capped stick model. The gray spheres indicate the active site cavity. A hypothetical membrane topology is presented showing the N-terminal helix and the HF/HG loop in contact with the hydrophobic membrane environment. (From Ref. 83.)

sis and experimental validation of 7-methoxy-4-(aminomethyl)coumarin as a novel and very selective substrate for high-throughput screening purposes (MAMC, Fig. 11) [127]. In line with computational predictions using the substrate and protein models of CYP2D6, the affinity of MAMC was very high for CYP2D6 when compared to nine other human CYPs; moreover, the metabolic

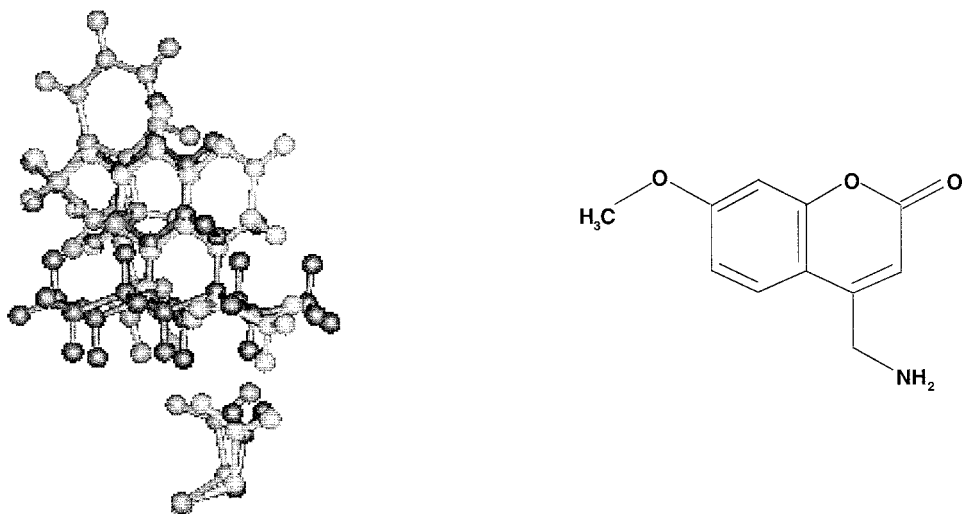


**Figure 11** Substrate and protein modeling in the case of CYP2D6 has led to the design of 7-methoxy-4-(aminomethyl)-coumarin (MAMC, right). MAMC has been superimposed on debrisoquine and dextromethorphan (left). (From Ref. 127.)

product, anticipated from the computer models, was fluorescent, thus making metabolic assays and drug–drug interaction assays feasible in a microplate reader setup.

## 5. CYP3A4

Cytochrome P450 enzymes of the CYP3 family are associated with the metabolism of a large variety of structurally diverse chemicals with considerable variations in molecular size, ranging from steroids like testosterone (MW = 288) and progesterone (MW = 314), carcinogens like aflatoxin B<sub>1</sub> (MW = 312), and drugs like nifedipine (MW = 346) to large antibiotics like erythromycin (MW = 734) and cyclosporin A (MW = 1202). Therefore, the CYP3A4 binding site is considered to be relatively large and open in order to accommodate such large substrates. A first molecular model of the CYP3A4 was built by Ferenczy et al. shortly after the first crystal structure of bacterial CYP101 (P450<sub>cam</sub>) [117,30], describing the modeled orientations of nifedipine, testosterone, quinidine, and *S*-benzphetamine within the binding site. Another CYP3A4 model was built later based on the crystal structure of CYP102 (P450<sub>BM3</sub>), being a class II cytochrome P450 [129]. In this 3A4 model, the heme pocket is also characterized by a relatively large and open substrate-binding site. A ‘palisade’ of aromatic residues (Phe 181,

Phe 263, and Tyr 266) reside on one side of the pocket, allowing the binding of relatively planar molecules, such as aflatoxin B<sub>1</sub> and benz(a)pyrenes. As more crystal structures of CYP appeared, a consensus homology modeling strategy was used by Sklarz and Halpert and recently by De Rienzo et al. to build CYP3A4 using the coordinates of four bacterial CYPs: CYP101, CYP102, CYP107, and CYP108 [61,62,83]. According to the authors, especially the inclusion of CYP107 (P450<sub>crIF</sub>) as a template resulted in a structure of the B'-helix that provided an enlarged 3A4 active site that enables the enzyme to accommodate large substrates such as erythromycin. From these studies, several active site residues are indicated to be interesting for site-directed mutagenesis studies [61,62,83].

## 6. CYP19

CYP19 (CYP aromatase) catalyzes the conversion of C19 steroids to estrogens. A model for CYP19 [56] was constructed using the core structure of the three crystallized bacteria CYPs using a structure-based alignment [9] based on a combination of previously reported alignments from Hasemann et al. [53] and Ravichandran et al. [8]. Molecular mechanics and molecular dynamics were used to optimize the homology model [56]. The active site was formed by the heme moiety, the loop between helices B' and C, the I-helix, and  $\beta$ -sheets 1 and 4 [56]. The loop between helices B and B' was not in the active site of this homology model [56], in contrast with an earlier homology model for CYP19 [84] based solely on CYP101 and in contrast with the homology model for CYP2D6 [31] based on the crystal structures of CYP101, CYP102, and CYP108, as described earlier. Two enantiomers of vorozole, a known inhibitor of CYP19, were docked into the active site of the protein model, explaining experimentally observed results [56], like the necessity for a kink in the I-helix, which can be accomplished by either a proline residue or two glycine residues. Residues indicated by site-directed mutagenesis experiments to be important for catalytic activity, i.e., Glu302 [65], Asp309 [85,86], Thr310 [85,86], and Ile474 [87], were indeed part of the active site [56]. Regions important for binding of CYP19 and its redox partner were also predicted, indicating that CYP19 cannot be classified as a class I or a class II CYP, but is an intermediate CYP type [56]. Two other complete models of CYP19 based on CYP101 and CYP102, respectively, have also been constructed [88]. Three steroidal inhibitors, four nonsteroidal inhibitors, and two flavone phytoestrogens were docked into the active sites. In this case, the authors preferred to evaluate the results based on the CYP101 template, where the F- and G-helices have more important contributions to the structure of the active site [88].

## G. Summary

All homology models of mammalian CYPs based on crystal structures presently available indicate certain regions in the CYP isoenzymes that can be modeled

with relative ease and high accuracy (e.g., the oxygen-binding domain near the heme, the helices D, E, I, and L, and some  $\beta$ -sheets) [31,40,56], and certain regions in which the models are less reliable due to large differences between the available bacterial CYP crystal structures in these four regions (e.g., the B'-helix, the loops between the C- and D-helices, the region spanning the F- and G-helices, and some parts of the  $\beta$ -sheets) [31,40,56].

Generally, very useful information concerning amino acids important for substrate and/or inhibitor binding can be obtained using homology models, although due to the relative low homology in the substrate/inhibitor binding site region between the various CYPs, these predictions should always be considered carefully and verified experimentally. Homology models can therefore be very useful to guide site-directed mutagenesis or site-specific modification experiments, but they cannot completely replace them. Concerning amino acids responsible for the catalytic activity of a certain CYP, homology models can merely be used to verify whether the observed differences can be rationalized using the modeled structure, because kinetic information on catalytic activities can as yet not be obtained from theoretical interaction studies.

## V. COMPUTATIONAL PREDICTION OF TOXICITY

Out of almost 2 million substances registered in the *Chemical Abstracts*, only 5000 are included in the Royal Society of Chemistry's *Dictionary of Substances and Their Effects* [89]. DOSE contains data on metabolism and pharmacokinetics, acute and subacute and long-term toxicity, carcinogenicity, teratogenicity, and reproductive effects, etc. Therefore, and because it is generally felt that toxicological animal tests have to be replaced by fast, reliable and cheaper approaches predicting toxic effects, several toxicological endpoints have been described using so-called computational predictive toxicology (CPT) methods. Chemical carcinogenesis has been the main focus in this regard. The available CPT techniques range from statistical modeling techniques to methods based on mechanistic knowledge derived from a wide range of sources.

### A. Selected Computational Predictive Toxicology Methods

A Computer-Optimized Molecular Parametric Analysis of Chemical Toxicity (COMPACT) program has been developed at the School of Biological Sciences of the University of Surrey (Table 2). COMPACT predictions of toxicity are based on mechanisms of activation and on induction of cytochrome CYP1A and 2E, resulting in mutagens and reactive oxygen species that can initiate and promote tumors. The approach is based on relatively simple computer-calculated molecular descriptors such as:  $\text{area/dept}^2$ , collision diameter,  $\Delta E$



**Table 2** COMPACT Flowchart

- 
1. Construct molecule
  2. Minimize geometry
  3. Measure molecular geometry
  4. Calculate electronic structure
  5. Compare molecular parameters with training set (2D or 3D)
  6. Predict CYP isoenzyme selectivity
  7. Predict potential toxicity
- 

Source: Adapted from Ref. 92.

(LUMO-HOMO), and  $\log P$ . Cluster analysis on these descriptors, for a 100-compound training set, yielded structural requirements for active compounds. Criteria for CYP1A, 2B, 2E substrates and inducers have been described by COMPACT. Results obtained with COMPACT have been combined with *HazardExpert* predictions to improve the predictability by including metabolism [90–92].

The authors relate CYP selectivity to potential toxicity mechanisms: CYP1A, strong evidence of toxicity (reactive intermediates); CYP2E, suspected toxicity (oxygen radicals); CYP3A, possible weak toxicity; CYP4A, likely rodent toxicity (peroxisome proliferation); and CYP2B, low level of toxicity. A rigid evaluation of the predictive value of COMPACT is still missing, however.

The Computer Automated Structure Evaluation (CASE) program was developed by Klopman et al. in early 1980 at Case Western University in Cleveland, based on methods developed by Cramer et al. and Hodes et al. [93–95]. It uses topological descriptors found statistically relevant to correlate with toxicological properties. Substructural fragments derived from training sets are used to describe toxicological properties or to predict such properties for compounds outside the training sets. A quantitative form of CASE, in which the toxicity of compounds was provided in CASE units on a continuous scale, was presented in 1985. Preselected descriptors were evaluated in a linear regression analysis to produce QSARs. In later versions of CASE, calculated  $\log P$  and  $(\log P)^2$  as well as (imported) quantum mechanical molecular parameters were used to derive QSARs. In the early 1990s, CASE was superseded by MultiCASE, which contains CASE as an option and handles databases in a hierarchical way. MultiCASE uses the concepts of biophores and modulators and breaks up training sets into subsets closer to premises used by a chemist than CASE does [95]. With the introduction of MultiCASE, the *cis*-/*trans*-geometry of fragments, fragment environments, and expanded and composite fragments were introduced [95]. An example describing the mutagenicity of pyrene is given in Figure 12. CASE and

C2CC2DD2C/D2DD2C/D2DC/2DD2D/

PYR

FORMULA

1 2 3 4 5 6 7 9 10 11 12 13 14 15 16

-----  
 C )  
 )  
 =C )  
 -C )  
 =CH-CH=C -CH=CH-CH=C -CH=CH-C =CH-CH=CH

Experimental Activity = 10

94 % chances of being ACTIVE due to substructure (Conf.level= 99%) :

C . =CH -CH =C . -CH =CH -CH =C . -

78 % chances of being INACTIVE due to substructure (Conf.level= 97%) :

CH =CH -C . =CH -CH =C . -CH =CH -

\*\*\* OVERALL probability of being a MUTAGEN. is 57.0% \*\*\*

\*\* HOWEVER, QSAR predicts the activity to be NEGLIGIBLE \*\*

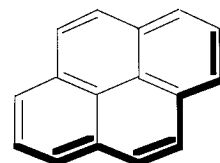
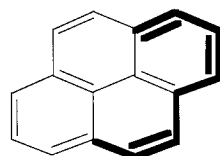


**Figure 12** CASE prediction for mutagenicity of pyrene showing activating (right, top) and deactivating (right, bottom) fragments. (Redrawn from Ref. 128.)

MultiCASE have been compared as to their ability to predict carcinogenicity when trained on the same database.

The Toxicology Prediction by Komputer Assisted Technology (TOPKAT) program was initially developed by Health Design Inc. [96] and later taken over by Oxford Molecular Group Inc. TOPKAT utilizes QSTR methodology for assessing specific adverse health effects, e.g., rodent carcinogenicity, Ames mutagenicity, developmental toxicity, skin sensitization, daphnia magna EC50s. The program computes probable toxic effects of chemicals solely from their chemical structure. The data (chemical structure, CAS numbers, experimental toxicity values, reference citations) used to develop the models has been accumulated, evaluated, and standardized by statisticians, toxicologists, computational chemists, and computer programmers specializing in QSTR/QSARs. The descriptors used in TOPKAT models quantify the electronic (E-states), shape (14 indices per molecule), and symmetry (7 indices per molecule) attributes of a molecular structure. TOPKAT computes probability values for the toxicity of a chemical using a linear QSTR equation. TOPKAT does not consider inorganic compounds, organometallic compounds, or mixtures of compounds. TOPKAT has been implemented with the TSAR QSAR package from Oxford Molecular enabling a general toxicity estimate with QSARs. A typical TOPKAT prediction for lidocaine is presented in Figure 13 [96].

All Validation Criteria Satisfied.

Computed Chronic LOAEL = 6.5 mg/kg

95% Confidence Limits: 879.5 ng/kg and 47.4 mg/kg

Chronic LOAEL (Single Benzene) Model

	Product
Constant Term	3.601
Symmetry Index #4 - Ratio # of Classes to # of C and H Ats	-0.251
Specific E-State Of [ *CH2* ] * [ Aliphatic H ]	1.345
Specific E-State Of [ -CH2- ] - [ =C< ]	-0.405
Average E-State Of [ Aliphatic C ] * [ Aliphatic O ]	-0.550
E-State Of [ -CH3 ] * [ Aromatic C ]	0.570
E-State Of [ *C(=)* ] * [ Aliphatic N ]	0.341
E-State Of [ Aromatic C ] : [ :c(*) : ]	-0.541
E-State Of [ :cH : ] : [ :c(-) : ]	0.449
Computed Chronic LOAEL, Log (1/Moles)	4.560

Lidocaine

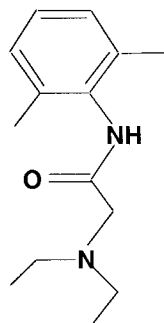


**Figure 13** TOPKAT prediction sheet of the rat oral LOAEL for lidocaine. (Redrawn from Ref. 96.)

The Deductive Estimation of Risk from Existing Knowledge (DEREK) system was initially developed by Sanderson and Earnshaw [97] and was based on the LHASA synthesis-planning program developed by Corey's group at Harvard University. DEREK is interactive and rule based. The rule starts with references to toxicophores, and the second part of the rule concerns a "computational" description of rule. The DEREK rule base can be separated into three subsets of rules describing several toxicological endpoints.

*HazardExpert* (HEX) is another program, by CompuDrug initially developed in 1987 as "a model of chemical toxicity in a compartmentalized system" and to predict toxicity of chemicals. Originally, a knowledge base collected by the EPA was used to predict several classes of toxicity, including oncogenicity, mutagenicity, and neurotoxicity, in various biosystems, e.g., including mammals, fish, and plants. The knowledge base has been further developed based on lists of toxic fragments reported by more than 20 leading experts. The values used by HEX can be set by the user to create additional biosystems and rules [92]. To predict toxicity, HEX uses an active fragment approach. CompuDrug meanwhile developed other expert systems, notably *MetaboloExpert* and *Prolog P*, to predict metabolites and log *P* values, respectively. Initially, these programs were based

on artificial intelligence languages. But more recently, HEX was combined with neural network technology to form a “hybrid” system. Rigid validation tests of HEX have not yet been reported, although recently 456 compounds have been pulled through HEX evaluation using experimental carcinogenicity data taken from an IARC database. Although HEX has been presented as a quantitative form of DEREK, its toxicity predictions are semiquantitative, predicting one of five concern levels.

Very recently, SciVision offered a comprehensive toxicological information system, TOXSYS. TOXSYS contains a wealth of toxicological information on over 230,000 compounds. It also uses neural net analysis to predict potential toxicity of compounds. Because of its size and potential applicability TOXSYS is worthwhile mentioning here, although the experience with this program in toxicological research is minimal so far ([www.scivision.com](http://www.scivision.com)).

## **B. Comparison of Different Computational Predictive Toxicology Methods**

The most well-known methods presently available make use of some sort of a noncongenericity correction and can then roughly be divided into two groups, i.e., rule-based and correlative methods. In Table 3, a comparative description of the CPT methods briefly discussed is presented. The CASE/MultiCASE and TOPKAT methods are both based on correlative models. The CASE and MultiCASE programs are developed as data-mining systems to find (new) SARs. MultiCASE is particularly useful as a discovery tool, while TOPKAT is more aimed at validated assessments of toxicity [96]. The philosophy of the ADAPT system is more closely related to that of CASE/MultiCASE than to TOPKAT and is using standard techniques with descriptors that can also be applied to predict properties other than toxicity, such as retention times on a column [98–100].

DEREK, HazardExpert, and OncoLogic [101] are all rule-based systems, but their specific background as well as their applicability differ. DEREK and HazardExpert are semiquantitative, and no further description of the supposed toxicity mechanism is needed. DEREK and HazardExpert include rules on several toxicological endpoints, while OncoLogic [101] just describes carcinogenicity.

Ideally, the goals for CPT methods should be: (1) to generate with a known reliability or confidence limit, (2) to be applicable to all types of potentially toxic agents (including organic, inorganic, polymeric compounds, minerals, and mixtures, and (3) to accelerate the performance of risk assessment and the experimental toxicity-assessment programs. As yet there is no ideal CPT method available, however. Moreover, a solid evaluation and validation of the various CPT methods

**Table 3** Brief Description of Some Computational Predictive Toxicology (CPT) Methods

Name	Modeling type	Method	Ref.
CASE MultiCASE	Derives (Q)SARs via fragment-based automatic data mining; previously derived models can be used for predictions	Correlative	95
TOPKAT	Uses topologically based (Q)SARs derived by expert guided data mining	Correlative	96
ADAPT	Uses fragment-based human guided pattern-recognition modeling tools	Correlative	98–100
DEREK	Expert system based on (bioactivating) toxicophores	Rule based	97
Oncologic	Expert system utilizing a wide range of user-provided compound properties	Rule based	101
HazardExpert	Expert system using positive and negative conditions/toxicophores supported by metabolism data and calculated log <i>P</i> , pKa, and log <i>D</i> values	Rule based	92
COMPACT	Expert-derived SARs of toxicities mediated by cytochrome P450 metabolism.	Correlative + rule based	90
TOXSYS	Toxicological information system with neural net analysis to predict toxicity	Correlative	

is not yet available. Negative predictions are neither appropriately evaluated nor validated at this moment, mainly because of lack of knowledge in general or of knowledge on negative indicators of toxicity. As long as this is the case, CPT methods will not become a major tool in decision-making processes in drug discovery or environmental risk assessment. The current status of the various CPT methods seems to divide investigators into believers and nonbelievers, as can be derived from several reports in the literature.

## VI. CONCLUSIONS

A number of pharmacophore models have been derived for CYPs, based either on suitable template molecules or on a variety of substrates or inhibitors when a single compound was inappropriate as a template molecule. Several of these pharmacophore models have been shown to have a good predictive value concerning metabolism and substrate/inhibitor selectivity, a property especially rele-

vant for isoenzymes that are subject to genetic polymorphisms (e.g., CYP2D6 [10,11,25]). Despite the potential benefits (especially for the chemical and pharmaceutical industry), the development of small molecule (pharmacophore) models for biotransformation enzymes has received relatively little attention so far, in contrast to pharmacophore models for receptor ligands.

The homology models for CYPs indicate that certain regions in the proteins can be modeled with relative ease and high accuracy (e.g., the oxygen-binding domain near the heme, the helices D, E, I, and L, and some  $\beta$ -sheets [31,34,40,56]), while in certain other regions the homology models are less reliable due to large differences between available crystal structures and the modeled CYPs (e.g., the B'-helix, the loops between the C- and D-helices, the region spanning the F- and G-helices, and some parts of the  $\beta$ -sheets [31,34,40,56]). The topology of homology models is generally prejudiced by the template crystal structure. However, due to crystal-packing effects, the crystal structure conformation might differ from the conformation of the protein in solvent. For this reason additional information from three-dimensional NMR techniques would be useful to supplement the crystal structures.

Generally, useful information concerning amino acids important for substrate and/or inhibitor binding can be obtained using homology models, although due to the relatively low homology in the case of CYPs in the substrate binding site region these predictions have to be considered carefully and should be verified experimentally. Homology models can be used to guide site-directed mutagenesis and site-specific modification experiments, but cannot completely replace them. As for the role of amino acids in the catalytic activity of a certain CYP, homology models can merely be used to verify whether the observed differences can be rationalized using the modeled structure, since information on catalytic activities cannot be obtained from these theoretical interaction studies. Cautious indications of substrate selectivity can be given in specific cases, although these predictions also have to be considered carefully and verified experimentally.

For the purpose of computational predictions of toxicity, there are multiple computer programs as well. Ideal programs, i.e., generating predictions with a high reliability, possessing a broad applicability, and really accelerating the risk assessment programs, however, are not available yet. Comparison of programs and validation (including sufficient negative predictions) are still missing as well. As long as this is the case, CPT methods will probably not become a major tool in drug discovery and risk assessment processes. Generally speaking, it may be concluded that computational approaches (often named *in silico* or *in computro* approaches as well), parallel to high(er)-throughput experimental technologies, are gradually becoming one of the newer and faster-developing approaches in drug metabolism, drug discovery, and toxicology. When new links with other recent developments, such as in neural network computing, genomics, pro-

teomics, and bioinformatics, can be created, *in silico* methods to predict drug metabolism and toxicity are likely to be of great scientific and practical utility.

## REFERENCES

1. EM van der Aar, KT Tan, JNM Commandeur, NPE Vermeulen. Strategies to characterize the mechanisms of action and the active sites of glutathione *S*-transferases. *Drug Metab Rev* 1998, 30(3), 569–643.
2. DR Nelson, T Kamataki, DJ Waxman, FP Guengerich, RW Estabrook, R Feyereisen, FJ Gonzalez, MJ Coon, IC Gunsalus, O Gotoh, K Okuda, DW Nebert. The P450 superfamily—update on new sequences, gene-mapping, accession numbers, early trivial names of enzymes, and nomenclature. *DNA Cell Biol* 1993, 12, 1–51.
3. NPE Vermeulen. Role of metabolism in chemical toxicity. In: C Ioannides, ed. *Cytochromes P450: Metabolic and Toxicological Aspects*. CRC Press, Boca Raton, FL, 1996, pp. 29–53.
4. S Graham-Lorence, JA Peterson. P450s: structural similarities and functional differences. *FASEB J* 1996, 10, 206–214.
5. FP Guengerich. Reactions and significance of cytochrome P-450 enzymes. *J Biol Chem* 1991, 266, 10019–10022.
6. AR Goeptar, H Scheerens, NPE Vermeulen. Oxygen and xenobiotic reductase activities of cytochrome P450. *Crit Rev Toxicol* 1995, 25, 25–65.
7. B Testa. In: *The Metabolism of Drugs and Other Xenobiotics—Biochemistry of Redox Reactions*. Academic Press, London, 1995, pp. 215–235.
8. KG Ravichandran, SS Boddupalli, CA Hasemann, JA Peterson, J Deisenhofer. Crystal structure of hemoprotein domain of P450BM-3, a prototype for microsomal P450's. *Science* 1993, 261, 731–736.
9. CA Hasemann, RG Kurumbail, SS Boddupalli, JA Peterson, J Deisenhofer. Structure and function of cytochromes P450: a comparative analysis of three crystal structures. *Structure* 1995, 2, 41–62.
10. MJ de Groot, GJ Bijloo, BJ Martens, FAA van Acker, NPE Vermeulen. A refined substrate model for human Cytochrome P450 2D6. *Chem Res Toxicol* 1997, 10(1), 41–48.
11. LMH Koymans, NPE Vermeulen, SABE van Acker, JM te Koppele, JJP Heykants, K Lavrijsen, W Meuldermans, GM Donné-Op den Kelder. A predictive model for substrates of cytochrome P450-debrisoquine (2D6). *Chem Res Toxicol* 1992, 5, 211–219.
12. FH Allan, O Kennard. Integrate rD-search facilities for the Cambridge Structural Database (CSD). *Chemical Design Automation News* 1993, 8, 31–38.
13. KR Korzekwa, JP Jones. Predicting the cytochrome P450 mediated metabolism of xenobiotics. *Pharmacogenetics* 1993, 3, 1–18.
14. MJ de Groot, GM Donné-Op den Kelder, JNM Commandeur, JH van Lenthe, NPE Vermeulen. Metabolite predictions for para-substituted anisoles based on *ab initio* CASSCF-calculations. *Chem Res Toxicol* 1995, 8, 437–443.

15. MJ de Groot, EM van der Aar, PJ Nieuwenhuizen, RM van der Plas, GM Donné-Op den Kelder, JNM Commandeur, NPE Vermeulen. A predictive substrate model for rat glutathione *S*-transferase 4-4. *Chem Res Toxicol* 1995, 8, 649–658.
16. DM Jerina, DP Michaud, RJ Feldman, RN Armstrong, KP Vyas, DR Thakker, H Yagi, PE Thomas, DE Ryan, W Levin. In: R Sato, R Kato, eds. *Microsomes, drug oxidations, and drug toxicity*. Japan Scientific Societies Press, Tokyo, 1982, pp. 195–201.
17. FF Kadlubar, GJ Hammons. In: FP Guengerich, ed. *Mammalian cytochromes P450*. CRC Press, Boca Raton, FL, 1987, pp. 81–130.
18. SK Yang. Stereoselectivity of cytochrome P-450 isozymes and epoxide hydrolase in the metabolism of polycyclic aromatic hydrocarbons. *Biochem. Pharmacol* 1988, 37, 61–70.
19. LHM Koymans, GM Donné-Op den Kelder, JM te Koppele, NPE Vermeulen. Cytochromes P450: their active-site structure and mechanism of oxidation. *Drug Metab Rev* 1993, 25, 325–387.
20. DFV Lewis, C Ioannides, DV Parke. Molecular orbital studies of oxygen activation and mechanisms of cytochromes P-450-mediated oxidative metabolism of xenobiotics. *Chem-Biol Interact* 1989, 70, 263–280.
21. A Mancy, P Brotto, S Dijols, PM Dansette, D Mansuy. The substrate binding site of human liver cytochrome P450 2C9: an approach using designed tienilic acid derivatives and molecular modeling. *Biochemistry* 1995, 34, 10365–10375.
22. A Mahgoub, JR Idle, LG Dring, R Lancaster, RL Smit. Polymorphic hydroxylation of debrisoquine in man. *Lancet* 1977, 11, 584–586.
23. M Armstrong, K Fairbrother, JR Idle, AK Daly. The cytochrome P450 CYP2D6 allelic variant CYP2D6J and related polymorphisms in a European population. *Pharmacogenetics* 1994, 4, 73–81.
24. T Wolff, LM Distlerath, MT Worthington, JD Groopman, GJ Hammons, FF Kadlubar, RA Prough, MM Martin, FP Guengerich. Substrate specificity of human liver cytochrome P-450 debrisoquine 4-hydroxylase probed using immunochemical inhibition and chemical modeling. *Cancer Res* 1985, 45, 2116–2122.
25. GR Strobl, S von Kreudener S, J Stckigt, FP Guengerich, T Wolff. Development of a pharmacophore for inhibition of human liver cytochrome P-450 2D6: molecular modeling and inhibition studies. *J Med Chem* 1993, 36, 1136–1145.
26. R Raag, TL Poulos. Crystal structures of cytochrome P-450CAM complexed with camphane, thiocamphor, and adamantane: factors controlling P-450 substrate hydroxylation. *Biochemistry* 1991, 30, 2674–2684.
27. UA Meyer, J Gut, T Kronbach, C Skoda, UT Meier, T Catin, P Dayer. *Xenobiotica* 1986, 16, 449.
28. SA Islam, CR Wolf, MS Lennard, MJE Sternberg. *Carcinogenesis* 1991, 12, 2211.
29. TL Poulos, BC Finzel, AJ Howard. Crystal structure of substrate-free *Pseudomonas putida* cytochrome P-450. *Biochemistry* 1986, 25, 5314–5322.
30. TL Poulos, BC Finzel, IC Gunsalus, GC Wagner, J Kraut. The 2.6-Å crystal structure of *Pseudomonas putida* cytochrome P-450. *J Biol Chem* 1985, 260, 16122–16130.
31. MJ de Groot, NPE Vermeulen, JD Kramer, FAA van Acker, GM Donné-Op den



- Kelder. A three-dimensional protein model for human cytochrome P450 2D6 based on the crystal structures of P450 101, P450 102 and P450 108. *Chem Res Toxicol* 1996, 9(7), 1079–1091.
32. LMH Koymans, NPE Vermeulen, A Baarslag, GM Donné-Op den Kelder. A preliminary 3D-model for cytochrome P450 2D6 constructed by homology model building. *J Comp-Aided Mol Design* 1993, 7, 281–289.
  33. SW Ellis, GP Hayhurst, G Smith, T Lightfoot, MMS Wong, AP Simula, MJ Ackland, MJE Sternberg, MS Lennard, GT Tucker, CR Wolf. Evidence that aspartic acid 301 is a critical substrate-contact residue in the active site of cytochrome P450 2D6. *J Biol Chem* 1995, 270, 29055–29058.
  34. MJ de Groot, GJ Bijloo, FAA van Acker, C Fonseca Guerra, JG Snijders, NPE Vermeulen. Extension of a predictive substrate model for human cytochrome P450 2D6. *Xenobiotica* 1997, 27(4), 357–368.
  35. MJ de Groot, MJ Ackland, VA Horne, AA Alex, BC Jones. Novel approach to predicting P450-mediated drug metabolism: development of a combined protein and pharmacophore model for CYP2D6. *J Med Chem* 1999, 42(9), 1515–1524.
  36. MJ de Groot, MJ Ackland, VA Horne, AA Alex, BC Jones. A novel approach to predicting P450 mediated drug metabolism. CYP2D6 catalyzed *N*-dealkylation reactions and qualitative metabolite predictions using a combined protein and pharmacophore model for CYP2D6. *J Med Chem* 1999, 42(20), 4062–4070.
  37. SS Boddupalli, CA Hasemann, KG Ravichandran, JY Lu, EJ Goldsmit, J Deisenhofer JA Peterson, Crystallization and preliminary x-ray diffraction analysis of P450terp and the hemoprotein domain of P450BM-3, enzymes belonging to two distinct classes of the cytochrome P450 superfamily. *Proc Natl Acad Sci USA* 1992, 89, 5567–5571.
  38. TF Havel, MF Snow. A new method for building protein conformations from sequence alignments with homologues of known structure. *J Mol Biol* 1991, 217(1), 1–7.
  39. A Sali, TL Blundell. Comparative protein modelling by satisfaction of spatial restraints. *J Mol Biol* 1993, 234(3), 779–815.
  40. GD Szklarz, YA He, JR Halpert. Site-directed mutagenesis as a tool for molecular modeling of cytochrome P450 2B1. *Biochemistry* 1995, 34, 14312–14322.
  41. CA Ouzounis, WT Melvin. Primary and secondary structural patterns in eukaryotic cytochrome P-450 families correspond to structures of the helix-rich domain of *Pseudomonas putida* cytochrome P-450cam. Indications for a similar overall topology. *Eur J Biochem* 1991, 198, 307–315.
  42. BC Jones, G Hawksworth, VA Horne, A Newlands, MS Tute, DA Smith. Putative active site model for P4502C9 (tolbutamide hydroxylase). *Br J Clin Pharmacol* 1993, 34, P143–P144.
  43. BC Jones, G Hawkesworth, VA Horne, A Newlands, J Morsman, MS Tute, DA Smith. Putative active site template model for cytochrome P4502C9 (tolbutamide hydroxylase). *Drug Metab Dispos* 1996, 24, 260–266.
  44. PR Ortiz de Montellano. Arylhydrazines as probes of hemoprotein structure and function. *Biochimie* 1995, 77, 581–593.
  45. S Modi, MJ Paine, MJ Sutcliffe, LY Lian, WU Primrose, CR Wolf, GCK Roberts.

- A model for human cytochrome P450 2D6 based on homology modeling and NMR studies of substrate binding. *Biochemistry* 1996, 35, 4540–4550.
46. R Raag, TL Poulos. The structural basis for substrate-induced changes in redox potential and spin equilibrium in cytochrome P-450CAM. *Biochemistry* 1989, 28, 917–922.
  47. TL Poulos, AJ Howard. Crystal structures of metyrapone- and phenylimidazole-inhibited complexes of cytochrome P-450cam. *Biochemistry* 1987, 26, 8165–8174.
  48. R Raag, H Li, BC Jones, TL Poulos. Inhibitor-induced conformational change in cytochrome P-450CAM. *Biochemistry* 1993, 32, 4571–78.
  49. N Ishida, Y Aoyama, R Hatanaka, Y Oyama, S Imajo, M Ishigura, T Oshima, H Nakazato, T Noguchi, US Maitra, VP Mohan, DB Sprinson, Y Yoshida. A single amino acid substitution converts cytochrome P450(14DM) to an inactive form, cytochrome P450SG1: complete primary structures deduced from cloned DNAs. *Biochem Biophys Res Commun* 1988, 155, 317–323.
  50. HY Li, TL Poulos. Modeling protein–substrate interactions in the heme domain of cytochrome P450 (BM3). *Acta Crystallogr D-Biol Cryst* 1995, 51, 21–32.
  51. JR Cupp-Vickery, HY Li, TL Poulos. Preliminary crystallographic analysis of an enzyme involved in erythromycin biosynthesis: cytochrome P450eryF. *Protein-Struct Funct Genet* 1994, 20, 197–201.
  52. JR Cupp-Vickery, TL Poulos. Structure of cytochrome P450eryF involved in erythromycin biosynthesis. *Nature Struct Biol* 1995, 2, 144–153.
  53. CA Hasemann, KG Ravichandran, JA Peterson, J Deisenhofer. Crystal structure and refinement of cytochrome P450terp at 2.3-Å resolution. *J Mol Biol* 1994, 236, 1169–1185.
  54. SY Park, H Shimizu, S Adachi, Y Shiro, T Iizuka, A Nakagawa, I Tanaka, H Shoun, H Hori. Crystallization, preliminary diffraction and electron paramagnetic resonance studies of a single crystal of cytochrome P450nor. *FEBS Lett* 1997, 412(2), 346–350.
  55. KN Degtyarenko. Structural domains of P450-containing monooxygenase systems. *Protein Engineering* 1997, 8(8), 737–747.
  56. S Graham-Lorence, B Amarneh, RE White, JA Peterson, ER Simpson. A three-dimensional model of aromatase cytochrome P450. *Protein Sci* 1995, 4, 1065–1080.
  57. TL Poulos. Cytochrome P450. *Curr Opin Struct Biol* 1995, 5, 767–774.
  58. T Lightfoot, SW Ellis, J Mahling, MJ Ackland, FE Blaney, GJ Bijloo, MJ De Groot, NPE Vermeulen, GM Blackburn, MS Lennard, GT Tucker. Regioselective hydroxylation of debrisoquine by cytochrome P4502D6: implications for active site modeling. *Xenobiotica* 2000, 30, 219–233.
  59. LM Podust, TL Poulos, MR Waterman. Crystal structure of cytochrome P450 14 alpha-sterol demethylase (CYP51) from *Mycobacterium tuberculosis* in complex with azole inhibitors. *PNAS* 2001, 48, 3068–3073.
  60. M Spatzenegger, QM Wang, YQ He, MR Wester, EF Johnson, JR Halpert. Amino acid residues critical for differential inhibition of CYP2B4, CYP2B5, and CYP2B1 by phenylimidazoles. *Mol Pharm* 2001, 59, 475–484.
  61. GD Szklarz, JR Halpert. Molecular modeling of cytochrome P450 3A4. *J Computer Aided Mol Design* 1997, 11, 265–272.

62. GD Szklarz, JR Halpert. Use of homology modeling in conjunction with site-directed mutagenesis for analysis of structure-function relationships of mammalian cytochromes P450. *Life Sciences* 1997, 61(26), 2507–2520.
63. S Modi, DE Gilham, L-Y Sutcliffe, WU Primrose, CR Wolf, GCK Roberts. 1-methyl-4-phenyl-1,2,3,6-tetrahydropyridine as a substrate of cytochrome P450 2D6: allosteric effects of NADPH-cytochrome P450 reductase. *Biochemistry* 1997, 36, 4461–4470.
64. G Smith, S Modi, I Pilla, L-Y Lian, MJ Sutcliffe, MP Pritchard, T Friedberg, CK Roberts, CR Wolf. Determinants of the substrate specificity of human cytochrome P-450 CYP2D6: design and construction of a mutant with testosterone hydroxylase activity. *Biochem J* 1998, 331, 783–792.
65. S Graham-Lorence, MW Khalil, MC Lorence, CR Mendelson, ER Simpson. Structure-function relationships of human aromatase cytochrome P-450 using molecular modeling and site-directed mutagenesis. *J Biol Chem* 1991, 266, 11939–11946.
66. D Lin, LH Zhang, E Chiao, WL Miller. Modeling and mutagenesis of the active site of human P450c17. *Mol Endocrinol* 1994, 8, 392–402.
67. GD Szklarz, RL Ornstein, JP Halpert. Application of 3-dimensional homology modeling of cytochrome P450 2B1 for interpretation of site-directed mutagenesis results. *J Biomolec Struct Dynamics* 1994, 12, 61–78.
68. DFV Lewis. Three-dimensional models of human and other mammalian microsomal P450s constructed from an alignment with P450102 (P450bm3). *Xenobiotica* 1995, 25, 333–366.
69. DFV Lewis, BG Lake. Molecular modelling of members of the P4502A subfamily: application to studies of enzyme specificity. *Xenobiotica* 1995, 25, 585–598.
70. JR Halpert, Y He. Engineering of cytochrome P450 2B1 specificity. Conversion of an androgen 16-beta-hydroxylase to a 15-alpha-hydroxylase. *J Biol Chem* 1993, 268, 4453–4457.
71. T Aoyama, K Korzekwa, K Nagata, M Adesnik, A Reiss, DP Lapenson, J Gillette, HV Gelboin, DJ Waxman, F.J. Gonzalez. Sequence requirements for cytochrome P-450IIB1 catalytic activity. Alteration of the stereospecificity and regioselectivity of steroid hydroxylation by a simultaneous change of two hydrophobic amino acid residues to phenylalanine. *J Biol Chem* 1989, 264, 21327–21333.
72. KM Kedzie, CA Balfour, GY Escobar, SW Grimm, Y He, DJ Pepperl, JW Regan, JC Stevens, JR Halpert. Molecular basis for a functionally unique cytochrome P450IIB1 variant. *J Biol Chem* 1991, 266, 22515–22521.
73. YA He, CA Balfour, KM Kedzie, JR Halpert. Role of residue 478 as a determinant of the substrate specificity of cytochrome P450 2B1. *Biochemistry* 1992, 31, 9220–9226.
74. Y He, Z Luo, PA Klekotka, VL Burnett, JR Halpert. Structural determinants of cytochrome P450 2B1 specificity: evidence for five substrate recognition sites. *Biochemistry* 1994, 33, 4419–4424.
75. JA Hasler, GR Harlow, GD Szklarz, GH John, KM Kedzie, VL Burnett, YA He, LS Kaminsky, JR Halpert. Site-directed mutagenesis of putative substrate recognition sites in cytochrome P450 2B1: importance of amino acid residues 114, 290, and 363 for substrate specificity. *Mol Pharmacol* 1994, 46, 338–345.

76. YQ He, YA He, JR Halpert. *Escherichia coli* expression of site-directed mutants of cytochrome P450 2B1 from six substrate recognition sites: substrate specificity and inhibitor selectivity studies. *Chem Res Toxicol* 1995, 8, 574–579.
77. DFV Lewis, BG Lake. Molecular modelling of mammalian CYP2B isoforms and their interaction with substrates, inhibitors and redox partners. *Xenobiotica* 1997, 27(5), 443–478.
78. R Dai, MR Pincus, FK Friedman. Molecular modeling of cytochrome P450 2B1: mode of membrane insertion and substrate specificity. *J Protein Chem* 1998, 17(2), 121–129.
79. M Eichelbaum, N Spannbrucker, B Steincke, HJ Dengler. Defective *N*-oxidation of sparteine in man: a new pharmacogenetic defect. *Eur J Clin Pharmacol* 1979, 16, 183–187.
80. SW Ellis, K Rowland, JR Harlow, AP Simula, MS Lennard, HF Woods, GT Tucker, CR Wolf. Regioselective and enantioselective metabolism of metoprolol by 2 human cDNA-derived CYP 2D6 proteins. *Br J Pharmacol* 1994, 112, 124.
81. SW Ellis, K Rowland, MJ Ackland, E Rekka, AP Simula, MS Lennard, CR Wolf, GT Tucker. Influence of amino acid residue 374 of cytochrome P-450 2D6 (CYP2D6) on the regio- and enantio-selective metabolism of metoprolol. *Biochem J* 1996, 316, 647–654.
82. T Wolff, LM Distlerath, MT Worthington, FP Guengerich. Human liver debrisoquine 4-hydroxylase: test for specificity toward various monooxygenase substrates and model of the active site. *Arch Toxicol* 1987, 60, 89–90.
83. F de Rienzo, F Fanelli, MC Menziani, PG de Benedetti. Theoretical investigation of substrate specificity for cytochromes P450 IA2, P450 IID6 and P450 IIIA4. *J Comp-Aided Mol Design* 2000, 14(1), 93–116.
84. CA Laughton, MJ Zvelebil, S Neidle. A detailed molecular model for human aromatase. *J Steroid Biochem Mol Biol* 1993, 44, 399–407.
85. S Chen, D Zhou. Functional domains of aromatase cytochrome P450 inferred from comparative analyses of amino acid sequences and substantiated by site-directed mutagenesis experiments. *J Biol Chem* 1992, 267, 22587–22594.
86. B Amarneh, CJ Corbin, JA Peterson, ER Simpson, S Graham-Lorence. Functional domains of human aromatase cytochrome P450 characterized by linear alignment and site-directed mutagenesis. *Mol Endocrinol* 1993, 7, 1617–1624.
87. D Zhou, LL Cam, CA Laughton, KR Korzekwa, S Chen. Mutagenesis study at a postulated hydrophobic region near the active site of aromatase cytochrome P450. *J Biol Chem* 1994, 269, 19501–19508.
88. S Chen, YC Kao, CA Laughton. Binding characteristics of aromatase inhibitors and phytoestrogens to human aromatase. *J Steroid Biochem Mol Biol* 1997, 61(3–6), 107–115.
89. RSC. In: *The Dictionary of Substances and their Effects*. The Royal Society of Chemistry, Cambridge, UK, 1994.
90. DFV Lewis, C Ioannides, DV Parke. Further evaluation of COMPACT, the molecular orbital approach for the prospective safety evaluation of chemicals. *Mut Res* 1998, 412, 41–54.
91. DFV Lewis, M Dickins, RJ Weaver, PJ Eddershaw, PS Goldfarb, MH Tarbit. Molecular modelling of human CYP2C subfamily enzymes CYP2C9 and CYP2C19:

- rationalization of substrate specificity and site-directed mutagenesis experiments in the CYP2C subfamily. *Xenobiotica* 1998, 28(3), 235–268.
92. DFV Lewis. In: KB Lipkowitz, DB Boyd, eds. *Reviews in Computational Chemistry*. VCH, New York, 1992, p. 173.
  93. RD Cramer III, G Redl, CE Berkoff. Substructural analysis. A novel approach to the problem of drug design. *J Med Chem* 1974, 17, 533–535.
  94. L Hodes, GF Hazard, RI Geran, S Richman. A statistical-heuristic method for automated selection of drugs for screening. *J Med Chem* 1977, 20, 469–475.
  95. G Klopman. A hierarchical computer automated structure evaluate program 1. *Quant Struct Activ Rel* 1992, 11, 176–184.
  96. K Enslein. In: C Reiss, S Parvez, G Labbe, H Parvez, eds. *Advances in Molecular Toxicology VSP*, Zeist, The Netherlands, 1998, pp. 141–164.
  97. DM Sanderson, CG Earnshaw. Computer prediction of possible toxic action from chemical structure: the DEREK system. *Hum Exp Toxicol* 1993, 10, 261–273.
  98. PC Jurs, JT Chou, M Yuan. Computer-assisted structure–activity studies of chemical carcinogens. A heterogeneous data set. *J Med Chem* 1979, 22, 476–483.
  99. K Yuta, PC Jurs. Computer-assisted structure–activity studies of chemical carcinogens. Aromatic amines. *J Med Chem* 1981, 24, 241–251.
  100. AM Richard, JR Rabinowitz, MD Waters. Strategies for the use of computational SAR methods in assessing genotoxicity. *Mutation Res* 1989, 181–196.
  101. Y Woo, DY Lai, MF Argus, JC Arcos. Development of structure–activity relationship rules for predicting carcinogenic potential of chemicals. *Toxicol Lett* 1995, 79, 219–228.
  102. DFV Lewis, H Moereels. The sequence homologies of cytochromes P-450 and active-site geometries. *J Comp-Aided Design* 1992, 6, 235–252.
  103. MJ Zvelebil, CR Wolf, MJ Sternberg. A predicted three-dimensional structure of human cytochrome P450: implications for substrate specificity. *Protein Eng* 1991, 4, 271–282.
  104. DFV Lewis, C Ioannides, DV Parke. Molecular modelling of cytochrome CYP1A1: a putative access channel explains differences in induction potency between the isomers benzo(*a*)pyrene and benzo(*e*)pyrene, and 2- and 4-acetylaminofluorene. *Toxicol Lett* 1994, 71, 235–243.
  105. DFV Lewis, BG Lake. Molecular modelling of CYP1A subfamily members based on an alignment with CYP102: rationalization of CYP1A substrate specificity in terms of active site amino acid residues. *Xenobiotica* 1996, 26(7), 723–753.
  106. DFV Lewis, M Dickins, BG Lake, PJ Eddershaw, MH Tarbit, PS Goldfarb. Molecular modelling of the human cytochrome P450 isoform CYP2A6 and investigations of CYP2A substrate selectivity. *Toxicology* 1999, 133(1), 1–33.
  107. JJ Lozano, E Lopez de Brinas, NB Centeno, R Guigo, F Sanz. Three-dimensional modelling of human cytochrome P450 1A2 and its interaction with caffeine and MeIQ. *J Comp-Aided Mol Des* 1997, 11(4), 395–408.
  108. R Dai, S Zhai, X Wei, MR Pincus, RE Vestal, FK Friedman. Inhibition of human cytochrome P450 1A2 by flavones: a molecular modeling study. *J Protein Chem* 1998, 17(7), 643–650.
  109. DFV Lewis, BG Lake, SG George, M Dickins, PJ Eddershaw, MH Tarbit, AP Beresford, PS Goldfarb, FP Guengerich. Molecular modelling of human CYP2E1

- by homology with the CYP102 haemoprotein domain: investigation of the interactions of substrates and inhibitors within the putative active site of the human CYP2E1 isoform. *Toxicology* 1999, 139(1–2), 53–79.
110. YT Chang, OB Stiffelman, IA Vakser, GH Loew, A Bridges, L Waskell. Construction of a 3D model of cytochrome P450 2B4. *Protein Engineering* 1997, 10(2), 119–129.
  111. TL Domanski, KM Schultz, F Roussel, JC Stevens, JR Halpert. Structure–function analysis of human cytochrome P-450 2B6 using a novel substrate, site-directed mutagenesis, and molecular modeling. *J Pharmacol and Exper Ther* 1999, 290(3), 1141–1147.
  112. VA Payne, YT Chang, GH Loew. Homology modeling and substrate binding study of human CYP2C9 enzyme. *Proteins—Structure Function Genetics* 1999, 37(2), 176–190.
  113. VA Payne, YT Chang, GH Loew. Homology modeling and substrate binding study of human CYP2C18 and CYP2C19 enzymes. *Proteins—Structure Function Genetics* 1999, 37(2), 204–217.
  114. DFV Lewis, PJ Eddershaw, PS Goldfarb, MH Tarbit. Molecular modelling of cytochrome P4502D6 (CYP2D6) based on an alignment with CYP102: structural studies on specific CYP2D6 substrate metabolism. *Xenobiotica* 1997, 27(4), 319–339.
  115. DFV Lewis, MG Bird, DV Parke. Molecular modelling of CYP2E1 enzymes from rat, mouse and man: an explanation for species differences in butadiene metabolism and potential carcinogenicity, and rationalization of CYP2E substrate specificity. *Toxicology* 1997, 118, 93–113.
  116. DFV Lewis, MG Bird, M Dickins, BG Lake, PJ Eddershaw, MH Tarbit, PS Goldfarb. Molecular modelling of human CYP2E1 by homology with the CYP102 haemoprotein domain: investigation of the interactions of substrates and inhibitors within the putative active site of the human CYP2E1 isoform. *Xenobiotica* 2000, 30(1), 1–25.
  117. GG Ferenczy, GM Morris. The active site of cytochrome P-450 nifedipine oxidase: a model-building study. *J Mol Graphics* 1989, 7, 206–211.
  118. DFV Lewis, BG Lake. Molecular modelling of CYP4A subfamily members based on sequence homology with CYP102. *Xenobiotica* 1999, 29(8), 763–781.
  119. YT Chang, GH Loew. Homology modeling and substrate binding study of human CYP4A11 enzyme. *Proteins—Structure Function and Genetics* 1999, 34(3), 403–415.
  120. S Vijayakumar, JC Salerno. Molecular modeling of the 3-D structure of cytochrome P-450scc. *Biochim Biophys Acta* 1992, 1160, 281–286.
  121. DF Burke, CA Laughton, S Neidle. Homology modelling of the enzyme P450 17 alpha-hydroxylase/17,20-lyase—a target for prostate cancer chemotherapy—from the crystal structure of P450BM-3. *Anti-Cancer Drug Design* 1997, 12(2), 113–123.
  122. RJ Auchus. The use of computational chemistry in the study of sex steroid biosynthesis. *Endocrine Res* 1998, 24(3–4), 541–547.
  123. LM Koymans, H Moereels, H Vanden Bossche. A molecular model for the interaction between vorozole and other non-steroidal inhibitors and human cytochrome P450 19 (P450 aromatase). *J Steroid Biochem Mol Biol* 1995, 53, 191–197.

124. PE Boscott, GH Grant. Modeling cytochrome P450 14 alpha demethylase (*Candida albicans*) from P450cam. *J Mol Graphics* 1994, 12, 185–192.
125. DFV Lewis, A Wiseman, MH Tarbit. Molecular modelling of lanosterol 14 alpha-demethylase (CYP51) from *Saccharomyces cerevisiae* via homology with CYP102, a unique bacterial cytochrome P450 isoform: quantitative structure–activity relationships (QSARs) within two related series of antifungal azole derivatives. *J Enzyme Inhib* 1999, 14(3), 175–192.
126. JA Braatz, MB Bass, RL Ornstein. An evaluation of molecular models of the cytochrome P450 *Streptomyces griseolus* enzymes P450SU1 and P450SU2. *J Comp-Aided Mol Design* 1994, 8, 607–622.
127. RCA Onderwater, J Venhorst, JNM Commandeur, NPE Vermeulen. Design, synthesis and characterization of MAMC as a novel and selective cytochrome P450 2D6 substrate suitable for high-throughput screening. *Chem Res Tox* 1999, 12(7), 555–559.
128. HS Rosenkranz, CS Mitchell, G Klopman. Artificial intelligence and Bayesian decision theory in the prediction of chemical carcinogens. *Mutation Res* 1985, 150, 1–11.
129. DFV Lewis, PJ Eddershaw, PS Goldfarb, MH Tarbit. Molecular modelling of CYP3A4 from an alignment with CYP102: identification of key interactions between putative active site residues and CYP3A-specific chemicals. *Xenobiotica* 1996, 26(10), 1067–1086.
130. S Ekins, G Bravi, S Binkley, JS Gillespie, BJ Ring, JH Winkel, SA Wrighton. Three- and four-dimensional quantitative structure activity relationship analyses of cytochrome P-450 3A4 inhibitors. *J Pharmacol Exp Ther* 1999, 290(1), 429–438.
131. C Minoletti, S Dijols, PM Dansette, D Mansuy. Comparison of the substrate specificities of human liver cytochrome P450s 2C9 and 2C18: application to the design of a specific substrate of CYP 2C18. *Biochemistry* 1999, 38(24), 7828–7836.
132. J Cosme, EF Johnson. Engineering microsomal cytochrome P4502C5 to be a soluble, monomeric enzyme—mutations that alter aggregation, phospholipid dependence of catalysis, and membrane binding. *J Biol Chem* 2000, 275, 2545–2553.
133. PA Williams, J Cosme, V Sridhar, EF Johnson, DE McRee. Microsomal cytochrome P4502C5: comparison to microbial P450s and unique features. *J Inorg Biochem* 2000, 81, 183–190.

# 14

## Development of a Metabolic Drug Interaction Database at the University of Washington

**Sonia P. Carlson, Isabelle Ragueneau-Majlessi, and René H. Levy**  
*University of Washington, Seattle, Washington*

**Thomas E. Bougan**  
*Applied Technical Systems, Bremerton, Washington*

### I. INTRODUCTION

The primary tool available to minimize patient exposure to interacting drug combinations has traditionally been memorization of interacting drugs. Monographs, handbooks [1], charts, and databases were compiled by physician, pharmacists, nurses, and dentists to assist them to retrieve dangerous drug combinations, but unfortunately the availability of these tools did not alleviate the problem [2]. In the last decade, the developing field of metabolically based drug interactions (see previous chapters) has opened new possibilities. There now exists a framework, based on *in vitro* studies, to anticipate some drug interactions. It became apparent to scientists in the pharmaceutical industry that the most effective approach to decrease the interaction potential of a drug candidate is during the earliest stages of drug development—at the level of drug discovery. New guidelines were issued in 1997 by regulatory agencies in the United States [3] and Europe outlining the need for *in vitro* studies for any new chemical entity and the possibility of providing “class labeling.” The pharmaceutical industry created new programs in the early phases of drug discovery and development to characterize, decrease, and, in some cases, eliminate the drug interaction potential of drug candidates.



These changes have had an impact on a broad array of health care providers and scientists. For clinicians, a new enzyme-based approach to drug interactions, with all its intricacies and nuances, has to be learned in order to take advantage of the rational, class-labeling system [4]. For scientists in academia, regulatory agencies, and the pharmaceutical industry, the progress accomplished in the prediction of metabolically based *in vivo* drug interactions means that research has to be undertaken to define the boundaries of quantitative predictions based on *in vitro* data. Implementation of the new approach requires rapid access to a decade of new literature on metabolic isozymes, substrates, inducers, and inhibitors. For example, those working in discovery need to understand whether inhibition of a particular metabolic enzyme (i.e., CYP2C9) with an  $IC_{50}$  in the micromolar range implies that a drug candidate should not be considered further. Those performing *in vitro* studies with human tissue fractions or cloned enzymes must resolve issues pertaining to incubation conditions: amount of enzyme, substrate/inhibitor depletion, microsomal binding, mechanisms of inhibition, inhibition parameters, and substrate independence of inhibition [5]. Scientists designing protocols for representative drug interaction studies in healthy subjects or patients must question the relative usefulness of different enzyme probes [6]. All this information is spread in a large body of literature that is relatively recent but expanding at a fast pace.

Changes in the field of drug interactions have drastically altered the need for and functions of drug interaction databases [7]. The metabolic drug interaction (MDI) database pioneered at the University of Washington utilizes an object-oriented approach. A prototype, which includes *in vitro* and *in vivo* inhibition models and information from approximately 500 peer-reviewed published articles, has been built. The utility of the prototype, as well as examples of queries and sample outputs of the MDI database, are presented in this chapter.

## II. DATABASE DESIGN

### A. Defining the Problem

A fundamental issue in database construction is to define endpoints of information management. The primary purpose of this database is to serve as a tool for researchers and clinicians interested in correlating *in vitro* and *in vivo* findings on interactions associated with metabolic enzymes (cytochromes P450, UDP-glucuronosyl transferase [UDPGTs]) and transporters (P-glycoprotein). The unit of information is the original research article. *In vitro* studies define the role of particular metabolic enzymes in the various metabolic pathways of substrates and the inhibition and induction spectra of drugs toward metabolic enzymes. Particular attention is paid to experimental conditions—enzyme kinetic param-

ters, including  $K_m$ ,  $K_i$ , and  $IC_{50}$ . In vivo studies include pharmacokinetic studies with blood level measurements, pharmacokinetic-pharmacodynamic studies, as well as case reports.

## B. Technical Approach: Object-Oriented vs. Relational Databases

Data has been collected and stored in computers for over 30 years. Gleaning knowledge from an accumulated data store has remained the domain of information technology professionals well versed in SQL (Sequel Query Language) and other retrieval languages. The relational data model, developed in the 1970s, was designed for the most important task at that time, which was data collection. Currently, the focus has turned to “mining” these vast collections of data for knowledge; the retrieval methods of the relational model are no longer sufficient.

A basic tenet of database design is that databases are optimized for ease of data entry or ease of knowledge extraction but not both. This is because a database designed to facilitate data entry must minimize possible contention between multiple users by having thousands or millions of small records, thereby decreasing the chance that multiple users will access the same record at the same time. The records are then “normalized” by the process of breaking the data into its smallest practicable unique elements. The relational model then connects these records by common keys stored in the separate records for related data elements. Thus, the contextual relationships among the data are dismantled and are reconstructed according to a defined set of rules only when queried by the user.

The relational model is therefore an efficient way to collect and store large quantities of data. It facilitates multiple-user entry, and eases the propagation of data updates throughout all of the records. However, the relational model becomes less efficient when users attempt to retrieve meaningful, contextual information from the accumulated store. In part, this is because the retrieval process assumes the user understands the dismantled relationships among the data and is able to formulate an SQL-type query that will correctly reconstruct and filter the data. This implies that the user needs to anticipate the expected answer to the question before asking it. Since a malformed query can return an empty set of results, the user may be led to conclude that the actual answer to the question is empty. This type of query design is therefore not conducive to extracting scientific knowledge because a user cannot anticipate all possible outcomes of a question.

The Contiguous Connection Model (CCM) (Applied Technical Systems, Bremmerton, WA) [8] is an object-oriented database that takes a different approach to data storage. Rather than decomposing the data and rebuilding the relationships according to a set of rules, CCM relies on maintaining and storing

the relationships *among* the data elements for quick retrieval. That is, CCM stores the data description in conjunction with the data value. This conjunctive relationship is referred to as a *data instance*. The relationships among the data instances (description and value) are then represented as a hierarchical tree, where the level of indenture signifies the dependencies of the data relationships. This is in contrast to the relational model, where the data description is stored separately in an accompanying data dictionary.

The CCM structure is flexible, powerful, and conducive to “mining” the accumulated store of published metabolic drug interaction literature. After the literature data has been collected and the hierarchical models determined, meaningful and contextual information can be extracted. For example, any descriptive parameter, such as  $K_i$  value, is always hierarchically connected to its source article and, therefore, to all other information contained in the source article. Since each article acts as a unit of information, and data relationships are maintained, the common data relationships among articles can then be gathered and compiled. This allows a multidimensional search *across* several articles and simultaneously *within* several articles for any descriptive parameter, such as  $K_i$ . Furthermore, relating  $K_i$ , for example, only to a particular drug or enzyme can refine the data even more. Cataloging articles in this way allows the scientific context to be retained.

This design provides the ability to accommodate the requirements for organizing and managing a growing and complex knowledge base. The use of a World Wide Web platform allows for easy access to the database as well as facilitating information upgrades. Display is dependent on the user’s choice of Internet browser.

### C. Connectivity Models and Data Collection

Connectivity models were developed to allow multidimensional “mining” of the database according to CCM. The articles belong to one or many of several categories: in vivo case reports; single-drug pharmacokinetics; pharmacokinetic interactions; pharmacodynamic effects; in vitro enzymatic information on cytochromes P450 involved in metabolism of individual drugs; enzymes affected by inducers, inhibitors, and activators; interactions associated with transporters (e.g., P-glycoprotein). Each article is assigned an *Accession Number*, i.e., a unique identifier that matches the Medline<sup>®</sup> Accession Number. The first two digits represent the year the article became electronically available, and they can be used to organize articles in chronological order.

The appropriate descriptive parameters to capture in vitro and in vivo studies are defined as follows:

*Comment:* Text associated with the content of an article. Comments are either summary points as presented by the author or directly related to the method of information extraction. Editorial comments will be noted as such.

*Object:* A compound that acts as the modified agent (i.e., substrate).

*Precipitant:* A compound that acts as the causative agent. A precipitant can be an inhibitor, an inducer, or an activator or may have no effect at all.

The use of object/precipitant language allows the user to examine a drug in multiple roles.

The category *overall effect* was introduced and defined differently for in vitro and in vivo interactions:

*Overall effect* in vitro applies to each object, precipitant, enzyme grouping.

*Overall effect* in vivo is defined to distinguish precipitants that exhibited an effect >20% from those that did not. It describes the overall effect of the precipitant on the object, i.e., a change in area under the curve (AUC) or total body clearance (Cl).

Linking an overall effect in vivo to a given enzyme can be problematic. Because Cl is often dependent on multiple enzymes, it was decided that the overall effect could not be attributed to individual enzymes unless metabolites were quantified and there was independent evidence that the formation of a given metabolite was attributable to a specific enzyme. The *attributed enzyme* category was introduced for studies involving in vivo probes such as (*S*)-mephenytoin, (*S*)-warfarin, theophylline, and midazolam, which reliably reflect the activity of specific enzymes. *Attributed* could also be assigned to transporters such as P-glycoprotein in cases where there is strong supporting in vitro evidence (e.g., digoxin/quinidine [9,10] or digoxin/itraconazole [11]).

Some assumptions were made for the inhibition models:

The in vitro cutoff for classification as an inhibition interaction applies to object/precipitant pairs that show >25% inhibition. For example, sparteine, diclofenac, and caffeine at a concentration of 60  $\mu\text{M}$  were shown to inhibit terfenadine metabolism, but only to 16%, 10%, and 13% of control, respectively [12]. These three precipitants were classified as non-inhibitory in vitro. If a  $K_i$  was determined, then the interaction is labeled as inhibitory, even if the experiment was conducted at heroic concentrations.

The in vivo cutoff for classification as an inhibition interaction applies to object/precipitant pairs that show (unless otherwise noted) statistically significant inhibition greater than 20%. This value is based on AUC differences considered significant in bioavailability studies.

### III. EXAMPLES OF QUERIES AND OUTPUT

To access information, users launch their Internet browser, connect to the MDI database, and then choose from three possible modes of entry. First, there is a set of standard queries, as illustrated in the *Query Designer* screen (Fig. 1). These queries represent common questions and cover a range of information that approaches the data from many different perspectives. For example, a user may ask for a list of enzymes involved in the metabolism of a particular drug, a list of precipitants affecting a particular object, or a list of interactions between an object/precipitant pair. There is also a *Word Wheel* mechanism. The Word Wheel lists all of the data categories in the database, such as journal, metabolite, and author. The user can select a category and then display an alphabetical list of all of the items within the category, or go directly to the item of interest within the list. A user may also construct specialized queries and save them for reuse in an individual user profile.

#### A. Standard Query

As an illustration of how the MDI Database functions, let us assume that a user is interested in inhibitors of CYP2C19 in vitro. The user can enter the database

The screenshot shows a web browser window with the title "Query Designer". Below the browser window is a table titled "Standard Queries" with the subtitle "-- Each query is a separate line in the table." The table contains four rows of query definitions, each with a "Query" button.

Standard Queries		-- Each query is a separate line in the table.	
(1)	Find drugs which are <input type="text" value="Precipitants"/> of Enzyme <input type="text" value="CYP2C19"/> Condition <input type="text" value="In Vitro"/>	<input type="button" value="Query"/>	
(2)	Find Enzymes which metabolize Object <input type="text" value="(R)-metoprolol (R)-warfarin (S)-acenocoumarol (S)-mephenytoin"/> Condition <input type="text" value="Both"/>	<input type="button" value="Query"/>	
(3)	Find Precipitants which <input type="text" value="Inhibit"/> <input type="text" value="Do Not Inhibit"/> Object <input type="text" value="(S)-mephenytoin"/> Condition <input type="text" value="In Vivo"/>	<input type="button" value="Query"/>	
(4)	Find Enzymes which are <input type="text" value="Inhibited"/> <input type="text" value="Induced"/> <input type="text" value="Activated"/> by Precipitant <input type="text" value="alpha-naphthoflavone alprazolam amiodarone amitriptyline"/> <input type="text" value="In Vitro"/>	<input type="button" value="Query"/>	

Figure 1 *Query Designer* screen from the Metabolic Drug Interaction Database prototype.

through the first standard query: “Find drugs which are precipitants of Enzyme CYP2C19 in vitro.” The query results are displayed in a browser window, with hierarchically arranged folder icons. For example, the *Enzyme: CYP2C19* folder icon contains a list of precipitants that were tested for inhibitory properties against CYP2C19 (Fig. 2). Additionally, each precipitant in the list has its own folder icon containing more detailed information about each precipitant, such as whether or not it was found to inhibit CYP2C19. The *Accession Number* of the source article is also displayed. The list of precipitants includes both inhibitors and non-inhibitors. Additionally, the user can at any time click the *View Text* button to view the abstract, the *Drug List* button to examine reference information (e.g.,

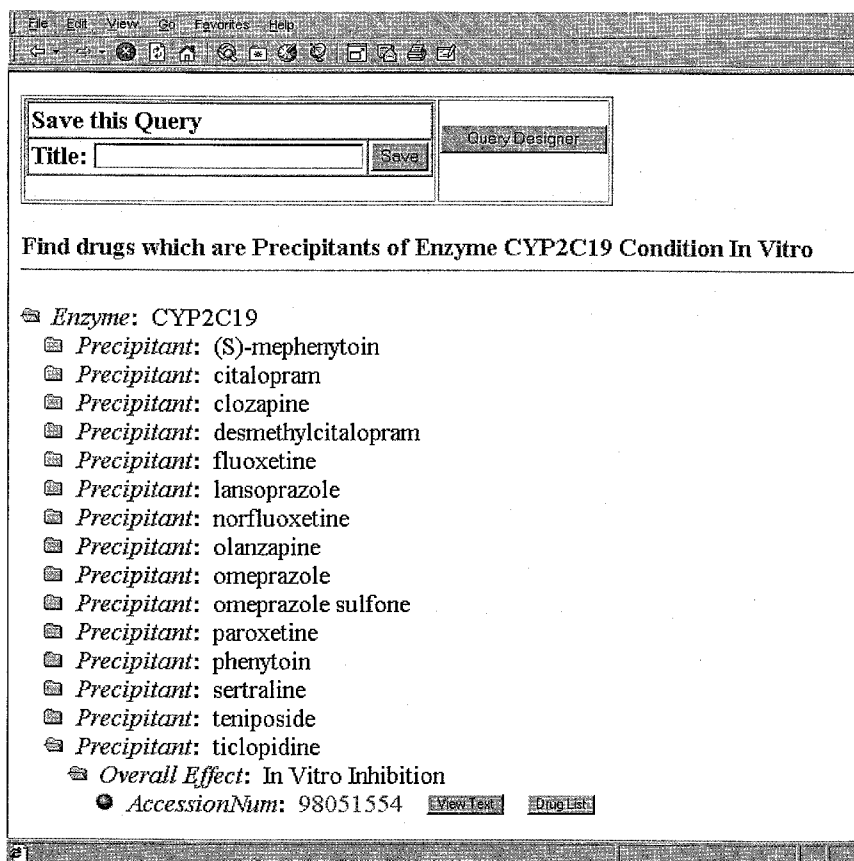


**Figure 2** List of Precipitants of Enzyme CYP2C19 as displayed by the Metabolic Drug Interaction Database prototype.

therapeutic concentration, plasma binding), or the *back* or *forward* browser button or return to *Query Designer* to ask another query or pursue a different approach. The user has the option to begin with a more refined query, which will perform filter operations to customize the results display.

From the precipitant list, the user can continue to pursue the answer to the original query: “*Find drugs which are precipitants of Enzyme CYP2C19 in vitro.*” In this example, we will assume that the user wishes to explore the effect of the last drug on the list, ticlopidine, on CYP2C19 [13]. The user opens the *ticlopidine* folder icon (Fig. 2). The display shows that ticlopidine is classified as an inhibitor and the *Accession Number* is given. By clicking directly on the source article number, the user is then transported directly to the contents of that article. Once the user reaches the article of interest, folder icons within the article can be hierarchically opened to provide progressively more detailed information.

For example, the user can view the citation information for the article (authors, title, etc.) and also the list of objects that were used with the precipitant ticlopidine (i.e., (*S*)-mephenytoin and tolbutamide). The use of these probes of CYP2C19 and CYP2C9, respectively, is logical because the article pertains to an interaction with phenytoin, which is metabolized by both enzymes. By pursuing the hierarchy further, the user will find that the  $K_i$  of ticlopidine found in this study for CYP2C19 (3.7  $\mu\text{M}$ ) is within the drug’s therapeutic range (1–3  $\mu\text{M}$ ), while the  $K_i$  toward CYP2C9 is an order of magnitude higher than the therapeutic plasma concentrations of ticlopidine. In the *comment*, the authors conclude that the interaction between ticlopidine and phenytoin can be attributed principally to inhibition of CYP2C19.

## B. Word Wheel Query

In addition to compiling information to answer specific queries, the MDI Database provides a convenient way to navigate other branches of information. From the *Word Wheel*, the user can select a data category of interest (under *data type*) and then select a particular value (under *data value*) from the list of all of the *data instances* in that category. For example, from the *Word Wheel*, the user may select *Therapeutic Class* as a data category. The values associated with this category are then shown in alphabetical order (Fig. 3). The user can then select the data value of interest, e.g., *Hypnotics and Sedatives*. The query is then submitted to the database and a list of all *Hypnotics and Sedatives* and their respective roles as *objects* or *precipitants* is displayed.

## C. Specialized Query

The foregoing example with ticlopidine and CYP2C19 illustrated a one-dimensional use of the MDI Database; a particular inhibitor of interest was pursued in an individual article and followed to a singular conclusion. Let us assume that

**Word Wheel Query**

- 1 Select a data type.
- 2 Choose Show Values.
- 3 Select a value.
  - To browse a long list of values, choose Next 50.
  - To find a value, enter it into the input field and choose Show Values.
  - Caution!** This field is case sensitive!
- 4 Choose your Submit option, Sim Query, Simx Query, or Query.
  - Sim Query uses the sim. operator for an inverted links analysis.
  - Simx Query uses the extended. simx. operator for a more in depth inverted links analysis.
  - Query submits the type and value pair you entered to open that Array

**CCM Database: database**

Data Type	Data Value
TherapClass	<input type="text"/> Show Values
PrincipalInvestigator	Gastrointestinal prokinetic Agents
ProteinConc	Glucocorticoids
PubDate	H1 Receptor Antagonists
ReliabilityComments	H2 Receptor Antagonists
System	HMG CoA reductase inhibitor
TherapClass	Hypnotics and Sedatives
TimeOfDay	Hypoglycemic Agents
Title	Immunosuppressive Agents
Submit->	Query

**Figure 3** View of the *Word Wheel* query page that lists data values of *Therapeutic Class* as displayed by the Metabolic Drug Interaction Database prototype.

the user wishes to gain a broader perspective of the inhibitory effects of compounds on CYP2C19 in vitro and perhaps examine the inhibition by ticlopidine in the context of other inhibitors of CYP2C19. The user can return to the *Query Designer* and ask a more advanced, multidimensional query such as; “*Find inhibitory compounds of CYP2C19 and list their respective  $K_i$  values in vitro.*”

The display as shown in Figure 4 provides a list of inhibitory precipitants of CYP2C19 with (*S*)-mephenytoin as the object and their respective  $K_i$  values. The  $K_i$  value for each precipitant is displayed by opening the respective folder icon, as shown for sertraline ( $K_i = 2.0 \mu\text{M}$  [14]) and clozapine ( $K_i = 69 \mu\text{M}$  [15]). As elsewhere in the database, the user can click the *Drug List* button to examine in vivo information (e.g., therapeutic plasma concentrations, extent of protein binding) for any of the compounds listed. Other observations can be extracted from this list of  $K_i$  values. For example, there are three different  $K_i$  values listed for omeprazole,  $2.0 \mu\text{M}$  [16],  $4.1 \mu\text{M}$  [15], and  $3.1 \mu\text{M}$  [17], as reported in three different articles. At one glance, the user can acquire a grasp of the range of reported  $K_i$  values for a particular inhibitor.

#### D. Hopping: The Ability to Roam

Like other Web applications, the MDI database uses hyperlinks, so the user can at any time “hop” onto a drug of choice simply by clicking on the highlighted



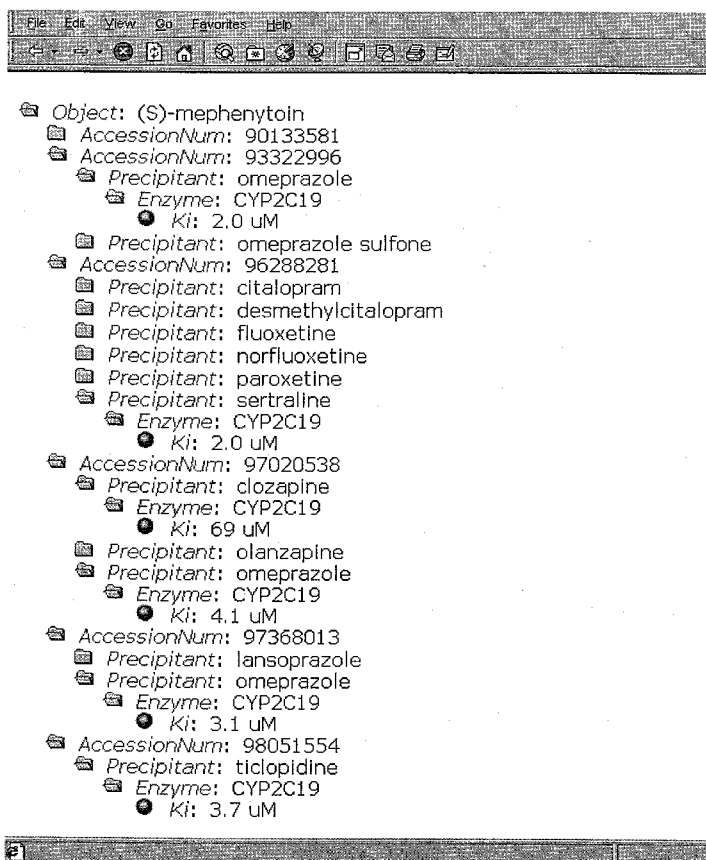


**Figure 4** List of inhibitory precipitants of CYP2C19 with (S)-mephenytoin as the object and their respective  $K_i$  values as displayed by the Metabolic Drug Interaction Database prototype.

name of the drug. In the previous ticlopidine example, we clicked on the folder icon to provide more detailed information about a particular pathway. But by clicking on the actual name of the drug, we expand the information by asking the database for all information about that drug. For example, from the list of *Hypnotics and Sedatives*, we can click on the drug name *alprazolam* and obtain a list of all articles in the database that have alprazolam as an object. Now, from this list of alprazolam articles, the user may decide to “hop” onto another compound. For example, the user may now be interested in fluoxetine. By clicking on the drug name fluoxetine, the user is then given a list of all articles in the

database that contain fluoxetine as a precipitant. So, although the user entered the database using the *Word Wheel* for *Hypnotics and Sedatives*, the hopping option led to examination of articles related to fluoxetine.

This feature is available throughout the database and can be executed at any time simply by clicking on any highlighted link. Hopping is a quick way to navigate through the database or to compile sets of information (e.g., a list can be compiled of all studies that were performed using a particular in vitro system such as reconstituted enzyme simply by clicking on *reconstituted enzyme*).

## E. In Vivo Examples

All of the foregoing features are also applicable to in vivo studies. As shown in Figure 2, the first query can be useful to select compounds that have been tested clinically as objects or precipitants of a particular isozyme. If the user asks the query, “*Find drugs which are precipitants of enzyme CYP3A4 in vivo,*” the query result (Fig. 5) provides an alphabetical list of all the drugs that have been used as precipitants. By opening the first folder, the user can immediately determine

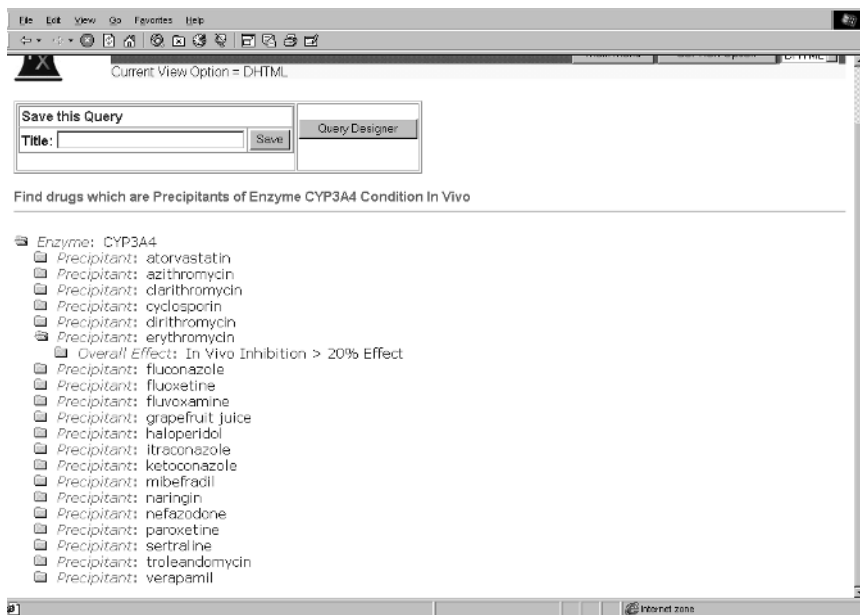


**Figure 5** List of precipitants of enzyme CYP3A4 in vivo and their overall inhibitory effect as displayed by the Metabolic Drug Interaction Database prototype.

whether an effect of more than 20% was observed, i.e., a change of more than 20% in the pharmacokinetic parameters of the object.

As in the previous examples, by clicking on an *Accession Number*, the user gains access to the individual article that reveals all the information extracted from the article and entered in the database. For in vivo articles, this includes a description of the study design and protocol, study population (e.g., healthy volunteers, patients, number of subjects), details of treatment administration (route, dose, duration of treatment, time), pharmacokinetic and pharmacodynamic results, and reported side effects. As described earlier, the user may also “hop” onto other hyperlinks, such as study design. In that case, the database provides a list of all studies with the same design as the hyperlink “hop.” Information from both in vitro and in vivo studies can also be accessed through an enzyme search using the second standard query (Fig. 1).

#### IV. DISCUSSION

To date, the MDI Database at the University of Washington has been developed to the prototype stage for inhibition-based drug interactions. It contains in vitro and in vivo studies and is intended to serve as a tool for researchers and health care providers interested in the evolving field of in vitro/in vivo correlations. As a research tool, it can contribute to the investigation of several unresolved issues. For example, “What is the degree of substrate independence for inhibition of a given isozyme by certain inhibitors?” This question has both an in vitro and an in vivo dimension. In vitro, the mechanism of inhibition must be evaluated. In the case of in vivo studies, evaluating substrate independence includes an analysis of various in vivo probes for a given isozyme. Additionally, the degree of substrate independence may be inhibitor specific. Similarly, the assignment of enzymes to the formation of given metabolites is another issue that requires the projection of data obtained in vitro to an in vivo situation. Evaluating the contribution of minor enzymes in given drug interactions is particularly challenging for induction as well as inhibition interactions.

In the area of quantitative prediction of inhibition interactions based on in vitro  $K_i$  values, it is necessary to know whether a given microsomal  $K_i$  value takes into consideration the extent of nonspecific binding or whether plasma concentrations of the inhibitor have been measured and the value of the fraction unbound in plasma. Known values for fraction unbound, therapeutic concentrations, and fractions metabolized can be found in the reference table by clicking the *Drug List* button. Information about nonspecific binding in vitro is extracted from the article. Accurate quantitative prediction of inhibition interactions also requires knowledge of whether the inhibitor is the sole inhibitory species or whether circulating metabolites are present, and whether or not their inhibitory

potential has been evaluated. This information is abstracted from the article and included in the display or is commented upon. *Comments* are written and reviewed by senior investigators. Users also act as reviewers by testing the stability and reproducibility of query results, and are able to report errors or alternative interpretations of the literature.

The design choice of the MDI database for Web accessibility has several advantages. Users can access the database via Web interface; this permits access from any computer with an Internet connection. It also allows for real-time discourse among users about articles in the database and their implications to the field of study. Each user will have the option to post comments about a particular article or issue and examine other opinions while simultaneously viewing a conglomerate of actual data. Web accessibility will also allow instantaneous upgrades of information so that information upgrades can be transmitted to users without delay. Furthermore, with the increase in electronic availability of information, additional links to online journals and other databases are anticipated. Users may wish to export the compiled lists of data from the query results from their Web browser into a desktop application, such as a spreadsheet for mathematical manipulation or graphical representation. The design analysis for this upcoming feature involves the selection of a suite of desktop applications to determine the standards for output formatting.

The flexibility of a Web application allows for multiple views of the same data. Depending on the interest of the user, customized data displays can be built to show the desired snapshots of the data. This necessitates the creation of individual user profiles that are password protected and customized for the user's needs. In a user's profile, there will be information about her group association, customized standard queries, and previously saved specialized queries. An additional feature of the customized user profile will be to provide direct links to electronic journals or other databases that the user frequently visits. Information about users is kept in strict confidence.

Unresolved issues regarding the growth of scientific knowledge databases still remain, the most prominent being limited public access to data. At present, the MDI database includes only published, peer-reviewed information. It is not clear whether unpublished studies and negative results that pharmaceutical companies have available in their own databases should be included. The value of a database, which encompasses a large knowledge base, including negative and positive data associated with failed compounds and unpublished studies, would be increased. Additionally, in many cases a considerable time delay exists between the time that studies are conducted and the time they are published. As electronic technology grows, the gap between traditional and electronic publishing should be exponentially decreased.

A database should be dynamic and unbiased and have the ability to quickly evolve with advances in research and computer technology. Additionally, as the

number of independent specialized databases increases, the capability to link to other databases via an accessible, user-friendly interface will become increasingly important. Consideration must also be given to the ease with which new information can be incorporated into the database. An object-oriented model, as chosen for the MDI Database, can incorporate new attributes, such as chemical structure, without being dependent on the details of the attribute itself. Our immediate goals, however, focus on populating the MDI Database one isozyme at a time, beginning with the most recent CYP2C9 and CYP2C19 literature.

## ACKNOWLEDGMENTS

We wish to express our thanks to, and acknowledge the contributions of, Philip D. Hansten, Pharm.D., William F. Trager, Ph.D., Kenneth E. Thummel, Ph.D., Fred L. Wurden, and Gary G. Mather, D.V.M., Ph.D.

## REFERENCES

1. PD Hansten, JR Horn. *Managing Clinically Important Drug Interactions*. Applied Therapeutics, Inc. Vancouver, WA. 1998.
2. NJ Cavuto, RL Woosley, M Sale. Pharmacies and prevention of potentially fatal drug interactions [letter; comment]. *JAMA* 275:1086–1087, 1996.
3. US FDA. *Guidance for Industry: Drug Metabolism/Drug Interaction Studies in the Drug Development Process, Studies In Vitro*. Washington, DC: U.S. Government Printing Office, April 1997.
4. R Levy. Cytochrome P450 isoenzymes and antiepileptic drug interactions. *Epilepsia* 36:S8–S13, 1995.
5. R Yuan, T Parmelee, JD Balian, RS Uppoor, F Ajayi, A Burnett, LJ Lesko, P Marroum. In vitro metabolic interaction studies: experience of the Food and Drug Administration. *Clin Pharmacol Ther* 66:9–15, 1999.
6. MT Kinirons, D O'Shea, RB Kim, JD Groopman, KE Thummel, AJ Wood, GR Wilkinson. Failure of erythromycin breath test to correlate with midazolam clearance as a probe of cytochrome P4503A [In Process Citation]. *Clin Pharmacol Ther* 66: 224–231, 1999.
7. P Bonnabry, J Sievering, T Leemann, P Dayer. Quantitative drug interactions prediction system (Q-DIPS): a computer-based prediction and management support system for drug metabolism interactions. *Eur J Clin Pharmacol* 55:341–347, 1999.
8. FL Wurden. Content is king (if you can find it): a new model for knowledge storage and retrieval. *Proceedings of the 13th International IEEE Conference on Data Engineering*, University of Birmingham, Birmingham, UK. Publisher Los Alamitos, CA: IEEE Computer Society, April 7–11, 1997, pp. 149–157.
9. SF Su, JD Huang. Inhibition of the intestinal digoxin absorption and exsorption by quinidine. *Drug Metab Dispos* 24:142–147, 1996.

10. U Mayer, E Wagenaar, B Dorobek, JH Beijnen, P Borst, AH Schinkel. Full blockade of intestinal P-glycoprotein and extensive inhibition of blood–brain barrier P-glycoprotein by oral treatment of mice with PSC833. *J Clin Invest* 100:2430–2436, 1997.
11. KM Jalava, J Partanen, PJ Neuvonen. Itraconazole decreases renal clearance of digoxin. *Ther Drug Monit* 19:609–613, 1997.
12. M Jurima-Romet, K Crawford, T Cyr, T Inaba. Terfenadine metabolism in human liver. In vitro inhibition by macrolide antibiotics and azole antifungals. *Drug Metab Dispos* 22:849–857, 1994.
13. SR Donahue, DA Flockhart, DR Abernethy, JW Ko. Ticlopidine inhibition of phenytoin metabolism mediated by potent inhibition of CYP2C19. *Clin Pharmacol Ther* 62:572–577, 1997.
14. K Kobayashi, T Yamamoto, K Chiba, M Tani, T Ishizaki, Y Kuroiwa. The effects of selective serotonin reuptake inhibitors and their metabolites on *S*-mephenytoin 4'-hydroxylase activity in human liver microsomes. *Br J Clin Pharmacol* 40:481–485, 1995.
15. BJ Ring, SN Binkley, M Vandenbranden, SA Wrighton. In vitro interaction of the antipsychotic agent olanzapine with human cytochromes P450 CYP2C9, CYP2C19, CYP2D6 and CYP3A. *Br J Clin Pharmacol* 41:181–186, 1996.
16. K Chiba, K Kobayashi, K Manabe, M Tani, T Kamataki, T Ishizaki. Oxidative metabolism of omeprazole in human liver microsomes: cosegregation with *S*-mephenytoin 4'-hydroxylation. *J Pharmacol Exp Ther* 266:52–59, 1993.
17. JW Ko, N Sukhova, D Thacker, P Chen, DA Flockhart. Evaluation of omeprazole and lansoprazole as inhibitors of cytochrome P450 isoforms. *Drug Metab Dispos* 25:853–862, 1997.



# 15

## Drug–Drug Interactions: Clinical Perspective

**David J. Greenblatt and Lisa L. von Moltke**

*Tufts University School of Medicine and New England Medical Center,  
Boston, Massachusetts*

### I. INTRODUCTION

During the last 15–20 years the general problem of pharmacokinetic drug interactions has received increasing attention. Over this period a number of new and unique classes of medications have been introduced into clinical practice. These include the selective serotonin reuptake inhibitor (SSRI) and related mixed-mechanism antidepressants, the azole antifungal agents, newer macrolide antimicrobial agents, and the highly active antiretroviral therapies (HAART) used against human immunodeficiency virus (HIV) infection and the acquired immunodeficiency syndrome (AIDS). While these and other classes of agents have had a major beneficial impact on the therapy on some serious and life-threatening illnesses, many of the agents have the secondary pharmacologic property of inducing or inhibiting the human cytochrome P450 (CYP) enzymes responsible for oxidative metabolism of most drugs used in clinical practice (Table 1) [1–16]. As such, pharmacokinetic drug interactions have become a clinical issue of increasing concern.

One principal objective of the drug development process is the generation of scientific information on drug interactions so that treating physicians will have the data necessary to proceed with safe clinical treatment involving more than one medication. However, complete attainment of this objective is seldom possible, because the number of possible drug interactions is very large, and time and resources available for implementation of controlled clinical pharmacokinetic



**Table 1** Representative Drugs Having Large and Clinically Important Effects on the Human Cytochrome P450 (CYP) Enzymes

	Inhibition of:	Induction of:
<i>Azole antifungals</i>		
Ketoconazole	CYP3A	
Itraconazole	CYP3A	
Fluconazole	CYP3A, 2C9	
Terbinafine	CYP2D6	
<i>Antidepressants</i>		
Fluoxetine	CYP2D6	
Paroxetine	CYP2D6	
Fluvoxamine	CYP1A2, 2C19	
Nefazodone	CYP3A	
<i>Anticonvulsants</i>		
Carbamazepine		CYP3A
<i>Anti-infectives</i>		
Erythromycin	CYP3A	
Clarithromycin	CYP3A	
Ciprofloxacin	CYP1A2	
Rifampin	CYP3A	CYP3A
<i>Viral protease inhibitors</i>		
Ritonavir	CYP3A	CYP3A
<i>Non-nucleoside reverse transcriptase inhibitors</i>		
Delavirdine	CYP3A	
Nevirapine		CYP3A
<i>Cardiovascular agents</i>		
Quinidine	CYP2D6	
<i>Antiulcer agents</i>		
Cimetidine	CYP3A	
Omeprazole	CYP2C9	

studies are inevitably limited. Some needed drug interaction studies will therefore be postponed until after a new drug is marketed, and some studies may be bypassed altogether. As such, *in vitro* data are becoming increasingly important as an approach to identifying which drug interactions are probable, possible, or unlikely, and thereby allow more informed planning of actual clinical studies [9,10,17–29].

## II. CLINICAL CONSIDERATIONS IN EVALUATION OF DRUG INTERACTIONS

### A. Nomenclature

A useful although legalistic nomenclature system refers to the agent causing the drug interaction as the “perpetrator,” while the drug being affected by the interaction is the “victim” (Fig. 1). A pharmacokinetic drug interaction implies that the perpetrator causes a change in the metabolic clearance of the victim, in turn either decreasing or increasing concentrations of the victim drug in plasma and presumably also at the site of action. This change may or may not alter the clinical activity of the victim drug. A pharmacokinetic interaction “variant” is one in

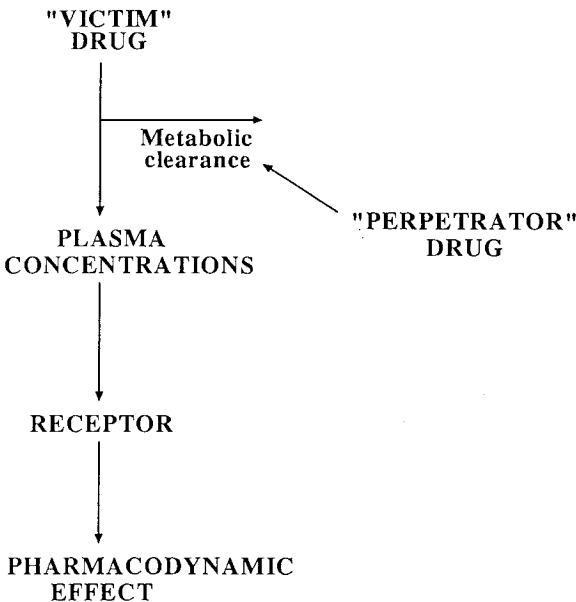


**Figure 1** Schematic representation of the mechanism of pharmacokinetic drug interactions. Plasma concentrations of the “victim” drug are determined by its dosing rate and metabolic clearance. Plasma levels, in turn, determine drug concentrations at the receptor site and ultimately its pharmacodynamic effect. A pharmacokinetic drug interaction involves the effect of the “perpetrator” on the metabolic clearance of the victim. When the perpetrator is an inducer, clearance of the victim is increased, plasma levels diminish, and pharmacological effect is reduced. Conversely, when the perpetrator is an inhibitor, clearance of the victim is reduced, plasma levels increase, and pharmacodynamic effect is enhanced.

which the perpetrator does not change the systemic clearance or plasma levels of the victim, but rather modifies the access of the victim to its pharmacologic receptor site. A familiar example is the antagonism of benzodiazepine activity by flumazenil; a less familiar example is benzodiazepine receptor antagonism by ketoconazole [30].

A pharmacodynamic interaction involves either inhibition or enhancement of the clinical effects of the victim drug as a consequence of similar or identical end-organ actions. Examples are the increase or decrease of the sedative-hypnotic actions of benzodiazepines due to coadministration of ethanol or caffeine, respectively.

## B. Inhibition vs. Induction of Metabolism

Mechanistically different processes are involved in drug interactions involving inhibition as opposed to induction of metabolism mediated by CYP enzymes (Table 2) [9,10,21,22,31–35]. Chemical inhibition is an immediate phenomenon. The effect becomes evident as soon as the inhibitor comes in contact with the enzyme, and is in principle reversible when the inhibitor is no longer present (an exception is “mechanism-based” inhibition, see Chap. 10) [13,36]. The magnitude of inhibition—that is, the size of the interaction—depends on the concentration of the inhibitor at the site of the enzyme relative to the intrinsic potency of the inhibitor. Inhibition potency can be measured using *in vitro* systems yielding quantitative estimates such as the inhibition constant ( $K_i$ ) or the 50% inhibitory concentration ( $IC_{50}$ ). Methods of calculating  $K_i$  and  $IC_{50}$ , including the limitations and drawbacks inherent in the calculations, are reviewed elsewhere [9,10,17–22,29,35]. Our current technological capacity to determine  $K_i$  or  $IC_{50}$  using *in vitro* systems is more advanced than our understanding of how to apply the numbers to quantitative predictions of drug interaction *in vivo*, which require knowledge of the effective concentration of inhibitor that is available to the enzyme. A generally applicable scheme to relate total- or unbound-plasma concentrations

**Table 2** Mechanistic Comparison of CYP Inhibition and Induction

	Inhibition	Induction
Mechanism	Direct chemical effect on enzyme	Indirect effect through enhanced quantities of CYP protein
Onset and reversibility	Rapid	Slow
Immediate exposure	Needed	Not needed
Prior exposure	Not needed	Needed
<i>In vitro</i> study	Straightforward	Difficult

of inhibitor to effective enzyme-available concentration has not been established. Nevertheless it now is abundantly clear, based on numerous examples, that the theoretical assumption of equality of unbound-plasma concentrations and enzyme-available intrahepatic concentrations is incorrect in reality and will frequently yield underestimates of observed *in vivo* drug interactions by as much as an order of magnitude or even more [18,29,37,38].

Induction of CYP-mediated metabolism requires prior exposure to a chemical inducer of the hepatocyte's CYP-synthesis mechanism. The inducer signals the synthetic mechanisms to upregulate the production of one or more CYP isoforms, a process that takes time. Consequently, evidence of increased CYP activity is of slow onset following initiation of exposure to the inducer, and conversely slowly reverts to baseline after the inducer is removed. Enhancement of CYP expression/activity due to chemical induction therefore reflects prior but not necessarily current exposure to the inducer. The quantitative extent of CYP induction depends on the dosage (concentration) of the inducer and on the duration of exposure. However, the induction process, in contrast to inhibition, is not straightforwardly studied *in vitro*, since induction requires intact cellular protein synthesis mechanisms as available in cell culture models [39–41].

Inducers and inhibitors of CYP3A can be expected to influence both hepatic and gastrointestinal CYP3A (see Chap. 9), although not necessarily to the same extent [22,42]. Nonetheless, profound changes in both hepatic and gastrointestinal CYP3A will be caused by very strong inhibitors (such as ketoconazole) or very strong inducers (such as rifampin). A uniquely complex situation arises for drugs such as ritonavir that are both inhibitors and inducers of CYP3A. Interactions of ritonavir with CYP3A substrate drugs will be time dependent. Initial exposure to ritonavir will produce CYP3A inhibition. But as the duration of exposure proceeds, CYP3A induction may counterbalance the inhibitory effects of acute exposure [43,44]. The net outcome may be unpredictable and variable among individuals.

### C. Clinical Importance of Drug Interactions

Given the prevalence of polypharmacy in clinical practice, noninteractions of drugs are far more common than interactions. The usual outcome of coadministration of two drugs is no detectable pharmacokinetic or pharmacodynamic interaction. That is, the pharmacokinetic disposition and clinical activity of each drug proceed independent of each other. Less common is the occurrence of a kinetic interaction that is detectable using controlled study design methods but is of no clinical importance under usual therapeutic circumstances because (1) the interaction, while statistically significant, is not large enough in magnitude to produce a clinically important change in dynamics of the victim drug; (2) the therapeutic index of the victim drug is large enough that even a substantial change in plasma

levels of the victim will not alter therapeutic effects or toxicity; or (3) kinetics and response to the victim drug is so variable that changes in plasma levels due to the drug interaction are far less important than inherent variability. Even less common are clinically important interactions that require modification in dosage of the perpetrator, the victim, or both. The most unusual consequences of a drug interaction is a situation in which the drug combination is so hazardous as to be contraindicated, as in the case of ketoconazole and terfenadine. These situations are rare, but unfortunately they receive disproportionate attention in the public media.

Many secondary sources are available to clinicians as guidelines to anticipate and avoid drug interactions. These compendia often serve as excellent and comprehensive collections of published data on drug interactions, but they generally are less helpful to clinicians in critically sorting out the literature and deciding

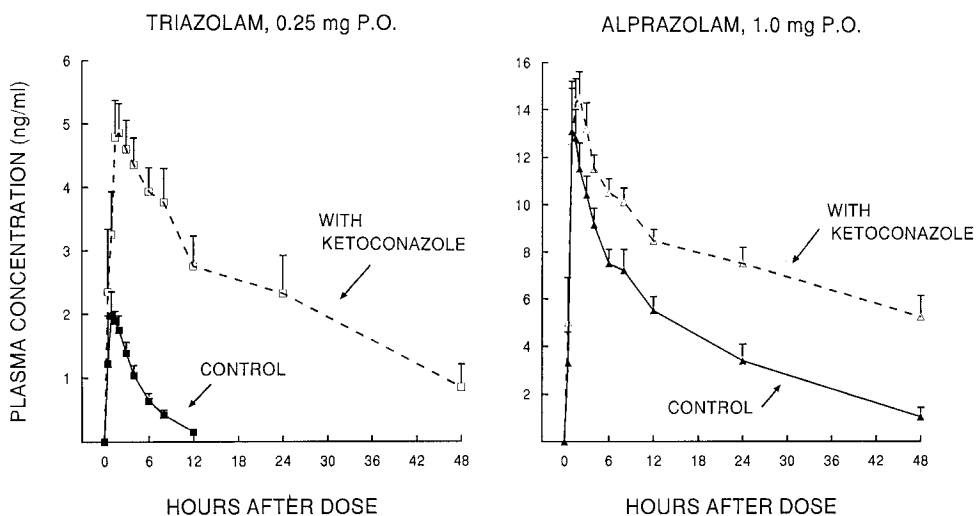


**Figure 2** Mean ( $\pm$ SE) plasma concentrations of triazolam (left) or alprazolam (right) in a series of healthy individuals who participated in a clinical pharmacokinetic study. In one phase of the study, they ingested a single 0.25-mg oral dose of triazolam with ketoconazole, 200 mg twice daily, or with placebo to match ketoconazole (control). In the second phase of the study, they took 1.0 mg of alprazolam orally, either with the same dosage of ketoconazole or with placebo to match ketoconazole (control). Note that ketoconazole increases AUC and reduces clearance of both triazolam and alprazolam. For triazolam (a high-extraction compound), the effect is evident as reduced presystemic extraction, increased  $C_{max}$ , and prolonged half-life. However, for alprazolam (a low-extraction compound) the effect of ketoconazole is evident only as a prolongation of half-life. (Adapted in part from Ref. 46.)

what interactions are actually of real concern in the course of drug therapy. A useful general guideline for clinicians is that drug interactions are more likely to be important when (1) the perpetrator drug produces a very large change in the kinetics and plasma levels of the victim drug, that is, the perpetrator is a powerful inducer or inhibitor; (2) the therapeutic index of the victim is narrow. Case (1) is exemplified by powerful inducers or inhibitors of CYP3A (ketoconazole, ritonavir, rifampin) coadministered with CYP3A substrates, or powerful inhibitors of CYP2D6 (quinidine, fluoxetine, paroxetine) coadministered with CYP2D6 substrates. Case (2) is exemplified by victim drugs such as phenytoin, warfarin, and digoxin, for which small changes in plasma levels could have important clinical consequences.

The intrinsic kinetic properties of the victim drug also influence the potential clinical consequences of an interaction. For orally administered medications that undergo significant presystemic extraction, impairment of clearance by a CYP inhibitor may produce increases in bioavailability (reduced presystemic extraction) as a consequence of reduced clearance [18,21,22,31,35,42]. The effects may be particularly dramatic for CYP3A substrates (such as triazolam or midazolam) that undergo both hepatic and gastrointestinal presystemic extraction [44,45]. As an example, coadministration of the CYP3A inhibitor ketoconazole with triazolam produced very large increases in area under the plasma concentration curve (AUC) and increases in peak plasma concentration ( $C_{max}$ ) of triazolam (Fig. 2). Cotreatment of ketoconazole with alprazolam, also a CYP3A substrate, produced a large increase in AUC for alprazolam [46]. However, alprazolam is a low-extraction compound, with bioavailability ordinarily in the range of 90%. As such, the reduction in alprazolam clearance caused by ketoconazole was evident mainly as prolonged elimination half-life but without a significant change in  $C_{max}$ .

### III. INTEGRATING KINETIC AND DYNAMIC STUDY OBJECTIVES

#### A. Background

Clinical pharmacokinetic drug interaction protocols are increasingly incorporating pharmacodynamic endpoints into the study design such that the dynamic consequences of drug interactions may be estimated concurrently with the usual pharmacokinetic outcome measures. The level of complexity of an integrated kinetic-dynamic study depends on the nature of the pharmacodynamic actions of the drug under study as well as the type of pharmacodynamic outcome measures that are required. A number of methodological principles and dilemmas are illustrated by kinetic-dynamic design options for drug interaction studies involving

**Table 3** Options for Pharmacodynamic Endpoints in Kinetic-Dynamic Studies of GABA-Benzodiazepine Agonists

Classification (with examples)	Relevance to primary therapeutic action	Influence of placebo	Influence of adaptation/practice	“Blind” conditions needed	Quantitative approach
<i>Subjective</i> Global assessments; rating scales	Close	Yes	Yes	Yes	Transformation of ratings into numbers
<i>Semi-objective</i> Psychomotor function tests; memory tests	Linked to adverse effect profile	Yes	Yes	Yes	Test outcomes are quantitative
<i>Objective</i> Electroencephalography	Not established	No	No	No	Fully objective computer-determined quantitation

sedative-hypnotic and anxiolytic drugs acting on the GABA-benzodiazepine receptor system [47]. For this category of drugs, a variety of outcome measures is available, but the approaches may differ substantially in their relevance to the principal therapeutic actions of the drug, the stability of the measure in terms of response to placebo or changes caused by practice or adaptation, the objective or subjective nature of the quantitative assessment, and the comparability of results across different investigators and different laboratories (Table 3). The extent to which the various pharmacodynamic measures provide unique information, as opposed to being overlapping or redundant, is not clearly established. For this reason most kinetic-dynamic studies of GABA-benzodiazepine agonists utilize multiple parallel dynamic outcome measures.

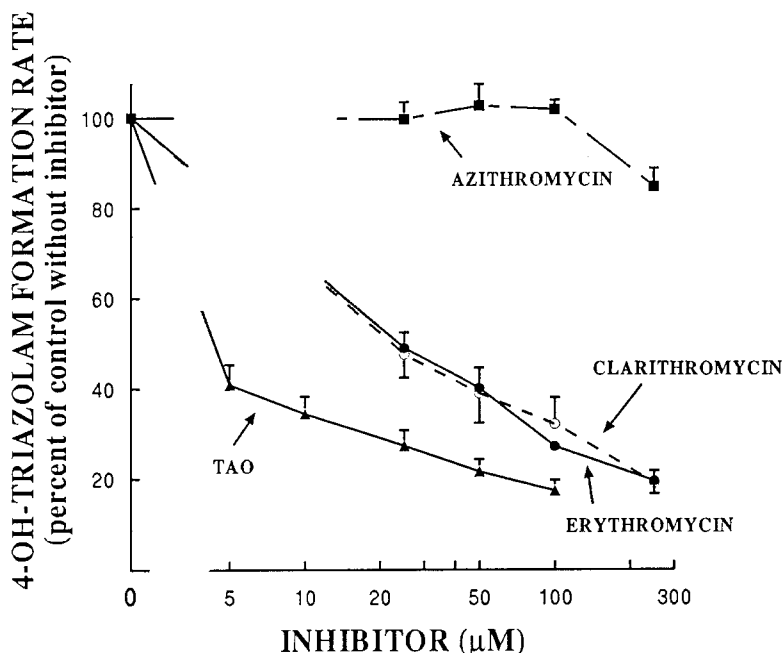


**Figure 3** Rates of formation of 4-*OH*-triazolam from triazolam (250 μM) by human liver microsomes *in vitro*. Each point is the mean ( $\pm$ SE) of four microsomal preparations. Reaction velocities when preparations were preincubated with the macrolide agents are expressed as a percentage of the control velocity with no inhibitor present (Inhibitor = 0). Mean 50% inhibitory concentrations ( $IC_{50}$ ) were: troleandomycin (TAO), 3.3 μM; erythromycin, 27.3 μM; clarithromycin 25.2 μM; azithromycin, >250 μM. (Adapted in part from Ref. 48.)



## B. Clinical Application

The kinetic and dynamic interaction of the triazolobenzodiazepine triazolam with various macrolide antimicrobial agents illustrates a number of these principles [48]. The “victim” drug in this model, triazolam, is established as a relatively “pure” substrate for human CYP3A isoforms [49,50] and is extensively prescribed in clinical practice as a hypnotic agent. The principal biotransformation pathways for triazolam involve parallel hydroxylation at two sites on the molecule, yielding  $\alpha$ -OH-triazolam and 4-OH-triazolam as principal metabolites. Previous studies have established that triazolam biotransformation is strongly inhibited in vitro and in vitro by CYP3A inhibitors such as ketoconazole, itraconazole, ritonavir, and nefazodone [44,50–55]. Some, but not all, of the macrolide antimicrobial agents also are CYP3A inhibitors [12]. The mode of inhibition by this class of compounds is described as “mechanism-based,” in that the parent compound binds to the metabolically active site on the CYP3A enzyme, yielding a metabolic intermediate that irreversibly inactivates the enzyme [36].

TRIAL	DAY 1		DAY 2		
	AM	PM	8AM	9AM	PM
A	PL	PL	PL	PL	PL
B	PL	PL	PL	TRZ	PL
C	AZ-500	PL	AZ-250	TRZ	PL
D	ERY	ERY	ERY	TRZ	ERY
E	CLAR	CLAR	CLAR	TRZ	CLAR

PL = PLACEBO

TRZ = TRIAZOLAM, 0.125 mg

AZ-500 = AZITHROMYCIN, 500 mg

AZ-250 = AZITHROMYCIN, 250 mg

ERY = ERYTHROMYCIN, 500 mg

CLAR = CLARITHROMYCIN, 500 mg

**Figure 4** Schematic representation of the design of the clinical study.

An *in vitro* model, using human liver microsomes, provided data that was qualitatively predictive of the clinical findings, as discussed shortly. Varying concentrations of four macrolide antimicrobial agents (troleandomycin [TAO], erythromycin, clarithromycin, azithromycin) were preincubated with liver microsomes and appropriate cofactors, followed by addition of a fixed concentration (250  $\mu$ M) of triazolam. At the completion of the 20-minute incubation period, samples were processed and concentrations of  $\alpha$ -OH- and 4-OH-triazolam determined by HPLC [50,51]. Rates of formation of the metabolites with coaddition of inhibitor were expressed as a percentage of the control velocity with no inhibitor present. The reaction velocity ratio versus inhibitor concentration relationship was used to determine a 50% inhibitory concentration ( $IC_{50}$ ). TAO, erythromycin, and clarithromycin all produced significant *in vitro* inhibition of triazolam hydroxylation

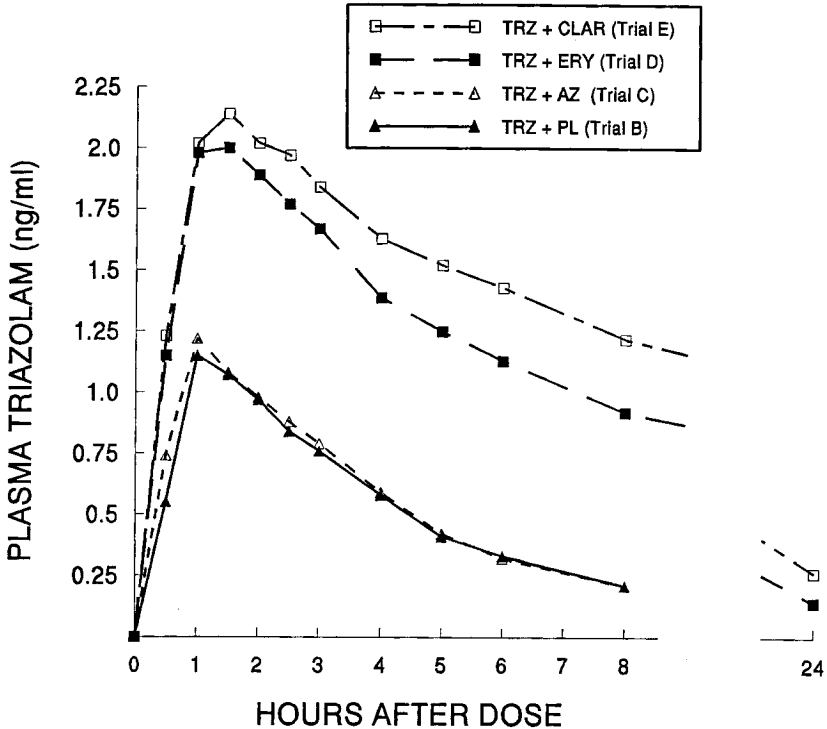


**Figure 5** Mean plasma triazolam concentrations following a single 0.125-mg oral dose of triazolam administered in Trials B, C, D, and E, as described in the text and in Fig. 4. Abbreviations: TRZ, triazolam; CLAR, clarithromycin; ERY, erythromycin; AZ, azithromycin; PL, placebo. (From Ref. 48.)

and would appear to have the potential to produce a significant interaction with triazolam in vivo (Fig. 3). However, azithromycin was a very weak inhibitor of triazolam in vitro, and is anticipated to produce no significant interaction in vivo.

The clinical pharmacokinetic-pharmacodynamic study had a double blind, randomized, five-way crossover design, with at least 7 days elapsing between trials. Twelve healthy volunteers participated and the treatment conditions were:

- A. Triazolam placebo plus macrolide placebo
- B. Triazolam (0.125 mg) plus macrolide placebo
- C. Triazolam (0.125 mg) plus azithromycin
- D. Triazolam (0.125 mg) plus erythromycin
- E. Triazolam (0.125 mg) plus clarithromycin

Dosage schedules of the coadministered macrolides were chosen to be consistent with usual dosage recommendations (Fig. 4).

Following each dose of triazolam (or placebo to match triazolam), multiple venous blood samples were drawn over a period of 24 hours, and multiple phar-

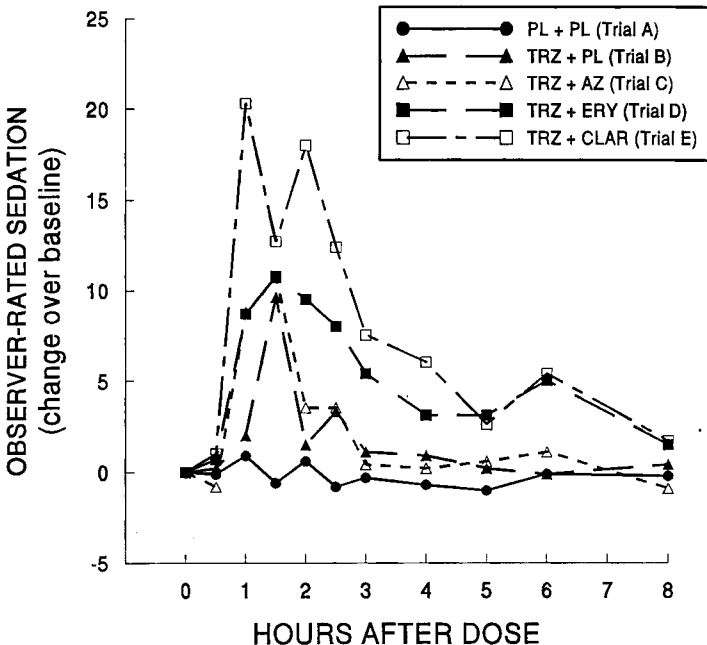


**Figure 6** Mean changes over baseline in observer-rated sedation during each of the five trials, as described in the text and in Fig. 4. Abbreviations are as given in Fig. 5. (From Ref. 48.)

macodynamic testing procedures were performed. These included subjective measures (observer's ratings and subjects' self-ratings of sedation and mood), a semiobjective measure of psychomotor performance (the digit-symbol substitution test, or DSST), and the fully objective quantitative of electroencephalographic (EEG) amplitude falling in the "beta" (13–30 cycles per second) frequency range [46–48,50]. Note that for purposes of a kinetic-dynamic study of a CNS-active agent, Trial A is necessary, whereas for a purely pharmacokinetic study, Trial A would not be necessary. Even so, the five-way crossover design still does not rule out the possibility, although very unlikely, of CNS pharmacodynamic effects attributable to the macrolide agents alone. This would have required three additional trials: triazolam placebo plus azithromycin, triazolam placebo plus erythromycin, and triazolam placebo plus clarithromycin.

Triazolam plasma concentrations were determined by gas chromatography with electron capture detection [50,56]. The pharmacokinetic results demonstrated that mean clearance during Trials B and C were nearly identical (413 and 416 ml/min, respectively); that is, coadministration of azithromycin had no effect on the pharmacokinetics of triazolam (Fig. 5). However, triazolam clearance was

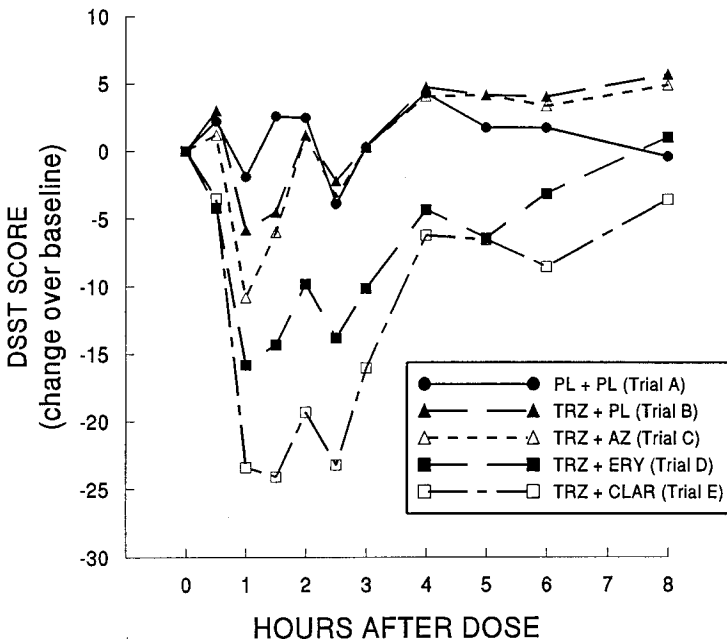


**Figure 7** Mean changes over baseline in scores on the digit-symbol substitution test (DSST) during each of the five trials, as discussed in the text and in Fig. 4. Abbreviations are as given in Fig. 5. (From Ref. 48.)

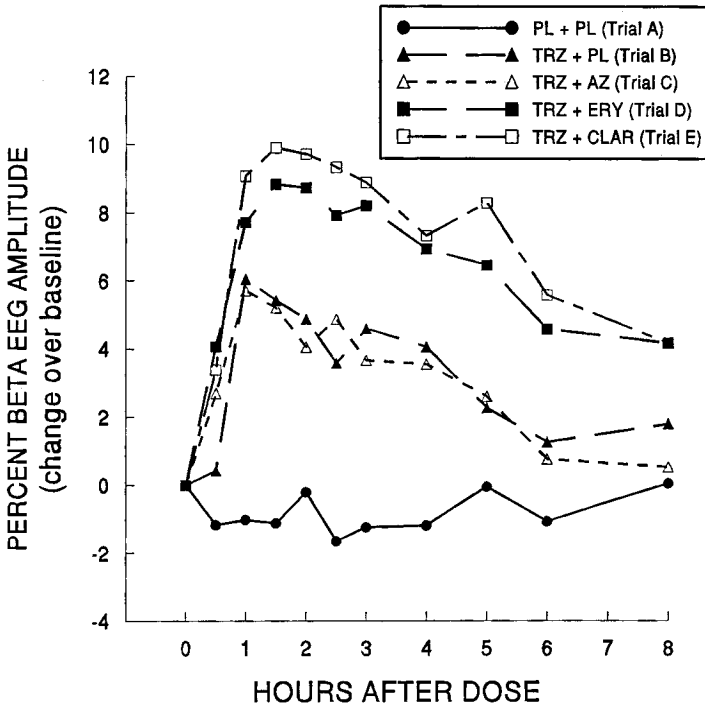


**Figure 8** Mean changes over baseline in percentage of EEG amplitude falling in the beta frequency range (13–30 cycles/sec) during each of the five trials, as discussed in the text and in Fig. 4. Abbreviations are as given in Fig. 5. (From Ref. 48.)

significantly reduced to 146 ml/min by erythromycin (Trial D) and to 95 ml/min by clarithromycin (Trial E). Thus, the *in vivo* kinetic results are highly consistent with the *in vitro* data.

The pharmacodynamic data indicated that the benzodiazepine agonist effects of triazolam plus placebo (Trial B) and of triazolam plus azithromycin (Trial C) were similar to each other and greater than the effects of placebo plus placebo (Trial A). However, coadministration of erythromycin (Trial D) or clarithromycin (Trial E) augmented the pharmacodynamic effects of triazolam when compared to Trials B and C. The outcome was similar based on subjective measures, a semiobjective measure (the DSST), or the fully objective measure (the EEG) (Figs. 6–8). Kinetic-dynamic modeling indicated that the augmentation in benzodiazepine agonist effects of triazolam caused by coadministration of erythromycin or clarithromycin was fully consistent with the increase in triazolam plasma

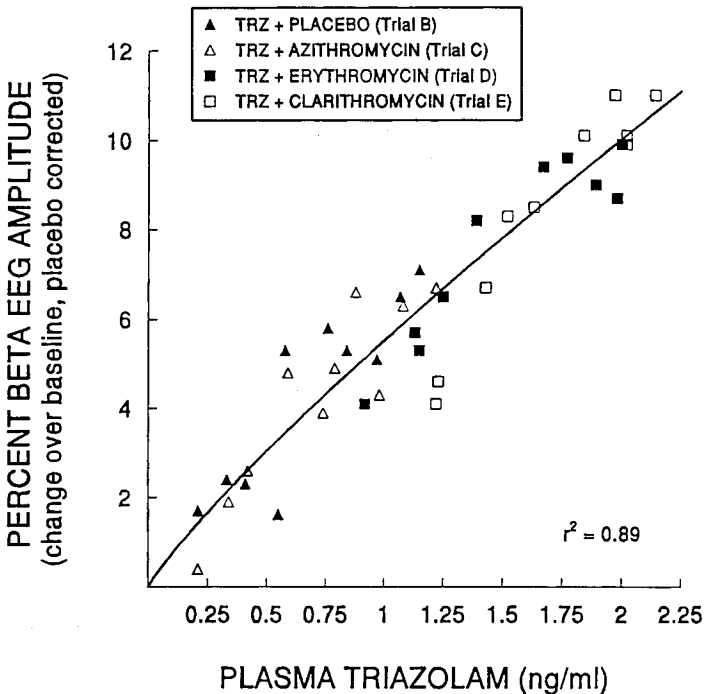


**Figure 9** Mean changes over baseline in percentage of EEG amplitude falling in the beta frequency range (normalized for placebo-associated changes) in relation to mean plasma triazolam concentrations at corresponding times. The line represents a function of the form  $y = Bx^4$  determined by nonlinear regression. (From Ref. 48.)

concentrations (Fig. 9). As anticipated, there was some redundancy among the various pharmacodynamic measures, in that the changes in these outcome measures at corresponding times were significantly intercorrelated (Fig. 10).

#### IV. COMMENT

The basic and clinical scientific issues underlying pharmacokinetic drug interactions are becoming increasingly complex as polypharmacy becomes more common and more drugs with enzyme-inducing or -inhibiting properties are introduced into clinical practice. A well-planned, integrated approach is needed to address the clinical problems. Ideally the approach should incorporate the collaborative participation of individuals with expertise in molecular pharmacology,

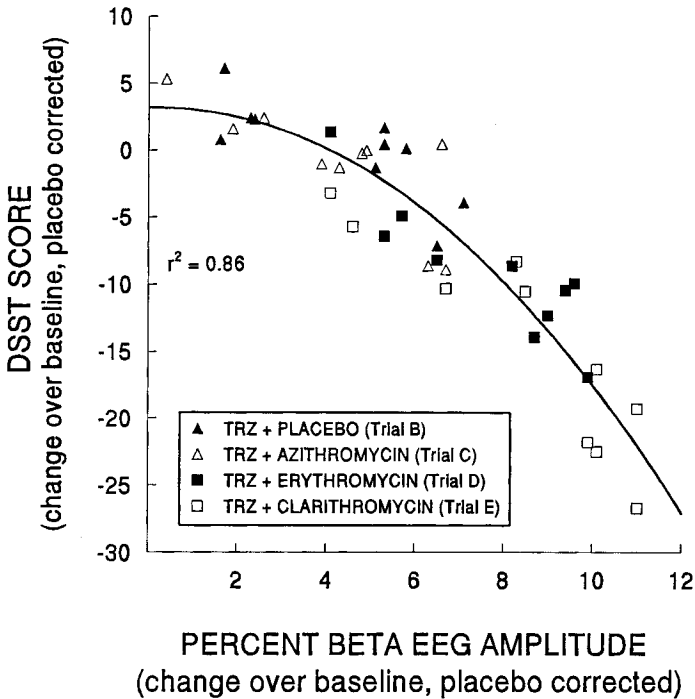


**Figure 10** Mean changes over baseline in percentage of EEG amplitude falling in the beta frequency range in relation to mean changes over baseline in DSST score at corresponding times. Both measures were normalized for placebo-associated changes. The line represents a function of the form  $y = Bx^A$  determined by nonlinear regression. (From Ref. 48.)

cytochrome biochemistry, in vitro metabolism, clinical pharmacokinetics-pharmacodynamics, and clinical therapeutics.

## ACKNOWLEDGMENTS

We are grateful for the collaboration and assistance of Dr. Richard I. Shader, Jerold S. Harmatz, Karthik Venkatakrishnan, and Brian W. Granda. The work is supported by Grants MH-34223, MH-01237, DA-05258, DA-13209, MH-58435, and RR-00054 from the U.S. Department of Health and Human Services.

## REFERENCES

1. Harvey AT and Preskorn SH. Cytochrome P450 enzymes: interpretation of their interactions with selective serotonin reuptake inhibitors. *Journal of Clinical Psychopharmacology* 1996; 16:273–285, 345–355.
2. DeVane CL. Metabolism and pharmacokinetics of selective serotonin reuptake inhibitors. *Cell Mol Neurobiol* 1999; 19:443–466.
3. Preskorn SH. Clinically relevant pharmacology of selective serotonin reuptake inhibitors. *Clin Pharmacokinet* 1997; 32 (Supp. 1):1–21.
4. Mitchell PB. Drug interactions of clinical significance with selective serotonin reuptake inhibitors. *Drug Safety* 1997; 17:390–406.
5. Richelson E. Pharmacokinetic drug interactions of new antidepressants: a review of the effects on the metabolism of other drugs. *Mayo Clin Proc* 1997; 72:835–847.
6. Sproule BA, Naranjo CA, Bremner KE and Hassan PC. Selective serotonin reuptake inhibitors and CNS drug interactions: a critical review of the evidence. *Clinical Pharmacokinetics* 1997; 33:454–471.
7. Baker GB, Fang J, Sinha S and Coutts RT. Metabolic drug interactions with selective serotonin reuptake inhibitor (SSRI) antidepressants. *Neurosci Biobehavioral Rev* 1998; 22:325–333.
8. Baumann P. Pharmacokinetic-pharmacodynamic relationship of the selective serotonin reuptake inhibitors. *Clin Pharmacokinet* 1996; 31:444–469.
9. Greenblatt DJ, von Moltke LL, Harmatz JS and Shader RI. Drug interactions with newer antidepressants: role of human cytochromes P450. *J Clin Psychiatry* 1998; 59 (Supp. 15):19–27.
10. Greenblatt DJ, von Moltke LL, Harmatz JS and Shader RI. Human cytochromes and some newer antidepressants: kinetics, metabolism, and drug interactions. *J Clin Psychopharmacol* 1999; 19 (Suppl. 1):23S–35S.
11. Venkatakrishnan K, von Moltke LL and Greenblatt DJ. Effects of the antifungal agents on oxidative drug metabolism in humans: clinical relevance. *Clin Pharmacokinet* 2000; 38:111–180.
12. Periti P, Mazzei T, Mini E and Novelli A. Pharmacokinetic drug interactions of macrolides. *Clin Pharmacokinet* 1992; 23:106–131.
13. Gillum JG, Israel DS and Polk RE. Pharmacokinetic drug interactions with antimicrobial agents. *Clin Pharmacokinet* 1993; 25:450–482.
14. Barry M, Gibbons S, Back D and Mulcahy F. Protease inhibitors in patients with HIV disease. Clinically important pharmacokinetic considerations. *Clin Pharmacokinet* 1997; 32:194–209.
15. Barry M, Mulcahy F, Merry C, Gibbons S and Back D. Pharmacokinetics and potential interactions amongst antiretroviral agents used to treat patients with HIV infection. *Clin Pharmacokinet* 1999; 36:289–304.
16. Hsu A, Granneman GR and Bertz RJ. Ritonavir. Clinical pharmacokinetics and interactions with other anti-HIV agents. *Clin Pharmacokinet* 1998; 35:275–291.
17. Tucker GT. The rational selection of drug interaction studies: implications of recent advances in drug metabolism. *Int J Clin Pharmacol Ther Toxicol* 1992; 30:550–553.



18. Bertz RJ and Granneman GR. Use of in vitro and in vivo data to estimate the likelihood of metabolic pharmacokinetic interactions. *Clin Pharmacokinet* 1997; 32:210–258.
19. Rodrigues AD and Wong SL. Application of human liver microsomes in metabolism-based drug–drug interactions: in vitro–in vivo correlations and the Abbott Laboratories experience. *Adv Pharmacol* 1997; 43:65–101.
20. Rodrigues AD. Use of in vitro human metabolism studies in drug development. *Biochem Pharmacol* 1994; 48:2147–2156.
21. Lin JH and Lu AY. Inhibition and induction of cytochrome P450 and the clinical implications. *Clin Pharmacokinet* 1998; 35:361–390.
22. Thummel KE and Wilkinson GR. In vitro and in vivo drug interactions involving human CYP3A. *Annu Rev Pharmacol Toxicol* 1998; 38:389–430.
23. Guengerich FP. Cytochrome P-450 3A4: regulation and role in drug metabolism. *Annu Rev Pharmacol Toxicol* 1999; 39:1–7.
24. Clarke SE. In vitro assessment of human cytochrome P450. *Xenobiotica* 1998; 28:1167–1202.
25. Smith G, Stubbins MJ, Harries LW and Wolf CR. Molecular genetics of the human cytochrome P450 monooxygenase superfamily. *Xenobiotica* 1998; 28:1129–1165.
26. Smith DA, Abel SM, Hyland R and Jones BC. Human cytochrome P450s: selectivity and measurement in vivo. *Xenobiotica* 1998; 28:1095–1128.
27. Glue P and Clement RP. Cytochrome P450 enzymes and drug metabolism—basic concepts and methods of assessment. *Cell Mol Neurobiol* 1999; 19:309–323.
28. Crespi CL and Penman BW. Use of cDNA-expressed human cytochrome P450 enzymes to study potential drug–drug interactions. *Adv Pharmacol* 1997; 43:171–188.
29. von Moltke LL, Greenblatt DJ, Schmider J, Wright CE, Harmatz JS and Shader RI. In vitro approaches to predicting drug interactions in vivo. *Biochem Pharmacol* 1998; 55:113–122.
30. Fahey JM, Pritchard GA, von Moltke LL, Pratt JS, Grassi JM, Shader RI and Greenblatt DJ. The effects of ketoconazole on triazolam pharmacokinetics, pharmacodynamics and benzodiazepine receptor binding in mice. *J Pharmacol Exp Ther* 1998; 285:271–276.
31. Ito K, Iwatsubo T, Kanamitsu S, Ueda K, Suzuki H and Sugiyama Y. Prediction of pharmacokinetic alterations caused by drug–drug interactions: metabolic interaction in the liver. *Pharmacol Rev* 1998; 50:387–412.
32. Waxman DJ and Azaroff L. Phenobarbital induction of cytochrome P-450 gene expression. *Biochem J* 1992; 281:577–592.
33. Park BK, Kitteringham NR, Piromohamed M and Tucker GT. Relevance of induction of human drug-metabolizing enzymes: pharmacological and toxicological implications. *Br J Clin Pharmacol* 1996; 41:477–491.
34. Halpert JR. Structural basis of selective cytochrome P450 inhibition. *Annu Rev Pharmacol Toxicol* 1995; 35:29–53.
35. Lin JH and Lu AYH. Role of pharmacokinetics and metabolism in drug discovery and development. *Pharmacological Rev* 1997; 49:403–449.
36. Silverman R. Mechanism-based enzyme inactivators. *Meth Enzymol* 1992; 249:241–282.

37. Greenblatt DJ and von Moltke LL. Can in vitro models predict drug interactions in vivo? A review of methods, problems, and successes. In: W Hori, ed. *Drug-Drug Interactions: Analyzing In Vitro-In Vivo Correlations*. Southboro, MA: International Business Communications, 1997, pp 2.2.1-2.2.28.
38. von Moltke LL, Greenblatt DJ, Duan SX, Daily JP, Harmatz JS and Shader RI. Inhibition of desipramine hydroxylation (cytochrome P450-2D6) in vitro by quinidine and by viral protease inhibitors: relation to drug interactions in vivo. *J Pharmaceut Sci* 1998; 87:1184-1189.
39. Li AP and Jurima-Romet M. Applications of primary human hepatocytes in the evaluation of pharmacokinetic drug-drug interactions: evaluation of model drugs terfenadine and rifampin. *Cell Biol Toxicol* 1997; 13:365-374.
40. Maurel P. The use of adult human hepatocytes in primary culture and other in vitro systems to investigate drug metabolism in man. *Advanced Drug Deliv Rev* 1996; 22:105-132.
41. George J, Goodwin B, Liddle C, Tapner M and Farrell GC. Time-dependent expression of cytochrome P450 genes in primary cultures of well-differentiated human hepatocytes. *J Lab Clin Med* 1997; 129:638-648.
42. Hall SD, Thummel KE, Watkins PB, Lown KS, Benet LZ et al. Molecular and physical mechanisms of first-pass extraction. *Drug Metab Dispos* 1999; 27:161-166.
43. Gass RJA, Gal J, Fogle PW, Detmar-Hanna D and Gerber JG. Neither dapsone hydroxylation nor cortisol 6 beta-hydroxylation detects the inhibition of CYP3A4 by HIV-1 protease inhibitors. *Eur J Clin Pharmacol* 1998; 54:741-747.
44. Greenblatt DJ, von Moltke LL, Daily JP, Harmatz JS and Shader RI. Extensive impairment of triazolam and alprazolam clearance by short-term low-dose ritonavir: the clinical dilemma of concurrent inhibition and induction. *J Clin Psychopharmacol* 1999; 19:293-296.
45. Tsunoda SM, Velez RL, von Moltke LL and Greenblatt DJ. Differentiation of intestinal and hepatic Cytochrome P450 3A activity with use of midazolam as an in vivo probe: effect of ketoconazole. *Clin Pharmacol Therapeut* 1999; 66:461-471.
46. Greenblatt DJ, Wright CE, von Moltke LL, Harmatz JS, Ehrenberg BL, Harrel LM, Corbett K, Counihan M, Tobias S and Shader RI. Ketoconazole inhibition of triazolam and alprazolam clearance: differential kinetic and dynamic consequences. *Clin Pharmacol Therapeut* 1998; 64:237-247.
47. Laurijssens BE and Greenblatt DJ. Pharmacokinetic-pharmacodynamic relationships for benzodiazepines. *Clin Pharmacokinet* 1996; 30:52-76.
48. Greenblatt DJ, von Moltke LL, Harmatz JS, Counihan M, Graf JA, Durol ALB, Mertzanis P, Duan SX, Wright CE and Shader RI. Inhibition of triazolam clearance by macrolide antimicrobial agents: in vitro correlates and dynamic consequences. *Clin Pharmacol Therapeut* 1998; 64:278-285.
49. Kronbach T, Mathys D, Umeno M, Gonzalez FJ and Meyer UA. Oxidation of midazolam and triazolam by human liver cytochrome P450III A4. *Molec Pharmacol* 1989; 36:89-96.
50. von Moltke LL, Greenblatt DJ, Harmatz JS, Duan SX, Harrel LM, Cotreau-Bibbo MM, Pritchard GA, Wright CE and Shader RI. Triazolam biotransformation by human liver microsomes in vitro: effects of metabolic inhibitors, and clinical confirma-

- tion of a predicted interaction with ketoconazole. *J Pharmacol Exper Therapeut* 1996; 276:370–379.
51. von Moltke LL, Greenblatt DJ, Duan SX, Harmatz JS and Shader RI. Inhibition of triazolam hydroxylation by ketoconazole, itraconazole, hydroxyitraconazole and fluconazole in vitro. *Pharmacy Pharmacol Commu* 1998; 4:443–445.
  52. von Moltke LL, Greenblatt DJ, Grassi JM, Granda BW, Duan SX, Fogelman SM, Daily JP, Harmatz JS and Shader RI. Protease inhibitors as inhibitors of human cytochromes P450: high risk associated with ritonavir. *J Clin Pharmacol* 1998; 38: 106–111.
  53. Barbhaiya RH, Shukla UA, Kroboth PD and Greene DS. Coadministration of nefazodone and benzodiazepines: II. A pharmacokinetic interaction study with triazolam. *J Clin Psychopharmacol* 1995; 15:320–326.
  54. Varhe A, Olkkola KT and Neuvonen PJ. Oral triazolam is potentially hazardous to patients receiving systemic antimycotics ketoconazole or itraconazole. *Clin Pharmacol Therapeu* 1994; 56:601–607.
  55. Rickels K, Schweizer D, Case WG, DeMartinis N, Greenblatt DJ, Mandos LA and España FG. Nefazodone in major depression: adjunctive benzodiazepine therapy and tolerability. *J Clin Psychopharmacol* 1998; 18:145–153.
  56. Friedman H, Greenblatt DJ, Burstein ES, Harmatz JS and Shader RI. Population study of triazolam pharmacokinetics. *Br J Clin Pharmacol* 1986; 22:639–642.

# 16

## Drug–Drug Interactions: Toxicological Perspectives

**Sidney D. Nelson**

*University of Washington, Seattle, Washington*

### I. INTRODUCTION

One of the major problems facing the pharmaceutical industry is unanticipated adverse drug reactions after the introduction of a new drug into clinical practice. Although in most cases the new drug itself is metabolically activated to a haptenic product that leads to immunotoxicity, in some cases the new drug may be the precipitator or perpetrator of toxicity of another drug by altering its metabolism and/or disposition, or the new drug may be the object or victim of altered metabolism and/or disposition caused by a drug already on the market. In many instances, the object or victim is a drug with a narrow therapeutic index, window, or ratio (for a recent discussion, see Ref. 1). Several definitions have been applied to this terminology, including the qualitatively simple one of a drug “for which relatively small changes in systemic concentrations lead to marked changes in pharmacodynamic response” [2]. The FDA has defined narrow therapeutic ratio to include those drugs for which there is less than a twofold difference in median lethal dose ( $LD_{50}$ ) and median effective dose ( $ED_{50}$ ), or for which there is less than a twofold difference in the minimum toxic concentrations and minimum effective concentrations in the blood, or for which safe and effective use of the drug requires careful titration and patient monitoring [3].

This chapter will focus on those metabolic drug–drug interactions that have led or can lead to serious toxicological consequences in humans. Most of the chapter will describe examples of metabolic drug–drug interactions that have caused serious toxicities. As discussed in Chapter 15, the majority of drug–drug interactions of clinical significance have occurred through interactions at the level

of cytochromes P450. Since substantial information is now either available or readily obtainable about induction and inhibition of these enzymes, as well as the kinetic parameters associated with the metabolism of drugs and other probe substrates, many metabolic drug–drug interactions can be predicted prior to clinical trials. However, because the situation *in vivo* is complicated by a variety of genetic and environmental factors that affect drug absorption, distribution, and metabolism, and because the physiological response to a toxic insult may vary from one individual to another, it is often difficult to predict that a particular drug–drug interaction will lead to a toxic insult. Nonetheless, the results of pre-clinical studies should provide the basis for more informed planning of clinical studies.

## **II. DRUGS AND CLASSES OF DRUGS AS OBJECTS (VICTIMS) OF CYTOCHROMES P450-MEDIATED DRUG–DRUG INTERACTIONS THAT LEAD TO TOXICITIES**

### **A. Warfarin**

Because of its narrow therapeutic window and extensive oxidation to inactive metabolites by cytochromes P450, warfarin (and the closely related drug acenocoumarol) is subject to many metabolic drug–drug interactions that can place patients at severe risk of either hyper- or hypocoagulability. Drug interactions with warfarin have recently been reviewed [4,5], and it is clear that most interactions occur through either induction or inhibition of CYP2C9, which forms the major 7-hydroxylation metabolite of the most active (*S*)-warfarin enantiomer [6].

Several inducers of cytochromes P450, including rifampin, several barbiturates, aminoglutethimide, primidone, phenytoin, and carbamazepine increase requirements for warfarin dosing, though mechanisms for most of these interactions have not been thoroughly investigated [4,5]. Clinically, this becomes manifest either when a patient stabilized on warfarin adds one or more of these drugs to his or her therapy or, more commonly, when the patient removes one of these drugs from his or her therapy after stabilization on the combination therapy. Rifampin induces several P450s, including CYP2C9, and has been shown to increase the formation clearance of the major hydroxylated metabolites of (*S*)-warfarin [7]. Substantial clinical and other indirect data implicates enhanced clearance of (*S*)-warfarin by CYP2C9 as one mechanism of the interaction [8], though increased glucuronidation may also play a role.

Several inhibitors of cytochromes P450 can substantially decrease requirements for warfarin dosage that, if not attended to, can lead to life-threatening bleeding episodes. Some drugs, such as sulfaphenazole, metronidazole, danazol, cotrimoxazole (trimethoprim-sulfamethoxazole), miconazole, and fluconazole,

contain heterocyclic rings with  $sp^2$ -hybridized nitrogen, a structural unit known to bind to the heme iron of P450s, and investigations implicate inhibition of CYP2C9 oxidation of (*S*)-warfarin as the mechanism for the drug–drug interactions caused by several of these drugs [5].

However, the presence of a nitrogen-containing heterocyclic ring in a drug is not sufficient for potent inhibition of CYP2C9. Cimetidine contains an imidazole moiety, but it is a much better inhibitor of the metabolism of (*R*)-warfarin [9], the least potent enantiomer, such that only at high doses of cimetidine is an effect on warfarin therapy observed [10]. Also, other potent inhibitors of CYP2C9 that inhibit (*S*)-warfarin metabolism and thereby increase the hypoprothrombinemic response to warfarin, such as phenylbutazone, sulfapyrazone, and amiodarone [5], do not contain such structures. Although many case reports have appeared of interactions between warfarin and a variety of other drugs with many different drug structures [11], only a few of these have resulted in serious toxic effects, and mechanisms are largely unknown. Because of their increased use, further investigations with some of these drugs, such as tamoxifen [12,13], seems warranted.

## B. Theophylline

General aspects of the drug–drug interactions involving theophylline are similar to those described for warfarin, because it too is a drug with a narrow therapeutic index. Increases in its rate of metabolism, either by some inducers of cytochromes P450 or by removal of an inhibitor of those P450s given concomitantly with theophylline, leads to diminution of therapeutic effect, resulting in increased dyspnea. Conversely, decreases in its rate of metabolism by inhibitors of P450s involved in the metabolism of theophylline or removal of an inducer given concomitantly can lead to serious toxicities, including convulsions and heart arrhythmias that can be serious enough to cause death.

The major P450 involved in the oxidation of theophylline to inactive metabolites is CYP1A2 (see Ref. 14 for a review). Interestingly, there are no reports of serious toxicity resulting from interactions of CYP1A2 inducers, such as cigarette smoking, even though theophylline clearance is increased [15]. Several case reports have appeared of increased theophylline clearance by barbiturates, carbamazepine, phenytoin, and rifampin, which are thought to induce CYP3A4 with little effect on CYP1A2, and adjustments to theophylline dosage are often required for optimal therapeutic effect.

In contrast, decreases in theophylline metabolism by selective inhibitors of CYP1A2, such as fluoxamine and some quinolone antibiotics, or by selective and potent inhibitors of CYP3A4, such as the macrolide antibiotics, decrease the metabolism of theophylline and have resulted in serious theophylline toxicity [14]. It is postulated that taken over time, the macrolide antibiotics act as mecha-

nism-based inhibitors of CYP isoforms other than just CYP3A4. Some nonselective inhibitors of P450s, such as cimetidine, some beta-blockers and calcium channel blockers, and others [11,14], also appear to inhibit the metabolism of theophylline enough to cause toxicity.

### C. Nonsedating Antihistamine Drugs

Terfenadine and astemizole were removed from the market in 1997 and 1999, respectively, because of drug interactions that led to QT interval prolongation [16]. Both of these drugs are prodrugs that are metabolized primarily by CYP3A4 to their therapeutically active metabolites (for a review, see Ref. 17). Inhibition of CYP3A4 by azole antifungal agents [17,18] and most macrolide antibiotics [17,19] can lead to sufficient increases in terfenadine concentrations to cause *torsades des pointes* as a result of the prodrug's ability to inhibit delayed rectifier potassium currents [20]. Similar interactions occur with astemizole [17,21]. Neither loratidine nor cetirizine, nor the active metabolites of terfenadine (fexofenadine) and astemizole (norastemizole), cause this cardiotoxic effect to any significant extent [17].

### D. Cisapride

More recently, the promotility agent cisapride was removed from the market because of over 300 reports of heart rhythm abnormalities similar to those caused by terfenadine, including 80 deaths [22]. Cisapride also is metabolized extensively by CYP3A4, and the same macrolide antibiotics, azole antifungal agents, and other inhibitors of this enzyme, such as grapefruit juice [23,24], sustain high enough concentrations of the parent drug to cause heart problems such as *torsades des pointes*.

### E. Cyclosporine

The widely used immunosuppressive agent cyclosporine is significantly metabolized by CYP3A4 (and to a lesser extent by CYP3A5) in human intestine and liver [25], and therefore it is subject to similar metabolic drug–drug interactions as described for terfenadine. However, in the case of cyclosporine, induction of its metabolism can lead to loss of its immunosuppressive activity to the point of transplant organ rejection, and inhibition of its metabolism can lead to kidney damage as a major toxicity. Cyclosporine is also pumped out of intestinal epithelial cells by P-glycoprotein, and many of the drugs that inhibit or induce CYP3A4 also inhibit or induce this transporter [25,26]. Thus, this effect also contributes, in part, to many of the observed drug–drug interactions with cyclosporine. It is noteworthy that ketoconazole, an azole antifungal agent that increases cyclosporine blood concentrations by its inhibition of CYP3A4 and P-glycopro-

tein, can be used concurrently to decrease the high cost of cyclosporine therapy in transplant recipients [27]. Tacrolimus, a newer immunosuppressive agent related to cyclosporine, apparently is subject to similar drug interactions as cyclosporine, though it has not been in use as long, and limited data is available [25].

## F. The Statins

Of the statin HMG-CoA reductase inhibitors on the market in the United States, lovastatin, simvastatin, atorvastatin, and cerivastatin are metabolized mainly by CYP3A4, whereas fluvastatin is metabolized by CYP2C9, and pravastatin by phase II pathways [28,29]. Most toxic drug interactions caused by the statins (myopathies and rhabdomyolysis) are related to supratherapeutic concentrations achieved as a result of inhibition of CYP3A4 by macrolide antibiotics, the azole antifungal agents, and cyclosporine [28,29], though some have resulted from combined therapy with other lipid-lowering agents, such as niacin and gemfibrozil [30]. Most recently, mibefradil, a unique benzimidazole-containing calcium channel blocking drug, was removed from the market because of its potent inhibition of the metabolism of several drugs and resultant toxicities, including life-threatening rhabdomyolysis in patients on lovastatin and simvastatin [31]. In fact, lovastatin and simvastatin are the two drugs that achieve the highest blood concentrations and appear to be the most susceptible to these kinds of drug interactions and resultant toxicity [29,32].

## G. Calcium Channel Blockers

The dihydropyridine class of calcium channel blockers undergoes extensive first-pass oxidation by CYP3A isoforms to their pyridine metabolites, and several studies have shown that inducers and inhibitors of these P450s respectively decrease and increase the blood concentrations of the active dihydropyridine structures [33]. The calcium channel blockers verapamil and diltiazem are unrelated structures that also undergo significant metabolism by cytochromes P450 of the CYP3A family [33]. However, apparently in only very few cases has this caused significant enough loss of antihypertensive activity (in the case of concomitant administration of inducers of CYP3A isoforms) or hypotension and edema (in the case of concomitant administration of inhibitors of CYP3A isoforms) to cause toxic drug reactions [11,33]. More commonly, it is the ability of these drugs to inhibit CYP3A isoforms that leads to toxicities caused by some other object drug.

## H. Sedative-Hypnotic and Anxiolytic Agents

The benzodiazepine derivatives are the most widely used drugs in this class, and most are metabolized extensively by enzymes of the CYP3A family, except



oxazepam, lorazepam, and temazepam, which are mostly glucuronidated [34]. Again, several studies have shown that inducers and inhibitors of CYP3A can markedly alter plasma concentrations of some benzodiazepines, but in only a few cases have toxic effects, such as deep unconsciousness, been reported [11,34,35]. Nonetheless, patients on these drugs should probably be monitored carefully, particularly the elderly, who may suffer severe physical injury as a result of falls suffered from impairment of psychomotor function.

### **I. Antidepressants**

Toxicities associated with antidepressant drugs have been most commonly reported for the tricyclic antidepressants as a result of inhibition of cytochromes P450, particularly CYP2D6 [36]. They include bradycardia, seizures, and delirium. Inhibitors of CYP2D6, such as paroxetine, fluoxetine, perfenazine, quinidine, and  $\beta$ -blockers, have all been shown to significantly increase plasma concentrations of tricyclic antidepressants such as imipramine and desipramine, in some cases with overt signs of toxicity [36–38]. However, in other cases toxicity is minimized, either because other pathways of metabolism involving CYP3A4, CYP2C19, and CYP1A2 are not affected or because of genetic polymorphisms of CYP2D6 [39–41] that decrease its activity.

### **J. $\beta$ -Blockers**

The  $\beta$ -adrenoceptor antagonists ( $\beta$ -blockers) are widely used drugs that are metabolized by cytochromes P450, particularly CYP2D6 [42]. Fortunately, these drugs have a rather large therapeutic index, and only a few instances of severe toxicity have been reported, which in part may be related to CYP2D6 polymorphism [43]. Reports of cardiac effects ranging from significant decreases in heart rate to orthostatic hypotension to cardiac arrest have occurred with  $\beta$ -blockers when combined with inhibitors of P450 metabolism, such as amiodarone [44], quinidine [45], propafenone [46], and fluoxetine [47]. The over-the-counter antihistamine diphenhydramine has recently been shown to cause bradycardia and other hemodynamic changes in subjects on metoprolol who were CYP2D6 extensive metabolizers but not poor metabolizers [48].

### **K. Anesthetics**

The volatile “flurane” anesthetics are metabolized primarily by CYP2E1, with lesser involvement by CYP2A6 and CYP3A4 [49]. A severe idiosyncratic immune-mediated toxic effect of most of these agents is liver necrosis as a result of oxidative dehalogenation of the anesthetics by CYP2E1 to form acyl halides that acylate hepatic proteins yielding antigens [50–52]. Thus, it might be anti-

pated that inducers of CYP2E1 would increase the risk of hepatotoxicity caused by the flurane anesthetics, and inhibitors of CYP2E1 would decrease the risk. The only evidence to support this is that obesity induces CYP2E1 activity [53] and is an increased risk factor for halothane hepatitis [54]. Obesity also leads to increased halothane oxidation in humans [55]. An interesting suggestion has been put forth to use disulfiram, a CYP2E1 inhibitor, in patients administered fluranes, because it markedly decreases the oxidation of halothane in humans to the proposed toxic metabolite [56].

The only other anesthetic to cause serious toxicity for which a metabolic drug interaction has been reasonably well characterized is the local anesthetic and antiarrhythmic agent lidocaine. Amiodarone decreased lidocaine systemic clearance in a patient (primarily by inhibition of CYP3A4 *N*-dealkylation of lidocaine) and yielded concentrations of lidocaine that led to seizures [57,58].

## L. Antiepileptics

### 1. Carbamazepine

Carbamazepine is considered a relatively safe antiepileptic drug that is subject to dose-related neurologic toxicities (e.g., drowsiness, vertigo, loss of coordination) in adults and children [59]. Since a major route of elimination of carbamazepine is via epoxidation catalyzed by CYP3A4 [60], there are several reports and studies that demonstrate CNS toxic effects of carbamazepine in individuals who also take CYP3A4 inhibitors [61].

The most serious toxicities associated with carbamazepine use are idiosyncratic skin rashes, hematological disorders, hepatotoxicity and teratogenicity [59]. Based on studies in mice, teratogenicity is most likely related to formation of arene oxide and/or quinone-like metabolites of carbamazepine [62], and studies in humans suggest that a reactive iminoquinone of 2-hydroxystilbene is formed [63]. It is known that coadministration of cytochrome P450 inducers (e.g., phenobarbital) with carbamazepine increases the risk of serious toxic effects [64–66].

### 2. Phenytoin

Phenytoin, like carbamazepine, causes dose-related neurological toxicities [67]. Since phenytoin is cleared mostly via CYP2C9 and CYP2C19 aromatic oxidation to *p*-hydroxyphenytoin [68], inhibitors of CYP2C9 (e.g., pyrazole nonsteroidal antiinflammatory agents, some azole antifungal agents, amiodarone, isoniazid, and sulfa drugs) and inhibitors of CYP2C19 (e.g., cimetidine, felbamate, omeprazole, and ticlopidine) can increase concentrations of phenytoin and increase the incidence of CNS-related toxicities [61].

As with carbamazepine, phenytoin also causes idiosyncratic toxic effects, including hematological and connective tissue toxicities, hepatotoxicity, and tera-

togenicity [67]. Although some of these toxicities have been hypothesized to be caused by P450 oxidative metabolism [69–70] or peroxidase-mediated reactions [71–72], mechanisms for these toxic effects in humans are unknown.

### 3. Valproic Acid

The two most serious toxic effects of valproic acid are hepatocellular injury [73] and teratogenesis [74]. Since CYP2A6 and CYP2C9 are known to oxidize valproic acid to a 4-ene metabolite that is hepatotoxic, inducers of these isoforms, including other antiepileptic agents, are likely to increase the risk of hepatotoxicity [75]. However, valproic acid also is metabolized by several other pathways that may be involved in causing its toxicities [76].

## M. Antineoplastic Agents

Several drugs used to treat cancer are metabolized by cytochromes P450, and it would be anticipated that if the parent drug were the cytotoxic species, inhibition of its metabolism would enhance cytotoxicity, which could either be beneficial if controlled or cause severe toxicity to bone marrow, the nervous system, etc., if concentrations of the parent drug became too high [77].

Alternatively, P450 inducers may decrease therapeutic effectiveness of the drugs [78]. Interestingly, only a few cases of toxicities to patients due to such drug–drug interactions have been reported, probably because most chemotherapy regimens are administered until some undesired toxic effect (e.g., leukopenia) limits the dosing. CYP3A isoforms appear to play the most significant role in the metabolism of many of the drugs (including paclitaxel, docetaxel, vincristine, vinblastine, etoposide, teniposide, cyclophosphamide, and tamoxifen), and in many cases P-glycoprotein transport is also affected [79]. For example, (*R*)-verapamil is an inhibitor both of CYP3A isoforms and of P-glycoprotein, and it significantly reduces the clearance and increases the hematological toxicity of paclitaxel [80]. The same reasoning applies to cases of severe neurotoxicity when itraconazole is administered with vincristine [81,82].

## III. DRUGS AND CLASSES OF DRUGS AS OBJECTS (VICTIMS) OF NONCYTOCHROME P450-MEDIATED PHASE I DRUG–DRUG INTERACTIONS THAT LEAD TO TOXICITIES

### A. Antidepressant Serotonergic Drugs and Sympathomimetics

These two classes of drugs are subject to life-threatening interactions (e.g., mania, convulsions, hypertension, heart arrhythmias) with MAO inhibitors, such as iso-

carboxazide, phenelzine, selegiline, and tranylcypromine, because they inhibit the metabolism of serotonin and sympathomimetic amines [11,83]. This is one of the earliest toxic drug–drug interactions to be recognized; however, these interactions are not often observed because the MAO inhibitors are now used sparingly.

## B. Digoxin

Digoxin is a narrow therapeutic index drug whose primary drug–drug interactions appear to involve the P-glycoprotein transporter [84]. An additional drug–drug interaction may occur at the level of reduction of the lactone ring double bond by intestinal microbial reductases that yields an inactive metabolite. Some antibiotic drugs can kill these microbes and lead to increases in digoxin concentrations [85].

## C. Arylamine Sulfonamides and Hydrazine Drugs

Several of these drugs can cause immune-mediated idiosyncratic toxicities, such as immune hemolysis, agranulocytosis, aplastic anemia, drug-induced lupus, and severe skin rashes [86,87]. It is well known that for most drugs in these classes acetylation of the amine or hydrazine group protects against the toxic effects based on significantly higher incidences of toxicity in individuals that genetically are slow acetylators [88]. However, there are no reported drug–drug interactions with the *N*-acetyltransferases. Oxidation products of the arylamino or hydrazine groups are implicated as the haptenic reactive metabolites [86–94], and both cytochromes P450 and peroxidases have been implicated in the oxidation process [87,92,93]. Although it might be anticipated that inducers and inhibitors of these enzymes would affect toxicities associated with the drugs, no reports of such drug–drug interactions on toxicity have appeared. The idiosyncratic nature of the toxicities make them very difficult to study.

## D. 6-Mercaptopurine and Azathioprine

Both of these drugs are metabolized by xanthine oxidase, and concomitant administration of the xanthine oxidase inhibitor allopurinol leads to elevated plasma concentrations of 6-mercaptopurine that can cause significant bone marrow depression [95,96].

## IV. DRUG–DRUG INTERACTIONS WITH PHASE II METABOLIC ENZYMES THAT LEAD TO TOXICITIES

There are only a few published reports of serious toxicities caused by drugs as a result of drug–drug interactions with Phase II metabolic enzymes. This in part

may reflect less attention given to these enzymes and/or lesser extents of induction and inhibition of these enzymes by drugs (Chap. 4).

In addition to being cleared by xanthine oxidase (see Sec. III.D), 6-mercaptopurine, is cleared by *S*-methylation catalyzed by the genetically polymorphic thiopurine methyltransferase [97]. This enzyme is inhibited by the drug sulfasalazine, leading to bone marrow suppression as a result of increased 6-mercaptopurine concentrations [98,99].

Valproic acid is extensively glucuronidated, and the coadministration of valproate with other drugs eliminated extensively by glucuronidation, such as lamotrigine [100] and zidovudine [101] can significantly decrease the clearance of these latter two drugs with resultant toxicities. Sertraline has been found to cause a similar effect with lamotrigine [102], and fluconazole with zidovudine [101].

## **V. DRUG-DRUG INTERACTIONS THAT AFFECT HEPATOTOXICITY CAUSED BY ACETAMINOPHEN: A COMPLEX EXAMPLE**

Acetaminophen is a widely used analgesic-antipyretic agent, and several instances of drug interactions have been reported [103]. However, in only a few cases have these interactions apparently increased the risk of hepatotoxicity, the major serious toxicity observed in humans who ingest this drug [104]. In part, this may be a consequence of multiple pathways of metabolism for acetaminophen and in part because relatively high concentrations of the drug ( $>1$  mM) are usually required to cause hepatotoxicity, which is an order of magnitude greater than therapeutic concentrations.

The major toxic metabolite of acetaminophen is *N*-acetyl-*p*-benzoquinone imine (NAPQI), which is an oxidation product formed by several human cytochromes P450 (for a review see Ref. 104). Therefore, it would be anticipated that inducers of cytochromes P450 would increase the rate of formation of NAPQI and thereby increase the risk for hepatotoxicity. Surprisingly, only a few cases of hepatotoxicity, caused by the use of normal doses of acetaminophen in patients on anticonvulsant drugs that are inducers of cytochromes P450, have been reported [105–107]. This may be due to the ability of these same drugs to induce glucuronosyl transferases, which would increase the formation of acetaminophen glucuronide, a nontoxic metabolite [108,109].

Human CYP2E1 is one of the most efficient P450s to catalyze the oxidation of acetaminophen to NAPQI [110–112]. Ethanol and isoniazid cause a time-dependent inhibition and induction of acetaminophen oxidation to NAPQI in humans [113,114] that can decrease risk for hepatotoxicity over the interval of concurrent administration and increase risk for hepatotoxicity a few hours after removal of ethanol or isoniazid. The latter induction phase of CYP2E1 may in

part be responsible for cases of acetaminophen hepatotoxicity associated with the use of ethanol [115–118] or isoniazid [119–121]. However, the induction is modest (2–3-fold); therefore, other factors, such as decreased glutathione stores and nutritional status, are likely to play an important role as well [122–124].

## VI. SUMMARY

Toxicities caused by drugs often limit their usefulness, and drug–drug interactions can cause enough of a change in tissue concentrations of some drugs, particularly those with a narrow therapeutic index, to cause serious toxic effects. Most of these interactions occur at the level of metabolism, though interactions with transporters, such as P-glycoprotein, are also becoming better recognized.

Unfortunately, we still do not have a good enough understanding either of the metabolism of some drugs or of mechanisms of toxicity (particularly immune-mediated idiosyncratic toxicities) to be able to predict whether or not a drug will cause toxic effects and under what conditions. For example, several nonsteroidal anti-inflammatory drugs have caused idiosyncratic toxicities that may be related to acyl glucuronide formation and/or cytochrome P450 activation [125–127]. Therefore, it would be anticipated that other drugs that affect these pathways might either increase or decrease the risk of toxicities, but no data is available because of the idiosyncratic nature of the toxicities and lack of understanding of immune-mediated mechanisms of drug-induced toxicity. The same reasoning applies to hepatic injury caused by the recently released drugs trovofloxacin [128] and troglitazone [129]. There is very little published information about whether it is the drugs themselves or their metabolites that are responsible for the observed toxicity.

On the other hand, in cases like that of mibefradil, the basic science of drug–drug interactions has progressed enough to make informed benefit/risk decisions. Thus, it is important to continue basic and clinical investigations of drug–drug interactions as well as studies of mechanisms of toxicity to effect safer drug therapy.

## REFERENCES

1. G Levy. What are narrow therapeutic index drugs? *Clin Pharmacol Ther* 63:501–505, 1998.
2. LZ Benet, JE Goyan. Bioequivalence and narrow therapeutic index drugs. *Pharmacotherapy* 15:433–440, 1995.
3. RL Williams. FDA position on product selection for “narrow therapeutic index” drugs. *Am J Health Syst Pharm* 54:1630–1632, 1997.

4. JO Miners, DJ Birkett. Cytochrome P4502C9: an enzyme of major importance in human drug metabolism. *Brit J Clin Pharmacol* 45:525–538, 1998.
5. WF Trager. Oral anticoagulants: In: RH Levy, KE Thummel, WF Trager, PD Hansten, M Eichelbaum, eds. *Metabolic Drug Interactions*. Philadelphia: Lippincott Williams and Wilkins, 2000, pp 403–413.
6. AE Rettie, KR Korzekwa, KL Kunze, RL Lawrence, AC Eddy, T Aoyama, HV Gelboin, FJ Gonzalez, WF Trager. Hydroxylation of warfarin by human cDNA-expressed cytochrome P450: a role for P-4502C9 in the etiology of (S)-warfarin-drug interactions. *Chem Res Toxicol* 5:54–59, 1992.
7. LD Heimark, M Gibaldi, WF Trager, RA O'Reilly, DA Goulart. The mechanism of the warfarin-rifampin drug interaction in humans. *Clin Pharmacol Ther* 42:388–394, 1987.
8. JS Cropp, HI Bussey. A review of enzyme induction of warfarin metabolism with recommendations for patient management. *Pharmacotherapy* 17:917–928, 1997.
9. I Niopas, S Toon, M Rowland. Further insight into the stereoselective interaction between warfarin and cimetidine in man. *Br J Clin Pharmacol* 32:508–511, 1991.
10. S Toon, KJ Hopkins, FM Garstang, M Rowland. Comparative effects of ranitidine and cimetidine on the pharmacokinetics and pharmacodynamics of warfarin in man. *Eur J Clin Pharmacol* 32:165–172, 1987.
11. PD Hansten, JR Horn. *Hansten and Horn's Drug Interactions Analysis and Management*. St. Louis: Facts and Comparisons, 1999.
12. R Lodwick, B McConkey, AM Brown. Life-threatening interaction between tamoxifen and warfarin. *Brit Med J* 295:1141, 1987.
13. P Tenni, DL Lalich, MJ Byrne. Life-threatening interaction between tamoxifen and warfarin. *Brit Med J* 298:93, 1989.
14. DJ Birkett, JO Miners. Methylxanthines. In: RH Levy, KE Thummel, WF Trager, PD Hansten, M Eichelbaum, eds. *Metabolic Drug Interactions*. Philadelphia: Lippincott Williams and Wilkins, 2000, pp 469–482.
15. JJ Grygiel, DJ Birkett. Cigarette smoking and theophylline clearance and metabolism. *Clin Pharmacol Ther* 30:491–496, 1981.
16. M Gibaldi. *Gibaldi's Drug Therapy 2000*. New York: McGraw-Hill, 2000, p 120.
17. DD Shen, S Madani, C Banfield, RP Clement. H<sub>1</sub>-Receptor Antagonists. In: RH Levy, KE Thummel, WF Trager, PD Hansten, M Eichelbaum, eds. *Metabolic Drug Interactions*. Philadelphia: Lippincott Williams and Wilkins, 2000, pp 435–446.
18. BP Monahan, CL Ferguson, ES Killeavy, BK Lloyd, J Troy, LR Cantilena Jr. Torsades des pointes occurring in association with terfenadine use. *J Am Med Assoc* 264:2788–2790, 1990.
19. PK Honig, DC Wortham, K Zamani, LR Cantilena. Comparison of the effect of macrolide antibiotics erythromycin, clarithromycin and azithromycin on terfenadine steady-state pharmacokinetics and electrocardiographic parameters. *Drug Invest* 7:148–156, 1994.
20. RL Woosley, Y Chen, JP Freiman, RA Gillis. Mechanism of the cardiotoxic actions of terfenadine. *J Am Med Assoc* 269:1532–1536, 1993.
21. RL Woosley. Cardiac actions of antihistamines. *Annu Rev Pharmacol Toxicol* 36:233–252, 1996.

22. JE Henney. Withdrawal of troglitazone and cisapride. *J Am Med Assoc* 283:2228, 2000.
23. TA Bedford, DJ Rowbotham. Cisapride: drug interactions of clinical significance. *Drug Safety* 15:167-175, 1996.
24. AS Gross, YD Goh, RS Addison, GM Shenfield. Influence of grapefruit juice on cisapride pharmacokinetics. *Clin Pharmacol Ther* 65:395-401, 1999.
25. MF Hebert. Immunosuppressive Agents. In: RH Levy, KE Thummel, WF Trager, PD Hansten, M Eichelbaum, eds. *Metabolic Drug Interactions*. Philadelphia: Lippincott Williams and Wilkins, 2000, pp 499-510.
26. KS Lown, RR Mayo, AB Leichtman. Role of intestinal P-glycoprotein (mdr1) in interpatient variation in the oral bioavailability of cyclosporine. *Clin Pharmacol Ther* 62:1-13, 1997.
27. MR First, TJ Schroeder, P Weiskittel, SA Myre, JW Alexander, AJ Pesce. Concomitant administration of cyclosporin and ketoconazole in renal transplant recipients. *Lancet* 2:1198-1201, 1989.
28. Y Horsmans. Cholesterol-lowering agents and cardiac glycosides. In: RH Levy, KE Thummel, WF Trager, PD Hansten, M Eichelbaum, eds. *Metabolic Drug Interactions*. Philadelphia: Lippincott Williams and Wilkins, 2000, pp 379-390.
29. RJ Herman. Drug interactions and the statins. *Can Med Assoc J* 161:1281-1286, 1999.
30. RP Bermingham, TB Whitsitt, ML Smart, DP Nowak, RD Scalley. Rhabdomyolysis in a patient receiving the combination of cerivastatin and gemfibrozil. *Am J Health-Syst Pharm* 57:461-464, 2000.
31. JC Krayenbühl, S Vozeh, M Kando-Ostreicher, P Dayer. Drug-drug interactions of new active substances: mibefradil example. *Eur J Clin Pharmacol* 55:559-565, 1999.
32. MA Marcano. Selected drug interactions with the statins. *Pharmacy Times*, August 1999, pp 38-40.
33. DR Jones, SD Hall. Calcium Channel Blockers. In: RH Levy, KE Thummel, WF Trager, PD Hansten, M Eichelbaum, eds. *Metabolic Drug Interactions*. Philadelphia: Lippincott Williams and Wilkins, 2000, pp 333-345.
34. DJ Greenblatt, LL von Moltke. Sedative-hypnotic and anxiolytic agents. In: RH Levy, KE Thummel, WF Trager, PD Hansten, M Eichelbaum, eds. *Metabolic Drug Interactions*. Philadelphia: Lippincott Williams and Wilkins, 2000, pp 259-270.
35. A Hiller, KT Olkkola, P Isohanni, L Saarnivaara. Unconsciousness associated with midazolam and erythromycin. *Br J Anaesth* 65:826-828, 1990.
36. K Chiba, K Kobayashi. Antidepressants. In: RH Levy, KE Thummel, WF Trager, PD Hansten, M Eichelbaum, eds. *Metabolic Drug Interactions*. Philadelphia: Lippincott Williams and Wilkins, 2000, pp 233-243.
37. RF Bergstrom, AL Peyton, L Lemberger. Quantification and mechanism of the fluoxetine and tricyclic antidepressant interaction. *Clin Pharmacol Ther* 51:239-248, 1992.
38. SH Preskorn, J Alderman, M Chung, W Harrison, M Hessig, S Harris. Pharmacokinetics of desipramine coadministered with sertraline and fluoxetine. *J Clin Psychopharmacol* 14:90-98, 1994.



39. LJ Cohen, CL DeVane. Clinical implications of antidepressant pharmacokinetics and pharmacogenetics. *Ann Pharmacother* 3:1471–1480, 1996.
40. K Brøsen, JG Hansen, KK Nielsen, SH Sindrup, LF Gram. Inhibition by paroxetine of desipramine metabolism in extensive but not poor metabolizers of sparteine. *Eur J Clin Pharmacol* 44:349–355, 1993.
41. M Eichelbam, AS Gross. The genetic polymorphism of debrisoquin/sparteine metabolism—clinical aspects. *Pharmacol Ther* 46:377–394, 1990.
42. MS Lennard.  $\beta$ -Adrenoceptor antagonists. In: RH Levy, KE Thummel, WF Trager, PD Hansten, M Eichelbaum, eds. *Metabolic Drug Interactions*. Philadelphia: Lippincott Williams and Wilkins, 2000, pp 347–358.
43. MS Lennard, GT Tucker, JH Silas, HF Woods. Debrisoquine polymorphism and the metabolism and action of metoprolol, timolol, propranolol and atenolol. *Xenobiotica* 16:435–437, 1986.
44. LJ Lesko. Pharmacokinetic drug interactions with amiodarone. *Clin Pharmacokin* 17:130–140, 1989.
45. NR Loon, CS Wilcox, W Folger. Orthostatic hypotension due to quinidine and propranolol. *Am J Med* 81:1101–1104, 1986.
46. F Wagner, D Kalushce, D Trenk, E Jahnchen, H Roskamm. Drug interaction between propafenone and metoprolol. *Br J Clin Pharmacol* 24:213–220, 1987.
47. WM Drake, GD Gordon. Heart block in a patient on propranolol and fluoxetine. *Lancet* 343:425, 1994.
48. BA Hamelin, A Bouayad, J Methót, J Jobin, P Desgagnés, P Poirier, J Allaire, J Dumesnil, J Turgeon. Significant interaction between the nonprescription antihistamine diphenhydramine and the CYP2D6 substrate metoprolol in healthy men with low or high CYP2D6 activity. *Clin Pharmacol Ther* 67:466–477, 2000.
49. ED Kharasch, AE Ibrahim. Volatile, intravenous, and local anesthetics. In: RH Levy, KE Thummel, WF Trager, PD Hansten, M Eichelbaum, eds. *Metabolic Drug Interactions*. Philadelphia: Lippincott Williams and Wilkins, 2000, pp. 271–295.
50. LR Pohl, H Satoh, DD Christ, JG Kenna. The immunologic and metabolic basis of drug hypersensitivities. *Annu Rev Pharmacol Toxicol* 28:367–387, 1988.
51. LR Pohl. An immunochemical approach to identifying and characterizing protein targets of toxic reactive metabolites. *Chem Res Toxicol* 6:786–793, 1993.
52. M Bourdi, W Chen, R Peter, JL Martin, JTM Buters, SD Nelson, LR Pohl. Human cytochrome P450 2E1 is a major autoantigen associated with halothane hepatitis. *Chem Res Toxicol* 9:1159–1166, 1996.
53. D O’Shea, SN Davis, RB Kim, GR Wilkensen. Effect of fasting and obesity in humans on the 6-hydroxylation of chlorzoxazone, a putative probe of CYP2E1 activity. *Clin Pharmacol Ther* 56:359–367, 1994.
54. MJ Cousins, JL Plummer, PM Hall. Risk factors for halothane hepatitis. *Aust NZ J Surg* 59:5–14, 1989.
55. JB Bentley, RW Vaughan, AJ Gandolfi, RC Cook. Halothane biotransformation in obese and nonobese patients. *Anesthesiology* 57:94–97, 1982.
56. ED Kharasch, D Hankins, D Mautz, KE Thummel. Identification of the enzyme responsible for oxidative halothane metabolism: implications for prevention of halothane hepatitis. *Lancet* 347:1367–1371, 1996.

57. JB Siegmund, JH Wilson, TE Imhoff. Amiodarone interaction with lidocaine. *J Cardiovasc Pharmacol* 21:513-515, 1993.
58. HR Ha, R Candinas, B Steiger, UA Meyer, F Follath. Interaction between amiodarone and lidocaine. *J Cardiovasc Pharmacol* 21:533-539, 1996.
59. GL Holmes. Carbamazepine toxicity. In: RH Levy, RH Mattson, BS Meldrum, eds. *Antiepileptic Drugs*. 4th ed. New York: Raven Press, 1995, pp 567-579.
60. BM Kerr, KE Thummel, CJ Wurden. Human liver carbamazepine metabolism. Role of CYP3A4 and CYP2C8 in 10,11-epoxide formation. *Biochem Pharmacol* 47: 1969-1979, 1994.
61. GG Mather, RH Levy. Anticonvulsants. In: RH Levy, KE Thummel, WF Trager, PD Hansten, M Eichelbaum, eds. *Metabolic Drug Interactions*. Philadelphia: Lippincott Williams and Wilkins, 2000, pp 217-232.
62. BM Amore, TF Kalhorn, GL Skiles, AP Hunter, GD Bennett, RH Finnell, SD Nelson, JT Slattery. Characterization of carbamazepine metabolism in a mouse model of carbamazepine teratogenicity. *Drug Metab Dispos* 25:953-962, 1997.
63. C Ju, JP Uetrecht. Detection of 2-hydroxy iminostilbene in the urine of patients taking carbamazepine and its oxidation to a reactive iminoquinone intermediate. *J Pharmacol Exp Ther* 288:51-56, 1999.
64. D Lindhout, RJA Hoppener, H Meinardi. Teratogenicity of antiepileptic drug combinations with special emphasis on epoxidation of carbamazepine. *Epilepsia* 25:77-83, 1984.
65. S Kaneko, K Otani, Y Fukushima, Y Ogawa, Y Nomura, T Ono, Y Makane, T Teranishi, M Goto. Teratogenicity of antiepileptic drugs: analysis of possible risk factors. *Epilepsia* 29:459-467, 1988.
66. JGC Omzigt, FJ Los, JWA Meijer, D Lindhout. The 10,11-epoxide-10,11-diol pathway of carbamazepine in early pregnancy in maternal serum, urine, and amniotic fluid: effect of dose, comedication, and relation to outcome of pregnancy. *Ther Drug Monit* 15:1-10, 1993.
67. J Bruni. Phenytoin toxicity. In: RH Levy, RH Mattson, BS Meldrum, eds. *Antiepileptic Drugs*. 4th ed. New York: Raven Press, 1995, pp 345-350.
68. M Bajpai, LK Roskos, DD Shen, RH Levy. Roles of cytochrome P4502C9 and cytochrome P4502C19 in the stereoselective metabolism of phenytoin to its major metabolite. *Drug Metab Dispos* 24:1401-1403, 1996.
69. JS Leeder, RJ Riley, J Cook, S Spielberg. Human anti-cytochrome P450 antibodies in aromatic anticonvulsant induced hypersensitivity reactions. *J Pharmacol Exp Ther* 263:360-366, 1992.
70. LX Zhou, B Pihlstrom, JP Hardwick, SS Park, SA Wrighton, JL Holtzman. Metabolism of phenytoin by the gingiva of normal humans: the possible role of reactive metabolites of phenytoin in the initiation of gingival hyperplasia. *Clin Pharmacol Ther* 60:191-198, 1996.
71. S Kubow and P Wells. In vitro bioactivation of phenytoin to a reactive free radical intermediate by prostaglandin synthase, horseradish peroxidase and thyroid peroxidase. *Mol Pharmacol* 35:1-8, 1989.
72. J Uetrecht. Drug metabolism by leukocytes and its role in drug-induced lupus and other idiosyncratic drug reactions. *Toxicology* 20:213-235, 1990.
73. DJ Porubek, MP Grillo, RK Olsen, TA Baillie. Toxic metabolites of valproic acid:

- inhibition of rat liver acetoacetyl-CoA thiolase by 2-*n*-propyl-4-pentenoic acid ( $\Delta^4$ -VPA) and related branched chain carboxylic acids. In: RH Levy, JK Penry, eds. *Idiosyncratic Reactions to Valproate: Clinical Risk Patterns and Mechanisms of Toxicity*. New York: Raven Press, 1991, pp 53–58.
74. U Bojic, MMA Elmazaar, R-S Hauck, H Nau. Further branching of valproate-related carboxylic acids reduces the teratogenic activity, but not anticonvulsant effect. *Chem Res Toxicol* 9:866–870, 1996.
  75. AJM Sadeque, MB Fisher, KR Korzekwa, FJ Gonzalez, AE Rettie. Human CYP2C9 and CYP2A6 mediate formation of the hepatotoxin 4-ene-valproic acid. *J Pharmacol Exp Ther* 283:698–703, 1997.
  76. TA Baillie, PR Sheffels. Valproic acid chemistry and biotransformation. In: RH Levy, RH Mattson, BS Meldrum, eds. *Antiepileptic Drugs*, 4th ed. New York: Raven Press, 1995, pp 589–604.
  77. HL McLeod. Clinically relevant drug–drug interactions in oncology. *Brit J Clin Pharmacol* 45:539–544, 1998.
  78. MV Relling, C-H Pui, JT Sandlund, GK Rivera, ML Hancock, JM Beyett, EG Schuetz, WE Evans. Adverse effect of anticonvulsants on efficacy of chemotherapy for acute lymphoblastic leukemia. *Lancet* 356:285–290, 2000.
  79. JB Mangold, V Fischer. Antineoplastic agents. In: RH Levy, KE Thummel, WF Trager, PD Hansten, M Eichelbaum, eds. *Metabolic Drug Interactions*. Philadelphia: Lippincott Williams and Wilkins, 2000, pp 545–554.
  80. AW Tolcher, KH Cowan, D Solomon. Phase I crossover study of paclitaxel with *R*-verapamil in patients with metastatic breast cancer. *J Clin Oncol* 14:1173–1184, 1996.
  81. A Böhme, A Ganser, D Hoelzer. Aggravation of vincristine-induced neurotoxicity by itraconazole in the treatment of adult ALL. *Ann Hematol* 71:311–312, 1995.
  82. J Gillies, KA Hung, E Fitzsimons, R Soutar. Severe vincristine toxicity in combination with itraconazole. *Clin Lab Haematol* 20:123–124, 1998.
  83. MU Shad, SH Preskorn. Antidepressants. In: RH Levy, KE Thummel, WF Trager, PD Hansten, M Eichelbaum, eds. *Metabolic Drug Interactions*. Philadelphia: Lippincott Williams and Wilkins, 2000, pp 563–577.
  84. JA Silverman. P-Glycoprotein. In: RH Levy, KE Thummel, WF Trager, PD Hansten, M Eichelbaum, eds. *Metabolic Drug Interactions*. Philadelphia: Lippincott Williams and Wilkins, 2000, pp 135–144.
  85. J Lindenbaum, DG Rund, VP Butler Jr, D Tse-Eng, JR Saha. Inactivation of digoxin by the gut flora: reversal by antibiotic therapy. *N Engl J Med* 305:789–794, 1981.
  86. BK Park, NR Kitteringham. Drug–protein conjugation and its immunological consequences. *Drug Metab Rev* 22:87–144, 1990.
  87. J Uetrecht. Drug metabolism by leukocytes and its role in drug-induced lupus and other idiosyncratic drug reactions. *Crit Rev Toxicol* 20:213–235, 1990.
  88. UA Meyer. Molecular mechanisms of genetic polymorphisms. *Annu Rev Pharmacol Toxicol* 37:269–296, 1997.
  89. M Bourdi, M Tinel, PH Beaune, D Pessayre. Interactions of dihydralazine with cytochromes P4501A: a possible explanation for the appearance of anti-cytochrome P4501A2 autoantibodies. *Mol Pharmacol*. 45:1287–1295, 1994.
  90. AE Cribb, BL Lee, LA Trepanier, SP Spielberg. Adverse reactions to sulphonamide

- and sulphonamide-trimethoprim antimicrobials: clinical syndromes and pathogenesis. *Adverse Drug Reactions Toxicol Rev* 15:9-50, 1996.
91. TP Reilly, PM Woster, CK Svensson. Methemoglobin formation by hydroxylamine metabolites of sulfamethoxazole and dapsone: implications for differences in adverse drug reactions. *J Pharmacol Exp Ther* 288:951-959, 1999.
  92. RE Bluhm, A Adedoyin, DG McCarver, RA Branch. Development of dapsone toxicity in patients with inflammatory dermatoses: activity of acetylation and hydroxylation as risk factors. *Clin Pharmacol Ther* 65:598-605, 1999.
  93. HJ Gill, MD Tingle, BK Park. *N*-Hydroxylation of dapsone by multiple enzymes of cytochrome P450: implications for inhibition of haemotoxicity. *Br J Clin Pharmacol* 40:531-538, 1995.
  94. M Pirmohamed, S Madden, BK Park. Idiosyncratic drug reactions: metabolic bioactivation as a pathogenic mechanism. *Clin Pharmacokin* 31:215-230, 1996.
  95. DG Poplack, FM Balis, S Zimm. The pharmacology of orally administered chemotherapy. A reappraisal. *Cancer* 58:473-480, 1986.
  96. DT Kennedy, MS Hayney, KD Lake. Azathioprine and allopurinol: the price of an avoidable drug interaction. *Ann Pharmacother* 30:951-954, 1996.
  97. RM Winshelbom, SL Sladek. Mercaptopurine pharmacogenetics: monogenic inheritance of erythrocyte thiopurine methyltransferase activity. *Am J Hum Genet* 32:651-662, 1980.
  98. C Szumlanski, RM Winshelbom. Sulphasalazine inhibition of thiopurine methyltransferase: possible mechanism for interaction with 6-mercaptopurine and azathioprine. *Br J Clin Pharmacol* 39:456-459, 1995.
  99. LD Lewis, A Benin, C Szumlanski. Olsalazine and 6-mercaptopurine-related hematologic suppression: a possible drug-drug interaction. *Clin Pharmacol Ther* 62:464-475, 1997.
  100. AW Yuen, G Land, BC Weatherley, AW Peck. Sodium valproate acutely inhibits lamotrigine metabolism. *Br J Clin Pharmacol* 33:511-513, 1992.
  101. CB Trapnell, RW Klecker, C Jamis-Dow, JM Collins. Glucuronidation of 3'-azido-3'-deoxythymidine (zidovudine) by human liver microsomes: relevance to clinical pharmacokinetic interactions with atovaquone, fluconazole, methadone, and valproic acid. *Antimicrob Agents Chemother* 42:1592-1596, 1998.
  102. KR Kaufman, R Gerner. Lamotrigine toxicity secondary to sertraline. *Seizure* 7:163-165, 1998.
  103. LF Prescott. Paracetamol (Acetaminophen): A Critical Bibliographic Review. London: Taylor and Francis, 1996.
  104. SD Nelson. Analgesic-antipyretics. In: RH Levy, KE Thummel, WF Trager, PD Hansten, M Eichelbaum, eds. *Metabolic Drug Interactions*. Philadelphia: Lippincott Williams and Wilkins, 2000, pp 447-455.
  105. JN Wright, LF Prescott. Potentiation by previous drug therapy of hepatotoxicity following paracetamol overdose. *Scott Med J* 18:56-58, 1973.
  106. JT Wilson, V Kasantikul, R Harbison, D Martin. Death in an adolescent following an overdose of acetaminophen and phenobarbital. *Am J Dis Child* 132:466-473, 1978.
  107. NA Minton, JA Henry, RJ Frankel. Fatal paracetamol poisoning in an epileptic. *Hum Toxicol* 7:33-34, 1988.

108. JO Miners, J Atwood, DJ Birkett. Determinants of acetaminophen metabolism: effects of inducers and inhibitors of drug metabolism on acetaminophen's metabolic pathways. *Clin Pharmacol Ther* 35:480–486, 1984.
109. LF Prescott, JAJH Critchley, M Bulali-Mood, B Pentland. Effects of microsomal enzyme induction on paracetamol metabolism in man. *Br J Clin Pharmacol* 12: 149–153, 1981.
110. JL Raucy, JM Lasker, CS Lieber, M Black. Acetaminophen activation by human liver cytochromes P450IIE1 and P450IA2. *Arch Biochem Biophys* 271:270–283, 1989.
111. CJ Patten, PE Thomas, RL Guy, ML Lee, FJ Gonzalez, FP Guengerich, CS Yang. Cytochrome P450 enzymes involved in acetaminophen activation by rat and human liver microsomes and their kinetics. *Chem Res Toxicol* 6:511–518, 1993.
112. W Chen, LL Koenigs, SJ Thompson, RM Peter, AE Rettie, WF Trager, SD Nelson. Oxidation of acetaminophen to its toxic quinone imine and nontoxic catechol metabolites by baculovirus-expressed and purified human cytochromes P4502E1 and 2A6. *Chem Res Toxicol* 11:295–301, 1998.
113. KE Thummel, JT Slattery, H Ro, JY Chien, SD Nelson, KE Lown, PB Watkins. Ethanol and production of the hepatotoxic metabolite of acetaminophen in healthy adults. *Clin Pharmacol Ther* 67:591–599, 2000.
114. R Zand, SD Nelson, JT Slattery, KE Thummel, TF Kalhorn, SP Adams, JM Wright. Inhibition and induction of cytochrome P450 2E1 catalyzed acetaminophen oxidation by isoniazid in humans. *Clin Pharmacol Ther* 54:142–149, 1993.
115. CJ McClain, JP Kromhaut, FJ Peterson, JL Holtzman. Potentiation of acetaminophen hepatotoxicity by alcohol. *J Am Med Assoc* 244:251–253, 1980.
116. LB Seeff, BA Cuccherini, HJ Zimmerman, E Adler, SB Benjamin. Acetaminophen toxicity in the alcoholic: a therapeutic misadventure. *Ann Intern Med* 104:399–404, 1986.
117. HJ Zimmerman, WC Maddrey. Acetaminophen (paracetamol) hepatotoxicity with regular intake of alcohol: analysis of instances of therapeutic misadventure. *Hepatology* 22:762–777, 1995.
118. SC Johnston, LL Pelletier. Enhanced hepatotoxicity of acetaminophen in the alcoholic patient: two case reports and a review of the literature. *Medicine* 76:185–191, 1997.
119. R Murphy, R Scartz, PB Watkins. Severe acetaminophen toxicity in a patient receiving isoniazid. *Ann Intern Med* 113:799–800, 1990.
120. TS Moulding, AG Redeker, GC Kanel. Acetaminophen, isoniazid, and hepatic toxicity. *Ann Intern Med* 114:431, 1991.
121. CM Nolan, RE Sandblom, KE Thummel, JT Slattery, SD Nelson. Hepatotoxicity associated with acetaminophen usage in patients receiving multiple drug therapy for tuberculosis. *Chest* 105:408–411, 1994.
122. BH Lauterburg, ME Velez. Glutathione deficiency in alcoholics: risk factor for paracetamol hepatotoxicity. *Gut* 29:1153–1157, 1988.
123. DC Whitcomb, GD Block. Association of acetaminophen hepatotoxicity with fasting and ethanol use. *J Am Med Assoc* 272:1845–1850, 1994.
124. JT Slattery, SD Nelson, KE Thummel. The complex interaction between ethanol and acetaminophen. *Clin Pharmacol Ther* 60:241–246, 1996.

125. H Spahn-Langguth, LZ Benet. Acyl glucuronides revisited: Is the glucuronidation process a toxification as well as detoxification mechanism? *Drug Metab Rev* 24: 5–48, 1992.
126. S Shen, MR Davis, GA Doss, LR Pohl. Metabolic activation of diclofenac by human cytochrome P4503A4: role of 5-hydroxydiclofenac. *Chem Res Toxicol* 12: 214–222, 1999.
127. W Tang, RA Stearns, RW Wang, SHL Chiu, TA Baillie. Roles of human hepatic cytochrome P450s 2C9 and 3A4 in the metabolic activation of diclofenac. *Chem Res Toxicol* 12:192–199, 1999.
128. HJL Chen, KJ Boch, JA MacLean. Acute eosinophilic hepatitis from trovofloxacin. *N Eng J Med* 342:359–360, 2000.
129. The Pink Sheet, March 27, 2000, p 4.



# 17

## An Integrated Approach to Assessing Drug–Drug Interactions: A Regulatory Perspective

**Shiew-Mei Huang, Peter Honig, Lawrence J. Lesko, and Robert Temple**

*U.S. Food and Drug Administration, Rockville, Maryland*

**Roger Williams**

*U.S. Pharmacopeia, Rockville, Maryland*

### I. INTRODUCTION

Change in one or more safety and efficacy outcomes of a drug by concomitant administration of another drug that interacts with it has become of increasing interest in the last decade. This increased interest has arisen in part because of many documented adverse clinical consequences of drug–drug interactions, coupled with improved understanding as to their cause. Interest in drug–drug interactions has also increased because of the rise in polypharmacy, where patients may take many drugs in the course of a day. The following regimen would not be uncommon today in patients over 50 years of age: one or more antihypertensive agents, a lipid-lowering drug, a hypnotic, an antihistamine, an antidepressant, one or more oral hypoglycemics, several over-the-counter (OTC) agents, and, if the patient is female, hormone replacement therapy, possibly with another drug to prevent osteoporosis. Depending on various short-term conditions, an antibiotic, antifungal, antiarrhythmic, analgesic, antianginal, or platelet inhibitor might be added.

To avoid serious harm, health care practitioners must be aware of and manage potential important interactions. To provide optimum information in product labeling for practitioners and patients, drug development and regulatory scientists should work cooperatively to ensure that each approved new drug is well characterized with respect to its metabolic vulnerability as a substrate and its action as an inhibitor or inducer. Further, product labeling for older drugs should be up-



dated as additional information about their potential for manifesting important drug–drug interactions becomes available.

Pharmacokinetic drug–drug interactions result from alteration in the dose/systemic exposure relationship, as reflected in a blood or plasma concentration–time curve, when an interacting drug induces or inhibits one or more routes of elimination of a substrate drug. Inhibition of metabolism may be associated with increased blood levels and pharmacological activity of the substrate, but if the substrate is a prodrug, pharmacological activity may be reduced; in some cases, when the parent drug and its metabolite have equal effects, there may be no change in pharmacological activity despite large changes in blood levels of parent and metabolite (Chaps. 1 and 15). The magnitude of clinical effect of an inhibitor depends on the magnitude of the effect of the inhibitor on clearance of the substrate, which in turn depends on the extent of inhibition and the extent to which the substrate is cleared by the affected pathway. A well-known interacting drug is ketoconazole, a powerful inhibitor of cytochrome P450 3A4 metabolism that has recently also been shown to inhibit transport mechanisms [1]. Coadministration of ketoconazole or a similar drug, itraconazole, increases the blood levels of many drugs, including dihydropyridine calcium channel blockers, short-acting benzodiazepines, some HMG Co-A reductase inhibitors, astemizole, and cisapride [2–4]. Drugs that induce metabolic pathways and reduce systemic exposure may result in loss of effectiveness (Chaps. 1 and 6).

While most literature reports have focused on metabolic drug–drug interactions involving the cytochrome P450 enzyme systems, every possible clearance pathway for a substrate may be altered by an interacting drug, including active renal secretion, drug degradation in the gut, biliary excretion, and secretion based on cellular transport mechanisms (Chaps. 5 and 8). Examples include the inhibition of the renal tubular secretion of penicillins by probenecid, which results in major increases in penicillin blood levels [5], or the increase in digoxin blood levels by the coadministration of quinidine, presumably by the inhibition of digoxin renal tubular secretion through inhibition of the P-glycoprotein transporter [6]. While these nonmetabolic examples of drug–drug interactions may be common, clearance pathways by the cytochrome P450 enzymes of the liver and gut have proved especially vulnerable and are the focus of this chapter. Many of the drug–drug interactions that result in large (>50%) changes in exposure do so through inhibition or induction of cytochrome P450 enzymes in liver or gut.

Less commonly recognized than pharmacokinetic interactions—perhaps because fewer studies have been performed to detect them—are pharmacodynamic drug–drug interactions, changes in response to a drug caused by alteration in exposure/response relationships. This type of drug–drug interaction may arise when the substrate and interacting drug affect the same physiologic system or when one drug prevents an appropriate response to the other. As an example of the former, both organic nitrates and sildenafil inhibit NO-mediated vasoconstriction and together cause marked hypotension [7]. As an example of the latter,

marked hypotension was observed in patients switched from the calcium channel blocker mibefradil to a dihydropyridine calcium channel blocker, apparently because residual mibefradil inhibited the usual compensatory tachycardia caused by the dihydropyridine. The effect may have been exaggerated by the increased levels of the dihydropyridine resulting from mibefradil's inhibition of the CYP3A4 route of elimination [8]. Both pharmacokinetic and pharmacodynamic drug–drug interactions are not unexpected and should be considered when two or more drugs are administered concurrently.

In considering many drug development and public health policy issues, it is important to focus on: (1) what the primary question is; (2) what may be assumed in addressing the question based on prior knowledge; and (3) how much confidence is needed in the answer. For drug–drug interactions, the primary question is: Does the dose of a substrate drug need to be adjusted in the presence of the interacting drug? More specifically, is the pharmacokinetic and/or pharmacodynamic change in the substrate drug in the presence of the interacting drug of sufficient magnitude to require adjustment of the substrate dose (or avoidance of the interacting drug)? With respect to assumptions, if we are willing (as we frequently are) to assume that exposure/response relationships for the substrate drug are undisturbed in the presence of a pharmacokinetically interacting drug, then we can rely on systemic exposure pharmacokinetic measures such as AUC and  $C_{max}$  to determine whether the dose of the substrate needs to be altered in the presence of the interacting drug. Further, if we assume that the dose/systemic exposure and systemic exposure/response relationships in healthy subjects are altered in the same way they would be in patients (again, as we frequently do), then we can rely on pharmacokinetic studies in healthy individuals to determine whether the substrate dosage should be adjusted in patients in the presence of an interacting drug. Finally, how confident we need to be in the answer depends on the nature of interaction and the consequences of error. These questions relate importantly to the general goals of risk assessment (determination of whether an important drug–drug interaction is present), risk management (adjustment in the substrate dosing in the presence of the interacting drug), and risk communication (provision of a labeling statement to indicate how to manage the risk). In terms of risk management, the magnitude of the interaction may be so great or the effect of the interacting drug so pervasive that special actions may be required; e.g., one drug may be removed from the market, or labeling may state that the interacting drug and the substrate drug should not be given concurrently.

## II. METHODS TO ASSESS METABOLIC DRUG–DRUG INTERACTIONS

Assessment of a potential drug–drug interaction begins with an understanding of the absorption, distribution, and elimination processes for both substrate and

interacting drugs. Based on this information, the potential importance of one or more metabolic routes of elimination in contributing to a clinically important drug–drug interaction can be estimated. Even when a metabolic route is important to the elimination of a substrate and is affected by an interacting drug, additional studies may be needed to understand whether a metabolic drug–drug interaction has clinical impact. Various methods may be used to develop the requisite information, including *in vitro* studies, *in vivo* pharmacokinetic and pharmacodynamic studies, population pharmacokinetic studies, clinical safety and efficacy studies, and postmarketing observational studies. All of these approaches can generate useful information about potentially important drug–drug interactions, and each has special strengths and limitations. Many of these approaches are described in three recently published FDA guidances for industry [9–11]. Metabolic drug–drug interactions involving CYP3A4 may require special consideration because they may occur in the wall of the gastrointestinal tract and/or the liver. Interactions in the gastrointestinal tract can increase bioavailability, as reflected in  $C_{\max}$  and AUC, but may cause little or no effect on half-life. Interactions in the liver may have only a small effect on single-dose  $C_{\max}$  but may alter half-life and accumulation index. Interpretation of drug–drug interaction data is sometimes complicated when a substrate drug is actively transported from the serosal to the mucosal side of the gastrointestinal tract by transporters such as P-glycoprotein. Like CYP3A4, these transporters are subject to inhibition/induction.

### III. GENERAL APPROACHES

As discussed in Sec. II, early *in vitro* and *in vivo* investigations can enhance the quality and efficiency of drug development, in some cases fully addressing a question of interest, in others providing information to guide further studies (Chaps. 6 and 7). The early elucidation of drug metabolism, for example, permits *in vitro* investigations of drug–drug interaction that in turn provide information useful in guiding the clinical program and possibly avoiding some clinical studies. Metabolism data can also provide information on the relevance of preclinical metabolism and toxicological data and permit early identification of drugs that are likely to have large interindividual pharmacokinetic variability due to genetically determined polymorphisms in drug-metabolizing enzymes or drug–drug interactions. An integrated approach is most useful, one in which evidence for and against a drug–drug interaction is examined at all stages of drug development, including: (1) preclinical *in vitro* studies of drug metabolism and drug–drug interactions to determine which *in vivo* studies should be conducted; (2) early-phase *in vivo* studies to assess the most important potential drug–drug interactions sug-

gested by in vitro data; (3) late-phase drug development population pharmacokinetic studies to expand the range of potential interactions studied, including unexpected ones, and to allow examination of pharmacodynamic drug–drug interactions. The further sections of this chapter provide more specific information about these approaches.

### A. In Vitro Methodologies

Pharmaceutical sponsors now frequently conduct in vitro studies in the preclinical phase of drug development programs to assess the contribution of cytochrome P450 or other enzymes to the metabolic elimination of an investigational drug and the ability of an investigational drug to inhibit specific metabolic pathways. The utility of these studies has been enhanced by the availability of specific enzyme preparations, microsomal preparations, and liver cell preparations, together with standard substrates and inhibitors/inducers. Information from in vitro metabolic studies can suggest not only that a substrate drug is or is not likely to be a candidate for certain metabolic drug–drug interactions but also whether a drug's metabolism will be affected by genetic polymorphisms.

If a drug is not metabolized or its metabolism is not mediated by cytochrome P450 enzymes, in vivo metabolic drug interactions with P450 enzyme inhibitors and inducers are not needed. If a drug does not inhibit any of the P450 enzymes, in vivo interaction studies with P450 substrate are not needed. Detection of the involvement of certain metabolic pathways, notably CYP1A2, CYP3A4, CYP2D6, CYP2C9, and CYP2C19, from in vitro studies suggests the possibility of important drug–drug interactions and usually results in significant effort to detect and define them. Thus in vivo studies may be avoided through an in vitro study showing that an investigational drug metabolism is not affected by furafylline (CYP1A2), ketoconazole (CYP3A4), quinidine (CYP2D6), sulfaphenazole (CYP2C9) (no potential effect on the substrate) and that the drug does not affect the metabolism of caffeine (CYP1A2), midazolam (CYP3A4), dextromethorphan (2D6), *S*-warfarin (CYP2C9), or *S*-mephenytoin (2C19) (no potential inhibition/induction). An April 1997 FDA guidance for industry entitled *Drug Metabolism/Drug Interactions in the Drug Development Process: Studies in Vitro* [9] describes the techniques and approaches to in vitro study of metabolic-based drug–drug interactions, in vitro and in vivo correlations, the timing of these studies, and the labeling of drug products based on in vitro metabolism and drug–drug interaction data. This guidance emphasizes the value of in vitro studies in human biomaterials in ruling out important metabolic pathways in a drug's metabolism or the possibility of the drug's ability to affect certain enzyme systems. The guidance further notes, however, that in vitro studies cannot define the clinical importance of an observed effect of an interacting drug on other therapy or of other therapy on the drug.

Previous chapters have detailed the relative advantages and disadvantages of various *in vitro* techniques in providing information pertinent to drug–drug interactions. These include the following preparations:

1. Cellular-based *in vitro* models, such as isolated hepatocytes and precision-cut liver preparations
2. Subcellular elements, such as microsomes or S9 (cytosolic) fractions
3. Expressed human drug-metabolizing enzymes

These systems can be used to define a drug's metabolic pathway, to assess its potential to inhibit the metabolism of other drugs, and to determine whether other drugs influence its metabolism.

The complex interrelationship of cellular transport mechanisms and drug-metabolizing enzymes, particularly CYP3A, in mediating systemic drug availability and drug–drug interactions is under increasing study. P-Glycoprotein is the best-understood cellular transporter. It is abundantly present in the intestinal epithelium and serves as an efflux pump for a variety of drugs and xenobiotics. It is also highly expressed in bile canaliculi, the apical membrane of the renal tubule epithelium, and other tissues. Many inhibitors of P-glycoprotein also inhibit CYP3A metabolism, and many, although not all, substrates for CYP3A are also actively transported by P-glycoprotein. For this reason, the relative contribution of P450 and transporter effects to a drug–drug interaction may be difficult to quantify. *In vitro* models currently available allow investigation of transporter-mediated drug–drug interactions, including a human colon carcinoma cell line, Caco-2.

## **B. In Vitro–In Vivo Correlation**

A complete understanding of the relationship between *in vitro* findings and *in vivo* results of metabolism/drug–drug interaction studies is still emerging. Quantitative prediction of the magnitude of clinical drug–drug interactions based on *in vitro* methodologies has been the topic of numerous publications and is described in earlier chapters. Although excellent quantitative concordance of *in vitro* and *in vivo* results has been shown, in some cases *in vitro* data may also under- or overestimate the clinical effect [12], and at present an observed *in vitro* effect needs further elucidation in *in vivo* studies. The bases for *in vitro*/*in vivo* disassociations have been described and include: (1) irrelevant substrate concentrations and inappropriate *in vitro* model systems; (2) mechanism-based inhibition; (3) activation/induction phenomena; (4) physical-chemical effects on absorption; (5) parallel elimination pathways that decrease the importance of the *in vitro*–assessed pathway; and (6) modulation of an important cellular transport mechanism.

### C. Specific Clinical Investigations

If metabolism is an important mechanism of clearance and in vitro studies suggest that metabolic routes can be inhibited, or if they suggest the drug may inhibit important clearance pathways of other drugs, in vivo studies are needed to evaluate the extent of these potential interactions. A 1999 FDA guidance for industry entitled *In Vivo Drug Metabolism/Drug Interaction Studies—Study Design, Data Analysis and Recommendations for Dosing and Labeling* [10] provides recommendation on study design, study population, choice of interacting drugs, route of administration, dose selection, and statistical considerations for clinical drug–drug interaction studies. As with in vitro studies, in vivo studies can often use a screening approach involving probe drugs. For example, if ketoconazole, a powerful CYP3A4 inhibitor, does not have a significant effect on the pharmacokinetics of a drug with some evidence of CYP3A4 metabolism in vitro, further interaction studies with other CYP3A4 inhibitors are not necessary. Similarly, if the drug does not affect the pharmacokinetics of a sensitive CYP3A4 substrate, such as midazolam, it will not pose problems with other CYP3A4-metabolized drugs. Where interactions are found, the studies of probe drugs and other drugs will provide a basis for specific recommendations on product labeling as to what concomitant uses should be avoided or what dosage adjustments to make. A critical determination for substrate effects is the size of the effect, measured in the in vivo interaction study, and the importance of the effect. Thus a 50% increase in blood levels of a well-tolerated drug with little dose-related toxicity may require no dosage adjustment. The same degree of increase for a drug with a narrow therapeutic range might require careful adjustment in dose or avoidance of coadministration. The issues in the areas of study design and data analysis are discussed in more detail in the following section.

If in vitro studies and other information suggest a need for in vivo metabolic drug–drug interaction studies, the following general issues and approaches should be considered. Depending on the study objectives, the substrate and interacting drug may be investigational agents or approved products.

#### 1. Study Design

In general, interaction studies compare substrate levels with and without the interacting drug. Several different study designs have been used to study drug–drug interactions. Any may be suitable, depending on the specific objectives of the study and the desired outcome. The study may use a randomized crossover (Tables 1 and 2), a one-way (fixed sequence) crossover (Table 3), or a parallel design (Table 4). Depending on circumstances, the studies can use various durations of exposure for substrate and interacting drug: single dose/single dose, single dose/multiple dose, multiple dose/single dose, and multiple dose/multiple dose. The details of the study design depend upon a number of factors for both the substrate

**Table 1** Example of Randomized (Two-Way) Crossover Design

Sequence	Period 1	Period 2
1	S	S + ID
2	S + ID	S

S: substrate; ID: interacting drug.

and interacting drug, including: (1) pharmacokinetic and pharmacodynamic characteristics of the substrate and interacting drugs; (2) the need to assess induction as well as inhibition (induction generally needs longer study duration); and (3) safety considerations, including whether the substrate is likely to be a narrow therapeutic range (NTR) or non-NTR drug. In general, the inhibiting/inducing drugs and the substrates should be dosed so that the exposure of both drugs is relevant to their clinical use. The following specific examples may be useful in choosing among study designs.

a. A substrate drug intended for chronic administration should generally be given until steady state is attained, with assessment of pharmacokinetics over one or more dosing intervals followed by administration of the interacting drug, also given until steady-state concentration is reached, again with collection of pharmacokinetic data on the substrate. The studies of erythromycin–terfenadine and ketoconazole–terfenadine interactions in healthy volunteers [13–14] are examples of this one-way, or fixed-sequence, crossover design.

b. If the substrate drug has a long half-life and accumulates, the probability of seeing an effect may be enhanced by giving the substrate drug as a single dose while the interacting drug is given as multiple doses. One example of this design is the study of the effect of terfenadine on the pharmacokinetics of buspirone, a CYP3A4 substrate, where a randomized two-way crossover design was utilized [15]. Note that although sensitivity to detecting inhibitory effect may be

**Table 2** Example of Randomized (Three-Way) Crossover Design

Sequence	Period 1	Period 2	Period 3
1	S	S + ID	ID
2	S + ID	ID	S
3	ID	S	S + ID

S: substrate; ID: interacting drug.

**Table 3** Example of Fixed (One-Sequence) Crossover Design

Sequence	Period 1	Period 2
1	$S$	$S + ID$
2	$S$	$S + \text{placebo}$

$S$ : substrate; ID: interacting drug.

Sequence 2 (optional) can be used as a control to ensure that no time-dependent changes occur between periods 1 and 2; if this is already established, comparison of periods 1 and 2 within sequence 1 is used as a basis for the evaluation of an interaction.

increased, it could be argued that effect on steady-state  $C_{\max}$  and AUC is more relevant.

c. When the substrate has complex metabolism (e.g., a long-acting active metabolite) or the interacting drug has a long half-life or active metabolite, attainment of steady state may pose problems. Multiple-dose studies would generally be necessary to be sure that relevant metabolites can be assessed and that the relevant dose of the interacting drug is used, but special approaches may also be useful. For example, a loading dose of the potential inhibitor may allow relevant levels to be obtained more rapidly and selection of a one-way (fixed-sequence) crossover or a parallel design, rather than a randomized crossover study design, may also help. Using a one-way crossover design, a recent study [16] showed that multiple-dose administration of sertraline inhibited the clearance of desipramine to a considerably greater extent than did a single-dose administration (Fig. 1). The long half-lives and the nonlinear accumulation of sertraline and its desethyl metabolite, both of which are CYP2D6 inhibitors, appeared to have contributed to the higher exposure of these two components and thus greater inhibition effects after multiple dosing.

**Table 4** Example of Parallel Design

Sequence	Period 1
1	$S$
2	$S + ID$

$S$ : substrate; ID: interacting drug.



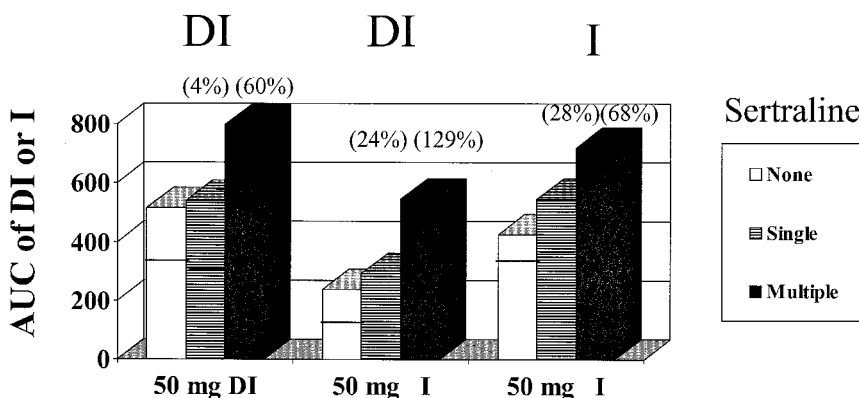


**Figure 1** AUC values of imipramine (I) or desipramine (DI) when 50 mg of I or DI was given with sertraline (150-mg single dose or 8 daily doses of 150 mg/day) and when given alone. The percent values shown indicate the percentage increase in the AUC values of DI or I when DI or I was given with sertraline as compared to when given alone. (Data from Ref. 16.)

d. The dosing duration depends on whether inhibition or induction is to be studied. Inducers may take several days or longer to exert their effects, while inhibitors generally exert their effects more rapidly. For this reason, a more extended period of exposure to interacting drug may be necessary if induction is to be assessed. The study design should also allow assessment of how long the inhibition or induction effect will last after an interacting drug has been removed from the dosing regimen. This can be observed in the randomized crossover design and in the one-sequence or parallel designs by adding an additional period in which the interacting drug is withdrawn. A recent publication [8] describing serious adverse events (including one death) observed when dihydropyridine calcium channel blockers (CYP3A4 substrates) were given to patients immediately after mibefradil (a CYP3A4 inhibitor) was withdrawn illustrates the importance of this consideration.

e. For an inhibitor drug that induces its own metabolism, a multiple-dose study design should be used so that the extent of interaction is not overestimated. Multiple doses of ritonavir have been shown to have smaller inhibitory effects on other CYP3A substrates [17–18] than a single dose. This may be partially explained by the lower exposure to ritonavir after multiple doses than after a single dose.

f. When a pharmacodynamic effect is also being measured, attainment of steady state for the parent or metabolite, whose pharmacodynamic effects are being measured, is important. In addition, inclusion of a period of the interacting

drug alone in the sequence (Table 2) is often advisable so that its contribution to the pharmacodynamic effects can be assessed. For example, erythromycin is known to prolong Q-T intervals at some doses. The assessment of Q-T interval change due to substrate accumulation resulting from erythromycin inhibition of CYP3A4 metabolism cannot be evaluated without an erythromycin-alone group to examine the effect of erythromycin in the population.

g. Studies can usually be open label (unblinded), unless pharmacodynamic endpoints (e.g., adverse events whose interpretation is potentially subject to bias) are part of the assessment of the interaction.

## 2. Study Population

Clinical drug–drug interaction studies can generally be performed in healthy volunteers unless safety considerations preclude their participation. Sometimes, use of subjects/patients for whom the substrate drug is intended offers advantages, including the opportunity to study pharmacodynamic endpoints not present in healthy subjects. If metabolic polymorphisms for a pathway being studied exist, the availability of genotype or phenotype information may be important, for inhibitors or inducers may have no effect or little effect in slow metabolizers, an observation that is particularly important for substrates eliminated by the CYP2D6, CYP2C9, and CYP2C19 pathways.

## 3. Choice of Substrates and Interacting Drugs

A recent survey [19] reviewed the interacting drugs used in 89 clinical drug interaction studies included in 14 New Drug Applications (NDAs) of new molecular entities to be marketed in oral, immediate-release formulations that were submitted to the FDA between December 1995 and November 1996. Forty-nine interacting drugs were used in these 89 studies. The most common substrates studied were digoxin (8 NDAs, or 57%), warfarin (7 NDAs, or 50%), oral contraceptives and nifedipine (4 NDAs each, or 28%), theophylline, terfenadine, and atenolol (3 NDAs each, 21%). The most commonly used interacting drug was cimetidine (7 NDAs, 50%). The selection of the substrates appeared to be based on whether coadministration was likely and the clinical consequences of an interaction, were there to be one, as well as past FDA guidance [20–21] that suggested a particular interest in digoxin, warfarin, and oral contraceptives. While past experience revealed a reasonable number of interactions with such drugs as digoxin and warfarin, the drugs used in these interaction studies generally did not indicate a clear understanding of interaction potential related to P450 enzyme inhibition. Improved understanding of the metabolic basis of drug–drug interactions allows the use of more informative approaches to choosing substrates and potential interacting drugs. Figure 2 describes a decision-making process [19] for the conduct

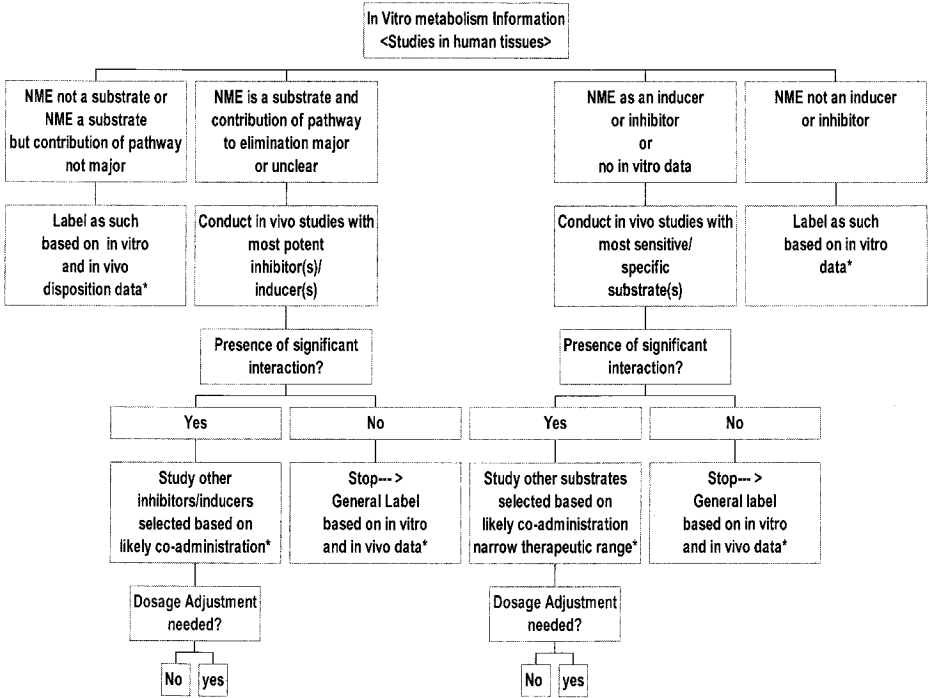


**Figure 2** Integrated approach in the evaluation of drug–drug interactions. \*Additional population pharmacokinetic analysis may assist the overall evaluation. (Reproduced from Ref. 19.)

of in vivo drug interaction studies once a new drug is characterized as a substrate for a particular metabolic pathway or an inhibitor of that pathway.

*a. Substrates for an Investigational Drug to Test Inhibition or Induction.*

In studying an investigational drug as the interacting drug (inhibitor or inducer), the choice of substrates for initial in vivo studies depends on the P450 enzymes affected by the drug. In testing for inhibition, the initial substrate selected should be one whose metabolism by a specific enzyme is markedly inhibited by known inhibitors (i.e., an especially sensitive substrate should be chosen). Examples include: (1) midazolam, buspirone, simvastatin, or lovastatin for a CYP3A4 inhibitor; (2) theophylline for a CYP1A2 inhibitor; (3) warfarin for a CYP2C9 inhibitor; and (4) desipramine for a CYP2D6 inhibitor. Tables 5–6 show some reported AUC ratios of these substrates with and without inhibitors. If the initial study of these sensitive substrates shows inhibition, further studies of other sub-

**Table 5** AUC Ratios of Substrates for CYP3A4 When Given with Inhibitors and When Given Alone

P450 enzyme	Substrate	Inhibitors	AUC ratios	Refs.
CYP3A4	Midazolam	Ketoconazole	16	27
		Itraconazole	11	27
		Erythromycin	4	28
	Buspirone	Itraconazole	19	29
		Erythromycin	6	29
		Verapamil	3	30
		Diltiazem	6	30
		Fluvoxamine	2.4	31
	Lovastatin	Itraconazole	20 (20)	32
		Diltiazem	4	33
	Simvastatin	Itraconazole	10 (19)	34
		Erythromycin	6	35
		Verapamil	4.6	35
	Triazolam	Ketoconazole	11, 22	36, 37
		Itraconazole	27	37
		Diltiazem	2, 3	38, 39
	Alprazolam	Ketoconazole	3	36
Felodipine	Itraconazole	6	40	
	Erythromycin	2.5	41	

Values in parentheses are AUC ratios of the statin acid metabolite.

**Table 6** AUC Ratios of Substrates for Various Cytochrome P450 Enzymes When Given with Inhibitors and When Given Alone

P450 enzyme	Substrate	Inhibitors	AUC ratios	Refs.
CYP1A2	Theophylline	Enoxacin	2.1	47
		Ciprofoxacin	1.3	47
CYP2C9	Warfarin	Fluconazole	3	48
	Losartan	Fluconazole	1.7, 1.3	49, 50
	Phenytoin	Fluconazole	1.8	51
CYP2D6	Desipramine	Quinidine	7	52
		Fluoxetine	11	53
		Sertraline	1.5	16
		Fluvoxamine	1.1	54
		Paroxetine	5.2	55

strates may be useful, representing a range of substrates based on the likelihood of coadministration. For example, possible substrates for further study of a CYP3A4-inhibitory drug might include dihydropyridine calcium channel blockers and triazolobenzodiazepines or, for a CYP2D6-inhibiting investigational drug, might include metoprolol. If the initial study is negative with the most sensitive substrates, less sensitive substrates may also be presumed to be unaffected and no further studies would be needed.

*b. Investigational Drug as Substrate for P450 Enzymes.* In testing an investigational substrate drug for the possibility that its metabolism is inhibited or induced, selection of the interacting drugs should be based on *in vitro* or other metabolism studies identifying the enzyme systems that metabolize the drug. The choice of interacting drug should then be based on known, important inhibitors or inducers of the pathway under investigation. For example, if the investigational drug is shown to be metabolized by CYP3A4, the choice of inhibitor and inducer could be ketoconazole and rifampin, respectively, because of the powerful effects of these interacting drugs on CYP3A4 metabolism (i.e., they are the strongest inhibitor and inducer recognized). If they show no inhibition or induction, further studies are not needed, and the substrate drug can be identified as having no clinically important drug–drug interaction for the pathway studied. If the clinical study of the most potent specific inhibitor/inducer is positive and the sponsor wishes to show a lack of an interaction between the test drug and less potent inhibitors or to give advice on dosage adjustment, further clinical studies would be needed. Tables 5 and 7 show reported inhibition and induction effects of sev-

**Table 7** AUC Ratios of Substrates for CYP3A4 Enzymes When Given with Inducers and When Given Alone

Substrate	Inducers	AUC ratios	Reference
Midazolam (15 mg)	Rifampin	0.04	42
Triazolam (0.5 mg)	Rifampin	0.05	43
	Dexamethasone	0.81	44
Nifedipine (20 mg)	Rifampin	0.07	45
Buspirone (30 mg)	Rifampin	0.09	46
Ethinyl estradiol (35 µg)	Rifampin	0.34	56
	Rifabutin	0.65	56
Norethindrone (1 mg)	Rifampin	0.49	56
	Rifabutin	0.87	56

Rifampin dose was given as 600 mg/day for 5 days (14 days for the ethinyl estradiol and norethindrone studies).

Dexamethasone was given as 1.5 mg/day for 4 days.

Rifabutin was given as 300 mg/day for 14 days.

eral commonly used CYP3A4 inhibitors and inducers. Certain approved drugs are not optimal selections as the interacting drug. For example, cimetidine, while frequently used, is not an optimal choice, because it inhibits multiple pathways.

#### 4. Route of Administration

For an investigational agent used as either an interacting drug or substrate, the route of administration should generally be the one being studied in trials. If only oral dosage forms will be marketed, studies with an intravenous formulation are not usually necessary, although information from oral and intravenous dosings may be useful in discerning the relative contributions of alterations in absorption and/or presystemic clearance to the overall effect observed for a drug interaction. For example, the interaction studies conducted of clarithromycin and intravenous or oral doses of midazolam enabled Gorski et al. to estimate the changes in the intestinal and hepatic availability of midazolam in the presence of clarithromycin [22]. Sometimes the use of certain routes of administration may reduce the utility of information from a study. For example, intravenous administration of a substrate or inhibitor would not reveal an effect on intestinal CYP3A activity that markedly altered oral bioavailability.

#### 5. Dose Selection

For both substrate and interacting drug, testing should maximize the possibility of finding an interaction. In general, the maximum doses of the interacting drug should be used. Doses smaller than those to be used clinically may be needed for substrates on safety grounds and should provide an adequate assessment of an interaction. The differential effects of different doses of ritonavir on the plasma levels of saquinavir [17] (Fig. 3) demonstrate the dose effect of an interacting drug.

#### 6. Endpoints

*a. Pharmacokinetic Endpoints.* The following measures and parameters are recommended to assess changes in substrate pharmacokinetic endpoints: (1) systemic exposure measures, such as AUC,  $C_{\max}$ , time to  $C_{\max}$  ( $T_{\max}$ ), and others as appropriate; and (2) pharmacokinetic parameters such as clearance, volumes of distribution, and half-lives. In some cases, these measures may be of interest for the inhibitor or inducer as well, notably where the study is intended to assess possible interactions between both study drugs. Additional measures may help in steady-state studies (e.g., trough concentration,  $C_{\min}$ ) to demonstrate that dosing strategies were adequate to achieve steady state before and during the interaction. In certain instances, an understanding of the relationship between dose, blood levels, and response may lead to a special interest in particular pharmacokinetic measures/parameters. For example, if a clinical outcome is most closely related

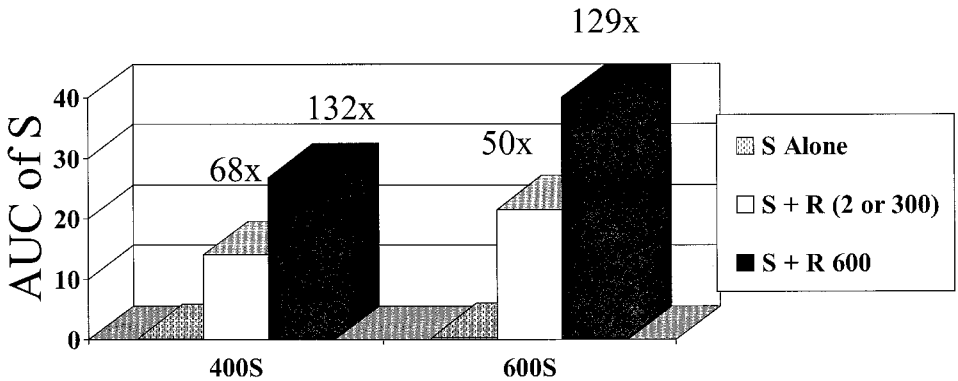


**Figure 3** AUC values of saquinavir (S, 400 or 600 mg) when given with ritonavir (R, 200, 300, or 600 mg) and when given alone. The AUC ratios of S with and without R are shown in the graph. (Data from Ref. 17.)

to peak concentration (e.g., tachycardia with sympathomimetics),  $C_{\max}$  or another early-exposure measure might be of particular interest. If the clinical outcome is related more to the extent of absorption, AUC would be more important. The frequency of sampling should be adequate to allow accurate determination of the relevant measures/parameters for the parent and metabolites. For the substrate, determination of the pharmacokinetics of both active and toxic metabolites is important.

*b. Pharmacodynamic Endpoints.* Pharmacodynamic measures can provide information about the consequences of the interaction when a pharmacokinetic/pharmacodynamic relationship for the substrate is not established or when pharmacodynamic changes do not result solely from pharmacokinetic interactions (e.g., additive cardiovascular effect of quinidine and tricyclic antidepressants). When an approved drug is studied as a substrate, the impact of a given change in blood level ( $C_{\max}$ , AUC) caused by an investigational drug should be well known, although this may not always be the case for older drugs.

## 7. Sample Size and Statistical Considerations

For both investigational drugs and approved drugs, when used as substrates and/or interacting drugs in drug–drug interaction studies, the general objective of the analysis should be to conclude that a certain type of drug–drug interaction is or is not present and, if present, to describe its magnitude. These conclusions should be based on the use of pharmacokinetic measures most relevant to understanding the relationship between exposure and therapeutic outcome. A confidence interval

approach, as opposed to a significance test, is preferred, to understand the magnitude of metabolic drug–drug interactions. Selection of the number of subjects for a given study will depend on how small an effect it is clinically important to detect or rule out. These should be known from information on the therapeutic range, concentration–response relationships, and the degree of the pharmacokinetic variability already present from factors other than interactions. In general, the sponsor should be able to recommend specific therapeutic equivalence boundaries based on information available for both the investigational agent and the approved drugs used in the studies. If the 90% confidence interval of the ratio of the pharmacokinetic measures/parameters with and without the interacting drug falls completely within the therapeutic equivalence boundary, a conclusion may be reached that no clinically significant drug–drug interaction was present. In the absence of other information to determine a therapeutic equivalence boundary, a standard interval of 80–125% may be employed for both the investigational drug and the approved drugs used in the interaction studies. When large intrasubject variability is present in the pharmacokinetic parameters that cause the observed equivalence interval to fall outside the standard interval without employing a large number of subjects, a scaled equivalence interval may be considered [23].

#### **D. Population Pharmacokinetic Screens**

Population pharmacokinetic analyses of data obtained from blood samples collected infrequently (sparse sampling) in clinical studies [20–21] conducted in the later phase of drug development can be valuable in detecting unsuspected drug–drug interactions. Because population pharmacokinetic studies are conducted as part of phase 2–3 clinical trials where comedication is expected to occur, they may provide added clinically relevant information. Population pharmacokinetic data can also be valuable in confirming the absence of a metabolic drug–drug interaction when interactions are not suggested by *in vitro* metabolism studies. The use of sparse sampling strategies to detect drug–drug interactions has been infrequent to date, and it is unlikely that population analysis can be used to prove the absence of an interaction that is strongly suggested by information arising from *in vitro* or *in vivo* studies specifically designed to assess a drug–drug interaction. Sparse plasma sampling approaches allow examination of the impact of a variety of covariates (age, sex, race, concomitant illness or concomitant drug use) on the pharmacokinetics of a drug. The quality of a population pharmacokinetic study depends on the number of samples, the precision of dosing and sample-collection time information, and the number of patients with relevant covariates. With attention to these factors, population pharmacokinetic data can provide definitive evidence of drug–drug interactions (or lack of them) that may not have been studied formally in specific clinical studies. In some cases, results for a



population study may suggest a need for further, more definitive investigations. A February 1999 FDA guidance for industry entitled *Population Pharmacokinetics* [11] describes when to use a population pharmacokinetic approach in drug development and considers pragmatic issues, such as study design and execution, data handling and analysis, and use of the information in labeling.

#### IV. REGULATORY CONSIDERATIONS

Information gathered in properly conducted in vitro and clinical studies of drug metabolism, drug absorption, and drug–drug interactions provides critical data for drug development decisions. For example, early knowledge that a candidate drug with a relatively narrow therapeutic range has high interindividual variability in pharmacokinetics due to oxidative metabolism by a polymorphically distributed cytochrome P450 enzyme might influence the decision to invest in further development. Increasingly, also, these factors can affect the regulatory decision to approve such a drug and/or how it is labeled. Section 505 of the Food Drug and Cosmetic Act requires that, for approval, a drug must be demonstrated to be both effective and safe when used as labeled. Safety is not an absolute measure but rather it reflects a conclusion that the drug's benefits outweigh its risks. Among the risks that must be considered is the presence of individuals who are at particular risk because of individual characteristics (e.g., poor metabolizers) or because of concomitant drug administration. It is striking that several important drugs—terfenadine, mibefradil, astemizole, and cisapride—have been removed from the market at least partly because of drug–drug interaction problems [24–26]. The importance of both mean and between- and within-individual variability must be assessed in light of many factors. These include the toxicity of the drug (wide therapeutic range drugs may not be harmful even if their pharmacokinetics are very variable, e.g., propranolol, loratidine), the disease being treated, the availability of alternative therapy, the value of treatment, and the consequences of treatment failure resulting from inadequate drug concentrations. Thus, development of a drug to treat seasonal allergic rhinitis that shows significant cardiac toxicity when taken with a CYP3A4 inhibitor would not be prudent. In the context of a non-life-threatening condition for which numerous safe and effective alternative therapies exist, such a drug would be unlikely to be approved for marketing today. In contrast, the potential for serious toxicities due to drug interactions is not an insurmountable impediment for drugs intended to treat severe or life-threatening conditions, particularly when alternative treatments are not available. In these instances, close attention to labeling and other aspects of risk management will be needed to inform practitioners and patients about the likelihood and consequences of interactions and the ways to avoid them.

## V. LABELING

Labeling for drug products in the United States must be in the format specified in the Code of Federal Regulations (21 CFR 201.56). Drug absorption, metabolism, and excretion and drug–drug interaction information appears, as appropriate, in some or all of the following sections of the approved product label: Clinical Pharmacology, Contraindications, Precautions, Warnings, Adverse Reactions, or Dosage and Administration. Certain basic pharmacokinetic information is almost always included (e.g., bioavailability, food effects, clearance, and half-life), as is all available information about drug–drug interactions, often including negative results. Clinically important interactions are emphasized and discussed in more detail. Potential interactions based on metabolic pathways may also be included. Recently approved product labels have reflected the increased understanding of the pathways and consequences of drug metabolism by health care practitioners. Newer labels almost always include mention of the drug’s effect on specific cytochrome P450 enzymes as well as the clinical consequences of their perturbation on coadministered drugs and the influence of concomitantly administered drugs on the drug itself. The following section describes the appropriate location for drug metabolism and drug–drug interaction information. The role of P-glycoprotein and other transporter mechanisms and their relationship to drug-metabolizing enzymes remain to be fully understood, and the effects on P-glycoprotein-mediated transport is often not reflected in labeling at this time. It is easy to envision, however, that the role of transporters and the clinical consequences of their modulation will soon be better understood and studied such that information on these systems will begin to appear in labeling.

### A. Information Appropriate for the Approved Product Label

#### 1. Drug Metabolism Information

In vitro and in vivo information on the metabolic pathways and metabolites is described briefly in the Clinical Pharmacology section of the labeling. Important clinical consequences of this information would be placed in Warnings, Precautions, and Dosage and administration sections, as appropriate.

#### 2. Metabolic Drug–Drug Interactions

Results of in vitro and in vivo metabolic drug–drug interaction studies describing the drug’s effects on other substrate drugs and the effects of inhibitors and inducers on the drug should be presented in some detail in the Drug–Drug Interactions section of the labeling in the Clinical Pharmacology section. It is important

to include both positive and important relevant negative findings. Ideally, the types of studies on which statements are based should be identified briefly in the labeling. If findings indicate a known or potential interaction of clinical significance or lack of an important interaction that might have been expected, these should be mentioned briefly in the Clinical Pharmacology: Interactions section and described more fully in the Interaction section under Precautions, with advice on how to adjust treatment placed in Warnings, Precautions, Dosage and Administration, and Contraindications, as appropriate. For example, results of a study of a drug–drug interaction involving an antihistamine that shows increased exposure and consequently increased somnolence would be described in brief under Clinical Pharmacology: Interactions. The clinical implications of this finding would then be described under Warnings and Precautions, citing the potential influence on driving or cognitive performance, with a further recommendation in the Dosage and Administration sections to lower the dose in the presence of an interacting drug. If there were no satisfactory way to adjust dose and the adverse events resulting from the interaction were important, there would generally be a Contraindication to concomitant use, if the drug were approved.

In certain cases, information in Warnings and Precautions could be based on extrapolation from other studies. For example, a strong inhibitor of CYP3A4 does not need to be tested with all CYP3A4 substrates to include a Warnings against an interaction of the inhibitor with CYP3A4 substrates. Similarly, a substrate strongly affected by one CYP3A4 inhibitor would be presumed to be altered by other inhibitors and appropriate warnings provided.

## **B. Drug Metabolism/Drug–Drug Interaction Outcomes and Appropriate Representation in Labeling Sections**

### **1. Clinical Pharmacology Section; Drug–Drug Interaction Section**

*Case 1.* In vivo drug–drug interaction studies adding the new drug to a prototypical substrate indicate little or no pharmacokinetic effect of the new drug:

(Labeling Representation): Data from a drug–drug interaction study involving (*the new drug*) and (*the prototypical CYP3A4 substrate*) in \_\_\_\_\_ patients/healthy individuals indicate that the pharmacokinetics of (*the prototypical CYP3A4 substrate*) are not altered when the drugs are co-administered. This indicates that (*the new drug*) does not inhibit CYP3A4 and will not alter the metabolism of drugs metabolized by this enzyme.

(Rationale): The use of a highly specific and sensitive substrate and the clinical finding of no interaction allow extrapolation to other substrates of the same P450 enzyme.

*Case 2.* In vivo drug–drug interaction studies adding the new drug to a prototypical inducer/inhibitor indicate little or no pharmacokinetic effect of the new drug:

(Labeling Representation): Data from a drug–drug interaction study involving (*the new drug*) and (*the prototypical CYP3A4 inducer/inhibitor*) in \_\_\_\_\_ patients/healthy individuals indicate that the pharmacokinetics of (*the new drug*) is not altered when the drugs are coadministered. This indicates that inhibitors/inducers of (*CYP3A4*) do not affect (*the new drug*).

(Rationale): The use of a potent inhibitor/inducer of a specific CYP enzyme and the clinical finding of no interaction allow extrapolation to other inhibitor/inducer of the same P450 enzyme.

*Case 3.* In vivo drug–drug interaction studies adding the new drug to a prototypical substrate indicate a clinically significant pharmacokinetic interaction:

(Labeling Representation): The effect of (*the new drug*) on the pharmacokinetics of (*the prototypical CYP3A4 substrate*) has been studied in \_\_\_\_\_ patients/healthy subjects. The  $C_{\max}$ , AUC, half-life, and clearances of (*the prototypical CYP3A4 substrate*) were increased/decreased by \_\_\_\_\_% (90% confidence interval: \_\_\_\_\_ to \_\_\_\_\_%) in the presence of (*the new drug*). This indicates that (*the new drug*) can inhibit/induce the metabolism of drugs metabolized by CYP3A4 and can increase/decrease blood concentrations of such drugs. [Depending on the seriousness of the interaction, CYP3A4-metabolized drugs might also be labeled to warn of the interaction.]

(Rationale): The use of a highly specific and sensitive substrate allows a reasonable suspicion that the clinical finding of a positive interaction may be extrapolated to other substrates of the same P450 enzyme. This is particularly important information if the clinical consequences of such an interaction are important and/or the likelihood of coadministration is high. As appropriate, this information and the extrapolated conclusions should be represented in the Contraindications, Warnings, Precautions, and Dosage and Administration sections of the inhibiting/inducing and substrate drugs.

*Case 4.* In vivo drug–drug interaction studies adding the new drug to a prototypical inhibitor/inducer indicate a clinically significant pharmacokinetic interaction:

(Labeling Representation): The effect of (*the prototypical inhibitor/inducer*) on the pharmacokinetics of (*the new drug*) has been studied in \_\_\_\_\_ patients/healthy subjects. The  $C_{\max}$ , AUC, half-life, and clearances of (*the new drug*) were increased/decreased by \_\_\_\_\_% (90% confidence interval: \_\_\_\_\_ to \_\_\_\_\_%) in the presence of (*the prototypical inhibitor/inducer*). This indicates that the blood concentrations of (*the new drug*) may be increased in the presence of other inhibitors/inducers of CYP3A4. [De-

pending on the seriousness of the interaction, other inhibitors/inducers of CYP3A4 might also be labeled to warn of the interaction.]

{Rationale}: The use of a potent inhibitor/inducer allows a reasonable suspicion that the clinical finding of a positive interaction may be extrapolated to other inhibitors/inducers of the same P450 enzyme. This is particularly important information if the clinical consequences of such an interaction are important and/or the likelihood of coadministration is high. As appropriate, this information and the extrapolated conclusions should be represented in the Contraindications, Warnings, Precautions, and Dosage and Administration sections of the inhibiting and substrate drugs.

*Case 5.* In vitro interaction has been studied, but no in vivo studies have been conducted to confirm or refute the in vitro finding.

a. In vitro interaction has been demonstrated:

{Labeling Representation}: In vitro drug metabolism studies reveal that the metabolism of (*the new drug*) is by CYP3A4 and can be inhibited by the CYP3A4 inhibitor ketoconazole. No clinical studies have been performed to evaluate this finding. Based on the in vitro findings, it is likely that ketoconazole, itraconazole, and other CYP3A4 inhibitors will lead to substantial increase in blood concentrations of (*the new drug*).

{Rationale}: In vitro drug metabolism and interaction data characterizing the enzyme responsible for the metabolism of the candidate drug and demonstrating an interaction with a specific enzyme modulator allow a reasonable suspicion that known modulators of that enzyme are likely to affect the pharmacokinetics of the new drug. This is particularly important information if the clinical consequences of such an interaction are important and/or the likelihood of coadministration is high. As appropriate, this information and the extrapolated conclusions should be represented in the Contraindications, Warnings, Precautions, and Dosage and Administration sections.

b. In vitro interaction has not been demonstrated:

{Labeling Representation}: In vitro drug interaction studies reveal no inhibition of the metabolism of (*the new drug*) by the CYP3A4 inhibitor ketoconazole. No clinical studies have been performed to evaluate this finding. However, based on the in vitro findings, a metabolic interaction with ketoconazole, itraconazole, and other CYP3A4 inhibitors is not anticipated.

{Rationale}: The finding of no interaction with a specific and potent enzyme inhibitor is strong evidence that there would be no metabolism-based interaction with other less potent and specific enzyme inhibitors.

*Case 6.* Through in vitro investigations, specific enzymes have been identified as metabolizing the test drug, but no in vivo or in vitro drug interaction studies have been conducted:

⟨Labeling Representation⟩: In vitro drug metabolism studies reveal that (*the new drug*) is a substrate of the CYP \_\_\_\_\_ enzyme. No in vitro or clinical drug interaction studies have been performed. However, based on the in vitro data, blood concentrations of (*the new drug*) are expected to increase in the presence of inhibitors of the CYP \_\_\_\_\_ enzyme such as \_\_\_\_\_, \_\_\_\_\_, or \_\_\_\_\_.

⟨Rationale⟩: In vitro metabolism data characterizing the sole or primary enzyme responsible for the metabolism of the drug in question allows a reasonable suspicion that known modulators of that enzyme are likely to affect drug concentrations, especially if metabolism constitutes the major elimination of the new drug. Depending on the clinical consequences of increased concentrations and the likelihood of coadministration, this information and the extrapolated conclusions could be represented in the Contraindications, Warnings, Precautions, and Dosage and Administration sections.

*Case 7.* Neither in vitro nor in vivo drug–drug interaction studies have been conducted, and there is no significant metabolism of the drug:

⟨Labeling Representation⟩: Neither in vitro nor in vivo drug–drug interaction studies have been conducted. Because (*the new drug*) is minimally metabolized (approximately 90% of the administered dose of (*the new drug*) is excreted in the urine as unchanged drug), metabolic interactions would not be expected. Whether (*the new drug*) can inhibit or induce metabolic enzymes or whether other drugs may influence the pharmacokinetics of (*the new drug*) through other mechanisms (e.g. effects on absorption or elimination) is not known.

⟨Rationale⟩: The absence of in vitro and in vivo metabolism information is usually not important for drugs whose clearance is largely by renal elimination, perhaps excepting unusual cases in which there is a very narrow therapeutic range. It should be remembered, however, that even renally excreted drugs (e.g., fluconazole) can inhibit P450 enzymes, and that not all drug–drug interactions are metabolism based, and the possible effects of transporter modulation are potentially very significant. For this reason, if the new drug has a relatively narrow therapeutic range or significant toxicities at higher exposures, more information (e.g., in vitro metabolism, clinical drug–drug interactions, etc.) usually will be needed.

## 2. Contraindications, Warnings, and/or Precautions Sections

*Case 1.* An interacting drug causes increased levels of the substrate, but it is important to be able to use both drugs, and a dose adjustment that allows safe and effective concomitant use has been defined. Results of the studies are described in “Clinical Pharmacology, Drug–Drug Interactions, Warnings, and/or Precautions.”

(Labeling Representation): (Drug \_\_\_\_\_/class of drug) causes significant increases in concentrations of (*the new drug*) when coadministered, so that dose of (*the new drug*) must be adjusted (see Dosage and Administration).

*Case 2.* An interacting drug causes significant risk by increasing concentrations of the substrate, and there is no documented reliable way to adjust the dose of substrate so that it can be used safely and effectively. After describing the interaction in the Clinical Pharmacology section, there should be a Contraindications section and possibly a boxed warning if the risk is serious.

(Labeling representation): Drug \_\_\_\_\_/class of drug can cause significant increases in concentrations of drug \_\_\_\_\_ when coadministered. The two drugs/drug and members of the \_\_\_\_\_ class should not be used together.

### 3. Dosage and Administration Section

*Case 1.* An interacting drug causes increased risk because of increased concentrations of the substrate, but dosage adjustment will allow safe and effective use of both drugs.

(Labeling representation): (Drug \_\_\_\_\_/class of drug) leads to significant increases in blood concentrations of (*the new drug*) by \_\_\_\_\_%. The dose of (*the new drug*) should be decreased by \_\_\_\_\_% when the patient is also taking (\_\_\_\_\_ or other drug in this class).

## VI. SUMMARY

In vitro and in vivo metabolism and drug–drug interaction data are critical for the complete evaluation and labeling of a drug. The information provided by these studies needs to be appreciated and understood by prescribers and utilized in individualizing pharmacotherapy. An integrated approach to studying and evaluating drug–drug interactions during the drug development and regulatory review process and incorporating language into labeling has been described. This integrated approach should be based on good understanding and utilization of the primary question, our willingness to rely on in vitro and in vivo pharmacokinetic and pharmacodynamic data, and our understanding of the degree to which an observed change in substrate measures caused by an interacting drug is or is not clinically important. Future efforts in assessing, managing, and communicating the risks of drug–drug interactions may focus on: (1) improved uses of in vitro tests, e.g., to rule in or rule out induction of the metabolism of a substrate by an interacting drug; (2) better use of in vitro data as a surrogate for in vivo findings, e.g., through in vitro/in vivo correlations; (3) better use of pharmacokinetic and pharmacodynamic data in understanding the clinical consequences of drug–drug

interactions; and (4) better ways to communicate information about important drug–drug interactions to patients and practitioners.

## ACKNOWLEDGMENTS

The authors would like to acknowledge the following FDA working group members who contributed to the development of the CDER/CBER guidance for industry entitled “In vivo metabolism/drug interactions: study design, data analysis and recommendations for dosing and labeling”: F. Ajayi, S. A1-Habet, J. Balian, G. Barnette, R. Baweja, J. Collins, B. Gillespie, M.D. Green, P. Hepp, K. Higgins, S. Machado, S. Madani, P. Marroum, A. Rahman, K. Reynolds, H. Sun, C. Trapnell, X. J. Wei, and R. Yuan

## REFERENCES

1. Kim RB, Cvetkovic M, Fromm MF, Leake B, Wilkinson G. OATP and P-glycoprotein mediate the uptake and excretion of fexofenadine. *Clin Pharmacol Ther* 65:111 (1999).
2. Bedford TA, Rowbotham DJ. Cisapride. Drug interactions of clinical significance. *Drug Safety* 15:167–175 (1996); published erratum appears in *Drug Safety* 17:196 (1997).
3. Albengres E, Le Louet H, Tillement JP. Systemic antifungal agents. Drug interactions of clinical significance. *Drug Safety* 18:83–97 (1998).
4. Neuvonen PJ, Kantola T, Kivisto KT. Simvastatin but not pravastatin is very susceptible to interaction with the CYP3A4 inhibitor itraconazole. *Clin Pharmacol Ther* 63:332–341 (1998).
5. Barza M, Weinstein L. Pharmacokinetics of the penicillins in man. *Clin Pharmacokin* 1:297–308 (1976).
6. Fromm MF, Kim RB, Stein CM, Wilkinson GR, Roden DM. Inhibition of P-glycoprotein-mediated drug transport: A unifying mechanism to explain the interaction between digoxin and quinidine. *Circulation* 99:552–557 (1999).
7. Webb DJ, Freestone S, Allen MJ, Muirhead GJ. Sildenafil citrate and blood-pressure-lowering drugs: results of drug interaction studies with an organic nitrate and a calcium antagonist. *Am J Cardiol* 83:21C–28C (1999).
8. Mullins ME, Horowitz BZ, Linden DH, Smith GW, Norton RL, Stump J. Life-threatening interaction of mibefradil and beta-blockers with dihydropyridine calcium channel blockers. *JAMA* 280:157–158 (1998).
9. Guidance for Industry: Drug Metabolism/Drug Interactions in the Drug Development Process: Studies in vitro. Internet: <http://www.fda.gov/cder>, April 1997.
10. CDER MPCC/CPS In vivo Drug–Drug Interaction Working Group. Guidance for industry: in vivo metabolism/drug interactions: study design, data analysis and rec-



- ommendations for dosing and labeling. Internet: <http://www.fda.gov/cder>, December 1999.
11. CDER MPCC/CPS Population PK Working Group. Guidance for industry: population pharmacokinetics. Internet: <http://www.fda.gov/cder>, February 1999.
  12. Davit B, Reynolds K, Yuan R, Ajayi F, Conner D, Fadiran, E, Gillespie B, Sahajwalla C, Huang, S-M, Lesko LJ. FDA evaluations using in vitro metabolism to predict and interpret in vivo metabolic drug–drug interactions: impact on labeling. *J Clin Pharmacol* 39:899–910 (1999).
  13. Honig PK, Woosley RL, Zamani K, Conner DP, Cantilena LR. Changes in the pharmacokinetics and electrocardiographic pharmacodynamics of terfenadine with concomitant administrations of erythromycin. *Clin Pharmacol Ther* 52:231–238 (1992).
  14. Honig PK, Wortham DC, Sarmani K, Conner DP, Mulin JC, Cantilena LR. Terfenadine–ketoconazole interactions: pharmacokinetic and electrocardiographic consequences. *JAMA* 269:1513–1518 (1993).
  15. Lamberg TS, Kivisto KT, Neuvonen PJ. Lack of effect of terfenadine on the pharmacokinetics of the CYP3A4 substrate buspirone. *Pharmacol Toxicol* 84:165–169 (1999).
  16. Kurtz DL, Bergstrom RF, Goldberg MJ, Cerimele BJ. The effect of sertraline on the pharmacokinetics of desipramine and imipramine. *Clin Pharmacol Ther* 62:145–156 (1997).
  17. Hsu A, Granneman G, Cao G, Carothers L, el-Shourbagy T, Baroldi P, Erdman K, Brown F, Sun E, Leonard JM. Pharmacokinetic interactions between two HIV-protease inhibitors, ritonavir and saquinavir. *Clin Pharmacol Ther* 63:453–464 (1998).
  18. Hsu A, Granneman GR, Sun E, et al. Assessment of single- and multiple-dose interactions between ritonavir and saquinavir. XI International Conference on AIDS, 1996 July 7–12: Vancouver, B. C., Canada.
  19. Huang S-M, Lesko, LJ, Williams RL. Assessment of the quality and quantity of drug–drug interaction studies in recent NDA submissions: study design, data analysis issues. *J Clin Pharmacol* 39:1006–1014 (1999).
  20. ICH E7 Guideline for industry: studies in support of special populations: geriatrics. Internet: <http://www.ifpma.org/ich1.html> or <http://www.pharmweb.net>, August 1994.
  21. Guideline for the study of drugs likely to be used in the elderly. Internet: <http://www.fda.gov/cder>, November 1989.
  22. Gorski JC, Jones DR, Haehner-Daniels BD, Hamman MA, O'Mara EM Jr, Hall SD. The contribution of intestinal and hepatic CYP3A to the interaction between midazolam and clarithromycin. *Clin Pharmacol Ther* 64:133–143 (1998).
  23. CDER BCC Population and Individual Bioequivalence Working Group. Guidance for industry: statistical approaches to establishing bioequivalence. Internet: <http://www.fda.gov/cder>, January 2001.
  24. Friedman MA, Woodcock J, Lumpkin MM, et al. The safety of newly approved medicines: Do recent market removals mean there is a problem? *JAMA* 281:1728–1734 (1999).
  25. Huang S-M, Booth B, Fadiran E, Uppoor RS, Doddapaneni S, Chen M, Ajayi F, Martin T, Lesko LJ. What have we learned from the recent market withdrawal Of terfenadine and mibefradil? Presentation at the 101st Annual Meeting of American

- Society of Clinical Pharmacology and Therapeutics, March 15–17, 2000, Beverly Hills, CA; abstract in *Clin Pharmacol Ther* 67(2):148 (2000).
26. FDA. Talk paper: Janssen pharmaceuticals stops marketing cisapride in the US. <http://www.fda.gov/bbs/topics/ANSWERS/ans01007.html>.
  27. Olkkola KT, Backman JT, Neuvonen PJ. Midazolam should be avoided in patients receiving the systemic antimycotics ketoconazole or itraconazole. *Clin Pharmacol Ther* 55:481–485 (1994).
  28. Okkola KT, Aranko K, Luurila H, Hill A, Saarnivaara L, Himberg JJ, Neuvonen PJ. A potentially hazardous interaction between erythromycin and midazolam. *Clin Pharmacol Ther* 53:298–305 (1993).
  29. Kivisto KT, Lamberg TS, Kantola T, Neuvonen PJ. Plasma buspirone concentrations are greatly increased by erythromycin and itraconazole. *Clin Pharmacol Ther* 62:348–354 (1997).
  30. Lamberg TS, Kivisto KT, Neuvonen PJ. Effects of verapamil and diltiazem on the pharmacokinetics and pharmacodynamics of buspirone. *Clin Pharmacol Ther* 63:640–645 (1998).
  31. Lamberg TS, Kivisto KT, Laitila J, Martensson K, Neuvonen PJ. The effect of flvoxamine on the pharmacokinetics and pharmacodynamics of buspirone. *Eur J Clin Pharmacol* 54:761–766 (1998).
  32. Neuvonen PJ, Jalava KM. Itraconazole drastically increases plasma concentrations of lovastatin and lovastatin acid. *Clin Pharmacol Ther* 60:54–61 (1996).
  33. Azie NE, Brater DC, Becker PA, Jones DR, Hall SD. The interaction of diltiazem with lovastatin and pravastatin. *Clin Pharmacol Ther* 64:369–377 (1998).
  34. Neuvonen PJ, Kantola T, Kivisto KT. Simvastatin but not pravastatin is very susceptible to interaction with the CYP3A4 inhibitor itraconazole. *Clin Pharmacol Ther* 63:332–341 (1998).
  35. Kantola T, Kivisto KT, Neuvonen PJ. Erythromycin and verapamil considerably increase serum simvastatin and simvastatin acid concentrations. *Clin Pharmacol Ther* 64:177–182 (1998).
  36. Greenblatt DJ, Wright CE, von Moltke LL, Harmatz JS, Ehrenberg BL, Harrel LM, Corbett K, Counihan M, Tobias S, Shader RI. Ketoconazole inhibition of triazolam and alprazolam clearance: differential kinetic and dynamic consequences. *Clin Pharmacol Ther* 64:237–247 (1998).
  37. Varhe A, Olkkola KT, Neuvonen PJ. Oral triazolam is potentially hazardous to patients receiving systemic antimycotics ketoconazole or itraconazole. *Clin Pharmacol Ther* 56:601–607 (1994).
  38. Kosuge K, Nishimoto M, Kimura M, Umemura K, Nakashima M, Ohashi K. Enhanced effect of triazolam with diltiazem. *Br J Clin Pharmacol* 43:367–372 (1997).
  39. Varhe A, Olkkola KT, Neuvonen PJ. Diltiazem enhances the effects of triazolam by inhibiting its metabolism. *Clin Pharmacol Ther* 59:369–375 (1996).
  40. Jalava KM, Olkkola KT, Neuvonen PJ. Itraconazole greatly increases plasma concentrations and effects of felodipine. *Clin Pharmacol Ther* 61:410–415 (1997).
  41. Bailey DG, Bend JR, Arnold JM, Tran LT, Spence JD. Erythromycin–felodipine interaction: magnitude, mechanism, and comparison with grapefruit juice. *Clin Pharmacol Ther* 60:25–33 (1996).

42. Backman JT, Olkkola KT, Neuvonen PJ. Rifampin drastically reduces plasma concentrations and effects of oral midazolam. *Clin Pharmacol Ther* 59:7–13 (1996).
43. Villikka K, Kivisto KT, Backman JT, Olkkola KT, Neuvonen PJ. Triazolam is ineffective in patients taking rifampin. *Clin Pharmacol Ther* 61:8–14 (1997).
44. Villikka K, Kivisto KT, Neuvonen PJ. The effect of dexamethasone on the pharmacokinetics of triazolam. *Pharmacol Toxicol* 83:135–138 (1998).
45. Holtbecker N, Fromm MF, Droemer HK, Ohnhaus EE, Heidermann H. The nifedipine–rifampin interaction. *Drug Metab Dispos* 24:1121–1123 (1996).
46. Lamberg TS, Kivisto KT, Neuvonen PJ. Concentrations and effects of buspirone are considerably reduced by rifampicin. *Br J Clin Pharmacol* 45:381–385 (1998).
47. Wijnands WJ, Vree TB, van Herwaarden CL. The influence of quinolone derivatives on theophylline clearance. *Br J Clin Pharmacol* 22:677–683 (1986).
48. Black DJ, Kunze KL, Wienkers LC, Gidal BE, Seaton TL, McDonnell ND, Evans JS, Bauwens JE, Trager WF. Warfarin—fluconazole. II. A metabolically based drug interaction: in vivo studies. *Drug Metab Dispos* 24:422–428 (1996).
49. Kazierad DJ, Martin DE, Blum RA, Tenero DM, Ilson B, Boike SC, Etheredge R, Jorkasky DK. Effect of fluconazole on the pharmacokinetics of eprosartan and losartan in healthy male volunteers. *Clin Pharmacol Ther* 62:417–425 (1997).
50. Kaukonen KM, Olkkola KT, Neuvonen PJ. Fluconazole but not itraconazole decreases the metabolism of losartan to E-3174. *Eur J Clin Pharmacol* 53:445–449 (1998).
51. Blum RA, Wilton JH, Hilligoss DM, Gardner MJ, Henry EB, Harrison NJ, Schentag JJ. Effect of fluconazole on the disposition of phenytoin. *Clin Pharmacol Ther* 49:420–425 (1991).
52. Brosen K, Gram LF. Quinidine inhibits the 2-hydroxylation of imipramine and desipramine but not the demethylation of imipramine. *Eur J Clin Pharmacol* 37:155–160 (1989).
53. Bergstrom RF, Peyton AL, Lemberger L. Quantification and mechanism of the fluoxetine and tricyclic antidepressant interaction. *Clin Pharmacol Ther* 51:239–248 (1992).
54. Spina E, Pollicino AM, Avenoso A, Campo GM, Perucca E, Caputi AP. Effect of fluvoxamine on the pharmacokinetics of imipramine and desipramine in healthy subjects. *Ther Drug Monit* 15:243–246 (1993).
55. Alderman J, Preskorn SH, Greenblatt DJ, Harrison W, Penenberg D, Allison J, Chung M. Desipramine pharmacokinetics when coadministered with paroxetine or sertraline in extensive metabolizers. *J Clin Psychopharmacol* 17(4):284–291 (1997).
56. Barditch-Crovo P, Trapnell CB, Ette E, Zacur HA, Coresh J, Rocco LE, Hendrix CW, Flexner C. The effects of rifampin and rifabutin on the pharmacokinetics and pharmacodynamics of a combination oral contraceptive. *Clin Pharmacol Ther* 65(4):428–438 (1999).

# 18

## Drug–Drug Interactions: Marketing Perspectives

**Kevin J. Petty and José M. Vega**

*Merck Research Laboratories, Blue Bell, Pennsylvania*

### I. INTRODUCTION

The number of drugs available to treat patient illness is steadily increasing as drug development benefits from advances in molecular biology and from increasing automation of drug screening through the use of robotics and combinatorial chemistry. This ever-expanding pharmaceutical arsenal is available to physicians to treat a large number of diseases (both human and veterinary). As the mean age of industrialized nations increases, in part due to advances in medical care, the need to treat multiple disease processes simultaneously increases the probability that large numbers of people will receive concomitant therapy with multiple drugs. Consequently, there is an increased risk of adverse drug–drug interactions as more drugs are used to treat a variety of conditions in the same patient.

Identifying the potential for adverse drug–drug interactions is increasingly difficult when patients are cared for by multiple specialists, each primarily concerned with one organ system, without overall coordination of the patient's management by one person. In many situations, the potential for drug–drug interactions can be minimized by appropriate choices of agents, particularly when options exist with different mechanisms of action, sites of metabolism, and routes of excretion. There are, unfortunately, situations where interactions may not be avoidable and the risks and benefits must be carefully assessed. For instance, the treatment of cancer, AIDS, or other life-threatening diseases might require treatment with a drug known to inhibit enzymes that metabolize other drugs (e.g., HIV protease inhibitor inhibition of cytochrome P450 3A4). Thus, drug–drug interactions must be evaluated in light of the therapeutic class and the risk/benefit

ratio. These interactions can have a significant impact on the marketing of drugs. This chapter will focus on drug–drug interactions and their effect on the marketplace.

## II. MARKET SIZE

The prescription drug market is large and continuously growing. Prescription drug sales (retail pharmacies) in the United States in 1997 totaled \$81.2 billion [1]. Each of the ten top-selling prescription drugs in 1997 had U.S. sales of over \$800 million and ranged from \$804.8 million for Augmenting® to \$2.28 billion for Prilosec®. Prilosec® became the first prescription drug to exceed \$5 billion, with worldwide sales in 1998 of \$5.14 billion [2]. The six top-selling drugs in 1997 (Prilosec®, Prozac®, Zocor®, Epogen®, Zolofit®, and Zantac®) each had U.S. sales greater than \$1 billion. New products launched in 1997 produced \$3.28 billion in U.S. sales, led by Lipitor® (\$587 million) and Rezulin (\$325 million). In 1998, U.S. retail pharmaceutical sales were \$86.6 billion, and 25 drugs achieved worldwide annual sales of at least \$1 billion. Worldwide (North America, Europe, Japan, Latin America, Australia) retail pharmacy sales totaled more than \$185 billion in 1998 [3].

This enormous market is influenced by a complex array of factors. Among the most significant of those factors are the efficacy and safety of a given drug. Those two factors are the most important considerations in the process by which drugs receive approval from regulatory agencies to allow their marketing. Those factors are also important for drugs after they gain entry to the market, together with additional factors, such as dosing convenience and cost when more than one drug is available to treat the same condition.

There are many ways in which drugs can interact to produce adverse events. Perhaps the most common type of interaction is where one drug alters the pharmacokinetics of a second drug. Alteration of pharmacokinetics can include inhibition by one drug of the metabolism of a second drug (e.g., erythromycin inhibition of warfarin metabolism), leading to accumulation of the second drug with its resultant toxicity [4]. Conversely, induction of metabolism of one drug by another can also produce untoward effects if plasma levels of the second drug become subtherapeutic. An example of such an interaction was the reported interaction of rifampin with oral contraceptives containing ethinyl estradiol, where concomitant use of rifampin accelerated the metabolism of ethinyl estradiol, resulting in decreased efficacy as a contraceptive and unwanted pregnancies [4].

Since 1964, approximately 60 drug products have been withdrawn from the U.S. market because they were found to be ineffective or unsafe [5]. Most of the compounds withdrawn primarily for safety had toxicities directly attributable to the compound. Only two of these drugs (terfenadine and mibefradil) were

withdrawn primarily for their high incidence of adverse drug–drug interactions. The discussion that follows will describe the experience with these two drugs and the experience with cimetidine where drug–drug interactions have had a significant impact on its market position.

## A. Terfenadine

Terfenadine was introduced into the marketplace as the first nonsedating histamine-1 ( $H_1$ ) receptor antagonist. It was launched in the United States in 1985 under the brand name Seldane®. Its patent protection was near expiration when the drug was voluntarily withdrawn from the antihistamine market in 1997.

### 1. Clinical Background

During its early development, terfenadine was found to act as a competitive antagonist for histamine binding to the  $H_1$  receptor with a 50% inhibitory concentration ( $IC_{50}$ ) of 0.7  $\mu$ M. It was thought that the antihistaminic effect of terfenadine was due to direct interaction with the  $H_1$  receptor. Subsequent studies revealed that terfenadine was completely metabolized *in vivo* to fexofenadine, a metabolite entirely responsible for the antihistaminic effect [6]. The unique property of fexofenadine compared to first-generation antihistamines (diphenhydramine, chlorpheniramine) was its inability to cross the blood–brain barrier, thereby avoiding the sedation seen with the first-generation antihistamines. Terfenadine was indicated for use in allergic rhinitis (both seasonal and perennial), and the recommended dose was 60 mg twice daily.

### 2. Clinical Pharmacology

Terfenadine is at least 70% absorbed after oral administration but is rapidly metabolized by first-pass metabolism to fexofenadine (terfenadine carboxylate) and an inactive dealkylated product. Metabolism appears to be mediated entirely by the cytochrome P450 (CYP3A4). Fexofenadine is about 70% protein bound and exhibits biphasic elimination with an initial plasma half-life of 3.5 hours and a terminal plasma half-life of 6–12 hours. Fexofenadine is excreted mostly unchanged (80% in feces, 12% in urine), with <10% converted to inactive metabolites [7]. Fexofenadine excretion can be affected by compounds (e.g., ketoconazole) that interact with the P-glycoprotein transporter because fexofenadine is a substrate for this transporter [8].

### 3. Drug–Drug Interactions

Terfenadine itself has no effect on CYP activity and thus does not affect metabolism of other CYP substrates. The drug–drug interactions of significance were

due to inhibition of CYP3A4 by other drugs, leading to toxic accumulation of terfenadine in plasma where it normally would only be found in trace amounts [9,10].

#### 4. Adverse Experiences

The first published report of a serious adverse event due to an interaction of terfenadine with another drug was that of a young woman who was taking terfenadine and who subsequently began taking ketoconazole. Within a few days after beginning ketoconazole therapy, she experienced syncopal episodes and was found to have *torsade de pointes* (polymorphic ventricular tachycardia) [11]. *Torsade de pointes* was also seen in patients with liver failure who took terfenadine and in patients who simultaneously received erythromycin and terfenadine [12]. Based on the initial reports of *torsade* with terfenadine, a “Dear Doctor” letter was issued by the manufacturer of Seldane® in 1990. A retrospective analysis of concomitant drug use within a large cohort of Medicaid patients revealed that there was a significant correlation between terfenadine toxicity and concomitant use of either erythromycin or ketoconazole (both potent CYP3A4 inhibitors) [13]. Additional reports of *torsade de pointes* in 1992 prompted the need for the manufacturer to incorporate a black box warning in the Seldane® label that contraindicated concomitant use of terfenadine with CYP3A4 inhibitors, including the azole antifungals (ketoconazole, itraconazole) and macrolide antibiotics (erythromycin, clarithromycin, troleandomycin), and use in patients with hepatic insufficiency.

The occurrence of cardiac toxicity was closely correlated with terfenadine use, and subsequent *in vitro* studies confirmed that terfenadine (but not fexofenadine) efficiently blocks cardiac potassium channels [14]. A study in healthy volunteers treated concomitantly with terfenadine and ketoconazole found a linear relationship between trough terfenadine concentrations and QT<sub>c</sub> intervals. The QT<sub>c</sub> interval lengthened up to 110 msec at the highest plasma concentrations of ~45 ng/ml [9]. Thus, the direct inhibitory effect of terfenadine on cardiac potassium channels results in prolongation of cardiac repolarization, which is a well-known cause of ventricular arrhythmias. In one death in which terfenadine was implicated, plasma level of the drug was 55 ng/ml several hours after the last ingestion of the drug (when it normally should be undetectable).

While fexofenadine is also metabolized primarily by CYP3A4 and its levels can be elevated in the presence of potent inhibitors of CYP3A4, its lack of effect on cardiac potassium channels allows for higher fexofenadine levels to be safely tolerated without QT<sub>c</sub> interval prolongation and without an increased risk of ventricular arrhythmias.

#### 5. Market Dynamics

Seldane® held market exclusivity as a nonsedating antihistamine from its launch in 1985 until 1989, when astemizole (Hismanal®) entered the market. Hismanal®

did not penetrate significantly into the market because of perceived inferior efficacy (longer onset of action) and cardiac toxicities similar to Seldane® [7]. Based on its nonsedating property, efficacy, and convenient dosing, Seldane® maintained market leadership, with a ranking of the fifth most commonly prescribed drug in the United States in 1990. In 1991, 17 million prescriptions were issued, and there were more than 100 million users of Seldane® worldwide. It had peak U.S. retail pharmacy sales of \$540 million and 54% market share in 1992 (combined antihistamine and cold markets). Despite the black box warning, Seldane® had worldwide sales of \$700 million in 1994 and held up to 29% market share in the United States in 1995. With the launch of Zyrtec® in 1996 (promoted as safer and equally effective), market share of Seldane® plummeted to 2.5% in 1997, when it was withdrawn from the market.

When it was recognized that fexofenadine was the active metabolite, efforts were begun to register it as a separate entity. Due to existing patent coverage of fexofenadine by Sepracor, Hoechst obtained the licensing rights for its development. Fexofenadine was approved (as Allegra®) for marketing in the United States in July 1996.

## B. Mibefradil

Mibefradil (Posicor®) was launched in the United States in June 1997 by Roche. It was promoted as a unique calcium channel blocker (CCB) that affected both transient (T) and long (L) calcium channels. At the time of launch, it was projected to eventually provide 1–3% of Roche's sales. It was withdrawn from the market in June 1998.

### 1. Clinical Background

Mibefradil is a tetralol derivative developed as a unique calcium channel blocker. Its efficacy as an antihypertensive was demonstrated in phase III trials where doses of 50–100 mg were compared to other calcium channel blockers (nifedipine SR, diltiazem CD, nifedipine GITS, amlodipine). Mibefradil was shown to be equally effective as or more effective than nifedipine SR, diltiazem CD, nifedipine GITS, or amlodipine in reducing blood pressure in mild to moderate hypertension. Average reductions of diastolic blood pressure of as much as 15 mm Hg were seen with the 100-mg dose. It was also found to be effective in the treatment of chronic stable angina. Thus, it was indicated for use in hypertension and stable angina at doses of 50 or 100 mg once daily [15].

Studies to support its registration included 2636 patients. It was reported to be well tolerated, with the most common adverse experiences being headache, leg edema, dizziness, and fatigue at incidences similar to those with placebo. The incidence of leg edema with mibefradil was found to be lower than with other CCBs, which was an attribute important in its registration and marketing.



Compared to other CCBs, mibefradil was found to have more negative chronotropic effects, with a significant incidence of dose-dependent first-degree AV block and sinus bradycardia. No effect on QT intervals was detected in the phase III studies.

## 2. Clinical Pharmacology

Oral bioavailability of mibefradil is dose dependent and ranges from 37% to over 90% with doses of 10 mg or 160 mg, respectively. The plasma half-life is 17–25 hours after multiple doses, and it is more than 99% protein bound [15]. The metabolism of mibefradil is mediated by two pathways: esterase-catalyzed hydrolysis of the ester side chain to yield an alcohol metabolite and CYP3A4-catalyzed oxidation. After chronic dosing, the oxidative pathway becomes less important and the plasma level of the alcohol metabolite of mibefradil increases. In animal models the pharmacological effect of the alcohol metabolite is about 10% compared to that of the parent compound. After metabolic inactivation, mibefradil is excreted into the bile (75%) and urine (25%), with less than 3% excreted unchanged in the urine.

Studies in human liver microsomal preparations have demonstrated that mibefradil is a powerful inhibitor of liver CYP3A4, with both competitive and mechanism-based effects on this enzyme at therapeutically relevant concentrations [16]. In particular, the potency of competitive inhibition of CYP3A4 is such that the  $IC_{50}$  value ( $<1 \mu\text{M}$ ) falls within the therapeutic plasma concentrations of mibefradil and is comparable to that of ketoconazole. However, the inhibition of CYP3A4 by mibefradil, unlike that of ketoconazole, is at least partially irreversible. Based on the *in vitro* results, mibefradil is one of the most potent mechanism-based inhibitors of CYP3A4 reported to date. Therefore, it should have been anticipated that clinically significant drug–drug interactions would likely ensue when mibefradil was coadministered with the large number of agents metabolized primarily by CYP3A4. In addition, *in vitro* studies by the manufacturer demonstrated an inhibitory effect of mibefradil on CYP2D6 and CYP1A2, thus suggesting the possibility of additional potential drug–drug interactions.

## 3. Clinical Drug–Drug Interactions

Prior to registration, several clinical drug–drug interaction studies were done. In those studies, mibefradil or its metabolites were found to inhibit CYP3A4 and CYP2D6 but not CYP1A2. Coadministration of mibefradil with metoprolol (a substrate for CYP2D6) in healthy subjects resulted in a twofold increase in the peak plasma concentrations of total (*R*- and *S*-enantiomeric) metoprolol and a four- to fivefold increase in AUC. Coadministration of terfenadine (a substrate for CYP3A4) and mibefradil in healthy subjects resulted in elevated plasma concentrations of terfenadine up to 40 ng/ml.

Twice-daily dosing of 60 mg terfenadine increased the mean  $QT_c$  interval 12%. The levels of cyclosporine A (another CYP3A4 substrate) increased about twofold with concomitant treatment with 50 mg mibefradil for 8 days. In healthy volunteers, elevations in peak quinidine (a CYP3A4 substrate) plasma levels (15–19%) and in AUC (50%) were found during coadministration of single doses of mibefradil at doses of 50 mg and 100 mg. Despite *in vitro* evidence of inhibition of CYP1A2, no pharmacokinetic interaction was observed with theophylline, a CYP1A2 substrate. It was also reported that no clinically important interaction was seen between mibefradil and cimetidine, digoxin, angiotensin-converting enzyme (ACE) inhibitors, nonsteroidal anti-inflammatory agents, long-acting nitrates, or warfarin [15].

#### 4. Adverse Experiences

Within several weeks of its launch, numerous serious adverse events involving mibefradil were being reported on a regular basis. These included severe bradycardia when used concomitantly with  $\beta$ -blockers, cardiogenic shock when switching from Posicor® to dihydropyridine CCBs [17], and rhabdomyolysis when used with HMG CoA reductase inhibitors [18].

On the basis of these postmarketing adverse experiences, the manufacturer issued a “Dear Doctor” letter in which it was mentioned that mibefradil was found to interfere with the metabolism of 26 other medicines and that concomitant use of mibefradil with several of these medications was contraindicated.

In a second “Dear Doctor” letter in June 1998, mibefradil was voluntarily withdrawn from the market by Roche due to “complexities” of drug interactions. The withdrawal apparently was precipitated by the analysis of the results of a study of ~2500 patients with congestive heart failure (Mortality Assessment in Congestive Heart failure or MACH-1 trial). This was a three-year study in which patients were treated with mibefradil, an ACE inhibitor, or placebo. The study reportedly found no difference between mibefradil and placebo in treating CHF but it “provided further information on drug interactions” [19]. It is likely that most of the interactions involved drugs metabolized by CYP3A4 and 2D6, but details of the study and its results have not yet been published.

#### 5. Market Dynamics

Although the CCB market is sizable (more than \$4 billion in U.S. retail sales in 1998), it is occupied by a variety of compounds, both branded and generic. Thus, Posicor® was launched in a very competitive market, and it had virtually no impact on that market. Before its withdrawal, it had been prescribed to ~200,000 patients worldwide and generated <\$27 million in U.S. retail sales during its brief time on the market.

### C. Cimetidine

Cimetidine was the first histamine-2 ( $H_2$ ) receptor antagonist in the antiulcerant market. It was introduced to the U.S. market as Tagamet® in 1977, and its patent expired in May 1994. It was approved for over-the-counter (OTC) marketing in September 1995, and it currently remains available on both the prescription and OTC markets.

#### 1. Clinical Background

Cimetidine is a specific antagonist of the  $H_2$  receptor. It binds to the  $H_2$  receptor on gastric parietal cells and competitively blocks the action of histamine in the signaling pathway that regulates gastric acid secretion (both basal and stimulated). It is indicated for the treatment of duodenal and gastric ulcers, gastroesophageal reflux disease (GERD), and hypersecretory conditions such as Zollinger–Ellison syndrome and systemic mastocytosis. It is also indicated for prevention of upper gastrointestinal bleeding in critically ill patients.

Controlled clinical trials supporting the registration of cimetidine found that it was significantly better than placebo in achieving healing of duodenal ulcers. Subsequent studies also found cimetidine was effective in controlling symptoms of peptic ulcer disease and GERD. In addition, it significantly decreased the duration of GI bleeding in patients with peptic ulcers [20]. During phase III studies, cimetidine was generally well tolerated. A variety of adverse experiences were reported with cimetidine but not an incidence greater than placebo. Drug–drug interactions were not significant when cimetidine was used concomitantly with sedatives, analgesics, thiazide diuretics, bronchodilators, digoxin, or propranolol in the phase III studies.

More extensive experience with cimetidine showed that it was reasonably well tolerated. Postmarketing adverse experiences included dizziness and somnolence, reversible confusional states (in severely ill patients), mild diarrhea, gynecomastia, impotence, neutropenia, thrombocytopenia, increased hepatic transaminases, and increased serum creatinine (due to competition by the drug of renal tubular secretion of creatinine). Most of these adverse experiences are uncommon (occurring in <1% of patients) and dose related. Gynecomastia has been reported in as many as 4% of patients taking prolonged high doses of cimetidine for hypersecretory conditions (Zollinger–Ellison syndrome).

#### 2. Clinical Pharmacology

Cimetidine is over 90% absorbed with ~50% bioavailability after oral administration. The plasma half-life is 2 hours with a volume of distribution of 1 L/kg. In patients with renal failure, plasma half-life is prolonged to ~5 hours. It has relatively low plasma protein binding (13–25%) and is readily removed by hemodialysis. Nearly 50% of the drug is excreted unchanged in urine after an oral

dose, and 75% is excreted unchanged in the urine after an intravenous dose. The remaining drug after oral dosing is metabolized primarily to cimetidine sulfoxide and to a lesser extent to 5-hydroxymethyl cimetidine and guanylurea cimetidine, which are excreted in urine. Less than 2% of the drug is excreted unchanged in bile.

Although cimetidine itself does not appear to be a significant substrate for cytochrome P450 (CYP) enzymes, it has been shown to inhibit several enzymes to varying degrees, including CYP1A2, 2C19, and 3A4. The inhibitory effect of cimetidine on these enzymes is the basis for its drug–drug interaction profile.

### 3. Drug–Drug Interactions

Drugs metabolized by CYP that interact with cimetidine include, but are not limited to, the following: lidocaine, quinidine, midazolam, triazolam, nifedipine, verapamil, and fentanyl [4]. In each instance, inhibition of CYP by cimetidine results in reduced metabolic clearance and increases in serum concentrations of the other drug, which can lead to the expected toxicity and adverse experiences characteristic of the other drug.

### 4. Market Dynamics

Cimetidine was launched in the United States as a first-in-class compound in 1977. It held virtually 100% of the U.S. prescription antiulcerant market from 1977 to 1981. In 1982, Carafate captured 4% of the U.S. market, and it was not until 1983 that the second H<sub>2</sub> antagonist (Zantac®) became available. The market share of Tagamet® decreased steadily from 1983 until it went off patent in 1994 (Fig. 1). The U.S. retail pharmacy sales of Tagamet® peaked at \$534 million in 1986, when it comprised 56% of the dispensed prescriptions in the U.S. market. Zantac® held the greatest U.S. market share of dispensed prescriptions from 1988 (44%) through 1996 (33%), with peak sales of \$1.95 billion in 1994. The U.S. prescription antiulcerant market is currently led by Prilosec®, which has been the largest-selling drug in the world from 1996 through 1998.

Several factors contributed to Tagamet®'s market decline. Dosing convenience (twice a day) made Zantac® much more attractive than Tagamet® (four times a day) to physicians and patients. Tagamet® was eventually approved for twice-daily dosing, but not in time to prevent the market uptake of Zantac®. However, the adverse drug–drug interactions attributed to Tagamet® also played a prominent role in the marketing strategy and success of Zantac® and other competitors. Despite being the first H<sub>2</sub> blocker in the prescription market and the first to apply for approval for OTC marketing, the approval for OTC marketing for Tagamet® did not occur until September 1995 (more than one year after patent expiration), and another H<sub>2</sub> receptor antagonist (Pepcid®) actually launched first in the OTC market. The concern of drug–drug interactions continues to be a

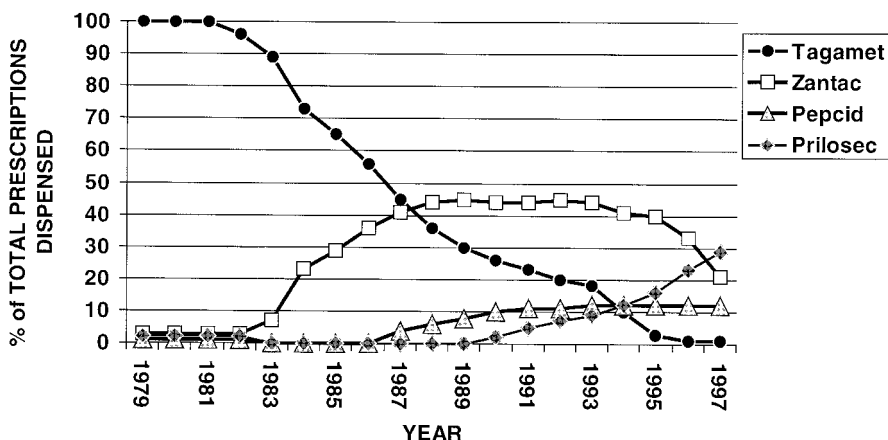


**Figure 1** Antilucerant market share, 1979–1997. The market share (expressed as percent of total prescriptions dispensed) of the antilucerant market is shown over the period from 1979 to 1997. Only four products (Tagamet®, Zantac®, Pepcid®, and Prilosec®) are shown. Other products in this market not shown here are Carafate®, Acid®, Cytotec, Propulsid®, Prevacid®, and generic cimetidine and ranitidine. Note that the initial increase in market share for Zantac® (1983–1986) came exclusively at the expense of Tagamet® and that further erosion of Tagamet® market share occurred as additional products were introduced into the market. Patent expiration for Tagamet® was in 1994, at which time it held 10% of the market. (Data derived from the National Prescription Audit, IMS America.)

factor in marketing efforts against cimetidine in both the prescription and OTC markets.

### III. CONCLUSIONS

Drug–drug interactions have always been important in the development of safe and effective drug therapies. The increasingly competitive marketplace requires that every possible advantage be highlighted, particularly with the more extensive use of direct-to-consumer advertising. The potential impact of drug–drug interactions must be considered at all phases of drug development.

### REFERENCES

1. F Mirasol. Pharma industry is poised for double-digit growth. *Chemical Market Reporter* 253:14–16, 1998.

2. P Galewitz. Ulcer drug is world's top seller. Associated Press, February 16, 1999.
3. IMS Health Drug Monitor, 12 months to December 1998.
4. EL Michalets, Pharm. D. Update: clinically significant cytochrome P-450 drug interactions. *Pharmacotherapy* 18:84–112, 1998.
5. Federal Register, Vol. 63, No. 195, October 8, 1998.
6. A Markham, AJ Wagstaff. Fexofenadine. *Drugs* 55:269–274, 1998.
7. MA Gonzalez, KS Estes. Pharmacokinetic overview of oral second-generation H<sub>1</sub> antihistamines. *Int J Clin Pharm Ther* 36:292–300, 1998.
8. M Cvetkovic, B Leake, MF Fromm, GR Wilkinson, RB Kim. OATP and P-glycoprotein transporters mediate the cellular uptake and excretion of fexofenadine. drug metabolism and disposition 27(8):866–871, 1999.
9. PK Honig, DC Wortham, K Zamani, DP Conner, JC Mullin, LR Cantilena. Terfenadine-ketoconazole: pharmacokinetic and electrocardiographic consequences. *JAMA* 269:1513–1519, 1993.
10. PK Honig, RL Woosley, K Zamani, DP Conner, LR Cantilena. Changes in the pharmacokinetics and electrocardiographic pharmacodynamics of terfenadine with concomitant administration of erythromycin. *Clin Pharm Ther.* 52:231–238, 1992.
11. BP Monahan, CL Ferguson, ES Killeavy, BK Lloyd, J Troy, LR Cantilena. Torsades de pointes occurring in association with terfenadine use. *JAMA* 264:2788–2790, 1990.
12. JW Slater, AD Zechnich, DG Haxby. Second-generation antihistamines, a comparative review. *Drugs* 57:31–47, 1999.
13. Cm Pratt, RP Hertz, BE Ellis, SP Crowell, W Louv, L Moye. Risk of developing life-threatening ventricular arrhythmia associated with terfenadine in comparison with over-the-counter antihistamines, ibuprofen and clemastine. *Am J Cardio* 73: 346–352, 1994.
14. RL Woosley, Y Chen, JP Freiman, RA Gillis. Mechanism of the cardiotoxic actions of terfenadine. *JAMA* 269:1532–1537, 1993.
15. RN Brogden, A Markham. Mibefradil, a review of its pharmacodynamic and pharmacokinetic properties, and therapeutic efficacy in the management of hypertension and angina pectoris. *Drugs* 54:774–793, 1997.
16. T Prueksaritanont, B Ma, C Tang, Y Meng, C Assang. Metabolic interactions between mibefradil and HMG-CoA reductase inhibitors: an in vitro investigation with human liver preparations. *Br J Clin Pharmacol* 47:291–298, 1999.
17. ME Mullins, BZ Horowitz, DHJ Linden, J Stump, GW Smith, RL Norton. Life-threatening interaction of mibefradil and [beta]-blockers with dihydropyridine calcium channel blockers. *JAMA* 280:157, 1998.
18. D Schmassman, R Bullingham, R Gasser, J Schmutz, WE Haefeli. Rhabdomyolysis due to interaction of simvastatin with mibefradil. *Lancet* 351:1929–1230, 1998.
19. F-D-C Reports, Inc. Roche Posicor withdrawn due to “complexities” of drug interactions, Roche says; FDA cites 25 drugs “dangerous” in combination with the calcium channel blocker. June 9, 1998.
20. RN Brogden, RC Heel, RM Speight, GS Avery. Cimetidine: a review of its pharmacological properties and therapeutic efficacy in peptic ulcer disease. *Drugs* 15:93–131, 1978.



# Index

- Absorption, 2, 23, 321
  - fraction ( $f_A, F_A$ ), 128, 360, 419
- Acetaminophen, 594
- Activation, 42
- Alprazolam, 570
- Alprenolol:
  - drug interaction, 6
- Area under the plasma concentration–time curve (AUC), 3, 6, 13, 19, 360, 364, 402, 420
- Autoactivation, 42
- Bioavailability:
  - hepatic, 419
  - oral, 25
- Biotransformation, 217
- Blood-brain barrier, 123
- Breath test, 77, 445, 452, 477
- Caffeine:
  - cytochrome P450 1A2, 68, 449
- Canalicular multispecific organic anion transporter (cMOAT/MRP2), 150, 158
- Cells:
  - brain capillary endothelial, 133, 311
  - [Cells]
    - Caco-2, 130, 309
    - Madine–Darby canine kidney (MDCK), 310
    - LLC-PK1, 132
    - OK, 132
  - Cerivastatin:
    - cyclosporin A and, 158
  - Cimetidine, 566, 640
  - Cisapride, 58
  - Clarithromycin, 370, 391, 405, 566, 573, 575
  - Clearance (CL), 4, 5, 7, 9, 61, 360, 442
    - hepatic, 9, 362, 419
    - intrinsic, 10, 12, 13, 61, 360, 402, 415, 418, 421
    - systemic, 4, 360, 419, 442
    - transport, 125
  - Concentration:
    - fifty percent inhibition ( $IC_{50}$ ), 242, 423
    - plasma, 4, 20
  - Correlation:
    - in vitro–in vivo, 196, 256, 283, 320, 610
    - liver bank, 260, 269



- Cyclosporin, 158, 330, 335, 367, 376, 407, 588
- Cytochromes P450 (CYP) 33, 36, 55, 189, 221, 359, 415, 439, 565
  - abundance, 57
  - active sites, 47, 509, 518
  - cycle, 36
  - induction, 189, 439
  - inhibition, 224, 439
  - in vivo probes, 440
  - microsomal, 36
  - models, 505
  - purified, 236
  - recombinant, 36, 235, 279
  - subfamilies, 57, 221
  - superfamily, 56, 221
  - tissue distribution, 57
- Cytochrome P4501A1 (CYP1A1), 43, 57
  - pharmacophore, 510
- Cytochrome P4501A2 (CYP1A2), 57, 65
  - induction, 67
  - inhibition, 67, 233, 587
  - in vivo probes, 449
  - pharmacophore, 511
  - selectivity, 65
  - substrates, 68, 233
- Cytochrome P450 2A6 (CYP2A6)
  - in vivo probe, 456
- Cytochrome P450 2B1 (CYP2B1)
  - homology model, 527
  - induction, 191, 192
  - pharmacophore, 512
- Cytochrome P450 2B6 (CYP2B6), 233
- Cytochrome P450 2C8 (CYP2C8):
  - homology model, 528
  - paclitaxel, 233
  - quercetin, 233
  - substrates, 233
- Cytochrome P450 2C9 (CYP2C9):
  - homology model, 528
  - inhibition, 69, 233, 586, 591
  - intestinal, 371
  - in vivo probes, 459
  - pharmacophore, 512
  - polymorphism, 69, 460
- [Cytochrome P450 2C9 (CYP2C9)]
  - selectivity, 68
  - substrates, 70, 233
- Cytochrome P450 2C19 (CYP2C19), 57
  - homology model, 528
  - inhibition, 71
  - intestinal, 371
  - in vivo probes, 462
  - polymorphism, 71, 462
  - selectivity, 70
  - substrates, 71, 233
- Cytochrome P450 2D6 (CYP2D6), 57
  - homology model, 528
  - inhibition, 73, 233, 566, 590
  - intestinal, 371
  - in vivo probes, 467
  - pharmacophore, 512
  - polymorphism, 73, 467
  - selectivity, 72
  - substrates, 73, 233
- Cytochrome P450 2E1 (CYP2E1), 57
  - in vivo probes, 472
- Cytochrome P450 3A2 (CYP3A2), 192, 207, 208
- Cytochrome P450 3A4 (CYP3A4), 42, 44, 57, 131, 220
  - homology model, 531
  - induction, 75
  - inhibition, 76, 566, 570, 573, 575, 587, 589
  - intestinal, 57, 366-371
  - in vivo probes, 475
  - MI complex, 370
  - pharmacophore, 517
  - selectivity, 74
  - substrates, 76, 233
- Cytochrome P450 3A5 (CYP3A5), 366, 475
- Cytosol, 218
- Dapsone, 477
- Database, 549
  - design, 550
  - object, 551
  - query, 554
  - relational, 551

- Debrisoquine:
  - cytochrome P450 2D6, 73, 469
- Dexamethasone:
  - cytochrome P450 induction, 194, 618
- Dextromethorphan:
  - cytochrome P450 2D6, 74, 470
- Digoxin:
  - interaction, 155, 163, 334, 593
- Diltiazem, 391, 400, 617
- Displacement, 25
- Disposition, 2
- Distribution, 14, 322
- Dosing:
  - bolus, 16
  - frequency, 24
  - infusion, 16
  - multiple, 16
  - route, 619
- Drug:
  - labeling, 623
  - marketing, 634, 636, 639, 641
  - perpetrator, 567
  - victim, 567, 586, 592
- Drug–drug interactions:
  - clinical, 439, 565, 605,
  - marketing and, 633
  - regulatory agency and, 605
  - toxicity and, 585
- Excretion, 327
- Expression:
  - protein, 192
  - RNA, 201, 204
- Extraction, 8, 421
- Erythromycin:
  - breath test, 77, 477
  - cytochrome P450 3A4, 77, 258, 477, 566
- First pass, 9, 359
  - intestinal, 360, 362, 404
  - liver, 362, 419
- Flavin-containing monooxygenase (FMO), 219, 269
- Fluvoxamine, 67, 233, 407, 566
- Gestodene, 258
- Grapefruit juice, 57
- Gut, 361
  - blood flow, 361
  - cytochrome P450 2C9, 371
  - cytochrome P450 2C19, 371
  - cytochrome P450 2D6, 371
  - cytochrome P450 3A4, 366, 404
  - cytochrome P450 3A5, 366
  - first pass, 360, 404
  - inhibition, 369
  - induction, 368
  - sulfotransferase, 373
  - UDP-glucuronosyltransferase, 373
- Half life ( $t_{1/2}$ ), 5, 20
- Hepatic clearance, 9, 362, 419
- Hepatocytes, 190
  - cultured, 133, 191, 237
  - induction in, 192, 208
- Hepatotoxicity, 594
- Homology model:
  - CYP3A1, 527
  - CYP2C8, 528
  - CYP2C9, 528
  - CYP2C19, 528
  - CYP2D6, 528
  - CYP3A4, 531
- Inactivation:
  - half maximal rate of ( $K_I$ ), 393, 395, 403
  - maximal rate of ( $k_{inact}$ ), 393, 395, 403
- Infusion, 15, 25
- Induction, 189, 192, 568
  - gut cytochrome P450 3A4, 368
  - measurement of, 201-206
  - screening, 197, 210
- Inhibition, 40, 62, 224, 226, 568
  - competitive, 126, 228, 230, 257
  - noncompetitive, 126, 228, 230, 257
  - partial, 42
  - screening, 63, 241, 251
  - suicide inactivation (mechanism-based), 225, 242, 257, 387-392, 417
  - uncompetitive, 228, 230, 257

- Inhibition constant ( $K_i$ ), 18, 19, 34, 41, 42, 126, 227, 242, 362, 418, 423
- Inhibitor:  
concentration, 18, 19, 41, 239, 362, 418, 428  
index, 18, 19, 28
- Interactions, 33, 365  
drug–drug, 6, 33, 98, 101, 152, 415, 565, 635, 638, 641  
prediction of, 102, 125, 162, 196, 256, 283, 320, 401, 415, 505, 610
- Intrinsic clearance, 10, 12, 13, 61, 360, 402, 415, 418, 421
- Imipramine:  
cytochrome P450 2C19, 72  
cytochrome P450 2D6, 614
- In vitro:  
assays, 197, 233, 314  
kinetics, 36, 229, 263, 395, 424  
models, 190, 232–237, 305, 308, 316, 319, 506, 518  
studies, 38, 42, 102, 128, 193, 240, 258, 261, 284, 395, 609
- Ketoconazole:  
cytochrome P450 3A4 inhibition, 76, 233, 369, 376, 420, 422, 425, 566, 570, 617
- Kinetics:  
atypical, 51  
biphasic, 46  
data analysis, 39, 230, 255, 265, 395  
in vitro, 36, 229, 263, 395, 424  
mechanism-based inhibition, 392, 395  
Michaelis–Menten, 34, 40  
non-Michaelis–Menten, 42, 43  
sigmoidal, 44
- Liver:  
bank, 269  
blood flow, 1, 2, 8, 13, 128, 361, 419  
microsomes, 232, 246  
perfusion, 317  
slices, 206, 237
- Macrolides:  
cytochrome P450 3A4 inhibition, 391, 573, 575
- Marketing, 634  
cimetidine, 640  
mibefradil, 637  
terfenadine, 635
- Mephenytoin:  
cytochrome P450 2C19, 71, 463
- Metabolism, 217, 324  
acetylation, 219  
fraction ( $f_m$ ), 19, 60, 402, 431  
glucuronidation, 89, 219, 373  
hydrolysis, 218  
methylation, 219  
oxidation, 218  
reduction, 218  
sulfation, 218, 373
- Metabolic intermediate (MI) complex, 370, 390
- Metabolic ratio:  
plasma, 444  
urinary, 443, 453, 463, 464
- Metoprolol:  
cytochrome P450 2D6, 74, 469
- Mibefradil, 637
- Michaelis constant ( $K_m$ ), 11, 18, 35, 123, 126, 227, 263, 418
- Midazolam:  
cytochrome P450 3A4, 77, 366, 422, 478, 617  
gut first pass, 359, 367  
kinetics, 426
- Models:  
hepatic, 9  
homology (protein), 518, 522  
P-glycoprotein, 306  
pharmacophore, 506, 509
- Multidrug resistance-associated protein 1 (MRP1), 149, 298
- Nifedipine:  
cytochrome P450 3A4, 77  
gut first pass, 359

- OCTN, 146
- Omeprazole:  
cytochrome P450 2C19, 72, 465
- Organic anion transporter (oat), 145
- Organic anion transporting polypeptide (oatp), 137, 158
- Organic cation transporter (oct), 137
- Organic solvents, 252
- Peptide transporter (PEPT), 147
- Perfusion:  
brain, 318  
kidney, 317  
liver, 317  
intestinal, 316
- P-glycoprotein (Pgp, MDR1), 130, 220, 295, 359  
expression, 297, 298  
gut, 374  
knockout mice, 149, 319  
methods to study, 314  
models of, 306  
nomenclature, 296  
recombinant, 313  
sister of (SPGP), 299  
structure, 301
- Pharmacodynamics, 1, 27, 571
- Pharmacokinetics, 1, 59, 360, 571  
alprazolam, 570, 617  
alprenolol, 6  
midazolam, 368, 478, 617, 618  
population, 621  
triazolam, 570, 575, 579, 617, 618  
warfarin, 6, 617
- Pharmacophore:  
CYP1A1, 510  
CYP1A2, 511  
CYP3A1, 512  
CYP2C9, 512  
CYP2D6, 512  
CYP3A4, 517
- Phenobarbital;  
alprenolol and , 6  
cytochrome P450 3A4 induction, 198
- Phenytoin:  
cytochrome P450 2C9, 70, 591  
cytochrome P450 3A4 induction, 198
- Polymerase chain reaction (PCR), 201
- Pregnane X receptor (PXR), 75, 207
- Primary active transporters, 137
- Probenecid:  
interaction, 99, 159, 160, 165
- Proguanil:  
cytochrome P450 2C19, 466
- Protein binding:  
plasma, 13
- Quinidine:  
P-glycoprotein, 156, 163, 331  
cytochrome P450 2D6, 73, 233, 566
- Reaction phenotyping, 258, 282  
chemical and antibody inhibitors, 260, 276  
correlation analysis, 260, 269  
recombinant enzymes, 260, 279
- Reaction velocity:  
maximal ( $V_{max}$ ), 18, 35, 126, 263  
initial, 253
- Retinoic acid receptor (RXR), 207
- Ribonuclease protection, 204
- Rifampicin:  
warfarin and, 6  
cytochrome P450 3A4 and, 77, 198, 204, 368, 566, 618
- Ritonavir:  
cytochrome P450 3A4, 391, 398, 566  
P-glycoprotein, 156
- Saquinavir:  
P-glycoprotein, 156
- Secondary active transporters, 137
- Sparteine, 468
- Study design:  
clinical, 571, 574, 611  
in vitro, 38, 42, 193, 240, 241, 260, 314

## Substrate:

concentration ([S]), 34, 38, 41, 237, 418

inhibition, 42, 46

## Sulfotransferase:

gut, 373

metabolism by, 219, 373

Systemic clearance, 4, 360, 419, 442

Terfenadine, 359, 367, 635

Tertiary active transporters, 137

## Theophylline:

cytochrome P450 1A2, 450, 587

interaction, 587, 617

## Tolbutamide:

cytochrome P450 2C9, 70, 461

interaction, 162, 166

## Toxicity:

drug–drug interactions and, 585

prediction of, 533

Transport clearance, 125

Transporters, 22, 123, 135

blood–brain barrier, 124

canalicular multispecific organic anion (cMOAT/MRP2), 150, 158

drug–drug interactions and, 152, 167, 329–335, 375, 593

intestinal, 124, 374

in vitro methods, 128

kidney, 124

multidrug resistance-associated protein 1 (MRP1), 149, 298

OCTN, 146

organic anion (oat), 145

organic anion transporting polypeptide (oatp), 137, 158

organic cation (oct), 137

peptide (PEPT), 147

primary active, 137

P-glycoprotein (Pgp), 22, 148, 152, 295, 296, 299, 301

secondary active, 137

## [Transporters]

sodium phosphate cotransporter (NPT1), 147

tertiary active, 137

## Triazolam:

cytochrome P450 3A4, 617

kinetics, 426

pharmacokinetics, 368, 570, 575, 579, 617, 618

## Unbound:

fraction ( $f_u$ ), 10, 13, 15

UDP-glucuronosyltransferase (UGT), 89

families, 90

gut, 373

induction, 103

inhibition, 593

probenecid, 99

UGT1A1, 91

UGT1A3, 92

UGT1A4, 92

UGT1A6, 94

UGT1A7, 94

UGT1A8, 94

UGT1A9, 94

UGT1A10, 96

UGT2B7, 97

zidovudine, 100

## Verapamil:

P-glycoprotein, 330

Volume, 3, 5, 7, 23

body ( $V_T$ ), 14, 15

plasma ( $V_p$ ), 14, 15

## Warfarin:

cytochrome P450 2C9, 68

drug interactions, 6, 586, 617

## Zidovudine:

interactions, 100